SECOND
INTERNATIONAL CONFERENCE ON

Nuclear Data for Reactors

CONFERENCE PROCEEDINGS
HELSINKI,
15-19 JUNE 1970

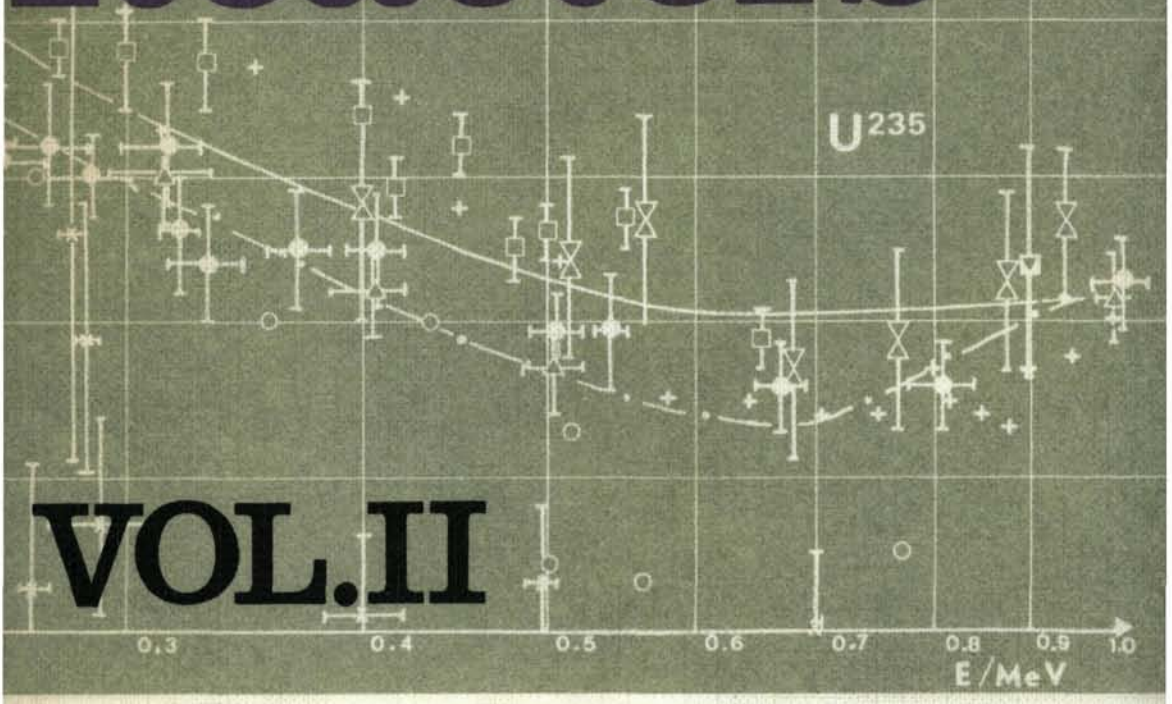

VOL. II

INTERNATIONAL ATOMIC ENERGY AGENCY, VIENNA, 1970

NUCLEAR DATA FOR REACTORS

VOL. II

The following States are Members of the International Atomic Energy Agency:

AFGHANISTAN
ALBANIA
ALGERIA
ARGENTINA
AUSTRALIA
AUSTRIA
BELGIUM
BOLIVIA
BRAZIL
BULGARIA
BURMA
BYELORUSSIAN SOVIET SOCIALIST REPUBLIC
CAMBODIA
CAMEROON
CANADA
CEYLON
CHILE
CHINA
COLOMBIA
CONGO, DEMOCRATIC REPUBLIC OF
COSTA RICA
CUBA
CYPRUS
CZECHOSLOVAK SOCIALIST REPUBLIC
DENMARK
DOMINICAN REPUBLIC
ECUADOR
EL SALVADOR
ETHIOPIA
FINLAND
FRANCE
GABON
GERMANY, FEDERAL REPUBLIC OF
GHANA
GREECE
GUATEMALA
HAITI
HOLY SEE
HUNGARY
ICELAND
INDIA
INDONESIA
IRAN
IRAQ
IRELAND
ISRAEL
ITALY
IVORY COAST
JAMAICA
JAPAN
JORDAN
KENYA
KOREA, REPUBLIC OF
KUWAIT
LEBANON
LIBERIA
LIBYAN ARAB REPUBLIC
LIECHTENSTEIN
LUXEMBOURG
MADAGASCAR
MALAYSIA
MALI
MEXICO
MONACO
MOROCCO
NETHERLANDS
NEW ZEALAND
NICARAGUA
NIGER
NIGERIA
NORWAY
PAKISTAN
PANAMA
PARAGUAY
PERU
PHILIPPINES
POLAND
PORTUGAL
ROMANIA
SAUDI ARABIA
SENEGAL
SIERRA LEONE
SINGAPORE
SOUTH AFRICA
SPAIN
SUDAN
SWEDEN
SWITZERLAND
SYRIAN ARAB REPUBLIC
THAILAND
TUNISIA
TURKEY
UGANDA
UKRAINIAN SOVIET SOCIALIST REPUBLIC
UNION OF SOVIET SOCIALIST REPUBLICS
UNITED ARAB REPUBLIC
UNITED KINGDOM OF GREAT BRITAIN AND NORTHERN IRELAND
UNITED STATES OF AMERICA
URUGUAY
VENEZUELA
VIET-NAM
YUGOSLAVIA
ZAMBIA

The Agency's Statute was approved on 23 October 1956 by the Conference on the Statute of the IAEA held at United Nations Headquarters, New York; it entered into force on 29 July 1957. The Headquarters of the Agency are situated in Vienna. Its principal objective is "to accelerate and enlarge the contribution of atomic energy to peace, health and prosperity throughout the world".

Printed by the IAEA in Austria
November 1970

PROCEEDINGS SERIES

NUCLEAR DATA FOR REACTORS

PROCEEDINGS OF THE
SECOND INTERNATIONAL CONFERENCE ON
NUCLEAR DATA FOR REACTORS
HELD BY THE
INTERNATIONAL ATOMIC ENERGY AGENCY
IN HELSINKI, 15 - 19 JUNE 1970

In two volumes

VOL. II

INTERNATIONAL ATOMIC ENERGY AGENCY
VIENNA, 1970

NUCLEAR DATA FOR REACTORS
IAEA, VIENNA 1970
STI/PUB/259

FOREWORD

The Second International Conference on Nuclear Data for Reactors, held in Helsinki at the invitation of the Finnish Government, was convened by the International Atomic Energy Agency from 15 to 19 June 1970. The Conference, held as a result of recommendations made by the International Nuclear Data Committee, was attended by 163 participants from 28 countries and four international organizations, and 21 invited and 98 contributed papers were presented.

This Conference was the second held by the IAEA on Nuclear Data for Reactors. Almost four years have elapsed since the first was held in Paris in 1966. During these years gratifying progress has been made by reactor, nuclear and evaluation physicists, whose collaboration has been greatly enhanced. As a result, many laboratories have concentrated their efforts on items of particular importance for reactor research and development, and many measurements are now available.

The main purpose of this Conference was to provide an opportunity to review results of recent basic neutron-physics investigations against a background need for basic information, especially concerning reactors.

The Conference itself, together with the preparatory meetings of IAEA experts in Studsvik on the status of $\alpha(^{239}\mathrm{Pu})$ and the $\bar{\nu}$-values for fissionable nuclei, showed an emphasis on the nuclear data aspects most important for nuclear technology.

Most contributors dealt with the measurement and analysis of neutron cross-sections. This extensive new cross-section information can be attributed to several factors, the most important being the development and systematic exploitation of high-intensity neutron sources, such as modern linear accelerators, modern cyclotrons and underground nuclear explosions, improvements in instrumentation and in sample preparation techniques, and other technical improvements.

Compared with the first IAEA Conference on Nuclear Data for Reactors this one has many more contributions on neutron data evaluation. Many papers are concerned with systematic evaluation of fission, capture and inelastic-scattering cross-sections of the most important fissile and fertile nuclei and of capture cross-sections of the main structural materials.

The vivid interest of the participants is clearly indicated by the extensive discussions, and pertinent problems still to be solved have been revealed, which constitute a challenge for the future.

The Agency wishes to thank the Finnish authorities as well as the authors and participants for their valuable contributions and the Chairmen of the individual sessions for their effort in organizing lively discussions.

EDITORIAL NOTE

The papers and discussions incorporated in the proceedings published by the International Atomic Energy Agency are edited by the Agency's editorial staff to the extent considered necessary for the reader's assistance. The views expressed and the general style adopted remain, however, the responsibility of the named authors or participants.

For the sake of speed of publication the present Proceedings have been printed by composition typing and photo-offset lithography. Within the limitations imposed by this method, every effort has been made to maintain a high editorial standard; in particular, the units and symbols employed are to the fullest practicable extent those standardized or recommended by the competent international scientific bodies.

The affiliations of authors are those given at the time of nomination.

The use in these Proceedings of particular designations of countries or territories does not imply any judgement by the Agency as to the legal status of such countries or territories, of their authorities and institutions or of the delimitation of their boundaries.

The mention of specific companies or of their products or brand-names does not imply any endorsement or recommendation on the part of the International Atomic Energy Agency.

CONTENTS OF VOL. II

NUCLEAR DATA ABOVE THE RESONANCE ENERGY: A > 220 (Section V)

NUCLEAR DATA ABOVE THE RESONANCE ENERGY: A < 220 (Section VI)

RELATIONSHIPS OF MICROSCOPIC AND INTEGRAL DATA
(Section VII)

EVALUATION PROBLEMS AND METHODS I (Section VIII)

EVALUATION PROBLEMS AND METHODS II (Section IX)

Section V

NUCLEAR DATA ABOVE THE RESONANCE ENERGY: A >220

Chairman
W.G. DAVEY (USA)

Invited Paper

RECENT EXPERIMENTAL DATA FOR HEAVY NUCLEI*

W.P. POENITZ
Applied Physics Division,
Argonne National Laboratory,
Argonne, Ill.,
United States of America

Abstract

RECENT EXPERIMENTAL DATA FOR HEAVY NUCLEI.

Nuclear data for ^{235}U, ^{238}U, and ^{239}Pu are of major importance for the development of fast reactor systems. Many experimental techniques developed in the past and successfully applied to lighter and non-fissile nuclei are complicated by the complex characteristics of the fissile nuclei. The precision the needed data are demanding of these older techniques often requires new experimental approaches.

Though the determination of total cross-sections using the transmission method is, in principle, not difficult, large discrepancies exist in the resulting cross-sections. For example, large discrepancies in the total cross-section of ^{238}U have been resolved only recently, and there still remain uncertainties of several per cent. The measurements of elastic and inealstic cross-sections of fissile and fertile nuclei are strongly affected by low-lying levels, by the large level density and by their fissile properties. Investigations of the level schemes of these nuclei by measurements of the γ-de-excitation of levels occupied either in the (n, n')-process or the α-decay support theoretical calculations of the inelastic scattering cross-sections.

The time-of-flight method has frequently been used in recent experiments to determine the fission cross-sections of ^{233}U, ^{239}Pu, and ^{238}U relative to that of ^{235}U. Such ratio measurements for ^{239}Pu confirm previous experiments with continuous neutron beams in the higher keV energy range but discrepancies of 10-15 per cent still exist in the energy range below 100 keV. The capture cross-sections of ^{235}U and ^{239}Pu are accessible through α-measurements. The results obtained for ^{239}Pu using different techniques are still discrepant. The measurements of prompt γ-rays to determine the capture cross-section of ^{238}U is difficult due to the low binding energy and the contribution from the γ-radiation emitted in the fission processes. The activation method seems to be more appropriate. Absolute values of the capture cross-sections of ^{238}U and the fission cross-section of ^{235}U have been obtained with different experimental techniques; however, the discrepancies are still of the order of 10-30 per cent.

Experiments for the determination of $\bar{\nu}$ (E) of ^{235}U suggest deviations from the linear behaviour previously assumed by about 2-3 per cent in the keV energy range.

INTRODUCTION

It is the purpose of this contribution to critically review the present knowledge of experimental nuclear data of fertile and fissile nuclei above the resonance energy region. Recent request lists for nuclear data have been more and more demanding of the accuracy of such data as the capture cross section of U-238 and the fission cross sections of U-235 and Pu-239. This situation reflects the importance of such cross sections in fast reactor calculations and design. Because of the large amounts of data involved the present review will be mainly restricted to those heavy nuclei and their properties which have the strongest influence on the neutronics of fast reactors.

* Work supported by the United States Atomic Energy Commission.

Therefore, the consideration for nuclear data of U-235, U-238, and Pu-239 will be emphasized. The capture and fission cross sections as well as $\bar{\nu}$ of these nuclei represent the negative and positive sources of neutrons in a reactor and are thus of predominant importance. Measurements of the average number of neutrons per fission are closely related to the problem of the Cf-252 standard, therefore only certain features of their energy dependence will be considered here. The importance of the inelastic scattering cross sections lies in their influence on the neutron energy spectra in a reactor. It has been suggested by Campbell [1] that the inelastic scattering cross section of U-238 might be too high and cause the underevaluation of k_{eff} which previously had been removed by lowering the capture cross section of U-238. This has been further substantiated by subsequent investigations by Zolotar et al. [2].

Consideration is here given to the energy range 10 keV - 10 MeV, however, this range is extended or reduced where it was felt that certain features of the data would be demonstrated more clearly by doing so. It is not the intention of the present review to present all the available data but to show certain features related to experimental techniques and to give an understanding of the precision and reliability of presently available data. Therefore, in the figures presented for some of the data eye-guide curves have been used instead of the original experimental points. Some data have been rejected as being immaterial for the particular feature under discussion.

FAST NEUTRON TOTAL AND SCATTERING CROSS SECTIONS

The Total Cross Section of Uranium

Measurements of absolute total cross sections have always been considered to be relatively easy because no determination of the absolute neutron flux or the detector efficiency has to be carried out. However, even with this consideration, discrepancies up to 15 per cent exist between different measurements. Particularly notable were the low total cross section data reported for uranium and thorium in Ref. [3] and some new high resolution data for several elements in Ref. [4] which are discrepant up to 15 per cent compared to previous measurements which had been considered to be reliable. This situation has been somewhat improved since the former measurements have been replaced by new data by Divadeena [5] and correction factors are available for the latter. However, discrepancies still exist which are difficult to understand in view of the basic experimental method. The total cross section of uranium might be a good example of the presently available accuracy of total cross sections of heavy elements.

Data are shown in Fig. 1 for the energy range 100-1200 keV. The new data by Divadeenam [5] are by about 10-15 per cent higher than the previous results given in Ref. [3]. The difference has been explained by in-scattering of neutrons due to a small distance between the sample and the neutron source. The new values by Divadeenam agree very well with measurements by Henkel [6] and by Barschall [7]. Measurements by Meads [8], Uttley et al. [9], and Whalen [10] yield values which are, in the energy range from 200-400 keV, up to 6 per cent higher. The data from both groups join at 100 keV, the values measured by Hibdon and Langsdorf [11]. Above 500 keV both groups are also in agreement. Recently, Smith [12] applied an experimental technique which usually is used in conjunction with scattering, fission or capture cross section measurements. In this measurement monoenergetic neutrons have been obtained from a thin Li-target and the time-of-flight technique has been applied for background suppression. Several different sample thicknesses and sizes have been used. The results confirm in the higher energy range both the measurements by Henkel

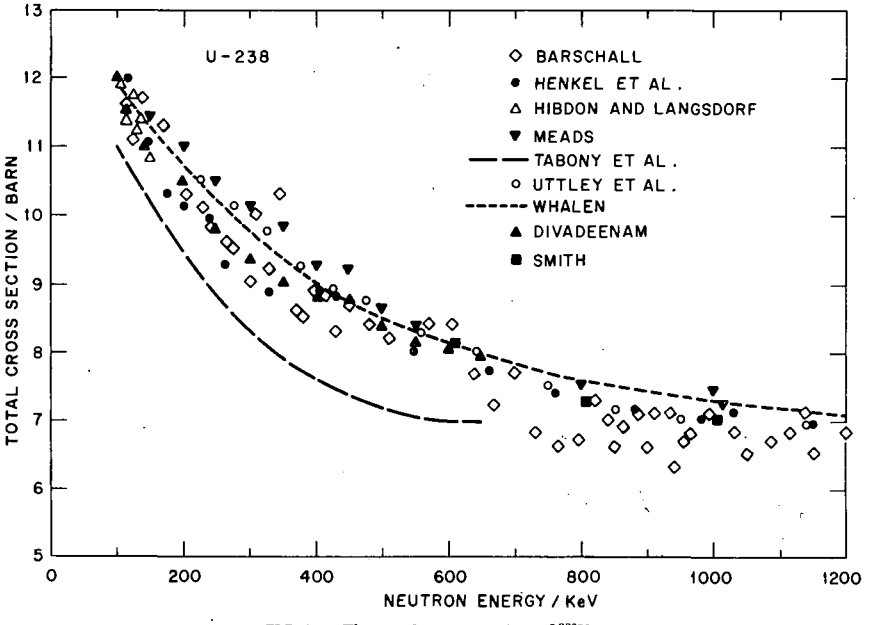

FIG. 1. The total cross-section of ^{238}U.

[6] and Uttley et al. [9] which are, however, discrepant at lower energies. On the basis of the data shown in Fig. 1 it seems feasible to suggest values for the total cross section for uranium with an approximate uncertainty of 3 per cent.

The measurements by Whalen [10] have been carried out with a resolution of about 5 keV. These measurements show little if any structure in the total cross section of uranium in the energy range from 100-1500 keV.

Experimental Techniques for Fast Neutron Scattering

Measurements of scattering cross sections have been tremendously improved in recent years by the use of the time-of-flight method to separate elastically and inelastically scattered neutrons. Sufficiently strong neutron sources are available with the $Li^7(p,n)$ and $T(p,n)$ reactions for the investigation of the inelastic scattering cross sections associated with low lying levels in a nucleus. Usually, organic scintillators are employed to detect the scattered neutrons because of their fast response. A time resolution of about 3 nsec can be achieved for a reasonable detector thickness, sample size, and a primary pulsed proton beam bunched to about 1 nsec width. The detector efficiency at lower neutron energies can be improved by using two multipliers in coincidence or the now available low noise bi-alkali multipliers. The use of pulse-shape discriminators for γ-background reduction is common for such experimental apparatus. Whereas most of the inelastic scattering cross section data were obtained at only one angle, usually at 90^0 (e.g. Barnard et al. [13] for U-238) some data have been taken at up to 10 angles simultaneously (Smith [14]). Measurements of inelastic scattering cross sections usually are carried out relative to the well known elastic scattering cross sections of carbon or hydrogen.

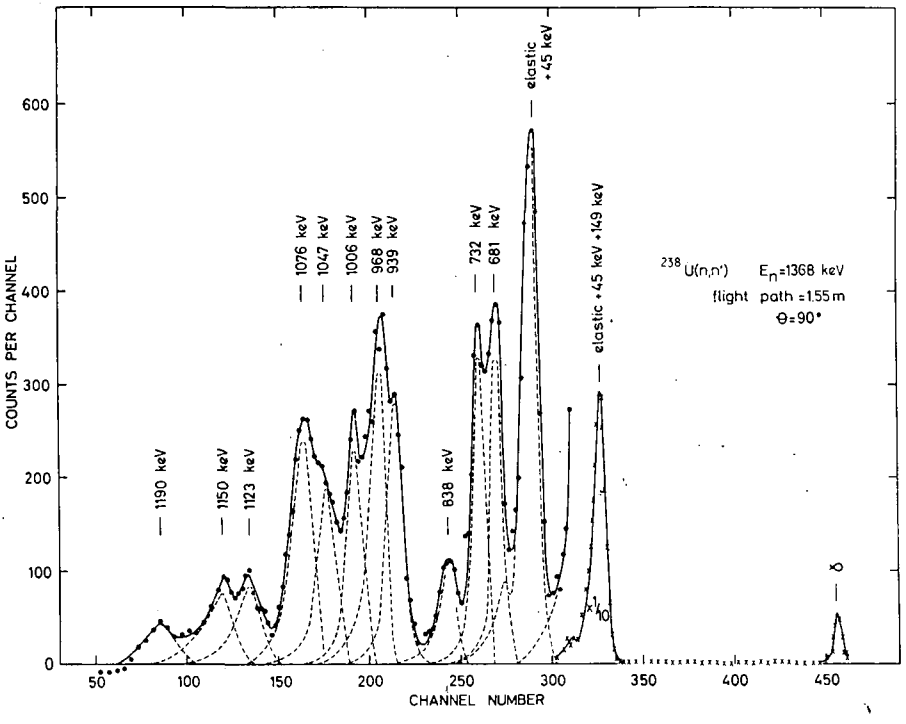

FIG. 2. Time-of-flight spectra for scattering on ^{238}U (Barnard et al. [13]).

Fig. 2 shows a time-of-flight spectrum for U-238, measured recently by Barnard et al. [13]. The incident neutron energy is 1.37 MeV. Besides the strong intensities for elastically scattered neutrons one obtains several groups of inelastically scattered neutrons. The figure shows that the determination of neutron cross sections requires some knowledge of the level scheme. Lack of such knowledge could lead to a distribution of the measured intensities to levels only as far as they have been assigned, and the intensities associated to missing levels would be accounted for by elevated cross sections for other levels. When the level density gets very high an arbitrary grouping according to different energy ranges is the only reasonable way to describe the inelastic scattering process. Even this procedure is hampered by the presence of fission neutrons, and new approaches must be attempted.

A knowledge of the level scheme which allows the theoretical calculation of the inelastic cross sections is very helpful. Different techniques are in use to investigate the level schemes of heavy nuclei; e.g. the level scheme of U-235 has been investigated by careful measurements of the α- and γ-spectrum from the decay of Pu-239 by Baranov et al. [15] and by Horsch [16]. Due to the long half life of the parent-isotope Pu-242 this method cannot be applied in the case of U-238. Coulomb-excitation with heavy ions has been used by Stephens et al. [17], however, not all levels which contribute to the inelastic neutron scattering were excited by this process.

Measurements of the γ-rays associated with the inelastic neutron scattering process is a technique in use for some time. The application of lithium drifted-germanium-detectors lead to a tremendous improvement of the energy resolution in such measurements. The determination of cross sections from such

measurements is complicated for heavy nuclei by the uncertainty of the electron conversion and branchings for most of the transitions. However, helpful information can be obtained to supplement data obtained from measurements detecting the inelastically scattered neutrons. In such experiments the sample is positioned close to the target and bombarded with monoenergetic neutrons. The γ-rays from the sample are detected with a Ge(Li)-detector positioned 30-60 cm

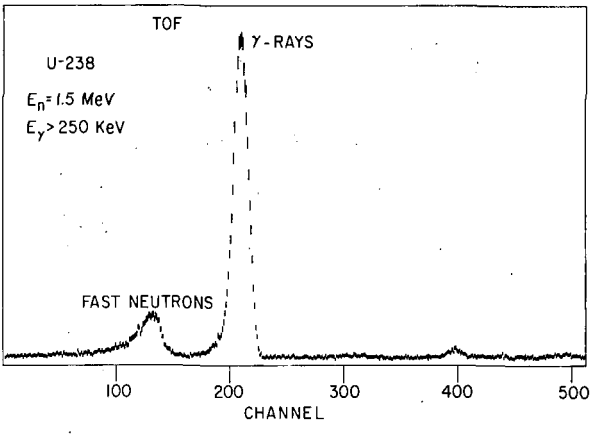

FIG. 3. Time-of-flight spectra for γ-rays of ^{238}U using a Ge (Li)-detector.

away from the sample and shielded against direct neutron bombardment. The time-of-flight method is used to separate the prompt γ-rays of the inelastic scattering process from background γ-rays due to fast neutrons. Fig. 3 shows a time-of-flight spectrum recently measured for U-238 at Argonne using a 7 ccm Ge(Li)-detector. The time resolution in such measurements is a function of the measured γ-energies and certain features of the detector. The use of rise time correction techniques reduces the spread of the prompt γ-peak in the TOF spectra. For E_γ > 200 keV a resolution better than 4 nsec has been achieved with the planar drifted 7 ccm detector. The remaining background under the prompt γ-peak can be properly subtracted by determining the spectrum found in an equally large time interval adjacent to the prompt peak. The resulting γ-spectra are shown in Fig. 4. This demonstrates very well the superiority of the energy resolution of such measurements compared to the time-of-flight neutron detection technique. The energy resolution is only indirectly influenced by the energy spread of the primary neutron beam. Therefore, thicker targets can be used and count rates similar to those obtained with the neutron detection technique can be achieved. For the determination of cross sections, the use of primary scattering standards like carbon and hydrogen is not possible, and measurements have to be carried out relative to another less accurately known inelastic scattering cross section. In some instances additional spectroscopic information such as spins can be deduced from γ-ray angular distribution measurements.

Inelastic Scattering Cross Sections

Some new measurements for the inelastic scattering cross sections of Pu-239 by Cavanagh et al. [20] and Pu-240 by Smith [19] are shown in Fig. 5. These figures demonstrate the difference between the inelastic cross section for even-even nuclei like Pu-240 and odd nuclei like Pu-239. Only three levels exist below 500 keV for Pu-240, all are members of the ground state rotational

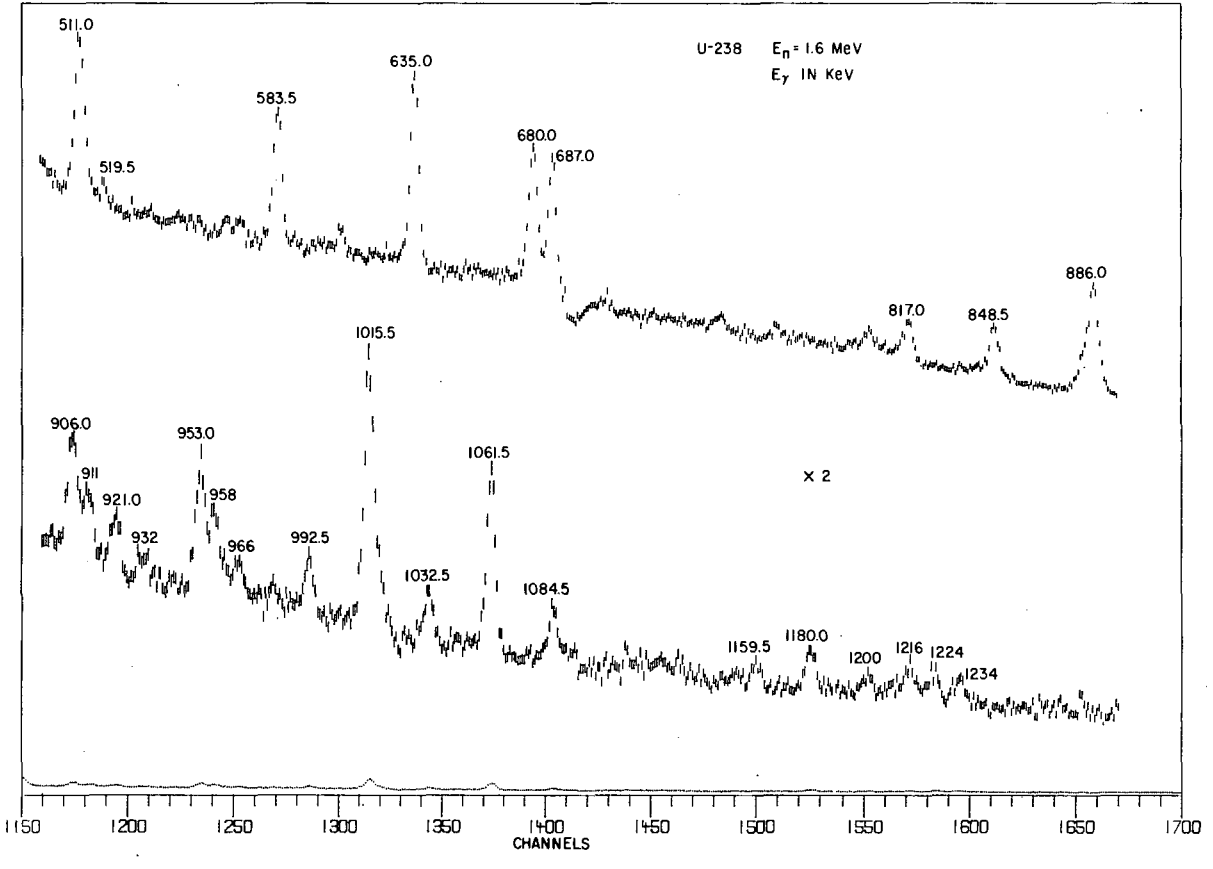

FIG. 4. γ-ray energy spectra of ^{238}U.

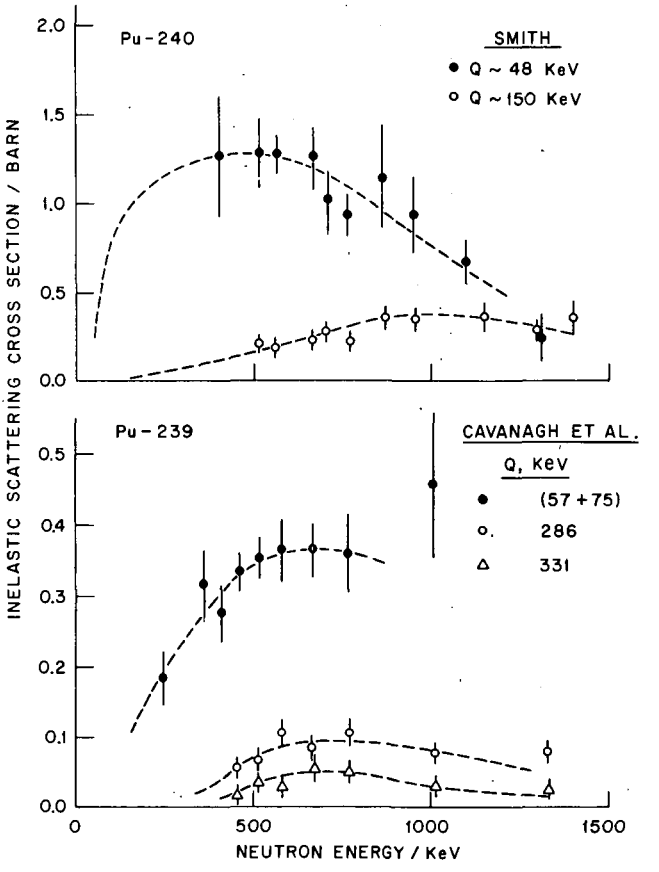

FIG. 5. Inelastic scattering cross-sections of ^{239}Pu and ^{240}Pu.

band, and the cross sections are sufficiently large to be well separated from the fission neutron background. In the same energy range about 15 or more levels exist for Pu-239 but only some of them can be measured and not all were resolved sufficiently. The cross sections are very small, therefore the background causes tremendous problems.

The inelastic scattering cross section of U-238 appears to be the best measured of any nuclei with A > 220. Extensive measurements have been reported by Barnard et al. [13]. These measurements have been carried out with sufficient resolution to resolve most of the important levels up to about 1.1 MeV. An appreciable contribution to the inelastic scattering process has been observed from two levels at 930 and 960 keV unknown from Coulomb-excitation experiments. Recent Ge(Li)-detector measurements confirmed the existence of these levels (930.5 and 966.5 keV) and showed the presence of a third level in the same energy region (950.5 keV) (Poenitz [18]). For energies above 1.1 MeV Barnard et al. [13] reported several levels which contribute about 1.2 barn to the total inelastic cross section at 1.6 MeV.

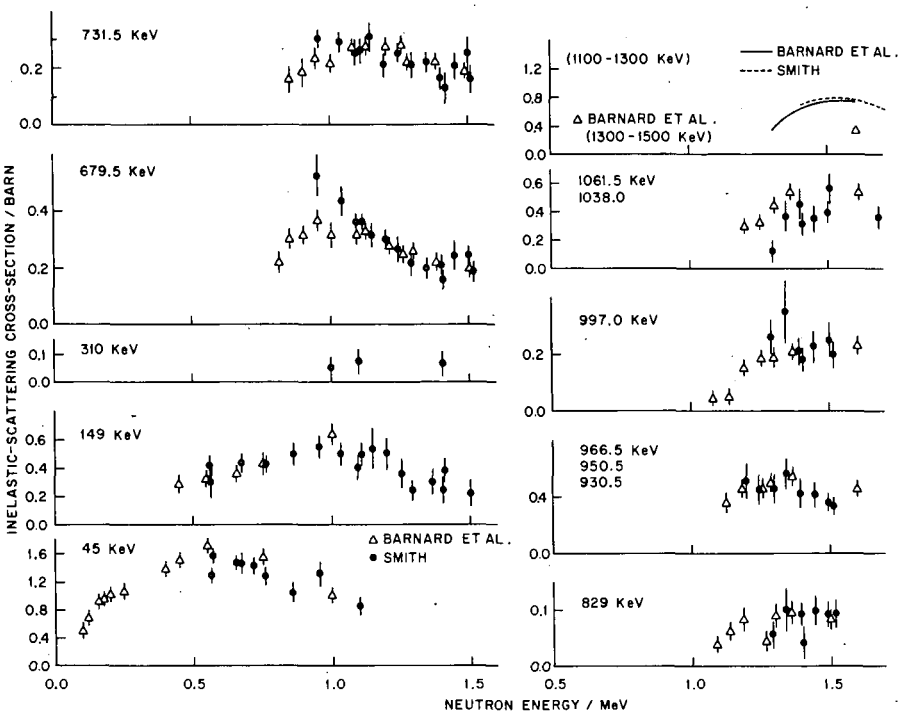

FIG. 6. Inelastic-scattering cross-sections of ^{238}U.

TABLE I. INELASTIC-SCATTERING CROSS-SECTIONS OF ^{238}U AT 1.6 MeV

Q/keV	Barnard et al[13] (a)	Smith[19]
45	b)	b)
149	0.16	0.18
310	0.06	0.05
680	0.17	0.17
731	0.17	0.15
829	0.09	0.08
930-966	0.45	0.34
977	0.21	0.22
1038-1061	0.55	0.41
1100-1300	0.84	0.81
1300-1500	0.44	0.36(d)
1500-1600	0.10(c)	0.10(c)
	3.24	2.87

a) Analysis by Schmidt [46].
b) Value cannot be obtained from measurements. 0.0 barn has been extrapolated in Ref. 46.
c) Value is from analysis of other available data given in Ref. 46.
d) Value has not been measured. The value given by Barnard et al. has been used and corrected for an assumed error in the detector efficiency.

The measurements by Barnard et al. [13] have been carried out at 90° only. The cross sections reported at that angle have been multiplied by 4π, and are shown in Fig. 6. The energies given in Fig. 6 are from Ge(Li)-detector γ-ray measurements (Poenitz [18]). Recent measurements by Smith [19] at 8 angles showed that the anisotropy does not exceed 10 per cent. These new measurements by Smith are also shown in Fig. 6. In addition, Smith measured cross sections for the sum of several levels which indicate that the values obtained by Barnard et al. [13] at 1.6 MeV for several cross sections might be too high. The agreement between the two sets of measurements shown in Fig. 6 is good. This may, however, be deceptive because the sum of the elastic and inelastic scattering cross section as measured by Barnard et al. [13] exceeds by 10-30 per cent the total cross section. A comparison for the total inelastic cross section at 1.6 MeV has been given in Tab. I. The values given under Barnard et al. [13] are based upon an analysis by Schmidt [46]. The values measured by Smith [19] have been corrected for missing levels above 1.3 MeV as indicated in Tab. I. The sum of the total inelastic scattering cross section and the elastic scattering cross section as measured by Smith is 6.57 barn which compares very well with 6.60 barn for the total scattering cross section as measured by Lane et al. [47] and Langsdorf et al. [48]. Adding 0.40 barn for the fission cross section and 0.08 barn for the capture cross section, one obtains 7.05 barn which compares well with the total cross section of 7.10 barn as measured by Henkel et al. [6] and Leroy et al. [49]. The values obtained from Barnard et al. [13] do not fit the total cross section quite as well, though they agree within the error bars.

FAST NEUTRON CAPTURE AND FISSION CROSS SECTIONS

Experimental Methods and Techniques

The basic experiment to measure a capture or fission cross section is to expose a sample in a neutron flux, $\emptyset$, and to count the events, C, corresponding to the type of reaction under consideration. The equation used to determine the cross section is $\sigma = C/N \cdot \emptyset$, where N is a constant which includes the mass of the sample. Such a measurement is considered "absolute" if both the reaction rate and the neutron flux have been determined absolutely. The usual way to avoid the absolute neutron flux measurement is to carry out a similar measurement for a sample material with a cross section which is supposed to be well known and defined "standard". A cross section determined in such experiment has been measured "relative" to another cross section. It should be emphasized that in such experiment the originally measured quantity is a cross section ratio and not the cross section itself which is determined from the equation $\sigma = N' \cdot R \cdot \sigma_{ST}$. N' is again a constant, R the measured ratio, and σ_{ST} the standard cross section. In the fast energy range the cross sections for the reactions H(n,n), $B^{10}(n,\alpha)$, $Li^{6}(n,\alpha)$, Au(n,γ), and U-235(n,f) have been accepted as standards. Among these standards the H(n,n) cross section is the best known cross section. This does not, however, mean that a cross section measured relative to this standard is the most reliable one because the measurement of the ratio is in this case much more difficult than for other standards. As it will be seen, measurements of cross sections relative to the H(n,n) cross section do not give consistent results.

Measurements of the ratio of two cross sections of the same type should be easiest to be carried out. In such instances similar geometrical conditions can be achieved, and the uncertainties of the efficiencies for counting the two reaction rates are likely to cancel out in first order. But still, care has to be taken to account for scattered neutrons and to correct for neutrons

of different energies. A very appropriate technique to apply is the time-of-flight method in order to separate background from the primary energy neutrons. Whereas the measurement of capture to fission ratios is still feasible, some problems exist for measurements of fission or capture cross sections relative to the cross sections for the reactions $Li^6(n,\alpha)$, $B^{10}(n,\alpha)$, H(n,n). The former two are usually applied in the lower keV energy range in time-of-flight measurements at a Linac where the counting efficiency can be eliminated by the well known thermal cross sections or resonance parameters. If such a procedure is not possible, as in measurements at a Van de Graaff, the shape of the cross section ratio may be the more reliable result. For ratio measurements involving the H(n,n)-cross section one has to be aware of the completely different energy dependence of the cross sections and of the different behavior of the effective efficiency of the detectors involved. It is unfortunate that the time-of-flight method is only applicable with many restrictions to the measurement of recoil protons. In spite of such difficulties uncertainties as low as 2 per cent have been reported for cross section measurements relative to the H(n,n) cross section. This is amazing as differences on the order of 10 times these uncertainties exist between different measurements of this type. Some improvement can be expected by the use of surface-barrier counters to detect the recoil protons. Such counter would allow a fast timing and improve the measurements to some extent. A recent suggestion to extend measurements relative to the H(n,n) cross section to a few per cent of a keV cannot be achieved with presently known techniques. A reasonable limit for the proton recoil counters presently used seems to be 10 keV.

Measurements of absolute capture and fission cross sections are based mainly on two different methods for the neutron flux determination. The neutron flux integration technique utilizes the well known thermal cross sections by the slowing down of the fast neutrons and measuring their capture at thermal energies. The most famous detector belonging to this group is the $MnSO_4$-bath. The best application of this technique for the determination of fast neutron fluxes is the use of the $MnSO_4$-bath to determine the source strength of a radioactive neutron source which in turn can be utilized to calibrate detectors. The calibration of collimated neutron fluxes seems to be also feasible if a sufficient shielding can be provided. The associated particle or the associated activity technique uses the detection of the charged particles or the residual activity from the neutron source reaction to measure the absolute neutron flux. The detection of the associated particles is very straight-forward in the case of the $T(d,n)He^4$ reaction. A very sophisticated technique is needed in the case of $T(p,n)He^3$ reaction which provides neutrons in the keV energy range. For the determination of the associated activities usually a high accuracy can be achieved. Some doubt about the branching ratio for the decay of associated activities like Be^7, Cr^{51}, and Zn^{65} has recently been removed.

The problem of the determination of absolute fission rates can be considered as solved. Using deposits of about 100 mg/cm^2 fissile material and ionization or gas scintillation counters an efficiency of about 98 per cent can be achieved, thus the uncertainty of the correction contributes very little to the final error. The use of gas scintillation counters is preferable due to their fast time response. Fast timing of ionization chambers has been applied in several recent experiments. The determination of capture rates by the activation method is certainly not up-to-date considering the advantage of prompt γ-ray detection using large liquid scintillators or Moxon-Rae-detectors. However, the accuracy which can be achieved with the activation method for the absolute measurements of the capture rate is in some cases superior to the detection of prompt γ-rays. This applied especially for U-238 where the proper extrapolation to zero pulse height is difficult due to high background and low neutron binding energy of U-238.

One of the major problems in absolute measurements as well as some ratio measurements arises from the presence of scattered neutrons of different than primary energy. In the case of U-235 fission, the presence of as little as two tenth of a per cent thermal neutrons leads to count rates equal to those obtained at 500 keV neutron energy. Thermal neutrons can be eliminated by cadmium shields, more difficult is a proper accounting for other low energy neutrons. Fast time-response of the detectors is one approach to these problems, low background arrangements the other.

Capture Cross Section Ratios

The ratio of the capture cross section of U-238 to the fission cross section of U-235 is next to α of Pu-239 the most important capture cross section ratio for fast reactor applications. Direct measurements of σ_γ(U-238)/σ_f(U-235) were carried out in 1944 by Linenberger et al. [21] using the activation method. Additional values for this ratio can be obtained from measurements of the U-238 capture cross section relative to the capture and fission cross section of U-235 by De Saussure et al. [22] and by Diven et al. [23], if one corrects for the contribution of the capture in U-235 using α-measurements. Measurements reported by Barry et al. [24] as relative to the hydrogen scattering cross section should be considered as ratio measurements relative to the fission cross section of U-235 if one uses the fission cross section reported by White [25], as Barry et al. sandwiched U-238 foils between two of White's fission counters and did not measure recoil protons. They measured the Np-239 activity of the U-238 sample after chemical separation, using a 4πβ-counter. The chemical separation was avoided in a recent measurement of the ratios σ_γ(U-238)/σ_f(U-235) and σ_γ(U-238)/σ_f(Pu-239) by Poenitz [26] using a high resolution Ge(Li)-detector to measure the 228 keV and 278 keV γ-rays which

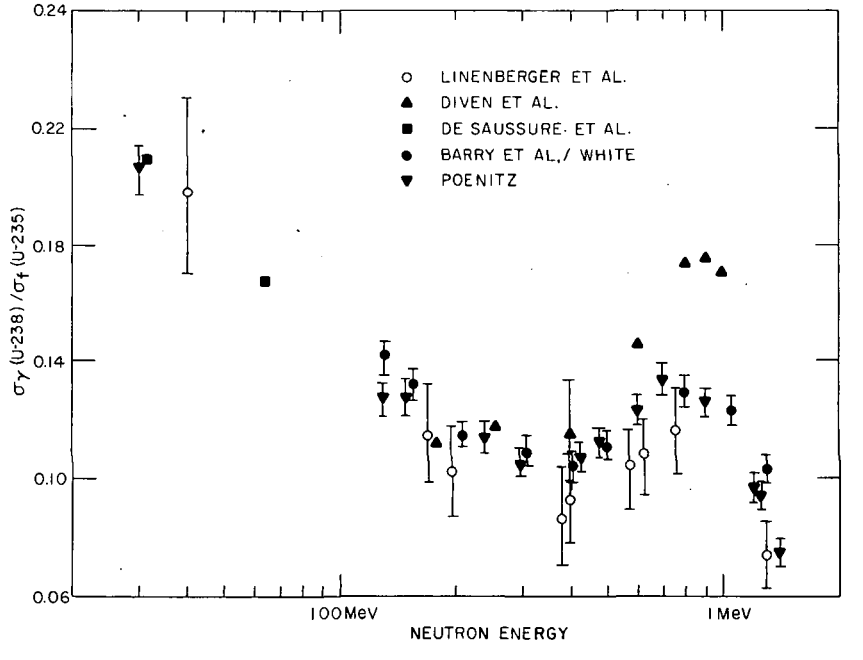

FIG. 7. The ratio $\sigma_\gamma(^{238}U)/\sigma_f(^{235}U)$.

occur in the decay of Np-239. Values for the ratio σ_γ(U-238)/σ_f(U-235) are shown in Fig. 7. The available values below 100 keV are too few to draw a conclusion about the shape as well as the amplitude. Above 130 keV the ratios measured by Barry et al. [24] and Poenitz [26] are in good agreement; the values measured in 1944 by Linenberger et al. [21] agree within error bars or overlap at least with their error bars the former two. Therefore, there is no justification to renormalize these data as had been done recently. The values derived from the measurements of Diven et al. [23] agree very well below and at 400 keV but deviate with increasing energy. This deviation may be due to the change of the effective efficiency of a large scintillator tank as a function of neutron energy and the influence of fission γ-rays. For U-238 such change might be large due to its low neutron binding energy. One should, however, note that Diven et al. [23] assigned large uncertainties to their value at 400 keV. Above 1 MeV the values measured by Barry et al. are somewhat higher than those measured by Poenitz. The latter still overlap with the results by Linenberger et al. [21]. The figure indicates a clear need for additional data in the lower keV energy range where data are most important for fast power reactors. Such measurements should be carried out with a prompt capture γ-ray detector as the activation method may not supply accurate data in a region where background from scattered neutrons is usually high.

One of the most exciting nuclear data problems of recent times was the measurement of the capture-to-fission ratio of Pu-239 in the energy range 0.1-30 keV. There have been many indirect and direct measurements made after Schomberg et al. [27] presented, in 1967, preliminary results which indicated much higher values than were previously assumed. So many evaluations, reviews and discussions have been presented recently that it is hard to add any new point of view. In Fig. 8 some recent measurements of α(Pu-239) are shown.

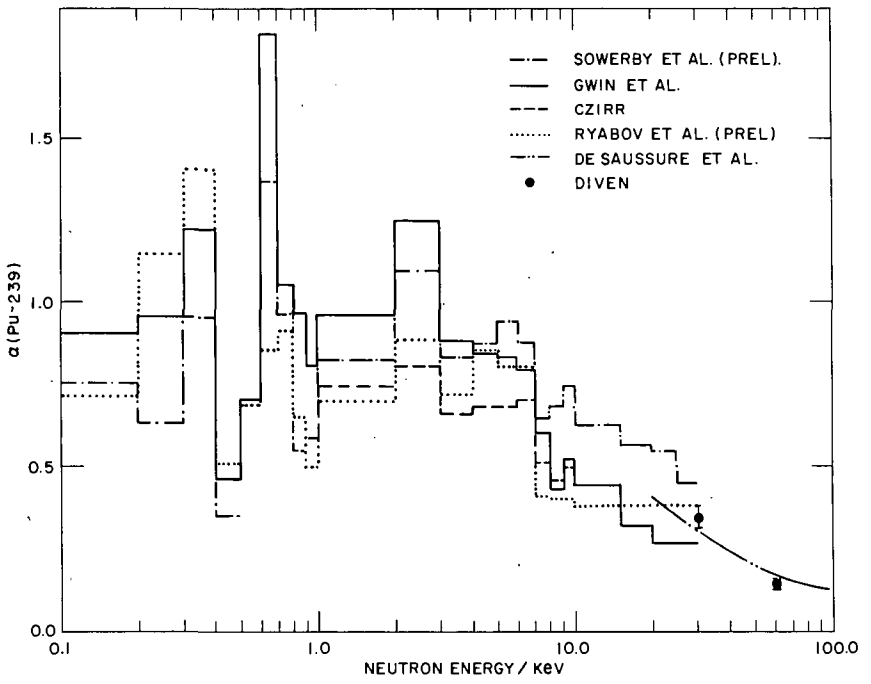

FIG. 8. The capture-to-fission ratio of ^{239}Pu.

The difference of the values measured by Gwin et al. [28] using a large liquid scintillator and by Sowerby et al. [29] using a low efficiency counter on the other hand in the energy range above 10 keV is obvious. It had been suggested that this difference might be due to a different normalization of the two data sets. Because of the good agreement of the data measured by Hopkins and Diven [30] and by De Saussure [31] in the higher keV energy range it would be reasonable to renormalize in the 20-30 keV energy range to these data. The advantage of such renormalization would be that the data measured by Sowerby et al. [29] would then agree above 0.5 keV with the new data measured by Ryabov et al. [32] as well as with measurements by Czirr [33]. The data measured by Gwin et al. [28] would be exceedingly large compared to these other renormalized values. Below 0.5 keV the agreement is better between the values reported by Ryabov et al. [32] and Gwin et al. [28]. The values for the absorption cross section measured by Gwin et al. [28] and those obtained by Uttley [30] from measurements of the total and the elastic scattering cross sections agree very well. However, in a more recent analysis Pitterle et al. [31] obtained consistently lower values for the absorption cross section. It is remarkable that both the measurements by Gwin et al. [28] and Ryabov et al. [32] have been obtained with a large liquid scintillator. The detector used by Ryabov had only half the volume of that used by Gwin and a coincidence between two halfs of the detector had been used to reduce the background. Currently, the issue appears to have settled down somewhat, though the accuracy needed for reactor applications has not yet been achieved.

Fission Cross Section Ratios

The overwhelming majority of the fission cross sections have been measured relative to the U-235 fission cross section. Of major importance are the ratios of U-233, U-238, and Pu-239 to U-235. The latter involves some difficulty due to the high α-activity associated with its short half life, but this problem can be solved.

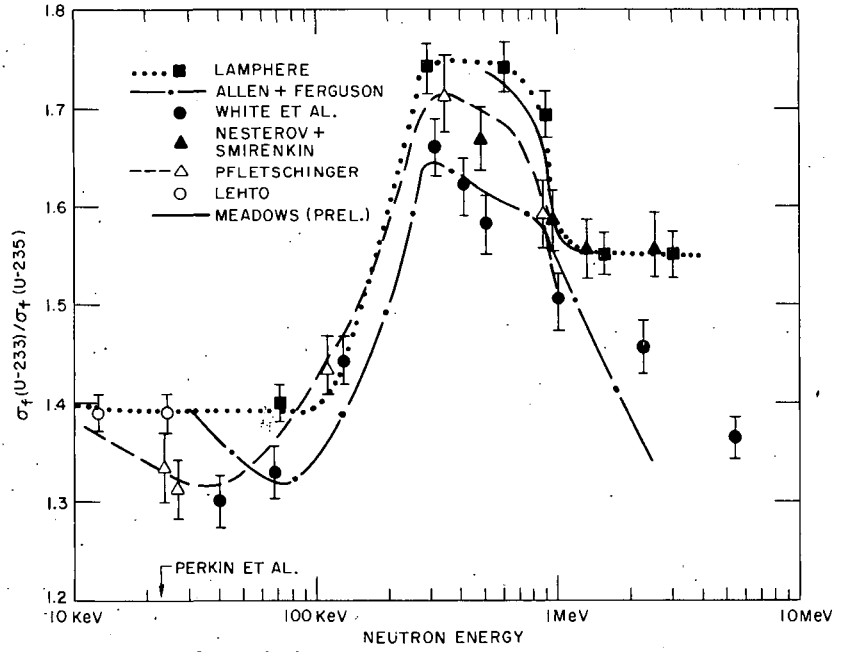

FIG. 9. The fission cross-section ratio $\sigma_f(^{233}U)/\sigma_f(^{235}U)$.

In Fig. 9 some data for the ratio σ_f(U-233)/σ_f(U-235) are shown. The basis for this selection was that for all data shown about the same accuracy has been quoted. Measurements by Smirenkin et al. [34] can be considered to be superceded by the new measurements by Nesterov and Smirenkin [35]. Values evaluated from the absolute measurements by Dorofeev and Dobrynin [36] are in good agreement with the results reported by Lamphere [37] but do not allow an exclusion of any of the values shown. Gorlove et al. [38] measured somewhat higher values than Lamphere [37], but they agree within error bars.

A comparison of the values drawn in Fig. 9 shows differences which exceed by far the given error bars. The values reported by White et al. [40], which are in good agreement with the results by Allen and Ferguson [39], had been generally accepted and were the base of suggested cross sections. Such selected cross section ratios have been revised in the energy range above 1 MeV after the measurements by White and Warner [41] were reported. The measurements by White et al. [40,41] have been considered as very reliable because the same fission counters have been used as in the U-235 fission cross section measurement relative to the H(n,n) cross section of White [25]. However, the new measurements by Nesterov and Smirenkin [35] in the energy range 1 - 2.5 MeV agree with the values measured by Lamphere [37], a value at 500 keV is outside error bars low. Time-of-flight measurements by Pfletschinger and Kaeppeler [42], are, with exception of the 100 - 250 keV range, about 3 per cent lower than the results from Lamphere [37]. A similar discrepancy of the Karlsruhe data can be noted for the Pu-239 to U-235 ratio. A good agreement with the Lamphere data at the low energy side is obtained in the measurements by Letho [43] and in the energy range 500 - 1500 keV with the measurements by Meadows [44]. The latter are time-of-flight measurements using monoenergetic neutrons and a two-dimensional recording of fission fragement energy versus neutron time-of-flight. Special care has been taken to obtain an accurate mass assignment. In the energy range considered in Fig. 9 the values measured by Lamphere [37] seem to be strongly supported by the newest results. A possible reason for the low value derived from the absolute measurements by Perkin et al. [45] using a Sb-Be source might be fluctuations in the fission cross sections of U-233 and U-235, however, it is hard to suggest a reason for the discrepancy of the values reported by White et al. [40,41] by up to 5 times their error bars and the similar low values for data reported by Allen and Ferguson [39].

The ratio of the Pu-239 to the U-235 fission cross section in the energy region 100 keV - 10 MeV is shown in Fig. 10. A recent time-of-flight measurement by Poenitz [26] using back to back scintillation counters confirmed previous DC measurements by Allen and Ferguson [39], Smirenkin et al. [34], and White et al. [40] in the energy range below 1 MeV. In the energy range from 1 MeV to 2 MeV these measurements are in good agreement with the new results reported by Nesterov and Smirenkin [35]. The new Karlsruhe measurements by Pfletschinger and Kaeppeler [42] are lower by about 3 - 4 per cent; however their error bars overlap in the energy range from 200 keV - 1 MeV. Below 200 keV the latter data change from values lower to values higher than those reported by White et al. [42].

The step in the cross section ratio at 900 keV is due to a 10 per cent step of the U-235 fission cross section at that energy. A similar step has been obtained for the ratio of the fission cross section of U-233 to U-235. From the measurements by Poenitz [26] as well as from those by Pfletschinger and Kaeppeler [42] it follows that this step in the ratio is about 10 per cent. It appears less distinctly in older measurements by Smirenkin et al. [34] presumably due to the poorer resolution of their measurements. Because of the good agreement in the 200 - 800 keV energy range, the large spread at 1 MeV is hard to understand and has been shown in a separate block of Fig. 10 as a function of the date of the measurements.

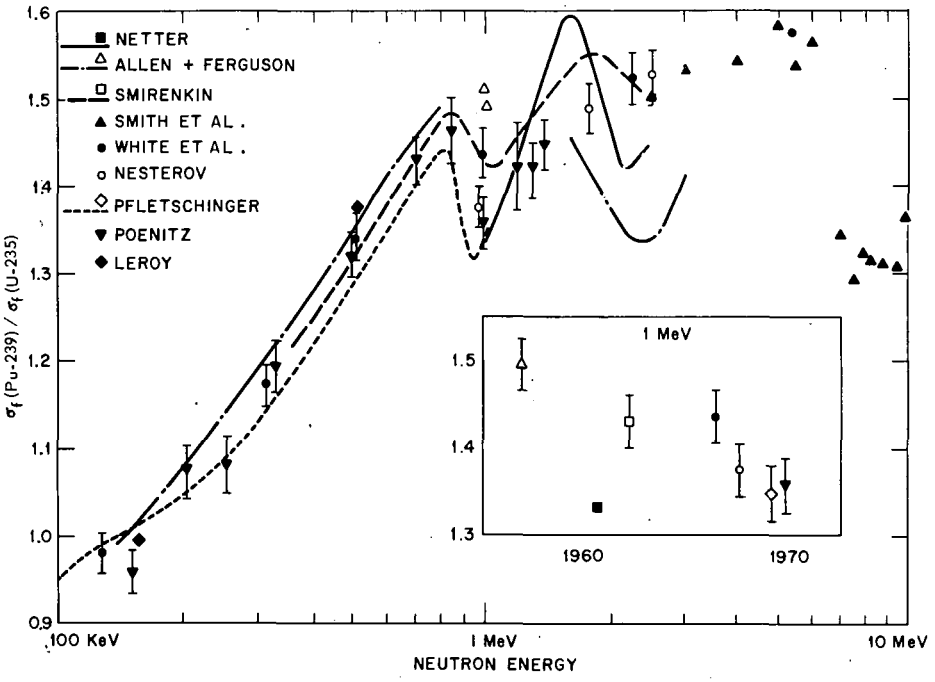

FIG. 10. The fission cross-section ratio $\sigma_f(^{239}Pu)/\sigma_f(^{235}U)$.

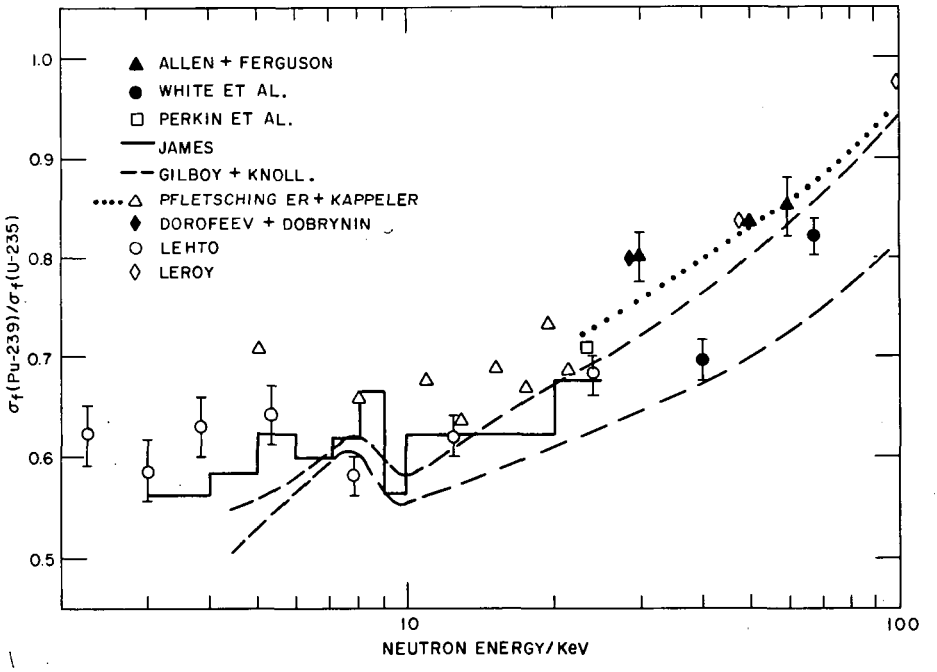

FIG. 11. The fission cross-section ratio $\sigma_f(^{239}Pu)/\sigma_f(^{235}U)$.

The lower energy range has been shown in Fig. 11. Here the agreement is not as good as in the higher keV energy range. Measurements by Gilboy and Knoll [75] resulted in two different sets of values. It should be mentioned that these authors suggested a correction for their higher curve. This would reduce these values and bring them in relatively good agreement with a value reported by White et al. [40] at 40 keV which is as much as 4 - 5 times their error bar lower than measurements from Allen and Ferguson [39]. The latter were more likely supported by the new measurements from Pfletschinger and Kaeppeler [42] and Leroy [49] than those from White et al. [40]. However, the values reported by Letho [43] and by James [50] lie more in line with a reasonable extrapolation of the two diverging groups. The need for additional measurements in this region is obvious.

An interesting question in connection with the results for U-233 arises if one considers the ratio for σ_f(U-238)/σ_f(U-235). This ratio has also been measured by Lamphere [37]. Measurements by Stein et al. [51] using a time-of-flight method and monoenergetic neutrons are about 8 per cent lower. A measurement by Smirenkin et al. [34] strongly supports the results of Lamphere, however, less accurate data by Kalinin and Ponkratov [52] as well as revised data by Smith et al. [53] agree better with the results reported by Stein et al. [51].

Measurements by White and Warner [41] agree with Stein et al. and have resulted the values reported by Lamphere being multiplied by 0.94 in some cross section compilations. This procedure may be questionable in the view of the situation for U-233.

Absolute Capture and Fission Cross Sections

Only very few absolute measurements of the capture cross section of U-238 are available. Other data based on reliable features of certain reference cross sections supplement these data. In Fig. 12 results of this type are presented.

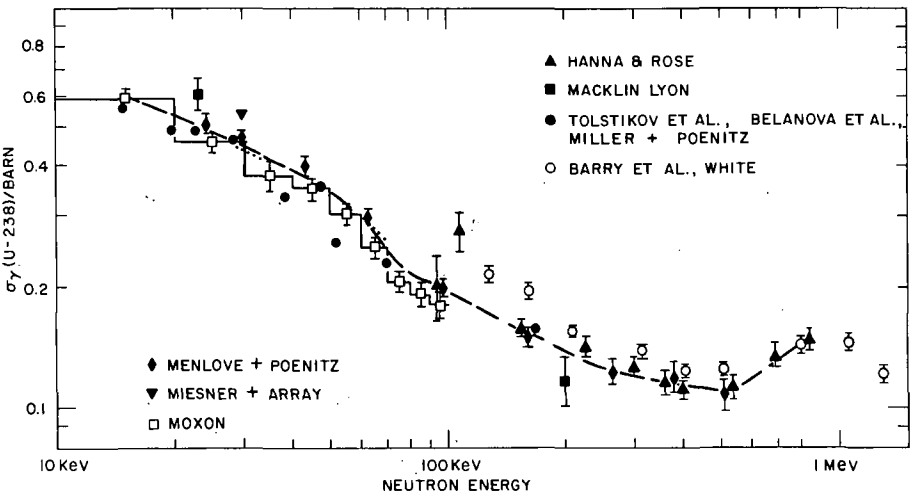

FIG. 12. The capture cross-section of ^{238}U.

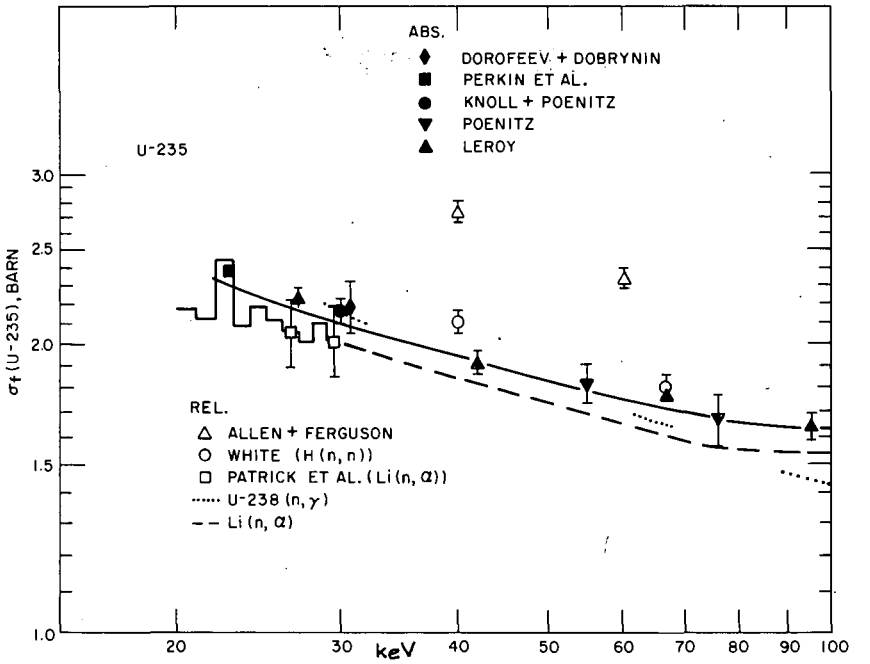

FIG. 13. The fission cross-section of ^{235}U below 100 keV.

Measurements by Macklin et al. [53] and Lyon and Macklin [54] are based on calibrated photo neutron sources. Hanna and Rose [55] used the H(n,n) cross section as a reference cross section and measured the β-activity of the irradiated U-238 samples. The measurements by Barry et al. [25] used the same determination of the capture rate but based on the calibration of a fission detector by White [25] and therefore must be considered a cross section ratio.

Menlove and Poenitz [56] measured the shape of the capture cross section using a large liquid scintillator tank and a beam catcher-flux integration type neutron-detector. The absolute value was measured at 30 keV using the associated activity method for the determination of the neutron flux from the $Li^7(p,n)Be^7$ source reaction. The activation method was used at that energy for the measurement of the capture rate in U-238. Tolstikov et al. [57] also used the activation technique for measurements in the energy range 5 - 200 keV. They utilized the shape of the $B^{10}(n,\alpha)$ reaction and normalized to the result from a shell transmission experiment by Belanova et al. [58] for which a new Monte Carlo evaluation had been carried out recently by Miller and Poenitz [59]. The values reported by Tolstikov et al. [57] were remarkably scattered which the authors noted in their publication. However, measurements by Moxon and Chaffey [60] showed fluctuations in the capture cross section which explained the scattering of the Tolstikov data. Newer measurements by Moxon [61] essentially confirmed the absolute values of their older results. The values shown in Fig. 12 allow the suggestion of a cross section which satisfies essentially all sets of measurements with the exception of the values reported by Barry et al. [24] which are systematically higher below 700 keV. It should be noted that the adjustment of the shape as measured in good agreement by Moxon [61], Tolstikov et al. [57] and by Menlove

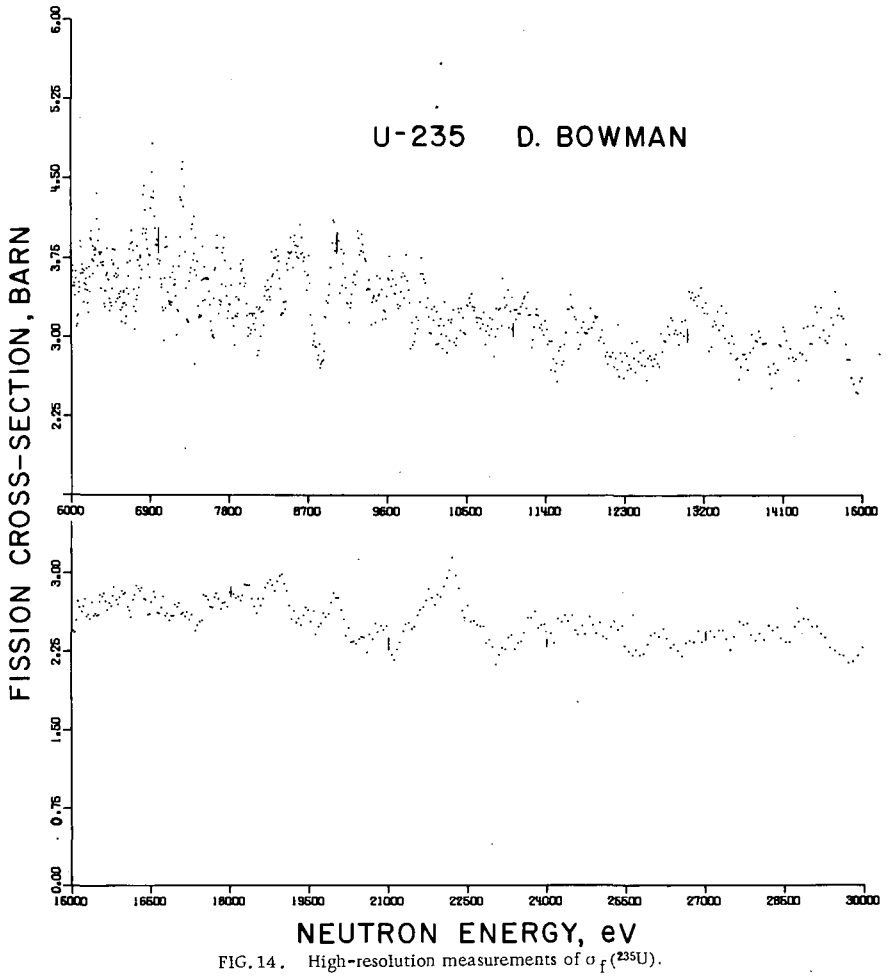

FIG. 14. High-resolution measurements of σ_f(^{235}U).

and Poenitz [56] to the values measured by Barry et al. [24] leads to values at lower energies never measured so high for U-238(n,γ) in an absolute cross section experiment.

Fig. 13 shows the fission cross section of U-235 in the energy range from 10 - 100 keV. The cross section had been assumed to show a smooth dependence on energy despite the strong scattering of values measured by Yeater et al. [62] in the lower energy range. Recent measurements by Patrick et al. [63] relative to the Li(n,α) cross section showed strong fluctuations of the cross section in the range 10 - 30 keV. Such fluctuations exceed 30 per cent and have a half width of about 1 keV. Similar structure is shown in measurements by Bowman [80] who measured up to 500 keV with a resolution of 0.7 nsec/m. Results from the latter measurements in the energy range 6 - 30 keV are shown in Fig. 14. Strong fluctuations had also been reported by Alberts [64] in the higher keV energy range; however, subsequent investigations by Smith and Whalen [65] and Macklin and Gibbons [66] did not confirm such fluctuations. Due to the small width of the observed fluctuations there should be no effect on the available absolute or relative cross section measurements which are considered here because they have been measured with a much broader

energy resolution. An exception are measurements with a Sb-Be source which has less than 2 keV half width for the primary neutrons. From the measurements by Patrick et al. [63] one would expect that values obtained with the Sb-Be source should be higher than other absolute values in the same region. However, such conclusion depends strongly on the validity of the value 22.8 keV for the neutron energy of the Sb-Be source. The usefulness of the Sb-Be source in absolute cross section measurements may be questioned because of the problems introduced by the fluctuations in capture and fission cross sections. Around 500 keV several different measurements display a similar non-smooth variation with energy which may indicate fluctuations within 2 - 3 per cent. A careful investigation of the energy dependence of the U-235 fission cross section in this range would be desirable.

Measurements using absolute calibrated Sb-Be sources by Perkin et al. [45] and by Doroffeev and Dobrynin [36] are in very good agreement with the value obtained by Knoll and Poenitz [67] using the associated activity method. The latter measurement has been extended by Poenitz [68] to the higher energy range using a shape measurement basing on a beam catcher neutron flux integration detector. A very good confirmation of these measurements in the lower keV energy range is given by recent absolute measurements by Leroy which will be reported at this conference. Additional values for the U-235 fission cross section can be derived from measurements relative to the Li(n,α) and H(n,n) cross sections. Barry [69] measured the ratio of the Li(n,α) cross section relative to the U-235 fission cross section in the energy range 25 - 100 keV. His results are in good agreement with older measurement by Bame and Curbitt [70]. In the energy range up to 100 keV independent and absolute measurements of the Li(n,α) cross section are available from measurements by Schwarz et al. [71] and from total cross section measurements by Uttley [72]. These values are in good agreement with a single point at 100 keV measured by Condé [73]. σ_f(U-235) values obtained from the measured ratios and the absolute Li(n,α) cross sections are shown in Fig. 13. The uncertainty of the dashed line is about ± 7 per cent and thus about of the

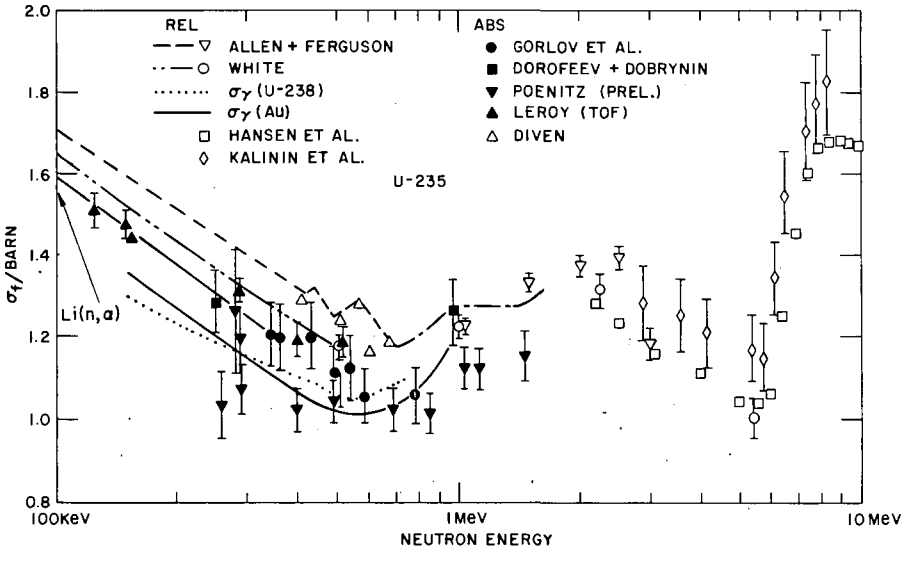

FIG. 15. The fission cross-section of ^{235}U above 100 keV.

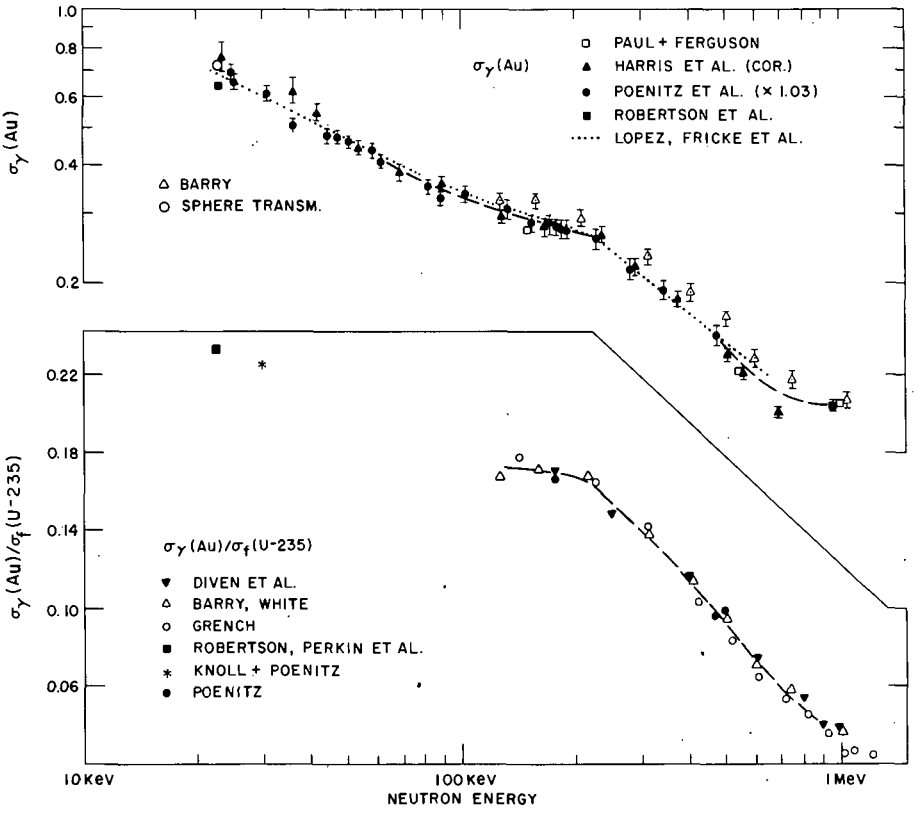

FIG. 16. The capture cross-section of Au (n, γ) and the ratio $\sigma_{\gamma}(Au)/\sigma_{f}(^{235}U)$.

same size as for the measurements by Patrick et al. [63], who quote an estimated uncertainty of ± 8 per cent. Therefore, the values based on the $Li^6(n,\alpha)$ cross section overlap very well with the available absolute measurements. Values obtained relative to the H(n,n) cross section suffer from the disagreement between different measurements of the ratio $\sigma_f(U\text{-}235)/\sigma_n(H)$. Fig. 13 shows a higher degree of probability for the measurements by White [25] although his 40 keV value is about 2 - 3 times his error bars higher than the value suggested by the absolute measurements and the measurements relative to the $Li^6(n,\alpha)$ cross section.

Fig. 15 shows the higher energy part of the U-235 fission cross section. At 100 keV the value relative to the Li(n,α) cross section has been indicated. Measurements relative to the hydrogen scattering cross section are also inconsistent in this energy range. Measurements by Diven [74] essentially confirm the results from Allen and Ferguson [39], however, the results reported by White [25] agree better with the absolute measurements by Gorlove et al. [38] and Leroy [49]. Preliminary measurements by Poenitz [68] resulted in still lower values which are, however, in agreement with the results by Gorlove et al. [75] and compatible with the absolute values for U-238(n,γ) and the Au(n,γ) standard cross section. The use of the latter is especially appealing because in contrast to the ratio measurements of $\sigma_f(U\text{-}235)/\sigma_n(H)$, a sufficiently high degree of agreement has been reached by several experimenters

TABLE II. DIFFERENCES IN ABSOLUTE CROSS-SECTIONS

Group	Reference	Measured Cross Section	Experimental Method	Energy Range/keV	Diff. in % Rel. to III
I	Fort, Leroy [93]	Li(n,α)	Ass. Particle	150-300	+ 15
	Cox [94]	Li(n,α)	Shell Transm.	10-100	+ 10 to 15
	Weston [95]	Au(n,γ)	Flux Integr.	30, 64	+ 15
	Allen, Ferguson [39]	U5(n,f)	Rel. H(n,n)	30-1000	+ 12 to 25
	Diven [74]	U5(n,f)	Rel. H(n,n)	400-1600	+ 12
II	White [25]	U5(n,f)	Rel. H(n,n)	40-1000	+ 5 to 8
	Leroy [49]	U5(n,f)	Sev. Abs. Techn.	300, 500	+ 4,8
III	Gorlov [38]	U5(n,f)	Flux Integr.	3-800	
	Doroffeev, Dobrynin [36]	U5(n,f)	Flux Integr.	250	
	Leroy [49]	U5(n,f)	Sev. Abs. Techn.	25-400	
	Perkin [45]	U5(n,f)	Flux Integr.	22.8	
	Knoll, Poenitz [67]	U5(n,f)	Ass. Activity	30	
	Robertson [86]	Au(n,γ)	Flux Integr.	22.8, 960	
IV	Ferguson, Paul [87]	Au(n,γ)	Rel. H(n,n)	150-1000	- 0 to 10
	Harris [84]	Au(n,γ)	Ass. Activity	15-650	- 5 to 8
	Poenitz [85]	Au(n,γ)	Flux Integr.	25-500	- 5 to 8
	Menlove, Poenitz [56]	U8(n,γ)	Ass. Act./FI	25-500	- 5
	Hanna, Rose [55]	U8(n,γ)	Rel. H(n,n)	100-700	- 0 to 5
	Poenitz [68]	U5(n,f)	Flux Integr.	30-1400	- 0 to 10
	Lyon, Macklin [54]	U8(n,γ)	Flux Integr.	250	
	Lopez [80]	Au(n,γ)	Rel. H(n,n)	≤700	- 3 to 8
V	Schwartz [71]	Li(n,α)	Abs.	3-500	- 8
	Condé [73]	Li(n,α)	Rel. C(n,n)	100	- 8
	Moxon [61]	U8(n,γ)	Rel. B(n,α)	≤100	- 12

[23,81,82,83] for the ratio σ_γ(Au)/σ_f(U-235). Also measurements of the absolute cross section by several different experimental methods are in good agreement [84-88]. The cross section value obtained from sphere transmission experiments depends on the interpretation of the measured transmission values. The latest evaluation by Semler [89] does not agree with the value obtained by Robertson et al. [86] in an activation experiment. The latter value is better supported by the interpretation of the shell transmission by Froehner [32]. The absolute values of σ_γ(Au) and the ratio σ_γ(Au)/σ_f(U-235) are shown in Fig. 16. The overlap and the agreement is good in the energy range from 150 - 500 keV which should result in reasonable U-235 fission cross sections. The estimated uncertainty of such values as shown in Fig. 15 is 5 per cent. It is noticeable that the cross sections for U-238 capture and Au capture which have been used to derive the U-235 fission cross sections in Fig. 15 are well supported or based on measurements relative to the H(n,n) cross section.

Discrepancies between the absolute cross sections obtained from different experiments as well as from different reference cross sections are obvious. In Tab. II a grouping of the different absolute levels has been attempted. Such systematic classification may be questioned in details, but can serve as a help for an understanding of existing discrepancies.

In the energy range above 1 MeV a remarkable difference exists around 5 MeV between data measured by White [25] and by Kalinin and Ponkratov [52]. Previous values reported by Smith et al. [79] agreed with the latter. After a recent revision they support the result by White. However, it had been noted recently by Hart [96] that the revised data by Smith et al. are not supported by the very well known value at 14 MeV.

FISSION PROPERTIES

In previous compilations the energy dependence of $\bar{\nu}$ (E) has usually been considered linear. In Fig. 17, $\bar{\nu}$ (E) measurements by a number of experimentors are shown. These are renormalized values discussed by Fillmore [76] in a

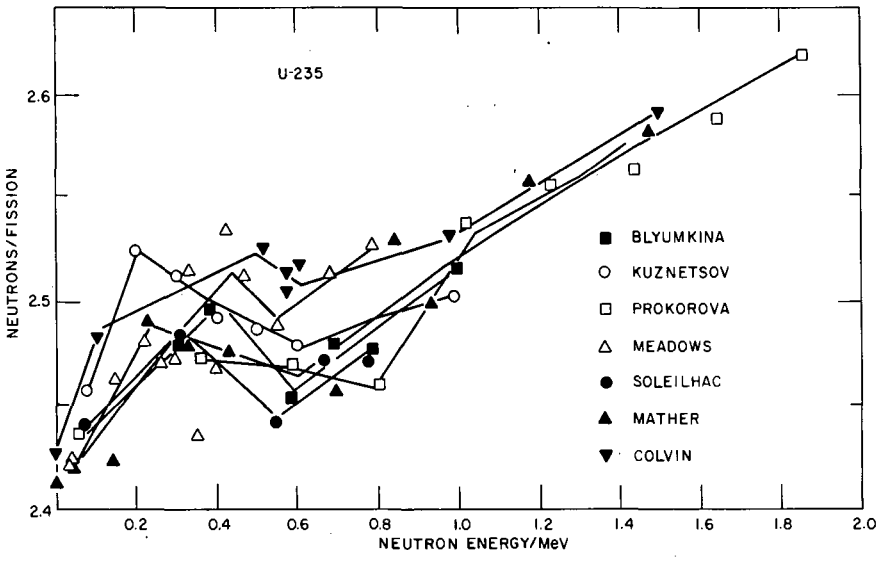

FIG. 17. The energy dependence of $\bar{\nu}$ (^{235}U).

recent review. Straight lines have been drawn between several points from each experimentor. This procedure may be very rough, but it cleary demonstrates the need for a more differential approach to the energy dependence of $\bar{\nu}$. It is remarkable that the deviation from a linear dependence of $\bar{\nu}$ as established by measurements at higher energy is about 2 - 3 per cent in the region around 400 keV. It is surprising that the observed nonlinearity has apparently never been taken into account in data compilations, althoug the effect is well known and has been discussed for nearly 10 years in fission physics. The $\bar{\nu}$ (E) - values in nuclear data sets like the ENDF(B) data file are clearly underestimated in this region which contributes appreciably to the neutronics of fast reactors. This underevaluation of $\bar{\nu}$ in the energy region around 400 keV is independent of the problem of absolute $\bar{\nu}$ values of Cf-252 for which two different groups of values are available which disagree by more than their error bars.

Another fission property of importance for the fast reactor calculations is the energy spectra of the primary fission neutrons. Recent experiments by Grundl [77] and Fabry [78] indicated much harder fission spectra than previously assumed. The average energy resulting from these experiments is about 2.2 MeV. The measurements by Grundl also suggest a lower value for the ratio of the average fission spectra energies for Pu-239 to U-235. These new values depend, however, on many other cross sections or cross section ratios which may not be random uncertain but might be systematically in error. Results from the more direct microscopic measurements using the time-of-flight technique yield values $\sim$ 2.0 MeV for the average energy of the fission spectra of U-235. However, a recent time-of-flight experiment by Belov et al. [75] supports the ratio for the average energies of the fission spectra for Pu-239 to U-235 as measured by Grundl [77].

CONCLUSIONS

In consideration of discrepancies up to a factor of two in some nuclear data, tremendous improvements have been achieved in the last ten years. This

was essentially possible due to the introduction of new experimental methods and techniques. Unfortunately, discrepancies still exist - now for different magnitudes of uncertainties.

Differences on the order of 15 per cent for the total cross sections of heavy elements have been resolved and the present uncertainties are about 5 per cent or less and thus sufficiently low for reactor applications. Because of its influence on the spectra of fast reactors, an improvement of the accuracy of the inelastic scattering cross sections of fertile nuclei from presently 5 - 10 per cent is desireable. The situation for fissile nuclei is much less favorable, and additional work is required.

Discrepanices in fission cross section ratios are suprisingly large; however, an improvement has been obtained in recent experiments. For some ratios and limited energy ranges the uncertainty is as small as 2 per cent, however, it exceeds 5 per cent in other regions. Capture to fission cross section ratios are usually less accurate due to difficulties in the capture detection techniques.

Several more or less distinct groups exist for absolute cross sections. The values of these groups are different by as much as 40 per cent, however, recent improvements allow to suggest an absolute fission cross section for U-235 in the energy range from 20 keV to 2 MeV with an uncertainty of 5 - 8 per cent.

Discrepancies observed in any kind of cross section value often exceed by far the quoted uncertainties, a fact which should not be underestimated because of the signification of the quoted uncertainties as a criterion of judgement about the reliability of a measurement. The usual method to evaluated the uncertainty of a measurement is that valid for statistical errors. The majority of estimated uncertainties of quantities and corrections involved in a cross section measurement are, however, not of this nature. Therefore, the interpretation of a value $A \pm \Delta A$ quoted by an experimentor, that "the real value is with 68 per cent probability between $A - \Delta A$ and $A + \Delta A$ (with higher probability at A than at the limits)" is already very optimistic. Hard to understand is the use of the value A with the interpretation that "this would be the real value as measured by the experimentor."

The discrepancies between different experimental results outside of their respective error bars do not only indicate a necessary modification of the error evaluation method but require as well to search for another criteria than the given uncertainty limits to judge about the reliability of a set of measured cross section values. The use of the agreement obtained between different measurements as such a criteria is also very problematic. E.g., the agreement obtained in ratio measurements by White et al. [40,41] and Allen and Ferguson [39] for the fission cross section of U-233 relative to that of U-235 did not warrant their final validity. The same seems to be almost sure for the U-235 fission cross section as measured relative to the H(n,n) cross section for which good agreement has been obtained for the values reported by Allen and Ferguson [39] and Diven [74]. The age of a measurement which has been used as a criteria for the validity of a measurement is also an insufficient indication. An example is the measurements for the ratio σ_γ(U-238)/σ_f(U-235) by Linenberger et al. [21] from 1944 which are in contrast to later measurements supported by most recent experiments.

A comparison of the differences which appear in the ratio measurements, and those present in the absolute cross section values, shows that the existing discrepancies may not be essentially caused by difficulties in the absolute neutron flux measurements as previously assumed.

ACKNOWLEDGEMENT

The author is indebted to those who contributed their recent experimental results to this review prior to publication.

REFERENCES

[1] CAMPBELL, C. G., EACRP-A-80 (1968).

[2] ZOLOTAR, B. A. et al., Transactions ANS 12 (1969) 742.

[3] TABONY, R. H., Dissertation, Duke University (1966); TABONY, R. H. et al., BNL-325.

[4] CIERJACKS, S. et al., KFK-1000 (1968).

[5] DIVADEENAM, M., Dissertation, Duke University (1969).

[6] HENKEL, R. L. et al., Phys. Rev. 94 (1954) 141.

[7] ADAIR, R. K. et al., LA-1060 (1950).

[8] MEADS, R. E., AERE-NP/R-1643 (1955).

[9] UTTLEY, C. A. et al., Conf. on Nucl. Data, CN-23/36 Paris (1966).

[10] WHALEN, J. F., private communication (1969).

[11] HIBDON, C. T. and LANGSDORF, A. S., private communication to Brookhaven Sigma Center (1953).

[12] SMITH, A. B., private communication (1970).

[13] BARNARD, E. et al., Nucl. Phys. 80 (1966) 46.

[14] SMITH, A. B. and LISTER, D., Conf. on Nucl. Data, CN-23/49, Paris (1966).

[15] BARANOV, S. A. et al., Nucl. Phys. 41 (1963) 95.

[16] HORSCH, F., Z. f. Physik 183 (1965) 352.

[17] STEPHENS, F. S. et al., Conf. on React. Between Complex Nuclei, E-8, Asilomar (1963).

[18] POENITZ, W. P., unpublished (1970).

[19] SMITH, A. B., private communication (1970).

[20] CAVANAGH, P. E. et al., AERE-R 5972 (1969).

[21] LINENBERGER, G. A. et al., LA-179 (1944).

[22] DE SAUSSURE, G. et al., ORNL-3360 (1962).

[23] DIVEN, B. C. et al., Phys. Rev. 120 (1960) 556.

[24] BARRY, J. F. et al., J. Nucl. Energy 18 (1964) 481.

[25] WHITE, P. H., J. Nucl. Energy 19 (1965) 325.

[26] POENITZ, W. P., Nucl. Sci. Eng., 40 (1970) 383.

[27] SCHOMBERG, M. G. et al., Conf. on Fast Reactor Physics, SM-101/41, Karlsruhe (1967).

[28] GWIN, R. et al., ORNL-TM-2598 (1969).

[29] SOWERBY, M. G., see Ref. [28].

[30] HOPKINS, J. C. and DIVEN, B. C., Nucl. Sci. Eng. 12 (1962) 169.

[31] DE SAUSSURE, G. et al., Conf. on Nucl. Data for Reactors, Prol. Vol. II (1966) 233.

[32] RYABOV, UY. V. et al., this conference (1970).

[33] CZIRR, J. B., Transactions ANS 12 (1969) 261.

[34] SMIRENKIN, G. N. et al., Atomnaya Energiya 13 (1962) 366.

[35] NESTEROV, V. G. and SMIRENKIN, G. N., Atomnaya Energiya 24 (1968) 185.

[36] DOROFFEEV, G. A. and DOBRYNIN, Y. P., J. Nucl. Energy 5 (1957) 217.

[37] LAMPHERE, R. W., Phys. Rev. 104 (1956) 1654.

[38] GORLOV, G. V. et al., J. Nucl. Energy 12 (1960) 79.

[39] ALLEN, W. D. and FERGUSON, A. T. G., Proc. Phys. Soc. A70 (1957) 573.

[40] WHITE, P. H. et al., Conf. on Phys. and Chem. of Fission, SM-60/14, Vienna (1965).

[41] WHITE, P. H. and WARNER, G. P., J. Nucl. Energy 21 (1967) 671.

[42] PFLETSCHINGER, L. and KAEPPELER, F., Nucl. Sci. Eng., 40 (1970) 375. (1970).

[43] LEHTO, W. K., Nucl. Sci. Eng. 39 (1970) 361.

[44] MEADOWS, J. W., private communication (1970).

[45] PERKIN, J. L. et al., J. Nucl. Energy 19 (1965) 423.

[46] SCHMIDT, J. J., KFK-120 (1966).

[47] LANE, R. O. et al., Ann. Phys. 12 (1961) 135.

[48] LANGSDORF, A. et al., Phys. Rev. 107 (1957) 1077.

[49] LEROY, J. L., this conference (1970).

[50] JAMES, G. D., ANL-7320 (1966).

[51] STEIN, W. E. et al., Conf. on Neutron Cross Sect. and Tech., Vol. I (1968) 627.

[52] KALININ, S. P. and PONKRATOV, V. N., 2nd Geneva Conf., Vol. 16 (1958) 136.

[53] MACKLIN, R. L. et al., Phys. Rev. 107 (1957) 504.

[54] LYON, W. S. and MACKLIN, R. L., Phys. Rev. 114 (1959) 1619.

[55] HANNA, R. C. and ROSE, B., J. Nucl. Energy 8 (1959) 197.

[56] MENLOVE, H. O. and POENITZ, W. P., Nucl. Sci. Eng. 33 (1968) 24.

[57] TOLSTIKOV, V. A. et al., J. Nucl. Energy 18 (1964) 599.

[58] BELANOVA, T. S. et al., J. Nucl. Energy 20 (1966) 411.

[59] MILLER, L. B. and POENITZ, W. P., Nucl. Sci. Eng. 35 (1969) 295.

[60] MOXON, M. C. and CHAFFEY, C. M., private communication to Brookhaven Sigma Center (1963).

[61] MOXON, M. C., AERE-R 6074 (1969).

[62] YEATER, M. L. et al., KAPL-1109 (1954).

[63] PATRICK, B. H. et al., EANDC(UK) 119 AL (1970).

[64] ALBERT, R. D., Phys. Rev. Letters 15 (1965) 637.

[65] SMITH, A. B. and WHALEN, J. F., Phys. Rev. Letters 16 (1966) 576.

[66] MACKLIN, R. L. and GIBBONS, J. H., Phys. Rev. Letters 16 (1966) 248.

[67] KNOLL, G. F. and POENITZ, W. P., J. Nucl. Energy 21 (1967) 643.

[68] POENITZ, W. P., Conf. on Neutron Cross Sect. and Tech., Vol. I (1968) 503.

[69] BARRY, J. F., Conf. on Neutron Cross Sect. and Tech., Vol. II (1966) 763.

[70] BAME, S. J. and CUBITT, R. L., Phys. Rev. 114 (1959) 1580.

[71] SCHWARZ, S. et al., Nucl. Phys. 63 (1965) 593.

[72] UTTLEY, C. A., see SOWERBY, M. C. et al., CN-26/26, this conference (1970).

[73] Conde, H. et al., Arkiv Fysik 29 (1965) 45.

[74] Diven, B. C., Phys. Rev. 105 (1957) 1350.

[75] BELOV, L. M. et al., Sov. J. Nucl. Phys. 9 (1969) 421.

[76] FILLMORE, F. L., J. Nucl. Energy 22 (1967) 79.

[77] GRUNDL, J., Nucl. Sci. Eng. 30 (1967) 39; Nucl. Sci. Eng. 31 (1968) 191.

[78] FABRY, A., Nukleonik 10 (1967) 280.

[79] SMITH, R. K. et al., Bull. Am. Phys. Soc. 2 (1957) 196.

[80] LOPEZ, W. et al., private communication (1970).

[81] BARRY, J. F., J. Nucl. Energy 18 (1964) 491.

[82] GRENCH, H. A. et al., private communication (1969).

[83] POENITZ, W. P., unpublished (1969).

[84] HARRIS, K. K. et al., Nucl. Phys. 69 (1965) 37; GRENCH, H. A., private communication (1970).

[85] POENITZ, W. P. et al., J. Nucl. Energy 22 (1968) 515.

[86] ROBERTSON, J. C. et al., J. Nucl. Energy (1966).

[87] FERGUSON, A. T. G. Paul, A., J. Nucl. Energy (1959).

[88] RYVES, T. B. et al., J. Nucl. Energy 20 (1966) 249.

[89] SEMLER, T. T., Transactions ANS 11 (1968) 162.

[90] UTTLEY, C. A., EANDC(UK) 40 "L" (1964).

[91] PITTERLE, T. A. et al., Conf. on Neutron Cross Sect. and Tech., Washington (1968).

[92] FROEHNER, F. H., GA-8072 (1967).

[93] FORT, E. and LEROY, J. L., Conf. on Nuclear Data for Reactors, Paris, Vol. I (1966) 267.

[94] COX, S. A., Conf. on Neutron Cross Sect. and Tech., Washington, Vol. II (1966) 701.

[95] WESTON, L. W. and LYON, W. S., Phys. Rev. 123 (1961) 948.

[96] HART, W., AHSB(S)R (1969) 169.

DISCUSSION

J.S. STORY: I would like to refer first to your observations on the inelastic data for ^{238}U. Even if the resolution by time-of-flight of the inelastic cross-sections is imperfect and inexact, it is conceivable that the measurements should be able to determine with reasonable precision, by integration over the observed secondary spectrum, the mean energy loss at each incident energy. If this assumption is valid, I think the measurement should in fact include the calculation and tabulation of this valuable integral characteristic. On the other hand, it seems inexcusable that the measurers apparently did not bother to check whether their partial cross-sections were consistent with the total cross-section.

Secondly, as regards Pfletschinger's data for the $^{239}Pu/^{235}U$ fission ratio (see Ref. [42]), these values cross those of White at about 150 keV. At this energy, however, Pfletschinger made some change either in sample or method, I forgot which. I do not know whether this had any effect on the result.

Lastly, in relation to your Fig. 17 for $\bar{\nu}$ (^{235}U), why does your eye-guide line through Meadow's data miss several of the points by a large margin

(the point at 0.35 MeV, for example)? This omission would bias the conclusions.

W.P. POENITZ: I think your first point was a comment, and one with which I completely agree.

The change in the shape of $\sigma_f(^{239}Pu)/\sigma_f(^{235}U)$ in the measurements by Pfletschinger and Kappeler around 150 keV could be related to a change in the experimental technique. Below this energy they used a whole-spectrum time-of-flight technique for background suppression. However, there is an overlap of the two experimental techniques and, therefore, they believe that they have a means of checking for possible errors. Moreover, I have noted that recent measurements by Leroy show the same change relative to White's values. Hence, this may be a real difference due to the White data.

As far as the $\bar{\nu}(E)$ curves are concerned, I mentioned in the oral presentation that the eye-guide curves represent only a very rough approximation. I realize that the data of Meadows and Whalen show some fluctuation. However, they also conform to the general picture for this region, in which nearly all values are higher than the values in ENDF(B), where a linear behaviour is assumed.

J.L. LEROY: The situation as regards the results of measurements on the fission cross-section of ^{235}U is very unsatisfactory, especially between 100 keV and 500 keV, since there are considerable discrepancies between a number of recent measurements in this range: for example, between those of Poenitz and those made at Cadarache. This is particularly disturbing in that these two sets of measurements are in fairly good agreement between 30 keV and 60 keV. Similarly, both sets make use of flat-response neutron detectors for measuring flux. It seems to me that it is essential to look for the reason for this disagreement while the experimental devices are still in existence, since this will be more difficult later on, when nothing will be available except the published descriptions.

MESURE DES SECTIONS EFFICACES TOTALES NEUTRONIQUES DU CARBONE, DU NICKEL, DE L'URANIUM-235, DE L'URANIUM-238 ET DU PLUTONIUM-239 ENTRE 0,1 MeV ET 6 MeV

J. CABE, M. CANCE, A. ADAM,
M. BEAUFOUR, M. LABAT
CEA, Centre d'études
de Bruyères-le-Châtel,
France

Présenté par M. Soleilhac

Abstract — Résumé

MEASUREMENT OF TOTAL NEUTRON CROSS-SECTIONS OF CARBON, NICKEL, ^{235}U, ^{238}U AND ^{239}Pu BETWEEN 0.1 MeV AND 6 MeV.

The authors measured the total neutron cross-sections of carbon, natural nickel, uranium-235, uranium-238 and plutonium-239 between 100 keV and 6 MeV with energy spreads of ± 2 keV to ± 40 keV depending on the element and the energy range. The error in the absolute values was less than 3%. The neutrons were obtained by the $T(p, n)^3He$ reaction, using protons (accelerated either by a 2-MeV Van-de-Graaff or by a 12-MeV pulsed-source tandem accelerator) to bombard a target of tritium adsorbed on a thin layer of titanium. The neutrons were detected by a 1 × 1.5 in. stilbene crystal used in combination with a 56 DVP 03 photomultiplier. The cross-section was derived, after appropriate correction, from the measurement of the transmission coefficient of the sample under study.

MESURE DES SECTIONS EFFICACES TOTALES NEUTRONIQUES DU CARBONE, DU NICKEL, DE L'URANIUM-235, DE L'URANIUM-238 ET DU PLUTONIUM-239 ENTRE 0,1 MeV ET 6 MeV.

Les auteurs ont mesuré les sections efficaces totales neutroniques du carbone, du nickel naturel, de l'uranium-235, de l'uranium-238 et du plutonium-239 entre 100 keV et 6 MeV, avec des dispersions en énergie comprises entre ± 2 keV et ± 40 keV suivant les corps et les gammes d'énergies. L'erreur sur la valeur absolue est inférieure à 3%. Les neutrons sont obtenus par la réaction $T(p, n)^3He$ en bombardant par des protons (accélérés soit par un Van de Graaff de 2 MeV soit par un tandem de 12 MeV à source pulsée) une cible de tritium adsorbé dans une couche mince de titane. Les neutrons sont détectés par un cristal de stilbène de 1 × 1,5 pouces couplé à un photomultiplicateur 56 DVP 03. La section efficace se déduit, après les corrections convenables, de la mesure du coefficient de transmission de l'échantillon étudié.

1. INTRODUCTION

Ces mesures de sections efficaces totales font suite à de nombreuses mesures de sections efficaces totales neutroniques sur des noyaux légers, moyens et lourds entreprises entre 100 keV et 1200 keV et ayant déjà fait l'objet de nombreuses publications.

Nous avons effectué ces expériences à l'aide d'un Van de Graaff de 2 MeV en utilisant le faisceau direct, et à l'aide d'un Van de Graaff tandem de 12 MeV à source pulsée en utilisant la méthode du temps de vol.

Une partie des mesures a été réalisée avec une dispersion en énergie de ± 2 keV et ensuite en utilisant des cibles épaisses dont la dispersion en

énergie était comprise entre ± 15 keV et ± 40 keV suivant l'énergie. Nous avons ainsi entre 100 keV et 1200 keV deux séries de mesures, l'une donnant la valeur moyenne de la section efficace, l'autre la structure fine quand elle existe comme dans le cas du nickel. Au-dessus de 1200 keV nous avons utilisé surtout des cibles épaisses.

2. DISPOSITIF EXPERIMENTAL

a) Avec le flux direct

Nous utilisons cette technique sur le Van de Graaff de 2 MeV pour obtenir une bonne définition en énergie du faisceau et un courant important sur la cible. Le bruit de fond à cette énergie est faible; on le détermine en plaçant un cône d'ombre à la place de l'échantillon. La distance source-détecteur est d'environ 90 cm, l'échantillon étant à mi-distance. Cette méthode est complètement décrite dans la référence [1]. Elle nous a permis, grâce à la faible dispersion en énergie des neutrons, d'obtenir la structure fine dans les différentes mesures de sections efficaces totales [2]. Cette méthode a été possible grâce à l'utilisation d'une discrimination de forme neutron-gamma d'excellente efficacité [3].

b) Avec le faisceau pulsé

Avec l'accélérateur Van de Graaff tandem de 12 MeV à source pulsée nous employons la méthode du temps de vol. Cette technique permet de déterminer avec précision le bruit de fond dû aux neutrons diffusés par les matériaux voisins et d'éliminer le flux des gamma directs produits par réaction sur la cible.

Dans les deux méthodes les neutrons sont produits par la réaction $T(p, n)^3He$, le tritium étant adsorbé sur du titane déposé sur un support en or. Ce support est choisi pour diminuer la production de neutrons parasites et minimiser l'importance des gamma. Le poids du tritium sur les cibles est choisi de façon à obtenir la dispersion en énergie souhaitée. Quant à la dispersion due à l'angle sous-tendu par le détecteur, elle est inférieure à 0, 3 keV, tandis que l'inhomogénéité du faisceau conduit à une dispersion inférieure à 10^{-3} en valeur relative.

L'étalonnage en énergie du Van de Graaff de 2 MeV a été fait à l'aide des résonances (p, γ) sur le ^{19}F et des seuils des réactions $T(p, n)^3He$ et $^7Li\ (p, n)^7Be$. Celui du Van de Graaff tandem de 12 MeV a été vérifié à l'aide des réactions (p, n) sur le ^7Li, le bore et l'aluminium. Ces mesures de seuils ont été réalisées par la méthode des deux compteurs.

L'énergie des protons est mesurée sur les deux accélérateurs par un ensemble gaussmètre à résonance nucléaire et fréquencemètre.

Les neutrons sont détectés par un scintillateur de stilbène de 2, 5 × 3, 7 cm couplé à un photomultiplicateur 56 DVP 03. Une discrimination de forme neutron-gamma rend le détecteur peu sensible aux gamma [3]. Le bruit de fond dû aux neutrons diffusés par les murs et matériaux environnants est réduit à l'aide de discriminateurs à seuils placés sur les différentes voies lentes.

Le contrôle est assuré par la mesure du courant intégré sur la cible ainsi que par un ensemble photomultiplicateur 58 DVP - scintillateur

NE 213 qui est vu par la cible sous un angle de 30° environ par rapport au faisceau de protons incidents.

Chaque cycle de mesure est entièrement automatique, et après chaque mesure les résultats acquis sur les blocs mémoires sont transférés dans la mémoire du calculateur CAE 510 où un programme d'exploitation nous permet d'obtenir les résultats définitifs (calcul de l'aire des pics, soustraction du bruit de fond, corrections des diffusions aux petits angles vers l'avant).

3. RESULTATS EXPERIMENTAUX

La valeur de la section efficace totale σ_T se déduit de la mesure du coefficient de transmission d'un échantillon du corps étudié. Les mesures sont corrigées du bruit de fond et de la contribution des diffusions élastiques aux petits angles [4]. L'erreur commise sur σ_T est due à la statistique et à l'incertitude sur les constantes physiques (poids, position, etc.). Dans tous les cas elle est de l'ordre de 3%.

3.1. Carbone

L'échantillon cylindrique a 3 cm de diamètre et 2 cm de long, ce qui correspond à une transmission voisine de 50%. Les mesures ont été réalisées entre 160 keV et 1200 keV avec une dispersion en énergie variant de ± 40 keV à ± 30 keV. Nos résultats (fig. 1) sont en bon accord avec ceux de Seth et al. [5] et Huddleston et al. [6] entre 160 keV et 700 keV. Entre 700 keV et 1200 keV les valeurs sont inférieures (de l'ordre de 50 mb à 100 mb) à celles de [6] et identiques à celles de Freier [7].

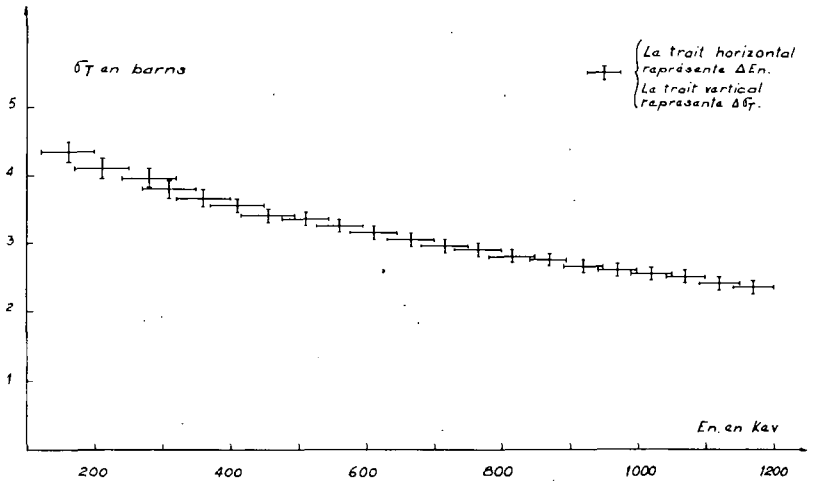

FIG. 1. Résultats obtenus: carbone.

3.2. Nickel

Les échantillons de nickel naturel sont cylindriques, d'un diamètre de 3 cm et de longueur telle que la transmission soit de l'ordre de 50%. Dans la gamme d'énergie de 100 keV à 1200 keV les mesures ont été réalisées, d'une part avec une dispersion en énergie de ± 2 keV pour mettre en évidence la structure fine, d'autre part avec un $\Delta E_n = \pm 35$ keV pour obtenir une bonne valeur moyenne de la section efficace.

Les résultats sont présentés sur la figure 2. La variation de la section efficace totale présente des fluctuations de très grande amplitude entre 100 keV et 350 keV, dues à des résonances plus ou moins résolues. A plus haute énergie, les fluctuations dans la section efficace sont moins importantes. Une analyse de ces fluctuations de la section efficace en termes de fluctuations statistiques ou de structure intermédiaire est en cours. Une mesure complémentaire de la diffusion élastique paraît nécessaire.

De nombreuses mesures ont été réalisées dans cette gamme d'énergie. On peut citer celles de Barshall et al. en 1948 [8] avec un $\Delta E_n = \pm 20$ keV, de Miller et al. en 1952 [9], de Newson et al. en 1959 [10], de Perrin et al. [11], Rainwater [12] et Cabé et al. en 1963 [13], de Rainwater et al. [14] et Smith en 1965 [15]. La comparaison entre elles de toutes ces mesures est difficile. Suivant la dispersion en énergie utilisée et le pas de la mesure, on met en évidence un plus ou moins grand nombre de fluctuations avec des amplitudes plus ou moins grandes dans la section efficace. Toutefois, les valeurs moyennes sont en bon accord avec les mesures de Smith [15] et nos anciennes mesures [13] réalisées à partir de 0,5 MeV.

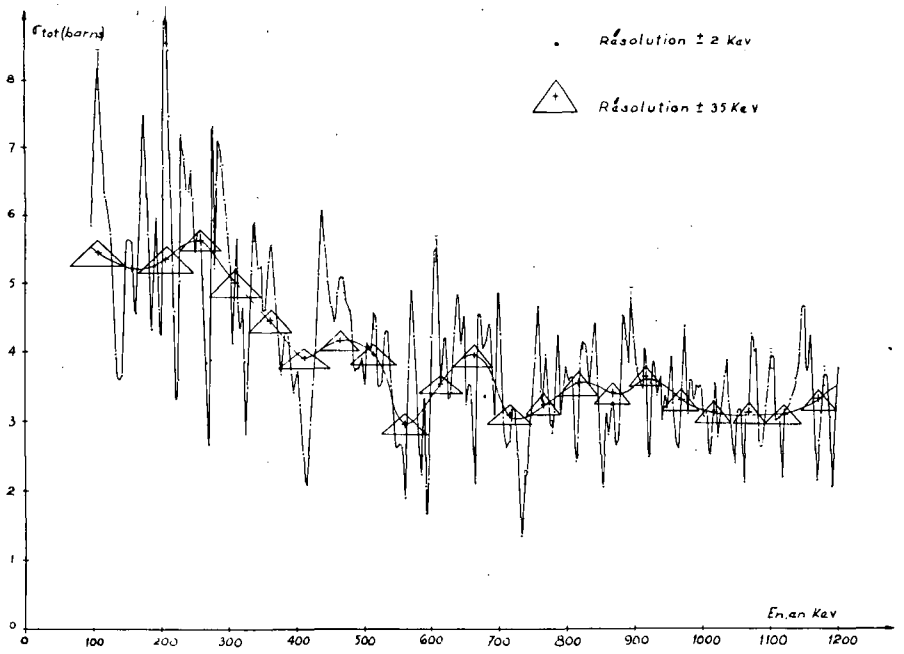

FIG. 2. Résultats obtenus: nickel.

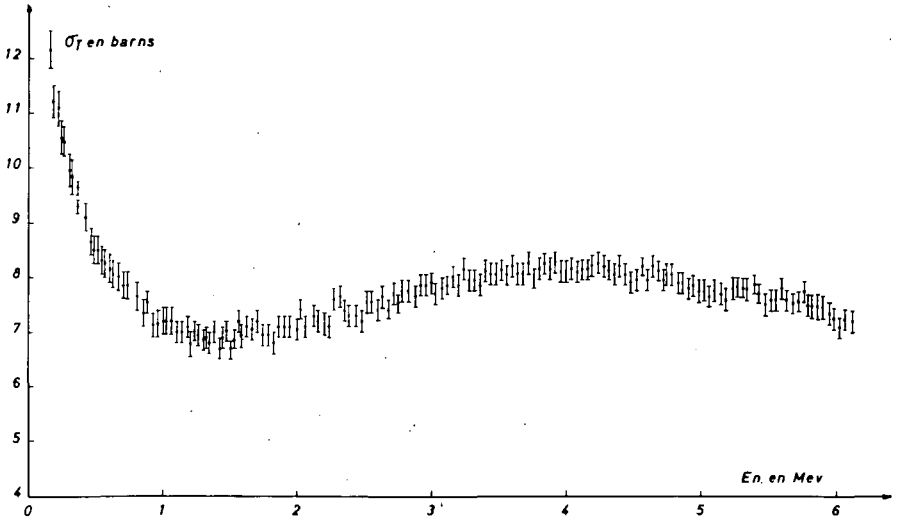

FIG. 3. Résultats obtenus: uranium-238.

3.3. Uranium-238

L'échantillon utilisé est un cylindre de 3 cm de diamètre et 2 cm de long. La dispersion en énergie est comprise entre ± 20 keV et ± 40 keV suivant l'énergie des neutrons. Les résultats sont présentés sur la figure 3. Les valeurs que nous obtenons sont supérieures à celles publiées par Tabony et al. [16] entre 30 keV et 650 keV. L'accord est bon avec les mesures des autres auteurs, en particulier entre 100 keV et 6 MeV (Smith [17], Barshall [18], Henkel et al. [19], Uttley [20], Nereson et Darden [21] et Leroy et al. [22]).

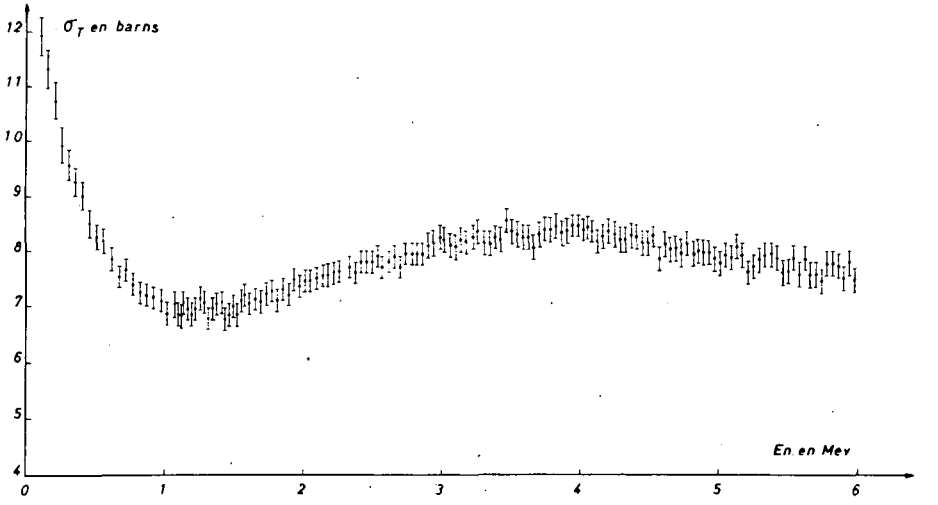

FIG. 4. Résultats obtenus: uranium-235.

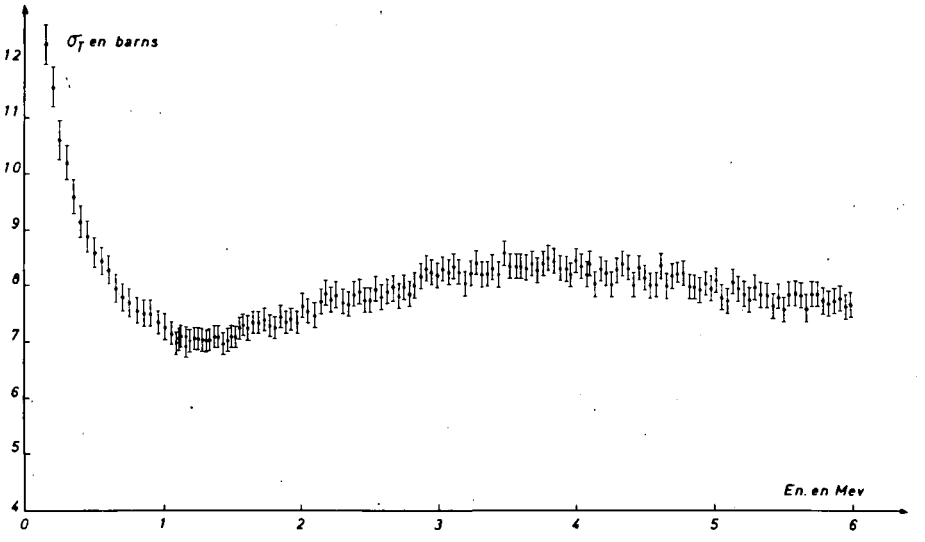

FIG. 5. Résultats obtenus: plutonium-239.

3.4. Uranium-235

Les conditions expérimentales sont identiques à celles utilisées pour l'uranium-238. Nous présentons nos résultats sur la figure 4. Leurs valeurs sont supérieures à celles obtenues par Henkel [23] et sont identiques aux valeurs supérieures obtenues par Smith [24]. Toutefois nos mesures sont moins dispersées et paraissent plus homogènes.

3.5. Plutonium-239

Les résultats sont présentés sur la figure 5. Ils ont été obtenus entre 160 keV et 6 MeV et sont en bon accord avec les mesures de Los Alamos [23].

4. CONCLUSION

Le but de ces mesures était de fournir des valeurs précises de sections efficaces intervenant dans les calculs de réacteurs. Nous espérons avoir répondu en partie aux diverses demandes formulées et sommes prêts à procéder à d'autres mesures si le désir en est exprimé.

REFERENCES

[1] CABE, J., Rapport CEA-3279, Thèse de Doctorat ès sciences physiques, Paris (1967).
[2] CABE, J., LAURAT, M., YVON, P., BARDOLLE, G., Nucl. Phys. A 102 1 (1967) 92.
[3] ADAM, A., CABE, J., CANCE, M., LAURAT, M., PONCE, J.C., J. Phys. appl. 4 2 (juin 1969) 262.
[4] VERVIER, J.S., Nucl. Instrum. 2 (1958) 53.

[5] SETH, K.K., BILPUCH, E.G., NEWSON, H.W., Nucl.Phys. 47 (1963) 137.
[6] HUDDLESTON, C.M., LANE, R.O., LEE, L.L., MOORING, F.P., Phys. Rev. 117 (1960) 1055.
[7] FREIER, G., FULK, M., LAMPI, E., WILLIAMS, J.H., Phys. Rev. 78 5 (1950) 508.
[8] BARSHALL, H., et al., Phys. Rev. 73 (1948) 659.
[9] MILLER, D.W., et al., Phys. Rev. 88 (1952) 83.
[10] NEWSON, H.W., et al., UCRL-5226 (1959).
[11] PERRIN, A., et al., J. Phys. Radium, Paris 24 (1963).
[12] RAINWATER, J., et al., Bull. Am. phys. Soc. 8 (1963) 334.
[13] CABE, J., et al., EANDC-(E) 49-L (1964).
[14] RAINWATER, J., et al., Communication privée (1965).
[15] SMITH, A.B., Communication privée (1965).
[16] TABONY, R.H., SETH, K.K., BILPUCH, E.G., Communication privée (1964).
[17] SMITH, A.B., Communication privée (1964).
[18] BARSHALL, H.H., LA-1060 (1950).
[19] HENKEL, R.L., et al., Phys. Rev. 94 (1954) 141.
[20] UTTLEY, C.A., AERE PR/NP 9 (1966) 4.
[21] NERESON, N., DARDEN, S., Phys. Rev. 89 (1953) 775.
[22] LEROY, J.L., et al., J. Phys. Radium, Paris 24 (1963) 826.
[23] HENKEL, R.L., LA-1493 (1952).
[24] SMITH, A.B., Communication privée (1964).

NEW TOTAL NEUTRON CROSS-SECTION MEASUREMENT OF URANIUM BETWEEN 0.5 - 4.35 MeV

D. KOPSCH, S. CIERJACKS, G.J. KIROUAC
Institut für Angewandte Kernphysik,
Kernforschungszentrum Karlsruhe,
Federal Republic of Germany

Abstract

NEW TOTAL NEUTRON CROSS-SECTION MEASUREMENT OF URANIUM BETWEEN 0.5 - 4.35 MeV.

The total neutron cross-section of natural uranium was measured with the neutron time-of-flight facility at the Karlsruhe Isochronous Cyclotron (KIC). The measurement covers the energy range between 0.5 and 4.35 MeV with a resolution of 0.03 ns/m; this corresponds to an energy resolution between 290 eV at 0.5 MeV and 7.4 keV at 4.35 MeV. In the energy region 1.1 - 4.35 MeV the statistical error was between 1% and 0.5%, below 1.1 MeV the error increases up to 2.7% at 0.5 MeV. An extensive comparison with new available data is given. The existence of fluctuations in the cross-section in the lower energy range is investigated.

1. INTRODUCTION

For the design of fast reactor assemblies, high-resolution total cross-sections of medium-weight and heavy nuclei, mainly in the keV and MeV region, are needed. These cross-section measurements should have considerably less than 5% uncertainty in order to be useful for reactor calculations. In addition, the resolution should be high enough to allow reproduction of the actual cross-section in satisfactory detail.

The knowledge of the fast-neutron total cross-section for uranium has been improved by extensive experimental work during the last few years [1-8]. Nevertheless, there remain some discrepancies in the absolute values, mainly in the energy region below 650 keV, and in the question of the existence of significant cross-section fluctuations.

Because of these discrepancies, the evaluated accuracy of the recommended σ_T values has been rather low; i.e. ±10% between 100-700 keV, ±6% between 0.7 and 2 MeV and ± 4 - 5% from 2 - 10 MeV [9].

The purpose of this work was to perform a high-resolution total cross-section measurement on natural uranium with good statistics. In section 2 of this paper a brief review of the experimental set-up is given. In section 3 our results and comparisons with other available data are shown and discussed. Finally, the question of fluctuations in the cross-section is considered.

2. EXPERIMENTAL DESCRIPTION

The measurement was performed with the neutron time-of-flight facility at the Karlsruhe isochronous cyclotron using a flight path of 187.5 m [10]. The neutron beam was collimated at 1 m, 10 m and 37 m

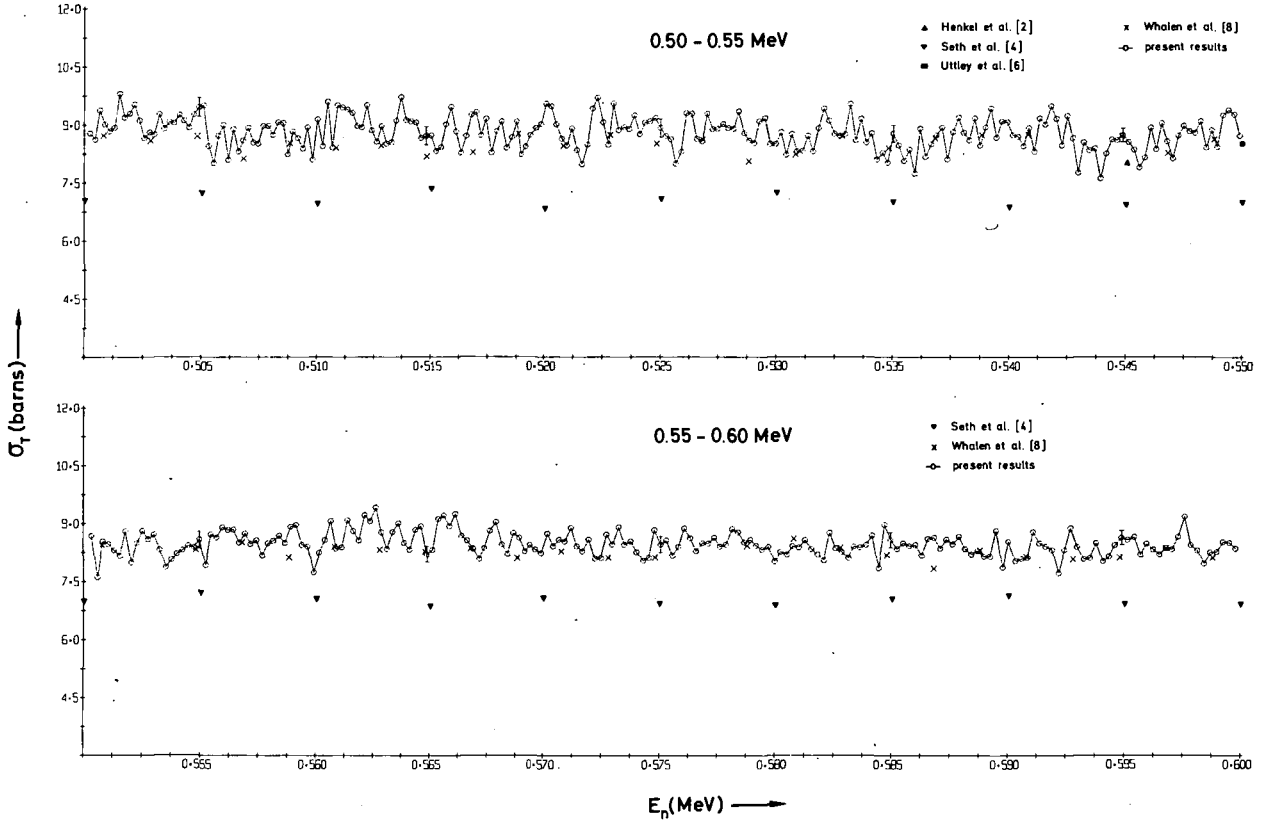

FIG. 1. Neutron total cross-section of uranium from 0.5 - 0.6 MeV.

from the source to about 2×10^{-6} sr. The sample, natural uranium with thickness 0.09542 at/barn, was positioned 1.50 m from the source. Normalization difficulties for sample-in and sample-out measurements were eliminated by alternating the sample-in and -out of the beam on a 250 sec-cycle. The effects of sample impurities were ascertained to contribute less than 3‰ uncertainty to the cross-section. Neutrons were detected by a 25-cm dia., 1-cm thick proton recoil scintillator, NE 102A, viewed simultaneously by two XP-1040 phototubes. The average counting rate for the detector was ~ 0.4 neutrons per machine burst when the sample was out of the beam. The measurement spans an energy region of 0.5 to 4.35 MeV in a total time-of-flight interval of ~ 16 μs with 1 ns channel width. Up to three counts per machine burst could be accepted by the time analyser and data acquisition system. Corrections for dead-time losses were performed in the data-reduction computer code.

The overall time resolution obtained in this measurement was 5.48 ns. This resolution of 0.029 ns/m corresponds to an energy resolution of ~ 290 eV at 0.5 MeV and 7.44 keV at 4.35 MeV. Since the measurement was performed with 1-ns channel width, a 4-channel compression could be applied after the measurement to improve the counting statistics, keeping a high resolution. The resolution width in the final reduced data corresponds to 1.37 times the point spacing. The statistical uncertainty lies between 0.45% at 4.35 MeV and 2.58% at 0.5 MeV.

3. RESULTS AND COMPARISON

Since more than 3000 data points were obtained in this measurement, a partition into several subintervals has been chosen for clearness of presentation. In Figs 1-5 our data are presented together with the data from other authors [1-8] available from CCDN, Saclay. As an insert in each drawing the symbols used for the different authors are given.

In Fig.1 and Fig.2, in the energy range 0.5 to 0.6 MeV and 0.6 to 0.7 MeV, respectively, the data are illustrated on an elongated energy scale. In these two figures our data points are connected by straight lines. In this region the energy resolution was ~ 0.29 keV at 0.5 MeV and ~ 0.48 keV at 0.7 MeV, respectively. The lines between the data points are definitely not intended to represent meaningful physical structure in all cases. They have been drawn to allow the viewer to appreciate the existence of some real structure. To give an impression of the statistical accuracy, the error bars are shown every 10 keV. The existence of real structure is discussed in detail in the next section. In the energy range 0.5 - 0.55 MeV, our data are compared with the results from Henkel et al. [2], Seth et al. [4], Uttley et al. [6] and the more recent and very extensive work performed by Whalen et al. [8]. Only one data point from Henkel et al. was available. These authors performed their measurement in 1954 with the Electrostatic Accelerator at Los Alamos using the $T(p, n)^3He$ reaction as a neutron source in the energy range 160 keV to 3.8 MeV. The energy resolution obtained in this region was within 20 - 40 keV; the statistical error ~ 200 mb. The agreement of this data point at 0.545 MeV with our measurement is satisfying. Also Uttley et al. measured only at one energy in this region. These authors performed a time-of-flight measurement at the Harwell booster pulsed-neutron source in 1966 with an energy

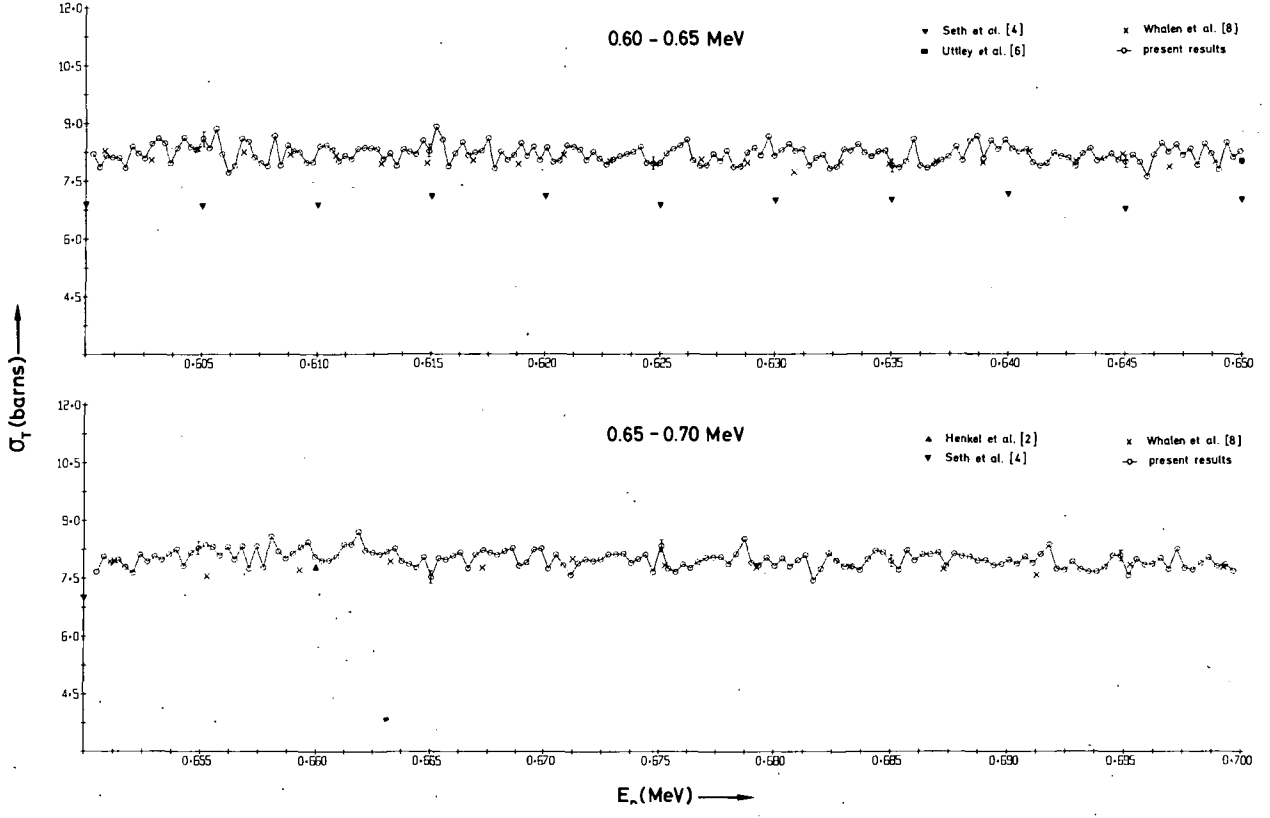

FIG. 2. Neutron total cross-section of uranium from 0.6 - 0.7 MeV.

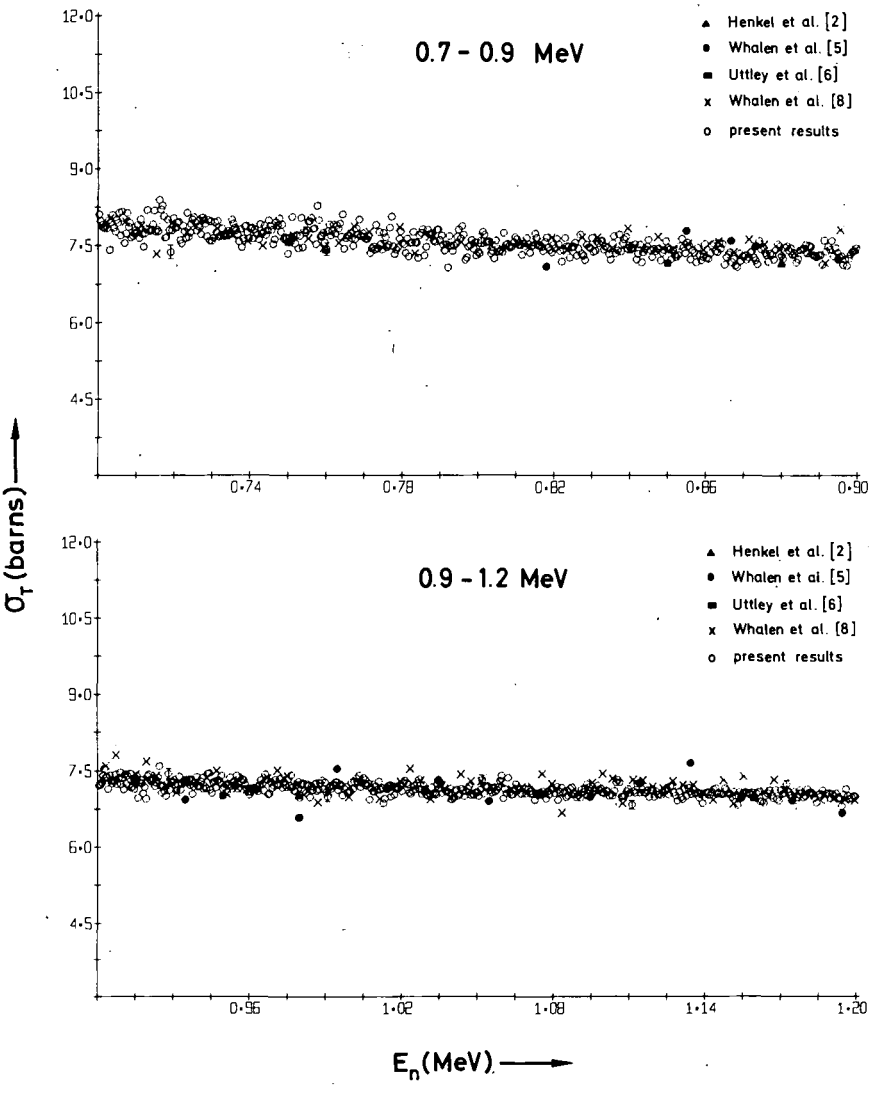

FIG. 3. Neutron total cross-section of uranium from 0.7 - 1.2 MeV.

resolution of ~ 50 keV for energies higher than 0.5 MeV. This data point also agrees with our measurement within the statistical error. The cross-section data from Seth et al. do not agree with our results; these data are ~ 15% lower than ours. The measurement was performed in 1964 in the energy range 30 to 650 keV with a resolution of 5 to 10 keV and a statistical error of ~ 200 mb. As previously shown by Schmidt [9], these data also do not agree with the earlier recommended cross-sections. In addition, the p-wave strength function deduced from this measurement is much lower than that derived by Uttley et al. The recent results from Whalen et al.

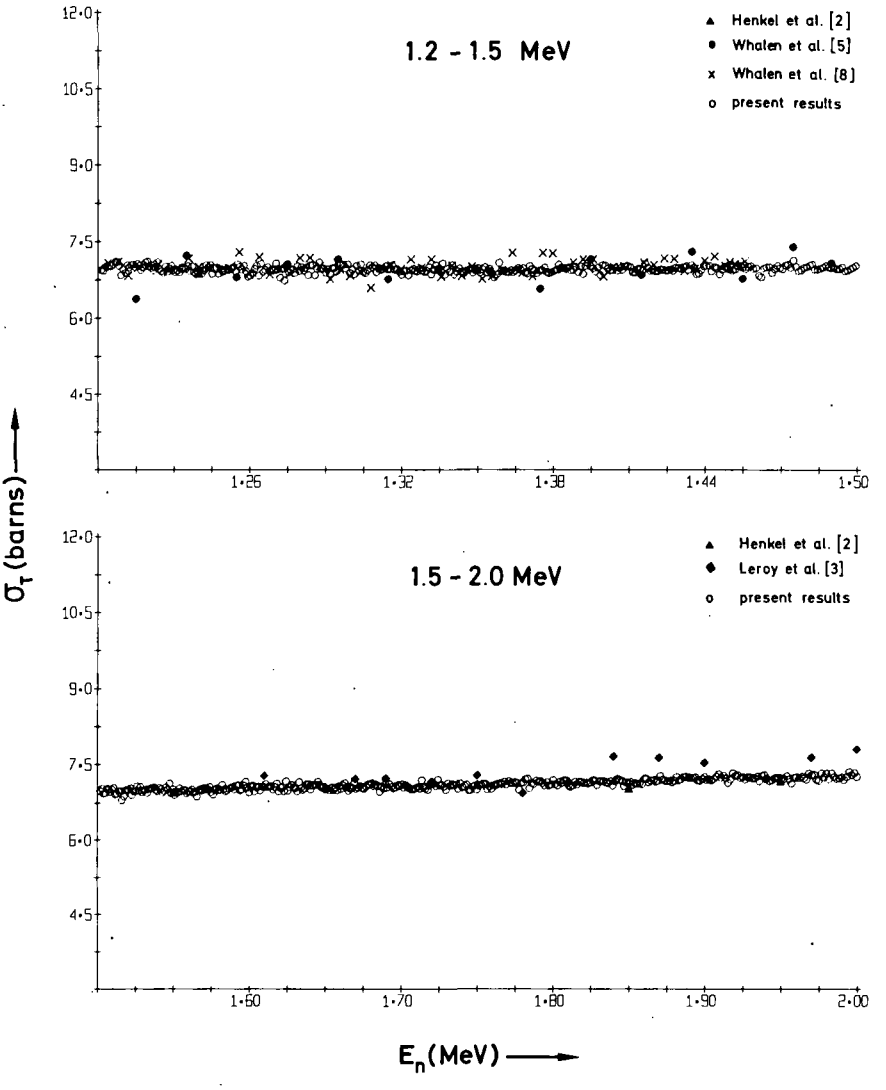

FIG. 4. Neutron total cross-section of uranium from 1.2 - 2.0 MeV.

performed at ANL in 1969 with a statistical error of 140 mb agree quite well with our results within the quoted errors. Also the suggestion of meaningful physical structure is present. We could not find any specific reference to this data, but we assume that this measurement had been performed under conditions similar to the other total-cross-section measurements carried out at ANL, i.e. with an energy resolution of 1.5 - 2.5 keV. In the energy range 0.55 - 0.6 MeV only data from Seth and Whalen were available. Here the situation is similar to the energy region 0.50 - 0.55 MeV.

In the upper part of Fig. 2, one value from Uttley, 11 values from Seth and 25 values from Whalen were available for comparison. There is still disagreement between Seth's values and ours while the agreement with the other values is excellent. In the region 0.65 - 0.70 MeV only a comparison between the Whalen data and the present results is possible because Seth's values run out at 0.65 MeV, and only one value is given by Henkel.

Starting with the energy region 0.7 - 0.9 MeV in Fig. 3, the present results are no longer connected by straight lines but are given as open circles. In the higher-energy regions, the evidence of fluctuations is not as significant as in the low-energy part. Furthermore, the density of data points is higher because of a compression of the energy scale. In this energy range, an extensive comparison between Whalen's results and the present results is possible. In addition, two values from Henkel and two from Uttley are shown. Again the agreement between these measurements and the present work is good. Furthermore, some earlier results measured by Whalen et al. [5] in 1965 are shown. The agreement between this measurement and the recent results from Whalen is good. In the energy region 0.9 - 1.2 MeV, the most extensive results available are again those from Whalen [8]. In addition, some other results are presented [2, 5, 6]. In the region 0.7 - 1.2 MeV, the statistical error of our data lies between 140 mb and 60 mb, respectively.

Figure 4 shows the energy range 1.2 - 2.0 MeV. From 1.2 - 1.5 MeV, approximately 70 data points from Whalen [8] are presented for comparison. The measurement extends to an energy of 1.5 MeV. Owing to an error on the CCDN data tape, data are not shown between 1.46 and 1.5 MeV. The agreement between Whalen's data and ours again is excellent. The error bars of our measurement in this energy range are equal to or less than the point size. Also the data from Henkel (3 points) and the earlier data from Whalen (15 points) agree quite well with our results. Between 1.5 and 2 MeV only values reported by Henkel and by Leroy et al. [3] were available. In 1963, Leroy et al. measured the cross-section of natural uranium in the energy range 1.61 -9.92 MeV using a 600 keV accelerator and the time-of-flight technique. To obtain a broad neutron spectrum the T-target was surrounded by an uranium sphere. The energy resolution between 2 and 4 MeV was ~ 60 to ~ 160 keV. The statistical error was ~250 mb for this region. The agreement between these results and ours is adequate up to 1.8 MeV. From 1.8 to 2 MeV their data are ~ 400 mb higher than our results while the agreement between Henkel's results and ours remains good.

In the last figure, data are presented in the energy range of 2 - 4.5 MeV. In the upper part of this figure, our results are shown together with those from Henkel, Leroy and Foster et al. [7]. In 1967, Foster et al. performed their pulsed-beam time-of-flight measurement on ^{238}U using a 2 MeV Van de Graaff. Their measurement spans an energy range 2.25 - 15 MeV with a resolution of 50 keV at 2.25 MeV and 115 keV at 4.5 MeV, respectively. The statistical precision quoted is between 200 mb and 80 mb in this region. The agreement between this measurement and the present results is good. The consistency between our data and the data from Leroy is not a severe test because of the large scatter of the latter data. Again the agreement between Henkel's data and ours is very good.

In the lower part of Fig. 5 data are shown from 3 MeV to 4.35 MeV. A comparison is made with the data from Henkel, Leroy Nereson et al.

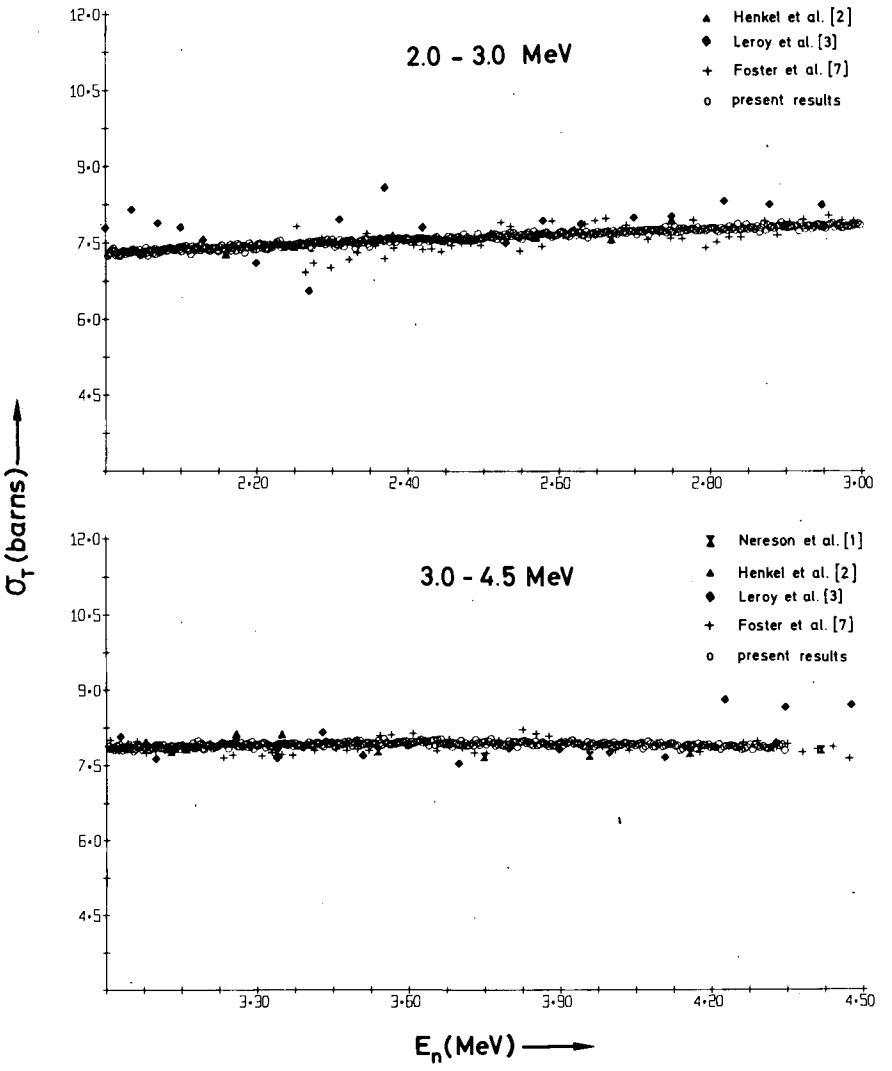

FIG. 5. Neutron total cross-section of uranium from 2.0 - 4.5 MeV.

[1] and Foster. The Foster data are the most extensive and recent data available for this comparison; only seven data points measured by Nereson et al. can be presented. The measurement performed by Nereson et al. in 1953 at the Los Alamos Fast Reactor has an overall accuracy of better or equal than ± 10% and was carried out with an energy resolution of ~ 300 keV. The consistency between the Foster data and our results is excellent. Leroy's data agree well with ours with the exception of the last three points between 4.20 and 4.50 MeV. Nereson's data are lower by about ~ 150 mb while the agreement between our data and those of Henkel is within the statistical accuracy.

4. DISCUSSION

The question of resolvable structure in the total cross-section of uranium below 1 MeV is of considerable interest and has been approached with caution in this work. To approach this problem quantitatively, we have calculated the actual variance of the total cross-section, i.e. the mean square deviation of single data points with reference to an average cross-section. The averaging interval was such that the residual statistical error is vanishing, but the gross structure (~ 100 keV) remains. The average cross-section was represented by a value obtained by smoothing the original data over an interval containing 100, 200, 300 or 400 data points. The average values obtained in this manner did not differ significantly for the four intervals.

The variance in four separate regions (0.50 - 0.55, 0.55 - 0.60, 0.60 - 0.65 and 0.65 - 0.70 MeV) was then compared with the variance based only on counting statistics, and the significance level of the ratio was investigated (F-test).

The statistical counting uncertainty used for this comparison properly includes the counting statistics of sample-in, sample-out and background measurements. We found that the variance is 2.7 times larger than that based on the statistical error for the energy range 0.50 to 0.55 MeV. This factor decreases smoothly to 1.6 for energies between 0.65 to 0.70 MeV. If, as we assume, the additional component of the actual variance is caused by significant cross-section fluctuations of very narrow width, then the variation of the ratio quoted above is in accordance with our decreasing resolution with increasing energy. The present measurement has a resolution of ~ 1.4 times the point spacing. Thus, only the question of counting statistics remained. The F-values of 2.7 and 1.6 correspond to a probability of > 99, 95% and > 99%, respectively, that the hypothesis of significant fluctuations is correct.

Summmarizing, we can say that the present results are in good agreement with other data with the exception of some older measurements. Our about 3000 data points provide good definition for the uranium total cross-section from 0.5 - 4.35 MeV. The analysis of fluctuations indicates meaningful physical structure in the energy range of 0.5 - 0.7 MeV though these fluctuations show only small amplitudes.

REFERENCES

[1] NERESON, N., DARDEN, S.E., data referenced in CCDN-NW/11 (Oct.69) 283; see also Phys. Rev. 89 (1953) 775.
[2] HENKEL, R.L., CRANBERG, L., JARVIS, G.A., NOBLES, R., PERRY, J.E., Jr., data referenced in CCDN-NW/11 (Oct.69) 283, see also Phys. Rev. 94 (1954) 141.
[3] LEROY, J.L., BERTHELOT, F.C., POMELAS, E., data referenced in CCDN-NW/11 (Oct.69), see also J. Physique 24 (1963) 826.
[4] SETH, K.K., et al., data referenced in CCDN-NW/11 (Oct.69) 283.
[5] WHALEN, J.F., SMITH, A.B., MEADOWS, J.W., data referenced in CCDN-NW/11 (Oct.69) 295, also ANL-7110 (1965) 15.
[6] UTTLEY, C.A., et al., data referenced in CCDN-NW/11 (Oct.69) 295.
[7] FOSTER, D.G., et al., data referenced in CCDN-NW/11 (Oct.69) 295.
[8] WHALEN, J.F., et al., data referenced in CCDN-NW/11 (Oct.69) 295.
[9] SCHMIDT, J.J., Rep. KFK 120 (EANDC-E-35 U) (1966) 14.
[10] CIERJACKS, S., DUELLI, B., FORTI, P., KOPSCH, D., KROPP, L., LÖSEL, M., NEBE, J., SCHWEICKERT, H., UNSELD, H., Rev. scient. Instrum. 39 (1968) 1279.

DISCUSSION

TO PAPERS IAEA-CN-26/68, 12

C. M. NEWSTEAD: The fact that Dr. Kopsch has apparently found that the Seth cross-section is somewhat lower than that of Uttley et al. and the one obtained in his own measurements would help explain one of the discrepancies in connection with the p-wave strength function pointed out by Dr. Muradyan in the presentation of his paper (CN-26/109), as it is from these total cross-section data at somewhat lower energies that one extracts the p-wave strength function. This was a rather large discrepancy - Seth obtained 0.5 whereas Uttley and I obtained 2.5. However, it would take more than a 15% difference in the cross-section to explain this difference: what it would really depend upon is the magnitude in the 200 keV range. It should be noted that Dr. Soleilhac, also, refers to a difference in values from those of Seth in the ^{238}U total cross-section.

РАДИАЦИОННЫЙ ЗАХВАТ НЕЙТРОНОВ ЯДРОМ ^{238}U

Ю. Я. СТАВИССКИЙ, В. А. ТОЛСТИКОВ,
В. Б. ЧЕЛНОКОВ
Физико-энергетический институт, Обнинск,

А. А. БЕРГМАН, А. Е. САМСОНОВ
Физический институт Академии наук СССР,
Москва,
Союз Советских Социалистических Республик

Presented by A.I. Abramov

Доклад представлен А.И. Абрамовым

Abstract — Аннотация

RADIATIVE CAPTURE OF NEUTRONS BY ^{238}U NUCLEI.

The authors present the results of measurements of the energy dependence of average cross-sections for the radiative capture of neutrons by uranium-238 nuclei in the energy range 5 eV-30 keV. The measurements were made at the Lebedev Physics Institute of the USSR Academy of Sciences with a neutron spectrometer using the phenomenon of slowing-down in lead. The radiative capture of the neutrons was recorded by measuring the prompt capture gamma rays with a proportional gas-discharge counter in which the efficiency of gamma ray recording was linearly dependent on the gamma ray energy. Cylindrical samples of uranium-238 (U_3O_8) of different effective thicknesses ($\bar{n}_1 = 7.10 \times 10^{21}$ nuclei/cm^2, $\bar{n}_2 = 3.93 \times 10^{21}$ nuclei/cm^2 and $\bar{n}_3 = 1.29 \times 10^{21}$ nuclei/cm^2) were used. Normalization was carried out using the first resonance in the cross-section for radiative capture by uranium-238 ($E_0 = 6.67 + 0.02$ eV) and the cross-section for radiative capture by gold-197. The results are compared with those obtained by other authors.

РАДИАЦИОННЫЙ ЗАХВАТ НЕЙТРОНОВ ЯДРОМ ^{238}U.

В работе изложены результаты измерений энергетической зависимости усредненных сечений радиационного захвата нейтронов ядром ^{238}U в области энергий от 5 эв до 30 кэв. Измерения выполнены на нейтронном спектрометре ФИАН СССР по времени замедления в свинце. Эффект радиационного захвата нейтронов регистрировался по мгновенным γ-лучам захвата пропорциональным газоразрядным счетчиком с линейной зависимостью эффективности регистрации γ-квантов от их энергии. В измерениях использованы цилиндрические образцы ^{238}U (U_3O_8) различной эффективной толщины ($\bar{n}_1 = 7{,}10 \cdot 10^{21}$ яд/см^2 ; $\bar{n}_2 = 3{,}93 \cdot 10^{21}$ яд/см^2 и $\bar{n}_3 = 1{,}29 \cdot 10^{21}$ яд/см^2). Нормировка проводилась по первому реэонансу в сечении радиационного захвата ^{238}U, $E_0 = 6{,}67 + 0{,}02$ эв, и по сечению радиационного захвата ^{197}Au. В работе проведено сравнение полученных данных с результатами измерений других авторов.

ВВЕДЕНИЕ

Сечение радиационного захвата нейтронов ядром ^{238}U представляет интерес для теории ядра и реакторостроения. В настоящее время опубликован ряд работ [5-18], в которых сечение радиационного захвата для ^{238}U измерено различными методами и с разным энергетическим разрешением в области энергий нейтронов ниже ~100 кэв.

В данной работе изложены результаты измерений усредненного сечения радиационного захвата для ^{238}U в области энергий от ~5 эв до ~30 кэв, выполненные на нейтронном спектрометре по времени замедления в свинце ФИАН СССР. Принцип работы спектрометра подробно описан ранее, например в работах [1,2].

МЕТОД ИЗМЕРЕНИЯ

В рабочем канале свинцового замедлителя исследуется зависимость счета детектором мгновенных γ-лучей радиационного захвата от времени замедления $I_\gamma(t)$ и плотность нейтронов $I_\beta(t)$ с помощью детектора, эффективность которого пропорциональна $1/v$ (например, борная камера). Тогда, как показано в работе [2]:

$$\frac{I_\gamma(t)}{I_\beta(t)} = k_x \sigma_c(E)\, v(t) \qquad (1)$$

где:
$$k_x = k_x(\bar{n}_x, M, \epsilon_x) \qquad (2)$$

здесь: k_x – нормировочный коэффициент, зависящий от эффективной толщины образца $\bar{n}_x$, счета монитора M и эффективности регистрации акта захвата ϵ_x;

$\sigma_c(E)$ – среднее сечение радиационного захвата для ядер исследуемого образца;

$v(t)$ – средняя скорость нейтронов в момент времени замедления t.

Средняя энергия нейтронов E (кэв) и время замедления (мксек) связаны эмпирическим соотношением:

$$E = \frac{183}{(t + 0{,}3)^2} \qquad (3)$$

ДЕТЕКТОР

В качестве детектора мгновенных γ-лучей захвата в данной работе использован газовый пропорциональный счетчик. Окружение стенок счетчика свинцом (с полной толщиной $\alpha \geqslant Re$, где Re пробег вторичного электрона, образованного γ-квантом радиационного захвата) и наполнение счетчика до высокого давления (10 атм $Ar + 4\% CO_2$) позволяют приблизить зависимость эффективности регистрации γ-лучей от их энергий E_γ к линейной:

$$\epsilon_\gamma \simeq \text{const}\, E_\gamma \qquad (4)$$

В этом случае эффективность регистрации акта радиационного захвата ϵ_x определяется только энергией связи нейтрона в ядре B_n^x:

$$\epsilon_x \approx \text{const}\, B_n \qquad (4\text{-а})$$

и не зависит от спектра захватных γ-лучей, который от одного нейтронного резонанса к другому может меняться.

Оценить точность равенства (4) можно из измерений на пропорциональном γ-счетчике с образцами, отличающимися спектром захватных γ-лучей. Действительно, из определения нормировочного коэффициента (2) следует, что k_x, вычисленный по параметрам резонансов, либо по тепловому сечению, и приведенный к толщине образца $\bar{n}_x$ и нейтронному потоку, зависит только от эффективности регистрации акта захвата ϵ_x.

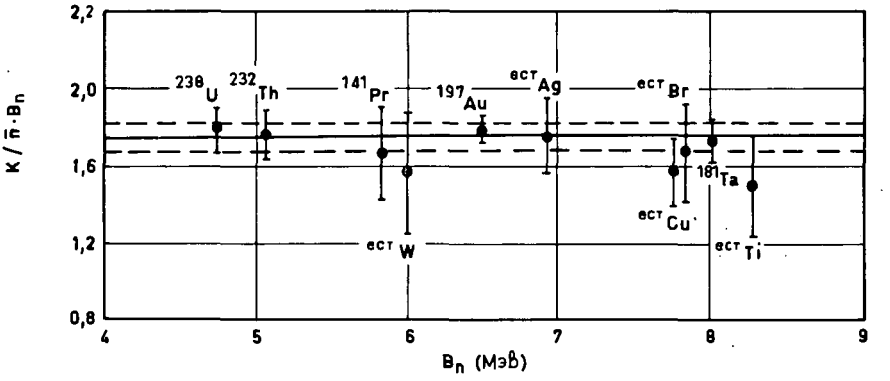

Рис. 1. Зависимость приведенного нормировочного коэффициента от энергии связи B_n.

Поэтому оказывается возможным определить зависимость $\epsilon_x(B_n)$, которая является следствием равенства (4).

Значения приведенных нормировочных коэффициентов, полученные из измерений с пропорциональным γ-счетчиком для образцов с различными захватными γ-спектрами, представлены на рис. 1. Обработка числовых значений по методу наименьших квадратов оценивает справедливость равенства (4-а) с точностью $\pm 4\%$.

ОБРАЗЦЫ И ОБРАБОТКА РЕЗУЛЬТАТОВ ИЗМЕРЕНИЙ

Энергетическая зависимость $\sigma_c(E)$ для ^{238}U последовательно измерялась с образцами (L_3O_8) трех различных эффективных толщин ($7{,}10\,10^{21}$ ат/см^2; $3{,}93\cdot10^{21}$ ат/см^2 и $1{,}29\cdot10^{21}$ ат/см^2). С целью повышения надежности данных, измерения с исследуемыми образцами чередовались с измерениями с образцом ^{197}Au ($\bar{n}_{Au} = 6{,}18\cdot10^{20}$ ат/см^2), для которого сечение радиационного захвата на спектрометре по времени замедления хорошо изучено [3]. Таким образом, относительные измерения энергетической зависимости сечения можно было отнормировать не только по резонансным параметрам собственных низкорасположенных уровней, но и по сечению радиационного захвата ^{197}Au.

Измерения проведены при частоте нейтронной вспышки f = 625 гц, что соответствует длительности цикла 1600 мксек. Поскольку плотность нейтронов в замедлителе спектрометра значительно убывает со временем замедления [2]:

$$I_\beta(t) = \text{const}\; t^{-0,35}\cdot e^{-\frac{t}{T}} \qquad (5)$$

(где T – среднее время жизни нейтронов ~890 мксек в свинцовом замедлителе), а тепловое сечение ^{238}U сравнительно мало, то поправка на вклад от нейтронов предыдущей вспышки не существенна и не вводилась в результаты измерений. Длительность нейтронной вспышки устанавливалась минимальная (~0,5 мксек) в тех сериях измерений, когда важно было получить данные о ходе сечения в области энергий нейтронов ~30 кэв (малые времена замедления).

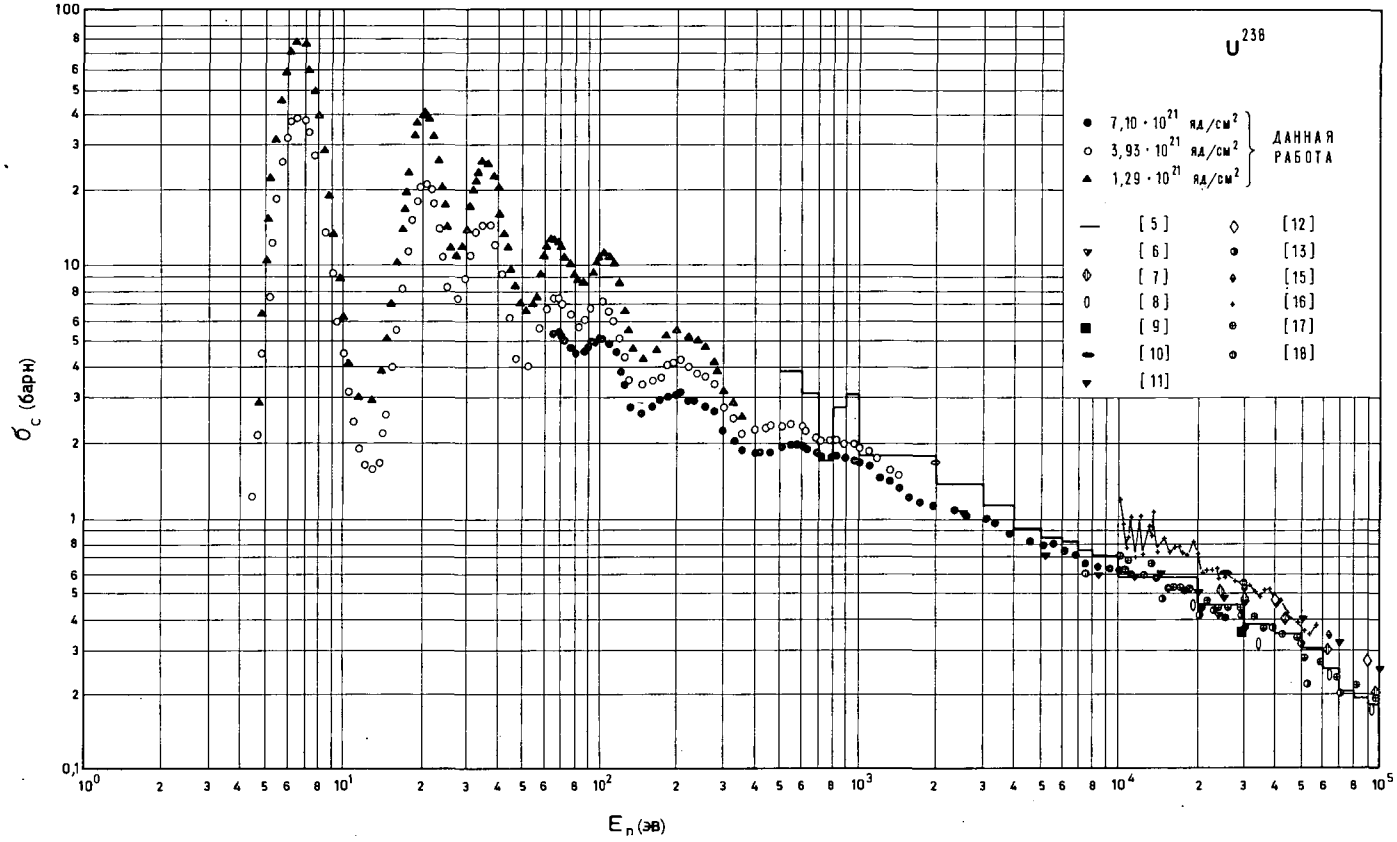

Рис. 2. Результаты измерений сечений радиационного захвата, полученные в данной работе, в сравнении с данными других авторов.

При измерениях с образцом и без образца активация детектора поддерживалась в насыщении (счетчик облучался до начала каждой серии около 10 мин), что позволяет исключить ее при обработке результатов. Активация самого образца (с периодами $\geqslant 1$ мин) оценивалась в отдельных измерениях по изменению естественного фона облученного образца и составляла $\sim 2\%$ от естественного фона. Измерения с образцом и без образца в нейтронном потоке чередовались с измерениями естественного фона каждого образца на дезактивированном счетчике.

В результаты измерений вводилась поправка на просчеты электронной регистрирующей аппаратуры, связанная с конечным временем разрешения ($\tau = 3$ мксек) счетной системы и перегрузками счета вблизи нейтронной вспышки. Значение поправки оценивалось по формуле [4]:

$$\eta = \frac{1}{f \cdot \Delta k} \cdot \int_{t-\tau}^{t} m(t)\,dt \qquad (6)$$

где $m(t)$ – средняя скорость счета в канале, расположенном в интервале времени от t до $t + \Delta k$.

Поправка на просчеты оказывается существенной только при малых временах замедления. Оценка по формуле (6) дает $\eta \simeq 10\%$ при $E \simeq 30$ кэв и $\eta \simeq 0{,}5\%$ при $E = 10$ кэв.

РЕЗУЛЬТАТЫ И ИХ ОБСУЖДЕНИЕ

Результаты измерения энергетической зависимости сечения радиационного захвата для ^{238}U приведены на рис. 2 в сравнении с данными работ других авторов [5-18].

Нормировка кривых зависимости сечений от энергии нейтронов проведена по резонансу $E_0 = 6{,}67 + 0{,}02$ эв и по сечению радиационного захвата ^{197}Au. При вычислении нормировочного коэффициента по резонансу для определения эффективного резонансного интеграла поглощения использованы рекомендованные значения резонансных параметров из работы [19] и графики, учитывающие эффект резонансной экранировки [20]. Нормировка по резонансам $E_0 = 21{,}0 + 0{,}2$ эв и $E_0 = 36{,}7 + 0{,}3$ эв не может быть проведена надежно вследствие слабого разрешения спектрометра, однако, нормировочный коэффициент, определенный по ним, находится в согласии, в пределах ошибок, с вычислениями по резонансу $E_0 = 6{,}67 + 0{,}02$ эв.

Среднеквадратичная ошибка результатов измерений не превышает 7-8% и обусловлена, главным образом, ошибкой нормировки.

Результаты работ, с которыми проводится сравнение данных настоящей работы, приведены, в основном, в оригинальном неперенормированном виде. Необходимо отметить, что при сравнении данных нужно обращать внимание на толщины образцов, с которыми проводились измерения, поскольку от толщины образца значительно зависит эффект блокировки.

В работе [21] введена поправка на эффект блокировки в результате работы Т. С. Белановой и др. [6]. Однако эта поправка кажется завышенной. Проводя предварительную оценку эффекта блокировки, вместо ранее опубликованного значения, авторы работы [6] предлагают значение 439 ± 31 мб для $E = 24$ кэв. Результаты нашей работы [13] приведены на рис. 2 перенормированными к этому значению. Результаты работы [14] не нанесены, так как совпадают с другими данными.

ЛИТЕРАТУРА

[1] БЕРГМАН, А. А., ИСАКОВ, А. И., МУРИН, И. Д., ШАПИРО, Ф. Л., ШТРАНИХ, И. В., КАЗАРНОВСКИЙ, М. В., Материалы Женевской конф. по мирному использованию атомной энергии 4 1955, стр. 166.
[2] ШАПИРО, Ф. Л., Труды ФИАН СССР 24 (1964) 3.
[3] КЕНКЕ, В. А., ПОПОВ, Ю. П., ШАПИРО, Ф. Л., ЖЭТФ 46 (1964), 80.
[4] МАТАЛИН, Л. А., ЧУБАРОВ, С. И., ИВАНОВ, А. А., Многоканальные анализаторы ядерной физики. Атомиздат, 1964.
[5] MOXON, M.C., "The Neutron Capture Cross-Section of ^{238}U in the Energy Region 0,5 to 100 keV", AERE-R-6074, 1969.
[6] БЕЛАНОВА, Т. С., ВАНЬКОВА, А. А., МИХАЙЛУС, Ф. Ф., СТАВИССКИЙ, Ю. Я., Атомная энергия 19 (1965), 3-8.
[7] MENLOVE, H.O., POENITZ, W.P., Nucl.Sci. and Eng. 23 (1968) 24.
[8] BERCGVIST, J., Arkiv för Fysik, Band 23, Häfte 5 (1963) 425.
[9] HANNA, R.C., ROSE, B., Journal of Nucl. Energy 8 (1959) 197.
[10] MACKLIN, R.L., LAZAR, N.H., LYON, W.S., Phys. Rev. 107 (1957) 504.
[11] BILPUCH, E.G., WESTON, L.W., NEWSON, H.W., Annals of physics 10 4 (1960) 455.
[12] LINENBERGER, G.A., MISKEL, J.A., Los-Alamos, LA-467 (1946).
[13] ТОЛСТИКОВ, В. А., ШЕРМАН, Л. Е., СТАВИССКИЙ, Ю. Я., Атомная энергия 15 (1963) 44.
[14] GIBBONS, J.H., MACKLIN, R.L., MILLER, P.D., NEILER, J.H., Phys. Rev. 122 (1961) 182.
[15] SAUSSURE, G. de, WESTON, L.W., KINGTON, J.D., SMIDDIE, P.D., LYON, W.S., ORNZ-3360 (1962) 51.
[16] MACKLIN, R.L., GIBBONS, J.H., Private communication (1964), Oak-Ridge, Moxon-Rac detector.
[17] MOXON, M.C., CHAFFEY, C.M., Private communication (1963), Harwell, Moxon – Rac detector.
[18] ARAI, E., MIESSNER, H., BECKURTZ, K.H., Nucl. Sci. Eng. 26 (1966) 573.
[19] STEH, J.R., GOLDBERG, M.D. et al., Neutron Cross Sections, BNL-325, Suppl. 2, Second Edition, 1965.
[20] ЕФИМОВ, В. Н., ШЕЛОНЦЕВ, И. И., Препринт ОИЯИ, Р-641, Дубна, 1961.
[21] MILLER, L.B., POENITZ, W.P., Nucl. Sci. Eng. 35 (1969) 295.

РАДИАЦИОННЫЙ ЗАХВАТ НЕЙТРОНОВ ^{238}U В ДИАПАЗОНЕ ЭНЕРГИЙ 24 ÷ 145 кэв

Ю. Г. ПАНИТКИН, В. А. ТОЛСТИКОВ,
Ю. Я. СТАВИССКИЙ
Физико-энергетический институт, Обнинск,
Союз Советских Социалистических Республик

Presented by A.I. Abramov

Доклад представлен А.И. Абрамовым

Abstract — Аннотация

RADIATIVE CAPTURE OF NEUTRONS BY ^{238}U IN THE ENERGY RANGE 24-145 keV.

Measurements were made of the cross-section for the radiative capture by uranium-238 of neutrons in the energy range 24-145 keV, using a Van de Graaff generator and neutrons produced in the reaction $^{7}Li(p,n)^{7}Be$. The target thickness was about 20 keV for protons of threshold energy. The induced activity was determined by measuring the gamma rays occurring in uranium-239 decay. The gamma radiation was detected by a Ge(Li) semiconductor detector. The neutron flux was monitored during the irradiation of uranium-238 samples. In the course of subsequent processing of the results a correction was introduced for fluctuations of the neutron flux during irradiation. The authors also measured the background of neutrons scattered in the target and in surrounding structural materials.

РАДИАЦИОННЫЙ ЗАХВАТ НЕЙТРОНОВ ^{238}U В ДИАПАЗОНЕ ЭНЕРГИЙ 24 ÷ 145 кэв.

В работе измерено сечение радиационного захвата нейтронов ядрами ^{238}U в диапазоне энергий нейтронов 24 ÷ 145 кэв. Измерения выполнены на генераторе Ван-де-Граафа, источником нейтронов служила реакция $^{7}Li(p,n)^{7}Be$. Толщина мишени составляла около 20 кэв при пороговой энергии протонов. Наведенная активность измерялась по γ-квантам, возникающим при распаде ^{239}U. Детектирование γ-излучения производилось полупроводниковым Ge(Li) детектором. Во время облучения образцов ^{238}U производилось мониторирование нейтронного потока и при последующей обработке результатов измерений вводилась поправка на флуктуации потока во время облучения. Проведены измерения фона от нейтронов, рассеянных на мишени и рассеянных от помещения.

1. ВВЕДЕНИЕ

Сечение радиационного захвата нейтронов ^{238}U имеет большое значение для расчета реакторов. Несмотря на это, сечение данной реакции еще недостаточно хорошо известно. Захват нейтронов ^{238}U является наиболее эффективным в быстрых реакторах, в диапазоне энергий нейтронов 20 ÷ 200 кэв, и требуемая в настоящее время точность сечения — порядка одного процента.

Рассмотрение работ, выполненных до настоящего времени, обнаруживает довольно значительные расхождения как в абсолютных значениях сечений радиационного захвата нейтронов, так и в ходе сечения радиационного захвата нейтронов в зависимости от энергии нейтронов. Например, имеются различия в ходе сечения радиационного захвата между работами [1], [2] и недавно проделанной работой [3].

В данной работе измерен ход сечения радиационного захвата нейтронов ^{238}U в диапазоне энергий нейтронов 24 ÷ 145 кэв. Был использован

активационный метод; монитором нейтронного потока была камера деления с ^{235}U. Измерялось рассеяние потока нейтронов на конструкции мишени и флуктуации потока нейтронов во время облучения образцов. Регистрация наведенной активности производилась Ge(Li) детектором по γ-линии с энергией 74 кэв, образующейся при распаде ^{239}U в ^{239}Np.

2. МЕТОД

Основными неопределенностями, возникающими при относительных измерениях активационным методом сечения радиационного захвата нейтронов ^{238}U в данной области энергий, являются:

1. Неопределенность в измерении наведенной активности в присутствии естественного фона образца ^{238}U.
2. Неопределенность при мониторировании потока нейтронов, падающих на образец, в присутствии фона, возникающего при рассеянии нейтронов на конструкции мишени и в мишенной камере ускорителя.
3. Неопределенность, возникающая из-за различия в потоках нейтронов, падающих на образец и монитор потока.

В данной работе для регистрации наведенной активности образца был использован Ge(Li) детектор, позволяющий существенно уменьшить влияние естественной активности образца на точность измерений. Отношение эффекта к фону было более 10.

Для уменьшения неопределенности, связанной с фоном рассеянных нейтронов, рассеяние нейтронов на конструкции мишени измерялось во всем энергетическом диапазоне измерений сечения радиационного захвата нейтронов. Относительные вклады рассеянных нейтронов в счет камеры деления и наведенную активность образца ^{238}U различны и меняются в зависимости от энергии, падая с 16% при $E_n = 24$ кэв до 5% при $E_n = 100$ кэв и возрастая затем до 6% при $E_n = 145$ кэв. Учет этого фактора приводит к изменению в относительном ходе сечения радиационного захвата на 2 ÷ 3%.

Камера деления со слоем ^{235}U и образец ^{238}U были расположены таким образом, что поток нейтронов, проходящий через них, был тождественным.

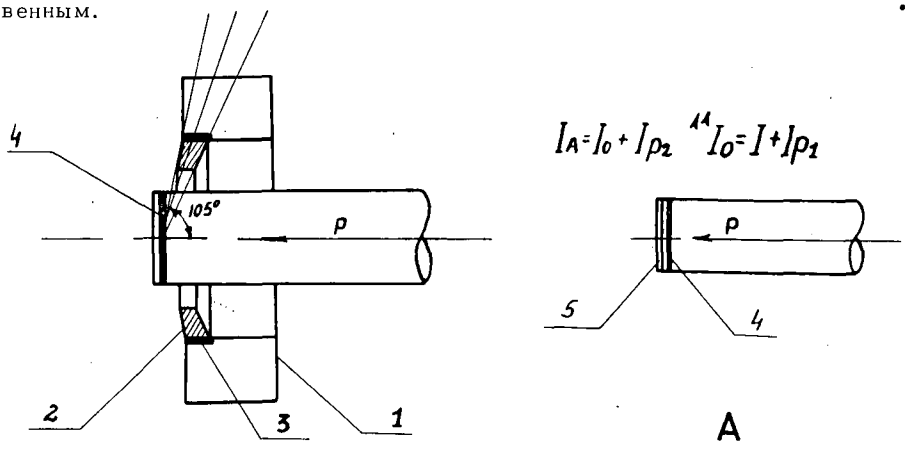

Рис. 1. Геометрия, использовавшаяся в процессе измерений: 1 – камера деления; 2 – образец ^{238}U; 3 – слой ^{235}U; 4 – мишень LiF; 5 – "добавка" на торец мишени.

3. ОБЛУЧЕНИЕ ОБРАЗЦОВ ^{238}U И ИЗМЕРЕНИЯ ФОНА РАССЕЯННЫХ НЕЙТРОНОВ

Облучение образцов производилось на электростатическом ускорителе с максимальной энергией протонов 2,5 Мэв. Источником нейтронов являлась реакция $^{7}Li(p,n)^{7}Be$. Толщина мишени из LiF составляла 22 кэв. Активация производилась под углом 105° по отношению к направлению падения пучка протонов. Геометрия, использовавшаяся в процессе измерений, показана на рис. 1.

Измерение рассеяния нейтронов от конструкции мишени производилось при помощи идентичного торца мишени, заполненного водой и помещенного на торец рабочей мишени. Вклад рассеянных на торце мишени нейтронов, в таком случае, определяется разностью двух экспериментально измеряемых величин: активацией образца и счетом камеры деления на рабочей мишени и активацией образца и счетом камеры деления при рабочей мишени с добавкой (рис. 1а). Доля рассеянных нейтронов будет:

$$I_{P1}/I_0 = (I_A/I_0 - 1)e^{an\sigma}$$

где:

$$I_0 = I + I_{P1}; \quad I_A = I_0 + I_{P2}$$

I_0 – счет камеры деления и активация образца при рабочей мишени,

I – счет камеры и активация образца от "прямых" нейтронов мишени,

I_{P1} – счет камеры деления и активация образца от нейтронов, рассеянных на конструкции рабочей мишени,

I_A – счет камеры деления и активация образца при рабочей мишени с "добавкой",

I_{P2} – счет камеры деления и активация образца, обусловленные рассеянием на "добавке",

a – константа, зависящая от геометрии облучения,

$n\sigma$ – макроскопическое сечение поглощения нейтронов материалами конструкции мишени на пути рассеянного нейтрона от места рождения к точке облучения.

Фон нейтронов, рассеянных в мишенной камере, измерялся как отклонение от закона обратных квадратов (I/R^2) при размещении камеры деления и образца на различных расстояниях от мишени. Этот фон был не более 0,1% от измеряемого эффекта.

Во время облучения образца ^{238}U производился контроль флуктуаций нейтронного потока. Поправка обусловленная этим эффектом, не превышала 0,6% .

4. РЕЗУЛЬТАТЫ ИЗМЕРЕНИЙ И ИХ ОБСУЖДЕНИЕ

Результаты измерений приведены в таблице 1 и на рис. 2. Ошибка в выведенном сечении радиационного захвата нейтронов ^{238}U является среднеквадратичной ошибкой эксперимента и не учитывает ошибки в сечении деления ^{235}U и в опорном сечении ^{238}U .

В качестве опорного сечения радиационного захвата нейтронов ^{238}U использовалось сечение радиационного захвата при 24,4 кэв, равное 516 mδ, взятое из работы [4]. Сечение деления ^{235}U взято из работы [5].

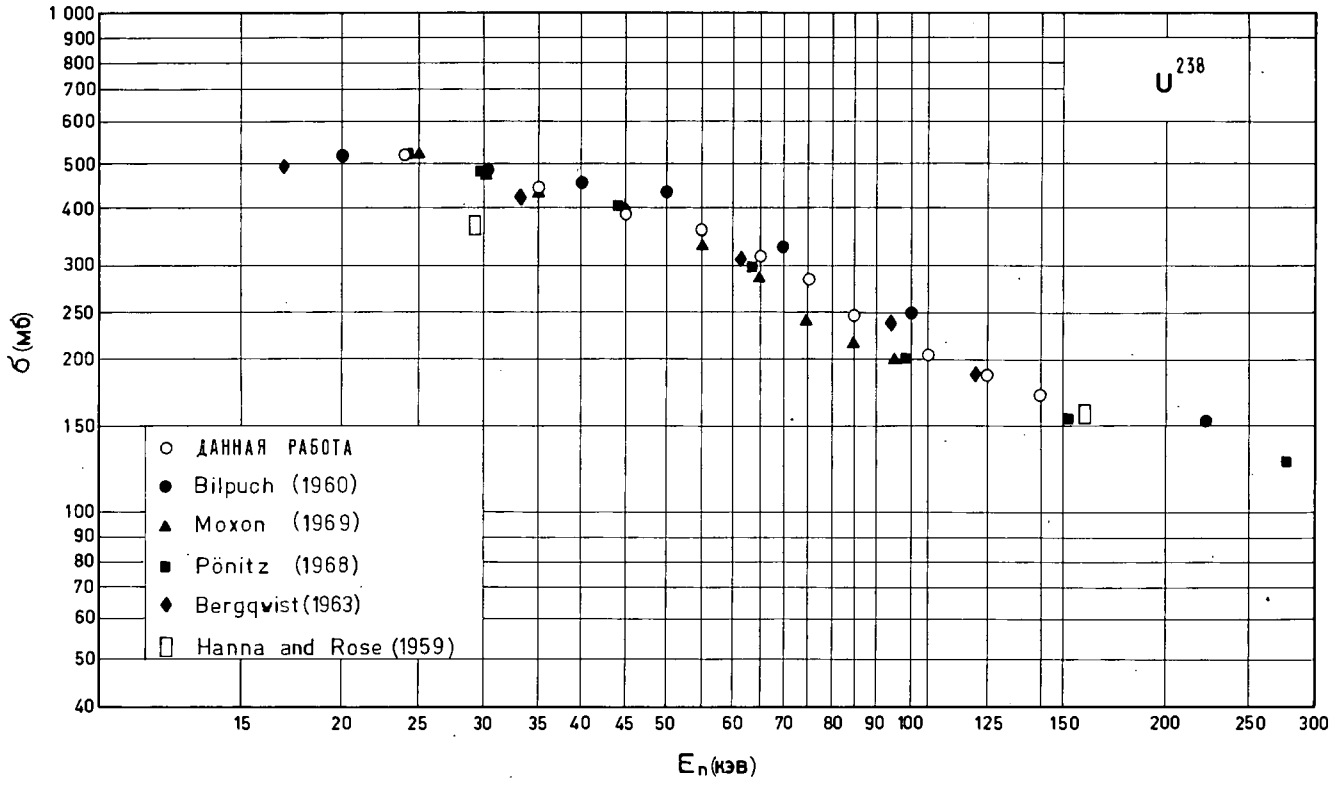

Рис. 2. Результаты измерений сечения радиационного захвата нейтронов ^{238}U [1-4, 6].

ТАБЛИЦА 1. ХОД СЕЧЕНИЯ РАДИАЦИОННОГО ЗАХВАТА НЕЙТРОНОВ ^{238}U В ДИАПАЗОНЕ ЭНЕРГИЙ 24 ÷ 145 кэв.

№ п/п	E_n [keV]	$\frac{N_8}{N_5}$	σ_5 [barns]	σ_8 [mb]
1	24 ± 8	1,66 ± 0,03	2,45	516 ± 10
2	35 ± 8	1,58 ± 0,04	2,19	439 ± 12
3	45 ± 8,5	1,51 ± 0,02	2,00	382 ± 5
4	55 ± 9	1,53 ± 0,03	1,90	366 ± 8
5	65 ± 10	1,34 ± 0,01	1,82	310 ± 4
6	75 ± 10,5	1,28 ± 0,01	1,76	284 ± 2
7	85 ± 11	1,15 ± 0,02	1,70	248 ± 4
8	105 ± 11,5	1,03 ± 0,01	1,62	211 ± 2
9	125 ± 12,5	0,95 ± 0,01	1,56	186 ± 2
10	145 ± 13,5	0,89 ± 0,01	1,51	170 ± 3

На том же рис. 2 приведены данные работ других авторов. Из рассмотрения рис. 2 видно, что ход сечения радиационного захвата нейтронов ^{238}U, измеренный в данной работе, лучше совпадает с ходом кривой сечения радиационного захвата, измеренным в работе [4]. При сравнении же с результатами работ других авторов имеются различия.

ЛИТЕРАТУРА

[1] BERGQVIST, I., Ark. Fis. 23 (1963) 425.
[2] BILPUCH, E.G., WESTON, L.W., NEWSON, H.W., Ann. Phys. 10 (1960) 455.
[3] MOXON, M.C., Report AERE-R 6074 (1969).
[4] MENLOVE, H.O., POENITZ, W.P., Nucl. Sci. Eng. 33 (1968) 24.
[5] HART, W., Fission Cross Section Data Files for ^{232}Th, ^{233}U, ^{234}U, ^{235}U, ^{236}U, ^{238}U, ^{237}Np, ^{339}Pu, ^{241}Pu and ^{242}Pu in the Energy Range 1 keV to 14 MeV (1967).
[6] HANNA, R.C., ROSE, B., Nucl. Energy 8 (1959) 197.

DISCUSSION

TO PAPERS IAEA-CN-26/78, 77

H. W. KÜSTERS: In normalizing your recent measurements to the 24-keV value of Poenitz you get excellent agreement with the Poenitz data up to 200 keV. This could mean that inconsistent results are due exclusively to differences in normalization. In Fig. 2 of paper CN-26/77 it will be seen that Moxon's data also agree with your data in the 25-keV range but are definitely lower above 50 keV, so that it seems to me there is also a difference in shape. Could you comment on this? I would also appreciate it if Dr. Moxon could say a few words on the subject.

A. I. ABRAMOV: As indicated in the paper, the relative errors in the measurement of the shape of the curve showing the dependence of $\sigma_\gamma(^{238}U)$ on neutron energy is of the order of 2%. However, the absolute errors were probably considerably higher. The results of this study and of the measurements of Poenitz and Moxon show the greatest discrepancy in the range of 75 keV, but even here the observed differences do not exceed ± 10%, which may be within the limits of the overall errors of these experiments.

M. C. MOXON: There is a difference in magnitude of only some 10% between my data on ^{238}U capture cross-sections and those of Menlove and Poenitz. There appears to be no disagreement in the shape in the energy region 10 to 100 keV.

W. P. POENITZ: I, too, think that Dr. Küsters may have misinterpreted the results presented here. As far as shape is concerned the results seem to confirm Moxon's values and our own; in absolute values, they agree with Moxon's results. It should be noted, however, that these results are in disagreement with the fission cross-section of ^{235}U as measured by White and with Davey's recent compilation relating to $\sigma_\gamma(^{238}U)$, which is based exclusively on White's fission cross-section.

W. G. DAVEY: The lead slowing-down spectrometer is, I believe, a poor-resolution device above a few tens of keV. Can this lead to differences in both the shape of the measured curve and the absolute values?

A. I. ABRAMOV: It is true that this is a low-resolution spectrometer, but sometimes this shortcoming turns into an advantage when we are dealing with average cross-section measurements used directly in reactor calculations. Moreover, this spectrometer can be used for making measurements over a very wide energy range and this affords an opportunity for making absolute normalizations of data both on thermal neutron cross-sections and on individual resonances.

W. G. DAVEY: The lower resolution may indeed have virtues but neither of the sets of results showed, for example, the dip in the ^{238}U-curve found by Moxon. In addition, the lower resolution makes it more difficult to carry out comparisons with other measurements.

THE keV FISSION CROSS-SECTION OF ^{235}U MEASURED WITH HIGH RESOLUTION †

C.D. BOWMAN, M.L. STELTS, R.J. BAGLAN
Lawrence Radiation Laboratory,
University of California,
Livermore, Calif.,
United States of America

Presented by W. Havens

Abstract

THE keV FISSION CROSS-SECTION OF ^{235}U MEASURED WITH HIGH RESOLUTION.

The fission cross-section of ^{235}U has been measured with a resolution of 1 ns/m from 1.5 to 500 keV. Structure in the cross-section was detected at neutron energies as high as 200 keV. It is shown that while the structure has had no appreciable effect on the accuracy of other keV-measurements carried out with nearly monoenergetic sources of neutrons, care will be necessary in future attempts to satisfy requests for cross-section accuracy of a few percent or less. The resolution of the experiment probably is sufficient to reveal much more structure than was actually observed. The structure which is observed, therefore, might be interpreted as intermediate structure in the average cross-section.

1. INTRODUCTION

The importance of the keV fission cross-section of ^{235}U to reactor design and its increasing use as a standard for measurements in the keV- and MeV-region have brought about high-priority requests for cross-sections with an accuracy of 1% throughout the keV- and MeV-range. Most attempts to satisfy such requests have been carried out at a relatively few points using monoenergetic neutron sources. The possibility of fine structure in the ^{235}U fission cross-section in the keV-region clearly could introduce point scatter into such experiments, and also influence the usefulness of ^{235}U as a standard. In fact, the concept of a double-humped fission barrier implies the existence of such structure at much higher energies than was expected previously.

An experiment was undertaken at the Livermore 30-MeV electron linac to measure the ^{235}U fission cross-section with both high resolution and good statistics. The measurements extended from 1.5 keV to 500 keV. The detector was of a unique design which allowed detection of fission with high efficiency via detection of triple or higher-order coincidence between neutrons and/or γ-rays. No attempt was made to compete with earlier experiments in terms of accuracy in absolute cross-section.

† Work performed under the auspices of the US Atomic Energy Commission.

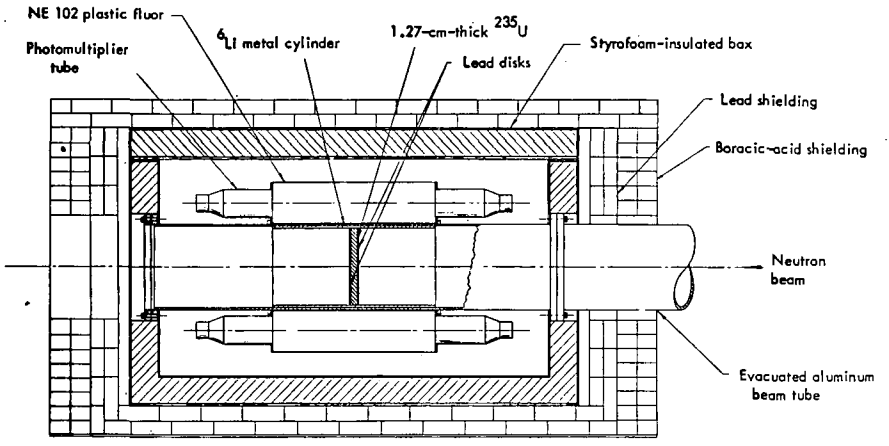

FIG. 1. Sectional view of the detection positron around the aluminium flight tube. The 1.27-cm-thick ^{235}U disk required when the device is used as a neutron detector has been replaced by a 0.125-cm-thick ^{235}U disk for this experiment.

2. MEASUREMENTS

The fission cross-section was measured by detecting either a triple coincidence between prompt γ-rays released in fission or by a triple coincidence between two γ-rays and one neutron. The detector used in the experiment is shown in Fig. 1. It consists of an annular cylinder of plastic scintillator surrounding a 25-cm-diameter ^{235}U plate. The cylinder is 60 cm long, 60 cm in outside diameter and divided into four quarters. The detector was originally developed for use as a neutron detector in the keV-region for threshold photo-neutron measurements and has been used extensively for this work [1]. In that application a 1.25-cm-thick plate of ^{235}U is used. Neutrons are detected via a triple coincidence between prompt gamma rays from neutron-induced fission events. As a neutron detector it has the advantage of a useful efficiency from 1 keV into the MeV region thus filling the gap in neutron energy between neutron-induced charged particle reactions at low energies and proton-recoil detectors at high energies. The detector is relatively fast (10 ns), insensitive to gamma flash and possesses a large sensitive area. The detector is described in more detail elsewhere [2].

A wide variety of fission detection modes are possible since a four-fold coincidence is possible and both neutrons and γ-rays can be detected. Under proper circumstances fission neutrons can be recognized in the detector owing to the differences in time-of-flight between neutrons and γ-rays. Simply as a result of the size of the detector prompt neutrons interact in the scintillator on the average about 20 ns later than prompt γ-rays. Also the amplitude of the pulses can be used as a parameter in the coincidence. In this experiment fission was detected either via a triple and higher-order coincidence between γ-ray pulses regardless of size, or by a double coincidence between two "large" γ-ray pulses followed by a "small" neutron pulse. Arrangements which have been used in other experiments include (1) three small prompt and one small delayed pulse,

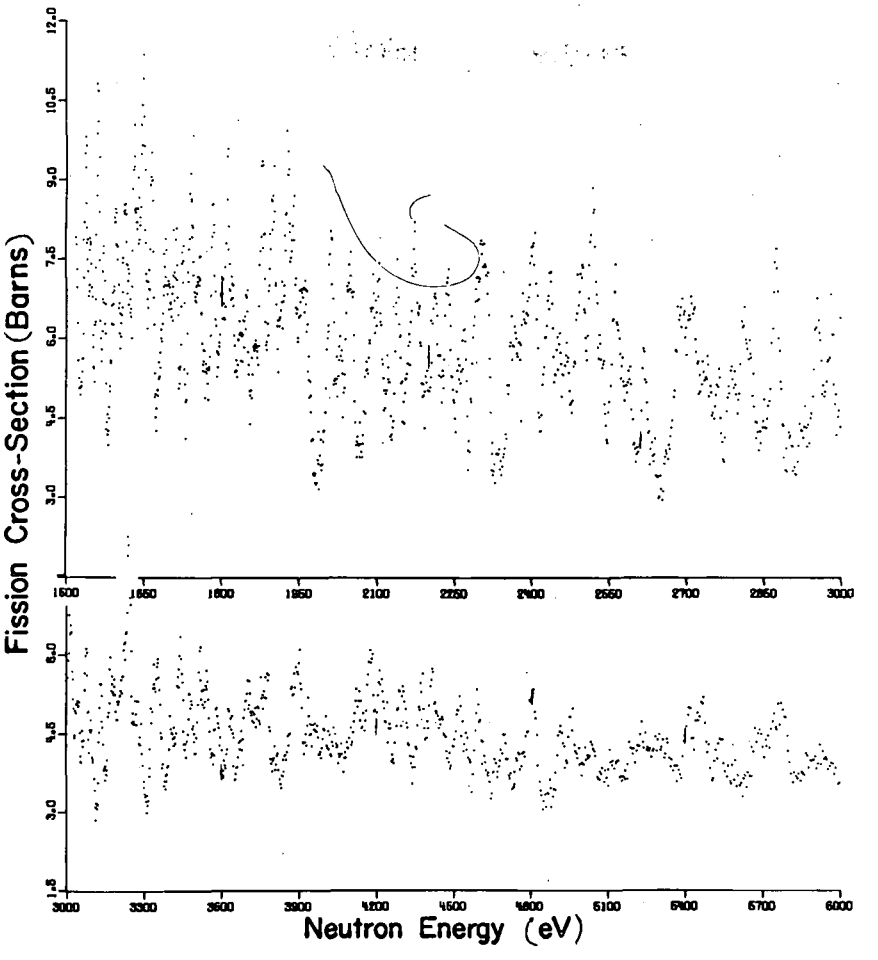

FIG. 2. Fission cross-section of ^{235}U. The flags on the points of the figure show the counting statistics. These data are useful only to the extent that they show fine structure. No new information on the absolute cross-section can be obtained from the data (see text).

(2) a prompt two-fold coincidence between large pulses, (3) a prompt three-fold coincidence between large pulses, (4) prompt four-fold coincidence between pulses large or small, and (5) one large prompt and two small delayed pulses.

The measurements reported here were carried out with a 0.125 cm thick by 25-cm-diameter ^{235}U plate which weighed 1300 g and which was located 17 m from the neutron source. The neutrons were produced by stopping the electron beam from the Livermore 30-MeV electron linac in a platinium target located outside of the neutron line-of-sight. Neutrons were scattered into the beam by a 0.6 cm thick layer of polyethylene located in the neutron line-of-sight. The primary contributors to the resolution were the channel width of 15 ns, the detector timing uncertainty of 10 ns, and the beam burst width of 8 ns, these conditions allowed a resolution of 1 ns.

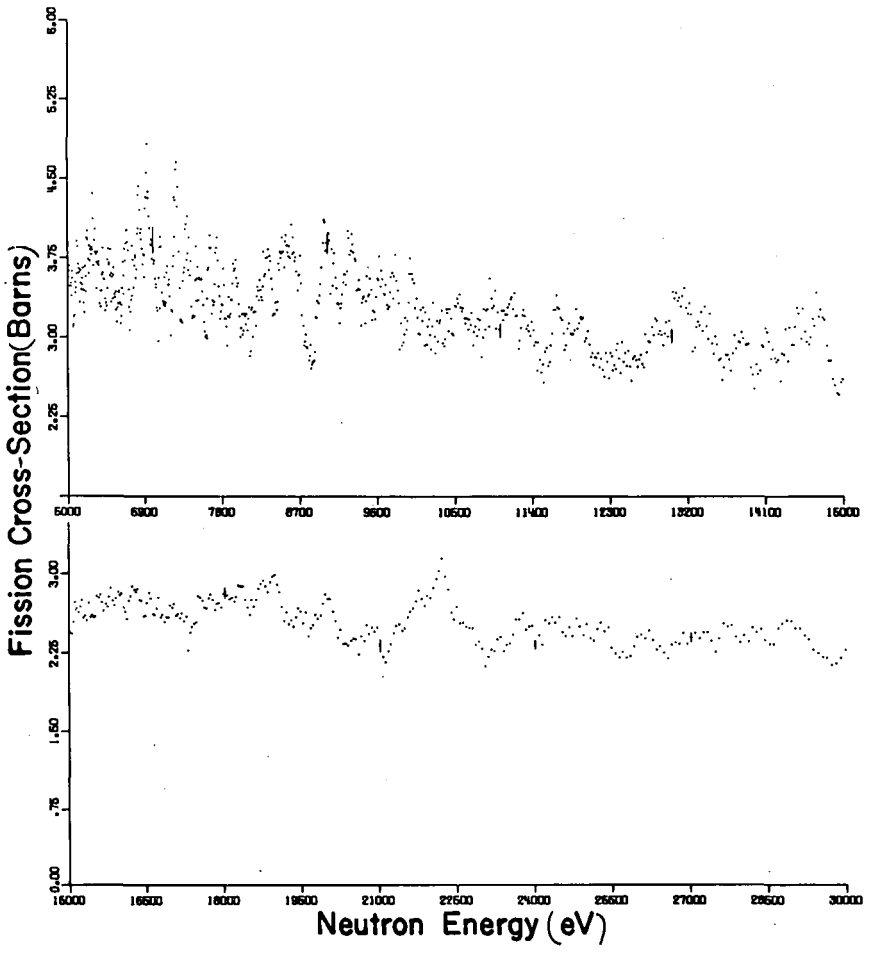

FIG. 3. Fission cross-section of ^{235}U. The flags on the points of the figure show the counting statistics. These data are useful only to the extent that they show fine structure. No new information on the absolute cross-section can be obtained from the data (see text).

The results of the measurements are shown in Figs 2-4. The data displayed here represent results from two measurements separated by about one year. The data from 1.5 to 15 keV were measured using the three-prompt-coincidence mode. The efficiency for this mode was measured by placing a fission ionization chamber inside the detector and recording coincidences between fission fragments and triple coincidences. The measured efficiency for this mode is about 20%. Neutron capture events in ^{235}U also can be detected. However, in the same measurements, it was shown that the efficiency for detection of a capture event is smaller by a factor of five than that for fission. Since the ratio of capture-to-fission cross-section is about 0.35, the neutron detection efficiency in the 1.5 to 15 keV range from neutron capture is only 7% of the efficiency from neutron-induced fission.

The data from 15 keV to 500 keV were taken via a triple coincidence between two prompt γ-rays and one neutron. This technique promised to offer somewhat better time resolution than the previously described mode. In addition, no capture events are detected. Also the efficiency is about the same as in the previously described coincidence. The standard deviation in counting statistics is shown in the figures by the small vertical lines centred on selected data points. Although greater statistical accuracy perhaps would have been helpful, it does not appear that structure has been obscured by inadequate statistics.

Since the experiment was directed primarily at a search for fine structure, no neutron flux measurements, which would have allowed an absolute cross-section determination, were made. Instead the data were normalized to Davey's [3] evaluated data set, in effect, by calculating the neutron flux required to give agreement with his evaluated curve. This procedure was carried out by averaging the measured spectrum over rather broad energy intervals before comparing with Davey's curve. Of course, care was taken so as not to introduce errors at the boundaries of the intervals chosen for the normalization procedure.

The usefulness of the ^{235}U fission cross-section as a standard depends, among other things, on the energy dependence of the cross-section. Of principal concern is the amplitude of fine structure and its influence on cross-sections obtained using it as a standard. There is probably some energy below which the cross-section is fluctuating too violently to be of any use as a standard. The determination of such an energy must be based on measurements of sufficient resolution and statistical uncertainty so as to show all the structure present in the fission cross-section. The resolution of the measurements reported here equals the Doppler spread only at the lowest energy of these measurements, so that they represent only a step in the direction suggested.

When the fully resolved cross-section is used as a standard for some other cross-section measurement, the influence of fluctuations in the ^{235}U fission cross-section can, in principle, be taken into account if the experimenter knows the resolution function of the apparatus used for his experiment. The degree of detail in the knowledge of the resolution function depends on the energy region in which the ^{235}U fission is used as a standard. Obviously, little such information is required if the resolution function width is much greater than the spacing of ^{235}U fine structure, particularly if the amplitude of the oscillations is small.

In fact, these are implicit assumptions already made in ratio measurements and even in absolute ^{235}U fission cross-section measurements carried out with charged-particle accelerators. Poenitz's [4] keV- and MeV-measurements are normalized to the fission cross-section at 30 keV measured by Knoll and Poenitz [5]. The Poenitz cross-section lies 15% below that of White's [6] absolute measurements at 300 keV, but the two measurements are much closer together in the lower keV range. The differences might be caused by the influence of fluctuations on Pœnitz's normalization at 30 keV or by uncertainties in the other points in both White's and Pœnitz's measurements below 100 keV where Figs 2 and 3 indicate fluctuations of 10-20%.

A comparison of the resolution used in those measurements with the fine structure observed in the present experiment, however, shows that significant errors were not introduced by the ^{235}U fine structure. The absolute measurement of Knoll and Pœnitz was carried out with a resolution

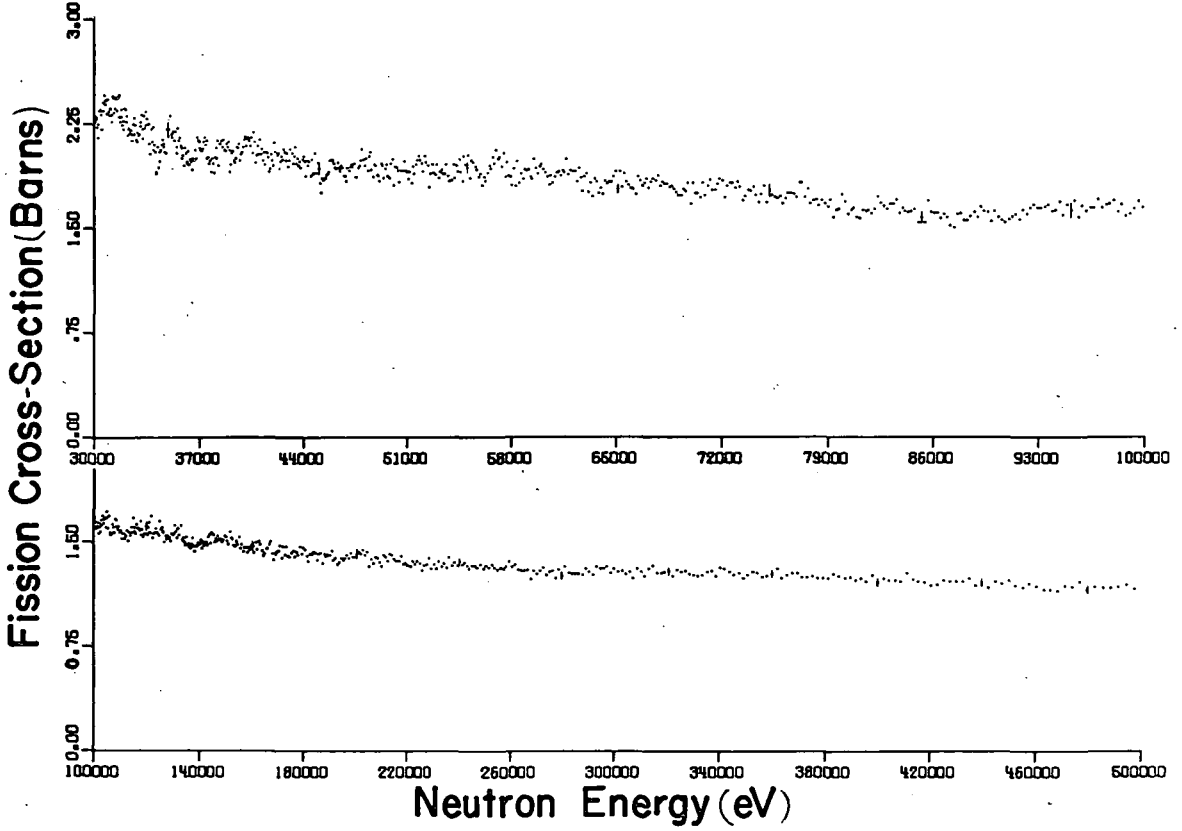

FIG. 4. Fission cross-section of ^{235}U. The flags on the points of the figure show the counting statistics. These data are useful only to the extent that they show fine structure. No new information on the absolute cross-section can be obtained from the data (see text).

of 30% so that the resolution function extended from 25 to 35 keV. A cursory consideration of Figs 3 and 4 indicate that errors of only a few percent could be introduced by insufficient averaging of the fine structure, an order of magnitude smaller than the 15% discrepancy at 300 keV. Similar considerations which are summarized later, of Poenitz's points at 55 and 75 keV and White's data at 40 and 70 keV indicate errors of only a few per cent from this source so that the difference at 300 keV must be associated with some other effect.

Another absolute experiment supporting Pœnitz's and White's data in the lower keV region has been carried out by Perkin et al. [7] using an Sb-Be photoneutron source for measurements at 24 keV. The precise energy of the neutrons is significant since in Fig. 3 it is clear that a 30% peak to valley fluctuation occurs in a region centered at 22 keV. Perkin et al. quote the neutron energy as 24.8 keV. A more recent evaluation [8] has given 23.3 keV. The energy distribution is flat ranging from 22.1 to 24.6 as a result of reaction kinematics; a small tail towards the low energies is present owing to scattering of the neutrons in the source. The average of the data in Fig. 3 from 22.1 to 24.6 is only 1% higher than the average from 15 keV to 32.5 keV so that the Perkin point apparently represents the average of the fission cross-section. Of course, this conclusion must be qualified somewhat by the uncertainty in the Sb-Be neutron energy.

These considerations are summarized in Table I. The neutron energy is given in the second column and the range in energy obtained from the quoted resolution is given in the third column. The fourth column shows an interval over which the present cross-section was averaged which is, at best, twice as wide as the resolution. The fifth column is the ratio of the average of the LRL data taken over the interval of the third column divided by the average of the LRL data over the interval of the fourth column. In the worst case only a 3% effect is introduced by fluctuations.

Therefore, it appears that no appreciable uncertainty was introduced into any of the standard measurements discussed above since the resolution was sufficiently broad compared to the fine structure. While the fine structure has not been a bothersome problem to past experiments, it clearly will be of concern to future absolute measurements undertaken to satisfy requests for fission cross-sections to an accuracy of 1%. The normalization procedures used in the past will need to be reviewed with the intention of eliminating any effect of the appreciable fine structure in ^{235}U.

3. FINE STRUCTURE AND THE DOUBLE-HUMPED FISSION BARRIER

The double-humped barrier for fission has been invoked to explain strong fluctuations in nuclei exhibiting sub-threshold neutron fission. To a lesser extent structure should also be present in the thermally fissile targets so long as the available fission channels are not completely open. However, it is not easy to show that fine structure observed is anything other than statistical effects in the matrix elements governing the reaction.

One step in this direction is a comparison of the standard deviation in the fission cross-section measured in the keV-region with that predicted from eV-measurements where multi-level fits are possible. Such a comparison requires the selection of a proper averaging interval for the keV-data.

TABLE I. COMPARISON OF SEVERAL EXPERIMENTS

Investigator	Energy (keV)	Range in ΔE (keV)	LRL Averaging Interval	Ratio
Knoll and Poenitz [a]	30 ± 2	25.5 - 34.5	20 - 40	1.02
Poenitz [b]	55 ± 3	50 - 60	45 - 65	1.01
Poenitz [b]	76 ± 3	68 - 83.5	60 - 90	1.00
Perkin [c]	23.3	22.1 - 24.6	15 - 32	1.01
White [d]	40	38 - 42	35 - 45	1.03
White [d]	67	64.5 - 69.5	60 - 75	0.986

[a] Ref. [5]

[b] Ref. [4]

[c] Ref. [7]

[d] Ref. [6]

TABLE II. COMPARISON OF OBSERVED STRUCTURE AT DIFFERENT ENERGIES

E_n (keV)	Observed spacing (keV)	Resolution [a] (keV)	Doppler effect (keV)	$\frac{\Delta\bar{\sigma}}{\bar{\sigma}}$ (Observed)	$\frac{\Delta\bar{\sigma}}{\bar{\sigma}}$ (Adler)	$\frac{\Delta\bar{\sigma}}{\bar{\sigma}}$ (R-Matrix)
2	0.0375	0.03	0.001	0.14	0.22	0.21
4.5	0.075	0.06	0.0014	0.14	0.16	0.148
9.5	0.300	0.12	0.002	0.13	0.079	0.074
18	0.300	0.22	0.003	0.10	0.079	0.074
36	1.400	0.40	0.004	0.09	0.036	0.034
120	7.000	1.3	0.007	0.07	0.015	0.015
300	-	3.0	0.012	-	-	-

[a] These figures represent upper limits to the FWHM of the resolution function (see text). The resolution in keV corresponding to 1 ns/m is in most cases considerably less than the above figures.

Ordinarily, this would be the resolution of the experiment or the Doppler width, whichever is larger. Table II shows a comparison of observed structure at different energies with the resolution and Doppler effect. The observed spacing shown in the second column was obtained by counting the structures in an energy interval around the energy listed in column one and then dividing the number of structures into the width (in keV) of the energy interval.

The standard deviation (S.D.) of the measured data divided by the average cross-section is given in column 5 of Table II. It was obtained by determining the error limits (2 S.D.) which enclose 70% of the points of the graph. This standard deviation also was calculated in two ways from low energy resolved resonance data.

The first method used the Adler-Adler [9] formalism for fitting resonance data. According to their prescription the fission cross-section can be written as

$$\sigma_f(E)\sqrt{E} = \sum_k \frac{G_k \nu_k + H_k(\mu_k - E)}{(\mu_k - E)^2 + \nu_k^2} \qquad (1)$$

The first term in the sum represents a sum of symmetric terms and the second a sum of asymmetric terms. The average cross-section, therefore, can be written:

$$\overline{\sigma_f(E)\sqrt{E}} = \frac{1}{\Delta E}\sum_k \left[G_k \nu_k \int_{\Delta E} \frac{dE}{(\mu_k - E)^2 + \nu_k^2} + H_k \int_{\Delta E} \frac{(\mu_k - E)\,dE}{(\mu_k - E)^2 + \nu_k^2} \right] \qquad (2)$$

Since $\Delta E \gg \overline{\nu}_k$, the second integral is zero, and the resulting cross-section is simply $\sigma_f\sqrt{E} = \pi \langle G \rangle / \langle D \rangle$. The standard deviation in the average cross-section is then simply the standard deviation in the ratio $\langle G \rangle / \langle D \rangle$ which is determined by the number of resonances in the averaging interval.

The average value of G_k was obtained from parameters resulting from the fit of de Saussure et al. [10] of Eq. (1) to the fission cross-section between 1 and 30 eV. This value was found to be 37 barn-eV$^{3/2}$; the standard deviation in $\langle G \rangle$ from the same fit is 55.5 barn-eV$^{3/2}$. One can then make use of the central limit theorem [11] to obtain the standard deviation S.D. for $\langle G \rangle$ averaged over n resonances. This becomes S.D. $= 55.5/\sqrt{n}$ so that $\langle G \rangle = 37\,(1 \pm 1.5/\sqrt{n})$. Assuming a Wigner distribution for spacing $\langle D \rangle$ is found to be 0.697 $(1 \pm 1/\sqrt{2n})$ eV. The resulting value for S.D./$\overline{\sigma} = 1.65/\sqrt{n}$ is shown in column six of Table II.

The standard deviation also can be predicted from the multi-level fits based on the R-Matrix formalism. In this formalism, the average cross-section can be written

$$\overline{\sigma}_f = 2\pi^2 \lambda^2 g \langle \Gamma_n^0 / D \rangle \langle \Gamma_f / \Gamma \rangle$$

where the various parameters have their usual notation. In the case of ^{235}U, $\langle \Gamma_f / \Gamma \rangle$ varies slowly compared to $\langle \Gamma_n / D \rangle$ since Γ_f is usually larger than any of the other partial widths. The standard deviation in $\overline{\sigma}_f$ is given, therefore, by the standard deviation in $\langle \Gamma_n / D \rangle$. It can be shown from a Porter-Thomas distribution for Γ_n and a Wigner distribution for spacing that S.D./$\overline{\sigma} \equiv \delta\overline{\sigma}/\overline{\sigma} = 1.58/\sqrt{n}$. Therefore, both procedures give essentially the same fluctuation. The fine structure level density, ρ_s, required for calculating n is taken from de Saussure [10] et al. in the former case and from Cramer's R-Matrix analysis [12] in the 17 to 70 eV range in the latter case. The fluctuation in the cross-section depends on the value of n which is calculated from the relationship $n = \rho_s D_{obs}$ where D_{obs} is the observed spacing given in column 2 of Table II. The results are given in column 6 and 7 of Table II.

Satisfactory agreement is obtained between the predicted and measured fluctuations when n is calculated from the observed level spacing in the keV-region. However, the predicted fluctuation should be calculated not from the observed spacing of fluctuations but from the width of the resolution function for the experiment. The resolution given in column 3 of Table II does not correspond to 1 ns/m. These values were measured in several threshold photo-neutron experiments [1] from observed widths of very narrow isolated resonances. They represent an upper limit to the resolution since the detector for those experiments contained the 1.25-cm-thick ^{235}U plate rather than the 0.125 cm thickness used for these experiments. The largest contribution to the resolution with the thicker plate arises from multiple scattering in the ^{235}U. This effect is essentially absent with the much thinner plate. Therefore, the expected resolution of 1 ns/m is actually considerably smaller than the numbers in column three of the table. In fact, at the lower energies the expected resolution is smaller by almost an order of magnitude than the observed spacing. If the resolution is actually that small, the structure observed is clearly intermediate structure of some sort. Unfortunately, more definite statements regarding the presence of intermediate structure cannot be made owing to the uncertainty about the actual resolution in the experiment.

For measurements now planned with the new Livermore 100-MeV electron linac at a flight path of 255 m, the resolution will be improved by a factor of 15 with no loss in counting rate. However, some compromise might be made in resolution to significantly improve the statistics. The detection of little additional structure with much higher resolution would provide strong evidence that the fluctuation in the average cross-section is not statistical but represents intermediate structure.

REFERENCES

[1] Papers reporting data using the device as a neutron detector include:
BOWMAN, C.D., BAGLAN, R.J., BERMAN, B.L., Phys. Rev. Lett. 23 (1969) 796.
BERMAN, B.L., VAN HEMERT, R.L., BOWMAN, C.D., Phys. Rev. Lett. 23 (1969) 386.
BERMAN, B.L., BAGLAN, R.J., BOWMAN, C.D., Phys. Rev. Lett. 24 (1970) 319.
BAGLAN, R.J., BOWMAN, C.D., PHILLIPS, T.W., STELTS, M.L., BERMAN, B.L. Accepted by Phys. Rev. Lett. (1970).

[2] VAN HEMERT, R.L., BOWMAN, C.D., BAGLAN, R.J. BERMAN, B.L., "A New Detector for keV Neutrons" submitted to Nucl. Instrum. Meth;
VAN HEMERT, R.L., Ph.D. thesis, "Threshold Photoneutrons for Light Nuclei," UCRL-50501, Lawrence Radiation Laboratory, Livermore, Calif. (1968).

[3] DAVEY, W.G., Nucl. Sci. Engng 26 (1966) 149.

[4] POENITZ, W.P., in Nuclear Cross-Sections and Technology (Proc. Conf. Washington, 1968) NBS-299, 503.

[5] KNOLL, G.F., POENITZ, W.P., J. nucl. Energy A/B 21 (1967) 643.

[6] WHITE, P.H., J. nucl. Energy A/B 19 (1965) 325.

[7] PERKIN, J.L. et al., J. nucl. Energy A/B 19 (1965) 423.

[8] BERMAN, B.L., VAN HEMERT, R.L., BOWMAN, C.D., Phys. Rev. 163 (1967) 958.

[9] ADLER, D.B., ADLER, F.T., in Breeding Economics and Safety in Large Fast Power Reactors (Proc. Conf. 1963), ANL-6792, 695.

[10] De SAUSSURE, G., GWIN, R., WESTON, L.W., INGLE, R.W., FULLWOOD, R.R., HOCKENBURY, R.W., ORNL-TM-1804 (1967).

[11] A brief discussion of the theorem can be found in:
MOOD, A.F., Introduction to the Theory of Statistics,
McGraw-Hill Book Co. Inc., New York, N.Y. (1950) 136.

[12] CRAMER, J.D., Nucl.Phys. A126 (1969) 471.

DISCUSSION

M.G. SOWERBY: The distribution of neutron energies in measurements at the $^{7}Li(p,n)$ threshold is not uniform over the quoted energy range. Therefore, the conclusion in Table I may well be incorrect and the 30-keV measurements may not be as representative of the cross-section from 20-40 keV as suggested in the paper.

The mean energy of the neutrons produced by an Sb-Be source is not known to be better than 1 keV. It is shown in paper CN-26/34 that the mean fission cross-section over the source energy spectrum varies by 8% when the mean energy changes from 22.5 to 24 keV. This means that ^{235}U-measurements made with Sb-Be-sources are of limited value at the present time.

W. HAVENS: I agree. The microscopic ^{235}U-fission cross-section as a function of energy must be integrated over the energy interval weighted by the energy distribution of the neutron source to determine the effects of the fluctuations on the fission cross-section measurements using Van-de-Graaff accelerators.

A MEASUREMENT OF THE FISSION CROSS-SECTION OF ^{241}Pu RELATIVE TO ^{235}U*

F. KÄPPELER, E. PFLETSCHINGER**
Institut für Angewandte Kernphysik,
Kernforschungszentrum Karlsruhe,
Federal Republic of Germany

Abstract

A MEASUREMENT OF THE FISSION CROSS-SECTION OF ^{241}Pu RELATIVE TO ^{235}U.

The fission cross-section ratio ^{241}Pu : ^{235}U has been measured as a function of neutron energy between 5 keV and 1 MeV by means of a pulsed 3-MeV Van-de-Graaff accelerator. The neutron energy was determined by time-of-flight technique. Fission events were detected in two identical argon-filled gas scintillation chambers in 4π - geometry. The accuracy of the cross-section ratios is estimated to be between 2.5 and 4%.

1. INTRODUCTION

The importance of accurate data for the design of fast reactors motivated this measurement of the fission cross section ratio ^{241}Pu : ^{235}U. In the neutron energy region between 10 keV and 1 MeV only a few measurements exist until now and therefore it seemed worthwhile to establish a new data set with improved accuracy.

The present work was performed with the experimental technique described in a previous paper on measurements of the fission cross sections of ^{239}Pu and ^{233}U relative to ^{235}U [1] . Therefore, only a general survey of the technique is given together with the modifications required by the high activity of ^{241}Pu.

2. EXPERIMENTAL METHOD

Two identical gas scintillation chambers containing the samples of ^{241}Pu and ^{235}U were exposed to the neutron flux in symmetric positions. Continually flowing Argon was used as scintillator gas. The chambers were divided by the opaque samples in two optically decoupled halves. From every fission event both fragments could be detected because the backings of the samples were so thin that the fragments could penetrate them. A coincidence requirement between the halves of each chamber provided good discrimination against α-background. In the case of low α-activity as for ^{241}Pu and ^{235}U it is possible to set the thresholds as low as the pulse height caused by alpha-particles. The coincidence width was 40 nsec.

---

* Work performed within the association in the field of fast reactors between the European Atomic Energy Community and Gesellschaft für Kernforschung mbH, Karlsruhe.

** Present address: Italglas, Piazza Rosetti 4-18, Genova, Italy.

The neutrons were produced via the $^{7}Li(p,n)^{7}Be$ reaction with the Karlsruhe 3-MV pulsed Van de Graaff accelerator. The pulse width of the accelerator was 1 nsec and the repetition frequency 10^{6} Hz. The time-of-flight technique served to discriminate against background and to determine the neutron energy. The scintillation chambers had a time resolution of 3.3 nsec, and with a flight path of 37.7 cm the time resolution of 9 nsec/m was accurate enough for the energy determination below 300 keV. At higher energies a ^{6}Li-glass detector at 1.82 m distance from the target and with 1.4 nsec/m time resolution was used. The thickness of the metallic ^{7}Li-targets varied between 20 keV and 90 keV for points between 140 keV and 1.2 MeV. ^{7}Li-targets of more than 130 keV thickness were used from 280 keV down to 10 keV. Thus a broad overlap exists between data obtained with thin and thick ^{7}Li-targets which confirms that there is no systematic difference in the results of the two types of measurements.

The zero point of the time-of-flight spectra was calculated from the position of the γ peak produced by the γ-flash of the accelerator. A second neutron group corresponding to population of ^{7}Be at 470 keV could be distinguished from the main group in the time-of-flight spectra but did not distort the results.

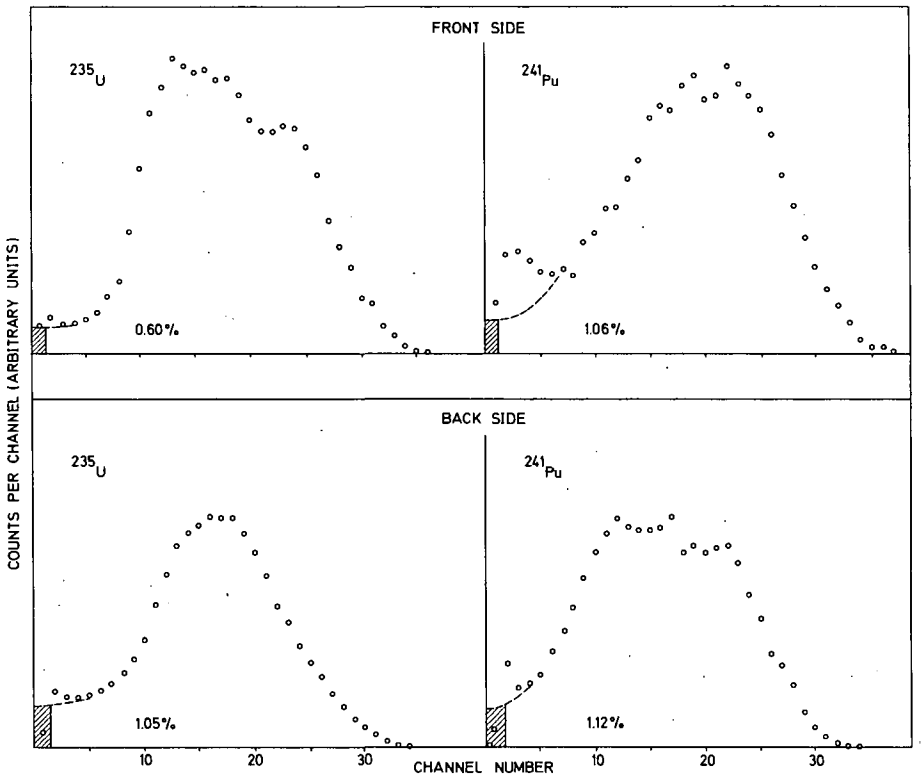

FIG.1. Pulse-height distributions. The dashed area corresponds to the extrapolated fraction.

The electronics were the same as described in Ref. [1] . The only change was the elimination of the pulse height discrimination trigger parallel to the time determination trigger, because the coincidence between both halves of a chamber was sufficient for discrimination against α-background.

The activity of the ^{241}Pu sample was about 70 mC. With respect to the very thin backing we could not risk a damage of the sample by interchanging it between the scintillation chambers by means of the removable transport chamber. Therefore it was not possible to eliminate remaining asymmetries in the neutron flux and the electronic thresholds by a measurement with interchanged samples. A very careful adjustment relative to the ^{7}Li-target and the direction of the incoming proton beam defined by a system of slits and diaphragms was made to arrange the chambers in symmetric positions. The symmetry could be checked with good accuracy by comparing the time-of-flight spectra of both chambers at the relatively low neutron energy of 80 keV. No differences between the flight times to the two chambers (about 100 ns) could be observed. If there was any difference, it was less than 0.4 nsec, corresponding to an uncertainty in the neutron flux of 0.8 % . Moreover, in a test run before the 241-Pu measurement, the ratio ^{235}U : ^{235}U was determined to be 1.0 within the statistical error of 1.5 %, including all other uncertainties, e.g. those from mass determination and electronic thresholds.

Asymmetries in the electronic thresholds were determined as indicated in Fig. 1. With the moderated neutrons of a ^{241}Am-Be-source pulse height spectra were obtained from both sides of each sample. An extrapolation to zero pulse height gives the undetected fraction of fission events. Because of the low thresholds the resulting correction is comparably small. The deviations of the pulse height spectra from one another and from the real energy distribution of fission fragments is due to the characteristics of the photomultipliers and to the chamber geometry. For the accuracy of the results these effects do not have any importance.

3. SAMPLES

The samples were prepared at the CBNM/EURATOM laboratory in Geel, Belgium. On a 90 $\mu g/cm^2$ thick Vyns[1] backing metallized with 30 $\mu g/cm^2$ Al a uranium or plutonium acetate layer is deposited by electrospraying as described by Verdingh and Lauer [2] . The mass determination will be carried out in Geel, too. Unfortunately it was not possible to finish the final mass determination to this date. Until now only mass values can be given which are calculated from the α-activities of the samples [3] . So far all fission cross section ratios presented in this paper are preliminary. The quantitative measurements were carried out with the samples marked by asterisks.

---

[1] Vyns consists of 85 % PVC and 15 % Polyvinyl acetate. It was delivered by Union Carbide Europe, Brussels.

4. CORRECTIONS AND UNCERTAINTIES

The corrections and uncertainties which result from this experiment are described in detail in Ref. [1] . Therefore only the characteristic values for this measurement are given here.

4.1 Background

The time-independent background was found to be about 2 % for ^{241}Pu and 0.6 % for ^{235}U. The resulting uncertainty is included in the statistical error and always smaller than 0.9 % except at energies below 20 keV. The time-correlated background, measured by withdrawing the fissile samples from the detectors into the transport chambers, was observed in the ^{235}U detector only. It does not exceed 2 %, introducing an uncertainty of about 0.4 %.

4.2 Finite Foil and Backing Thickness

The energy loss in the fissile layer and the backing increases with increasing angle between the direction of the fission fragments and the incident neutron beam. Therefore not all fission events could be detected. Following the calculation of Rossi and Staub [4] the fraction of fragments which cannot escape from the samples was determined. The values necessary for this calculation are the thickness of the various layers of the sample (uranium acetate, aluminum and vyns) and the range and energy loss of fission fragments in these materials [5,6,7,8,9,10,11] . The result was averaged between light and heavy fragments and shows that 5.1 % of the ^{241}Pu and 6.2 % of the ^{235}U fission fragments were absorbed in the samples. The main error sources of this correction are thickness uncertainties of the aluminum (20 %) and vyns layer (20 %). The vyns backings were made by a standard method but not at the same time. Therefore these uncertainties are taken into account. During the final mass analysis a more accurate determination of the backing thickness is tried by measuring the energy loss of the α-particles passing through the backing. Uncertainties in the fragment ranges cancel when the ratio is formed because they influence the calculation in the same way for both samples. The preliminary absorption correction is 0.989 ± 1.5 %.

The electronic threshold correction was determined by extrapolating the pulse height distributions from both sides of the samples to zero pulse height (see Fig. 1). It was found to be 1.005 ± 0.2 %.

4.3 Electronic Corrections

The electronics were checked with a pulse generator several times during the experiment to confirm that no pulses were lost or uncorrectly routed. The measurement at 535 keV was repeated at constant intervals to ensure that there was no systematic drift in the electronics. A dead time correction was necessary neither for ^{241}Pu nor for ^{235}U.

4.4 Sample Mass and Isotopic Composition

Due to the complex calculation from the α-activities via the isotopic composition and the α-halflives to the sample masses the uncertainties are about 10 % for the ^{241}Pu and 2 % for the ^{235}U sample mass. The final determination which is being prepared now will give the masses with an accuracy of about 1 %. The preliminary mass values and the isotopic composition of the samples are listed in Table I.

TABLE I. MASS AND ISOTOPIC COMPOSITION OF SAMPLE

Mass (mg) (preliminary)	
2.345 ± 2 %	0.522 ± 10 %
*2.099 ± 2 %	*0.562 ± 10 %
*2.027 ± 2 %	0.559 ± 10 %
	0.612 ± 10 %

Isotopic Composition (at. %)			
^{234}U	0.169	^{239}Pu	1.83
^{235}U	99.45 ± 0.05	^{240}Pu	5.83
^{236}U	0.027	^{241}Pu	91.18 ± 1.0
^{238}U	0.353	^{242}Pu	1.14
		$\frac{^{241}Am}{Pu\ tot}$	6.94 ± 1.4 %

TABLE II. CONSTANT UNCERTAINTIES

Source of Uncertainty	$\sigma_f{}^{241}Pu / \sigma_f{}^{235}U$	
Correction for (n,γ)-background	^{235}U	0.4 %
	^{241}Pu	-
Absorption losses in the samples	^{235}U	1.2 %
	^{241}Pu	1.0 %
Electronic threshold correction	^{235}U	0.1 %
	^{241}Pu	0.2 %
Sample Mass	^{235}U	2.0 %
	^{241}Pu	10.0 %
Asymmetry in Neutron Flux		0.8 %

TABLE III. FISSION CROSS SECTION RATIO $\frac{\sigma_f{}^{241}Pu}{\sigma_f{}^{235}U}$

En (keV)	$\frac{\sigma_f{}^{241}Pu}{\sigma_f{}^{235}U}$	Statistical Uncertainty (%)	En (keV)	$\frac{\sigma_f{}^{241}Pu}{\sigma_f{}^{235}U}$	Statistical Uncertainty (%)
13.7	1.143	3.0	192 ± 16	1.263	1.8
15.7	1.167	2.7	230 ± 19	1.243	1.4
17.6	1.204	2.5			
19.5	1.100	2.4	273 ± 20	1.264	1.5
21.5	1.192	2.3	324 ± 29	1.262	1.9
23.9	1.116	1.8	388 ± 18	1.154	1.7
			436 ± 22	1.151	1.6
26.8	1.227	1.7	486 ± 25	1.206	1.4
29.7	1.149	1.6			
32.5	1.135	1.7	535 ± 32	1.195	0.9
35.4	1.133	1.6	584 ± 23	1.169	1.1
38.9	1.168	1.5	633 ± 29	1.216	1.5
42.7	1.178	1.4	678 ± 33	1.186	1.3
46.7	1.169	1.3	740 ± 31	1.241	1.8
51.7	1.133	1.3	790 ± 38	1.220	1.9
56.9	1.130	1.3	870 ± 32	1.223	1.7
63.2	1.119	1.2	945 ± 40	1.141	1.7
69.8	1.192	1.3			
77.4	1.200	1.3	1035 ± 40	1.174	2.1
84.6	1.193	1.4	1133 ± 49	1.178	2.1
93.6	1.198	1.2			
103.8	1.222	1.2			
125.2	1.255	1.4			
137.3	1.236	1.5			
151.1	1.222	1.6			
166.9	1.243	1.7			

The errors of the isotopic corrections are included in the statistical uncertainty.

For ^{241}Pu a correction of the fission count rate has to be made because of fission events from the other Pu isotopes and from ^{241}Am. For ^{241}Am the fission cross sections were taken from Seeger et al. [12] and from Bowman et al. [13] , for the Pu isotopes the evaluated data of Davey [14] were used. The correction for the Pu isotopes is (1.2 ± 0.1)% at 13 keV and increases to (8.9 ± 0.9)% at 1.1 MeV. That for ^{241}Am decreases from a value of (1.9 ± 0.5)% at 13 keV to nearly zero between 50 and 500 keV. At higher energies the correction increases again up to (4.7 ± 1.2)% at 1.1 MeV. The uncertainties of these corrections are included in the statistical error.

All other constant uncertainties are listed in Table II.

5. DISCUSSION

The results of this measurement are listed in Table III. Only the statistical error is given there, because the mass values are preliminary. The neutron-energy spread at the points below 200 keV is about 10 % of the neutron energy. In Fig. 2 our values are plotted together with those of several authors [15,16,17,18,19] and the evaluated curve of Davey [14].

A systematic difference of about 10 % was found between the existing values and this work, which may be due to the preliminary mass values. Apart from this the shape of our measurement does not agree with the other data. The values of Butler and Sjoblom [15] and those from Smith, Smith and Henkels [16] were accurate to about 5 % and the neutron energy spread for most of the points was greater than 100 keV. Therefore any structure in the cross section ratio may be smoothed out. But there is still a remaining discrepancy between the measurement of White, Hodgkinson and Wall (accuracy 2.5 %, neutron energy spread 7 to 15 keV) [17] and this work.

A distinct structure in the cross section ratio can be seen below 70 keV, which was reproduced by several runs. One can assume that the structure is mainly due to the fission cross section of ^{241}Pu because it is absent in the ratios ^{239}Pu : ^{235}U and ^{233}U : ^{235}U of Ref. [1], measured under nearly identical conditions. The same is valid for the dip between 300 and 400 keV, while that between 900 and 1100 keV seems to be due to a raise in the fission cross section of ^{235}U.

An investigation with better energy resolution may yield more detailed information about this structure, as was obtained for the fission cross section of ^{235}U by Patrick, Sowerby and Schomberg [20].

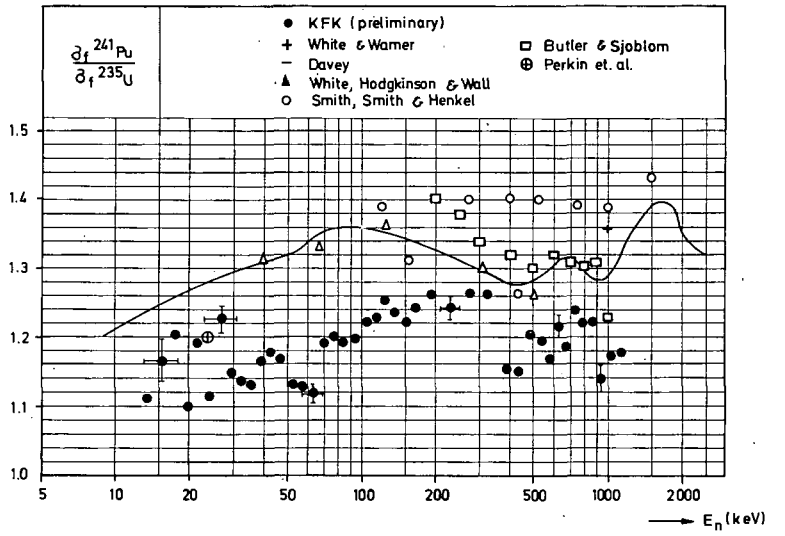

FIG.2. Fission cross-section ratio $^{241}Pu/^{235}U$.
Full circles: present work,
solid line : Davey [14].

ACKNOWLEDGEMENT

The authors are indebted to Prof. Beckurts for his permanent interest in this work. They wish to thank Drs. Lauer and Verdingh for the careful preparation of the samples and the preliminary mass analysis as well as the operateurs of the Van de Graaff accelerator for their help.

REFERENCES

[1] PFLETSCHINGER, E., and KÄPPELER, F., to be published in Nuc. Sci. Eng. (June 1970).

[2] VERDINGH, V., and LAUER, K.F., Nucl. Instr. Meth. 21 (1963) 161.

[3] LAUER, K.F., priv. comm.

[4] ROSSI, B.B., and STAUB, H.H., Ionization Chambers and Counters, McGraw-Hill, New York (1949) 227.

[5] NASYROV, F., and LINEV, S.V., Atomnaya Energiya 20 (1966) 464.

[6] LAMPHERE, R.W., Fast Neutron Physics-I (J.B. Marion and J.L. Fowler, Eds.), Intersci., N.Y. (1963) 456.

[7] KAHN, G., and FORGUE, V., Nucl. Sci. Eng. 23 (1958) 8.

[8] CUMMING, J.B., and CRESPO, V.P., Phys. Rev. 161 (1967) 287.

[9] HYDE, E.K., The Nuclear Properties of the Heavy Elements III, Prentice-Hall, Englewood Cliffs, New Jersey (1964) 195.

[10] NIDAY, J., Phys. Rev. 121 (1961) 1471.

[11] MÜNZEL, H., HOLLSTEIN, M., and ISHIMORI, T., Physics and Chemistry of Fission, IAEA, Vienna (1965) 573.

[12] SEEGER, P.A., HEMMENDINGER, A., and DIVEN, B.C., LA-3586 (1966).

[13] BOWMAN, C.D., and AUCHAMPAUGH, G.F., Nuclear Data for Reactors-II, IAEA, Vienna (1967) 149.

[14] DAVEY, W.G., Nucl. Sci. Eng. 32 (1968) 35; also DAVEY, W.G., Nucl. Sci. Eng. 26 (1966) 149.

[15] BUTLER, DANIEL K., and SJOBLOM, RUTH K., Phys. Rev. 124 (1961) 1129.

[16] SMITH, H.L., SMITH, R.K., and HENKEL, R.L., Phys. Rev. 125 (1962) 1329.

[17] WHITE, P.H., HODGKINSON, J.G., and WALL, G.J., Physics and Chemistry of Fission, IAEA, Vienna (1965) 219.

[18] WHITE, P.H., and WARNER, G.P., J. Nucl. Energy 21 (1967) 671.

[19] PERKIN, J.L., et al., J. Nucl. Energy 19 (1965) 423.

[20] PATRICK, B.H., SOWERBY, M.G., and SCHOMBERG, M.G., EANDC(UK)119AL.

DISCUSSION

H. W. KÜSTERS: In fast reactors under design we have about 4-5% ^{241}Pu compared to the ^{239}Pu content. Thus, a lowering of the fission cross-section of ^{241}Pu by 10-20% in the main energy range of fast reactors, as indicated in your paper, would have a considerable effect. Can you make any statement as to why the data should be lower than in the Davey evaluation, or are your results too preliminary to draw any conclusion?

F. KÄPPELER: It is true that the values given here are too preliminary in character. However, a final mass determination will soon be available and then the figures can be presented with good accuracy.

FISSION NEUTRON SPECTRUM FROM 0.01 TO 1.0 MeV

L. JÉKI, Gy. KLUGE, Gy. KOZMA, A. LAJTAI
Central Research Institute for Physics
of the Hungarian Academy of Sciences,
Budapest, Hungary
and
P.P. DYACHENKO, B.D. KUZMINOV
Institute of Physics and Power Engineering,
Obninsk, Union of Soviet Socialist Republics

Abstract

FISSION NEUTRON SPECTRUM FROM 0.01 TO 1.0 MeV.

Measurements of fission neutron spectra from 0.01 to 1 MeV for spontaneous fission of ^{252}Cf and thermal-neutron-induced fission of ^{235}U by time-of-flight technique are reported. A ^{6}Li-loaded glass scintillator and a gas scintillation detector (80% Ar + 20% Ni) are used for the detection of fission neutrons and fragments, respectively. The results are discussed in terms of the evaporation model.

INTRODUCTION

It is well known that, immediately after the scission of the fissioning nucleus, fission fragments are formed in states of high excitation energies. It has been established from the measured energy and angular distributions of the neutrons emitted during the de-excitation process of fission fragments from the spontaneous fission of ^{252}Cf and the thermal-neutron-induced fission of ^{235}U that, for energies higher than 0.5 MeV, the majority of neutrons are emitted isotropically from the fully accelerated fragments, while 10 - 15% may be emitted in the act of nuclear scission isotropically in the laboratory system.

It has been shown [1] that the energy spectrum of the neutrons emitted in the laboratory system can be described in terms of the nuclear evaporation theory, with an allowance for the distribution of the nuclear temperatures of the fission fragments, by the Maxwellian form

$$N(E) \propto E^{1/2} \exp(-E/T)$$

A large number of experimental data [2-5] are now available which show good agreement with this type of spectrum. Unfortunately, however, very few data have been reported in the range below 0.3 - 0.5 MeV.

The spontaneous-fission neutron spectrum of ^{252}Cf from 0.003 MeV to 15 MeV has been measured by Meadows [5] with the use of the time-of-flight technique and a hydrogenous liquid-scintillator detector at the higher and a ^{6}Li-loaded glass scintillator at the lower neutron energies. He pointed out that the lower-energy part of the experimental spectrum shows some deviation from the Maxwellian shape, while the agreement was found to be excellent for the spectra above 0.5 MeV.

The measurements at low energies are of particular importance since they are expected to yield relevant information on the physical characteristics of the evaporation process and also highly useful data for reactor physicists.

Our experiments were started with the measurement of the energy spectrum of neutrons in the range from 0.01 to 1.0 MeV, originating from the spontaneous fission of ^{252}Cf. Actually, we repeated the measurement of Meadows with the ultimate aim of using ^{252}Cf as a reference source with standard parameters in the experiments on the thermal-neutron-induced fission of ^{235}U.

EXPERIMENTS

A schematic drawing of the experimental apparatus is shown in Fig. 1. The energy of the fission neutrons was evaluated from the flight time measured over a given distance. The neutrons were detected by a 7.6-cm-diameter-by-0.3-cm-thick Nuclear Enterprises glass scintillator containing 7.3% lithium, enriched to 96% in ^{6}Li. The glass scintillator has nearly 100% efficiency for thermal neutrons, and its efficiency rapidly decreases with increasing neutron energies.

The ^{252}Cf fission source with 1.7×10^{5} fissions per minute on thin stainless steel foil, was mounted in the centre of a gas scintillator cell which was 10 cm in diameter and 6 cm long. The gas scintillation counter contained a mixture of 80% argon and 20% nitrogen gas at a pressure of 1 atm. The gas was let from the scintillation counter into the air by which the complicated procedures of gas purification could be avoided, and the gas could be kept free from possible contamination. A gas scintillation counter was chosen to prevent the counting of other than fission events in spite of the large background contribution from alpha, neutron and gamma radiation.

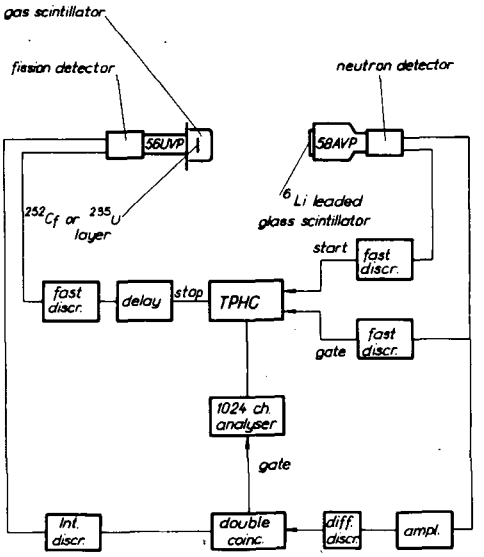

FIG. 1. Block diagram of the apparatus.

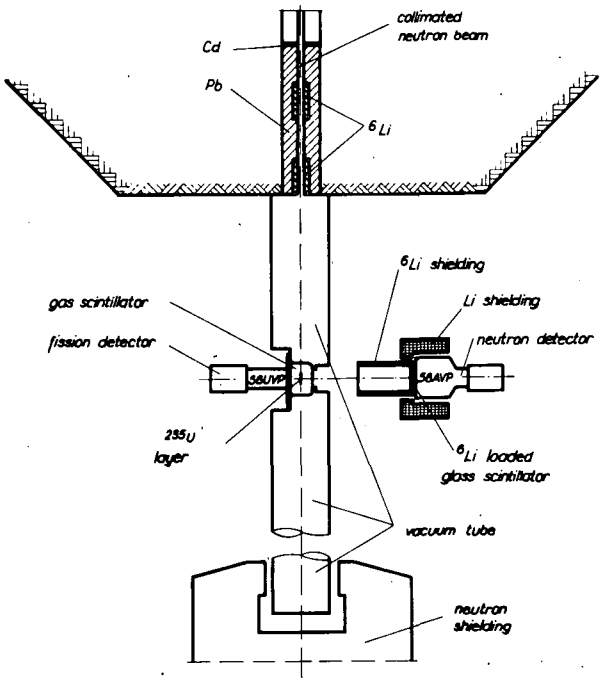

FIG. 2. Schematic drawing of the geometrical arrangement for the measurement on ^{235}U.

The flight path was 30 cm and the flight times up to 400 ns were measured by a time-to-pulse-height converter. Because of the high count rate of the fission detector, the neutron detector was used for triggering the time converter. The stop signal was provided by the fission detector. The limited signals from the fission detector were sent through a delay line of 400 ns. The zero time was determined from the position of the prompt gamma-ray peak with a correction for the gamma-ray flight time. The time scale was calibrated by recording the position of this peak at different values of the delay varied by the use of calibrated delay lines. The channel time was 0.39 ns. The time resolution, determined by the width of the prompt gamma ray, was 4.5 ns. The time calibration, the detector pulse heights and bias levels were checked daily and adjusted, if necessary.

A serious problem was caused in the measurement on ^{235}U fission neutrons by the high efficiency of the detector for thermal neutrons. This necessitated the shielding of the neutron detector against the scattered thermal neutrons.

The measurements were performed at the tangential channel of the VVRS-type research reactor. The experimental arrangement is shown in Fig. 2. A 2.5 m long collimator was built into the reactor channel. To decrease the scattering by air of the collimated neutron beam, a vacuum tube, 16 cm in diameter, was prepared to lead from the exit slit of the channel to the neutron trap. The fission detector was mounted into the vacuum tube. The ^{235}U target, enriched to 96% with ^{235}U, 16 cm^2

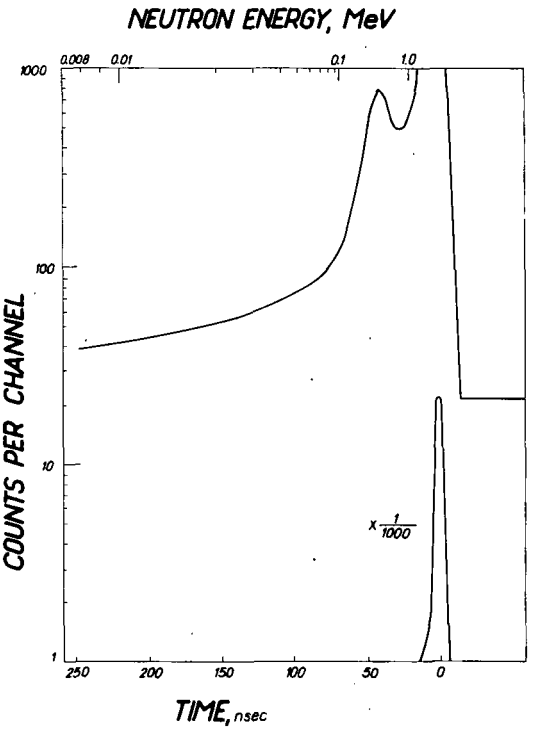

FIG.3. Time-of-flight spectrum of neutrons and gamma rays from the fission of ^{252}Cf taken with a ^{6}Li glass scintillator for 30 cm flight path.

in surface and of 2 mg/cm^2 thickness was located at 50 cm from the exit slit of the reactor channel. The fission fragments were detected by a gas scintillation counter. The neutron detector was shielded by a 1 cm thick cylindrical sheet, prepared from lithium enriched in ^{6}Li, surrounded by another cylindrical plate of 3 cm thickness, prepared from natural lithium carbonate, and finally enveloped by a 5 cm thick lead shield.

This large shielding may naturally cause some distortion in the measured neutron spectra. To reduce the scattered background, the detector was prepared from light material, using 0.1 cm aluminium and for the window of the fission chamber 0.03 cm aluminium. Nevertheless, some corrections have to be taken for the effect of scattered neutrons. To evaluate the necessary corrections measurements will be performed by replacing the ^{235}U by ^{252}Cf source in the same geometry. The difference between the data obtained on ^{252}Cf under the possibly optimum experimental conditions and on ^{252}Cf under reactor conditions is expected to yield the necessary corrections.

We started simultaneous measurements on ^{235}U and ^{252}Cf. The results on ^{235}U show a very large statistical error because of the background conditions discussed above. Recently we have achieved a considerable decrease in the random background counts. The measured ^{252}Cf fission

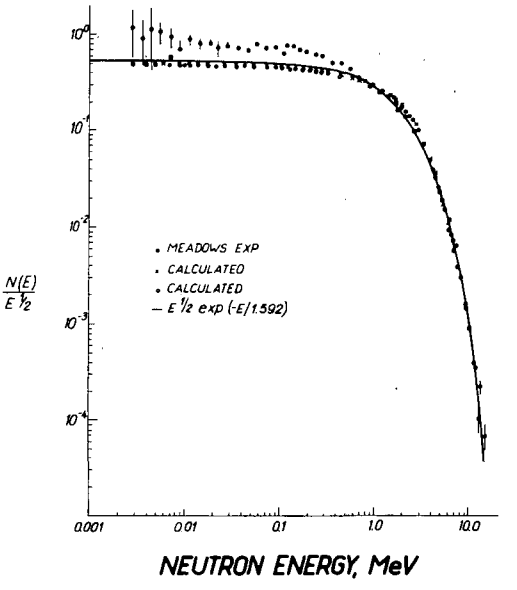

FIG. 4. ^{252}Cf fission-neutron-energy spectra
● experimental data from Ref. [5]
× calculated values – sum of Bowman's spectra
○ calculated values – sum of Maxwellian spectra

$$\frac{N(E)}{E^{\frac{1}{2}}} \propto \exp\left(-\frac{E}{1.592}\right)$$

neutron spectrum is shown in Fig. 3. The statistical accuracy is worse than that of Meadows' measurement, but the first preliminary calculations seem to be consistent with these data. The simultaneous measurements are still in progress since some unforeseen difficulties prevented their completion by this time.

Some calculations were made simultaneously with the experiments to reproduce the experimental data.

The total neutron-energy spectrum is calculated as a sum of contributions from individual fragments weighted, by their frequency of occurrence and the number of neutrons emitted. The emission of neutrons from individual fragments is evaluated by assuming isotropic evaporation in a frame of reference moving with the fragment. Two types of emission spectra are considered: one is a Bowman type [6], the other of Maxwellian form. The parameters, namely the average number and energy of neutrons, can be obtained from the earlier statistical-model calculations [7].

It is evident from Fig. 4 that these calculations without any free parameters "microscopically" reproduce the Maxwellian spectrum with a temperature T = 1.592 MeV estimated by Meadows from the experimental data. Only the neutron yields at lower neutron energies seem to be somewhat lower than predicted. It is hoped that on completion of the present measurement it will be possible to explain the small deviations in the low-energy part of the neutron spectrum.

REFERENCES

[1] TERRELL, J., Phys. Rev. 113 (1959) 527.
[2] HYDE, E.K., "The Nuclear Properties of the Heavy Elements", Prentice-Hall Inc., New-Yersey 3 (1964) 237.
[3] BARNARD, E., FERGUSON, A.T.G., MURRAY, W.R., VAN HEERDAN, I.J., Nucl. Phys. 71 (1965) 228.
[4] CONDE, H., DURING, G., Arkiv Fysik 29 (1965) 313.
[5] MEADOWS, J.W., Phys. Rev. 157 (1967) 1076.
[6] BOWMAN, H.R., THOMPSON, S.B., MILTON, J.C.D., SWIATECKI, W.J., Phys. Rev. 126 (1962) 2120.
[7] KLUGE, Gy., LAJTAI, A., Physics Lett. 30B (1969) 311.

DISCUSSION

L.A.R. DIERCKX: Up to now it has been assumed that neutron emission is isotropic in the fission process. Has this theory been established with certainty or would it not be necessary to conduct experiments in order to demonstrate it?

L. JÉKI: There are various indications at present which support the assumption of isotropic or partly anisotropic emission in the fission process. A final decision between the existing possibilities could be made if the angular distribution of the low energy neutrons were measured.

M.S. MOORE: What steps are you taking to calibrate the Li-glass detector in an absolute sense? This is especially important because of scattering effects near the 250-keV resonance.

L. JÉKI: Our preliminary calculations were carried out using the same efficiency curve as in Meadow's measurement [5].

M.S. MOORE: These are standard detectors then?

L. JÉKI: Yes.

A. ATEN: Mr. H. Pauw, one of my collaborators at Amsterdam, has recently measured the intensity of the low-energy neutrons ($E < 1.5$ MeV) in the ^{252}Cf-spectrum by an activation method. This is possible since the cross-section curve for the reaction $^{115}\mathrm{In}(n,\gamma)^{116}\mathrm{In}^{m}$ is approximately flat between 0.2 and 1.5 MeV. The intensity of the low-energy part of the spectrum observed in this way is in good agreement with the exponential spectral distribution with a nuclear temperature T=1.41 MeV.

However, it is also possible to obtain information concerning the lower part of the spectrum. This is done by means of the process $^{197}\mathrm{Au}(n,\gamma)^{198}\mathrm{Au}$ for which σ varies appreciably with the energy. These measurements indicate that a small fraction of the neutrons below 1.5 MeV have their energies displaced to energies lower than required by the exponential equation. Our Cf-source is canned in a fairly thick nickel-copper container, but, as far as we can see at the moment, energy loss by scattering is insufficient to account for this difference.

NEUTRON ENERGY SPECTRA FROM NEUTRON-INDUCED FISSION OF ^{238}U AT 1.35 AND 2.02 MeV

E. ALMÉN, B. HOLMQVIST, T. WIEDLING
AB Atomenergi, Studsvik, Nyköping,
Sweden

Abstract

NEUTRON ENERGY SPECTRA FROM NEUTRON-INDUCED FISSION OF ^{238}U AT 1.35 AND 2.02 MeV.

The shapes of fission neutron spectra are of interest for power reactor calculations. Recently it has been suggested that the neutron-induced fission spectrum of ^{235}U should be harder than was earlier assumed. For this reason, measurements of the neutron spectra of some fissile isotopes are in progress at the authors' laboratory. This report will present results from a study of the energy spectrum of the neutrons emitted in the neutron-induced fission of natural uranium.

The measurements were performed at incident neutron energies of 1.35 and 2.02 MeV using time-of-flight techniques. The time-of-flight spectra were analysed only above the position of the neutron elastic-scattering peaks. Corrections for neutron attenuation in the uranium sample were calculated using a Monte-Carlo program.

The corrected fission neutron spectra were fitted to Maxwellian temperature distributions. A temperature of 1.29 ± 0.03 MeV was obtained at 1.35 MeV incident neutron energy compared with 1.29 ± 0.02 MeV at 2.02 MeV. These values are consistent with previous results of ^{238}U. There are, thus, no indications that the ^{238}U fission spectra do not follow the generally observed temperature trend, at least within the energy region considered in this investigation.

1. INTRODUCTION

The intensity distribution of a neutron fission spectrum is of primary importance in a nuclear reactor in connection with its influence on the reactivity. An accurate knowledge of the shape of the neutron spectrum is thus of interest in reactor physics calculations. Such spectra have been studied several times for a number of fissile isotopes undergoing spontaneous fission as well as neutron induced fission at thermal and fast neutron energies [1 - 17]. Most experimental fission spectrum data obtained at well defined primary neutron energies and published up to now are compiled in Table I giving the Maxwellian temperature as a characteristic parameter of the spectral shape. With some exceptions several experiments have been made for each individual nucleus. When studying the table one is struck by the observation that in spite of the relatively small quoted errors there is in many cases rather large scattering between the values of each isotope indicating large systematic uncertainties. There is, for instance, a recent result of ^{235}U giving a Maxwellian temperature, 1.49 MeV, remarkably different from the other ones and indicating an appreciably harder fission spectrum. Such a temperature value would really mean that all results of calculations on thermal reactor cores would have to be revised.

The present fission spectrum measurement of ^{238}U is part of an extended study of fission spectra of several nuclei at fast neutron primary energies. The program was initiated when observing the discrepency between recent ^{235}U results when using the multiple foil activation iterative method [4] and earlier measurements performed with time-of-flight techniques and other methods. The main purpose of our experiment has been merely to check the spectrum shape for the presence of any extraordinary

TABLE I. A COMPILATION OF MAXWELLIAN TEMPERATURES OF FISSION SPECTRA OF URANIUM, PLUTONIUM, CURIUM AND CALIFORNIUM ISOTOPES

Fissile nuclide	Incident neutron energy (MeV)	Maxwellian temperature (MeV)	Average number of neutrons per fission*	Reference
^{233}U	Thermal	1.36	2.47	[1]
	Thermal	1.25±0.03	-"-	[2]
	Thermal	1.32	-"-	[3]
^{235}U	Thermal	1.33±0.03	2.43	[1]
	Thermal	1.29	-"-	[3]
	Thermal	1.49	-"-	[4]
	Slow	1.29	-"-	[5]
	0.04	1.24±0.04	-"-	[6]
	0.100	1.297±0.030	-"-	[7]
	1.50	1.25±0.04	2.55	[6]
	14.3	1.36±0.04	4.56	[8]
^{238}U	2.086	1.285±0.030	2.64	[7]
	4.908	1.422±0.030	3.09	[7]
	13.9±0.1	1.85±0.28	4.53	[9]
	14.3	1.46±0.04	4.59	[8]
^{239}Pu	Thermal	1.385	2.83	[1]
	Thermal	1.34	-"-	[3]
	Thermal	1.83±0.28	-"-	[9]
	Thermal	1.35±0.04	-"-	[10]
	Thermal	1.34	-"-	[11]
	Thermal	1.33	-"-	[12]
	0.04	1.34±0.04	-"-	[6]
	0.130	1.407±0.020	-"-	[7]
	0.150-1.5	1.214	-"-	[13]
	1.5	1.41±0.05	3.05	[14]
	1.9	1.45±0.04	3.12	[14]
	2.0	1.35±0.08	3.13	[15]
	2.3	1.52±0.04	3.17	[14]
	4.0	1.51±0.07	3.48	[14]
	4.5	1.69±0.06	3.55	[14]
	5.0	1.61±0.07	3.62	[14]
	5.5	1.61±0.05	3.69	[14]
^{240}Pu	Spontaneous	1.189	2.19	[1]
^{241}Pu	Thermal	1.335±0.034	2.95	[16]
^{242}Pu	Spontaneous	1.21±0.07		[10]
^{244}Cm	Spontaneous	1.37±0.04		[10]
^{252}Cf	Spontaneous	1.367	3.77	[1]
	Spontaneous	1.39±0.04	-"-	[6]
	Spontaneous	1.565	-"-	[17]

* These numbers are from references [18 - 19]

effects of importance in reactor physics and observable with the method used, i.e. time-of-flight technique, at 1.35 and 2.02 MeV primary neutron energies. A previous report has been published concerning data of ^{238}U in this energy range by Barnard et al. [7] who have described experiments made at 2.09 and 4.91 MeV.

The measurements and analyses of fission spectra at fast neutron energies become complicated because of the interference between the continuous fission spectrum and neutrons emitted in competing elastic and inelastic processes. With present technique and energy resolution it is thus difficult to resolve the close lying neutron groups from inelastic scattering events and to be able to observe that part of the fission spectrum on which they are superposed. As regards the measurement of the fission spectrum of ^{238}U there is also the difficulty involved in the fission cross section, which drops rather fast below 2 MeV primary neutron energy. In connection with low primary neutron intensities and long measuring times the background difficulties may become excessive.

2. EXPERIMENTAL ARRANGEMENTS

The measurements were made by using a time-of-flight spectrometer in conjunction with a 6 MV Van de Graaff accelerator provided with a pulsed ion source and a klystron bunching system [20]. Pulses having about 2 ns width at half height and a repetition rate of 1 MHz have been used. The neutron detector consisted of an organic scintillator* (10 cm in diameter and 5 cm thick) viewed by a photomultiplier. The detector was enclosed in a large collimating shielding [21] and placed at a distance of 300 cm from the uranium sample.

Neutrons were produced by the $^{3}T(p, n)^{3}He$ reaction using a gas target giving a neutron energy spread of 50 keV. The relative neutron flux from the target was monitored by a long counter [21].

Since the fission cross section is comparatively small at 1.35 MeV neutron energy, a rather large sample (height 5 cm, outer diameter 2.5 cm, inner diameter 0.95 cm) of natural uranium was chosen for the measurements at this energy. The fission cross section at 2 MeV is appreciably larger and a smaller sample (height 3 cm, outer diameter 1.8 cm, inner diameter 0.95 cm) could be used, thus minimizing neutron absorption and multiple scattering.

3. EXPERIMENTAL PROCEDURE

The 1.35 MeV measurements were performed with the detector positioned at an angle of 90° relative to the incident neutron beam. At 2.02 MeV, however, three detector angles, namely 40°, 90° and 150°, were chosen in order to observe if there were any systematic deviations due to angle dependent scattering effects.

The intensity effect of room scattered neutrons interacting with the sample was measured with a tantalum scatterer replacing the uranium source. The measurements were then alternatively repeated with the tantalum and uranium samples as well as without any scatterer.

It is very important in measurements of this type, requiring accurate determinations of intensities in different energy intervals covering a large energy range, that the energy scale as well as the energy dependence of the neutron detector are very well known. The energy calibration of the time-to-pulse-height converter of the neutron spectrometer was performed by observing the positions of a large number of peaks corresponding to elastic and inelastic neutron scattering from different elements together with the positions of peaks obtained by neutron scattering from hydrogen at different angles, as well as the position of the gamma ray peak. These data points were obtained in a separate inelastic neutron scattering project

* Nuclear Enterprises, NE 104

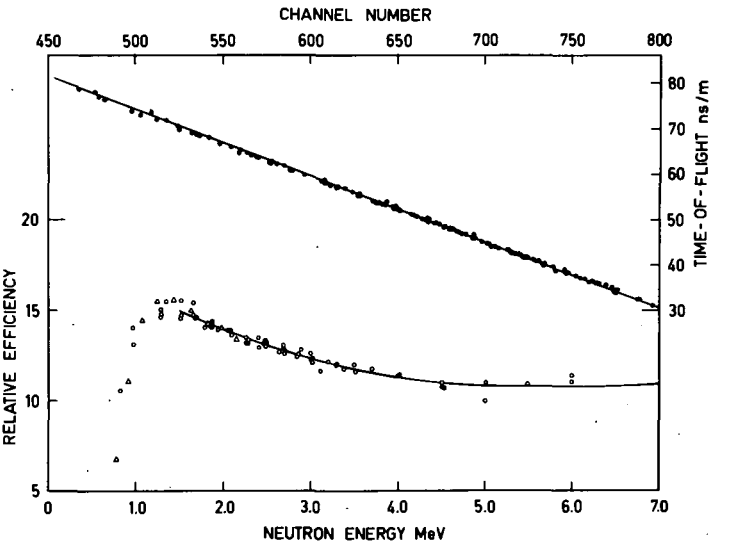

FIG.1. The relative efficiency of the neutron detector as measured with the n-p (circles) and $^{3}T(p,n)^{3}He$ (triangles) processes. The curve represents a least-squares fit to the experimental points in the energy range 1.5 to 6 MeV and is extrapolated to energies above 6 MeV. The figure also illustrates the energy calibration curve of the time-of-flight spectrometer (filled circles). The line through the points is the least-squares-fit representation.

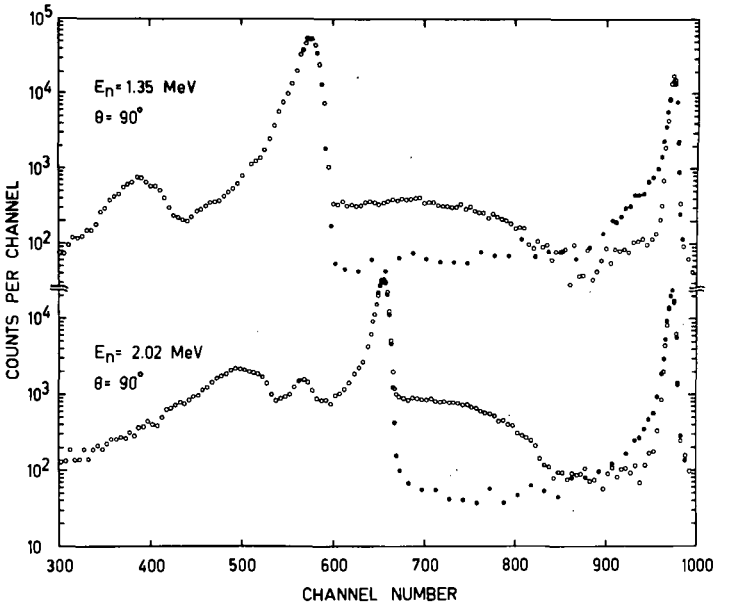

FIG.2. Time-of-flight spectra from neutron-induced reactions in uranium (circles) and tantalum (filled circles). Backgrounds observed without any scatterers have been subtracted from each spectrum.

[22] (Fig. 1). The points are on or close to the straight line representing a least squares fit. There are a few points which are somewhat scattered, which is probably explained by less accurate determinations of the energies of the corresponding nuclear levels. Anyway, the linearity of the time-to-pulse height converter is, as demonstrated, well within the accuracy needed for an accurate analysis of a fission spectrum and the slope of the line is determined with a relative error smaller than 1 per cent in the energy interval 0.5 to 7 MeV. The calibration curve is thus known with high enough accuracy within the energy range of the fission spectrum which is of primary interest in this investigation.

The relative efficiency of the neutron detector was determined up to about 6 MeV by measuring neutron scattering from hydrogen at different angles and at different primary neutron energies using a polythene sample (height 3.0 cm, outer diameter 0.95 cm, inner diameter 0.6 cm). The low energy part of the efficiency curve has also been measured by detecting neutrons from the $^{3}T(p, n)^{3}He$ reaction at angles between 15° and 125° and at a proton energy of 3.00 MeV. Fig. 1 shows the results of these measurements. The uncertainties of the experimental points are about 2 per cent, which include the statistical errors in the number of counts of the different elastic scattering peaks of the time-of-flight spectra as well as an error of about 1 per cent in the H(n, n) cross section [23]. The uncertainty of the points obtained by measuring neutrons from the T(p, n) reaction was about 4 per cent because of the error of 3 per cent in the differential reaction cross section [24]. In the energy range 1.5 to 6.0 MeV a least squares fit procedure has been applied to the experimental points. The result is represented by the curve drawn in Fig. 1. For energies above 6 MeV where no experimental data exist the efficiency curve has been extrapolated in a linear way.

4. EXPERIMENTAL RESULTS, DATA ANALYSES AND CORRECTIONS

The observed velocity spectra resulting from fission in ^{238}U induced by neutrons of 1.35 and 2.02 MeV energy are shown in Fig. 2. These measurements were made at an angle of 90° relative to the incident neutron beam. The figure shows the peaks due to gammas from fission and inelastic events. There are also the peaks resulting from the elastic and a number of unresolved inelastic groups appearing at the low energy end of the fission neutron continuum. Backgrounds recorded without scatterers are subtracted from each spectrum.

The spectrum obtained at 1.35 MeV incident neutron energy is the result of eleven individual measurements with a total running time of about twenty hours and that obtained at 2.02 MeV is the result from seven measurements during about twelve hours.

The fission spectra are expected to drop to approximately zero intensity at high energies. The curves in the figure do not demonstrate such a trend, probably because of the scattering by the uranium sample of secondary room scattered neutrons into the detector. The effect is generally small but far from negligible in this type of experiment. Because of the low fission cross section the recording of the 1.35 MeV fission spectrum is of course more sensitive to such a background effect than that of 2.02 MeV. The intensity distribution measured at 1.35 MeV primary energy is thus significantly distorted in the whole energy range, contrary to the 2.02 MeV exposure which is influenced mostly in the high energy region. To be able to correct for this inscattering, a ^{181}Ta sample was chosen for separate measurements at the corresponding primary neutron energies. Fig. 2 shows the background corrected spectra of these separate measurements. Tantalum is convenient for this purpose since, on the one hand, it is rather heavy and on the other, like ^{238}U, it has many low lying excited states. The main neutron scattering peaks are the ones corresponding to elastic

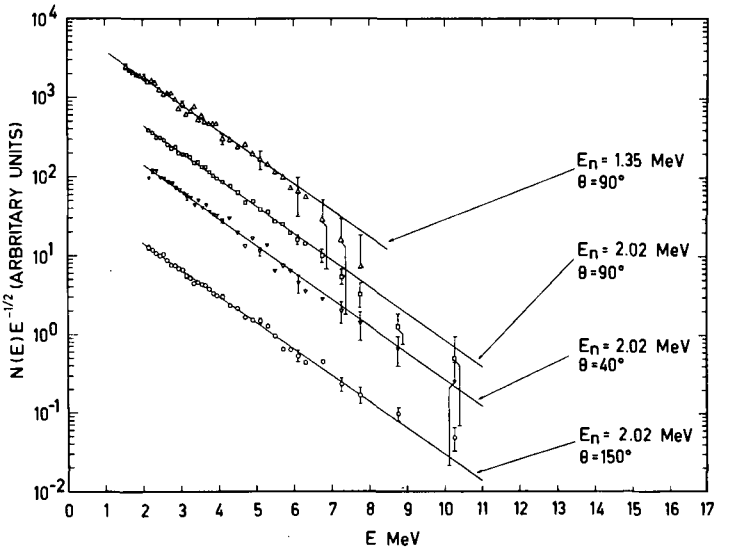

FIG.3. The fission neutron spectra obtained at 1.35 and 2.02 MeV primary neutron energies. The lines are least-squares fits to the experimental points.

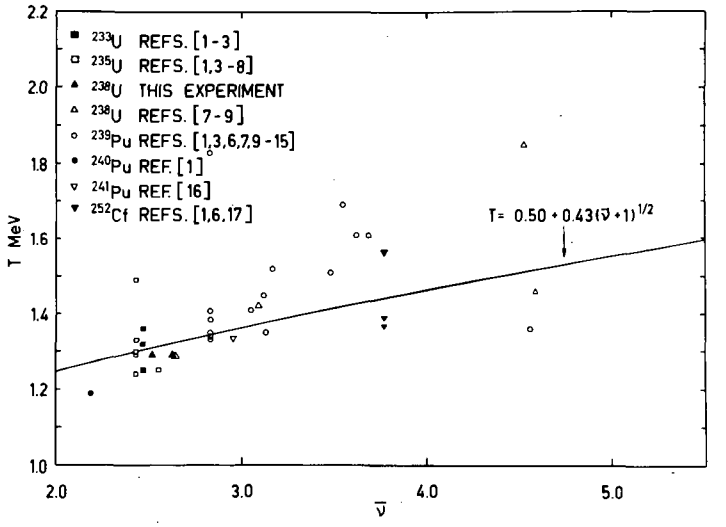

FIG.4. The Maxwellian temperature plotted versus the average number of neutrons per fission for the isotopes listed in Table I as well as the data obtained in the present work.

scattering, which also include some contributions from neutron transitions to the low lying states. The tantalum and uranium spectra were normalized with respect to the "elastic" peaks, also including inelastic contributions, as well as with respect to the gamma peaks. The tantalum spectrum fits in rather well also in the valleys between the end points of fission spectra and the gamma peaks. The energy resolution of the neutron spectrometer puts a limit on the range of a fission spectrum possible to study. The high en-

ergy end may be somewhat influenced by the low energy tail of the gamma peak. The low energy range is superposed by the unresolved peaks from elastic and inelastic events. The influence from the gamma peak has been somewhat diminished in this experiment by reducing the gamma flux, which to a large extent consists of low energy gamma quanta from fission and inelastic scattering processes in ^{238}U, by putting a lead absorber (1 cm thickness) in front of the gamma sensitive neutron detector, which, however, results only in a minor reduction (10 per cent) of the neutron detection efficiency. (The pulse shape discrimination method could as well have been used.) After application of these methods the fission spectra were analyzed up to 8 MeV (the 1.35 MeV measurement) and 11 MeV (the 2.02 MeV measurement), respectively.

The fission spectra were corrected for the efficiency of the neutron detector. The uncertainty of the relative efficiency of the neutron detector is small in comparison with the statistical error in the number of neutron fission pulses in each energy interval, which for instance in the measurement at 2.02 MeV incident neutron energy goes from 4 per cent at 2.1 MeV to 15 per cent at 6 MeV and is therefore of small importance for the shape of the fission neutron spectrum.

Corrections for flux attenuation and source to sample geometry for the uranium samples were calculated using Monte Carlo techniques [25]. The correction factor goes with increasing fission neutron energy from 1.35 to 1.31 and from 1.21 to 1.18 in the 1.35 and 2.02 MeV measurements, respectively. The fission spectra are evidently roughly corrected by the same factor over the whole energy region.

5. DISCUSSION

A Maxwellian distribution $N(E) \sim E^{1/2} \exp(-E/T_m)$ has been fitted to the experimental neutron fission spectra (N(E) is the intensity of the fission neutrons having the energy E). A semi-logarithmic presentation of the fission neutron spectra of the present investigation is shown in Fig. 3. The values of the parameter T_m, the Maxwellian temperature, are obtained by least squares fit procedures. At 1.35 MeV incident neutron energy a temperature of 1.29 ± 0.03 MeV was obtained. The fission neutron spectra observed at angles of 40°, 90° and 150° at 2.02 MeV give the individual temperature values 1.28 ± 0.02, 1.28 ± 0.02 and 1.30 ± 0.02 MeV, respectively, and show no significant differences indicating any angle dependent effects. The mean value of the three measurements is $1.29 \pm \pm 0.02$ MeV. The results show that the Maxwellian distribution describes the energy distribution of the fission neutrons well as predicted by Terrell [26] on the basis of Weisskopf's nuclear evaporation theory.

The only previously reported measurement of the neutron spectrum from fission of natural uranium induced by neutrons having an energy in the vicinity of those in this work is that of Barnard et al. [7] at 2.09 MeV incident neutron energy. Their value of the Maxwellian temperature is 1.29 ± 0.03 MeV, being in good agreement with the results of the present work. The value of 1.49 MeV reported for thermal induced fission of ^{235}U obtained by using the multiple foil activation method is thus evidently higher. There are thus no indications that the ^{238}U fission spectra do not follow the generally observed temperature trend, at least within the fission neutron energy region considered in this investigation.

A good overall view of the present status of the quality of fission spectrum measurements published until now is obtained from Fig. 4, demonstrating the temperature variation with $\bar{\nu}$, the average number of neutrons per fission. When letting Terrell's [27] theoretical relation between T and $\bar{\nu}$ represent a guide for an expected trend, one is struck by the observation

of the large scatter between the data points. It seems at present rather unjustified to try to make any comparisons and to draw any serious conclusions about the T-$\bar{\nu}$ relationship. At the best one can say that the T-$\bar{\nu}$ relation demonstrates somewhat of a trend but also demonstrates a need for new accurate fission spectrum measurements with a serious evaluation of all important error sources.

REFERENCES

[1] BONNER, T. W., Nucl. Phys. 23 (1961) 116.

[2] SMITH, A.B., FIELDS, P.R. SJÖBLOM, R.K., ROBERTS, J.H., Phys. Rev. 114 (1959) 1351.

[3] GRUNDL, J.A., Nucl. Sci. Engng. 31 (1968) 191.

[4] MC ELROY, W.N., Rep. BNWL-SA-1794 (1968).

[5] CRANBERG, L., FRYE, G., NERESON, N., ROSEN, L., Phys. Rev. 103 (1956) 662.

[6] CONDÉ, H., DURING, G., Arkiv Fysik 29 (1965) 313.

[7] BARNARD, E., FERGUSON, A.T.G., MCMURRAY, W.R., VAN HEERDEN, I.J., Nucl. Phys. 71 (1965) 228.

[8] VASIL'EV, YU.A., ZAMYATNIN, YU.S., IL'IN, YU.I., SIROTININ, E.I., TOROPOV, P.V., FOMUSHKIN, É.F., Soviet Physics JETP 11 (1960) 483.

[9] DIDIER, D., MOUILHAYRAT, G., PERRAULT, F., International conference on the nuclear structure study with neutrons, Antwerp, Belgium (1965).

[10] BELOV, L.M., BLINOV, M.V., KAZARINOV, N.M., KRIVOKHATSKY, A.S., PROTOPOPOV, A.N., INDC-260 E (1969) 94.

[11] GRUNDL, J.A., NEUER, J.R., Bull. Am. phys. Soc. 1 (1956) 95.

[12] NERESON, N., Phys. Rev. 88 (1952) 823.

[13] BOYCE, D.A., CAVANAGH, P.E., COLEMAN, C.F., GARD, G.A., HARDACRE, A.G., KERR, J.C., TURNER, J.F., Rep. AERE-PR/NP 14 (1968).

[14] COPPOLA, M., KNITTER, H.H., Private communication.

[15] BATCHELOR, R., WYLD, K., Rep. AWRE 055/69.

[16] SMITH, A.B., SJÖBLOM, R.K., ROBERTS, J.H., Phys. Rev. 123 (1961) 2140.

[17] MEADOWS, J.W., Phys. Rev. 157 (1967) 1076.

[18] HOPKINS, J.C., DIVEN, B.C., Nucl. Phys. 48 (1963) 433.

[19] BOSCHUNG, P., GAGNEUX, S.T., HOOP Jr, B., HUBER, P., LEWANDOWSKI, Z., WAGNER, R., Helvetica Physica Acta 42 (1969) 225.

[20] TYKESSON, P., WIEDLING, T., Nucl. Instr. and Meth. 77 (1970) 277.

[21] HOLMQVIST, B., Arkiv Fysik 38 (1968) 403.

[22] ALMÉN, E., ETEMAD, M.A., HOLMQVIST, B., WIEDLING, T., "Fast neutron inelastic scattering in the energy range 2 to 4.5 MeV" to be presented at this conference.

[23] HORSLEY, A., Nuclear Data, Sect. A, 2 (1966) 243.

[24] PAULSEN, A., LISKIEN, H., Conf. Proc. Nuclear Data for Reactors, Paris (ed. IAEA, Vienna), 1 (1967) 217.

[25] HOLMQVIST, B., GUSTAVSSON, B., WIEDLING, T., Arkiv Fysik 34 (1967) 481.

[26] TERRELL, J., Phys. Rev. 113 (1959) 527.

[27] TERRELL, J., Physics and Chemistry of Fission II IAEA, Vienna (1965) 3.

DISCUSSION

A.M. FABRY: I would first like to make a brief comment. A proper understanding of $T(\bar{\nu})$ correlations requires elucidation of the origin of fission neutrons (possible influence of "central" or "scission" neutrons). As far as measurements of the total fission neutron spectrum are concerned, this in turn suggests that the energy range covered by differential experiments should be as large as possible, extending in any case towards energies lower than 1 MeV, as attempted in Dr. Jéki's work.

I would then like to ask the following question: is your laboratory planning to investigate such matters as coincidence between fragments and emitted neutrons?

T. WIEDLING: I agree very much with your statement concerning the importance of performing the measurements in as large a neutron energy interval as possible.

In reply to your question, I can say that we do have plans for continuing these neutron spectra measurements but no final decisions have yet been taken as to which methods should be applied in the future.

At this point, I would also like to mention the results of a recent measurement on ^{235}U at 0.95 MeV primary neutron energy. According to this experiment, the Maxwellian temperature is 1.27 ± 0.01 MeV.

H. ALTER: Can you please comment on the value of 1.83 MeV for the Maxwellian temperature of thermal neutron induced fission in ^{239}Pu? This value was one of several shown on your first slide.

T. WIEDLING: I have no comment on this specific temperature value of ^{239}Pu. I mentioned in my presentation that for many of the isotopes there is a rather large scatter between the Maxwellian temperature values and there seems to be a need for new, carefully performed measurements.

INELASTIC SCATTERING OF FAST NEUTRONS FROM ^{238}U

E. BARNARD, J.A.M. DE VILLIERS, D. REITMANN
Atomic Energy Board*, Pelindaba,
Transvaal, Republic of South Africa

Abstract

INELASTIC SCATTERING OF FAST NEUTRONS FROM ^{238}U.

The cross-sections for inelastic scattering of fast neutrons from ^{238}U are of considerable importance in reactor calculations. In spite of this fact, relatively few detailed measurements of these quantities have been reported. The need for another independent measurement of the excitation function for inelastic scattering from threshold up to several MeV has been pointed out on several occasions. The present experiment was undertaken in an attempt to check the accuracy of existing data in the energy region below about 1.2 MeV.

Neutrons with an energy spread of less than 10 keV were obtained from a pulsed 3 MV Van-de-Graaff accelerator and the ^{7}Li (p, n) ^{7}Be reaction. Time-of-flight techniques were employed and care was taken to ensure sufficient resolution of the neutron groups corresponding to the excitation of different energy levels in ^{238}U. Results were obtained for the levels at approximately 45, 150, 680 and 730 keV. All cross-sections were determined relative to the known cross-section for elastic scattering from carbon. Corrections were applied for flux attenuation and multiple scattering.

The excitation curve for the first excited state in ^{238}U, measured in steps of 10 keV (or less) in incident energy, rises fairly smoothly with energy and only slight indications of structure were observed. The absolute values of the 90° differential inelastic-scattering cross-section for all the energy levels agree fairly well with the detailed results published by the Harwell group in 1966. In view of the completely different methods of cross-section normalization employed in these two experiments, this agreement is encouraging.

Introduction

The accuracy of existing cross sections for the inelastic scattering of fast neutrons from ^{238}U has often been questioned. This is due to the lack of consistency between different sets of measurements, to the fact that the sum of the partial cross sections exceed the total cross section in some energy regions, and to the disagreement between measured spectra from fast critical assemblies and those calculated from the existing microscopic cross sections. These considerations have prompted the present investigation.

The most detailed sets of experimental cross-sections for inelastic scattering of neutrons from ^{238}U which have been published, are those of Smith [1] and Barnard et al. [2]. In general the values obtained by Barnard et al. are slightly larger than those of Smith and have been preferred in evaluations like that of Schmidt [3]. On the other hand, the discrepancies mentioned in the previous paragraph seem to indicate that existing inelastic scattering cross sections are too large.

While absolute cross sections for inelastic scattering in the experiment by Barnard et al. [2] were determined in a direct way (by comparing the incident neutron flux with the scattered flux as measured by the same detector), it was considered useful to repeat these measurements employing a different technique for absolute normalization. In the present experiment all cross sections were measured relative to the known elastic scattering cross sections for carbon [4], which was also used as a standard by Smith [1].

* Mail address: Private Bag 256, Pretoria, Republic of South Africa.

Experimental method

Neutrons of well-defined energy were produced by bombarding thin targets (5 to 10 keV) of Li metal with protons from the 3 MV pulsed van de Graaff at Pelindaba. Beam pulses were between 1 and 2 ns long, the repetition frequency was 3 MHz and average currents of about 10 μA were used. A hollow right cylinder of pure natural uranium was used as scattering sample. The height was 25 mm, the outside diameter 25 mm and the inside diameter 17.2 mm. This particularly "thin" sample was chosen in order to keep flux attenuation and multiple scattering effects small. For the same reasons, the carbon sample had the same outside dimensions but a wall thickness of less than 2 mm. These samples were suspended at about 8 cm from the Li target and scattered neutrons were detected in a well-shielded plastic scintillator, 10 cm in diameter and either 1 cm or 2.5 cm thick, viewed by an XP-1040 photomultiplier tube. Flight paths varied between 1.2 and 3 metres, depending on the resolution required.

Considerable care was taken to ensure proper separation of the different neutron groups in the time-of-flight spectra by the choice of target and detector thickness and flight path. In those cases where the neutrons scattered inelastically from the 45 keV level were not clearly resolved from the elastic group, the shape of the elastic peak was determined by elastic scattering from a Pb sample with the same macroscopic cross section as the U sample.

The incident neutron flux was monitored by a "long counter" and corrections were applied for its (slight) variation in efficiency as a function of neutron energy as well as for the effect of the second neutron group from the $^{7}Li(p,n)^{7}Be^{*}$ reaction.

All experimental results were fully corrected for flux attenuation in U and C, as well as for multiple scattering in U by means of an expression derived from semi-analytical considerations and Monte Carlo calculations [5]. Data on elastic scattering were, for the purpose of these corrections, taken from the complete set of Smith [1]. Flux attenuation corrections were all smaller than 20% for U and smaller than 10% for C, while the multiple scattering corrections were of the order of 10%. The resultant overall correction to the raw data was in no case larger than 5%.

Excitation curves for the levels at 44.9, 148.4, 680.0 and 731.9 keV were measured from as close to their respective thresholds as the detector efficiency would allow up to the highest energies where the resolution was considered sufficient. Small steps in incident energy (10 or even 5 keV) were taken at low energies in order to ensure that existing differences could not be explained by structure in the excitation curves. Inelastic scattering angular distributions were measured for each of these four levels at one or two incident energies. No attempt was made to determine accurate level energies from the neutron time-of-flight spectra. The energy values adopted were obtained by McMurray et al. [6] from their $(n,n'\gamma)$ studies on ^{238}U. No attempt was made to obtain detailed results on the very small cross section for inelastic scattering from the level at about 310 keV.

Results

The differential inelastic scattering cross sections at 90^{o}, obtained in the present experiment, are indicated in fig. 1 together with the Harwell-results [2] and those of Smith [1], calculated by dividing his total inelastic cross sections by 4π. The solid curve indicates the "recommended values" from Schmidt's evaluation [3] similarly reduced to differential values under the assumption of angular isotropy. The dotted lines indicate the results of the Hauser-Feshbach calculation, taken directly from the paper by Barnard et al. [2]. Errors indicated on the experimental points include the statistical errors on the determination of the areas under peaks in the time-of-flight spectra, as well as a 5% allowance for uncertainties in the determination of the detector efficiency. No allowance was made for possible systematic errors in the carbon cross sections used as standard.

The largest differences between the present results and the other two sets exist in the case of the 45 keV level. The present values are systematically higher by 20 to 30% over most of the energy range, but do seem to approach the older values towards higher energies. The shape of the excitation curves are quite similar, apart from the fact that the present data appear to reflect more structure, which may be attributed to the smaller spread in incident energy and the smaller step size employed here.

The excitation curves for the levels at 148, 680 and 732 keV agree remarkably well in shape and absolute magnitude with both earlier sets of results.

The angular distributions obtained in the present experiment are indicated in fig. 2. Within experimental errors they are very nearly isotropic except in the case of the 45 keV level, measured at 550 keV. Comparison of this particular angular distribution with that obtained at the same energy by Barnard et al. reveals remarkable agreement. Fitting a series of Legendre polynomials to each of the angular distributions from the present experiment indicated that the error introduced by multiplying the 90° differential inelastic cross sections by 4π to obtain total inelastic scattering cross sections (i.e. by assuming isotropy), was in only one case larger than 8%.

Discussion

The good agreement between the present results and those of Barnard et al. and Smith for the excitation of the levels at 148, 680 and 732 keV confirms the reliability of each of the three sets of measurements and practically rules out the possibility of gross systematic errors.

The rather poor agreement between the three sets of results for the 45 keV level is difficult to explain. Neutrons scattered inelastically from this level are difficult to resolve clearly from the elastically scattered group and long flight paths and very good time resolution are essential. Even under the best conditions some allowance has to be made for a "tail" of the elastic peak under the inelastic peak in the time spectrum. In the present experiment

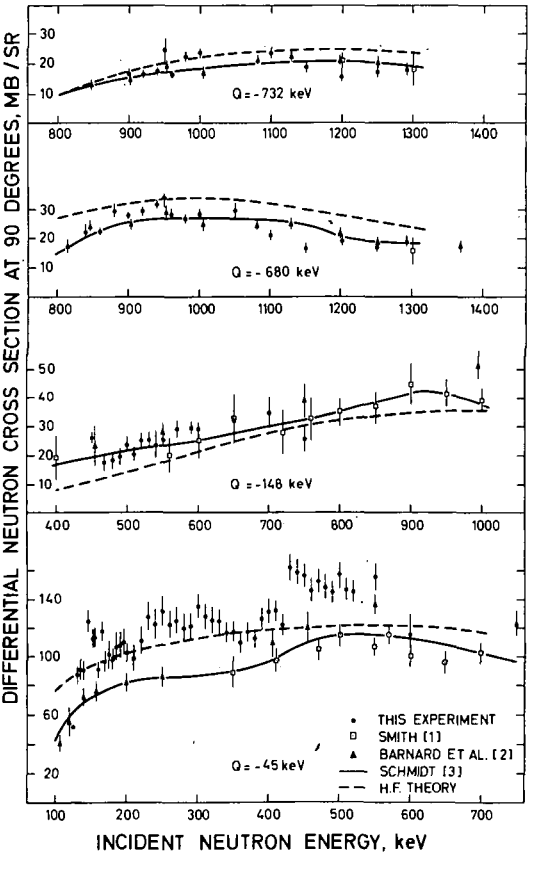

FIG. 1. Differential inelastic-scattering cross-sections at 90° for four levels in ^{238}U.

this effect was kept as small as possible by using a thin Li target, a small scattering sample, long flight paths and optimum time resolution. The use of a Pb scattering sample to determine the shape of the elastic peak assisted in the stripping procedure. In spite of all these precautions, it is still possible that the effects of the elastic "tail" may have been underestimated in the present experiment. It is also possible that this effect may have been overcorrected for in the two earlier experiments. It is unlikely, however, that this alone could be responsible for the discrepancies. Other effects which may play a role, are connected with the fact that the largest differences exist where the scattered neutrons have fairly low energies. In general, plastic scintillator efficiencies drop rapidly towards low energies and accurate knowledge of accelerator energy calibration becomes increasingly important.

The fact that good agreement exists for the three other excitation curves practically rules out systematic errors in the various corrections applied, in the long counter efficiency curves or in the carbon standard values. In any case, the experiment of Barnard et al. did not rely on the latter data.

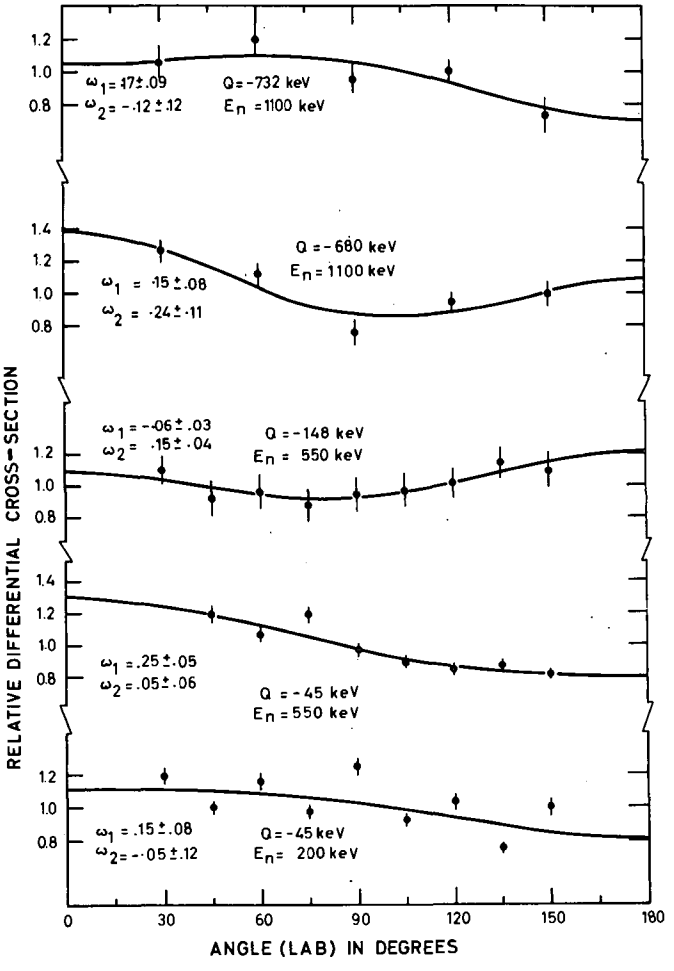

FIG. 2. Angular distributions for inelastic scattering of neutrons from four levels in ^{238}U. The smooth curves represent the expression $(1 + \omega_1 P_1 + \omega_2 P_2)$ where P_1 and P_2 are Legendre polynomials.

In conclusion, it is fair to say that the present results indicate that the recommended excitation curves of Schmidt [3] and hence the results of Barnard et al. [2] and Smith [1] are reasonably reliable in the energy range under discussion. The only exception to this is the excitation curve for the 45 keV level, which may have been somewhat too low. There is no indication that the accepted inelastic scattering cross sections are generally too high, as has sometimes been suggested. It is encouraging to note that, at neutron energies up to 1300 keV, the sums of all inelastic scattering cross sections (as taken from Schmidt's evaluation) added to the very recent elastic scattering cross sections measured by Smith [7] fall just below Smith's latest values for the total cross section [7]. The agreement between the sum of partial cross sections and the total cross section in the energy range from about 300 to 1300 keV remains quite good if an additional 0.3 barn (corresponding to 20 to 30 mb/sr) as suggested by the present results, is added to the cross section for excitation of the 45 keV level.

REFERENCES

[1] SMITH, A.B., Nucl. Phys. 47(1963)633.
[2] BARNARD, E., FERGUSON, A.T.G., McMURRAY, W.R., VAN HEERDEN, I.J., Nucl. Phys. 80(1966)46.
[3] SCHMIDT, J.J., Neutron cross sections for fast reactor materials, KFK 120(EANDC-E-35U).
[4] LANGSDORF, A., Jr., LANE, R.O., MONAHAN, J.E., ANL Report ANL-5567(1961) revised.
[5] ENGELBRECHT, C.A., To be published in Nucl. Instr. & Methods.
[6] McMURRAY, W.R., VAN HEERDEN, I.J., SPITZ, L.M., VAN DER MERWE, P., Southern Universities Nuclear Institute Annual Report 1969.
[7] SMITH, A.B., Private communication.

DISCUSSION

H.H. KNITTER: Did you also evaluate the fission neutron energy spectra?

D. REITMANN: No, but I believe fission plays a very small part at the incident neutron energies used in our experiment.

J.L. ROWLANDS: Dr. Reitmann has said that his experiments do not support the suggestion which has been made that inelastic scattering in ^{238}U in current evaluations is too large. Integral measurements of $^{238}U/^{235}U$ fission ratios have suggested that the ^{238}U inelastic scattering above the ^{238}U fission threshold at 1.5 MeV may be too high, but this is above the energy range of Dr. Reitmann's measurements. The paper presented at this Conference by Dr. Campbell (CN-26/116) shows that other explanations for these discrepancies between integral measurements and calculation are possible. Integral measurements also suggest the necessity for higher inelastic-scattering cross-section values for ^{238}U at lower energies.

W.G. DAVEY (Chairman): My comment is similar to that made by Dr. Story earlier in this session. Perhaps the greatest need, from the point of view of reactor physics calculations, is to obtain energy transfer cross-sections. Thus, discrepancies in the differential cross-sections for a low-lying level (such as that at 45 keV in ^{238}U) are perhaps not as important as they seem, unless this cross-section is then subtracted from the total inelastic scattering cross-section to give the remaining cross-sections, in which case errors may be introduced.

MESURE DES SECTIONS EFFICACES DES REACTIONS (n, 2n) ET (n, 3n) DES MATERIAUX FISSILES PAR LA TECHNIQUE DU GROS SCINTILLATEUR LIQUIDE

J. FREHAUT, J. GAURIAU, G. MOSINSKI, M. SOLEILHAC
CEA, Centre d'études
de Bruyères-le-Châtel,
France

Abstract — Résumé

MEASUREMENTS OF (n, 2n) AND (n, 3n) REACTION CROSS-SECTIONS OF FISSIONABLE MATERIALS USING A LARGE LIQUID SCINTILLATOR.

Working with the technique involving the use of a large liquid scintillator, the authors developed a method for measuring (n, 2n) and (n, 3n) cross-sections relative to fission cross-section in fissionable materials. The method consists in using the preferential time distribution of the instants at which the emitted neutrons are detected. By comparing the probability of detecting two (or three) neutrons with the previously measured probability of the emission of two (or three) fission neutrons, the authors derive the relative cross-sections. They present the first results obtained, and, more particularly, those for ^{238}U.

MESURE DES SECTIONS EFFICACES DES REACTIONS (n, 2n) ET (n, 3n) DES MATERIAUX FISSILES PAR LA TECHNIQUE DU GROS SCINTILLATEUR LIQUIDE.

En utilisant la technique du gros scintillateur liquide les auteurs ont mis au point une méthode de mesure des sections efficaces des réactions (n, 2n) ou (n, 3n) relatives à la section efficace de fission pour les matériaux fissiles. La méthode consiste à utiliser la répartition privilégiée dans le temps des instants de détection des neutrons émis. En comparant la probabilité de détecter deux (ou trois) neutrons à la probabilité déjà mesurée d'émission de deux (ou trois) neutrons de fission les auteurs déduisent les sections efficaces relatives. Ils présentent les premiers résultats obtenus notamment sur ^{238}U.

1. INTRODUCTION

Nous mettons actuellement au point une méthode de détection des réactions émettant au moins deux neutrons (fission, réactions (n, 2n), (n, 3n)) qui est une application particulière de la technique classique de détection des neutrons avec un gros scintillateur liquide.

La plupart des méthodes de mesure de sections efficaces (n, 2n) ou (n, 3n) sur matériaux fissiles ont utilisé des techniques radiochimiques, car les techniques classiques de physique nucléaire ne permettent pas de distinguer les neutrons de fission des neutrons (n, Nn).

La technique que nous proposons peut aussi être utilisée pour mesurer des sections efficaces (n, Nn) sur matériaux non fissiles. La mesure récente de Holmberg [1] en est un exemple.

2. PRINCIPE

La méthode consiste à utiliser la répartition privilégiée dans le temps, par rapport à l'instant de la réaction, des époques de détection des neutrons émis.

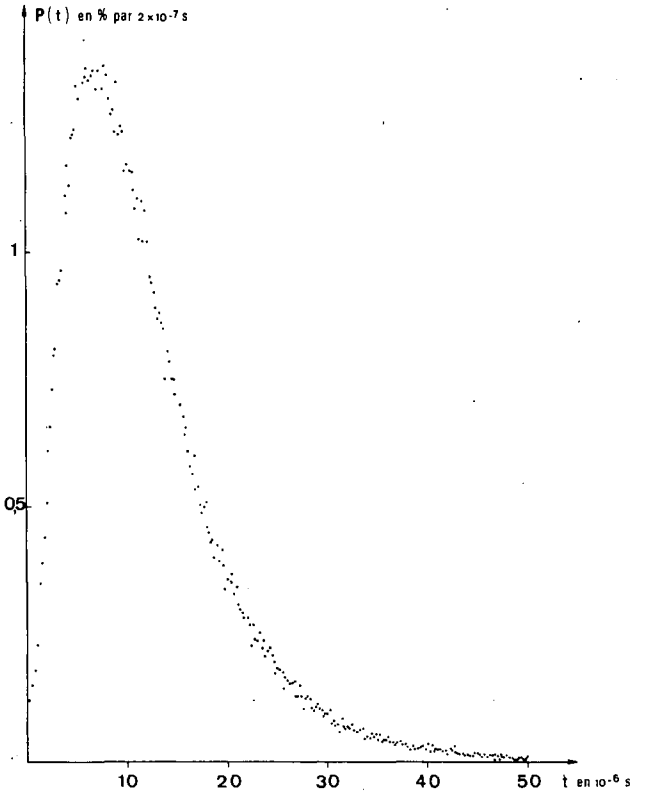

FIG.1. Probabilité de détection d'un neutron en fonction du temps suivant son émission.

En comparant la probabilité de détecter deux (ou trois) neutrons à la probabilité mesurée par ailleurs d'émission de deux (ou trois) neutrons de fission, nous en déduisons les sections efficaces relatives.

3. DETECTEUR DE NEUTRONS

Le détecteur de neutrons utilisé est un gros scintillateur liquide de 250 litres décrit dans la référence [2].

Le processus de détection des neutrons est bien connu: Rappelons simplement que les neutrons, d'abord thermalisés par chocs successifs sur les noyaux d'hydrogène, sont, après migration dans le liquide, capturés par le gadolinium dissous dans celui-ci. Les gamma de capture émis sont détectés par 12 photomultiplicateurs.

La probabilité de détection en fonction du temps d'un neutron émis à l'instant 0 au centre de la sphère est donnée sur la figure 1. L'efficacité de détection est de l'ordre de 80%.

4. CAS DES REACTIONS (n, Nn)

Alors que la fission est accompagnée d'une émission de deux fragments et d'environ 9 MeV de gamma prompts dont la détection permet une bonne identification du phénomène, dans le cas des réactions (n, Nn), l'émission des neutrons est rarement accompagnée de gamma détectables.

L'instant de la réaction ne peut donc être déterminé par l'un de ses produits; il faut alors utiliser des bouffées de neutrons incidents et analyser à chaque bouffée ce que détecte le scintillateur.

Le temps d'analyse étant de l'ordre de 50 μs (fig. 1) il est donc nécessaire d'utiliser une période de pulsation de l'accélérateur supérieure. Dans ces conditions le flux de neutrons que l'on peut obtenir est très faible. Pour retrouver une statistique suffisante il faut augmenter la masse de matériau et on ne peut plus le placer alors dans une chambre à fission.

A chaque bouffée de neutrons incidents on enregistrera donc des impulsions correspondant à l'un des cas:

bruit de fond
réaction (n, n) ou (n, n') + bruit de fond
réaction (n, 2n) + bruit de fond
réaction (n, 3n) + bruit de fond
fission + bruit de fond.

Si l'on peut soustraire le bruit de fond, on connaîtra, compte tenu de l'efficacité de détection, le nombre de fois où N = 1, 2, 3 ... etc. neutrons ont été émis.

Pour N > 3 il ne peut s'agir que de neutrons de fission. Nous avons mesuré avec une précision de 5% [2] les probabilités $P(\nu)$ d'émission de ν neutrons par fission.

Ces résultats et les données pour N > 3 nous permettent donc de calculer le nombre de fissions analysées.

Le nombre de réactions (n, 2n) sera la différence entre le nombre d'événements où deux neutrons ont été émis et le nombre de fissions à deux neutrons. On détermine de la même façon le nombre de réactions (n, 3n).

5. PROBLEME DU BRUIT DE FOND

Dans nos conditions expérimentales, le bruit de fond moyen est d'environ 0,1 coup par 30 μs. Compte tenu du flux de neutrons incidents et de la masse de matériau fissile utilisée (10 g), pour les cas où nous détectons deux impulsions nous n'avons qu'une probabilité de 3% de détecter deux neutrons.

On ne peut donc espérer faire de mesures sérieuses en se contentant de compter le nombre d'événements détectés.

Nous avons mis au point une méthode de discrimination neutron-bruit de fond qui rend possible des mesures acceptables de sections efficaces σ(n, Nn) dans des conditions expérimentales difficiles.

6. DISCRIMINATION NEUTRON-BRUIT DE FOND

Nous mesurons la probabilité f(t) de détecter à l'instant t un neutron émis à l'instant 0. Dans le même domaine de temps, un bruit de fond a une probabilité h(t) d'arrivée dans le temps, à peu près constante (s'il suit une loi proche de la loi de Poisson). Il est possible de calculer les probabilités $P_i^n(t)$ que le $i^{ème}$ neutron de n émis à l'instant 0 soit détecté à l'instant t. De même on peut calculer (et mesurer) les probabilités $B_i^n(t)$ que le $i^{ème}$ bruit de fond de n détectés arrive à l'instant t.

La discrimination s'obtient en mesurant, à l'aide d'un codeur de temps d'événements multiples [3], l'instant d'arrivée, par rapport à la bouffée de neutrons incidents, de chacune des impulsions détectées pendant un temps donné T. On dispose ainsi des probabilités $R_i^n(t)$ que la $i^{ème}$ impulsion de n comptées arrive à l'instant t.

7. CALCUL DES PROBABILITES $P_i^n(t)$

On peut montrer facilement que

$$P_i^n(t) = nC_{n-1}^{i-1} f(t) \{F(t)\}^{i-1} \{1 - F(t)\}^{n-i}$$

où f(t) représente la probabilité d'arrivée en temps d'un neutron émis à l'instant zéro et $F(t) = \int_0^t f(\theta)d\theta$. La normalisation choisie est $F(T) = 1$.

Lorsque le bruit de fond est poissonien la loi $B_i^n(t)$ a la même forme que la loi $P_i^n(t)$ avec $f(t)dt = \lambda e^{-\lambda t}\, dt$.

En pratique un bruit de fond arrivant par paquets d'impulsions se superpose à un bruit de fond du type poissonien.

8. CALCUL DES PROBABILITES $R_i^n(t)$

La probabilité d'arrivée dans le temps de la $i^{ème}$ impulsion de n impulsions comptées peut s'écrire

$$R_i^n(t) = \sum_{j=0}^{n} G_{j,n-j}^n \left\{ \sum_{\ell=0}^{n-j} C_{n-j}^{\ell} C_j^{i-\ell} P_{i-\ell}^{i-\ell}(t) \int_t^T P_1^{j-i+\ell}(\theta)\, d\theta \int_0^t B_\ell^\ell(\theta)\, d\theta \int_t^T B_1^{n-j-\ell}(\theta)\, d\theta \right.$$

$$\left. + \sum_{k=0}^{j} C_j^k C_{n-j}^{i-k} B_{i-k}^{i-k}(t) \int_t^T B_1^{n-j-i+k}(\theta)\, d\theta \int_0^t P_k^k(\theta)\, d\theta \int_t^T P_1^{j-k}(\theta)\, d\theta \right\}$$

La sommation sur j permet d'envisager tous les cas où sur n impulsions on a j neutrons et n-j bruits de fond détectés. Pour une telle répartition, dont la probabilité est $G_{j,n-j}^n$, deux cas se présentent:

- la $i^{ème}$ impulsion correspond à la détection d'un neutron et ℓ bruits de fond sont détectés avant le temps t
- la $i^{ème}$ impulsion correspond à la détection d'un bruit de fond et k neutrons sont détectés avant l'instant t.

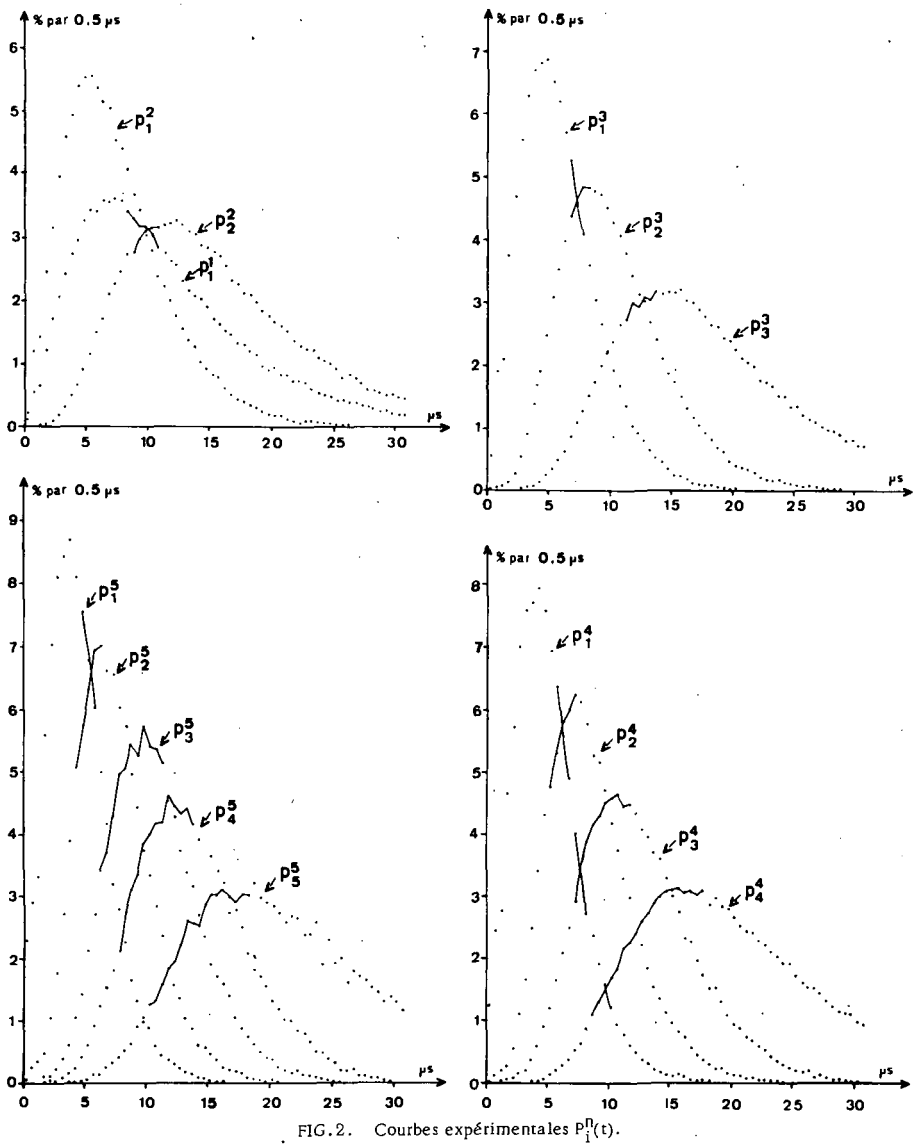

FIG. 2. Courbes expérimentales $P_i^n(t)$.

A chacun de ces deux cas correspond une sommation entre les accolades.

On montre que l'on peut écrire $R_i^n(t)$ sous la forme

$$R_i^n(t) = \sum_{j=0}^{n} G_{j,n-j}^n \, A(n, i, j, t)$$

où les quantités A(n, i, j, t) sont entièrement calculables à partir des résultats expérimentaux.

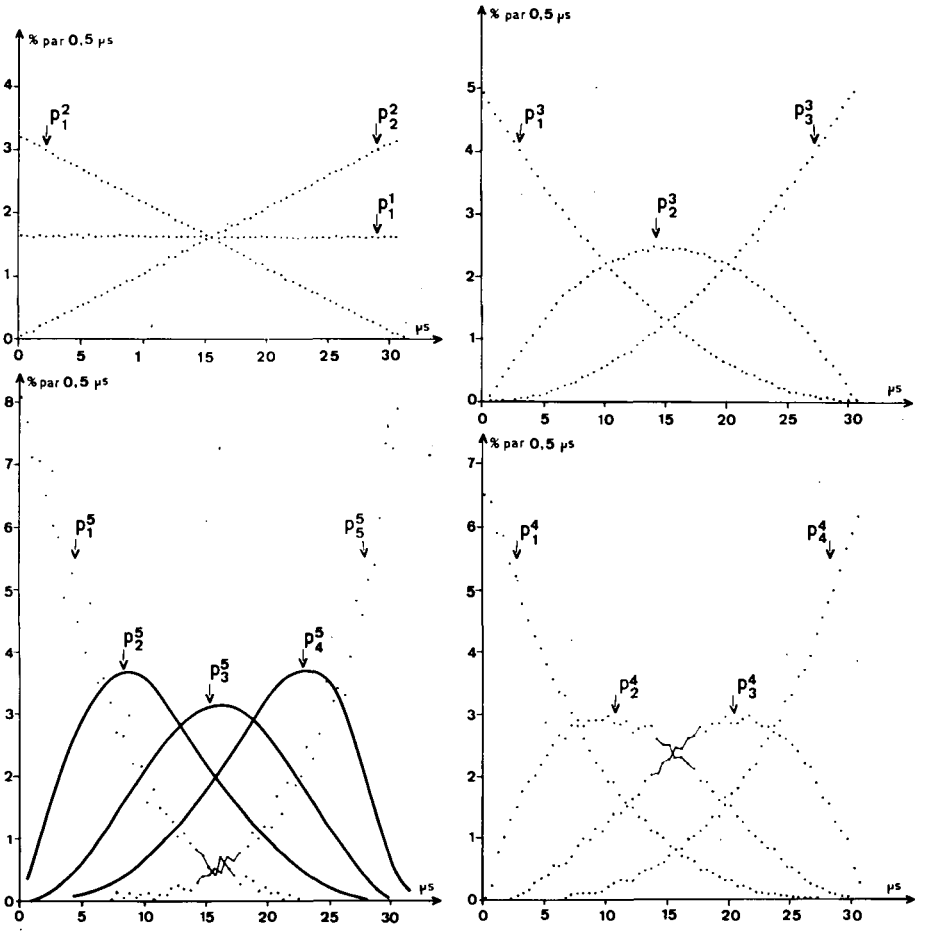

FIG. 3. Bruit de fond poissonien.

9. CORRECTION DU BRUIT DE FOND

Pour chaque valeur de n on dispose de n équations $R_i^n(t)$. Le nombre de coefficients $G_{j,n-j}^n$ à déterminer est n+1 mais il existe également la relation de normalisation

$$\sum_{j=0}^{n} G_{j,n-j}^n = 1$$

Les solutions $G_{j,n-j}^n$ sont indépendantes du temps; ce fait permet une détermination plus précise de ces coefficients en ajustant les courbes théoriques $R_i^n(t)$ sur les courbes expérimentales par la méthode des moindres carrés.

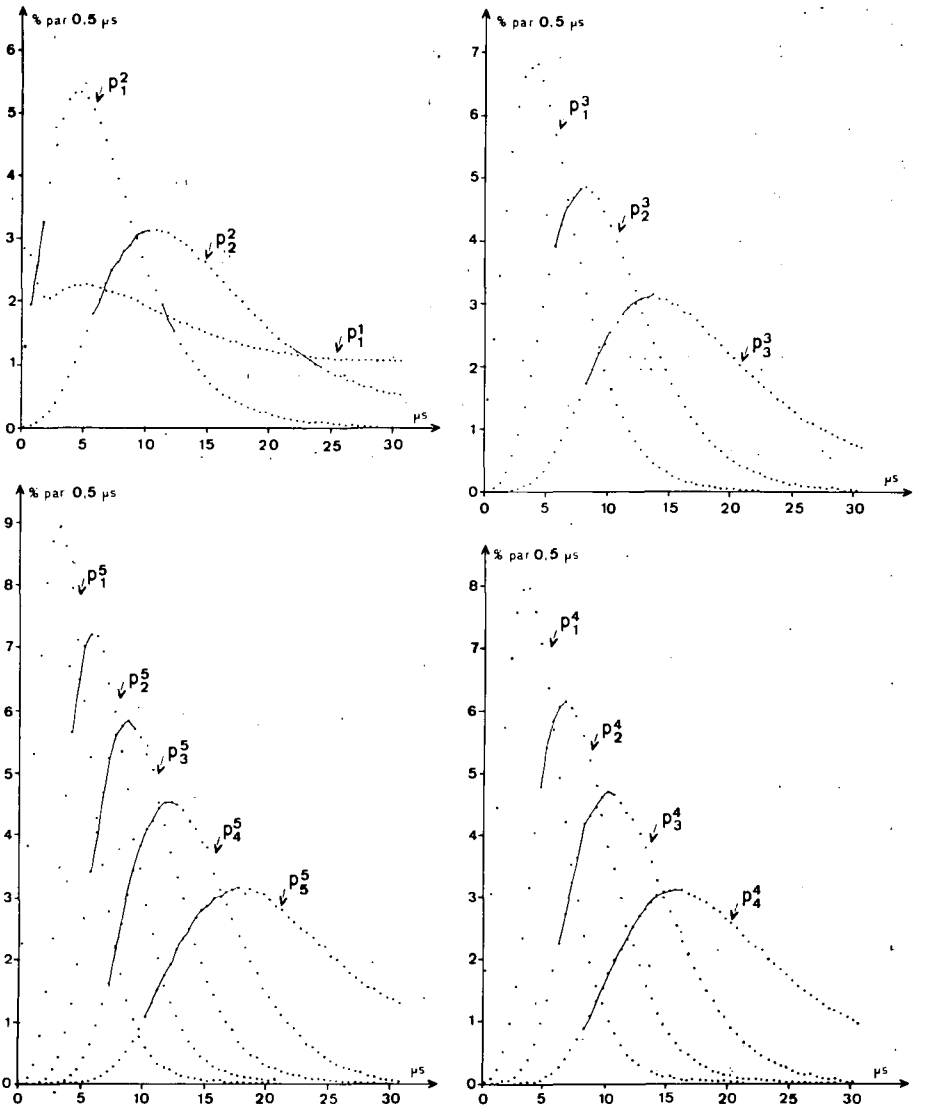

FIG. 4. Mesures de $\bar{\nu}$ du ^{252}Cf sans détection du fragment de fission.

Le nombre de fois où l'on a détecté j neutrons est donné par la relation

$$Q(j) = \sum_{n=j}^{n\,max} N(n)\, G^{n}_{j,\,n-j}$$

où N(n) est le nombre de fois où l'on a compté n impulsions.

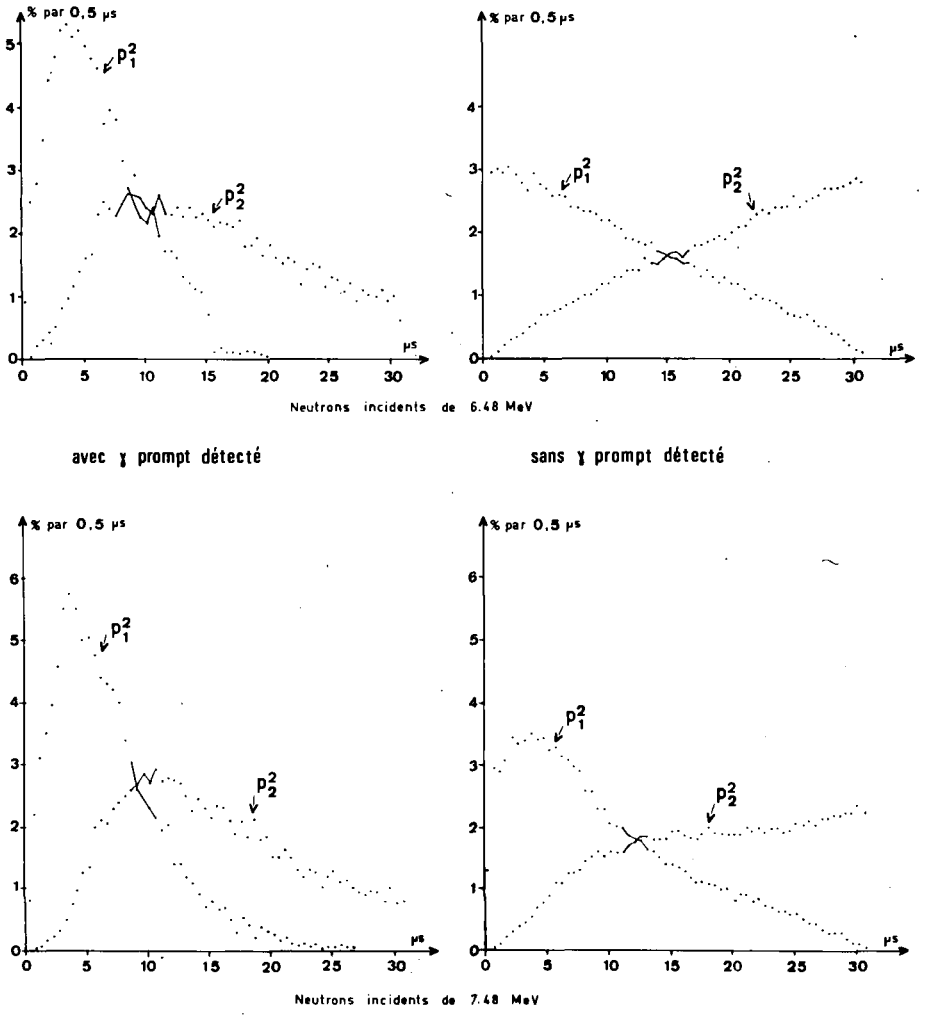

FIG.5. Mise en évidence de la réaction (n,2n) sur ^{238}U.

10. RESULTATS PRELIMINAIRES

La figure 2 représente les courbes $P_i^n(t)$ mesurées avec les neutrons de fission du ^{252}Cf, l'instant initial étant défini par la détection des gamma prompts et d'un des deux fragments. Ces courbes vérifient la loi du paragraphe 7.

La figure 3 représente les courbes $B_i^n(t)$ mesurées lorsque le bruit de fond est poissonien. Les lois obtenues sont en parfait accord avec les lois théoriques, ce qui permet de tester le bon fonctionnement du système de mesure.

La figure 4 donne un exemple d'utilisation de la méthode où, cette fois, nous mettons en évidence les neutrons de fission du ^{252}Cf sans détecter le fragment de fission; nous déclenchons le système d'analyse sur toute impuslion en provenance du scintillateur liquide à condition qu'aucune impulsion ne soit apparue dans les 50 μs qui précèdent.

Enfin la figure 5 met en évidence l'influence du phénomène (n, 2n) dans le cas du ^{238}U sur les courbes $R_i^n(t)$ pour deux énergies de neutrons, l'une inférieure au seuil (6, 48 MeV), l'autre supérieure (7, 48 MeV).

Nous avons distingué à gauche de la figure les cas où il existe des gamma prompts en coïncidence avec la bouffée de neutrons incidents (fission et une partie des réactions (n, 2n)).

Lorsqu'il n'y a pas de coïncidence (courbes de droite) et lorsqu'on est en dessous du seuil (n, 2n), on obtient pratiquement les courbes $B_i^n(t)$ pour le bruit de fond naturel; lorsqu'on est au-dessus du seuil, on voit se superposer une composante correspondant à l'apparition des deux neutrons (n, 2n) pour lesquels on n'a pas détecté de gamma synchrones.

11. CONCLUSION

Cette méthode de mesure est en cours de développement; elle doit permettre de réaliser des mesures d'activités neutroniques de neutrons de fission ou des mesures de sections efficaces (n, 2n) ou (n, 3n) sur matériaux fissiles avec un précision comprise entre 5 et 10%.

REFERENCES

[1] HOLMBERG, M., Nucl. Phys. A 129 (1969) 327.
[2] SOLEILHAC, M., FREHAUT, J., GAURIAU, J., J. nucl. Energy 23 (1969) 257.
[3] LAGET, J.P., et al., C.r. Coll. int. sur l'électronique nucléaire II, Versailles (1968) 80.

Invited Paper

STATUS OF IMPORTANT HEAVY-ELEMENT NUCLEAR DATA ABOVE THE RESONANCE REGION

W.G. DAVEY
Argonne National Laboratory,
Idaho Falls, Idaho,
United States of America

Abstract

STATUS OF IMPORTANT HEAVY-ELEMENT NUCLEAR DATA ABOVE THE RESONANCE REGION.

The status of $\bar{\nu}$-values, capture, and fission cross-sections for the most important heavy elements, ^{235}U, ^{238}U, ^{239}Pu, ^{240}Pu, and ^{241}Pu is evaluated to determine both the accuracy to which the data are known and to what degree the needs of reactor physicists are satisfied. Ratios of other fission cross-sections to that of ^{235}U are reasonably well known but the absolute value of the reference ^{235}U cross-section is very unsatisfactorily defined above 100 keV. The capture cross-section of ^{238}U is uncertain to about 15% below 100 keV if both ^{10}B (n, α) and ^{235}U (n, f) cross-sections are used as references. The ratio relative to ^{235}U (n, f) alone shows better consistency but even if this standard is correct the absolute capture cross-section suffers due to the stated uncertainties in ^{235}U (n, f) data.

The ratio of capture-to-fission (α) in ^{235}U and ^{239}Pu is satisfactorily known, but the α-values for ^{240}Pu and ^{241}Pu remain unmeasured.

Best values of $\bar{\nu}$ for the heavy isotopes at thermal energies are related to $\bar{\nu}$ for ^{252}Cf, but are not strongly affected by its precise value and tend to be incompatible with the ^{252}Cf data. The best values for $\bar{\nu}$ for ^{252}Cf have tended to lie in two groups differing by approximately 2% and a recent precise measurement gives additional support for the lower data which further emphasizes the incompatibility with the heavy element $\bar{\nu}$-data.

Even if thermal-neutron $\bar{\nu}$-values are satisfactory, the variation of $\bar{\nu}$ with neutron energy may be of comparable importance for fast-reactor physicists. The evidence for non-linear dependence of $\bar{\nu}$ for ^{235}U with neutron energy below 1 MeV is fairly clear, but better definition of the energy dependence for ^{235}U is needed. It is important to determine if similar behaviour occurs in the $\bar{\nu}$-values for the other isotopes, particularly ^{239}Pu, but present experimental data are not sufficiently detailed to show if this occurs.

1. INTRODUCTION

Although several cross sections of many, heavy, medium, and moderately light, nuclei enter into the physics of fast reactors, among the heavy elements, those reactions which involve the absorption and creation of neutrons are by far the most important in reactor design.

This is true because these cross sections determine to the greatest degree the critical sizes, breeding ratios, and power distributions in the reactors. By contrast, the total, elastic- and inelastic-scattering cross sections of the structural, coolant, and other diluent materials present in the reactor tend to obscure the effects of similar cross sections in the heavy fissile and fertile materials, at least in power reactors, although not always in zero-energy critical experiments where diluents are minimized.

For this reason, the capture and fission cross sections of the fissile and fertile materials, and the number of neutrons generated per fission, are the parameters of pre-eminent importance and are considered in this review.

2. THE ^{235}U FISSION CROSS SECTION BETWEEN 20 keV AND 20 MeV

Although there have been many measurements of this cross section, only those data which have been made using precise, well-defined, flux-measuring techniques and which are well documented should be considered. A review which discusses most of the experimental data has been given by Davey [1,2].

The measurements worthy of serious consideration at the present time are as follows:

(a) Those measured relative to the (n,p) cross section,

1. Allen and Ferguson [3], over the range 30 keV to 3.0 MeV, using hydrogen- and methane-filled proportional counters for flux determination.

2. Diven [4], over the range 403 keV to 1.62 MeV, using a solid, hydrogenous, radiator to monitor the flux and provide an absolute determination at 1.27 MeV.

3. White [5], over the range 40 keV to 14.1 MeV, using a hydrogen-filled proportional counter to measure the flux up to 505 keV, and a solid, hydrogenous, radiator at higher energies.

4. Smith, Henkel, and Nobles [6], as revised by Hansen, McGuire, and Smith [7], over the range 2.2 MeV to 20.5 MeV, using a proton-recoil telescope to measure the flux.

(b) That measured using an energy-insensitive detector,

5. Poenitz [8,9,10], over the range 30 keV to 1.47 MeV, using a beam-catcher, "grey", neutron detector to monitor the flux and normalizing at 30 keV to an absolute measurement by Knoll and Poenitz [11]. The "grey" detector counts the capture gamma rays in a hydrogen catcher; the normalization at 30 keV is based primarily upon a knowledge of the total emission of neutrons from a ^{7}Li target by measurement of the resulting ^{7}Be activity.

(c) That measured using a known-strength source,

6. Perkin, et al [12], at 24 keV, using an antimony-beryllium photoneutron source calibrated in a manganese-bath and in an oil-bath, and also related to the A.E.R.E., Harwell, boron-pile.

Of these measurements, the four made relative to the (n,p) cross section must take a pre-eminent place since this cross section is known so precisely. Of this group of four, the White data must constitute the standard by which the others should, at least at first, be judged since they cover the entire energy range and were performed most recently with the most careful attention to the problems of relating the proton-recoil measurements to the neutron flux. Although, at the present time, White's data are, in the author's opinion, in this position, it is not an inviolate one since, as subsequent discussion will show, there are several minor, and one major discrepancy with White's values.

We will now discuss the individual measurements, largely with reference to White's work, in order to show areas of agreement and disagreement. All the experimental data are presented in Fig. 1. For clarity, the experimental errors are not shown.

Allen and Ferguson's results are in very good agreement with those of White in shape above 120 keV but they are uniformly 6% larger. The disagreement in magnitude is somewhat outside the combined experimental errors and is significant from the viewpoint of reactor design, but in view of the more sophisticated techniques available to White, it is possible that this difference reflects the improvements possible with time. However, it is disconcerting to note that the Diven data, which are in excellent agreement in shape with those of Allen and Ferguson, and in good agreement in shape with White's, lie 5% above White's and thus in excellent agreement with Allen and Ferguson in magnitude as well as shape.

Below 120 keV, the Allen and Ferguson values are in very strong disagreement with White, being about 25% larger, and this can be construed as disagreement in shape when considering the entire common energy range. Since the disagreement in shape is only evident when including the lowest-energy points where there is greatest difficulty in determining the flux from the proton-recoil distribution, it is possible that the shape disagreement only reflects the improvements in flux measurements between the earlier and later measurements. On this interpretation, the Allen and Ferguson data at 30 and 60 keV would be rejected.

The Poenitz measurements are in opposition to the above viewpoint since there is reasonable agreement in shape between Allen and Ferguson, and Poenitz over the entire range 30 keV to 1.5 MeV although the disagreement in magnitude is 20 to 25%. The Poenitz data are in good agreement in magnitude with White below 100 keV but are about 10% lower than White from about 300 keV to 1.5 MeV. The agreement in shape with White in this higher energy range is good. This discrepancy could arise if the efficiency of the Poenitz "grey" detector with energy were incorrect, but measurements by Poenitz [10] have generally substantiated his earlier calculations [9] of the detector efficiency. Alternatively, the absolute measurements of Allen and Ferguson, Diven, and White, in the few hundred keV to few MeV range would have to be incorrect or the normalization of Poenitz's data at

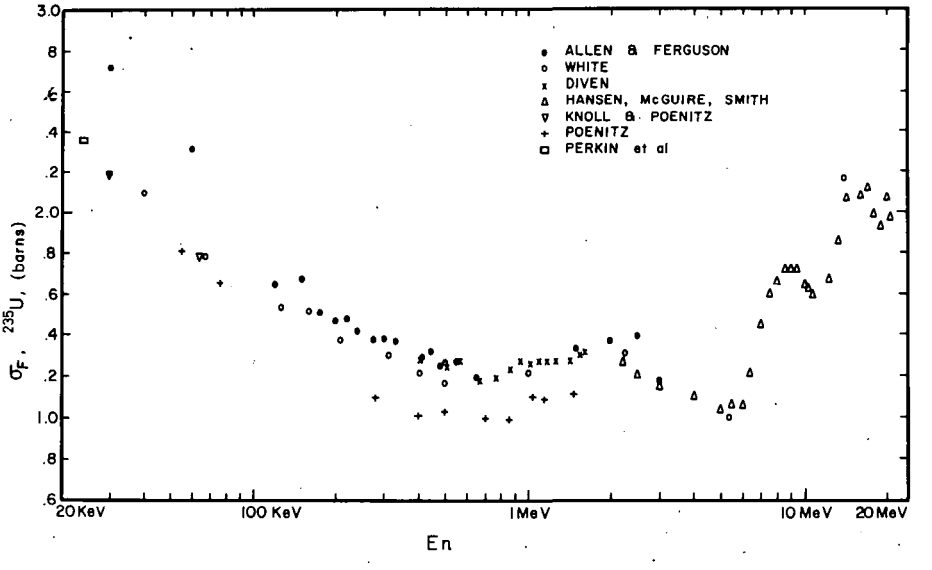

FIG. 1. The fission cross-section of ^{235}U from 20 keV to 20 MeV.

30 keV would have to be incorrect. The cross section measured at 24 keV by Perkin, et al, is however in good agreement with the Poenitz normalization at 30 keV and consistent with White's measurement at 40 keV so that the lower values are well supported at the low-energy end of the range. Furthermore, a ^{235}U fission cross section as low as one barn in the few hundred keV to 1 MeV range would be difficult to reconcile with the critical sizes of ^{235}U-fueled fast reactors.

At the highest energies, the revised data of Hansen, McGuire, and Smith are in quite good agreement with the White values although they cannot be said to be in disagreement with the slightly higher values of Allen and Ferguson and also Diven, or the lower values of Poenitz since the energy ranges either do not overlap or only overlap slightly.

The Los Alamos data prior to revision do not agree with White and some concern may be expressed at the propriety of applying calculated revisions many years after completion of the original measurements. In the present author's view, this procedure is perfectly legitimate if the original experimental conditions are well known, and this certainly appears to be true in the present instance.

In summary, there are considerable areas in which it appears that this vital question of the ^{235}U fission cross section may be close to resolution, but that there are also pressing problems which must be resolved. First, the question of the correctness of Poenitz's low data in the several hundred keV to few MeV region (supported by agreement in shape with Allen and Ferguson) must be resolved. The correctness or incorrectness of the two high values of Allen and Ferguson at 30 and 60 keV may be viewed as part of the same problem. Second, assuming resolution of the first question, the 5% to 6% discrepancy between White, and Allen and Ferguson, and Diven must be removed. Third, better confirmation of the corrected Los Alamos data at high energies is needed.

The inescapable conclusion is that additional measurements are needed, and that it is essential that:

(a) these should be measured relative to the best standard available, the (n,p) cross section;

(b) they must have a precision approaching 2%; and

(c) they should cover the entire energy range from a few tens of keV up to 10 MeV or higher in order to avoid questions of non-overlapping data.

This is the most important single question in the area of nuclear data above the resonance region and the five to ten man years effort probably needed to resolve it is completely justified. Indeed, in view of the great importance of these data, it is by no means clear that a single new measurement would suffice, and several laboratories should be encouraged to perform this work.

3. FISSION CROSS SECTIONS OF THE PLUTONIUM ISOTOPES

The fission cross sections of ^{239}Pu, ^{240}Pu, ^{241}Pu, and ^{242}Pu are best defined by their ratios to the fission cross section of ^{235}U. The uncertainties in these plutonium isotope cross sections are consequently determined not only by the errors in the cross section ratios but also by those in the ^{235}U cross section already discussed.

These cross sections have been completely discussed and evaluated by the author in 1966 and 1968 (Davey [1,2]), and the few additional measurements since these dates generally confirm these evaluations so that the discussion here will be limited to comments upon these published evaluations.

3.1 $^{239}Pu/^{235}U$ Ratio

In 1968, this ratio was defined by the data of Allen and Ferguson [3] (30 keV to 3 MeV), White, Hodgkinson, and Wall [13] (40 keV to 500 keV), Perkin, et al [12] (24 keV), White and Warner [14] (1.0, 2.25, and 5.4 MeV), and Smith, Henkel, and Nobles [15] (2.5 MeV to 10 MeV). The low-precision data of Dubrovina and Shigin [16] were used to make an approximate extrapolation below 24 keV.

On the basis of these data, the fission ratio appeared to be well-defined (about + 3%) from 24 keV to about 1 MeV, uncertain to about 10% between 1 MeV and 3 MeV, and defined to about 3% between 3 MeV and 10 MeV. Only one measurement of White, Hodgkinson, and Wall (at 40 keV), and three points of Allen and Ferguson (2 MeV to 3 MeV) appear to be discrepant.

Since 1968, we have the additional measurements of Lehto [17] (0.24 keV to 24 keV), Poenitz [18] (150 keV to 1.4 MeV), and Pfletschinger and Käppeler [19] (5 keV to 1 MeV). Both Poenitz, and Pfletschinger and Käppeler pay particular attention to, and identify, a dip (of about 7%) in the ratio between about 800 keV and 1.2 MeV. This dip occurs because of a rise in the ^{235}U cross section in this energy range. With the exception of this dip, all three additional measurements provide reasonably good confirmation of the earlier work, at least down to about 3 keV. Below this energy, Lehto's work shows a significant rise in the ratio. A discussion of the data in this region is beyond the scope of the present paper.

Taking all data, the ratio is defined to about 3% to 4% accuracy from about 10 keV to 800 keV, to slightly less than this between 800 keV and 1.5 MeV, it shows discrepancies of perhaps 10% between 1.5 MeV and 3 MeV, and it is known to about 3% to 5% accuracy between 3 MeV and 10 MeV.

3.2 $^{240}Pu/^{235}U$ Ratio

No additional measurements have been made since the 1968 evaluation and the conclusion reached at that time therefore still stands.

The subthreshold plateau between 10 keV and about 200 keV is defined to a satisfactory precision (since the cross section is so low) of about 10% to 20%, principally by the data of Perkin, et al, and Gilboy and Knoll [20]. From 200 keV to 1 MeV, where the cross section rises steeply, there is good consistency between the results of Nesterov and Smirenkin [21], and Henkel, Nobles, and Smith [22], but the true accuracy is probably not better than 10% and the agreement is partly accidental. From 1 MeV to 10 MeV, the measurements of White and Warner, Nesterov and Smirenkin, and Henkel, Nobles, and Smith are in reasonable agreement in shape and the accuracy is no worse than 10% and may be as good as 5%.

3.3 $^{241}Pu/^{235}U$ Ratio

Here too there have been no additional measurements since the 1968 evaluation (and there was only one between the 1966 and 1968 studies).

There is reasonable consistency between the results of Smith, Smith, and Henkel [23], Butler and Sjoblom [24], White, Hodgkinson, and Wall,

and Perkin, et al, which together cover the range 24 keV to 10 MeV and the ratio may be defined as well as 5% over this range, but the number of measurements is few and the degree of overlap is not great so that this may be an optimistic view. Between 24 keV and a few keV there are no measurements.

3.4 $^{242}Pu/^{235}U$ Ratio

The only measurement of this ratio is that made by Butler [25] in 1960. The energy range covered is 100 keV to 1.7 MeV and the quoted accuracy is 5%.

4. FISSION CROSS SECTION OF ^{238}U

Here too, there have been no additional measurements since the 1968 evaluation.

The ^{238}U cross section is defined by the ratio measurement $^{238}U/^{235}U$, and the precise ratio data of Stein, Smith, and Grundl [26] (1.5 MeV to 5.0 MeV) and White and Warner (2.25 MeV and 5.4 MeV) form the basis for the evaluation. The data of Lamphere [27], normalized by multiplication by a factor 0.94, were used to define the shape over the threshold region and up to 3 MeV, and the results of Hansen, McGuire, and Smith provided an extension of the other data up to 10 MeV.

The Stein, Smith, and Grundl ratios have a quoted accuracy of approximately 2%, and thus the error in the ^{238}U cross section appears to lie almost entirely in the uncertainty in the ^{235}U fission cross section. In this regard, it is disconcerting to note that the derived ^{238}U cross section when averaged over the Watt form of the ^{235}U thermal-neutron induced fission spectrum is 0.282b [2] which is in poor agreement with the mean experimental value of 0.309b obtained from the measurements of Leachman and Schmitt [28], Richmond [29], and Nikolaev, et al [30]. This disturbing disagreement could clearly arise from a number of sources, but it again emphasizes the need for establishment of the ^{235}U fission cross section.

5. NECESSARY FISSION RATIO MEASUREMENTS

The $^{239}Pu/^{235}U$ ratio is apparently defined to about 3% or better except for the limited range 1.5 MeV to 3.0 MeV where a small number of measurements would be useful. The ratios for the three other plutonium isotopes show no significant inconsistencies but the ratios are not known to better than 5% to 10% accuracy and additional data are needed for all three isotopes over the entire energy range. The $^{238}U/^{235}U$ fission ratio is defined to a few percent accuracy. It must be noted that even when the ratios are well known, the derived fission cross sections are completely dependent upon the ^{235}U fission cross section.

6. CAPTURE CROSS SECTION OF ^{238}U

This cross section has recently been evaluated by the author (Davey [31]) and this work may be consulted for a complete discussion of the principal discussions and conclusions.

The objective of the study was to provide evaluated data which could be used in the analysis of fast reactor experiments and, for this purpose, it is of great importance to insure that all data are derived on a consistent basis. Hence, the ^{238}U capture cross sections were evaluated using, as far

as possible, the same reference cross sections as were used for the previous fission cross section evaluations [1,2], and these selected fission data were used where necessary to re-normalize ^{238}U capture data. For the same reason, the capture measurements of Barry, Bunce, and White [32] played a dominant role in the evaluation since the neutron flux was determined using instruments and techniques developed by White for his precise measurements of the ^{235}U fission cross section. The importance of White's fission measurements has been emphasized earlier in the discussion.

After a careful study of all the individual measurements, it was found that some experimental data had to be rejected completely, some on the basis of identification of probable errors in technique, some on the basis of inadequate and inconsistent reporting, and some simply on the basis of incompatibility with well-defined reference data such as those of Barry, Bunce, and White. The data remaining was grouped into three categories which include:

(a) "absolute" (as opposed to shape) measurements alone (defined as measured relative to the (n,p) or ^{235}U fission cross section,

(b) good shape measurements, and

(c) less reliable "absolute" and shape data.

Here we will only discuss the information in the first two categories since these alone were used in deriving the final recommended cross sections.

In Category (a), we have the following:

1. Barry, Bunce, and White (127 keV to 7.6 MeV) for which the reference was essentially the (n,p) cross section and White's ^{235}U fission cross section; the original data were revised slightly above 1.3 MeV to give accord with selected ^{235}U data [1,2].

2. Belanova, et al [33], (24 keV) measured with a Sb-Be source, as corrected by Miller and Poenitz [34].

3. deSaussure, et al [35], (30 keV and 64 keV) relative to the capture-plus-fission cross section of ^{235}U; these were re-normalized to Davey's ^{235}U cross sections.

4. Gibbons, et al [36], (30 keV and 65 keV) which were normalized to absolute measurements made at 24 keV by Schmitt and Cook [37].

5. Macklin, Gibbons, and Pasma [38], (8 keV to 58 keV) made relative to the capture cross section of Ta but indirectly related to the ^{235}U absorption cross section.

6. Macklin, Lazar, and Lyon [39], (25 keV) using an absolutely calibrated Sb-Be photoneutron source.

7. Menlove and Poenitz [40], (25 keV to 500 keV) which was absolute at 30 keV and in which the variation in neutron flux was measured using the "grey" neutron detector described by Poenitz [9]; these data disagreed with those of Barry, Bunce, and White by 17% in a similar manner to the disagreement between Poenitz's and White's ^{235}U fission cross sections (see the previous discussion of the ^{235}U data) and hence ^{238}U capture/^{235}U fission ratios were formed using the Poenitz ^{235}U data, and ^{238}U capture cross sections were subsequently derived from the ratios using Davey's ^{235}U fission cross sections.

8. Perkin, O'Connor, and Coleman [41], (14.5 MeV) using an accelerator source of known flux.

9. Poenitz [42], (30 keV to 900 keV) where the ratio to the ^{235}U fission cross section was measured; Davey's ^{235}U data were used to derive ^{238}U capture values.

In Category (b), good shape measurements, is only one experiment, that of Moxon [43] (500 eV to 100 keV). Here the measurements were made relative to the gamma-ray production cross section in ^{10}B using a Moxon-Rae detector. These measurements should be regarded as absolute since the ^{10}B cross section is presumably well-known, but Moxon's results lie systematically 15% below the Category (a) data and hence were multiplied by a factor 1.15 to be consistent with them. Moxon's results are particularly valuable since they cover a wide energy-range, are detailed in their energy-resolution, and have good relative precision. They are discussed further below.

All these data are shown in Fig. 2.

We will now examine some additional aspects of the "absolute" (Category (a)) data. These data exhibit good consistency with each other within the experimental errors (which are sometimes quite large). Apart from the two data points of Barry, Bunce, and White at 127 keV and 160 keV, all the points lie on a relatively smooth curve. The lower-energy values of Macklin, Gibbons, and Pasma tend to be high, but the experimental errors (which are not shown) are large and there is no real discrepancy with other data. In considering the data defined here as "absolute" it should be noted that most of the experimental data are related directly or indirectly to the ^{235}U

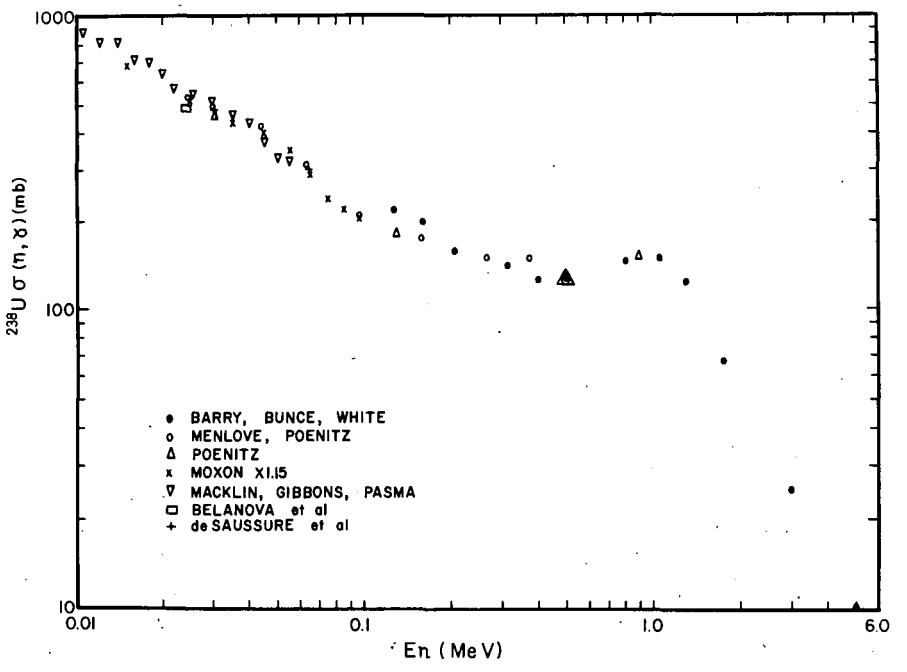

FIG. 2. The capture cross-section of ^{238}U from 10 keV to 6 MeV.

fission cross section; this is true particularly of the most important measurements of Barry, Bunce, and White; Menlove and Poenitz; and Poenitz; and the ^{238}U capture cross sections given here must be regarded as having significance only with regard to the author's evaluated ^{235}U fission cross sections. In particular, the use of Poenitz's ratio measurements, and the revision of Menlove and Peonitz's data on the basis of a presumed inaccuracy in the "grey" neutron detector is subject to the uncertainties in the absolute ^{235}U fission data discussed earlier in this paper.

In brief, the ratios of the ^{238}U capture data given here and Davey's evaluated ^{235}U fission data are essentially what have been defined in this study and not the absolute values.

This need to obtain ^{238}U capture values which are consistent with fission data is essentially the only justification for accepting Moxon's data only in a shape sense and re-normalizing them to the Category (a) data. It should be emphasized that it is by no means certain that Moxon's values are not equally good in an absolute sense, only that they are less consistent relative to the ^{235}U fission cross section. As can be seen, Moxon's data are exceedingly valuable in defining the shape of the curve and show, for example, the dip associated with the onset of inelastic scattering in the 45 keV level in ^{238}U.

For interest, it should be noted that the ^{238}U data derived here are consistent with resonance parameters derived at 4 keV and lower energies, and calculated cross sections (up to 40 keV) using the resonance parameters selected by Schmidt [44] (including Γ_γ = 24.8 meV, p-wave strength function = 2.5×10^{-4}) are within 5% to 10% of the present curve. The present data would be less consistent with the lower data suggested by Glass, et al [45], (Γ_γ = 19.1 ± 2.0 meV, p-wave strength function = $(1.8 \pm 0.3 \times 10^{-4})$, and the agreement with resonance-parameter data should be considered to be tentative.

With regard to accuracies, the situation is uncertain but it would appear unwise to assume better than 5% in the ratio of ^{238}U capture and ^{235}U fission.

There is a clear need for ^{238}U capture-to-^{235}U fission ratio measurements over the energy range from about 1 keV to a few MeV.

7. CAPTURE IN ^{235}U AND THE PLUTONIUM ISOTOPES

The capture cross sections in these materials above the resonance region are defined by measurements of α, the capture-to-fission ratio. In this energy region, measurements exist only for ^{235}U and ^{239}Pu; data for the other important isotopes, ^{240}Pu, ^{241}Pu, and ^{242}Pu are completely lacking.

For ^{235}U and ^{239}Pu, a quite complete presentation of all the experimental α values has been included by deSaussure, et al [46], in the presentation of their own experimental data and here we will only present a summary of the situation.

The important subject of the α values of ^{239}Pu from a few hundred eV up to 30 keV (see, for example, Gwin, et al [47], and Schomberg, et al [48]) is more properly considered a part of the resonance region and will not be discussed here.

In ^{235}U, the measured α-values lie in a smooth curve dropping from about 0.37 at a few tens of keV down to about 0.1 at 1 MeV. The principal experiments in this range are those of deSaussure, et al, Weston, et al [49], and Hopkins and Diven [50], and all the data are consistent within the experimental uncertainties of approximately 10%. As noted by deSaussure, et al, the measurements were made using very similar techniques and there is a possibility of similar systematic errors in all the results.

In ^{239}Pu, the situation is quite similar to that for ^{235}U with α decreasing smoothly from about 0.4 at a few tens of keV to about 0.03 at 1 MeV. There are only two measurements which may be compared over significant energy ranges, those of deSaussure, et al, and Hopkins and Diven, and here too the data agree within the 10% experimental errors. As with ^{235}U, the possibility of similar systematic errors exists.

For both ^{235}U and ^{239}Pu, the status of the existing α-data is that there exist no discrepancies that indicate serious uncertainties in the existing information but that the current uncertainty (about 10%) and the similarity in the experimental techniques used show that additional measurements are needed to a higher precision and preferably with different methods.

For ^{240}Pu, ^{241}Pu, and ^{242}Pu, the complete lack of information above the resonance energy region is an omission which could have serious consequences in the design of fast reactors which contain significant amounts of these isotopes.

TABLE I. $\bar{\nu}$ FOR ^{252}Cf (TAKEN FROM HANNA, ET AL. [51])

Author	Reassessed Value	Adopted Mean (For Each Category)
Liquid Scintillator		
Asplund-Nilsson, et al	3.830 ± 0.037	
Hopkins and Diven	3.793 ± 0.031	3.807 ± 0.024
Boron Pile		
Colvin and Sowerby	3.713 ± 0.015	3.713 ± 0.024
Dependent on NPL Manganese Bath		
Moat, et al	3.727 ± 0.056	
Colvin, et al	3.700 ± 0.031	
White and Axton	3.796 ± 0.031	
Axton, et al	3.700 ± 0.020	3.713 ± 0.024
ANL Bath		
DeVolpi and Porges	3.739[(a)] ± 0.017	3.739[(a)] ± 0.024
	Weighted Mean	3.743[(a)] ± 0.016
	Fitted Value	3.7653 ± 0.0104

(a) A revised value of 3.725 ± 0.015 has been given by DeVolpi and Porges; a revised weighted mean including this measurement (with an assigned error of 0.024) is 3.740; see text for discussion.

8. $\bar{\nu}$ VALUES

The status of the $\bar{\nu}$ values for the uranium and plutonium isotopes is best examined in two parts:

(a) that of the absolute values, and

(b) the variation of $\bar{\nu}$ with the incident neutron energy.

8.1 Absolute $\bar{\nu}$ Status

The $\bar{\nu}$ data for the relevant uranium and plutonium isotopes is strongly connected with that of ^{252}Cf since this source is widely used in experiments as a reference and frequently the ratio of $\bar{\nu}$ for a given isotope to that of ^{252}Cf is measured. However, the $\bar{\nu}$ for ^{252}Cf is not the exclusive reference since, for example, precise values of η and α are available for the thermally fissile isotopes and these must be included in any comprehensive study. Such a study has very recently been made in Hanna, Westcott, Lemmel, Leonard, Story, and Atree's [51] revision of the 2200 m/s constants for ^{233}U, ^{235}U, ^{239}Pu, and ^{241}Pu, and the following discussion is taken largely from this work.

The current situation can be exemplified by considering the absolute ^{252}Cf $\bar{\nu}$ measurements in relationship to the ratio of $\bar{\nu}$ values for ^{235}U and ^{252}Cf, and the $\bar{\nu}$, η, and α, and other nuclear data for ^{235}U. The procedure adopted by Hanna, et al, was to consider the individual data separately and first derive weighted means for the individual parameters and then to use these as input data for a fitting scheme from which a set of fitted, consistent, parameters is obtained. The consistency between the input and output data is a measure of the consistency of the measurements of related parameters.

First, with regard to the measured values of $\bar{\nu}$ for ^{252}Cf, Hanna, et al, divide the eight measurements into four categories depending upon the method of measurement, derive a mean for each category, and then obtain a weighted mean of the results from the four categories. These are shown in Table I together with the final-fitted value which considers all related nuclear data. This table reflects the fact that the ^{252}Cf measurements tend to fall into two separate groups with values close to 3.7 and 3.8 respectively despite the apparent high accuracies of the measurement. The situation is perhaps even slightly worse than presented here since DeVolpi and Porges have revised their result to 3.725 ± 0.015 which further emphasizes the separation into two divergent sets of data.

Second, the fitted value of $\bar{\nu}$, 3.7653 ± 0.0104, is not particularly close to the weighted mean and this reflects the fact that the fitted $\bar{\nu}$ (^{252}Cf) is strongly dependent upon the highly accurate η and α values for the fissile isotopes and the precisely measured ratios of $\bar{\nu}$ for the fissile isotopes to the ^{252}Cf value (to illustrate, the weighted mean and fitted values of $\bar{\nu}$ (^{235}U)/$\bar{\nu}$(^{252}Cf) are 0.6417 ± 0.0018 and 0.6433 ± 0.0015 respectively). This point is further demonstrated by the derivation of a $\bar{\nu}$(^{252}Cf) of 3.784 ± 0.014 if all the absolute $\bar{\nu}$ values are omitted from the fitting procedure. For this reason, the fitted value of $\bar{\nu}$(^{252}Cf) should only change very slightly by the use of the revised DeVolpi and Porges result.

Hanna, et al, conclude that the measurements of η are apparently in serious conflict with the very low values of $\bar{\nu}$(^{252}Cf), and yet, in the present author's view, it is becoming increasingly more difficult not to accept that the low values are not correct, particularly with the revision of

DeVolpi and Porges' result. In this regard, it is only the inclusion of the high, liquid-scintillator, $\bar{\nu}(^{252}Cf)$ result which prevents an even clearer and more disturbing discrepancy.

In summary, at the present time, an uncertainty possibly as large as a per cent lies over $\bar{\nu}(^{252}Cf)$ and the $\bar{\nu}$ values for the uranium and plutonium isotopes.

8.2 Variation of $\bar{\nu}$ with Neutron Energy

From the viewpoint of fast reactor physics, the energy-dependence of $\bar{\nu}$ is of comparable importance to the absolute value of $\bar{\nu}$ at the normalizing, thermal, energy. A linear dependence over the energy range in which only the (n,f) reaction is permissible, and a similar linear dependence, but with a different slope, over the higher energy range where the (n,n'f) reaction (that is, fission after inelastic scattering of the incident neutron) also occurs has been widely assumed for many years. Indeed, in 1963, Hopkins and Diven [52] proposed such a "universal curve" for the energy dependence of $\bar{\nu}$ which fitted most, if not all, the available data for all isotopes by the expedient of assuming suitable displacements of the energy scales for different isotopes. However, even at this time, there was some clear evidence for a non-linear energy dependence below about 1.5 MeV in the ^{235}U studies of Moat, Mather, and Fieldhouse [53]. This trend has been clearly confirmed by the studies of Blyumkina, et al [54], Meadows and Whalen [55], and others and is of importance to fast reactor physics since the major deviations from the previously assumed linearity occur in the several hundred keV region where the majority of the neutron spectrum lies.

Since most of the information has been obtained for ^{235}U fission, it is beneficial to discuss this isotope first. We will also restrict the discussion to the data of Blyumkina, et al, and Meadows and Whalen.

The experimental data are of three kinds; Meadows and Whalen determined $\bar{\nu}$ relative to that of ^{252}Cf over the range 39 keV to 1 MeV; Blyumkina, et al, determined, first, the relative values of $\bar{\nu}$ for ^{235}U from 80 keV to 1 MeV and normalized their results at 0.39 MeV and, second, inferred the variation of $\bar{\nu}$ from the measured difference, ΔE_k, in the total kinetic energy of the fission fragments from that in thermal fission assuming a linear dependence of $\bar{\nu}$ on the internal (or excitation) energy, E_i, of the fission fragments. The difference between $\bar{\nu}$ (E) and $\bar{\nu}$ (thermal) is then proportional to $E_n - \Delta E_k$. In this latter method, the $\bar{\nu}$ (E) values are related to the thermal value but a proportionality constant must be assumed.

Figure 3 shows these three sets of data. The Meadows and Whalen results have been re-normalized to a $\bar{\nu}_p$ (prompt) for ^{252}Cf of 3.756 [51], and the Blyumkina, et al, relative $\bar{\nu}$ measurements were then normalized to the Meadows and Whalen values. The Blyumkina, et al, fission fragment results were converted to $\bar{\nu}$ data assuming $\bar{\nu}_p$ (thermal) for ^{235}U was 2.4071 [51] and $d\bar{\nu}/dE_i = 0.1293$ (Soleilhac, et al [56]).

A histogram has been drawn through the Meadows and Whalen data to illustrate the possible structure in the energy dependence of $\bar{\nu}$. The Meadows and Whalen results were chosen for this purpose because the energy-resolution is about ± 25 keV which is approximately a factor of two better than the Blyumkina, et al, ratio data and a factor of four better than the fission-fragment energy data. Thus, neither set of Blyumkina data could be expected to show the structure found by Meadows and Whalen. The energy-width of each component corresponds approximately to the energy-resolution of the measurement up to about 0.6 MeV. Above this energy, the experimental

resolution is much finer than is illustrated by the histogram. The experimental errors in $\bar{\nu}$, which are not shown in the interests of clarity, are generally in the range $\pm$ 0.020 to $\pm$ 0.030 and are very approximately the same for all the points shown except for the fission-fragment data where the errors are approximately $\pm$ 0.040.

The smooth curve shown is based upon a weighted fit to all the experimental data and it can be seen that some evidence of structure at 350 keV is retained. Below 500 keV, this curve lies uniformly above the straight line fit to the data ($\bar{\nu}(E) = 2.407 + 0.1293\ E_n$) and between 500 keV and 1 MeV, the curve lies below this line.

It can be seen that, for example, the $\bar{\nu}_p$ value at 300 keV may be as high as about 2.50 rather than 2.445 which would be predicted on the basis of an increase in $\bar{\nu}$ arising from the neutron energy, 300 keV, alone. This difference of approximately 2% in $\bar{\nu}$ is highly significant since it is reflected directly in calculations of the multiplication constant, k, for fast reactors (and thus also in the critical mass) and could be a major reason for the current inability to predict critical masses for ^{235}U-fueled fast reactors.

The complexity of the situation is further shown by the available evidence for ^{233}U where fission fragment energy measurements by Blyumkina, et al, and relative $\bar{\nu}$ measurements of Kuznetsov and Smirenkin [57] show that $\bar{\nu}$ for ^{233}U first decreases in going from thermal energies to about 300 keV and then rises on going to higher energies. Thus, if the fast reactor physicist is studying a series of reactors fueled either with ^{235}U or ^{233}U, the sign of the discrepancy in critical mass will be different for these two fuels unless the structure in $\bar{\nu}$ is properly known.

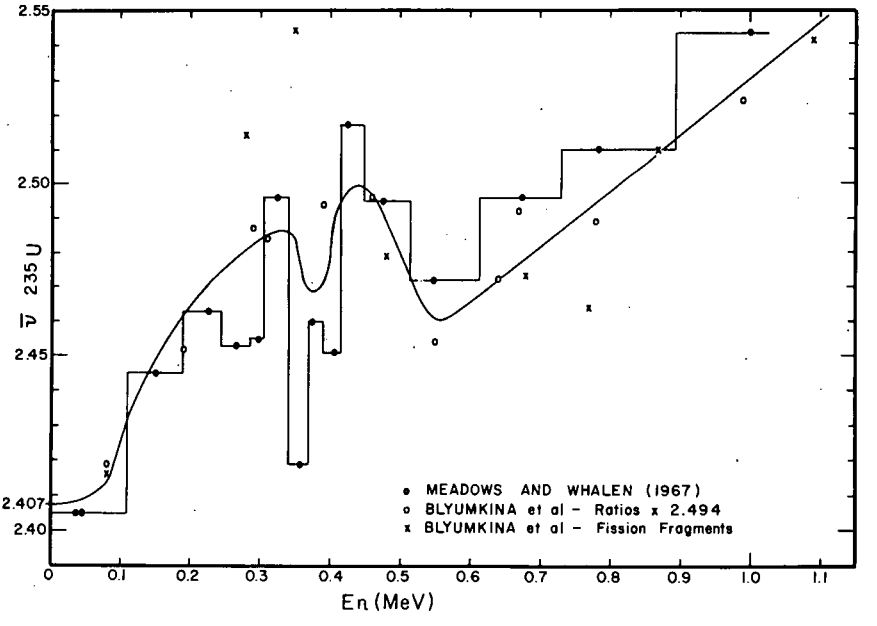

FIG.3. The energy-dependence of $\bar{\nu}$ for ^{235}U below 1.1 MeV.

Further evidence for this type of structure in $\bar{\nu}$ is given by data for ^{232}Th near the threshold (Conde and Holmberg [58], and Prokhorova, Smirenkin, and Shpak [59]).

Similar information on the most important fast reactor fuel, plutonium, is essentially completely lacking and it is vital that this deficiency should be corrected, particularly for ^{239}Pu, ^{240}Pu, and ^{241}Pu. Similar studies would also be justified for ^{238}U although the need here is considerably less pressing.

With regard to the energy dependence of $\bar{\nu}$ from about 1 to 15 MeV, the situation appears to be much more satisfactory since the evidence shows that a series of linear fits to the data appear to be satisfactory. Such fits are given in a recent evaluation by Fillmore [60]. However, the confidence generated by the detailed study of ^{235}U, ^{238}U, and ^{239}Pu by Soleilhac, et al, who determined $\bar{\nu}$ at approximately 0.5 MeV intervals from 1.36 MeV to 15 MeV shows that such detailed energy dependence should be obtained for all the major isotopes.

In summary, the possibility of significant structure in $\bar{\nu}$ below a few MeV makes detailed measurements essential. Such studies are particularly urgent for the major plutonium isotopes, ^{239}Pu, ^{240}Pu, and ^{241}Pu. The energy-resolution needed at these lower energies should be determined, of course, by the experimental results themselves, but would seem to be of the order of 25 keV to 50 keV over at least part of the energy range. Absolute $\bar{\nu}$ measurements, relative measurements, and fission-fragment, kinetic-energy measurements would all be of value in this respect. At higher energies, the energy intervals chosen should not be more than approximately 0.5 MeV and information similar to that obtained for ^{235}U, ^{238}U, and ^{239}Pu should be determined for the other major isotopes.

9. CONCLUSIONS

Of the data examined in this review, there is no doubt that the single most important parameter which must be established with accuracy and certainty is the fission cross section of ^{235}U since it serves as a reference for so many other measurements.

Other data which are urgently needed are well-established values of the capture cross section of ^{238}U to remove current ambiguities and uncertainties, and capture-to-fission ratios for ^{240}Pu, ^{241}Pu, and ^{242}Pu where no data currently exist.

Finally, it is important to establish whether or not structure occurs in the $\bar{\nu}$ values for ^{239}Pu, ^{240}Pu, and ^{241}Pu below about 1.5 MeV similar to that which occurs with ^{233}U and ^{235}U.

REFERENCES

[1] DAVEY, W. G., Nucl. Sci. Engng., 26, (1966) 149.

[2] DAVEY, W. G., Nucl. Sci. Engng., 32, (1968) 35.

[3] ALLEN, W. D., FERGUSON, A. T. G., Proc. Phys. Soc., 70, (1957) 573.

[4] DIVEN, B. C., Phys. Rev., 105, (1951) 1350.

[5] WHITE, P. H., J. Nucl. Energy, 19, (1965) 325.

[6] SMITH, R. K., HENKEL, R. L., NOBLES, R. A., Bull. Am. Phys. Soc., 2, (1957) 196.

[7] HANSEN, G., McGUIRE, S., SMITH, R. K., To be submitted to Nucl. Sci. Engng. also Private communication (1967).

[8] POENITZ, W. P., Proc. Conf. on Neutron Cross Sections and Technology, Washington, D.C., NBS Special Publication 299, 1, (1968) 503.

[9] POENITZ, W. P., Nucl. Instr. and Method, 58, (1968) 39.

[10] POENITZ, W. P., Nucl. Instr. and Method, 72, (1969) 120.

[11] KNOLL, G. F., POENITZ, W. P., J. Nucl. Energy, 21, (1967) 643.

[12] PERKIN, J. L., WHITE, P. H., FIELDHOUSE, P., AXTON, E. J., CROSS, P., ROBERTSON, J. C., J. Nucl. Energy, 19, (1965) 423.

[13] WHITE, P. H., HODGKINSON, J. G., WALL, G. J., Proc. Salzburg Conf. Physics and Chemistry of Fission, IAEA Salzburg, Austria (1965).

[14] WHITE, P. H., WARNER, G. P., J. Nucl. Energy, 21 (1967) 671.

[15] SMITH, R. K., HENKEL, R. L., NOBLES, R. A., Bull. Am. Phys. Soc., 2, (1957) 196.

[16] DUBROVINA, S. M., SHIGIN, V. A., Dokl. Akad. Nauk. USSR, 157, (1964) 561.

[17] LEHTO, W. K., Nucl. Sci. Engng. 39, (1970) 361.

[18] POENITZ, W. P., Trans. Am. Nucl. Soc., 12 (1969) 742.

[19] PFLETSCHINGER, E., KAPPELER, F., To be published Nucl. Sci. Engng. (1970).

[20] GILBOY, W. B., KNOLL, G., "The Fission Cross Sections of Some Plutonium Isotopes in the Neutron Energy Range 5-150 keV," KFK-450, Kernforschungszentrun, Karlsruhe (1966).

[21] NESTEROV, V. G., SMIRENKIN, G. N., Reactor Sci. Tech., 16, (1962) 51.

[22] HENKEL, R. L., NOBLES, R. A., SMITH, R. K., "Neutron Induced Fission Cross Section of ^{240}Pu," AECD-4256, Los Alamos Scientific Laboratory (1957).

[23] SMITH, H. L., SMITH, R. K., HENKEL, R. L., Phys. Rev., 125, (1962) 1329.

[24] BUTLER, D. K., SJOBLOM, R. K., Phys. Rev., 124, (1961) 1139.

[25] BUTLER, D. K., Phys. Rev., 117 (1960) 1305.

[26] STEIN, W. E., SMITH, R. K., GRUNDL, J. A., Proc. Conf. on Neutron Cross Sections and Technology, Washington D.C., NBS Special Publication 299, 1, (1968) 627.

[27] LAMPHERE, R. W., Phys. Rev., 104, (1956) 1654.

[28] LEACHMAN, R. B., SCHMITT, M. W., J. Nucl. Energy, 4, (1957) 38.

[29] RICHMOND, R., Unpublished, Results quoted by ALLEN, W. D., HENKEL, R. L., Progress in Nuclear Energy, Series 1, 2, pp. 1-50, Pergamon Press, New York (1957).

[30] NIKOLAEV, M. N., GOLUBEV, V. I., BONDARENKO, I. I., J. Expt. Theoret. Phys., 7, (1958) 517.

[31] DAVEY, W. G., Nucl. Sci. Engng. 39, (1970) 337.

[32] BARRY, J. F., BUNCE, J., WHITE, P. H., J. Nucl Energy A/B, 18, (1964) 481.

[33] BELANOVA, T. S., VANKOV, A. A., MIKHAILUS, F. F., STAVISKII, YU. YA., J. Nucl. Energy, 20, (1958) 411.

[34] MILLER, L. B., POENITZ, W. P., Nucl. Sci. Engng., 35, (1969) 295.

[35] deSAUSSURE, G., WESTON, L. W., KINGTON, J. D., SMIDDIE, R. D., LYON, W. S., "Neutron Physics Division Annual Report for Period Ending September 1, 1962," p. 51 ORNL-3360, Oak Ridge National Laboratory (1963).

[36] GIBBONS, J. H., MACKLIN, R. L., MILLER, P. D., NEILER, J. H., Phys. Rev., 122, (1961) 182.

[37] SCHMITT, H. W., COOK, C. W., Nuclear Phys., 20, (1960) 207.

[38] MACKLIN, R. L., GIBBONS, J. H., PASMA, P. J., WASH-1046, (1963) 88; and Private communication (1968).

[39] MACKLIN, R. L., LAZAR, N. H., LYON, W. S., Phys. Rev., 107 (1957) 504.

[40] MENLOVE, H. O., POENITZ, W. P., Nucl. Sci. Engng., 33, (1968) 24.

[41] PERKIN, J. L., O'CONNOR, L. P., COLEMAN, R. F., Proc. Phys. Soc., 72, (1958) 505.

[42] POENITZ, W. P., Trans. Am. Nucl. Soc., 12, (1968) 279.

[43] MOXON, M. C., "The Neutron Capture Cross Section of ^{238}U in the Energy Region 0.5 to 100 keV," AERE-R-6074, (1969) Atomic Energy Research Establishment, Harwell, England.

[44] SCHMIDT, J. J., "Neutron Cross Section for Fast Reactor Materials, Part 1; Evaluation," KFK-120, (1966) Kernforschungszentrun, Karlsruhe.

[45] GLASS, N. W., SCHELBERG, A. D., TATRO, L. D., WARREN, J. H., Proc. Conf. on Neutron Cross Sections and Technology, Washington, D.C., NBS Special Publication 299, 1, (1968) 587.

[46] deSAUSSURE, G., WESTON, L. W., GWIN, R., INGLE, R. W., TODD, J. H., HOCKENBURY, R. W., FULLWOOD, R. R., LOTTIN, A., Proc. Conf. Nuclear Data for Reactors, Paris, 1966, IAEA Vienna, 2, (1967) 233.

[47] GWIN, R., WESTON, L. W., deSAUSSURE, G., INGLE, R. W., TODD, J. H., GILLESPIE, F. E., HOCKENBURY, R. W., BLOCK, R. C., Measurements of the neutron fission and absorption cross sections of ^{239}Pu over the energy region 0.02 eV to 30 keV, To be published in Nucl. Sci. Engng. (1970).

[48] SCHOMBERG, M. G., SOWERBY, M. G., EVANS, F. W., Proc. Conf. Fast Reactor Physics, Karlsruhe, 1967, IAEA, Vienna, 1, (1968) 289.

[49] WESTON, L. W., deSAUSSURE, G., GWIN, R., Nucl. Sci. Engng., 20, (1964) 80.

[50] HOPKINS, J. C., DIVEN, B. C., Nucl. Sci. Engng., 12, (1962) 169.

[51] HANNA, G. C., WESTCOTT, C. H., LEMMEL, H. D., LEONARD, B. R., Jr., STORY, J. S., ATTREE, P. M., "Revision of Values for the 2200 m/s Neutron Constants for Four Fissile Nuclides," Atomic Energy Review, Vol. VII, No. 4, p. 3, IAEA, Vienna (1969).

[52] HOPKINS, J. C., DIVEN, B. C., Nucl. Phys., 48 (1963) 433.

[53] MOAT, A., MATHER, D. S., FIELDHOUSE, P., Proc. Seminar - Physics Fast and Intermediate Reactors, IAEA, Vienna, Vol. 1, (1962) 139.

[54] BLYUMKINA, YU. A., BONDARENKO, I. I., KUZNETSOV, V. F., NESTEROV, V. G., OKOLOVITCH, V. N., SMIRENKIN, G. N., USACHEV, L. N., Nucl. Phys., 52, (1964) 648.

[55] MEADOWS, J. W., WHALEN, J. F., J. Nucl. Energy, 21, (1967) 157.

[56] SOLEILHAC, M., FREHAUT, J., GAURIAU, J., J. Nucl. Energy, 23, (1969) 257.

[57] KUZNETSOV, V. F., SMIRENKIN, G. N., Proc. Inter. Conf. on Nuclear Data, Paris, 1966, IAEA, Vienna, Vol. 2, (1967) 75.

[58] CONDE, H., HOLMBERG, M., Arkiv for Fysik, 29, (1965) 33.

[59] PROKHOROVA, L. I., SMIRENKIN, G. N., SHPAK, D. L., Proc. Inter. Conf. on Nuclear Data, Paris, 1966, IAEA, Vienna, Vol. 2, (1967) 67.

[60] FILLMORE, F. L., J. Nucl. Energy, 22, (1968) 79.

DISCUSSION

H. W. KÜSTERS: Could someone comment from the nuclear-physics point of view on the structure in the energy dependence of $\bar{\nu}(E)$?

M. S. MOORE: The simplest mechanism is that invoked by Blyumkina in 1964, when the evidence for this structure was first noted, namely, channel effects connected with p- and d-wave neutrons.

M. C. MOXON: I would like to make a comment on Dr. Davey's renormalization of my ^{238}U capture data. First, I think an increase of 15% is a bit large. At 30 keV my value is 425 ± 29 mb, while a weighted mean of all the other data, after consideration of various renormalizations and extrapolations to 30 keV using the slope of my data, is 468 ± 10 mb, i. e. there is an increase of < 10%.

The errors on the $^{7}Li(p,n)$ threshold measurements and shell transmission are small and suggest that they are increased by ~ 5% to take into account possible fluctuations in the cross-section and lack of knowledge of the shape of the energy distribution of the neutron flux. An

average value of ~445 ± 25 mb is then obtained by taking into account this additional error. This latter value is < 5% greater than my absolute value and within the quoted uncertainties.

W. G. DAVEY: I think this is a very valid comment and I certainly agree that 15% is a bit much. As regards reference to the weighted mean near 30 keV, there is some room for interpretation here and one has to be careful which values one uses. There are a number of measurements made at this energy and they have to be renormalized before you can use them because they are based on fairly old data. I believe an intermediate position between yours and mine has been taken by Pitterle (CN-26/83)

W. P. POENITZ: My comment concerns Fig. 3 of your paper, which shows $\bar{\nu}(E)$. The curve you have drawn through the data of Blyumkina shows a dip which does not seem to be supported by the available data.

The second comment concerns the renormalization of the ^{238}U capture which you used to obtain agreement with the Barry-White values. You have to renormalize not only the data of Moxon and of Menlove and Poenitz but also all other absolute cross-sections available for ^{238}U-$\sigma_{n\gamma}$. In fact there are two papers being presented at this Conference (CN-26/77 and 43) which report measurements of the capture cross-section for ^{238}U and these, too, would have to be renormalized if you wanted to achieve consistency with White's data.

W. G. DAVEY: On your first comment, the dip in the averaged data at about 300 to 400 keV arises only from inclusion of Meadows and Whalen's $\bar{\nu}$ values, which show a dip here. No other experiments show this dip. With regard to your second point, as stated in my published evaluation and in the text of the present paper, it is essentially the ratio of ^{238}U capture and ^{235}U fission which is defined by my study. If White's fission cross-sections are incorrect then the ^{238}U capture cross-sections given here are also not correct.

V. A. KONSHIN: You did not mention the recent measurements of $\bar{\nu}$ for ^{235}U by Soleilhac et al. These were carried out with a high resolution and appear to be fairly accurate. The measurements were made in a more wide energy region, from above 200 keV to 28 MeV. The results seem to show definite structure below 2 MeV. Could you comment on this?

W. G. DAVEY: I was not aware of the Soleilhac results until last week and therefore I cannot comment on them at this time.

M. SOLEILHAC: I can say that our recent low-energy measurements of $\bar{\nu}$ for ^{235}U are in good agreement with the results of Meadows et al. which suggest the presence of structure. We used equivalent energy resolutions. Our results would appear to disagree with those of Boldeman, although these discrepancies may be attributable to statistical fluctuations. I think it may be necessary to make a control measurement using a linear accelerator.

M. G. SOWERBY: I would like to make three points. The first is that in your paper you discuss the disagreement between the ^{235}U fission cross-section measurements of Allen and Ferguson and of White. In our evaluation (CN-26/34) we accepted only the two absolute measurements of Allen and Ferguson, because the efficiency of the fission chamber used for their relative measurements is probably sensitive to changes in the fission fragment angular distribution. Secondly, in your conclusions on the ^{235}U fission cross-section, you state that it is essential to make new measurements relative to the (n, p) cross-section. We would consider that it is more important to use alternative techniques. Lastly, the aim in

your evaluation is to provide ratios of the cross-sections relative to ^{235}U (n, f). Would it not be better to use the direct ratio measurements than to have to adjust the values of so many experiments?

W.G. DAVEY: I shall reply only to your third point, since the first two were comments. In my published evaluation it is clearly stated that it is the ratio of ^{238}U capture and ^{235}U fission cross-sections that are defined. Perhaps it would be more convenient only to quote ratios. These ratios are indeed tabulated in detail in my Nuclear Science and Engineering article published in March 1970.

J.S. STORY: You made a comparison with the fission-spectrum averaged values for the ^{238}U fission cross-section. This is a very important integral reference standard and I think it would be valuable to have new measurements. Richmond used a very ingenious method for his measurement, but the work was never fully documented. However, the results reported in the literature depend on the value adopted for the thermal value for the prompt $\bar{\nu}$ of ^{235}U. I discussed this with Richmond some time ago and he told me he thought he had used a rather low value for $\bar{\nu}$, namely, 2.39. If you use the current value for the prompt $\bar{\nu}$, Richmond's result for the fission-spectrum average of the ^{238}U fission cross-section would have to be reduced by 1 or 2 per cent.

W.G. DAVEY: This is a comment with which I agree. There is a need for further measurements of the ^{238}U fission cross-section averaged over the ^{235}U fission spectrum.

J.L. LEROY: Like Dr. Sowerby, I think it is difficult to use the recoil proton method for obtaining absolute values of flux, especially at low energies, because in this case the gamma radiation obliges one to eliminate a considerable part of the pulse height spectrum of the recoil neutrons. The correction, which may be of the order of 30%, is obtained by calculation and, in unfavourable cases, may certainly lead to errors of several per cent. The problem does not arise in such acute form when one is trying to determine the shape of the neutron energy operation in a massive medium, especially if the counter is used with an electronic device capable of separating the pulses due to neutrons from those due to gammas.

As regards the accurate determination of the fluxes of monokinetic neutrons having energies of several tens of keV, I think the manganese bath method is the most reliable one as it involves only very slight corrections.

THE VALUE $\bar{\nu}$ OF ^{235}U AND ^{239}Pu IN A FAST-REACTOR SPECTRUM

H. CONDÉ, L. WIDÉN
Research Institute of National Defense, Stockholm, Sweden

Abstract

THE VALUE $\bar{\nu}$ of ^{235}U AND ^{239}Pu IN A FAST-REACTOR SPECTRUM.

The average number of prompt neutrons per ^{235}U and ^{239}Pu fission are being measured at the fast zero-power reactor (FRO) at Studsvik, Sweden. Special attention is paid to the fission resonance region where earlier measurements with good energy resolution have given different $\bar{\nu}$-values for different groups of resonances. As fission neutron detector a large liquid scintillator is used. The reactor neutron energy spectrum is measured in separate time-of-flight and proton-recoil detector experiments. The experimental technique is described, and preliminary $\bar{\nu}$-values averaged over the fast reactor spectrum from 0 - 70 keV are given.

1. INTRODUCTION

The average number of neutrons emitted in the neutron-induced fission of ^{235}U and ^{239}Pu has been measured with good energy resolution in the neutron energy region from 30 keV to 14 MeV [1, 2] but also recently in the fission resonance region [3, 4].

The energy dependences of $\bar{\nu}$ for ^{235}U and ^{239}Pu including the thermal values and values over about 100 keV are within 1 - 2% represented by straight lines.

In the fission resonance region Weinstein et al. [3] have measured the variation of $\bar{\nu}$ among the resonances in the energy regions 0.01 eV to 100 eV for ^{239}Pu, 0.01 to 25 eV for ^{235}U and 0.01 eV to 5.5 eV for ^{233}U. They found that the $\bar{\nu}$-values fall into two different groups which they correlated with the spins of the individual resonances. For ^{239}Pu the high ($J = 0$) and the low group ($J = 1$) differed about 3% while for ^{235}U the difference between the two spinstates ($J = 3$ and 4) was less pronounced. In addition, they measured the variations of $\bar{\nu}$ in the thermal regions. For ^{239}Pu they found 1% decrease compared to the thermal value at 0.198 eV while for ^{235}U they found 0.6% increase at 0.3 eV.

Ryabov et al. [4] have also recently measured the variation of $\bar{\nu}$ for different resonances in the fission of ^{239}Pu and ^{235}U. The results for many of the resonances disagree with the results of Weinstein et al. The differences between the $\bar{\nu}$-values for the two spin groups of ^{239}Pu and ^{235}U were 6.8% and 2% respectively.

In calculations on fast reactors one has usually assumed a linear energy dependence from thermal values up to 14 MeV. In practice, this means that one has assumed a $\bar{\nu}$-value equal to the thermal value in the fission resonance region. The measurements by Weinstein et al. and Ryabov et al. point out that within a few per cent this might not be a good approximation.

To find the $\overline{\nu}$-value for ^{235}U and ^{239}Pu averaged over a fast-reactor spectrum up to 50 - 100 keV an experiment was set up at the fast reactor FRO at Studsvik, Sweden. The measurements presented in this paper are made with a critical reactor and the $\overline{\nu}$-values are corrected for fission induced by neutrons above about 70 keV. Along with the measurement of $\overline{\nu}$ a measurement of the neutron-energy spectrum in the same energy range of 0-100 keV is in progress utilizing a pulsed sub-critical reactor and time-of-flight technique.

2. EXPERIMENTAL TECHNIQUE AND PROCEDURE

The experimental set-up is shown in Fig. 1. The fast zero-power reactor FRO [5] was used as a neutron source. The present experiment was carried out with a critical reactor. The cylindrical reactor core consisting of uranium (20 per cent enrichment) and moderator materials (graphite and polyethylene) was surrounded by a copper reflector. The neutron-energy spectrum corresponding to the actual reactor configuration is shown in Fig 2. The neutrons were extracted through a narrow hole from the centre of the core region and entered the 13-meter long evacuated beam tube through aluminium windows. Inside the beam-tube two collimators of borated paraffin were placed to give a well defined neutron beam through the central channel in the cylindrical scintillator tank. The tank was shielded by 10 cm of lead and 30 cm of borated paraffin.

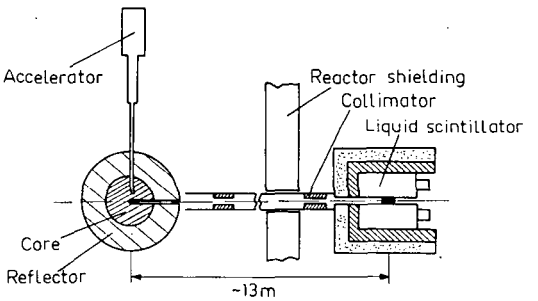

FIG. 1. Experimental arrangement.

Fission chambers containing 450 mg of ^{235}U and 20 mg of ^{239}Pu (< 0.1 per cent ^{240}Pu) were put in the middle of the central channel through the scintillator tank. The fissionable materials were electro-deposited onto thin platinum plates and housed in thin-walled (0.2 millimeters of aluminium) ionization chambers. The $\overline{\nu}$-value for the spontaneous fission of ^{252}Cf was used as a standard. A fission chamber similar to those described above contained a ^{252}Cf-source giving about 20 spontaneous fissions per minute.

The experimental arrangement for the liquid scintillator and the experimental procedure are described elsewhere [6]. In the present experiment the cylindrical scintillator tank, 50 cm in diameter and 50 cm in length, contained about 100 litres of a Gd-loaded liquid scintillator.

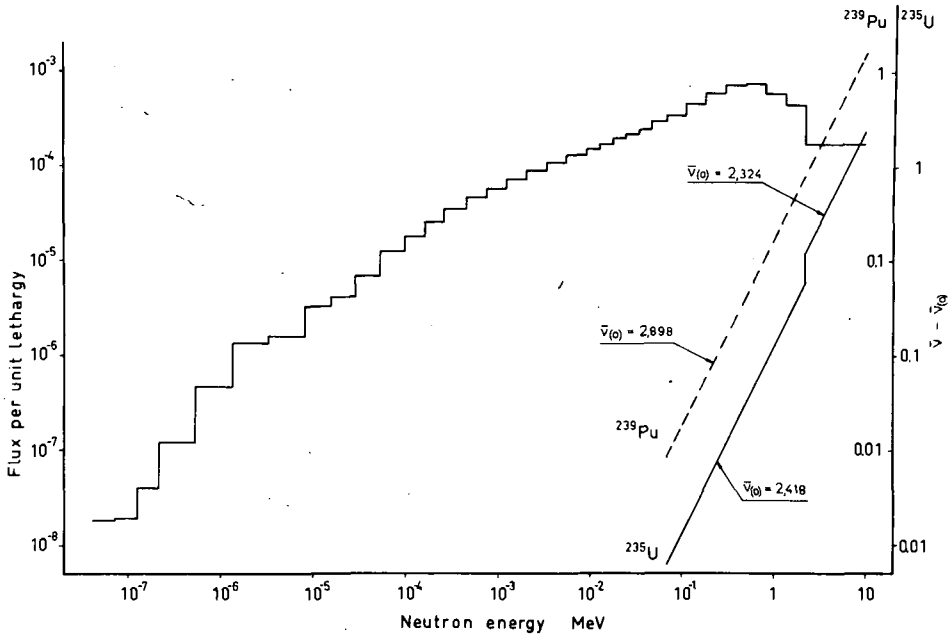

FIG. 2. The reactor neutron-energy spectrum and the energy dependence of $\bar{\nu}$ for ^{239}Pu and ^{235}U.

TABLE I. CORRECTIONS IN PER CENT APPLIED TO THE INTEGRAL $\bar{\nu}$-VALUES OF ^{239}Pu AND ^{235}U

Correction	^{239}Pu	^{235}U
Spontaneous fission	+ 2.0	-
Pile-up correction	+ 0.5	+ 0.8
Accidental coincidences	+ 0.2	+ 0.5
Different fission neutron spectra	- 0.3	- 0.6
Total correction	+ 2.4	+ 0.7

The pulses from the liquid scintillator were counted on a fast scaler. The scaler was gated by a pulse from a coincidence circuit, which was triggered by the fission chamber and scintillator prompt pulses. The gate was opened for 45 μs, long enough to count the capture pulses of the fission neutrons. About 200 μs after each fission event the gate was opened again to count the number of background pulses.

To obtain a reasonable counting rate, the ^{239}Pu runs were made with a higher reactor effect than the ^{235}U runs. The fission counting rates in the ^{239}Pu and ^{235}U measurements were about two and ten fissions per minute, respectively.

The $\bar{\nu}$-value of ^{252}Cf and the ratio between the gate-length of the fission neutron counter and the background counter were checked several times during each run.

The number of spontaneous ^{240}Pu fission events in the ^{239}Pu runs were estimated by placing the ^{239}Pu fission chamber in the scintillator tank and counting the fission events without a neutron beam from the reactor.

The time distribution of the background pulses in the scintillator caused by the reactor was checked. No time correlation of the background pulses could be observed.

3. DATA HANDLING

The observed $\bar{\nu}$-values were integral values over the actual reactor neutron-energy spectrum. The corrections to the observed integral $\bar{\nu}$-values are given in Table I. The corrections were applied according to Asplund-Nilsson et al. [6]. The contribution from the spontaneous fission of ^{240}Pu was calculated from a separate measurement as described above and gave a correction of about 2% in $\bar{\nu}$ for ^{239}Pu.

To calculate the $\bar{\nu}$-values in the resonance region use was made of a theoretical 34-group reactor spectrum as calculated from the one-dimensional diffusion theory program MONDAY [7]. A measurement of the reactor spectrum by a time-of-flight technique is in progress.

Linear approximations of the $\bar{\nu}$-values according to Fillmore [1] have been used in the weighting of $\bar{\nu}$-values against the reactor spectrum.

$$\bar{\nu}\,(^{239}Pu) = 2.898 + 0.1275\ E_n$$

$$\bar{\nu}\,(^{235}U) = \begin{cases} 2.418 + 0.1146\ E_n & 0 < E_n < 2.22\ \text{MeV} \\ 2.324 + 0.1569\ E_n & 2.22\ \text{MeV} < E_n < 10\ \text{MeV} \end{cases}$$

Figure 2 shows the theoretical 34-group reactor spectrum and the linear energy dependence of $\bar{\nu}$. The observed $\bar{\nu}$-values were corrected for fissions induced by neutrons with an energy above 67.4 keV or by neutrons with an energy corresponding to the eight high-energy groups in the 34-group spectrum.

Thus, the final corrected $\bar{\nu}$-values are averages over the fast-reactor spectrum from 0 - 67.4 keV.

To investigate the dependence of the calculated $\bar{\nu}$-values on the slopes of the linear approximations of $\bar{\nu}$, calculations have been performed for three different slopes of the $\bar{\nu}$ (^{239}Pu)-energy dependence. Besides the value 0.1275 n/MeV, 0.1200 n/MeV and 0.1400 n/MeV were also used. The observed differences in the calculated $\bar{\nu}$-values were for the slope 0.1200 n/MeV an increase of 0.4% and for the slope 0.1400 n/MeV a decrease of 0.7% relative to the calculated value of $\bar{\nu}$ from the slope 0.1275 n/MeV recommended by Fillmore.

4. RESULTS AND DISCUSSION

Table II gives the prompt $\bar{\nu}$-values averaged over the total reactor spectrum and over the reactor spectrum from 0 - 67.4 keV. The statistical errors in the measurements of $\bar{\nu}$ for ^{239}Pu and ^{235}U are 1.9 per cent and

TABLE II. PROMPT $\bar{\nu}$-VALUES WITH STATISTICAL ERRORS AVERAGED OVER THE TOTAL REACTOR SPECTRUM (INTEGRAL VALUE) AND OVER THE REACTOR SPECTRUM FROM 0 - 67.4 keV (CALCULATED VALUE)

	Energy region	$\bar{\nu}$ (^{239}Pu)	$\bar{\nu}$ (^{235}U)
Integral value	$E_{Th} < E < 10$ MeV	2.902 ± 0.055	2.481 ± 0.037
Calculated value	$E_{Th} < E < 67.4$ keV	2.704 ± 0.051	2.411 ± 0.036

1.5 per cent, respectively. The $\bar{\nu}$-values are based on $\bar{\nu}$ = 3.756 for the spontaneous fission of ^{252}Cf [8]. In comparison with the thermal values of $\bar{\nu}$ recommended by Fillmore the present $\bar{\nu}$-values in the energy region 0 - 67.4 keV are 6.7 and 0.3 per cent below the corresponding thermal values for ^{239}Pu and ^{235}U, respectively.

Because of the uncertainties primarily in the reactor neutron-energy spectrum the results of the present investigation must be regarded as preliminary. A time-of-flight measurement of the energy spectrum is in progress as well as $\bar{\nu}$-measurement where the fissions induced by neutrons above about 100 keV-energy will be eliminated by a time-of-flight arrangement.

REFERENCES

[1] FILLMORE, F.L., J. nucl. Energy 22 (1968) 79.
[2] CONDÉ, H., HOLMBERG, M., J. nucl. Energy 22 (1968) 53.
[3] WEINSTEIN, S., REED, R., BLOCK, R.C., in Physics and Chemistry of Fission (Proc. 2nd Symp. Vienna, 1969) IAEA, Vienna (1969) 477.
[4] RYABOV, Yu. V., DONSICK, So., CHICKOV, N., IANEVA, N., Report D-3893, Joint Inst. for nucl. Research, Dubna, 88.
[5] ANDERSSON, T.L., HELLSTRAND, E., LONDEN, S-O. and TIRÉN, L.I., Report AE-195, part 1.
[6] ASPLUND-NILSSON, I., CONDÉ, H., STARFELT, N., Nucl. Sci. Engng 20 (1964) 527.
[7] LINDE, S., TPM-RFN-259 (1967). (In Swedish).
[8] HANNA, G.C., WESTCOTT, C.H., LEMMEL, H.D., LEONARD, B.R., STORY, J.S., ATTREE, P.M., At. Energy Rev. IAEA Vienna, 7 4 (1969) 3.

NOMBRE MOYEN DE NEUTRONS PROMPTS ET SECTIONS EFFICACES RELATIVES POUR LA FISSION DE L'URANIUM-235 ET DU PLUTONIUM-239 ENTRE 0, 3 ET 1, 4 MeV

M. SOLEILHAC, J. FREHAUT,
J. GAURIAU, G. MOSINSKI
CEA, Centre d'études
de Bruyères-le-Châtel,
France

Abstract — Résumé

MEAN NUMBER OF PROMPT NEUTRONS AND RELATIVE CROSS-SECTIONS FOR THE FISSION OF ^{235}U AND ^{239}Pu BETWEEN 0.3 AND 1.4 MeV.

Using a spectrum of neutrons produced by the ^{7}Li (p, n)^{7}Be reaction on a thick lithium target, the authors made simultaneous measurements of $\bar{\nu}$ and of relative fission cross-sections on ^{235}U and ^{239}Pu. The energy of the incident neutrons was determined by the time-of-flight method, using a beam of pulsed protons at a frequency of 2.5 Mc/s. The energy resolution obtained varied from 10 keV to 50 keV between 0.3 and 1 MeV. The data were recorded on magnetic tape. The measurements of $\bar{\nu}$ are a follow-up of the results between 1.3 and 15 MeV which were published earlier. The authors' findings are in agreement with most of the earlier measurements and confirm the non-linear variation of $\bar{\nu}$ between 0.3 and 1 MeV.

NOMBRE MOYEN DE NEUTRONS PROMPTS ET SECTIONS EFFICACES RELATIVES POUR LA FISSION DE L'URANIUM-235 ET DU PLUTONIUM-239 ENTRE 0, 3 ET 1, 4 MeV.

En utilisant un spectre de neutrons produits par réaction ^{7}Li (p, n)^{7}Be sur une cible épaisse de lithium les auteurs ont mesuré le $\bar{\nu}$ et les sections efficaces relatives de fission simultanément sur ^{235}U et ^{239}Pu. L'énergie des neutrons incidents a été déterminée par la méthode du temps de vol en utilisant un faisceau de protons pulsé à une fréquence de 2, 5 MHz. La résolution en énergie obtenue varie de 10 keV à 50 keV entre 0, 3 et 1 MeV. L'enregistrement des données a été effectué sur bande magnétique incrémentale. Les mesures de $\bar{\nu}$ obtenues prolongent les résultats déjà publiés pour la gamme comprise entre 1, 3 et 15 MeV. Les résultats des auteurs sont en accord avec la plupart des mesures antérieures et confirment la variation non linéaire de $\bar{\nu}$ entre 0, 3 et 1 MeV.

1. INTRODUCTION

De nombreuses mesures de $\bar{\nu}_p$ pour des fissions induites par des neutrons d'énergie comprise entre 0, 1 et 1, 5 MeV existent pour ^{235}U [1-14]. Leur compilation paraît indiquer que la variation de $\bar{\nu}_p$ avec l'énergie n'est pas linéaire aux environs de 0, 4 MeV. Pour ^{239}Pu les données expérimentales sont par contre assez rares dans cette gamme d'énergie [1, 14-17].

Il nous a semblé intéressant de réaliser des mesures dans ce domaine d'énergie, d'une part pour essayer de préciser la variation de $\bar{\nu}$ pour ^{235}U, d'autre part pour vérifier si un phénomène analogue se retrouve pour ^{239}Pu.

Nous avons effectué ces mesures simultanément sur les deux matériaux fissiles contenus dans une même chambre à fission déjà décrite [14]. Nous avons pu aussi mesurer les sections efficaces relatives de fission de ^{235}U et ^{239}Pu.

2. SOURCE DE NEUTRONS

Pour mettre éventuellement en évidence des structures dans la loi $\overline{\nu}_p = f(E)$ il nous a paru intéressant d'utiliser une cible épaisse pour produire avec un accélérateur pulsé des bouffées de neutrons couvrant une large gamme d'énergie que l'on analyse ensuite par temps de vol.

Nous utilisons la réaction $^{7}Li(p, n)^{7}Be$ avec un accélérateur tandem Van de Graaff de 12 MeV pulsé à fréquence de 2,5 MHz auprès duquel se trouve installé le scintillateur liquide.

Pour obtenir le flux maximal de neutrons dans la plage étudiée, l'énergie des protons a été réglée successivement à 3,1 MeV puis à 2,8 MeV.

3. TECHNIQUE EXPERIMENTALE

Nous utilisons la technique du gros scintillateur liquide pour détecter les neutrons [14]. Par rapport à la référence [14] seule la technique d'enregistrement des données, qui s'effectue maintenant sur bande magnétique incrémentale, a été modifiée.

Les paramètres enregistrés pour chaque fission sont:
- l'adresse du corps où la fission s'est produite
- le nombre de neutrons et de coups de bruit de fond détectés
- le nombre de coups de bruit de fond détectés
- le temps de vol du neutron qui a provoqué la fission (1 ns par canal)
- l'amplitude de l'impulsion de détection du fragment de fission.

4. EXPLOITATION DES RESULTATS - CORRECTIONS

En plus des corrections «classiques» [14]: bruit de fond, temps mort et efficacité, nous effectuons dans le cas présent quatre corrections supplémentaires.

4.1. Correction du spectre de temps de vol

Les spectres de temps de vol (pulsation - fragment de fission) se trouvent entachés d'une erreur qui dépend de l'amplitude de l'impulsion détectée. Cette correction n'est faite que pour le ^{235}U pour lequel huit électrodes sont additionnées dans la chambre à fission. La mesure de l'amplitude du fragment de fission nous permet de corriger le spectre de temps de vol expérimental.

4.2. Corrections des fissions induites par des neutrons d'énergie dégradée

Un inconvénient de la technique de production des neutrons est l'apparition de nombreux neutrons d'énergie très faible. La différence de temps de 400 ns entre deux bouffées entraîne un léger recouvrement des spectres de temps de vol dont il faut tenir compte (fig. 1). Nous devons également tenir compte de la linéarité différentielle de la chaîne de codage en temps.

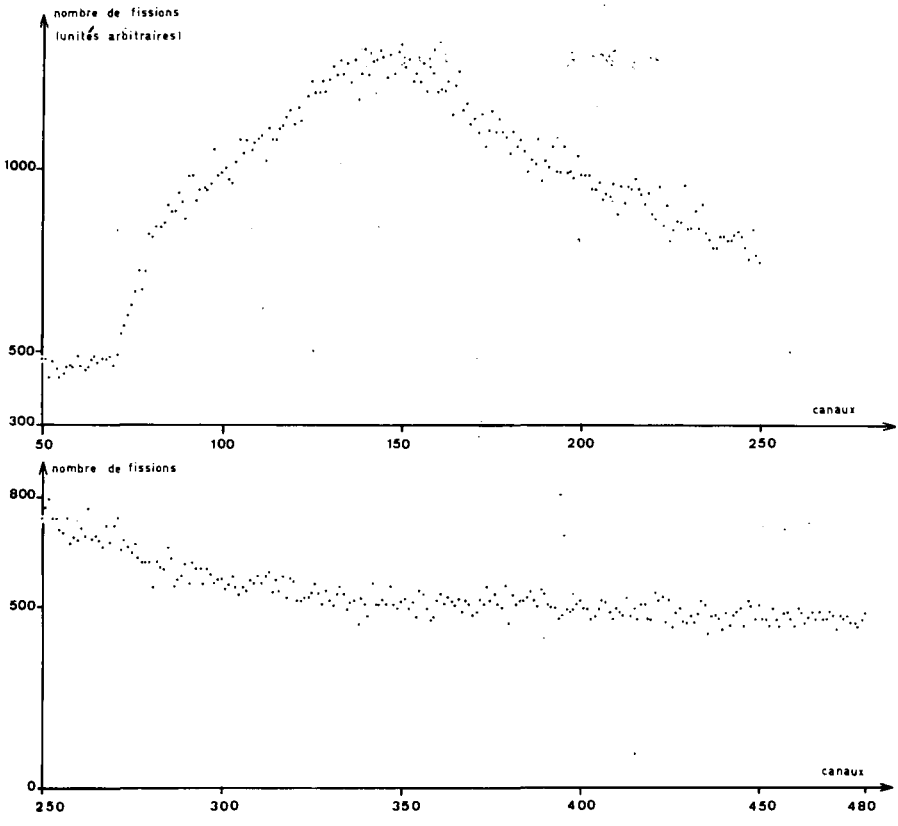

FIG. 1. Spectre de temps de vol des fissions induites par les neutrons de la réaction $^{7}Li(p, n)^{7}Be$ pour des protons de 2,7 MeV.

4.3. Etalonnage en énergie du spectre de temps de vol

L'étalonnage en énergie a été obtenu en enregistrant, dans les mêmes conditions expérimentales, un spectre de temps de vol de neutrons produits par la réaction $T(p, n)^{3}He$ sur cible mince. L'étalonnage a été effectué pour des neutrons de 1,36 MeV.

L'étalonnage en temps de la chaîne d'analyse permet alors de calculer l'énergie en chaque point du spectre. La largeur de la bouffée de neutrons incidents (4 ns) entraîne un mélange des énergies qui atteint 50 keV à 1 MeV et descend à 10 keV pour 0,3 MeV. Nous avons donc découpé le spectre en bandes de 50 keV au-dessus de 0,7 MeV et de 20 keV au-dessous.

4.4. Correction due à la diffusion des neutrons par le matériau support de cible (nécessaire pour déduire les sections efficaces)

Les neutrons incidents sont diffusés par le platine. L'uranium-235, situé derrière le ^{239}Pu par rapport au faisceau incident, reçoit un flux de neutrons plus faible que ce dernier.

TABLEAU I. RESULTATS OBTENUS POUR L'URANIUM-235

E_n (MeV)	N_F	$\bar{\nu}$	$\pm \Delta\bar{\nu}$
1,36	34509	2,565	0,010
1,375	8222	2,5826	0,0317
1,325	3388	2,5588	0,0399
1,275	3463	2,6378	0,0396
1,225	5571	2,5779	0,0300
1,175	5784	2,5769	0,0292
1,125	6234	2,5786	0,0277
1,075	8122	2,5782	0,0242
1,025	8526	2,5471	0,0233
0,975	14907	2,5539	0,0194
0,925	16361	2,5498	0,0173
0,875	17383	2,5473	0,0166
0,825	20861	2,5347	0,0151
0,775	25328	2,5215	0,0136
0,725	27314	2,4958	0,0129
0,690	10861	2,4920	0,0195
0,670	14772	2,4998	0,0168
0,65	14894	2,5108	0,0167
0,63	15576	2,4921	0,0162
0,61	16003	2,4928	0,0168
0,59	20093	2,4725	0,0142
0,57	19916	2,4885	0,0143
0,55	19338	2,4725	0,0146
0,53	17953	2,5140	0,0155
0,51	16663	2,4960	0,0162
0,49	17654	2,5004	0,0163
0,47	15246	2,4562	0,0179
0,45	15506	2,4764	0,0184
0,43	13195	2,4969	0,0206
0,41	13275	2,5326	0,0212
0,39	11546	2,4788	0,0229
0,37	11464	2,4736	0,0232
0,35	11525	2,5165	0,0237
0,33	11164	2,4455	0,0242
0,31	10714	2,4699	0,0257
0,29	7900	2,4607	0,0292
0,27	8281	2,4930	0,0307
0,25	6706	2,4635	0,0371
0,23	6251	2,4471	0,0410
0,21	3780	2,4307	0,0535

E_n énergie des neutrons incidents

N_F nombre de fissions

$\bar{\nu}$ nombre moyen de neutrons prompts

$\Delta\bar{\nu}$ erreur sur la valeur de $\bar{\nu}$.

Notre mesure étant relative, ce phénomène ne doit être pris en considération que si la section efficace de diffusion du platine $\sigma(E)$ varie dans la gamme d'énergie étudiée. C'est le cas pour cette étude: Si le ^{239}Pu reçoit un flux unité, le ^{235}U reçoit un flux $1 - b\sigma(E)$. Nos valeurs expérimentales doivent donc être multipliées par le facteur

$$\frac{1 - b\,\sigma(E)}{1 - b\,\sigma(E_0)}$$

où b est une constante qui dépend de la géométrie et E_0 l'énergie à laquelle on normalise nos résultats sur les mesures existantes (0,61 MeV).

Le coefficient b a été déterminé en retournant la chambre par rapport à la direction du flux incident. Cette correction est de 6% à 0,2 MeV; au-dessus de 0,9 MeV elle est constante et égale à 1,2%.

5. RESULTATS

Le point situé sur les figures à 1,36 MeV correspond à une mesure antérieure [14] effectuée en réaction (p, T).

5.1. $\bar{\nu}_p$ pour ^{235}U

Le tableau I et la figure 2 présentent nos résultats pour ^{235}U; nos valeurs sont normalisées à 3,782 pour le ^{252}Cf. Sur la figure 3 se trouvent rassemblées toutes les mesures réalisées entre 0 et 2 MeV pour ce même matériau fissile.

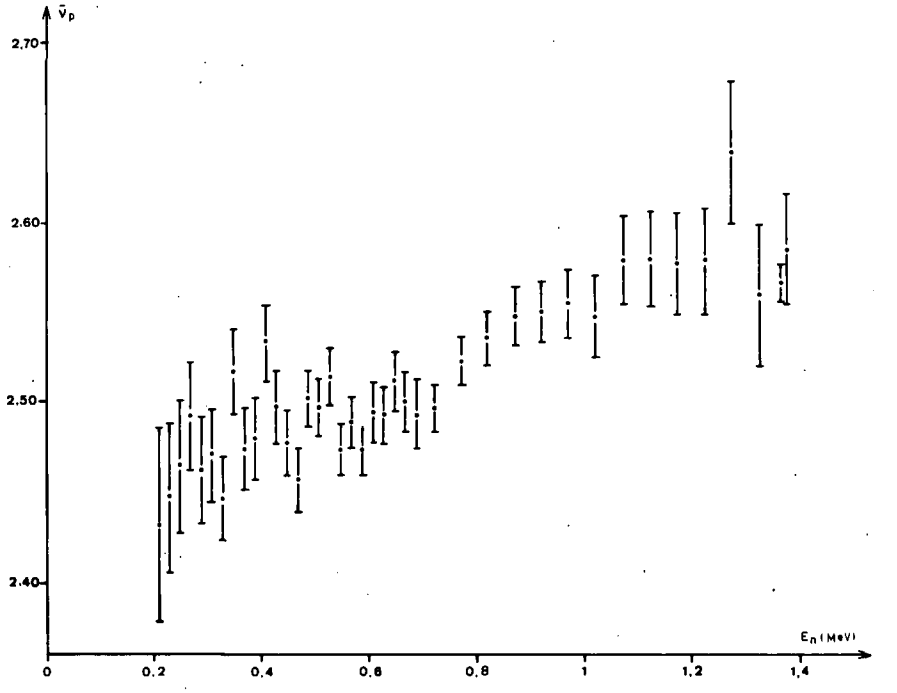

FIG. 2. $\bar{\nu}_p = f(E_n)$ pour ^{235}U.

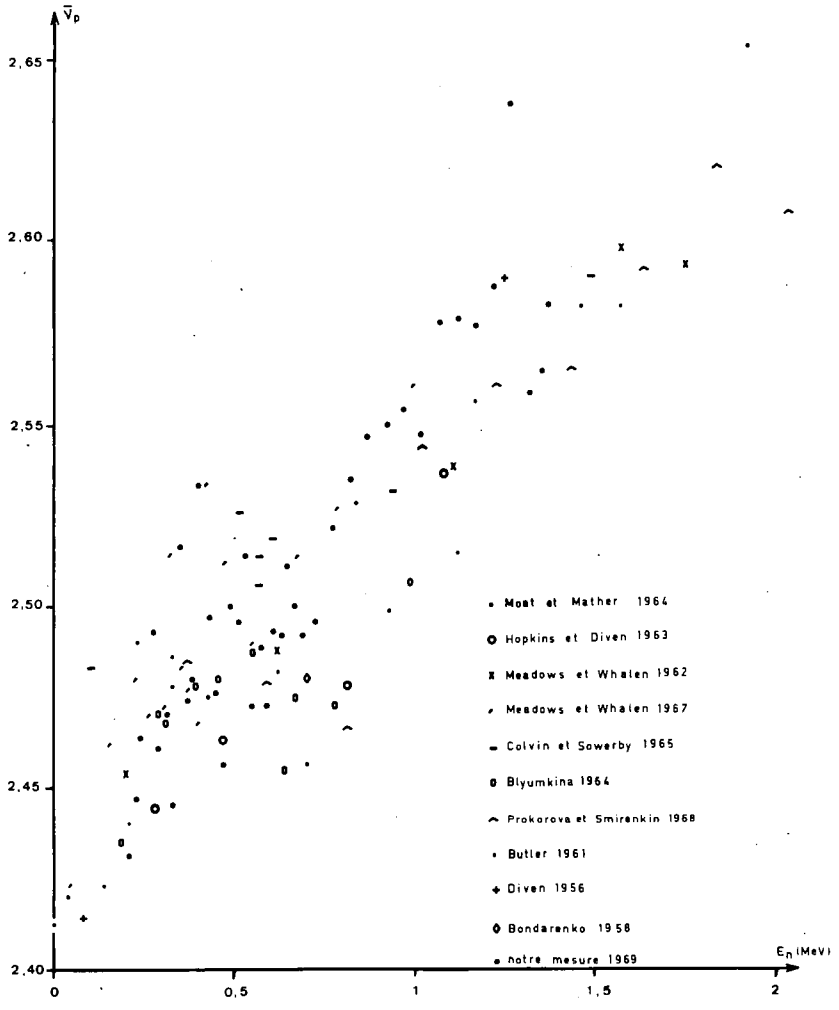

FIG. 3. $\bar{\nu}_p = f(E_n)$ pour ^{235}U.

Les tracés de la figure 4 permettent de comparer les courbes moyennes obtenues dans la gamme d'énergie étudiée dans les trois cas suivants:

Courbe 1: nos résultats
Courbe 2: toutes les autres mesures existantes
Courbe 3: l'ensemble des points de 1 et 2.

La droite que nous avons tracée sur cette même figure a été déterminée par la méthode des moindres carrés à partir de nos points de mesure compris entre 1, 36 et 3, 5 MeV [14].

Pour une énergie de neutrons inférieure à 0, 7 MeV, nos résultats semblent confirmer ceux des mesures précédentes et l'existence d'une

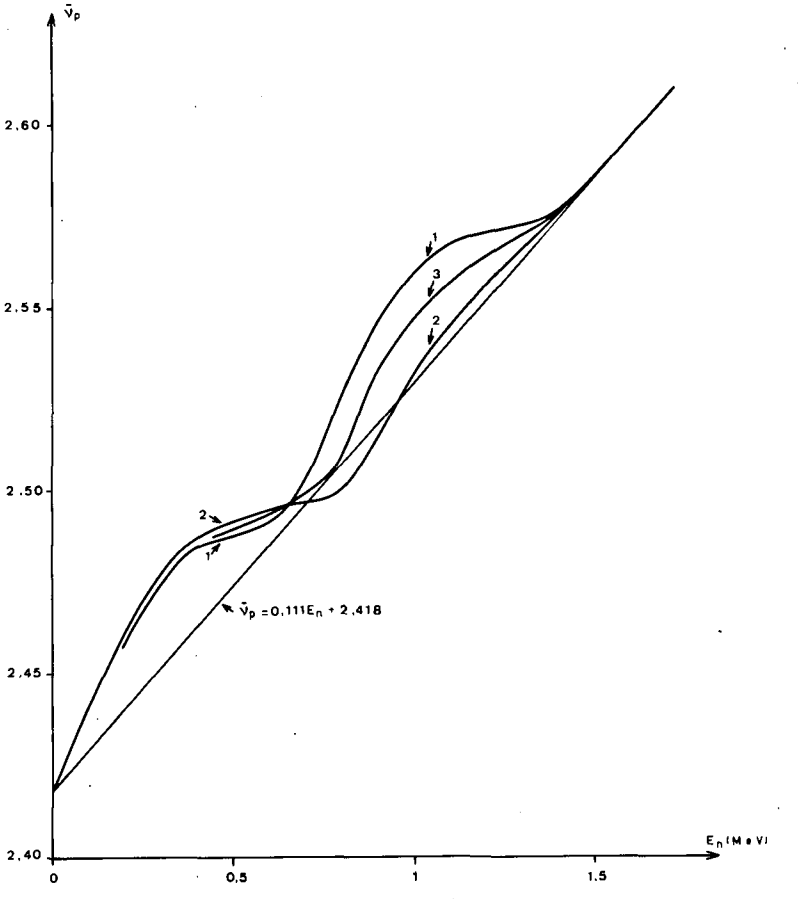

FIG. 4. $\bar{\nu}_p = f(E_n)$ pour ^{235}U.

«bosse» pour la loi $\bar{\nu}_p = f(E)$ par rapport à la droite précédemment déterminée. L'écart maximal par rapport à la droite se situe vers 0,4 MeV et est de l'ordre de 1%.

Entre 0,7 et 1,4 MeV apparaît une deuxième bosse dont l'écart maximal par rapport à la droite est d'environ 1,2%. Mais des mesures complémentaires sont nécessaires pour confirmer cette structure.

5.2. $\bar{\nu}_p$ pour ^{239}Pu

Le tableau II et la figure 5 présentent les résultats pour ce matériau. La droite de la figure 5 a été déterminée par la méthode des moindres carrés à partir de nos points de mesure compris entre 1,36 et 5,06 MeV et entre 12,41 et 14,85 MeV [14]. Cette droite traduit bien la variation $\bar{\nu}_p = f(E)$ que nous avons mesurée au-dessus de 500 keV.

Une structure analogue à celle observée pour ^{235}U semble apparaître vers 400 keV, mais avec une amplitude plus faible de l'ordre de 0,6%.

TABLEAU II. RESULTATS OBTENUS POUR LE PLUTONIUM-239

E_n (MeV)	N_F	$\bar{\nu}$	$\pm \Delta\bar{\nu}$
1,36	43 040	3,0708	0,0100
1,375	7 700	3,0446	0,0421
1,325	4 094	3,1439	0,0473
1,275	5 220	3,1027	0,0381
1,225	4 245	3,0835	0,0406
1,175	5 919	3,0310	0,0343
1,125	6 796	3,0614	0,0288
1,075	5 411	3,0457	0,0307
1,025	6 761	3,0177	0,0263
0,975	18 273	2,9885	0,0206
0,925	15 006	2,9858	0,0209
0,875	21 330	3,0035	0,0176
0,825	19 607	2,9674	0,0180
0,775	27 622	2,9912	0,0153
0,725	29 662	2,9712	0,0145
0,69	15 860	2,9781	0,0189
0,67	12 129	2,9719	0,0190
0,65	16 389	2,9562	0,0184
0,63	16 887	2,9686	0,0181
0,61	21 280	2,9702	0,0162
0,59	17 099	2,9358	0,0178
0,57	20 920	2,9605	0,0164
0,55	20 120	2,9600	0,0169
0,53	19 230	2,9281	0,0173
0,51	20 413	2,9683	0,0176
0,49	17 815	2,9202	0,0193
0,47	8 302	2,9577	0,0220
0,45	15 039	2,9366	0,0228
0,43	13 384	2,9641	0,0249
0,41	11 381	2,9345	0,0275
0,39	12 800	2,9592	0,0270
0,37	10 873	2,9367	0,0295
0,35	10 601	2,9467	0,0300
0,33	10 897	2,9576	0,0306
0,31	10 543	2,9307	0,0324
0,29	8 432	2,8795	0,0359
0,27	7 313	2,8883	0,0420
0,25	6 470	2,8537	0,0493
0,23	5 738	2,9185	0,0588
0,21	2 836	2,8969	0,0941

E_n énergie des neutrons incidents

N_F nombre de fissions

$\bar{\nu}$ nombre moyen de neutrons prompts

$\Delta\bar{\nu}$ erreur sur la valeur de $\bar{\nu}$.

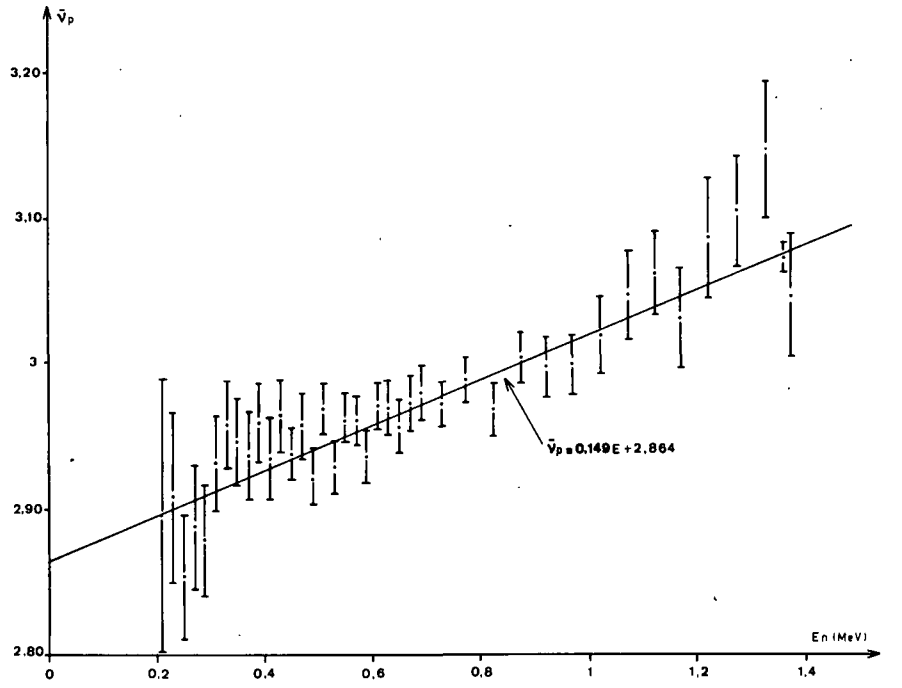

FIG. 5. $\bar{\nu}_p = f(E_n)$ pour ^{239}Pu.

5.3. Sections efficaces relatives de fission

Le tableau III et la figure 6 présentent nos résultats. Ces résultats sont obtenus à partir du nombre de fissions détectées compte tenu de la correction signalée au paragraphe 4.4.

Nos points sont normalisés à 0,61 MeV sur la valeur $\sigma_{F\,^{239}Pu} / \sigma_{F\,^{235}U} = 1,354$ recommandée dans le rapport KFK-750 [18].

Nous avons représenté sur la figure 6 les évaluations données dans KFK-750 [18] et par Davey [19] et Hart [20] avec la même normalisation.

6. CONCLUSION

En ce qui concerne les mesures de $\bar{\nu}$ nos résultats confirment la possibilité d'une structure au voisinage de 0,4 MeV sans toutefois clarifier la situation. Seule une précision statistique nettement améliorée permettrait de conclure. Pour le ^{239}Pu, la variation $\bar{\nu} = f(E)$ est linéaire à mieux que 1% dans toute la gamme d'énergie étudiée.

Les mesures de sections efficaces relatives confirment la plupart des évaluations existantes jusqu'à 0,9 MeV; au-delà nous nous rapprochons de l'évaluation de Hart jusqu'à 1,1 MeV et nous en écartons de nouveau pour des énergies plus élevées.

TABLEAU III. RESULTATS OBTENUS: SECTION EFFICACE RELATIVE ($\sigma_{F\ ^{239}Pu}/\sigma_{F\ ^{235}U}$)

E_n (MeV)	σ	$\Delta\sigma$
1,36	1,277	0,020
1,375	1,203	0,082
1,325	1,310	0,069
1,275	1,419	0,067
1,225	1,291	0,055
1,175	1,307	0,050
1,125	1,321	0,045
1,075	1,351	0,045
1,025	1,376	0,043
0,975	1,351	0,033
0,925	1,389	0,033
0,875	1,397	0,030
0,825	1,397	0,029
0,775	1,389	0,026
0,725	1,372	0,024
0,69	1,379	0,034
0,67	1,389	0,033
0,65	1,382	0,030
0,63	1,370	0,030
0,61	1,354	0,028
0,59	1,326	0,027
0,57	1,308	0,026
0,55	1,323	0,027
0,53	1,356	0,030
0,51	1,288	0,028
0,49	1,265	0,029
0,47	1,286	0,033
0,45	1,243	0,033
0,43	1,271	0,038
0,41	1,234	0,039
0,39	1,227	0,041
0,37	1,216	0,043
0,35	1,228	0,044
0,33	1,247	0,046
0,31	1,240	0,049
0,29	1,179	0,053
0,27	1,158	0,058
0,25	1,155	0,071
0,23	1,092	0,078
0,21	0,891	0,095

E_n énergie des neutrons incidents

σ $\sigma_{F\ ^{239}Pu}/\sigma_{F\ ^{235}U}$

$\Delta\sigma$ erreur sur la valeur de σ.

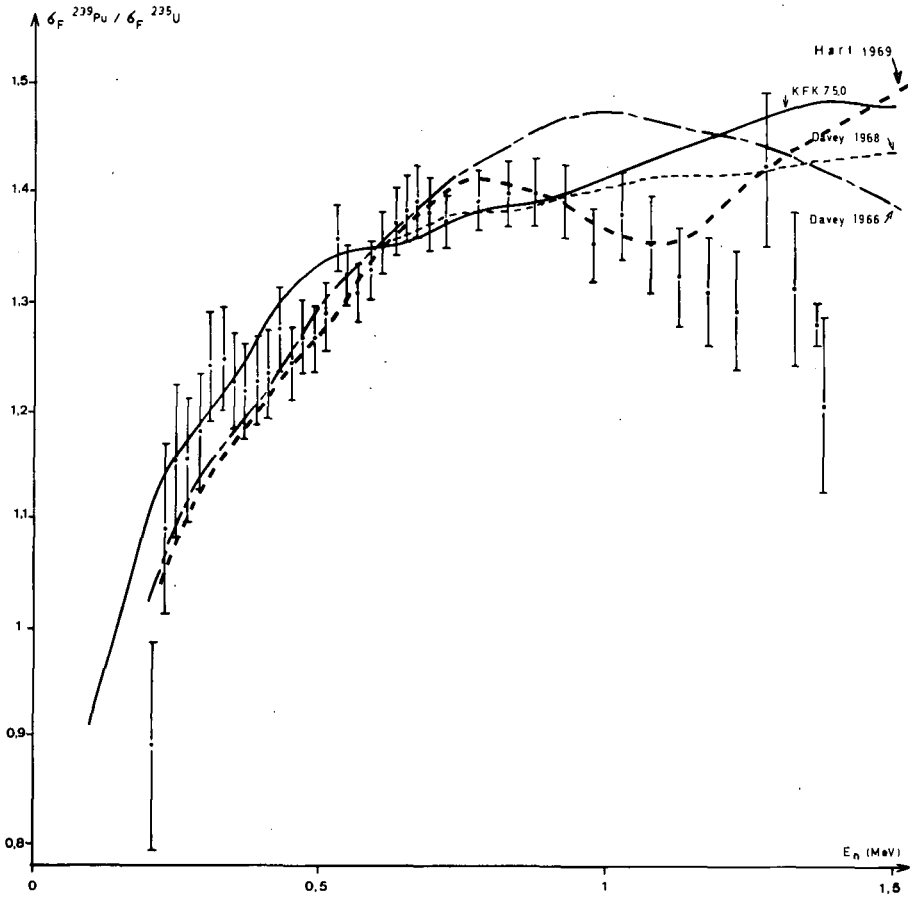

FIG. 6. Section efficace relative de fission de ^{239}Pu par rapport à celle de ^{235}U.

REFERENCES

[1] FILLMORE, F.L., J. nucl. Energy 22 (1968) 79.
[2] MEADOWS, J.W., WHALEN, J.F., J. nucl. Energy 21 (1967) 157.
[3] MATHER, D.S., FIELDHOUSE, P., MOAT, A., Phys. Rev. 133B (1964) 1403.
[4] COLVIN, D.W., SOWERBY, M.G., «Boron pile $\bar{\nu}$ measurements», Physics and Chemistry of Fission (C.r. Coll. Salzbourg, 1965) II, AIEA, Vienne (1965) 25.
[5] HOPKINS, J.C., DIVEN, B.C., Nucl. Phys. 48 (1963) 433.
[6] MEADOWS, J.W., WHALEN, J.F., Phys. Rev. 126 (1962) 197.
[7] MOAT, A., MATHER, D.S., MacTAGGART, M.H., Reactor Sci. Technol. (J. nucl. Energy A/B) 15 (1961) 102.
[8] FOWLER, J.L., Rep. ANL-5800 (1963).
[9] BUTLER, D., et al., «Experimental studies of fission properties utilized in reactor design», Physics of Fast and Intermediate Reactors (C.r. Sém. Vienne, 1961) I, AIEA, Vienne (1962) 125.
[10] BLYUMKINA, Yu.A., et al., Nucl. Phys. 52 (1964) 648.
[11] DIVEN, B.C., et al., Phys. Rev. 101 (1956) 1012.

[12] KALASHNIKOVA, V.I., et al., C.r. 1ère Conf. int. Acad. Sci. URSS Util. pacif. Energ. atom., Moscou, juillet 1955, p. 127.
[13] PROKHOROVA, L.I., SMIRENKIN, G.N., Proc. Conf. Nuclear Data for Reactors (Paris, 1966) II, AIEA, Vienne (1967) 67.
[14] SOLEILHAC, M., FREHAUT, J., GAURIAU, J., J. nucl. Energy 23 (1969) 257.
[15] MATHER, D.S., FIELDHOUSE, P., MOAT, A., Nucl. Phys. 66 (1965) 149.
[16] DIVEN, B.C., et al., Phys. Rev. 101 (1956) 1012.
[17] HOPKINS, J.C., DIVEN, B.C., Nucl. Phys. 48 (1963) 433.
[18] LANGNER, I., SCHMIDT, J.J., WOLL, D., KFK-750 (1968).
[19] DAVEY, W.G., Nucl. Sci. Engng 32 (1968) 35.
[20] HART, W., AHSB R-169 (1969).

СРЕДНЕЕ ЧИСЛО МГНОВЕННЫХ НЕЙТРОНОВ ПРИ ДЕЛЕНИИ ^{235}U, ^{239}Pu, ^{240}Pu БЫСТРЫМИ НЕЙТРОНАМИ

М. В. САВИН, Ю. А. ХОХЛОВ,
Ю. С. ЗАМЯТНИН, И. Н. ПАРАМОНОВА
Государственный комитет по использованию
атомной энергии СССР, Москва,
Союз Советских Социалистических Республик

Presented by S.I. Sukhoruchkin
Доклад представлен С.И. Сухоручкиным

Abstract — Аннотация

THE AVERAGE NUMBER OF PROMPT NEUTRONS IN FAST-NEUTRON-INDUCED FISSION OF ^{235}U, ^{239}Pu AND ^{240}Pu.

The authors report measurements of $\bar{\nu}$ made during fission of ^{235}U, ^{239}Pu and ^{240}Pu by fast neutrons with energies of 0.6 to 5 MeV. The measurements were carried out in a linear electron accelerator. The fission neutron detector was a liquid scintillator with a capacity of 400 l. The fission neutron counting efficiency was approximately 70%. Virgin neutrons were selected by the time-of-flight method with a resolution of 1 nsec/m. The instant of fission was recorded from prompt fission gamma-ray pulses. The information was recorded by a two-dimensional AI-4096 amplitude analyser (16 x 256). The measurements were based on comparison with the $\bar{\nu}$ value for spontaneous fission of ^{252}Cf ($\bar{\nu}$ = 3.772). The measured values are accurate to within 1-3% for ^{235}U and ^{239}Pu and 3-5% for ^{240}Pu. The energy dependence of $\bar{\nu}$ for ^{235}U reveals a number of the irregularities noted previously. The average $(d\bar{\nu}/dE_n)$ value for ^{239}Pu as measured in the present work is 0.15 MeV^{-1}.

СРЕДНЕЕ ЧИСЛО МГНОВЕННЫХ НЕЙТРОНОВ ПРИ ДЕЛЕНИИ ^{235}U, ^{239}Pu и ^{240}Pu БЫСТРЫМИ НЕЙТРОНАМИ.

Сообщаются результаты измерений $\bar{\nu}$ при делении ^{235}U, ^{239}Pu и ^{240}Pu нейтронами с энергией 0,6 - 5 Мэв. Измерения проводились на линейном ускорителе электронов. Нейтроны деления регистрировались жидкостным сцинтилляционным детектором объемом 400 л. Эффективность регистрации нейтронов деления составляла 70%. Селекция первичных нейтронов осуществлялась по методу времени пролета с разрешением 1 нсек/м. Момент деления регистрировался по импульсам от мгновенных γ-лучей деления. Для записи информации использовался амплитудный анализатор АИ-4096 в двумерном режиме (16×256). Величины $\bar{\nu}$ получены путем сравнения со значением $\bar{\nu}$ = 3,772 спонтанного деления ^{252}Cf. Точность измерений $\bar{\nu}$ составляла 1-3% для ^{235}U и ^{239}Pu и 3-5% – для ^{240}Pu. Энергетическая зависимость $\bar{\nu}$ для ^{235}U обнаруживает ряд нерегулярностей, замеченных ранее. Среднее значение $(d\bar{\nu})/(dE_n)$ для ^{239}Pu, полученное в данной работе, составляет 0,15 Мэв$^{-1}$.

ВВЕДЕНИЕ

Главной целью данной работы являлось исследование относительного хода энергетической зависимости $\bar{\nu}(E_n)$ при делении ядер ^{235}U, ^{239}Pu и ^{240}Pu быстрыми нейтронами. Эти изотопы играют особенно важную роль в реакторостроении. Однако для ^{239}Pu величины $\bar{\nu}(E_n)$, полученные различными авторами, существенно расходятся [1, 2], а для ^{240}Pu измерений величины $\bar{\nu}$ крайне малы [3]. С другой стороны, в последние годы точные и подробные измерения $\bar{\nu}$ показали, что принимавшаяся ранее линейная зависимость $\bar{\nu}$ от энергии нейтронов с $(d\bar{\nu})/(dE_n) = 0{,}11 \div 0{,}16$ Мэв$^{-1}$ не отражает существенных деталей этого роста. Группой Смиренкина были обнаружены скачки в $\bar{\nu}$ ^{235}U при $E_n = 1$ Мэв и $E_n = 2$ Мэв [4, 5]. Было показано [5], что подобные скачки коррелируют с поведением $K^2(E_n)$ – средним квадратом проекции углового момента

на ось ядра. Четно-четное составное ядро ^{236}U обладает энергетической щелью (Δ) в спектре внутренних возбуждений. Эффект скачкообразного изменения $\bar{\nu}$ был объяснен скачкообразным изменением числа возбужденных квазичастиц при изменении энергии возбуждения в интервале нескольких Δ [6]. Поэтому представляло значительный интерес как повторение измерений $\bar{\nu}$ для ядра мишени ^{235}U, так и проведение подобных измерений для ^{239}U, для которого также можно ожидать проявления каналовых эффектов в зависимости $\bar{\nu}(E_n)$.

В данной работе энергетическая зависимость $\bar{\nu}$ для ^{239}Pu, ^{235}U и ^{240}Pu была измерена с помощью методики времени пролета, позволяющей получить высокую относительную точность результатов.

МЕТОДИКА И АППАРАТУРА

Первичные нейтроны возникали в свинцовой мишени линейного ускорителя, облучавшейся импульсами электронов с энергией $E_e \approx 17$ Мэв. Частота повторения импульсов составляла 2000 сек$^{-1}$, длительность импульсов на полувысоте ~30 нсек. На расстоянии 35 м от мишени ускорителя за защитной стенкой с коллиматором устанавливался жидкостный сцинтилляционный детектор. Внутрь детектора помещался исследуемый образец. При делении ядер детектор регистрировал мгновенные γ-кванты деления и нейтроны деления по γ-излучению, возникавшему после захвата замедлившегося нейтрона кадмием, содержавшимся в растворе сцинтиллятора. Импульс от γ-квантов деления использовался для регистрации акта деления, а по числу задержанных во времени импульсов определялось число нейтронов, образовавшихся при делении. Селекция нейтронов, вызвавших деление, велась методом времени пролета. Момент вылета нейтрона из мишени отмечался по импульсу с высокочастотного резонатора, установленного на выходе ускорителя. Монитором нейтронного потока служил всеволновый счетчик.

Жидкостный сцинтилляционный детектор и аппаратура подробно описаны в работе [7]. Детектор заполнен раствором на основе толуола с добавлением пропионово-кислого кадмия (среднее время жизни нейтрона в сцинтилляторе 10 мксек). Световые вспышки в сцинтилляторе регистрировались 12 фотоумножителями типа ФЭУ-49Б, которые были подобраны так, чтобы при одинаковом коэффициенте усиления среднее время пролета электронов для различных экземпляров не отличалось более чем на 5 нсек. Сцинтиллирующий раствор разделен светонепроницаемой перегородкой на 2 равные части. Выделяя события, совпадающие по времени в обоих половинах, удается более чем в 100 раз снизить собственный фон детектора без существенного уменьшения регистрации актов деления [7, 8]. Блок-схема электронной аппаратуры дана на рис. 1.

Чтобы исключить амплитудные перегрузки регистрирующей аппаратуры импульсами от тормозного излучения и связанные с перегрузками искажения временных распределений, предусмотрены линейные схемы пропускания $СП_1$ и $СП_2$, которые блокируются на время тормозного излучения ускорителя. Выход с преобразователя "Время-амплитуда" $t \to A$ подключен к блоку амплитудного преобразователя ($БАП_2$) анализатора АИ-4096, работавшего в двумерном режиме с разбиением адресного устройства (АУ) на 16 плоскостей (сечений) по 256 каналов. Выбор плоскости осуществлялся импульсами от нейтронов деления с дискриминатора $Д_3$.

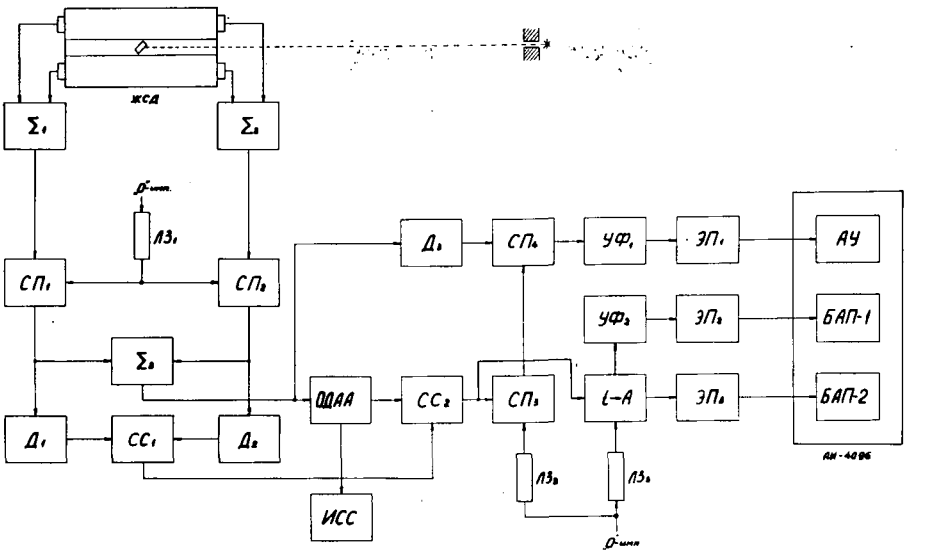

Рис. 1. Блок-схема аппаратуры.

Время регистрации этих импульсов (30 мксек) задавалось схемой пропускания $СП_4$. Мертвое время нейтронного канала ($Д_3$-АУ) определялось быстродействием триггеров АУ ($f_{max} = 4{,}2 \cdot 10^6$ гц). Калибровка временной шкалы осуществлялась с помощью калиброванной линии задержки. Временное разрешение аппаратуры определялось по полуширине пика от тормозного излучения ускорителя и составляло 35 нсек. Ноль шкалы времени задавался положением пика тормозного излучения.

Измерения эффективностей регистрации γ-лучей и нейтронов деления проводилось с помощью камеры деления со слоем ^{252}Cf ($\bar{\nu} = 3{,}772 \pm \pm 0{,}000$), установленной в центре внутреннего канала детектора. В этом случае импульс с камеры деления использовался в качестве "старт"-импульса для преобразователя "время-амплитуда", в качестве "стоп"-импульса использовался импульс от γ-квантов деления со схемы совпадений $СС_2$.

При выбранных порогах дискриминаторов $Д_1$, $Д_2$ (0,3 Мэв по энергии γ-лучей), порогов одноканального дифференциального амплитудного анализатора (ОДАА) (2,0 Мэв и 9 Мэв) и порога дискриминатора $Д_3$ (1,5 Мэв) эффективность регистрации γ-квантов деления составляла $\epsilon_\gamma = 0{,}347 + 0{,}002$, эффективность регистрации нейтронов деления $\epsilon_n = 0{,}789 \pm 0{,}004$. Собственный фон детектора по нейтронному каналу при этом был меньше 0,1 импульса на один 30-микросекундный интервал регистрации нейтронов.

Вес образцов, использованных в измерениях, составлял: ^{235}U – 30,7 г (обогащение 90%), ^{239}Pu – 24,21 г (обогащение 98%), ^{240}Pu – 10 г (^{240}Pu – 81,47%, ^{239}Pu – 9,17%; ^{241}Pu – 9,36%). Образцы из ^{235}U и ^{239}Pu представляли наборы металлических дисков диаметром 15 мм и толщиной 1 мм. Образец ^{240}Pu был в виде двуокиси, которая помещалась в контейнер из оргстекла. Во внутренний канал детектора вставлялась свинцовая труба толщиной 3 мм для защиты детектора от мягкого γ-излучения образцов ^{239}Pu и ^{240}Pu.

Эксперимент состоял из цикла одинаковых измерений с исследуемыми образцами, образцом свинца и без образца. Измерения со свинцом проводились для учета упругого и неупругого рассеяния нейтронов на исследуемых изотопах. При этом исследуемый образец делящегося изотопа для сохранения скорости счета оставался в канале детектора, но не в пучке.

На рис. 2 приведены временные распределения для четырех плоскостей ($\nu = 0, 1, 2, 3$), полученные в одной из серий измерений на ^{235}U.

Сплошные кривые представляют усредненный фон, измеренный с образцом свинца. Этот фон существенен в первых плоскостях ($\nu = 0$ и 1) и уменьшается с ростом номера плоскости. Возрастание фона в области энергий нейтронов $E_n = 4$ Мэв – 7 Мэв соответствует регистрации γ-квантов, возникших при неупругом рассеянии нейтронов. При энергии ниже 4 Мэв уровень этого фона снижается из-за малой вероятности регистрации γ-квантов неупругого рассеяния по каналу схемы совпадений CC_1

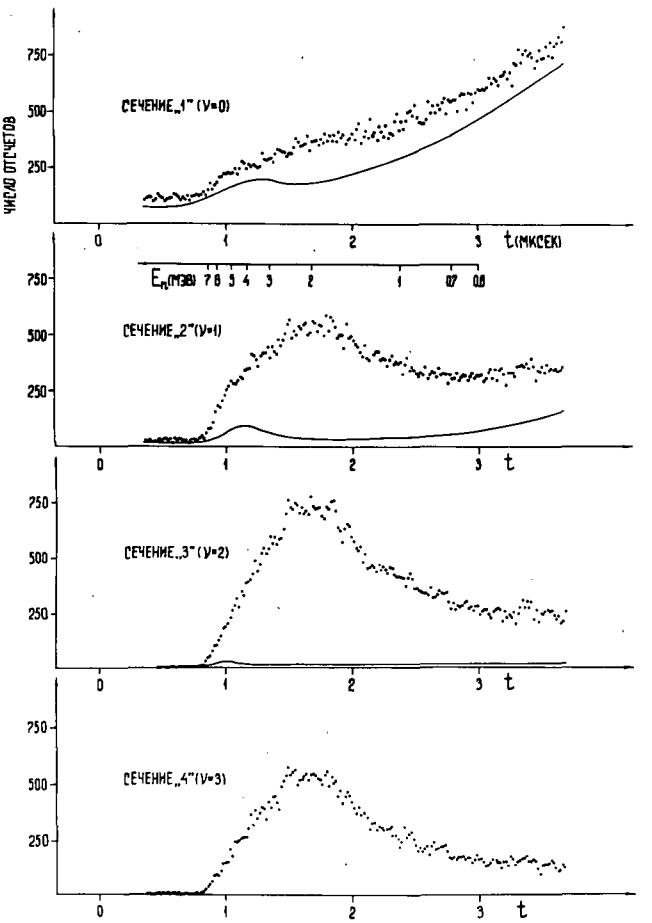

Рис. 2. Временные распределения в четырех плоскостях, полученные в эксперименте с ^{235}U.

и высокого порога ОДАА. При $E_n < 0,7$ Мэв фон плавно возрастает со временем за счет регистрации упруго и неупруго рассеянных нейтронов. Этот фон определяется временным распределением нейтронов из мишени линейного ускорителя, полным сечением рассеяния нейтронов и временным распределением вероятности захвата нейтронов в сцинтилляторе f(t) [8].

В соответствии с ростом вероятности захвата нейтрона со временем, уровень фона от упруго и неупруго рассеянных нейтронов становится существенным при $t > 2,8$ мксек ($E_n < 0,7$ Мэв).

Ошибка за счет вычитания фонов при $E_n > 5$ Мэв и $E_n < 0,7$ Мэв существенно возрастает. Поэтому экспериментальные результаты обрабатывались в энергетическом интервале 0,6-5 Мэв (для ^{235}U в данной работе приводятся также значения и при $E_n > 5$ Мэв). В этом диапазоне фон от рассеянных нейтронов составлял 2-7% от эффекта. Разница в полных сечениях рассеяния на Pb и исследуемых изотопах в указанном диапазоне энергий нейтронов не превышает 20%. Поэтому величина ошибки, вносимой в конечный результат из-за неточного определения фона, меньше 1% в случае ^{235}U и ^{239}Pu и меньше 1,5% для ^{240}Pu. Ошибки за счет разницы энергетических и угловых распределений рассеянных нейтронов на свинцовом и исследуемых образцах значительно меньше ошибок, обусловленных неопределенностями в сечениях рассеяний, ввиду слабой энергетической и угловой чувствительности подобного детектора к нейтронам [9]. В измерениях с образцом ^{240}Pu основной фон во временных распределениях определялся фоном спонтанного деления ^{240}Pu, который составлял ~ 50% зарегистрированного числа делений.

ОБРАБОТКА РЕЗУЛЬТАТОВ ИЗМЕРЕНИЙ

Из временных распределений были вычтены: фон случайных совпадений (измерения без образца, приведенные по потоку нейтронов из мишени) и фон упруго и неупруго рассеянных нейтронов (измерения со свинцовым образцом, нормированные, после вычитания фона случайных совпадений, на поток нейтронов и отношение числа ядер в образцах).

В полученные после вычитания фонов временные распределения в каждой плоскости анализатора были внесены поправки на запуски временного канала нейтронами деления, возможные вследствие просчета импульсов от γ-лучей деления. Величина этой поправки возрастала с увеличением времени регистрации делений в соответствии с поведением f(t). Максимальная величина поправки была при $E_n = 0,7$ Мэв, где она составляла 2% от общего числа зарегистрированных делений.

Во временных распределениях импульсов в первом сечении ($\nu = 0$) присутствовала часть импульсов, обусловленных γ-лучами радиационного захвата нейтронов в образцах. Для определения числа делений с $\nu = 0$ в в каждом канале "k" (N_0^k) мы принимали, что все N_0^k при $E_n = 3 \div 5$ Мэв обусловлены делением, так как в этой области сечение захвата нейтронов мало, вследствие сильной конкуренции деления и испускания нейтронов.

Используя энергетическую зависимость $N_0^k / \sum_{n=1}^{n=n_{max}} N_n^k$ (после поправок на

фон) в интервале $E_n = 3 \div 5$ Мэв, определялось число нейтронов N_k^0, принадлежавших делению при $E_n < 3$ Мэв.

После введения во временные распределения вышеуказанных поправок среднее число нейтронов на акт деления определялось по методу, предложенному в работе [9].

Просчет импульсов в нейтронном канале учитывался с помощью соотношения:

$$F'_n = F_n\left(1 - \frac{n!}{(n-2)!\,2!}\cdot r\right) + F_{n+1}\, r\,\frac{(n+1)!}{(n-1)!\,2!}\cdot r \qquad (1)$$

где $F'_n = N_n \Big/ \sum_{n=1}^{n=n_{max}} N_n$ есть вероятность регистрации "n" нейтронов, полученная в эксперименте, а F_n – вероятность регистрации "n" импульсов без просчетов в регистрирующей аппаратуре, k – номер канала. Коэффициент "r" в формуле (1) есть вероятность того, что 2 импульса не разрешаются аппаратурой:

$$r = 2\tau \int_0^\infty f^2(t)\,dt$$

где τ – мертвое время аппаратуры, а $f(t)$ – временное распределение вероятности захвата нейтрона в детекторе.

Фон в нейтронном канале учитывался с помощью соотношения:

$$F_n = B_0 C_n + B_1 C_{n-1} + \ldots + B_n C_0$$

где B_n – вероятность регистрации "n" фоновых импульсов; C_n – вероятность регистрации "n" импульсов от нейтронов деления в отсутствие фона. Распределение фона по нейтронному каналу B_n измерялось следующим образом. Импульс от специального генератора, синхронизированный с нейтронным импульсом ускорителя, открывал схему пропускания $СП_4$ в нейтронном канале. Одновременно тот же импульс генератора использовался в качестве "стоп"-импульса преобразователя "время-амплитуда". При этом на анализаторе регистрировались в основном фоновые распределения по плоскостям, так как частота повторения импульсов генератора была равна $f = 2000$ сек$^{-1}$, а скорость делений в образце ≈ 5 дел/сек.

Такая процедура повторялась несколько раз во время измерений. Распределения B_n, полученные подобным образом для ^{235}U и ^{239}Pu, совпадали с распределениями B_n, полученными в измерениях со свинцом из интервала 0,2-0,7 мксек.

Было обнаружено, что фон по нейтронному каналу был одинаков во всем измеряемом интервале E_n, что связано с тем, что временной интервал регистрации нейтронов (30 мксек) много больше интервала регистрации γ-лучей деления (2,5 мксек).

Среднее значение B_n составляло в измерениях с ^{235}U 0,3 импульса, с ^{239}Pu – 0,5 импульса и с ^{240}Pu – 0,9 импульса на один 30 мксек интервал регистрации нейтронов.

Среднее число нейтронов на акт деления находилось так:

$$\nu = \frac{\sum_{n=1}^{n=n_{max}} C_n \cdot n}{\epsilon_n}$$

Так как порог регистрации актов делений составлял 2 Мэв, то можно было ожидать различной эффективности регистрации делений с разными значениями ν. Этот эффект мог бы привести в первую очередь к искажению $P(\nu)$ – вероятности образования при делении ν нейтронов.

Полученное нами из калибровочных измерений распределение $P(\nu)$ для ^{252}Cf сравнивалось с измерением $P(\nu)$ ^{252}Cf [10], в котором акты деления регистрировались по осколкам делений. Результаты, полученные в данной работе и [10] в пределах ошибки совпадали. Поэтому предполагалось, что эффективность регистрации делений с различными ν постоянна. При вычислении $\bar{\nu}$ учитывались:

1) угловая корреляция нейтрон деления – падающий нейтрон, возникшая вследствие угловой анизотропии осколков;

2) изменение средней энергии нейтронов деления с ростом $\bar{\nu}$ и отличие спектра нейтронов деления ^{252}Cf, использованного для калибровки, от спектра нейтронов деления исследуемых изотопов;

3) размножение образовавшихся нейтронов в исследуемых образцах;

4) содержание в образцах посторонних изотопов. При введении поправок в $\bar{\nu}$ ^{240}Pu на содержание ^{239}Pu использовались результаты данной работы. При введении поправок на содержание в образцах ^{238}U, ^{241}Pu и ^{236}U использовались результаты работы [3].

На рис.3 представлены результаты измерений $\bar{\nu}(E_n)$ для ^{238}U, ^{239}Pu и ^{240}Pu. Значения $\bar{\nu}$ для ^{235}U усреднены по трем сериям измерений, для ^{239}Pu – по двум сериям, проведенным в разное время. Статистическая точность каждой серии составляла 1-1,5%. Отклонения от средних по сериям величин $\bar{\nu}$, приведенных на рис.3, при одинаковых E_n, в каждой точке составляли 0,5-0,7%. Указанные ошибки являются среднеквадратичными. При вычислении ошибок учитывались:

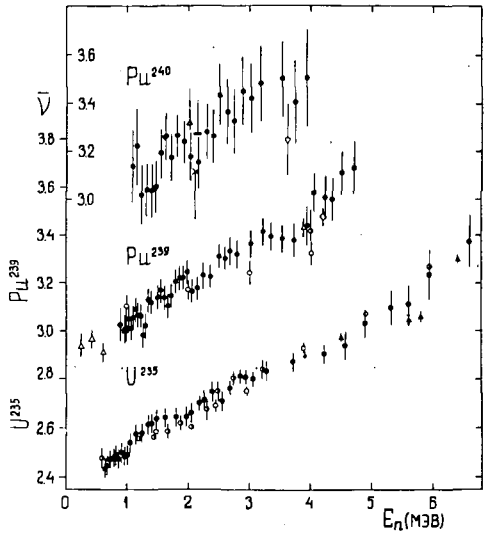

Рис.3. Сравнение результатов измерений данной работы с данными других авторов: ◑ – [5, 17], ○ – [1, 11], ▲ – [12], △ – [2], ◇ – [14], ▽ – [16], ◭, ✕, ▬ – Barton, Sanders, Engl.(из обзора [3]).

1) статистические флуктуации;

2) изменение эффективности регистрации нейтронов, вследствие нестабильности аппаратуры (≈0,5%);

3) ошибки, обусловленные неточностью определения фона с помощью свинцового образца (≈0,5%);

4) ошибки поправок на запуски временного канала нейтронами деления (≈0,5%) при E_n = 0,7-0,9 Мэв.

Относительные ошибки измерений определялись только статистическими флуктуациями и поправками при E_n < 1 Мэв на запуски временного канала нейтронами деления и составляли 0,8% для ^{235}U и 1% для ^{239}Pu в диапазоне E_n = 0,7 ÷ 4,5 Мэв.

ОБСУЖДЕНИЕ РЕЗУЛЬТАТОВ

На рис. 3 полученные авторами результаты для ^{235}U, ^{239}Pu и ^{240}Pu сравниваются с некоторыми наиболее точными данными других авторов.

Измеренные в данной работе величины $\bar{\nu}$ ^{235}U находятся в хорошем согласии с результатами, опубликованными ранее [5, 11, 12]. Характерные особенности зависимости $\bar{\nu}$ от E_n в области от 1 до 3 Мэв хорошо повторяют результаты, полученные Прохоровой и Смиренкиным. Их интерпретация подробно обсуждается в работе [5]. Вся совокупность приведенных на рис. 3 данных свидетельствует, что после монотонного возрастания $\bar{\nu}$ в интервале от 3 до 5 Мэв наклон $(d\bar{\nu})/(dE_n)$ при E_n > 5,5 Мэв увеличивается, что связано, очевидно, с началом реакции (n, n) [13].

Зависимость $\bar{\nu}$ от E_n для ^{239}Pu обнаруживает значительно более быстрый рост $\bar{\nu}$ от E_n, чем измеренный в работе Мазера и др. [1]. Значения $\bar{\nu}$ при E_n = 1 Мэв и E_n = 4 Мэв хорошо совпадают с данными работы [2] и выше 4 Мэв – с результатами, опубликованными Конде [14], если учесть различие калибровочных значений $\bar{\nu}$ ^{252}Cf (в работе [14] использовано значение $\bar{\nu}$ = 3,768 ^{252}Cf).

Относительная точность измерений $\bar{\nu}$, достигнутая в данной работе, позволяет говорить о наличии структуры в зависимости $\bar{\nu}(E_n)$ для ^{239}Pu на участке 0,7-3 Мэв.

Данные, приведенные на рис. 3, обнаруживают два отчетливых скачка в значениях $\bar{\nu}$ при E_n = 1,3 Мэв и E_n = 2,5 Мэв. Эти скачки коррелируют с поведением $K_0^2(E_n)$, вычисленным из углового распределения осколков в реакции ^{239}Pu (d, p_f) в предположении величины энергетической щели в спектре внутренних возбуждений 2Δ = 2,6 Мэв [15]. Используя метод, развитый Струтинским и Павлинчуком для объяснения зависимости $\bar{\nu}(E_n)$ для ^{235}U [6], можно, по-видимому, объяснить поведение $\bar{\nu}$ и K^2 и корреляцию между ними для ^{239}Pu без привлечения предположения об аномально большой величине щели Δ.

Величины $\bar{\nu}$ ^{240}Pu, полученные в данной работе, показывают, что $\bar{\nu}$ для различных изотопов Pu не отличаются в пределах экспериментальных ошибок. Обращает на себя внимание аномалия в значениях $\bar{\nu}$ ^{240}Pu при E_n = 1,2-1,5 Мэв, но так как статистическая ошибка измерений $\bar{\nu}$ велика (из-за спонтанного деления ^{240}Pu), то для уточнения детального хода $\bar{\nu}(E_n)$ требуются дополнительные измерения как на более интенсивных источниках нейтронов, так и с помощью других методик.

ЛИТЕРАТУРА

[1] MATHER, D.S., FIELDHOUSE, P., MOAT, A., Nucl. Phys. 66 (1965) 149.
[2] HOPKINS, J.C., DIVEN, B.C., Nucl. Phys. 48 (1963) 433.
[3] FILLMORE, F.I., Nucl. Energy 22 (1968) 79.
[4] BLYAMKINA, Yu.A., BONDARENKO, I.I., KUZNETSOV, V.F., NESTEROV, V.G., OKOLOVITCH, V.N., SMIRENKIN, G.N., USACHEV, L.N., Nucl.Phys. 52 (1964) 648.
[5] ПРОХОРОВА, Л.И., СМИРЕНКИН, Г.Н., ШПАК, Д.Л., Nucl. Data for Reactors, v.II, IAEA, Vienna, 1967, p.67.
[6] СТРУТИНСКИЙ, В.М., ПАВЛИНЧУК, В.А., Physics and Chemistry of Fission, v.I, IAEA, Vienna, 1965, p.127.
[7] САВИН, М.В., ХОХЛОВ, Ю.А., ИЛЬИН, Ю.И., ШЕИН, Ю.В., ПТЭ №6 (1969) 21.
[8] ВАН-ШИ-ДИ, РЯБОВ, Ю.В., ПТЭ №4 (1965) 63.
[9] DIVEN, B.C. et al., Phys. Rev. 101 (1956) 1012.
[10] BARON, E., FREHAUT, J., OUVRY, F., SOLEILHAC, M., Nuclear Data for Reactors, v.II, IAEA, Vienna, 1967, p.57.
[11] MATHER, D.S., FIELDHOUSE, P., MOAT, A., Phys. Rev. 139 (1964) 1403.
[12] MEADOWS, J.W., WHALEN, I.F., ANL – 7028 (1965), ANL – 7010 (1964).
[13] ВАСИЛЬЕВ, Ю.А., ЗАМЯТИН, Ю.С. и др. ЖЭТФ 38 (1960) 673.
[14] CONDE, H., HANSEN, J., HOLMBERG, M., Nucl. Energy 22 (1968) 53.
[15] BRITT, H.C., CIBBS, W.R., GRIFFIN, J.J., STOKES, R.H., Phys.Rev. 139 (1965) 354.
[16] КУЗМИНОВ, В.Д., Сб. "Нейтронная физика", Атомиздат, М., 1961, стр.246.
[17] СМИРЕНКИН, Г.Н., БОНДАРЕНКО, И.И. и др., Атомная энергия IV (1958) 187.

СРЕДНЕЕ ЧИСЛО МГНОВЕННЫХ НЕЙТРОНОВ ПРИ ДЕЛЕНИИ УРАНА-235 И ПЛУТОНИЯ-239 НЕЙТРОНАМИ

В. Г. НЕСТЕРОВ, Б. НУРПЕИСОВ,
Л. И. ПРОХОРОВА, Г. Н. СМИРЕНКИН,
Ю. М. ТУРЧИН
Физико-энергетический институт, Обнинск,
Союз Советских Социалистических Республик

Presented by S.I. Sukhoruchkin

Доклад представлен С.И. Сухоручкиным

Abstract — Аннотация

AVERAGE NUMBER OF PROMPT NEUTRONS IN THE FISSION OF URANIUM-235 AND PLUTONIUM-239 BY NEUTRONS.

Results are given for measurements of the fission cross-section and the average number of prompt neutrons in the fission of ^{235}U and ^{239}Pu induced by neutrons. The fission cross-section was measured by a relative method used in conjunction with track methods in the 10 keV to 1 MeV neutron energy range. The fission cross-section of ^{235}U was taken as a reference. Between 0.3 and 5 MeV the average number of secondary neutrons was measured by means of ^{3}He counters in a paraffin block and between 0.08 and 0.7 MeV with a threshold detector (multilayer thorium chamber).

СРЕДНЕЕ ЧИСЛО МГНОВЕННЫХ НЕЙТРОНОВ ПРИ ДЕЛЕНИИ УРАНА-235 И ПЛУТОНИЯ-239 НЕЙТРОНАМИ.

Сообщаются результаты измерений эффективного сечения деления и среднего числа мгновенных нейтронов при делении ^{235}U и ^{239}Pu нейтронами. Сечение деления измерено относительным методом с помощью трековой методики в диапазоне энергий нейтронов 10 кэв – 1 Мэв. В качестве опорного сечения использовалось сечение деления ^{235}U. Измерения среднего числа вторичных нейтронов произведены в диапазонах энергий нейтронов 0,3 – 5 Мэв с помощью ^{3}He-счетчиков в парафиновом блоке и 0,08 – 0,7 Мэв – с помощью порогового детектора (многослойной ториевой камеры).

ВВЕДЕНИЕ

Начиная с 1955 года, когда были опубликованы экспериментальные данные и результаты расчетов [1,2] среднего числа нейтронов деления $\bar{\nu}$ с ростом возбуждения ядра, ведутся интенсивные исследования энергетической зависимости $\bar{\nu}(E_n)$. Накопленные в течение первых 5 лет данные [3,4] подтвердили, что среднее число нейтронов, испускаемых при делении, с ростом энергии бомбардирующих нейтронов E_n возрастает в пределах достигнутой в то время точности эксперимента (3÷5%) так, как того можно было бы ожидать в предположении независимости средней кинетической энергии осколков E_k от энергии возбуждения:

$$\bar{\nu}(E_n) = \bar{\nu}(0) + \frac{d\bar{\nu}}{dE_n} E_n; \quad \frac{d\bar{\nu}}{dE_n} \approx 0{,}13 - 0{,}15 \text{ Мэв}^{-1} \qquad (1)$$

В последующие годы были выполнены более детальные исследования $\bar{\nu}$ и E_k [5-17], которые дали свидетельства в пользу существования небольших, но вполне заметных отступлений от линейной зависимости $\bar{\nu}(E_n)$ (1).

По-видимому, они носят нерегулярный и достаточно сложный характер, однако из-за малости эффектов и недостаточной точности и детальности измерений большинство авторов предпочитает экспериментальные данные описывать упрощенно [6,9,18,19], пользуясь различными модификациями (1). Имеющиеся теоретические представления о зависимости $\bar{\nu}(E_n)$ весьма бедны [7,20], однако, они подтверждают идею о нерегулярном характере изменения $\bar{\nu}$ и связывают происхождение нерегулярностей в ходе $\bar{\nu}(E_n)$ с каналовыми эффектами – проявлениями дискретной структуры спектра переходных состояний.

Данная работа предпринята с целью изучения поведения $\bar{\nu}$ ^{235}U и ^{239}Pu в низкоэнергетической области E_n, которая имеет наибольшее практическое значение и где наблюдение структурных эффектов наиболее вероятно.

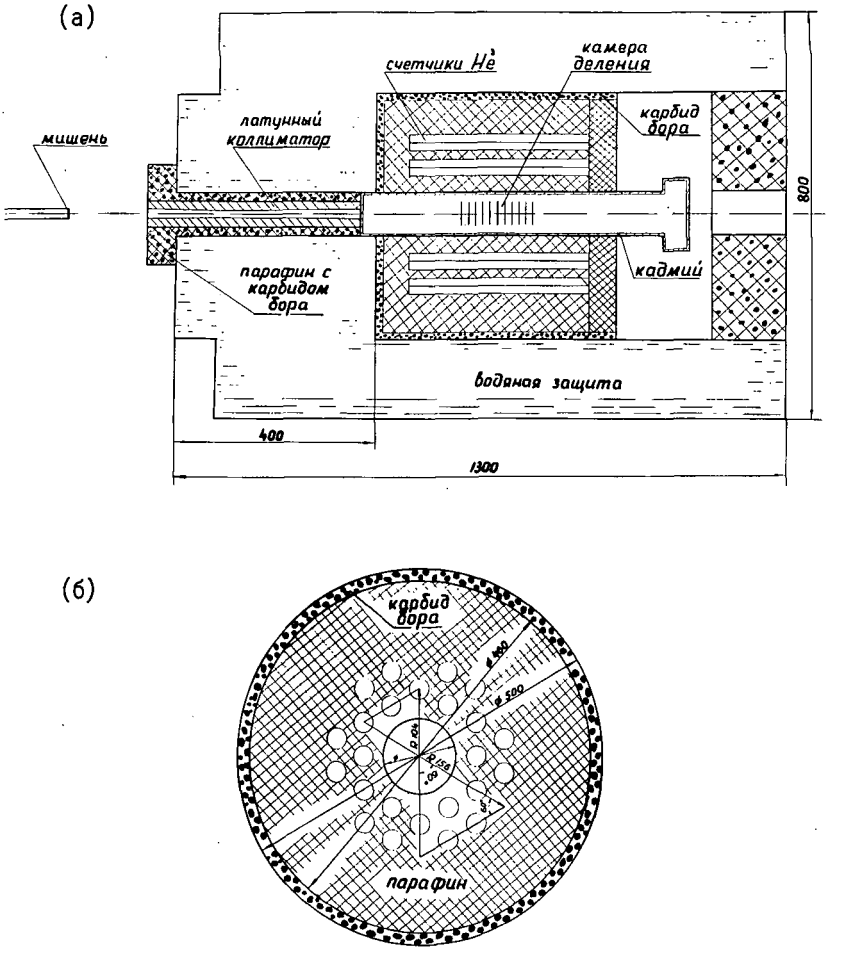

Рис. 1. Схема опыта (а) и вертикальный разрез детектора нейтронов (б)

МЕТОД ИЗМЕРЕНИЙ

Измерения производились на электростатическом генераторе с использованием в качестве источников нейтронов реакций T(p,n) и Li(p,n). В эксперименте использовался наиболее прямой и распространенный метод измерения $\bar{\nu}$ – регистрация совпадений между импульсами от детекторов нейтронов и осколков деления. Схема опыта изображена на рис. 1(а).

Детектор нейтронов представляет собой цилиндрический блок из парафина высотой 50 см и диаметром 50 см со сквозным центральным каналом диаметром 9 см для помещения внутрь него детектора осколков деления – многослойной ионизационной камеры. В отверстия в парафине, расположенные вокруг центрального канала, помещались ^{3}He-счетчики длиной 31 см и диаметром 3,2 см, наполненные ^{3}He – 4 атм. Использование 24 счетчиков, расположенных как показано на рис. 1(б), обеспечило эффективность регистрации нейтронов деления 21%. Среднее время жизни нейтронов в детекторе ≈ 50 мксек.

Детектором актов деления служила многослойная ионизационная камера. Слои делящегося вещества (^{235}U, 90% –обогащения, и ^{239}Pu с примесью ^{240}Pu 1,8%) толщиной ~0,5 мг/см^2 в виде U_3O_8 и PuO_2 наносились с обеих сторон тонких алюминиевых фольг. Общее количество ^{235}U в камере составило 200 мг, ^{239}Pu – 100 мг. Посередине сборки из слоев исследуемого вещества размещалась камера со слоем ^{252}Cf (500 делений в минуту), для спонтанного деления которого $\bar{\nu}$ служила эталоном. Вся сборка слоев в камере в обоих случаях имела протяженность около 8 см. В плутониевой камере слои делящегося вещества были поровну разделены на 10 групп, каждая из которых имела независимый выход, предварительный усилитель, дискриминатор. После дискриминации α-частиц и их наложений производилось суммирование сигналов от всех ячеек камеры делений. Детектор делений ^{235}U работал в обычном режиме многослойной камеры с единой системой собирающих электродов.

Рис. 1 дает достаточно полное представление о защитной системе; отметим только, что весь трактат, формирующий пучок нейтронов, падающих на детектор актов деления, был защищен от медленных нейтронов слоем карбида бора; на камеру, кроме того, одевался кадмиевый чехол.

Применялась процедура измерений, обычная для экспериментов с умеренной эффективностью к нейтронам. В канале совпадений непрерывно велось суммирование числа отсчетов в продолжение длительности ворот $T \sim 2\tau$. Одновременно с помощью задержки импульсов в нейтронном канале регистрируются случайные совпадения. Основные параметры регистрирующей аппаратуры: длительность ворот T = 100 мксек, время задержки – 250 мсек, разрешающее время нейтронного детектора, т. е. эффективная длительность импульса, $T_0 \approx 3{,}5$ мксек.

Отношение числа истинных совпадений к числу делений $\rho = N/N_f$ с точностью до небольших поправок пропорционально $\bar{\nu}$. Из измерений этих отношений для деления ^{235}U нейтронами и спонтанного деления ^{252}Cf получаем:

$$\frac{\bar{\nu}(E_n)}{\bar{\nu}_0} = A(E_n)\,\frac{\rho(E_n)}{\rho_0} \qquad (2)$$

где A ≈ 1 – поправочный фактор, учитывающий ряд аппаратурных эффектов, которые связаны с изменением условий регистрации нейтронов деления исследуемого изотопа и эталона, как то:

1) зависимость эффективности регистрации от положения источника нейтронов в детекторе;

2) энергетическая зависимость и угловая анизотропия эффективности детектора нейтронов $\eta(\epsilon)$;

3) дискриминация части актов деления;

4) просчеты импульсов при регистрации совпадений.

Приведенный перечень поправок необходимо дополнить фоновыми эффектами, которые обусловлены недостаточной изотопной чистотой ^{235}U и делением под действием рассеянных нейтронов.

Измерения $\bar{\nu}/\bar{\nu}_0$ были выполнены для нескольких энергий нейтронов в диапазоне 0,08 – 1,5 Мэв, а также для нейтронов, полученных замедлением быстрых нейтронов (E_n = 0,3 Мэв) в парафиновом блоке. Спектр их характеризуется кадмиевым отношением ~15. Более подробно методика данных измерений описана в работе [21].

РЕЗУЛЬТАТЫ ИЗМЕРЕНИЙ

Результаты измерений представлены в табл. 1, где последовательно приведены: среднее значение и разброс энергии нейтронов $E_n \pm \Delta E$, экспериментальное отношение $\rho(E_n)/\rho_0$, значения $\bar{\nu}(E_n)/\bar{\nu}_0$ и $\bar{\nu}(E_n)$. В ошибку включена погрешность, найденная из разброса результатов отдельных циклов измерений и неопределенность поправочного коэффициента A, со-

ТАБЛИЦА 1. РЕЗУЛЬТАТЫ ИЗМЕРЕНИЙ $\bar{\nu}$ ^{235}U И ^{239}Pu В ДАННОЙ РАБОТЕ

E_n (Мэв)	$\rho(E_n)/\rho_0$ эксп.	$\bar{\nu}(E_n)$
Уран-235		
0,0	0,6438 ± 0,0028	2,412 ± 0,014
0,080	0,6426 ± 0,0100	2,404 ± 0,014
0,214 ± 0,040	0,6566 ± 0,0047	2,467 ± 0,020
0,322 ± 0,043	0,6540 ± 0,0048	2,457 ± 0,020
0,408 ± 0,042	0,6580 ± 0,0052	2,474 ± 0,024
0,510 ± 0,039	0,6602 ± 0,0067	2,484 ± 0,027
0,686 ± 0,039	0,6519 ± 0,0063	2,452 ± 0,025
0,810 ± 0,038	0,6663 ± 0,0048	2,514 ± 0,020
0,910 ± 0,037	0,6670 ± 0,0064	2,518 ± 0,026
1,002 ± 0,062	0,6797 ± 0,0060	2,588 ± 0,025
1,112 ± 0,035	0,6814 ± 0,0054	2,578 ± 0,022
1,314 ± 0,035	0,6797 ± 0,0057	2,574 ± 0,024
1,515 ± 0,035	0,6764 ± 0,0062	2,572 ± 0,025
Плутоний-239		
0,0	0,7561 ± 0,0050	2,872 ± 0,025
0,400 ± 0,051	0,7624 ± 0,0065	2,904 ± 0,031
0,677 ± 0,048	0,7538 ± 0,0081	2,871 ± 0,035
0,902 ± 0,045	0,7561 ± 0,0087	2,882 ± 0,037
1,103 ± 0,045	0,7668 ± 0,0109	2,926 ± 0,043
1,306 ± 0,043	0,7931 ± 0,0076	3,034 ± 0,039
1,404 ± 0,043	0,8166 ± 0,0100	3,115 ± 0,040
1,483 ± 0,042	0,8144 ± 0,0095	3,128 ± 0,039
1,607 ± 0,042	0,8169 ± 0,0116	3,138 ± 0,055

ставляющая 0,4 – 0,5%. Для удобства сравнения с другими данными в качестве эталона взято часто употребляемое значение $\bar{\nu}_0 = 3{,}782$ [6,13,19], неопределенность которого при вычислении ошибок $\bar{\nu}(E_n)$ во внимание не принималась.

УРАН-235

На рис. 2 полученные значения $\bar{\nu}$ ^{235}U сравниваются с результатами других работ [6,7,11-13,19,22-26], измеренными в опытах с моноэнергетическими нейтронами с точностью не хуже 2%. Соответствующая выборка зарубежных данных взята из обзора Филмора [19]. Использовавшаяся Филмором информация дополнена данными французской группы [25] и новыми результатами измерений Савина с сотрудниками на селекторе быстрых нейтронов [26], перенормированными в соответствии с принятым стандартом для $\bar{\nu}_0$.

В нижней части рис. 2 приведена гистограмма значений $\langle \bar{\nu} \rangle$ ^{235}U, полученных усреднением совокупности экспериментальных данных в области $E_n \leqslant 3{,}5$ Мэв, где имеется достаточно подробная экспериментальная

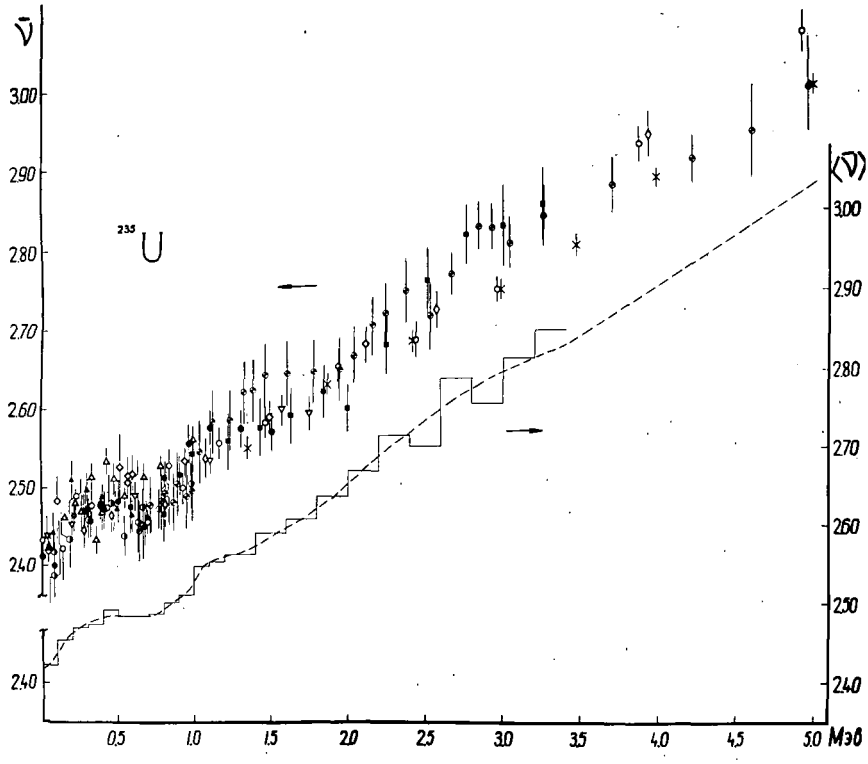

Рис. 2. Вверху – совокупность данных о среднем числе мгновенных нейтронов деления $\bar{\nu}$ ^{235}U($E_n \leqslant 5$ Мэв): △ – [13]; ▽ – [22]; ○ – [6]; ◇ – [23]; ◊ – [8]; × – [25]; ⊛ – [26]; ◑ – [7]; ▲ – [11]; ■ – [12]; ● – данная работа; ⊗ – значение $\bar{\nu}(E_n^0)$, к которому принормированы результаты относительных измерений в [7,11,12]. Внизу – усредненные значения $\langle \bar{\nu}(E_n) \rangle$ (гистограмма).

информация. Усреднение производилось по узким интервалам энергии $\Delta E_n = 0{,}1$ Мэв ($0 \leqslant E_n \leqslant 1{,}2$ Мэв) и 0,2 Мэв ($1{,}2 \leqslant E_n \leqslant 3{,}4$ Мэв) с весами, обратно пропорциональными квадратам ошибок σ. В табл. 2, кроме значений $\langle \bar{\nu} \rangle$, приводятся погрешности:

$$\sigma_I = \sqrt{\frac{\Sigma(\bar{\nu}_i - \langle \bar{\nu} \rangle)^2 \frac{1}{\sigma_i^2}}{(n-1)\Sigma \frac{1}{\sigma_i^2}}} \quad \text{и} \quad \sigma_{II} = \frac{1}{\sqrt{\Sigma \frac{1}{\sigma_i^2}}}$$

первая из которых отражает разброс значений $\bar{\nu}_i$ внутри данного интервала ΔE_n, вторая – точность генерального среднего $\langle \bar{\nu} \rangle$ при условии совместности усредняемых величин. Величины ошибок σ_I и σ_{II}, за исключением нескольких интервалов, отличаются мало. Это показывает, что рассеяние данных имеет преимущественно случайную статистическую природу. Отметим также, что результаты данной работы (табл. 1) хорошо согласуются со средними значениями $\langle \bar{\nu} \rangle$.

При энергиях $E_n > 3$ Мэв процедура усреднения данных разных авторов для выработки рекомендованной кривой $\bar{\nu}(E_n)$ становится неэффективной по двум причинам. Во-первых, сильно уменьшается плотность данных. Во-вторых, среди них при усреднении преобладают относительно редкие значения французской группы [25], которые имеют наименьшую

ТАБЛИЦА 2. УСРЕДНЕННЫЕ РЕКОМЕНДОВАННЫЕ ЗНАЧЕНИЯ $\bar{\nu}$ ^{235}U

E_n (Мэв)	$\langle \bar{\nu} \rangle$	σ_I	σ_{II}	$\bar{\nu}(E_n)$[a]
0 – 0,1	2,423	0,005	0,007	2,425
0,1 – 0,2	2,455	0,010	0,014	2,455
0,2 – 0,3	2,471	0,006	0,007	2,472
0,3 – 0,4	2,475	0,010	0,007	2,481
0,4 – 0,5	2,493	0,011	0,008	2,486
0,5 – 0,6	2,485	0,010	0,009	2,485
0,6 – 0,7	2,485	0,009	0,008	2,485
0,7 – 0,8	2,488	0,016	0,009	2,488
0,8 – 0,9	2,502	0,009	0,010	2,501
0,9 – 1,0	2,512	0,007	0,010	2,515
1,0 – 1,1	2,549	0,007	0,010	2,547
1,1 – 1,2	2,555	0,011	0,011	2,558
1,2 – 1,4	2,564	0,010	0,011	2,566
1,4 – 1,6	2,591	0,007	0,010	2,586
1,6 – 1,8	2,609	0,014	0,015	2,609
1,8 – 2,0	2,638	0,007	0,010	2,636
2,0 – 2,2	2,671	0,019	0,020	2,673
2,2 – 2,4	2,716	0,020	0,023	2,706
2,4 – 2,6	2,702	0,011	0,010	2,736
2,6 – 2,8	2,788	–	0,022	2,764
2,8 – 3,0	2,756	0,016	0,009	2,786
3,0 – 3,2	2,814	–	0,027	2,806
3,2 – 3,4	2,848	–	0,029	2,826

[a] В последней колонке приведены значения $\bar{\nu}(E_n)$, соответствующие рекомендованной плавной кривой для середин указанного интервала энергии. Выше 3,5 Мэв она соответствует выражениям (3) и (4).

ошибку, но проходят на 1-1,5% ниже основной массы точек $\bar{\nu}_i$. Эти обстоятельства из-за подавляющего веса данных [25] приводят к "дрожанию" гистограммы в зависимости от того, есть значение [25] в данном интервале ΔE_n или нет, что, например, уже отчетливо проявилось на участке 2,5-3,5 Мэв.

Пунктиром на рис. 2 показана рекомендуемая нами плавная зависимость $\bar{\nu}(E_n)$ ^{235}U, которая также отражена в таблице 2 и ниже 2 Мэв довольно точно следует гистограмме $\langle \bar{\nu} \rangle$. При $E_n > 2$ Мэв рекомендованная кривая по указанным причинам содержит бóльший элемент произвола. Однако, как показано в [21], возникающие при этом неточности не имеют серьезного практического значения из-за резкого падения с ростом энергии нейтронов требуемой точности ядерных констант.

Зависимость $\bar{\nu}(E_n)$ на участке 1,2-5 Мэв для многих прикладных целей может быть упрощена и описана линейной зависимостью (1):

$$\bar{\nu}(E_n) = (2{,}3954 \pm 0{,}0330) + (0{,}1274 \pm 0{,}0092) E_n \qquad (3)$$

конкретный вид которой установлен с помощью метода наименьших квадратов. При более высоких энергиях удобно воспользоваться эмпирическими выражениями, приведенными в [25]:

$$\bar{\nu}(E_n) = \begin{cases} 2{,}028 + 0{,}200\ E_n & 5{,}0 < E_n < 7{,}5 \text{ Мэв} \\ 2{,}485 + 0{,}139\ E_n & 7{,}5 < E_n < 15 \text{ Мэв.} \end{cases}$$

ПЛУТОНИЙ-239

Данные о $\bar{\nu}$ ^{239}Pu для низкоэнергетического участка $E_n < 2$ Мэв представлены на рис. 3. По числу и точности измерений они заметно уступают ^{235}U. В данной работе разница в точности измерений $\bar{\nu}$ ^{239}Pu и ^{235}U определялась главным образом наличием фона спонтанных делений ^{240}Pu в плутониевом образце. Этот фон в обычных для измерений $\bar{\nu}$ ^{235}U условиях превосходил полезный эффект. Путем изменения геометрии опыта и увеличения доли случайных совпадений до 35-50% (в 2-3 раза больше, чем на ^{235}U) фон спонтанных делений в эксперименте с плутонием был доведен до уровня 20-30%.

В дальнейшем измерения будут продолжены на более кондиционном ^{239}Pu, поэтому результаты данного эксперимента мы рассматриваем как предварительные.

Результаты данных измерений обнаруживают приблизительное постоянство $\bar{\nu}$ до 1 Мэв с резким последующим скачком более чем на 5%. При самых низких энергиях нейтронов они согласуются с единственными данными [8], но заметно отклоняются вниз от группы точек [8,26] в диапазоне 0,9 – 1,2 Мэв, хотя в дальнейшем снова неплохо согласуются с данными [25,26].

Таким образом, данные других работ в том числе и информация о зависимости $\bar{\nu}(E_n)$, основанная на анализе энергетического баланса деления $^{239}Pu(n,f)$ [27], свидетельствуют о более плавном росте $\bar{\nu}$ с увеличением E_n в сравнении с тем, что следует из результатов данного эксперимента.

Это расхождение данных, важное как с практической точки зрения, так и для интерпретации хода $\bar{\nu}(E_n)$ [10,20], явится предметом ближайших исследований.

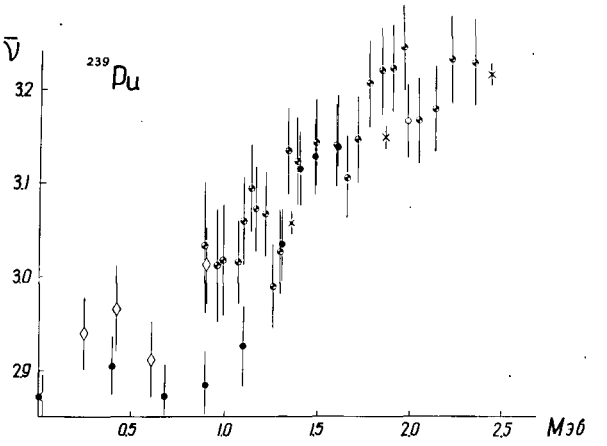

Рис. 3. Совокупность данных о среднем числе мгновенных нейтронов деления $\bar{\nu}$ ^{239}Pu ($E_n \leqslant 2$ Мэв): O – [6]; ◇ – [8]; X – [25]; ⊕ – [26]; ● – данная работа.

Резюмируя изложенное, можно заключить следующее:

1. Совокупность результатов измерений $\bar{\nu}$ ^{235}U разными авторами непротиворечива. Ее анализ показывает, что в среднем в наиболее важной для практики области E_n достигнута точность относительного хода $\bar{\nu}(E_n)$ 0,3-0,5% (табл. 2), что уже, по-видимому, отвечает разумному уровню требований к точности современного расчета реакторов.

2. Информация о $\bar{\nu}$ ^{239}Pu бедна и явно недостаточна для обеспечения потребностей практики, в особенности при низких энергиях < 1,5 Мэв.

3. Экспериментальные данные поддерживают представления о наличии тонкой структуры зависимости $\bar{\nu}(E_n)$ ступенчатого типа [20]. Упрощение зависимости $\bar{\nu}(E_n)$ при оценке данных и составлении многогрупповых констант для расчета реакторов в настоящее время нецелесообразно.

Авторы выражают признательность А. И. Лейпунскому за интерес к работе, Л. Н. Усачеву и Ю. Я. Стависскому – за полезные обсуждения и поддержку исследований, Ю. Е. Багдасарову, И. И. Котухову, Н. Н. Щадину – за участие на отдельных этапах эксперимента, персоналу, обслуживающему ускоритель, – за четкую работу установки.

ЛИТЕРАТУРА

[1] КАЛАШНИКОВА, В. И., ЗАХАРОВ, В. П., КРАСНУШКИН, А. В., ЛЕБЕДЕВ, В. И., ПЕВЗНЕР, М. И., Сессия АН СССР по мирному использованию атомной энергии (отд. физ.-мат. наук) Издание АН СССР, 1955, стр. 156.

[2] LEACHMAN, R.B., Phys. Rev. 101 (1956) 1005.

[3] LEACHMAN, R.B., Int. Conf. peaceful Uses atom. Energy (Proc. Conf. Geneva, 1958) 15 (1958) 229.

[4] BONDARENKO, I.I., KUZMINOV, B.D., KUTSAEVA, L.S., PROCHOROVA, L.I., SMIRENKIN, G.N., Int. Conf. peaceful Uses atom. Energy (Proc. Conf. Geneva, 1958) 15 (1958).

[5] MOAT, A., MATHER, D.S., FIELDHAUSE, P.F., Proc. of the Seminar of the Physics of Fast and Intermediate Reactor, IAEA, Vienna (1961) 139;
BONDARENKO, I.I., ditto 3 (1961) 451.

[6] MATHER, D.S., FIELDHAUSE, P.F., MOAT, A., Phys. Rev. B1403 (1964) 133.
[7] BLJUMKINA, Yu.A., BONDARENKO, I.I., KUZNETSOV, V.F., NESTEROV, V.G., OCOLOVICH, V.N., SMIRENKIN, G.N., USACHEV, L.N., Nucl.Phys. 52 (1964) 648.
[8] HOPKINS, I.C., DIVEN, B.C., Nucl. Phys. 48 (1963) 433.
[9] БОНДАРЕНКО, И. И., КУЗНЕЦОВ, В. Ф., НЕСТЕРОВ, В. Г., ПАВЛИНЧУК, В. А., ПРОХОРОВА, Л. И., РАБОТНОВ, Н. С., СМИРЕНКИН, Н. С., УСАЧЕВ, Л. Н., Доклад №/С 336 на Международном конгрессе по ядерной физике, Париж, 1964.
[10] ПРОХОРОВА, Л. И., СМИРЕНКИН, Г. Н., ШПАК, Д. Л., Nuclear Data for Reactors, Paris, IAEA, 2 (1967) 67.
[11] КУЗНЕЦОВ, В. Ф., СМИРЕНКИН, Г. Н., Nuclear Data for Reactors, Paris, IAEA, 2 (1967) 75.
[12] ПРОХОРОВА, Л. И., СМИРЕНКИН, Г. Н., ЯФ 7 (1968) 961.
[13] MEADOWS, J.W., WHAVEN, J.F., Journ. Nucl. Energy 21 (1967) 157.
[14] БОЛЬШОВ, В. И., КУЗНЕЦОВ, В. Ф., СМИРЕНКИН, Г. Н., ЕРМАГАМБЕТОВ, С. Б., ОКОЛОВИЧ, В. И., ЯФ 6 (1967) 1162.
[15] ДЬЯЧЕНКО, П. П., КУЗЬМИНОВ, Б. Д., ТАРАСКО, М. З., ЯФ 8 (1968) 286.
[16] MATHER, D.S., FIELDHAUSE, P., MOAT, A., Nucl. Phys. 66 (1965) 149.
[17] СЕРГАЧЕВ, А. И., ВОРОБЬЕВА, В. Г., КУЗЬМИНОВ, Б. Д., МИХАЙЛОВ, В. Б., ТАРАСКО, М. З., ЯФ 7 (1968) 778.
[18] Neutron Cross Sections, BNL-325, Second Edit. Suppl., 2 No. 2, 1965.
[19] FILMORE, F.L., Journ. Nucl. Energy 22 (1968) 79.
[20] СТРУТИНСКИЙ, В. М., ПАВЛИНЧУК, В. А., Physics and Chemistry of Fission, IAEA, Vienna, 1 (1965) 127.
[21] ПРОХОРОВА, Л. И., БАГДАСАРОВ, Р. Е., АЭ (в печати).
[22] CONDE, H., Arkiv Fisic. 29 (1965) 293.
[23] MEADOWS, I.W., WHALEN, I.F., Phys. Rev. 126 (1962) 197.
[24] COLWIN, D.W., SOWERBY, M.G., Proc. IAEA Physics and Chemistry of Fission, 2 (1965) 25.
[25] SOLEILHAE, M., FREHAUT, J., GAURIAU, J., Journ. Nucl. Energy 23 (1969) 257.
[26] САВИН, М. В. и др., II конф. по ядерным данным для расчета реакторов, Хельсинки, 1970, CN-26/40.
[27] ВОРОБЬЕВА, В. Г. и др., II конф. по ядерным данным для расчета реакторов, Хельсинки, 1970, CN-26/88.

АНАЛИЗ ЗАВИСИМОСТИ $\bar{\nu}$ ОТ ЭНЕРГИИ НЕЙТРОНОВ НА ОСНОВЕ ЭНЕРГЕТИЧЕСКОГО БАЛАНСА ПРИ ДЕЛЕНИИ ЯДЕР

В. Г. ВОРОБЬЕВА, П. П. ДЬЯЧЕНКО,
Н. П. КОЛОСОВ, Б. Д. КУЗЬМИНОВ,
А. И. СЕРГАЧЕВ, Л. Д. СМИРЕНКИНА
Физико-энергетический институт, Обнинск,
Союз Советских Социалистических Республик,
А. ЛАЙТАИ
Центральный институт физических исследований,
Будапешт,
Венгерская Народная Республика

Abstract — Аннотация

ANALYSIS OF THE NEUTRON ENERGY DEPENDENCE OF $\bar{\nu}$, ON THE BASIS OF THE ENERGY BALANCE IN NUCLEAR FISSION.

On the basis of experimental data relating to fission fragment yields and kinetic energies the authors discuss the energy balance in thorium-232, uranium-235, uranium-238 and plutonium-239 fission by neutrons with energies in the 0-6 MeV. Their findings, together with earlier results of direct measurements of $\bar{\nu}$, are used to plot a curve showing the dependence of $\bar{\nu}$ on neutron energy.

АНАЛИЗ ЗАВИСИМОСТИ $\bar{\nu}$ ОТ ЭНЕРГИИ НЕЙТРОНОВ НА ОСНОВЕ ЭНЕРГЕТИЧЕСКОГО БАЛАНСА ПРИ ДЕЛЕНИИ ЯДЕР.

На основе экспериментальных данных о выходах и кинетических энергиях осколков в работе обсуждается энергетический баланс при делении ^{232}Th, ^{235}U, ^{238}U и ^{239}Pu нейтронами с энергией 0-6 Мэв. Полученные сведения совместно с существующими результатами прямых измерений $\bar{\nu}$ используются при построении кривой зависимости $\bar{\nu}$ от энергии нейтронов.

Существующие экспериментальные данные, характеризующие зависимость среднего числа вторичных нейтронов от энергии нейтронов, вызывающих деление, достаточно полно представлены в последнем обзоре Филлмора [1]. К сожалению, очень часто различие экспериментальных результатов разных авторов превышает приписываемую ошибку измерений. Это обстоятельство затрудняет понимание деталей зависимости $\bar{\nu}$ от E_n. В ряде работ [2, 3] для выяснения энергетической зависимости $\bar{\nu}$ привлекались некоторые модельные представления о механизме процесса деления. В работах [3-5] исследовалась корреляция зависимости $\bar{\nu}$ и средней кинетической энергии осколков E_k от энергии нейтронов E_n.

В данной работе зависимость $\bar{\nu}$ от E_n анализировалась на основе энергетического баланса с привлечением результатов измерений распределений осколков по массам и кинетическим энергиям при делении ^{232}Th, ^{235}U, ^{238}U и ^{239}Pu нейтронами с энергией $0 \leq E_n \leq 6$ Мэв [6-9]. Метод измерений и обработка результатов подробно описаны в работах [6-9]. Требования, предъявляемые к точности измерения $\bar{\nu}$ (0,5-1%), означают, что при рассмотрении энергетического баланса следует учитывать каждые 100-200 кэв. Измерения распределений осколков по массам и кинетическим энергиям, результаты которых ис-

пользовались для анализа энергетического баланса, выполнены с учетом этих требований. В применении к нашему эксперименту энергетическую зависимость $\bar{\nu}(E_n)$ удобно представить в следующем упрощенном виде:

$$\bar{\nu}(E_n) = \bar{\nu}(E_n^0) + \alpha(\Delta E_n - \Delta \bar{E}_k + \Delta E_f^Z) + \Delta \bar{\nu} \qquad (1)$$

где $\Delta E_n = E_n - E_n^0$, $\Delta E_k = \int \Delta E_k(M)\, Y(M)\, dM$, $\Delta \bar{\nu}_Y = \int \nu_0(M)\, \Delta Y(M)\, dM$;

$\nu_0(M)$ – зависимость $\bar{\nu}$ от массы при энергии нейтронов E_n^0,

$\Delta E_k(M) = E_k(M, E_n) - E_k(M, E_n^0)$,

$Y(M)$ – выход осколков с массой M,

$\Delta Y(M) = Y(E_n, M) - Y(E_n^0, M)$,

ΔE_f – изменение средней энергии деления за счет перераспределения зарядов между осколками.

На вариации кинетической энергии пары осколков может повлиять ряд причин: изменение деформации ядра в момент разрыва, вклад энергии коллективных движений (энергия вращения и колебаний, кинетическая энергия деформации), перераспределение заряда между осколками. В последнем случае одновременно происходит и изменение полной энергии деления. Причем, величине $\Delta Z = \pm 1$ соответствует $\Delta E_k \approx 1{,}5$ Мэв и $\Delta E_f^Z = 4$ Мэв (расчеты по таблицам Зигера [10]).

К сожалению, полученные результаты измерений не позволяют непосредственно установить, имеет ли место перераспределение зарядов между осколками в рассматриваемом диапазоне изменений E_n. Об этом приходится судить лишь на основе косвенных соображений.

Изменение выходов осколков ведет к изменению средней энергии деления и, следовательно, к изменению $\bar{\nu}$.

Для ^{235}U и ^{239}Pu имеются прямые измерения зависимости $\bar{\nu}$ от масс осколков при делении этих ядер тепловыми нейтронами [11]. Используя систематику Террела [12], можно сконструировать соответствующую кривую и для изотопов с пороговым ходом сечения деления.

Основная часть энергии возбуждения, затрачиваемой на испускание нейтронов осколками, обусловлена деформацией осколков в момент их образования. Кинетическая энергия осколков также определяется конфигурацией делящегося ядра в момент его развала на два осколка. В интервале энергий нейтронов $0 \leq E_n \leq 6$ Мэв средняя кинетическая энергия меняется всего на 1% (см. рис. 1). Из этого можно заключить, что зависимость $\bar{\nu}(M)$ также мало меняется. Вклад же в энергию возбуждения осколков, вносимый нейтронами, не зависит от отношения масс осколков.

Таким образом, зная изменения выходов осколков, можно подсчитать соответствующие изменения $\bar{\nu}$.

Величина α, характеризующая количество испускаемых нейтронов на единицу энергии возбуждения осколков, в данном анализе принималась постоянной. Следует отметить, что имеется целый ряд факторов, которые могут привести к изменению этой величины: изменение нуклонного состава осколков, изменение выходов осколков, изменение температуры осколков и т. д.

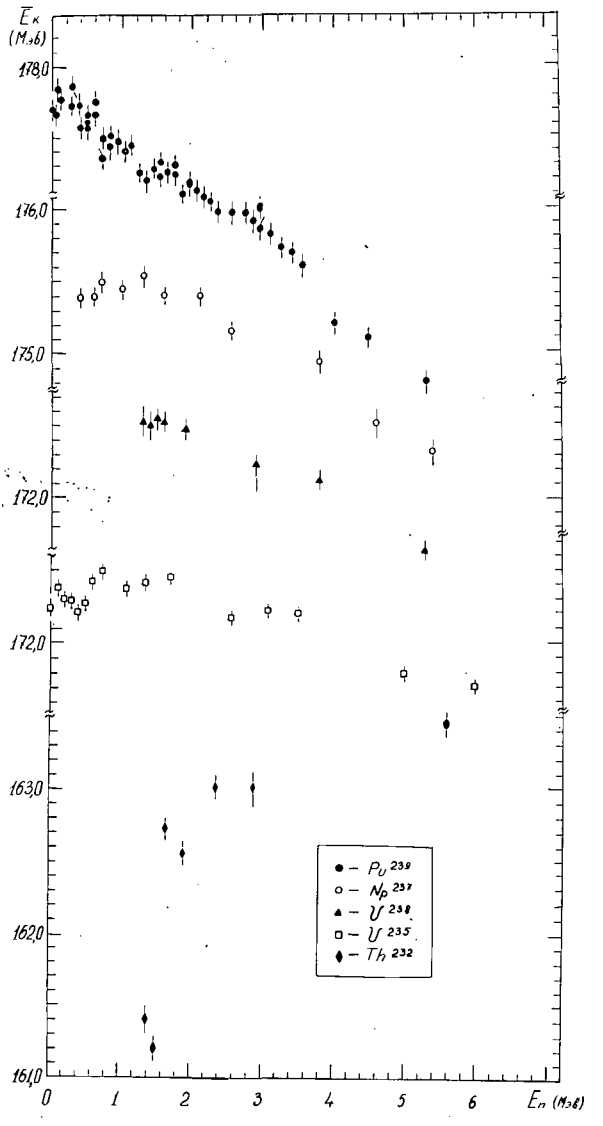

Рис. 1. Зависимость средней кинетической энергии осколков деления от энергии нейтронов.

ТАБЛИЦА 1. ЗНАЧЕНИЯ α И $\bar{\nu}$

Ядро-мишень	E_n^0, Мэв	$\bar{\nu}(E_n^0)$	α, Мэв$^{-1}$
^{239}Pu	тепл.	2,898	0,104
^{235}U	тепл.	2,418	0,125
^{238}U	1,50	2,540	0,140
^{232}Th	1,65	2,118	0,175

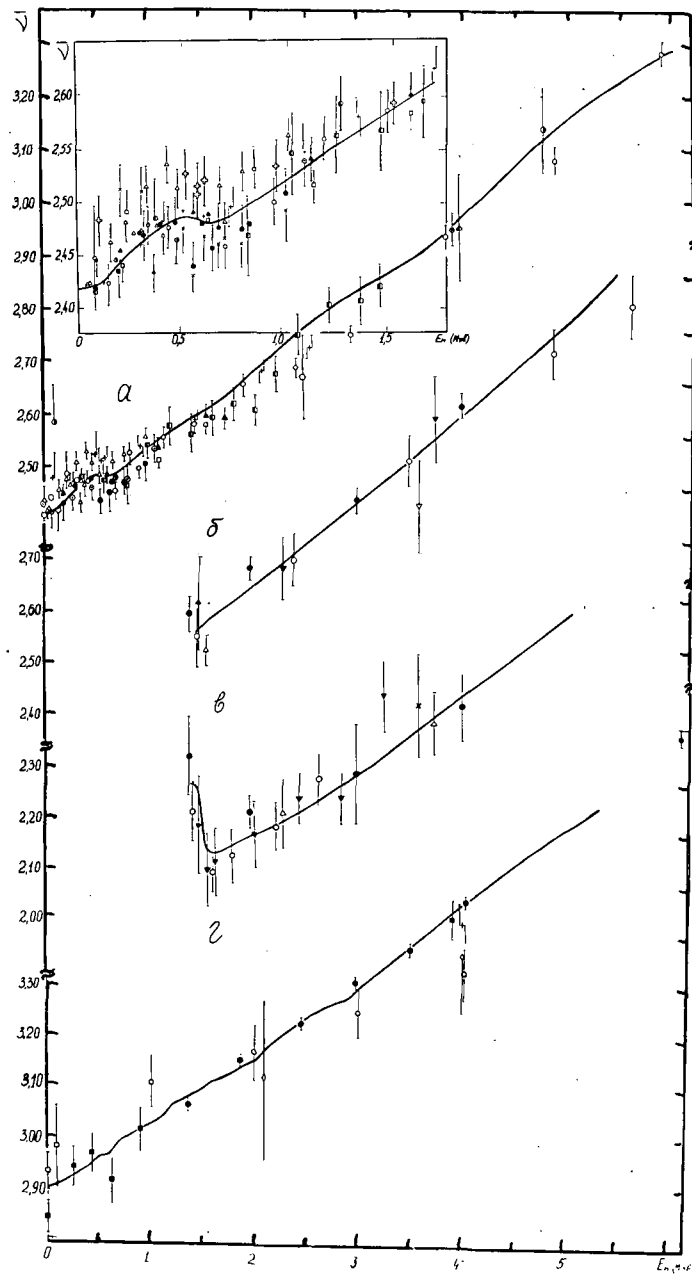

Рис. 2. Зависимость среднего числа нейтронов от энергии нейтронов:
а) уран-235, в) торий-232,
б) уран-238, г) плутоний-239.
На вставке – $\bar{\nu}$ для урана-235 в интервале энергий нейтронов 0 ÷ 1,5 Мэв. Экспериментальные значения $\bar{\nu}$ взяты из работы [1]. Для плутония-239 черными кружками обозначены результаты работы [13].

Величина α определялась методом наименьших квадратов с использованием совокупности всех результатов прямых измерений $\bar{\nu}$. Поскольку при малых ΔE_n роль α невелика, полученные значения величин α более характерны для области больших ΔE_n. Для пороговых изотопов определялась также и величина $\bar{\nu}(E_n^0)$. Во всех расчетах принималось $\Delta E_f^Z = 0$. Наиболее убедительно достоверность этого предположения можно показать на примере ^{232}Th. При переходе от $E_n = 1{,}6$ Мэв к $E_n = 1{,}5$ Мэв средняя кинетическая энергия осколков уменьшается на 1,5 Мэв. Если это изменение обусловлено перераспределением зарядов между осколками, то, как отмечалось выше, оно сопровождалось бы изменением энергии деления на величину $\Delta E_f^Z \approx 5$ Мэв. Однако, рассчитанная кривая $\bar{\nu}$ хорошо описывает результаты прямых измерений в этой области энергий нейтронов, что служит аргументом в пользу предположения о равенстве нулю величины ΔE_f^Z.

В таблице 1 приведены значения α и $\bar{\nu}(E_n^0)$, полученные методом наименьших квадратов для ядер ^{232}Th, ^{235}U, ^{238}U и ^{239}Pu.

Применявшийся метод определения α может затушевать влияние неучтенных в анализе факторов, если они вносят достаточно плавную компоненту в кривую зависимости $\bar{\nu}(E_n)$ при больших ΔE_n. В частности, полученное из анализа значение $\alpha = 0{,}104$ для ^{239}Pu, представляется слишком малым и может указывать на наличие некоторого процесса, снижающего эту величину.

Кривые, обозначенные сплошной линией на рис. 2, можно рассматривать как рекомендованные энергетические зависимости $\bar{\nu}$ для ^{232}Th, ^{235}U, ^{238}U и ^{239}Pu, полученные в результате анализа энергетического баланса при делении этих ядер. Следует иметь в виду, что достоверность этих кривых ограничивается предположениями, использованными при анализе. Имеется ряд особенностей процесса деления, которые не учтены в данном анализе и вероятность проявления которых тем выше, чем больше ΔE_n. Рассмотренный метод достаточно чувствителен к проявлению локальных изменений величины $\bar{\nu}$ ($\sim 0{,}5\%$).

Авторы признательны профессору Л. Н. Усачеву за интересные обсуждения, Н. И. Акимову, В. Н. Кабенину, Л. С. Куцаевой и М. З. Тараско – за помощь в работе.

ЛИТЕРАТУРА

[1] FILLMORE, F.L., Journ. of Nucl. Energy 22 (1968) 79.
[2] АНДРЕЕВ, В.Н., Тезисы докладов на конф. по физике деления ядер. Ленинград, Изд. АН СССР, 1961.
[3] BLUMKINA, Yu.A. et al., Nucl. Phys. 52 (1964) 648.
[4] БОЛЬШОВ, В.И., КУЗНЕЦОВ, В.Ф., СМИРЕНКИН, Г.Н. и др., Ядерная физика 6 (1967) 1162.
[5] КУЗНЕЦОВ, В.Ф., СМИРЕНКИН, Г.Н., Материалы конф. по ядерным данным. Париж, 1966, CN-23/97.
[6] DYACHENKO, P.P., KUZMINOV, B.D., LAJTAI, A., Phys. Letters 31B (1970) 122.
[7] СЕРГАЧЕВ, А.И., ВОРОБЬЕВА, В.Г., КУЗЬМИНОВ, Б.Д. и др., Ядерная физика 7 (1968) 778.
[8] ДЬЯЧЕНКО, П.П., КУЗЬМИНОВ, Б.Д., ТАРАСКО, М.З., Ядерная физика 8 (1968) 286.
[9] ВОРОБЬЕВА, В.Г., КУЗЬМИНОВ, Б.Д., СЕРГАЧЕВ, А.И., ТАРАСКО, М.З., Ядерная физика 9 (1969) 296.
[10] SEEGER, A., Nucl. Phys. 25 (1961) 1.
[11] АПАЛИН, В.Ф. и др., Атомная энергия 8 (1960) 15.
[12] TERRELL, Y., Phys. Rev. 127 (1962) 880.
[13] SOLEILHAC, M., FREHAUT, I., GAURIAU, Y., Journ. Nucl. Energy 23 (1969) 257.

ИЗМЕРЕНИЕ ЭНЕРГЕТИЧЕСКИХ СПЕКТРОВ И СРЕДНЕГО ЧИСЛА $\bar{\nu}$ МГНОВЕННЫХ НЕЙТРОНОВ ДЕЛЕНИЯ АКТИНИДНЫХ ЭЛЕМЕНТОВ

Ю. С. ЗАМЯТНИН, Н. И. КРОШКИН,
А. К. МЕЛЬНИКОВ, В. Н. НЕФЕДОВ,
Научно-исследовательский институт
атомных реакторов, Мелекесс,
Союз Советских Социалистических Республик

Presented by S.I. Sukhoruchkin

Доклад представлен С.И. Сухоручкиным

Abstract — Аннотация

MEASUREMENT OF THE ENERGY SPECTRA AND THE AVERAGE NUMBER $\bar{\nu}$ OF PROMPT NEUTRONS PRODUCED IN THE FISSION OF ACTINIDE ELEMENTS.

Using the time-of-flight method the authors measure the spectra of prompt neutrons produced in the spontaneous fission of ^{244}Cm and ^{252}Cf and in the induced fission of ^{229}Th, ^{235}U, ^{238}Pu, ^{242m}Am, ^{245}Cm, ^{249}Cf by thermal neutrons. The pulse produced by the fission fragments in a gas-filled scintillation chamber is used as the starting signal. The neutrons are recorded by plastic detectors and by scintillation glass containing ^{6}Li. Using the expression $N(E) \sim \sqrt{E}\, e^{-E/T}$ to approximate the spectra the authors obtain the following values of the parameter T for ^{244}Cm, ^{252}Cf, ^{229}Th, ^{238}Pu, ^{242m}Am, ^{245}Cm, ^{249}Cf, respectively: 1.38±0.03; 1.48±0.03; 1.24±0.04; 1.35±0.04; 1.42±0.03; 1.50±0.05; 1.55±0.04 Mev. The values obtained for the average number $\bar{\nu}$ of neutrons for the above nuclei are, respectively: 2.77±0.08; 3.77±0.08; 2.05±0.10; 2.92±0.12; 3.28±0.10; 3.83±0.16 and 4.60±0.21. The measurements are performed relative to ^{235}U, it being assumed that T = 1.29 MeV and $\bar{\nu}$ = 2.426 for this nuclide. The low-energy neutrons produced in the spontaneous fission of ^{252}Cf are measured by means of scintillation glass containing ^{6}Li. The spectrum is measured down to 5 keV. In the energy region below 100 keV it was noted that the neutron spectrum exceeds the expected distribution $N(E) \sim E^{\frac{1}{2}}$. Spectrum peaks are found at 80-90 keV, 0.5 MeV and 0.7-0.8 MeV.

ИЗМЕРЕНИЕ ЭНЕРГЕТИЧЕСКИХ СПЕКТРОВ И СРЕДНЕГО ЧИСЛА $\bar{\nu}$ МГНОВЕННЫХ НЕЙТРОНОВ ДЕЛЕНИЯ АКТИНИДНЫХ ЭЛЕМЕНТОВ.

Методом времени пролета измерены спектры мгновенных нейтронов спонтанного деления ^{244}Cm, ^{252}Cf и вынужденного деления ^{229}Th, ^{235}U, ^{238}Pu, ^{242m}Am, ^{245}Cm, ^{249}Cf тепловыми нейтронами. В качестве стартового сигнала использовался импульс от осколков деления в газовой сцинтилляционной камере. Для регистрации нейтронов применялись пластмассовые детекторы и сцинтилляционные стекла, содержащие изотоп ^{6}Li. При аппроксимации спектров выражением $N(E) \sim \sqrt{E} \cdot e^{-E/T}$ значения параметра T были получены равными (1,38±0,03), (1,48±0,03), (1,24±0,04), (1,35±0,04), (1,42±0,03), (1,50±0,05) и (1,55±0,04) Мэв для ^{244}Cm, ^{252}Cf, ^{229}Th, ^{238}Pu, ^{242m}Am, ^{245}Cm и ^{249}Cf, соответственно. Значения $\bar{\nu}$ среднего числа нейтронов для названных ядер оказались равными соответственно: 2,77±0,88; 3,77±0,08; 2,05±0,10; 2,92±0,12; 3,28±0,10; 3,83±0,16 и 4,60±0,21. Измерения проводились относительно ^{235}U, причем считалось, что для ^{235}U T = 1,29 Мэв и $\bar{\nu}$ = 2,426. Низкоэнергетическая часть нейтронов спонтанного деления ^{252}Cf измерена с помощью сцинтилляционного стекла, содержащего ^{6}Li. Спектр измерен до 5 кэв. В области ниже 100 кэв отмечено превышение спектра нейтронов по сравнению с ожидаемым распределением $N(E) \sim E^{1/2}$. На спектре обнаружены максимумы, расположенные при энергиях 80-90 кэв, 0,5 Мэв и 0,7-0,8 Мэв.

ВВЕДЕНИЕ

Среди различных характеристик мгновенных нейтронов деления большой интерес представляют их энергетические спектры и среднее число нейтронов, испускаемых в акте деления. Исследованию этих характеристик нейтронов деления как при спонтанном делении ядер, так и при делении ядер тепловыми и быстрыми нейтронами посвящено значительное число работ. Результаты этих исследований позволили установить некоторые закономерности изменения $\bar{\nu}$ в зависимости от различных параметров делящегося ядра (A, Z, E*) и показали, что форма спектров нейтронов достаточно хорошо согласуется с моделью испарения нейтронов из движущихся осколков [1, 2].

Однако, за исключением энергетических спектров нейтронов деления ^{233}U, ^{235}U, ^{239}Pu тепловыми нейтронами [3, 4] и спонтанного деления ^{252}Cf [5-9], данные по спектрам нейтронов деления весьма ограничены.

Очень мало данных также по спектрам мгновенных нейтронов деления в области малых энергий (меньше 0,1 Мэв) [9]. Поэтому представляют значительный интерес опыты по измерению $\bar{\nu}$ и спектров мгновенных нейтронов для более широкого круга изотопов, а также измерения спектров мгновенных нейтронов деления в области энергий меньше 0,1-0,2 Мэв.

В данной работе выполнены измерения $\bar{\nu}$ и энергетических спектров мгновенных нейтронов в области 0,4-6 Мэв при спонтанном делении ^{244}Cm и ^{252}Cf и при делении ^{229}Th, ^{238}Pu, ^{242m}Am, ^{245}Cm и ^{249}Cf тепловыми нейтронами. Для спонтанно делящегося изотопа ^{252}Cf выполнены измерения спектра мгновенных нейтронов в интервале до 5 кэв. При выполнении измерений спектра нейтронов в области малых энергий особое внимание уделялось выяснению вопроса о существовании нерегулярностей в спектре нейтронов. В нашей работе [10] на спектрах мгновенных нейтронов деления ^{235}U и ^{252}Cf было обнаружено несколько максимумов, имеющих энергии 0,75 Мэв, 1,2 Мэв, 1,6 Мэв и 2,6 Мэв. Есть указание о наличии максимумов и при более низких энергиях. Было показано, что обнаруженные максимумы образованы нейтронами, испускаемыми за время порядка $10^{-9} - 10^{-8}$ сек после момента деления.

Выполненные в данной работе измерения спектра мгновенных нейтронов спонтанного деления ^{252}Cf в области 0,005-2 Мэв позволили получить ответ о наличии таких максимумов при более низких энергиях.

МЕТОДИКА ИЗМЕРЕНИЙ

Измерение спектров мгновенных нейтронов производилось методом времени пролета. Блок-схема электронной аппаратуры приведена на рис. 1. Пролетное расстояние в опытах составляло 50 см. Кроме того, при измерении спектра нейтронов ^{252}Cf в области малых энергий использовались пролетные расстояния 30 и 15 см. Полное разрешающее время спектрометра, определенное на полувысоте пика от мгновенных γ-квантов деления, составляло 4 нсек.

В качестве детектора осколков деления использовалась газовая сцинтилляционная камера, которая позволяла выполнять измерения со слоями, обладающими α-активностью до 10^8 α-част./сек. Это достигалось регистрацией световой вспышки, создаваемой обоими осколками на начальном участке их пробега. Камера имела рабочий объем ϕ 40 $\times$ 40 мм

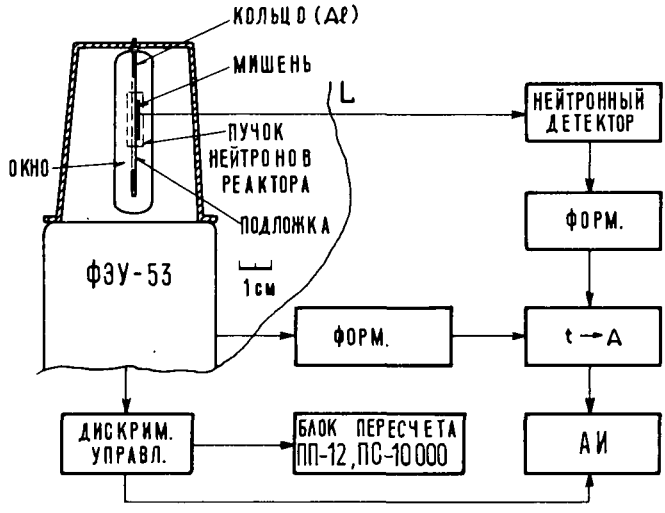

Рис. 1. Блок-схема электронной аппаратуры.

и заполнялась техническим аргоном или гелием до давления 2000 мм рт. ст. Световые вспышки, возникающие в газовом объеме детектора, регистрировались фотоумножителем ФЭУ-53. Исследование рабочих характеристик камеры показало, что импульсы осколков полностью отделяются от импульсов α-частиц.

В случае вынужденного деления мишени облучались выведенным пучком (1,5×15 мм) нейтронов горизонтального канала реактора СМ-2.

Диаметр мишеней не превышал (5-15 мм), количество вещества мишени для всех исследованных изотопов было не более 50 мкг. Подложка мишеней представляла собой золотую фольгу толщиной ~ 150 мкг/см^2, которая крепилась на алюминиевом кольце диаметром 40 мм. Исключение составляли мишень ^{229}Th (количество вещества ~ 15 мкг) на платиновой подложке толщиной 14 мк [11], мишень ^{249}Cf (количество вещества ~0,2 мкг) на титановой подложке толщиной 100 мк и мишень ^{252}Cf интенсивностью $6 \cdot 10^4$ делений/сек, нанесенная на алюминиевую подложку толщиной 0,5 мм, которая использовалась в измерениях с литиевым стеклом.

Изотопный состав образцов плутония, америция и кюрия исследовался как с помощью полупроводникового α-спектрометра, так и на масс-спектрометре и приведен в табл. 1.

Регистрация нейтронов в области энергий 0,4-6 Мэв осуществлялась пластмассовым сцинтиллятором размером ϕ 100×30 мм с фотоумножителем ФЭУ-63 (диаметр фотокатода 100 мм). Для снижения фона γ-квантов деления и γ-квантов, рассеиваемых подложкой мишени, сцинтиллятор был защищен слоем свинца толщиной 15 мм. Порог нейтронного детектора с пластмассовым сцинтиллятором постоянно контролировался по γ-квантам ^{241}Am(E_γ = 59,6 Мэв).

Измерения спектра мгновенных нейтронов спонтанного деления ^{252}Cf в области малых энергий проводились с помощью сцинтилляционного стекла, содержащего изотоп литий-6. Стекло диаметром 70 мм и

ТАБЛИЦА 1. ИЗОТОПНЫЙ СОСТАВ МИШЕНЕЙ, %

Мишень			
№1 (^{244}Cm + ^{245}Cm)	№2 (^{244}Cm + ^{245}Cm)	^{242m}Am (152г)	^{238}Pu
Количество вещества, мкг			
20	4	30	50
^{242}Cm - 0,05 ^{243}Cm - < 0,35 ^{244}Cm - 96,38 ^{245}Cm - 1,75 ^{246}Cm - 1,47	^{242}Cm - 3,90 ^{244}Cm - 95,40 ^{245}Cm - 0,40 ^{246}Cm - 0,30	^{241}Am - 88,97 ^{242m}Am - 1,03 ^{243}Am - 10,00	^{238}Pu - 100

высотой 11 см содержало 5,8% лития, обогащенного до 90,4% изотопом литий-6. Регистрация нейтронов таким стеклом осуществлялась за счет экзотермической реакций ^{6}Li (n, α)^{3}H + 4,78 Мэв, что обеспечивало измерение спектров нейтронов в диапазоне от нескольких мегаэлектронвольт до нескольких килоэлектронвольт [9, 12]. Сечение реакции ^{6}Li(n, α)^{3}H хорошо известно, что позволяет получать достаточно точные результаты при измерении спектров нейтронов методом времени пролета. При измерениях порог нейтронного детектора устанавливался на уровне регистрации импульсов от γ-лучей с энергией 0,8 ÷ 1 Мэв.

Измерения спектров нейтронов в диапазоне 0,4-6 Мэв производились попеременно с измерением спектра нейтронов деления ^{235}U тепловыми нейтронами. Фон случайных совпадений точно учитывался и был незначительным при спонтанном делении ^{244}Cm (рис. 2) и ^{252}Cf. При делении ^{229}Th, ^{235}U, ^{238}Pu, ^{242m}Am, ^{245}Cm и ^{249}Cf тепловыми нейтронами фон составлял 10-15% и лишь на границах интервала измерений возрастал до 35-40%.

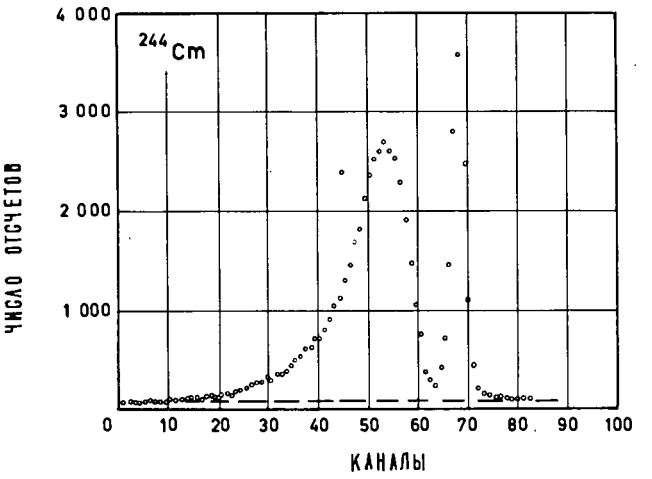

Рис. 2. Аппаратурный спектр нейтронов деления.

В предположении, что спектр нейтронов ^{235}U известен и определяется выражением

$$N(E) \sim \sqrt{E} \cdot e^{-E/T} \quad (1)$$

при значении параметра T = 1,29 Мэв [1-4], находилась эффективность детектора нейтронов в зависимости от их энергии.

Так как нейтронный пучок реактора СМ-2 имеет довольно жесткий спектр [13], измерения на пучке нейтронов выполнялись с кадмием и без кадмия. В результате этих измерений определялся чистый эффект от деления тепловыми нейтронами. При делении ^{229}Th тепловыми нейтронами скорость счета составляла 100 делений/сек, кадмиевое отношение равнялось 3. Используемый в измерениях ^{238}Pu был получен в результате α-распада ^{242}Cm. В измерениях с мишенями из ^{238}Pu и ^{242m}Am кадмиевые отношения были равны 7 и 20, соответственно. Образец ^{244}Cm (мишень №1, см. табл. 1) был получен путем облучения ^{242}Pu в реакторе СМ-2 и содержал равновесное количество ^{245}Cm. Примеси ^{243}Am и ^{238}Pu составляли $<0,3\%$ каждая. Число спонтанных делений ^{244}Cm равнялось (60 ÷ 80) делений/сек, в зависимости от уровня дискриминации осколков. Эта мишень использовалась для изучения мгновенных нейтронов спонтанного деления ^{244}Cm, а также нейтронов деления ^{244}Cm тепловыми нейтронами. Оценка вклада делений за счет других изотопов кюрия показала, что доля делений ^{244}Cm составляет небольшую величину ($\sim 6\%$); существенной могла быть доля делений ^{244}Cm тепловыми нейтронами, так как сечение деления для ^{244}Cm тепловыми нейтронами дается различными авторами в интервале 0 ÷ 20 барн. Для оценки значения сечения деления ^{244}Cm тепловыми нейтронами была приготовлена путем кратковременного облучения образца ^{243}Am другая мишень ^{244}Cm с меньшим содержанием ^{245}Cm (мишень №2, см. табл. 1). Результаты измерений с двумя мишенями с кадмием и без кадмия на одном и том же пучке нейтронов дали значение сечения деления ^{244}Cm тепловыми нейтронами $\sigma_f = (1 \pm 1)$ барн, причем считалось, что сечение деления ^{245}Cm тепловыми нейтронами составляет 1700 барн. В табл. 2 приведены скорости счета для двух мишеней кюрия (делений/сек).

Образец ^{249}Cf получен в результате β-распада ^{249}Bk. Скорость счета составляла 80 делений/сек. При изучении спектра нейтронов спонтанного деления ^{252}Cf скорость счета составляла ~ 600 делений/сек.

ТАБЛИЦА 2. ДАННЫЕ ДЛЯ ДВУХ МИШЕНЕЙ КЮРИЯ

Номер мишени	Спонтанное деление	На нейтронном пучке	На нейтронном пучке с кадмием
1	59,6	240	75
2	16,9	30	18,2

Калибровочные спектры вынужденного деления ^{235}U (90%) измерялись при скорости счета 5000 делений/сек.

С каждым изотопом выполнено несколько серий измерений продолжительностью 4 ÷ 6 суток каждая. В процессе измерений периодически

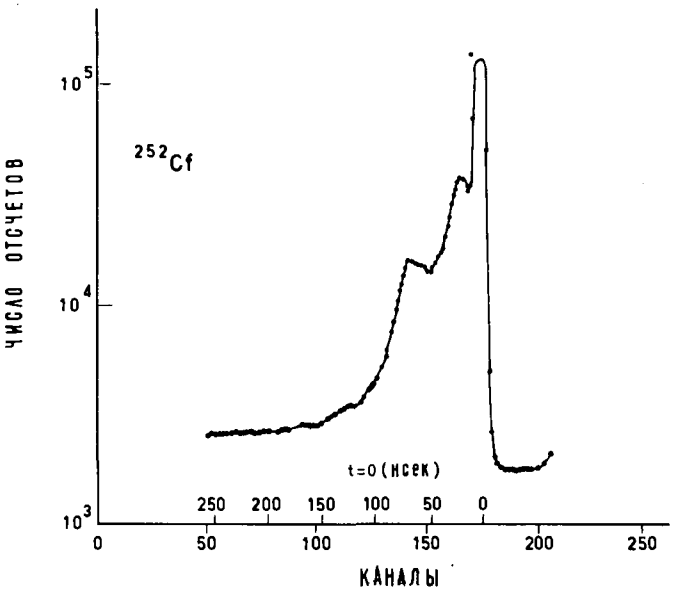

Рис. 3. Аппаратурный спектр мгновенных нейтронов деления ^{252}Cf. Измерения проведены с помощью сцинтилляционного стекла, содержащего литий-6. Пролетное расстояние – 50 см.

контролировались пороги детекторов осколков и нейтронов и осуществлялась регистрация полного числа актов деления. В результате измерений получены временные спектры мгновенных нейтронов деления. На рис. 2 и 3 представлены аппаратурные спектры мгновенных нейтронов спонтанного деления кюрия-244 и калифорния-252, измеренные на пролетной базе L = 50 см.

В опытах большое внимание уделялось определению фона. В измерениях по времени пролета спектров мгновенных нейтронов деления фон состоит из трех составляющих:

1) фон случайных совпадений;

2) фон от нейтронов, рассеянных окружающими предметами и зарегистрированных детектором нейтронов;

3) фон от запаздывающих γ-квантов деления.

При измерениях спектров нейтронов в диапазоне 0,4-6 Мэв, выполненных с пластмассовым детектором, учитывался только фон случайных совпадений.

В опытах по измерению спектра мгновенных нейтронов спонтанного деления ^{252}Cf в области низких энергий учитывались все три составляющих фона.

Фон случайных совпадений может быть легко определен из экспериментальных кривых.

Фон рассеянных нейтронов зависит от условий эксперимента. Для уменьшения этой составляющей фона спектрометр располагался в центре помещения на расстоянии в 1,8 м от пола. Для определения фона от рассеянных нейтронов проводились специальные измерения, в которых между детектором осколков деления и детектором нейтронов располагался затеняющий конус из железа длиной 20 см.

При больших временах пролета значительный вклад в измеряемый эффект дают запаздывающие γ-кванты деления. Из работы Юханссона [14] известно, что около 6% γ-квантов деления имеют период полураспада около 15-100 нсек. Поэтому при обработке результатов измерений необходимо учитывать эффект от запаздывающих γ-квантов деления. Этот эффект определялся экспериментально, для чего выполнялись измерения при расстоянии между детектором нейтронов и мишенью из калифорния, равным 1,5 см. При таком пролетном расстоянии нейтроны и мгновенные γ-кванты деления регистрируются в нескольких каналах вблизи нуля отсчета времени. Для времен задержки, больших 10-30 нсек, измеряемый эффект в основном (>90%) обязан запаздывающим γ-квантам. Для еще больших времен эффект полностью отвечает регистрации запаздывающих γ-квантов. Возможным вкладом от задержанных нейтронов при временах, больше 30 нсек, можно пренебречь, так как время испускания их — $10^{-9} \div 10^{-8}$ сек, а эффективность регистрации нейтронов ниже эффективности регистрации γ-квантов стеклянным сцинтиллятором. Эти измерения использовались для нахождения фона при обработке результатов измерений спектров нейтронов на разных пролетных расстояниях.

Обработка экспериментальных результатов заключалась в обычном преобразовании временных спектров нейтронов в энергетические с учетом эффективности детектора нейтронов. Эффективность нейтронного детектора рассчитывалась по величине сечения реакции $^{6}Li(n, \alpha)^{3}H$, взятой из работ Форта и др. [15] и Шварца и др. [16]. Данные Шварца нормировались так, чтобы получить согласие с данными других авторов [17].

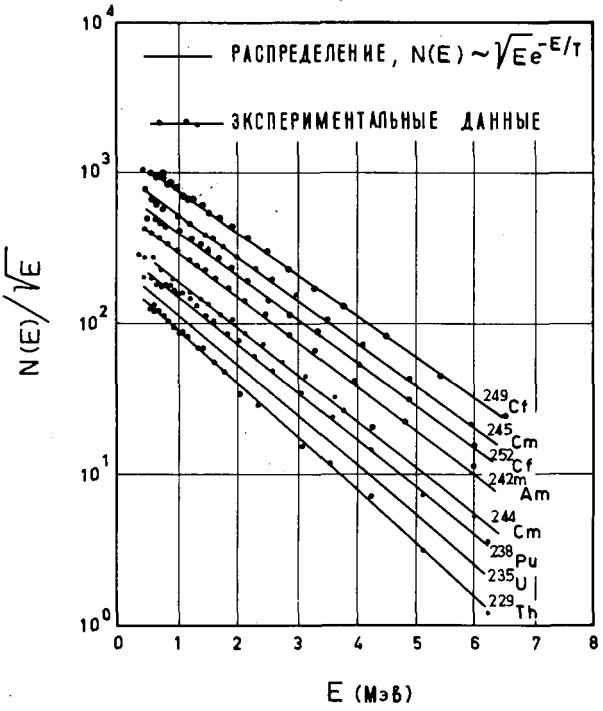

Рис. 4. Спектры нейтронов деления.

РЕЗУЛЬТАТЫ ИЗМЕРЕНИЙ

В результате измерений были получены спектры нейтронов спонтанного деления ^{244}Cm, ^{252}Cf и деления ^{229}Th, ^{238}Pu, ^{242m}Am, ^{245}Cm и ^{249}Cf тепловыми нейтронами.

Данные измерений показывают, что спектры всех указанных изотопов хорошо аппроксимируются выражением (1), при этом заметно увеличение жесткости спектра при переходе от ^{229}Th к более тяжелым ядрам (рис. 4-5, табл. 3).

На рис. 4 приведены ненормированные спектры нейтронов деления. Из сравнения спонтанного деления и деления ядер тепловыми и быстрыми нейтронами видно увеличение T с ростом энергии возбуждения делящегося ядра E* (рис. 6).

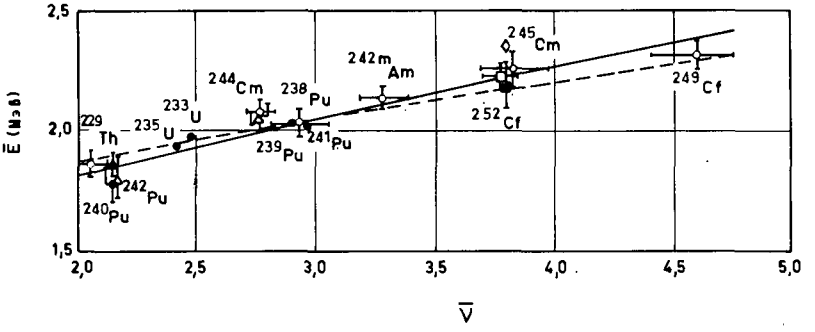

Рис. 5. Связь средней энергии $\bar{E}$ нейтронов деления с $\bar{\nu}$:
— — — кривая типа $\bar{E} = \bar{E}_f + b\sqrt{\bar{\nu}+1}$, рассчитанная Терреллом ($\bar{E}_f = 0{,}75$, $b = 0{,}65$); ——— кривая, проведенная методом наименьших квадратов через экспериментальные точки ($\bar{E}_f = 0{,}25$, $b = 0{,}90$).
Экспериментальные данные взяты из работ: ◊ – [9], ●■ – [26], △ – [27], ▲ – [28], ○□ – данная работа.

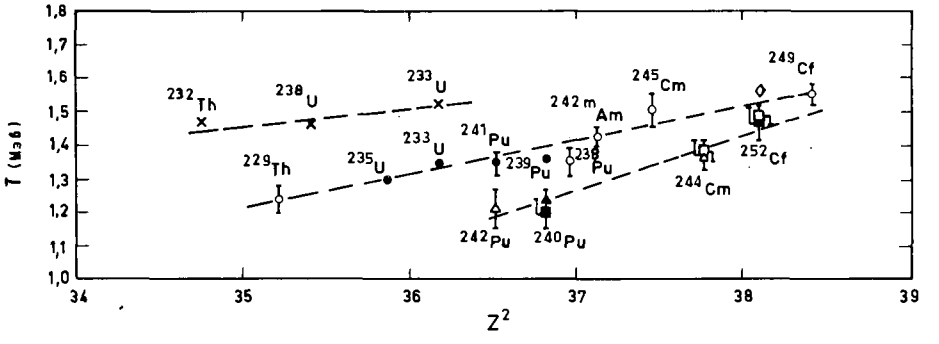

Рис. 6. Зависимость жесткости нейтронного спектра от параметра Z^2/A:
◊ △ ▲ ■ □ – данные при спонтанном делении ядер, ◊ – [9], ■ – [26], △ – [27], ▲ – [28], □ – данная работа;
○ ● – данные при делении ядер тепловыми нейтронами, ● – [26], ○ – данная работа;
X – данные при делении ядер нейтронами с энергией 14,3 Мэв [29-31].

Для всех исследованных ядер было определено среднее число нейтронов деления относительно значения $\bar{\nu}(^{235}U) = 2{,}426$. Для определения $\bar{\nu}$ производилось интегрирование спектров нейтронов деления. Полученный результат относился к числу делений, зарегистрированных во время измерений. Ошибка относительных измерений $\bar{\nu}$ составляла ~3%. Результаты измерений $\bar{\nu}$ также приводятся в табл. 3. Ошибка абсолютного значения $\bar{\nu}$ дается как среднеквадратичная по пяти сериям измерений для каждого изотопа. Приведенное в табл. 3 значение $\bar{\nu}$ для спонтанного деления ^{252}Cf хорошо согласуется с данными других авторов (см., например, работу [18]). Значения $\bar{\nu}$ при делении ^{242m}Am и ^{245}Cm тепловыми нейтронами представлены в трех кратких сообщениях [19-21]; данные по $\bar{\nu}$ для деления ^{238}Pu и ^{249}Cf тепловыми нейтронами отсутствуют; значения $\bar{\nu}$ для ^{229}Th даны в двух работах [22, 23].

Теоретическое истолкование наблюдаемых энергетических спектров нейтронов деления может быть получено на основе модели испарения нейтронов из возбужденных осколков.

Террелл [24-26], рассматривая ядро как ферми-газ входящих в него нуклонов и основываясь на экспериментальных данных, нашел простое полуэмпирическое соотношение, связывающее среднюю энергию мгновенных нейтронов деления с числом нейтронов, испускаемых на акт деления:

$$\bar{E} = \bar{E}_f + b\sqrt{\bar{\nu} + 1} \text{ Мэв} \qquad (2)$$

где параметры: $\bar{E}_f = 0{,}75$, $b = 0{,}65$. В выражении (2) $\bar{E}_f$ соответствует средней энергии нейтрона, движущегося со скоростью осколка.

Необходимо отметить, что выражение (2) получено на основе ограниченного экспериментального материала. Кроме того, в одной из последних работ по среднему спектру нейтронов ^{252}Cf автор работы [9] приводит $\bar{E} = 2{,}348$ Мэв. Это значение находится в хорошем согласии с результатами Смита и др. (2,35 Мэв) [5] и Боумана и др. (2,34 Мэв) [7] и значительно больше величины $\bar{E}$, измеренной авторами работ [6] и [8] и использованной Терреллом [26].

Следует также добавить, что выражение (2) получено при некоторых упрощающих предположениях, в частности без учета зависимости параметра плотности уровней a от A и Z осколков.

ТАБЛИЦА 3. РЕЗУЛЬТАТЫ ИЗМЕРЕНИЙ ЭНЕРГЕТИЧЕСКИХ СПЕКТРОВ И СРЕДНЕГО ЧИСЛА $\bar{\nu}$ МГНОВЕННЫХ НЕЙТРОНОВ ДЕЛЕНИЯ

Изотоп	Тип деления	T, Мэв	$\bar{E}$, Мэв	$\bar{\nu}$	Число зарегистрированных нейтронов
^{229}Th	Тепловое	1,24 ± 0,04	1,86 ± 0,06	2,05 ± 0,10	$6\cdot10^4$
^{235}U	"	1,29	1,935	2,426	$5\cdot10^5$
^{238}Pu	"	1,35 ± 0,04	2,03 ± 0,06	2,92 ± 0,12	$1\cdot10^5$
^{242m}Am	"	1,42 ± 0,03	2,13 ± 0,05	3,28 ± 0,10	$9,2\cdot10^4$
^{244}Cm	Спонтанное	1,38 ± 0,03	2,07 ± 0,05	2,77 ± 0,08	$4\cdot10^4$
^{252}Cf	"	1,48 ± 0,03	2,22 ± 0,05	3,77 ± 0,08	$8\cdot10^4$
^{245}Cm	Тепловое	1,50 ± 0,05	2,25 ± 0,08	3,83 ± 0,16	$5\cdot10^4$
^{249}Cf	"	1,55 ± 0,04	2,32 ± 0,06	4,60 ± 0,21	$1\cdot10^5$

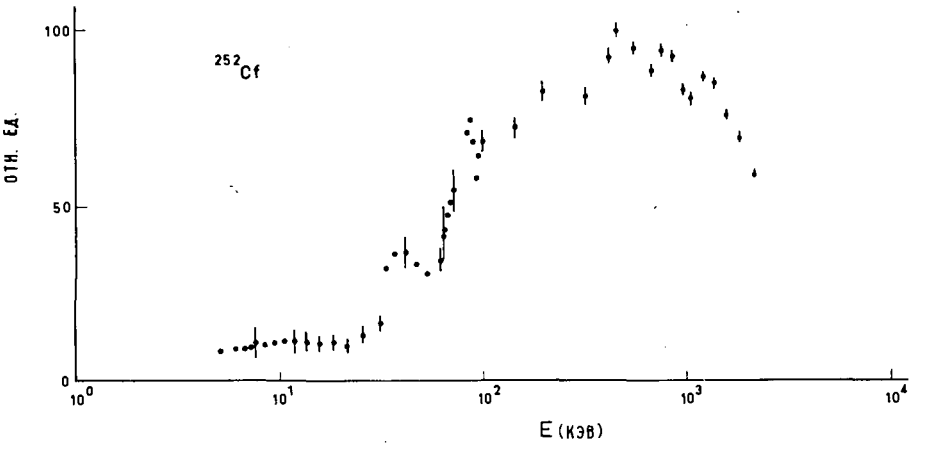

Рис. 7. Энергетический спектр мгновенных нейтронов деления ^{252}Cf в области 5 кэв – 2 Мэв.

Результаты данных измерений и измерений $\bar{E}$ и $\bar{\nu}$, выполненных другими авторами за последнее время (см. рис. 5), дают возможность уточнить зависимость $\bar{E}$ от $\bar{\nu}$. С этой целью методом наименьших квадратов были определены значения параметров $\bar{E}_f$ и b в выражении (2). Наилучшее согласие с экспериментальными данными получается при значениях $\bar{E}_f = 0{,}25 \pm 0{,}16$, $b = 0{,}90 \pm 0{,}08$. Уточненное значение $\bar{E}_f$ значительно меньше средней энергии нейтрона, движущегося со скоростью осколка. Это свидетельствует о том, что зависимость $\bar{E}$ от $\bar{\nu}$ является сложной и, по-видимому, требует учета распределения осколков по массе, кинетической энергии и энергии возбуждения, понижения температуры осколка при испускании им нейтрона и других факторов.

В результате обработки данных измерений был получен спектр нейтронов калифорния-252 в диапазоне 0,005 ÷ 2 Мэв. Спектр приведен на рис. 7. Ошибки, приведенные на спектре, представляют собой суммарные статистические ошибки измерений спектра нейтронов, фона рассеянных нейтронов и эффекта от запаздывающих γ-квантов деления. Из рис. 7 видно, что на спектре нейтронов наблюдаются несколько максимумов. Кроме максимумов с энергией 0,75 Мэв и 0,2 Мэв, обнаруженных нами ранее [10], наблюдаются максимумы, расположенные при энергиях 85 кэв, 0,18-0,2 Мэв и 0,45 Мэв. Эти максимумы наблюдаются в измерениях на различных пролетных расстояниях (50 и 30 см), что подтверждает реальность их существования.

Обнаруженные максимумы с энергией 85 кэв, 0,2 Мэв и 0,45 Мэв, по-видимому, имеют общую природу с максимумами 0,7 Мэв, 1,2 Мэв, 1,6 Мэв и 2,6 Мэв, описанными в работе [10].

В заключение авторы выражают благодарность Г. Н. Смиренкину за интерес к работе и ее обсуждение, Б. В. Курчатову и В. А. Пчелину, любезно предоставившим образец ^{229}Th, В. Я. Габескирия – за проведение изотопного масс-спектрального анализа, В. А. Ермакову, Г. А. Тимофееву – за химическое отделение элементов, В. Н. Козыренко – за составление программ при расчетах на вычислительной машине БЭСМ-3М, а также сотрудникам лаборатории, обеспечившим проведение измерений.

ЛИТЕРАТУРА

[1] БОНДАРЕНКО, И.И. и др., В кн. "Труды Второй Междунар. конф. по мирному использованию атомной энергии (Женева, 1958)". Доклады советских ученых, Госатомиздат, М., 1, 1959, стр. 438.
[2] ЗАМЯТНИН, Ю.С., В сб. "Физика деления атомных ядер". Госатомиздат, М., 1962, стр. 98.
[3] ЕРОЗОЛИМСКИЙ, Б.Г., В сб. "Физика деления атомных ядер". Госатомиздат, М., 1957, стр. 74.
[4] ЛИЧМЕН, Р.Б., В кн. "Труды Второй Междунар. конф. по мирному использованию атомной энергии (Женева, 1958)". Избранные доклады иностранных ученых. Госатомиздат, М., 2, 1959, стр. 342.
[5] SMITH, A.B., FIELDS, P.R., ROBERTS, J.H., Phys. Rev. 108 (1957) 411.
[6] BONNER, T.W., Nucl. Phys. 23 (1961) 116.
[7] BOWMAN, H.R. et al., Phys. Rev. 126 (1962) 2120.
[8] CONDE, H., DURING, G., Proc. Symp. on Phys. and Chem. Fission (Salzburg) Vienna, IAEA 2, 1965, p. 93.
[9] MEADOWS, I.W., Phys. Rev. 157 (1967) 1076.
[10] НЕФЕДОВ, В.Н., Препринт НИИАР П-52 (1969).
[11] БОРИСОВ, Н.И. и др., Ядерная физика 8 (1968) 695.
[12] FIRK, J., Nucl. Instr. and Meth. 13 (1961) 313.
[13] ФЕЙНБЕРГ, С.М. и др., Атомная энергия 17 (1964) 452.
[14] JOHANSSON, S.A.E., Nucl. Phys. 64 (1965) 147.
[15] FORT, E., LEROY, J.L., Nucl. Data for Reactors, Vienna, IAEA 1, 1967, p. 267.
[16] SCHWARZ, S. et al., Nucl. Phys. 63 (1965) 539.
[17] COX, S.A., PONTET, F.R., J. Nucl. Energy 21 (1967) 271.
[18] FILLMORE, F.L., J.Nucl. Energy 22 (1968) 79.
[19] VON GUNTEN, H.R., FLYNN, K.F., GLENDENIN, L.E., Phys. Rev. 161 (1967) 1192.
[20] ЮИЗЕНГА, Дж., ВАНДЕНБОШ, Р., В кн. "Ядерные реакции". Госатомиздат, М., 2, 1964, стр. 51.
[21] PERKINS, S. et al., Nucl. Sci. and Engng. 32 (1968) 131.
[22] JAFFEY, A., LERNER, J., BNL-325, Second Edition, Supplement 2 (1965) 9.
[23] ЛЕБЕДЕВ, В.И., КАЛАШНИКОВА, В.И., ЖЭТФ 35 (1958) 535.
[24] TERRELL, J., Phys. Rev. 113 (1959) 527.
[25] TERRELL, J., Phys. Rev. 127 (1962) 880.
[26] TERRELL, J., Proc. Symp. on Phys. and Chem. Fission (Salzburg) Vienna, IAEA 2, 1965, p. 3.
[27] БЕЛОВ, Л.М. и др., Ядерная физика 9 (1969) 727.
[28] БОЛЬШОВ, В.И. и др., В сб. "Физика деления атомных ядер", Госатомиздат, М., 1962, стр. 127.
[29] ЗАМЯТНИН, Ю.С. и др., Атомная энергия 4 (1958) 337.
[30] ВАСИЛЬЕВ, Ю.А. и др., ЖЭТФ 38 (1960) 671.
[31] ВАСИЛЬЕВ, Ю.А. и др., В сб. "Физика деления атомных ядер". Госатомиздат, М., 1962, стр. 121.

THE NUMBER OF NEUTRONS PER FISSION, $\bar{\nu}$, FROM THERMAL TO 15 MeV

D.W. COLVIN
UKAEA, Harwell, Didcot, Berks,
United Kingdom

Report on the IAEA Consultants Meeting, Studsvik, Sweden, 10-11 June 1970, and the papers on $\bar{\nu}$ presented at this Conference

I INTRODUCTION

I have been asked to review the principal papers submitted to this Conference on the parameter $\bar{\nu}$, the number of neutrons per fission, from thermal to 15 MeV: at the same time, to present findings of the IAEA Consultants Meeting on this subject, held at Studsvik in Sweden last week. As well as the Conference papers, /1/ - /6/, a number of other papers and results, /7/ - /16/, were presented at this Meeting, which should be mentioned to complete the input data for our two days of discussion. To cover this in a logical fashion, I should like to consider the information under the headings of 'thermal and absolute values', '$\bar{\nu}$ as a function of energy', recent 'evaluation work on $\bar{\nu}$ as a function of energy', and some suggestions, or recommendations, of the Meeting for future work.

I shall attempt to cover all this material as fairly as possible in the time available, and apologise in advance for possible inadequacies, or the omission of important results. In view of the very high quality of the work which went into these papers, I hope to leave enough time at the end of this presentation to permit the individual authors to answer questions, or fill in gaps, as necessary.

Before going any further, I wish to echo most sincerely on behalf of all the participants of the Meeting, Dr. Sukhoruchkin's sentiments of yesterday, on the generous hospitality of our hosts at Studsvik. Some of the defects in this review may well be traced to the entertainment, but I hope at the end of the talk to demonstrate just how fruitful the assistance of our Swedish hosts was in providing fresh results for this Conference.

Participants in the Meeting were as follows:

H. Condé	FOA	Sweden
W.G. Davey	ANL	U.S.A.
J.A. Farrell	LASL	U.S.A.
J. Frehaut	CEA	France
G.C. Hanna	Chalk River	Canada
V.A. Konshin	Nuclear Data Section	IAEA
D.S. Mather	AWRE	U.K.
J.J. Schmidt	Nuclear Data Section	IAEA
M. Soleilhac	CEA	France
S.I. Sukhoruchkin	IETP	U.S.S.R.
A. de Volpi	ANL	U.S.A.

and the present writer, who, as Chairman, thanks the individual participants for their patience and help.

II THERMAL AND ABSOLUTE $\bar{\nu}$ VALUES

Values of $\bar{\nu}$ for the important fissile and fertile isotopes are strongly linked to the absolute value of the spontaneous $\bar{\nu}$ for ^{252}Cf, and values of η and α for the thermally fissile isotopes of uranium and plutonium. The most recent, and most thorough, review of this material is that of Hanna et al [17] and it has been discussed in the paper by Davey this morning [18]. In reviewing his paper, Hanna emphasised again that the authors had to make several arbitrary decisions, particularly with regard to the drastic down-weighting of Cf values and that, as there is little room for manoever in α values, a correct weighting of the Cf values could only lead to suspicion of values of η.

De Volpi and Porges' recent adjustment [7] of the Argonne ^{252}Cf $\bar{\nu}$ value [19] [20] to

$$3.725 \pm 0.015 \text{ n/fiss. (Total)}$$

further emphasises the trend to low $\bar{\nu}$ values for ^{252}Cf, although as Davey showed in his Table 1, this only brings the IAEA weighted mean down to 3.740 from 3.743. The Argonne workers have gone into very extensive checking procedures since their first publications, following the philosophy that a minimum of correction calculations based on other cross sections, coupled with a major investment in experimental checks and verification of procedures, is the only path to 'accuracy', and a body of consistent data. In this they follow earlier workers in this field [21]. These verification procedures are fully discussed in their papers and forthcoming publications [8] [22] but incidentally lead to possible re-evaluation of certain η experiments. The three factors of sulphur and oxygen parasitic absorption, neutron escape, and resonance absorption in manganese when combined, lead, in De Volpi's opinion, to a reduction of $\frac{1}{3}\%$ in Macklin [23] and Smiths' [24] results, a trend again consistent with the pressure of lower ^{252}Cf values of $\bar{\nu}$ on the over-determined set of fundamental fission parameters analysed in the IAEA sponsored evaluation [17]. Several members of the Studsvik Meeting were unhappy about the artificial down-rating of the ^{252}Cf $\bar{\nu}$ values and pointed out that a more realistic weighting would serve to constrain η to a lower value. In this connection it seems a pity that the results of De Volpi's own η measurements have not yet been analysed, owing to budgetary restrictions.

A very fruitful discussion of these correction procedures has taken place between De Volpi and Axton of the National Physical Laboratory in England, and others, and it is clear that, although the recent Argonne and NPL measurements of $\bar{\nu}$ for ^{252}Cf are in reasonable agreement, the remaining measure of disagreement over procedures and corrections may yet result in two additional highly accurate $\bar{\nu}$ values being added to the very small set presently used. This was evident from Axton's letter [9] to the Meeting and, although it was unfortunate that he could not attend in person, it is hoped that the discussion will be continued in a seminar at the end of this month at Harwell. Up-dating and completion of Axton's most recent measurements [17] of $\bar{\nu}$ for ^{252}Cf, which yield a low value consistent with the Boron Pile, should take place by the end of 1970.

The influence on absolute $\bar{\nu}$ values of the lack of information on delayed γ rays from Cf fission, and new uncertainties about the fission neutron spectrum were again pointed out.

TABLE I. EVALUATIONS OF $\bar{\nu}_p(E_n)$ FOR ^{239}Pu: LEAST SQUARES STRAIGHT LINE FITS TO EXPERIMENTAL DATA 1963 – 1970

Row	Energy Range (MeV)	Intercept	Slope x 10^2	No. of Data Pts.	Author Year	Ref.
a	0 -14.5	0.7507 ± 0.0101	4.243	7	Hopkins '63	45
b	0 - 4.5	0.7639 ± 0.0037	3.464 ± 0.212	22	Mather '65	46
c	0 -15	0.7662 ± 0.0016	3.387 ± 0.117	21	Fillmore '68	30
d	0 -15	0.7665	3.642	~22	Condé '68	37
e	0 -15	0.7655 ± 0.0020	3.649 ± 0.098	23	Colvin '68	15
f	0 -15	0.7637 ± 0.0016	3.911 ± 0.026	50	Colvin '68	16
g	0 - 4.22	0.7658 ± 0.0018	3.543 ± 0.108	22		
h	6.77-15	0.7844 ± 0.0068	3.740 ± 0.063	25		
i	Thermal	0.7651 ± 0.0024	(Output of Total L.Sq. Fit)		Hanna '69	17
j	0 -28	0.7632 ± 0.0011	3.885 ± 0.021	156	IAEA Studsvik Meeting June 1970	
k	0 -15	0.7613 ± 0.0008	3.966 ± 0.016	150		
l	0 - 5.06	0.7620 ± 0.0009	3.869 ± 0.057	122		
m	1 - 4.7	0.7655 ± 0.0027	3.775 ± 0.105	62		
n	6.77-11	0.7567 ± 0.0084	4.068 ± 0.094	13	Colvin '70	
o	12.41-15	0.7867 ± 0.0457	3.718 ± 0.336	10		

Interesting new results for spontaneous and thermal fission were presented in a paper entitled 'Measurement of the energy spectra and average number of prompt neutrons $\bar{\nu}_p$ from the fission of actinide elements' by Zamyatnin et al. of the Atomic Reactor Research Institute, Melekess, U.S.S.R. [67]. Past studies of these parameters have provided functions of $\bar{\nu}$ in terms of parameters of the fissioning nucleus (A, Z, E* - the excitation energy of the fissioning nucleus) and show agreement for the shape of the neutron spectra as derived from a model of neutron evaporation from moving fission fragments. Unfortunately, apart from ^{233}U, ^{235}U, ^{239}Pu and ^{252}Cf, spectral data are limited, and particularly so at low energies (less than 0.1 MeV). Measurements were reported here for $\bar{\nu}$ and energy spectra of prompt neutrons in the range 0.4 to 6 MeV for spontaneous ^{244}Cm and ^{252}Cf, and for thermally induced fission in ^{229}Th, ^{238}Pu, ^{242m}Am, ^{245}Cm, and ^{249}Cf. For ^{252}Cf the prompt neutron spectrum was measured from 2 MeV down to 5 keV.

The time of flight method used is fully discussed in the Conference paper. Flight paths of 15 to 50 cms were used with a resolving time for the spectrometer of 4 ns. The fission fragments and neutrons were detected in a gas-filled scintillation counter, and plastic scintillator respectively. For ^{252}Cf at low energies, ^{6}Li glass was used. The efficiency of the neutron detector as a function of neutron energy was based on the ^{235}U neutron spectrum, assumed known and determined by the expression

$$N(E) \propto \sqrt{E}\, e^{-E/T} \quad \text{for } T = 1.29 \text{ MeV}$$

Careful correction was made for background and delayed fission gamma rays.

The data are shown in figures 4 & 5 of the paper. The first figure shows the un-normalised fission neutron spectra and the second the relationship between mean fission neutron energy $\bar{E}$ and $\bar{\nu}$. The spectra of all the isotopes are well represented by the expression above and there is pronounced hardening of the spectrum from ^{229}Th to heavier nuclei. Figure 5 shows plots of the Terrell curve [25], the hatched line

$$\bar{E} = \bar{E}_f + b\sqrt{\bar{\nu}+1} \text{ MeV}$$

where $\bar{E}_f$ is the mean energy of a neutron moving with the same velocity as a fission fragment, and the continuous line is a least square's fit to all experiments giving

$$\bar{E}_f = 0.25 \pm 0.16 \quad \& \quad b = 0.90 \pm 0.08$$

(significantly less than the Terrell values of

$$\bar{E}_f = 0.75 \quad \& \quad b = 0.65)$$

$\bar{\nu}$ relative to $\bar{\nu}(^{235}U) = 2.426$ was determined for all the nuclei by integrating the neutron spectra giving results for the relative measurements of order 3% accuracy. Table 2 of the paper gives all the results for $\bar{\nu}$ as well as the fission neutron spectra. There are no previous $\bar{\nu}$ data available for thermally induced fission of ^{238}Pu and ^{249}Cf.

The $\bar{\nu}$ measurements do not agree with calculations [26] in the United States by Clark of Du Pont-SRL on critical masses of fissile transplutonium isotopes and this will show up as discrepancies in critical mass determinations.

Figure 7 of this paper presents the results for the energy spectrum of prompt neutrons from ^{252}Cf fission in the range 5 keV to 2 MeV. Peaks can be seen at 85 keV, 0.18 to 0.2 MeV, and 0.45 MeV, as well as peaks found previously at 0.75 MeV and 1.2 MeV and appear to be of the same type found by Nefedov [27] at 0.7, 1.2, 1.6, and 2.6 MeV.

Perhaps the most interesting contribution to the Meeting, and certainly to the discussion of absolute $\bar{\nu}$ values, was the very recent discovery by Soleilhac of the CEA, Centre D'Etudes de Bruyeres le Chatel, France, of anomalies in the detecting procedures used in liquid scintillation measurements of $\bar{\nu}$. As these are the very measurements which give, as a set, the high absolute $\bar{\nu}$ values, this possible systematic error is a matter of fundamental importance, which should be resolved with urgency. It is interesting to note that the discovery did not stem from a direct attack on the problem it could help to solve, but from an on-going programme of measurements of $\bar{\nu}$ as a function of

TABLE II. EXPERIMENTAL DATA FROM SOLEILHAC SCINTILLATOR USING ^{252}Cf SOURCE AND 3 BANKS OF 4 PHOTOMULTIPLIERS

Parameters %	Bias* (1)	(2)	(3)	(4)	(5)	(6)
$\bar{\varepsilon}_\gamma$	96.81	96.37	95.14	93.75	91.64	88.58
ε_n^γ	80.19	79.75	78.66	77.21	75.58	73.12
ε_n^o	71.48	70.77	71.42	70.49	69.62	67.95
ε_n	79.91	79.42	78.32	76.82	75.08	72.53
$\frac{\varepsilon_n^\gamma - \varepsilon_n}{\varepsilon_n}$	0.35	0.42	0.44	0.51	0.66	0.81

* Numbers (1) - (6) referring to decreasing gain on the photomultipliers, correspond to numbers in Fig.2.

energy, a point to be noted by the Directors of any overall programme of work directed and restricted to specific ends.

A brief discussion of this 'French' effect is given in Appendix 1. Condé in Sweden and Mather in the U.K. have made recent attempts to check the effect with disparate results. Provisionally the former finds 0.1 - 0.2% effect and the latter a small, but definite, effect. It is difficult to apply corrections from one scintillator to another, and for old measurements where experimental information is no longer available, perhaps impossible, but Soleilhac suggests that for the Swedish ^{252}Cf $\bar{\nu}$ experiment, where one bank of detectors was used at a neutron efficiency of 0.69 there could be a 1.1% error changing $\bar{\nu}$ (^{252}Cf) from 3.799 to 3.757 n/fiss. Soleilhac is of the opinion that, if the effect is found to be genuine, new scintillator absolute $\bar{\nu}$ measurements will be required; however he feels that these should not be carried out at present because the correction can not be measured sufficiently accurately to give a better than 1% accurate $\bar{\nu}$.

III DATA FOR ν AS A FUNCTION OF ENERGY, $\bar{\nu}_p(E_n)$

The extensive new data reported for average neutron yield as a function of energy for the isotopes ^{235}U, ^{239}Pu, and ^{240}Pu demonstrate a greatly improved situation since the first IAEA Conference on Nuclear Data for Reactors at Paris in October, 1966, and even since the IAEA Symposium on the Physics and Chemistry of Fission held last year in Vienna.

No new data were reported, however, for $\bar{\nu}$ in the fission resonance region where the earlier measurements of Weinstein et al. [28] and Ryabov et al. [29], carried out with good energy resolution, gave different values for different groups of resonances for ^{235}U and ^{239}Pu. $\bar{\nu}$ was also measured in the thermal region by the former workers and found 1% less and 0.6% greater than thermal values for ^{239}Pu and ^{235}U respectively.

No resolution of the discrepancies was suggested at the Meeting but Obninsk scientists were reported as considering it time to make new measurements for ^{239}Pu. The problem has important consequences for fast reactor design where linear dependence has been assumed from thermal on up, which implies using a thermal value in the resonance region.

An interesting and important experiment to resolve some of these difficulties is described in the paper [2] by Condé and Widén from the Research Institute of National Defence, Stockholm on '$\bar{\nu}$ of ^{235}U and ^{239}Pu in a fast reactor spectrum'. The fast zero-power critical pulsed assembly, FRO, at Studsvik, has been used along with fission chambers in the central channel of a scintillation tank, and a ^{252}Cf source as standard ($\bar{\nu}_p$ = 3.756, [17]). The measured $\bar{\nu}$ values are integral values over the actual reactor neutron energy spectrum shown in Figure 2 of their paper (deduced from a theoretical 34-group calculation using one dimensional diffusion theory. A measurement of the actual spectrum is in progress using time of flight methods). Linear approximations of Fillmore [30] to $\bar{\nu}$ as a function of energy for ^{239}Pu and ^{235}U were used in weighting $\bar{\nu}$ values against the reactor spectrum and are shown in the same figure. The observed $\bar{\nu}$ values were corrected for fissions induced by neutrons of energy greater than 67.4 keV, or corresponding to the eight high energy groups, giving final corrected values of $\bar{\nu}$ averaged over the fast reactor spectrum from 0 to 67.4 keV. Table 2 of the paper gives preliminary results showing, in comparison with Fillmore's thermal value recommendations, $\bar{\nu}$ values in the region 0 to 67.4 keV, 6.7% and 0.3% lower for ^{239}Pu and ^{235}U respectively: (Statistical errors at present, 1.9 and 1.5% respectively).

It is clear that a successful conclusion of this experiment (where future accuracy is hoped to be of order 1 to 1.5%) should do much to resolve current uncertainty as to whether the present differential $\bar{\nu}$ data to be discussed below are sufficiently precise for fast reactor design.

Another approach to the provision of ^{239}Pu data for reactor design was given in a paper [10] by Mather and co-workers of the Atomic Weapons Research Establishment, U.K. This was to identify the requirements of the user who would decide the useful energy bands within which to work. The experiment then consisted of producing uniform distributions of neutrons over each energy band in which $\bar{\nu}$ was to be measured. Structure as such, if it existed, was not being examined. In order to get some idea of how much resolution smearing of fine structure is permissible, a series of reactivity computations was carried out at the Winfrith Atomic Energy Establishment by Rowlands for a typical fast reactor assembly. A form of $\bar{\nu}$ energy variation for ^{239}Pu similar to that reported for ^{235}U was adopted, and calculations were made with this exact representation followed by histograms formed by averaging $\bar{\nu}$ over 50, 100, and 200 keV intervals. The overall conclusion was that 100 keV wide bands were satisfactory.

The experimental details are described in the AWRE report and a previous paper [31]. A tritium gas cell was used to avoid uncertainty in the distribution of tritium in solid targets. Constancy in neutron yield of 6% across a band was predicted. The $^{7}Li(p,n)$ reaction, with which there is less uncertainty than for solid tritide targets, was used below 300 keV. The large liquid scintillator used previously by this group was set up with new electronics on a 6 MeV Van de Graaff. The detailed corrections nowadays applied to $\bar{\nu}$ measurements of this type are thoroughly discussed in the paper.

Energy bands were 40-115 keV, 115-285 keV and 100 keV wide from 300 keV to 1.2 MeV with relative accuracy of 1%. In addition, confirmatory measurements were made in the region 25-75 keV with 50 keV neutron spread. A straight line fit confirming a previous evaluation of the speaker [16] was obtained and extrapolation to thermal energies agreed with the IAEA [17] best values. Mather concluded that, for practical purposes, linear dependence is an adequate representation at the present moment, although he did find some evidence of structure at around 500 keV.

At the Meeting Davey and Mather emphasised the importance of understanding the underlying physics of such anomalies, and, while doubting any adverse effects caused by $\bar{\nu}_p(E_n)$ difficulties, pointed out that reactivity calculations were not sensitive to many things.

A companion piece of work, with yet another approach, was presented by Soleilhac [3] who reported new French data on $\bar{\nu}$ for ^{235}U and ^{239}Pu for neutrons between 0.3 and 1.4 MeV. The experimental set-up closely resembled that used in their previous work [32], with the addition of on-line magnetic tape recording of data. Time of flight analysis of pulsed neutrons from the $^{7}Li(p,n)$ reaction in a thick target on a Tandem Van de Graaff set at 3.1 MeV and 2.8 MeV, was the method adopted. Energy bands of $\pm$ 20 keV up to 700 keV and $\pm$ 50 keV above this energy were used. Simultaneous measurements were made, of $\bar{\nu}_p(E_n)$ for the two fissile isotopes, and the relative fission cross-sections; the latter were mentioned in this morning's Session 5 by Dr. Soleilhac.

^{235}U results, with ^{252}Cf as a standard at 3.782, are shown in figure 2 of their paper. We see two possible humps at 400 keV, and between 0.7 and 1.4 MeV, confirming previous measurements. Deviations from a straight line are of order 1% and 1.2%. Fig.3 shows all previous results, and the interesting Fig.4 allows one to compare smooth fits from the two previous figures, with a smooth fit to the totality of measurements. The straight line is a least squares fit between 1.36 and 3.5 MeV, taken from their own previous measurements up to 15 MeV. Fig.5 gives results for ^{239}Pu; again the straight line is taken from their previous measurements, fitted by a least squares procedure from 1.36 to 5.06 MeV and 12.41 to 14.85 MeV, and gives a good fit to the low energy results with but the barest minimum of evidence (a deviation of 0.6%) for a slight hump at 400 keV, which may be compared with similar evidence from Mather's work.

Soleilhac concludes that the inevitable next step is to carry out measurements on a linear accelerator. He intends further to make $\bar{\nu}_p(E_n)$ measurements for ^{240}Pu from 1 MeV to 15 MeV at the end of this year, as well as relative measurements of the fission cross section.

In a paper [4] by Smirenkin et al. of Obninsk, on 'Some characteristics of the fission process in ^{235}U and ^{239}Pu induced by fast neutrons' data are presented for $\bar{\nu}$ from thermal to 1.6 MeV, measured using multi-layer ion chambers in a paraffin pile with ^{3}He detectors, 24 in number, giving an efficiency of 21%. The reference isotope used was ^{252}Cf and the authors concluded that, (1) values for ^{235}U of order 0.3-0.5% accuracy meet reasonable requirements for fast reactors, (2) their preliminary results with ^{239}Pu demonstrate inadequacies in the data below 1.5 MeV, and (3) the fine structure which would be predicted by the Strutinsky model is confirmed by the experimental data. The data for ^{235}U appear in their Fig.2 where the hatched line represents an evaluation of the totality of results and the histogram,

averages over 100 keV and 200 keV steps; the filled in circles are the authors' data. We note here the qualitative similarity of this fit to that of Soleilhac. In Fig.3 we see what must be emphasised as preliminary results for ^{239}Pu. These results appear to conflict with the measurements of other workers, but a more careful comparison is necessary which takes account of energy spreads used in different measurements.

In the paper [5] by Kusminov et al., again from Obninsk, an analysis is made of the dependence of $\bar{\nu}$ on neutron energy, on the basis of the energy balance in fission. The experimental results of these workers, which allow of an indirect determination of $\bar{\nu}_p(E_n)$, led them to conclude that no irregularity of the type shown by the work of Smirenkin can be confirmed on the basis of indirect assumptions. The experimental results which are shown in Fig.2 demonstrate for ^{239}Pu, where strong irregularities in $\bar{\nu}$ should be reflected in the kinetic energy results, that this is not the case. (The derived $\bar{\nu}_p(E_n)$ values for ^{239}Pu are shown as the lowest curve in Fig.1.)

A further extensive set of measurements of $\bar{\nu}$ for ^{235}U, ^{239}Pu and ^{240}Pu, was given in the paper [1] by Savin et al. of the Kurchatov Institute, in the range of energies 0.6-5 MeV. These measurements were of especial interest being performed by time-of-flight on a linear accelerator, the fission neutrons being detected in the large split liquid scintillator used in previous work [3]. ^{252}Cf, $\bar{\nu}$ = 3.772, was used as standard, and the error in the measurements was 1-3% for ^{235}U and ^{239}Pu and 3-5% for ^{240}Pu. It was valuable to have new $\bar{\nu}_p(E_n)$ measurements for ^{240}Pu for which measurements have been all too sparse in the past. Again, details of the measurement, corrections, and processing of the results, are given in full in the paper.

The results of this experiment are compared with some of the more accurate data of other workers in Fig.3 of their paper, and we saw a similar comparison of this work for ^{235}U and ^{239}Pu in Figs.2 and 3 of Smirenkin's work [4]. The ^{235}U measurements were in good accord with previous results and the ^{239}Pu measurements support the greater slope for $\bar{\nu}_p(E_n)$ presently accepted, in contrast with older measurements and evaluations. Again there was evidence of structure in the region 0.7-3 MeV. The results for ^{240}Pu were less accurate and the evidence is not entirely clear for anomalies between 1.2-1.5 MeV. Additional measurements will be required for this isotope.

In view of the mass of evidence above, albeit somewhat conflicting, it was somewhat disconcerting to hear that the results contained in two preprints [11] [12] submitted to the Meeting by the Australian workers at Lucas Heights, led by Boldeman, appeared to establish that no structure is apparent in $\bar{\nu}_p(E_n)$ for ^{235}U in the energy range 0 to 2 MeV. No effects related to the discreet nature of the low-lying fission channels were observed. The method adopted was similar to previous experiments [35], using a large liquid scintillator with ^{252}Cf as $\bar{\nu}$ standard ($\bar{\nu}_p$ = 3.782), and targets of $^{7}Li(p,n)$ and $^{3}H(p,n)$ on a 3 MeV Van de Graaff. Spreads in neutron energy, E_n, of $\pm$ 25 to $\pm$ 70 keV were used. A statistically consistent linear fit was obtained,

$$\bar{\nu}_p = (2.412 \pm 0.005) + (0.114 \pm 0.008)\ E_n\ (MeV),$$

and the authors claim "there is no evidence whatsoever in the data points of any deviation which could be interpreted as fine structure". They go on to analyse the so-called discrepant data of previous workers and conclude that, excluding the data of Meadows and Whalen [36], a straight line fit,

$$\bar{\nu}_p = (2.416 \pm 0.004) + (0.107 \pm 0.004)\ E_n\ (\text{MeV}),$$

provides an excellent representation of all $\bar{\nu}_p(E_n)$ data, [11].

In addition, measurements of the average total kinetic energy of fragments in the fission of ^{235}U by neutrons of energy 200-900 keV, which could be expected to reflect structure in $\bar{\nu}_p(E_n)$, proved to be independent of the incident neutron energy and, within the experimental error, did not show the reported discontinuity around 300 keV of Blyumkina [34]. Data from this early experiment are compared with those of later workers and appear to be the only disparate results (Fig.3 of [12]). It was concluded that there is no significant dependence of the average total fission fragment kinetic energy on the excitation energy of the fissioning nucleus and no indication of channel effects, within the limits of experimental error.

It was further reported by Soleilhac that Boldeman had made some recent measurements for ^{239}Pu which agreed with his own, i.e. the Australian and French workers disagreed for ^{235}U while agreeing for ^{239}Pu.

There was extended discussion of these results by the Meeting, but no conclusions could be drawn without more detailed examination of all the evidence. Again, it was unfortunate that Boldeman was prevented from attending the Meeting.

IV COMPILATION AND EVALUATION

One of the most useful reference documents presented to the Meeting was a compilation [13] by Konshin and Manero of the energy dependent $\bar{\nu}$ values for ^{235}U, ^{239}Pu, ^{233}U, ^{240}Pu, and ^{241}Pu, and the status of $\bar{\nu}$ for spontaneous fission isotopes, in draft form only. This compilation of almost all previous $\bar{\nu}$ data, and data submitted to the Meeting, in the form of experimental details for the major measurements, tables of values and different forms of graphical display, became a working document of the Meeting. Without any proper evaluation of the results the authors were nevertheless able, from an inspection of the renormalised data, to draw useful conclusions as to the present status of $\bar{\nu}$, and the appropriate fields for future work. I seriously recommend this compilation to workers in the $\bar{\nu}$ field; the Meeting looked forward to seeing it in its final form.

An even more monumental work [14], but this time an evaluation, was presented by Davey covering $\bar{\nu}$ for the principal plutonium, uranium and thorium isotopes. Apart from thermal neutron data, all experimental values for $\bar{\nu}$ for ^{232}Th, ^{233}U, ^{234}U, ^{235}U, ^{238}U, ^{239}Pu, ^{240}Pu and ^{241}Pu over the energy range from 0-15 MeV were analysed to derive best available evaluated data sets, primarily for fast reactor design. Data were re-normalised to $\bar{\nu}_p$ for Cf of 3.756. The lower energy data for ^{233}U and ^{235}U revealed structure of significance for fast reactor analysis, but it was not clear at the time of Davey's evaluation that equally important structure did not exist in the important Pu isotopes. Above several MeV linear energy dependence remains valid but the occurrence of the (n,n'f) and (n,2nf) reactions in addition to the (n,f) reaction, introduces possibly significant non-linear behaviour. A model of first, second and third chance fission fitted the single case in which a test could be made, and the model was applied to the evaluation of other isotopes. This work, which was in a sense complimentary to the IAEA compilation, likewise concludes with more than three pages of recommendations for future work.

Three slides from this evaluation are all I have time to show. The first, Fig.6, shows the status of low energy ^{235}U data prior to the Meeting, the second, Fig.11, the paucity of data for ^{241}Pu and the third, Fig.7, ^{239}Pu data, again prior to the Meeting. You will note that the author has decided, on principle, to use the comprehensive early French set of data [32] as a guide to shape.

We may compare these evaluations for $\bar{\nu}_p(E_n)$ with data shown earlier for the most recent French work [3]. This paper, when updated to include the Helsinki material, is expected to be submitted to a journal. Davey was at a loss to understand the results of Boldeman and felt somewhat reluctant to make any kind of fit to the low energy $\nu_p(E_n)$ values.

The final piece of work reported to the Meeting was an evaluation of $\bar{\nu}_p(E_n)$ for ^{239}Pu [15] [16]. For the purposes of the fast reactor programme in the U.K. we took a careful look in 1968 at the available data to decide whether the reactor requests were met and, if not, which would be the most fruitful areas for future work. Fillmore's evaluation [30] was the most recent but it did not include the results of Condé et al. [37]; moreover, from the point of view of an experimentalist, it was felt that the limited evidence available merited closer examination.

The same experiments were considered as in Fillmore's work, with the addition of Condé's; all material was carefully examined and corrected where possible, using up to date cross-sections, etc. For example, Fillmore's value from Diven et al. [38] is not understood but Leroy's data [39] were improved to give slightly better accuracy and fit. The experiments of Bonderenko, Flerov, Graves, and Bethe [40], were neglected, either through difficulties in misquotation, inadequate documentation, or inability to re-normalize; they all appear to be transmission type experiments and are difficult to normalize to ^{252}Cf. (An attempt to up-date the values of Bonderenko and Flerov, and to normalize them to ^{252}Cf, $\bar{\nu}_p = 3.779$ (the Westcott value derived from η and α [40]), gave improved fits compared to Fillmore, but the results were not included.) To avoid the constant re-normalization, which goes on in this type of work, values were quoted as ratios, $\bar{\nu}_p^{239}Pu/\bar{\nu}_p^{252}Cf$, and the results [15] are given as intercept and slope of a least squares linear fit in Table 1(e) for comparison with Fillmore's earlier evaluation (c). Better, and more realistic, fits were obtained using two straight lines of different slope in the ranges 0-5 and 5-15 MeV, but were not fully justified.

Early data [41] [42] [43] from Soleilhac were not used in the above analysis because of discrepancies in the reported results, and lack of information on errors. With clarification of the position [44] the French results were included in the evaluation, Table 1(f,g,h) [16]. It could be seen that this detailed and careful set of measurements nicely confirmed the earlier results of Condé et al. [37] and Hopkins and Diven [45] and lent support to the higher slope c.f. Fillmore. The low slope suggested by the AWRE group [46] was no longer valid, although individual points are consistent with other data.

At this point it was evident that the U.K. reactor request for $\pm$ 1% accuracy in $\bar{\nu}_p(E_n)$ for ^{239}Pu as a reactor spectrum averaged value, which implies $\pm$ 1% differential data in the range 40 keV to 4 MeV, was met, provided absolute values could be derived through the ^{252}Cf standard, an independent problem. Even the preliminary evaluation provided $\frac{1}{4}$-$\frac{1}{2}$% accuracy from thermal energies to 4 MeV, for ratios to ^{252}Cf (without

error). Although no evidence existed for structure in $^{239}Pu\bar{\nu}_p(E_n)$, in this energy region, the possible effects could be allowed for by making measurements of the type described earlier, [10].

At the conclusion of the Studsvik Meeting I decided that it might be of interest to present some of the results to this Conference to show where we stand today in $\bar{\nu}_p(E_n)$ for an isotope of great interest in reactor design. All the results for ^{239}Pu submitted to the Meeting were re-normalized and added to the previously adjusted values of the older data [16]. The IAEA report [13] was useful in this work, but some of the measurements which I have used are not yet in this compilation, and some have been corrected since. Through the great courtesy of the Director at Studsvik, and the programmer Claes Lissing, I was able to have six linear least squares fits made to all this data, and these are presented at the bottom of Table 1 (j-o).

In the second paper delivered to the Conference [47] Hutchins gave us some 1975 accuracy goals for important nuclear data; in the case of ^{239}Pu $\bar{\nu}$ we can see from Table 1 that the approach to this goal may no longer lie in further measurements for ^{239}Pu, but in a continuing attack on the vexatious problem of the absolute accuracy of the standard, ^{252}Cf. The same remarks may well soon apply to many of the $\bar{\nu}$ items remaining in the request lists, [48].

V CONCLUSIONS OF THE STUDSVIK MEETING

The Meeting concluded by making a series of suggestions, or recommendations for future work, covering only the more important problems relating to $\bar{\nu}_p(E_n)$, as follows:

1. In general evaluators must be much more cautious in their handling of weighting. Not all participants in the Meeting were happy about the methods employed in the IAEA least squares fit but did agree that there was no other obvious approach.

2. More measurements are required on the energy spectra of fission neutrons.

3. Fresh measurements are urgently required for $\bar{\nu}$ in the resonance region, to resolve the present almost complete lack of agreement between the two principal experiments.

4. Although it was not clear what attempts should be made to resolve the discrepancies in findings on $\bar{\nu}_p(E_n)$ structure, principally between the Boldeman set for ^{235}U and results of other workers, clearly meaningful structure details must be discovered, if they exist. Stable energy and stable resolution experiments are needed in this work.

5. Additional experiments are required to complement the interesting $\bar{\nu}$ results for Cf and Cm found by Russian workers, [6].

6. Further measurements are required below 200 keV for $\bar{\nu}_p(E_n)$ for ^{235}U and ^{239}Pu, as well as more measurements in general for ^{240}Pu and ^{241}Pu.

7. There is an urgent necessity to verify the 'French' prompt effect by users of scintillator techniques. If possible, measurements should be made of the prompt pulse efficiency along with $\bar{\nu}$.

It would be of interest for Russian workers to attempt to verify this effect with their large split scintillator with gadolinium loading.

If this effect is confirmed, careful measurement of gamma ray energy distributions will be required.

8. Measurements on delayed fission gamma rays are still required, particularly for ^{252}Cf.

9. A better theoretical approach is required to the energy dependence of $\bar{\nu}$ to provide a guide to what we might expect.

APPENDIX 1

Consider a typical scintillator experiment for measuring $\bar{\nu}$, as shown in Fig.1. To the normal outputs of coincidence between prompt pulse and fission fragment, and fission neutron numbers ($P(\nu)$, we add an output recording lack of coincidence between the fission fragments and prompt pulse, when the latter is not detected. The photomultipliers may be connected in several banks.

Define:

N_γ^n = Total number of fissions detected with coincident prompt pulse, n neutrons, + background.
N_o^n = Total number of fissions detected without a prompt signal, and n neutrons, + background.
ε_n^γ = Neutron efficiency for fission neutrons detected with a prompt pulse.
ε_n^o = Neutron efficiency for fission neutrons detected without a prompt pulse.
ε_n = Neutron efficiency for neutrons from all fissions.
$\bar{\varepsilon}_\gamma$ = Prompt pulse efficiency.

Then

$$\bar{\varepsilon}_\gamma = \frac{\sum_{n=o}^{\infty} N_\gamma^n}{\sum_{n=o}^{\infty} N_\gamma^n + \sum_{n=o}^{\infty} N_o^n}$$

Soleilhac reported at the Meeting in Studsvik that he had measured the prompt pulse efficiency as a function of the number of neutrons detected per fission and the results are shown in Fig.2. Classically one would expect a horizontal line showing no variation with the number of neutrons detected. Fig.2 shows the effect for three banks of photomultipliers, connected four to a bank. Similar effects are found for two banks of six, and one bank of 12. The curves labelled 1 to 6 were measured for different gains, 1 being the highest.

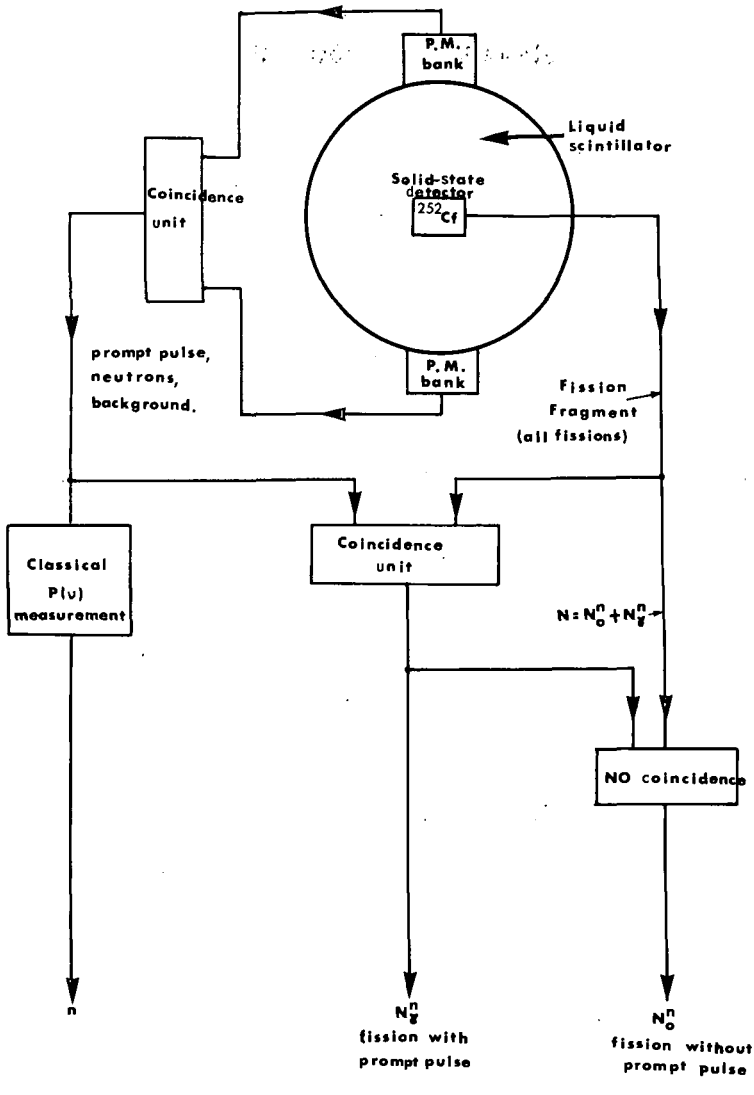

FIG.1. Typical scintillator experiment.

Fig.3 shows the variation of the neutron efficiency of the detector for neutrons detected with the prompt pulse plotted against the prompt-pulse efficiency, and in Fig.4 as a function of the background in a 50 μs gate.

Finally in Fig.5 we plot the error in efficiency and consequently in absolute $\bar{\nu}$, which can be expected, with this particular detector, as a function of its prompt-pulse efficiency, if the effect were to be neglected. The law seems to apply to the three different arrangements of photomultipliers. Table 2 gives some numerical results.

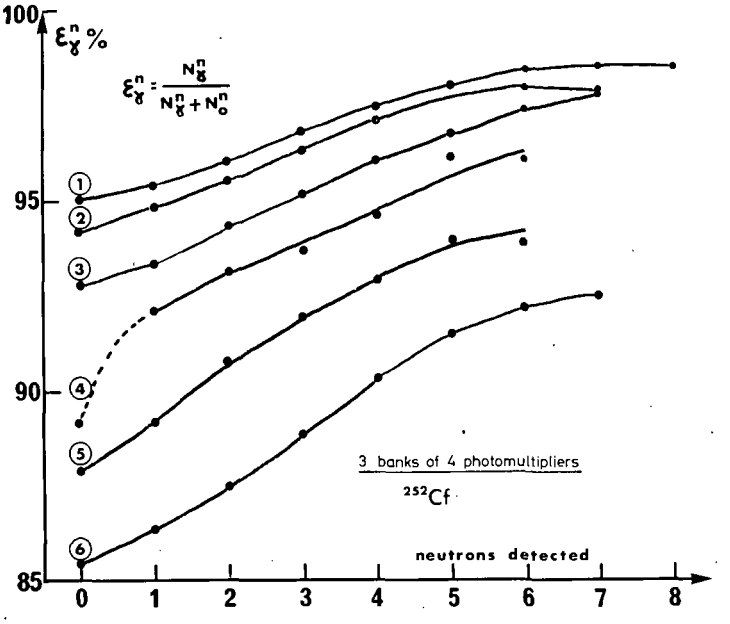

FIG.2. Prompt pulse efficiency as a function of the number of neutrons detected.

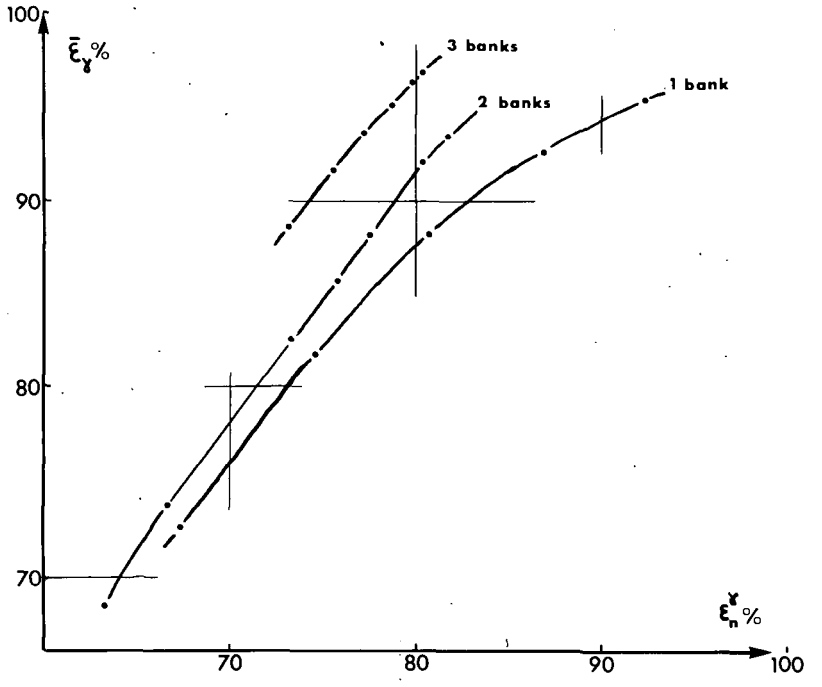

FIG.3. Neutron efficiency of detector for neutrons detected with the prompt pulse versus prompt-pulse efficiency.

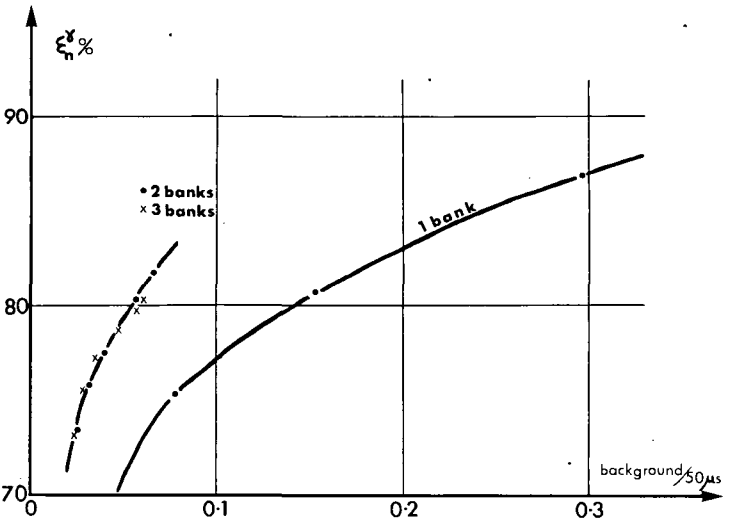

FIG.4. ϵ^{γ}_{n} (%) versus background in a 50-μs gate.

The physical explanation of this phenomenon is not certain, and would require further investigation, but clearly, if it is genuine, it will not be possible to correct old absolute measurements for which the apparatus has been dismantled, without an understanding of the mechanism. In Diven's original measurement [45] the ^{252}Cf neutron efficiency was 0.86, and in Condé's 0.69 [49]; correction to the former should be small but for the latter, carried out with one bank of detectors, an error of 1.1% is suggested by Soleilhac, which would reduce the ^{252}Cf value for $\bar{\nu}_p$ from 3.799 to 3.757.

The magnitude of the effect will depend on the diameter of the scintillator and its shape. (N.B. the Diven detector was cylindrical.) A new large scintillator has been constructed at Saclay, which can be divided into two halves, and this shows the same effect but of half the magnitude when the two halves are connected together; the photomultiplier geometry is however different from the Soleilhac chamber.

Condé reported to the meeting that when he had measured $\bar{\nu}$ as a function of the prompt pulse height an effect of 0.1 to 0.2% was found. However he had recently repeated the French experiments on his present scintillator and found the same phenomenon that Soleilhac had discovered, although figures were not yet available.

Mather reported that he had tried to repeat the measurements of Soleilhac on the AWRE scintillator, which was very similar to the French one, but with a different connection of the banks of photomultipliers. $\bar{\nu}$ was measured directly using two gates, one connected to the fission chamber and the other to a coincidence between the fission chamber and the prompt pulse. This arrangement should demonstrate the same effect. He had found a 0.1% effect which increased to 0.18% when the gain was reduced by 20 db; in this latter condition the neutron counting efficiency was reduced from 83-84% to 37%. This measurement was carried out with 3 banks of 4 photomultipliers and when repeated with 2 banks of 6 gave corresponding figures of 0.08% increasing to 0.32% for a 20 db gain change which altered the efficiency from 87% to 45%.

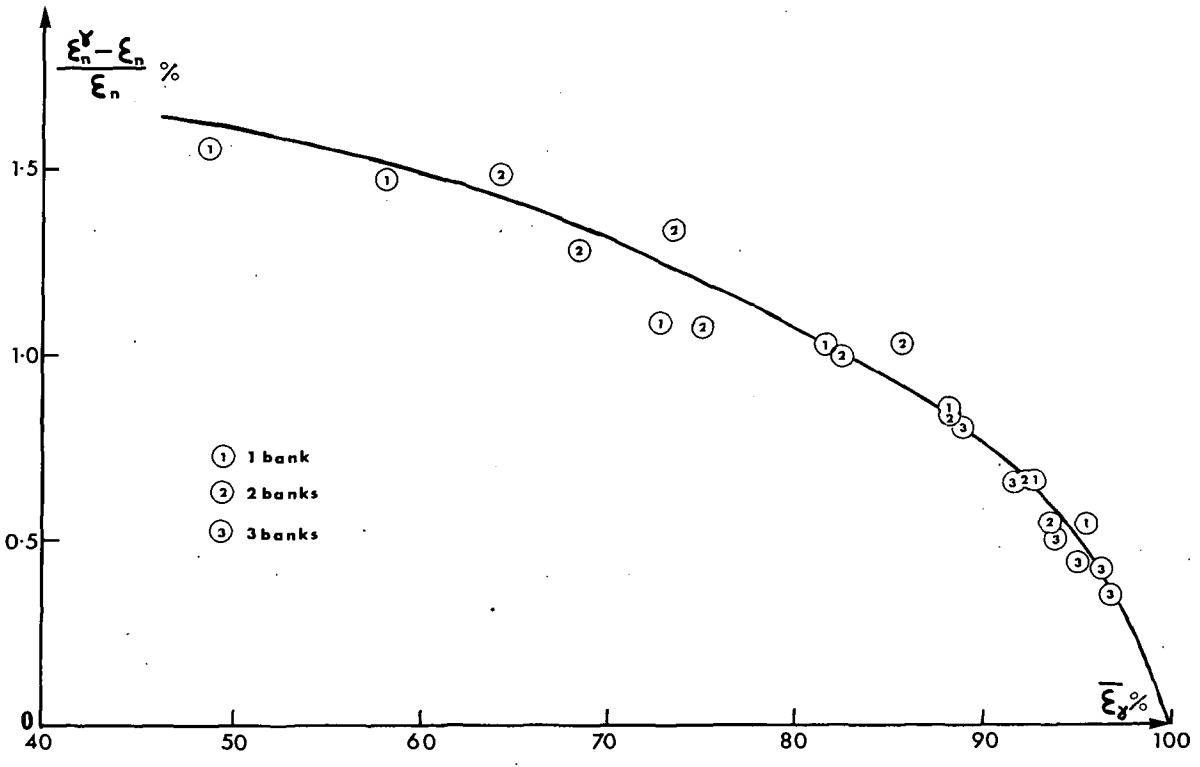

FIG.5. Error in efficiency versus prompt-pulse efficiency.

All the above measurements were carried out with a ^{252}Cf source, and there was unlikely to be any effect on $\bar{\nu}$ ratios but Soleilhac is attempting to measure the effect for ^{240}Pu, a difficult experiment. Preliminary results indicate a law of similar slope but different magnitude. Depending on the physical explanation measurements may be required on gamma spectra as a function of $\bar{\nu}$. In the split detector used by Savin et al. [1] the gamma ray efficiency for ^{252}Cf gammas is 0.347, and for fission neutrons 0.789. With such low efficiency for gamma rays $\bar{\nu}$ ratios may just be affected.

Although conflicting evidence was submitted to the Meeting Soleilhac repeated that had he carried out an absolute measurement of $\bar{\nu}$ with the detection efficiency approximately 0.80, he would now consider the result to be approximately 1.5% too high. As this is the order of magnitude of the discrepancy between the absolute measurements carried out with scintillators and the majority of others no doubt remained in the minds of participants of the Meeting that further investigations should be carried out with urgency.

REFERENCES

[1] SAVIN, M.V., KHOKHLOV,YU.A., ZAMYATNIN, YU.S., PARAMONOVA, I.N., IAEA Conference on 'Nuclear Data for Reactors', Helsinki, Finland, (15-19 June 1970), Paper IAEA/CN-26/40.

[2] CONDE, H., WIDEN, L., ibid. Paper CN-26/59.

[3] SOLEILHAC, M., FREHAUT, J., GAURIAU, J., MOSINSKI, G., ibid. Paper CN-26/67.

[4] KUZNETSOV, V.F., NESTEROV, V.G., PROKHOROVA, L.I., BAGDASAROV, R.E., FURSOV, B.I., SHPAK, D.L., SMIRENKIN, G.N., ibid. Paper CN-26/74.

[5] VOROBEVA, V.G., DYACHENKO, P.P., KUZMINOV, B.D., SERGACHEV, A.I., SMIRENKINA, L.D., ibid. Paper CN-26/88.

[6] ZAMYATNIN, YU.S., KROSHKIN, N.I., MELNIKOV, A.K., NEFEDOV, V.N., ibid. Paper CN-26/90.

[7] DE VOLPI, A., PORGES, K.G., Private Communication to IAEA Consultants Meeting, Studsvik, Sweden, (10-11 June 1970)

Part I: "Verification of accuracy in measurements of neutron yield from ^{252}Cf."
A. De Volpi and K.G. Porges.

Part II: "Remarks concerning accuracy in neutron yield measurements."
A. De Volpi.

[8] DE VOLPI, A., Private Communication to IAEA Consultants Meeting, Studsvik, Sweden, (10-11 June 1970)

"Neutron escape from water moderated tanks", (April 1970), Submitted to Journal of Nuclear Energy.

[9] AXTON, E.J., Private Communication (4 June 1970) to J.J. Schmidt for IAEA Consultants Meeting, Studsvik, Sweden, (10-11 June 1970).

/10/ MATHER, D.S., BAMPTON, P.F., JAMES, G., NIND, P.J., Private Communication to IAEA Consultants Meeting, Studsvik, Sweden, (10-11 June 1970)

"Measurement of $\bar{\nu}$ for ^{239}Pu between 40 keV and 1.2 MeV" (February 1970), to be published as AWRE Report No. AWRE 042/70.

/11/ BOLDEMAN, J.W., WALSH, R.L., Private Communication to IAEA Consultants Meeting, Studsvik, Sweden, (10-11 June 1970)

"The energy dependence of $\bar{\nu}_p$ for neutron induced fission of ^{235}U below 2.0 MeV", (November 1969), to be published.

/12/ AJITANAND, N.N., BOLDEMAN, J.W., Private Communication to IAEA Consultants Meeting, Studsvik, Sweden, (10-11 June 1970)

"Precise measurements of the average kinetic energy of fragments in the fission of ^{235}U by fast neutrons", (February 1970), to be published.

/13/ KONSHIN, V.A., MANERO, F., INDC(NDS)-19/N (Draft Version). (June 1970)

"Energy dependent $\bar{\nu}$-values for ^{235}U, ^{239}Pu, ^{233}U, ^{240}Pu, ^{241}Pu, and the status of $\bar{\nu}$ for spontaneous fission isotopes".

/14/ DAVEY, W.G., Private Communication to IAEA Consultants Meeting, Studsvik, Sweden, (10-11 June 1970)

"An evaluation of $\bar{\nu}$ for the principal Plutonium, Uranium and Thorium Isotopes", Draft, (May 1970), to be published.

/15/ COLVIN, D.W., HNDC(68)P.64, (3 July 1968).

/16/ COLVIN, D.W., HNDC(68)P.69, (28 October 1968).

/17/ HANNA, G.C., WESTCOTT, C.H., LEMMEL, H.D., LEONARD, B.R., STORY, J.S., ATTREE, P.M., Atomic Energy Review, VII, No.4, 3, (1969), IAEA, Vienna.

/18/ DAVEY, W.G., IAEA Conference on 'Nuclear Data for Reactors', Helsinki, Finland, (15-19 June 1970), Paper IAEA/CN-26/112.

/19/ DE VOLPI, A., PORGES, K.G., Metrologia 5, 128, (1969)

/20/ DE VOLPI, A., PORGES, K.G., Phys. Rev. C 1, 683, (1970).

/21/ COLVIN, D.W., SOWERBY, M.G., MACDONALD, R.I., Nuclear Data for Reactors, (Proc. Conf. Paris, 1966) I, IAEA, Vienna (1967), 307.

/22/ DE VOLPI, A., "International comparison of ^{56}Mn activity in 1968" ANL-7642 (to be published).

/23/ MACKLIN, R.L., DESAUSSURE, G., KINGTON, J.D., LYON, W.S., Nucl. Sci. Eng. 8, 210, (1960).

/24/ SMITH, J.R., REEDER, S.D., FLUHARTY, R.G., IDO-17083, (1966).

/25/ TERRELL, J., Physics & Chemistry of Fission, (Proc. Symp. Salzburg, 1965), II, IAEA, Vienna (1965), 3.

/26/ CLARK, H.K., Trans. Am. Nucl. Soc. 12, 886, (1970).

/27/ NEFEDOV, V.N., NIIAR Preprint P-52, (1969).

/28/ WEINSTEIN, S., REED, R., BLOCK, R.C., 'Physics & Chemistry of Fission' (Proc. Symp. Vienna, 1969), IAEA, Vienna, (1969), 477.

/29/ RYABOV, YU.V., DONSICK, SO., CHICKOV, N., IANEVA, N., Report D-3893, JINR, Dubna, p.88.

/30/ FILLMORE, F.L., J. Nucl. Eng. 22, (1968), 79.

/31/ MATHER, D.S., FIELDHOUSE, P., MOAT, A., Phys. Rev. 133, B, (1964), 1403.

/32/ SOLEILHAC, M., FREHAUT, J., GAURIAU, J., J. Nucl. En., 23, (1969), 257.

/33/ SAVIN, M.V., KHOKHLOV, YU.A., ILIN, YU.I., SHEIN, YU.V., Pribory Tekh. Eksp., 6, (1969), 21.

/34/ BLYUMKINA, YU.A., BONDARENKO, I.I., KUZNETSOV, V.G., NESTEROV, V.G., OKOLOVITCH, V.N., SMIRENKIN, G.N., USACHEV, L.N., Nucl. Phys., 52, (1964), 648.

/35/ BOLDEMAN, J.W., J.Nucl. En., 22, (1968), 63.

/36/ MEADOWS, J.W., WHALEN, J.F., J. Nucl. En., 21, (1967), 157.

/37/ CONDE, H., HANSEN, J., HOLMBERG, M., J. Nucl. En., 22, (1968), 53.

/38/ DIVEN, B.C., MARTIN, H.C., TASCHEK, R.F., TERRELL, J., Phys. Rev. 101, (1956), 1012.

/39/ LEROY, J., J. Phys. Radium, 21, (1960), 617.

/40/ For these references, see Fillmore /30/.

/41/ FREHAUT, F., GAURIAU, J., LABAT, M., PERCHEREAU, J., SOLEILHAC, M., EANDC(E) 76 "U", (1967), 186.

/42/ SOLEILHAC, M., Colloque de Phys. Nucleaire, French Phys. Soc., Bordeaux, (1967).

/43/ FREHAUT, F., GAURIAU, J., LABAT, M., PERCHEREAU, J., SOLEILHAC, M., EANDC(E) 89 "U", (1968), 221.

/44/ Private Communications, M. Soleilhac to D.W. Colvin, (Sept - Oct, 1968), and Ref. /32/.

/45/ HOPKINS, J.C., DIVEN, B.C., Nucl. Phys., 48, (1963), 433.

/46/ MATHER, D.S., FIELDHOUSE, P., MOAT, A., Nucl. Phys., 66, (1965), 149.

/47/ GREEBLER, P., HUTCHINS, B.A., COWAN, C.L., IAEA Conference on 'Nuclear Data for Reactors', Helsinki, Finland, (15-19 June 1970), Paper IAEA/CN-26/102.

/48/ EANDC 85 "U", (April 1970), pages 69, 75, 81, 90, 103, etc.

/49/ ASPLUND-NILSSON, I., CONDE, H., STARFELT, N., Nucl. Sci. Eng., 16, (1963), 124.

DISCUSSION

TO PAPERS IAEA-CN-26/40, 59, 67, 74, 88, 90, 99

A. DE VOLPI: I should like to make a few remarks on Dr. Colvin's report. In the first place, two contrasting interpretations have been made regarding the utility of the least squares fit by Hanna et al.: one, that the fit represents the best available values of the thermal fission cross-sections and parameters; the other, that the fit should be disregarded because there is an incompatibility between the input and output values of $\bar{\nu}(^{252}Cf)$ of the order of 1%. I suggest that the proper interpretation is that the least squares fit has accomplished an essential purpose: namely, defining a serious and sustained systematic discrepancy amongst the fundamental fission constants. Accordingly, one should be cautious in using the thermal set with a confidence greater than 1%.

There have been brought out at this Conference and at the preparatory meeting in Studsvik three factors which may lead to a possible resolution of this dilemma: briefly, (1) that the lower values of $\bar{\nu}(^{252}Cf)$ are indeed valid (as corroborated by the fact that the most recent absolute measurements are lower and by the isolation of plausible causes for systematic discrepancy in the higher values of liquid scintillator measurements); (2) that $\eta(^{252}U)$ should be lower by perhaps one-third of a per cent; and (3) that the fission cross-section for ^{235}U (as reported at this Conference by Deruytter) should be higher by about 1%.

Section VI

NUCLEAR DATA ABOVE THE RESONANCE ENERGY: A < 220

Chairman
F. H. FRÖHNER (FRG)

Invited Paper

NEUTRON TOTAL, SCATTERING AND (n, x)-REACTION CROSS-SECTIONS ABOVE THE RESONANCE REGION

S. CIERJACKS
Institut für Angewandte Kernphysik,
Kernforschungszentrum Karlsruhe,
Federal Republic of Germany

Abstract

NEUTRON TOTAL, SCATTERING AND (n, x)-REACTION CROSS-SECTIONS ABOVE THE RESONANCE REGION.
In this review, the present status of neutron facilities used for fast-neutron cross-section measurements is considered. A few topics are then discussed in some detail. In the important area of total neutron cross-sections, several examples of new high-resolution data are shown. Comparisons of other data with optical-model calculations are also considered. Scattering-cross-section measurements are reviewed, and the sphere-transmission method, the associated γ-ray method and the time-of-flight method are discussed. Finally, the (n, x)-reaction cross-sections are briefly reviewed. Concluding remarks are made concerning the accuracy of the data available at present.

1. INTRODUCTION

It is a well-known fact that the threshold of the range above the resonance region varies from nucleus to nucleus. The beginning of this region may be above several MeV for light nuclei, but can also be reached at about several keV in the heavy-mass region. In addition, there is no well-defined energy separating the two regions from one another. There is, rather, an intermediate range in which individual levels become more and more overlapping. We shall take the energy range between about 100 keV and 10 MeV as the region of interest and refer to it as the fast-neutron region.

This area of cross-section measurements is very large and numerous groups are engaged in this work. Preparing this contribution, we had to choose between the two possibilities of either touching on as many experiments as possible in a very brief fashion or discussing only a few points in some detail. We decided in favour of the latter, although we feel quite unhappy in view of the numerous contributions offered to us on request by various groups from many countries. Furthermore, it seemed proper at this Conference to pay attention primarily to experimental and applied aspects of fast-neutron cross-sections rather than to the physical interpretation of cross-section behaviour.

Bearing in mind these facts, we shall concentrate our review on the following topics: present neutron facilities used in the fast-neutron region, measurements and some interpretations of total, (n, x)- and scattering cross-sections. Finally, a few remarks concerning the accuracy of available data will be added.

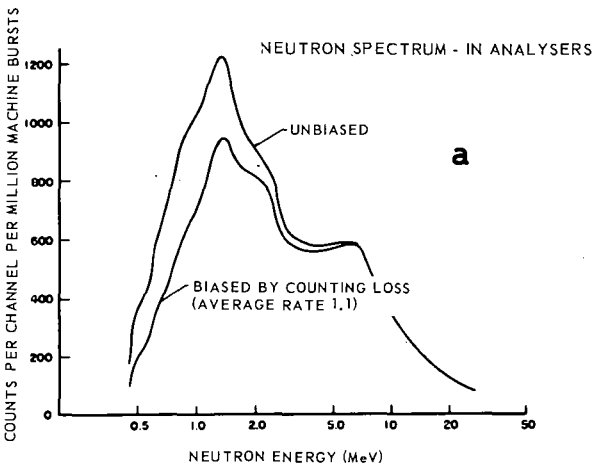

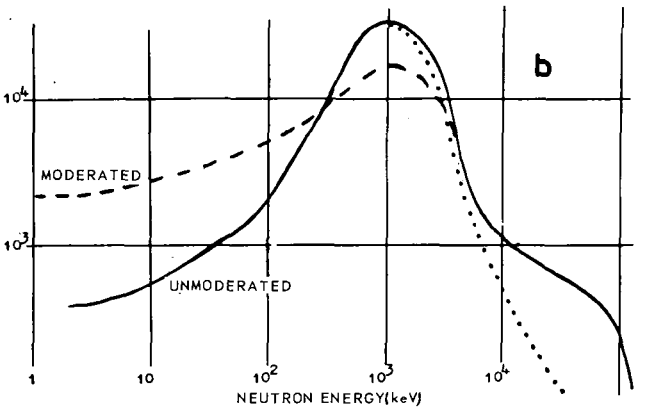

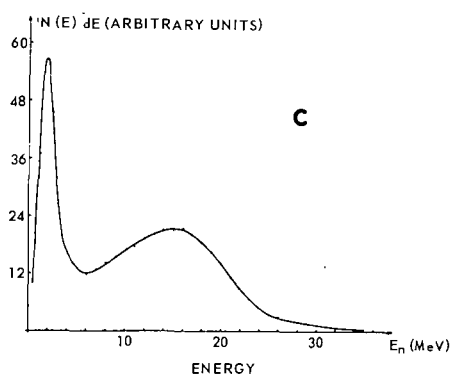

FIG. 1. Typical neutron spectra obtained with
a) an electron linear accelerator,
b) a 140-MeV proton cyclotron,
c) an isochronous cyclotron.

2. NEUTRON FACILITIES USED FOR FAST-NEUTRON CROSS-SECTION MEASUREMENTS

The facilities presently used for cross-section measurements above the resonance region can be divided into two main groups according to the different types of neutron sources involved:

1. Facilities using charged-particle reactions with light nuclei to produce nearly monoenergetic neutrons, such as ^{7}Li (p, n) ^{7}Be.
2. Devices producing wide continuous neutron spectra by interaction of high-energy electrons or charged particles with heavy nuclei.

Van-de-Graaff accelerators and Cockcroft-Walton machines belong to the first category of devices. They can be operated either in the continuous or the pulsed-beam mode. In the following, we shall only consider the latter application since usually this is the most favoured mode for fast-neutron cross-section work. Van-de-Graaff accelerators with top terminal pulsing and pulse compression systems can be used to produce pulses of about 10 mA of protons with 1 ns duration. Several machines with 3, 5, 6 and 8 million volts are in use. In general, monoenergetic neutrons in the energy region between 0.1-10 MeV are produced by the following reactions:

^{7}Li (p, n) ^{7}Be between $0.1 \leq E_n \leq 0.6$ MeV with $E_p \leq 2.3$ MeV
T (p, n) ^{3}He between $1.5 \leq E_n \leq 4.2$ MeV with $E_p \leq 5$ MeV
D (d, n) ^{3}He between $4.5 \leq E_n \leq 11$ MeV with $E_d \leq 8$ MeV

where the projectile energies correspond to neutron observation in the forward direction.

Of course, each of these reactions can also be used to produce neutrons of higher energy than that indicated here, but in typical monoenergetic-neutron experiments there arise some complications because of (i) the second neutron group in the Li (p, n) reaction above $E_p \approx 2.25$ MeV, (ii) the secondary processes in the T (p, n) reaction above $E_p \approx 5$ MeV, and (iii) the deuteron break-up processes in the D (d, n) reaction above $E_d \approx 5$ MeV: the optimum energy resolutions which could be observed in some experiments with monoenergetic neutrons are 1 - 2 keV, 2 - 5 keV, and 20 keV, respectively, in the abovementioned three regions.

Most of the devices using linear accelerators, proton or deuteron cyclotrons as pulsed neutron sources have been utilized in the field of fast-neutron cross-section measurements for the last few years only. Nevertheless, a tremendous amount of total cross-sections has already been determined with these facilities. Electron linear accelerators provide neutron bursts of 5 - 10 ns duration and a time-averaged neutron intensity of up to $\sim 10^{14}$ neutrons/s [1], proton and deuteron cyclotrons bursts of 1 - 3 ns duration and a time-averaged neutron intensity of up to $\sim 2 \times 10^{14}$ neutrons/s [2] which allow high-resolution and precision time-of-flight measurements using flight path lengths of typically 200 m. The resulting energy resolutions show the well-known $E^{3/2}$-dependence. With the electron linac at GGA, Carlson [3] has obtained energy resolutions ranging from 0.3 keV at 500 keV to ~30 keV at 10 keV. With the new 190-m flight path installed at the Karlsruhe isochronous cyclotron, the corresponding energy resolutions obtained so far range between 0.2 keV and 20 keV. If we exclude the subject of energy resolution which may

not be the critical point at all, it should be clear that these continuous-spectra-type facilities combine the advantages of extremely high neutron intensities and broad neutron spectra.

With some of these facilities [1, 2] neutron fluxes even at the end of a 200-m flight path are up to 3 - 4 orders of magnitude higher than those obtained with Van-de-Graaff accelerators in a distance of 1 m from the target if an equivalent energy spread of the neutrons from a monoenergetic source is taken into account. This fact is advantageous mainly for (n, x) and scattering cross-section measurements which were stimulated at a number of laboratories some time ago and which have just now shown some first results [4, 5].

In Fig. 1 three typical neutron spectra are shown which have been obtained with the RPI 140-MeV electron linac (a), with the 140 MeV proton synchrocyclotron at Harwell (b), and the Karlsruhe isochronous cyclotron (c) [6]. All intensities are given in relative units.

3. TOTAL NEUTRON CROSS-SECTIONS

The measurements of total neutron cross-sections are, in principle, reasonably easy to perform because the transmission method does not require a determination of the neutron flux from the source.[1] Most of the measurements of total neutron cross-sections are made with proton recoil detectors though there are some exceptions [7, 8]. In Fig. 2, the geometry of the time-of-flight facility used with the Karlsruhe isochronous cyclotron is shown. This arrangement is used for total neutron cross-section measurements in the region from 0.5 - 32 MeV. Neutrons are detected with a 25-cm-diameter, 1-cm-thick plastic scintillator. For beam monitoring, a small liquid scintillator is placed at an angle of ~6° to the main flight path. The neutron beam is suitably collimated by two collimators inside the vacuum tube of 1 m diameter. Similar arrangements are used on other neutron time-of-flight spectrometers.

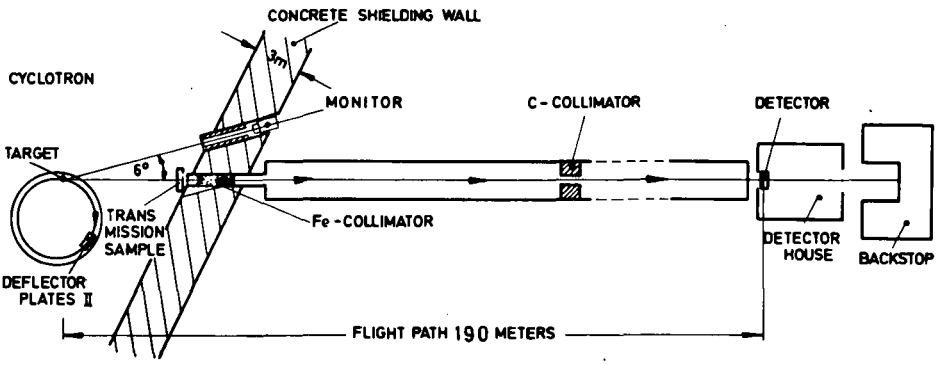

FIG. 2. Arrangement of the time-of-flight spectrometer used with the Karlsruhe isochronous cyclotron.

[1] Nevertheless, some kinds of difficulties arise in high-resolution and high-precision measurements from either the determination of the absolute energy scale [10], of in-scattering effects or dead-time considerations [11].

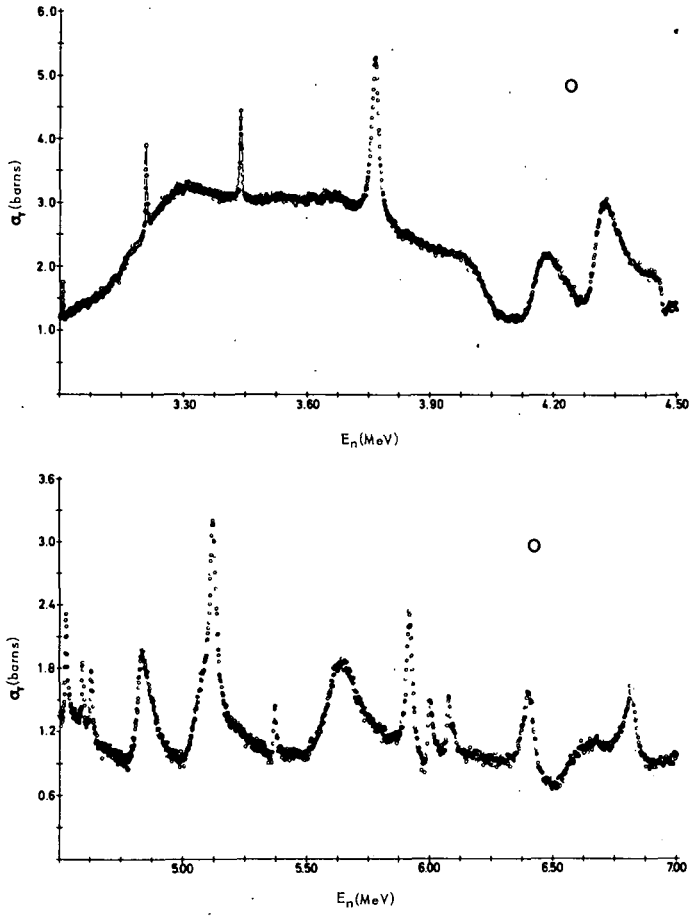

FIG. 3. Total neutron cross-sections of oxygen measured at Karlsruhe.

A recent re-measurement of the total neutron cross-section of oxygen at Karlsruhe using the new 190-m flight path is shown in Fig. 3. These data clearly illustrate the presence of separated resonances, typical of the light nuclei in the MeV-region. In addition to the well-known broader resonances, these new measurements show several narrow resonances which either have not been seen or not been fully resolved in the measurement with the 60-m flight path. Among these, there are also some resonances which were previously seen only in other reactions. This is, for instance, true for the level at 1.690 and the level at 2.888 MeV, with widths smaller than 0.5 and 1.5 keV, respectively.

As an example of a medium-weight nucleus, Fig. 4 shows the excellently resolved cross-section data of iron from a measurement of Carlson and co-workers at GAA [9]. At 500 keV, this nucleus still shows isolated resonances with widths comparable to the level spacings. With increasing energy we can observe more and more overlapping of levels.

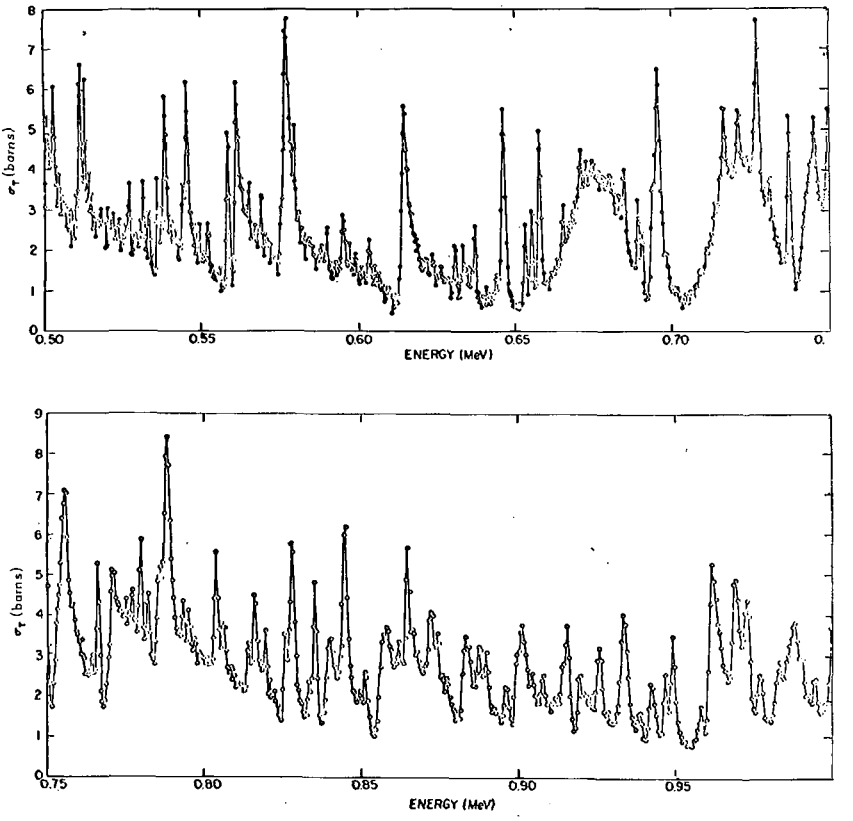

FIG.4. Total neutron cross-sections of iron measured by Carlson [9] at GGA.

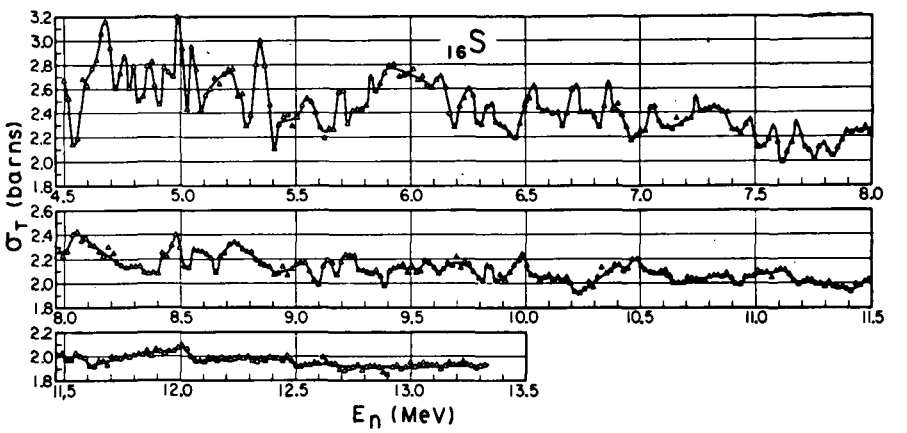

FIG.5. Total neutron cross-section data obtained by Carlson and Barshall [12].

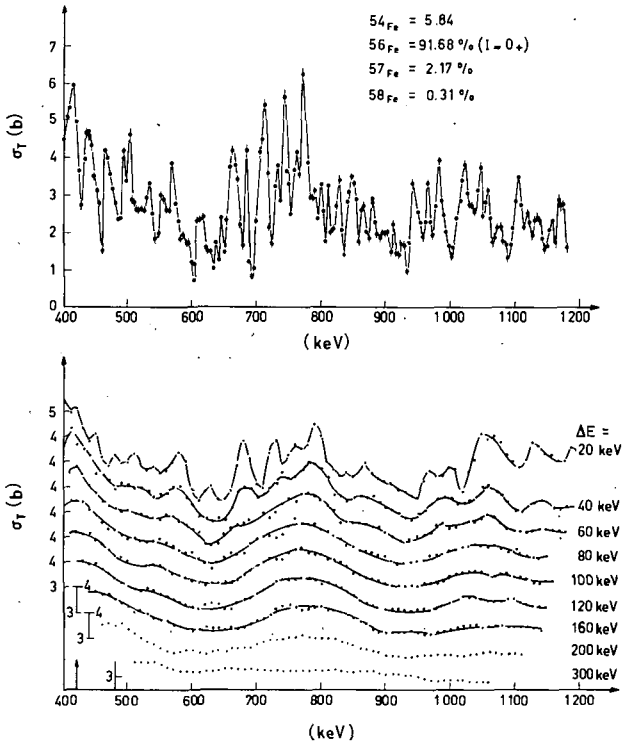

FIG. 6. a) Measured total neutron cross-sections of iron,
b) Averaged total neutron cross-section data of Cabé et al. [13].

To investigate the presence of intermediate structure for several medium- and heavy-weight nuclei, Carlson and Barshall [12] measured the cross-sections of 18 elements from Mg to Bi in the region between 4.5 and 14 MeV with high resolution and precision. Their results for S are shown in Fig. 5. All fluctuations found in this energy region for some medium-weight nuclei could be explained satisfactorily in terms of statistical fluctuations of the level widths and the level spacings.

Cabé et al. at Saclay measured total neutron cross-sections for some light- and medium-weight nuclei from 0.4 - 1.2 MeV [13, 14]. Figure 6 illustrates their results obtained for iron. In addition to the fine structure (Fig. 6a) which arises from the many resonance states of the compound nucleus, a phenomenon known as "intermediate structure" is seen (Fig. 6b). This structure having spacings of ~200 - 300 keV and widths of about 50 - 100 keV is reported to result from the initial formation of simple compound nuclear states such as (2p, 1h)-states. Though structure of this type has been observed in the scattering cross-sections of several elements [15] so that its existence is not questioned, some care must be taken in the interpretation if only the total cross-sections are considered. Therefore, we shall come back to this topic in the discussion of the neutron-scattering data.

Figure 7 illustrates some moderately resolved data from a variety of 78 naturally occuring elements and 14 separated isotopes obtained by Foster and Glasgow [16] in the energy region between 3 and 15 MeV. The large body of data observed under identical experimental conditions has been used to check the predictions of the non-local model of Perey and Buck [17]. The solid circles in this figure demonstrate a seven-point sliding average of the original data. The solid curves are obtained from optical-model calculations. Good agreement between experiments and theory is observed for spherical nuclei (only some of them are shown). However, the experimental results systematically deviate from the predictions for highly deformed nuclei. This result supports the previous assumption that the spherical non-local optical potential should adequately describe the energy variation of σ_T for spherical nuclei, but yields less accurate results in the region of high deformation.

Unfortunately, the above conclusions can not be extrapolated to the regions of lower or higher energies. At Karlsruhe, we have just finished a similar analysis for a variety of 19 elements and one separated isotope in the extended region from 0.5 - 32 MeV [18]. Some of our results are shown in Fig. 8. It can be seen from this figure that the agreement between experiment and theory, mainly below 3 MeV but also above 20 MeV, is less satisfactory also for spherical nuclei. This result is in accordance with the observations made for neutron-scattering cross-sections near 1 MeV [19-22], where the data cannot be matched with this potential. In this region, good agreement could, however, be obtained with the Moldauer potential [23].

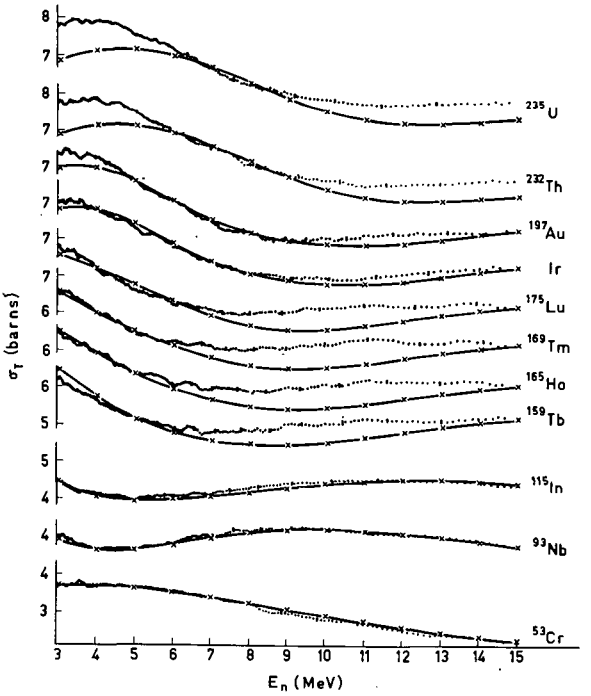

FIG. 7. Comparison of total neutron cross-section values with the predictions of the optical model, Ref. [16].

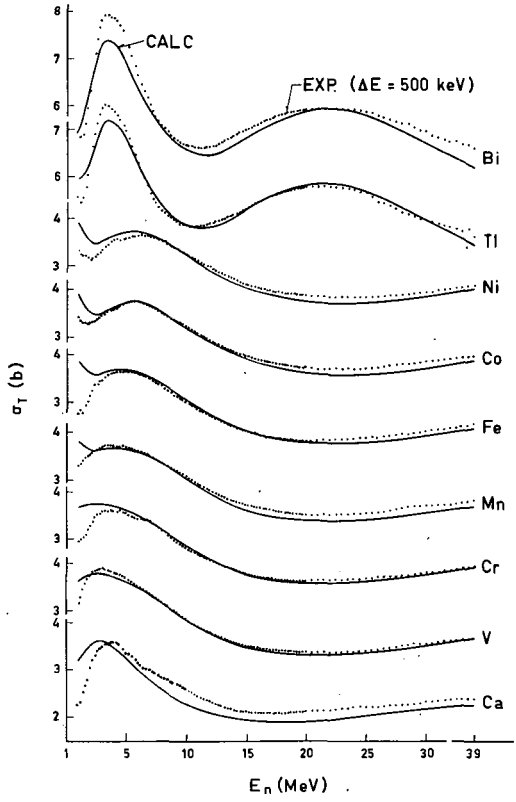

FIG.8. Comparison of total neutron cross-section values with the predictions of the optical model, Ref.[18].

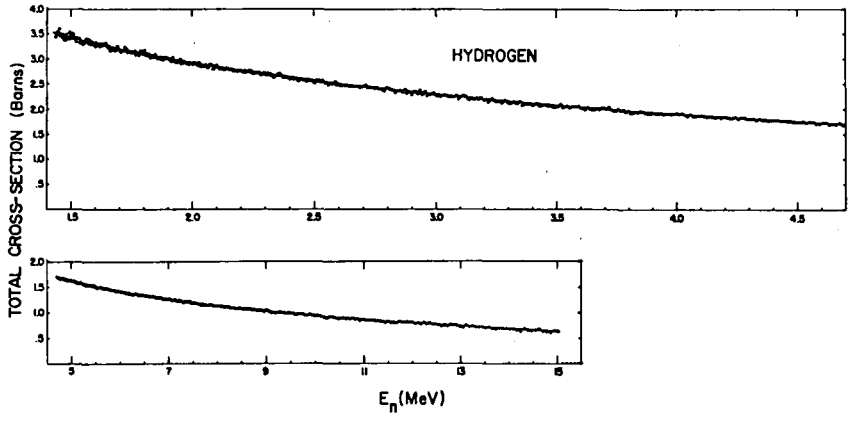

FIG.9. (n,p)-scattering cross-sections between 1.5 and 15 MeV [25].

It was recently reported [24] that the total (n, p)-scattering cross-section shows small but statistically significant oscillation in the energy dependence. This has stimulated some new high-precision cross-section measurements in the fast-neutron region. As an example, the results obtained by Schwartz et al. at NBS [25] are illustrated in Fig. 9. In accordance with the results of some other laboratories [26-28], no significant structure was found.

4. NEUTRON SCATTERING CROSS-SECTIONS

A large amount of accurate fast-neutron scattering data have been measured during the last few years [28-34]. These data range in the total-energy region between about 0.1 - 10 MeV though there is an overwhelming portion in the region below 1.5 MeV. There are two important reasons for acquiring scattering cross-section data: The accurate knowledge of fast-neutron scattering cross-sections (i) is essential for the design of advanced nuclear reactors, and (ii) allows the predictions of suitable nuclear models to be checked. Having such models not only gives better understanding of nuclear reactions, but also provides the reactor physicists with a tool for calculating unknown cross-sections.

There is a lot of techniques used for the fast-neutron scattering cross-section measurements. Only three of the most important methods should be mentioned:

4.1. The sphere transmission method

This is a very elegant method for determining the non-elastic cross-sections which often are equivalent to the inelastic-scattering cross-section. The essential point in this method is the self-cancellation of the elastic scattering from all portions of the sphere shell surrounding either the source or the detector. The observed transmission of this shell can be simply related to the non-elastic-scattering cross-section. The application of this method, however, is limited by the spectroscopic quality of the detectors and the possibility of determining complex correction factors.

4.2. The associated γ-ray method

This method deals with the registration of γ-rays emitted during the de-excitation of the residual nucleus formed by fast-neutron scattering reactions. It can be used to determine accurate γ-ray production cross-sections, which often can be related to the neutron-inelastic-scattering cross-sections. If Ge(Li) detectors are used, relative intensities, energy and angular distributions for all occurring γ-transitions can be determined very accurately from a single experiment. With the exact knowledge of these measurements if there is no transition of the secondary neutrons to the continuum of the residual nucleus. This condition holds for a variety of light- and medium-weight nuclei up to several MeV incident neutron energy.

4.3. The fast-neutron time-of-flight method

Most of the presently available elastic- and inelastic-scattering cross-section data have been determined by this method. An example of a neutron time-of-flight facility used in this field is shown in Fig. 10 [35]. The arrangement consists of a pulsed monoenergetic neutron source, usually a Van-de-Graaff accelerator. The scattering sample is placed close to the neutron-producing target. The energies of the scattering neutrons are determined by the time-of-flight between the scatterer and the neutron detectors positioned at several angles around the scatterer.

Figure 11a gives an example of a measurement done with the latter type of apparatus. This figure shows elastic- and inelastic-neutron-scattering cross-sections obtained for vanadium which were measured by A. B. Smith at Argonne [35]. In this Figure 11a, the experimental total neutron cross-sections, total elastic-scattering cross-sections (lower part) and the first five Legendre polynomial coefficients obtained from a least squares fit to the angular distribution measurements (upper part) are illustrated. Figure 11b contains the measured inelastic-scattering cross-section for the excitation of the 0.32 and the 0.93 MeV levels of ^{51}V. All observed cross-sections are characterized by both a fine and an intermediate energy-dependent structure. The intermediate structure can be described by a width and a spacing large compared to that of the compound nuclear states, but small relative to that of the single-particle or diffraction "giant resonances".

The observed structures in the elastic and inelastic channels were found to be correlated in scattering angle. Structure of this type can be interpreted in terms of doorway-state processes such as mentioned in the preceding section. To reproduce not only the smooth energy dependence but also the observed structure, the authors analysed their data with an intermediate optical potential. This potential has been interpreted to be a conventional optical potential modified only by the presence of two energy-dependent

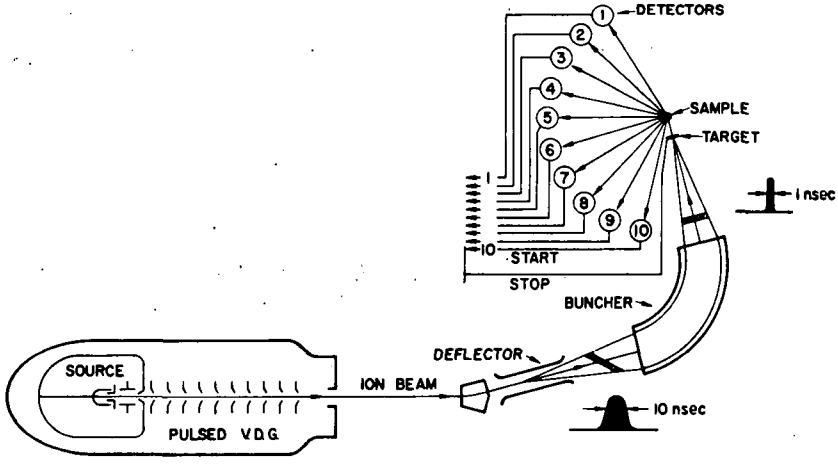

FIG. 10. Time-of-flight facility for fast-neutron scattering experiments [35].

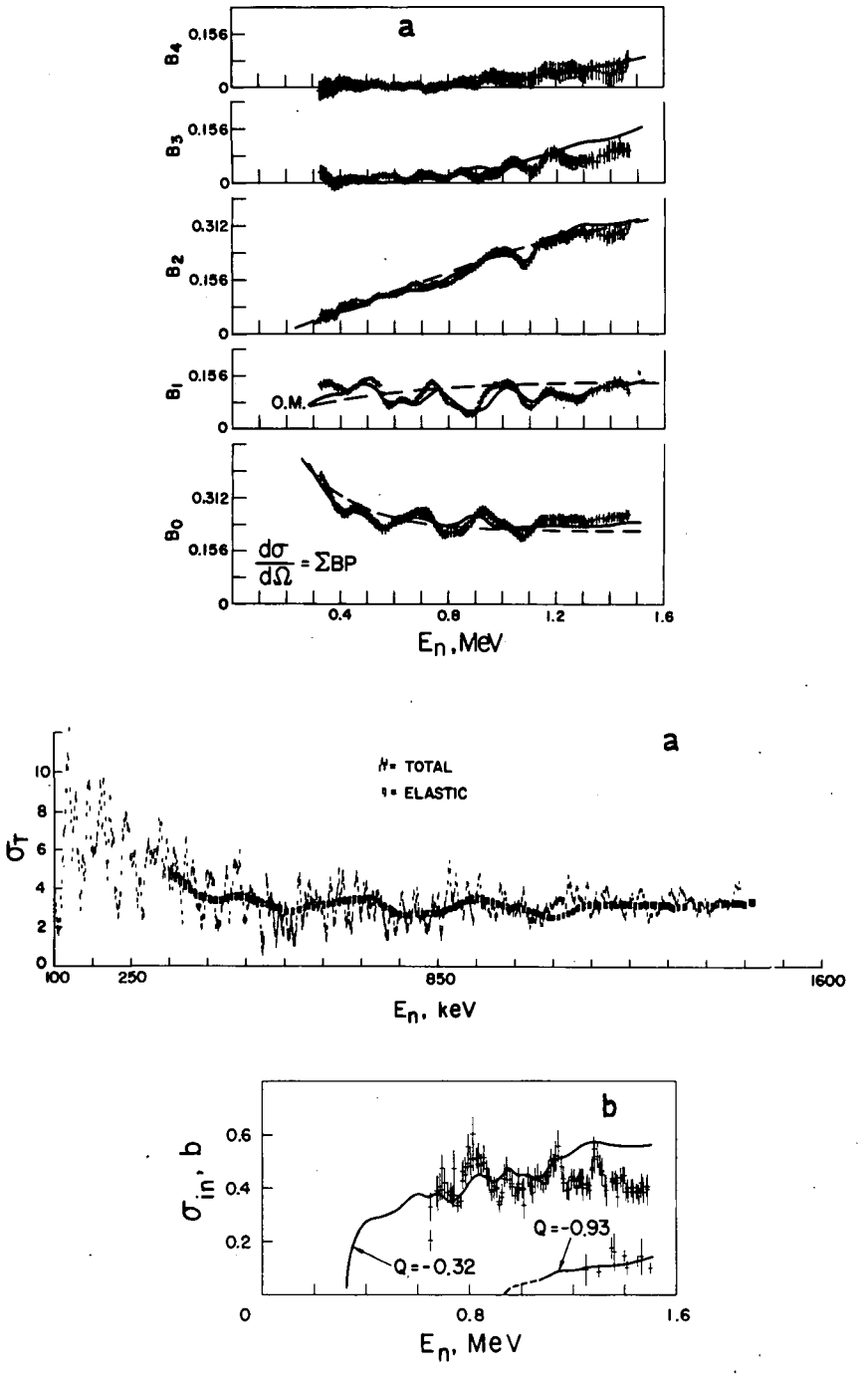

FIG. 11. a) Some neutron scattering data on vanadium obtained by A.B. Smith [35], (two parts, see text).
b) Inelastic-scattering cross-sections of ^{51}V for the excitation of the 0.32 and 0.93 MeV levels.

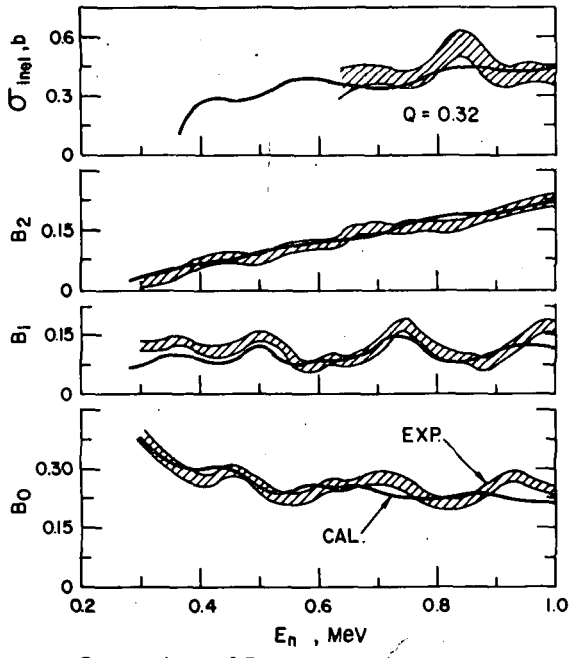

Comparison of Experimental Elastic Scattering Angular Distributions and Inelastic Cross Sections, EXP., of Vanadium with Those Calculated from the Intermediate Optical Potential and Statistical Theory, CAL.

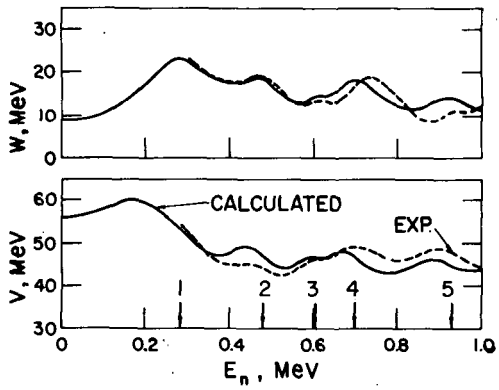

Real (V) and Imaginary (W) Portions of the Intermediate Optical Potential (Eq. 20), Calculated, Compared with the Phenomenological Optical Potential Derived from a Fit to the Measured Elastic Scattering Distributions, EXP. Positions of doorway states are indicated by arrows referring to Table IV values.

FIG. 12. Comparison of experimental results with the calculations from the intermediate optical model [35].

factors classifying a limited number of doorway states. Each of these is characterized by its resonance energy, a decay width of the doorway to the compound nucleus and a strength of the interaction with the doorway. The adjustment of the parameters needed for a general application of such a potential was accomplished by a detailed fit to the measured elastic distribution restricting the number of doorway states to ≤ 5/MeV. The resulting intermediate potential was then used to calculate elastic and inelastic distributions for direct comparison with the measured values. The results of calculation were in qualitative agreement with the experimental results (compare Fig. 12). A wider application of this method may become a useful tool in the determination of statistical properties of doorway states.

Other large bodies of data have been obtained by Holmqvist and Wiedling and coworkers at Studsvik [36] and by Tsukada et al. at Tokai-mura [29]. These two groups investigated the elastic and inelastic neutron scattering for a variety of nuclei in the region between 1.5 - 8 and 0.5 - 8 MeV, respectively, with an experimental arrangement similar to that shown in Fig. 10. New results and the analysis of the data from these two groups will be presented in this session and, therefore, should only be mentioned here.

One example of the use of a Ge(Li) detector in the fast-neutron inelastic-scattering studies is given in Fig. 13a. This figure is from a recent publication of Roger et al. [37] and shows the excitation function for neutron inelastic scattering to the 367-keV level in ^{45}Sc. The corresponding decay scheme of the residual nucleus obtained simultaneously from the measurement is shown in Fig. 13b. The excitation function in Fig. 13a was obtained by summing the γ-ray production cross-section for the 364-and the 376-keV levels, since no cascading transitions to this level were observed. In a similar manner, these authors determined the excitation functions for the inelastic scattering to six other levels up to 1412 keV. In some cases, e.g. for the level at 544 keV, the cascading contributions from higher levels had to be subtracted.

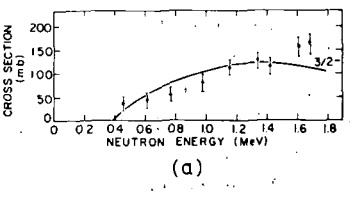

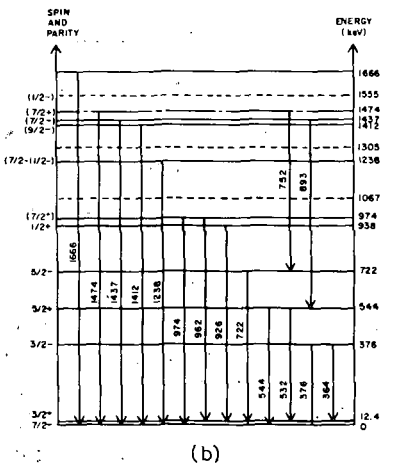

FIG. 13. a) Excitation function for the 376-keV level in ^{45}Sc [37],
b) Decay scheme of ^{45}Sc.

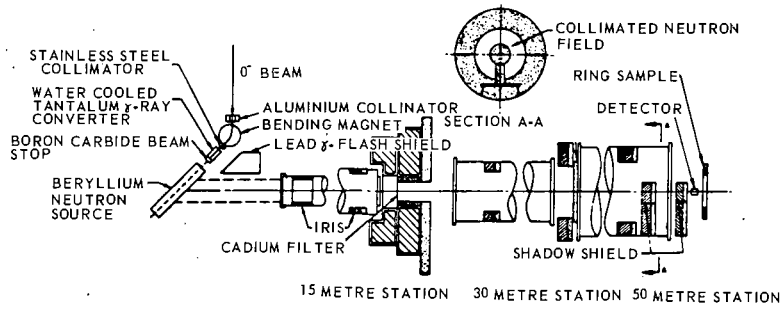

(a)

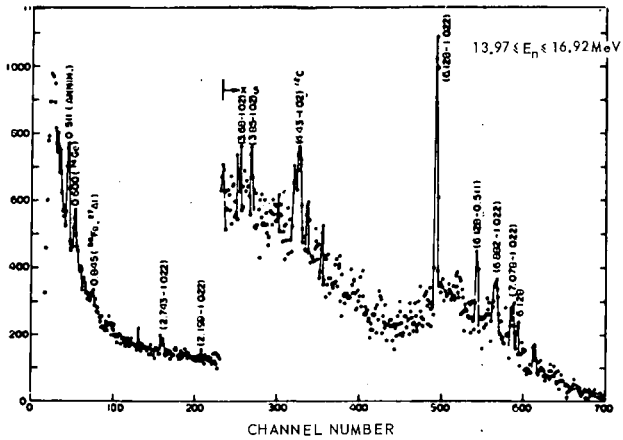

(b)

FIG. 14. a) Arrangement of the time-of-flight spectrum at GGA,
b) γ-ray spectrum from (n, xγ)-reactions in oxygen [4].

With the knowledge of the angular distributions of the γ-rays which were taken from other experiments the excitation functions for several inelastic channels were obtained from the γ-ray-production cross-sections by correcting for cascading transitions.[2] A fascinating aspect in this context is the application of the associated γ-ray method to continuous-spectra-type pulsed sources which was recently demonstrated by Carlson et al. at GGA [4]. Their experimental arrangement is shown in Fig. 14a. The use of the 140-MeV electron linear accelerator as pulsed neutron source allowed

[2] The results of Roger et al. for the lowest inelastic channels are in good agreement with some new unpublished measurements of Reitmann et al. at Pelindaba. These authors determined the inelastic-scattering cross-sections of ^{45}Sc at the 3-MeV pulsed Van-de-Graaff by measuring the neutrons by the fast time-of-flight method. This information is due to a private communication from Dr. Reitmann immediately before the Helsinki Conference.

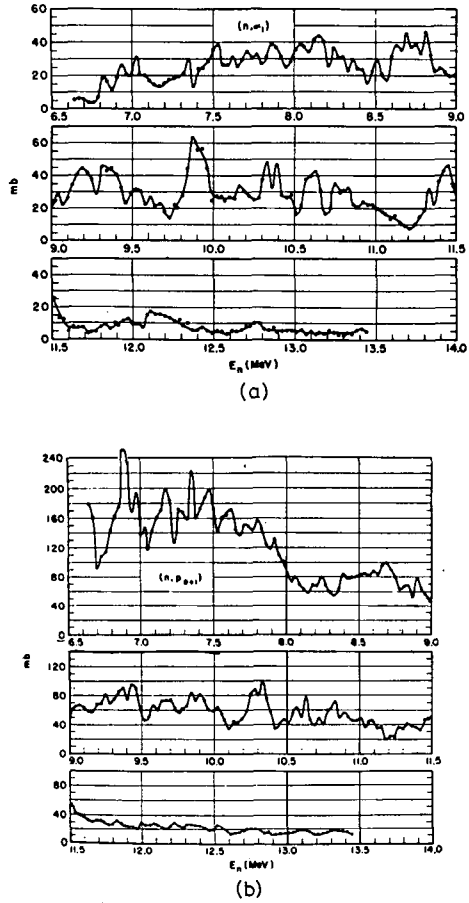

FIG. 15. Excitation functions for reaction cross-sections of Si [44].

a simultaneous measurement of the γ-ray production cross-section in the total energy range from the threshold up to 15 MeV in a single run. The γ-ray energies and intensities are measured using a Ge(Li) detector and the corresponding neutron energy is determined by time-of-flight in a two-parameter experiment. First results for O were obtained at a backward angle of 125° using a ring sample (Fig. 14b). The installation of a similar arrangement is nearly completed at the Karlsruhe isochronous cyclotron.

5. (n, x)-REACTION CROSS-SECTIONS

Neutron-induced charged-particle reactions such as (n, p)- and (n, α)-reactions and (n, 2n)-reactions are mainly threshold reactions and have been used for neutron-flux determination as well as for neutron-spectra measurements. These applications and nuclear-structure studies are the main reasons why detailed and accurate data of those cross-sections from

the threshold up to more than 10 MeV are desirable. While there is a large amount of data centred around 14 MeV [38-43], only comparatively few measurements have been made in the region below. The measurements of threshold reactions in this range often suffer from low neutron intensity.

Most of the available data have been obtained by use of the activation technique. Activation measurements have two advantages: first, large quantities of sample material can be used and, second, the constituent isotopes of an element can be distinguished. The disadvantage of this method is obvious. Such measurements yield the excitation functions only. If more detailed information such as angular and energy distributions of the reaction products are wanted either the nuclear-emulsion technique or direct counting of the emitted particles are necessary. Both methods deal with extremely small amounts of target material, and only a few measurements of this kind could be done in some favourable cases [44, 45].

An experiment belonging to the latter category was recently reported by Grimes [44]. Some of his results are shown in Fig. 15. (n, α)- and (n, p)-reaction cross-section were obtained for the favourable case of Si, where the silicon could serve as the scattering sample as well as the detector. Excitation functions have been determined for some separated α- and proton-groups characterizing the decay of the compound nucleus into some of the first low-lying levels in ^{25}Mg and ^{27}Al, respectively.

In this context, we should like to mention some recent measurements of the (n, α)-reaction cross-section of ^{9}Be done at Karlsruhe by Kropp et al. [5]. Using the isochronous cyclotron as a pulsed source of fast neutrons gave reasonable intensity to measure double-differential cross sections in a four-parameter time-of-flight experiment with good sensivity and resolution. These first results promise that the continuous-spectra-type facilities may become a very powerful tool for the measurement of detailed (n, p)- and (n, α)-reaction cross-sections in the near future.

In the high-energy region, the measured cross-sections do not only include data obtained at ~14 MeV, which were carried out with Cockcroft-Walton accelerators. For several measurements between 1 and 20 MeV, Van-de-Graaff accelerators operated in the continuous beam mode have also been employed [45-48]. In this case, neutrons were produced additionally by the DT-reaction. In Fig. 16, two examples are given of energy-dependent cross-section measurements of threshold reactions between 1 and 20 MeV. One is the ^{60}Ni-(n, p)-reaction taken from a report of Paulsen [43], the other one is the ^{27}Al-(n, α)-reaction measured by H. Schmitt et al. [46] at Oak Ridge. From an examination of the cross-section fluctuations in Al, it can be seen that it is necessary to take data at energy intervals smaller than the energy spread of the incident beam if the true average energy dependence of the cross-section is to be obtained.

With respect to the measurements of (n, 2n)-reactions it seems worthwhile to mention the so-called "Fermi-Water-Tank Method" [49] which does not require that the residual nucleus is radioactive. This method is a valuable tool for bridging those regions where the activation method can not be applied. Surrounding a shell-sphere fast-neutron source combination by a large watertank allows the (n, 2n)-reaction to be calculated if the total non-elastic cross-section is known. Therefore, neutron-flux measurements in water are made at various distances from the target. This allows separation of the neutron flux due to evaporation neutrons from the primary fast neutrons emitted from the source. Feicht and Vonach have obtained several values in good agreement with other measurements.

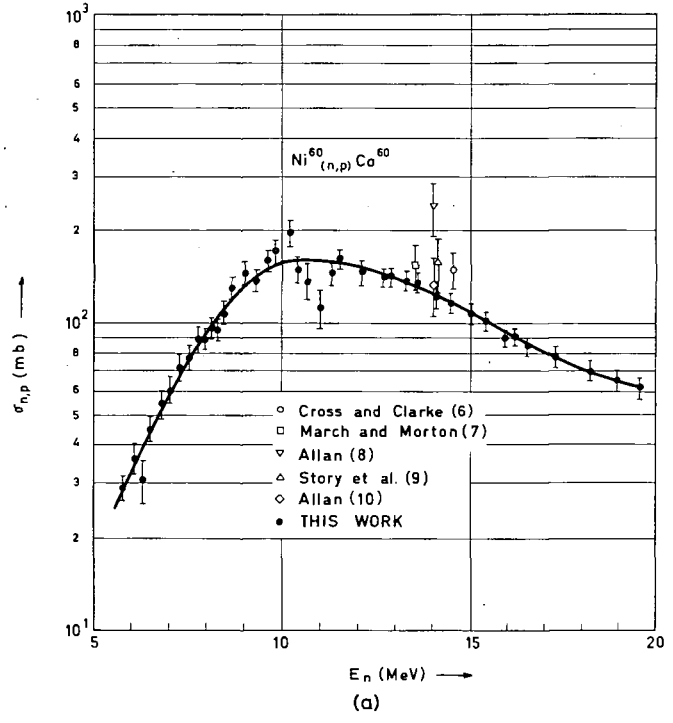

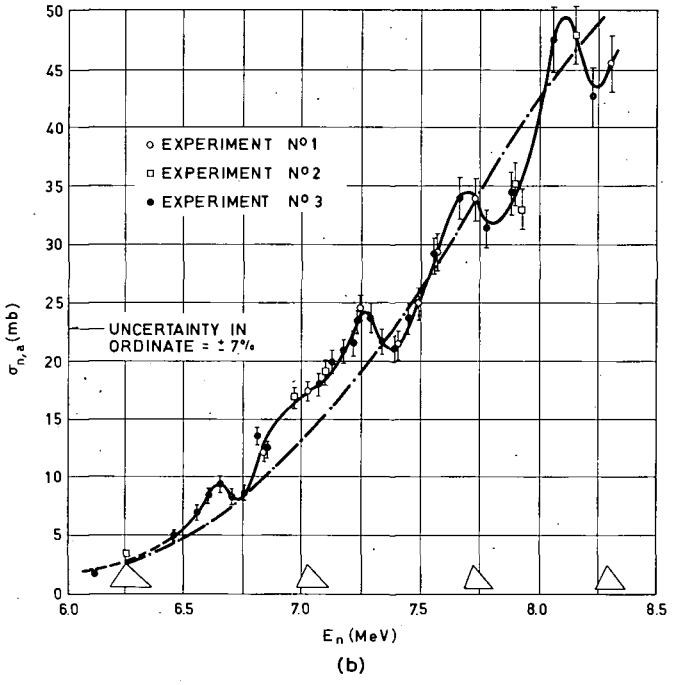

FIG. 16. Excitation functions for reaction cross-sections of
a) Ni (n, p) Ref. [43],
b) ^{27}Al (n, α) Ref. [46].

In addition to the observation of systematic trends found in (n, p)- and (n,α)-reactions [50], S. and A. Chatterjee recently observed some similar effects for (n, 2n)-reactions [51]. The observation of systematic trends in these reactions can be of great importance in calculating unknown threshold reaction cross-sections which are of interest for different kinds of reactor and engineering applications, and will, therefore, be discussed briefly. In the above-mentioned publication, Chatterjee plotted available (n, 2n)-reaction cross-sections at three selected excitation energies versus the mass excess $(N-Z)_R$ of the residual nucleus. This is shown in Fig. 17 which contains the data in the mass-excess range from 0 - 30 and for the excitation energy of U = 6 MeV. A gross trend curve A can be drawn through the most abundant target elements.[3] Effects due to shell closures can be seen in the dips marked by A_1A_2, A_3A_4 and A_5A_6 which shows an anomalous behaviour of the (n, 2n)-reaction cross-section at the magic neutron numbers A = 28, 50 and 82. In addition, remarkable effects are indicated by the weak solid straight lines and the dotted straight lines.

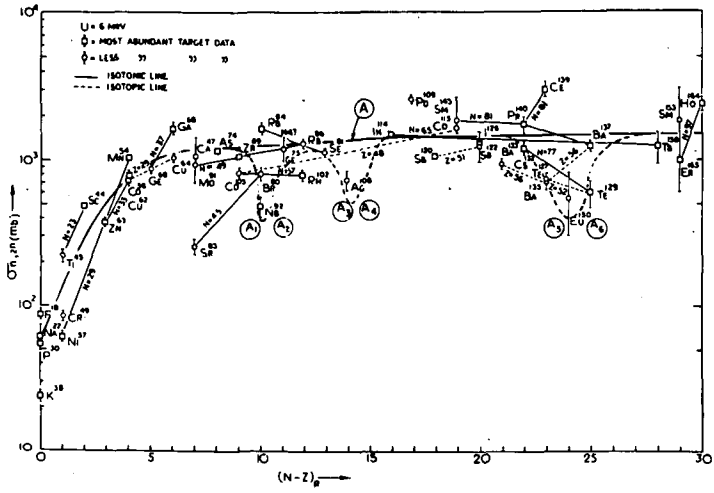

FIG. 17. Experimentally measured (n, 2n)-reaction cross-sections plotted against neutron excess of the residual nuclei.

The lines of constant N (residual isotones, weak solid straight lines) seem to align themselves approximately parallel to gross trend A. This trend, already known as "Csiai-Petro", shows that generally an isotone at lower residual Z value has a higher cross-section than its higher isotopic member. Similarily, there is the same trend for isotopes (dotted straight lines): a heavier isotope usually has a higher cross-section than the lighter one. According to S. and A. Chatterjee, all three trends can be understood semi-quantitatively as a compound nuclear decay process where the available residual excitation of a suitably shifted Fermi gas is properly treated.

[3] Effects due to shell closures can be observed from some cross-section dips.

6. ACCURACY AND RELIABILITY OF PRESENTLY AVAILABLE DATA

Primarily, the users of neutron cross-sections are interested in accurate data for research purposes. Therefore, it should be considered appropriate to this Conference to add some remarks concerning the accuracy to be obtained with the present techniques and man power. A characterization of the accuracy and the reliability should include both the typical uncertainties quoted for some advanced measurements and the comparison of various cross-sections published in the literature. Of course, the comparison of cross-section data in the regions of rapidly varying cross-sections will be complicated by the effects of different energy resolutions obtained in different measurements. In these regions, comparison can only be done in those cases where the effect of energy resolution is small.

In the case of total-cross-section data, the major portion of the more recent measurements has been carried out with a statistical accuracy of ~1% for most of the data points. Absolute uncertainties additionally must include errors due to background, in-scattering or dead-time corrections. Typical values quoted for these measurements are 2 - 3%. A comparison of total neutron cross-section data, which have been collected in various previous compilations [52], often indicated systematic differences of several percent in the measurements made by different

TABLE I. RESONANCE-PEAK POSITIONS (keV)

Cierjacks et al. [53]	Davis and Noda [10]	Johnson et al. [54]
	Carbon	
4933 ± 5	4935 ± 4	
5369 ± 6	5368 ± 5	
6293 ± 8	6294 ± 5	
7755 ± 11	7759 ± 8	
	Oxygen	
1651 ± 1		1651 ± 2
1690 ± 1		1689 ± 2
1833 ± 1		1833 ± 2
1906 ± 1		1906 ± 2
2352 ± 2		2353 ± 2
3211 ± 3		3213 ± 2
3440 ± 3		3443 ± 2
3765 ± 4	3765 ± 3	
5122 ± 4	5122 ± 4	
5906 ± 7	5914 ± 5	
6386 ± 8	6395 ± 7	
6806 ± 9	6807 ± 7	
7193 ± 9	7200 ± 8	

laboratories. Many dicrepancies gradually disappeared as measurements with better resolution superseded the older data. In addition, several discrepancies vanished after some corrections were applied to a few data measured at Wisconsin [10] and at Karlsruhe [11]. A re-calibration of the analysing magnet at Wisconsin caused a correction of their absolute energy scale. A careful re-investigation of the dead-time introduced by the digital time analyser used with the Karlsruhe time-of-flight spectrometer indicated that dead-time effects were overcompensated in some of our earlier measurements.

Table I shows some resonance-peak-position determinations done independently at Wisconsin, Oak Ridge, and Karlsruhe. As the sources of errors are entirely different in the three measurements, the good

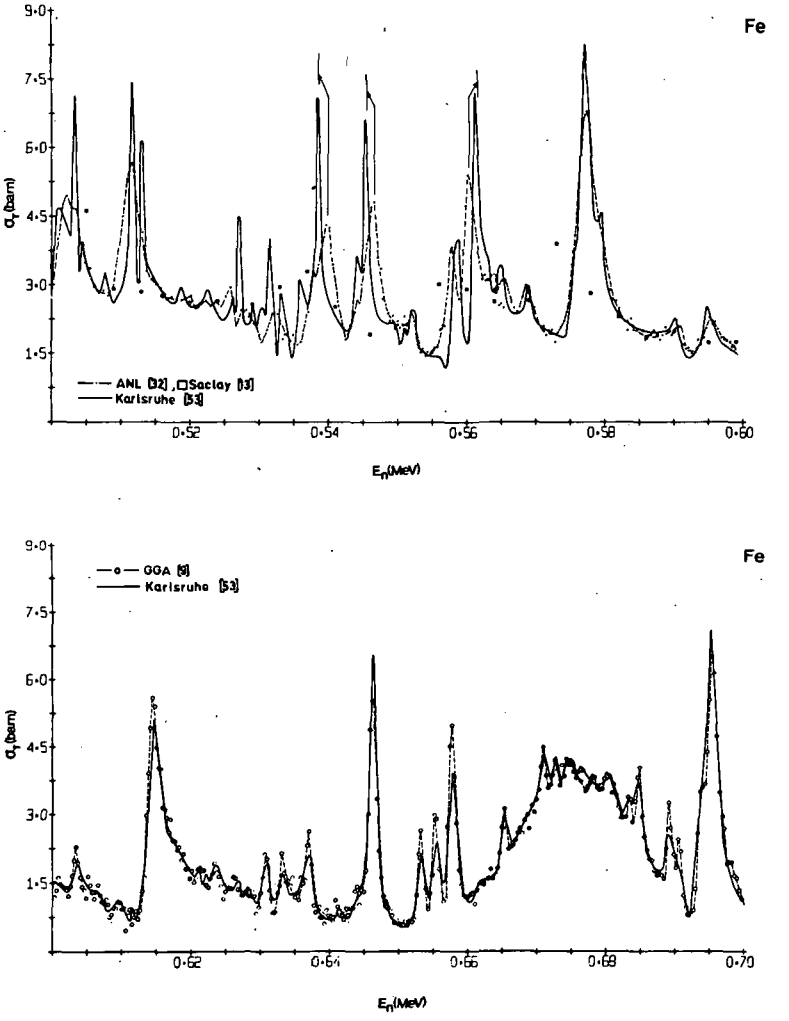

FIG. 18. Comparison of recent iron total cross-section data [11].

agreement is particularly significant. A comparison of some recently measured cross-sections of iron in the region between 0.5 - 0.7 MeV is shown in Fig. 18. Good agreement was observed between the Karlsruhe and the GGA data. The iron data of Smith are less well resolved than our data. In addition, there is a systematic shift of about 5 keV, indicated by the arrows, but a shift of this amount does not represent an actual disagreement. In the Argonne data an uncertainty of several keV is quoted for the absolute energy scale.

In the case of scattering data, the uncertainties associated with the individual cross-section measurements are complex composites of statistical and experimental effects and often have to be estimated subjectively [35]. This, especially, is true for the inelastic-scattering cross-sections. Typical estimated uncertainties for elastic- and inelastic-scattering cross-sections are quoted to be about 5 and 10%, respectively. A recent measurement and a comparison of available elastic- and inelastic-scattering cross-sections for six nuclei between C and Co was made by Perey and co-workers at Oak Ridge [31]. As an example in Fig. 19 some results obtained for Fe are shown. With some exceptions there is general agreement for the total elastic and the total inelastic cross-sections from different laboratories. For inelastic-scattering cross-sections, only very few measurements have been published in overlapping energy regions.

The accuracy with which neutron reaction cross-sections can be determined depends on several factors. The statistical accuracy may be quite poor applying direct counting of charged particles, while in activation measurements sufficient counting rates can be obtained. In the latter case, the experimental uncertainty is largely governed by factors such as the separation of different half-lives, the determination of the detector efficiency or the knowledge of decay schemes. Presently reported cross-sections measured by the activation method quote average total uncertainties of several per cent in favourable cases, inclusive of uncertainties in the reference standard cross-section.

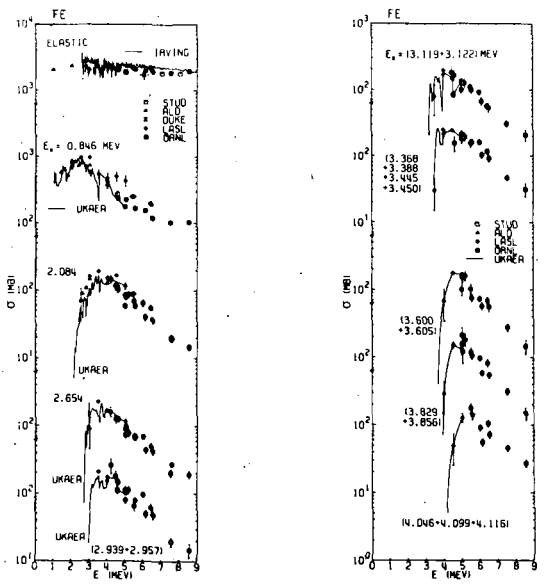

FIG. 19. Comparison of elastic and inelastic cross-sections for iron [31].

7. CONCLUSION

In the last few years, a large amount of cross-section data has been measured which could not all be mentioned here. There have been large advances in the resolution and precision by both the improvement of existing facilities and the installation of new efficient fast-neutron spectrometers. In addition, there are advances in the precision of standard cross-sections such as the (n, p)-scattering cross-section and the ^{10}B (n, α) reaction cross-section. In the field of neutron-scattering cross-sections, a fundamental change is visible: experimentally, the measurers are going to make the transition from the knowledge of a few cases to a more systematic study of scattering processes. All activities in the fast-neutron area not only promise a better knowledge of cross-section values, but also a better fundamental understanding of nuclear reactions. Much activity is presently devoted to the use of linear accelerators and cyclotrons in nearly all fields of fast-neutron cross-section measurements. Several technological improvements may also be expected from new aspects and developments in the area of data processing and data acquisition. A consideration of all these facts may indicate that the users and evaluators will be supplied with a large amount of further and more precise data. We have, however, some doubt that it will be always exactly the data and the precision which is wanted by the users. In any case, as an experimentalist, the author knows that the measurers will do their best to satisfy the requests as far as possible.

REFERENCES

[1] LOPEZ, W.M., FRIESENHAHN, S.J., FRÖHNER, F.H., Report GA-7820 (1967).
[2] CIERJACKS, S., DUELLI, B., FORTI, P., KOPSCH, D., KROPP, L., LÖSEL, M., NEBE, J., SCHWEICKERT, H., UNSELD, U., Rev. scient. Instrum. 39 (1968) 1279.
[3] *CARLSON, A.D., private communication.*
[4] ORPHAN, V.J., HOOT, C.G., CARLSON, A.D., JOHN, J., BEYSTER, J.R., Nucl. Instrum. Meth. 73 (1969) 1.
[5] KROPP, L., FORTI, P., Report KFK 1190 to be published.
[6] YERGIN, P.F., MARTIN, R.C., WINHOLD, E.J., MEDICUS, H.A., MOYER, W.R., AUGUSTSON, R.H., KAUSHAL, N.N., FULLWOOD, R.R., in Neutron Cross-Sections and Technology (Proc. Conf. Washington D.C., March 1966) CONF.-660303 (1966) 690.
[7] RÖSSLE, E., TAUBER, M., Nuclear Structure Study with Neutrons (Proc. Conf. Antwerp, 1965) North-Holland Publishing Company, Amsterdam (1966) 281.
[8] STÜWER, D., GENZ, H., BORMANN, M., Nucl. Phys. 62 (1965) 165.
[9] CARLSON, A.D., private communication.
[10] DAVIS, J.C., NODA, F.T., Nucl. Phys. A 134 (1969) 361.
[11] CIERJACKS, S., Report EANDC (E) 122 "AL" (1969).
[12] CARLSON, A.D., BARSHALL, H.H., Phys. Rev. 158 (1967) 1142.
[13] CABÉ, J., LAURAT, M., YVON, P., BARDOLLE, G., Nucl. Phys. A 102 (1967) 92.
[14] CABÉ, J., Report CEA-R 3279 (1967).
[15] FESHBACH, H., KERMAN, A.K., LEMMER, R.H., Ann. Phys. 41 (1967) 230;
FARREL, J.A., KYKER, G.C., BILPUCH, E.G., NEWSON, H.W., Phys. Lett. 17 (1965) 286;
MONAHAN, J.E., ELWYN, A.J., Nucl. Phys. A 123 (1969) 33;
BOWMAN, C.D., BILPUCH, E.G., NEWSON, H.W., Ann. Phys. 17 (1962) 319;
LEJENNE, A., MAHAUX, C., Z. Physik 207 (1967) 35.
[16] GLASGOW, D.W., FOSTER, D.G., Jr., Phys. Rev. Lett. 22 (1969) 139.
[17] PEREY, F., BUCK, B., Nucl. Phys. 32 (1962) 353.

[18] CIERJACKS, S., NEBE, J., TSIEN, T., Optical-Model Analysis of Total Neutron Cross-Sections (publication in progress).
[19] DE VILLIERS, J.A.M., ENGELBRECHT, C.A., VONACH, W.G., SMITH, A.B., Z. Phys. 183 (1965) 323.
[20] VONACH, W.G., SMITH, A.B., MOLDAUER, P.A., Phys. Lett. 11 (1964) 331.
[21] ENGELBRECHT, C.A., FIEDELDEY, H., Ann. Phys. 42 (1967) 262.
[22] LANE, A.M., LYNN, J.E., MELKONIAN, E., RAE, E.R., Phys. Rev. Lett. 2 (1959) 424.
[23] MOLDAUER, P.A., Nucl. Phys. 47 (1963) 65.
[24] HREHUSS, G., CZIBÓK, T., Phys. Lett. 28 B (1969) 585.
[25] SCHWARTZ, R.B., SCHRACK, R.A., HEATON, H.T., Phys. Lett. 30 B (1969) 36.
[26] CLEMENTS, P.J., LANGSFORD, A., Phys. Lett. 30 B (1969) 25.
[27] CLEMENTS, P.J., LANGSFORD, A., Report, AERE-PR/NP 16 (1970).
[28] CIERJACKS, S., FORTI, P., KIROUAC, G.J., KOPSCH, D., KROPP, L., NEBE, J., Phys. Rev. Lett. 23 (1969) 866.
[29] TSUKADA, K., TANAKA, S., TOMITA, Y., MARUYAMA, M., Nucl. Phys. A 125 (1969) 641;
MARUYAMA, M., Nucl. Phys. A 131 (1969) 145;
KIKUCHI, S., YAMAMUTI, Y., NISHIMURA, K., J. Phys. Soc. Japan 28, 4 (1970) in press.
[30] MENLOVE, H.O., COOP, K.L., GRENCH, H.A., Phys. Rev. 163 (1967) 1299.
[31] PEREY, F.G., private communication.
[32] SMITH, A.B., WHALEN, J.F., BARNARD, E., de VILLIERS, J.A.M., Report ANL-7636 (1969) and to be published in Nucl. Sci. and Engng;
BARNARD, E., de VILLIERS, J.A.M., ENGELBRECHT, C.A., REITMANN, D., Nucl. Phys. A 118 (1968) 321.
[33] HOLMQVIST, B., WIEDLING, T., Report AE-366 (1969);
HOLMQVIST, B., Ark. Fysik, 38 25 (1968) 403;
HOLMQVIST, B., JOHANNSSON, S.G., LODIN, G., WIEDLING, T., Report AE-375 (1969).
[34] HOLMQVIST, B., JOHANNSSON, S.G., LODIN, G., SALAMA, M., WIEDLING, T., Report AE-385 (1969).
[35] SMITH, A.B., WHALEN, J.F., TAKEUCHI, K., Report ANL-7564 (1969) and to be published in Phys. Rev.
[36] HOLMQVIST, B., WIEDLING, T., in Neutron Cross-Sections and Technology (Proc. Conf. Washington D.C., March 1968), NBS Special Publication 299 (1968) 845.
[37] ROGERS, V.C., BEGHIAN, L.E., CLIKEMAN, F.M., Nucl. Phys. A 137 (1968) 85.
[38] BORMAN, M., DREYER, F., SEEBECK, U., VOIGTS, W., Z. Naturforschung 21 A (1966) 988.
[39] VONACH, H.K., VONACH, W.G., in Neutron Cross-Sections and Technology (Proc. Conf. Washington D.C., March 1968), NBS Special Publication 299 (1968) 885.
[40] COLLI, L., private communication to the CCDN Saclay (1969).
[41] RANAKUMAR, R., KONDAIAH, E., FINK, R.W., Nucl. Phys. A 122 (1968) 679;
TIWARI, P.N., KONDAIAH, E., Phys. Rev. 167 (1968) 1091.
[42] CSIKAI, J., Atomki Közl. 8 (1966) 79.
[43] PAULSEN, A., Nukleonik 10 (1967) 91.
[44] GRIMES, S.M., Nucl. Phys. A 124 (1969) 369.
[45] BASS, R., Report EANDC/E-89 (1966);
SPIRA, C., ROBSON, J.M., Nucl. Phys. A 127 (1969) 81.
[46] SCHMITT, H.W., HALPERIN, J., Phys. Rev. 121 (1961) 827.
[47] PAULSEN, A., LISKIEN, H., Nukleonik 8 (1966) 315.
[48] BORMANN, M., BEHREND, A., RIEHLE, I., VOGEL, O., Nucl. Phys. A 115 (1968) 309.
[49] FEICHT, E., VONACH, H., Nukleonik 10 (1967) 58.
[50] CHATTERJEE, A., Nucl. Phys. 49 (1963) 686; Nucl. Phys. 60 (1964) 273.
[51] CHATTERJEE, S., CHATTERJEE, A., Nucl. Phys. A 125 (1969) 593.
[52] SCHMIDT, J.J., Report KFK 120 (EANDC-E-35U) (1966).
[53] CIERJACKS, S., FORTI, P., KOPSCH, D., KROPP, L., NEBE, J., UNSELD, H., Report KFK 1000 (EUR 3963e, EANDC (E)-111 "U") (1968).
[54] JOHNSON, C.H., HAAS, F.H., FOWLER, J.L., MARTIN, F.D., KERNELL, R.L., COHN, H.O., in Neutron Cross-Sections and Technology (Proc. Conf. Washington D.C., March 1968), NBS Special Publication 299 (1968) 851.

DISCUSSION

C. J. CSIKAI: In connection with the fast-neutron total cross-sections, I should like to mention our present result at 14 MeV, as shown in Fig. A. The ratio of measured cross-sections and those calculated by the "black nucleus" formula shows a sinusoidal form in the function of $A^{1/3}$. This oscillation can be explained by the optical model, and a simple expression can be found if we determine the phase shift on the basis of the nuclear Ramsauer effect. The dashed curve in the figure was calculated using the same potential values. The energy dependence of the total cross-sections above a few MeV can also be described by this simple formula. In the case of light nuclei a correlation exists between r_0 and the binding energy per nucleon. This suggests that the higher cross-section values are connected with a loose nuclear structure.

R. F. TASCHEK: At present, the main reactor interest in cross-sections above 1 MeV or so is for (n, n') and (n, n'γ) reactions. These, and especially the spectrum of (n, n'), still require the use of monoenergetic neutron sources for their derivation. I do not think that the white sources can be used for carrying out the necessary experiments.

S. W. CIERJACKS: I can only answer that I believe it should be possible to make double time-of-flight measurements with these machines. At the moment we do not have enough manpower to devote to this project but we are making preparations for such an experiment. We have very large neutron intensities at the end of the 200-m flight path, too, and I think it would be possible in this case to make double time-of-flight measurements as well.

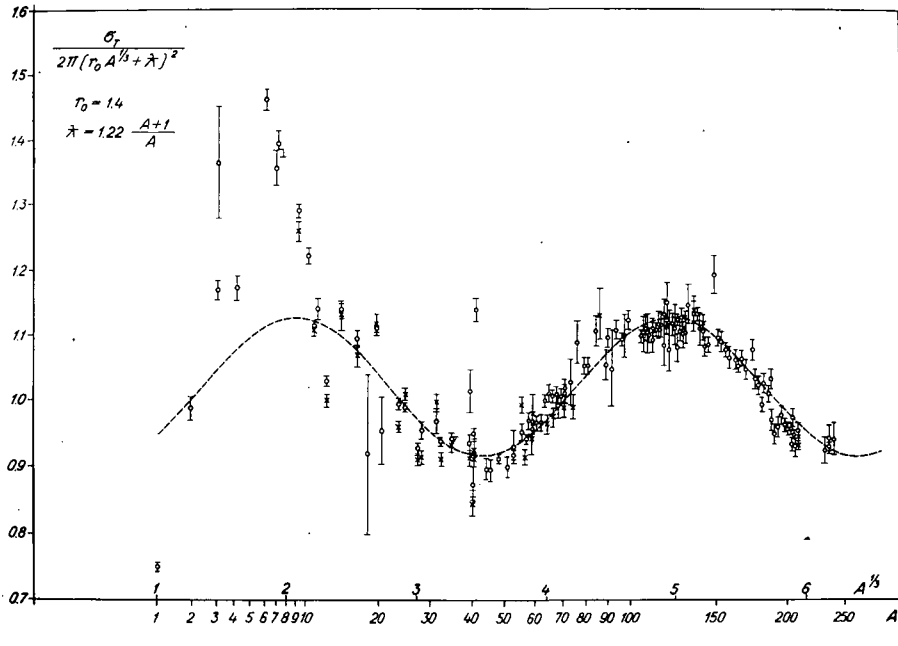

FIG. A. Fast-neutron total cross-sections.

H. W. KÜSTERS: In your presentation you mentioned that, thanks to more precise measurements with higher energy resolution, it has been possible to eliminate inconsistencies in the experimental results. Can you elaborate on this?

S. W. CIERJACKS: What I said was that many discrepancies that had originally been present had disappeared with the availability of new measurements made with better resolution and better statistical accuracy. In addition, several discrepancies vanished after certain corrections were applied to the data measured at Karlsruhe and at Wisconsin.

СЕЧЕНИЯ РАДИАЦИОННОГО ЗАХВАТА НЕЙТРОНОВ ДЛЯ ЯДЕР С A < 220 ВЫШЕ РЕЗОНАНСНОЙ ОБЛАСТИ

А. И. АБРАМОВ
Физико-энергетический институт, Обнинск,
Союз Советских Социалистических Республик

Abstract — Аннотация

RADIATIVE NEUTRON CAPTURE CROSS-SECTIONS FOR NUCLEI WITH A < 220 ABOVE THE RESONANCE REGION.

A review of our state of knowledge of radiative neutron capture cross-sections for nuclei with A < 220 in the non-resonance energy region (mainly above 1 keV) is given. The possibilities of various experimental methods and the results of the most recent measurements are considered.

СЕЧЕНИЯ РАДИАЦИОННОГО ЗАХВАТА НЕЙТРОНОВ ДЛЯ ЯДЕР С A < 220 ВЫШЕ РЕЗОНАНСНОЙ ОБЛАСТИ.

Проводится обзор состояния сведений по сечениям радиационного захвата нейтронов ядрами с A < 220 в нерезонансной области энергий (в основном, выше 1 кэв). Рассматриваются возможности различных экспериментальных методик и результаты последних измерений.

1. ВВЕДЕНИЕ

В данном докладе делается попытка в самых общих чертах рассмотреть состояние дел в области экспериментальных данных по сечениям радиационного захвата быстрых нейтронов и те изменения, которые произошли в уровне имеющихся сведений по этим сечениям и в применяемой измерительной технике после первой конференции по ядерным данным для реакторов, состоявшейся в Париже, т. е. за период времени с 1967 г. по 1969 г.

В предыдущем докладе отмечалось, что границы между областями разрешенных и неразрешенных резонансов весьма условны и их положение во многом зависит как от свойств изучаемых ядер, так и от достижений экспериментальной техники. В настоящее время эта граница проходит для средних ядер где-то в районе 100 кэв. При более высоких энергиях ширина аппаратурной линии самых лучших методик оказывается больше расстояний между уровнями, благодаря чему удается измерять лишь сечения, усредненные по многим близко расположенным резонансам.

Может показаться, что измерение усредненных сечений захвата не является особенно интересным ни для ядерной физики (поскольку усреднение по многим резонансам не позволяет получать детальную информацию о свойствах отдельных ядерных уровней), ни для расчета реакторов (поскольку сечения захвата в этой области энергий малы и составляют незначительную долю от полного сечения). Однако на самом деле это далеко не так.

В данном докладе могут оказаться затронутыми некоторые сведения о сечениях захвата, детально рассматриваемые в других докладах, представленных на данную конференцию. Речь будет идти об усредненных се-

чениях радиационного захвата, полученных в экспериментах с монохроматическими нейтронами при энергиях, начиная с нескольких десятков или даже единиц кэв. Результаты измерений на широких спектрах нейтронов (например, на спектре деления) в данной работе вообще не рассматриваются.

Как известно, в области неразрешенных резонансов абсолютная величина сечений радиационного захвата нейтронов невелика и составляет обычно несколько десятков мбарн. Поэтому особенно большой интерес к информации об этом процессе со стороны реакторостроения проявился лишь сравнительно недавно, в связи с развитием работ по энергетическим реакторам на быстрых нейтронах. Правда, при расчете и конструировании таких реакторов в первую очередь и с наибольшей точностью нужны сведения о захвате нейтронов тяжелыми элементами с $A > 220$ (торием, ураном, плутонием). Однако и для более легких элементов информация о сечениях захвата крайне необходима. Выбор оптимальных конструкционных материалов, выдерживающих высокие тепловые и радиационные потоки и тем самым обеспечивающих получение высоких значений к. п. д. при незначительном снижении реактивности системы и коэффициента воспроизводства ядерного горючего, расчеты активации теплоносителя и различных узлов реактора, а также расчеты защиты в значительной степени опираются на данные о сечениях радиационного захвата быстрых нейтронов ядрами легких и средних элементов. Значительный интерес к радиационному захвату нейтронов проявляется также со стороны специалистов ряда других направлений науки и техники, а также самими физиками-ядерщиками.

Этот интерес находит определенное отражение в запросах на ядерные данные, поступающих от расчетчиков в различные ядерные центры. На рис. 1 показана требуемая точность по сечениям захвата нейтронов с энергиями выше 1 кэв для различных элементов [1]. На этом же рис. 1 стрелками отмечены элементы, для которых информация требуется в первую очередь. Из рассмотрения рис. 1 можно сделать два основных вывода:

1. Число элементов, сведения о которых необходимы реакторостроителям в первую очередь, сравнительно невелико, хотя полный перечень элементов, на которые поступили запросы, довольно широк и охватывает более половины элементов с $Z \leqslant 83$.

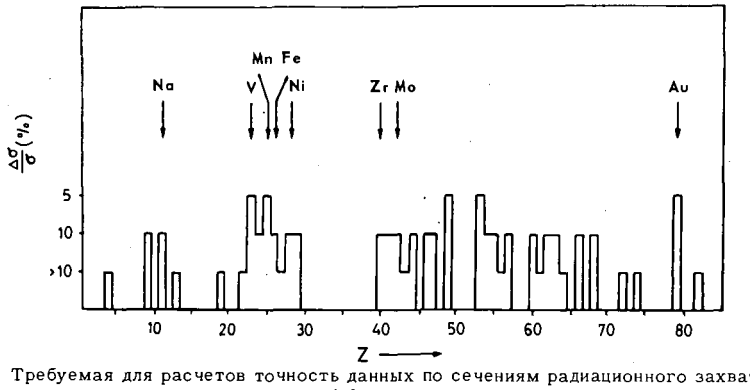

Рис. 1. Требуемая для расчетов точность данных по сечениям радиационного захвата нейтронов с энергиями выше 1 кэв согласно [1]. Для In, I и Au указана повышенная точность (5%), поскольку эти элементы используются в качестве стандартов.

2. Требования к точности знания сечений радиационного захвата быстрых нейтронов ядрами элементов с $Z \leqslant 83$ весьма умеренны, и ошибки, не выходящие за пределы $\pm 5\%$, удовлетворили бы подавляющее большинство запросов.

2. ИЗМЕРЕНИЯ СЕЧЕНИЙ ЗАХВАТА БЫСТРЫХ НЕЙТРОНОВ

Как известно, для измерений сечений радиационного захвата быстрых нейтронов используют, в основном, три метода измерений: метод измерения пропускания образцов в сферической геометрии, метод регистрации мгновенного гамма-излучения и активационный метод.

1. Метод сферической геометрии

Основное преимущество данного метода – возможность получения абсолютных значений сечений поглощения нейтронов из относительных измерений. Кроме того, и статистические ошибки, и ошибки, связанные с расчетом сечения из измеренного пропускания образца, могут быть весьма малыми – порядка одного процента или даже еще меньше [2]. Поэтому результаты опытов в сферической геометрии, казалось бы, могут дать надежные значения сечений в ряде точек, которые затем можно было бы использовать для нормировки данных, получаемых при относительных измерениях другими методами. Однако, ограниченность интервала энергий, в котором возможно проведение измерений (24-900 кэв), низкое энергетическое разрешение и необходимость введения большого числа трудно рассчитываемых поправок, вносящих довольно большую неопределенность в окончательные результаты (до 5% и более [2,3]), сдерживали развитие данного метода измерений, и в течение последних лет он практически не использовался. Тем не менее, углубленное понимание физических процессов и успехи в развитии техники расчетов распространения нейтронов в средах позволяют надеяться, что в будущем экспериментаторы смогут вновь вернуться к этому методу, как к одному из самых надежных методов получения абсолютных значений сечений из относительно простых измерений.

2. Метод регистрации мгновенного гамма-излучения

Этот метод имеет несколько разновидностей, из которых наибольшее распространение приобрели измерения с использованием техники времени пролета. После 1966 года стало известно довольно большое число работ, выполненных этим методом в ряде научных институтов и лабораторий многих стран мира.

В Карлсруэ продолжались измерения на импульсном ЭСГ с использованием в качестве детектора большого жидкого сцинтиллятора. По сравнению с результатами, представленными на Парижскую конференцию [4], было значительно улучшено энергетическое разрешение – с 7 до 2,5 нсек/м [9], что позволило получить ряд новых данных о резонансной структуре сечений захвата. Другим примером работ этой группы могут служить измерения энергетической зависимости сечения захвата для золота [6,7]. Результаты трех серий измерений, выполненных относительно бора-10, лития-6 и "серого" детектора нейтронов, прекрасно согласуются между собой и позволяют выявить структуру в кривой $\sigma_\gamma = \sigma_\gamma(E)$ при энергиях вплоть до нескольких десятков килоэлектронвольт (рис. 2).

Группой Моксона в Харуэлле после реконструкции линейного ускорителя был проведен цикл измерений сечений захвата для ряда элементов в интервале энергий до 100 кэв с использованием детектора Моксона-Рея. При измерениях с бустером полная временная неопределенность выше 1 кэв составляла ~250 нсек, что на пролетной базе 32,5 м позволяло получить номинальное разрешение 8 нсек/м [10].

Значительно улучшено энергетическое разрешение и на установке Ренселлеровского политехнического института. Последние работы группы Блока на этой установке выполнены с разрешением 0,6 нсек/м, которое в настоящее время является, по-видимому, самым высоким разрешением при измерениях сечений радиационного захвата [13]. Высокое разрешение позволило обнаружить ряд новых резонансов (рис. 3), многие из которых с малой шириной являются, возможно, p-резонансами.

Группой Вейгмана в Гиле разработан новый детектор гамма-квантов [17], эффективность которого в диапазоне энергий до 10 Мэв пропорциональна энергии гамма-излучения и в то же время в 4 раза выше эффективности обычного детектора Моксона-Рея. С помощью этого детектора и линейного ускорителя электронов были измерены сечения захвата для меди и молибдена в интервале энергий нейтронов до 25 кэв [18,19].

Новый детектор – так называемый детектор полной энергии – на основе сцинтилляционного счетчика гамма-квантов с безводородным сцинтиллятором был разработан и применен для измерений сечений захвата в Ок-Ридже [20].

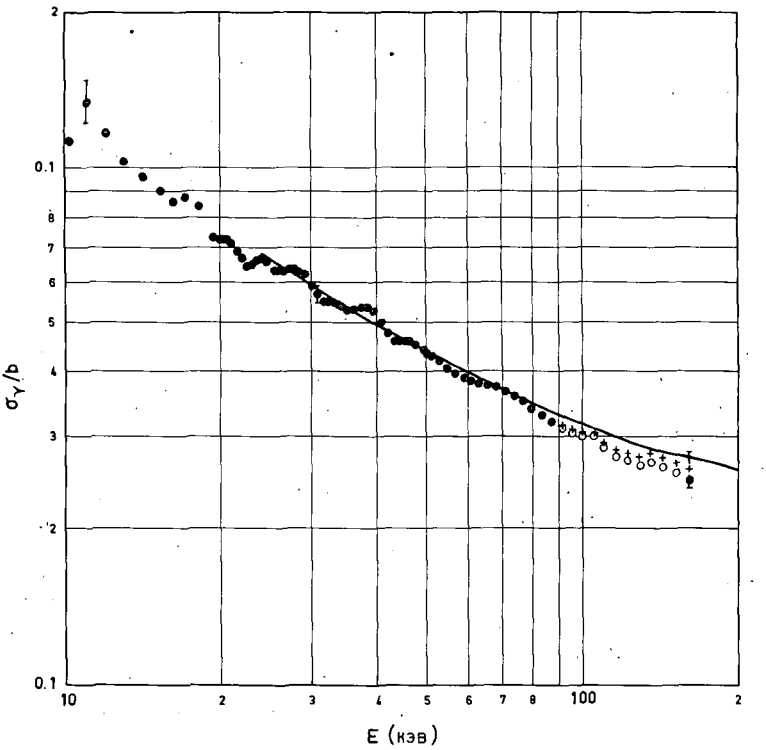

Рис. 2. Результаты измерений $\sigma_\gamma(^{197}Au)$ в Карлсруэ [7].

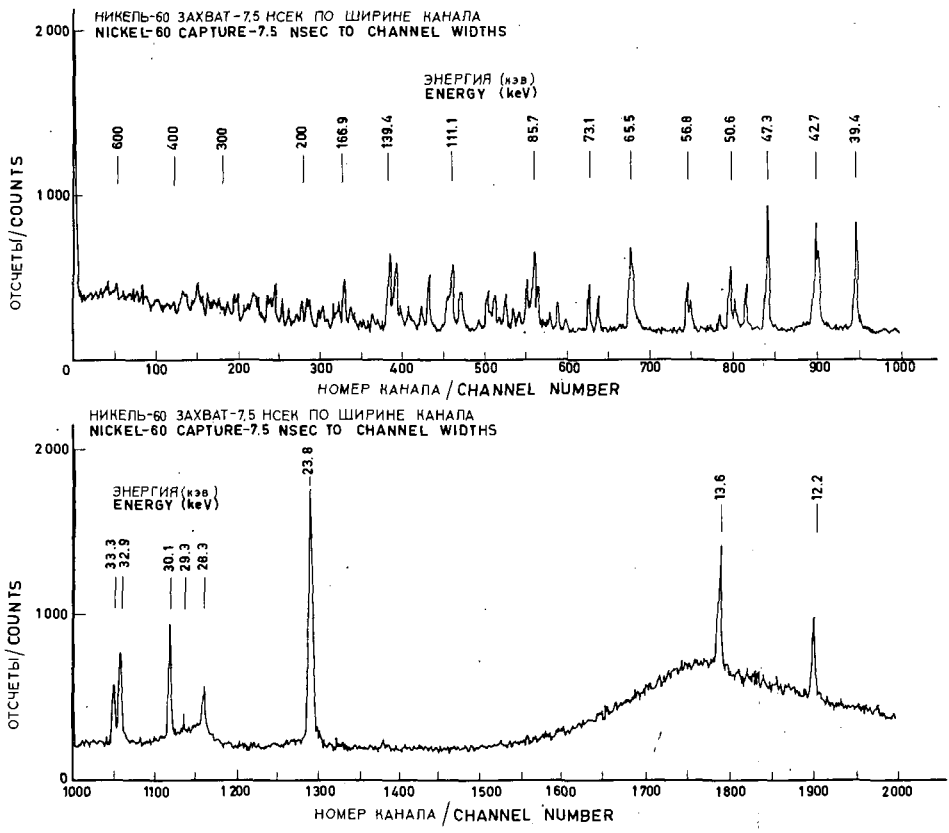

Рис. 3. Результаты измерений σ_γ (^{60}Ni) в РПИ [13].

Особо следует отметить возможности измерений методом времени пролета с использованием подземных ядерных взрывов. Во время испытаний "Персиммон" (февраль 1967) и "Поммард" (март 1968) с очень высоким разрешением были измерены сечения радиационного захвата нейтронов ядрами некоторых изотопов прометия, европия и лютеция [21-23].

Более подробные сведения о перечисленных выше и некоторых других измерениях с использованием техники времени пролета приведены в табл. 1.

Из других разновидностей методики регистрации гамма-лучей можно отметить измерения, проводимые в ФИАН им. Лебедева в Москве на спектрометре по времени замедления нейтронов в свинце. Как известно, этот спектрометр обладает очень низким энергетическим разрешением, позволяющим проводить измерения лишь усредненных сечений даже в области малых энергий, однако благодаря ряду достоинств – широте диапазона энергий, допускающей в одном опыте калибровку по тепловым сечениям и по резонансам, возможности применения широкого круга детекторов, возможности создания многоканальных систем и весьма низкому фону – этот прибор находит применение и поныне [30].

ТАБЛИЦА 1. НЕКОТОРЫЕ ИЗМЕРЕНИЯ СЕЧЕНИЙ ЗАХВАТА НЕЙТРОНОВ С ПРИМЕНЕНИЕМ ТЕХНИКИ ВРЕМЕНИ ПРОЛЕТА (1967-1969 гг.)

Место проведения измерений	Авторы работ	Методика	Интервал энергий (кэв)	Разрешение (нсек/м)	Исследованные элементы	Литература
Карлсруэ, ФРГ	Компе, Френер и др.	ЭСГ + БЖС[a]	5 – 500	2,5	Fe, Ni, Mo, Au и др.	[5 – 9]
Харуэлл, Англия	Моксон и др.	ЛУЭ + МР	1 – 200	8	Si, In, Sn, Au и др.	[10 – 12]
Трой, США	Блок и др.	ЛУЭ + БЖС	до 850	0,6	Na, Fe, Ni, Zr и др.	[13 – 16]
Гил, Бельгия	Вейгман и др.	ЛУЭ + СД	1 – 25	1	Cu, Mo	[18, 19]
Ок-Ридж, США	Маклин и др.	ЭСГ + СДПЭ	30 – 220	4	V, Fe, Ni, Au и др.	[20]
Лос-Аламос, США	Гласс и др.	ПЯВ + МР	до 10		Pm, Eu, Lu	[21 – 23]
Кейптаун, ЮАР	Брукс и др.	ЭСГ + МР	8 – 120		Mn, Ni, Nb, Au и др.	[24]
Стокгольм, Швеция	Бергквист и др.	ЭСГ +	20 – 8300	3,5	F, Mg, Al, Ni и др.	[25, 26]
Галф, США	Лопез и др.	ЛУЭ + БЖС	1 – 700	9,5	Gd, W, Re, Au	[27, 28]
Колумбийский университет, США	Хэвенс и др.	СНХ + МР	до нескольких кэв	1	Mn, In, Cu, Zr, Au	[29]

[a] ЭСГ – электростатический генератор (ускоритель Ван де Граафа), ЛУЭ – линейный ускоритель электронов, СНХ – синхротрон, ПЯВ – подземный ядерный взрыв, БЖС – большой жидкий сцинтиллятор, МР – детектор Моксона и Рея, СД – сцинтилляционный детектор Вейгмана, СДПЭ – сцинтилляционный детектор полной энергии.

Очень интересную информацию о механизме реакции может дать изучение спектров гамма-лучей захвата. Несмотря на то, что рассмотрение этой области исследований выходит за рамки настоящего доклада, уместно отметить возможности получения парциальных сечений, соответствующих переходам в определенные состояния конечного ядра, что позволяет оценить относительную роль статистического и прямого процессов. Измерения такого рода проводились во многих странах [25,31-34].

3. Метод активации

Несмотря на ряд ограничений по сравнению с методом регистрации мгновенного гамма-излучения (применимость к ограниченному кругу ядер, низкое разрешение в области нескольких кэв, необходимость монохроматических источников нейтронов и др.), метод активации широко применяется при измерениях сечений захвата, начиная от энергий нейтронов порядка 5-10 кэв, а в диапазоне выше 1 Мэв этот метод оказывается основным.

На протяжении многих лет в Физико-энергетическом институте в г. Обнинске под руководством проф. Стависского ведется комплексное изучение радиационного захвата быстрых нейтронов с применением различных методов исследований, в том числе и активационного [35-42]. Эти исследования проводятся на монохроматических нейтронах от реакции T(p,n) и Li(p,n), идущих на мишенях электростатистических ускорителей на 2,5 и 5 Мв. Все последние измерения проводились относительно сечения деления урана-235. По сравнению с прежними работами этой же группы, в последнее время была значительно улучшена методика измерений: регистрация бета-частиц торцевыми счетчиками была заменена регистрацией гамма-квантов сцинтилляционными и полупроводниковыми Ge-Li счетчиками.

Ряд работ активационным методом был проведен также в Институте физики АН УССР в г. Киеве [43].

Большой комплекс активационных измерений выполнен группой Гренча в Пало Альто (США). Разработанная ранее методика измерений путем сравнения активностей ванадиевой мишени ускорителя и исследуемого образца [44] была значительно улучшена (применен новый кристалл NaI(Tl) с более точной калибровкой эффективности, исключено присутствие посторонних материалов около образца и др.), и с ее помощью были проведены новые измерения сечений захвата для золота при энергии нейтронов 575 кэв [48]. Сечения захвата нейтронов золотом в интервале энергий от 0,14 до 1,22 Мэв были недавно измерены этой же группой другим методом, относительно $\sigma_f(^{235}U)$ и известных сечений для тепловых нейтронов [49]. Кроме этого, были проведены измерения и для ряда других элементов [45-47].

Абсолютное измерение сечения захвата для золота при энергии нейтронов 966 кэв было выполнено в Англии [50] с использованием калиброванного Na-Be источника и абсолютного бета-счета (ранее аналогичное измерение было проведено при E = 24,8 кэв [51]). Такое внимание к золоту говорит о том, что несмотря на неоднократно обсуждавшиеся и до сих пор остающиеся расхождения результатов отдельных измерений, многими экспериментаторами золото рассматривается в качестве одного из возможных стандартов при проведении относительных измерений. В частности, относительно золота измерялись сечения захвата для большого числа ядер на пучке квазимонохроматических нейтронов с энергией 2 кэв,

ТАБЛИЦА 2. НЕКОТОРЫЕ ИЗМЕРЕНИЯ СЕЧЕНИЙ ЗАХВАТА НЕЙТРОНОВ МЕТОДОМ АКТИВАЦИИ (1967-1969 гг.)

Место проведения измерений	Авторы работ	Интервал энергий (Мэв)	Исследованные элементы	Литература
Обнинск, СССР	Толстиков и др.	0,01 – 3,15	Mn, Cu, Ga, Ge, Se, Rb, Mo, Os и др.	[35 – 42]
Киев, СССР	Заикин и др.	0,18 – 3,1	Ti, V, Cu, W	[43]
Пало Альто	Гренч и др.	0,14 – 19,4	Na, Mn, Y, In, Ho, Au	[45 – 49]
Теддингтон, Англия	Робертсон и др.	0,966	Au	[50]
Айдахо, США	Шуман	0,002	Na, Mn, Co, Cu, Zr, Cd, Ta, Ir и др.	[52]
Карлсруэ, ФРГ	Кнолль и др.	0,03 и 0,064	Au	[53]
Ок-Ридж, США	Маклин и др.	0,01 – 0,2	Pb	[54]
Аргонн, США	Ступеджна и др.	0,005 – 17	V, Mn, Mo и др.	[55,56]
Варшава, Польша	Брзоско и др.	0,03 – 5,1	Ta	[57,58]
Дебрецен, Венгрия	Чикаи и др.	14,7	Na, Al, Sc, Ca, Ti, V, Mn, Y и др.	[59,60]
Алигарх, Индия	Чаубей и др.	0,024	Na, Mo и др.	[61,62]
Лахор, Пакистан	Квайм и др.	14,7	I	[63]

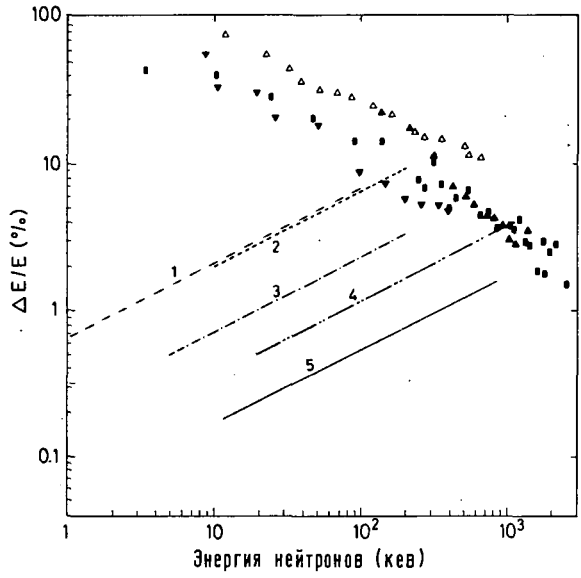

Рис. 4. Энергетическое разрешение при измерениях сечений радиационного захвата. Прямые линии показывают номинальное разрешение при измерениях методом времени пролета: 1 – Харуэлл (1968) 7,8 нсек/м [10], 2 – Карлсруэ (1966) 7 нсек/м [4], 3 – Карлсруэ (1969) 2,5 нсек/м [9], 4 – РПИ (1966) 1,3 нсек/м, 5 – РПИ (1969) 0,6 нсек/м [13].
Точками показано разрешение при измерениях методом активации: Δ – Харрис (1965); ▲ – Гренч (1969) [49], ▼ – Довбенко, Толстиков (1969) [42], ▮ – Ступеджиа (1968) [55].

полученных фильтрацией нейтронов из реактора MTR через Sc [52]. Сведения о некоторых других активационных измерениях приведены в табл. 2.

В качестве одного из итогов рассмотрения экспериментов по измерениям сечений захвата за последние годы можно отметить значительный прогресс в повышении энергетического разрешения применяемых методик, особенно метода времени пролета (рис. 4), в результате чего границы области неразрешенных резонансов значительно сдвинулись в сторону больших энергий.

3. ПОЛНОТА И ДОСТОВЕРНОСТЬ ДАННЫХ ПО СЕЧЕНИЯМ ЗАХВАТА

После Парижской конференции 1966 года было проведено и опубликовано большое количество экспериментальных работ по измерениям сечений радиационного захвата быстрых нейтронов, причем, как можно видеть по рис. 5, наибольшее внимание уделялось элементам, применяемым в реакторостроении или используемым в качестве стандартов. В результате этих работ получена весьма ценная информация, уточняющая имевшиеся ранее сведения об абсолютных значениях и энергетической зависимости сечений захвата для основных реакторных материалов. Характерным примером современной ситуации в области полноты информации по сечениям захвата может служить рис. 6. Из рассмотрения подобных рисунков можно заключить, что в настоящее время в области энергий до 1 Мэв, к которой относится подавляющее число запросов [1], общие представления

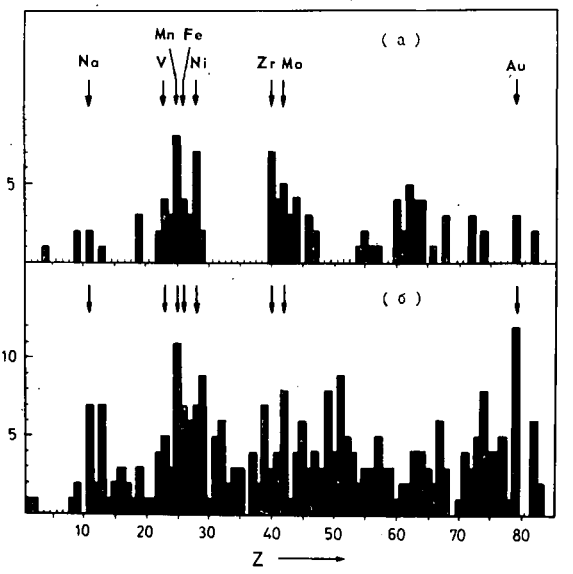

Рис. 5. Сравнение числа запросов [1] на сечения радиационного захвата нейтронов с энергиями выше 1 кэв (а) с числом экспериментальных работ, опубликованных за период 1967-1969 гг. (б).

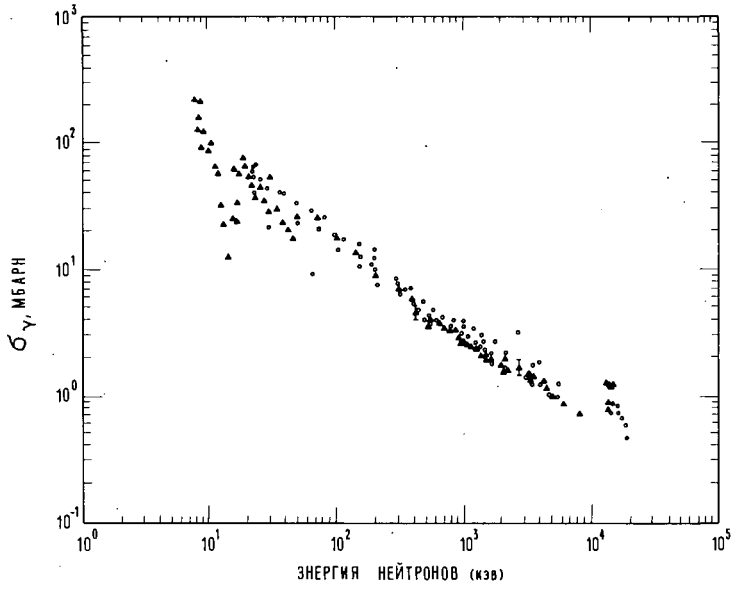

Рис. 6. Сечения радиационного захвата нейтронов для марганца. Светлые кружки – результаты измерений, опубликованных по 1966 г., черные треугольники – результаты измерений, опубликованных за период 1967-1969 гг.

о сечениях захвата имеются для всех элементов, находящих наиболее широкое применение в ядерных реакторах.

В то же время, реальная точность полученных данных еще весьма далека от желаемой. При измерениях как методом регистрации гамма-излучения, так и методом активации, сечение в конечном счете находится из соотношений типа:

$$\sigma_\gamma = \frac{N}{\Phi n \epsilon} C$$

где N – число зарегистрированных импульсов за вычетом фона, Φ – поток нейтронов, n – число ядер в образце, ϵ – полная эффективность регистрирующей установки (включая собственную эффективность детектора, геометрический фактор и т. п.) и C – коэффициент, учитывающий всевозможные поправки. Отсюда ясно, что предельная точность измерения сечений захвата определяется точностью, с которой известна каждая из этих пяти величин.

Очень часто для избежания трудностей, связанных с абсолютными измерениями потоков нейтронов, прибегают к так называемым относительным измерениям, при которых в одном и том же потоке измеряется отношение эффектов на образцах из исследуемого материала и стандарта. Чаще всего в качестве стандартов используются $\sigma_f(^{235}U)$, $\sigma_{n\alpha}(^{10}B)$, $\sigma_\gamma(^{197}Au)$, $\sigma_{n\alpha}(^{6}Li)$, $\sigma_\gamma(In)$, сечение рассеяния нейтронов протонами, или же для измерений потока применяются детекторы с постоянной чувствительностью типа длинного счетчика, позволяющие "привязаться" к известному значению сечения самого исследуемого изотопа при одной какой-то энергии. Комбинация использования такого известного сечения и стандарта позволяет исключить из расчетной формулы не только потоки нейтронов, но и эффективности счетных установок, однако при этом возникает необходимость знания абсолютных значений опорных сечений. Таким образом, проведение относительных измерений не открывает прин-

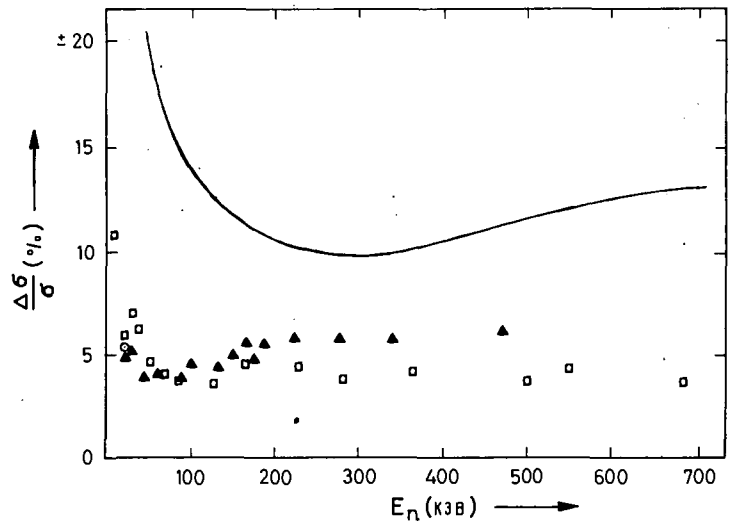

Рис. 7. Сравнение ошибок, указываемых авторами различных работ (отдельные точки с наблюдаемым разбросом $\sigma_x(^{197}Au)$ (сплошная линия).

ципиально новых путей повышения точности эксперимента, а лишь перекладывает трудности и ответственность за возможные ошибки на авторов работ, поставляющих данные по опорным сечениям, добавляя при этом к их ошибкам свои собственные.

Анализ возможных погрешностей при проведении измерений содержится практически в каждой экспериментальной работе, а некоторые исследования посвящались этому вопросу специально (см., например, [64]). Несмотря на некоторые различия в оценке роли отдельных факторов, в большинстве таких работ делается вывод о возможности в настоящее время проводить измерения сечений радиационного захвата нейтронов в области десятков сотен кэв, по крайней мере, для некоторых ядер с точностью до 3-5%. Именно такую точность указывают авторы ряда некоторых последних работ по измерениям сечений захвата для золота (см. рис. 7). Однако, к сожалению, очень часто различия данных из разных работ оказываются значительно больше указываемых экспериментальных ошибок, что можно видеть на том же рис. 7.

Вряд ли было бы возможно в одной работе пытаться решить все проблемы, связанные с отысканием причин таких расхождений. Тем не менее, стоит, по крайней мере, назвать некоторые из них.

1. Погрешности в стандартных сечениях

При проведении относительных измерений экспериментатор обычно выбирает наиболее удобный для себя стандарт и применяет значения сечений для этого стандарта из наиболее достоверной, с его точки зрения, работы вместе с указанными там ошибками. Но кто может поручиться за достоверность этих ошибок? На примере золота, часто используемого в качестве стандарта, мы только что видели, сколь велик разброс данных из разных работ. То же относится и к другим стандартам. Всем известны, например, драматические изменения сечений деления урана-235 за последние годы. Ситуация усугубляется еще и тем, что использование в разных работах различных стандартов, не связанных друг с другом достаточно надежными прямыми измерениями, может привести к сильному разбросу получаемых результатов и одновременно сделать невозможным их объективное сравнение, побуждая тем самым оценщиков к проявлениям субъективного подхода и волюнтаризма.

2. Погрешности при введении поправок

Большинство поправок при обработке результатов измерений определяется достаточно надежно, их абсолютная величина часто оказывается небольшой, благодаря чему они не могут внести существенных непредвиденных ошибок в получаемые сечения. Однако, существует один эффект, который может по-разному проявляться в различных экспериментах для одних и тех же ядер и при одних и тех же энергиях нейтронов, и расчет которого до сих пор вызывает существенные трудности: это – эффект так называемой резонансной самоэкранировки сечений. Величина этого эффекта существенно зависит от толщины и геометрии образцов и от присутствия в них посторонних веществ, поэтому неправильный учет данного эффекта может привести к значительному различию результатов из разных работ. Анализу эффекта резонансной самоэкранировки уделялось немало внимания [65-68], однако и поныне этот эффект причиняет экспериментаторам немало хлопот.

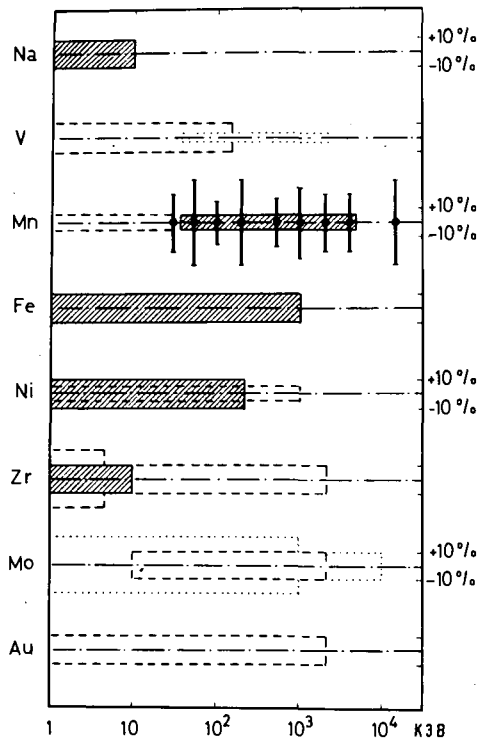

Рис. 8. Требуемая точность данных по сечениям захвата для восьми из наиболее важных для реакторостроения элементов [1]. Сплошными линиями со штриховкой показаны запросы с приоритетом [1], штрихами – с приоритетом [2] и точками – с приоритетом [3]. Для марганца вертикальными линиями отмечен разброс экспериментальных данных, приведенных на рис. 6.

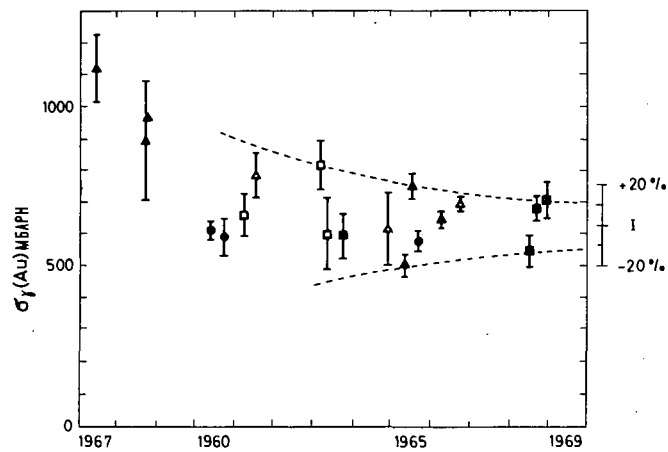

Рис. 9. Изменения разброса значений $\sigma_\gamma(^{197}Au)$ при энергии нейтронов 24,5 ± 0,5 кэв со временем. Треугольники – активационные измерения, квадраты – измерения с регистрацией гамма-лучей, кружки – измерения в сферической геометрии. Черными значками показаны результаты измерений непосредственно при указанной энергии, светлыми значками – результаты пересчета данных, полученных при других энергиях (главным образом при 30 кэв).

Наконец, даже в наиболее тщательно выполненных работах самых опытных экспериментаторов нельзя полностью исключить возможность появления прямых ошибок. Поэтому реально достигнутую точность данных по сечениям захвата разумно оценивать не по ошибкам, указываемым в отдельных экспериментальных работах, и даже не по ошибкам, получающимся при перенормировках и оценках старых работ, а по наблюдаемому разбросу значений сечений, полученных различными методами измерений [69]. Для золота этот разброс сейчас в области 30 кэв составляет около ±10%, для многих других элементов – еще больше, что значительно хуже точности, требуемой расчетчиками реакторов (см. рис. 8). Однако вполне можно согласиться с Коксом [70] в том, что, если несколько лет назад ситуация выглядела довольно-таки безнадежно, то сейчас появились некоторые основания для оптимизма, что подтверждается, в частности, рис. 9.

4. ЭКСПЕРИМЕНТ И ТЕОРИЯ

Данный доклад посвящен экспериментальным аспектам проблемы сечений радиационного захвата быстрых нейтронов. Однако полезно, по крайней мере, перечислить основные моменты, по которым экспериментаторам и теоретикам приходится соприкасаться при анализе получаемых данных и планировании новых опытов.

1. При энергиях нейтронов ниже 1-2 Мэв энергетическая зависимость усредненных сечений захвата обычно удовлетворительно описывается в общих чертах статистической теорией ядерных реакций. При этом в процессе подгонки теоретических кривых под экспериментальные данные открывается возможность определить вклад в величину сечения захвата каждой парциальной волны падающих нейтронов, соответствующей определенному значению орбитального момента ℓ, а также получить целый ряд весьма важных параметров типа S_0, S_1, S_2, S_γ и a (рис. 10). Специальный метод определения силовых функций d-нейтронов для четно-четных ядер по сбросам сечений в районах уровней 2^+ исходных ядер был предложен в работе [71]. Следует отметить, что некоторые из перечисленных величин, и в частности – S_2, невозможно или очень трудно измерить непосредственно в области разрешенных резонансов. Однако, несмотря на относительное благополучие, даже в этой области энергий периодически отмечались отдельные сюрпризы. Так, например, сообщалось, что используя обычный метод Мольдауэра [72], не удалось воспроизвести наблюдаемую энергетическую зависимость сечений захвата ряда элементов выше 100 кэв, несмотря на разумные вариации параметров плотности уровней, различный выбор параметров оптического потенциала и учет эффекта сильной связи между упругим и неупругим каналами [73]. Теорию и эксперимент удалось согласовать лишь при искусственном допущении быстрого уменьшения полной радиационной ширины с ростом энергии возбуждения составного ядра. На необходимость введения уточнений и проводимые расчеты указывает также результат недавних работ по обнаружению различия значений силовых функций для s-нейтронов, соответствующих двум возможным значениям спина составного ядра [74]. Для уточнения теоретических представлений и методов расчета сечений в этой области энергий желательно иметь более полные и надежные данные об энергетической зависимости сечений захвата для разных ядер.

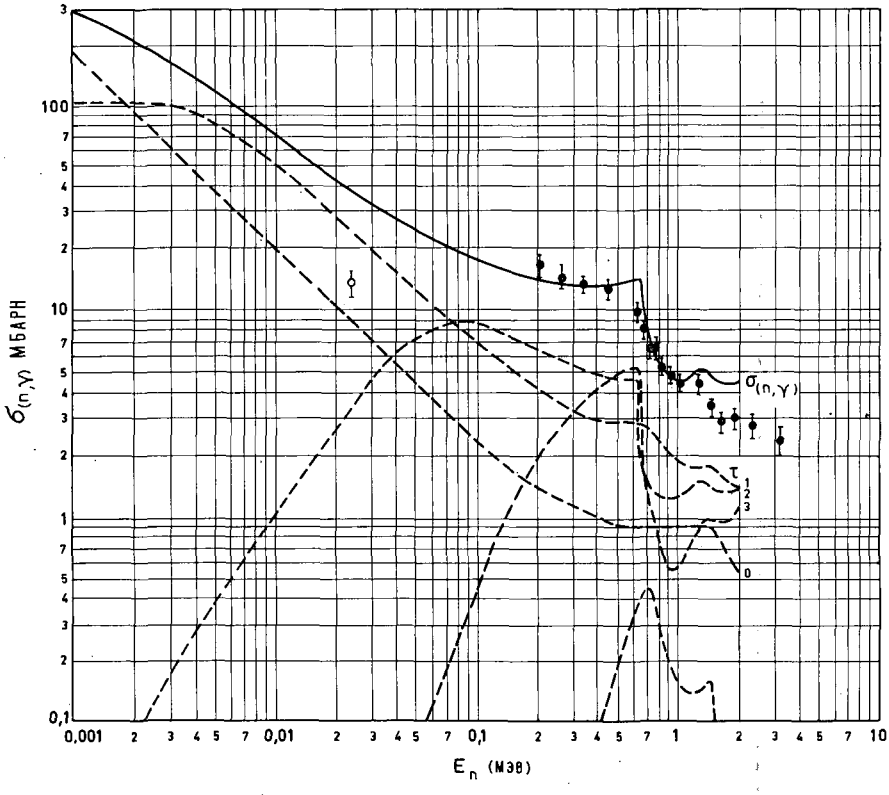

Рис. 10. Анализ данных по $\sigma_\gamma(^{80}Se)$ с помощью статистической теории [37].

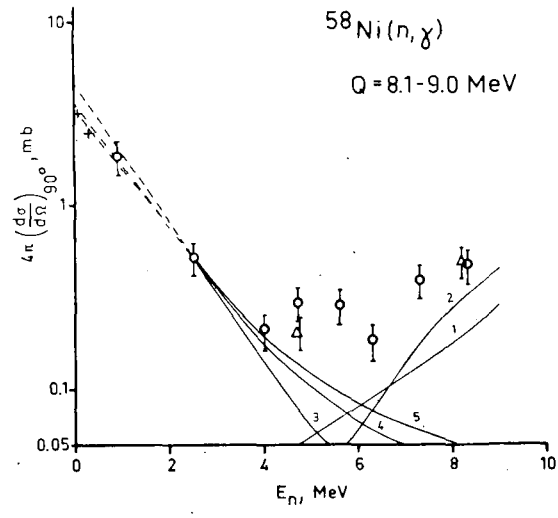

Рис. 11. Сравнение экспериментальных данных по $\sigma_\gamma(^{58}Ni)$ с расчетами по теории полупрямого захвата (1,2) и по теории составного ядра (3,4,5) [25].

2. Выше 2-3 Мэв расчеты в рамках статистической теории не дают удовлетворительных результатов, что связано, главным образом, с двумя причинами: отсутствием достаточно полной информации по параметрам возбужденных уровней исходных ядер и вступлением в игру новых механизмов реакции, которые с ростом энергии быстро становятся превалирующими. Возможность использования теории полупрямого захвата [75,76] для описания сечений в области энергий 6-8 Мэв с учетом спин-орбитального взаимодействия продемонстрирована, в частности, в работах группы Бергквиста [25] (рис.11). Крайняя скудность экспериментальных данных при энергиях нейтронов выше 7-8 Мэв в значительной мере задерживает дальнейшее развитие представлений о механизме радиационного захвата в этом интевале энергий. Как уже отмечалось, очень ценные сведения о прямых и полупрямых процессах может дать изучение спектров гамма-лучей захвата [85,86], однако обсуждение этого вопроса выходит за рамки данного доклада.

3. Интересные сведения можно ожидать также от сравнения экспериментальных и теоретических данных по энергетической зависимости отношений вероятностей переходов на основной и первые возбужденные уровни конечного ядра, которые обычно называются изомерными отношениями. Измерение и теоретический анализ изомерных отношений проводились в последние годы во многих лабораториях, и в частности – в Физико-энергетическом институте [37,47,77,78].

4. Наконец, весьма интересная информация, существенно дополняющая сведения, получаемые при исследовании реакции (n,γ), была в последние годы приобретена при изучении обратной реакции (γ,n). В работе [79] было показано, что изучение спектров нейтронов при фотоядерных реакциях, идущих при небольших превышениях энергии фотонов над порогом, открывает возможность исследования тех же самых уровней выше энергии связи нейтрона, которые обычно исследуются по резонансам, наблюдаемым при радиационном захвате нейтронов. При этом, исследование реакции (γ,n) обладает рядом специфических преимуществ. Так, например, оно позволяет непосредственно измерить парциальную ширину Γ_γ^0, соответствующую прямому переходу из возбужденного в основное состояние ядра; изучение реакции (γ,n) на ядре с массовым числом A эквивалентно изучению радиационного захвата нейтронов ядром A-1, которое может оказаться радиоактивным, и тогда прямое измерение сечения захвата для него практически невозможно; изучение спектров нейтронов при несколько больших энергиях фотонов открывает возможность с высоким энергетическим разрешением измерять спектры нейтронов, соответствующих переходам на первое возбужденное состояние конечного ядра, что эквивалентно захвату нейтронов возбужденным ядром, наблюдать который непосредственно также невозможно. Это, в свою очередь, позволяет получать сведения о ядерных уровнях с новыми спиновыми параметрами, не проявляющихся при радиационном захвате. Некоторые из отмеченных возможностей были в последние годы использованы в работах Лоуренсовской лаборатории (см., например, [80]), а также в других местах [84]. Далее, значительное повышение энергетического разрешения при измерениях сечений фотоядерных реакций, достигнутое, например, группой Московского университета на основе использования оригинального и высокоэффективного способа автоматической смены энергии [81] позволило получить детальные сведения о структуре гигантского резонанса для средних и тяжелых ядер, которые могут быть использованы для расчета

сечений радиационного захвата в наиболее трудной для измерений и наиболее интересной для развития теории полупрямых процессов области энергий.

Обычно от теории ожидают возможности предсказания величин сечений в случаях отсутствия экспериментальных данных. Широко известными примерами практических потребностей такого рода являются оценка захвата нейтронов радиоактивными осколками деления в ядерных реакторах [82] и анализ роли захвата в теории происхождения элементов [83]. Сравнение выполненных расчетов с имеющимися экспериментальными данными в области энергий до 2-3 Мэв показывает, что в настоящее время, даже в тех случаях, когда о свойствах ядра совсем ничего не известно, с помощью различных систематик можно получать усредненные сечения захвата с отклонением от их истинных значений не более чем в два-три раза.

5. ЗАКЛЮЧЕНИЕ

На основании изложенного, по нашему мнению, можно сделать следующие выводы:

1. В настоящее время по всем наиболее важным реакторным материалам имеется основная информация об энергетической зависимости сечений радиационного захвата нейтронов до энергий 1-2 Мэв, однако точность этой информации остается пока ниже требуемой. Выше 2-3 Мэв сведений о сечениях захвата значительно меньше, а выше 5-6 Мэв имеются лишь отдельные точки для некоторых ядер (не считая данных для 14 Мэв); правда, эта область энергий имеет значительно меньшее значение для реакторов.

2. Реальная достоверность имеющихся сведений о ядерных константах определяется наблюдаемым разбросом точек из различных работ, поэтому желательно проведение новых экспериментов с применением различных методов измерений и последующим сравнением результатов с целью анализа возможных причин наблюдаемых расхождений и их устранения.

3. Для облегчения оценок результатов различных экспериментов и их последующих перенормировок было бы полезно выбрать один или, по крайней мере, ограниченное число рекомендуемых стандартов, хорошо пронормированных относительно друг друга. Такой стандарт должен удовлетворять ряду физических и технологических требований, которые могут быть обсуждены уже сегодня.

4. Ощущается необходимость в разработке надежного и универсального метода введения поправок на эффект резонансной самоэкранировки сечений для различных вариантов проведения экспериментов (толстые и тонкие образцы, цилиндрическая, сферическая и плоская геометрия и т. п.).

5. Представляется весьма перспективным комплексный подход к исследованиям процессов (n,γ) и (γ,n), в связи с чем должны приветствоваться любые контакты между соответствующими группами специалистов, включая специальные совещания по обсуждению общих проблем.

В заключение мне очень приятно выразить искреннюю признательность физикам из различных стран – Бергквисту, Блоку, Вейгману, Гренчу, Дэви, Компе, Рею, Ташеку, Толстикову, Френеру, Шмидту и другим, приславшим мне весьма ценную информацию для данного доклада, а также поблагодарить проф. Стависского за полезные обсуждения и советы.

ЛИТЕРАТУРА

[1] RENDA, A Compilation of Needed Neutron Data, Vienna, 1968.
[2] БЕЛАНОВА, Т.С. и др., Атомная энергия 19 (1965) 3.
[3] SCHMITT, H.W., COOK, C.W., Nucl. Phys. 20 (1960) 202.
[4] KOMPE, D., Nuclear Data for Reactors, IAEA, Vienna, 1 1967, p.513.
[5] BECKURTS, K.H. et al., Fast Reactor Physics. Vienna, 1 1968, p.67.
[6] POENITZ, W.P., KOMPE, D., MENLOVE, H.O., J. Nucl. En. 22 (1968) 505.
[7] KOMPE, D., Nucl. Phys. A133 (1969) 513.
[8] KOMPE, D., ERNST, A, FRÖHNER, F.H., Nucl.Phys. A141 (1970) 602.
[9] FRÖHNER, F., Частное сообщение, 1970.
[10] MOXON, M.C., Thesis for M.Sc. AERE, Harwell, 1968.
[11] ASGHAR, M., CHAFFEY, C.M., MOXON, M.C., Nucl.Phys. A108 (1968) 535.
[12] MOXON, M.C., HUGHES, M.B., AERE-PR/NP 16 (1969) 10.
[13] BLOCK, R.C., Сообщение на 2-м совещании МКЯД в Брукхэвене, 1969.
[14] BLOCK, R.C. et al., Частные сообщения, 1968-1969 гг.
[15] BARTOLOME, Z.M. et al., Nucl.Sci.Eng. 37 (1969) 137.
[16] HOCKENBURY, R.W. et al., Phys.Rev. 178 (1969) 1746.
[17] WEIGMANN, H., CARRARO, G., BÖCKHOFF, K.H., Nucl.Instr.Meth. 50 (1967) 265.
[18] WEIGMANN, H., SCHMID, H., Nucl.Phys. 104 (1967) 513.
[19] WEIGMANN, H., WINTER, J., Z.Physik 213 (1968) 411.
[20] MACKLIN, R.L., GIBBONS, J.H., Phys.Rev. 159 (1967) 1007.
[21] HARLOW, M.V. et al., Neutron Cross Section and Technology, Washington 2 1968, p.837.
[22] BEERY, J.G., CODDING, J.W., Bull.Am.Phys.Soc. 13 (1968) 1391.
[23] GLASS, N.W. et al., Частное сообщение, 1969.
[24] SPITZ, L.M., BARNARD, E., BROOKS, F.D., Nucl.Phys. A121 (1968) 655.
[25] BERGQVIST, I. et al., Nucl.Phys. A120 (1968) 161.
[26] NYSTRÖM, G., LUNDBERG, B., BERGQVIST, I., Частное сообщение, 1970.
[27] FRIESENHAHN, S.J. et al., J.Nucl.Energy 22 (1968) 191.
[28] LOPEZ, W.M. et al., Частное сообщение, 1968.
[29] RAHN, F. et al., Частное сообщение, 1968.
[30] КОНКС, В.А., ПОПОВ, Ю.П., ФЕНИН, Ю.И., Ядерная физика 7 (1968) 493.
[31] BIRD, J.R. et al., Phys.Lett. 27B (1968) 638.
[32] ALLEN, B.J. et al., Nucl.Phys. 122 (1968) 220.
[33] AUCHAMPAUGH, G.F., Bull.Am.Phys.Soc. 13 (1968) 893.
[34] WASSON, O.A. et al., Phys.Rev. 176 (1968) 1314.
[35] ТОЛСТИКОВ, В.А. и др., Атомная энергия 23 (1967) 151.
[36] ДОВБЕНКО, А.Г. и др., Атомная энергия 23 (1967) 566.
[37] ТОЛСТИКОВ, В.А., КОРОЛЕВА, В.П., КОЛЕСОВ, В.Е., Атомная энергия 24 (1968) 187.
[38] ТОЛСТИКОВ, В.А., КОРОЛЕВА, В.П., Атомная энергия 24 (1968) 576.
[39] ДОВБЕНКО, А.Г. и др., Атомная энергия 25 (1968) 529.
[40] КОЛЕСОВ, В.Е. и др., Англо-советский семинар в Дубне, 1968.
[41] ДОВБЕНКО, А.Г. и др., Атомная энергия 26 (1969) 67.
[42] ДОВБЕНКО, А.Г. и др., Атомная энергия 27 (1969) 406.
[43] ЗАИКИН, Г.Г. и др., Атомная энергия 23 (1967) 67; 25 (1968) 526.
[44] HARRIS, K.K. et al., Nucl.Phys. 69 (1965) 37.
[45] GRENCH, H.A. et al., Nucl.Phys. A94 (1967) 157.
[46] MENLOVE, H.O., COOP, K.L., GRENCH, H.A., Phys.Rev. 163 (1967) 1299.
[47] GRENCH, H.A., MENLOVE, H.O., Phys.Rev. 165 (1968) 1298.
[48] GRENCH, H.A., VAUGHN, F.J., Частное сообщение, 1968.
[49] GRENCH, H.A. et al., Частное сообщение, 1970.
[50] ROBERTSON, J.C. et al., J.Nucl.Energy 23 (1969) 205.
[51] RYVES, T.B. et al., J.Nucl.Energy AB20 (1966) 825.
[52] SCHUMAN, R.P., Частное сообщение, 1969.
[53] KNOLL, G.F., PÖNITZ, W.P., J.Nucl.Energy 21 (1967) 643.
[54] MACKLIN, R.L., GIBBONS, J.H., Phys.Rev. 181 (1969) 1639.
[55] STUPEGIA, D.C. et al., J.Nucl.Energy 22 (1968) 267.
[56] DUDEY, N.D., HEINRICH, R.R., MADSON, A.A., J.Nucl.Energy 23 (1969) 443.
[57] BRZOSKO, J.S. et al., Acta Phys.Pol. 35 (1969) 417.
[58] BRZOSKO, J.S. et al., Nucl.Phys. A123 (1969) 603.
[59] CSIKAI, J. et al., Nucl.Phys. A95 (1967) 229.
[60] PETO, G., MILIGY, Z., HUNYADI, I., J.Nucl.Energy 21 (1967) 797.

[61] HASAN, S.S., CHAUBEY, A.K., SEHGAL, M.L., Nuovo Cim. 58, 2B (1968) 402.
[62] CHAUBEY, A.K., SEHGAL, M.L., Nucl.Phys. A117 (1968) 545.
[63] QAIM, S.M., EJAZ, M., J.Inorg.Nucl.Chem. 30 (1968) 2577.
[64] RAE, E.R., Англо-советский семинар в Дубне, 1968. Доклад UK/21.
[65] DRESNER, L., Nucl.Instr.Meth. 16 (1962) 176.
[66] АБАГЯН, Л.П. и др., "Групповые константы для расчета реакторов", М., 1964.
[67] BOGART, D., Nuclear Data for Reactors, IAEA, Vienna 1 1967, p.503.
[68] MILLER, L.B., PÖNITZ, W.P., Nucl.Sci.Eng. 35 (1969) 295.
[69] АБРАМОВ, А.И. и др., Nuclear Data for Reactors, Vienna 1 1967, p.459.
[70] COX, S.A., Neutron Cross Sections and Technology. Washington 2 1968, p.701.
[71] КОНОНОВ, В.Н., Ядерная физика 5 (1967) 129.
[72] MOLDAUER, P.A., Rev.Mod.Phys. 36 (1964) 1079.
[73] FRICKE, M.P., LOPEZ, W.M., Частное сообщение, 1969.
[74] NEWSTEAD, C.M. et al., Частное сообщение, 1969.
[75] BROWN, G.E., Nucl.Phys. 57 (1964) 339.
[76] CLEMENT, C.F., LANE, A.M., ROOK, J.R., Nucl.Phys. 66 (1965) 273.
[77] PÖNITZ, W.P., Частное сообщение, 1968.
[78] PAULSEN, A., Z.Physik 205 (1967) 226.
[79] BOLLINGER, L.M., Neutron Cross Section Technology. Washington 2 1966, p.1064.
[80] BOWMAN, C.D., SIDHU, G.S., BERMAN, B.L., Phys.Rev. 163 (1967) 951.
[81] ИШХАНОВ, Б.С. и др., Изв. АН СССР, сер. физ. 33 (1969) 2074.
[82] BENZI, V., Neutron Cross Sections and Technology. Washington 1 1968, p.311.
[83] ШОРИН, В.С., КАПЧИГАШЕВ, С.П., КОЛЕСОВ, В.Е., Ядерная физика 6 (1967) 769.
[84] BROOMHALL, G.J., BIRD, J.R., Nucl.Phys. A121 (1968) 329.
[85] Dinter. Nucl. Phys. A111 (1968) 360.
[86] CVELBAR, F. et al., Nucl.Phys. A130 (1969) 401.

MEASUREMENTS OF CROSS-SECTIONS FOR THE RADIATIVE CAPTURE OF 1-keV TO 1-MeV NEUTRONS BY Mo, Rh, Gd, Ta, W, Re, Au AND ^{238}U *

M.P. FRICKE, W.M. LOPEZ,† S.J. FRIESENHAHN, A.D. CARLSON, D.G. COSTELLO

Gulf General Atomic Incorporated,
San Diego, Calif.,
United States of America

Abstract

MEASUREMENTS OF CROSS-SECTIONS FOR THE RADIATIVE CAPTURE OF 1-keV TO 1-MeV NEUTRONS BY Mo, Rh, Gd, Ta, W, Re, Au AND ^{238}U.

Neutron average capture cross-sections have been measured for eight elements in the energy range 1 keV to 1 MeV with a neutron time-of-flight spectrometer consisting of an electron-linear-accelerator pulsed-neutron source, a 230-metre evacuated neutron flight path, and a large liquid scintillator to detect the capture γ-rays. The intensity and energy dependence of the incident neutron flux were monitored during the capture measurements with ^{3}He-gas proportional counters calibrated against other counters containing boron tri-fluoride and methane. The measured energy variation of the neutron flux is, thus, based upon the cross-section for the $^{10}B(n, \alpha_0 + \alpha_1)^{7}Li$ reaction at neutron energies below 80 keV, and upon the n+p scattering cross-section at energies above 80 keV. The measurements extend to very low energies (~ 2 eV), and absolute capture cross-sections were obtained by normalization to the observed capture areas of resolved resonances. In most instances, a "saturated" resonance was available, which provides a normalization that does not depend strongly upon resonance parameters. These measurements yield a set of radiative capture cross-sections which span an exceptionally large neutron-energy interval with a relative accuracy of about 10% over the full range.

1. INTRODUCTION

Radiative capture cross sections for neutrons of energy 1-1000 keV are known to be very important in determining the performance and economy of fast-breeder reactor systems. They are also of considerable interest in establishing statistical properties of nuclei at high excitation energies and for calculations of heavy-element nucleosynthesis in studies of nuclear astrophysics.

Measurements of capture cross sections at these energies have been made in a number of different ways, using different types of neutron sources, different methods to detect the capture events and incident neutrons, and different schemes to establish both the normalisation of the

* Work supported in part by the U.S. Atomic Energy Commission and by the U.S. National Aeronautics and Space Administration.

† Present address: University of California at San Diego, La Jolla, California 92037, USA.

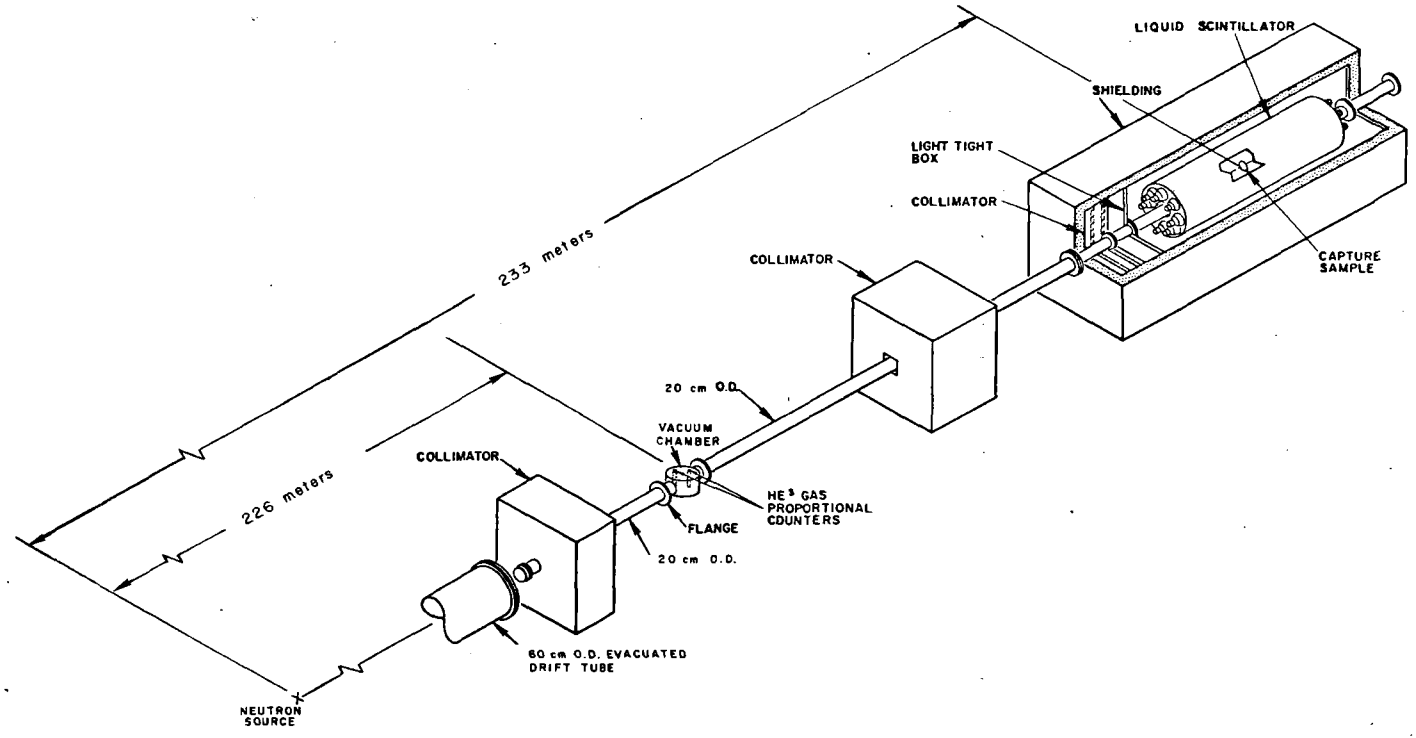

FIG. 1. Facility for capture cross-section measurements.

cross section and the shape of the excitation function. Previous capture data from any one measurement have spanned only a portion of the neutron energy region 1-1000 keV, and the results of different measurements have been determined relative to several different standard neutron cross sections. When separate data sets have energies in common, discrepancies of 20-50% in the cross-section values are often observed. In the energy region ~100 keV - 1 MeV it is particularly difficult to accurately establish the incident neutron flux relative to a well-known, primary standard cross section. Capture data for gold in this region that have been based on the ^{235}U fission cross section of Ref. [1] or [2] have tended [3] to be consistently higher than results normalised by other means. The data above 100 keV are also relatively sparce and have been obtained almost exclusively from measurements made with van de Graaff accelerators. These energies are above those covered by lead slowing-down spectrometers, and previous measurements made with electron linear accelerators have been confined to neutron energies below 200 keV.

In the present paper we describe measurements of capture cross sections which have reduced a number of the uncertainties involved in some of the previous data. The present measurements yield absolute average capture cross sections for eight heavy elements at continuous neutron energy intervals over the region ~ 1-1000 keV. The excitation functions are normalised directly to low-energy (eV) resonances, and their shapes above 80 keV are based directly on the well-known hydrogen scattering cross section. A theoretical interpretation of these and other recent data is presented in the following paper (CN-26/44).

2. EXPERIMENT

Time-of-flight measurements were made with short bursts of photoneutrons produced by bombarding a tungsten-alloy target with 45-MeV electrons from the Gulf General Atomic linear accelerator. The electron target is surrounded by a cylinder of uranium or lead to moderate the neutrons by inelastic scattering and also to shield the detection apparatus from bremsstrahlung. The neutrons are slowed further in a 2.5-cm slab of polyethylene, and a ^{10}B filter is used to prevent overlap of very low-energy neutrons produced from different accelerator bursts.

The neutrons traverse an evacuated flight path containing the collimators and anti-scattering baffles illustrated in Fig. 1. The capture sample is located 230 metres from the neutron-producing target at the centre of a large liquid scintillator used to detect the capture gamma rays. During a capture experiment, the incident neutron flux is monitored by sampling the outer edge of the neutron beam with two ^{3}He gas proportional counters located ahead of the final collimators shown in Fig. 1. This portion of the neutron beam is not viewed by the capture sample. Determinations of the neutron flux and capture γ-ray yield are discussed further in this Section.

The samples used for the capture measurements were all high-purity metal disks approximately 11 cm in diameter and ranged in thickness from 0.1 to 0.25 cm. Except for the ^{238}U sample which was composed of depleted uranium (99.8% ^{238}U), the isotopic composition of the samples was that of the naturally occurring element.

2. 1. Neutron flux

The energy distribution of the incident neutron flux is determined by the time history of counts from the ^{3}He gas proportional counters. The ^{3}He counter was a convenient monitor for use during the capture measurements since it has a high detection efficiency and adequate timing resolution over most of the neutron energy region of interest here. The relative efficiency of the ^{3}He counters for detecting neutrons of different energies was calibrated above 80 keV against that of a methane (CH_4)-filled proportional counter and, at lower energies, against

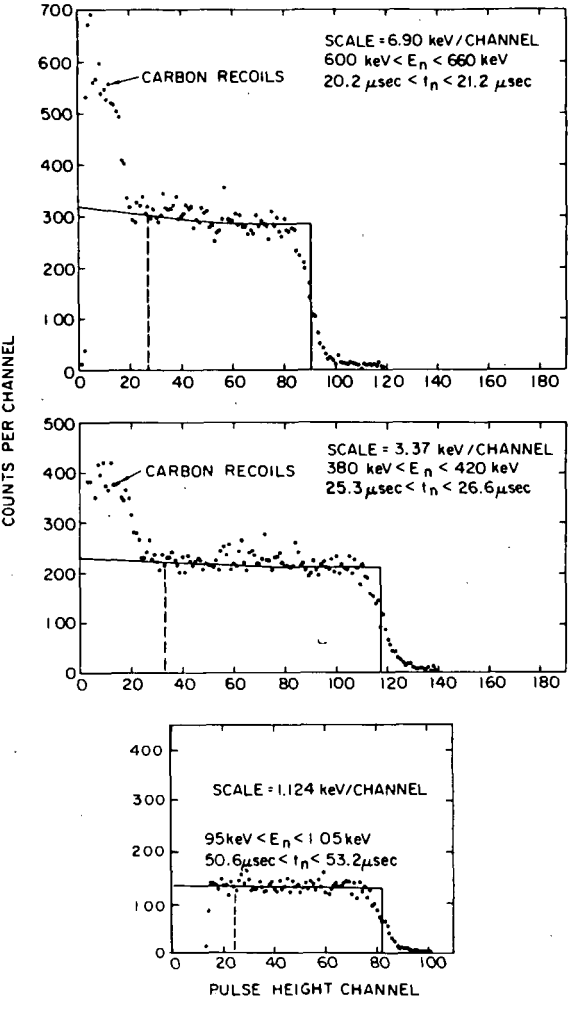

FIG. 2. Proton-recoil pulse-height spectra from methane-gas proportional counter. The solid curves are the results of Monte-Carlo calculations [7], and the broken lines denote the threshold pulse heights described in the text.

that of another gas counter filled with $^{10}BF_3$. Consequently, the measured energy variation of the neutron flux, and hence the shape of the excitation function for radiative capture, is based upon the cross section* for the $^{10}B(n, \alpha_0 + \alpha_1\gamma)^7Li$ reaction at neutron energies below 80 keV and upon the n+p scattering cross section [4] at higher energies. These cross sections are widely considered to be the best standards presently available for partial neutron cross-section measurements at these energies.

To supplement the flux data obtained from the ^3He monitor counters, separate measurements of the flux were made either before or after a capture determination with the methane counter placed in the centre of the neutron beam near the liquid scintillator. These measurements have an overall resolution of 3 ns/m (about four times better than the ^3He measurements) and provide more detailed information on the neutron spectrum at higher energies. The ^3He monitors were also used during the measurements with the methane counter to verify that the flux spectrum was the same as that observed during the capture measurements. The flux data from the methane counter were used at energies above 80 keV.

For all three types of proportional counters used in this work, the corrections made for backgrounds, self-shielding and multiple scattering in the gas, transmission through end windows, and wall-scattering and misalignment effects are well understood and were kept small. The active volume of the counters and their timing resolution were determined experimentally. Full details of the construction and instrumentation of these counters are given in Ref. [5].

The methane counter was implemented for time-of-flight measurements by using a computer-based data acquisition system [6] to record both the pulse height and neutron flight time associated with each event in the counter. Pulse-height spectra from the methane counter for four flight-time intervals are shown in Fig. 2. The solid curves in the figure are the results of Monte Carlo calculations [7] of the proton-recoil spectrum which were made to extrapolate the spectra to zero pulse height. The spectrum for a given interval of flight time is summed only above a threshold pulse height (see broken lines in Fig. 2) taken at three-tenths of the maximum proton-recoil pulse height, which eliminates the smaller pulses due to ^{12}C recoils. The relative efficiency of the counter, which then varies little with incident neutron energy, is established directly from the fraction of the proton-recoil spectrum that lies above the threshold pulse height. The implementation of the ^3He and $^{10}BF_3$ counters is more straightforward since a fixed electronic threshold can be used that will eliminate ^3He and ^{10}B recoils, respectively, at all neutron energies of interest. Some two-parameter (pulse-height and

*This cross section was taken to vary as (1/v) from the thermal value [2] to 80 keV.

time-of-flight) data were also taken for the ^{3}He counter to determine the ^{3}He(n, p)T cross section relative to the ^{3}He total cross section in the neutron energy region 0.3 to 1.16 MeV [8].

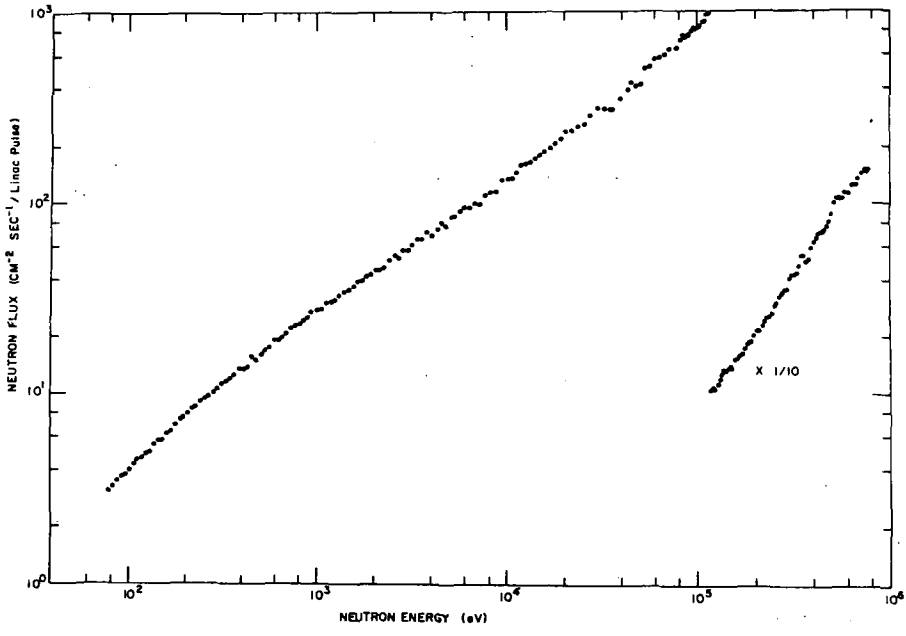

FIG. 3. Neutron flux per unit time of flight measured with ^{3}He and methane proportional counters.

Neutron flux data with an overall uncertainty of about 5% in relative intensity were obtained routinely over the neutron energy region ~100 eV - 1 MeV. A typical time-of-flight flux spectrum is shown in Fig. 3. Although absolute flux data are illustrated in this figure, only the relative energy variation (or time history) of the incident flux is required in our experiment. Normalisation of the radiative capture yields is discussed in the next Section.

2.2. Capture yields

For most of the data reported here, a 600-litre liquid scintillator viewed by photomultipliers (illustrated in Fig. 1) was used to detect the capture gamma rays. This scintillator has recently been enlarged to a volume of 2400 ℓ to improve the signal-to-background ratio by increasing the efficiency for summing capture γ-ray cascades. This improvement was particularly important in the measurements for ^{238}U due to the low excitation energy (~ 4.8 MeV) of the compound nucleus. Both scintillator configurations used in this work were similar in construction to that described in Ref. [9].

The photomultiplier outputs were summed to produce a pulse proportional to the total γ-ray energy deposited in the liquid. A pulse-height window discriminator was normally set to accept events depositing

a total energy in the range 4 to 10 MeV, and the time history of accepted events was stored by a multi-channel analyser. In recent measurements made with the enlarged scintillator, three types of data were obtained simultaneously. Two data channels used different lower limits (3.5 and 4.5 MeV) for the discriminator and provided a useful check on the variation of the detection efficiency with neutron energy (see below). In the third data channel a 3.5-MeV level was used, but a coincidence was required which assured that at least 1 MeV of energy was deposited in each of the two optically isolated halves of the scintillator. This requirement selects many of the multi-gamma cascades which are usually produced by capture and eliminates many single-gamma events that are usually associated with background. This increased the signal-to-background ratio by about one order of magnitude, and comparison of the data taken for several samples both with and without the coincidence requirement has failed to reveal any dependence on the γ-ray cascade mode (or energy spectrum) introduced by the requirement. Moreover, the γ-ray energy spectrum is not expected to vary markedly with neutron energy when the measurement averages over many resonances of the compound nucleus. Figure 4 illustrates the very acceptable signal-to-background ratio achieved with the coincidence mode for ^{238}U, which has the poorest signal-to-background ratio of the nuclei measured here. Gain shifts in each data channel were checked by verifying a constant (flight-time independent) difference of counts between capture yields measured with and without a ^{24}Na γ-ray source placed near the sample but outside the neutron beam. This difference (the count rate from the ^{24}Na source) is very sensitive to gain shifts since the total γ-ray energy from ^{24}Na is close to the sum-signal discriminator threshold.

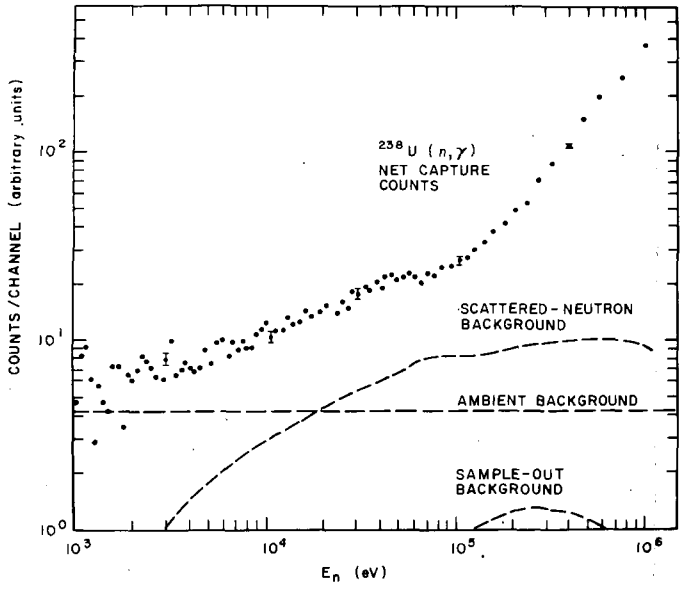

FIG. 4. Time-of-flight neutron capture data and γ-ray backgrounds described in the text.

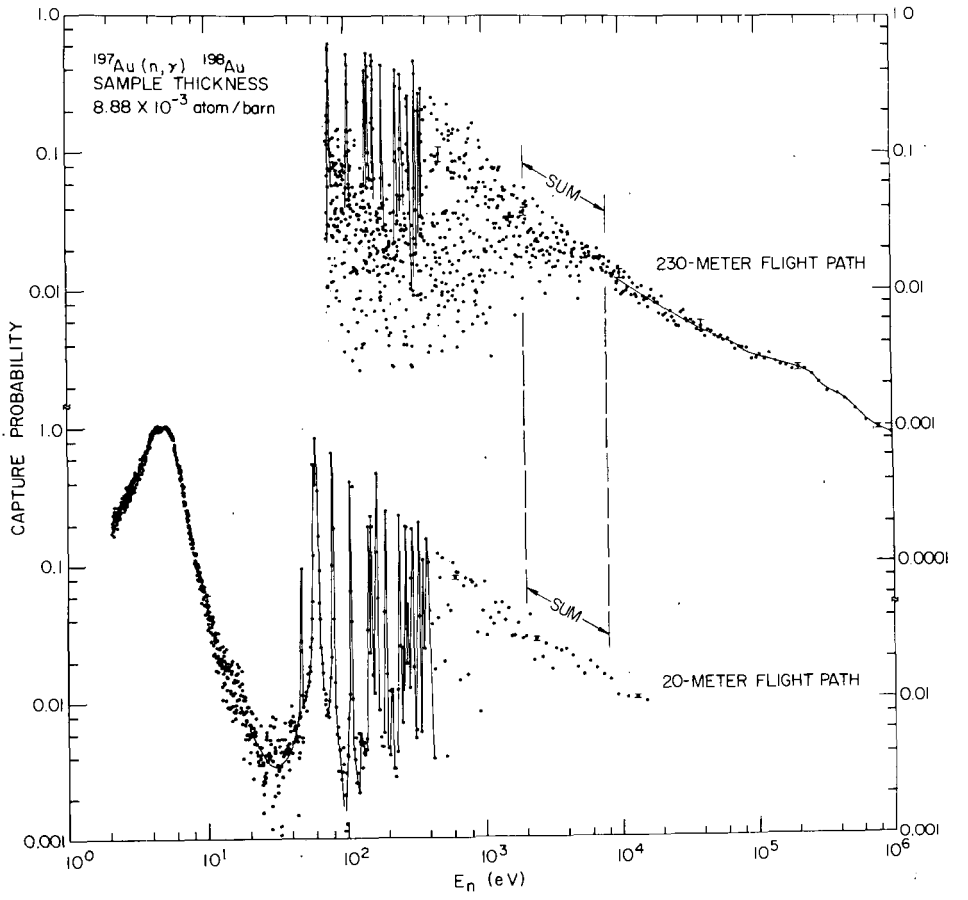

FIG. 5. Capture probabilities measured with 230-m and 20-m neutron flight paths. The scatter of points is primarily due to partially-resolved resonance structure.

The ambient background shown in Fig. 4 is the constant background arising principally from cosmic-ray interactions with the scintillator. The sample-out background varies with neutron flight time and is primarily due to neutrons scattered and captured in the vicinity of the collimator nearest to the scintillator. The scattered-neutron background results from neutrons scattered by the sample and then captured in the scintillator materials. A measure of this background was obtained by substituting a lead or carbon sample (where capture is negligible) and scaling the observed γ-ray counts by the ratio of scattering probabilities at a representative neutron energy that takes into account the mean lifetime of neutrons in the scintillator. An overall check of the background subtractions is made by introducing a thick sodium "notch" filter in the beam ahead of the capture sample. The count rate observed at the bottom of the transmission dip at the 2.85-keV resonance in ^{23}Na+n has always agreed within a few percent with the sum of the individually deter-

mined backgrounds. The statistical precision of the net capture counts (summed over 5% energy intervals under 50 keV) is ±10% or better for all elements at all neutron energies.

A typical capture yield (net capture counts divided by the incident neutron flux) obtained for gold with the 230-m flight-path facility is shown by the points in the upper portion of Fig. 5. The data are usually taken with a 2-μs accelerator burst width and a 2-μs channel width for the time analyser, which results in an overall energy resolution of about 1% at 1 keV and 20% at 1 MeV. The data extend downward in neutron energy to about 70 eV, and known [2] resonances in ^{197}Au+n below 300 eV are indicated in the figure. When accurate resonance parameters are available, the yields can be normalised from the observed and calculated areas of capture resonances in the energy region ~100 eV. By scaling the measured yield to produce the calculated area, the capture probability for a given sample thickness can be normalised without recourse to a determination of the absolute detection efficiency for either the capture γ-rays or the incident neutrons.

To improve the precision of the normalisation, capture yields at lower neutron energies were measured for each sample with a 20-m neutron flight-path facility using a 4000-ℓ scintillator [9] to detect the capture γ-rays and a ^{3}He gas proportional counter to detect the incident neutrons. Data were obtained with this facility from about 2 eV - 20

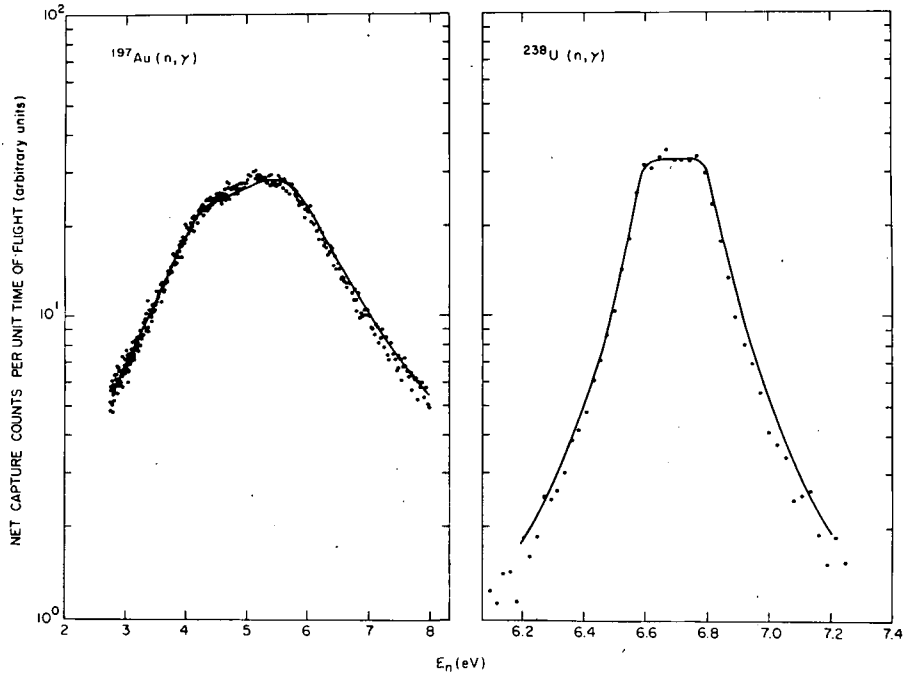

FIG.6. Data and calculations for saturated resonances in gold and uranium.

keV, and the results for Au are shown in the lower portion of Fig. 5. At these lower energies most of the elements studied have resonances that, for the sample thickness used, become "saturated"; i.e. they have a neutron interaction probability near unity. When the resonance is also weak ($\Gamma_n << \Gamma_\gamma$), the area of the resonance calculated near its peak then becomes essentially independent of the values of the resonance parameters, and the yields measured with the 20-m facility can be normalised with an accuracy of 1-2%. The yields determined with the 230-m facility were then normalised to the absolute 20-m results in the region where the two data sets overlap. This is normally done by matching the integrals of the yields from 2-8 keV, as is indicated in the figure.

Typical fits to saturated resonances are shown in Fig. 6 for ^{197}Au(n, γ) and ^{238}U(n, γ). The resonance shapes were calculated with a Monte Carlo code [10] that includes Doppler and resolution broadening, multiple neutron scattering, and incoherent contributions from adjacent resonances. Existing resonance parameters were used without any adjustment to produce detailed fits in the wings of the resonances, and the calculated capture probabilites were used only at energies near the peak of the resonance. In most cases several resonances of a given nuclide, although not saturated, were suitable for normalisation; and the absolute yield could therefore be determined at more than one energy. This provides a check on the flux spectrum measured at low energies, as is illustrated in Fig. 7. The curve in this figure was obtained from a

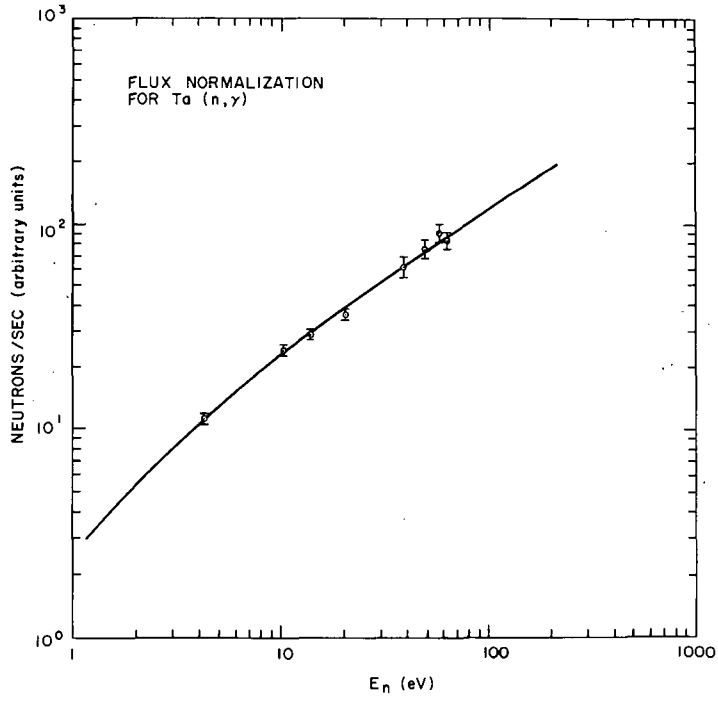

FIG.7. Flux normalization deduced from eight resonances in tantalum. The curve was obtained from a least-squares fit to the flux data and was normalized to three saturated resonances below 15 eV.

least-squares fit to the flux data measured with the ^{3}He counters, and the points denote the relative flux deduced from the ratio of observed and calculated capture areas of eight resonances in $^{181}Ta+n$. The normalisation of the yields for Rh, Ta, Au and ^{238}U measured with the 230-m flight path is judged to be determined within ± 5%.

Normalisation of the yields for Mo, Gd, W, and Re is less straightforward since the effective γ-ray detection efficiency for samples that are not essentially monoisotopic involves an average of the different efficiencies for each isotope weighted by both the isotopic abundance and the average isotopic capture cross section. The latter were taken from recent data and, in some cases, were estimated from statistical-model calculations. An additional difficulty is present for the molybdenum isotopes, where existing resonance parameters produced very poor agreement with many of the observed capture resonances, and where none of the resonances was saturated for a sample thickness of 0.25 cm. This difficulty was partially overcome by comparing capture γ-ray pulse-height distributions for resonances in different isotopes and deducing relative detection efficiencies from the observed spectrum fractions above the discriminator threshold. Full details of the normalisation are given in Ref. [11] for Gd, Ref. [5] for W and Re, and Ref. [12] for Mo. The normalisation of the yield is judged to be determined to within ±10% for Gd, W, and Re and within ± 20% for Mo.

The average capture cross sections were obtained from the normalised yields measured with the 230-m flight path facility by taking into account the variation of γ-ray detection efficiency at the higher incident neutron energies and the finite-sample effects of multiple scattering and self-shielding. For all samples the capture data obtained with no coincidence requirement were used at the higher energies, and the efficiency variation was calculated from the change in the spectrum fraction of scintillator pulses above the sum-signal discriminator threshold. The pulse-height distributions at high energies were deduced from those measured in the resolved-resonance region with the assumption that the distribution is stretched linearly with the initial excitation energy of the compound nucleus. (The spectra $f(E_\gamma)$ measured at low neutron energies were replaced by the spectra $g(E_\gamma) = f[E_\gamma B_n/(B_n + E_n)]$, where E_γ is the γ-ray energy, B_n the neutron separation energy, and E_n the incident neutron energy.) For multi-isotopic samples, the efficiency correction was obtained from an average weighted by isotopic capture cross sections. At 700-keV incident energy, this correction was ~10% or less for all samples except ^{238}U, where it was about 20%. Corrections for resonance self-shielding and multiple scattering were determinted with the code SESH [13] which uses Monte Carlo methods to generate a Doppler-broadened resonance environment at each collision in the sample. This environment is produced by sampling distributions of resonance widths and spacings calculated from specified values of neutron strength functions, average level spacings, and average radiation widths. The total correction to the data for finite-sample effects was ⩽15% for all samples at neutron energies above 5 keV.

3. RESULTS

Our capture cross-section results for Mo, Rh, Gd, Ta, W, and Re are shown in Fig. 8 together with some previous data from other laboratories. The other data chosen for illustration were selected somewhat at random. The data of Gibbons et al. [14] and Diven et al. [15] are perhaps representative of "early" (1960-62) measurements made with liquid scintillators and pulsed van de Graaff neutron sources. The data of Kompe [16] obtained with a liquid scintillator and van de Graaff, and those* of Moxon [17] measured with a Moxon-Rae detector and electron

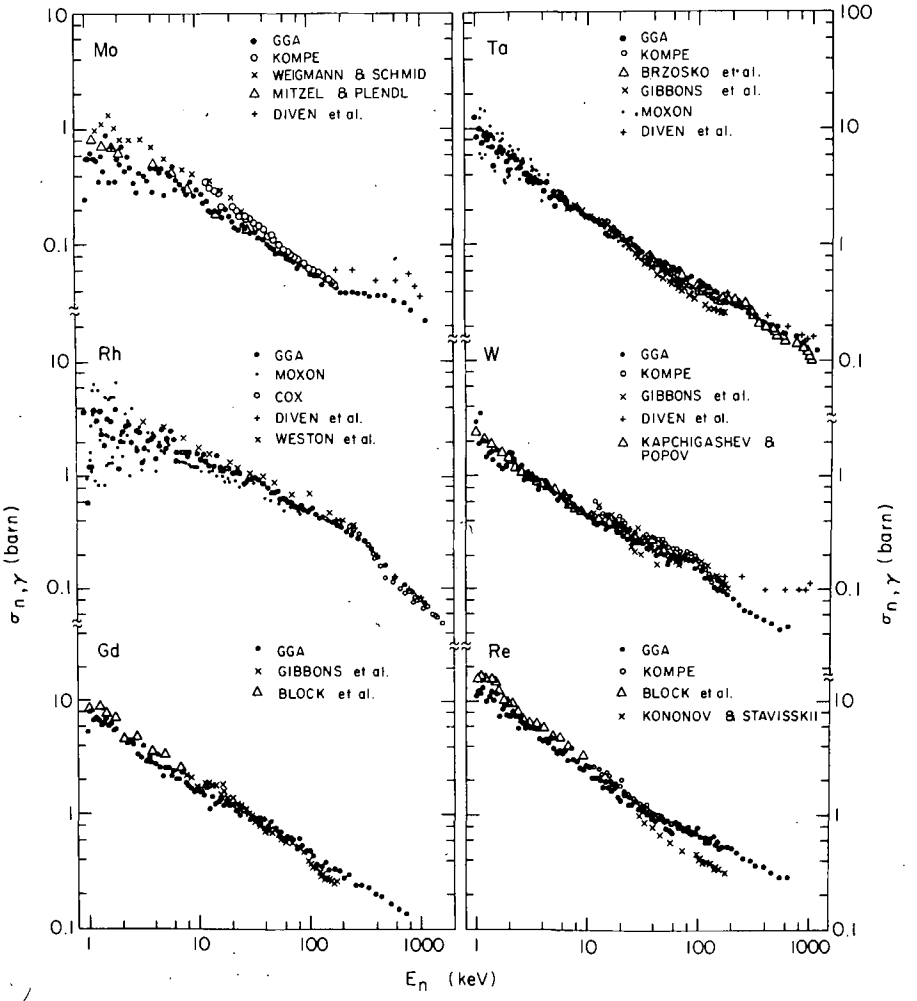

FIG. 8. Capture data for Mo, Rh, Gd, Ta, W, and Re.

*The data of Ref. [17] are measured at very small energy intervals, and many of these points are not included in Figs. 8 and 9.

linear accelerator, have been published within the last two years. A variety of neutron flux measurement techniques and capture-yield normalisation procedures are represented, and several primary and secondary cross-section standards are involved.

Of our present results for eight elements, those for Mo(n, γ) appear to be in poorest agreement with previous data. The data of Weigmann and Schmid [18] are relative to $^{10}B(n, \alpha)^{7}Li^{*}$ and are normalised to saturated resonances in Ag, and these results agree well with those of Kompe [16] which are relative to the Au(n, γ) data of Poenitz et al. [3] (discussed below). The data of Mitzel and Plendl [19] are relative to $^{10}B(n, \alpha)$ and are normalised to Mo resonances. Even in view of some uncertainties in both the present and previous data which arise from poor resonance-parameter and isotopic cross-section information, it is difficult to account for the systematically smaller cross sections found here at the lower energies. Further measurements designed to definitively resolve these discrepancies for Mo(n, γ) are planned at this laboratory.

Our cross sections for Rh are about 20% higher (at least in the region 10-50 keV) than those determined by Moxon [17], which are relative to $^{10}B(n, \alpha)^{7}Li^{*}$ and normalised to saturated resonances. The present data for Gd near 100 keV do not fall off as fast with increasing neutron energy as those of Gibbons et al. [14], which are relative to their determination [14] of the excitation function for In(n, γ). A similar disagreement with the results of Gibbons et al. occurs for Ta and Au. Agreement of our Ta data with the other results illustrated is exceptionally good at all energies below 900 keV. Discrepancies in the average cross section exceed a few percent only in the region ~ 50-150 keV, where our results are ~ 10% higher than those of Kompe [16] and ~ 20% higher than those of Moxon [17].

Our data for W are ~ 20% lower than those of Kompe below 100 keV and are also lower than those of Gibbons et al. both below 20 keV and above 100 keV. The vast disagreement above 100 keV with the measurements of Diven et al. [15] relative to the ^{235}U capture-plus-fission cross section is not easily explained. Similar but smaller disagreements with the results of that experiment are also observed for Mo, Ta, W and ^{238}U but do not appear to be present for Rh and Au. Our excitation function for Re disagrees in shape with that measured by Kononov and Stavisskii [20] relative to the In(n, γ) cross section determined by Gibbons et al. Our Re data are about 10% lower than those of Kompe below 50 keV and about 20% lower than the results of Block [21], which are all at energies < 10 keV. The latter measurements were made relative to $^{10}B(n, \alpha)$ but were normalised without a detailed consideration of the capture γ-ray detection efficiency.

Capture data for Au and ^{238}U are shown in Fig. 9. Our data for gold agree within a few percent at all energies below 400 keV with the measurements of Poenitz et al. [3] made with a "grey" (flat-response) neutron detector and normalised at 30 keV to an absolute value of the

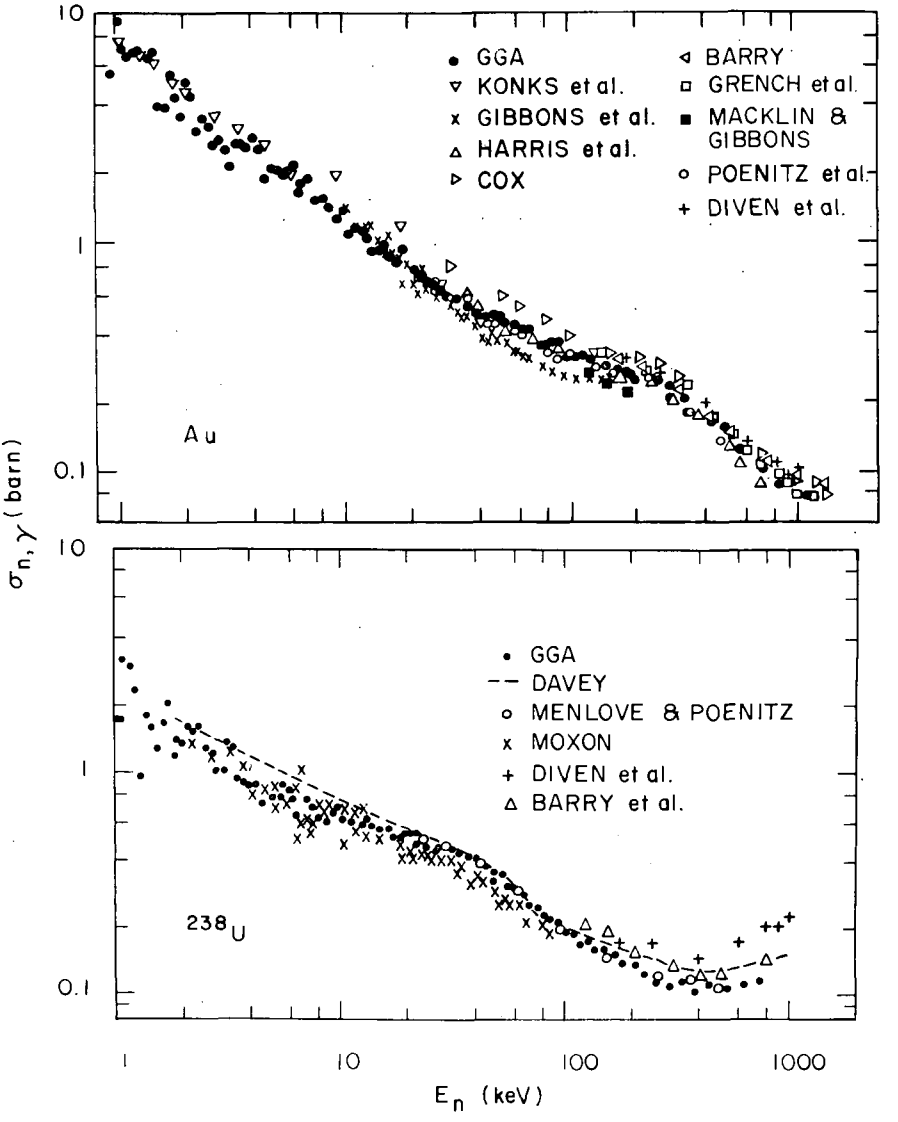

FIG. 9. Capture data for Au and ^{238}U.

cross section determined by five independent measurements. The cross section measured by Poenitz et al. at ~470 keV is about 10% lower than our data. Our data from ~40-200 keV are about 20% higher than the data of both Gibbons et al. and the later measurements of Macklin and Gibbons [22], which are relative to their previous results for Ta, In or I. Except near 500 keV, our data for Au(n, γ) are 10-20% lower than the activation measurements of Cox [23], which are relative to ^{10}B(n, α) below 200 keV and based on ^{235}U(n, f) above 200 keV. Our data above 400 keV are ~ 15% higher than the absolute activation measurements of Harris [24]

and agree closely above 400 keV with the measurements of Grench and Vaughn [2] relative to $^{235}U(n, f)$. Our gold data from 200-800 keV also agree within ~10% with the measurements of Barry [25] using a ^{235}U fission counter calibrated [1] against the n+p cross section.

Our data for ^{238}U are once again in best overall agreement with measurements by Menlove and Poenitz [26] using the grey detector and an absolute activation normalisation at 30 keV. Our results are somewhat lower than the evaluation of Davey [27] below 20 keV, and ~15% lower everywhere in the region 200-800 keV. The cross sections above 200 keV recommended by Davey are essentially equivalent to the activation measurements of Barry [28], which were relative to the ^{235}U fission cross section. Our results near 40 keV are about 20% higher than the data of Moxon [17], which were obtained relative to $^{10}B(n, \alpha)^{7}Li^{*}$ and were normalised to saturated resonances.

4. CONCLUSIONS

With the possible exception of the results for $Mo(n, \gamma)$, the present measurements considered together with previous data obtained over more limited regions of energy are believed to establish the absolute average capture cross sections discussed here to within 10-15% over the full energy region ~ 1-1000 keV. The present experiment is designed to yield cross-section values with an accuracy ~10% over a very large energy range. Consequently, it is difficult to judge whether our results lend support to previous indications that gold capture data based on the ^{235}U fission cross section are ~ 15% higher than other results above 200 keV. Our data for gold above 400 keV are in good agreement with one such measurement by Grench [2] and yet are also in good agreement with the data of Poenitz et al. [3] at lower energies. Our cross sections for $^{238}U(n, \gamma)$ agree best with those of Menlove and Poenitz [26], are consistently smaller above 200 keV than the recommended values of Davey [27], and do not support the lower capture cross sections obtained by Moxon [17] between 20 and 100 keV.

REFERENCES

[1] White, P. H., J. Nucl. Energy 19 (1965) 325.

[2] Brookhaven National Laboratory Report BNL 325, 2nd ed., Supplement 2 (1964-66).

[3] Poenitz, W. P., et al., J. Nucl. Energy 22 (1968) 505.

[4] Gammel, J. L., "The n-p Total and Differential Cross Sections in the Energy Range 0-40 MeV," Ch. V. T, Fast Neutron Physics, Part II (Marion, J. B., and Fowler, J. L., Eds.), Interscience, New York (1963).

[5] Lopez, W. M., et al., National Aeronautics and Space Administration Report NASA CR-72474 (1968).

[6] Lopez, W. M., Proceedings for the Skytop Conference on Computer Systems in Experimental Nuclear Physics, Conf - 690301, EANDC (U.S.) 121 u (1969).

[7] Parker, J. B., et al., Nucl. Instr. and Methods 23 (1963) 61.

[8] Costello, D. G., et al., Nucl. Sci. and Engr. 39 (1970) 409.

[9] Haddad, E., et al., Nucl. Instr. and Methods 31 (1964) 125.

[10] Fröhner, F. H., Gulf General Atomic Report GA-6906 (1966).

[11] Fricke, M. P., et al., USAEC Report GA-9275 (1969).

[12] Friesenhahn, S. J., et al., Gulf General Atomic Report GA-10081 (1970).

[13] Fröhner, F. H., Gulf General Atomic Report GA-8380 (1968).

[14] Gibbons, J. H., et al., Phys. Rev. 122 (1961) 182.

[15] Diven, B. C., et al., Phys. Rev. 120 (1960) 556.

[16] Kompe, D., Nucl. Phys. A133 (1969) 513.

[17] Moxon, M. C., "The Measurement of Average Neutron Capture Cross Sections in the Mass Region Above 100," thesis-London University, July 1968, HL68/3739.

[18] Weigmann, H., and Schmid, H., Nucl. Phys. A104 (1967) 513.

[19] Mitzel, V. F., and Plendl, H. S., Nukleonik 6 (1964) 371.

[20] Kononov, V. N., and Stavisskii, Yu. Ya., Atomnaya Energiya 19 (1965) 457.

[21] Block, R. C., et al., "Neutron Radiative Capture Measurements Utilizing a Large Liquid Scintillator Detector at the ORNL Fast Chopper," Neutron Time-of-Flight Methods (Saclay Conf.) (Spaepen, J., Ed.), EURATOM (1961).

[22] Macklin, R. L., and Gibbons, J. H., Phys. Rev. 159 (1967) 1007.

[23] Cox, S. A., Phys. Rev. 122 (1961) 1280.

[24] Harris, K. K., et al., Nucl. Phys. 69 (1965) 37.

[25] Barry, J. F., J. Nucl. Energy 18 (1964) 491.

[26] Menlove, H. O., and Poenitz, W. P., Nucl. Sci. and Engr. 33 (1968) 24.

[27] Davey, W. G., Nucl. Sci. and Engr. 39 (1970) 337.

[28] Barry, J. F., et al., J. Nucl. Energy 18 (1964) 481.

CALCULATIONS OF CROSS-SECTIONS FOR THE RADIATIVE CAPTURE OF FAST NEUTRONS *

M.P. FRICKE, W.M. LOPEZ †, S.J. FRIESENHAHN
A.D. CARLSON, D.G. COSTELLO
Gulf General Atomic Incorporated
San Diego, Calif.,
United States of America

Abstract

CALCULATIONS OF CROSS-SECTIONS FOR THE RADIATIVE CAPTURE OF FAST NEUTRONS.

The data of the other paper presented by the authors at the Helsinki Conference, together with some results of recent activation measurements, have been analysed in terms of the statistical model. It has not been found possible to reproduce most of the observed excitation functions using the customary energy dependence of the γ-ray penetrabilities. This result is independent of (1) different optical-model parameters used to describe the neutron channels and the effects of a non-spherical potential; (2) different level-density formulas and a wide variation in their parameters; (3) extreme assumptions of neutron width-fluctuation correlations; (4) extreme limits of the effect of the (n, γ n') process; and (5) of any plausible spin or parity dependence of the total radiation width. If the usual form is retained for the γ-ray penetrabilities, $T_\gamma \sim 2\pi < \Gamma_\gamma > /D$, then the most likely source of difficulty appears to lie with the conventional excitation-energy dependence of the average partial radiation widths that sum to $< \Gamma_\gamma >$.

1. INTRODUCTION

Reliable experimental information on average neutron capture cross sections, particularly at energies $\geq$ 100 keV, is virtually absent for some important fertile and fissile nuclei and completely absent for most fission-product nuclides. This places considerable emphasis on theoretical capabilities to predict these cross sections or to extrapolate them from energies where credible measurements have been made. For a critical examination of such capabilities, it is desirable to consider first the case where fission channels are closed.

The current theoretical description of average capture cross sections below one MeV was developed quite fully almost two decades ago [1]. The Hauser-Feshbach theory is used, and the shape of the excitation function for capture is fairly insensitive to different optical-model characterisations of the neutron channels. The main ingredient for capture cross sections is the radiative strength function, i.e. the ratio of the average total radiation width to the average level spacing. The average radiation width is calculated conventionally from the Weisskopf estimate [2], and the average level spacing is taken from standard level-density formulas. When radiation widths and level

* Work supported in part by the US Atomic Energy Commission.

† Present address: University of California at San Diego, La Jolla, California 92037, USA.

spacings have been measured for low-energy neutron resonances, or when the average capture cross section is known in the lower-keV region, the radiative strength function can be chosen to produce agreement with these data. The average capture cross section at higher energies is then determined principally by the variation of the radiative strength function with energy.

Such calculations have been compared to the data presented in the previous paper (CN-26/43) and also to recent measurements by Stupegia et al. [3]. We conclude that the conventional treatment of the capture reaction is in general unable to reproduce the observed excitation functions in the region ~ 100 keV - 1 MeV. Early results of this study were presented in Ref. [4].

2. THEORY

The average angle-integrated compound-nucleus cross section is given [5] by the following sum over all entrance (α) and exit (β) channel quantum numbers:

$$\sigma_{n,x} = \pi\lambda^2 \Sigma_{\alpha\beta} g_\alpha^J [F_{\alpha\beta} \langle\theta_{\mu\alpha}\rangle \langle\theta_{\mu\beta}\rangle / \langle\theta_\mu\rangle - \delta_{\alpha\beta} Q_\alpha \langle\theta_{\mu\alpha}\rangle^2 / 4] \qquad (1)$$

Here g_α^J is the spin statistical factor; $F_{\alpha\beta}$ the correction for width fluctuations; and $\langle\theta_\mu\rangle$ is a sum over all open channels ν of resonance parameters $\langle\theta_{\mu\nu}\rangle$, where the brackets denote an average over compound levels μ.

The average resonance parameters for the neutron channels are given by optical-model transmission coefficients T_α and a parameter Q_α which depends on statistical properties [5] of the compound levels:

$$\langle\theta_{\mu\alpha}\rangle = T_\alpha + (1/Q_\alpha)[1 - (1 - Q_\alpha T_\alpha)^{\frac{1}{2}}]^2 \qquad (2)$$

The optical-model parameters of Moldauer [6] were used in most of the calculations discussed here. By analogy with the treatment of particle channels at low energies, the average resonance parameters for the capture γ-ray channels are taken proportional to the radiative strength function,

$$\langle\theta_{\mu\gamma}\rangle = 2\pi \langle\Gamma_\gamma(U)\rangle / D_{J\pi}(U) \qquad (3)$$

where $D_{J\pi}$ is the average spacing of compound levels at the excitation energy U, and $\langle\Gamma_\gamma(U)\rangle$ is the average total radiation width. We refer to these quantities as γ-ray penetrabilities $T_\gamma \equiv \langle\theta_{\mu\gamma}\rangle$.

The energy dependence of $<\Gamma_\gamma>$ is calculated conventionally as a sum of partial widths for electric radiation that vary [2] with energy as $|Q|^2\epsilon^{2\ell+1}$, where ϵ is the gamma energy and $|Q|^2 \propto D(U)$. For a continuous distribution of levels, this gives

$$<\Gamma_\gamma(U)> \propto D(U)\int_0^U \epsilon^{2\ell+1}\rho(U-\epsilon)\,d\epsilon \qquad (4)$$

where $\rho = D^{-1}$ is the level density and is described here with the parameters of Gilbert and Cameron [7]. The present calculations are made with $\ell = 1$, and cross sections calculated with $\ell = 2$ differ negligibly at neutron energies below one MeV. The exit-channel penetrabilities were corrected for the (n, γn') process in the manner proposed by Moldauer [8,9]. This allows for the possibility of terminitating the gamma cascade by neutron emission (an event not recorded experimentally). The (n, γn') effect can be described approximately [9] by using an effective "capture width" in the exit channel which includes only those primary transitions to levels where the total neutron width for a given spin and parity is less than $<\Gamma_\gamma>$. In particular, the maximum possible effect of the (n, γn') process is realised for capture widths obtained by changing the lower limit of integration in Eq. (4) to equal the incident neutron energy.

The most favourable neutron energy region for a critical examination of the current treatment of the capture penetrability T_γ for heavy nuclei is the region between ~ 100 keV and 1 MeV. The situation is illustrated for Au(n, γ) in Fig. 1. Below 100 keV the excitation energy U of the compound nucleus is not appreciably different from the neutron separation energy U_0, and the excitation function is insensitive to the dependence $T_\gamma(U)$. Above 1 MeV the capture reaction becomes dominated by the (n, γn') process, which has all the unknowns of the capture reaction plus several more of its own. The curve in Fig. 1 labeled realistic (n, γn') was calculated with the method of Ref. [8]. The other curves were obtained with no correction for the (n, γn') process, and with the maximum possible effect discussed above. The latter corresponds to the extreme assumption that all primary gamma transitions ending above the neutron separation energy result in neutron emission. Another formidable complication at the higher energies is that one rarely knows all the levels that can be populated in heavy nuclei and, e.g., must approximate the (n, n') competition rather crudely by resorting to a continuous level-density expression for the residual target levels, the validity of which is quite dubious at excitation energies of only 1 MeV.

The disagreement found between the measured and calculated excitation functions is evident in Fig. 1. For most of the nuclei examined, the excitation function from 100 keV - 1 MeV is incorrectly reproduced; the calculated capture cross sections fall off too slowly with increasing neutron energy, even with the maximum effect of (n, γn'). We note that this discrepancy is opposite to that found at much higher energies, $E_n \gtrsim 10$ MeV, where a direct or collective capture mechanism is required to increase the calculated cross sections above those given by the compound-nucleus treatment. The discrepancy found here was also observed

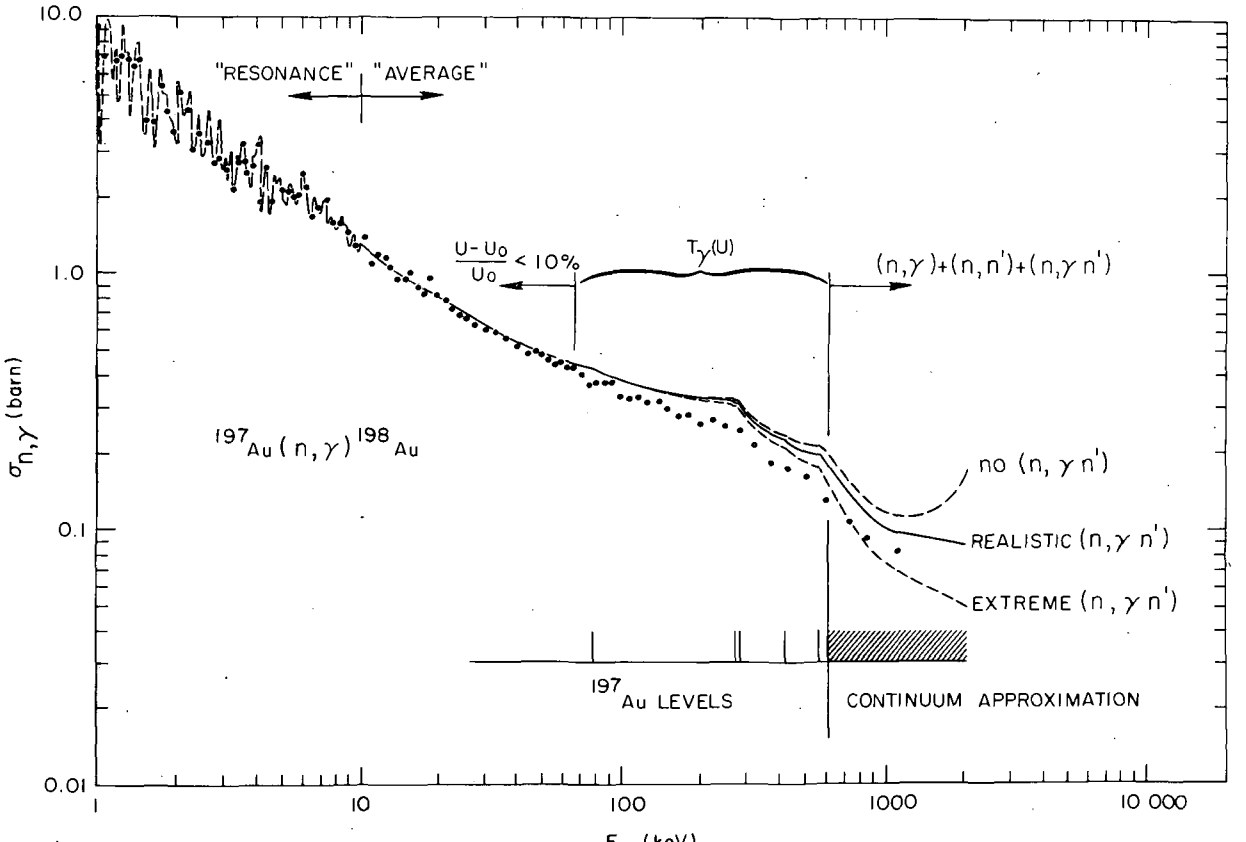

FIG. 1. Statistical-model calculations of the average capture cross-section for gold. In the region spanned by the bracket labeled T_γ (U), the competition from inelastic scattering can be treated rigorously for each level in ^{197}Au, and the effect of the (n, γ n') process is small. Below this region T_γ is approximately constant since the compound excitation energy $U = U_0 + E_n$ differs little from the binding energy U_0.

in the previous work of Stupegia et al. [3]. Of the nuclei examined in that study, the discrepancy was more pronounced for deformed nuclei; and it was speculated [3] that the source of difficulty might lie in the use of a spherical optical-model potential to describe the neutron scattering channels.

3. ANALYSIS

3.1. Trial calculations

Studies were carried out for a few nuclei in an attempt to reconcile theory and experiment by modifying ingredients of the calculation other than the form of the γ-ray penetrabilities. Some of these results are illustrated here, principally by calculations made for Au(n, γ); the data shown are those presented in the previous paper (CN-26/43). For convenience, the (n, γn') process was not included in these calculations at energies where it changes the gold capture cross section by ≤10%. The statistical-model calculations were made with a version [10] of the code NEARREX [8] and were verified to agree with sample calculations made with similar programs in use at four other laboratories. Several optical-model codes were used and intercompared.

The effects of width-fluctuation correlations were examined by varying the parameter Q_α from 0 to 2 (as T_α permits) and also by setting $F_{\alpha\beta} = 1$ to eliminate the width-fluctuation correction. Varying Q_α was determined to have no appreciable effect in the capture calculations. Eliminating the width-fluctuation correction increases the capture cross section almost uniformly by about 20% at energies below the first threshold for inelastic scattering and has little effect above the threshold. This, however, does not remove the discrepancy in the slope of the excitation function. The change produced is much too small, and for some nuclei (see below) the discrepancy can be observed below the first (n, n') threshold. The rest of the calculations discussed here include the correction for width fluctuations and use $Q_\alpha = 0$.

Results of calculations made with different sets [6, 11, 12] of optical-model parameters for the neutron elastic and inelastic scattering channels are shown in Fig. 2. The calculations were normalised by adjusting $T_\gamma(U_0)$ to produce agreement with the data at $E_n = 10$ keV. The values of $T_\gamma(U_0)$ varied $\sim \pm 20\%$ with the choice of optical potential and were in fair agreement (20-30%) with values of $\langle \Gamma_\gamma \rangle / D_{obs}$ deduced from s-wave resonance parameters. As can be seen in Fig. 2, the relative cross sections calculated with the different potentials agree within $\sim 20\%$ from 10-700 keV.

Possible changes in the excitation function produced by using a non-spherical optical-model potential were investigated by making coupled-channel calculations [13] of the neutron scattering amplitudes. Generalised transmission coefficients were then obtained from the scattering amplitudes in the manner indicated in Ref. [4]. Coupled-channel calculations were made with the code described in Ref. [14] for

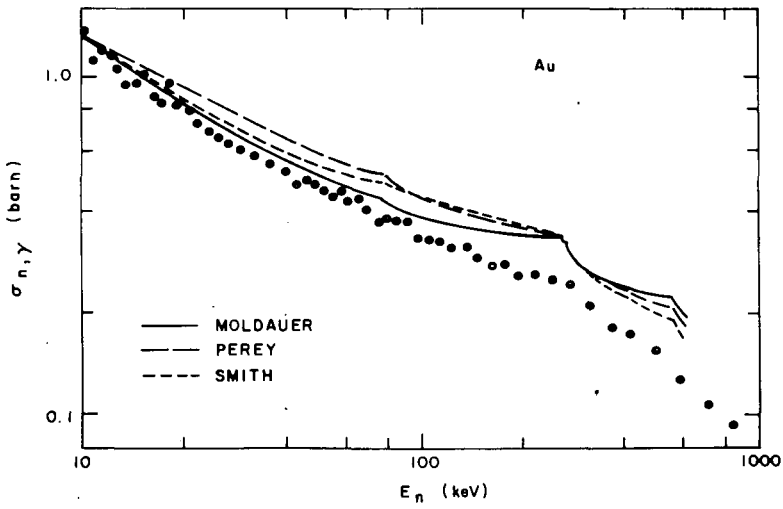

FIG. 2. Capture cross-sections for gold calculated with different optical-model parameters. The solid curve was calculated with the parameters of Ref. [6], the long-dash curve with Ref. [12], and the short-dash curve with Ref. [11].

^{197}Au+n including the first five positive-parity states in ^{197}Au. The four excited states $1/2^+$ - $7/2^+$ were assumed to result from coupling the $d_{3/2}$ valence proton to a one-quadrupole-phonon vibration of the core with a typical deformation parameter [13] of $\beta_2 = 0.2$. Coupled-channel calculations were also made for the tungsten isotopes $^{182, 183, 184, 186}$W assuming a quadrupole deformation of strength $\beta_2 = 0.24$. The 0^+ - 2^+ - 4^+ states were included for the even isotopes, and the ground-state band $1/2^-$ - $7/2^-$ was used for ^{183}W. Capture calculations were then made with these generalised transmission coefficients together with the usual transmission coefficients (obtained from a spherical potential) for any other open (n, n') channels. The capture calculations were essentially identical for generalised transmission coefficients obtained with "complex coupling", for which both real and imaginary parts of the optical potential are deformed [13], and "real coupling" where only the real part of the potential is allowed to contribute to the nonspherical interaction.

Results of capture calculations for gold and natural tungsten using the spherical and nonspherical optical potentials are shown in Fig. 3. The two results are essentially identical for both the vibrational nucleus Au and the rotational nucleus W. Although the nonspherical treatment for W changes the transmission coefficients considerably at the higher incident energies, the capture calculation is still largely unaffected. This can be understood as an approximate cancellation of the differences in transmission coefficients in the quantities $\langle\theta_{\mu a}\rangle/\langle\theta_{\mu}\rangle$.

It was thus found unlikely that the discrepancy in the shape of the capture excitation function could be attributed to the neutron channels, and the exit-channel parameters were then examined. In its present form (Eqs. 3 and 4), the energy dependence of the γ-ray penetrabilities

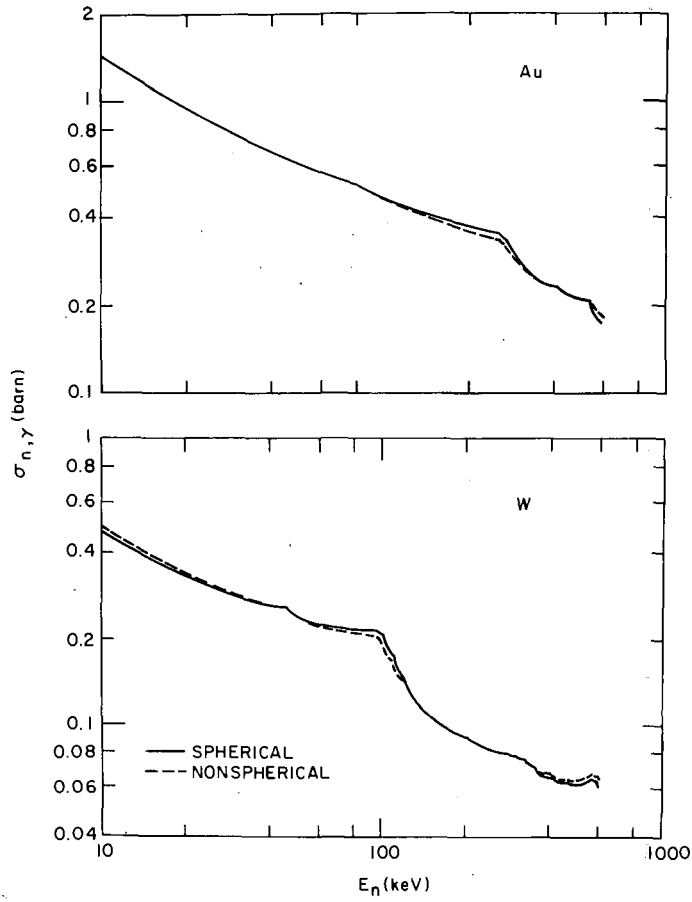

FIG. 3. Capture cross-sections calculated with neutron transmission coefficients obtained from spherical and non-spherical optical-model potentials. A vibrational model was assumed for Au and a rotational model for W.

is determined by the energy and angular-momentum dependence of the level density. Capture calculations were made using the composite level density of Gilbert and Cameron [7], a simple Fermi-gas form $\rho \propto \exp(4aU)^{\frac{1}{2}}$, and a constant-temperature model $\rho \propto \exp(U/T)$. For values of the parameters a and T given in Ref. [7], these three representations produce negligible differences in the cross section at neutron energies below 1 MeV. A pairing correction [7] was used in the Fermi-gas formula, but this also has a small effect. Figure 4 illustrates that, to force the calculation to fit the general shape of the excitation function for gold up to $\sim$ 700 keV, the inverse-temperature parameter a must take a value about one order of magnitude different from the expected value of 18 MeV^{-1}. The spin dependence of the level density also changes the shape of the excitation function, since higher-energy neutrons bring more angular momentum into the compound nucleus. The spin dependence is represented here by $\rho(J) \propto [f(J) - f(J+1)]$, where $f(x) = \exp(-x^2/2\sigma^2)$; and the

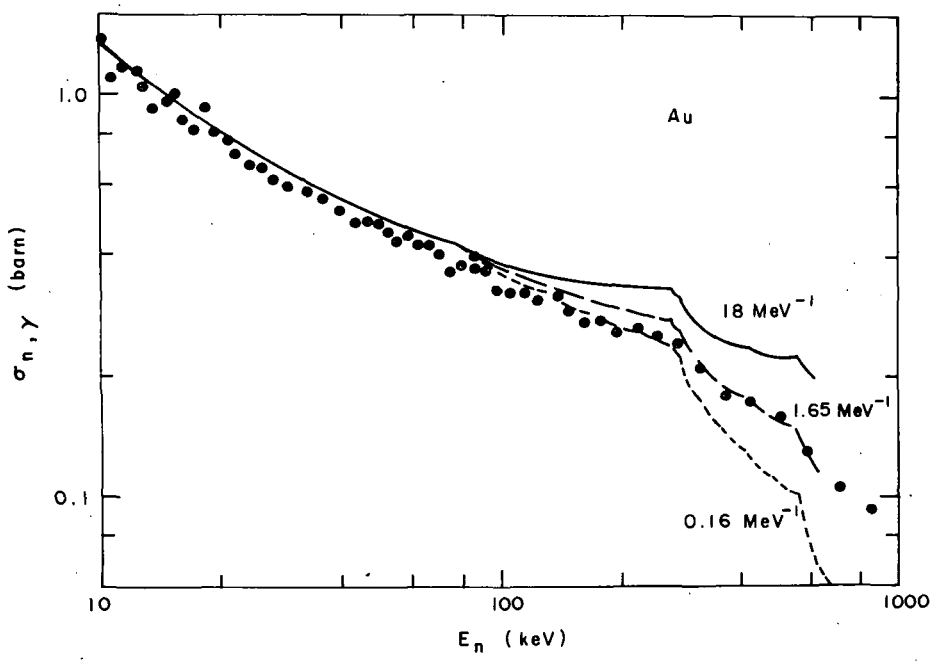

FIG. 4. Capture cross-sections for gold calculated with a reasonable value (18 MeV^{-1}) of the level-density parameter a and with lower values required to force agreement with the data.

parameter σ is taken from Ref. [7]. Qualitiative agreement with a few (but not all) of the exitation functions could be produced by eliminating the spin dependence altogether. None of these gross changes in the level-density representation is attractive.

The calculations in which the spin dependence of the level density was varied can also be interpreted as introducing a spin dependence of the total radiation width, since the capture calculation depends only on the ratio $<\Gamma_\gamma>/D_{J\pi}$. Thus, the limited agreement mentioned above could also have been achieved using a standard [7] level density but a total radiation width which had the spin dependence $[f(J) - f(J+1)]^{-1}$ or, approximately, $(2J+1)^{-1}$. There is no evidence of such a dependence from neutron resonance-parameter studies. Calculations were also made with an arbitrary dependence of the total radiation width on the parity of the initial compound state. For gold, the p-wave contribution to the capture cross section dominates the s- and d-wave components in the region 60-600 keV, and the observed excitation function there could be reproduced by using a constant value of $(\Gamma_\gamma^+/\Gamma_\gamma^-)$ other than unity and by adjusting Γ_γ^+ to also produce agreement at 10 keV. However, a fit could only be achieved with the very unlikely [15] ratio $(\Gamma_\gamma^+/\Gamma_\gamma^-) \sim 5$.

3.2. Results for several nuclei

Standard calculations (as described in Section 2) were then carried out systematically for the eight data sets presented in the previous paper

and also for ten excitation functions measured by Stupegia et al.[3] which also span the energy region of interest. The optical-model parameters were taken from Ref. [6], the level-density parameters from Ref. [7], and the (n, γn') process was included. The calculations were normalised by adjusting $T_\gamma(U_0)$ to approximately reproduce the data at the lowest energies. The normalisation is not critical for our present purposes since the shape of the exitation function changes little with wide variations in $T_\gamma(U_0)$. For ^{238}U, the fission competition was represented in the manner of Ref. [16] and is very small at energies below one MeV. The results are shown by the solid curves in Figs. 5 and 6. Within uncertainties in the data and reasonable variations of the parameters,

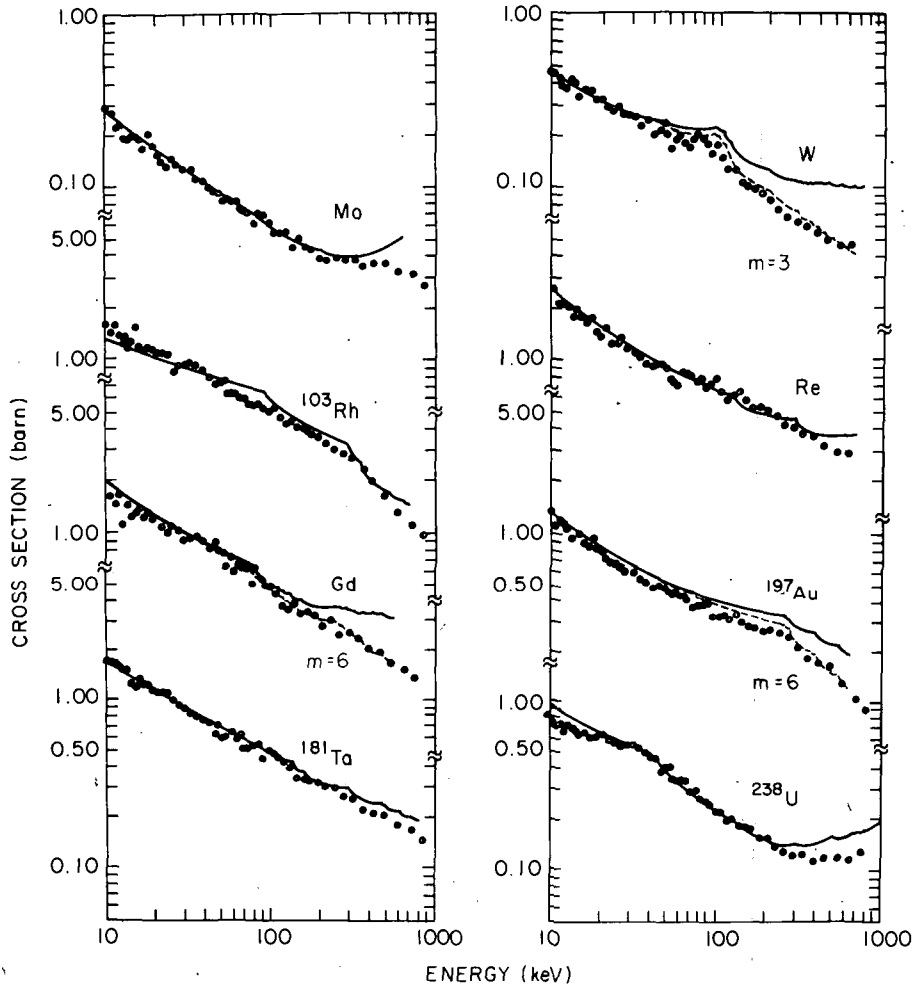

FIG. 5. Capture cross-section data of paper CN-26/43 versus statistical-model calculations. The solid curves were obtained with the standard theory and the broken curves with γ-ray penetrabilities proportional to a power m of the compound excitation energy.

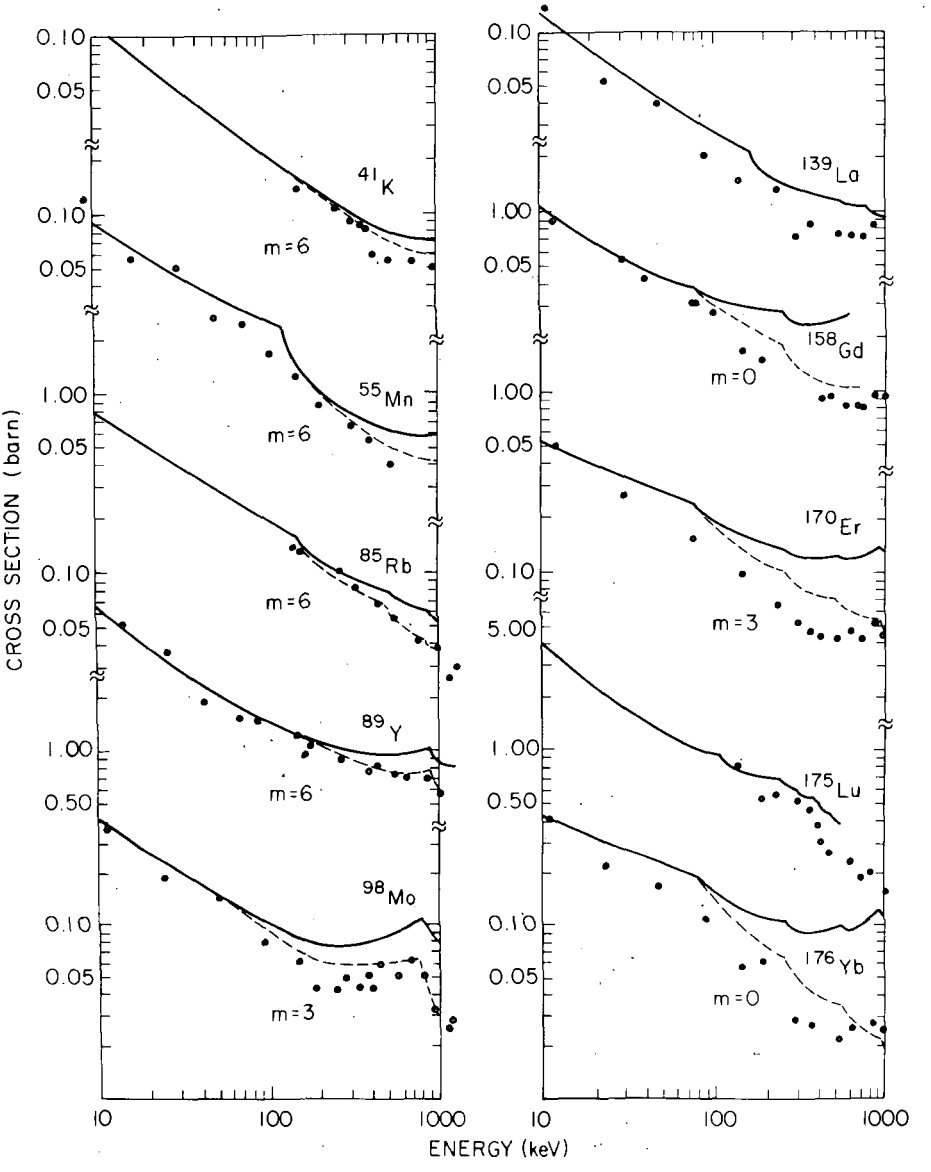

FIG. 6. Capture cross-section data of Ref. [3] versus statistical-model calculations. As in Fig. 5 the solid curves are standard calculations, and the broken curves use $T_\gamma \propto U^m$.

we conclude that the standard treatment produces fairly good agreement with the capture data for Rh, Ta and Re but that a persistent discrepancy, of varying magnitude but always in the same direction, can be seen in the excitation functions for all the nuclei examined. The discrepancy can be observed in regions where there are no open (n, n') channels, e. g. in ^{89}Y(n, γ) below 1 MeV. The agreement is exceptionally poor for ^{98}Mo, ^{158}Gd, natural Gd, ^{170}Er, ^{176}Yb and natural W. We find no consistent variation of the magnitude of the discrepancy for different nuclei with

such properties as $<\Gamma_\gamma(U_0)>$, $D(U_0)$, $<\Gamma_\gamma(U_0)>/D(U_0)$, U_0, even or odd A, characteristics of measured capture γ-ray energy spectra, extrema in the s- and p-wave neutron strength functions, or the ground-state quadrupole deformation parameter.

Some additional calculations are shown in Figs. 5 and 6 to illustrate the degree of disagreement with the present theory. The broken curves were calculated with a much more slowly-varying γ-ray penetrability which has the empirical form $T_\gamma = C(U-\Delta)^m[f(J) - f(J+1)]$, where Δ is the pairing energy [7] and where the constant C was adjusted to produce the same value of $T_\gamma(U_0)$ used in the standard calculation. The exponent m is a measure of the energy dependence of T_γ required to roughly fit the shape of the excitation function below 1 MeV. If we retain Eq. (3) and a conventional level-density expression, then m is a measure of the energy variation of $<\Gamma_\gamma> \propto T_\gamma(U)/\rho(U)$. For Au(n, γ) using the level density of Ref. [7], the value of $<\Gamma_\gamma(U)>/<\Gamma_\gamma(U_0)>$ calculated conventionally is about 1.2 at E_n = 700 keV, whereas it drops to about 0.6 for the empirical expression with m = 6.

4. CONCLUSIONS

The current statistical-model treatment of fast-neutron capture cross sections with parameters presently deemed reasonable does not reproduce the majority of the excitation functions examined. Even when normalised to data at energies up to 100 keV, the excitation functions calculated for some nuclei differ from the data by a factor of two at only 500 keV; and the discrepancy is always in the same direction. On phenomenological grounds, the most likely source of difficulty lies with the excitation-energy dependence of the γ-ray penetrability (or radiative strength function). Since there is no compelling reason to abandon Eq. (3) for the cases examined, and since such enormous departures from conventional level-density descriptions would otherwise be required to fit many of the cross sections with the standard calculation of $<\Gamma_\gamma(U)>$, it is tempting to speculate that the difficulty lies with the traditional estimate [2] of the excitation-energy dependence of the partial radiation widths. Although this estimate is obtained from very simple assumptions about the electromagnetic matrix elements and the distribution of single-particle strength at high excitation energies, it is still difficult to understand how the estimate could be so grossly incorrect. It thus seems clear that new, fundamental work on the capture mechanism will be required before theory can be applied with confidence to fill gaps in the data for capture cross sections at neutron energies ~100 keV - 1 MeV.

REFERENCES

[1] Margolis, B., Phys. Rev. 88 (1952) 327.

[2] Blatt, J. M., and Weisskopf, V. F., Theoretical Nuclear Physics, Wiley, New York (1952).

[3] Stupegia, D. C., et al., J. Nucl. Energy 22 (1968) 267.

[4] Fricke, M. P., and Lopez, W. M., Phys. Letters 29B (1969) 393.

[5] Moldauer, P. A., Rev. Mod. Phys. 36 (1964) 1079; Phys. Rev. 135 (1964) B642; Phys. Rev. 171 (1968) 1164.

[6] Moldauer, P. A., Nucl. Phys. 47 (1963) 65.

[7] Gilbert, A., and Cameron, A. G. W., Can. J. Phys. 43 (1965) 1446.

[8] Moldauer, P. A., et al., Argonne National Laboratory Report ANL-6978 (1964).

[9] Moldauer, P. A., Proc. Conf. on Neutron Cross Section Technology, 1966, Washington, D. C., p. 163.

[10] Dunford, C. L., Atomics International Report NAA-SR-MEMO 12530 (1967).

[11] Lister, D., et al., Phys. Rev. 162 (1967) 1077.

[12] Perey, F. G., and Kinney, W. E., Oak Ridge National Laboratory Report ORNL-TM-2159 (1968).

[13] Tamura, T., Rev. Mod. Phys. 37 (1965) 679.

[14] Tamura, T., Oak Ridge National Laboratory Report ORNL-4152 (1967).

[15] Cameron, A. G. W., Proc. Conf. on the Neutron Interactions with the Nucleus, Columbia Univ., 1957, USAEC Report TID-7547.

[16] Dunford, C. L., "Evaluation of Heavy Even-Even Nuclide Elastic and Inelastic Cross-Sections by Means of a Non-spherical Optical Model," Nuclear Data for Reactors (Paris Conf., 1966), IAEA, Vienna (1967).

DISCUSSION

TO PAPERS IAEA-CN-26/43, 44

M. ADIB: You used ^{3}He in proportional conditions as your means of detection. However, in this arrangement the distribution of output pulses is obtained from the ^{3}He recoil atoms, and this is influenced by the sensitivity of the detector to gamma background and to other background. Did you not use counters in corona conditions in order to avoid these difficulties?

M. P. FRICKE: No, we did not. For incident neutrons up to 300 keV, the ^{3}He-recoils can be eliminated by setting the lower level of the discriminator used with these counters to about one third of the proton peak energy produced by thermal neutrons. We actually set it at about 80% of the peak, and the spectrum fraction of proton pulses can be determined from two-parameter data (pulse-height and neutron-flight time) measured separately with the discriminator set very low.

In our experimental arrangement, the background from all sources was very small (about 2%) and was studied in special experiments with the ^{3}He-counters positioned just outside the beam.

I want to emphasize, however, that the ^{3}He-counters were only used as flux monitors during the capture measurements. They are calibrated against flux measurements made with methane and BF_3-counters above and below 80 keV respectively.

C. M. NEWSTEAD: You have stated that to fit the gold data it was necessary to assume a value of the parameter (the Fermi-level-density parameter) of 0.16 MeV^{-1}. Since this parameter is directly proportional to g, the single-particle level density near the Fermi surface, and since this quantity is considered to be well-behaved with respect to mass number except in the region of closed shells, this value you require (which is an order of magnitude smaller than the trend in this mass region) would seem to indicate that something very unusual is happening in gold.

M. P. FRICKE: I certainly did not wish to suggest that theory and experiment can be reconciled with a change in level density. On the contrary, my purpose was to illustrate what a drastic change in the temperature would be required to do this.

M. C. MOXON: Can you say what cross-section you used for the $^{10}B(n,\alpha)$ reaction? Did the neutron flux measured with the BF_3-counter agree with that measured with the methane counter in the region of overlap?

M. P. FRICKE: Let me answer your second question first. We have not yet made measurements of the type we consider necessary to relate the $^{10}B(n,\alpha)$ cross-section directly to the hydrogen-scattering cross-section with suitable accuracy in the region of overlap in the present experiment, i. e. 80-100 keV. However, such measurements are planned at our laboratory for the near future.

The $^{10}B(n,\alpha)$ cross-section we used to calibrate the ^{3}He detectors at energies below 100 keV was the (1/v)-cross-section, and this differs from the Harwell results by ±4% in this energy region. However, I would like to point out that some recently published work at Idaho Nuclear has indicated that the response of a methane counter is non-linear at lower incident neutron energies. We used a linear fit to our observed variation of the proton-recoil pulse height with neutron energy, but we have also

calculated spectrum fractions for the methane counter using the Idaho Nuclear results. The non-linearity would introduce an error of about 4% in the flux we measured with the methane counter near 100 keV, but in a direction such that this would just about exactly cancel any error produced by deviations of the $^{10}B(n,\alpha)$ cross-section from (1/v) according to the Harwell data. But whether or not either, both or none of these differences in $^{10}B(n,\alpha)$ and the methane response hold up, our present results will still be good within the 5% uncertainty we have assigned to the flux measurements.

РЕАКЦИЯ (n, n'γ) НА ЯДРАХ ФТОРА, ЖЕЛЕЗА, КОБАЛЬТА, НИКЕЛЯ И ТАНТАЛА

Д. Л. БРОДЕР, А. Ф. ГАМАЛИЙ, А. И. ЛАШУК, И. П. САДОХИН
Физико-энергетический институт, Обнинск, Союз Советских Социалистических Республик

Presented by A.I. Abramov

Доклад представлен А.И. Абрамовым

Abstract — Аннотация

INELASTIC NEUTRON SCATTERING – (n, n' γ) – BY FLUORINE, IRON, COBALT, NICKEL AND TANTALUM NUCLEI.

Using a Ge(Li) semiconductor spectrometer the authors measured the cross-sections for the formation of gamma rays in inelastic neutron scattering by various nuclei: fluorine – for gamma lines with energies 110 and 200 keV in the neutron energy range 0.14-3.14 MeV; iron – for gamma lines with energies 847, 1030, 1240, 1250, 1410, 1810, 2100, 2112, 2280, 2350, 2430, 2545, 2610, 2775 and 3210 keV in the neutron energy range 0.90-6.0 MeV; cobalt – for gamma lines with energies 1095, 1190, 1280 and 1400 keV in the neutron energy range 1.14-2.68 MeV; nickel – for gamma lines with energies 1000, 1170, 1332, 1450, 1795, 2150 and 2210 keV in the neutron energy range 1.20-6.0 MeV; tantalum – for gamma lines with energies 137, 153, 302 and 482 keV in the neutron energy range 0.17-2.86 MeV. On the basis of the experimental data and of the energy level schemes of these nuclei conclusions are drawn regarding the excitation of individual levels and the total cross-section for inelastic neutron scattering.

РЕАКЦИЯ (n, n' γ) НА ЯДРАХ ФТОРА, ЖЕЛЕЗА, КОБАЛЬТА, НИКЕЛЯ и ТАНТАЛА.

Полупроводниковым Ge(Li) спектрометром иэмерены сечения образования γ-квантов в реакции неупругого рассеяния нейтронов на ядрах фтора для γ-линий с энергией 110 и 200 кэв в диапазоне энергий нейтронов 0,14-3,14 Мэв; железа – для γ-линий с энергией 847, 1030, 1240, 1250, 1410, 1810, 2100, 2112, 2280, 2350, 2430, 2545, 2610, 2775 и 3210 кэв в диапазоне энергий нейтронов 0,90-6,0 Мэв; кобальта – для γ-линий с энергией 1095, 1190, 1280 и 1400 кэв в диапазоне энергий нейтронов 1,14-2,68 Мэв; никеля – для γ-линий с энергией 1000, 1170, 1332, 1450, 1795, 2150 и 2210 кэв в диапазоне энергий нейтронов 1,20-6,0 Мэв; тантала – для γ-линий с энергией 137, 153, 302 и 482 кэв в диапазоне энергий нейтронов 0,17-2,86 Мэв. На основании экспериментальных данных и схем энергетических уровней указанных ядер делаются заключения о возбуждении отдельных уровней и полном сечении неупругого рассеяния нейтронов.

Измерения спектров γ-квантов, возникающих в реакции (n, n', γ) выполнены на электростатических ускорителях. Для получения нейтронов использовались реакции T(p, n) ^{3}He и D(d, n) ^{3}He. Разброс нейтронов по энергии не превышает ±32 кэв для реакции T(p, n) ^{3}He и ±50 кэв для реакции D(d, n) ^{3}He.

Для измерений γ-спектров использовалась кольцевая геометрия [1]. Регистрация спектров осуществлялась 512- и 4096-канальным амплитудным анализатором.

В качестве детектора γ-квантов использовался полупроводниковый Ge(Li) детектор с толщиной активного слоя 5 мм, обладающий энергетическим разрешением γ-линии с энергией 1332 кэв ^{60}Co – 4,5 кэв и γ-линии с энергией 85 кэв ^{169}Tu – 2,1 кэв.

ТАБЛИЦА 1. СЕЧЕНИЯ ОБРАЗОВАНИЯ γ-КВАНТОВ В РЕАКЦИИ $^{19}F(n, n' \gamma)\ ^{19}F$

E_γ / E_n, Мэв	110 кэв σ, барн	200 кэв σ, барн	σ_{in} барн	E_γ / E_n, Мэв	110 кэв σ, барн	200 кэв σ, барн	σ_{in} барн
0,14	0,54	–	–	0,55	0,76	1,53	2,28
0,16	0,73	–	–	0,57	0,61	1,45	2,06
0,21	1,33	–	–	0,59	0,66	1,46	2,12
0,23	2,15	0,03	2,18	0,62	0,50	1,38	1,88
0,24	2,45	0,03	2,48	0,64	0,44	1,35	1,79
0,25	3,40	0,02	3,42	0,66	0,43	1,08	1,51
0,27	4,09	0,30	4,39	0,72	0,41	1,29	1,70
0,29	3,30	0,57	3,87	0,80	0,65	1,15	1,80
0,30	2,72	0,42	3,14	0,90	0,36	0,99	1,35
0,31	2,50	0,65	3,15	0,99	0,34	0,97	1,31
0,33	2,23	0,80	3,03	1,05	0,44	0,80	1,24
0,34	1,68	0,90	2,58	1,24	0,62	0,75	1,62
0,36	1,45	1,27	2,72	1,66	0,45	0,74	
0,37	1,23	1,52	2,75	2,12	0,29	0,89	
0,38	1,28	1,57	2,85	2,61	0,21	0,55	
0,40	1,32	1,95	3,27	3,14	0,12	0,58	
0,42	0,89	2,22	3,11				
0,46	0,72	1,81	2,53				
0,48	1,15	2,02	3,17				
0,51	1,21	1,94	3,15				
0,53	0,80	1,66	2,46				

ТАБЛИЦА 2. СЕЧЕНИЯ ОБРАЗОВАНИЯ γ-КВАНТОВ В РЕАКЦИИ Fe(n, n' γ)Fe, мб

E_n Мэв	847	1038	1240	1470	1770	1810	2096	2112	2274	2523	2610	2984	3449	3601	σ_{in}
0,93	290	–	–	–	–	–	–	–	–	–	–	–	–	–	290
1,16	616	–	–	–	–	–	–	–	–	–	–	–	–	–	616
3,40	1065	27	123	43	–	135	43	81	27	–	–	–	–	–	1108
3,54	1158	40	121	51	–	168	53	81	33	–	–	–	–	–	1209
3,67	1215	48	146	51	–	156	78	112	56	14	9	–	12	–	1278
3,79	1160	34	242	63	–	242	88	128	–	–	–	–	–	–	–
3,86	1155	62	218	67	–	249	109	133	127	27	55	–	37	33	1292
3,91	1150	49	230	76	–	227	78	125	107	85	64	–	28	53	1307
4,0	1180	57	230	65	16	265	48	140	109	102	140	–	45	52	1342
4,12	1145	82	254	86	39	242	102	137	127	100	85	38	44	57	1332
4,24	1134	54	215	56	32	231	59	98	97	89	112	–	40	50	1280
4,40	1020	54	247	61	44	193	33	92	99	108	72	38	42	69	1192
4,50	1085	45	222	86	45	176	59	120	145	77	100	21	54	70	1295
4,56	1158	67	203	63	–	197	–	–	–	–	–	–	40	–	–
4,62	1180	40	215	87	–	158	76	144	121	65	–	–	38	–	–
4,85	1128	62	272	71	49	186	56	125	127	–	108	–	42	47	1288
4,99	1150	–	213	107	–	238	–	–	–	–	–	–	31	–	–
5,17	1130	30	299	67	–	125	42	80	73	–	72	–	47	38	1282
5,42	1120	–	281	76	–	172	–	–	–	–	–	–	42	–	–
5,53	1110	20	250	122	–	149	39	112	–	–	102	–	40	56	1328
5,96	1240	–	250	99	84	280	–	–	–	–	–	–	27	–	–
6,59	1300	–	242	65	57	217	–	–	–	–	–	–	35	–	–
7,37	1310	–	364	92	80	300	–	–	–	–	–	–	–	–	–

ТАБЛИЦА 3. СЕЧЕНИЯ ОБРАЗОВАНИЯ γ-КВАНТОВ В РЕАКЦИИ Ni(n, n' γ)Ni

E_γ, кэв / E_n, Мэв	860	1000	1170	1332	1450	1795	2150	2240	3040	σ_{in}	σ_{in}
	мб	мб	мб	мб	мб	мб	мб	мб	мб	барн	[2]
1,81	–	–	41	0,21	0,40	–	–	–	–	–	–
2,52	–	–	65	0,35	0,59	–	–	–	–	–	–
2,87	–	13	70	0,45	0,60	–	–	–	–	–	–
2,98	–	15	71	0,44	0,65	–	–	–	–	–	–
3,52	80	43	77	0,43	0,75	–	–	–	–	–	–
3,79	–	51	70	0,49	0,62	38	15	63	–	1,20	1,25
3,90	68	50	70	0,44	0,75	–	–	–	–	–	–
3,97	59	53	70	0,46	0,64	–	–	–	–	–	–
4,01	–	52	70	0,49	0,65	30	16	60	17	1,24	1,25
4,12	65	54	70	0,50	0,65	–	–	–	–	–	–
4,22	70	51	68	0,48	0,61	–	–	–	–	–	–
4,32	83	55	72	0,49	0,63	–	–	–	–	–	–
4,39	–	54	70	0,50	0,63	28	15	48	14	1,23	1,19
4,42	60	61	77	0,52	0,67	–	–	–	–	–	–
4,50	–	45	73	0,42	0,55	30	15	40	16	1,25	1,18
4,56	62	64	76	0,47	0,63	–	–	–	–	–	–
4,62	57	59	81	0,43	0,65	–	–	–	–	–	–
4,84	–	50	78	0,46	0,64	35	16	34	15	1,21	1,15
4,99	79	66	74	0,49	0,61	–	–	–	–	–	–
5,17	–	47	75	0,49	0,60	31	15	34	15	1,19	1,12
5,42	–	74	80	0,41	0,51	30	16	59	16	1,03	1,10
5,96	–	57	81	0,50	0,61	–	–	–	–	–	–
6,59	–	60	73	0,39	0,51	–	–	–	–	–	–

ТАБЛИЦА 4. СЕЧЕНИЯ ОБРАЗОВАНИЯ γ-КВАНТОВ В РЕАКЦИИ $^{59}Co(n, n' \gamma)^{59}Co$

E_n Мэв	σ (1095 кэв) барн	σ (1190 кэв) барн	σ (1280 кэв) барн	σ (1400 кэв) барн	σ_{in} барн
1,14	0,07	–	–	–	0,07
1,21	0,15	0,21	–	–	0,36
1,24	0,16	0,28	–	–	0,44
1,27	0,17	0,26	–	–	0,43
1,35	0,23	0,36	–	–	0,59
1,44	0,19	0,40	0,08	–	0,60
1,57	0,17	0,43	0,15	–	0,75
1,65	0,20	0,56	0,13	0,06	0,90
1,74	0,21	0,50	0,13	0,14	0,98
1,83	0,27	0,55	0,15	0,11	1,08
1,91	0,24	0,52	0,18	0,12	1,56
2,00	0,19	0,49	0,15	0,16	0,99
2,10	0,17	0,58	0,18	0,18	1,11
2,20	0,18	0,53	0,20	0,18	1,08
2,28	0,16	0,59	0,28	0,29	1,26
2,36	0,19	0,68	0,27	0,21	1,35
2,54	0,20	0,66	0,35	0,23	1,44
2,61	0,21	0,66	0,32	0,24	1,43
2,68	0,22	0,64	0,34	0,29	1,49

ТАБЛИЦА 5. СЕЧЕНИЯ ОБРАЗОВАНИЯ γ-КВАНТОВ В РЕАКЦИИ $^{181}Ta(n, n' \gamma)^{181}Ta$

E_n, Мэв \ E_γ, Мэв	137 кэв барн	153 + 163 кэв барн	302 кэв мбарн	482 кэв барн	σ_{in} барн
0,17	0,05	–	–	–	0,05
0,21	0,07	–	–	–	0,07
0,23	0,04	0,07	–	–	0,11
0,25	0,07	0,07	–	–	0,14
0,26	0,11	0,09	–	–	0,20
0,28	0,13	0,13	–	–	0,26
0,34	0,13	0,15	–	–	0,28
0,35	0,20	0,17	–	–	0,37
0,38	0,18	0,19	15	–	0,38
0,41	0,15	0,17	11	–	0,33
0,44	0,25	0,19	15	–	0,45
0,47	0,31	0,18	10	–	0,50
0,51	0,40	0,19	25	0,05	0,66
0,53	0,29	0,17	20	0,04	0,52
0,57	0,37	0,17	19	0,07	0,63
0,59	0,43	0,19	54	0,11	0,78
0,66	0,39	0,20	50	0,15	0,79
0,71	0,54	0,21	40	0,21	1,00
0,77	0,64	0,18	54	0,25	1,12
0,81	0,66	0,17	48	0,24	1,12
0,90	0,75	0,21	75	0,39	1,42
0,97	0,83	0,25	110	0,40	1,59
1,04	0,86	0,26	130	0,44	1,69
1,08	1,02	0,40	140	0,47	2,03
1,15	1,10	0,59	145	0,56	2,39
1,20	1,32	0,73	150	0,60	2,80
1,27	1,27	0,75	140	0,64	2,80
1,48	1,38	–	130	0,74	
1,66	–	–	132	0,65	
1,88	–	–	122	0,70	
2,00	–	–	125	0,67	
2,12	–	–	113	0,64	
2,23	–	–	141	0,49	
2,36	–	–	150	0,68	
2,61	–	–	–	0,66	
2,86	–	–	–	0,77	

Суммарная ошибка в определении значений сечений выхода γ-квантов не превышает 5-7% для γ-линий с энергиями 110, 200 кэв для ядер фтора; 847, 1240, 1810, 2430 кэв – для ядер железа; 1332, 1450, 1795 кэв – для ядер никеля; 137 и 482 кэв – для ядер тантала, увеличиваясь до 12 ÷ 15% для других менее интенсивных гамма-линий.

В табл. 1-5 представлены результаты измерений сечений образования гамма-квантов для ядер фтора, железа, кобальта, никеля и тантала при неупругом рассеянии нейтронов.

ЛИТЕРАТУРА

[1] БРОДЕР, Д.Л., ЛАШУК, А.И., САДОХИН, И.П., Изв. АН СССР, сер. физ. 25 (1961) 309.

[2] SCHMIDT, J.J., Neutron Cross Sections for Fast Reactor Materials, Part I, KFK-120, Karlsruhe, 1966.

NEUTRON SCATTERING CROSS-SECTIONS OF IRON

Y. TOMITA, K. TSUKADA, M. MARUYAMA, S. TANAKA
Japan Atomic Energy Research Institute,
Tokai-mura, Naka-gun,
Ibaraki-ken,
Japan

Abstract

NEUTRON SCATTERING CROSS-SECTIONS OF IRON.

The differential cross-sections of elastic and inelastic scatterings by iron have been measured at incident neutron energies from 1.43 to 2.15 MeV in steps of 40 keV with an energy resolution of 50 keV. Scattered neutrons and gamma rays produced in the inelastic process were observed at the same time with a Mobley bunching system of the JAERI 5.5-MV Van de Graaff accelerator and a time-of-flight spectrometer. The neutron scattering cross-sections were measured relative to the p-n cross sections, and the neutron-energy standard was the 2.08-MeV resonance of carbon. The cross-sections of gamma-ray production were measured with the same liquid-scintillation detector as the neutron detector, and normalized to the neutron scattering cross-sections. Both neutron and gamma-ray cross-sections were corrected for multiple scattering and attenuation of neutrons in the scattering sample, and source-to-sample angular spread. The angular distributions of the neutron and gamma-ray cross-sections thus obtained were fitted with Legendre expansions of a form of $\frac{1}{4\pi}\sum_{\ell=0}^{L} B_\ell P_\ell (\cos\theta)$ ($\ell_{max} = 6$ for elastic scattering). Intermediate structures, which are similar to those observed by Elwyn and Monahan, and Barnard et al. in the energy region of 0.3 to 1.5 MeV, appear in the excitation functions of some of the expansion coefficients of the cross-sections, i.e. the coefficients of $\ell = 0$ to 4 for the elastic scattering, $\ell = 0$ for the inelastic scattering and $\ell = 0$ and 2 for the gamma-ray production. Energies of humps in the excitation functions are about 1.6 and 2.05 MeV.

1. INTRODUCTION

Since the proposal [1] of the concept of doorway states, many attempts have been made to find them among intermediate structures in neutron cross-sections. Although the identification of an intermediate structure as a doorway state needs caution, some of the structures observed in the cross-sections of lead isotopes [2, 3] and ^{56}Fe [4] have been shown to be consistent with the doorway-state picture.

For ^{56}Fe Monahan and Elwyn [4] measured the angular distributions and polarizations of scattered neutrons in the energy range 0.35 - 0.96 MeV, and with the help of the fine-structure data by Bowman et al. [5] found a possible doorway-state resonance at E_n = 0.36 MeV. Similar structures were observed by Cabé et al. [6] and by Bernard et al. [7] at energies below 1.5 MeV. The present authors [8] also noticed a dip at about 1.7 MeV in the excitation function of inelastic scattering to the first excited state. These were the motive for the present investigation.

In this work the differential cross-sections of elastic and inelastic scattering and the angular distributions of gamma rays associated with the decay of the first excited state were measured for iron in the energy range 1.43 - 2.15 MeV. Two structures with intermediate widths have been found at about 1.6 MeV and 2.05 MeV in the excitation functions.

2. EXPERIMENTAL PROCEDURE

The cross-sections were measured by the time-of-flight method. Neutrons were generated by the $^{3}H(p, n)^{3}He$ reaction using the JAERI 5.5-MV Van de Graaff accelerator and a Mobley beam-bunching system. The tritium target was a gas cell about 3 cm long and was filled with tritium gas at 42 cmHg. Scattering samples were placed at a distance of 11.5 cm from the centre of the cell. They were in the form of hollow cylinders; a natural iron sample 4 cm high with outside diameter 2.5 cm and inside diameter 1.5 cm, and a polyethylene sample 4 cm high with outside diameter 1.0 cm and inside diameter 0.8 cm. The latter was used as the cross-section standard by employing the known cross-sections of hydrogen. Scattered neutrons were observed by a detector consisting of an NE-213 liquid scintillator and an XP-1040 photo-multiplier placed at a distance of 3 m from the samples. Gamma rays were also detected by the neutron detector. Another detector with a small organic scintillator monitored the neutron yield by the time-of-flight method. All the measurements at the same energy were normalized by these monitor counts.

The experiment was performed at incident neutron energies between 1.43 and 2.15 MeV in steps of about 40 keV and at thirteen lab angles between 30° and 146°. Another measurement at 20° was added for several energies. The energy spread of the incident neutrons was about 50-keV FWHM. Incident neutron energies were calibrated by the 2.08-MeV resonance of ^{12}C. Since the excitation of the second level at 2.085 MeV could not take place or was negligible at the energy region investigated, the gamma rays detected were the 0.845-MeV gamma rays from the first level of ^{56}Fe with a small amount of admixture of the 1.409-MeV gamma rays from ^{54}Fe. Both the elastic and inelastic scattering cross-sections were corrected for the effect of flux attenuation and multiple scattering and for source-to-sample geometrical effect by the Monte-Carlo method. Absolute values of the $(n, n'\gamma)$ cross-sections were normalized to the (n, n') cross-sections. The effect of neutron multiple scattering on the gamma-ray angular distributions was corrected by an analytical method similar to the one used by Cox [9].

3. RESULTS

The measured angular distributions in the centre-of-mass system were fitted with Legendre polynomials of the form

$$\frac{d\sigma}{d\Omega} = \frac{1}{4\pi} \sum_{\ell=0}^{L} B_\ell P_\ell (\cos \theta)$$

where L was taken as 6 for elastic scattering and 4 for inelastic scattering and gamma rays. These coefficients are shown in Fig. 1 for elastic scattering, in Fig. 2 for inelastic scattering and in Fig. 3 for gamma rays as functions of incident neutron energies. Uncertainties shown in the figures include only those due to statistics in the measurement and in the Monte-Carlo calculations. The largest uncertainties not included will be those in

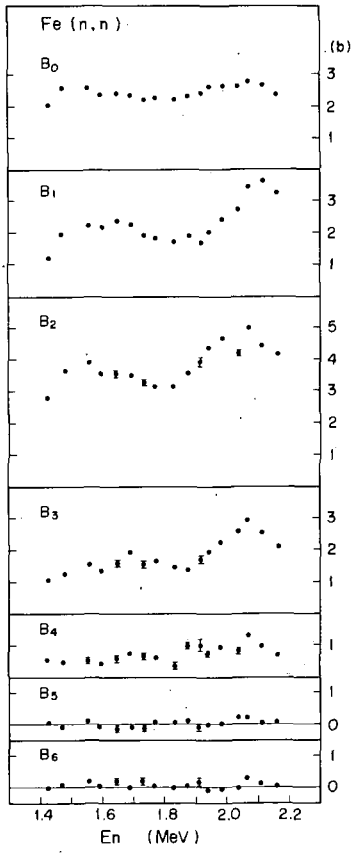

FIG. 1. Legendre expansion coefficients for the differential elastic scattering cross-sections of Fe.

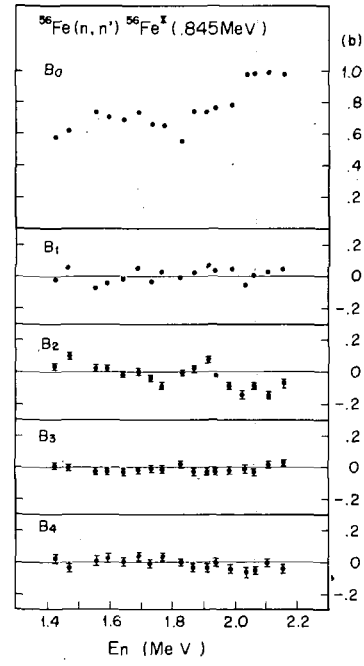

FIG. 2. Legendre expansion coefficients for the differential inelastic scattering cross-sections of ^{56}Fe.

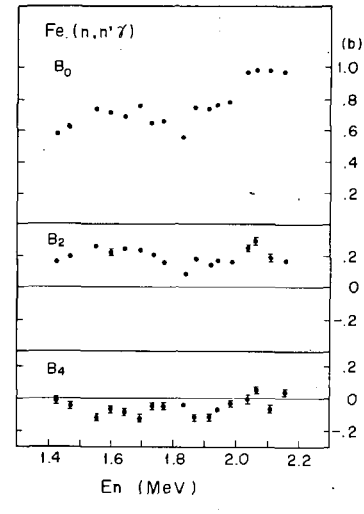

FIG. 3. Legendre expansion coefficients for the angular distributions of gamma rays from the first excited state of Fe.

the detector efficiency, which was determined by the use of the known cross-sections of the $^{3}H(p, n)^{3}He$ and $^{7}L(p, n)^{7}Be$ reactions. These uncertainties may amount to 5% or more. Strong structures are seen in the coefficients of $\ell = 1$ to 3 for elastic scattering at about 1.6 MeV and 2.05 MeV. They also appear to lesser degrees in the coefficients of $\ell = 0$ for elastic scattering, $\ell = 0$ and 2 for inelastic scattering and $\ell = 0$, 2 and 4 for gamma rays. The widths of the humps are about 200 MeV, which is of the same magnitude as were observed [4-6] for the structures at lower energies. It is of much interest whether or not each of the observed structures can be attributed to a single partial wave and be regarded as an intermediate resonance. If the weak structures seen in $\ell = 4$ for gamma rays are not statistical fluctuations and are due to intermediate resonances, their spins cannot be smaller than 5/2. But the structures are too irregular to draw such conclusion until the complete analysis of all cross-sections is made. An analysis on this point as well as an optical-model analysis will be published elsewhere.

REFERENCES

[1] RESHBACH, H., KERMAN, A.K., LEMMER, R.H., Annls Phys. (NY) 41 (1967) 230.
[2] FARRELL, J.A., KYKER, G.C., Jr., BILPUCH, E.G., NEWSON, H.W., Physics Lett. 17 (1965) 286.
[3] LEJEUNE, A., MAHAUX, C., Z. Phys. 207 (1967) 35.
[4] MONAHAN, J.E., ELWYN, A.J., Phys. Rev. Lett. 20 (1968) 1119; ELWYN, A.J., MONAHAN, J.E., Nucl. Phys. A123 (1969) 33.
[5] BOWMAN, C.D., BILPUCH, E.G., NEWSON, H.W , Annls Phys. (NY) 17 (1962) 319.
[6] CABÉ, J., LAURAT, K., YVON, P., BARDOLLE, G., Nucl. Phys. A102 (1967) 92.
[7] BARNARD, E., DE VILLIERS, J.A.M., ENGELBRECHT, C.A., REITMANN, D., SMITH, A.B., Nucl. Phys. A118 (1968) 321.
[8] TSUKADA, K., TANAKA, S., TOMITA, Y., MARUYAMA, M., Nucl. Phys. A125 (1969) 641.
[9] COX, S.A., Nucl. Instrum. Meth. 56 (1967) 245.

WIDTH-FLUCTUATION AND RESONANCE-INTERFERENCE EFFECTS IN NEUTRON SCATTERING CROSS-SECTIONS OF ALUMINIUM, COPPER AND ZINC

K. TSUKADA, Y. TOMITA, S. TANAKA, M. MARUYAMA
Japan Atomic Energy Research Institute,
Tokai-mura, Naka-gun,
Ibaraki-ken, Japan

Abstract

WIDTH-FLUCTUATION AND RESONANCE-INTERFERENCE EFFECTS IN NEUTRON SCATTERING CROSS-SECTIONS OF ALUMINIUM, COPPER AND ZINC.

Neutron scattering cross-sections of aluminium, copper and zinc have been analysed in the energy region of 1 to 8 MeV by means of optical and statistical models, the width-fluctuation effect and the resonance-interference effect being taken into account. Data of the cross-sections used in the analysis include those at 4.81, 5.96, 7.03 and 8.03 MeV for aluminium, at 1.71 and 2.24 MeV for copper and at 1.71, 2.24, 4.48, 5.92, 6.97 and 7.99 MeV for zinc which were measured in our laboratory, and data available in BNL-400 and CCDN. Best-fit sets of optical-model parameters are sought for the angular distributions of elastic scattering, the inelastic scattering cross-sections and the total cross-sections at each energy. By using a computer code STAX2, calculations on the basis of Hauser-Feshbach's formulation and Moldauer's formulation are performed. In the latter formulation, the calculations are carried out with the maximum and zero values of Moldauer's parameter Q. Difference in fitting among the three calculations appears in backward angles in a limited energy region. Systematic energy variations of the optical-model parameters are seen more or less in the region below 4 MeV for all cases. In the region above 4 MeV, where the Moldauer effect is ineffective, the energy variations are not so pronounced. Judging from these two, the calculation with the maximum value of Q is considered to be best among the three calculations to reproduce the measured data, though fluctuations in the cross-sections and simple forms of the angular distributions in the lower energy region make the choice ambiguous.

1. INTRODUCTION

The level width-fluctuation effect was taken into account in the statistical calculation of reaction cross-sections by Dresner [1] and Lane and Lynn [2], and it was formulated together with the resonance-interference effect by Moldauer [3]. Details of the effects, however, have not yet been clear, because of insufficient accuracy of available data, statistical fluctuations in the cross-sections, and ambiguity of the resonance and optical-model parameters used in the calculation of the cross-sections. In most analyses of low-energy neutron-scattering data, both effects have been taken into account only for inelastic scattering [4]. Since the effects have a large influence also upon the compound elastic-scattering component of the elastic scattering cross-section, they should be taken into account for both elastic and inelastic scattering cross-sections.

The following two methods of analysis are useful to see the effects:

(1) Comparison of fitness of the cross-sections calculated with and without the effects to the measured ones. The optical-model parameters used in the calculations are obtained by extrapolating the parameters obtained at higher energies where the effects are ineffective.
(2) The measured cross-sections are analysed with and without the effects to obtain the optical-model parameters. The energy dependences of the parameters obtained in both cases are examined. Some anomaly may be expected unless the effects are correctly taken into consideration.

In Moldauer's formulation, a parameter Q is defined [3] as a measure of the effects, and most analyses hitherto published [4] are with Q = 0 and

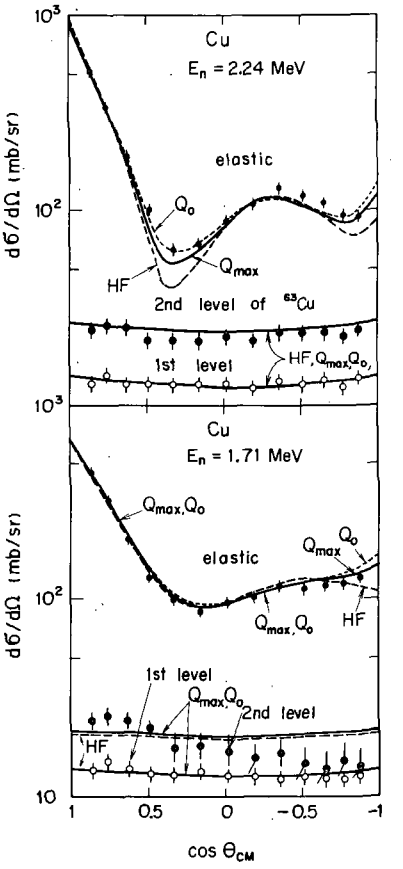

FIG. 1a. Differential elastic and inelastic scattering cross-sections of copper at 1.71 and 2.24 MeV; the errors are indicated by vertical bars; the curves show the angular distributions calculated with the best-fit sets of potential parameters. The symbols HF, Q_{max} and Q_0 are defined in the text.

its other extreme, $Q = 1$. As pointed out in our previous paper [5], however, the case $Q = 1$ sometimes leads to an unphysical result at a high energy, that is, $\sigma_{cc} < 0$, where σ_{cc} is the compound elastic scattering cross-section through a channel c. It is necessary to calculate an upper limit value of Q_c at each channel c instead of using $Q_c = 1$.

In the present paper, we analyse neutron total cross-sections, elastic scattering differential cross-sections, and inelastic scattering cross-sections of aluminium, copper and zinc in the energy range of 1 to 8 MeV by using the second method mentioned above. We have obtained the best-fit sets of optical-model potential parameters at 10 energies for aluminium, and at 12 energies for copper and zinc in three cases of Q_0 (the case $Q_c = 0$), Q_{max} (the case of the maximum Q_c) and HF (Hauser-Feshbach's case). The data used include the elastic and inelastic ones on copper and zinc which we have measured at 1.71 and 2.24 MeV and those of aluminium and zinc at 4.5 to 8 MeV reported in our other paper [6]. Energy dependences of the potential parameters obtained show some anomalies, a part of which seems to be due to the level width-fluctuation and resonance-interference effects.

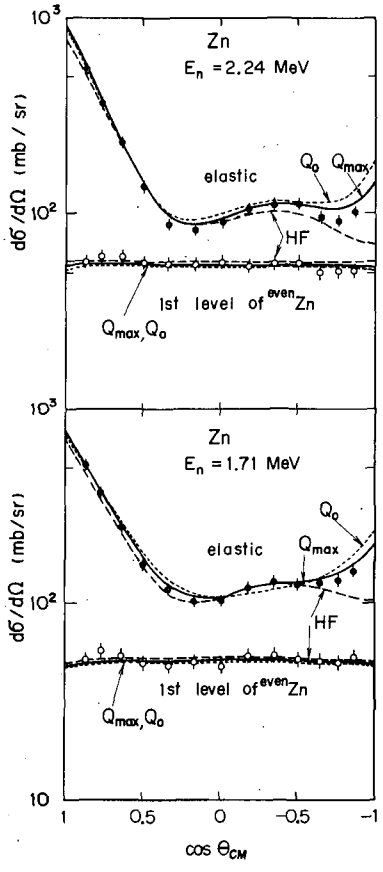

FIG.1b. Differential elastic and inelastic scattering cross-sections of zinc; same as in Fig.1a.

TABLE I. MEASURED CROSS-SECTIONS OF COPPER AND ZINC

E_n (MeV)	Cu σ_{total}[a] (b)	Cu σ_{ela} (b)	Cu σ_{inela} (b)	Zn σ_{total}[a] (b)	Zn σ_{ela} (b)	Zn σ_{inela} (b)
	3.1	2.00	1st (nat)	3.2	2.43	1st (^{e}Zn)
1.71			0.164			0.645
	±0.1	±0.05	±0.012	±0.2	±0.04	±0.013
			2nd (nat)			
			0.232			
			±0.033			
	3.1	2.02	1st (nat)	3.2	2.25	1st (^{e}Zn)
2.24			0.165			0.690
	±0.1	±0.04	±0.012	±0.2	±0.04	±0.013
			2nd (^{63}Cu)			
			0.294			
			±0.018			

[a] References [7] and [8].

2. NEUTRON CROSS-SECTIONS OF ALUMINIUM, COPPER AND ZINC

Neutron total cross-sections and scattering cross-sections which are used in the present analyses are those in Refs [7], [8] and [9] in addition to our data shown below.

The differential cross-sections of copper and zinc for elastic and inelastic scattering were measured at incident neutron energies of 1.71 and 2.24 MeV with an energy spread of about 90 keV and at scattering angles of 30° to 150° in 10° steps. The measurements were carried out with neutrons produced by the $^{3}H(p,n)^{3}He$ reaction and a 5.5-MV pulsed-beam Van de Graaff accelerator with a Mobley-type beam buncher. Both the elastic and inelastic cross-sections are relative to the $^{1}H(n,n)^{1}H$ cross-sections [7], and are corrected for multiple-scattering, flux-attenuation and source-to-sample geometrical effects in the scattering samples and polyethylene by using the Monte-Carlo computer code [10] MULT-1. The results are shown in Figs 1a and 1b; the errors of the cross-sections shown in the figure are mainly statistical. The integrated values are shown in Table I.

3. ANALYSES

Differential cross-sections for elastic scattering are analysed with neutron total and inelastic scattering cross-sections by using the optical model and the statistical model. The form of the optical potential used is

$$-V(r) = Vf(r) + iWg(r) + V_{so}\, 1/r\, h(r)\, \lambda_\pi^2 \vec{l}\cdot\vec{\sigma} \tag{1}$$

$$f(r) = (1 + \exp\{(r - R_0)/a\})^{-1}$$

$$g(r) = 4 \exp\{(r - R_s)/b\}\, (1 + \exp\{(r - R_s)/b\})^{-2}$$

$$h(r) = 1/a\, \exp\{(r - R_0)/a\}\, (1 + \exp\{(r - R_0)/a\})^{-2}$$

$$R_0 = r_0 A^{1/3},\quad R_s = r_s A^{1/3},\quad \lambda_\pi = \hbar/m_\pi c$$

The number of free parameters is seven: V, W, V_{so}, r_0, r_s, a and b. The best-fit potential parameter set is sought to make the χ^2-value defined below minimum

$$\chi^2 = W_{ela} \sum_i^N \left[\left\{ \left(\frac{d\sigma_{ela}}{d\Omega_i} \right)_{exp} - \left(\frac{d\sigma_{ela}}{d\Omega_i} \right)_{cal} \right\} / \Delta \left(\frac{d\sigma_{ela}}{d\Omega_i} \right)_{exp} \right]^2$$

$$+ W_{inela} \{ (\sigma_{inela,\,exp} - \sigma_{inela,\,cal}) / \Delta\sigma_{inela,\,exp} \}^2$$

$$+ W_{total} \{ (\sigma_{total,\,exp} - \sigma_{total,\,cal}) / \Delta\sigma_{total,\,exp} \}^2 \tag{2}$$

$$N W_{ela} + W_{inela} + W_{total} = 1$$

where W_{ela}, W_{inela} and W_{total} are weights of the data, and $\Delta(d\sigma/d\Omega_i)_{exp}$ and $\Delta\sigma_{exp}$ are their errors. The sub-indices exp and cal show measured and calculated values, respectively.

Compound elastic and inelastic cross-sections are calculated by the use of both Hauser-Feshbach's and Moldauer's formulations [1, 3, 11]. In Moldauer's formulation, the cross-section $\sigma_{cc'}$ through the compound process is expressed as

$$\sigma_{cc'} = \pi \lambda_{\mu c} \left(\frac{\Theta_{\mu c}\, \Theta_{\mu c}}{\Theta_\mu} \right) \left(- \delta_{cc'} \frac{1}{4} Q_c (\Theta_{\mu c})_\mu^2 \right) \tag{3}$$

$$\Theta_\mu = \frac{2\pi}{D} N_\mu^2 \Gamma_{\mu c} \tag{4}$$

$$Q_c = (2B_c/N^2) \left(1 - \Phi((\Theta_{\mu c})_\mu / 2\pi N^2) \right) \tag{5}$$

TABLE II. THE BEST-FIT SETS OF OPTICAL POTENTIAL PARAMETERS OF COPPER AND ZINC

	E_n(MeV)	Model	V(MeV)	a(fm)	W(MeV)	b(fm)	χ^2
Zn	1.71	HF	55.9	0.28	2.9	0.80	2.0
		Q_{max}	53.5	0.60	10.8	0.46	0.4
		Q_0	53.8	0.67	17.5	0.36	1.4
	2.24	HF	57.6	0.08	4.5	0.77	2.9
		Q_{max}	54.5	0.50	11.7	0.50	0.8
		Q_0	54.9	0.59	14.7	0.44	2.2
Cu	1.71	HF	57.6	0.22	2.5	0.75	2.2
		Q_{max}	54.5	0.52	9.0	0.43	1.5
		Q_0	53.7	0.60	13.8	0.35	2.2
	2.24	HF	51.4	0.63	5.1	0.60	4.5
		Q_{max}	51.2	0.71	8.3	0.51	2.7
		Q_0	51.3	0.76	11.2	0.45	2.6

The 1st term in the square bracket of Eq.(3) becomes closer to $(\Theta_{\mu c})_\mu (\Theta_{\mu c})_\mu / (\Theta_\mu)_\mu$, if $c \neq c'$, with increasing number of channels. For elastic scattering ($c = c'$), however, it is not the case. The second term expresses the resonance-interference effect, and it is not zero only for elastic scattering.

In these relations the factors N_μ and B_c defined by Moldauer [3] are

$$N_\mu = |g_{\mu c}|^2 / \Gamma_{\mu c} \geq 1 \tag{6}$$

$$B_c (= |b_c|^2) = |(g_{\mu c}{}^2)_\mu| / (|g_{\mu c}|^2)_\mu \tag{7}$$

$$= \begin{cases} 1 \text{ for the Porter-Thomas distribution of the partial widths of resonances,} \\ 0 \text{ for the Gaussian distribution of the partial widths.} \end{cases}$$

In addition to these factors, values of $Re(b_c b^*_{c'}/|b_c b^*_{c'}|)$ must be estimated for the calculation of differential cross-section [4]. In the present analysis we perform calculations with two extreme values of Q_c, that is, zero and maximum. This maximum value is obtained with

$$\left.\begin{aligned} N_\mu &= 1, \\ B_c &= 1, \end{aligned}\right\} \tag{8}$$

for all channels. We assume for all c and c'

$$Re(b_c b^*_{c'}/|b_c b^*_{c'}|) = 1 \tag{9}$$

The results with $Re(b_c b^*_{c'}) = 0$, however, are almost similar to the present ones.

A computer code [12] STAX2 is used in the calculations. As a result of preliminary studies where all seven free parameters of the optical

TABLE IIIA. THE VALUES OF χ^2 FOR THE BEST-FIT SETS OF POTENTIAL PARAMETERS OF ALUMINIUM

E_n(MeV)	Model	χ^2 [a]	E_n(MeV)	Model	χ^2 [a]
0.98	HF	0.3	3.50	HF	1.0
	Q_{max}	0.5		Q_{max}	1.4
	Q_0	0.4		Q_0	2.2
2.01	HF	0.9	4.00	HF	0.6
	Q_{max}	1.1		Q_{max}	0.7
	Q_0	3.7		Q_0	2.1
2.47	HF	2.7	4.81	HF	2.9
	Q_{max}	3.3	5.96	HF	10.3
	Q_0	3.7	7.02	HF	8.3
3.01	HF	0.4	8.03	HF	8.4
	Q_{max}	0.6			
	Q_0	0.1			

[a] Values of V, W, a and b are searched for the best fit.

TABLE IIIB. THE VALUES OF χ^2 FOR THE BEST-FIT SETS OF POTENTIAL PARAMETERS OF COPPER AND ZINC

E_n(MeV)	Model	Cu χ^2 [b]	Cu χ^2_c [c]	Zn χ^2 [b]	Zn χ^2_c [c]
1.30	HF	1.0[a]		0.1	
	Q_{max}	0.7[a]		0.5	
	Q_0	0.7[a]		0.4	
1.50	HF	0.5[a]		0.2	
	Q_{max}	0.8[a]		1.4	
	Q_0	1.2[a]		2.8	
1.71	HF	2.2[a]	163	2.0	6.5
	Q_{max}	1.5[a]	73	0.4	10.0
	Q_0	2.2[a]		1.4	14.0
2.24	HF	4.5[a]	18.9	2.9	7.7
	Q_{max}	2.7[a]	4.2	0.8	11.4
	Q_0	2.6[a]	4.4	2.2	17.6
2.47	HF	3.0[a]	14.2	2.3	10.4
	Q_{max}	1.4[a]	5.9	5.1	19.0
	Q_0	0.2[a]		12.7	
3.00	HF	3.2[a]		8.4	17.0
	Q_{max}			0.7	12.3
	Q_0			5.3	
3.50	HF	4.7[a]		0.9	
	Q_{max}			7.0	
	Q_0			33.8	
4.00	HF	2.6[a]		0.7	
4.5	HF	1.7[a]		5.7	
6.0	HF	2.3[a]		10.2	
7.0	HF	1.9[a]		12.3	
8.0	HF	1.8[a]		25.7	

[a] $\frac{d\sigma_{ela}}{d\Omega_i}$ $(i=1\sim N)$, σ_{total} and σ_{inela} for the 1st level are used in the analyses; in the cases without footnote mark, $\frac{d\sigma_{ela}}{d\Omega_i}$ and σ_{total} are used.

[b] Values of V, W, a and b are sought for the best fit.

[c] Values of all potential parameters are fixed.

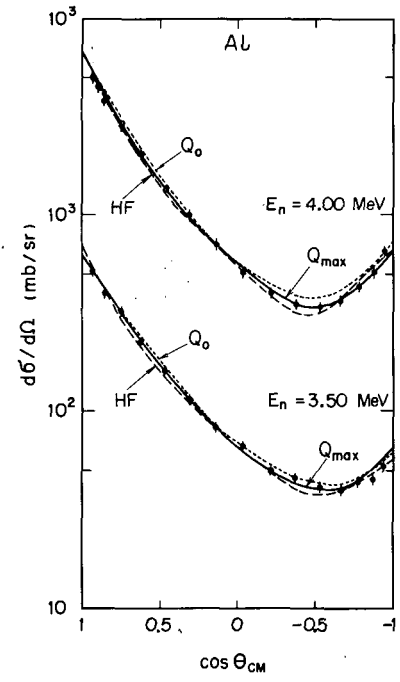

FIG. 2. Differential elastic-scattering angular distributions for aluminium at 3.50 and 4.00 MeV; the closed circles represent the results by Holmqvist; the curves show the calculated angular distributions.

potential were searched for the best-fit sets, values of the parameters r_0, r_s and V_{so} are fixed as in the following:

$$\begin{aligned} r_0 &= r_s = 1.2 \text{ fm} && \text{for all elements} \\ V_{s0} &= 10 - 3/8\ E && \text{in MeV for Al} \\ V_{s0} &= 9 - 3/8\ E && \text{in MeV for Cu} \\ V_{s0} &= 7 - 3/8\ E && \text{in MeV for Zn} \end{aligned} \qquad (10)$$

The weight factors in Eq.(2) are chosen so that the neutron total cross-section, the elastic scattering cross-section and the inelastic scattering cross-section equally contribute to the analysis. If the inelastic scattering cross-section is available

$$W_{inela} = W_{total}$$

In the case that the error $\Delta(d\sigma_{ela}/d\Omega_i)$ includes not only a statistical one but also systematic ones correctly

$$W_{total} = W_{ela}$$

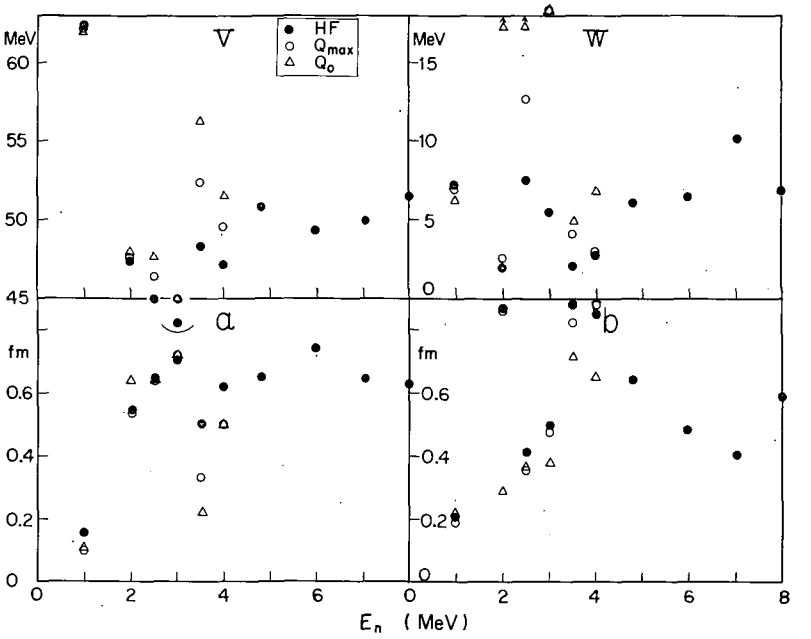

FIG.3a. Potential parameters V, W, a and b in the best-fit sets for aluminium; the other parameters V_{SO}, r_0 and r_S are shown in the text. The abscissa shows the incident neutron energy. The symbol ● refers to the sets with HF, ○ with Q_{max} and △ with Q_0.

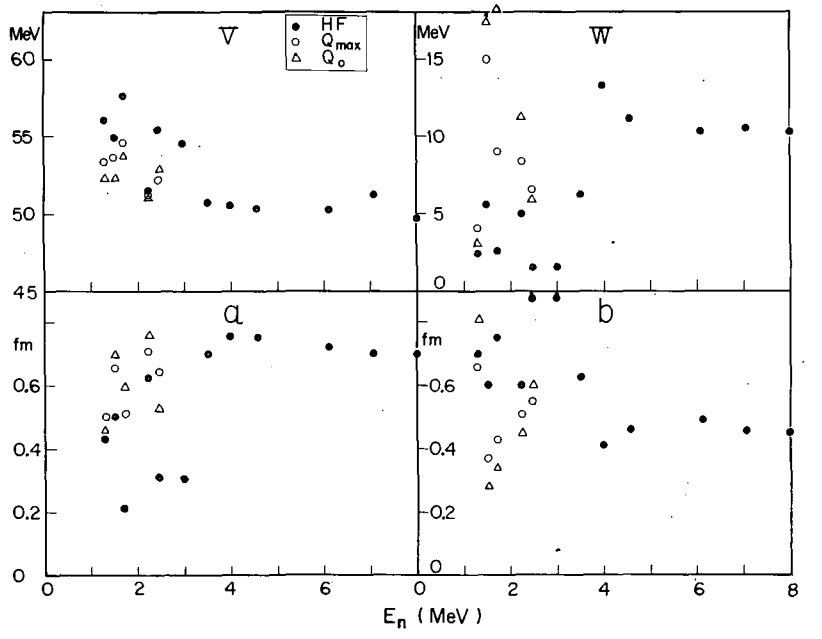

FIG.3b. Potential parameters V, W, a and b for copper; same as in Fig.3a.

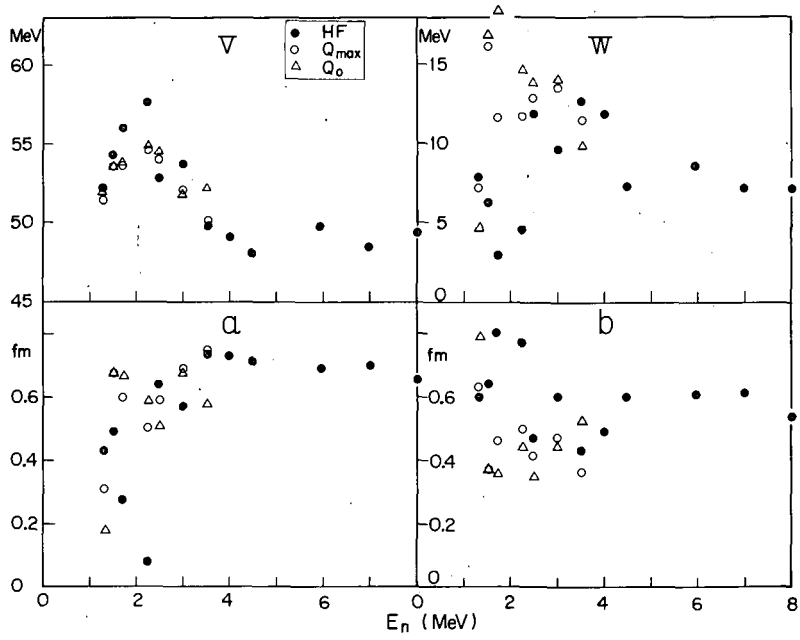

FIG.3c. Potential parameters V, W, a and b for zinc; same as in Fig.3a.

However, $\Delta(d\sigma_{ela}/d\Omega_i)$ usually does not include the systematic errors, as in the present measurement, and then

$$W_{total} = NW_{ela}$$

where N is number of angles observed. The best-fit sets obtained for copper and zinc at 1.71 and 2.24 MeV are shown in Table II. The values of χ^2 for all of the best-fit sets are shown in Tables IIIA and IIIB. Some of the calculated angular distributions of elastically scattered neutrons are shown in Figs 1a, 1b and 2. The values of the potential parameters, V, W, a and b in the sets are plotted as a function of incident neutron energy in Figs 3a-c.

4. DISCUSSIONS

None of the three cases, HF, Q_{max} and Q_0, leads to the minimum χ^2-value in the whole energy region as is seen in Table II. In our data on copper and zinc at 1.71 and 2.24 MeV, however, the case Q_{max} gives the minimum χ^2-value, though any difference between calculations with Q_{max} and Q_0 is not seen for copper at 2.24 MeV. Furthermore, some of the potential parameters in the best-fit sets with HF and Q_0 have rather unnatural values, as is seen in Table II and Figs 3a-c.

The shape of the angular distributions of the calculated elastic scattering shows some differences in the three cases HF, Q_{max} and Q_0

at most backward angles, and the backward cross-sections increase in the order. No appreciable differences exist in the inelastic angular distributions. As is seen in Figs 1a-b and 2, the case Q_{max} is a little better than the others in a limited energy region for each element. The angular distributions of copper and zinc at 1.3 and 1.5 MeV and aluminium at 0.98 and 2.0 MeV are too simple to discriminate fitness of calculations for HF, Q_{max} and Q_0.

The energy dependences of the potential parameters V, W, a and b in the best-fit sets are found not to be monotonic. The anomalies in the energy dependences of the potential parameters are less with Q_{max} than with HF except for aluminium, as is seen in Fig.3a. Differences between the calculations with Q_{max} and Q_0 are not distinguished. For aluminium, fluctuations are too large to discriminate the differences among the three cases. Some of the anomalies cannot be taken off by taking Moldauer's effect into consideration. In Tables IIIA and IIIB values of χ_c^2 which are obtained by using the potential parameters averaged in the region of 4.5 to 8 MeV are shown with values of χ^2 for the best-fit sets. Difference between values of χ_c^2 and χ^2 is appreciable at the anomalies.

Judging from the results of the three analyses shown above, the calculations in the case Q_{max} give more reasonable results than in HF and, though not definitely, more reasonable results than in the case Q_0. However, we cannot get rid of some of the anomalies seen in the lower-energy region, even if both the width-fluctuation effect and the resonance-interference effect are taken into consideration.

REFERENCES

[1] DRESNER, L., Proc. int. Conf. on neutron interactions with the nucleus, Columbia University Rep. CU-175 (1957) 71.
[2] LANE, A.M., LYNN, J.E., Proc. Phys. Soc. A70 (1957) 577.
[3] MOLDAUER, P.A., Phys. Rev. 135 (1964) B642.
[4] MOLDAUER, P.A., Rev. mod. Phys. 36 (1964) 1079.
[5] TSUKADA, K., TANAKA, S., TOMITA, Y., MARUYAMA, M., Nucl. Phys. A125 (1969) 641.
[6] TANAKA, S., TSUKADA, K., MARUYAMA, M., TOMITA, Y., "Fast neutron scattering from Al, Si, S and Zn", these Proceedings, IAEA-CN-26/31.
[7] HUGHES, D.J., SCHWARTZ, R.B., BNL 325, 2nd Ed. (1958).
[8] GOLDBERG, M.D., et al., BNL 325, 2nd Ed. Suppl. 2 (1966).
[9] TOWLE, J.H., GILBOY, W.B., Nucl. Phys. 39 (1962) 300.
[10] KOHSAKA, A., TOMITA, Y., private communication.
[11] HAUSER, W., FESHBACH, H., Phys. Rev. 87 (1952) 366.
[12] TOMITA, Y., JAERI 1191 (1970).

FAST-NEUTRON SCATTERING FROM Al, Si, S AND Zn

S. TANAKA, K. TSUKADA, M. MARUYAMA, Y. TOMITA
Japan Atomic Energy Research Institute,
Tokai-mura, Naka-gun,
Ibaraki-ken, Japan

Abstract

FAST-NEUTRON SCATTERING FROM Al, Si, S and Zn.

Differential cross-sections for elastic and inelastic neutron scattering have been measured for natural samples of Al, Si, S and Zn at incident energies from 4.5 to 8 MeV in about 1-MeV steps. Scattered neutrons were observed at angles from 30° to 150° in 10° steps with a Mobley bunching system of the JAERI 5.5-MV Van de Graaff accelerator and a time-of-flight spectrometer. The absolute differential cross-section scale was fixed with reference to the n-p scattering cross-section. The data were corrected for flux attenuation, multiple scattering in the samples and source-to-sample angular spread of neutron energy using a Monte-Carlo computer code. The differential cross-sections were analysed using the optical model for the elastic scattering, the statistical theory for the compound processes, and the coupled-channels and DWBA theories for the direct inelastic scattering. The optical-potential parameters were obtained by fitting the sum of the shape-elastic and compound-elastic scattering cross-sections to the measured elastic data. The inelastic data for low-lying levels are compared with the combined predictions by the Hauser-Feshbach and coupled-channels (or DWBA) calculations. The comparison shows good agreement for ^{27}Al and ^{32}S. For the first states in even isotopes of Zn, the direct processes are predominant in the energy region higher than 5.9 MeV.

1. INTRODUCTION

For the inelastic scattering of neutrons in the several-MeV region, it is expected that direct-interaction processes participate in competition with compound processes. Cranberg and Zafiratos [1] analysed their inelastic data on natural lead, ^{206}Pb and ^{209}Bi for the octupole-vibrational states at a neutron energy of 8 MeV using the DWBA calculation and deduced the values of deformation parameters. Martin et al. [2] analysed inelastic data using the direct-interaction theory as well as the statistical theory for the compound nucleus. They compared their data on ^{27}Al, ^{28}Si, ^{31}P and ^{32}S at 5.95 MeV with the Moldauer [3] plus coupled-channels [4] predictions and obtained good results for the latter three nuclei.

To study this problem further, we measured the elastic and inelastic scattering cross-sections of Al, Si, S and Zn at energies from 4.5 to 8 MeV and analysed the data with the optical model for the elastic scattering, the statistical theory for the compound processes, and the coupled-channels and DWBA theories for the direct inelastic scattering.

2. EXPERIMENTAL METHOD AND RESULTS

The measurements were done on the JAERI 5.5-MV Van de Graaff accelerator and a Mobley beam bunching system with a time-of-flight spectrometer. The target was a gas cell 3-cm long, filled with deuterium

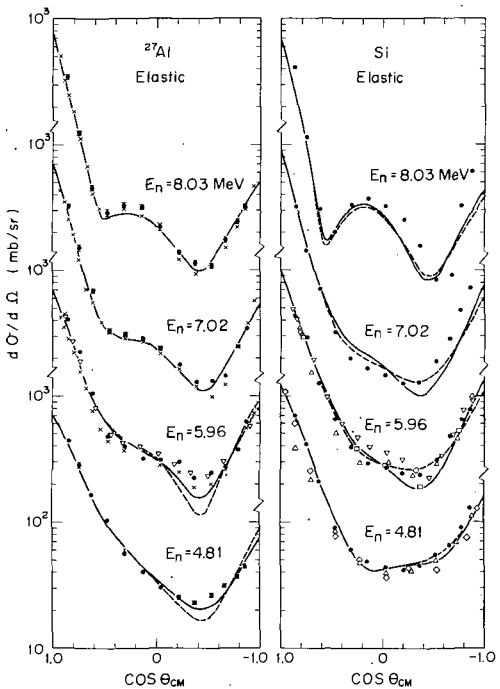

FIG. 1a.

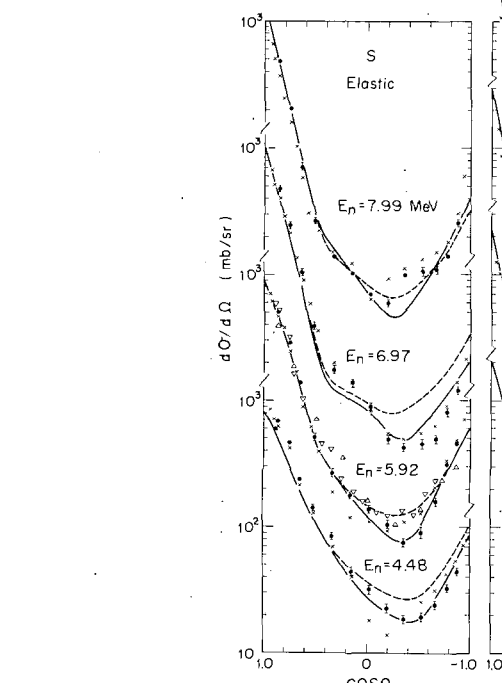

FIG. 1b.

FIG. 1c.

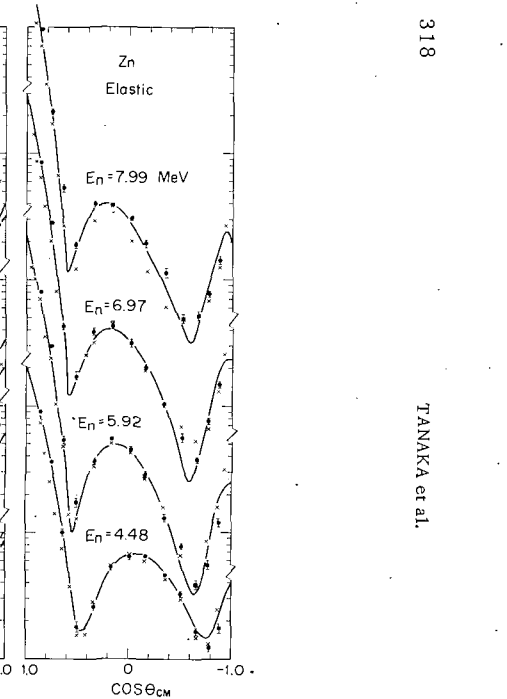

FIG. 1d.

FIGS 1a-d. Differential cross-sections for elastic scattering by Al (Fig. 1a), Si (Fig. 1b), S (Fig. 1c) and Zn (Fig. 1d). Data of other authors are plotted with various symbols: × Holmqvist and Wiedling [6]; △ Petitt et al. [7]; ◇ Knitter and Coppola [8]; ▽ Martin et al. [2] and □ Drake et al. [9]. For Al, Si and S, the solid and dashed curves respresent shape-elastic plus compound-elastic cross-sections calculated with the HF and corrected HF theories, respectively; for Zn the solid curves are shape-elastic cross-sections.

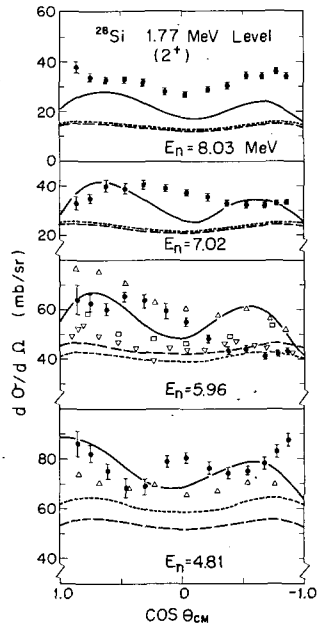

FIG. 2a.

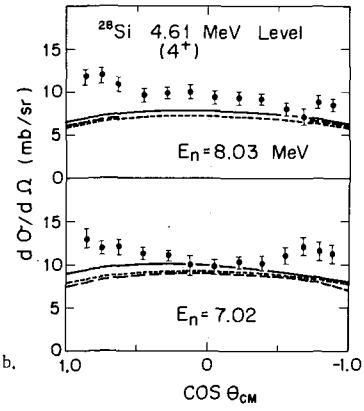

FIG. 2b.

FIGS 2a-b. Inelastic cross-sections for ^{28}Si (Fig. 2a at 1.77-MeV, Fig. 2b at 4.61-MeV level). The dotted and dashed curves are cross-sections calculated with HF and corrected HF theories, respectively. The solid curves are combined predictions by the c-c and HF calculations.

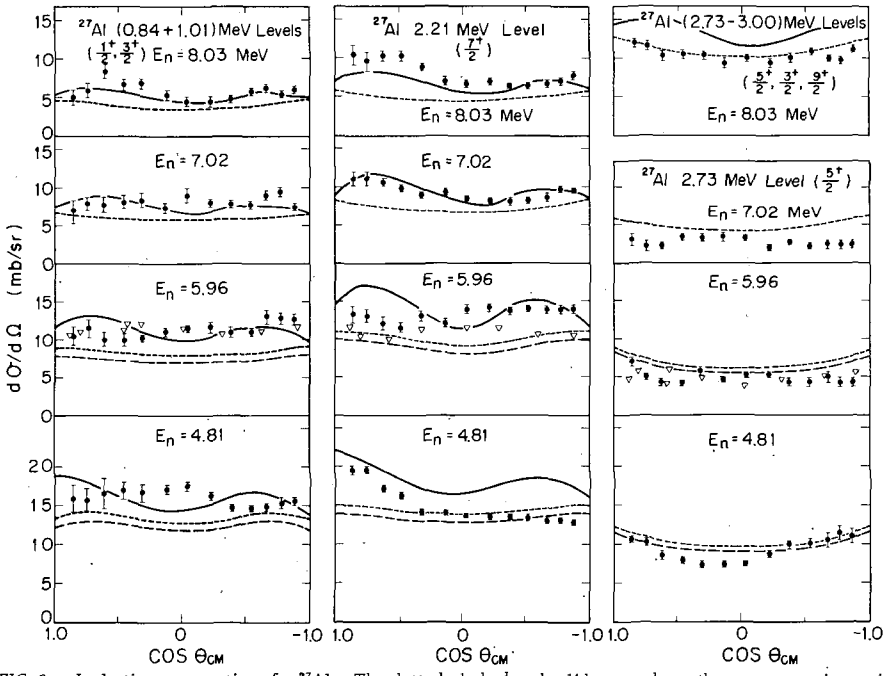

FIG. 3. Inelastic cross-sections for ^{27}Al. The dotted, dashed and solid curves have the same meaning as in Figs 2a-b.

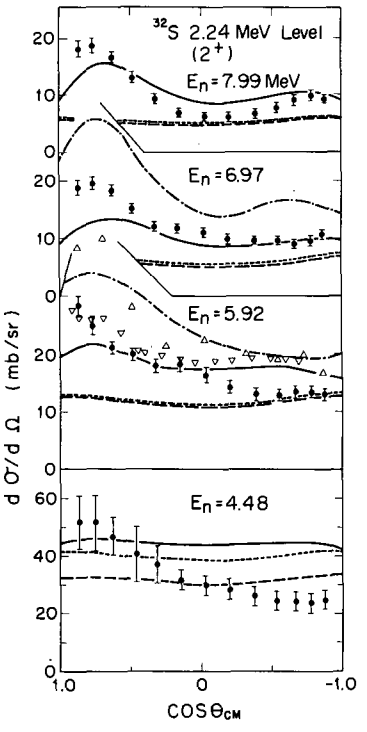

FIG. 4. Inelastic cross-sections for the first-level of ^{32}S. The dotted, dashed and solid curves have the same meaning as in Figs 2a-b. The dash-dot curves represent the HF plus DWBA predictions.

gas at 50 cm Hg. Scattering samples were placed at a distance of 10.1 cm from the centre of the gas cell. The energy spreads of the neutrons incident on the samples were about 150 keV in FWHM in the energy region above 5 MeV and 200 keV below this energy. Scattered neutrons were detected in an NE213 liquid scintillator. The detector was placed 2.89 or 3.89 m from the sample, at angles between 30° and 150° in 10° steps.

The absolute differential cross-section scale was fixed with reference to the ^{1}H (n, n) ^{1}H cross-section [5] by observing the neutron group scattered from hydrogen in a polyethylene sample with a 1.0-cm diameter. The energy variation of the detector efficiency was obtained from measurement of the neutron yield from the ^{3}H (p, n) ^{3}He and ^{2}H (d, n) ^{3}He reactions at 0° using the published cross-sections of the reactions.

Peaks unresolved in the time spectra were separated by a peeling-off method. The scattering cross-sections were corrected for flux attenuation, multiple scattering in the sample and for source-to-sample geometrical effect by the Monte-Carlo method.

The differential elastic and inelastic cross-sections thus obtained are shown by solid points in Figs 1-5. The error bars shown in the figures contain statistical errors and errors originating in the peeling-off process. For comparison, some data of other authors are also plotted. The differences in the incident energy between these data and ours are within 170 keV. The discrepancies in the values among the data of the different authors may, to a certain extent, be due to the fluctuation effect.

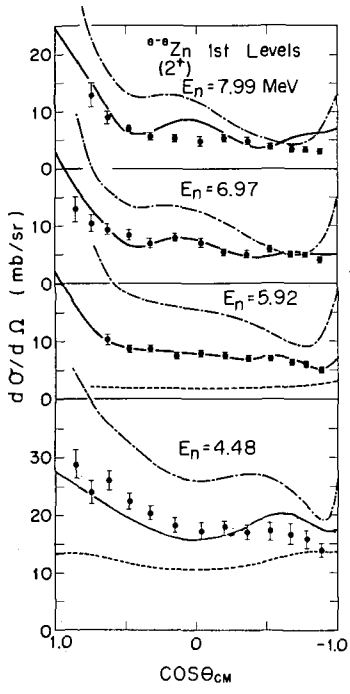

FIG. 5. Inelastic cross-sections for the first levels of the even isotopes of zinc. The dashed curves are the HF calculation. For the two higher energies, the HF prediction is assumed to be negligible. The solid and dash-dot curves have the same meaning as in Fig. 4.

3. THEORETICAL ANALYSES AND DISCUSSIONS

3.1. Elastic scattering and Hauser-Feshbach calculation

The calculations for shape-elastic and compound-elastic cross-sections were performed with computer codes STAX2 [10] and ELIESE-2 [11]. The optical-potential form used was of standard type with a Saxon-derivative imaginary part and with a spin-orbit coupling term. The compound-elastic cross-sections together with the compound-inelastic cross-sections were estimated by the Hauser-Feshbach (HF) [12] and Moldauer (corrected HF) [3] calculations. In the corrected HF calculation, the values of Moldauer's parameter Q were taken to be zero for ^{27}Al and to be the maximum values [10] for the other elements. After a preliminary survey of the optical parameters, the potential depths V and W were searched by means of an automatic parameter-searching routine, the other parameters being fixed as follows: r_0 = 1.20 fm, a = 0.66 fm, b = 0.47 fm, V_{so} = 7.2 MeV for Al, Si and S, and r_0 = 1.25 fm, a = 0.70 fm, b = 0.50 fm, V_{so} = 9.0 MeV for Zn. The values of V, W, χ^2 and total cross-sections σ_T are listed in Table I. In the calculation of χ^2, the experimental errors were assumed to be 10% of the cross-sections. The calculated cross-sections are shown by curves in Figs 1a-d.

TABLE I. OPTICAL-POTENTIAL PARAMETERS

	E_n	Compound part by HF				Compound part by corrected HF				$\sigma_{T,obs}$[a]
	(MeV)	V (MeV)	W (MeV)	χ^2	σ_T (b)	V (MeV)	W (MeV)	χ^2	σ_T(b)	(b)
Al	4.81	50.5	7.71	0.7	2.25	49.2	5.71	2.5	2.15	2.25
	5.96	49.9	6.21	3.4	1.94	49.5	4.85	6.0	1.87	2.10
	7.02	50.0	8.33	1.1	1.85					1.90
	8.03	51.3	7.88	1.2	1.80					1.80
Si	4.81	65.9	6.48	1.8	3.12	64.8	11.0	1.0	2.88	2.90
	5.96	53.4	5.47	3.1	2.28	54.2	13.2	1.3	2.28	2.20
	7.02	52.7	7.86	6.5	2.05	52.5	13.3	5.8	2.07	1.95
	8.03	46.7	8.51	11.5	1.70	44.2	11.3	10.6	1.73	1.90
S	4.48	46.8	8.86	4.4	2.45	46.4	10.3	14.4	2.42	2.70
	5.92	49.3	8.80	1.4	2.31	49.0	12.2	9.1	2.30	2.72
	6.97	49.8	18.0	6.7	2.23	51.2	16.9	31.6	2.27	2.39
	7.99	51.2	10.3	4.6	2.26	51.9	15.1	2.2	2.30	2.25
Zn	4.48	45.5	8.39	0.5	4.00					3.74
	5.92	46.4	10.13	0.8	3.94					3.84
	6.97	46.1	9.38	4.1	3.90					3.79
	7.99	46.6	8.73	5.3	3.83					3.70

[a] The values are taken from the Supplement of BNL 325.

In estimating a cross-section by the HF or corrected HF method, attention must be paid to missing levels in a residual nucleus and to reactions other than neutron scattering. For ^{28}Si and ^{32}S, contributions of the (n, p) and (n, α) reactions were not negligible and the calculated cross-sections were corrected for these contributions. In the case of the two higher energies for ^{27}Al, the three higher energies for ^{32}S and the two lower energies for the even isotopes of zinc, the effect of missing levels was serious. Therefore, the calculated results were normalized to 90° symmetric inelastic data for higher levels, which are not shown in this paper. For the higher two of the even isotopes of zinc, the compound inelastic scattering was neglected.

As seen in Figs 1a-d, the solid curves (HF for the compound elastic), in general, show rather a better agreement with the experimental data than the dashed curves (corrected HF for compound elastic). For this reason, the optical parameters obtained in the former case were employed in the calculation of the direct part of the inelastic scattering.

3. 2. Inelastic scattering

The direct-interaction components for the calculated inelastic scattering were added to the compound inelastic cross-sections assuming that there is no interference between compound and direct processes. The c-c calculation for the elastic scattering gave results that were a little different from the straightforward optical-model calculation. In some cases, such as for the highest energy of Si, the two higher energies of S, the former results showed a tendency to improve the fitness to the experimental data. However, only the results for the latter calculation are shown in Figs 1b and 1c.

The solid curves in Figs 2-5 show the sum of the c-c and HF predictions. Using the computer code JUPITOR-1 [4, 13], the c-c calculation was performed under the following assumptions: (1) coupling potentials are complex, and (2) ^{27}Al and ^{28}Si are deformed, and ^{32}S and $^{e-e}$Zn are vibrational. For the convenience of calculation, the spin-orbit term was neglected and for ^{28}Si the adiabatic approximation was used. The values of β_2 were taken as 0.40 for ^{28}Si, 0.37 for ^{32}S and 0.23 for $^{e-e}$Zn in accordance with previous data [14]. For ^{27}Al we adopted the core-excitation model considering this nucleus as a spin 5/2 proton hole weakly coupled to a ^{28}Si core [15]. Hence the cross-sections for direct excitation of the first 2^+ state in ^{28}Si were shared among the 1/2, 3/2, 5/2 and 9/2 levels of ^{27}Al with weighting factors of $(2J + 1)/30$.

For comparison, the sums of the DWBA and HF predictions are also shown by dash-dot curves in Figs 4 and 5. The DWBA calculation was made with the computer code DWBA2 [16]. The perturbation term was taken to be real and the same values of β_2 as in the c-c calculation were used.

The discrepancy between the DWBA and c-c predictions is remarkable. This is, however, because different coupling terms were used in these predictions. A trial calculation for ^{32}S revealed that, when a real coupling term same as in the DWBA case was used, the c-c calculation resulted in cross-section values quite close to the DWBA predictions.

In most cases, the combined predictions by the HF calculation and the c-c calculation with complex coupling potentials are in good agreement with measured inelastic data, though there are discrepancies between the measured and predicted angular distribution patterns for the first level of ^{28}Si. These discrepancies may be due to the fluctuation effect [17] in the compound inelastic scattering. Therefore, we may conclude that in the present energy region the measured inelastic cross-sections for ^{27}Al, ^{28}Si and ^{32}S are well described by the combined predictions of the statistical model and the direct-interaction mechanism, and that the excitation of the first states in even isotopes of zinc by inelastic scattering is mainly caused by direct processes in the energy region higher than 5.9 MeV.

REFERENCES

[1] CRANBERG, L., ZAFIRATOS, C. D., Phys. Rev. 142 (1966) 775.
[2] MARTIN, J., STEWART, D. T., CURRIE, W. M., Nucl. Phys. A113 (1968) 564.
[3] DRESNER, L., Columbia Univ. Report Cu-175 (1957) 71; LANE, A. M., LYNN, J. E., Proc. phys. Soc. A70 (1957) 557; MOLDAUER, P. A., Phys. Rev. 123 (1961) 968, 135 (1964) B462.
[4] TAMURA, T., Rev. mod. Phys. 37 (1965) 679.
[5] HUGHES, D. J., SCHWARTS, R. B., BNL 325 2nd Ed. (1958).
[6] HOLMQVIST, B., WIEDLING, T., AE-366 (1969).
[7] PETITT, G. A., BUCCINO, S. G., HOLLANDSWORTH, C. E., BEVINGTON, P. R., Nucl. Phys. 79 (1966) 231.
[8] KNITTER, H. H., COPPOLA, M., Z. Phys. 207 (1967) 56.
[9] DRAKE, D. M., HOPKINS, J. C., YOUNG, C. S., CONDÉ, H., SATTLER, A., Nucl. Phys. A128 (1969) 209.
[10] TOMITA, Y., JAERI 1191 (1970).
[11] IGARASI, S., private communication.
[12] HAUSER, W., FESHBACH, H., Phys. Rev. 87 (1952) 366.
[13] WAKAI, M., IGARASI, S., MIKOSHIBA, O., YAMAJI, S., JAERI Memo 3833 (1969).
[14] STELSON, P. H., GRODZINS, L., Nucl. Data Sect. A1 (1965) 21.
[15] e.g. CRAWLEY, G. M., GARVEY, G. T., Phys. Rev. 167 (1968) 1070.
[16] KAWAI, M., KUBO, K., YAMAMURO, G., DWBA manual, INS, Univ. of Tokyo, PT-9.
[17] GRIMES, S. M., Nucl. Phys. A124 (1969) 369.

DISCUSSION

TO PAPERS IAEA-CN-26/29, 30, 31

A. PRINCE: In determining your optical potentials did you use a χ^2 (chi-squared) parameter search for the inelastic or the elastic cross-section, or for both?

S. TANAKA: We made a least-squares fit only to the elastic data. We calculated the inelastic scattering by using the results of the optical analysis.

NEUTRON ELASTIC-SCATTERING CROSS-SECTIONS OF VANADIUM, CHROMIUM, IRON AND NICKEL

B. HOLMQVIST, T. WIEDLING
AB Atomenergi, Studsvik, Nyköping,
Sweden

Abstract

NEUTRON ELASTIC-SCATTERING CROSS-SECTIONS OF VANADIUM, CHROMIUM, IRON AND NICKEL.

The elements V, Cr, Fe and Ni play an important role as alloying components in construction materials for nuclear power reactors. For this reason, the fast-neutron elastic-scattering cross-sections have been requested with relatively high accuracy for energies from about 1 MeV up to 15 MeV.

The present report comprises a description, a compilation and finally a discussion of elastic-scattering data obtained from measurements made in the authors' laboratory in the energy range 1.8-8.1 MeV. Between 1.8 and 3.0 MeV these measurements have been performed at intervals of about 0.25 MeV while between 3.0 and 8.1 MeV, the corresponding intervals were generally 0.5 MeV.

As is the case with all elastic-scattering data collected in the authors' laboratory, time-of-flight techniques have been employed. The differential scattering cross-sections are standardized with respect to well-established n-p scattering cross-sections.

The experimental differential and total elastic cross-section data have been compared with results deduced from optical-model calculations involving a spherical optical potential.

Although it is well known that the total cross-sections of V, Cr, Fe and Ni show pronounced resonance structures at neutron energies below about 3 MeV, it has also been considered appropriate to analyse the measurements below 3 MeV in the light of the nuclear optical model. It is clearly advantageous for nuclear-reactor applications to have access to a standardized set of optical-model parameters when performing cross-section calculations at intermediate energies.

The experimental elastic-scattering data and the calculated differential cross-sections are presented diagramatically. The optical-model parameters, total elastic cross-sections and total cross-sections are tabulated.

1. INTRODUCTION

This work forms part of a neutron elastic scattering programme in the mass number region from the lightest to the very heaviest natural elements which has been going on for several years at our laboratory. The objective is the acquisition of cross section data at incident neutron energies between 1.8 and 8.1 MeV for reactor physics applications and the continuation of systematic investigations [1 - 3] of the characteristics of the optical model potential. Emphasis has been given to the important reactor constructional materials V, Cr, Fe and Ni for which elastic scattering angular distributions were measured at several energies in the above mentioned energy interval. Elastic scattering cross sections are requested [4] for these elements in the energy region 1 - 15 MeV in energy steps of about 50 keV in the low energy region and in steps of up to several hundred keV at higher energies. The angular distribution recordings are required at intervals of 5° to 10°.

The experimental differential cross sections were compared with cross sections calculated with a spherical optical potential in order to provide a basic understanding of the neutron scattering which can be used for interpolation and extrapolation of the measured values.

TABLE I. THE EXPERIMENTAL PARAMETERS CHARACTERISTIC OF THE ELASTIC-SCATTERING CROSS-SECTION MEASUREMENTS

Neutron source	$T(p, n)He^3$ for $E_n \leq 4.6$ MeV $D(d, n)He^3$ for $E_n > 4.6$ MeV
Gas target	Length of gas target cell 3 cm Nickel foil thickness 2.5 mg/cm^2 Gas pressure in the cell 1 kp/cm^2 (for T_2 as well as for D_2) Total energy spread $\pm$ 50 keV for $E_n \leq 4.6$ MeV Total energy spread $\pm$ 90 keV for $E_n > 4.6$ MeV
Accelerator beam	Beam pulse frequency 1 MHz Beam pulse width at half-height 2 ns Mean target current 1.5 μA
Sample size and purity	V to Ni, cylinders having lengths of 5.0 cm, 0.95 cm inner diameter and 2.5 cm outer diameter Polythene scatterer, 3.0 cm in length, 0.95 cm outer diameter and 0.65 cm inner diameter Sample purity $\geq$ 99.5 %
Target-scatterer-detector distances	Target-scatterer 10 cm Scatterer-detector 300 cm
Neutron time-of-flight detector	Scintillator NE102A, size 10 cm diameter and 5 cm length Spectrometer time resolution 3 ns
Neutron flux measurements	The neutron flux was monitored with a directional long counter
Angular interval	The angular distributions have been measured in the angular region 20° to 160° in 10° steps except in the foreward directions, where measurements were performed in 5° step
Background conditions	The signal-to-background ratio at the position of the eleastic peak was 7 to 1 in the most unfavourable case i.e. at 8 MeV neutron energy and at the forward scattering angles, but was much more favourable at lower energies
Counting statistics	Statistical errors for the number of counts in the elastic peaks of the time-of-flight spectra $\leq$ 2 % Statistical error for the number of monitor counts 0.3 %
Errors	The experimental cross section errors are 5 per cent except for Cr below 2.5 MeV and for Fe and Ni below 3 MeV, where the errors are about 10 per cent

2. EXPERIMENTAL DETAILS AND RESULTS

The angular distribution measurements were carried out concurrently with those reported earlier [1 - 3]. The cross sections were measured relative to the n-p cross sections [5].

The experimental parameters and data characteristic of the elastic cross section measurements are collected in Table I. Table II contains the total n-p cross section values at the different neutron energies for which the measurements were made.

TABLE II. THE TOTAL n-p CROSS-SECTIONS [5] USED AT THE NEUTRON ENERGIES FOR WHICH DIFFERENTIAL ELASTIC-SCATTERING MEASUREMENTS HAVE BEEN PERFORMED

E_n	MeV	1.77	2.02	2.27	2.52	2.76	3.00
σ_T	b	3.10	2.89	2.70	2.53	2.40	2.28
E_n	MeV	3.49	4.00	4.56	6.09	7.05	8.05
σ_T	b	2.07	1.88	1.73	1.40	1.25	1.11

Corrections of the experimental angular distributions have been applied for neutron multiple scattering in the sample under investigation as well as for neutron attenuation and geometrical effects caused by the size of the sample and its distances from target and detector [6].

The corrected experimental angular distributions are shown in Figs. 1 and 2. The cross sections for V are from reference [3], those of Cr at 2.47 MeV and higher energies are from references [1, 2] as are those at 3.0 MeV and higher energies for Fe and Ni.

3. THEORETICAL ANALYSES

The experimental elastic scattering angular distributions have been compared with cross sections calculated by using a local nuclear optical potential of the form

$$-V(r) = Uf(r) + iWg(r) + U_{so} \left(\frac{\hbar}{\mu_\pi c}\right)^2 1/r\ (d/dr)\ |\ f(r)\ |\ \bar{\sigma} \cdot \bar{l}$$

where U and W are the real and imaginary potential depths respectively and U_{so} the strength of the spin-orbit interaction. The diffuseness functions f(r) and g(r) are of the Saxon-Woods and derivative Saxon-Woods forms. The real and imaginary radii are defined by the relations $R_U = r_{oU} A^{1/3}$ and $R_W = r_{oW} A^{1/3}$, respectively. The corresponding diffuseness parameters are a and b.

In order to make a proper comparison between an optical model elastic scattering angular distribution and an experimental one, it is necessary to take the effect of compound eleastic scattering into account. This has been done by applying the Hauser and Feshbach formalism [7] together with the techniques described in reference [1]. However, as pointed out by Moldauer [8] the cross sections calculated with the Hauser-Feshbach theory must be corrected for the effect of level-width fluctuations, an effect which tends to increase the compound elastic cross sections but which decreases with increasing neutron energy.

The calculations with the optical potential have been performed in two different manners depending upon the incident neutron energy. Thus the optical potential parameters, i.e. U, W, r_{oU}, r_{oW} and a corresponding to the best fits to the experimental data, have been obtained by using the ABACUS II automatic five-parameter search routine except below 3 MeV neutron energy for the elements Fe and Ni and below 2.5 MeV for Cr where no parameter search procedures have been applied since resonance effects may be expected. But since it is of interest to obtain information concerning the ability of the optical model to describe the experimental results, potential depths were obtained in the low energy range 1.77 to 2.76 MeV by

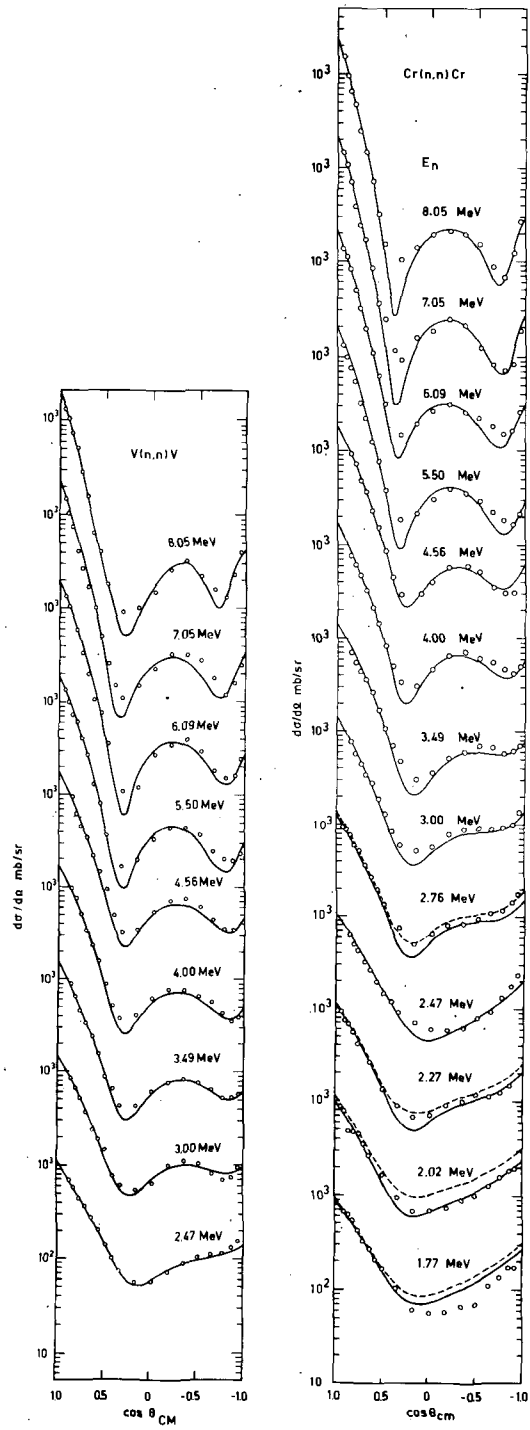

FIG. 1. The experimental differential elastic scattering cross-sections of V and Cr (circles). The solid lines represent optical-model calculations which take no account of width fluctuations and the dashed lines represent those with width fluctuation corrections included. The cross-sections for V are from Ref. [3], those of Cr at 2.47 MeV and higher energies are from Refs [1, 2].

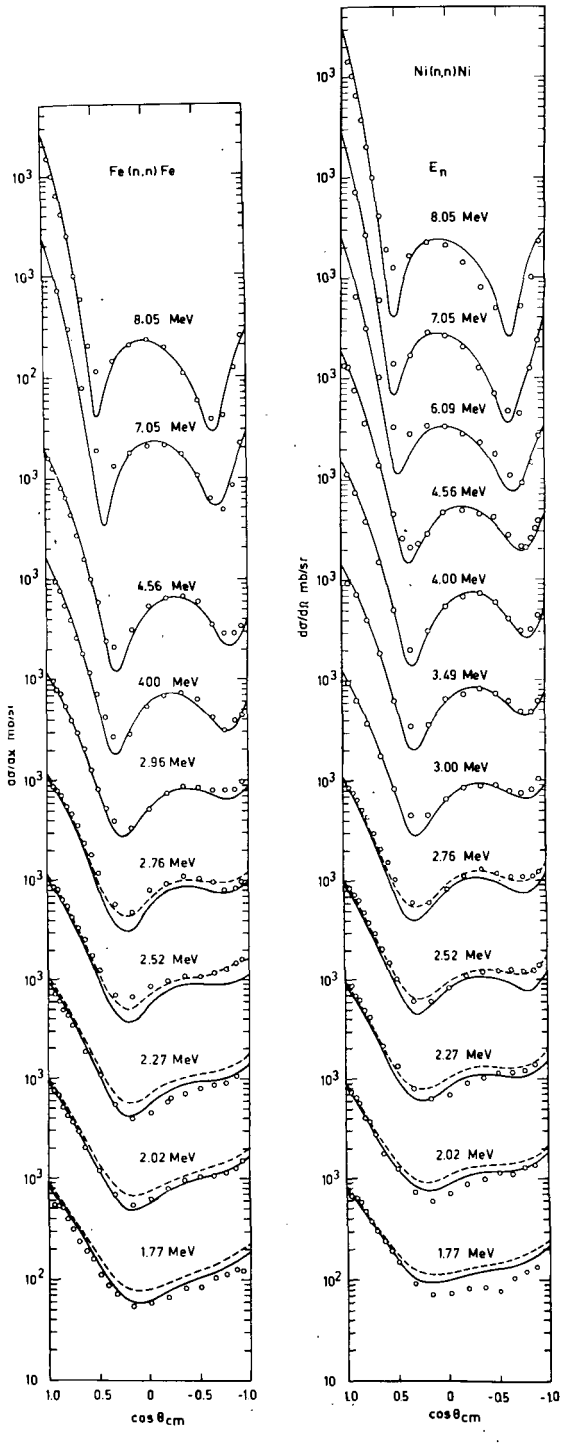

FIG. 2. The experimental differential elastic scattering cross-sections of Fe and Ni (circles). The solid lines represent optical-model calculations which take no account of width fluctuations and the dashed lines represent those with width-fluctuation corrections included. The cross-sections for Fe and Ni at 3.0 MeV and higher energies are from Refs [1, 2].

TABLE III. OPTIMUM VALUES OF THE OPTICAL POTENTIAL PARAMETERS FROM FIVE-PARAMETER ANALYSES OF VANADIUM. THE TOTAL ELASTIC CROSS-SECTIONS σ_{el} AND THE TOTAL CROSS-SECTIONS σ_T CALCULATED WITH THE OPTICAL POTENTIAL ARE ALSO INCLUDED, TOGETHER WITH THE CORRESPONDING EXPERIMENTAL QUANTITIES σ_{el}^{exp} AND σ_T^{exp}. THE COMPOUND ELASTIC CROSS-SECTIONS σ_{ce} HAVE BEEN CALCULATED WITH THE HAUSER-FESHBACH FORMALISM

E_n (MeV)	2.47	3.00	3.49	4.00	4.56	5.50	6.09	7.05	8.05
U (MeV)	51.3	47.4	48.6	48.1	49.2	52.3	51.8	50.7	46.6
W (MeV)	8.40	8.40	8.41	8.30	8.12	7.90	7.94	7.94	6.43
r_{oU} (fm)	1.19	1.26	1.24	1.25	1.23	1.19	1.19	1.21	1.23
r_{oW} (fm)	1.21	1.23	1.22	1.21	1.18	1.17	1.20	1.20	1.25
a (fm)	0.65	0.66	0.66	0.66	0.65	0.65	0.66	0.64	0.65
σ_T (b)	3.58	3.81	3.71	3.70	3.60	3.37	3.28	3.24	3.10
σ_{se} (b)	1.79	2.08	2.11	2.19	2.19	2.08	2.01	1.96	1.85
σ_A (b)	1.79	1.73	1.60	1.51	1.41	1.29	1.27	1.28	1.25
σ_{ce} (b)	0.67	0.60	0.31	0.23	0.17	0	0	0	0
σ_{el} (b)	2.46	2.68	2.42	2.42	2.36	2.08	2.01	1.96	1.85
σ_{el}^{exp} (b)	2.45±0.15	2.66±0.16	2.49±0.15	2.61±0.15	2.40±0.14	2.05±0.12	2.00±0.12	1.96±0.12	1.85±0.11
σ_T^{exp} (b)	3.92±0.14 [Ref. 11] 3.67±0.04 [Ref. 12]	3.77±0.09 [Ref. 11] 3.75±0.04 [Ref. 12]	3.75±0.07 [Ref. 11] 3.75±0.04 [Ref. 12]	3.83±0.07 [Ref. 11] 3.75±0.04 [Ref. 12]	3.74±0.06 [Ref. 11] 3.75±0.04 [Ref. 12]	3.64±0.07 [Ref. 11] 3.75±0.04 [Ref. 12]	3.51±0.07 [Ref. 11] 3.50±0.04 [Ref. 12]	3.32±0.07 [Ref. 11] 3.45±0.03 [Ref. 12]	3.14±0.08 [Ref. 11] 3.25±0.03 [Ref. 12]

TABLE IV. OPTIMUM VALUES OF THE OPTICAL POTENTIAL PARAMETERS FROM FIVE-PARAMETER ANALYSES OF CHROMIUM. THE TOTAL ELASTIC CROSS-SECTIONS σ_{el} AND THE TOTAL CROSS-SECTIONS σ_T CALCULATED WITH THE OPTICAL POTENTIAL ARE ALSO INCLUDED, TOGETHER WITH THE CORRESPONDING EXPERIMENTAL QUANTITIES σ_{el}^{exp} AND σ_T^{exp}. THE COMPOUND ELASTIC CROSS-SECTIONS σ_{ce} HAVE BEEN CALCULATED WITH THE HAUSER-FESHBACH FORMALISM

E_n (MeV)	2.47	3.00	3.49	4.00	4.56	5.50	6.09	7.05	8.05
U (MeV)	55.4	50.9	51.4	50.2	49.7	51.7	49.7	48.0	50.6
W (MeV)	8.81	8.33	8.45	8.15	7.49	8.74	9.49	9.77	9.13
r_{oU} (fm)	1.11	1.19	1.17	1.21	1.20	1.19	1.21	1.24	1.21
r_{oW} (fm)	1.15	1.15	1.20	1.16	1.25	1.18	1.15	1.23	1.21
a (fm)	0.63	0.66	0.64	0.66	0.65	0.68	0.68	0.64	0.61
σ_T (b)	3.34	3.69	3.53	3.62	3.68	3.42	3.41	3.27	3.07
σ_{se} (b)	1.66	2.00	1.99	2.15	2.34	2.03	1.99	1.85	1.76
σ_A (b)	1.68	1.69	1.54	1.47	1.34	1.39	1.42	1.42	1.31
σ_{ce} (b)	0.74	0.49	0.28	0.17	0.10	0	0	0	0
σ_{el} (b)	2.40	2.49	2.27	2.32	2.44	2.03	1.99	1.85	1.76
σ_{el}^{exp} (b)	2.39±0.12	2.50±0.13	2.24±0.11	2.21±0.11	2.44±0.12	1.99±0.10	2.00±0.10	1.83±0.09	1.78±0.09
σ_T^{exp} (b)	3.45±0.12 [Ref. 11]	3.49±0.07 [Ref. 11]	3.80±0.08 [Ref. 11]	3.75±0.06 [Ref. 11]	3.75±0.06 [Ref. 11]	3.66±0.07 [Ref. 11]	3.66±0.08 [Ref. 11]	3.38±0.08 [Ref. 11]	3.19±0.08 [Ref. 11]

TABLE V. OPTIMUM VALUES OF THE OPTICAL POTENTIAL PARAMETERS FROM FIVE-PARAMETER ANALYSES OF IRON. THE TOTAL ELASTIC CROSS-SECTIONS σ_{el} AND THE TOTAL CROSS-SECTIONS σ_T CALCULATED WITH THE OPTICAL POTENTIAL ARE ALSO INCLUDED, TOGETHER WITH THE CORRESPONDING EXPERIMENTAL QUANTITIES σ_{el}^{exp} AND σ_T^{exp}. THE COMPOUND ELASTIC CROSS-SECTIONS σ_{ce} HAVE BEEN CALCULATED WITH THE HAUSER-FESHBACH FORMALISM

E_n (MeV)	2.96	3.95	4.56	7.05	8.05
U (MeV)	51.1	53.8	49.2	46.7	49.3
W (MeV)	10.8	9.84	11.19	10.46	10.45
r_{oU} (fm)	1.21	1.16	1.24	1.24	1.23
r_{oW} (fm)	1.15	1.05	1.16	1.24	1.20
a (fm)	0.61	0.63	0.61	0.66	0.64
σ_T (b)	3.34	3.45	3.43	3.36	3.32
σ_{se} (b)	1.68	1.97	1.89	1.85	1.85
σ_A (b)	1.66	1.48	1.54	1.51	1.47
σ_{ce} (b)	0.38	0.13	0.09	0	0
σ_{el} (b)	2.06	2.10	1.98	1.85	1.85
σ_{el}^{exp} (b)	2.14±0.11	2.08±0.10	2.10±0.11	1.80±0.09	1.76±0.09
σ_T^{exp} (b)	3.40±0.07 [Ref. 11]	3.68±0.07 [Ref. 11]	3.67±0.07 [Ref. 11]	3.65±0.09 [Ref. 11]	3.31±0.09 [Ref. 11]

extrapolating the U and W values calculated for Cr, Fe and Ni at higher energies by the parameter search procedure. A least squares fit analysis was made for that purpose. The U-values were calculated from the relations, Cr: $U = 54.0 - 0.65\ E_n$, Fe: $U = 54.3 - 0.80\ E_n$ and Ni: $U = 58.7 - 1.60\ E_n$. The geometrical parameters, i.e. r_{oU}, r_{oW} and a, were taken to represent mean values for all energies studied in the five-parameter analyses. The values of b and U_{so} used throughout the calculations were 0.48 fm and 8 MeV, respectively. The parameters obtained from the search procedure of V, Cr, Fe and Ni are given in Tables III to VI and the extrapolated optical potential parameters of Cr, Fe and Ni in Tables VII to IX.

The calculated differential elastic scattering angular distributions are shown in Figs. 1 and 2. Distributions representing Hauser-Feshbach calculations with (dashed lines) as well as without (solid lines) width fluctuation corrections are illustrated. The agreements between the calculated and experimental elastic angular distributions are good. It is clear that optical potential parameters obtained from the search procedure for Cr, Fe and Ni are useful for extrapolation purposes to lower neutron energies. However, the fact that the agreements between the experimental and calculated

TABLE VI. OPTIMUM VALUES OF THE OPTICAL POTENTIAL PARAMETERS FROM FIVE-PARAMETER ANALYSES OF NICKEL. THE TOTAL ELASTIC CROSS-SECTIONS σ_{el} AND THE TOTAL CROSS-SECTIONS σ_T CALCULATED WITH THE OPTICAL POTENTIAL ARE ALSO INCLUDED, TOGETHER WITH THE CORRESPONDING EXPERIMENTAL QUANTITIES σ_{el}^{exp} AND σ_T^{exp}. THE COMPOUND ELASTIC CROSS-SECTIONS σ_{ce} HAVE BEEN CALCULATED WITH THE HAUSER-FESHBACH FORMALISM

E_n (MeV)	3.00	3.49	4.00	4.56	6.09	7.05	8.05
U (MeV)	53.2	54.1	53.4	50.0	48.5	51.5	45.7
W (MeV)	8.68	8.37	8.77	10.09	10.07	11.3	9.16
r_{oU} (fm)	1.18	1.14	1.15	1.17	1.21	1.18	1.25
r_{oW} (fm)	1.22	1.11	1.16	1.15	1.20	1.18	1.29
a (fm)	0.64	0.56	0.67	0.72	0.73	0.71	0.68
σ_T (b)	3.27	3.38	3.36	3.60	3.68	3.45	3.59
σ_{se} (b)	1.70	1.87	1.88	1.99	2.04	1.86	2.01
σ_A (b)	1.57	1.51	1.48	1.61	1.64	1.59	1.58
σ_{ce} (b)	0.41	0.23	0.12	0.09	0	0	0
σ_{el} (b)	2.11	2.10	2.00	2.08	2.04	1.86	2.01
σ_{el}^{exp} (b)	2.15±0.11	2.06±0.10	2.00±0.10	2.00±0.10	1.83±0.09	1.79±0.09	1.71±0.09
σ_T^{exp} (b)	3.27±0.08 [Ref. 11]	3.49±0.07 [Ref. 11	3.51±0.06 [Ref. 11]	3.63±0.06 [Ref. 11]	3.74±0.07 [Ref. 11]	3.57±0.08 [Ref. 11]	3.53±0.08 [Ref. 11]

TABLE VII. CROSS-SECTIONS AND EXTRAPOLATED VALUES OF THE OPTICAL-POTENTIAL PARAMETERS OF CHROMIUM. σ_T, σ_{se} AND σ_A ARE THE TOTAL CROSS-SECTION, THE TOTAL SHAPE-ELASTIC CROSS-SECTION AND THE TOTAL ABSORPTION CROSS-SECTION. σ_{ce}^{corr} AND σ_{ce}^{HF} ARE THE TOTAL COMPOUND ELASTIC CROSS-SECTIONS WITH AND WITHOUT LEVEL-WIDTH FLUCTUATION CORRECTIONS, RESPECTIVELY. σ_{el}^{corr} AND σ_{el}^{HF} ARE THE CORRESPONDING TOTAL ELASTIC CROSS-SECTIONS.

E_n (MeV)	1.77	2.02	2.27	2.76
U (MeV)	52.9	52.7	52.5	52.2
W (MeV)	8.70	8.70	8.70	8.70
r_{oU} (fm)	1.19	1.19	1.19	1.19
r_{oW} (fm)	1.19	1.19	1.19	1.19
a (fm)	0.65	0.65	0.65	0.65
σ_T (b)	3.43	3.45	3.47	3.51
σ_{se} (b)	1.45	1.54	1.63	1.80
σ_A (b)	1.98	1.91	1.84	1.71
σ_{ce}^{HF} (b)	1.11	1.02	0.82	0.58
σ_{ce}^{corr} (b)	1.40	1.30	1.12	0.84
σ_{el}^{HF} (b)	2.56	2.56	2.45	2.38
σ_{el}^{corr} (b)	2.85	2.84	2.75	2.64
σ_{el}^{exp} (b)	2.31±0.20	2.46±0.25	2.49±0.23	2.55±0.26
σ_T^{exp} (b)	3.25±0.33 [Ref. 13]	3.70±0.37 [Ref. 13]	3.20±0.32 [Ref. 13]	3.74±0.18 [Ref. 13]

differential cross sections (corrected for level-width fluctuations) are better at 2.52 and 2.76 MeV than at lower energies is probably fortuitous. One explanation is that in spite of the comparatively large energy spread (± 50 keV) in the neutron beam the resonance effects are not smoothed out and the statistical assumptions of the optical model are not completely satisfied experimentally. This explanation is confirmed by the results obtained from five parameter searches on Cr, Fe and Ni at 3 MeV. In the latter case the optical model parameters obtained differed somewhat from the mean values applied in calculations at lower energies, but appreciably better agreements were obtained between experiment and theory even without Moldauer corrections. Lister and Smith [9] have shown that cross sections for elastic and inelastic neutron scattering measured in the energy range 0.3 to 1.5 MeV for even mass number germanium isotopes tended to be

TABLE VIII. CROSS-SECTIONS AND EXTRAPOLATED VALUES OF THE OPTICAL-POTENTIAL PARAMETERS OF IRON. σ_T, σ_{se} AND σ_A ARE THE TOTAL CROSS-SECTION, THE TOTAL SHAPE-ELASTIC CROSS-SECTION AND THE TOTAL ABSORPTION CROSS-SECTION. σ_{ce}^{corr} AND σ_{ce}^{HF} ARE THE TOTAL COMPOUND ELASTIC CROSS-SECTIONS WITH AND WITHOUT LEVEL-WIDTH FLUCTUATION CORRECTIONS, RESPECTIVELY. σ_{el}^{corr} AND σ_{el}^{HF} ARE THE CORRESPONDING TOTAL ELASTIC CROSS-SECTIONS.

E_n (MeV)	1.77	2.02	2.27	2.52	2.76
U (MeV)	52.9	52.7	52.5	52.3	52.1
W (MeV)	10.55	10.55	10.55	10.55	10.55
r_{oU} (fm)	1.20	1.20	1.20	1.20	1.20
r_{oW} (fm)	1.16	1.16	1.16	1.16	1.16
a (fm)	0.63	0.63	0.63	0.63	0.63
σ_T (b)	3.33	3.31	3.31	3.31	3.32
σ_{se} (b)	1.40	1.44	1.50	1.56	1.61
σ_A (b)	1.93	1.87	1.81	1.75	1.71
σ_{ce}^{HF} (b)	0.79	0.69	0.62	0.55	0.46
σ_{ce}^{corr} (b)	1.09	0.98	0.88	0.79	0.68
σ_{el}^{HF} (b)	2.19	2.13	2.12	2.11	2.07
σ_{el}^{corr} (b)	2.49	2.42	2.38	2.35	2.29
σ_{el}^{exp} (b)	1.88±0.19	2.13±0.21	1.85±0.19	2.49±0.25	2.36±0.25
σ_T^{exp} (b)	2.85±0.14 [Ref. 13]	3.20±0.16 [Ref. 13]	3.20±0.16 [Ref. 13]	3.90±0.04 [Ref. 12]	3.25±0.04 [Ref. 12]

reasonably well described in terms of the Hauser-Feshbach statistical model without corrections for level-width fluctuations. Furthermore they found that the agreement between measured and calculated inelastic cross sections could be appreciably improved with a model properly accounting for vibrational effects. Also for the elements Cr, Fe and Ni consisting mainly of even mass number isotopes (9.5 per cent Cr^{53} can be neglected) it is likely [10] that the differential elastic cross sections are influenced by collective effects. There is a strong excitation of the 2+ state by inelastic nucleon scattering and it is possible that the coupling to this state is sufficiently strong to allow its virtual excitation to have an observable effect on the elastic scattering from even nuclei. These facts also demonstrate some of the difficulties in testing the usefulness of the Moldauer level-width theory.

TABLE IX. CROSS-SECTIONS AND EXTRAPOLATED VALUES OF THE OPTICAL-POTENTIAL PARAMETERS OF NICKEL. σ_T, σ_{se} AND σ_A ARE THE TOTAL CROSS-SECTION, THE TOTAL SHAPE ELASTIC CROSS-SECTION AND THE TOTAL ABSORPTION CROSS-SECTION. σ_{ce}^{corr} AND σ_{ce}^{HF} ARE THE TOTAL COMPOUND ELASTIC CROSS-SECTIONS WITH AND WITHOUT LEVEL-WIDTH FLUCTUATION CORRECTIONS, RESPECTIVELY. σ_{el}^{corr} AND σ_{el}^{HF} ARE THE CORRESPONDING TOTAL ELASTIC CROSS-SECTIONS.

E_n (MeV)	1.77	2.02	2.27	2.52	2.76
U (MeV)	55.9	55.5	55.1	54.8	54.3
W (MeV)	9.32	9.32	9.32	9.32	9.32
r_{oU} (fm)	1.19	1.19	1.19	1.19	1.19
r_{oW} (fm)	1.20	1.20	1.20	1.20	1.20
a (fm)	0.69	0.69	0.69	0.69	0.69
σ_T (b)	3.20	3.15	3.12	3.12	3.15
σ_{se} (b)	1.38	1.36	1.37	1.41	1.47
σ_A (b)	1.82	1.79	1.75	1.71	1.68
σ_{ce}^{HF} (b)	1.08	0.89	0.74	0.54	0.46
σ_{ce}^{corr} (b)	1.36	1.19	1.04	0.90	0.77
σ_{el}^{HF} (b)	2.46	2.25	2.11	1.95	1.93
σ_{el}^{corr} (b)	2.74	2.55	2.41	2.31	2.24
σ_{el}^{exp} (b)	2.23±0.22	2.20±0.22	2.37±0.24	2.36±0.24	2.35±0.24
σ_T^{exp} (b)	3.22±0.16 [Ref. 13]	3.20±0.16 [Ref. 13]	3.21±0.32 [Ref. 13]	3.22±0.16 [Ref. 13]	3.23±0.16 [Ref. 13]

With the exception of the real potential depth U, the optimum parameter values of V (Table III) from the five-parameter analyses are essentially independent of the neutron energy. However, the variations of U seem to be coupled to variations of r_{oU}, so that the well known Ur_{oU}^2 ambiguity is fulfilled (Table I). This is in agreement with earlier experience [1] of the same type of potential as the one given here. The present values of Ur_{oU}^2 [mean value 74 ± 1 MeV(fm)^2] agree well with those of the earlier investigation [mean value 72 ± 3 MeV(fm)^2] [1].

For the predominantly even mass number nuclei Cr, Fe and Ni (Tables IV to VI) the real potential depth decreases slowly with the neutron energy. The parameters r_{oU}, r_{oW}, a and W are generally independent of energy.

Satisfactory agreement has been obtained between the optical model total cross sections and the experimental ones given by Foster [11], Galloway [12] and those compiled by Schmidt [13].

REFERENCES

[1] HOLMQVIST, B., A systematic study of fast neutron elastic scattering in the energy region 1.5 to 8.1 MeV, Arkiv Fysik 38 (1968) 403.

[2] HOLMQVIST, B., WIEDLING, T., Neutron elastic scattering cross sections, experimental data and optical model cross section calculations, AB Atomenergi, Studsvik, Sweden Rep. AE-366 (1969).

[3] HOLMQVIST, B., JOHANSSON, S.G., LODIN, G., WIEDLING, T., Fast neutron elastic and inelastic scattering of vanadium, AB atomenergi, Studsvik, Sweden Rep. AE-375 (1969).

[4] HÄUSSERMANN, W., SCHWARZ, S., RENDA, Compilation of EANDE requests for neutron data measurements, EANDC 61 "U", Paris (1968).

[5] HORSLEY, A., Neutron cross sections of hydrogen in the energy range 0.001 eV to 20 MeV, Nucl. Data 2A (1966) 243.

[6] HOLMQVIST, B., GUSTAVSSON, B., WIEDLING, T., A Monte Carlo program for calculation of neutron attenuation and multiple scattering corrections, Arkiv Fysik 34 (1967) 481.

[7] HAUSER, W., FESHBACH, H., The inelastic scattering of neutrons, Phys. Rev. 87 (1952) 366.

[8] MOLDAUER, P.A., Average compound-nucleus cross sections, Rev. Mod. Phys. 36 (1964) 1079.

[9] LISTER, D., SMITH, A.B., Fast-neutron scattering from germanium, Phys. Rev. 183 (1969) 954.

[10] PEREY, F.G., Optical-model analysis of proton elastic scattering in the range of 9 to 22 MeV, Phys. Rev. 131 (1963) 745.

[11] FOSTER, D.G., Jr., Glasgow, D.W., (private communication) and Neutron Cross Sections, BNL 325, Second Ed., Suppl. 2 (1966).

[12] GALLOWAY, III. L.A., SHRADER, E.F., Neutron total cross section measurements using a "white" neutron source, COO-1573-6 (1966).

[13] SCHMIDT, J.J., Neutron cross sections for fast reactor materials, Part 3: Graphs, KFK-120 (1962).

FAST-NEUTRON ELASTIC SCATTERING AT 8 MeV

B. HOLMQVIST, T. WIEDLING
AB Atomenergi, Studsvik, Nyköping,
Sweden

Abstract

FAST-NEUTRON ELASTIC SCATTERING AT 8 MeV.

The aim of the present neutron-scattering study was to collect data for reactor physics application as well as to continue a study, being in progress for several years at the authors' laboratory, of the spherical optical model.

Fast-neutron elastic-scattering angular distributions have been measured for 22 natural elements, ranging from Al to Bi, at 8 MeV neutron energy. Using time-of-flight techniques, differential scattering cross-sections were measured in the angular interval 20° to 160° in steps of 10° except in the forward angular region, where 5° steps were used. The angular distributions were corrected for neutron attenuation in the sample, for neutron multiple scattering and for geometrical effects.

The experimental angular distributions are compared with distributions calculated using an optical potential with spherical symmetry. The potential parameters, i.e. the real and imaginary potential depths, the radii and the real diffuseness parameter have been calculated with an automatic parameter search routine. The remaining parameters, namely the imaginary diffuseness parameter and the spin-orbit potential depth were held constant throughout the calculations. The results of these investigations demonstrate that the experimental cross-sections can be described satisfactorily in terms of the optical model. The geometrical parameters of the potential obtained by a best-fit procedure show no marked variations with mass number. The real potential depth slowly decreases with mass number and neutron excess. This shows the existence of a potential term depending upon isobaric spin. Its strength is 50 ± 10 MeV. The imaginary potential depth also decreases with mass number for values of the latter larger than about 55. Below this mass number the imaginary potential depth exhibits pronounced fluctuations.

1. INTRODUCTION

The purpose of the present experiment was to measure differential neutron elastic scattering cross sections at 8 MeV for several (22) elements in the mass interval A = 27 - 209, these being of interest to reactor designers and engineers. This is a continuation of work which has been done at our Van de Graaff laboratory for several years. Throughout, the work has been oriented toward the need for cross section data for application to reactor physics problems. Some of the cross section data hitherto obtained have been reported elsewhere [1 - 3]. These papers also discuss the interpretation of the observations in terms of an optical model potential with five adjustable parameters showing that the experimental data can be well described by this model. A good basis is thus obtained for calculations of neutron cross sections of fairly good accuracy for intermediate energies as well as for nuclear masses where experimental data are lacking. By extracting information from scattering data some evidence has previously been obtained that the spherical optical potential should be dependent on the isobaric spin [1, 4]. The present study will contribute further knowledge supporting the existence of an isobaric spin term in the optical potential.

2. EXPERIMENTAL PROCEDURE AND RESULTS

The differential scattering cross section measurements were carried out using the techniques reported previously [1 - 3] except that the electronic equipment has recently been replaced by a standard commercial fast

TABLE I. THE EXPERIMENTAL PARAMETERS CHARACTERISTIC OF THE ELASTIC-SCATTERING CROSS-SECTION MEASUREMENTS

Neutron source	$D(d, n)He^3$
Neutron energy	8.05 MeV
Gas target	Length of gas target cell 3 cm Nickel foil thickness 2.5 mg/cm^2 Deuterium gas pressure in the cell 1 kp/cm^2 Total energy spread $\pm$ 90 keV
Accelerator beam	Beam pulse frequency 1 MHz Beam pulse width at half-height 2 ns Mean target current 1.5 μA
Sample size and purity	Al to Bi, cylinders having lengths of 5.0 cm, 0.95 cm inner diameter and 2.5 cm outer diameter Polythene scatterer, 3.0 cm in length, 0.95 cm outer diameter and 0.65 cm inner diameter Sample purity $\geq$ 99.5%
Target-scatterer-detector distances	Target-scatterer 10 cm Scatterer-detector 300 cm
Neutron time-of-flight detector	Scintillators NE102A and NE104 Scintillator size 10 cm diameter and 5 cm length Spectrometer time resolution 3 ns
Neutron flux measurements	The neutron flux was monitored with a directional long counter
Angular interval	The angular distributions have been measured in the angular region 20° to 160° in 10° steps except in the foreward directions, where measurements were performed in 5° steps
Background conditions	The signal-to-background ratio at the position of the elastic peak was 7 to 1 in the most unfavourable case i.e. at the forward scattering angles.
Counting statistics	Statistical errors for the number of counts in the elastic peaks of the time-of-flight spectra $\leq$ 2% Statistical error for the number of monitor counts 0.3%
Errors	The experimental cross section errors are about 5 per cent

neutron time-of-flight set up. The experimental parameters are summarized in Table I. The cross sections were measured relative to the n-p cross sections [5]. Corrections have been applied to the measured cross sections for neutron multiple scattering in the sample under investigation as well as for neutron attenuation and geometrical effects caused by the size of the sample and its distance from the target and the detector [6]. The corrected angular distributions are shown in Fig. 1.

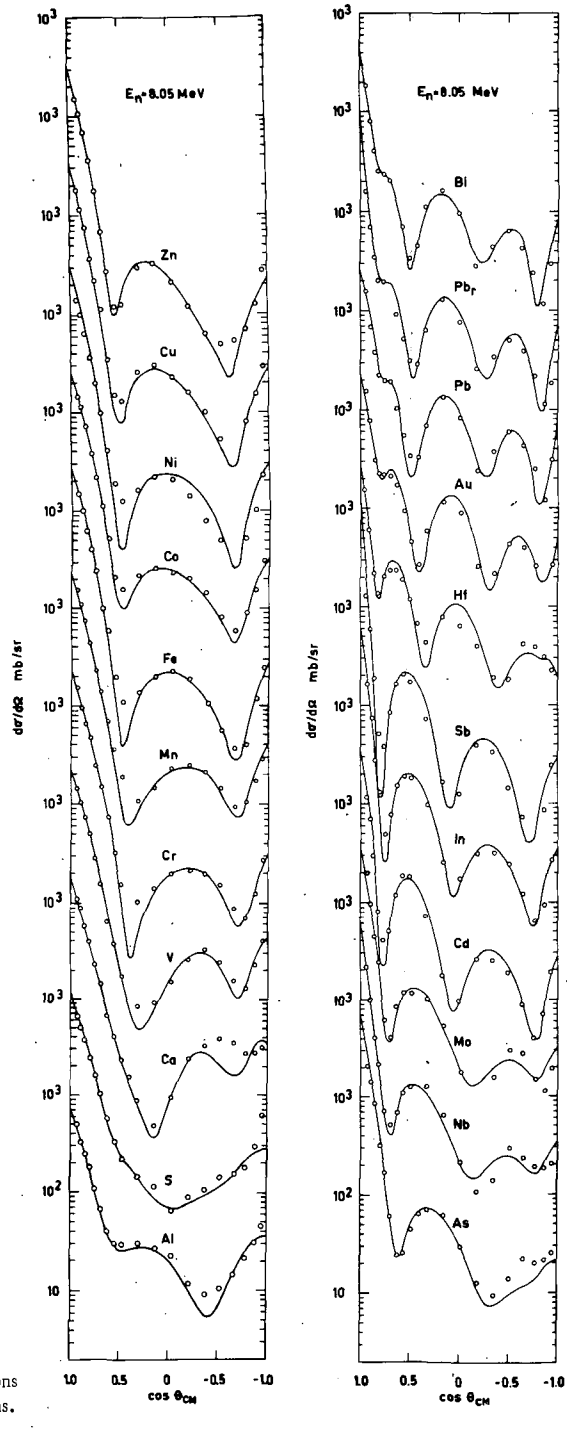

FIG. 1. The experimental (circles) and calculated (solid lines) angular distributions of elastically scattered 8.05 MeV neutrons.

TABLE II. OPTIMUM VALUES OF THE OPTICAL-POTENTIAL PARAMETERS OF THE ELEMENTS IN THE MASS NUMBER INTERVAL A = 27 - 209 AT 8.05 MeV NEUTRON ENERGY AND FROM THE FIVE-PARAMETER ANALYSES. THE TOTAL ELASTIC CROSS-SECTIONS σ_{el} AND THE TOTAL CROSS-SECTIONS σ_T CALCULATED WITH THE OPTICAL POTENTIAL ARE ALSO INCLUDED TOGETHER WITH THE CORRESPONDING EXPERIMENTAL QUANTITIES σ_{el}^{exp} AND σ_T^{exp}. THE EXPERIMENTAL TOTAL CROSS-SECTIONS HAVE BEEN TAKEN FROM REFERENCES [7, 8]

Element	Al	S	Ca	V	Cr	Mn	Fe	Co	Ni	Cu	Zn
U (MeV)	49.9	49.6	53.9	46.6	50.6	50.5	49.3	51.3	45.7	47.5	49.4
W (MeV)	7.14	8.20	5.93	6.43	9.13	8.04	10.45	10.04	9.16	10.11	10.80
r_{oU} (fm)	1.22	1.22	1.13	1.23	1.21	1.19	1.23	1.19	1.25	1.22	1.20
r_{oW} (fm)	1.24	1.18	1.41	1.25	1.21	1.17	1.20	1.17	1.29	1.18	1.19
a (fm)	0.65	0.68	0.78	0.65	0.61	0.65	0.64	0.66	0.68	0.68	0.70
σ_T (b)	1.78	2.21	2.86	3.10	3.07	3.21	3.31	3.36	3.59	3.58	3.62
σ_{el} (b)	0.77	1.02	1.60	1.85	1.76	1.89	1.85	1.90	2.01	2.01	2.00
σ_A (b)	1.01	1.19	1.26	1.25	1.31	1.32	1.47	1.46	1.58	1.57	1.62
σ_{el}^{exp} (b)	0.81±0.04	1.01±0.05	1.58±0.08	1.85±0.11	1.78±0.09	1.94±0.14	1.76±0.09	1.82±0.09	1.71±0.09	2.00±0.10	1.82±0.09
σ_T^{exp} (b)	1.68±0.05 [Ref. 7] 1.81±0.03 [Ref. 8]	2.20±0.06 [Ref. 7]	2.77±0.07 [Ref. 7] 2.76±0.04	3.14±0.08 [Ref. 7] 3.26±0.03 [Ref. 8]	3.19±0.08 [Ref. 7]	3.32±0.09 [Ref. 7]	3.31±0.09 [Ref. 7] 3.37±0.03 [Ref. 8]	3.52±0.08 [Ref. 7]	3.53±0.08 [Ref. 7]	3.63±0.05 [Ref. 7]	3.68±0.08 [Ref. 7]

Element	As	Nb	Mo	Cd	In	Sb	Hf	Au	Pb	Pb_r	Bi
U (MeV)	49.0	48.8	48.4	49.5	46.0	46.5	45.2	45.5	46.0	45.2	44.5
W (MeV)	9.73	9.76	9.78	9.55	8.15	8.49	6.74	6.29	6.30	6.69	6.21
r_{oU} (fm)	1.22	1.22	1.21	1.20	1.24	1.23	1.22	1.23	1.23	1.24	1.25
r_{oW} (fm)	1.17	1.13	1.14	1.27	1.26	1.29	1.26	1.27	1.28	1.26	1.28
a (fm)	0.67	0.68	0.68	0.68	0.66	0.66	0.66	0.65	0.65	0.64	0.65
σ_T (b)	3.79	4.04	4.05	3.97	4.15	4.17	4.51	4.93	5.39	5.33	5.51
σ_{el} (b)	2.18	2.20	2.20	1.98	2.22	2.14	2.29	2.60	2.95	2.88	3.04
σ_A (b)	1.62	1.84	1.85	1.99	1.93	2.03	2.23	2.32	2.44	2.45	2.46
σ_{el}^{exp} (b)	2.37±0.11	2.68±0.14	2.22±0.13	1.62±0.10	1.99±0.10	1.75±0.10	2.34±0.13	2.30±0.19	2.20±0.13	2.11±0.13	2.70±0.14
σ_T^{exp} (b)	4.00±0.05 [Ref. 7]	4.21±0.06 [Ref. 7]	4.23±0.08 [Ref. 7]	4.25±0.10 [Ref. 7]	4.33±0.08 [Ref. 7]	4.35±0.06 [Ref. 7]	5.01±0.11 [Ref. 7]	5.19±0.10 [Ref. 7]	5.42±0.10 [Ref. 7] 5.42±0.08 [Ref. 8]	5.40±0.05 [Ref. 7]	5.57±0.12 [Ref. 7]

Pb_r stands for radiogenic lead

3. THEORETICAL ANALYSES

The observed angular distributions have been compared with distributions calculated with a local nuclear optical potential of the form

$$-V(r) = Uf(r) + iWg(r) + U_{so}\left(\frac{\hbar}{\mu_\pi c}\right)^2 \frac{1}{r}\frac{d}{dr}\,|f(r)|\,\bar{\sigma}\cdot\bar{l}$$

The radial variation of the real potential is determined by the Saxon-Woods form factor f(r) and that of the imaginary potential by the derivative Saxon-Woods form factor g(r). The corresponding strengths of these potentials are U and W, respectively. The last term of the potential takes the spin-orbit interaction into account. Its strength is U_{so}. The real and imaginary radii are defined by the expressions $R_U = r_{oU}A^{1/3}$ and $R_W = r_{oW}A^{1/3}$. The diffuseness of the real and imaginary potential terms are determined by the parameters a and b, respectively.

Five of the potential parameters, i.e. U, W, r_{oU}, r_{oW} and a have been adjusted to obtain the best agreement with the measured elastic cross sections. The best fits to the experimental data have been acquired by using the ABACUS II automatic five-parameter search code. The spin-orbit potential depth was kept constant as also was the diffuseness parameter of the imaginary potential since the angular distributions are comparatively insensitive to variations in these parameters [1]. Their values were chosen to be 8.0 MeV and 0.48 fm, respectively.

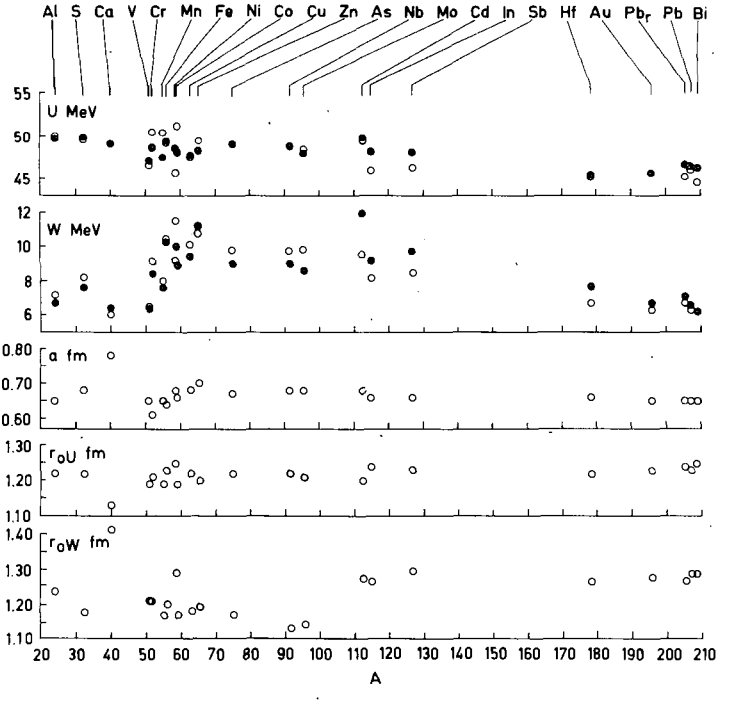

FIG. 2. The parameter values U, W, a, r_{0U} and r_{0W} plotted versus the mass number A (circles). The filled circles are the values of U and W from the two-parameter analyses.

The compound elastic cross sections are negligible for all the elements at 8 MeV neutron energy.

The angular distributions calculated with the five-parameter search procedure are shown in Fig. 1. It is clear that the experimental distributions are well described by distributions calculated with the simple spherical optical potential. Even the calculated distributions of the light elements Al, S and Ca agree surprisingly well with the measured ones.

The optical potential parameters corresponding to the best fits between the experimental and calculated angular distributions are given in Table II which also includes experimental and calculated total and total elastic cross sections. The agreements between the experimental and calculated cross sections are generally very good. Thus it is quite clear that the optical potential parameters corresponding to the optimum fits of the angular distributions are also relevant to calculations of the total cross sections of the elements.

The optimum potential parameters have been plotted versus the mass number (A) in Fig. 2. The geometrical parameters of the potential show no pronounced variations with the mass number except may be for r_{oW} which shows a tendency to increase somewhat with A. The real potential depth slowly decreases with A which is the case also for the imaginary potential at least for A > 55. Below that value the imaginary potential depth exhibits pronounced fluctuations.

Since the geometrical parameters have been obtained for a rather large number of elements and are essentially independent of A they have been used for mean value calculations representative of neutron scattering at 8 MeV in the mass interval $27 \leq A \leq 209$. The values obtained are: $\bar{r}_{oU} = \bar{r}_{oW} = 1.22 \pm 0.01$ fm, $\bar{r}_{oW} = 1.23 \pm 0.01$ fm and $\bar{a} = 0.67 \pm 0.01$ fm. These values are in good agreement with those ($\bar{r}_{oU} = \bar{r}_{oW} = 1.21 \pm 0.01$ fm and $\bar{a} = 0.66 \pm 0.01$ fm) obtained previously from a study of neutron scattering in the energy interval 1.5 to 8.1 MeV [1].

Using the mean values of the geometrical parameters, analyses in terms of two variable parameters, namely the well depths U and W, have been performed. The best fits are not essentially different from those of the five parameter analyses and are hardly visible on the scale of Fig. 1.

The optimum values of U and W from the two parameter calculations have been plotted in Fig. 2. It is seen that U and W obtained from the two analyses vary in the same way with A. However, the values of U obtained from the two parameter analyses show a smoother variation with A than those obtained from the five parameter analyses.

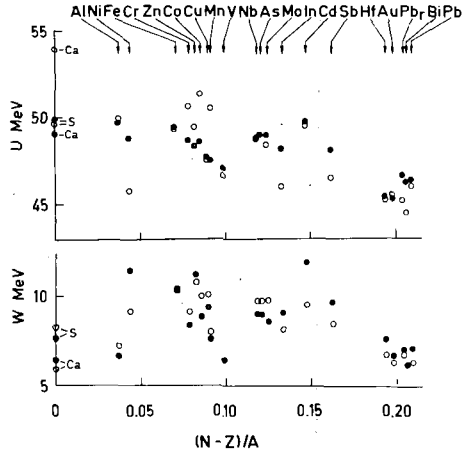

FIG. 3. The optimum values of U and W from the two-parameter (filled circles) and five-parameter (circles) analyses plotted as functions of the symmetry parameter (N-Z)/A.

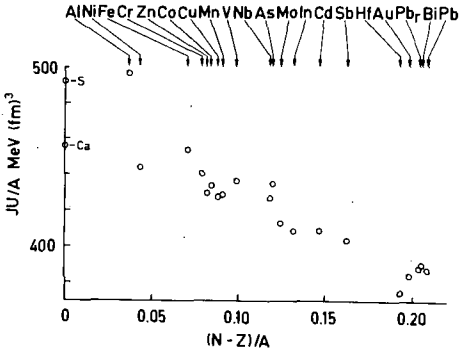

FIG.4. The quantity JU/A plotted as a function of the symmetry parameter (N-Z)/A.

The values of the parameters U and W have been plotted versus the symmetry parameter $\alpha = (N - Z)/A$ in Fig. 3 showing that U decreases smoothly with α in contrast to W which exhibits a large scatter. It is clear that the real part of the optical potential contains an isobaric spin dependent potential part. Its strength is conveniently determined from the expression $U = U_0 - U_1 (N - Z)/A$ where U_0 and U_1 are constants [1]. A least squares fitting gives a value of 50 ± 10 MeV for U_1. No isobaric spin dependence of W has been extracted from the data because of the large fluctuations of W with $(N - Z)/A$. However, because of the well-known ambiguity of U due to its dependence on r_{oU} it is better to use the volume integral (J) of the real potential as a measure of its strength than U in a study of the α dependence [1]. Thus the quantity $JU/A = 4\pi U/A \int_0^\infty f(r)\, r^2 dr$ was calculated from the data of the five parameter analyses. The values of JU/A have been plotted versus α in Fig. 4. A comparison between Figs. 3 and 4 shows that the fluctuations of JU/A are smaller than those of U. Assuming that JU/A is linearly dependent on α the strength of the isobaric spin potential has been calculated by the least squares method giving 470 ± 40 MeV $(fm)^3$.

REFERENCES

[1] HOLMQVIST, B., A systematic study of fast neutron elastic scattering in the energy region 1.5 to 8.1 MeV, Arkiv Fysik 38 (1968) 403.

[2] HOLMQVIST, B., WIEDLING, T., Neutron elastic scattering cross sections experimental data and optical model cross section calculations, AB Atomenergi, Studsvik, Sweden, Rep. AE-366 (1969).

[3] HOLMQVIST, B., JOHANSSON, S.G., LODIN, G., WIEDLING, T., Fast neutron elastic and inelastic scattering of vanadium, AB Atomenergi, Studsvik, Sweden, Rep. AE-375 (1969).

[4] HOLMQVIST, B., WIEDLING, T., Evidence for a symmetry term in the optical potential for neutrons, Phys. Letters 26B (1968) 620.

[5] HORSLEY, A., Neutron cross sections of hydrogen in the energy range 0.001 eV to 20 MeV, Nucl. Data 2A (1966) 243.

[6] HOLMQVIST, B., GUSTAVSSON, B., WIEDLING, T., A Monte Carlo program for calculation of neutron attenuation and multiple scattering corrections, Arkiv Fysik 34 (1967) 481.

[7] FOSTER, D.G., Private communication, and Neutron Cross Sections, BNL 325, 2nd ed., Suppl. No. 2 (1965).

[8] GALLOWAY III, L.A., SHRADER, E.F., Neutron total cross section measurements using a "white" neutron source. Case Institute of Technology, Technical Report No. COO-1573-6 (1966).

FAST-NEUTRON INELASTIC SCATTERING IN THE ENERGY RANGE 2 TO 4.5 MeV

E. ALMÉN, M.A. ETEMAD,*
B. HOLMQVIST, T. WIEDLING
AB Atomenergi, Studsvik, Nyköping,
Sweden

Abstract

FAST-NEUTRON INELASTIC SCATTERING IN THE ENERGY RANGE 2 TO 4.5 MeV.

A comprehensive investigation of fast-neutron inelastic scattering is in progress for a number of elements whose cross-sections have been requested for reactor-physics calculations.

The inelastic scattering cross-sections have been measured for 20 elements but the investigation of only six of them, i.e. Al, V, Mn, Fe, Nb, and Bi has been completed up to now. The measurements were made in the energy region 2 to 4.50 MeV in steps of roughly 0.25 MeV. Time-of-flight techniques were used. The inelastic cross-sections were determined relative to those established for the n-p reaction.

The experimental cross-sections have been corrected for the effects of the neutron-source anisotropy, attenuation of the neutron flux in the scatterer as well as for finite geometrical effects, using Monte-Carlo techniques.

The experimental excitation functions are compared with those calculated with the Hauser-Feshbach formalism. The effects of level-width fluctuation have also been taken into account. Optical-model parameters previously found in a systematic fast-neutron elastic-scattering investigation on the elements studied here have been used to obtain transmission coefficients for application in the Hauser-Feshbach calculations.

1. INTRODUCTION

These studies were made in order to collect information on neutron inelastic scattering cross sections to provide data, experimental as well as theoretical, for reactor physics calculations.

The project concerns the investigation of inelastic neutron scattering cross sections of a large number of elements. Measurements of 20 elements are in progress, i.e. Be, Mg Al, S, Ti, V, Cr, Mn, Fe, Co, Ni, Cu, Zn, Ga, Nb, In, Ta, Pb, Pb_r (radiogenic lead) and Bi. The measurements have been performed up to now over the energy range 2 to 4.5 MeV for 12 of these elements, i.e. Al, V, Cr, Mn, Fe, Co, Cu, Zn, Nb, In, Ta and Bi. Observations of the rest of the elements have only been made in the energy interval 2 to 3.25 MeV, but also these measurements are planned to be extended up to 4.5 MeV. Energy intervals of 0.25 MeV were chosen between the individual energy points, which was considered satisfactory from the reactor physics point of view.

Since relatively large amounts of sample material are needed in this type of measurements and enriched samples have not been put at our disposal and because of the complex level structures of the individual isotopes composing the natural elements, rather complex spectra have often been obtained.

The analyses of the experimental data have at present only been completed for the following elements: Al, V, Mn, Fe, Nb and Bi. The excitation curves for the inelastic transitions of these elements will be presented and will be compared with cross section predictions based on the Hauser-Feshbach (HF) statistical model corrected for level width fluctuations.

---

* On leave from Teheran University Nuclear Centre, Teheran, Iran.

2. EXPERIMENTAL

The experiments were made using the Studsvik 6 MV Van de Graaff accelerator supplied with a pulsed ion source with a klystron buncher [1]. The facilities and experimental methods have been described on several occasions [2, 3]. The main experimental data characteristic of the measurements are summarized in Table I.

The measurements have been made only at one angle, 125°. This is sufficient with regard to the angular distribution functions, which are usually either isotropic or only slightly unisotropic. Then the total inelastic

TABLE I. THE EXPERIMENTAL PARAMETERS CHARACTERISTIC OF THE INELASTIC-SCATTERING CROSS-SECTION MEASUREMENTS

Neutron source	$^{3}T(p, n)He^{3}$
Gas target	Length of gas target cell 3 cm Nickel foil thickness 2.5 mg/cm^2 Gas pressure in the cell 1 kp/cm^2 Total energy spread ± 50 keV
Accelerator beam	Beam pulse frequency 1 MHz Beam pulse width at half-height 2 ns Mean target current 1.5 μA
Sample size and purity	Al to Bi, cylinders having lengths of 5.0 cm, 0.95 cm inner diameter and 2.5 cm outer diameter Polythene scatterer, 3.0 cm in length, 0.95 cm outer diameter and 0.65 cm inner diameter Sample purity ≥ 99.5%
Target-scatterer-detector distances	Target-scatterer 10 cm Scatterer-detector 300 cm
Neutron time-of-flight detector	Scintillator NE 104, size 10 cm diameter and 5 cm length Spectrometer time resolution 3 ns
Neutron flux measurements	The neutron flux was monitored with a directional long counter
Scattering angle	125°
Errors	The experimental cross section errors are in general about 10 per cent

TABLE II. NEUTRON-PROTON TOTAL SCATTERING CROSS-SECTIONS USED IN THE EVALUATION OF THE INELASTIC-NEUTRON-SCATTERING CROSS-SECTIONS AT THE APPROPRIATE INCIDENT NEUTRON ENERGIES

E_n MeV	2.02	2.27	2.50	2.77	3.01	3.29	3.52	3.78	4.02	4.26	4.50
σ_T b	2.88	2.70	2.54	2.40	2.28	2.15	2.06	1.97	1.84	1.81	1.74

cross section is just 4π times the measured differential cross section when the angular distribution function is of the form $1 + a_2 P_2(\cos\theta)$. This Legendre function is a good approximation of most inelastic angular distributions.

The cross sections are expressed relative to the n-p cross sections [4]. The neutron-proton scattering cross sections applied are compiled in Table II.

The resolution of the time-of-flight spectrometer is demonstrated in Fig. 1, showing two typical spectra of scattering from Nb recorded at 2.50 MeV primary neutron energy and Bi at 3.78 MeV.

The experimental cross sections have been corrected for the effects of the neutron source anisotropy, attenuation of the neutron flux in the scatterer, as well as for finite geometrical effects, using Monte Carlo techniques. The effects of elastic-inelastic and inelastic-inelastic neutron processes have also been considered.

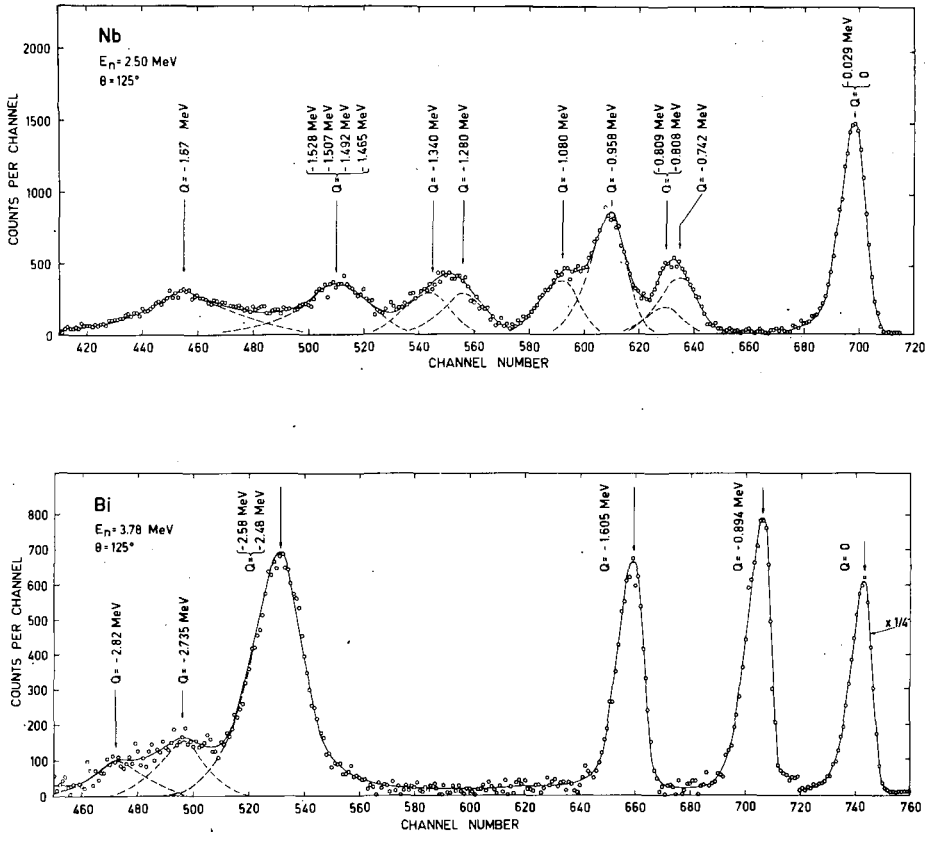

FIG. 1. The figure illustrates typical neutron time-of-flight spectra obtained for two elements, one with comparatively small level spacings, Nb, and one with large level spacings, Bi. The spectra were recorded at primary neutron energies of 2.50 and 3.78 MeV, respectively.

TABLE III. NUCLEAR OPTICAL-MODEL PARAMETERS USED IN THE CALCULATIONS OF THE TRANSMISSION COEFFICIENTS FOR APPLICATION IN THE HF-CALCULATIONS OF THE INELASTIC CROSS-SECTION OF Al, V, Mn, Fe, Nb AND Bi

Element	E_n (MeV)	U (MeV)	W (MeV)	r_U (fm)	r_W (fm)	a (fm)
Al	2.02	48.2	8.40	1.15	1.21	0.65
	2.50	48.4	8.30	1.15	1.22	0.65
	3.01	48.5	8.25	1.16	1.22	0.65
	3.52	48.6	8.20	1.17	1.22	0.65
	4.02	48.7	8.10	1.17	1.22	0.65
	4.50	48.8	8.04	1.18	1.23	0.65
V	2.50	51.3	8.40	1.19	1.21	0.65
	3.01	47.4	8.40	1.26	1.23	0.66
	3.52	48.6	8.41	1.24	1.22	0.66
	4.02	48.1	8.30	1.25	1.21	0.66
	4.50	49.2	8.12	1.23	1.18	0.65
Mn	2.02	52.5	8.34	1.18	1.15	0.66
	2.50	52.5	8.35	1.18	1.15	0.66
	3.01	52.4	8.35	1.18	1.15	0.66
	3.52	52.4	8.35	1.18	1.15	0.66
	4.02	52.3	8.35	1.18	1.15	0.66
	4.50	52.2	8.35	1.18	1.16	0.66
Fe	2.02	52.7	10.70	1.19	1.09	0.61
	2.50	52.3	10.70	1.20	1.10	0.61
	3.01	51.9	10.70	1.20	1.11	0.61
	3.52	51.5	10.65	1.21	1.12	0.62
	4.02	51.0	10.60	1.21	1.13	0.62
	4.50	50.7	10.60	1.21	1.14	0.63
Nb	2.02	45.6	7.82	1.29	1.24	0.64
	2.50	45.8	7.86	1.28	1.24	0.65
	3.01	45.9	7.91	1.28	1.25	0.65
	3.52	46.1	7.96	1.27	1.25	0.65
	4.02	46.3	8.00	1.27	1.25	0.65
	4.50	46.4	8.05	1.26	1.25	0.66
Bi	2.02	43.5	6.37	1.25	1.26	0.69
	2.50	43.6	6.35	1.25	1.27	0.68
	3.01	43.7	6.32	1.25	1.27	0.68
	3.52	43.8	6.30	1.25	1.27	0.68
	4.02	43.9	6.30	1.25	1.27	0.68
	4.50	44.0	6.28	1.25	1.27	0.67

3. RESULTS

The experimental results are shown in Figs. 2 to 4. Included in the figures are also data of some previously reported experiments [3, 5 - 9]. The agreement is in general good with the exception of the elements Al and V which show some discrepancies, probably explainable by somewhat worse energy resolution in the previous experiments.

The transmission coefficients used to calculate the inelastic scattering cross sections are those obtained with the optical model parameters shown in Table III. These parameters were evaluated from systematic optical model studies of elastic neutron scattering from a number of elements in the periodic table when using a local optical nuclear potential [10].

Theoretical excitation curves representing cross sections calculated with the HF formalism for neutron transitions to individual energy levels are shown in Figs. 2 - 4. The results of HF calculations corrected for level width fluctuations are shown in appropriate cases. Information on level energies, spins and parities were obtained from the following references: for Al [11, 12], V [3], Mn [11, 13], Fe [11, 14 - 16], Nb [17 - 20] and for Bi [8, 11].

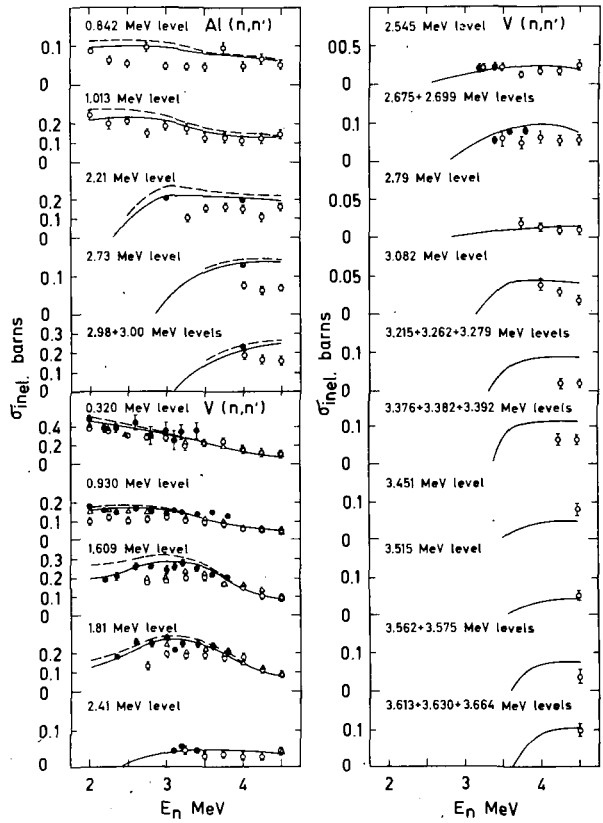

FIG. 2. Excitation functions for inelastic neutron scattering from the elements Al, and V. The experimental results (circles) are compared with cross-sections calculated by use of the HF-formalism (dashed lines) as well as with HF-cross-sections corrected for Moldauer level-width fluctuation (solid lines). Filled circles refer to results published by Towle et al. for Al [5] and V [7] and the triangles to Holmqvist et al. [3].

4. COMMENTS

Since it is not possible to discuss the results in detail, the discussion will be limited to some general remarks and comments. A comparison between the calculated excitation functions and the experimental points clearly demonstrates that the calculations give in some cases systematically too large cross sections. Such a trend is observed for Al, Nb and Bi, where the calculated cross sections of all transitions are well outside the experimental values. The experimental data of the elements V, Mn and Fe, on the other hand, seem to be better described by the HF formalism. This general behaviour of the inelastic neutron scattering process clearly demonstrates the need for future accurate and systematic investigations.

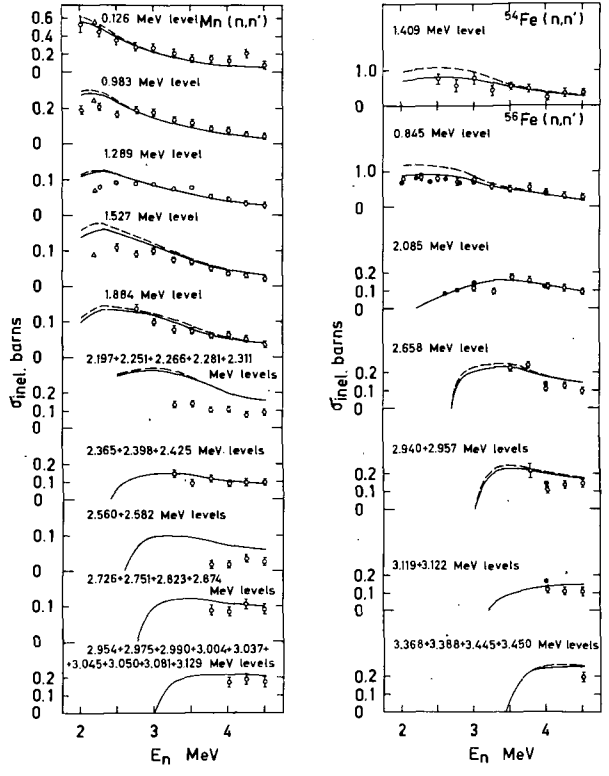

FIG. 3. Excitation functions for inelastic neutron scattering from the elements Mn and Fe. The experimental results (circles) are compared with cross-sections calculated by use of the HF-formalism (dashed lines) as well as with HF-cross-sections corrected for Moldauer level-width fluctuation (solid lines). Filled circles refer to results reported by Towle et al. [6] and triangles to Barrows et al. [9].

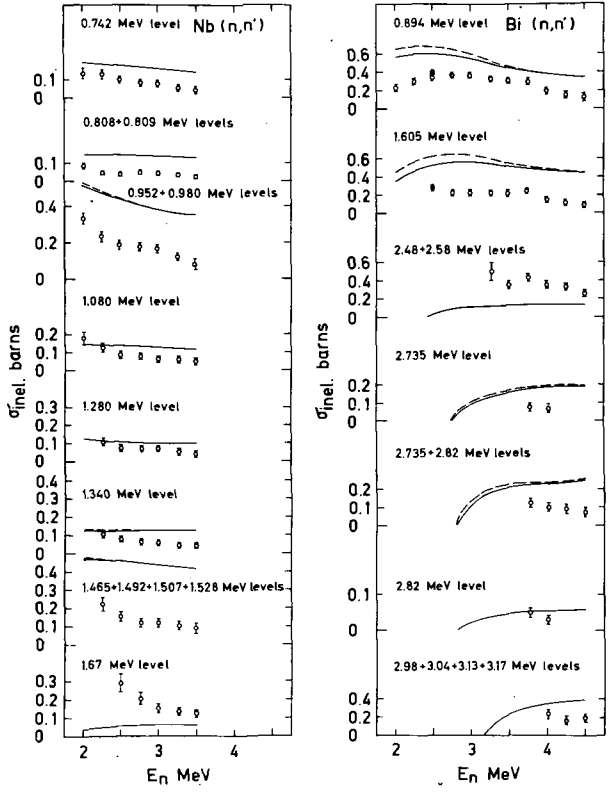

FIG. 4. Excitation functions for inelastic neutron scattering from the elements Nb and Bi. The experimental results (circles) are compared with cross-sections calculated by use of the HF-formalism (dashed lines) as well as with HF-cross-sections corrected for Moldauer level-width fluctuation (solid lines). Filled circles refer to Cranberg's data [8].

REFERENCES

[1] TYKESSON, P., WIEDLING T., Nucl. Inst. and Meth. 77 (1970) 277.

[2] HOLMQVIST, B., Arkiv Fysik 38 (1968) 403.

[3] HOLMQVIST, B., JOHANSSON, S.G., LODIN, G., WIEDLING, T., Fast Neutron Elastic and Inelastic Scattering of Vanadium, AB Atomenergi, Rep. AE-375 (1969).

[4] HORSLEY, A., Nuclear Data 2A (1966) 243, Academic Press, New York & London (1966).

[5] TOWLE, J.H., GILBOY, W.B., Nucl. Phys. 39 (1962) 300.

[6] GILBOY, W.B., TOWLE, J.H., Nucl. Phys. 64 (1965) 130.

[7] TOWLE, J.H., Nucl. Phys. A117 (1968) 657.

[8] CRANBERG, L., OLIPHANT, T.A., LEVIN, J., ZAFIRATOS, C.D., Phys. Rev. 159 (1967) 969.

[9] BARROWS, A.W., LAMB, R.C., VELKLEY, D., McELLISTREM, M.T., Nucl. Phys. A107 (1968) 153.

[10] HOLMQVIST, B., WIEDLING, T., Neutron Elastic Scattering Cross Sections, Experimental Data and Optical Model Cross Section Calculations, AB Atomenergi, Rep. AE-366 (1969).

[11] LEDERER, C.M., HOLLANDER, J.M., PERLMAN, I., Table of Isotopes, Wiley & Sons Inc. New York (1967).

[12] LOMBARD, R.M., BISHOP, G.R., Nucl. Phys. A101 (1967) 601.

[13] KATSANOS, A.A., HUIZENGA, J.R., Phys. Rev. 159 (1967) 931.

[14] MACDONALD, J.R., GRACE, M.A., Nucl. Phys. A92 (1967) 593.

[15] BROWN, G., HAIGH, J.G.B., MACGREGOR, A.E., Nucl. Phys. A97 (1967) 353.

[16] BROWN, G., WARREN, S.E., Nucl. Phys. 77 (1966) 365.

[17] ROGERS, V.C., BEGHIAN, L.E., CLIKEMAN, F.M., HOFMAN, F., WILENSKY, S., Nucl. Phys. A142 (1970) 100.

[18] SHARMA, H.C., NATH, N., Nucl. Phys. A142 (1970) 291.

[19] Nuclear Data Sheets, National Academy of Science, National Research Council, Washington D.C. (1960).

[20] SHARMA, H.C., NATH, N., Nuclear Physics and Solid State Physics (Proc. Symp. Bombay, 1968) 2 (1968) 12.

DISCUSSION

TO PAPERS IAEA-CN-26/53, 54, 55, 56

S. W. CIERJACKS: As I understand your paper, you analysed your data by fitting the optical parameters separately for each energy. Have you observed, in the case of certain intermediate nuclei, e. g. iron and vanadium, any fluctuation in the well depth of the real and the imaginary potential with energy? You may know that Smith at Argonne observed such fluctuations for vanadium at energies which are lower than the energy at which you start your analysis. However, I would like to know whether such fluctuations are completely damped in the higher-energy region.

B. HOLMQVIST: Fluctuations of this kind have not been observed. I think they are damped out in our energy region.

A. PRINCE: I noticed that there was a wide gap in the experimental data between antimony and hafnium. This is a region of high deformity. Have you made any measurements in this region and, if so, have you analysed them in the same manner?

B. HOLMQVIST: Thus far elastic neutron scattering has been measured for ^{181}Ta at several energies in the interval between 2. 5 and 8 MeV. The experimental data have been enalysed in terms of a non-spherical optical potential developed by Professor Benzi's group at CNEN in Bologna. A report has been accepted for publication in Nuclear Physics. Some neutron-elastic-scattering data measured at 8 MeV have also been submitted to this Conference (see paper CN-26/31).

НЕУПРУГОЕ РАССЕЯНИЕ БЫСТРЫХ НЕЙТРОНОВ НА ЯДРАХ Cr, Ni, Y, Zr, W

О. А. САЛЬНИКОВ, Г. Н. ЛОВЧИКОВА,
Г. В. КОТЕЛЬНИКОВА, Н. И. ФЕТИСОВ,
А. М. ТРУФАНОВ

Физико-энергетический институт, Обнинск,
Союз Советских Социалистических Республик

Presented by A.I. Abramov

Доклад представлен А.И. Абрамовым

Abstract — Аннотация

INELASTIC SCATTERING OF FAST NEUTRONS BY CHROMIUM, NICKEL, YTTRIUM, ZIRCONIUM AND TUNGSTEN NUCLEI.

The authors obtained the energy spectra of neutrons undergoing inelastic scattering by chromium, nickel, yttrium, zirconium, and tungsten nuclei for five scattering angles: 30°, 60°, 90°, 120° and 150°. The measurements were made with a KG-300 cascade generator using the time-of-flight method. The initial energy of the neutrons was 14.4 MeV and the resolution 3 nsec/m at the half-height of the gamma peak. Knowing the energy spectra of the inelastically scattered neutrons it was possible to determine the differential cross-section of the inelastically scattered neutrons for different spectrum energy intervals and to calculate the averaged temperature T_{eff} on the basis of the two neutron spectra from the reactions (n, n') and (n, 2n) and the temperature T of the residual nucleus after evaporation of the first neutron – i.e. the temperature characterizing inelastic scattering in a multi-level nucleon system. On the basis of the known angular distribution of the inelastically scattered neutrons the authors determined the relationship between the contributions of direct processes, characterized by small incident neutron energy losses, and of processes involving a compound nucleus.

НЕУПРУГОЕ РАССЕЯНИЕ БЫСТРЫХ НЕЙТРОНОВ НА ЯДРАХ Cr, Ni, Y, Zr, W.

Получены энергетические спектры неупруго рассеянных нейтронов на ядрах Cr, Ni, Y, Zr, W для пяти углов рассеяния: 30°, 60°, 90°, 120°, 150°. Измерения проводились методом времени пролета на каскадном генераторе КГ-300. Начальная энергия нейтронов составляла 14,4 Мэв, разрешение – 3 нсек/м на половине высоты γ-пика. Знание энергетических спектров неупруго рассеянных нейтронов дало возможность определить дифференциальное сечение неупруго рассеянных нейтронов для различных энергетических интервалов спектра, вычислить значение усредненной температуры $T_{эфф}$ по двум нейтронным спектрам из реакции (n,n') и (n,2n); температуры T, остаточного ядра после испарения первого нейтрона, т. е. температуры, характеризующей процесс неупругого рассеяния на многоуровневой нуклонной системе. На основании известного углового распределения неупруго рассеянных нейтронов определено соотношение между вкладами прямых процессов, характеризующимися малыми потерями энергии падающих нейтронов, и процессами, идущими через составное ядро.

ВВЕДЕНИЕ

В докладе изложены результаты изучения спектров нейтронов, испускаемых ядрами Cr, Ni, Y, Zr, W при бомбардировке их нейтронами с начальной энергией 14,4 Мэв и дифференциальные сечения реакций (n,n'), (n,2n) и (n,pn) на этих ядрах. Дифференциальные сечения и спектры измерялись под углами от 30° до 150° через каждые 30°.

ЭКСПЕРИМЕНТ

Измерение спектров и дифференциальных сечений проводилось методом времени пролета. Схема эксперимента показана на рис. 1. Нейтроны из реакции $^3T(d,n)^4He$ падали на рассеиватель под углом 66° ± 6° по отношению к направлению движения дейтонов. Энергия дейтонов равнялась 250 кэв. Вспышки нейтронов длительностью 5 нсек получались прерыванием пучка дейтонов до ускорения. Частота повторения вспышек была 2 Мгц, средний ток на мишени составлял 2 мка.

Рассеивателями служили полые цилиндры, внешний диаметр которых был равен 4,5 см, а внутренний – 1,5 см. Высота рассеивателей была в пределах 5-6 см. Учет многократного рассеяния в образце осуществлялся методом Монте-Карло на ЭВМ.

Расстояние от мишени до рассеивателя ℓ = 17 см, а пролетная база L = 200 см.

Суммарный энергетический разброс падающих на рассеиватель нейтронов, обусловленный толщиной мишени и конечностью размеров рассеивателя был равен ±0,14 Мэв, так что начальная энергия нейтронов равнялась 14,4 ± 0,14 Мэв.

Рассеянные нейтроны регистрировались жидкостным сцинтиллятором (ЖС-20) в сборке с двумя ФЭУ-36, включенными на совпадения. Детектор помещался в защитный коллиматор, конструкция которого показана на рис. 1. Порог регистрации нейтронов детектором был ~100 кэв. Относительная эффективность детектора измерялась на ускорителе Ванде-Граафа до энергии 3,5 Мэв с использованием реакций $^3T(p,n)^3He$ и $^3T(d,n)^4He$ (14 Мэв); промежутки кривой эффективности соединялись теоретической кривой [1].

Прямой поток нейтронов фиксировался двумя мониторами: всеволновым счетчиком и водородной ионизационной камерой.

В работе использовался цифровой кодировщик измеряемых интервалов времени, имеющий дифференциальную линейность не хуже 0,4%.

Ширина канала временного анализатора была равна 2,62 нсек, число каналов – 256.

Разрешение спектрометра, определяемое по ширине γ-пика на полувысоте, равнялось 7 нсек[1].

ИЗМЕРЕНИЯ И ОБРАБОТКА РЕЗУЛЬТАТОВ ИЗМЕРЕНИЙ

Процедура измерения заключалась в измерении под заданным углом спектра нейтронов от рассеивателя, что давало суммарный спектр полезных нейтронов и γ-лучей, и нейтронов фона, и в измерении спектра фона при удаленном рассеивателе. Затем фон вычитался. При вычитании фона производилась нормировка на счет монитора и вводилась поправка на просчеты из-за мертвого времени регистрирующей системы. Максимальная величина поправки на просчеты была для угла 31° и составляла 3%.

---

[1] Более полное описание спектрометра дано в статье, направленной в журнал "Ядерная физика", где приведены также результаты измерений спектров и дифференциальных сечений на ядрах Fe, Cu и Nb.

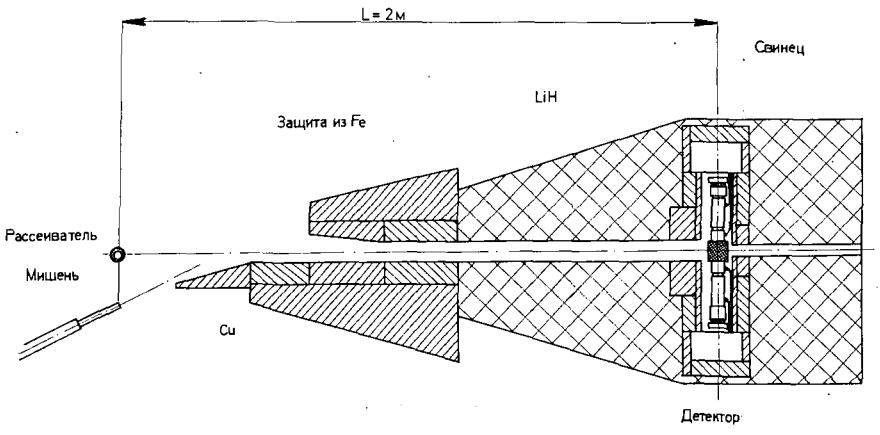

Рис. 1. Схема эксперимента.

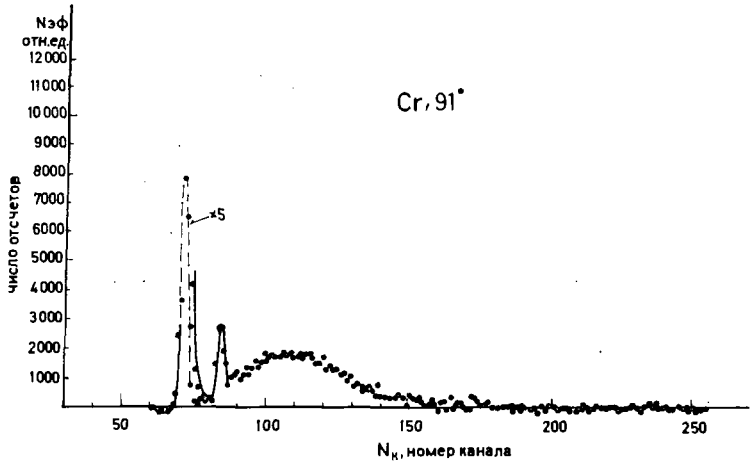

Рис. 2. Аппаратурный спектр нейтронов, рассеянных ядрами хрома. Угол рассеяния $\theta = 91°$.

На рис. 2 приведен для примера аппаратурный спектр нейтронов, рассеянных ядрами *Cr под углом* 91°.

На временном спектре проводилось отделение пика упруго рассеянных нейтронов, затем временной спектр пересчитывался в энергетический с учетом эффективности детектора к нейтронам разной энергии и вводилась поправка на многократное рассеяние в образце.

Полученные спектры нормировались по измеренному прямому потоку и по рассеянию на углероде. Дифференциальные сечения рассеяния на углероде брались из работы [2]. Оба метода нормировки дали совпадающие результаты.

Так как в зарегистрированный спектр нейтронов давали вклад реакции (n, n'), (n, 2n) и (n, pn), то суммарное число нейтронов нормированного спектра (площадь спектра) равно сумме $\sigma(n,n') + 2\sigma(n, 2n) + \sigma(n, pn)$. Значение этой суммы, полученной в нашей работе для ядер Cr, Ni, Y, Zr, W и в работах, собранных в [3], приведено в табл. 1.

Измеренные спектры разбивались на интервалы: (0-3) Мэв, (3-4,2) Мэв, (4,2-5,4) Мэв, (5,4-6,4) Мэв и (6,4-14,4) Мэв. Для каждого интервала вычислялось соответствующее дифференциальное сечение. Они приведены в табл. 2. На рис. 3 приведено для примера угловое распределение эмиссии нейтронов для Ni .

ТАБЛИЦА 1. СУММАРНОЕ ЧИСЛО НЕЙТРОНОВ

Элемент	$\sigma(n,n') + 2\sigma(n,2n) + \sigma(n,pn)$	
	данная работа	работа [2]
Cr	1,32 ± 0,03	1,44
Ni	0,98 ± 0,02	1,09
Y	2,40 ± 0,06	2,61
Zr	2,14 ± 0,04	2,32
W	3,23 ± 0,08	3,02

Спектры нейтронов эмиссии содержат нейтроны первого и второго каскада испарения, т. е. нейтроны из реакции (n, n'), (n, 2n) и (n, pn), где она возможна (Ni). Для описания этого общего спектра использовалось распределение Максвелла с параметром $T_{эфф}$ – эффективной температурой:

$$N(E)dE = const \cdot E \cdot e^{-\frac{E}{T_{эфф}}} dE$$

Однако большой интерес представляет температура ядра после испарения первого нейтрона – T_1 . Для хрома, никеля и иттрия она определялась, как это делалось в работах [4-5]: выбирался участок спектра, где заведомо нет нейтронов из реакции (n, 2n) и (n, pn), а влиянием прямых процессов еще можно было пренебречь, и на этом участке спектр описывался распределением Максвелла с температурой T_1 :

$$N(E)dE = const \cdot E \cdot \sigma_{inv} \cdot e^{-\frac{E}{T_1}} dE$$

где σ_{inv} – сечение обратной реакции, причем для него использовалось два значения: $\sigma_{inv} = const$ и $\sigma_{inv} = f(E)$, рассчитанное по оптической модели.

Из-за сравнительно низких порогов реакции (n, 2n) на некоторых изотопах Zr (8 Мэв), составляющих 50% , и особенно на W (7 Мэв), для этих ядер невозможно выбрать участок спектра, где не было бы нейтронов из реакции (n, 2n), а вкладом прямых процессов можно было бы пренебречь. Поэтому для этих ядер T_1 определялось методом Лекутера [6], где суммарный спектр нейтронов первого и второго каскада испарения описывается с помощью параметра $T_{1\lambda}$ выражением:

$$N(E)dE = const \cdot E^{\frac{5}{11}} \cdot exp\left\{-\frac{12}{11}\frac{E}{T_{1\lambda}}\right\}$$

Полученные значения $T_{эфф}$, T_1 и $T_{1\lambda}$ приведены в табл. 3. На рис. 4 и 5 показаны в полулогарифмической шкале спектры нейтронов, рассеянных ядрами Cr и Ni.

ТАБЛИЦА 2. ДИФФЕРЕНЦИАЛЬНЫЕ СЕЧЕНИЯ

Интервал энергий / θ	0 ÷ 3,0 Мэв σ, Мб/стерад	3,0 ÷ 4,2 Мэв σ, Мб/стерад	4,2 ÷ 5,4 Мэв σ, Мб/стерад	5,4 ÷ 6,4 Мэв σ, Мб/стерад	6,4 ÷ 14,4 Мэв σ, Мб/стерад
ХРОМ					
31°	62,7 ± 1,3	17,2 ± 0,9	10,3 ± 0,8	6,6 ± 0,7	18,3 ± 3,2
61°	69,5 ± 1,3	16,2 ± 0,8	10,1 ± 0,7	6,7 ± 0,7	20,4 ± 2,5
91°	63,3 ± 1,2	13,4 ± 0,7	7,8 ± 0,6	4,9 ± 0,6	13,9 ± 2,1
121°	56,9 ± 1,1	11,4 ± 0,6	6,3 ± 0,6	3,8 ± 0,5	9,7 ± 3,8
151°	63,6 ± 1,2	11,5 ± 0,6	6,3 ± 0,6	3,8 ± 0,5	10,9 ± 1,8
НИКЕЛЬ					
31°	56,0 ± 1,0	12,8 ± 0,6	7,5 ± 0,6	4,8 ± 0,5	14,2 ± 2,5
61°	54,0 ± 1,0	10,0 ± 0,5	5,5 ± 0,5	3,5 ± 0,4	11,0 ± 1,6
91°	45,4 ± 0,9	9,1 ± 0,5	5,2 ± 0,4	3,3 ± 0,4	9,4 ± 1,3
121°	47,4 ± 0,9	8,2 ± 0,4	4,4 ± 0,4	2,7 ± 0,4	7,2 ± 1,3
151°	49,1 ± 0,9	7,7 ± 0,4	4,5 ± 0,4	2,9 ± 0,3	9,1 ± 1,3
ИТТРИЙ					
31°	151,8 ± 3,3	22,5 ± 1,6	12,7 ± 1,5	8,0 ± 1,4	23,8 ± 6,3
61°	165,2 ± 3,4	17,1 ± 1,3	8,6 ± 1,2	4,8 ± 1,2	9,2 ± 4,4
91°	136,8 ± 3,0	17,5 ± 1,2	9,6 ± 1,1	5,7 ± 1,0	14,0 ± 3,8
121°	130,9 ± 3,0	13,8 ± 1,2	7,3 ± 1,1	4,3 ± 1,0	9,7 ± 3,9
151°	157,4 ± 3,7	14,6 ± 1,3	6,8 ± 1,2	3,5 ± 1,1	6,1 ± 4,1
ЦИРКОНИЙ					
31°	133,2 ± 2,4	19,0 ± 1,1	9,7 ± 1,0	5,8 ± 0,9	16,6 ± 2,3
61°	140,2 ± 2,4	15,6 ± 0,9	7,8 ± 0,8	4,6 ± 0,8	11,8 ± 2,9
91°	128,2 ± 2,3	14,9 ± 0,9	7,3 ± 0,8	4,3 ± 0,8	12,6 ± 2,8
121°	121,6 ± 2,1	14,2 ± 0,9	6,5 ± 0,7	3,6 ± 0,7	8,8 ± 2,5
151°	132,4 ± 2,2	14,5 ± 0,8	6,8 ± 0,7	3,8 ± 0,6	8,7 ± 2,3
ВОЛЬФРАМ					
31°	201,2 ± 4,0	32,3 ± 2,1	17,4 ± 2,0	10,6 ± 1,8	29,9 ± 8,0
61°	216,9 ± 3,9	26,6 ± 1,8	13,2 ± 1,6	7,6 ± 1,5	18,2 ± 5,8
91°	208,9 ± 3,8	23,8 ± 1,6	11,1 ± 1,5	6,2 ± 1,4	15,0 ± 5,1
121°	185,2 ± 3,5	18,2 ± 1,5	7,7 ± 1,3	3,9 ± 1,2	7,4 ± 4,6
151°	180,8 ± 3,6	16,5 ± 1,4	7,1 ± 1,2	3,8 ± 1,2	8,8 ± 4,3

Значение T_1 позволяет по суммарному спектру нейтронов определить дифференциальные сечения реакций (n, n') и $(n, 2n) + (n, pn)$, причем у обсуждаемых ядер $\sigma(n, pn)$ имеет существенное значение только для Ni, а у Cr и Y сечение $\sigma(n, pn) \sim 0$, так что для них определяется сечение реакции $(n, 2n)$. Для этого спектр Максвелла с температурой T_1 нормируется по участку экспериментального спектра, где определялась T_1, и вычитается из экспериментального спектра. Разность дает спектр вторых нейтронов из реакции $(n, 2n)$ для ядер Cr и Y, а, следовательно, и сечение реакции $(n, 2n)$, так как спектр нормирован. Зная $\sigma(n, 2n)$, находим и $\sigma(n, n')$.

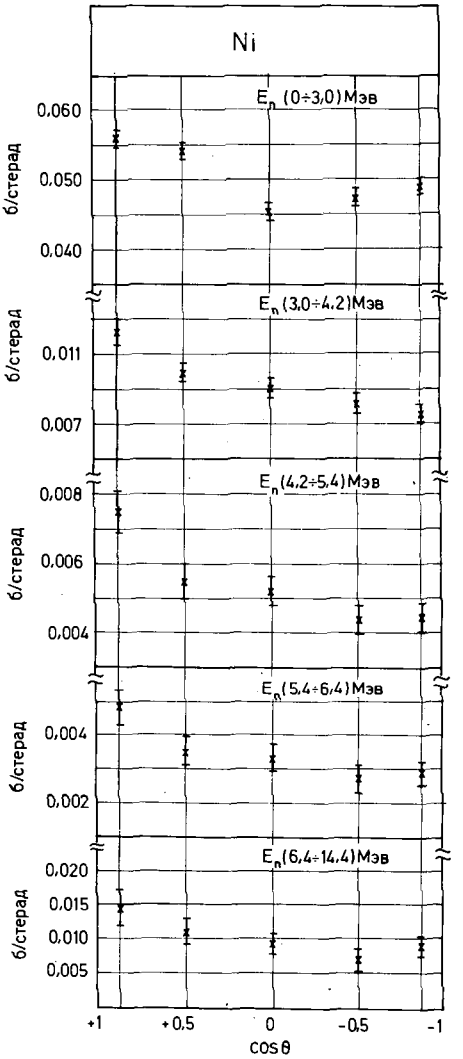

Рис. 3. Угловое распределение эмиссии нейтронов на никеле.

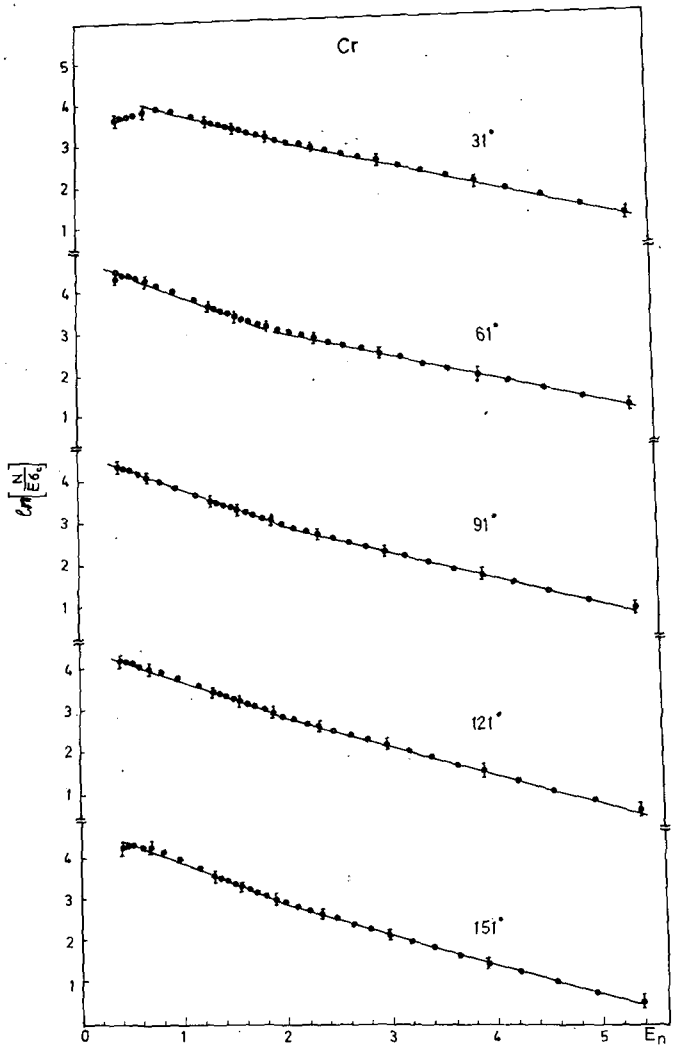

Рис. 4. Спектры нейтронов, рассеянных ядрами хрома.

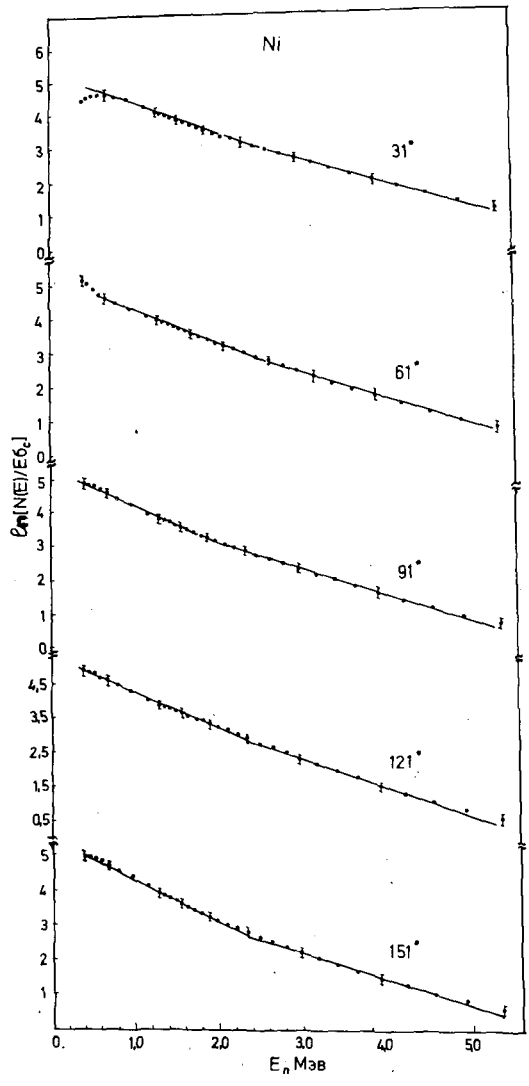

Рис. 5. Спектры нейтронов, рассеянных ядрами никеля.

Для Ni вычитание спектра Максвелла давало суммарный спектр вторых нейтронов из реакции (n, 2n) и нейтронов из реакции (n, pn).

Для углов $\theta = 91°$, 121° и 151° использовались значения T_1, полученные для тех же углов. Для углов 31° и 61° использовалось $\overline{T}_1'$, усредненное по углам 121° и 151° значение T_1.

Значения дифференциальных сечений реакций (n, n'), (n, 2n) и (n, 2n) + + (n, pn) приведены в табл. 4.

На рис. 6 приведены усредненные по углам спектры вторых нейтронов из реакции (n, 2n) для Cr и Y, а на рис. 7 – суммарный спектр вторых нейтронов из реакции (n, 2n) и нейтронов из реакции (n, pn) на Ni.

ТАБЛИЦА 3. ЗНАЧЕНИЯ $T_{эфф}$, T_1 И $T_{1\lambda}$

Ядро	$\theta°$	$E_1 \div E_2$ Мэв	$T_{эфф}$ Мэв	$E_1 \div E_2$ Мэв	T_1 Мэв
Ni	31°	0,80 ÷ 1,89	0,96 ÷ 1,05	2,8 ÷ 4,22	1,44 ÷ 1,38
	61°		0,92 ÷ 0,99		1,31 ÷ 1,26
	91°		0,90 ÷ 0,96		1,38 ÷ 1,32
	121°		0,86 ÷ 0,90		1,26 ÷ 1,21
	151°		0,78 ÷ 0,81		1,34 ÷ 1,28
	Среднее значение T по пяти углам рассеяния		0,88 ÷ 0,94	1,35 ÷ 1,29	
	Среднее значение T по углам 121° и 151°		–	1,30 ÷ 1,25	
Cr	31°	0,96 ÷ 1,71	1,13 ÷ 1,40	2,8 ÷ 4,22	1,52 ÷ 1,69
	61°		1,09 ÷ 1,03		1,55 ÷ 1,73
	91°		1,13 ÷ 1,11		1,42 ÷ 1,57
	121°		1,08 ÷ 1,12		1,33 ÷ 1,46
	151°		0,89 ÷ 0,97		1,29 ÷ 1,42
	Среднее значение T по пяти углам рассеяния		1,06 ÷ 1,13	1,42 ÷ 1,58	
	Среднее значение T по двум углам рассеяния 121° и 151°		–	1,31 ÷ 1,44	
Y	31°	0,96 ÷ 2,10	0,78 ÷ 0,81	2,8 ÷ 4,22	1,32 ÷ 1,50
	61°		0,68 ÷ 0,71		1,18 ÷ 1,32
	91°		0,64 ÷ 0,74		1,31 ÷ 1,48
	121°		0,64 ÷ 0,70		1,23 ÷ 1,38
	151°		0,76 ÷ 0,78		1,10 ÷ 1,22
	Среднее значение T по пяти углам рассеяния		0,71 ÷ 0,75	1,23 ÷ 1,38	
	Среднее значение T по двум углам рассеяния 121° и 151°		–	1,16 ÷ 1,30	

Ядро	$\theta°$	$E_1 \div E_2$ Мэв	$T_{эфф}$ Мэв	$E_1 \div E_2$ Мэв	T_1 Мэв
Zr	31°	0,96 ÷ 2,48	0,86 ÷ 0,88	0,96 ÷ 2,98	1,27
	61°		0,75 ÷ 0,76		1,09
	91°		0,79 ÷ 0,80		1,16
	121°		0,81 ÷ 0,82		1,17
	151°		0,80 ÷ 0,82		1,15
	Среднее значение по пяти углам рассеяния		0,80 ÷ 0,81	1,17	
	Среднее значение по углам 121° и 151°		–	1,16	
W	31°	0,59 ÷ 2,34	0,88 ÷ 0,82	0,96 ÷ 2,48	1,32
	61°		0,77 ÷ 0,72		1,15
	91°		0,77 ÷ 0,72		1,59
	121°		0,75 ÷ 0,70		1,04
	151°		0,70 ÷ 0,65		1,03
	Среднее значение по пяти углам рассеяния		0,77 ÷ 0,72	1,14	
	Среднее значение по углам 121° и 151°		–	1,03	

ПРИМЕЧАНИЕ: Разброс значений температур обусловлен выбором сечения образования составного ядра, первое значение соответствует σ_{inv} = const, второе – сечению, рассчитанному по оптической модели ядра.

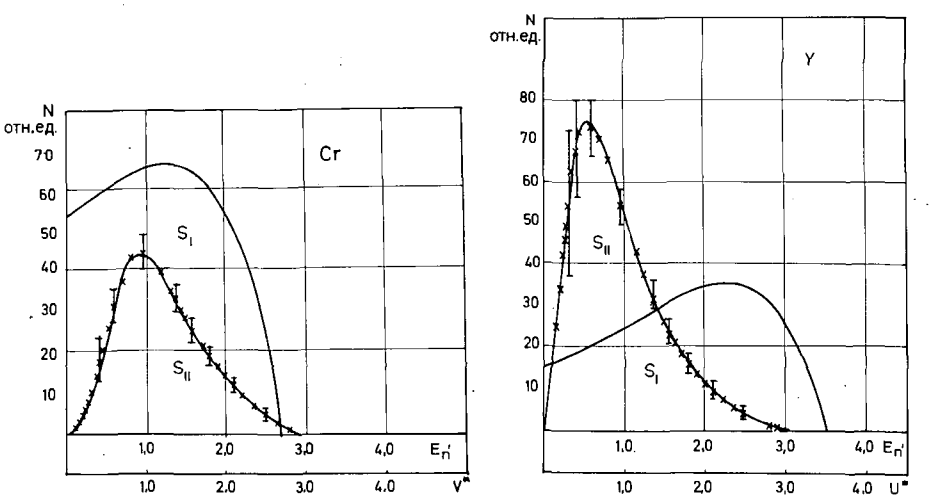

Рис. 6. Усредненные по углам спектры вторых нейтронов из реакции (n, 2n) на ядрах хрома и иттрия:

S_I – число возбужденных ядер, имеющих возможность испустить второй нейтрон,

S_{II} – число действительно испущенных вторых нейтронов.

ТАБЛИЦА 4. ЗНАЧЕНИЯ ДИФФЕРЕНЦИАЛЬНЫХ ЗНАЧЕНИЙ РЕАКЦИЙ (n, n'), (n, 2n) и (n, 2n) + (n, pn)

Элемент / θ	σ(n, 2n) + σ(n, pn), Мб/стерад.			σ(n, n') Мб/стерад.	
	Cr	Ni	Y	Cr	Ni
31°	17,5 ± 2,0	24,4 ± 2,6	63,7 ± 4,3	80,0 ± 4,0	70,9 ± 3,3
61°	24,2 ± 2,2	19,3 ± 2,2	87,3 ± 5,5	74,7 ± 3,5	64,7 ± 2,8
91°	15,1 ± 1,9	13 ± 2,0	67,9 ± 5,1	73,1 ± 3,2	59,5 ± 2,6
121°	13,4 ± 1,6	13,9 ± 2,1	71,2 ± 5,3	61,1 ± 2,4	56,1 ± 2,5
151°	17,9 ± 2,0	20,4 ± 2,4	81,0 ± 5,2	60,4 ± 2,3	52,9 ± 2,4

Дифференциальное сечение / Элемент	σ(n, 2n) + σ(n, pn), барны		σ(n, n'), барны	
	данная работа	работа [3]	данная работа	работа [3]
Cr	0,22 ± 0,02	0,26	0,88 ± 0,04	0,99
Ni	0,23 ± 0,02	0,27	0,76 ± 0,04	0,74
Y	0,97 ± 0;06	0,37	–	–

ОБСУЖДЕНИЕ РЕЗУЛЬТАТОВ

1. Сечение реакций (n, n'), (n, 2n) и (n, pn)

Из данных табл. 1 видно, что суммы σ(n, n') + σ(n, pn) + 2σ(n, 2n), получаемые в нашей работе (площади спектров) и получаемые на основе приведенных в работе [3] данных, совпадают в пределах ошибок измерений. Из работы [3] брались значения σ_x, σ(n, 2n), σ(n, p), σ(n, pn), σ(n, α), и площадь нашего спектра (суммарное число нейтронов) сравнивалась с алгебраической суммой:

$$\sigma_x + \sigma(n, 2n) - \sigma(n, p) - \sigma(n, \alpha)$$

Сечения реакций (n, 2n) и (n, pn) для Cr, Ni и Y также хорошо согласуются с данными других работ [3].

Угловые распределения нейтронов эмиссии для ядер Cr, Ni, Y, Zr и W показывают несимметричность относительно $\theta = 90°$ (см. табл. 2 и рис. 3.), начиная с энергии нейтронов 3 Мэв.

Так как порог реакции (n, 2n) для Cr, Ni и Y превышает 11,5 Мэв, то дифференциальные сечения эмиссии для этих ядер, начиная с интервала энергий (3-4,2) Мэв, есть дифференциальные сечения неупругого рассеяния нейтронов, и только интервал (0-3) Мэв содержит, кроме нейтронов из реакции (n, n'), еще и нейтроны из реакции (n, 2n), а для Ni еще и нейтроны (n, pn). Однако, если исходить только из энергии связи[2], то в реакции (n, pn) на ^{58}Ni возможно испускание и нейтронов с большей энергией, так как $Q_p = 7,17$ Мэв для ^{59}Ni и, следовательно, верхняя граница

[2] Данные по энергии связи брались из таблиц: Seeger, P. A., Nucl. Phys. 25 (1961) 1.

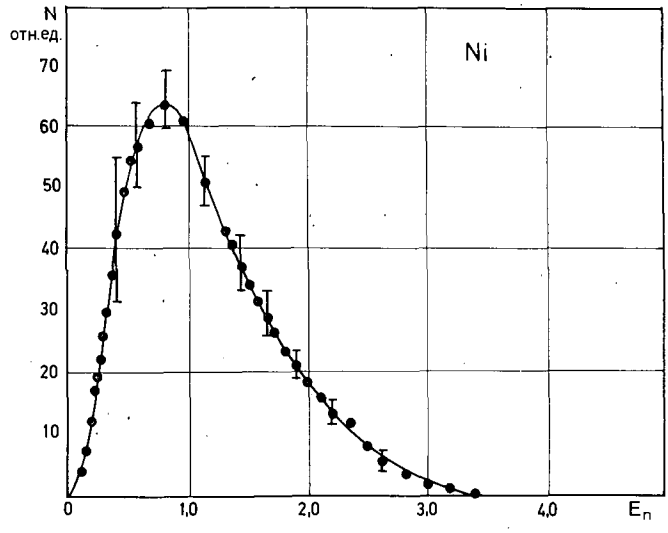

Рис. 7. Усредненный по углам суммарный спектр нейтронов из реакций (n, 2n) и (n, pn) на ядрах никеля.

энергии возбуждения ядра $^{58}Co^{*}$ равна 16,47 Мэв, но нуклоновский барьер реакции (n, p) на Ni = 7 Мэв, поэтому испускание протонов с энергией существенно меньшей, чем 7 Мэв, маловероятно, а так как $Q_n = 8{,}56$ Мэв для ^{58}Co, то вылетающий нейтрон не может иметь энергию больше 3 Мэв.

Для Zr и W, наоборот, только нейтроны из последнего интервала разбиения (6,4-14,4) Мэв полностью относятся к неупруго рассеянным нейтронам, а в остальных интервалах содержится смесь нейтронов реакций (n, n') и (n, 2n).

Оценка вкладов прямых процессов в реакцию(n,n'), полученная по разности спектра Максвелла с температурой T_1, нормированного по участку спектра, где эта температура определялась, и экспериментального спектра показывает, что этот вклад составляет 20% от числа нейтронов, прошедших стадию составного ядра, причем его относительная доля увеличивается с ростом энергии вылетающего нейтрона.

Сравнение дифференциальных сечений эмиссии нейтронов для ядер Zr и W, полученных в нашей работе, с результатами работы [2] при приведении к одинаковому энергетическому интервалу показывает очень хорошее согласие.

Угловые распределения вторых нейтронов из реакции (n, 2n), приведенные в табл. 4 и на рис. 8 для Cr и Y, отождествляются с дифференциальными сечениями реакции (n, 2n).

На рис. 6, где показаны усредненные по углам спектры вторых нейтронов из реакции (n, 2n) на Cr и Y, показаны также спектры ядер, энергия возбуждения которых достаточна для испускания вторых нейтронов. Сравнение числа таких возбужденных ядер с числом действительно испущенных вторых нейтронов позволяет определить отношение Γ_γ/Γ_n для этого интервала энергий:

$$\frac{\Gamma_\gamma}{\Gamma_n} = \frac{S_I - S_{II}}{S_{II}}$$

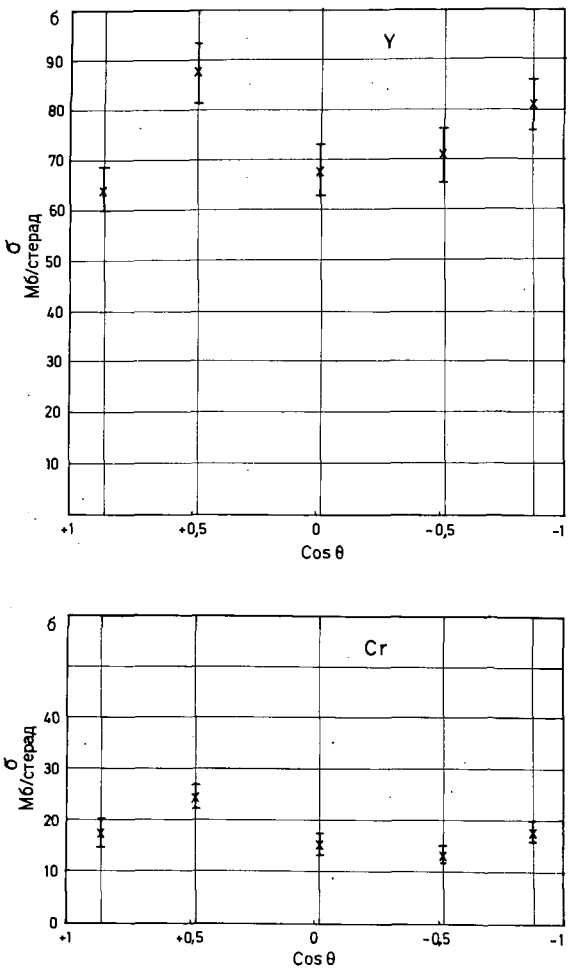

Рис. 8. Угловые распределения вторых нейтронов из реакции (n, 2n) на ядрах хрома и иттрия.

где: S_I – число возбужденных ядер, энергия возбуждения которых достаточна для испускания второго нейтрона,

S_{II} – число действительно испущенных вторых нейтронов.

Для $Cr \cdot \Gamma_\gamma / \Gamma_n = 1{,}52$, а для $Y \cdot \Gamma_\gamma / \Gamma_n = 0$, т. е. практически все ядра, имеющие возможность испустить второй нейтрон, его испускают. Такое большое различие может быть объяснено следующим. Во-первых, энергия связи нейтрона в ядре ^{52}Cr Q = 11,41 Мэв, а у ^{89}Y Q = 10,87 Мэв, т. е. несколько меньше, и реакция (n, 2n) для Cr ближе к порогу. Но, вероятно, это не главное. На спектр вторых нейтронов накладываются сильные ограничения законом сохранения углового момента: бомбардирующие ядро нейтроны с энергией 14,4 Мэв могут вносить в ядро большие угловые моменты (для Cr до 7h), а нейтроны из реакции (n, 2n) не могут унести больших орбитальных моментов, так как суммарная кинетическая энергия их

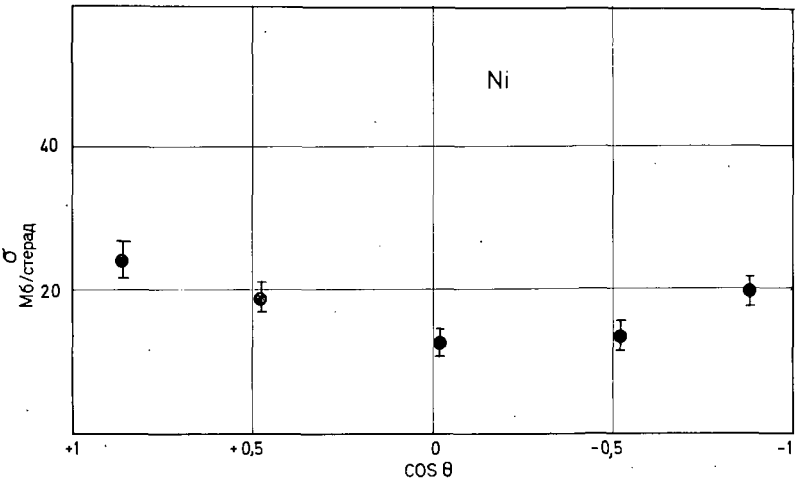

Рис. 9. Угловое распределение нейтронов из реакций (n, 2n) и (n, pn) на ядрах никеля.

для Cr ($E = E_{n_1} + E_{n_2}$) не может быть больше $E_0 - Q_n = 14{,}4\text{-}11{,}4 = 3$ Мэв. Если основное состояние конечного ядра имеет большой спин, то такой переход облегчен. Если же основное состояние конечного ядра имеет малый спин, то переход будет осуществляться с возбуждением промежуточного уровня с большим спином и последующим высвечиванием γ-излучением. Но уровней с большим спином в таком сравнительно узком интервале энергий, как 3 Мэв, будет немного и, возможно, у ^{51}Cr их и нет. У ^{88}Y такой уровень (или группа уровней) несомненно есть; его положение можно установить по соотношению между числом возбужденных ядер, могущих испустить второй нейтрон, и действительно его испускающих: превышение числа вторых нейтронов над числом ядер с соответствующей энергией возбуждения в некоторых энергетических интервалах может быть объяснено только потерей энергии при оставлении конечного ядра в возбужденном состоянии с энергией возбуждения:

$$E_{ур.} = E^* - Q_n - E_{n_2}$$

где: E^* – энергия возбуждения ядра-мишени после вылета первого нейтрона,

Q_n – энергия связи нейтрона в ядре-мишени,

E_{n_2} – кинетическая энергия второго нейтрона.

Анализ спектра вторых нейтронов из реакции (n, 2n) на Y показывает, что, вероятно, у ядра ^{88}Y имеется уровень (или группа уровней), энергия которого равна 2,0 + 0,2 Мэв, и реакция (n, 2n) на Y идет преимущественно с возбуждением этого уровня.

Спектры вторых нейтронов для Zr и W не определялись, так как мы считаем, что применение метода Лекутера для получения T_1 не совсем корректно для таких сравнительно низких энергий возбуждения.

Суммарный спектр вторых нейтронов из реакции (n, 2n) и (n, pn) на Ni, показанный на рис. 7, имеет максимум при 0,8 Мэв, что подтверждает предположение об испускании протонов с энергией порядка кулоновского барьера. Угловое распределение этих нейтронов симметрично относительно 90° (рис. 9), а полученное суммарное сечение очень хорошо согласуется с данными работы [3].

2. Температуры

Как видно из табл. 3, где приведены значения температуры T_1 и область ее определения, она остается одинаковой в пределах точности измерений для всех углов, кроме передних (31° и 61°), где, вероятно, сказывается влияние прямых процессов. Это же подтверждается и несимметричностью относительно 90° угловых распределений нейтронов из области спектра, где определялась температура T_1. Это и вызвало использование $\overline{T_1}$ для определения спектра вторых нейтронов для углов 31° и 61°, так как при рассеянии на задние углы вклад прямых процессов минимален.

Из данных табл. 3 и рис. 4 и 5 видно, что мы определяли T_1 в области энергий нейтронов до 5 Мэв. Может показаться, что определение T_1 в области энергий, настолько удаленной от точки разложения в ряд энтропии, некорректно и что линейность спектра в логарифмической шкале, проявляющаяся экспериментально, в этой области носит случайный характер, что она обусловлена вкладом прямых процессов и т. п. Однако опубликованная недавно работа В. С. Ставинского [7] показывает физическую основу такого поведения спектра нейтронов и возможность определения температуры в широком интервале энергетического спектра.

На величину получаемой температуры некоторое влияние оказывает принятое значение σ_{inv} – сечения обратной реакции, что необходимо учитывать при сравнении результатов различных работ.

Ошибка в определении температуры T_1, обусловленная статистической точностью измерений, точностью кривой эффективности и введенных поправок, оказалась равной 3%. Однако некоторый неизбежный произвол в выборе участка спектра для определения T_1 и неопределенность в оценке вклада прямых процессов заставляют нас указать вероятную ошибку в определении T_1 в ± 10%.

3. Плотность ядерных уровней

Рассматривая ядро как ферми-газ, но учитывая остаточное взаимодействие в виде энергии спаривания, в данной работе определялся параметр плотности ядерных уровней "a" в выражении для полной плотности состояний:

$$P(V) = \frac{\text{const}}{V^{5/4}} \cdot \exp\left\{2(aV)^{\frac{1}{2}}\right\}$$

через ядерную температуру T_1 с помощью выражения:

$$a = \left(\frac{1}{T_1} + \frac{5}{4V}\right)^2 \cdot V$$

Здесь: $V = E_0 + P_z + P_N - 2T_1$ – энергия возбуждения ядра после испарения первого нейтрона; P_z и P_N – энергии спаривания протонов и нейтронов, соответственно (их значения брались из работы [8]); $2T_1$ – средняя кинетическая энергия, уносимая первым нейтроном.

Так как часто для определения параметра "a" из таких же экспериментальных спектров используется выражение для плотности уровней с определенным значением спина, а оно отличается от приведенного выше выражения только предэкспоненциальным множителем (V^{-2} вместо $V^{-5/4}$),

ТАБЛИЦА 5. ПАРАМЕТРЫ ПЛОТНОСТИ ЯДЕРНЫХ УРОВНЕЙ "a" и "a'"

Ядро	[Данная работа] a'_p, Мэв$^{-1}$	[Данная работа] a''_p, Мэв$^{-1}$	a'_p, Мэв$^{-1}$ [9]	a'_p, Мэв$^{-1}$ [10]	a''_p, Мэв$^{-1}$ [11]
Ni	7,44 ÷ 8,02	8,87 ÷ 9,49	6,10 ^{59}Ni 7,20 ^{61}Ni	6,51 ^{58}Ni 7,75 ^{60}Ni 7,99 ^{62}Ni	——
Cr	7,32 ÷ 6,12	8,73 ÷ 7,44	6,25 ^{53}Cr	6,32 ^{52}Cr 5,10 ^{53}Cr 5,80 ^{54}Cr	——
Y	10,30 ÷ 8,28	11,82 ÷ 9,66	8,33 ^{90}Y	11,34 ^{89}Y	13,5 ÷ 21,7
Zr	9,82	11,36	11,40 ^{92}Zr 8,50 ^{91}Zr 11,15 ^{93}Zr	11,82 ^{90}Zr 10,85 ^{91}Zr 11,25 ^{92}Zr 12,16 ^{94}Zr 14,43 ^{96}Zr	——
W	12,27	13,89	20,3 ^{183}W 19,5 ^{185}W 22,5 ^{187}W	24,53 ^{182}W 22,95 ^{183}W 20,76 ^{184}W 21,42 ^{186}W	——

ПРИМЕЧАНИЕ: Разброс значений a'_p и a''_p тоже обусловлен выбором сечения образования составного ядра, первое значение соответствует σ_{inv} = const, второе – сечению, рассчитанному по оптической модели ядра.

то мы, для сравнения наших результатов с данными таких работ, вычислили и параметр плотности ядерных уровней для такого случая:

$$a' = \left(\frac{1}{T_1} + \frac{2}{V} \right)^2 \cdot V$$

Значения найденных нами параметров плотности ядерных уровней "a" и "a'" приведены в табл. 5. Там же приведены результаты определения этого параметра в других работах, в частности, из анализа нейтронных резонансов [9] и теоретических расчетов [10]. Видно, что наблюдается хорошее согласие для всех ядер, кроме W. Расхождение данных по W может быть связано с некорректностью определения T_1 по методу Лекутера.

В некоторых работах параметр плотности ядерных уровней определялся не через ядерную температуру T_1, а непосредственно подгонкой к экспериментальному спектру выражения

$$N(E)dE = \text{const} \cdot E \cdot \sigma_{inv} \cdot \frac{1}{V^2} \cdot e^{2(aV)^{\frac{1}{2}}} \cdot dE \qquad (1)$$

Однако в большинстве случаев экспериментальный спектр неупруго рассеянных нейтронов точнее и в более широкой энергетической области

описывается распределением Максвелла, т. е. постоянной T_1. Кроме того, попытки получить сечение реакции (n, 2n) продолжением спектра первого нейтрона в область, где присутствуют вторые нейтроны из этой реакции, с помощью выражения (1) дают неверный результат. Поэтому в данной работе параметр "а" получался с помощью температуры T_1.

В заключение авторы благодарят Л. Н. Усачева за внимание к работе и В. С. Ставинского за ценное обсуждение результатов.

ЛИТЕРАТУРА

[1] BATHELOR, R. et al., Nucl. Inst. S. Meth. 13 (1961) 70.
[2] BNL-400.
[3] BNL-325.
[4] АНУФРИЕНКО, В. Б., ДЕВКИН, Б. В. и др., Ядерная физика 2 5 (1965) 826.
[5] САЛЬНИКОВ, О. А., ЛОВЧИКОВА, Г. Н. и др., Ядерная физика 4 6 (1966) 1154.
[6] LE COUTER, K.I., LANG, D.W., Nucl. Phys. 13 (1959) 32.
[7] СТАВИНСКИЙ, В. С., Ядерная физика 11 3 (1970) 601.
[8] CAMERON, A.I.W., CAN, I., J.Phys. 36 (1958) 1040.
[9] МАЛЫШЕВ, А. В., ЖЭТФ 45 (1963) 316.
[10] ШУБИН, Ю. Н., Бюллетень информационного центра по ядерным данным, Атомиздат 4 (1967) 304.
[11] MARUJAMA, M., Nucl. Phys. A131 (1969) 145.

DISCUSSION

TO PAPERS IAEA-CN-26/79, 81

H.-H. KNITTER: What type of neutron time-of-flight detector did you use? From one of your slides it appeared that it was one with a very low threshold with respect to neutron energy. Was it a detector which uses the principle of coincidences between multipliers in order to suppress the noise?

A. I. ABRAMOV: As indicated in the paper, we used a scintillation detector with a liquid scintillator which was viewed by two photomultipliers in coincidence. The neutron recording threshold was around 100 keV.

Invited Paper

EVALUATION OF NUCLEAR DATA ABOVE THE RESONANCE ENERGY REGION: A < 220

V. BENZI
Comitato Nazionale Energia Nucleare, Centro di Calcolo,
Bologna, Italy

Abstract

EVALUATION OF NUCLEAR DATA ABOVE THE RESONANCE ENERGY REGION: A < 220.

The problem of nuclear data above the resonance energy region (A < 220) is discussed; total and elastic cross-sections, inelastic scattering, radiative capture and charged-particle and multiple-neutron emission are treated. Among other statements, the author expresses the opinion that in the near future the evaluators' effort should be directed towards the determination of reliable parameter sets on the basis of systematic analyses of large amounts of data.

1. INTRODUCTION

The problems of cross section evaluation for non-fissile nuclei above the resonance region are generally considered to belong to a privileged class with respect to other evaluation problems. This is due to the availability of a rather large amount of experimental data and to the existence of suitable nuclear models which can be used to fill the gaps, provided some parameters contained in the models are empirically known.

The situation about experimental data having been analyzed in the introductory and other papers belonging to this Section, this paper will be devoted to some remarks concerning "modelistics" and "parametrology" as tools for the evaluation job.

Before doing this, it might be worthwhile to have some idea of the requirements to be fulfilled, on the average, in evaluating nuclear data pertinent to the field here considered.

In Table I the number of requests contained in RENDA [1] for different kinds of cross-sections above resonances of non-fissile nuclei, is given.

In the Table the requests are subdivided into three groups, according to the accuracy desired. As can be seen, for about three-quarters of the requests the accuracy is no more than 10%. This immediately gives an idea of the important rôle covered by the nuclear models in the evaluation work. It is well known, in fact, that the nuclear models available to-day are quite well able to reproduce the energy dependence of the cross-section shape for several types of reactions. Thus, nuclear models can be reliably used for interpolation between experimental data, with considerable reduction in the amount of experimental work required to produce a complete nuclear data file.

Unfortunately, the capability of the nuclear models to predict cross sections when no data at all are available, cannot be equally well asserted in general, as will be briefly shown in the following sections.

2. TOTAL AND ELASTIC CROSS SECTIONS

The evaluation of total and shape-elastic cross sections is the realm of the optical model. No Conference on neutron cross sections has been held in the past without at least one paper demonstrating the capability of this model to give very good fits of experimental data.

TABLE I. NUMBER OF REQUESTS CONTAINED IN RENDA FOR MEASUREMENTS ABOVE THE RESONANCE REGION FOR NUCLEI WITH A < 220

Quantity (cross section)	Accuracy required (%)			Total
	<10	10-20	>20	
Total	5	5	-	10
Diff. elastic	2	55	-	57
Total inelastic	6	13	1	20
Diff. inelastic	16	49	4	69
Radiative cap.	13	76	1	90
Charged particle emission [(n,p), (n,α) etc.]	31	29	13	73
Multiple neutron emission [(n,2n),(n,3n) etc.]	11	13	-	24
Total	84	240	19	343

In its standard form, the optical model assumes a complex potential with radial symmetry. Such potential depends on some parameters, whose number ranges from a minimum of three (square-well) up to twenty and more. There are several recommended sets of parameters (normally, four to six parameters are considered), inferred from various analyses of a large number of experimental data. From the physical point of view the sets are more or less equivalent, differences being mainly due to the well known "geometrical" ambiguities ($V_o R^2$, Wb, etc...) [2] . These sets can be used with some confidence to predict total and elastic cross sections above the resonance region, provided the nucleus considered is not a very deformed one. In this case one has to modify the parameters considerably if the deformation is not explicitly taken into account.

Following Perey [3], however, the parameters applying to spherical nuclei can be used if the deformation is considered in the calculation. This would certainly be a very important feature of the optical model, because a systematic search of a "best set" for a non-spherical potential implies a great amount of computation time even using the large computers available today. Unfortunately, there are some aspects of non-spherical potential calculations which make the adoption "sic et simpliciter" of the parameters inferred from analyses of spherical nuclei rather questionable. We will examine here some of these aspects.

Let us consider a typical non-spherical potential, e.g.

$$V(r,\theta,\phi) = - V_c\, f(r,R,a) - 4i\, W_D\, g(r,\bar{R},b) - V_{so} \frac{\lambda^2}{r} (\underline{\sigma} \cdot \underline{\ell}) \frac{d}{dr} f(r,R,a) \quad (1)$$

Assuming an axially symmetric rigid rotor, the radii R and $\bar{R}$ appearing in the form factors $f(r,R,a)$ and $g(r,\bar{R},b)$ are given by

$$\begin{aligned} R &= R_{oa} \left[1+\beta\, Y_{2o}(\theta')\right] \\ \bar{R} &= R_{ob} \left[1+\beta\, Y_{2o}(\theta')\right] \end{aligned} \quad (2)$$

β being the deformation parameter. The angle θ' refers to the body-fixed system, whereas θ and ϕ are space-fixed coordinates.

To solve the appropriate Schrödinger equation with the above potential, two different approximations are frequently used. In the first kind of approx-

imation the potential is expanded in powers of β up to the first order [4], [5], [6]. The second kind of approximation assumes a Legendre polynomial expansion of the potential (in general up to ℓ=4) [7], [8]. Now, there may be rather large differences in the results depending on the approximation adopted.

As an example, Fig. 1 shows the results of calculations of the total cross-section of Gd-156 in the MeV energy range. The form factors and the parameters assumed for the optical potential are the same as those adopted by Agee and Rosen [9].

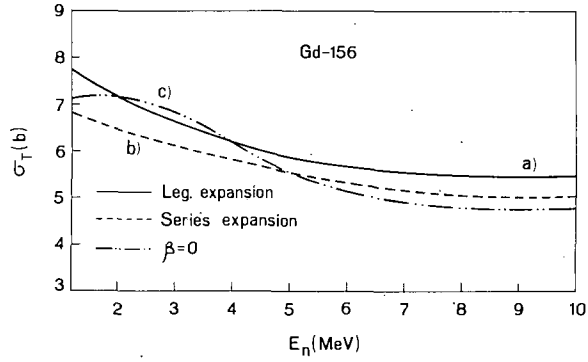

FIG. 1. Theoretical total cross-sections of ^{156}Gd calculated with the same set of parameters, but assuming different approximations for the generalized optical-model potential.

Curve (a) was calculated assuming a deformation parameter β=0.35 and strong coupling of the first excited 2^+ level. The potential was expanded in Legendre polynomials up to ℓ=4. Curve (b) was obtained using the same parameters of curve (a), but the potential was expanded in power series of β to the first order. It can be seen that there is a systematic difference between the two curves of ~10÷15 percent. The total cross-section calculated by assuming β=0 (spherical potential) is shown for comparison.

Quite large differences are also found for the shape-elastic angular distribution, as shown in Fig. 2.

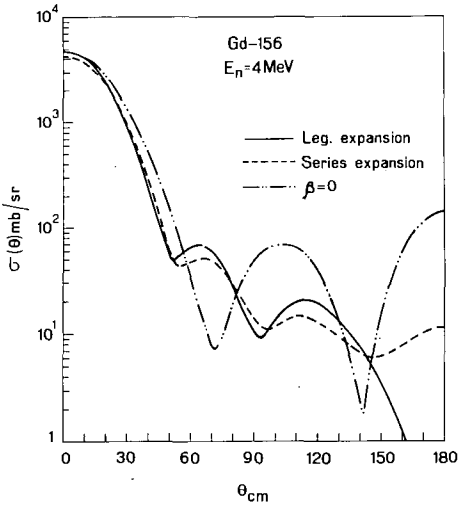

FIG. 2. Theoretical shape-elastic cross-sections of ^{156}Gd at 4 MeV calculated with the same set of parameters, but assuming different approximations for the generalized optical-model potential.

One of the effects of nuclear deformations is the damping of the diffraction pattern of the shape-elastic angular distribution. The same effect can be obtained, qualitatively, by using a spherical potential with a large value of the absorption potential W_D. Since a rather large number of nuclei are more or less deformed, a systematic analysis based on a spherical potential will result in a W_D-value which is too high for generalized potential calculations. In addition, the magnitude of the theoretical cross-sections given by the generalized optical model strongly depends on the coupling scheme used in each particular calculation. Therefore, the value of W_D to be adopted also depends greatly on the coupling scheme assumed.

In conclusion, it seems very unlikely that a W_D-value deduced by a systematic analysis of experimental data in terms of spherical potential, could be used when performing calculations based on a generalized optical potential. Because of the $W_D.b$ ambiguity, the same conclusion can be extended to the b-parameter.

Another parameter which may change drastically when deformation effects are taken into account is the depth of the spin-orbit potential V_{so}. The correlation between β and V_{so} has been discussed by Thompson et al. [10], who found a lower value of V_{so} than in spherical-potential calculations when the deformation is taken into account. This correlation mainly depends on the fact that the nuclear deformation effects predominate near the nuclear surface where the phenomenological spin-orbit potential also produces major effects.

From the above considerations it can be concluded that three parameters at least (i.e. W_D, b and V_{so}) have to be varied when changing from spherical to non-spherical optical model calculations. Thus, the prediction of an unknown cross-section obtained by using "standard" spherical optical model parameters and generalized potentials must be taken with care.

3. INELASTIC SCATTERING

As in elastic scattering, there are two components in an inelastic scattering process, namely the compound nucleus and the direct interaction component. In the energy range below a few MeV, however, the compound nucleus component in general prevails and, therefore, the situation is very different with respect to the elastic scattering, which is dominated by the direct process.

In principle, the average compound nuclear cross-sections can be calculated using the well known statistical theory of Hauser and Feshbach, incorporating some width-fluctuation correction when necessary.

The transmission coefficients corresponding to the energetically-allowed outgoing channels are obtained from optical model calculations, provided the number of channels is not too high. Otherwise, the optical model is used to calculate the reaction cross-section, and the required information on nuclear structure is summarized by a nuclear level density formula. The limitations of the H-F theory, in connection with the evaluation work, have been discussed in several papers (see e.g. ref. [3]) and it is not necessary to insist here on this point. It is generally admitted that H-F calculations are reliable in absolute magnitude within a factor of about two, even taking into account the correction for width fluctuation.

As the incident neutron energy increases, the direct interaction component becomes more and more important. For example, it was estimated by Cranberg and Zafiratos [11] that the compound nuclear contribution to the inelastic differential cross-section at 50° of Pb-206 to the 3^- state at 2.6 MeV falls from 7 mb/sr at 4 MeV to 0.7 mb/sr at 6 MeV. In the same energy interval the direct interaction rises from 3 mb/sr to about 7 mb/sr. Thus, in this particular case, the direct-to-compound cross-section ratio rises by a factor of about twenty-five in a 2 MeV energy interval.

A peculiar characteristic of the direct inelastic scattering at high energies is that the amplitude of the scattered waves will tend to be large for forward angles and small for backward angles. As a consequence, the angular distribution of the scattered particles will be neither isotropic nor symmetric around 90°, as happens for the compound inelastic scattering in the statistical region. Such an effect may be of some interest, especially in connection with shielding calculations.

Cross sections for direct inelastic scattering can be calculated within the framework of the coupled-channel theory by using a generalized optical potential. Unfortunately, the results are strongly affected by several factors, like the number of coupled channels considered, the adopted value of the imaginary part of the optical potential, etc... In Fig. 3 calculated angular distributions for the direct inelastic scattering of 1 MeV neutrons by the first 2^+ excited state of Gd-156 at 0.09 MeV are shown. All the curves were calculated using the same set of parameters, namely the set adopted for the calculations whose results were shown in Figs. 1 and 2. Curve (a) was obtained by assuming that only the first 2^+ excited state channel is strongly coupled with the elastic channel. Curve (b) was calculated under the hypothesis that the second (4^+) excited state too is strongly coupled. Curve (c) was calculated in adiabatic approximation, taking into account the coupling of all the excited levels belonging to the fundamental rotational band. It can be seen that there is a rather sensible dependence of the results on the coupling scheme assumed.

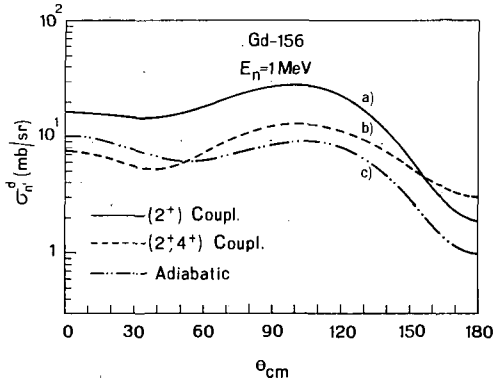

FIG. 3. Theoretical direct inelastic-scattering angular distributions for ^{156}Gd at 1 MeV. The curves were obtained under different hypotheses concerning the channel coupling.

Fig. 4 shows the effect of the "geometrical" W.b ambiguity. The curve labeled (a) shows the theoretical angular distribution of the inelastic cross-section for 1 MeV neutron scattered by the first 2^+ excited level of Gd-156 via compound nucleus. The parameters adopted to calculate the penetrabilities were those of ref. [9], with W_D = 5.75 MeV and b = 0.70 fm. The dots superimposed on the curve represent the results of a calculation carried out using the same parameters, but with W_D = 8.05 MeV and b = 0.5 fm. In both cases one has W_D.b = 4.025 MeV.fm, and the results are identical up to the third significant figure.

The angular distribution for direct inelastic scattering, however, differs sensibly in magnitude in the two cases, as can be seen in Fig. 4 itself.

At present, the large amount of uncertainty to which the theoretical cross-sections for direct inelastic scattering are subjected cannot be reduced on the basis of the experimental data. In fact, it is almost impossible to resolve the individual excitation functions in the energy region where the direct effects are prominent.

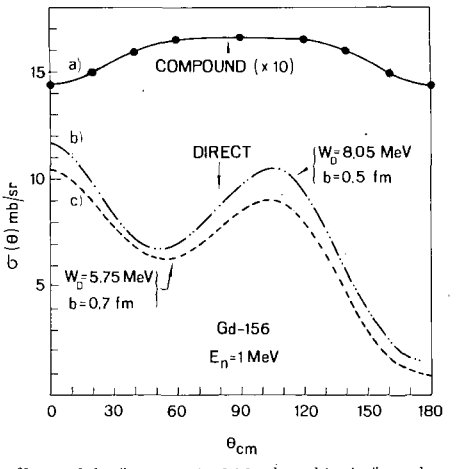

FIG. 4. An example of the effects of the "geometrical W_D, b ambiguity" on the calculation of the inelastic-scattering cross-sections.

4. RADIATIVE CAPTURE

The neutron radiative capture process is usually described in terms of three possible reaction mechanisms, namely the compound nucleus, direct and collective capture. In general, the compound nucleus process predominates up to a few MeV and the corresponding cross-section above the resonance region can be estimated by means of the statistical model. A large amount of experimental data was analyzed in the past by several authors using this model (see, for example, ref. [12]). The experience gained from these analyses can be summarized as follows:

i) Provided the level scheme of the target nucleus is well known, the shape of the theoretical cross-section agrees quite well with the experimental one.

ii) The magnitude of the theoretical cross-section weakly depends on the value of the penetrabilities T_ℓ. It has been shown [13] that if one increases or decreases all the T_ℓ by a factor of ~10, the cross-section does not vary more than by a factor of ~2, except at very low energies where it depends on T_o only. In addition, calculations based on T_ℓ obtained from three different sets of optical-model parameters were found to agree within 20% in the keV-to-MeV energy range [14].

iii) The magnitude of the theoretical cross-section strongly depends on the ratios $\langle\Gamma_\gamma/D\rangle_J = \xi_J$.

The quantities ξ_J can be factorized as the product of a constant ξ_o times an energy and spin-dependent factor $f(E;J)$. In this case ξ_o represents the ratio $\langle\Gamma_\gamma/D\rangle_{J=0}$ at ~0 neutron energy, whereas $f(E;J)$ takes into account the spin- and energy-dependence of the radiation width and the level spacing. When the theoretical formula is used to interpolate between experimental points, the constant ξ_o can be assumed as an adjustable parameter. Otherwise, the ξ_o-value for a particular nucleus can be guessed on the basis of a systematic analysis of the low-energy resonances, assuming some theoretical dependence of the average values of Γ_γ and D on J. The systematics on Γ_γ and D available at present, allow an estimate of ξ_o with an average uncertainty of ~50%, to be optimistic.

In the MeV energy range the level scheme of the target nucleus is in general not known, so that it is necessary to use a nuclear evaporation formula. The results obtained with these kinds of formulae lean heavily on the assumed dependence of Γ_γ and D on J and E.

As an example, Fig. 5 shows the results of three different theoretical estimates of $\sigma_{n,\gamma}$ (compound) for I-127 in the MeV energy-range.

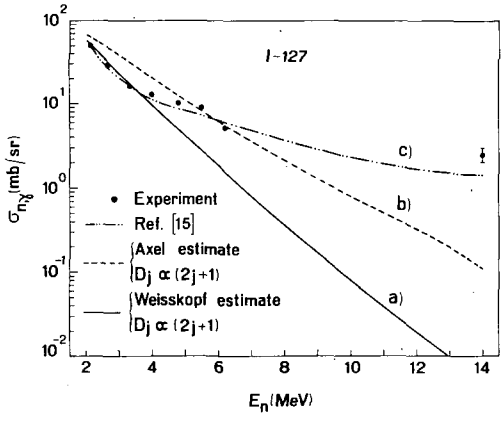

FIG. 5. Theoretical radiative-capture cross-sections in the MeV-energy range for ^{127}I, calculated under different assumptions.

Curve (a) was obtained by assuming the so-called "Weisskopf estimate" for the energy-dependence of $\bar{\Gamma}_\gamma$ and a (2J+1) dependence of $\bar{D}$ on J. Curve (b) was obtained by assuming a $\bar{\Gamma}_\gamma$ energy-dependence given by the "Axel estimate". Curve (c) was calculated by Sperber [15], assuming the "Axel estimate" for $\bar{\Gamma}_\gamma$ and a more sophisticated J-dependence of $\bar{D}$ than (2J+1). At 14 MeV the three curves differ among themselves by a factor ~10, and the value of curve (a) is smaller by a factor of about 400 in comparison with the experimental value.

It may be noted that the theoretical value given by Sperber at 14 MeV differs only by a factor ~2 with respect to the experimental value. This result is in contrast with the commonly accepted opinion that the compound nucleus mechanism fails completely to explain high energy capture cross-sections of medium and heavy nuclei [16].

As far as the direct and collective capture processes are concerned, a systematic analysis of the data available in the ~14 MeV region has been carried out by Longo and Saporetti [17]. The two processes appear reasonably

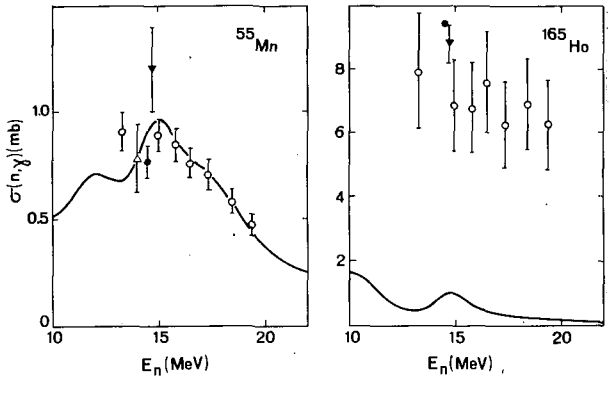

FIG. 6. Examples of radiative-capture cross-sections calculated by assumiug a direct and collective capture mechanism.

to explain the experimental (n,γ) cross-sections of heavy nuclei $(A>40)$ with magic or near-magic neutron number, but for deformed or "soft" nuclei the theoretical results are an order of magnitude lower than the measured one. Typical theoretical (n,γ) cross-sections obtained by using a model which takes into account the direct and collective capture mechanism are shown in Fig. 6. It can be seen that the model predicts a too low cross-section for the strongly deformed Ho-165 nucleus, whereas for Mn-55 the theoretical results are in good agreement with the experimental ones.

5. CHARGED PARTICLE AND MULTIPLE NEUTRON EMISSION

From the evaluator's point of view, the charged particle and multiple neutron emission processes can be discussed together, because the basic model used to analyze the data is the evaporation model for both classes of reactions.

As briefly mentioned in connection with the compound radiative capture in the MeV region, the limitations of this model as an evaluation tool are mainly due to the strong dependence of the numerical results on the energy and J-dependence assumed for the level density. The situation is rendered worse by the fact that in the energy region of interest for these kinds of reactions there are, in general, several competing processes whose particular features can be only roughly accounted for by the evaporation model. A clear example of the limitations of such a model is given by the results of an analysis of the (n,α) cross-section at 14 MeV carried out by Facchini et al. [18] for a large number of nuclei. It was found that a reasonable agreement between experiment and theory can be obtained only for nuclei with either neutron number $N\leq 50$ or magic.

The experimental cross-sections, however, were found to be $5\div 10$ times larger than the theoretical ones for $50\leq N\leq 82$, and $100\div 1000$ times larger for $N>82$. The increasing of the discrepancies with increasing N can probably be explained by the fact that for heavy elements the direct processes predominate over the compound nucleus processes. As was pointed out by Robertson [19], the direct process gives a reaction product particle with energy close to the maximum possible, whereas the statistical process will favour the emission of lower energy particles. Thus the Coulomb barrier prevents charged particle emission via compound nucleus more strongly than direct emission and the cross-section for the compound process decreases very rapidly as Z increases. There are very few analyses of experimental data in which the direct particle emission mechanism is taken into account. A systematic analysis of this kind, based for example on some refinement of the theory developed by Brown and Muirhead [20], would be very useful in order to estimate the importance of the direct component in charged particle emission.

The evaporation model is widely used to predict the energy distribution of the emitted particles. For single particle emission, a large number of empirical studies has shown that a Maxwellian formula like

$$\sigma(E_o;E) = \sigma_T(E_o)\,\frac{E}{T^2}\,\exp(-E/T) \qquad (3)$$

agrees quite well with the bulk of experimental data. In formula (3), $\sigma_T(E_o)$ is the cross-section for the formation of the compound nucleus at neutron energy E_o, and $T=T(E_o)$ is the so-called nuclear temperature.

A relationship like $T(E_o) = \text{const.}(E_o)^{\frac{1}{2}}$ is suggested by the experimental evidence, with the constant varying reasonably smoothly as a function of the mass number.

A Maxwellian formula, however, is not adequate if the direct process is important, as in the case of strongly deformed nuclei or high E_o-values. In these situations the predicted spectra are sensibly softer than the observed one.

Modified Maxwellian formulae are also used to predict the energy distribution of the emitted particles in multiple neutron-emission processes. There are several recipes for the "nuclear temperature" (or temperatures) to be used in connection with these formulae. None of them, however, was extensively tested, because of the scarcity of clean experimental data.

6. CONCLUSIONS

All the "theories" considered so far have a fundamental characteristic in common. In fact, none of them takes explicitly into account the dynamics of the nuclear many body system, but all are based on some models which simulate the real situation. Nevertheless, a very good agreement between theory and experiment can be obtained in particular cases with a suitable choice of the adjustable parameters which appear in the various models. The big problem, however, is not so much the fitting of measured data, but rather the prediction of missing data. A correct answer to this problem mainly depends on the availability of good sets of parameters obtained by means of systematic analyses of large amount of data. From this point of view the situation is not in general very good, as was briefly discussed in the previous Sections of this paper.

For the field here considered, therefore, it is the author's personal opinion that the main effort of the evaluators in the near future should be directed toward the determination of reliable parameter sets obtained on the basis of systematic analyses of large amounts of data rather than towards the determination of particular sets for specific nuclei.

As for other fields of reactor physics, the analogy of the three-legged stool can be applied very well to the evaluation of nuclear data above the resonance region. In this case the three legs are represented by the experimental data, the nuclear models and the parameters obtained from systematics. If these three legs are not well balanced, an evaluation will result in a mediumistic message rather than in a technical work.

REFERENCES

[1] RENDA - SCHWARZ, S., HÄUSSERMANN, W., Eds., EANDC-78 "AL" (1968).

[2] HOLMQVIST, B., Arkiv för Fysik, 38, 403, (1968).

[3] PEREY, F.G., Conf. Neutron Cross Section Tech., CONF-660303 (TID-4500) edited by P.B. Henning, Vol. I, page 236 (1966).

[4] YOSHIDA, S., Proc. Phys. Soc. (London) A 69 , 668, (1956)

[5] MARGOLIS, B., TROUBETZKOY, E.S., Phys. Rev., 106, 105, (1957).

[6] BUCK, B., Phys. Rev. 130, 712, (1963).

[7] CHASE, D.M., WILETS, L., EDMONDS, A.R., Phys. Rev. 110, 1080, (1958).

[8] TAMURA, T., Rev. Mod. Phys. 37, 679, (1965).

[9] AGEE, F.P., ROSEN, L., LA-3538-MS (1966).

[10] THOMPSON, W.J., EDWARDS, S., TAMURA, T., Nucl. Phys., A 105, 678, (1967).

[11] CRANBERG, L., ZAFIRATOS, C.D., Phys. Rev. 142, 775, (1966).

[12] BENZI, V., PANINI, G.C., REFFO, G., VACCARI, M., CNEN Report CEC(70)2 - - (1970).

[13] CAMERON, A.G.W., LAZAR, N.H., SCHMITT, H.W., Fast Neutron Physics, Part II, Ch. V.M. (MARION, J.B., FOWLER, J.L. Eds) Interscience, New York (1963).

[14] FRICKE, M.P., LOPEZ, W.M., Physics Letters, 29 B, 393 (1969).

[15] SPERBER, D., Phys. Rev., 184, 1201, (1969).

[16] LANE, A.M., LYNN, J.E., Nucl. Phys. 11, 646, (1959).

[17] LONGO, G., SAPORETTI, F., Nucl. Phys. A 127, 503, (1969).

[18] FACCHINI, U., SAETTA-MENICHELLA, E., TONOLINI, F., TONOLINI-SEVERGHINI, L., Nucl. Phys. 51, 460, (1964).

[19] ROBERTSON, J.C., Nucl. Phys., 49, 306, (1963).

[20] BROWN, G., MUIRHEAD, H., Phyl. Mag. 2, 473, (1957).

DISCUSSION

M. P. FRICKE: I certainly disagree with your statement that the capture cross-section is well described below 1 MeV. As regards your recently published calculations for a large number of nuclei, I am not sure that you make quite the same approximations as I do, but even so, for 6 out of the 7 nuclei we have in common, the excitation functions between 50 and 500 keV actually agree rather closely in shape; your calculations for natural molybdenum and ^{139}La fall off even more slowly than mine. So whether or not a discrepancy in shape is observed depends somewhat upon which data are used for comparison. I feel that the key place to make a careful comparison for heavy nuclei is in the one decade of energy from about 100 keV to 1 MeV.

C. M. NEWSTEAD: Could you please comment on the criteria one should use to determine W_D, the depth of the diffuse absorptive potential. Secondly, could you indicate how to choose between Legendre and Taylor series expansion to obtain the multipole terms of the deformed potential?

V. BENZI: It has been pointed out by Tamura that an unambiguous choice of W_D requires the coupling of a large number of excited states. This means that W_D strongly depends on the coupling assumed, and hence there is no general criterion for determining this quantity. As far as the Legendre and Taylor series expansions are concerned, it can be said that the Legendre polynomial expansion is a much better approximation than the power series expansion for values of β greater than $\simeq 0.20$, as explained by Tamura in a paper published in Review of Modern Physics, October 1965.

Section VII

RELATIONSHIPS OF MICROSCOPIC AND INTEGRAL DATA

Chairmen

B.A. HUTCHINS (USA)

Yu. F. CHERNILIN (USSR)

Invited Paper

THE RELATIONSHIP OF MICROSCOPIC AND INTEGRAL DATA

C.G. CAMPBELL, J.L. ROWLANDS
UKAEA, Reactor Group,
Atomic Energy Establishment,
Winfrith, Dorchester, Dorset,
United Kingdom

Abstract

THE RELATIONSHIP OF MICROSCOPIC AND INTEGRAL DATA.

The ways in which UK reactor physicists have acquired group-averaged macroscopic cross-sections for use in reactor design calculations are reviewed and the role of integral experiments in this work is identified.

The present adequacy of these data for reactor design calculations is reviewed with particular reference to fast reactors, and the proposed use of both integral and evaluated differential data in meeting current needs is discussed. The program of work required to meet the needs of fast reactors, bearing in mind the time scale for acquiring adequate information on cross-sections is reviewed.

Part 1 Review

Requirements

Performance predictions for power reactors ideally require an adequate model of the reactor together with an adequate solution of the neutron transport equation for the model, and adequate microscopic nuclear data. These data are used to calculate sets of group averaged cross-sections by weighting them with neutron spectra appropriate to the material compositions of the various regions of the reactor.

Because these ideal requirements so far have rarely, if ever, been met, it has been necessary to base predictions of power reactor performance on integral measurements made in zero-power test assemblies of similar geometry and composition to that of the power reactor.

Early use of integral data

This process began in the UK well over a decade ago in order to make predictions for the large UK natural uranium magnox reactors then being designed. These reactors, by modern standards, have a particularly simple lattice cell geometry, and sufficiently accurate predictions were made using simple two neutron group diffusion theory methods. Although this treatment

introduced approximations, the associated uncertainties were small compared with uncertainties arising from the nuclear data available at that time. The technique was to make integral experiments spanning the range of lattice cell geometries for which predictions were required. Exponential and other sub-critical assemblies were used for buckling and cell flux distribution measurements. These experimental lattices were analysed using the same methods of calculation as those adopted for prediction of the power reactor. Agreement with the integral measurements of buckling, for example, was obtained by choosing the η-value of U235 and the effective resonance integral of U238 to produce a good fit. Any other calculational or data inadequacies were thus thrown into biassing these two parameters, which could not therefore be regarded as a true measure of these quantities. Used with a consistent method of calculation, this technique was very successful in making accurate prediction of reactivity and other key parameters for these reactors.
A similar approach was used at this time in the UK for light water reactors except that a four neutron-group model was required to characterise sufficiently well the neutron spectra encountered in the range of designs studied.

Later developments for thermal reactors

At the first Geneva conference a great deal of differential nuclear data, previously classified, was released and at about this time digital computers were being applied to the numerical solution of the multi-group neutron transport equations. The enthusiasts were hopeful of calculating reactor performance by sophisticated methods with accurate models and adequate differential data. Quite simple calculations however dispelled such hopes. It was easily shown that to obtain a prediction of k-inf to 1%, the following accuracies are required for a typical thermal reactor:

η to $\sim \frac{1}{2}\%$
Capture in structural materials to $\sim 5\%$
Resonance capture in U238 to $\sim 2\%$
Fast fissions in U238 to $\sim 7\%$

Differential nuclear data, even now, do not meet such stringent demands, and many further integral checks of performance prediction have been needed.

In the case of the magnox reactors, the power reactor lattice cell was sufficiently simple that the multi-group treatment could effectively eliminate errors due to the model and method of solving the transport equation. Discrepancies were then due to inadequate nuclear data.

For the geometrically more complex cells of later thermal reactors, there was not such a clear-cut distinction between errors from the data and errors from calculation. However, with the advent of modern sophisticated lattice codes (eg WIMS, HAMMER) capable of representing complex geometries in some detail, this distinction has tended to disappear and reactor physics measurements from AGR, SGHW and PWR/BWR lattices have provided a considerable body of information confirming the data trends observed in the simpler lattices. This wide range of integral results, covering all the main moderators, makes it possible to check data changes shown by particular integral experiments and hence to eliminate errors arising from moderator data.

For thermal reactor studies the domination of individual items of data in particular neutron energy ranges is an additional help in identifying discrepancies. Thus U238 fission events dominate the fast energy part of the spectrum; U238 resonance capture largely controls events in the epithermal region and thermal events are dominated by U235 data. This has allowed nuclear data discrepancies, leading to failure to predict integral quantities, to be identified by studying changes to integral predictions resulting from changing variables one at a time, followed by seeking confirmation of suspected data errors in integral experimental results with different moderators. This technique has led to a gradual elimination of most of the major errors in thermal reactor data although some discrepancies remain to be solved.

Outstanding discrepancies between differential and integral data from thermal lattice tests

The most important discrepancies are as follows:

i Fast data

Multi-group WIMS transport theory calculations of fast fission ratio (U238/U235 fission) using the best available differential data for high energy U238 cross-sections have

consistently underpredicted measurements performed in liquid moderated systems by about 10%, and measurements in graphite lattices by somewhat less. Current studies of graphite moderated systems in the UK have shown that in such systems improved agreement can be obtained by hardening the fission spectrum in line with recent recommendations (the temperature of the Maxwellian being increased from 1.30 Mev to 1.43 Mev). However, a pitch dependent variation of about 5% in fast fission ratio remains unexplained.

ii Resonance data

For several years it has been found impossible to predict consistently the measured U238 capture rates in graphite, D_2O and H_2O moderated lattices using the U238 resonance integrals obtained from standard differential data which is incorporated in the library of the WIMS code. Satisfactory agreement can be found by making a consistent adjustment to the resonance cross-sections for U238.

The resonance methods adopted in WIMS have been extensively checked by comparison with Monte Carlo calculations. Using the latest differential data for the slowing down cross-sections of hydrogen, deuterium and carbon it has been found that consistently satisfactory predictions of relative conversion ratios for all three moderators can be obtained by applying a reduction of 0.1 barns to the U238 cross-sections between 4 ev and 9.1 Kev.

iii Thermal data

The graphite thermalisation matrix used in the WIMS code was derived, via a complex theoretical extrapolation process, from differential scattering measurements and checked against corresponding specific heat data. The standard WIMS matrix predicts too soft a spectrum when compared with measured Pu/U fission ratios and Lu/Mn capture ratios. A trial adjustment to the scattering data appears to result in accurate predictions of Pu/U fission ratios but to change a 3% underestimate of Lu/Mn ratios into a 3% overestimate. Further revisions are being made to the thermal scattering data. Calculations are being made using more recent evaluations and the calculations

are being correlated with a wide range of integral experiments.

When known errors in the calculation of U238 captures have been removed, WIMS reactivity estimates for a carefully selected range of lattices show little or no trend for a given moderator but do exhibit a trend between moderators which is correlated with the spectrum of U235 fission events. The effect is worst for D_2O moderated lattices which are on average 1½% underreactive. Rothenstein (12) has also carried out a survey of heavy water lattices using the HAMMER code and ENDF 'B' data for U235 and deduced a similar underestimate of reactivity.

iv Reactivity Coefficients

Measurements of temperature coefficients of reactivity, and also moderator and coolant void coefficients for water moderated systems provide another form of integral check of nuclear data and methods of calculation for thermal reactors. Experiments in which the temperature of uniform light water lattices was varied have indicated that the magnitude of the fuel plus coolant temperature coefficient is significantly overestimated by the best methods of calculation (by about - 2 mN/°C). A careful analysis of this problem in which measurements of changes of reaction rates, and the effects of density changes were separately investigated suggested that the difficulties stemmed from errors in calculating the change of leakage (ie for neutron energies above 1 MeV). Although it was clear that changes to inelastic scattering data for U238 for example would modify calculated leakages from high buckling systems, no satisfactory adjustment of nuclear data has yet been found to explain the discrepancy. Somewhat smaller discrepancies of the same sign appear to occur from the limited experimental evidence on graphite lattices, and also the SGHWR type of lattice exhibits a similar behaviour to the light water systems. Another suggestion has been that adjustment of the energy dependence of the capture and fission cross-sections for U235 in the thermal range would reduce these discrepancies.

The predicted void coefficient of reactivity in both light water and heavy water systems is sensitive to the assumptions relating to moderator slowing down cross-sections and U238 resonance data. The recommended adjustment of U238 cross-sections when used with the current scattering cross-sections for H_2O and D_2O does lead to good agreement with the measured void coefficient. The discrepancy on void coefficient in SGHWRs which arises when the unadjusted U238 cross-sections are used is significant in terms of the experimental accuracy.

Fast reactors

The situation for fast reactors is very different from that for thermal systems. The uncertainties in the nuclear data over the very wide range of neutron energies are large; there is an energy dependent competition between the important events at all neutron energies, and the checks available in the thermal reactor analysis from different moderators are not available in the same way. Any attempt to isolate particular fast reactor data discrepancies by varying a single parameter at a time cannot lead to useful results because of the uncertainties in competing events.

"High-accuracy" requests for data

The sensitivity of fast reactor performance to nuclear data uncertainties has been studied by most fast reactor teams, and all come to the conclusion that the differential nuclear data requires very considerable improvement. The target accuracies from such studies are listed in the so-called "high-accuracy" nuclear data requests. The nuclear data measurers advise that these high accuracy requests will in most cases be costly and time-consuming to achieve. The development of fast reactors in the UK is on a time-scale such that performance prediction cannot await the achievement of such accurate data measurements and alternative means have therefore been sought.

Data adjustment

These alternative means are based on the use of both evaluated differential data and integral information. The integral data uses results from clean-geometry fast lattices to minimise calculational errors, and covers neutron spectrum as well as all the important reaction rates measurable by integral techniques.

The compositions of the fast lattices studied are chosen to be sensitive to particular cross-sections within the limitation of allowing criticality.

The second part of this paper describes the manner in which the evaluated differential data and these integral results are being used in the UK to provide data fitted to all the useful information available. The data adjusted to fit these measurements are then generally of sufficient accuracy to meet the demands of fast reactor performance prediction. If the accuracy is insufficient, the sensitive data is identified for further differential or integral study.

It is recognised that the integral data, apart from the spectrum measurements made on zero power assemblies, lacks energy resolution but provides stringent bounds within which reaction rate ratios must lie. The coarse degree of energy resolution available arises from the extremes of spectrum in the lattices tested.

Judicious choice of material compositions in the fast test lattices provides a sensitive overall test of particular cross-sections. The differential data on the other hand is capable of providing great detail on the shape of cross-sections in broad energy ranges, but there are difficulties in relating the cross-sections accurately from one energy range to another.

The data adjustment technique adopted divides the spectrum into broad energy bands, and ten such bands have been used in the latest studies. The sensitivity of each item of data to each measured integral property is calculated (including the neutron spectrum). By using a least-squares fitting process the broad-group cross-sections are adjusted to give the best fit to both the integral and evaluated differential measurements. The fitting criterion chosen depends on the estimated accuracy of both the differential and integral measurements. These accuracies are not well documented and all groups adopting similar adjustment techniques will support a plea for the systematic and random errors in microscopic cross-sections and cross-section ratios to receive much more attention in data evaluation.

A feature of the UK work is that the fitting procedure provides an estimate of the accuracy of the adjusted cross-sections and

of the reactor properties calculated using them. The predictions of reactor properties obtained from the adjusted data are much more accurate than the predictions based on adjusted microscopic data, because of the constraints applied by the integral measurements to these properties. The accuracy of a few of the individual cross-sections are also significantly improved by the adjustment process, and this draws attention to possible systematic errors in the microscopic data. If data adjustments beyond the limit of the assigned uncertainties are required then it is likely that errors exist in data not included in the adjustment process.

In general it is our view that this approach is to be preferred to an alternative of testing various sets of evaluated nuclear data against integral results to identify which particular set performs best. Such a procedure lacks the systematic approach afforded by data adjustment. Moreover the technique does not provide an estimate of the accuracy of predicted reactor properties which is needed to accommodate uncertainties in prediction in design. There is however an exception to this general comment concerning spectrum measurements through resonances. Here it has proved very useful to test alternative evaluated cross-sections of single materials to identify which data gives the best fit to the detailed spectrum shape.

Further developments

The data adjustment techniques being used in the UK would benefit from further development. Not all the reactor properties of interest are yet incorporated into the predictions made. Furthermore the adjustment process does not yet automatically incorporate an allowance for resonance shielding. This must be calculated separately by methods which themselves are sufficiently free from errors in prediction.

Nevertheless sufficient experience has now been gained in these techniques to regard data adjustment with its prediction of uncertainties in the reactor properties of interest as a key process in utilising both differential and integral data measurements to allow prediction of performance of fast reactors on a short time-scale.

Part 2 Nuclear Data Adjustment

Brief Review of Methods of Adjusting Cross-sections

Methods of adjusting cross-sections to fit fast reactor integral experiments have been described by Cecchini et al (1), (2), Hemment and Pendlebury (3), Pazy et al (4) Barre and Ravier (5), and Rowlands and Macdougall (6). The dependence of the calculated value of an integral property on a cross-section change is assumed to be linear and the derivatives, or sensitivities, are obtained either by repeated calculations, changing each group cross-section in turn, or by means of perturbation theory. The generalised perturbation theory developed by Usachev (7) and further developed by Gandini (8) and others has played an important part in the calculation of cross-section sensitivities. The cross-sections are adjusted in a few broad energy groups although Pazy et al have formulated the solution in terms of cross-section adjustments which are a continuous function of energy.

In references (3), (4) and (6) the cross-section adjustments are obtained by minimising the sum of the squares of the cross-section adjustments and the residual discrepancies between the calculations using adjusted cross-sections and the integral measurements (all relative to their estimated standard deviations). Cecchini et al minimise the sum of the squares of the cross-section adjustments (relative to their standard deviations) and constrain the adjusted calculated values of the integral measurements to lie within fixed uncertainty ranges. Barre and Ravier determine the adjusted cross-sections which minimise the sum of the squares of the residual discrepancies between the adjusted calculated values and integral measurement. The cross-sections are permitted to be adjusted through a wide range of values. In this method the nuclear data is largely determined by the integral measurements a number of cross-sections being adjusted to the limits of the permitted uncertainty range.

The methods also differ in the treatment of the correlations between the errors in different cross-sections and between different energy ranges of the same cross-section. In reference (6) a simple treatment of correlations was included and more general methods have been described by Haggblom (9)

and by Mitani and Kuroi (10). However, the problem of assessing the numerical values of these correlations remains.
Pazy et al have given a formula for the accuracies of adjusted cross-sections and in reference (6) numerical values for these were obtained. It was shown that most individual cross-section adjustments were not significant. Since reference (6) was written further studies have been made of the dependence of adjusted cross-sections on assumed standard deviations and these will be described later in the paper.
In reference (6) an expression was given for the accuracies of reactor properties calculated using adjusted cross-sections. It was shown that the accuracies of prediction of such properties as the effective multiplication of the UK Prototype Fast Reactor and certain reaction rate ratios were about an order of magnitude higher than the values obtained using unadjusted cross-sections. Further studies which have been made have confirmed the importance of integral measurements in the prediction of such reactor properties and reactor spectra.

Mathematical formulation of the method of adjusting cross-sections

Cross-section adjustments are customarily made in a few broad energy groups, the cross-section for reaction x being increased by the constant factor $(1 + f_x)$ within the broad group. The initial fractional discrepancy, D_I, between the experimental, E_I, and calculated, C_I, values of the integral property I (where $D_I = (E_I - C_I)/C_I$) is changed to a fractional discrepancy d_I following the adjustment of the cross-sections. The approximation is made that the calculated value of the integral property C'_I varies linearly with the cross-section changes:

$$C'_I = C_I \left(1 + \sum_x S_{I,x} f_x\right) \qquad (1)$$

The sensitivities,

$$S_{I,x} = \left(\frac{\sigma_x}{C_I} \frac{\partial C_I}{\partial \sigma_x}\right) \qquad (2)$$

can be calculated using first order perturbation theory or from the difference between two calculations of the property

I (one with the standard cross-section set and the second with the cross-section σ_x increased by, say, 1%). The residual fractional discrepancies following the cross-section adjustments are given by the expressions:

$$d_I \equiv (E_I - C'_I)/C_I = D_I - \sum_x S_{I,x} f_x \qquad (3)$$

The cross-section adjustments can be chosen in different ways. When it is assumed that the errors in the cross-sections and in the integral measurements are independent and normally distributed, with standard deviations g_x and e_I, respectively, the method of least squares can be used. This requires the sum of the squares of the cross-section changes and the residual discrepancies, relative to their standard deviations, to be a minimum:

$$M = \sum_x \left(\frac{f_x}{g_x}\right)^2 + \sum_I \left(\frac{d_I}{e_I}\right)^2, \text{ is a minimum.} \qquad (4)$$

The requirement is then that the derivatives of M with respect to f_x should be zero:

$$\frac{f_x}{g_x^2} - \sum_I S_{I,x} \frac{d_I}{e_I^2} = 0 \qquad (5)$$

This can be written

$$\left(\frac{f_x}{g_x}\right) - \sum_I t_{I,x} \left(\frac{d_I}{e_I}\right) = 0 \qquad (6)$$

where

$$t_{I,x} = g_x \cdot S_{I,x} / e_I .$$

Calculation of the adjusted cross-sections and the residual discrepancies

The solution to equations (6) and (3) can be obtained either by eliminating d_I or f_x. Eliminating d_I the simultaneous equations which are obtained are

$$\sum_y C_{xy} \left(\frac{f_y}{g_y}\right) = \sum_I t_{I,x} \left(\frac{D_I}{e_I}\right) \equiv E_x \qquad (7)$$

where

$$C_{xy} = \delta_{xy} + \sum_I t_{I,x} . t_{I,y} \qquad (8)$$

and δ_{xy} is the Kronecker delta ($\delta_{xy} = 1$ if $x = y$. $\delta_{xy} = 0$ if $x \neq y$).

These equations can be solved by inverting the matrix. The cross-section adjustments are given by:

$$f_x = g_x \sum_y C^{-1}_{xy} E_y \qquad (9)$$

An alternative procedure is to solve the matrix equation which results when f_x is eliminated between equations (8) and (3), instead of d_I:

$$\sum_J G_{IJ} \left(\frac{d_J}{e_J}\right) = \frac{D_I}{e_I} \qquad (10)$$

where

$$G_{IJ} = \delta_{IJ} + \sum_x t_{I,x} . t_{J,x}$$

$$d_J = e_J \sum_J G^{-1}_{JI} \left(\frac{D_I}{e_I}\right) \qquad (11)$$

and

$$f_x = g_x \sum_J t_{J,x} \left(\frac{d_J}{e_J}\right) \qquad (12)$$

The matrix C_{xy} which is inverted in the first method has dimension m x m (where m is the number of cross-section variables plus systematic error variables) while the matrix G_{IJ} which is inverted in the second method has dimension n x n (where n is the number of integral measurements included in the fit). In the work described in reference (6) the first method

was used. In our studies the number of variables has exceeded the number of integral measurements by more than a factor of two and so the second method is to be preferred. The second method was adopted for the later ten group adjustment studies because this enabled the matrix to be stored and inverted in the fast store of the IBM 7030.

The accuracy of adjusted cross-sections

An estimate of the accuracy of the adjusted cross-section is given by the correlation matrix:

$$V_{xy} = E\left[(f_x - \hat{f}_x) \cdot (f_y - \hat{f}_y)\right] \qquad (13)$$

where E denotes the expectation value and the circumflex a true value (that is, $\hat{f}_x$ is the true fractional error in the cross-section x). The diagonal elements of the matrix V_{xy} are the variances of the adjusted cross-sections and the off-diagonal elements are the covariances.

In order to derive an expression for V_{xy} in terms of the sensitivities and the assumed standard deviations f_x is first expressed in terms of $\hat{f}_x$ and $\hat{d}_I$ (the fractional discrepancy between the measured value and the true value of the integral property I):

$$\hat{d}_I = (\dot{E}_I - \hat{E}_I)/C_I \qquad (14)$$

The fractional difference between the measured and calculated values of the integral property I can be expressed in terms of the measurement errors and the cross-section errors:

$$D_I = \hat{d}_I + \sum_x S_{I,x} \cdot \hat{f}_x \qquad (15)$$

Substituting this expression for D_I in one of the two equations for f_x (eqn. (9) or (12)) and assuming that the values of d_I and f_x are uncorrelated results in V_{xy} having one of the two alternative forms (depending on the method of solution chosen for f_x).

$$V_{xy} = g_x\, g_y\, C_{xy}^{-1} \qquad (16)$$

or

$$V_{xy} = g_x\, g_y\, (\delta_{xy} - \sum_I \sum_J t_{I,x}\, t_{J,y}\, G_{IJ}^{-1}) \quad , \tag{17}$$

The cross-section adjustments, f_x, depend on the relative values of the assumed standard deviations, e_I and g_x but the variances and covariances are proportional to the square of the absolute value of these standard deviations. These absolute values can be multiplied by a constant factor so that the distribution of the discrepancies between measured and calculated values of the integral experiments is consistent with the assumed standard deviations. The scaling factor can be obtained most conveniently by considering the expectation value of the sum of squares, M.

$$E\,[M] = \sum_{x=1}^{m} E\left[\left(\frac{f_x}{g_x}\right)^2\right] + \sum_{I=1}^{n} E\left[\left(\frac{d_I}{e_I}\right)^2\right] = n \tag{18}$$

where n is the number of integral measurements included in the fit and m is the number of cross-section variables.
When M/n is greater than unity the assumed standard deviations have been underestimated. (Alternatively there are sources of uncertainty other than the cross-sections, or the simple few group representations of the error is inadequate.) Increasing the standard deviations by the factor $\sqrt{M/n}$ will make them consistent with the distribution of the discrepancies between measurement and calculation. For this reason the correlation matrix is chosen to be

$$V_{xy} = \frac{M}{n} \cdot g_x \cdot g_y\, C_{xy}^{-1} \tag{19}$$

or

$$V_{xy} = \frac{M}{n}\, g_x\, g_y\, (\delta_{xy} - \sum_I \sum_J t_{Ix}\, t_{Jy}\, G_{IJ}^{-1}) \tag{20}$$

The square roots of the diagonal elements are the fractional standard deviations of the adjusted cross-sections:

$$\tau_x = \sqrt{V_{xx}} \tag{21}$$

Because of the factor M/n, τ_x can be larger than g_x.

The accuracy of calculations made using adjusted cross-sections

When the cross-section sensitivities, S_{px} of the calculated value of a reactor property, p, are known a correction factor can be obtained which is to be applied to the value calculated using the unadjusted cross-sections. This correction factor is $(1 + F_p)$ where

$$F_p = \sum_x S_{p,x} f_x$$

The variance of the adjusted value is the expectation value

$$E\left[(F_p - \hat{F}_p)^2\right] = E\left[\left(\sum_x S_{p,x} (f_x - \hat{f}_x)\right)\left(\sum_y S_{p,y} (f_y - \hat{f}_y)\right)\right]$$

$$= \sum_x \sum_y S_{p,x} \cdot S_{p,y} V_{xy}$$

and so the standard deviation of the adjusted calculated value is

$$\alpha_p = \sqrt{\sum_x \sum_y S_{p,x} \cdot S_{p,y} V_{xy}} \qquad (22)$$

The theory of prediction by least squares fitting is described in the text book by Linnik (11). Confidence intervals on the predictions are given by the Student distribution with n degrees of freedom. The number of integral properties included in the fit, n, is usually sufficiently large for the Student distribution to be approximately equal to a normal distribution with the above standard deviations.

Although the standard deviations of the adjusted cross-sections may not be significantly smaller than those assumed for the unadjusted cross-sections, the accuracy of the prediction of many reactor properties is radically improved because of the covariance components of the matrix, V. This is because the accuracies of cross-section groups and ratios are significantly improved by the fit.

Because the assumptions which have been made about the nature of the cross-section errors (and other sources of error) may be inaccurate it is necessary to test the correctness of the predictions and the uncertainty estimates by examing the predictions of integral properties which have been measured. Such

a test was described in reference (6). Each of 55 integral measurements was excluded from the fit in turn and the predicted value was compared with the measured value (relative to the combined measurement uncertainty and estimated accuracy of prediction). The distribution of predicted values was consistent with a normal distribution having the estimated standard deviations (combined with the estimated standard deviations of the integral measurements).

Accuracy of the numerical methods

The two methods of calculating adjusted cross-sections (eqns (9) and (12)) and standard deviations (eqns (19) and (20)) have been incorporated in an IBM 7030 computer programme called LSQ. In a five energy group adjustment study for 11 substances and 60 integral measurements the two methods of solution gave percentage cross-section adjustments and standard deviations which differed at most in the fourth place of decimals. The predicted correction factors to be applied to the standard calculations of integral properties and the estimated standard deviations obtained using the two methods agreed to within six places of decimals.

Treatment of systematic errors

Systematic errors in the integral measurements can be represented in the equations in the same way as cross-section errors. Denoting by $T_{I,y} \cdot h_y$ the contribution to the fractional experimental error in E_I caused by the systematic error, h_y (which has the estimated standard deviation j_y) then the expression (3) for the residual fractional discrepancy d_I becomes

$$d_I = D_I - \sum_x S_{I,x} \cdot f_x - \sum_y T_{I,y} h_y \qquad (23)$$

and the sum of the squares to be minimised becomes

$$M = \sum_I \left(\frac{d_I}{e_I}\right)^2 + \sum_x \left(\frac{f_x}{g_x}\right)^2 + \sum_y \left(\frac{h_y}{j_y}\right)^2 \qquad (24)$$

Usually $T_{I,y}$ will be either unity or zero depending upon whether the systematic error y applies to the integral measurement I. The quantity e_I is the standard deviation of the

random component of the fractional error in the measurement. An estimate of the systematic error, h_y, is obtained from the fit.

As an example of the treatment of systematic errors in the integral measurements consider neutron spectra measured using the same equipment on several different assemblies. We represent the spectrum measurements by the set of ratios of the neutron flux in energy group g + 1 to the flux in group g

$$S_\alpha (g + 1,g) = \phi_\alpha (g + 1)/\phi_\alpha (g) \qquad (25)$$

where S_α denotes the spectrum in assembly α.

The fractional error in the component S_α (g + 1,g) is equal to

$$t_\alpha (g + 1,g) - r_\alpha (g + 1) - r_\alpha (g) + s (g + 1,g) \qquad (26)$$

where

t_α (g + 1,g) is an error in the shape of the spectrum which is independent of the errors in other assemblies

r_α (g) is the random error in the measurement of the flux in group g and assembly α

s (g + 1,g) is a systematic error in the shape of the spectrum which is common to each assembly.

The errors r_α (g) for g not equal to the first or last group in the spectrum measurement enter the calculation as systematic errors because they appear in more than one integral measurement equation. The random error component is t_α (g + 1,g) in these groups (the random error is (t_α (2, 1) - r_α (1)) in the first group). More complex relationships are possible. For example, the systematic errors s (g + 1,g) may differ by a factor, T_α, in the different assemblies, and there may be correlations between the errors in s (g + 1,g) and s (g, g - 1).

An analysis has been made of the systematic errors occurring in the integral measurements made in the Zebra 8 series of zero leakage test zones. The measurements include k_∞, U238/U235 and Pu239/U235 fission ratios, U238 capture/Pu239 fission ratios and neutron spectra. Correlations exist between the errors in the different types of measurement made in the same test zone

(arising from the extrapolation of the measurements to the infinite medium values) and between the same type of measurement made in the different test zones (such as the thermal calibration of the U238 capture/Pu239 fission ratio measurements). These systematic errors are represented in the adjustment study described in the paper.

The treatment of correlations in the cross-section errors

The errors in the value of an evaluated cross-section in a particular energy range is correlated both with the errors in other energy ranges and in other cross-sections. The correlations exist because of correlations in the errors of measurement at different energies, and for different reactions, and because the shape of the cross-section may be to some extent defined by nuclear theory. For example, some cross-section are measured relative to a standard cross-section, such as B10 (n,α) or U235 (n,f), or the shape of the cross-section may be measured accurately over a certain energy range and normalised at some energy to a less accurate value of the cross-section. Some capture cross-sections are expected to be of 1/v form at low energies and the elastic scattering cross-sections are constant at these energies. In these cases the uncertainties are constant factors which are the same in all energy groups within the range for which the shape of the cross-section is known. Most of the important cross-sections of practical interest cannot be expressed in a simple form and the problem of assessing the correlations appears to be a formidable one. The problem of assessing likely correlations also faces the reactor physicist when estimating the required accuracies for microscopic cross-section measurements. Over what energy range is the error to be assumed systematic and for what ranges uncorrelated? For which cross-sections will the errors be correlated? When different assumptions are made about correlations, and when the requirements are partitioned between the different substances and reactions contributing to the overall errors in the integral quantities in different ways, the accuracy requirements can change by factors of 2 or 3.
Some recent evaluation studies have taken account of correlations in the errors in the cross-section measurements for different substances, by simultaneously fitting both direct

measurements of fission cross-sections and ratio measurements. Normalisation measurements have also been treated separately in the fits. More complex correlations between the measurements made at different energies have not been included. Nuclear theory predictions have not been taken into account in these evaluations.

We would like to ask nuclear data evaluators to give consideration to the assessment of the correlations in cross-section errors. The form in which these are given is not important provided that it enables the correlation between any pair of group cross-sections to be calculated.

In the mathematical formulation of the adjustment of cross-sections correlations in the cross-section errors can be allowed for by transforming the expression for the discrepancy between integral measurement and calculation, d_I, to be in terms of the independent cross-section variables f^*_x which have standard deviations g^*_x. In the cross-section adjustment studies, we have made correlations between the errors in different energy ranges of the same cross-section in a simple way by assuming a dependence of the form:

$$f_{s,\,r,\,g} = f^*_{s,\,r,\,g} + C_{s,\,r,\,g} \cdot f_{s,\,r(g+1)} \qquad (27)$$

The fractional adjustment to the cross-section for substance s and reaction r in group g consists of one term which is a fraction $C_{s,\,r,\,g}$ of the adjustment in the next lower group plus a second independent term, $f^*_{s,\,r,\,g}$. The standard deviation associated with the independent adjustment is given by

$$(g_{s,r,g})^2 = (g^*_{s,r,g})^2 + (C_{s,r,g} \cdot g_{s,r,(g+1)})^2 \qquad (28)$$

The sensitivity which is to be associated with the independent adjustment, $S^*_{I,s,r,g}$ is obtained by substituting the expression (27) for $f_{s,r,g}$ into eqn (3), $S^*_{I,s,r,g}$ being the coefficient of $f^*_{s,r,g}$:

$$S^*_{I,s,r,g} = S_{I,s,r,g} + C_{s,r,(g-1)} \cdot S^*_{I,s,r,(g-1)} \qquad (29)$$

The quantities f_x^*, g_x^* and $S_{I,x}^*$ are now used in the least squares and fractional discrepancy expressions in place of f_x, g_x and $S_{I,x}$.

When the shape of a cross-section is accurately known (for example, when the cross-section is known to be of $^1/v$ form) $g_{s,r,g}$ is the same in all energy groups and $C_{s,r,g}$ is unity. In this case $g_{s,r,g}$ is zero excepting for the lowest energy group, g_o, for which $g^*_{s,r,g_o} = g_{s,r,g_o}$ and

$$S^*_{I,s,r,g_o} = \sum_g S_{I,s,r,g} \tag{30}$$

The adjustment is essentially made in one energy group in this case. In the general case the correlation parameters, $C_{s,r,g}$ will increase as the width of the energy groups is reduced. Other forms of correlation are possible, for example, when the cross-section is known to vary linearly with energy the correlation has the form:

$$f_g = f_{g_o} + L_g (f_1 - f_{g_o}) \tag{31}$$

where L_g is a factor which depends on the mean energy in group g

$$L_g = (\bar{E}_g - \bar{E}_{go}) / (\bar{E}_1 - \bar{E}_{go}) \tag{32}$$

In this case there are only two variables representing the reaction. In general the correlation can be written in the form:

$$f_x = f_x^* + \sum_y C_{xy} f_y \tag{33}$$

but for some cases, such as the relationship (31), the standard deviation g_x^*, associated with some of the f_x^* may be zero. These variables are therefore omitted from the fit.

Method of allowing for differences between the standard cross-section set and the microscopic data

It has been implicit in the discussions so far that the cross-section set used in the calculations contains the best current evaluation of the microscopic cross-section data. However,

later measurements may have been made of some of the cross-sections in the set or some of the cross-sections may have been adjusted or selected to give a better fit to integral measurements. To allow for these differences in the adjustment of the cross-sections it is necessary to know the factors, $(1 + b_x)$, by which the microscopic cross-sections differ from the standard cross-section set. Since the object is to obtain cross-sections which are the best fit to the integral and microscopic measurements the quantity to be minimised is

$$M = \sum_x \left(\frac{f_x - b_x}{g_x}\right)^2 + \sum_I \left(\frac{d_I}{e_I}\right)^2 \qquad (34)$$

where g_x is the standard deviation of the differential cross-section measurements.

This minimisation is achieved by transforming the expression for d_I to be in terms of f_x^+, where

$$f_x^+ = f_x - b_x \qquad (35)$$

$$d_I = D_I - \sum_x S_{I,x} (f_x^+ + b_x)$$

$$= D_I^+ - \sum_x S_{I,x} f_x^+ \qquad (36)$$

and

$$D_I^+ = D_I - \sum_x S_{I,x} b_x \qquad (37)$$

is the discrepancy which would be obtained between measurement and calculation if the unadjusted differential cross-sections were used in the calculations.

Scope of recent cross-section adjustment studies

In reference 6 a five energy group adjustment study was described. Since that paper was written further studies have been made in five groups and a new study completed in which important cross-sections are adjusted in ten groups and less important cross-sections in six groups. The energy group structures are listed in Tables I and II.

TABLE I. ENERGY GROUP STRUCTURE USED IN THE FIVE-GROUP ADJUSTMENT STUDIES

Group	Lower energy (Kev)
1	821
2	111
3	15
4	0.748
5	thermal

TABLE II. ENERGY GROUP STRUCTURE USED IN THE TEN-GROUP ADJUSTMENT STUDIES

10 group structure	6 group structure	Lower energy (Kev)
1	1	1 350
2	2	498
3		183
4	3	67.4
5		24.8
6	4	9.12
7		3.35
8	5	1.23
9		0.454
10	6	thermal

The integral properties were calculated using the 2000 group cross-section set FGL4 described in reference 6.

The cross-sections of eleven substances are adjusted: U235, Pu239, U238, Pu240, C, O, Na, Fe, Cr, Ni and Al. The recent studies have included the mean energies of the fission spectra of U235, Pu239 and U238 as variables.

The transport cross-section, or $\bar{\mu}$, is taken to be a variable only in the high energy groups. The number of cross-section variables for carbon and oxygen has been reduced by assuming that the elastic scattering cross-sections can vary only by a constant factor below 183 Kev. The small radiative capture cross-sections in carbon and oxygen have also been eliminated from the fit. The uncertainty in the mean energy of the fission spectrum of U235 has in most cases been taken to be $\pm$ 10% and the adjustments to the mean energies of the fission spectra of Pu239 and U238 have been taken to be correlated with the adjustments to the U235 fission spectrum with uncertainties in the mean energies of $\pm$ 3% relative to the U235 adjustment. The standard FGL4 fission spectra are Maxwellian with temperatures of 1.30 Mev for U235, 1.39 Mev for Pu239 and 1.30 Mev for U238. Biases were applied to these values in the adjustment calculations to make them more consistent with Terrel's formula (which relates the fission spectrum temperature to $\bar{\nu}$).

The temperatures were increased by 1% for U235, - 1.5% for Pu239 and 3% for U238. The adjustments quoted later in the paper are relative to the FGL4 values, however.

The integral measurements used in the fit have been extended to include the measurements of k_∞ and reaction rate ratios in 4 further zero leakage test zones in the Zebra 8 series, the critical sizes of 13 small Los Alamos critical assemblies, and Grundl's measurement of U238/U235 fission ratio in a U235 fission spectrum. The spectrum measurements made in Zebra 8A, 8B, 8C and 8D are represented by the eight ratios $\emptyset(3)/\emptyset(2)$ to $\emptyset(10)/\emptyset(9)$ where $\emptyset(n)$ represents the flux measured in group n of the ten group structure.

In Table III typical values are given for the numbers of cross-section variables, systematic errors and integral measurements included in a fit.

TABLE III. TYPICAL VALUES FOR THE NUMBERS OF VARIABLES AND INTEGRAL MEASUREMENTS INCLUDED IN A FIT

Number of cross-section variables	220
Number of variables due to systematic errors connecting integral measurements	56
Total number of variables	276
Number of critical size measurements	49
Number of k_∞ measurements	7
Number of reaction rate ratio measurements	19
Number of items of neutron spectrum information (4 spectra)	32
Total number of integral measurements	107

Cross-section adjustments and their dependence on assumed standard deviations and integral measurements

The standard deviations assumed for the cross-sections and many of the earlier integral measurements of critical size are in many cases very approximate. Some were reassessed when it was found difficult to fit certain integral experiments. For example, the uncertainty assumed for the elastic scattering cross-section of sodium in the region of the 3 Kev sodium resonance was inconsistent with the reactor spectrum measurement

in Zebra 8D. The evaluation for sodium used in the FGL4 set is J J Schmidt's 1962 evaluation, (below the inelastic scattering threshold) and the 3 Kev resonance data in this evaluation is not now regarded as correct. The uncertainty was increased to ± 50% and a + 100% adjustment was obtained. A more recent evaluation is now being converted for use in our calculational scheme and the Zebra 8D spectrum will be recalculated using this revised data. It is expected that this will result in a much improved agreement with the measured spectrum. Integral measurements have also been reassessed and in some cases the assumed standard deviations increased following cross-section adjustment studies. One difference from the earlier work (reference 6) is that the moisture content of the graphite used in the Zebra 8 series of experiments and in Zebra 2 and 6 has been remeasured and found to be higher than was earlier thought. Other small revisions have been made to the composition data and integral measurements, the main result being that the spectrum measurements are not now so difficult to fit. Some inconsistencies remain but in these cases no explanation has yet been found. The cross-section correlations are also only approximate. The capture cross-sections of U235 and Pu239 have been correlated with the fission cross-sections, so that α is the independent variable. In recent studies the fission cross-section of Pu239 has been correlated with that of U235. The variations of the mean energies of the fission spectra of U235, Pu239 and U238 are also correlated. The correlation factor relating cross-section variations in adjacent energy groups has been taken to be 0.7 for cross-sections varied in 10 groups and 0.5 for cross-sections varied in 6 groups, excepting for regions where the uncertainty is thought to be uncorrelated. These values for the correlation factors reflect the absence of any proper evaluation of them but since some correlation does exist in most cases, an order of magnitude estimate was thought preferable to neglecting the correlation. The values of the cross-section uncertainties and the correlations used in the cross-section adjustment studies will continue to be refined and the present values must be regarded as preliminary estimates.

The cross-section adjustments are regarded as significant if they are larger than the assumed standard deviation of the

unadjusted data or if the standard deviation of the adjusted cross-section is lower than that assumed for the microscopic data. When the adjustment is approximately the same in all energy groups the adjustment to the spectrum averaged value may be significant although the adjustments to individual group values are not. These adjustments are also of interest.
Some of the cross-section adjustments which were described as being significant in reference 6 no longer appear to be significant. This has happened because the fission spectrum has been included in the fit and some assumed cross-section uncertainties have been changed; in particular, the fission cross-section accuracies have been relaxed and the accuracies for carbon and oxygen have been made higher.

The fission spectrum and U238 fission rates

The calculated value of the U238 fission rate (per fission in the reactor, or relative to U235 or Pu239 fission) depends upon the U238 fission cross-section and factors which affect the fraction of the reactor neutron spectrum above the U238 fission threshold at about 1.5 Mev. These factors include the mean energy of the fission spectrum and high energy moderation cross-sections, in particular, inelastic scattering in U238 and elastic scattering in carbon.
In reference 6 two cross-section adjustments which were noted as significant were a 16% $\pm$ 4% reduction to the U238 inelastic scattering cross-section and a 21% $\pm$ 6% reduction to the moderation cross-section of carbon. Such a large adjustment to the carbon cross-section was considered to be well outside the accuracy of the microscopic data.
A special study was therefore undertaken to investigate this situation further. The results of the steps taken in this study are illustrated in Table IV. The first five cases listed relate to adjustments made in 5 broad groups and case 6 is undertaken in 10 groups.
Case 1 is the standard case reported in reference 6. Table IV shows that the adjustment to the carbon cross-section resulted from inclusion of the single U238/U235 fission ratio for Zebra 8A in the fit. The value of C/E (calculation/experiment) for this ratio was over 10% lower than the C/E values for the ratio for Zebra 8B and 8C also included in the fit.

TABLE IV. ADJUSTMENTS TO CROSS-SECTIONS IN THE MeV ENERGY RANGE

	Assumed uncertainty (%)	Including Zebra 8A F8/F5		Excluding Zebra 8A F8/F5 (and Z8F F8/F5 in case 6)	
		Adjustment (%)	Accuracy (%)	Adjustment (%)	Accuracy (%)
1					
U238 σ_f	3	1.5	3.0	0.3	2.9
U238 σ_{mod}	20	-15.9	4.0	-17.9	3.9
C σ_{el}	10	-21.1	6.0	3.4	9.0
C σ_{tr}	10	10.0	8.6	8.7	8.3
2					
U238 σ_f	3	3.4	3.2	0.3	3.0
U238 σ_{mod}	20	-15.6	4.3	-18.4	3.9
C σ_{el}	5	- 8.1	4.5	1.7	4.8
C$(1 - \bar{\mu})$	3	1.9	3.6	1.2	3.2
3					
U238 σ_f	3	3.9	3.0	0.2	2.9
U238 σ_{mod}	20	-15.4	4.1	-18.0	3.8
C σ_{el}	3	- 5.9	2.5	- 3.2	2.4
C$(1 - \bar{\mu})$	2	0.6	2.3	0.3	2.1
4					
U238 σ_f	3	1.7	3.2	0.5	2.9
U238 σ_{mod}	20	- 8.5	5.6	-18.2	5.7
C σ_{el}	3	- 4.5	2.6	- 3.2	2.3
U235 T	10	7.7	4.3	1.3	4.2
Pu239 T		5.7		- 3.7	
5					
U238 σ_f	7	4.6	5.9	1.2	5.7
U238 σ_{mod}	20	- 5.3	6.0	-14.1	6.5
C σ_{el}	3	- 3.9	2.5	- 2.9	2.4
U235 T	10	6.9	4.9	3.1	4.8
Pu239 T		5.5		- 0.7	
6					
U238 σ_f	5	7.6	5.3	5.1	5.1
U238 σ_{mod}	20	- 0.5	6.8	-10.9	7.3
C σ_{el}	3	- 0.2	3.2	1.6	3.1
U235 T	10	8.3	5.4	3.2	5.4
Pu239 T		5.1		- 3.0	

Cases 2 and 3 show the effect of increasing the accuracy of the carbon data, case 3 representing what are considered to be realistic values. A strong correlation between the uncertainties in adjacent energy groups (a correlation factor of 0.866) is assumed for case 3.

These cases show how dependent the adjustments to carbon data are on the assumed uncertainties in the unadjusted cross-sections of carbon.

The residual discrepancies in the fitted values of the Zebra 8A U238/U235 fission ratios are not markedly worsened by constraining the adjustments to the carbon cross-section. (The residual discrepancy increases from - 1.2% to - 2.6%, the assumed relative standard deviation of the measurement (excluding systematic error components) being ± 1.2%.) There are compensating changes in several cross-sections, including U235 fission.

Case 4 introduces the mean energy of the fission spectrum as a new variable. The standard deviation of the mean energy of the U235 fission spectrum was assumed to be ± 10% and the mean energy of the U238 and Pu239 fission spectra were taken to be correlated with that of U235 with a relative standard deviation of ± 3%. The fission spectrum of U235 was hardened by 7.7%; the carbon data were fitted slightly better and the reduction required in U238 inelastic scattering data was approximately halved. However these adjustments depended very strongly on including the Zebra 8A fission ratio measurement in the fit.

Case 5 illustrates that when the 8A integral result is excluded from the fit, an increase in the uncertainty of the fission cross-section of U238 from 3% to 7% leads to a reduction in the change in the U238 inelastic cross-section from - 18% ± 4% to - 14% ± 6.5%.

Case 6 (a 10 group fit) includes new integral evidence on the fission ratio from Zebra 8F which is a test-zone of composition similar to 8A but a less heterogeneous structure. Furthermore, a range of small Los Alamos criticals is included in the fit in this case. The results confirm the increase in hardness of the U235 fission spectrum, suggested in Case 4, but show that the U238 fission cross-section should be increased by 7.6%, and that the U238 inelastic data should not be changed. When the 8A fission ratio is excluded from the fit the cross-section adjustments do not change markedly, but when both the 8A and 8F fission ratios are omitted the increase to the mean energy of the U235 fission spectrum is only 3% and an 11% ± 7% reduction to the U238 moderation cross-section is obtained.

Other integral measurements tend to support the 8% increase in the mean energy of the U235 fission spectrum. Measurements of the second moment of the spatial distribution of U235 fission

neutrons moderated in H_2O, D_2O and graphite (the neutron age to the indium resonance) are best fitted by a fission spectrum having a mean energy about 5% higher than the standard value in FGL4 and are not inconsistent with even higher values. Preliminary results from a direct measurement of the fission spectrum made at Winfrith using a Li6 spectrometer also support the higher mean energy. Measurements of the U238/U235 fission ratio now being made in an enriched uranium zero leakage test zone, Zebra 8H, should also provide a valuable integral check relating to the fission spectrum. This experiment seeks confirmation that the graphite data is not at fault.

U235 and Pu239 fission cross-sections

At the time the FGL4 cross-section set was produced (1967), the evaluated fission cross-sections of U235 and Pu239 were estimated to be accurate to about ± 3%. It was known at the time, however, that these data did not fit the integral fission ratio measurements, and for FGL4 the Pu239 fission cross-section was increased from the evaluated data by about 10% in the range 25 to 100 Kev.

More recent measurements have suggested that the 1967 evaluations may be 10% to 15% too high in the energy range 10 Kev to 700 Kev for both U235 and Pu239 fission.

In the recent 10 group adjustment studies, the U235 fission cross-section has been assumed to have a larger standard deviation of ± 10% and the Pu239 fission cross-section is assumed to be correlated to the U235 fission cross-section with a relative standard deviation ranging from 5% to 10%.

If the Zebra spectrum measurements are excluded from the fit, no significant adjustments to these fission cross-sections are required, the changes called for being in the range ± 5%.

It is known, however, that below about 10 Kev, the calculated spectra are more rapidly attenuated than the measured spectra. At these energies moderation in Zebra cores 8A and 8B is predominantly due to scattering in carbon, for which the cross-sections are well established. (Particular care had been taken to measure and allow for the water content of the graphite used in these measurements.) Because of these considerations, it was expected that absorption in the lattice must be reduced at these energies.

Including the Zebra spectra in the fit causes the U235 fission cross-section to be reduced by 20% to 26% below 10 Kev and the Pu239 fission cross-section to be reduced by between 14% and 23% in this energy range. The changes required to the U238 capture cross-sections and other data associated with the spectrum results are discussed in the sections considering these cross-sections.

The proposal to reduce the fission cross-sections by 10 to 15% in the energy range 10 Kev to 700 Kev has also been tested (with corresponding reductions to the U238 capture data). These data were all adjusted back to values close to those used in the FGL4 set, showing that such changes are inconsistent with the integral measurements.

The tentative conclusion reached is that the evidence from the Zebra spectrum measurements require the fission cross-sections of U235 and Pu239 to be significantly reduced below 10 Kev.

U238 capture

Earlier adjustment studies had indicated the need for a reduction of about 10% in the U238 capture cross-section at energies above 100 Kev (relative to the measurements of Barry et al) and an increase of about 5% in the range 1 to 15 Kev where Moxon's data are used. Since the uncertainties on the fission cross-sections have been increased the adjustments have changed and are no longer significant. The largest change is a reduction of 11% $\pm$ 13% in the energy range 10 to 25 Kev where Moxon's data are used. This adjustment resulted from the inclusion of spectrum measurements in the fit.

Iron capture

A reduction of about 30% in the iron capture cross-section (relative to the measurements of Moxon) is required to fit the k_∞ measurement made in Zebra 8C. The energy range in which this reduction is to be made is not defined because only one integral measurement relating to iron capture has been included in the fit. Small sample reactivity perturbation measurements are to be included in the fit and preliminary results show that these support the need for such a reduction in iron capture.

Pu239 alpha

All the cross-section adjustments studies have indicated that the value of Pu239 alpha in the FGL4 set is about 10% low,

although the adjustment to any one energy group is not significant and the standard deviation of the adjustment to the spectrum averaged value is only about ± 10%. When the results of fast reactor irradiation experiments are included in the fit more significant results should be obtained. The adjustments are consistent with the preliminary results of these irradiation experiments. The value of alpha in the FGL4 set is a smooth curve which passes approximately through an average of the Schomberg and Sowerby, Gwin and Czirr measurements. Spectrum averaged values are compared in Table V.

TABLE V. SPECTRUM-AVERAGED VALUES OF ^{239}Pu-ALPHA

Recommended curve of Schomberg and Sowerby	0.242
FGL4 unadjusted	0.246
Adjusted value	0.267

The accuracy of prediction of reactor properties

Although many of the adjustments to individual cross-sections are not significant the predicted values of PFR properties are significantly improved in precision by the use of the adjusted data.

In Table VI the values of effective multiplication, k, to be sought for the critical reactor using unadjusted FGL4 data are given. These values refer to the clean critical reactor at 300°K and do not include uncertainties due to extrapolation to the operating temperature or to fission product data. The cases quoted refer to the initial assumptions made in the corresponding cases of Table IV. Two main conclusions are shown from these results:

i Adjustment of data to fit the integral measurements improves the accuracy of prediction from 5% to 0.5%. (The 5% figure is based on the relaxed accuracies of the microscopic fission data now considered appropriate.)

ii The prediction and its accuracy based on adjusted data is not very sensitive to the uncertainties assumed in the unadjusted data, nor does it depend significantly on whether or not the Zebra 8A fission data (which controls the fit to the fission spectrum, inelastic data for U238 and fission cross-section of U238) is included.

In Table VII the percentage increase to the FGL4 values of the U238/Pu239 fission ratios used in PFR are illustrated. The cases again correspond to those of Table IV. All the cases show the need to increase this ratio, as a result of fitting to the integral data, by about 10% ± 3%. The accuracy of the unadjusted data ranged from ± 10% to ± 15%. Although this ratio is more dependent upon the assumed uncertainties in the unadjusted data than the k-values of Table VI, all the adjustments lie within the uncertainty of ± 3%.

Adjustments to be applied to the calculated values of the PFR neutron spectrum are given in Table VIII. It will be seen that the accuracy of prediction has been improved by about a factor of 2 below 10 Kev, that is, in the Doppler coefficient energy range, and that a 9% reduction in the flux in the energy range 1.23 to 3.36 Kev is followed by a 33% increase in the

TABLE VI. VALUE OF k TO BE USED IN FGL4 CALCULATIONS FOR PFR

Case	Including Z8A F8/F5		Excluding Z8A F8/F5 (and 8F F8/F5 in case 6)	
	Prediction	Accuracy of the unadjusted value	Prediction	Accuracy of the unadjusted value
1	1.0087 ± 0.0042	± 0.026	1.0073 ± 0.0041	± 0.026
2	1.0053 ± 0.0043	± 0.026	1.0055 ± 0.0039	± 0.026
5	1.0064 ± 0.0039	± 0.037	1.0056 ± 0.0037	± 0.037
6	1.0073 ± 0.0049	± 0.049	1.0061 ± 0.0047	± 0.049

TABLE VII. PERCENTAGE INCREASE TO BE APPLIED TO THE FGL4-CALCULATED VALUE OF THE $^{238}U/^{239}Pu$ FISSION RATIO IN PFR

Case	Including Z8A F8/F5	Excluding Z8A F8/F5 (and Z8F F8/F5 in case 6)
1	9.2	9.6
2	10.2	9.5
5	12.6	9.1
6	11.9	8.8

TABLE VIII. CORRECTIONS TO BE APPLIED TO THE FGL4-CALCULATED VALUE OF THE PFR NEUTRON SPECTRUM. PERCENTAGE INCREASE IN THE RATIO OF FLUXES IN ADJACENT BROAD ENERGY GROUPS, ϕ_{g+1}/ϕ_g

g	Including spectrum measurements in the fit	Excluding spectrum measurements from the fit	Accuracy of the unadjusted prediction
2	4.1 ± 8.0	3.0 ± 9.2	± 12.5
3	- 0.3 ± 7.8	1.3 ± 9.7	± 7.8
4	- 0.7 ± 5.6	- 2.0 ± 6.8	± 5.7
5	- 6.9 ± 3.1	- 2.9 ± 4.6	± 4.3
6	- 0.7 ± 3.7	- 3.2 ± 4.6	± 4.7
7	1.4 ± 4.7	- 6.8 ± 8.3	± 7.2
8	- 9.4 ± 4.5	- 2.8 ± 13.7	± 11.1
9	32.9 ± 7.0	- 8.2 ± 19.3	± 16.0
10	9.2 ± 7.6	-15.9 ± 12.5	± 11.8

range 0.748 to 1.23 Kev (relative to the value in the higher energy group). Such a change would bring the calculated Doppler coefficient into better agreement with experiment for the Zebra 5 Doppler loop measurements.

Conclusions

The following conclusions are drawn from experience so far obtained in adjusting nuclear data to fit simultaneously both the evaluated microscopic cross-sections and the results of integral experiments:

i Although the majority of the cross-section changes are not significant the accuracy of predicting reactor properties is radically improved as a result of using adjusted data. Reactivity of a clean cold PFR is predicted with an uncertainty of only ± ½% compared with 5% when unadjusted data are used, which compares favourably with the accuracy sought from the "high accuracy" nuclear data.

ii Additional data are required to predict burn-up and temperature effects and the use of alternative canning and structural materials. The data requests should emphasise measurements such as the resonance structure of cross-sections for which integral experiments lack resolution.

iii Adjustments to individual cross-sections depend significantly on the uncertainties assumed in the evaluated data. Greater attention in evaluation should be given to identifying these uncertainties and to correlations between the uncertainties in different cross-sections. The prediction of reactor properties, however, is not strongly dependent on uncertainties assumed for the unadjusted data.

iv Particular care is required when a single integral measurement is responsible for significant data changes. The adjustment process should be examined critically to ensure that sufficient data variables have been allowed and that the accuracies assumed for the unadjusted data are realistic. Independent confirmation of the integral result is clearly important.

v The range of integral measurements included in the fit should be extended whenever results of sufficient accuracy are available. Such extensions may include central perturbation measurements made in a calculable geometry and environment, irradiation experimental results conducted in operating power reactors, and measurements of distributed properties through zero power reactor assemblies.

vi Changes in individual items of data in the FGL4 library which at present appear significant are as follows:

An increase in the mean energy of the U235 fission spectrum by 8% $\pm$ 5% and corresponding increases for Pu239 and U238. (This adjustment is produced as a result of only two integral measurement but other integral measurements not included in the fit tend to support it.)

A reduction of about 20% in the U235 and Pu239 fission cross-sections below 10 Kev. (This reduction results from fitting four reactor neutron spectra.)

A 30% reduction in the iron capture cross-section (in the energy range 1 Kev to 100 Kev), relative to Moxon's measurements. This result is a consequence of a single integral measurement (k_∞ in Zebra 8C) but is supported by other integral measurements not included in the fit.

An increase in Pu239 alpha by about 10% $\pm$ 10%

relative to current evaluations. A number of integral measurements in different spectra indicate the need for such an increase.

Proposed reductions in the U235 and Pu239 fission cross-sections in the range 10 to 700 Kev, by 10% to 15%, are not consistent with the integral data (unless a wide range of compensating cross-section adjustments were also to be introduced).

vii Fast and thermal reactor integral data studies have used different evaluations of the microscopic measurements and so it has not been possible to combine the results of such studies. It is clearly desirable that there should be a standardisation of data sources and more effort should be made to adjust cross-sections to fit both types of integral data.

References

1 Cecchini G, Farinelli V, Gandini A and Salvatores M.
A/Conf 28/P 627, Geneva (1964).

2 Cecchini G, Gandini A, Dal Bono I and Faleschini B.
Fast Critical Experiments and their Analysis.
ANL-7320 (p 107) Argonne (October 1966).

3 Hemment P C E and Pendlebury E D.
ANL-7320 (p 88) Argonne (October 1966).

4 Pazy A, Rakavy G, Reiss Y and Yeivin Y.
ANL-7320 (p 270) Argonne (October 1966).

5 Barrē J Y and Ravier J.
Fast Reactor Physics (IAEA Karlsruhe Conference 1968).

6 Rowlands J L and MacDougall J D.
The Physics of Fast Reactor Operation and Design.
(BNES London Conference 1969).

7 Usachev L N.
Atomnaya Energiya 15 472 (1963).

8 Gandini A, Salvatores M, Sena G and Dal Bono I.
ANL-7320 (p 304) Argonne (October 1966).

9 Haggblom H.
Correlational Analysis of Integral and Differential Data in Reactor Physics.
TPM-RF-69-16 Aktiebolaget Atomenergi Sweden (1969).

10 Mitani H and Kuroi K.
On the correlation between group cross-sections to be adjusted by use of integral data.
Journal of Nuclear Science and Technology 7 1 60 (January 1970).

11 Linnik Yu V.
Method of Least Squares.
Pergammon Press, Oxford (1961)

12 Rothenstein W.
Analysis of heavy and light water moderated thermal reactor lattices using ENDF 'B' data and the HAMMER code system.
BNL RP 1001.

Invited Paper

THEORETICAL AND EXPERIMENTAL ANALYSIS OF FAST ZERO-POWER ASSEMBLIES with special consideration of nuclear-data check

R. BÖHME, E.A. FISCHER
Institut für Angewandte Reaktorphysik,
B. HINKELMANN, E. KIEFHABER, H. KÜSTERS, H. WERLE,
Institut für Neutronenphysik und Reaktortechnik,
Kernforschungszentrum Karlsruhe
Federal Republic of Germany

Abstract

THEORETICAL AND EXPERIMENTAL ANALYSIS OF FAST ZERO-POWER ASSEMBLIES.

The prediction of integral nuclear parameters for fast reactors is not yet so satisfactory as for thermal reactors. To clarify the uncertainties in nuclear cross-sections and in calculational methods, a large effort was started long ago with the investigation of the physics of fast reactors in zero-power facilities. Thorough analysis of the experiments was to yield reliable information on missing or uncertain nuclear data and the accuracy of theoretical methods in order that confidence in the prediction of the nuclear properties of large power reactors could be achieved.

In this paper the authors discuss the correlation between the microscopic data and integral quantities of interest for the reactor physicists, from a general point of view, mainly in connection with experiments in fast zero-power assemblies.

The paper comprehends the activities in the field of nuclear data and fast-reactor analysis performed in the Karlsruhe nuclear research centre. The following points are discussed in detail: 1. The procedure followed by the nuclear-data evaluator to select best data from the given experimental microscopic cross-sections (a comparison of some specific cross-sections in various evaluated data files is given). 2. The procedure in calculating multi-group constants from these best data. 3. The iufluence of data uncertainties on integral nuclear parameters as criticality, reactivity coefficients, reaction-rate traverses and reacrion-rate ratios. 4. The procedure and accuracy of the experimental assessment in spectrum measurements, reaction rate measurements, fine-structure measurements and in the determination of reactivity coefficienrs. 5. The evaluation of critical experiments with respect to checking the microscopic nuclear data and the possibility of improving these data by integral experiments.

INTRODUCTION

In the days of fast breeders of the first generation (EBRII, FERMI-REACTOR, DOUNRAY FAST REACTOR) critical assemblies were mostly designed as mock-ups. In the past few years, they have taken on a different role. The large size of breeder reactors currently under design, and the lack of inventory of materials used to simulate the power reactor in a critical assembly have given rise to the construction of critical assemblies with the purpose of checking nuclear data and calculational methods. Extrapolation to the power reactor is then done by analysis.

At the 1965 Conference on Safety, Fuels and Core Design in Large Fast Power Reactors at Argonne [1], Okrent presented the results of an

international inter-comparison on theoretical predictions of integral neutronic properties of some specified fast systems. It became evident that fast reactors could not be calculated reliably. In 1966, another inter-comparison on ZPRIII-48 [2] showed that the analysis of fast critical assemblies was far from satisfactory. It was assumed that the discrepancies were both due to the uncertainties in the microscopic data, and to inadequate theoretical methods. In the last few years, it was possible to improve the theoretical methods considerably and at the 1969 BNES Conference on the Physics of Fast Reactors [3] in London, it was generally agreed that the remaining differences between theoretical and experimental results are mainly caused by incorrect nuclear data.

In this paper, a review is given of the theoretical and experimental methods used at Karlsruhe to analyse critical assemblies. Special consideration is given to the possibility of checking microscopic data by integral experiments.

The situation of microscopic data uncertainties is briefly illustrated in section 1. Principles and problems in evaluating these data for the use in reactor calculations are discussed. In section 2, the main integral nuclear data to be predicted in the design of a fast reactor are stated and the possibility of checking these predictions in zero-power facilities is outlined. In section 3 the theoretical methods used to calculate fast power reactors and to analyse fast zero-power assemblies are described. The experimental methods and the accuracy of the measured integral data are discussed in section 4. In section 5, it is analysed whether these experiments can be used to check nuclear data. The concluding section shows how the information derived from critical experiments can be used to support the evaluation of microscopic data and to improve the physics design of fast power reactors.

1. PRINCIPLES AND PROBLEMS IN MICROSCOPIC DATA EVALUATION

The steady improvement and refinement of reactor-theory programs in the last few years has led to a situation where the reliability of the theoretical predictions of physical properties of fast reactors depends to a very great extent on the detailed and reliable knowledge of the microscopic nuclear data involved. The dominating influence of the heavy nuclei on the physical behaviour of fast reactors has provoked high-accuracy requests for the nuclear data of these materials so that the experimental methods for neutron cross-section measurements had to be more and more refined. Because of the large amount of data produced, the evaluator's task of deriving complete sets of so-called "best" data by taking into account all available experimental information and by judging its reliability has become more laborious and complicated.

1.1. Consistent experimental results

In the ideal case, different measurements reach agreement after reduction to the same experimental conditions, at least within the range of their mutual uncertainties. These data sets can then simply be averaged by least-squares and other adjustment procedures so that recommended values can be worked out.

Problems can arise here because of gaps in the available experimental information either because the experimental facilities are limited or because not all data have been determined experimentally owing to the fact that they might not until now have been urgently requested. For a cross-section smoothly depending on energy the gaps can be bridged in a fairly reliable fashion by numerical or graphical inter- or extrapolation, using theoretical models and empirical or semi-empirical systematics.

In most cases nuclear theory can only be applied successfully for interpolation if, at least, some of the theoretical parameters are determined from experiment. The reliability of the nuclear models is restricted to certain energy ranges, reactions and nuclei. For example, outside the resolved resonance region the optical model allows the prediction of total cross-sections without differentiation for the various exit channels like fission, radiative capture, etc. The various reaction cross-sections for elastic and inelastic scattering, fission, radiative capture, etc. can be predicted here by using a statistical theory for the decay of the compound nucleus. The evaporation model can serve for the completion of the data available for the energy distribution of inelastically scattered neutrons in the continuum range whereas the discrete-level inelastic model has to be used in the range of resolved excitation levels of the target nucleus. For the prediction and interpolation of cross-sections in the resonance region single-level and multi-level formulae are available. The necessary statistical parameters for the unresolved region can be derived from available resolved resonance data or, concerning the strength functions, from optical-model calculations. The Fermi-gas model, for example, here predicts the spin and energy dependence of the level densities, the Hill-Wheeler formula the energy dependence of the fission widths.

Gaps in the resolved resonance range can, in principle, not be closed in a similar way because at the moment no theory able to predict the position and properties of resonances exists. This shows clearly the limited scope of the various nuclear models and illustrates how problematic the closing of gaps can become even in the case of consistent experimental results simply because no unified nuclear theory exists. A more extensive survey about the possibilities for interpolation by nuclear theory is given in Ref.[4].

1.2. Discrepant experimental results

Instead of agreement between different data sets, however, one more often encounters discrepancies between the results by an amount larger than the uncertainties of the individual measurements, in spite of the corrections already applied. These discrepancies and inconsistencies represent the main problem in almost every evaluation regardless of neutron energy, reaction type and nucleus concerned. In the simplest case, the differences are due to normalization to different standard values. In other cases, however, their sources cannot be detected so easily, as they are very closely connected with the experimental facility and methods used.

An example of discrepancy due to different measuring techniques is given by the experiments for the mean number of neutrons released in the spontaneous fission of ^{252}Cf. This value is the most important standard for $\bar{\nu}$-measurements for all fissile and fertile materials. Neutron detection with liquid scintillators yields higher values for $\bar{\nu}_{sp}$ (^{252}Cf) than the boron

pile and the manganese-sulphate-bath measurements. The differences are larger than the uncertainties quoted for the individual measurements. This discrepancy may partly be attributed to the loss of fast neutrons because of other nuclear reactions in the manganese-sulphate bath, but the situation is still rather unsatisfactory.

Another well-known example of strong, not yet resolved, systematic discrepancies between different measurement series is given by the capture-cross-section measurements for ^{238}U.. For purposes of illustration, different measurements at 30 keV are quoted in Table I, together with the deviations relative to the experiment of de Saussure (arbitrarily chosen).

TABLE I. VARIOUS ^{238}U-CAPTURE MEASUREMENTS AT 30 keV

Neutron energy (keV)	$\sigma_{n\gamma}$ (mb)	Authors References given in Ref. [60]	Comments	Deviation relative to de Saussure (%)
30.0 ± 8	470 ± 38	de Sanssure, Weston et al.	relative to $(\sigma_{nf} + \sigma_{n\gamma})$ (^{235}U)	taken as reference
30.0 ± 7	473 ± 74	Gibbons, Macklin, Miller, Neiler	normalization to the absorption cross-section of Indium	+0.6
30.0 ± 1.5	479 ± 14	Menlove, Põnitz	"grey" detector, absolute measurement of σ_γ (^{238}U) at 30 keV	+2
30.0	467 ± 18	Põnitz	grey detector; relative to $\sigma_f(^{235}U)$	-0.6
30.1	549 ± 55	Macklin, Gibbons, Pasma	Moxon-Rae detector; relative to σ_γ(Ta)	+17
30.5	480	Bilpuch, Weston, Newson	normalized to those of other experimenters	+2
30	350[a] (±50)	Bergquist	relative to capture in Ag, normalized to σ_γ (Ag) at 24 keV	-26
30	373[a] (±77)	Hanna, Rose	relative to the hydrogen-elastic-scattering cross-section	-21
30	458[a] (±70)	Linenberger, Miskel	relative to σ_f (^{235}U)	-3
30	420[a] (±30)	Moxon	relative to the absorption cross-section of ^{10}B	-11
30	526[a]	Tolstikov et al.	normalized to the ^{10}B cross-section at 24 keV	+12

[a] linearly interpolated between neighbouring experimental points

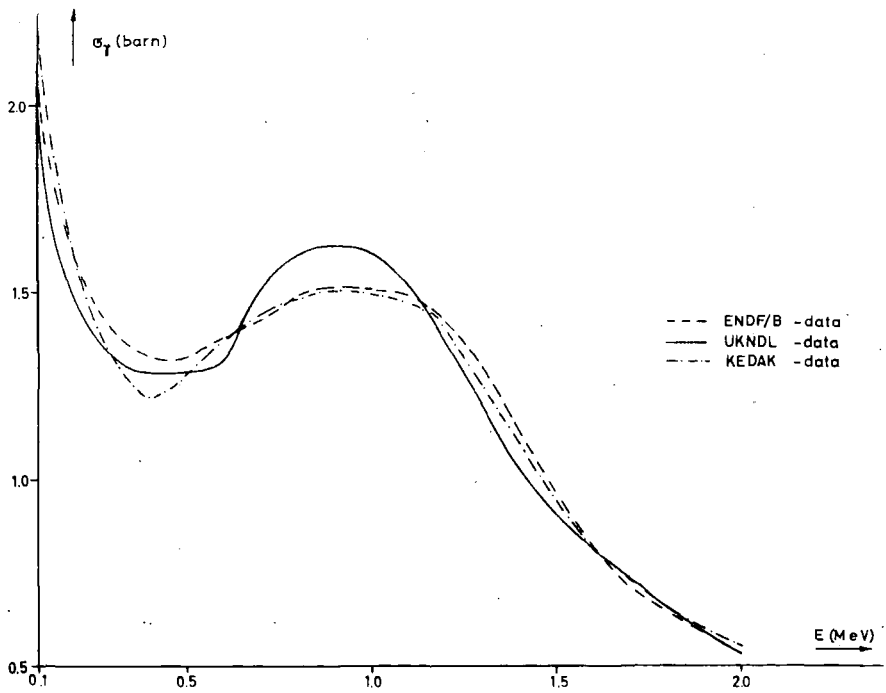

FIG. 1. ^{238}U capture cross-section.

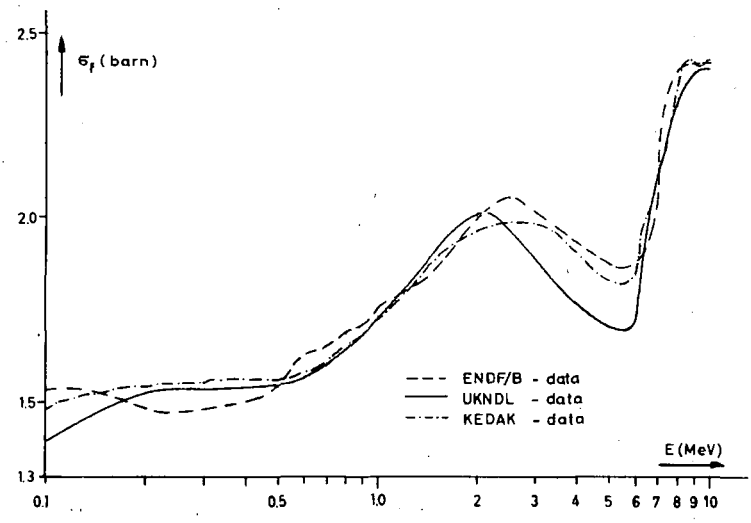

FIG. 2. ^{239}Pu fission cross-section.

Since some of these measurements have also been repeated with great care and have yielded the same results, it seems that the persistent deviations are, at least partly, due to the different experimental methods used. Each laboratory relies with greatest confidence on its own special detector although systematic errors might obviously be caused by it.

The consequence of such unresolved discrepancies is that the evaluated data will display uncertainties larger than the accuracies quoted for the individual experimental data in question. The evaluator is forced to make a decision on the reliability of the different discrepant experimental data sets in order to derive "best" values. Empirical and semi-empirical nuclear systematics are restricted in their reliability. Nuclear theory does not necessarily give an unambiguous answer because the individual series might all be well reproduced by nuclear theory if different sets of nuclear parameters or different models, some of which are quoted in the preceding section, are employed.

Thus, in the end, the evaluator's subjective judgement based on experience and understanding of physics plays an essential role in the evaluation procedure. Important aspects in this context are the reputation of the experimentalist and the laboratory where the measurements have been performed.

It is hence obvious that evaluations carried out by evaluators in different countries and scientific institutions may yield different results. To demonstrate this fact, we give a comparison of three evaluated data files in Fig. 1 for the capture cross-section of ^{238}U and in Fig. 2 for the fission cross-section of ^{239}Pu. We compared the American ENDF/B-file, the English UKAEA Nuclear Data Library and the German KEDAK-file in the versions available at CCDN, Saclay in April 1970.

1.3. Possible ways of reducing data discrepancies

The present situation with so many unresolved discrepancies in the important experimental nuclear-data information is rather unsatisfactory. Naturally, the continuous improvement of the experimental methods gradually reduces the discrepancies. But attention has to be paid to the fact that new precision measurements do not clarify the situation in any case. This is, for example, the case for the spontaneous-fission $\bar{\nu}$-measurements for ^{252}Cf, where recent measurements have not succeeded in resolving the discrepancies, but only in increasing the number of discrepant measurements. In some cases certainly more detailed considerations of the experimental conditions followed by a thorough re-evaluation could help. This procedure will become much easier in the near future since the compilation centres have started compiling physical and technical comments characterizing the measurement together with the experimental data sets. These comments will be structured according to the internationally agreed exchange format. The last discussion on this subject took place at the last Four-Centre-Meeting in November 1969. In a standardized form, information is given on the experimental facility, the experimental method, the sample properties, the detector, the standard used, the data analysis, the corrections applied, the error analysis, and other items. These compiled schematic descriptions of the experimental conditions of a measurement help the experimentalist to survey quickly what kind of information is required by the evaluator for a

comparison of his measurements with other measurements and for the judgement of it.

If large discrepancies arise the experimentalists themselves should meet to compare their experimental results and to re-consider the experimental conditions of their measurements in all details because they know best the difficulties in their measurements and the possible sources of errors in them. This procedure is considered highly efficient in detecting the deficiencies of various experiments and their analysis. Thus, improved techniques for measurement and analysis can be applied, a search for new independent experimental methods may be stimulated, the experimental equipment, or at least parts of it, can be exchanged and so all of these efforts should lead to more precise and consistent results. A close co-operation with the evaluators guarantees that the reactor physicists as users of these data can rely on successfully elaborated "best" data sets. An international organization such as the IAEA could have the important function of co-ordinating these activities.

2. THE INTEGRAL NUCLEAR DATA OF INTEREST IN FAST REACTORS

The neutronic properties to be predicted for the design of a fast reactor are:

(a) the fuel inventory,
(b) the power distribution,
(c) the conversion of fertile to fissile material during operation together with the build-up of fission products, and
(d) the behaviour of the system as a consequence of perturbations of the normal operating reactor.

The theoretical prediction is supported by information from critical experiments, but one must realize that the latter cannot deal directly with the transient behaviour, or with long-term effects. The check of methods and data by critical experiments is mainly devoted to the determination of critical mass, reaction-rate traverses and reaction-rate ratios, reactivity coefficients, reactivity worths of the materials or isotopes in question, and also the reactivity effect of higher Pu-isotopes and fission products.

If experimental investigation aims at clarifying nuclear-cross-section uncertainties, the theoretical methods used to analyse integral measurements as well as the experimental accuracy have to have high precision so that discrepancies between theoretical and experimental results can be attributed to cross-section uncertainties in a unique way.

3. THEORETICAL METHODS IN FAST-REACTOR CALCULATIONS

In the fast power reactors now under design the neutron mean free path over a wide energy range is larger than the core-lattice pitch. Therefore, each core zone can be treated as homogeneous for the calculation. In most cases, the diffusion approximation of Boltzmann's transport equation is sufficient to calculate the neutronic properties of the system. Higher-order transport approximations are normally used only to determine corresponding

corrections. Even control-rod calculations can be performed by diffusion theory with tolerable accuracy. The main effort in the calculation of fast reactors is therefore not so much made in obtaining the spatial distribution of neutrons, but rather the distribution in energy. With respect to the nuclear quantities of interest mentioned in chapter 2 energies from some MeV down to some hundred eV are equally important.

The analysis of experiments in fast critical or sub-critical assemblies definitely requires more sophisticated theoretical methods also for the spatial and angular distributions of neutrons, especially if it is desired to check the accuracy of nuclear data.

3.1. The multigroup procedure

Since no analytical solutions to the transport or diffusion equation exist for cases of interest, the neutron distribution has to be obtained numerically by discretization in all variables. With respect to energy, this means integrating the balance equation over a certain energy interval, the energy group. To preserve the reaction rates in one energy group, the cross-sections are averaged over the energy group with the true neutron flux density as a weighting function. This procedure implies two main problems:

(a) By definition, the group cross-section is not a constant because the weighting function depends on position and angle.
(b) A unique set of group cross-sections for reactor calculations does not exist because diffusion theory, S_N, P_N or collision-probability methods each require a different system of weighting functions.

To overcome the first difficulty, one usually assumes a separation of the neutron distribution in energy and the other variables, so that the group cross-sections become independent of space and angle. To account for the space variation of the neutron spectrum in homogeneous zones, these may be subdivided into several regions with different group constants. If the groups are broad, it is important to use the proper weighting spectrum, which is not easy to determine. In principle, it can be obtained from an iterative procedure.

In the resonance region of the cross-sections, the neutron spectrum varies strongly, across one resonance proportional to the inverse of the total macroscopic cross-section (narrow resonance (NR)-approximation). Therefore, group constants of one isotope depend on the material composition of a region. The resonance character of the cross-section also introduces the temperature as a variable in the group constants.

At Karlsruhe, we have adopted the scheme, developed at Obninsk [5], of splitting the effective group constant into

$$\sigma_{\mathrm{eff}}^{(i)} = \sigma_{\infty}^{i} \cdot f^{i} \text{ (composition, temperature)}$$

where σ_{∞}^{i} is the group constant for infinite dilution of the isotope in question. This splitting is especially advantageous in the unresolved-resonance range, because f^i is not too sensitive to uncertainties in the statistical resonance data and σ_{∞}^{i} can be calculated from measured values across the energy group.

The determination of the resonance self-shielding factors f^i is based on the single-level Breit-Wigner formula. Interference of potential and

resonance scattering and resonance overlap is taken into account. The interaction between resonances of different isotopes is neglected by definition. This is not a severe limitation in the energy range of interest in fast reactors.

Two different procedures are currently in use at Karlsruhe to account for the dependence of the resonance self-shielding on the composition of a reactor region:

(a) The total cross-sections of all isotopes except that whose resonance self-shielding is being calculated, are approximated by an appropriate value, called σ_0, within the group. Usually, one takes the total cross-sections for infinite dilution. We call this the σ_0-concept.

(b) Cross-sections for elastic moderation of neutrons by nuclei of structural and coolant materials are not approximated by the σ_0-concept, but are calculated exactly within the NR-approximation. The numerical procedure uses about 1000 energy points. In the case of anisotropic scattering in the CMS, experimental angular distributions are directly used. This procedure is called REMO (from elastic removal) [6]. It should be noted that reactor calculations are performed only in the broad group scheme.

This limitation is just being eliminated by 200 group fundamental-mode and space-dependent consistent P_1-calculations. Here, again the macroscopic elastic-removal constants are determined exactly, using as a basis about 1000 groups. A full documentation of the procedure used and the calculated results will be published shortly.

3.2. Number of energy groups

At Karlsruhe all design calculations of fast reactors are based on standardized 26-group sets [6], according to the scheme first introduced by Abagjan et al. [5]. The energetic fine structure due to resonances within a group is treated in NR-approximation so that the collision density is only weakly dependent on composition and energy. However, the group width is too broad for a standard collision-density weighting function to be used for all types of fast reactors, mainly because of a miscalculation of the neutron slowing-down. In consequence, we use different weighting spectra for most of the reactors calculated, especially if the REMO procedure is applied.

The desired goal is to perform reactor calculations with data sets which do not include any prescribed weighting function. Then both main problems stated in section 3.1 in establishing group constants are avoided. This is, for example, possible if the group width is so small that simple energetic averages of the cross-sections in the fine groups can be used. This condition leads to more than 10^5 groups, caused by the resonance structure of the heavy nuclei (e.g. ^{238}U). It is obvious that the application of reactor codes with such high energy resolution is restricted to very special investigations (GENEX [7], RABBLE [8]).

A condition, which can much more easily be fulfilled, is to request a constant collision density within a group. This leads to a group number of some hundred, which is mainly related to the resonance structure of medium-weight nuclei as coolant and structural material and, in case of a reactor

with plutonium oxide, also to the energy dependence of the oxygen cross-sections. This procedure requires the calculation of resonance self-shielding within the groups, especially for the heavy nuclei, for instance, according to the scheme described above, but not using the σ_0-concept for description of neutron down-scattering. To avoid immense tabulations on the composition-dependent resonance self-shielding factors for the heavy nuclei, an appropriate interpolation formula must be used. This group scheme can also deal satisfactorily with threshold-type cross-sections as σ_f (^{238}U).

These some hundred group calculations originated by Hummel and Rago [9] in fundamental-mode calculations can now be performed easily for one-dimensional problems on modern computers. The resulting spectra can then be used to condense the group constants regionwise in order to perform rough group calculations with multi-dimensional diffusion or transport codes.

Though the effect of a scattering resonance on the neutron spectrum in a homogeneous fast-reactor medium is restricted to energies around the resonance itself, the necessity of a proper treatment of these resonances stems from the fact that they are relatively broad and sometimes overlapping for structural materials (the main resonances cover a complete group in the 26-group scheme) and thus influence the absorption rates of neutrons by other nuclei in this energy range.

If one follows this calculational scheme, it is obvious that success in predicting integral nuclear parameters of fast reactors depends strongly on the accuracy of the various cross-sections, resonance data and also on the methods of generating group constants. From the physical nature of the effects to be studied in fast reactors, the following cross-sections are important:

(a) For neutron energies above some hundred keV:
fast fission of even-even nuclei (^{238}U, ^{240}Pu, ^{242}Pu), fission spectra, elastic- and inelastic-scattering data which influence the neutron spectrum and leakage (critical mass, shape of power distribution)

(b) For neutron energies above some 10 keV to some hundred keV:
fission and absorption of heavy nuclei, elastic-scattering resonance data (critical mass, breeding, coolant density and void effects)

(c) For neutron energies from some hundred eV to some 10 keV:
resonance parameters for fission and absorption of heavy nuclei, absorption in fission products (Doppler effect, critical mass, breeding, fission product poisoning)

Besides the above-mentioned unsatisfactory state of heavy-nuclei fission and absorption cross-sections, we want to emphasize that the gaps in the data for anisotropic elastic-scattering distribution should be closed.

3.3. Special theoretical methods of analysing experiments in zero-power facilities

In connection with the development of accurate experimental techniques at Karlsruhe it was recognized that adequate calculational methods had to be developed for an interpretation of the experiments. Special attention was paid to heterogeneity effects which are either due to the plate structure of the core or else arise in a sample experiment, such as material worth or Doppler experiment where one has to look at the heterogeneous configuration

of the sample in its environment. In all cases the collision-probability method was used, and resonance self-shielding was included [10-12]. Table II shows the influence of heterogeneity in

(a) a Na-void experiment [13], where the homogeneous results are lowered by about 20%;
(b) a Doppler experiment [14], where the resonance interaction between a hot sample and the cold environment is considerable at high energies;

TABLE II. EFFECT OF HETEROGENEITY IN DIFFERENT EXPERIMENTS

a) Na-Void Experiment (205 litres, SNEAK-6A), reactivity in cents

Experiment	2.32
Calculation, homogeneous	2.72
Calculation, heterogeneous	2.30

b) Doppler Experiment (25% enriched U in SNEAK-3A-2, depleted U in ZPR-6/4Z), relative units of reactivity change

Energy Range	Effect without interaction		Correction for hot sample cold-environment interaction	
	SNEAK	ZPR6	SNEAK	ZPR 6
Above 10 keV	- 16.5	- 25.5	- 3.5	-11.8
1 - 10 keV	- 42.4	- 46.1	- 2.6	- 3.2
Below 1 keV	- 28.1		+ 1.2	
Total	- 87.0	- 71.6	- 4.9	-15.0

c) Material-worth experiment SNEAK-5C

	Weight (g)	Position	Exper. ($\mu \$/g$)	Homogeneous calculated	Heterogeneous calculated
				Exp.	Exp.
^{238}U	60	1	-37.7	0.97	1.16
	60	2	-24.4	1.49	1.26
	5	1	-86	0.43	0.80
	5	2	-25	1.42	1.22
^{239}Pu	5	1	443	0.98	1.09
	5	2	390	1.13	1.19

Position 1 in the graphite region of the unit cell,
position 2 in the fuel region of the unit cell.

(c) material worth measurements [12], which are sensitive to the sample size and the environment. These experiments were done in SNEAK-5C, an assembly with $k_\infty = 1$ and a soft spectrum. Heterogeneity was very strong, which is reflected by the fact that the 5 g sample of ^{238}U was worth three times as much in the graphite as in the fuel. It is obvious that in such an assembly large corrections for heterogeneity are necessary.

3.4. Theoretical methods to be developed

From a theoretical point of view the following aspects are not yet included in our procedure outlined above. Across core-blanket or core-reflector interfaces the space dependence of heavy-isotope-resonance self-shielding has to be investigated more properly. Work is under way at Karlsruhe [14], to treat the plane-geometry case. The general case of space-dependent resonance shielding in multi-zoned reactor systems or cells involving transient neutron spectra is rather complicated and so far has only been treated approximately [10, 14, 15]. A re-investigation of the resonance parameters of fissile nuclei in terms of a multi-level formula and the corresponding determination of resonance self-shielding is important for soft-spectrum systems and high content of fissile material, both for criticality and for Doppler effect calculations. For fast reactors now under design the multi-level effect is not very important [11].

It was stated in section 3.1. that no unique set of group constants can be established for reactor calculations, with a generally acceptable number of groups. In any case, one has to make sure whether these group constants, which are originally prepared, for instance, for diffusion-theory calculations, can also be used in transport calculations or in the calculation of the adjoint flux. A thorough investigation of the effects on integral parameters, caused by this inconsistency (mainly neutron leakage is influenced) has not yet been made. Kiefhaber, for example, [16] showed that the use of flux-weighted group constants in adjoint calculations may have a non-negligible effect on the calculations of neutron life-time and material worths.

4. METHODS USED IN INTEGRAL EXPERIMENTS

At Karlsruhe two fast assemblies and a coupled fast-thermal assembly are available for checking fast-reactor calculations and the empirical determination of the behaviour of mocked-up fast reactors.

(a) The sub-critical fast assembly SUAK [17] is designed for pulsed neutron experiments on uranium- and plutonium-fuelled assemblies. The assembly is laid out for core volumes of up to 600 litres and multiplication constants $k_{eff} < 0.95$. It is pulsed either with a 200-keV Cockroft-Walton accelerator or a neutron flash tube. For time of flight (TOF) measurements flight channels of up to 100 m length are provided.

(b) The fast-thermal reactor STARK [18] consists of a 50-litre cylindrical zone with the composition of a uranium-fuelled fast reactor surrounded by a thermal driver zone. The fast zone of this reactor

is mainly used for checking experimental methods to be applied in SUAK and SNEAK and for supporting studies of fast-reactor lattices.

(c) In the fast critical facility SNEAK [19] experiments on clean physics cores and measurements on technical mock-ups of fast power reactors are performed. The maximum core size is limited by the fuel inventory, which is now 800 kg of ^{235}U-metal and 200 kg ^{239}Pu oxide fuel.

The fast cores of all three assemblies are built of fuel and diluent platelets of the dimensions 50.7 × 50.7 mm and thicknesses ranging from 1.6 to 6.3 mm. These platelets are contained in a stainless steel or aluminium matrix. Unit cells of less than 100 cm^3 volume can be constructed.

In the following sections the various experimental methods and their accuracies are discussed.

4.1. Determination of the critical mass

The most accurate but also most complex quantity determined in a critical experiment is the mass of fissile isotopes. The errors inherent in the critical mass m_{cr} are due to

(1) the content and the isotopic composition of fuel (usually of the order of 0.1 to 0.3% of m_{cr}). Especially, the Pu-content in oxide fuel is mostly not known exactly.
(2) corrections for partially inserted control rods and for detectors located in the core.

The critical mass can be given with a total uncertainty of less than 0.5% in m_{cr} or 0.3% in k_{eff}. For an evaluation detailed information on the reactor geometry has to be given in addition to m_{cr}.

Especially the irregular core boundaries and the internal heterogeneity of core zones may influence the critical mass substantially. For critical experiments carried out in the past this information is not always easily to obtain.

In SNEAK assemblies the shape correction is of the order of a few tenths of a percent.

Differences in the critical mass of different compositions may be obtained by progressive substitution experiments [20, 21]. These experiments yield information on the nuclear properties of reactor media which can be built in small zones in fast critical reactors of not too different compositions, especially of not too different diffusion constants. By this means only a small stock of about 200 kg Pu-fuel allows the investigation of core compositions as foreseen for large fast-breeder reactors. In SNEAK-3 experiments, the critical mass of a 500-litre plutonium-fuelled reactor was inferred with an accuracy of 2% ($\approx$ 0.3% $\Delta k/k$) from the substitution of a 230-litre Pu-zone in a uranium-fuelled reactor.

4.2. The measurement of reactivity changes

The uncertainties in reactivity measurements depend strongly on the magnitude of the reactivity change to be measured.

(a) Reactivity changes $\rho \gtrsim 2\$$ as measured for shut-down rods and in substitution experiments cannot be determined by reactivity compensation in SNEAK because of excess reactivity limitations. Therefore, such large reactivity changes are compensated by a change in critical mass.

(b) Reactivity changes in the range $2\$ > \rho \gtrsim 1\,¢$, as measured for sodium void effects in zones of the reactor, poisoning of a few elements etc., are determined with calibrated control rods. The control rods are calibrated by period measurements and/or the solution of the inverse kinetics equation after incremental movements of the rod. Calibration by inverse kinetics result in a systematic error up to about $\pm 3\%$ in control-rod worth [22], which is mostly due to the shift in statistical-weight distribution. An absolute limit in accuracy is given by the reproducibility of the geometrical arrangement and the temperature distribution after a change in loading. A single change in loading results in an uncertainty of about $\pm 0.2\,¢$. Careful elimination of error sources and repetitive measurements yielded small reactivity changes due to sodium loss with a precision of $\pm 0.05\,¢$.

(c) For measurements of reactivity changes $\rho \leq 1\,¢$ special techniques are developed which eliminate influences of temperature shift or loading changes. For material-worth measurements, a pile oscillator is used in connection with an automatic sample changer. The reactivity measurements are performed by recording either the flux signal while oscillating or the position of a auto-rod. This is a control rod, driven by a servo-mechanism to keep the flux level constant. The accuracy of these measurements is limited by statistics and the reproducibility in sample positioning. Both effects amount to an error of about 10^{-7} $\Delta k/k$.

An uncertainty in β_{eff} does not affect the accuracy of the techniques described above, but has to be taken into account, if reactivity measurements are compared with calculations or calculated corrections are applied to the critical mass.

Such a correction for the irregular core boundary is usually calculated by two-dimensional codes. More difficult to obtain is a calculated correction for the heterogeneity of the core. Bunching experiments, i.e. increasing the heterogeneity of a medium, give an experimental check of these calculations and allow an extrapolation to homogeneous-medium properties [22].

4.3. Reaction-rate measurements

Measured reaction rates yield valuable information on the neutron balance in critical reactors. They allow the sources of discrepancies in criticality calculations to be identified even if – owing to compensation – no effect on k_{eff} is noticeable. Of main importance are, of course, the fission and capture rates in the fuel. Since measurements in zero-power facilities do not yield the capture rates of ^{235}U or ^{239}Pu they are deduced from the neutron or reactivity balance equation [23, 24].

At the London Conference of BNES, 1969, detailed information on the techniques of measuring reaction rates were presented. It is now widely

accepted that accurate measurements have to consider the perturbation introduced by any detector very accurately. For capture- and fission-rate measurements minimum perturbation is achieved if the detectors themselves are part of the fuel. In practice, this is accomplished by activating foils made of fuel material inside the lattice [25, 26]. Fission chambers are mainly used in measurements of reaction-rate distributions, either to deduce material bucklings of large uniform zones or power distributions in complicated geometrical arrangements.

The precision of measurements of the fission rates in ^{235}U and ^{239}Pu and the capture rate in ^{238}U is quite high. But error margins quoted in literature do not always distinguish clearly between statistical and estimated systematic errors. Since there is still some doubt about systematic errors most laboratories are developing several independent techniques of measuring these rates. An extensive study aiming at intercalibrating the equipment for reaction-rate measurements used at Karlsruhe and Cadarache was started recently.

The techniques currently in use are summarized below.

4.3.1. Fission rate measurements with chambers

The evaluation has to take into account perturbations introduced by the chamber walls, the connections to the electronic equipment and any guide channel for the chamber itself. Then, the precision of the measurements is limited by the counting time available and the determination of the effective fissile mass of the chambers. Reaction-rate measurements are thus restricted to an accuracy of $\pm$ 1%. Bucklings can be obtained from traverse measurements with less than 0.5% standard deviation [27].

4.3.2. ^{235}U and ^{239}Pu fission rate measurements with foils

These measurements introduce very small perturbations only. They may be performed in different manners:

(a) Radiochemical analysis [28] of the samples.
Absolute β-counting of ^{99}Mo yields the fission rates of ^{235}U and ^{239}Pu with an error of about 1.5% and fission ratios with an accuracy of about 3% [23, 29].

(b) Comparison of the γ-activity due to fission products with the activity of foils irradiated in a thermal neutron spectrum [26, 29]. or inside a calibrated fission chamber. The accuracy quoted in these measurements is about 2% in fission ratios.

4.3.3. Fission rate measurements with solid-state track recorders [26, 30]

This method is still in the stage of development. The tracks produced by fission fragments emerging from thin layers of fissile isotopes are recorded in a suitable catcher foil. After etching, these tracks can be counted visually. Accuracies of 3% in the fission ratios were obtained. The main difficulty seems to arise in the construction of a reliable and fast automatic counting device.

TABLE III. ESTIMATED ACCURACIES OF INTEGRAL EXPERIMENTS

A) Reactivity measurements at SNEAK

Type of measurement	$1¢ \lesssim \rho \lesssim 2\$$	$\rho \lesssim 1¢$
Relative	±3%	-
Absolute	>±0.2¢	$\pm 2 \cdot 10^{-3}$ ¢

B) Recent reaction-rate-ratio measurements by foils

Reaction-rate ratio	Radiochemical analysis	Calibration in thermal flux	Calibration by fission chambers	Capture with Seufert-Stegemann method [31]
σ_f^5/σ_f^9		2.2% ANL [29]	2.2% ANL [29] 2.1% UKAEA [26]	
σ_f^8/σ_f^9	3.1% ANL [29]		2.9% ANL [29]	
σ_f^8/σ_f^5	3.3% ANL [29]		2.2% UKAEA [26] 3.1% ANL [29]	
σ_c^8/σ_f^9	3.6% ANL [29]	1.7% UKAEA [26] 1.4% ANL [29]		1.3% UKAEA [26] 1.6% UKAEA [32]
σ_c^8/σ_f^5	3.0% ANL [23]	1.5% ANL [29]		2.9% Khe [25]

4.3.4. ^{238}U capture rate measurements

Radiochemical analysis [28] and absolute β-counting of ^{239}Np yields capture rates with an accuracy of about 1.5% [23]. Widely used is the comparison of γ-rays and or X-rays emitted in the ^{239}U or the ^{239}Np decay after simultaneous irradiation of foils in a thermal- and the fast-neutron spectrum. The accuracy achieved is about 2% in the ratio of capture in ^{238}U to fission in either ^{235}U or ^{239}Pu [26, 29]. At Karlsruhe, coincidences of 106-keV γ-rays and 104-keV X-rays of ^{239}Np are counted in a fast electronic circuit. The sensitivity of the equipment is determined by means of a calibrated ^{234}Am-source, which also decays to ^{239}Pu via ^{239}Np [31]. An improved version of this technique [32] yields the capture rate of ^{238}U about 1% and the ratio of ^{238}U capture to ^{239}Pu fission with less than 2% accuracy.

In Table III the estimated accuracies of reactivity measurements and measured reaction-rate ratios are listed.

4.4. Spectrum measurements

The different techniques used to measure neutron spectra are discussed. The accuracy of these methods is stated in order to define the role of neutron spectra in checking nuclear data.

4.4.1. Proton-recoil-counters

The lower limit of the measurable energy range lies around 1 keV and is determined by the fact that 1-keV protons create only about 30 electron-ion pairs. In fact, it seems that already below about 5 keV results with reasonable accuracy cannot be obtained because of lacking knowledge on the detailed energy dependence of the energy loss per ion pair for hydrogen.

On the high-energy side, there is, in principle, no limit and it has been shown [33] that with large counters and moderate pressure (below 5 atm) measurements up to 10 MeV are possible. For in-core measurements, on the other hand, the dimensions of the counters are limited to some ten centimeters and, therefore, high pressures (above 10 atm) would be necessary to stop the high-energy protons. Because of the difficulties caused by these high pressures, in-core measurements are restricted to the energy range below about 2 MeV as yet.

The experimental errors in the proportional-counter measurements are currently assessed as follows [33, 34]:

Energy	5-30 keV	30-100 keV	100 keV-1 MeV	1-2 MeV	1-4 MeV	4-10 MeV
Statistics	2%	2%	2%	2%	2%	2%
Total systematic errors	20%	13%	10%	20%	10%	20%
Comments				(Small counters, In-core)	(large counters)	

A large part of the overall experimental error is due to uncertainties in the correction of the distortions in the measured proton-recoil distribution, which arise from the truncation of proton-recoil tracks by the counter walls, or by extension of tracks into the end region, where little or no multiplication occurs.

Two difficulties encountered with in-core proton-recoil measurements should be mentioned: First, owing to the relatively high efficiency, measurements in Pu-cores have been restricted up to now to the sub-critical region. The second problem, which is also common to some other reactor-physics experiments and complicates the comparison of measured and calculated data, is the void of some hundred cm^3 that is necessary to install the detectors.

4.4.2. ^6Li- and ^3He-semiconductor sandwich spectrometer

Both spectrometers are used above some hundred keV. Owing to the better signal-to-noise ratio, the ^3He-spectrometer seems to be more

favourable. A serious handicap for both spectrometers are the uncertainties of about 8% in the cross-sections, which contribute greatly to the total experimental error. For a typical measurement with a ^{6}Li-spectrometer, figures for the total experimental error are given below [33]:

Energy	0.4–2.5 MeV	2.5–4 MeV	4–10 MeV
Statistics	3%	10%	15%
Total systematic error	7%	10%	12%

4.4.3. The time-of-flight method

Measurements with the time-of-flight method are restricted to subcritical assemblies and comparison with the results from other methods are difficult if the beam spectrum is different from the angle-averaged spectrum.

The neutron detector used at Karlsruhe is a ^{6}Li-glas scintillator Ne 905. It was calibrated in the energy range 100 eV to 100 keV against a ^{10}B-NaJ-slab detector, the efficiency of which has been calculated by a Monte-Carlo code [35]. In the energy range between 60 keV and 320 keV, the ^{6}Li-detector was calibrated with monoenergetic neutrons from a Van-de-Graaf accelerator relative to a long counter. In the remaining energy range, the efficiency relies on calculations with the recommended ^{6}Li(n,α) cross-section.

The experimental error is mainly due to uncertainties in the detector efficiency. In the energy range where it relies on the Monte-Carlo calculation the error in the detector efficiency is assumed to be 10% and from 100 keV to 350 keV it may amount to 15%. Typical figures (12 hour run with flash tube at 100 pps and an energy resolution of 10%) for the errors in the measured spectra, are [33]:

Energy	200 keV	40 keV	10 keV	1 keV	0.1 keV
Statistics	< 1%	1%	3%	10%	50%
Total systematic error (Efficiency, zero time)	25%	15%	13%	10%	10%

4.4.4. Resonance foil activation in sandwich geometry

Up to twenty isotopes are used to determine the low-energy end of the neutron-spectrum by the resonance-foil-activation technique [26]. The energies of the main resonances range from 1 eV to 10 keV. The calibration factors, which depend on the γ-counter efficiency, are difficult to calculate and were determined experimentally in a $1/E$-neutron spectrum and by comparison with time-of-flight results at various SUAK assemblies. For the evaluation effective resonance integrals are calculated using the TRIX-1 program and most recent microscopic data.

The total experimental error depends strongly on the neutron spectrum. It amounts to 10–20% in the soft spectra of steam-cooled assemblies and to

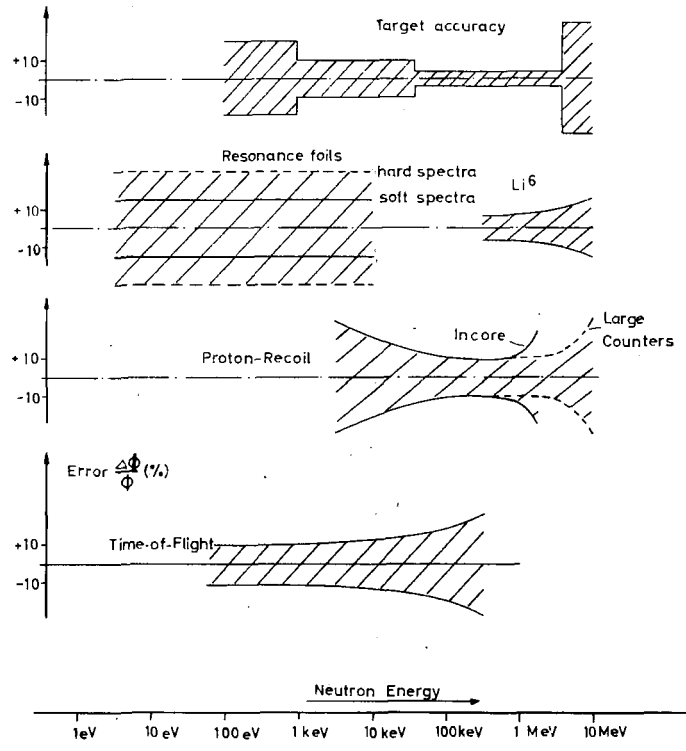

FIG.3. Tentative target accuracy and systematic errors for broad group neutron spectra.

20-40% in the harder spectra of sodium-cooled reactors and is composed mainly of the following contributions:

(a) Correction for activities not related to the main resonance:
Soft spectrum 10%, hard spectrum 20%.
(b) Resonance parameters and calculation of effective resonance integrals:
Soft spectrum 2%, hard spectrum 3%.
(c) Counting statistics:
Soft spectrum 4%, hard spectrum 8%.
(d) Other contributions: 2%.

4.4.5. Accuracy of spectrum measurements

Although an attempt has been made to use spectrum measurements for adjustment of neutron-cross-section data [37], in our opinion, this will be useful only after considerable improvement of the measurements and a more reliable estimation of errors is possible, as compared to the figures quoted in this paper.

If one starts, according to Ref.[34], with the required standard deviation for fast-reactor prediction of 0.01 in k, and 0.03 in breeding

gain, examination of a range of systems leads (as a rough guide) to the target accuracy for this amplitude of a broad group spectrum as indicated in the upper part of Fig. 3. Comparing this target accuracy with the quoted experimental errors - where the statistical errors, except for the resonance foils, are omitted because the uncertainties quoted in Fig. 3 are related to a broad group spectrum - one concludes that, at least in the energy range of 10 keV to 4 MeV, the experimental accuracy has to be improved considerably before spectrum measurements will be useful to improve the prediction for fast reactors.

TABLE IV. SOME IMPORTANT CLEAN CRITICAL EXPERIMENTS

Property	Bench-mark series ZPR-III/48, 49, 50, 53.	k_∞-series ZEBRA, 8A-8C, ZPR-III/55.	SNEAK-3 series	MASURCA 2A, 2B
Core-Geometry	cylindrical one-zone core, reflector	k_∞-zone, with degraded spectrum, driver and buffer	cylindrical one-zone core, reflector (3A-1, 3A-2) substitution of inner Pu-zone (3B-2)	cylindrical one-zone core reflector (2B) substitution of inner Pu-zone (2A)
Fuel	$Pu/^{238}U$	$Pu/^{238}U$	enriched U(3A) $Pu/^{238}U$ (3B-2)	enriched U(2B) $Pu/^{238}U$ (2A)
Cell-Geometry	complicated plate cell (three drawers)	relatively simple, but large cell	simple in the 3A-series (U) complicated in 3B-2 (inner Pu-zone)	simple rod cell (4 rods)
Important Measurements	k_{eff}, fission ratio with chambers (not with foils), reactivity worth with samples of various sizes	k_∞, ratios of reaction rates with foils across the fuel plates, spectrum (TOF, proton recoil)	k_{eff}, ratios of reaction rates (only in 3A-2 with foils), reactivity worths, spectrum (proton recoil, ^6Li, sandwich foils), Pu-α by Doppler experiment)	B^2, ratios of reaction rates (with foils across fuel rods)
Special Feature	composition similar to a mixed-carbide-fuelled, Na-cooled fast breeder; various modifications	degraded spectrum to emphasize the region where α_{Pu} was uncertain	composition similar to a steam-cooled UO_2 (or mixed oxide) fuelled fast reactor	
References	[29]	[26, 29]	[22, 38]	[42]

5. CHECK OF NUCLEAR DATA BY INTEGRAL EXPERIMENTS IN CRITICAL ASSEMBLIES

A check of nuclear data in critical assemblies poses strict requirements on both experimental and calculational techniques because a valid check of cross-sections by integral experiments is possible only under the following conditions:

(a) the experiments must be carried out with sufficient precision;
(b) a meaningful interpretation must be possible; this means that the measured effect can be calculated by well-established techniques for which errors are small.
(c) the result must be sensitive to the cross-section data of interest.

From these requirements, the following definition of a "clean" critical experiment suitable for data check can be given: it is a set of good precision measurements on a critical assembly in simple geometry such that errors due to calculational methods are small.

The characteristics of some important clean critical experiments are given in Table IV. Of course, none of them is ideally clean, but they all are either reflected single-zone cores, or have a large enough uniform test zone. An improvement would be desirable to reduce the heterogeneity effects: these are quite large, especially in the bench-mark series, and it would be useful to have, at least, a few experiments in a homogeneous zone.

The important techniques used in the experiments are:

(1) criticality measurements (critical mass, substitution),
(2) reaction rates (ratios of reaction rates at the centre, fission rate traverses to obtain B^2),
(3) reactivity worth measurements of absorbing materials,
(4) spectrum measurements.

The first three techniques give good experimental precision, typically 2% for reaction rates, 1% in the critical mass, and 10^{-7} $\Delta k/k$ for reactivity measurement. The accuracy of spectra measured is too low to be directly used for data check.

In the following the usefulness of these experiments for data check will be discussed under the aspects (b) and (c) above.

5.1. Criticality and ratios of reaction rates

The quantity k_{eff} of a critical configuration, though easy enough to measure, is rather difficult to interpret, mainly because of the many corrections. First, there are the corrections for irregular boundary, and for transport effects, which are fairly small in large cores, but may be sizeable in small cores. Obviously, they may be eliminated by experiment if either a $k_\infty = 1$ experiment is performed, or B^2 is obtained from measured fission rate traverses.

The main correction, however, is for heterogeneity. It is quite large for assemblies with metal fuel, and it is uncertain, especially for large and complicated plate cells, like in ZPR-III/48. In fact, the Δk due to heterogeneity was calculated to be 0.0182 by Broomfield and Palmer [43],

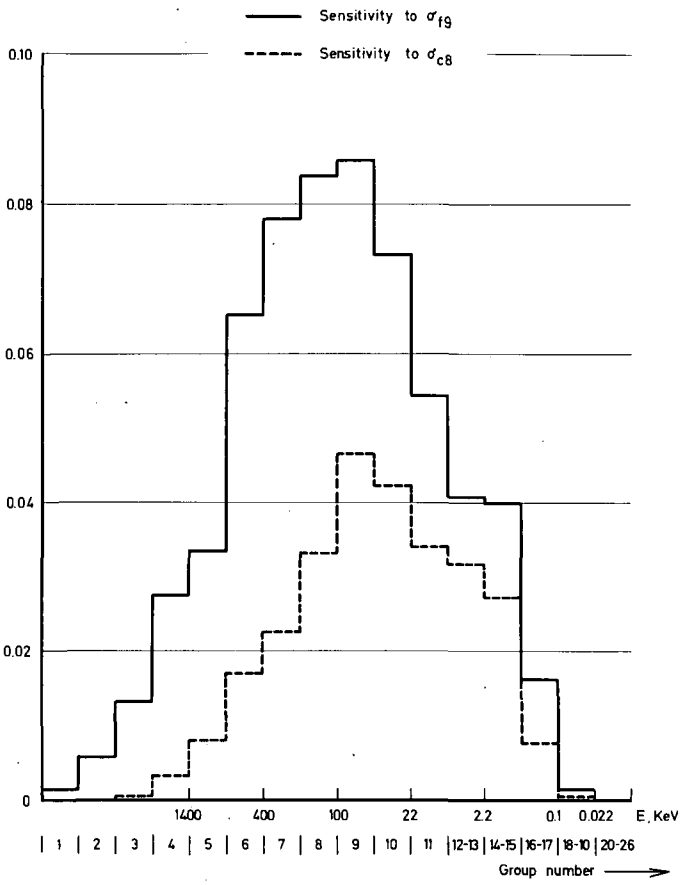

FIG. 4. Sensitivities $\frac{\sigma}{k}\frac{\partial k}{\partial \sigma}$ for a 5000-litre oxide breeder (after Zaritsky and Troyanov)

TABLE V. SENSITIVITIES OF SPECTRUM-AVERAGED CROSS-SECTIONS TO CHANGE OF -10% IN CROSS-SECTIONS (SNEAK 3A-SERIES)

Energy Groups (ABN)	σ_c^8			σ_f^9		
	3A-0	3A-1	3A-2	3A-0	3A-1	3A-2
1- 5	-0.006	-0.006	-0.006	-0.019	-0.019	-0.018
6- 8	-0.030	-0.024	-0.020	-0.046	-0.039	-0.031
9-11	-0.043	-0.037	-0.031	-0.030	-0.024	-0.019
12-16	-0.009	-0.020	-0.027	-0.027	-0.005	-0.021
Total	-0.088	-0.087	-0.084	-0.100	-0.097	-0.089

0.0126 by Fillmore et al. [38], whereas the Karlsruhe ZERA Code [10] gives 0.0151. The values scatter by more than 0.5% in Δk, and, therefore, the calculation of the heterogeneity effect is the dominating uncertainty in k_{eff}-calculations for a large cell. The bunching experiments at Argonne [44] gave only agreement in order of magnitude. Though it was found that the effect is much smaller and, therefore, probably less uncertain with oxide fuel, it is certainly worth while to build, for some typical cases, quasi-homogeneous assemblies where these effects are not present. Such experiments were carried out in England in an epithermal spectrum [49], and are being planned at Ispra in fast spectra.

The ratio of reaction rates can be measured with chambers or with foils. However, foil measurements can generally be well interpreted, and, therefore, qualify for good precision data check whereas chamber measurement should be used with caution. Foil measurements were carried out in the $k_\infty = 1$ assemblies on ZPR-III, and on ZEBRA, in SNEAK-3A-2, and in MASCURA.

TABLE VI. CROSS-SECTION VARIATION USED FOR THE CALCULATIONS

Group	Energy Range	Variation of σ_f (^{235}U) (%)	Variation of σ_γ (^{238}U) (%)
1	6.5 - 100.5 MeV	-10[a]	-10
2	4.0 - 6.5 "	-10	-10
3	2.5 - 4.0 "	-10	-10
4	1.4 - 2.5 "	-10	-10
5	0.8 - 1.4 "	-10	-10
6	0.4 - 0.8 "	+ 7	-10
7	0.2 - 0.4 "	+ 7	-20
8	100 - 200 keV	+ 7	-20
9	46.5 - 100 "	+ 7	-20
10	21.5 - 46.5 "	+ 7	-20
11	10.0 - 21.5 "	+ 7	-20
12	4.65 - 10.0 "	+ 7	-20
13	2.15 - 4.65 "	+ 7	-20
14	1.0 - 2.15 "	+ 7	-20
15	0.456 - 1.0 "	+ 7	-15
16	215 - 456 eV	+ 7	-15
17	100 - 215 "	+ 7	-15
18	46.5 - 100 "	+ 7	-15

[a] Since in group 1-5 σ_f (^{235}U) has as upper limit the KFK-SNEAK data the calculations are performed with the lower limit.

TABLE VII. INFLUENCE OF DATA UNCERTAINTIES ON INTEGRAL NUCLEAR PARAMETERS IN SNEAK-3A-2

Reactor parameter	KFK 793/KFK 776		Fundamental Mode Calculations[a]											
			$B^2 = 24.0 \times 10^{-4}$	$B^2 = 25.49 \times 10^{-4}$ cm^{-2}										
	Experiment	KFK SNEAK SET (twodim.)	KFK SNEAK SET	KFK SNEAK SET	$\sigma_\gamma(^{238}U)$ Low Gr.1-5	$\sigma_\gamma(^{238}U)$ Low Gr.6-9	$\sigma_\gamma(^{238}U)$ Low Gr.10-14	$\sigma_\gamma(^{238}U)$ Low Gr.15-18	$\sigma_f(^{235}U)$ Low Gr. 1-5	$\sigma_f(^{235}U)$ High Gr.6-9	$\sigma_f(^{235}U)$ High Gr.10-12	$\sigma_f(^{235}U)$ High Gr.13-15	$\sigma_f(^{235}U)$ High Gr.16-18	σ_γ (FE) Low Gr. 9-14
k_{eff}	1.000	0.9886	1.0047	0.9886	0.9897	0.9995	1.0101	0.9926	0.9811	1.0017	0.9961	0.9944	0.9916	0.9934
$\Delta k_L \times 10^2$	-7.0	-5.91	-6.32	-6.55	-6.54	-6.13	-7.04	-6.91	-6.63	-5.85	-6.42	-7.00	-6.83	-6.17
$\Delta k_{\rho/2} \times 10^2$	-3.8	-3.17	-3.30	-3.43	-3.43	-3.22	-3.54	-3.64	-3.48	-3.10	-3.35	-3.63	-3.62	-3.42
$\Delta k_{2\rho} \times 10^2$	+4.8	+3.74	+3.89	+4.09	+4.08	+3.86	+3.97	+4.34	+4.05	+3.76	+3.96	+4.21	+4.34	+4.04
R.S.D.C.$\times 10^2$	+5.8	+4.70	+4.54	+4.76	+4.75	+4.46	+4.76	+5.01	+4.83	+4.31	+4.61	+4.98	+5.06	+4.72
$-\Delta k(\Delta T) \times 10^2$	-	-	1.04	1.01	1.01	1.02	0.96	0.961	1.01	1.00	1.00	1.01	1.02	1.02
$25\sigma_\gamma / 25\sigma_f$	-	-	0.321	0.320	0.320	0.321	0.324	0.321	0.324	0.312	0.315	0.315	0.317	0.321
$28\sigma_\gamma / 25\sigma_f$	0.130	0.137	0.139	0.138	0.137	0.131	0.124	0.136	0.140	0.135	0.136	0.137	0.138	0.136
$49\sigma_\gamma / 25\sigma_f$	-	-	0.303	0.301	0.302	0.303	0.307	0.304	0.305	0.294	0.296	0.296	0.297	0.303
$28\sigma_f / 25\sigma_f$	0.0338	0.0297	0.0288	0.0291	0.0291	0.0288	0.0284	0.0290	0.0295	0.0287	0.0289	0.0289	0.0290	0.0290
$49\sigma_f / 25\sigma_f$	-	-	0.965	0.966	0.965	0.966	0.963	0.967	0.978	0.944	0.953	0.954	0.959	0.966

[a] With heterogeneity corrections from KFK 766.
$\delta k_{eff} = +0.46 \times 10^{-2}$; $\delta \Delta k_L = -0.3 \times 10^{-2}$; $\delta \Delta k_{\rho/2} = -0.14 \times 10^{-2}$; $\Delta k_{2\rho} = +0.32 \times 10^{-2}$

The multiplication factor k_{eff} is sensitive to $\nu\sigma_f - \sigma_a$, and errors in the different cross-sections may compensate in part. Typical sensitivities for a 5000-litre oxide breeder, as taken from Zaritsky and Troyanov [62] are given in Fig. 4. On the other hand, measurements of the ratios σ_f^5/σ_f^9 and σ_c^8/σ_f^5 are sensitive mainly to the cross-sections in the ratio, and such measurements help to resolve compensating errors in k_{eff}. This is clear from Table V, which shows some typical sensitivities of spectrum-averaged cross-sections in the SNEAK-3A-series, normalized to a change of -10% in the cross-sections. However, the table also shows that the sensitivities are not strongly spectrum-dependent, and a number of measurements in strongly different spectra would be required to allow conclusions in the 4-groups frame used in the table.

Broeders [61] has determined the influence of uncertainties in σ_f (^{235}U) and σ_γ (^{238}U) for integral parameters in SNEAK-3A-2, a uranium-fuelled assembly with soft neutron spectrum to simulate steam-cooled systems. The changes in the cross-sections are listed in Table VI, the basic group-constant set is the KFK-SNEAK set [6]. The results of fundamental-mode calculations, corrected for heterogeneity, are quoted in Table VII. It is: $\Delta k_L = k(N_H = 0) - k(N_H)$, where N_H is the normal hydrogen concentration in SNEAK-3A-2; $\Delta k_{\rho/2} = k(N_{H/2}) - k(N_H)$; $\Delta k_{2\rho} = k(2N_H) - k(N_H)$; RSDC = $(dk/k)/(d\rho/\rho)$.

It is realized from Table VII that the assumed uncertainties of about 10% in σ_f (^{235}U) and up to 20% in σ_γ (^{238}U) have rather large effects on most of the integral data quoted. From this it follows that the differential nuclear data have to have a much higher precision. It would, indeed, be a drastic and highly appreciated improvement if the data of independent differential measurements are consistent within a 5% margin though even a higher accuracy has been requested in literature.

5.2. Central-material-worth measurements

The interpretation of material-worth measurements is problematic. It should be mentioned first that the worth of materials with a strong slowing-down cross-section depends very much on the details of the adjoint spectrum so that they cannot be used presently for data check. Therefore, the following discussion will be restricted to absorbing or fissile materials.

The interpretation is complicated because of two problems:

(a) Uncertainties in the kinetic parameters, especially in β_{eff} for Pu-^{238}U-fuelled assemblies.
(b) Dependence of the reactivity worth on the sample size and on the heterogeneity of the environment.

The importance of the first problem in Pu-fuelled assemblies will be illustrated by the following results obtained in the U-fuelled core 3A-2 and in the partially Pu-fuelled core 3B-2 in SNEAK. The Pu-zone was substituted into 3A-2, and the difference in buckling was determined, and found to be small. The reactivity worth of 1 cm^3 core material in the centre is given by

$$\rho_c = \frac{(\phi^+ DB^2 \phi)}{F\beta_{eff}}$$

where F is the usual normalization integral. The ratio of calculated-over-experimental reactivity ρ_c was found to be

0.94 for SNEAK-3A-2
1.07 for SNEAK-3B-2

Although these results are only preliminary, the difference of 13% in going from the U-fuelled to the partially Pu-fuelled assembly seems to indicate an inconsistency between the kinetics parameters used for Pu-assemblies and for U-assemblies.

The results are in line with the observation published, for example, by Little and Hardie [46], that materials worths in Pu-fuelled assemblies are consistently overpredicted by 20-25%. The conclusion is that, so far, one can only use ratios of reactivity worths.

The second effect, namely the dependence of reactivity worth on the sample size and the environment, has been studied recently at Karlsruhe [12], and these effects are now understood to be heterogeneity effects. Thus, although material-worth measurements require a careful analysis they will probably give useful information on data of fuel and structural materials, which complements the information from reaction-rate measurements.

In several cases, material-worth measurements were used as integral checks in cases where large uncertainties in the cross-sections existed. For example, Oosterkamp has carried out experiments in SNEAK to check the data of ^{240}Pu. Reactivity measurements were made with two PuO_2UO_2 compositions which contained the same amount of ^{239}Pu, but different amounts of ^{240}Pu. The measured difference in reactivity in going from 8% to 22% in ^{240}Pu is shown in the table, and compared with calculations using the ABN-data [5], for σ_f and σ_c, and also data evaluated by Pitterle [47], which are based on recent differential measurements.

Difference in reactivity for two fuel compositions, in cents

	SNEAK-3B-2 (soft spectrum)	SNEAK-4B (hard spectrum)
Experiment	16.6	22.9
ABN-Set	11.3	13.3
Pitterle	20.0	21.8

The results in the hard spectrum clearly favour the Pitterle data, whereas the results in the soft spectrum show only a slight bias. It should be noted that σ_c values by Yiftah which are slightly higher than those by Pitterle would give better agreement in the soft spectrum.

An other example is taken from a paper by Barré et al. [40]. Worth measurements of nickel in the French reactor ERMINE, in addition to reflector worth measurements, give a check on the capture cross-section. The results are in good agreement with recent capture data by Spitz.

Differential-cross-section data on fission products were compiled by different authors, but are still highly uncertain [48]. On the other hand, data on the reactivity effect of fission products can be obtained by material worth measurements. The critical facility STEK in the Dutch research centre Petten [49] has been designed to measure highly radioactive samples

by the oscillator technique. Directly applicable results will be available soon.

5.3. Special experiments to check nuclear data

Measurements of the Doppler effect are sensitive to the low-energy spectrum and adjoint spectrum, which in turn depend on many cross-section data. For ^{238}U, in spectra of Na-reactors, discrepancies between Karlsruhe calculation and experiment are about 10% though somewhat better agreement is obtained in assemblies containing hydrogen.

Though the calculational methods are well developed now, such discrepancies are difficult to trace because too many cross-section data are involved. However, an interesting check on data was possible by means of the Doppler effect in ^{239}Pu [11]. The Doppler effect occurs mainly between 0.1 and 5 keV, and this is the energy range where the large discrepancy between the KAPL "low-α" data and the "high-α" data by Schomberg and Gwin existed. Experiments were carried out in SNEAK-3B-2 in the normal core, and in a boron environment, which was designed to suppress the absorption effect, but to retain the fission effect. The analysis of both experiments shows clearly that the calculation with "high-α" values is compatible with the experimental results within about 25%, which may be expected in a Pu Doppler experiment, whereas the calculation with "low-α" values is not. Table VIII shows the breakdown of the calculated values.

One could, in principle, try to use reaction-rate traverses for data check. There are disagreements in the SNEAK measurements in the vicinity of interfaces, and in the blankets, and there is evidence that a large portion of the disagreement is due to errors in cross-section data. However, the measurements depend on the cross-sections in a very complicated way, which certainly also involves the spectrum, and, therefore, they are not well suited to trace errors.

TABLE VIII. BREAK-DOWN OF THE CALCULATED REACTIVITY EFFECT IN A DOPPLER EXPERIMENT (SAMPLE: 450 g PuO_2, TEMPERATURE CHANGE 400°C) 10^{-6} $\Delta k/k$ FOR DIFFERENT ALPHA-VALUES FOR ^{239}Pu

	Normal Core		Boron Environment	
	Low Alpha	High Alpha	Low Alpha	High Alpha
Fission	+21.2	+19.9	+13.4	+11.0
Absorption	-18.7	-21.4	- 7.1	- 7.4
	+ 2.5	- 1.5	+ 6.3	+ 3.6
^{240}Pu	- 1.3	- 1.2	- 0.4	- 0.4
	+ 1.2	- 2.7	+ 5.9	+ 3.2
Expansion	- 0.6	- 0.6	- 0.1	- 0.1
Total calculated	+ 0.6	- 3.3	+ 5.8	+ 3.1
Experiment	-3.7±0.1		+2.5±0.1	

Also, for the same reason, the fine structure of reaction rates in a cell is not a good quantity to trace cross-section errors. Furthermore, the reactor physicist tries to design his experiments with small heterogeneity effects so that they may be considered to be a correction. Calculational methods, at the present stage, are just adequate to give an estimate of this correction, and there is still disagreement between heterogeneity calculations in different laboratories. To use heterogeneity effects for data check, one would have to design an experiment with large heterogeneity effects, and be sure that the calculations describe these effects adequately. This has probably not been carried out, as yet.

6. CONCLUSION

The foregoing discussion shows that in most cases the theoretical methods are adequate for an analysis of the experimental results in critical assemblies, which can be performed also with a relatively high accuracy. For a meaningful analysis to be performed one should make sure to use sufficiently accurate calculational methods and precise and reliable experimental results. Spectrum measurements definitely need more precision. On the other hand, it is generally agreed that the differential data presently available are not good enough to allow a reliable calculation of the reactor parameters with the accuracy desired. This is the main reason why critical experiments are still being carried out. The information obtained in critical experiments can be used for power-reactor design in different ways. The first, not very sophisticated, way is to use scaling factors obtained from calculated and measured integral data. This procedure is, nevertheless, useful and normally allows a sufficient prediction of the main characteristics of a power reactor if the scaling is based on engineering mock-up experiments [51].

The second way is to analyse the discrepancies between measured and predicted integral data in order, first, to locate the main responsible microscopic data uncertainties and, secondly, to give preference to specific cross-section measurements according to the direction indicated by the analysis of the discrepancies. It can be stated generally that only a systematic study of a variety of fast cores differing in geometry, material composition, and neutron energy distribution, combined with a thorough comparison and re-evaluation of the main microscopic data, can provide more definite conclusions on the reliability of nuclear data to be used in fast-reactor calculations. The results of such investigations performed at Karlsruhe were reported by Küsters [52] and Kiefhaber [53], and led for instance to the conclusion that lower ^{238}U-capture data should be preferred, to those used in our calculations (now, Moxon's data [54] are included). The low ^{235}U-fission cross-section measured by Pönitz [55] must be excluded. Our interpretation of the 1967 Schomberg data [56] for the α-value of plutonium should better be replaced by Gwin's data [57]. $\sigma_f(^{239}Pu)$ should be increased above White's results [58] to the Pfletschinger and Käppeler data [59]. Oosterkamp [12] could rule out the formerly used capture data of ^{240}Pu. The calculation of criticality for various assemblies as given in Table IX shows that a relatively good prediction is possible since for most Pu-fuelled assemblies investigated k_{eff} is underpredicted

TABLE IX. BEST AVAILABLE CRITICALITY VALUES CALCULATED FOR VARIOUS FAST ZERO-POWER ASSEMBLIES

Assembly	Best available value for k_{eff} (MØXTØT-set)	Experimental results	Δk Theory-Experiment
SUAK U1B	0.856	0.86 ±0.01	-0.004
SUAK UH1B	0.930	0.945±0.01	-0.015
ZPRIII-10	1.011	1.000	+0.011
ZPRIII-25	0.997	1.000	-0.003
SNEAK-series 3A0	0.937	0.930	+0.007
3A1	0.968	0.962	+0.006
3A2	1.000[a]	1.000	±0.000
3A3	1.036	1.048	-0.019
SNEAK-3A1	1.020	1.000	+0.020
SNEAK-3A2	1.013	1.000	+0.013
SNEAK-3B2	1.000	1.000	±0.000
ZPRIII-48	0.989	1.000	-0.011
ZPRIII-48B	0.987	1.000	-0.013
ZEBRA 6A	0.985	1.000	-0.015
SNEAK 5C	1.040	1.03±0.01[b]	+0.010
ZPRIII-55	0.983	1.000	-0.017

[a] Normalization point for the SNEAK-3A-series.
[b] Preliminary experimental results

by about 1 to 2%, while for most U-fuelled assemblies k_{eff} is overpredicted by nearly the same amount.

This procedure, in the end, will lead to and support those measured microscopic data which are consistent with the integral data obtained in critical facilities.

Finally, there is the third way of adjusting cross-sections to fit available integral data, i.e. using a least-squares fit technique. This way, in our opinion, is just a more systematic way than the first one to use integral data in reactor design. One has to be careful about certain pitfalls: The number of adjustments must be lower than the number of integral data, otherwise one gets meaningless oscillations in the adjusted cross-sections [50]. It must be realized that adjusted and non-adjusted cross-sections generally have about the same standard deviation so that the procedure does not yield additional information on a single cross-section except in cases where there are large uncertainties or errors in the original values. Thus, it is not surprising that the fitting procedure, when applied to different original values, does not necessarily lead to the same adjusted cross-sections. An example is given for adjusted values obtained by Barré and by Rowlands, as reported in [49]:

Cross-section adjustment:

	Energy Range keV	Barré Adjusted	Barré Adjusted value	Rowlands Adjusted	Rowlands Adjusted value	Difference % in adjusted values
^{238}U capture	302-498	-14.3%	0.111	-7.8%	0.120 ± 6%	8%
	24.8-40.9	-11 %	0.392	+3.8%	0.472 ± 6%	20%
	3.36-5.53	+ 6 %	0.927	+7.4%	0.949 ± 6%	2%
^{239}Pu alpha	0.768-9.12	+40 %	0.78	+11 %	0.94 ± 15%	20%

It is apparent that the difference of 20% in the adjusted data of ^{238}U capture in energy group 25-40 keV is rather large, and so is the difference in ^{239}Pu alpha which is also 20%. However, these differences are of the same order as the uncertainties in differential data (compare the difference between Moxon and Pönitz for ^{238}U-capture and the uncertainty of 15% quoted by Gwin for Pu-alpha), and if it is accepted that the cross-section fit does not improve differential data, there is no contradiction.

As a final remark, it should be emphasized that work with adjusted cross-sections does not ensure a meaningful extrapolation to integral data of assemblies which differ widely in composition or spectrum from those assemblies which are used in the fit.

REFERENCES

[1] OKRENT, D., Proceedings of the Conference on Safety Fuels and Core Design in Large Fast Power Reactors, ANL 7120 (1965) 3.

[2] Proceedings of the International Conference on Fast Critical Experiments and their Analysis, Argonne Rep. ANL 7320 (1966).

[3] The Physics of Fast Reactor Operation and Design, International BNES Conference, June 1969.

[4] SCHMIDT, J.J., Karlsruhe Rep. KFK 772 (1968).

[5] ABAGJAN, L.P. et al., translated in Karlsruhe Rep. KFK-tr-144 (1964)

[6] HUSCHKE, H., Karlsruhe rep. KFK 770 (1968).

[7] BRISSENDEN, R.J., DURSTON, C., UKAEA Rep. AEEW-M429 (1963).

[8] KIER, P.H., ROBBA, A.A., Argonne Rep. ANL 7326 (1967).

[9] HUMMEL, H., RAGO, A., in Physics of Fast and Intermediate Reactors (Proc. Sem. Vienna 1961) 1, IAEA, Vienna (1962) 231.

[10] WINTZER, D., Karlsruhe Rep. KFK 743 (1969).

[11] FISCHER, E.A., Karlsruhe Rep. KFK 844 (1969).

[12] OOSTERKAMP, W.J., Karlsruhe Rep. KFK 1036 (1969).

[13] FISCHER, E.A., unpublished note (1970).

[14] HUSCHKE, H., private communication (1970).

[15] FISCHER, E.A., McGRATH, P., private communication (1970).

[16] KIEFHABER, E., Nucl. Sci. Engng 38 2 (1969) 178.

[17] BORGWALDT, H. et al., Karlsruhe Rep. KFK 302 (1965).

[18] MEISTER, H. et al., Argonne Rep. ANL 7320 (1966) 137.

[19] ENGELMANN, P. et al., Argonne Rep. ANL 7320 (1966) 725.

[20] STORRER, F., CHAUMONT, J.M., Argonne Rep. ANL 7320 (1966) 439.

[21] HELM, F., Karlsruhe Rep. KFK 975 (1969).

[22] SCHROEDER, R. et al., Karlsruhe Rep. KFK 847 (1968).

[23] BRETSCHER, M.M., REDMAN, W.C., Nucl. Sci. Engng 39 (1970) 368.

[24] Reports on k_∞=1 experiments presented at the BNES Conference on the Physics of Fast Reactor Operation and Design, London (June 1969).

[25] BÖHME, R., SEUFERT, H., Nucl. Appl. Techn. 7 (1969).
[26] BROOMFIELD, A.M. et al., BNES Conference on Fast Reactors, London (1969).
[27] BARBERGER, M. et al., BNES Conference on Fast Reactors, London (1969).
[28] ARMANI, R., Argonne Rep. ANL 7210 (1966) 304.
[29] TILL, C.E. et al., Nucl. Sci. Engng 40 (1970) 132.
[30] GOLD, R. et al., Nucl. Sci. Engng 34 (1968) 1.
[31] SEUFERT, H., STEGEMANN, D., Nucl. Sci. Engng 28 (1967) 277.
[32] CHAWLA, R., BESANT, C.B., Journal of the BNES, 9 1 (1970) 28.
[33] BLUHM, H. et al., BNES Conference on Fast Reactors, London (1969).
[34] BROOMFIELD, A.M. et al., BNES Conference on Fast Reactors, London (1969).
[35] BRANDL, V., Karlsruhe Rep. KFK 1185 (1970).
[36] MÜLLER, M., to be published (1970).
[37] BALLANCE, B.M.O. et al., BNES Conference on Fast Reactors, London (1969).
[38] EDELMANN, M. et al., BNES Conference on Fast Reactors, London (1969).
[39] FILLMORE, F.L. et al., BNES Conference on Fast Reactors, London (1969).
[40] BARRE, J.Y. et al., BNES Conference on Fast Reactors, London (1969).
[41] ROWLANDS, J.L., MACDOUGALL, J.D., BNES Conference on Fast Reactors, London (1969), and Panel discussion, ibid., 277.
[42] CLOUET D'ORVAL, C. et al., Paper to the forthcoming 10. ANS Meeting, Los Angeles (1970).
[43] BROOMFIELD, A.M., PALMER, R.G., Trans. Act. ANS 11 1 (1968) 203.
[44] DANCE, K., KARAM, R.A., MARSHALL, J.E., Argonne Rep. ANL 7410 (1968) 140.
[45] FOX, W.N. et al., Journal of BNES 9 1 (1970) 15.
[46] LITTLE, W.W., HARDIE, R.W., Nucl. Sci. Engng 36 (1969) 115.
[47] SCHMIDT, J.J., Karlsruhe Rep. KFK 966 (1969).
[48] HÄFELE, W. et al., "Fast Breeder Reactors", to be published in Annual Review of Nuclear Science.
[49] BUSTRAAN, M., in Fast Reactor Physics (Proc. Symp. Karlsruhe, 1967) 1, IAEA, Vienna (1968) 349.
[50] CECCHINI, C. et al., International Conference on Fast Critical Experiments and their Analysis, Argonne rep. ANL 7320 (1966) 107.
[51] NOBLE, L.D. et al., General Electric Rep. GEAP 13588.
[52] KÜSTERS, H. et al., Karlsruhe Rep. KFK 793 (1968).
[53] KIEFHABER, E. et al., BNES Confereuce on Fast Reactors, London (1969) 94.
[54] MOXON, M.C., UKAEA Rep. AERE-R 6074 (1969).
[55] PÖNITZ, W.P., in Neutron Cross Sections and Technology (2nd Conf. Washington, 1968).
[56] SCHOMBERG, M.G., in Fast Reactor Physics (Proc. Symp. Karlsruhe 1967) 1, IAEA, Vienna (1968) 289.
[57] GWIN, R. et al., USAEC Rep. WASH 1093 (1968) 106.
[58] WHITE, P.H., Reactor Sci. Technology 19 (1965) 325.
[59] KÄPPELER, F., PFLETSCHINGER, E., to be published in Nucl. Sci. Engng, June 1970.
[60] DAVEY, W., Nucl. Sci. Engng 39 (1970) 337.
[61] BROEDERS, C.H.M., Karlsruhe Rep. KFK 939 (1969).
[62] ZARITSKY, S.M., TROYANOV, M.E., BNES Conference on Fast Reacrors, London (1969) 309.

DISCUSSION

TO PAPERS IAEA-CN-26/116, 117

H. HÄGGBLOM: In Stockholm we have developed a computer program, JOHN, similar to the LSQ program in Winfrith. Two preliminary calculations have been performed; the first with 22 and the second one with 26 integral values for cross-section adjustments. The integral data in the first calculation related only to FRO assemblies; in the second calculation ZEBRA-6A and ZPR III/48 data were also included. Figure A below shows the capture cross-sections used for ^{238}U and the adjustments obtained in the two calculations. Davey's evaluation in Nucl. Sci. Engng., March 1970 is also included. Figure B shows the slowing-down cross-section and the inelastic scattering cross-section for ^{238}U. In accordance with the earlier calculations of Rowlands et al., we obtained a negative adjustment of the slowing-down cross-section above 820 keV, but we have also obtained a positive correction between 15 and 100 keV. This may be connected with an increase in the cross-section corresponding to the 45-keV inelastic threshold according to the measurements of Reitmann et al. The estimated accuracy was improved compared to the assumed one.

For the fission cross-section of ^{235}U the corrections gave very low values in the whole energy region.

C.G. CAMPBELL: The significance of changes in the ^{238}U capture-cross-section data depends critically on the uncertainties assumed for the fissile cross-sections. When the ^{235}U fission cross-section was thought to be known to about 3%, significant changes to ^{238}U capture data were shown by the integral experiments. Now that the uncertainty of the fission cross-section of ^{235}U is increased to 10% or 15%, the significance of these ^{238}U capture data changes disappears.

J.L. ROWLANDS: I should like first to comment on Dr. Küster's statement in his oral presentation that reactor spectrum measurements are not sufficiently accurate to be useful at present. He based this statement on the relationship between spectrum variations and k_{eff} and breeding gain. We find that the accuracy of prediction of k_{eff} is not influenced significantly by the inclusion of reactor spectrum measurements in the cross-section adjustment calculations, but that the accuracy of prediction of the PFR reactor spectrum in the Doppler energy region is markedly improved.

Secondly, I should like to ask Dr. Campbell, Dr. Küsters and Dr. Hutchins whether they think that some nuclear data requirements could be met by integral measurements, thereby permitting a relaxation of the accuracy requirements for microscopic measurements. We have seen, for example, that k_{eff} can now be predicted to an accuracy of $\frac{1}{2}$% on the basis of integral measurements.

C.G. CAMPBELL: For the fissile and fertile materials, there exists so much confusing information that I suggest we do not know what are the correct differential measurements to make. The important requirement now is for the measurers to evaluate the existing information and to identify the random and systematic errors in the measurements. This is why the UK request list calls for an evaluation of data in the case of the fissile and fertile materials.

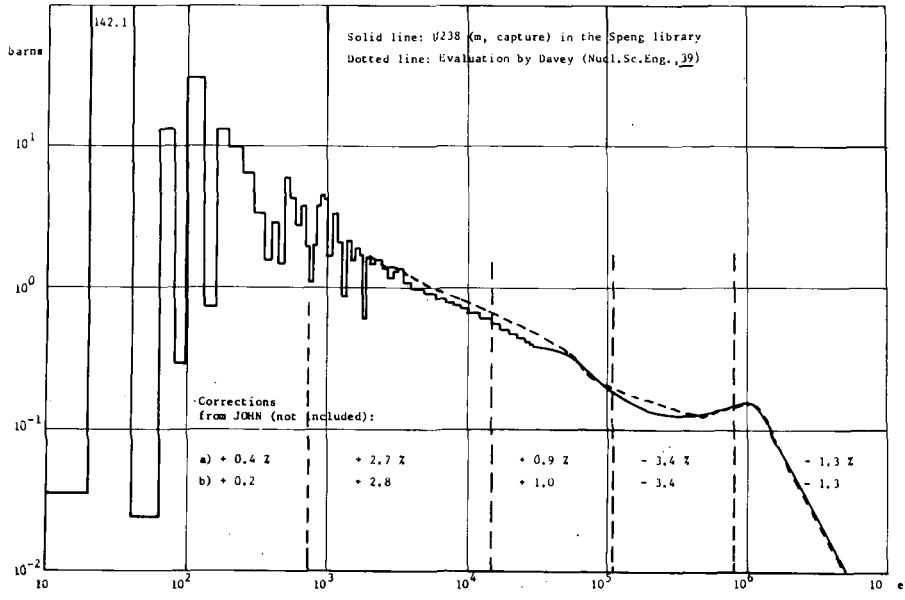

FIG. A. Capture cross-sections used for ^{238}U and adjustments obtained in two calculations.

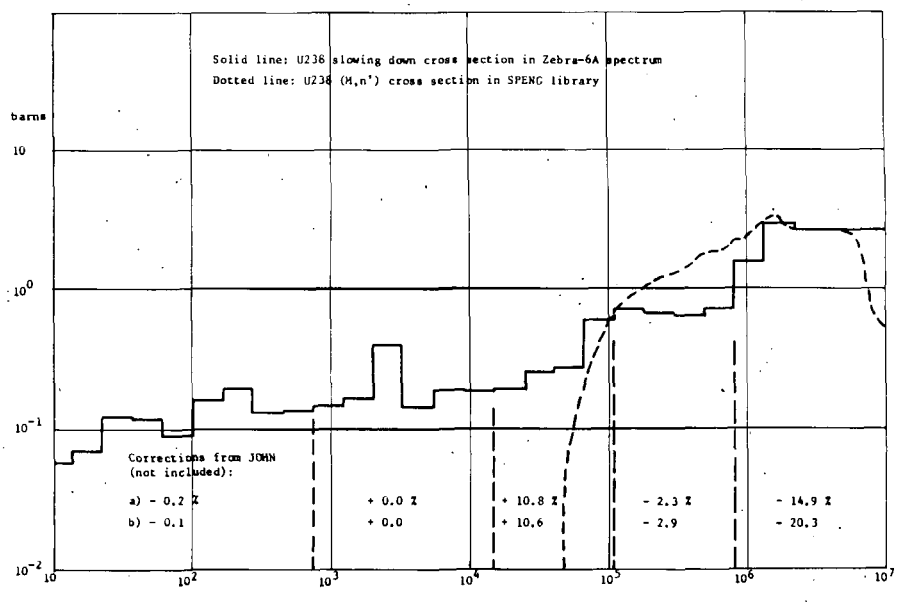

FIG. B. Slowing-down and inelastic-scattering cross-sections for ^{238}U.

Prior to this meeting, very little evidence on the cross-sections of possible canning and structural materials for fast reactors was available. For this reason, we need measurements of the resonance structure in the relevant capture cross-sections, to about 10% accuracy. This information cannot be obtained from integral experiments and differential data are required.

H. W. KÜSTERS: I agree fully with what Dr. Campbell has said. As I stated in my presentation, I believe that we should indeed relax some of our requests for high accuracies and try instead to obtain consistent results for the important cross-sections within a wider, but still acceptable, margin. On the basis of data adjustment or by making proper use of the results of investigations, we are able, as shown at Karlsruhe, at least to predict criticality or enrichment of fast reactors. I might add that there is, in particular, a lack of data on the angular distribution of elastically scattered neutrons.

I would also like to comment briefly on the spectrum measurement accuracies. As stated in our paper, these measurements are rather uncertain in the low-energy region, when the Doppler effect is important. However, if the calculated spectrum in this range deviates even by a much larger amount than the high experimental uncertainties, the use of the spectrum in a fit should result in an improvement. We did not have much trouble with interpretation of Doppler experiments, as can be seen from our paper.

W. G. DAVEY: As a reactor physicist and an evaluator, I cannot agree that evaluations and not additional experiments are needed at the present time. There are, for example, discrepancies in the ^{235}U cross-sections above 1 MeV which cannot be resolved by evaluation alone and more experiments are needed.

H. W. KÜSTERS: What is meant by evaluation here is that the experimentalists should reconsider all the details of their measurements in order to discover the possible reasons for inconsistent results. I think that only those who are doing the experiments can detect the deficiencies in their methods and analysis.

W. G. DAVEY: I agree that evaluation in that sense is needed at the present time.

H. ALTER: I would like to supplement Dr. Rowland's plea for more accurate reporting of differential data by requesting that results of integral measurements be reported in a more complete and less ambiguous manner. In addition, the experimenter's assessment of systematic errors in his measurements should be fully reported.

B. ROSE: I should say at the outset that I fully support Dr. Campbell's position that integral experiments are an indispensable weapon in predicting reactor performance. However, there are a number of points which I believe he understated. First, it seems to me that it is sometimes forgotten that integral experiments also have their experimental errors, including systematic ones. An example, which is to be found in Dr. Campbell's own paper, is the question of the unsuspected water content of graphite. Any new experimental technique must by its very nature involve new and incompletely understood types of errors. The differential people have in the past been very open about the errors that bedevil their measurements - indeed this is the very stuff of the scientific method. It is important that the same highly critical approach, with multiplicity of the same experiment, be adopted in integral experimentation. It is

not sufficient in this work to claim, say, an accuracy of 2%. We already have too much experience in the differential field of different experimenters claiming an absolute accuracy of 2% yet differing by 10%.

Second, anyone knows that interpolation is easy, so that one may predict the performance of reactor types or sizes intermediate between those already studied. But it is equally well known that extrapolation is a particularly dangerous process. Many of us will recall with pleasure Professor Abramov's interesting slide at the Paris meeting (1966) showing the improbability of being able to estimate the future height of ladies' hemlines from a study of data taken from a few selected epochs in the past. I personally would be very unhappy to see Dr. Campbell similarly revealed in all his nakedness or, at best, dressed in his Emperor's new clothes. We know that the error one can place on an extrapolated value increases dramatically with the length of the extrapolation - and indeed, the more arbitrary the parameters that are used to force a good fit over the range studied, the more uncertain becomes the extrapolated value.

In this connection, Dr. Campbell has stated that he can predict the reactivity performance of a clean, cold PFR to $\pm\frac{1}{2}\%$ using integral data adjustment from present differential values. What can he do for a dirty, hot CFR - and how does he propose to make a mock-up containing up to 10% of ^{241}Pu?

In Part 2 of his paper, in the section headed "The accuracy of calculations made using adjusted cross-sections", Dr. Campbell states that the accuracy of the prediction of many reactor properties is radically improved because of the correlation of errors. I do not see how this can possibly be a general statement; in general, as many parameters must have their errors increased as reduced.

C.G. CAMPBELL: I should like to reply to the points raised by Dr. Rose. First, as regards the question of systematic errors in integral measurements, the ZEBRA group has given very close attention to this. All the integral experiments are performed by two independent techniques and the results are accepted only when the identified random and systematic errors show that they are consistent. The integral measurers are in a strong position to criticise the lack of published information on systematic and random errors in cross-section measurements, but no one can afford to be complacent about this.

Second, the range of integral experiments embraces the material compositions and spectra of fast power reactors and the dangers of large extrapolations can be avoided.

Third, the significance of higher isotopes of plutonium can be assessed and if the uncertainties on performance of CFR's warrant it, the influence of higher isotopes can be measured in zoned integral assemblies. Irradiation experiments in operating fast assemblies also provide possibilities for valuable integral checks.

Fourth, the point here is that integral experiments measure and constrain combinations of cross-sections and these same combinations are important in performance predictions. That is why the accuracy is so dramatically improved.

W. HAVENS: This discussion gives me the feeling of watching a film that has now reached the point where I came in. In 1946, the general feeling of reactor designers was that detailed microscopic differential data were no longer necessary. Reactors have been constructed and

were operating satisfactorily. Integral data were all that was necessary to design new, more efficient reactors. However, late in 1946, there were some changes in reactivity of the Hanford reactors as a function of time which could not be explained. At approximately the same time we were measuring the transmission of plutonium with the Columbia neutron velocity spectrometer. We found that the cross-sections of two of the samples were not consistent near 1 eV. Tracing the history of the samples we found one had been irradiated for 50 MWd/t and the other for 100 MWd/t. This was the first evidence for the existence of the very strong resonance in ^{240}Pu at 1.06 eV which has a peak cross-section in excess of 100 000 b. The details of this resonance and its effects on reactor calculation would never have been properly determined without differential measurements. This is only one illustration of the value of differential measurements for reactor development. I could give many more if time permitted.

The conclusion I have reached after many years of work in this field is that integral results are excellent for interpolation but are not very valuable for extrapolation. After all, who would want to calculate the performance of a fast reactor using only the integral data available from thermal assemblies and reactors?

I believe that some of our difficulties occur because different people mean different things by the word evaluation. No amount of evaluation will remove an experimental discrepancy. The details of experiments which give discrepant results must be examined and the systematic error determined. This type of evaluation is much different from what is usually regarded as evaluation, namely, the examination of several sets of data to determine which of them is the best to use for a reactor calculation.

I agree with Dr. Küsters' description of the type of evaluation which it is most important to do now, but this is an extremely difficult task. For example, I spent a considerable amount of time trying to find what was wrong with the absolute fission cross-section measurements of ^{235}U in the epithermal region done at the Lawrence Laboratory in Livermore. The trouble was finally found to be due to the back-scattering in a thick aluminium plate placed behind the fission chamber. Hanna at Chalk River spent a lot of time trying to find out what was wrong with the 2200 m/sec measurements of the ^{235}U fission cross-section made by Bollinger of the Argonne National Laboratory. Those of us who had made absolute fission cross-section measurements were sure that Bollinger's measurements were wrong but we could find no reason for the error. The difficulty was finally cleared up by the experiments of Maslin at Aldermaston some years later: there was a correlation between the angular distribution of the neutrons and the fission fragments emitted in fission which had not been taken into consideration. It takes a great deal of work to find the systematic errors in an experiment and sometimes they never will be found.

There are obviously some systematic errors in the measurements of the fission cross-section of ^{235}U in the keV region. Poenitz' measurements do not agree with White's and the differences are much larger than the errors assigned. Obviously something is wrong with one set of measurements or the other or perhaps with both, because they should agree. The details of each experiment must be examined in an attempt to discover which systematic errors have been overlooked. I think it is the experimentalists who must do this type of evaluation. The theorist who evaluates data to obtain a self-consistent set is usually not interested in determining the

systematic experimental errors which have been overlooked, nor is he competent to do so.

R.F. TASCHEK: Experimentalists attempting to evaluate certain discrepant experiments often find that part or all of the original experiment needs to be redone, as for instance in the case of σ_f (^{235}U) at the thermal energies, measured by Bollinger a number of years ago. Very often the unique apparatus used no longer exists and the requirement cannot be met. This situation now obtains in the case of the important $\bar{\nu}$ discrepancy, where some results cannot be checked and the experimental devices have disappeared.

I should like to mention another aspect of evaluation: it needs to be realized that experimental results must sometimes be assigned low weighting factors because of insufficient direct evidence; in other words, the weighting must be made on a rather intuitive basis. At present, this is the situation as regards the fission cross-section of ^{235}U between about 500 keV and 1000 keV. It has not been possible to find the difficulty involved in the low Poenitz values but that they are incorrect appears rather certain. In this connection, there is a lot of information available which has never been reported in the published literature. For example, the old cross-section evidence in Los Alamos report LA 150 should be added to the data now in use for evaluations of the MeV values for σ_f(^{235}U).

M.S. MOORE: I should like to point out that discrepancies in nuclear data are usually not resolved by discussions between experimentalists, but rather as a result of a continuing program of measurements. A striking case in point is the effect discovered by Dr. Soleilhac in connection with measurements of $\bar{\nu}$ for spontaneous fission of ^{252}Cf in large liquid scintillators, as reported in paper CN-26/66.

J.J. SCHMIDT: I agree completely with the remarks of Dr. Havens which, incidentally, are in line with the conclusions drawn independently by Dr. Küsters, Dr. Campbell and myself in statements at this Conference. More generally, it seems to be recognized that the "classical" procedure of evaluation, which often had to be used in the past, particularly for the establishment of more comprehensive libraries of evaluated nuclear data, is no longer satisfactory. By "classical" evaluation procedure I mean the simple averaging of discrepant experimental data, in which the discrepancies do not arise from statistics but from systematic errors, and in which there is no attempt to remove those discrepancies. This is at least true of the more important types of nuclear data, such as heavy-element and standard cross-sections, where so many systematic discrepancies still exist.

Evaluation in the sense of searching for systematic errors in discrepant experiments can only be done by the experimentalists themselves, with the support of data compilers and reviewers in the four world neutron data centres. This was the idea behind the expert meetings on α(^{239}Pu) and $\bar{\nu}$. These meetings were convened by the IAEA at Studsvik in advance of this Conference for the specific purpose of identifying discrepancies and possible sources of systematic errors in the experimental results and of working out detailed recommendations regarding further experimental and evaluation work. These and similar meetings planned by the IAEA for the future are intended to stimulate close co-operation between experimentalists, compilers and reviewers, with the aim of improving the confidence level of those microscopic nuclear data which are of crucial importance for reactor design.

ROLE COMPLEMENTAIRE DES EXPERIENCES INTEGRALES PAR RAPPORT AUX MESURES DIFFERENTIELLES POUR UN PROJET DE REACTEUR A NEUTRONS RAPIDES
Cas des isotopes du plutonium

J.Y. BARRE, J. BOUCHARD*
CEA, Centre d'études
nucléaires de Cadarache,
France

Abstract — Résumé

COMPLEMENTARY ROLES OF INTEGRAL EXPERIMENTS AND DIFFERENTIAL MEASUREMENTS FOR A FAST-NEUTRON REACTOR PROJECT – THE CASE OF PLUTONIUM ISOTOPES.

Reactor physicists have two experimental sources at their disposal: differential measurements of the microscopic constants and results of integral experiments. The paper presents a general analysis of the complementary role of these two types of measurement for the case of fast reactors. The examples refer, above all, to plutonium isotopes. The essential conclusion is that the precision demanded by a project for the fundamental parameters (k_{eff}, breeding ratio) can be achieved by integral experiments and that, to obtain this result, it is not necessary to have very-high-precision differential measurements.

ROLE COMPLEMENTAIRE DES EXPERIENCES INTEGRALES PAR RAPPORT AUX MESURES DIFFERENTIELLES POUR UN PROJET DE REACTEUR A NEUTRONS RAPIDES – CAS DES ISOTOPES DU PLUTONIUM.

Les physiciens des réacteurs disposent de deux sources expérimentales: les mesures différentielles des constantes microscopiques et les résultats d'expériences intégrales. Une analyse générale du rôle complémentaire de ces deux types de mesure dans le cas des réacteurs rapides est présentée. Les exemples illustrent surtout le cas des isotopes du plutonium. On conclut essentiellement que les précisions demandées par un projet pour les paramètres principaux (k_{eff}, taux de surgénération) peuvent être atteintes à partir des expériences intégrales et qu'il n'est pas indispensable pour arriver à ce résultat d'obtenir des mesures différentielles de très haute précision.

1. INTRODUCTION

Le but concret de la physique des réacteurs rapides au CEA est actuellement de pouvoir prédire avec la meilleure précision les caractéristiques d'un réacteur à deux zones, réfléchi, au plutonium, et refroidi au sodium.

Pour atteindre ce but, le physicien dispose de deux bases expérimentales: les mesures différentielles des données élémentaires et les paramètres intégraux mesurés dans les expériences critiques. La part relative de ces deux ensembles de mesure dans la mise au point des calculs de réacteurs rapides est analysée. Les exemples choisis concernent essentiellement les isotopes du plutonium.

---

* CEA, Centre d'études nucléaires de Fontenay-aux-Roses, France.

Dans une première partie, l'examen des différentes données de base nécessaires montre que, si les constantes les plus importantes font l'objet de mesures différentielles, les incertitudes qui existent encore sur ces données fondamentales ne permettent pas d'atteindre les précisions demandées par un projet. De plus, la complexité des problèmes traités impose dans les calculs de réacteurs des approximations qui font qu'un test sur des paramètres intégraux est de toute manière nécessaire.

Dans l'analyse des expériences intégrales faites dans la seconde partie, on distingue deux classes d'expériences par leur but:

a) Expériences spécifiques d'une constante: les conclusions tirées des mesures des paramètres $\bar{\alpha}$ ^{239}Pu et $\bar{\alpha}$ ^{235}U effectuées soit par la méthode du signal local dans ERMINE, soit par irradiations dans OSIRIS (filtre en bore) ou RAPSODIE sont présentées; les mesures des taux de fission des isotopes du plutonium (^{239}Pu, ^{240}Pu, ^{241}Pu) rapportés à celui de ^{235}U permettent de tester les sections efficaces de fission.

b) Expériences orientées vers une analyse systématique de paramètres intégraux.

On présente les solutions actuellement retenues pour l'analyse de l'ensemble de ces expériences qui constitue la base de la physique des réacteurs.

Les résultats des méthodes d'ajustement développées précédemment ont été testés sur les résultats des expériences nouvelles faites à SNEAK ou MASURCA.

Les grandes lignes d'une méthode plus directe pour l'analyse des expériences intégrales indépendante des ajustements statistiques sont présentées.

On aboutit à la conclusion que les expériences intégrales permettent, sans la nécessité d'obtenir des mesures différentielles de haute précision, d'atteindre les précisions demandées par un projet.

2. MESURES DIFFERENTIELLES

Les données résultant des mesures différentielles constituent le point de départ des calculs de réacteur. Dans le cas des réacteurs rapides, le large domaine d'énergie couvert, les diverses réactions possibles et la gamme d'isotopes mis en jeu imposent la connaissance d'un très grand nombre de données fondamentales.

TABLEAU I. CARACTERISTIQUES DES DEUX CŒURS DU TYPE PHENIX UTILISES COMME EXEMPLES

	Cœur 1	Cœur 2	Teneur isotopique (% atomes)
Enrichissement (%)	19	27	^{240}Pu: 20,1
Composition volumétrique (%)			
combustible	37	37	^{241}Pu: 2,8
sodium	35	35	^{242}Pu: 0,4
acier	25	25	
gaz	3	3	

2.1. Données nécessaires

2.1.1. Domaine d'énergie

La limite basse du domaine d'énergie concerné peut être définie à partir de la répartition en fonction de l'énergie des productions ou des absorptions dans le cas des deux cœurs d'un réacteur du type PHENIX [1] utilisés comme exemples dans la suite (tableau I):

		Production	Absorption
Cœur 1:	E > 5 keV	91 %	85%
	E > 750 eV	99 %	98%
Cœur 2:	E > 5 keV	95 %	90%
	E > 750 eV	99,5%	99%

Si l'analyse du bilan permet théoriquement de limiter le domaine d'énergie utile à la gamme 1 keV - 15 MeV, d'autres causes nécessitent la connaissance des sections efficaces de capture et de fission des éléments lourds en dessous de 1 keV, comme par exemple:
- la détermination des paramètres de résonance pour le calcul des facteurs d'autoprotection utilisés dans la gamme des résonances non résolues
- le calcul des distributions de puissance en fin de couverture
- la normalisation à basse énergie des mesures faites à plus haute énergie.

2.1.2. Type de réaction

L'analyse du bilan, des distributions de puissance et du taux de surgénération est directement liée à la connaissance des taux de production et d'absorption (par capture et fission) donc à celle des sections efficaces de capture et de fission et du paramètre υ. La décomposition par isotope des taux de production et d'absorption au centre du cœur 1 (mode fondamental) met en évidence l'importance relative dans le bilan des isotopes supérieurs du plutonium (fission et capture pour le ^{240}Pu, fission pour le ^{241}Pu) par rapport à celle des autres isotopes (tableau II). Ces valeurs correspondent, pour ce type de cœur, à une contribution en k_{eff} de 6% pour le ^{240}Pu et 5% pour le ^{241}Pu.

La détermination de ces taux de production et d'absorption moyennés sur l'énergie implique la connaissance du spectre du flux de neutrons, donc, en plus des données précédentes, du spectre de fission et des sections efficaces de ralentissement. Dans le cœur 1, le nombre de neutrons ralentis en dessous de 100 keV, soit par diffusion inélastique (surtout ^{238}U), soit par diffusion élastique (surtout O et Na), est respectivement 19 et 80%, alors que le nombre de neutrons vierges de fission est 1%.

Le calcul des fuites qui équilibrent le bilan nécessite, en plus des sections de ralentissement, la connaissance des sections de diffusion. Dans le cœur 1 le bilan se décompose ainsi: production: 100%; absorption: 65,4%; fuites: 34,6%.

En dehors des données de base nécessaires pour le calcul des paramètres principaux (bilan, k_{eff}, distributions de puissance, taux de surgénération), des problèmes complémentaires demandent la connaissance d'autres données de base, par exemple:

TABLEAU II. TAUX DE PRODUCTION ET D'ABSORPTION AU CENTRE DU CŒUR 1

	Production (%)	Absorption (%)	Absorption par fission (%)
^{238}U	9,8	34,2	5,9
^{239}Pu	79,2	51,9	41,2
^{240}Pu	5,1	5,6	2,4
^{241}Pu	4,9	2,9	2,5
Structures		4,7	
O		0,3	
Na		0,3	
Total	100	100	

- sections efficaces des absorbeurs (barres de contrôle)
- sections efficaces de production d'hélium ou d'hydrogène dans les structures
- rendement en produits de fission et leur absorption.

2.1.3. Nature des données nécessaires

Il est bien sûr nécessaire de connaître en valeur absolue l'ensemble des données de base citées sur toute la gamme d'énergie mentionnée.

Cependant, le but poursuivi dans les mesures différentielles ne correspond pas toujours exactement aux besoins des physiciens des réacteurs.

Par exemple il est difficile, même dans un calcul de bilan en milieu infini, d'utiliser un découpage en énergie suffisamment fin pour décrire correctement les résonances de capture et de fission des éléments lourds. On utilise des sections efficaces moyennées sur un certain nombre de résonances et des facteurs d'autoprotection calculés à partir des paramètres de résonance. Cette méthode classique implique que les mesures différentielles conduisent à une bonne précision non seulement sur les paramètres de résonance, ce qui est généralement le but poursuivi par les expérimentateurs dans des expériences à haute résolution [2], mais aussi sur les sections efficaces moyennes.

Il est intéressant de choisir des conditions expérimentales telles que la précision sur la section moyenne soit améliorée, même si la résolution est plus mauvaise. Suivant le découpage en énergie utilisé dans le calcul, cette remarque peut également s'appliquer dans le cas de fluctuations des sections efficaces.

2.2. Imprécisions des paramètres d'un réacteur dues aux incertitudes sur les données de base

Les exemples sont nombreux pour montrer que les écarts entre les mesures d'une même donnée de base faites par différents expérimentateurs

TABLEAU III. SENSIBILITES DU k_{eff} ET DU TRI DU CŒUR 2 AUX SECTIONS EFFICACES MOYENNES DES ISOTOPES DU PLUTONIUM ($d\sigma/\sigma = +1\%$)

		$\frac{dk}{k}$ (10^{-5} k)	$\frac{dTRI}{TRI}$ (%)
^{239}Pu	capture	-54	-0,33
	fission	549	0,52
	ν	803	2,0
^{240}Pu	capture	-17	+0,09
	fission	42	0,11
	ν	61	0,15
^{241}Pu	capture	-2	-0,01
	fission	33	0,03
	ν	47	0,12
^{242}Pu	capture	0,4	-
	fission	0,7	
	ν	1,0	

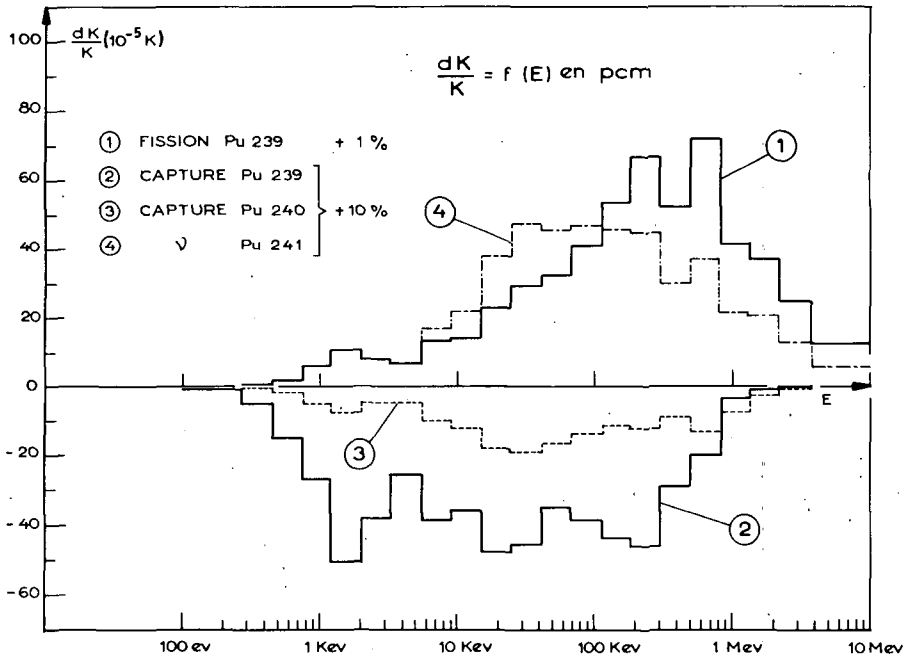

FIG. 1. Sensibilités de k_{eff} aux sections efficaces.

sont couramment supérieurs aux précisions annoncées par chaque expérimentateur. Les données de base évaluées sont entachées d'erreurs importantes qui se répercutent sur les paramètres d'un projet [3].

Dans le cas des isotopes du plutonium, les sensibilités aux sections efficaces de capture et de fission et au paramètre υ du k_{eff} et du taux de régénération interne (TRI: rapport des captures fertiles aux absorptions fissiles) sont calculées par la méthode classique des perturbations généralisées [3] pour le cœur 2. La criticité est rétablie par variation de l'enrichissement. L'importance relative des constantes du ^{240}Pu ($\upsilon\sigma_f$ et σ_c) et du ^{241}Pu ($\upsilon\sigma_f$) pour ces deux paramètres intégraux est mise en évidence dans le tableau III. Ces constantes ont été augmentées de +1% sur toute la gamme d'énergie.

Les variations en fonction de l'énergie des sensibilités de k_{eff} (fig. 1) et de TRI (fig. 2) aux constantes les plus importantes des isotopes du plutonium montrent le décalage en énergie du maximum de sensibilité entre la fission (100 keV - 2 MeV) et la capture (1 keV - 300 keV), en particulier pour le ^{239}Pu.

Bien que ce choix contienne une part d'arbitraire, on peut estimer un ordre de grandeur des incertitudes moyennes actuelles sur les constantes des isotopes du plutonium (tableau IV).

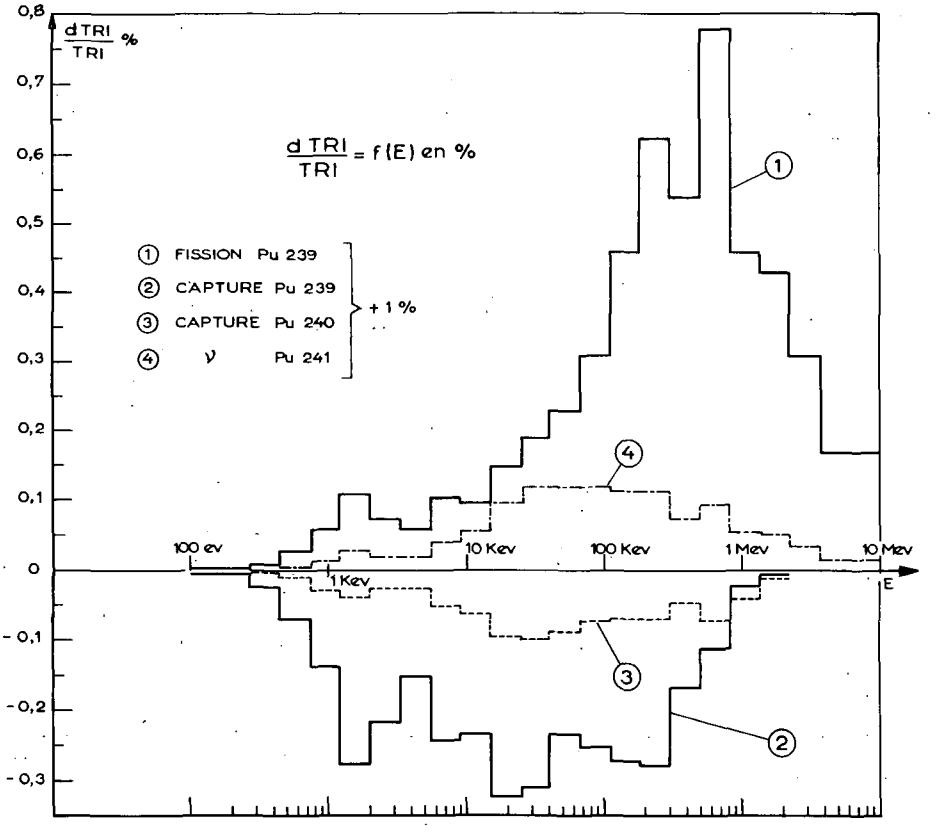

FIG. 2. Sensibilités du taux de régénération interne aux sections efficaces.

TABLEAU IV. ORDRES DE GRANDEUR DES INCERTITUDES SUR LES SECTIONS EFFICACES MOYENNES DES ISOTOPES DU PLUTONIUM ESTIMEES A PARTIR DES MESURES DIFFERENTIELLES

	Capture (ou α) (%)	Fission (%)	ν (%)
^{239}Pu	± 30	± 10	± 2
^{240}Pu	± 50	± 20	± 4
^{241}Pu	± 100	± 20	± 5
^{242}Pu	± 200	± 30	± 10

TABLEAU V. ECARTS QUADRATIQUES POUR QUELQUES ISOTOPES

Isotope	$\frac{dk}{k}$ (%)	$\frac{dTRI}{TRI}$ (%)
^{239}Pu	5,9	12
^{240}Pu	1,2	4,9
^{241}Pu	0,7	1,4
^{242}Pu	0,1	0,2
Total	6,1	13,0
Limite admise	1	3

Avec ces imprécisions évaluées et les sensibilités calculées, les écarts quadratiques moyens sur les deux paramètres intégraux obtenus, soit pour un isotope, soit globalement, sont largement supérieurs aux marges d'erreurs demandées par le projet (tableau V) [1].

Les limites admises sont valables pour l'optimisation de la filière, en particulier en ce qui concerne le taux de régénération pour son influence sur la variation de réactivité et de la distribution de puissance durant le cycle de combustible. Elles ne correspondent qu'aux incertitudes dues aux données de base et aux méthodes de calcul.

En supposant que l'incertitude sur le k_{eff} est due uniquement à la fission du ^{239}Pu par exemple, il faut obtenir à partir des mesures différentielles une précision inférieure à 2% sur cette section efficace.

2.3. Conclusion

Si on tient compte non seulement des isotopes du plutonium mais aussi de l'ensemble des isotopes présents, il est évident que les incertitudes sur les données de base ne permettent pas actuellement d'atteindre les précisions demandées sur les paramètres intégraux, et ne le permettront sans doute jamais (cas de la fission du ^{239}Pu par exemple).

De plus, on a supposé que ces données pouvaient être utilisées directement sans cause d'erreur supplémentaire dans un calcul de réacteur. Or les méthodes de passage des données de base aux données utilisables dans un calcul comprennent obligatoirement des approximations qui sont des sources d'erreurs supplémentaires, par exemple:
- facteurs d'autoprotection déjà cités
- flux de pondération nécessaire pour condenser les données de base en un nombre nécessairement limité d'intervalles d'énergie (pour des calculs de milieux finis) ou définir les sections efficaces de ralentissement élastique.

Enfin, les méthodes de calcul elles-mêmes comprennent des approximations, comme par exemple le calcul du coefficient de fuite.

Même en ne considérant que le calcul du bilan en milieu infini, cas le plus simple, la seule utilisation des données différentielles est totalement insuffisante pour atteindre les précisions demandées.

3. MESURES INTEGRALES

3.1. Généralités

Les nombreuses incertitudes sur les données fondamentales et les différentes approximations introduites dans les calculs rendent indispensables les expériences intégrales.

En réalité, pour le physicien de réacteur, le but final n'est pas de mieux connaître les données de base mais de mieux savoir calculer un certain nombre de paramètres intégraux.

Les données de base ne constituent qu'un intermédiaire. La mesure intégrale peut être considérée comme une mesure différentielle de très mauvaise résolution, mais c'est le résultat de ce type de mesure qui intervient dans le calcul d'un réacteur.

A la limite, les mesures précises de ces quantités intégrales dans une maquette rigoureuse du réacteur étudié résoudraient le problème. Cette solution demeure utopique car les maquettes ne sont jamais suffisamment proches des conditions cherchées pour pouvoir utiliser directement les résultats.

Par contre, on peut réaliser des expériences intégrales de caractère fondamental, facilement calculables, qui servent aux ajustements. Le seul problème réside alors dans la validité des transpositions des résultats des expériences critiques au cas réel. Cette transposition peut être faite avec le minimum de risques si les expériences sont judicieusement choisies.

On peut distinguer deux orientations principales pour les expériences intégrales:
- expériences spécifiques d'une constante
- expériences orientées vers une analyse systématique de paramètres intégraux.

3.2. Expériences spécifiques d'une constante

Ces expériences sont dirigées vers les constantes non directement accessibles aux mesures intégrales usuelles. Dans les expériences de ce type, la comparaison directe des paramètres intégraux calculés et

mesurés permet de choisir entre les diverses valeurs différentielles possibles.

3.2.1. Capture des éléments fissiles

Plusieurs techniques intégrales permettent d'accéder au paramètre $\bar{\alpha}$ (rapport capture sur fission) des éléments fissiles:
- méthode PCTR
- méthodes basées sur le coefficient de réactivité
- irradiations.

Deux expériences originales, basées sur les deux dernières techniques et réalisées au CEA pour mesurer $\bar{\alpha}$ ^{239}Pu et $\bar{\alpha}$ ^{235}U, sont présentées en détail dans ces comptes rendus [4].

3.2.1.1. Mesure du coefficient de réactivité

La mesure du coefficient de réactivité d'un échantillon fissile (signal de réactivité) fournit une relation entre le paramètre $\bar{\alpha}$ et le taux de fission de cet isotope. L'originalité de la méthode réside dans la mesure du taux de fission par une chambre à fission placée au voisinage de l'échantillon, sensible au taux de production par fission de cet échantillon (signal local). L'étalonnage de ces deux mesures se fait par l'intermédiaire d'une source de californium. Le paramètre $\bar{\alpha}$ peut alors être mesuré pour un même élément fissile à différentes dilutions.

L'accord observé entre les paramètres $\bar{\alpha}$ ^{239}Pu et $\bar{\alpha}$ ^{235}U obtenus par cette méthode et par deux autres méthodes pour lesquelles la répartition des erreurs dues aux termes calculés est très différente (méthode classique du bore [5] et méthode d'étalonnage absolu) permet de conclure à la faible importance d'erreurs systématiques [4].

L'expérience est effectuée au centre d'un bloc de graphite placé dans le cœur uranium U_2 dans ERMINE. Pour les échantillons de faible diamètre, le pourcentage de capture en dessous de 1 keV est fort ($\simeq$60%), pour les échantillons de fort diamètre, le calcul du flux perturbé dans l'échantillon est délicat. Pour un échantillon de 4 mm de diamètre, qui représente un bon compromis entre les deux inconvénients précédents (45% des captures dans le ^{239}Pu entre 1 et 20 keV), la comparaison des valeurs calculées avec le jeu Cadarache version 2 et mesurées montre un accord aux marges d'erreur près pour $\bar{\alpha}$ ^{235}U et une valeur calculée légèrement supérieure à la mesure pour $\bar{\alpha}$ ^{239}Pu:

	$\bar{\alpha}$ ^{235}U	$\bar{\alpha}$ ^{239}Pu
Expérience :	0,35 ± 0,04	0,37 ± 0,04
Calcul :	0,347	0,414
(E - C)/E (%):	1 ± 11	-10 ± 11

La précision obtenue sur $\bar{\alpha}$ par cette technique est du même ordre que celle donnée par la méthode PCTR [6].

3.2.1.2. Irradiations [4]

OSIRIS. L'irradiation dans OSIRIS d'échantillons de ^{239}Pu, ^{235}U et ^{238}U à l'intérieur d'un filtre en bore, choisi de telle manière que le pourcentage

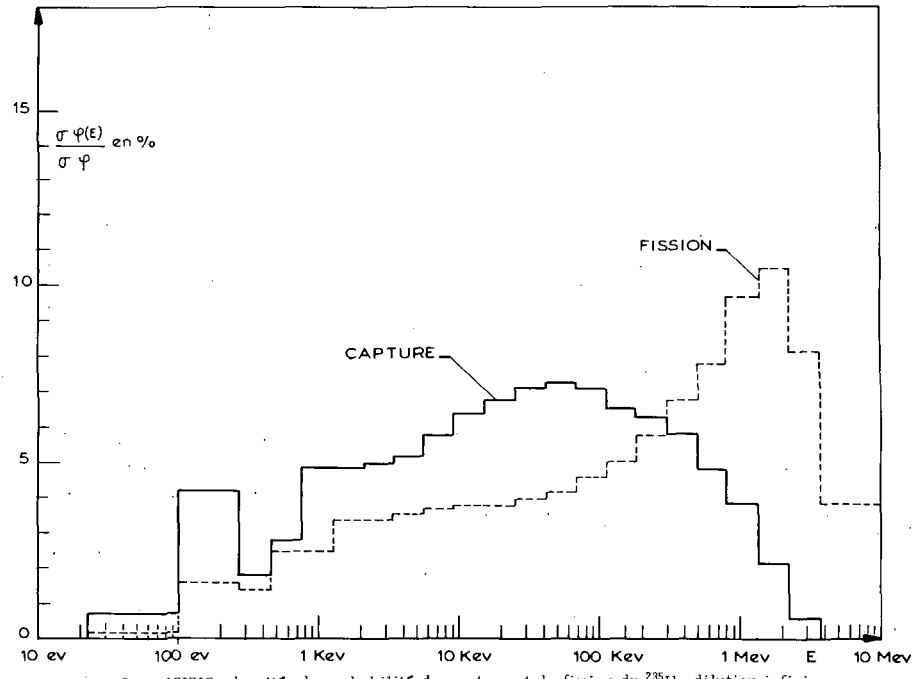

FIG.3. OSIRIS, densités de probabilité de capture et de fission du ^{235}U, dilution infinie.

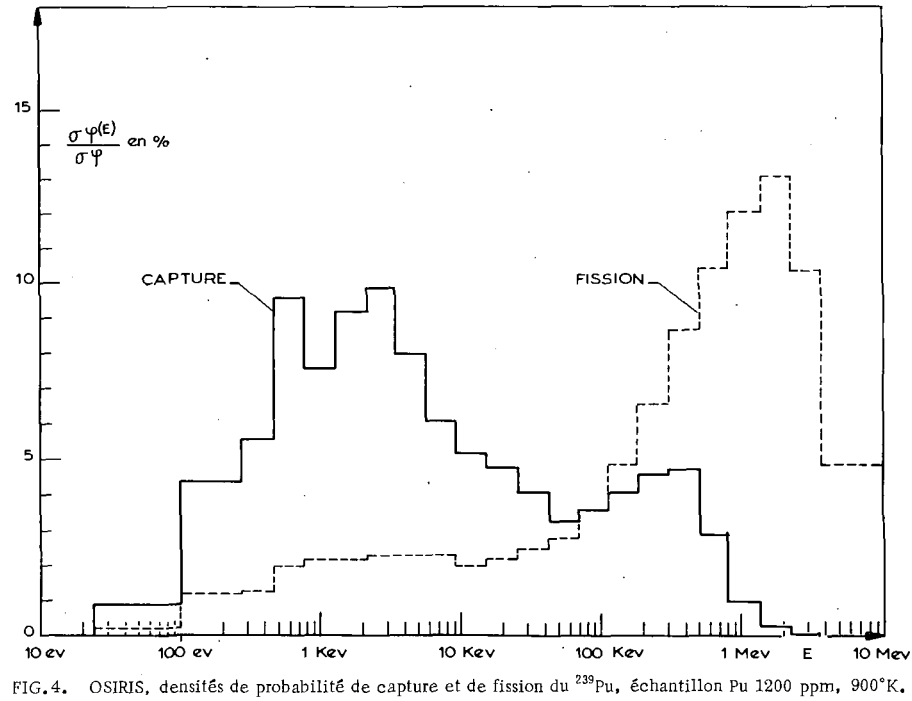

FIG.4. OSIRIS, densités de probabilité de capture et de fission du ^{239}Pu, échantillon Pu 1200 ppm, 900°K.

de capture dans le ^{239}Pu entre 1 et 20 keV soit maximal, permet d'obtenir les taux de capture du ^{239}Pu et du ^{238}U.

La mesure dans ISIS, maquette rigoureuse à puissance nulle d'OSIRIS, dans le même dispositif d'irradiation, de l'indice de spectre capture ^{238}U sur fission ^{239}Pu permet de déterminer le paramètre $\bar{\alpha}$:

$$\bar{\alpha}^{239}Pu = \frac{(\sigma_c^9 \phi t)}{(\sigma_c^8 \phi t)} \times \frac{\sigma_c^8}{\sigma_f^9}$$

Par cette technique qui ne fait pas intervenir les rendements de fission, les risques d'erreurs systématiques sur le paramètre $\bar{\alpha}$ mesuré sont très faibles car toutes les mesures sont classiques tant pour l'indice σ_c^8/σ_f^9 mesuré dans tous les cœurs étudiés que pour la mesure par spectrométrie de masse de $\sigma_c^9\phi t$ et $\sigma_c^8\phi t$.

La mesure du taux de fission de ^{235}U (par mesure de la disparition de ^{235}U et du taux de capture de ^{235}U) et de l'indice σ_f^9/σ_f^5 constitue une méthode complémentaire pour la détermination de $\sigma_f^9\phi t$ donc de $\bar{\alpha}^{239}Pu$.

Le paramètre $\bar{\alpha}^{235}U$ est obtenu par des méthodes similaires.

Les possibilités d'erreur sur le calcul du spectre au centre de la capsule sont limitées au maximum par les nombreux tests expérimentaux effectués dans ISIS [4].

Les répartitions suivant l'énergie des taux de capture et de fission de ^{235}U(fig. 3) ou de ^{239}Pu (fig. 4) à l'intérieur de la capsule justifient le choix du filtre:

	Capture ^{239}Pu	Capture ^{235}U
1 - 25 keV	51%	48 %
E < 100 eV	1%	0,7%

La valeur mesurée du paramètre $\bar{\alpha}^{235}U$ (précision ±6%) est en accord avec la valeur calculée par le jeu Cadarache version 2 (tableau VI). Le paramètre $\bar{\alpha}^{239}Pu$ mesuré est inférieur aux valeurs calculées par le jeu Cadarache version 2 de 8 ± 6%; la tendance est la même que celle obtenue par la méthode du signal local.

TABLEAU VI. PARAMETRES $\bar{\alpha}^{235}U$ ET $\bar{\alpha}^{239}Pu$ MESURES PAR IRRADIATION DANS OSIRIS

	Expérience	Calcul		(E - C)/E (%)
$\bar{\alpha}^{239}Pu$	0,199 ± 0,012	Jeu Cadarache version 2:	0,215	- 8 ± 6
		Valeurs basses entre 0,1 et 20 keV:	0,162	+19 ± 6
		Gwin [7] entre 0,1 et 20 keV:	0,223	-12 ± 6
		Sowerby [8] entre 0,1 et 20 keV:	0,221	-11 ± 6
$\bar{\alpha}^{235}U$	0,230 ± 0,012	Jeu Cadarache version 2:	0,227	1 ± 5

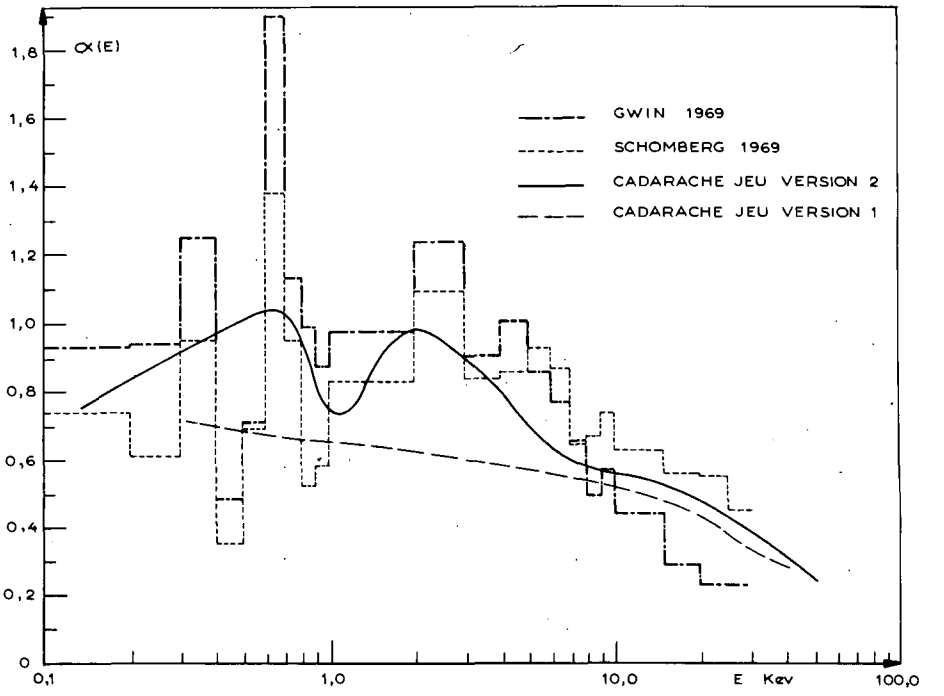

FIG. 5. $\alpha(E)$ du ^{239}Pu entre 0,1 et 100 keV.

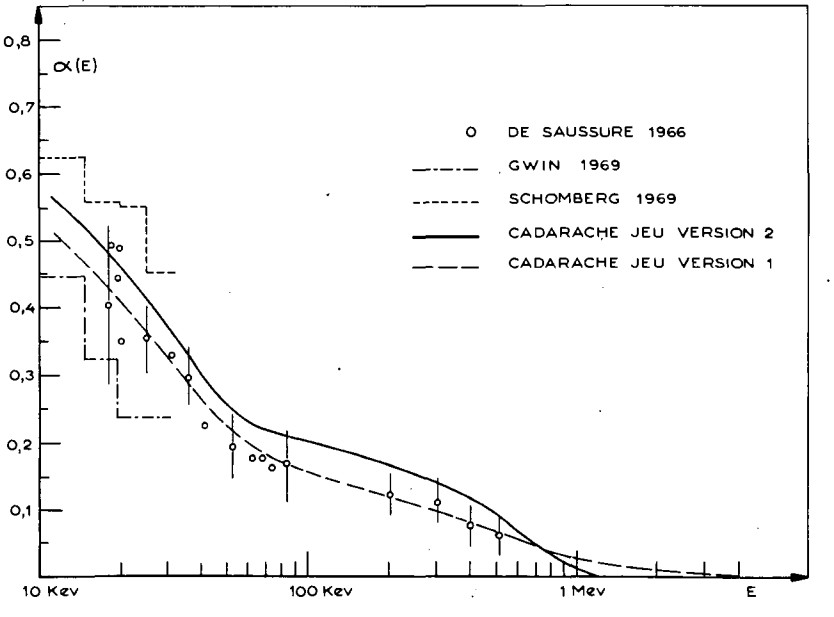

FIG. 6. $\alpha(E)$ du ^{239}Pu entre 10 keV et 10 MeV.

La comparaison des mesures avec les valeurs calculées à partir des différentes mesures différentielles de $\bar{\alpha}^{239}Pu$ (fig. 5 et 6), avec le même spectre et la même fission de ^{239}Pu (jeu Cadarache) permet de rejeter définitivement les valeurs basses admises précédemment entre 1 keV et 20 keV (jeu version 1) et montre que les mesures de Gwin [7] ou Sowerby [8] sont trop élevées en moyenne de 10% (fig. 5, tableau VI).

Les nouvelles applications de cette méthode porteront sur la mesure, avec une précision analogue, de $\bar{\alpha}^{240}Pu$ et $\bar{\alpha}^{241}Pu$ à partir d'échantillons purs.

RAPSODIE. L'analyse du combustible normal RAPSODIE (oxyde mixte 25% PuO_2, 75% UO_2 enrichi à 60%) donne le taux de capture de ^{235}U par mesure du ^{236}U formé et le taux de disparition de ^{235}U, donc le paramètre $\bar{\alpha}^{235}U$ avec une précision actuelle de ±5%. La comparaison avec les valeurs calculées par le jeu Cadarache version 2 indique que les données utilisées pour $\alpha^{235}U$ dans ce jeu au-delà de 25 keV sont légèrement trop élevées:

Expérience	Calcul	(E - C)/E (%)
$\bar{\alpha}^{235}U = 0,190 \pm 0,008$	0,203	-6,8 ±4
$\bar{\alpha}^{239}Pu = 0,099 \pm 0,007$	0,108	-9 ±7

Au centre de RAPSODIE, 97% des neutrons ont une énergie supérieure à 25 keV.

Le paramètre $\bar{\alpha}^{239}Pu$, obtenu à partir d'échantillons de ^{239}Pu pur irradiés dans RAPSODIE, est mesuré actuellement avec une précision de ±7%. Ce résultat, bien que préliminaire, montre que, si l'amplitude de l'augmentation de $\alpha^{239}Pu$ (E) au-delà de 10 keV proposée dans le jeu version 2 est trop forte (fig. 6), la tendance retenue est correcte: en effet, le paramètre $\bar{\alpha}^{239}Pu$ calculé en utilisant les valeurs basses de $\alpha^{239}Pu$ (E) (jeu version 1) est inférieur à la mesure de 10 ± 7%. Les analyses en cours permettront d'améliorer la précision sur ces paramètres $\bar{\alpha}$.

3.2.2. Section efficace de fission

Les taux de fission des différents isotopes du plutonium, rapportés par exemple à celui de ^{235}U, sont directement mesurés par chambres à fission dans les différents cœurs uranium ou plutonium étudiés à MASURCA et ERMINE avec une perturbation minime (diamètre 4 mm).

Les cœurs étudiés au CEA couvrent une très large gamme de spectres qui englobe largement les spectres des deux cœurs d'un réacteur du type PHENIX.

TABLEAU VII. INDICES DE SPECTRE $\bar{\sigma}_f^{239}Pu/\bar{\sigma}_f^{235}U$

Valeurs extrêmes	Expérience	Calcul	(E - C)/E (%)
Spectre dur	1,10 ± 0,015	1,10	0 ± 1,5
Spectre dégradé	0,92 ± 0,014	0,96	-4 ± 1,5
Cœur 1 PHENIX		0,97	
Cœur 2 PHENIX		1,02	

TABLEAU VIII. INDICES DE SPECTRE $\frac{\sigma_f{}^{240}Pu}{\sigma_f{}^{235}U}$ ET $\frac{\sigma_f{}^{241}Pu}{\sigma_f{}^{235}U}$

	A	B	C	D	Cœur 1	Cœur 2
$\sigma_f{}^{240}Pu/\sigma_f{}^{235}U$ Expérience	0,141 ± 0,012	0,262 ± 0,015	0,283 ± 0,017	0,394 ± 0,016		
Calcul jeu version 2	0,136	0,260	0,311	0,467	0,218	0,272
(E - C)/E (%)	3,5 ± 8	0,8 ± 6	-10 ± 6	-18 ± 4		
Calcul nouvelle évaluation	0,139	0,260	0,307	0,448		
(E - C)/E (%)	1,4 ± 8	0,8 ± 6	-8 ± 6	-14 ± 4		
$\sigma_f{}^{241}Pu/\sigma_f{}^{235}U$ Expérience	1,39 ± 0,03	1,36 ± 0,03	1,34 ± 0,03	1,36 ± 0,03		
Calcul jeu version 2	1,57	1,64	1,63	1,50	1,64	1,63
(E - C)/E (%)	-13 ± 2,5	-21 ± 2,5	-22 ± 2,5	-10 ± 2,5		
Calcul nouvelle évaluation	1,41	1,34	1,35	1,32		
(E - C)/E (%)	-1,4 ± 2,5	1,4 ± 2,5	-0,8 ± 2,5	-3 ± 2,5		

L'analyse systématique des écarts entre les valeurs calculées et les valeurs mesurées permet de tester les sections efficaces de fission utilisées sur tout le domaine d'énergie intéressant.

Plutonium-239. Cet indice est mesuré dans tous les cœurs étudiés (10 expériences) avec une précision de ± 1, 5%. Les valeurs extrêmes suivant le spectre encadrent largement les valeurs de ces indices dans les deux cœurs du type PHENIX. La comparaison des calculs faits avec le jeu Cadarache version 2 et des valeurs mesurées confirme la validité des constantes utilisées dans ce jeu (écart maximal - 4% pour un spectre dégradé) (tableau VII).

Plutonium-240, plutonium-241. Ces mesures n'ont été effectuées actuellement que dans quatre cœurs. Les indices dans ces cœurs encadrent cependant déjà les valeurs des deux cœurs PHENIX. La comparaison des valeurs calculées avec le jeu Cadarache version 2 et des valeurs mesurées est présentée du cœur A au cœur D dans l'ordre croissant de dureté du spectre (tableau VIII).

La précision sur l'indice ^{240}Pu est actuellement limitée par la teneur en ^{240}Pu des dépôts et sera améliorée prochainement par l'obtention d'échantillon pur. Cependant ces mesures apportent déjà un test probant de la validité des sections efficaces, soit utilisées dans le jeu, soit proposées dans une nouvelle évaluation [9] (fig. 7).

La précision sur l'indice ^{241}Pu vient pratiquement de la précision sur la valeur thermique de σ_f ^{241}Pu. La comparaison des indices mesurés et des valeurs calculées, soit avec le jeu Cadarache version 2, soit à partir d'une autre évaluation [10] (fig. 8), confirme sans équivoque l'amélioration apportée par ces dernières données.

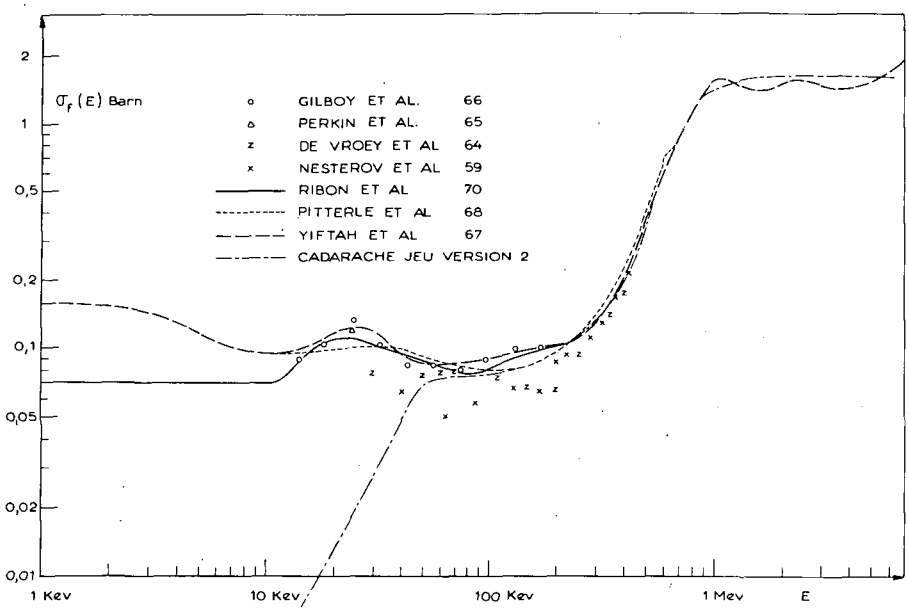

FIG. 7. Section efficace de fission du ^{240}Pu.

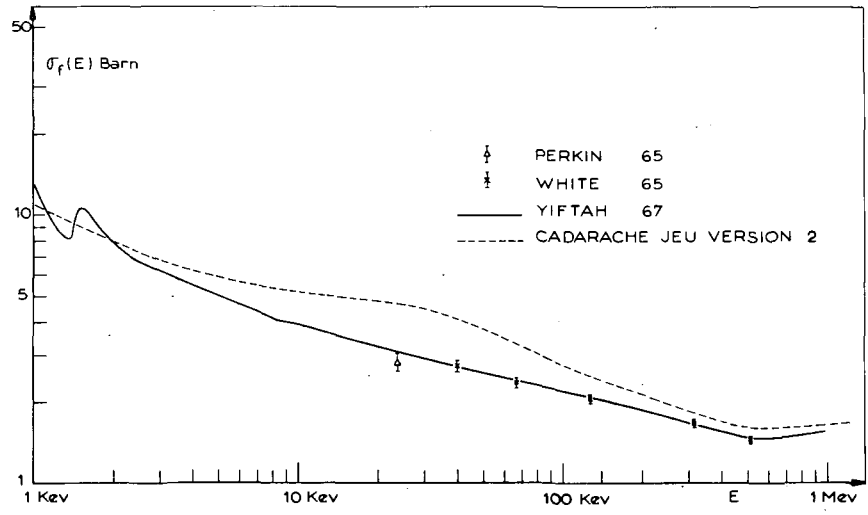

FIG. 8. Section efficace de fission du ^{241}Pu entre 1 keV et 1 MeV.

3.2.3. Conclusion

Toutes les expériences intégrales orientées vers une constante n'ont pas été décrites. On a seulement montré par ces exemples le rôle important de ces expériences intégrales spécifiques pour améliorer notre connaissance des données de base des isotopes du plutonium les plus importantes pour un projet: capture et fission du ^{239}Pu et du ^{240}Pu, fission du ^{241}Pu.

3.3. Analyse globale d'un ensemble d'expériences intégrales

3.3.1. Généralités

Une étape essentielle de la physique des réacteurs rapides est l'analyse du bilan en milieu infini et c'est vers cette analyse que sont orientés en priorité les programmes des expériences critiques en France [11] ou à l'étranger [12]. Ce bilan caractérise en effet un milieu indépendamment de sa forme et de son environnement et peut donc être étudié par des méthodes de calcul précises: les mesures des paramètres de ce bilan fournissent alors un très bon test des données de base.

Les paramètres caractéristiques des milieux multiplicateurs rapides varient dans des domaines limités: les expériences critiques sont centrées d'abord sur ces domaines et sur les causes les plus importantes de ces variations. Les variations mesurées des paramètres du bilan en fonction de l'enrichissement, but du programme expérimental actuel sur MASURCA et SNEAK, constituent la base des ajustements des méthodes de calcul.

Parmi ces paramètres, le laplacien matière (mesuré avec une précision de $\pm 1\%$) est considéré comme le plus important car il est proportionnel à la différence entre la production et l'absorption des neutrons et peut

être facilement relié à la masse critique du milieu nu. De plus, en dehors de l'intérêt direct pour le bilan, les mesures intermédiaires nécessaires pour mesurer ce paramètre permettent de tester le calcul des distributions de puissance et des gains de réflecteur. La mesure des rapports des taux de réaction σ_c^8/σ_f^5, σ_f^9/σ_f^5, σ_f^8/σ_f^5 (avec une précision moyenne ± 1, 5%) permet une analyse plus détaillée du bilan.

La priorité donnée au CEA aux laplaciens par rapport aux expériences $k_\infty = 1$ vient, en plus de l'intérêt déjà mentionné de ce paramètre, du fait que les laplaciens peuvent être mesurés dans des compositions de cœurs voisines de celles du projet (k_∞ de l'ordre de 1, 5) alors que l'obtention de la condition $k_\infty = 1$ impose des compositions très particulières. Cependant, ces deux types de mesure sont complémentaires: la méthode $k_\infty = 1$ mesure le rapport production/absorption indépendamment des fuites. Un programme $k_\infty = 1$ est d'ailleurs en cours dans ERMINE.

3.3.2. Exploitation des mesures intégrales pour un projet

3.3.2.1. Méthodes d'ajustement statistique

Le but de ces méthodes, très développées actuellement [13, 14] est de trouver l'ensemble des variations des sections efficaces jugées prépondérantes qui donne le meilleur accord entre les paramètres intégraux calculés par un jeu donné et mesurés dans des expériences critiques. La méthode et les conclusions obtenues pour le jeu Cadarache ont été déjà largement discutées [13].

Les résultats obtenus à partir de ce jeu version 2, qui tient compte des résultats des ajustements, sur des cœurs étudiés après la définition de ce jeu, montrent la validité de cette technique pour améliorer la prévision des paramètres intégraux.

Pour les principaux cœurs actuellement mesurés à MASURCA (combustible plutonium ou uranium, pourcentages volumétriques voisins de ceux de PHENIX au point de vue de l'acier et du sodium) les ordres de grandeurs des écarts relatifs expérience-calcul sont les suivants:

	Cœurs Uranium	Cœurs Plutonium
B^2m	-1 %	-3 %
k_{eff}	+0, 5%	-0, 5%
σ_f^8/σ_f^5	+1 %	+6 %
σ_f^9/σ_f^5	-1 %	-2 %

L'accord est bon en particulier pour le k_{eff}, pour lequel l'écart-type prévu pour le jeu version 2 par la méthode d'ajustement est 0, 7%.

L'écart constaté sur l'indice σ_f^8/σ_f^5 entre les cœurs plutonium et uranium (5%) peut s'expliquer par la différence des spectres de fission pour ces deux isotopes (rapport mesuré des énergies moyennes de fission $^{239}Pu/^{235}U = 1, 06 \pm 0, 02$ [15]). Le jeu Cadarache utilise actuellement le même spectre de fission pour les deux cœurs, celui de ^{235}U ($E_f = 1, 98$ MeV). Une augmentation de 6% du spectre de fission intervient peu sur la réactivité (+0, 6% en k_{eff}) mais accroît l'indice σ_f^8/σ_f^5 de +6%. Les autres indices mesurés sont très peu sensibles à ce paramètre. Par contre les informations

intégrales dont nous disposons actuellement ne nous permettent pas de confirmer l'augmentation proposée de la valeur absolue de E_f [15].

Les méthodes d'ajustement ont pour but principal d'améliorer globalement les prévisions des paramètres caractéristiques d'un réacteur. Les variations d'ensemble obtenues pour les sections efficaces sont donc certainement valables pour améliorer la prévision des paramètres d'un réacteur. Ceci est d'autant plus vrai que les paramètres du projet étudié sont dans la gamme des mesures intégrales utilisées.

Cependant ces méthodes permettent également de déterminer les tendances principales vers lesquelles les constantes du jeu doivent évoluer. Deux exemples importants choisis dans le cas du jeu Cadarache version 2 montrent que la tendance proposée par les ajustements est en accord avec les mesures différentielles les plus récentes postérieures à l'ajustement:

- pour tous les isotopes le paramètre ν utilisé dans ce jeu correspond aux valeurs basses du californium confirmées par les mesures les plus récentes [15]
- de même les données retenues dans ce jeu pour la capture du ^{238}U sont voisines des mesures proposées par Moxon [16] mais en désaccord avec l'évaluation proposée par Davey [17] (fig. 9).

Dans ces deux cas, la dispersion des mesures différentielles est trop importante pour les précisions souhaitées.

Il n'est pas question d'utiliser telles quelles les corrections issues des ajustements pour modifier un jeu de sections efficaces. Cependant les résultats de ces méthodes constituent une information supplémentaire importante pour effectuer les évaluations: c'est de cette manière que le jeu Cadarache version 2 a été réalisé.

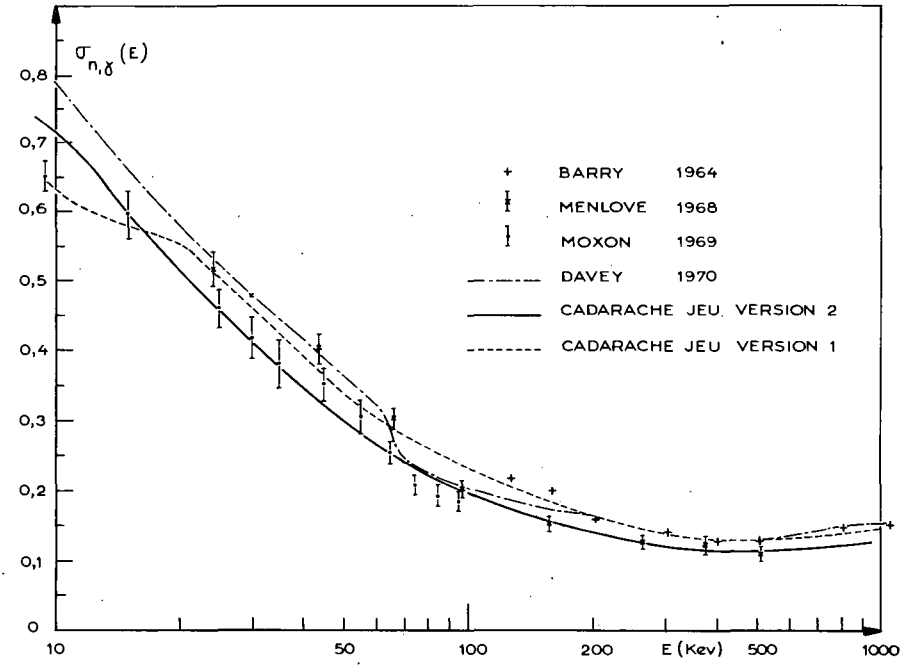

FIG. 9. Section efficace de capture du ^{238}U entre 10 keV et 1 MeV.

Il n'a pas été effectué de nouvel ajustement de ce jeu: le but actuel est l'obtention de mesures intégrales précises (erreurs systématiques éliminées aussi largement que possible), situées dans une gamme voisine de celle des deux cœurs PHENIX ou des réacteurs de filière et caractéristiques du spectre asymptotique (laplaciens et indices de spectre). Le développement prévu de la méthode BARRACA bénéficiera également des améliorations apportées dans les méthodes de calcul et comprendra l'introduction de nouveaux paramètres (par exemple spectre de fission) et des corrélations entre données ajustées.

3.3.2.2. Analyse directe des résultats intégraux

Seule la philosophie de la méthode envisagée sera présentée. En effet, le programme expérimental qui devrait permettre de l'appliquer est toujours en cours.

Le principe consiste à utiliser directement les mesures intégrales sans passer obligatoirement par l'intermédiaire des données différentielles comme dans la méthode précédente, pour ajuster un nombre limité de paramètres judicieusement choisis. Les ajustements se font sur les causes de variation les plus importantes qui sont mesurées dans les expériences intégrales: on peut alors faire confiance au calcul pour déterminer les effets secondaires même avec des données moins précises.

En effet les milieux multiplicateurs rapides forment des classes restreintes et, par suite, la quantité d'informations nécessaires pour connaître les paramètres essentiels est en réalité très inférieure à celle contenue dans les données élémentaires. On montre facilement que, dans la gamme intéressante, les sections efficaces moyennes des différents isotopes varient pratiquement linéairement en fonction du spectre caractérisé par un seul paramètre (section efficace moyenne de fission du ^{239}Pu par exemple). La variation est la même quelle que soit la cause de modification du spectre (enrichissement ou pas du réseau). Seules les sections efficaces à seuil font exception mais sont mesurées (indices $\sigma_f{}^{238}U/\sigma_f{}^{239}Pu$ et $\sigma_f{}^{240}Pu/\sigma_f{}^{239}Pu$).

Le but du programme expérimental actuel est d'ajuster les variations des sections efficaces moyennes dues à une variation de l'enrichissement: dans ce programme on mesure en réalité des différences, ce qui permet d'éliminer certaines causes d'erreurs systématiques. Dans les cœurs plutonium MASURCA $Z_2 - Z_1 - Z_3$ (variation de l'enrichissement entre 25 et 12%), les laplaciens et les taux de réactions capture ^{238}U, fission ^{238}U, fission ^{235}U rapportés au taux de fission du ^{239}Pu sont mesurés. Les mêmes mesures effectuées dans des cœurs uranium permettent des recoupements. En effet les mesures individuelles ne sont pas assez précises pour obtenir séparément toutes les données nécessaires. De plus le contrôle des transpositions calculées des effets secondaires doit être réalisé.

Il n'est pas possible de présenter ici des résultats concrets de ce type d'interprétation, les expériences étant encore en cours. Cependant cette analyse doit apporter une meilleure compréhension des phénomènes physiques et, associée à un programme expérimental bien choisi, permet d'espérer une amélioration de la précision sur les paramètres essentiels du projet (k_{eff}, distributions de puissance, taux de surgénération).

4. CONCLUSION

Les données de base issues des mesures différentielles constituent le point de départ des calculs des réacteurs rapides. La majorité des données nécessaires fait l'objet de ce type de mesure. Cependant les incertitudes qui existent sur ces constantes, dues essentiellement aux erreurs systématiques entre différentes expériences, sont trop importantes pour atteindre les précisions demandées sur les paramètres principaux par une étude de projet ou d'optimisation de filière. De plus, même si ces données de base étaient parfaitement connues, un test expérimental des paramètres intégraux calculés serait nécessaire.

En réalité le but des calculs de réacteur est de prédire des quantités intégrales: les données différentielles ne sont pas un but en elles-mêmes.

Les expériences intégrales spécifiques d'une constante permettent d'améliorer notre connaissance de données indirectement accessibles à une analyse systématique de paramètres intégraux et mal connues à partir des mesures différentielles, par exemple α^{239}Pu et α^{235}U par coefficient de réactivité ou irradiations, sections efficaces de fission des isotopes du plutonium.

C'est seulement l'analyse systématique des expériences intégrales, base de la physique des réacteurs, faite soit à partir d'ajustements statistiques soit à partir de méthodes plus directes, qui permet d'atteindre les précisions souhaitées sur les paramètres intégraux. Le fait utopique de disposer de données de base exactes permettrait d'avoir une confiance plus grande dans les ajustements mais ne supprimerait en aucun cas les tests expérimentaux des paramètres intégraux.

Les mesures différentielles contribuent essentiellement à définir des limites réalistes pour les valeurs absolues des données de base et à fournir les variations relatives de ces données en fonction de l'énergie: les calculs des transpositions des paramètres caractéristiques mesurés dans les expériences critiques à ceux des projets peuvent alors être faits avec le minimum d'erreur. Par contre, le recalage global des paramètres intégraux est fait sur les expériences critiques qui permettent d'atteindre les précisions souhaitées par un projet sans qu'il soit nécessaire d'obtenir les mesures différentielles de très grande précision.

REFERENCES

[1] CLAUZON, P.P., et al., «Some neutronic problems related to PHENIX», Paper 2.3, BNES Conf. London (1969) 222.

[2] BLONS, J., et al., «Mesure et analyse des sections efficaces de fission de l'uranium-235 et du plutonium-241, ces comptes rendus, IAEA-CN-26/60.

[3] BARRE, J.Y., RAVIER, J., «Imprécisions des paramètres caractéristiques d'un réacteur rapide de puissance dnes aux incertitudes actuelles concernant les données neutroniques», Fast Reactors Physics I (C.r. Coll. Karlsruhe, 1967), AIEA, Vienne (1968) 205.

[4] BOUCHARD, J., et al., «Mesures intégrales de alpha pour le plutonium-239 et l'uranium-235», ces comptes rendus, IAEA-CN-26/96.

[5] ADAMSON, J., et al., « ZEBRA 6, A dilute plutonium-fuelled assembly », Proc. Int. Conf. on Fast Critical Experiments and their Analysis, Argonne, ANL-7320 (1966) 216.

[6] TILL, C.E., et al., « The Argonne National Laboratory critical experiment programme », Paper 1.3, BNES Conf. London (1969) 40.

[7] GWIN, R., et al., Measurements of the neutron fission and absorption cross sections of ^{239}Pu over the energy region 0.02 eV to 30 keV, NSE-40 (1970) 306.

[8] Meeting of specialists on the value of plutonium α, Winfrith, UK, 30 June - 1 July, Summary Report IAEA/NPR/5 (1969).
[9] L'HERITEAU, J.P., RIBON, P., Examen critique des sections efficaces neutroniques du ^{240}Pu, EANDL-(E) 126-AL (1970).
[10] YIFTAH, S., et al., Nuclear data for ^{240}Pu, ^{241}Pu and ^{242}Pu, IA-1152 (December 1967).
[11] MEYER-HEINE, A., et al., « Analysis of experiments performed in MASURCA », Paper 1.2, BNES Conf. London (1969) 25.
[12] BROOMFIELD, A.M., et al., « Measurements of k infinity reactions rates and spectra in ZEBRA plutonium lattices », Paper 1.1, BNES Conf. London (1969) 5.
[13] BARRE, J.Y., et al., « Lessons drawn from integral experiments on a set of multigroup cross sections », Paper 1.15, BNES Conf. London (1969) 165.
[14] ROWLANDS, J.L., et al., « The use of integral measurements to adjust cross sections and predict reactor properties », Paper 1.16, BNES Conf. London (1969) 180.
[15] HANNA, G.C., et al., Revision of values for the 2200 m/s neutron constants for four fissile nuclides, Atom. Energy Review VII 4 (1969).
[16] MOXON, M.C., The neutron capture cross section of ^{238}U in the energy region 0.5 to 100 keV, AERE-R-6074 (1969).
[17] DAVEY, W.G., An analysis of the neutron capture cross section of ^{238}U between 1 keV and 15 MeV, NSE-39 (1970) 337-60.
[18] SAUSSURE, G., DE, et al., « Measurement of the neutron capture and fission cross-sections and of their ratio alpha for ^{233}U, ^{235}U and ^{239}Pu », Nuclear Data for Reactors II (C.r. Conf. Paris, 1966), AIEA, Vienne (1967) 233.

MESURES INTEGRALES DE ALPHA POUR LE PLUTONIUM-239 ET L'URANIUM-235

J. BOUCHARD, J.Y. BARRE*, M. DARROUZET,
R. BOYER, P. MENESSIER, R. VIDAL
CEA, Centre d'études nucléaires
de Fontenay-aux-Roses,
France

Abstract — Résumé

INTEGRAL MEASUREMENTS OF α FOR ^{239}Pu AND ^{235}U.

Two series of integral experiments on the α of ^{239}Pu have been carried out in the medium-energy range.

a) Reactivity and reaction-rate measurements. These measurements have been carried out in the coupled thermal-fast ERMINE assembly. An original method based on the use of a local chamber with a ^{238}U foil was developed to separate the capture and fission terms. This method, which is less sensitive to imprecision of $\bar{\nu}$ and to important ratios than the boron calibration method used previously, can be used to obtain α for the true dilution of the sample without need for extrapolation to infinite dilution.

b) Irradiation. Two irradiation experiments have been carried out, one in OSIRIS, a 70-MW, swimming-pool reactor, in a boron carbide capsule enriched such that the spectrum at the centre resulted in a high capture rate in the energy range between 1 and 20 keV, and the other one in RAPSODIE, a fast-reactor prototype, whose neutron spectrum corresponds to higher energies.

Various samples of ^{235}U, ^{239}Pu and ^{238}U were irradiated during the two runs, the integrated fluxes for the one having been about 5×10^{21} n/cm^2 and about 1.5×10^{22} n/cm^2 for the other. The classical determinations of the capture rates by measuring the variation of the isotopic contents were supplemented by spectral-index measurements which allowed one to do without knowledge of the yields in determining the fission rates. In the case of the OSIRIS capsules, for which several difficulties in the calculation of the spectrum could be expected, the experimental checks were performed in an identical capsule placed at the centre of the ISIS reactor, a faithful low-power model of OSIRIS.

The results of this set of experiments, some of which are still preliminary – particularly those of RAPSODIE – are compared with the calculations made by the multigroup cross-section set of CADARACHE. For ^{239}Pu the experimental values of α are seen to be, in general, slightly lower than the calculated ones.

MESURES INTEGRALES DE ALPHA POUR LE PLUTONIUM-239 ET L'URANIUM-235.

Deux séries d'expériences intégrales concernant le α du plutonium-239 dans les énergies intermédiaires ont été réalisées.

a) Mesures de réactivité et de taux de réaction. Ces mesures ont été effectuées dans l'assemblage couplé thermique-rapide ERMINE. Une méthode originale basée sur l'utilisation d'une chambre locale à dépôt de ^{238}U a été développée pour séparer les termes de capture et de fission. Moins sensible à l'imprécision sur $\bar{\nu}$ et sur les rapports d'importance que la méthode d'étalonnage par le bore qui a également été utilisée, elle permet de plus d'obtenir α pour la dilution réelle de l'échantillon sans nécessiter une extrapolation à dilution infinie.

b) Irradiations. Deux irradiations ont été effectuées, l'une dans OSIRIS, pile piscine de 70 MW, à l'intérieur d'une capsule en carbure de bore enrichi telle que le spectre au centre conduise à un taux de capture élevé dans le domaine d'énergie compris entre 1 et 20 keV, et l'autre dans RAPSODIE, prototype de réacteur rapide, dont le spectre des neutrons correspond à des énergies plus élevées.

Différents échantillons de ^{235}U, de ^{239}Pu et de ^{238}U ont été irradiés dans ces deux expériences, les flux intégrés étant respectivement de $5 \cdot 10^{21}$ n/cm^2 et de $1,5 \cdot 10^{22}$ n/cm^2. Aux déterminations classiques des taux de capture par mesure de la variation des teneurs isotopiques on a associé des mesures d'indices de spectre permettant de se dispenser de la connaissance des rendements pour la détermination des taux de fission. Dans le cas de la capsule d'OSIRIS, pour lequel on pouvait craindre quelques difficultés dans le calcul du spectre,

* CEA, Centre d'études nucléaires de Cadarache.

on a effectué les vérifications expérimentales dans une capsule identique placée au centre du réacteur ISIS, maquette fidèle, à faible puissance, d'OSIRIS.

Les résultats de cet ensemble d'expériences, dont certains sont encore préliminaires, en particulier ceux de RAPSODIE, sont comparés avec les calculs effectués avec le jeu de sections efficaces multigroupes de CADARACHE. On note pour le ^{239}Pu des valeurs expérimentales de α qui, dans l'ensemble, sont légèrement plus basses que les valeurs calculées.

INTRODUCTION

A la fin de 1967, l'incertitude sur les valeurs du rapport capture sur fission du Plutonium 239, dans les domaines d'énergie intéressant les réacteurs rapides, et principalement autour de 10 keV., était telle qu'un programme de mesures intégrales a été décidé, en deux phases :

- Mesures de α_5 et α_9 dans l'expérience critique ERMINE, à partir des effets en réactivité de petits échantillons, pour obtenir rapidement des valeurs avec une précision de l'ordre de 15%.

- Détermination de ces rapports par irradiations, dans le réacteur à neutrons rapides RAPSODIE et, sous un filtre de bore, dans le réacteur à neutrons thermiques OSIRIS, la première permettant d'obtenir des renseignements sur les valeurs de α pour les hautes énergies et la seconde dans le domaine 1 - 20 keV. Les résultats de ces irradiations qui sont très récents nous donnent des valeurs plus précises.

Les mesures d'ERMINE ont porté sur différentes tailles d'échantillons et, afin de diminuer les parts d'incertitude dues aux techniques expérimentales, aux valeurs de ν et aux calculs d'importance, on a utilisé trois méthodes indépendantes pour déterminer α à partir de l'effet en réactivité.

Par analyse d'échantillons irradiés, plusieurs méthodes permettent également d'obtenir α. On en présente trois, dont deux qui ne font pas intervenir des rendements de fission mais qui nécessitent des mesures d'indices de spectres à l'emplacement de l'irradiation ou dans une position équivalente.

ISIS, maquette à faible puissance du réacteur OSIRIS a permis d'effectuer de telles mesures d'indices, ainsi que de contrôler expérimentalement la validité des calculs effectués pour obtenir le spectre au centre de la capsule de bore.

Dans RAPSODIE, des analyses sur le combustible normal du réacteur, ainsi que sur des petits échantillons irradiés dans une aiguille spéciale, nous ont permis d'obtenir également α_5 et α_9.

Tous les résultats expérimentaux, qui sont présentés ici, sont comparés aux valeurs calculées avec la version la plus récente du jeu de sections efficaces de

CADARACHE dans laquelle, en particulier, l'évaluation de la capture du Pu 239 est basée essentiellement sur les résultats des mesures de GWIN et de SOWERBY.

I - DETERMINATION DE α DANS ERMINE

I.1 - ERMINE

ERMINE est une expérience critique couplée thermique-rapide installée dans la pile MINERVE du Centre de FONTENAY-AUX-ROSES. Après une expérience préliminaire, ERMINE I, [1] , dont les résultats ont montré la validité du principe, quatre milieux uranium-graphite et plutonium-graphite ont été étudiés dans ERMINE 2 [2] , puis, après une investigation sur des milieux uranium-sodium, le programme actuel porte essentiellement sur l'étude de réseaux à $k_\infty = 1$.

Réacteur piscine de puissance nulle, MINERVE a la particularité d'avoir une cavité centrale carrée de dimensions variables, qui se prête particulièrement bien aux expériences couplées. Le milieu à neutrons rapides placé au centre, d'un volume généralement compris entre 20 et 100 litres, est entouré d'une zone de transition comprenant un convertisseur de neutrons thermiques en neutrons rapides et un filtre adaptateur, ce dernier étant redéfini pour chaque milieu étudié.

I.2 - Principe des déterminations de α

A l'exception de ^{238}U, la capture des corps fissiles ne peut être atteinte, en expérience critique, que par des mesures d'effets en réactivité sur de petits échantillons ou par l'étude du bilan neutronique de milieux dans lesquels ces corps jouent un rôle prépondérant. Ces deux approches ont chacune leurs avantages et inconvénients et conduisent à des résultats affectés d'erreurs assez comparables [3, 4] . Le but essentiel de ces mesures étant, pour nous, d'obtenir des résultats assez rapidement, c'est la première approche, la plus simple à mettre en oeuvre, que nous avons choisie.

La mesure de l'effet en réactivité d'un échantillon de corps fissile conduit à un résultat qui peut s'exprimer, pour un atome, sous la forme :

$$\delta k = \frac{1}{J} [W_f \nu \sigma_f \phi - W_a \sigma_f (1 + \alpha) \phi]$$

en supposant δk corrigé des termes de transfert en énergie qui sont au demeurant très faibles.

Parmi les différents termes qui apparaissent dans cette équation, on peut distinguer :

- les constantes dépendant du corps mesuré, α , ν , σ_f

- la normalisation J

- les coefficients W_f et W_a qui correspondent à des valeurs moyennes de l'importance des neutrons, valeurs moyennes sur le spectre de fission pour W_f et sur le spectre d'absorption pour W_a.

Les méthodes utilisées pour déterminer α reposent sur les choix suivants :

- on calcule les coefficients W_f et W_a ou, plus exactement, le rapport W_a/W_f

- on supprime la normalisation J en mesurant δk en relatif par rapport à un autre effet en réactivité

- on cherche une autre relation permettant d'éliminer σ_f, ν étant supposé connu avec une certaine incertitude.

Trois méthodes ont été appliquées :

a) Méthode du bore

Déjà utilisée précédemment [4, 5] , elle consiste à mesurer deux grandeurs :

$$K = \frac{\delta k_X}{\delta k_B} \frac{N_X}{N_B} = \frac{W_f \nu_X \sigma_{fX} - W_a \sigma_{fX} (1 + \alpha_X)}{W_B \sigma_B}$$

$$R = \frac{\sigma_{fX}}{\sigma_B}$$

le résultat expérimental étant le rapport des deux, corrigé des nombres de noyaux, soit :

$$E_1 = \frac{K}{R} \times \frac{N_B}{N_X}$$

Cette méthode introduit une valeur moyenne de l'importance, W_B, qui est pondérée par le spectre d'absorption du bore, et qui est obtenue également par le calcul. A partir des différents termes mesurés ou calculés, on déduit :

$$\alpha_X = \frac{W_f}{W_a} \nu_X - \frac{W_B}{W_a} E_1 - 1$$

b) Méthode du signal local

Dans ce cas, on étalonne la réactivité avec une source de Californium 252 et on détermine le rapport de l'émission des neutrons produits par la fission dans l'échantillon à celle de la source au moyen d'une chambre à dépôt de ^{238}U placée au voisinage

de l'échantillon pendant les mesures d'effet en réactivité. Les deux quantités mesurées sont alors :

$$K = \frac{N_X}{S_{Cf}} \frac{\delta k_X}{\delta k_{Cf}} = \frac{N_X}{S_{Cf}} \frac{W_f \nu_X \sigma_{fX} \phi - W_a \sigma_{fX} (1 + \alpha_X) \phi}{W_f}$$

$$R = \frac{N_X}{S_{Cf}} \cdot \frac{\nu_X \sigma_{fX} \phi}{\chi}$$

S_{Cf} étant le nombre de neutrons émis par la source et χ le rapport d'efficacité, vis-à-vis de la chambre locale, des neutrons émis par la source et de ceux émis par la fission dans l'échantillon.

Le résultat expérimental se présente sous la forme :

$$E_2 = \frac{K}{R}$$

les nombres de noyaux s'éliminant dans le rapport.

L'expression de α est cette fois :

$$\alpha_X = \frac{W_f}{W_a} \nu_X (1 - E_2 \chi) - 1$$

c) Méthode des étalonnages absolus

On étalonne comme précédemment la réactivité avec une source de ^{252}Cf, mais on effectue ensuite deux mesures absolues, l'une pour déterminer le taux de fission, l'autre pour connaître le nombre de neutrons émis par la source.

On a donc cette fois trois résultats expérimentaux :

$$K = \frac{N_X}{S_{Cf}} \frac{W_f \nu_X \sigma_{fX} \phi - W_a \sigma_{fX} (1 + \alpha_X) \phi}{W_f}$$

$$R = N'_X \sigma_{fX} \phi \qquad \text{et} \qquad S_{Cf}$$

(N'_X étant le nombre de noyaux du dépôt de la chambre à fission)
qui peuvent se résumer en un seul :

$$E_3 = \frac{K}{R} \frac{N'_X S_{Cf}}{N_X}$$

la valeur de α étant alors obtenue par :

$$\alpha_X = \frac{W_f}{W_a} (\nu_X - E_3) - 1$$

1.3 - Mise en oeuvre expérimentale

a) Configuration (fig. 1)

Les mesures de α ont été effectuées dans un bloc de graphite de 8 cm d'arête, placé au centre du coeur U2 dans l'expérience ERMINE 2. Les compositions du réseau U2 sont données dans le tableau I.

Le choix du bloc de graphite a été guidé par la volonté d'obtenir un spectre suffisamment dégradé pour que le maximum du taux de capture soit au voisinage de 1 keV, et par la nécessité de découpler les structures fines aux énergies de résonance entre les barreaux combustibles du réseau et les échantillons placés au centre de la cavité.

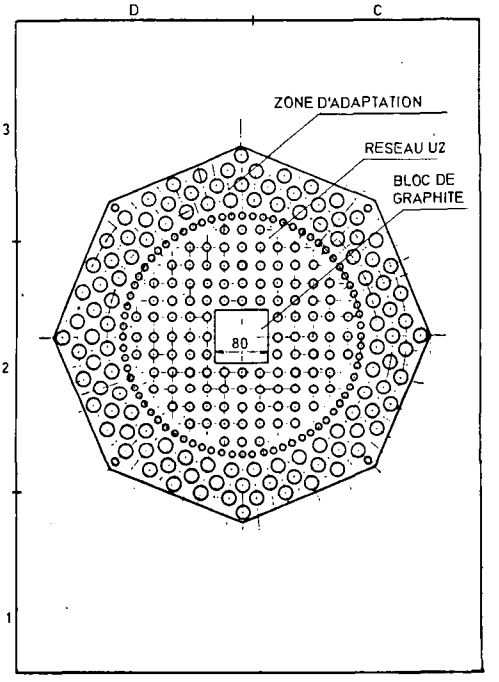

FIG.1. Schéma de la configuration.

TABLEAU I : COMPOSITIONS DU RESEAU U2

	^{235}U	^{238}U	C	Fe	Cr	Ni
Nombre d'atomes par cm^3 x 10^{-24}	$2,522.10^{-3}$	$5,810.10^{-3}$	$5,669.10^{-2}$	$4,120.10^{-3}$	$1,106.10^{-3}$	$0,911.10^{-3}$

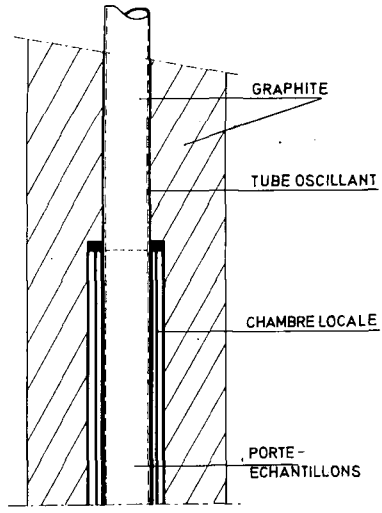

FIG.2. Dispositif expérimental.

b) Effets en réactivité

Ils sont mesurés par la technique d'oscillations avec une barre de pilotage automatique [6] . L'échantillon est placé dans un volume vide entre deux continuités de graphite, à l'intérieur d'un tube Ø 17 mm. Le schéma de ce dispositif est représenté sur la figure 2.

L'effet des neutrons émis par la source de Cf est mesuré en effectuant la détermination de l'effet en réactivité à plusieurs puissances.

c) Taux de réaction

L'indice $\sigma_{cB} / \sigma_{fX}$ utilisé dans la première méthode est mesuré à l'aide de chambres, avec étalonnage en colonne thermique. Les chambres à fission sont de type cylindrique avec un diamètre de 1,5 , 4, ou 10 mm, suivant l'utilisation. Pour la capture du bore, on utilise des compteurs à BF_3 ainsi que des chambres à dépôt du même type que les chambres à fission.

Dans tous les cas, les spectres d'impulsions délivrées par les chambres, obtenus grâce à un sélecteur d'amplitudes, sont enregistrés et une méthode de dépouillement de ces spectres a été mise au point pour s'affranchir des réglages et des dérives de l'appareillage électronique, et pour vérifier la validité des mesures ainsi effectuées [7] .

d) Signal local

Pour la mesure du signal local utilisé dans la seconde méthode, on utilise une chambre annulaire placée au centre du bloc, le tube oscillant la traversant de part en part (fig. 2). Cette chambre a été réalisée avec un dépôt d'uranium très appauvri en

^{235}U. Les impulsions qu'elle délivre sont amplifiées par une électronique rapide et analysées par le même appareillage que le signal de réactivité.

e) Etalonnages absolus

La troisième méthode nécessite deux mesures absolues. Pour le taux de fission, on détermine la masse du dépôt d'une chambre à fission, du type chambre plate, par comptages alpha. Le nombre de neutrons émis par la source de Californium est mesuré par la méthode du bain de sulfate de manganèse [8] .

f) Echantillons

Les principales caractéristiques des échantillons d'uranium et de plutonium utilisés pour ces mesures sont données dans le tableau II.

TABLEAU II : CARACTERISTIQUES DES ECHANTILLONS

Isotope mesuré	Nature de l'échantillon	Diamètre (mm) ou épaisseur	Longueur (mm)	$\overline{l}\,N$ (10^{21} cm^{-2})
^{235}U	U à 93% tube mince	0,1	100	1,79
^{235}U	U à 93% cylindre	1,9	101,6	8,43
^{235}U	U à 92% cylindre	4	50	17,0
^{235}U	U à 92% cylindre	6	50	25,0
^{235}U	U à 92% cylindre	9	50	36,4
^{235}U	U à 92% cylindre	12,7	50,8	49,8
^{239}Pu	Pu à 99% tube mince	0,1	100	1,70
^{239}Pu	Pu à 99% cylindre	1,9	100	6,9
^{239}Pu	Pu à 98% cylindre	4	50	18,2
^{239}Pu	Pu à 98% cylindre	6	50	26,8
^{239}Pu	Pu à 98% cylindre	12,1	30,5	47,8

$\overline{l} = \frac{4V}{S}$ = corde moyenne N = nombre d'atomes de l'isotope principal par cm^3 d'échantillon

1.4 - Précision

Les erreurs expérimentales sont présentées dans le tableau III et le tableau IV résume l'ensemble des causes d'incertitude, avec leur incidence sur le résultat pour les différentes méthodes, dans un cas particulier correspondant à une valeur de α de l'ordre de 0,5.

TABLEAU III : ERREURS EXPERIMENTALES (EN %)

Paramètre / Méthode	$\frac{\delta k_X}{\delta k_y}$	$\frac{\sigma B}{\sigma fX}$	$\frac{N_X \nu_X \sigma_{fX}^{\emptyset}}{S_{Cf}}$	$N'_X \sigma_{f_X}^{\emptyset}$	N_X	N_B	N'_X	N_{Cf}
bore	3 *	3	-	-	0,3	1	-	-
signal local	1 à 2	-	2 à 3	-	-	-	-	-
étalonnages absolus	3 *	-	-	0,5	0,3	-	2	2

* Les erreurs sont plus importantes en raison des extrapolations à dilution infinie

TABLEAU IV : PRECISION DES MESURES DE α (POUR $\alpha = 0,5$)

Paramètre	Précision %	Erreur sur α (%)		
		bore	local	Etalonnages
E	3		5,4	
	4,5	8,1		8,1
ν	1,5	7,2	4,5	7,2
a/b	2	9,6	6,0	9,6
c/b	1	1,8	-	-
X	3	-	5,4	-
Erreur totale sur α		15	11	15

Les précisions expérimentales sont celles qui ont été obtenues au cours de cette série de mesures [9] . Pour ν et X les précisions indiquées correspondent aux incertitudes actuelles sur les résultats des mesures différentielles et sont donc susceptibles d'amélioration. Enfin, pour les rapports d'importance, on s'est basé, pour évaluer les erreurs possibles, sur les résultats obtenus dans la mesure du rapport d'importance des neutrons émis respectivement par une source de ^{252}Cf et par une source Sb-Be.

1.5 - Discussion des méthodes

Ces méthodes ont une base commune, l'effet en réactivité. Pour ce qui les sépare, on peut comparer leurs avantages respectifs de plusieurs points de vue :

Dans la méthode du bore, comme dans celles des étalonnages absolus, le taux de fission est atteint à l'aide de chambres à fission, donc σ_f dans la seconde relation correspond à la dilution infinie. Il doit en être de même pour la première relation, ce qui implique que l'effet en réactivité soit mesuré pour la dilution infinie. Ainsi qu'on le verra dans les résultats, ceci est un inconvénient assez important.

Dans la seconde méthode, les deux valeurs expérimentales sont mesurées à partir des mêmes échantillons, ce qui évite ce problème, et on obtient alors des valeurs de α correspondant aux conditions de dilution des échantillons considérés. Cette méthode du signal local est également la seule pour laquelle le résultat ne fait intervenir aucun nombre de noyaux, ce qui entraîne que la connaissance des échantillons n'a pas besoin d'être très précise.

Par contre des corrections sont nécessaires pour obtenir les valeurs expérimentales sous la forme simplifiée adoptée dans cette présentation, le signal local n'étant pas exclusivement sensible à la fission.

Les incertitudes sur les valeurs de ν et sur les calculs d'importance ne sont éliminées dans aucun cas ; cependant, ainsi qu'on peut le voir dans le tableau IV, leur incidence sur le résultat est nettement plus faible dans la méthode du signal local.

Enfin, les spectres d'émission du Californium et de fission de l'Uranium ou du Plutonium n'étant pas rigoureusement identiques, un facteur de correction χ a été introduit dans la méthode du local, la réponse de la chambre étant particulièrement sensible à ces différences. Ce facteur ne peut être connu avec précision et l'erreur qui lui a été appliquée est importante pour le résultat.

Finalement, ces trois méthodes conduisent à des précisions voisines et leur mise en oeuvre simultanée a essentiellement permis de s'assurer que les erreurs sur un certain nombre de valeurs expérimentales ou calculées n'excèdaient pas celles qui avaient été prévues.

Les résultats intéressants pour l'interprétation sont ceux qui ont été acquis pour plusieurs échantillons par la méthode du signal local, qui, en raison de la cohérence des résultats, permet de garantir une précision de 10%.

I.6 - Résultats

a) Vérification des conditions de calcul du spectre

L'utilisation d'un bloc de graphite au centre de l'assemblage a nécessité de vérifier que les erreurs sur le calcul des conditions neutroniques au centre de ce bloc n'étaient pas supérieures à celles que l'on obtient normalement pour un réseau. On a donc comparé les rapports calcul sur expérience, pour quelques indices de spectre, au centre du bloc de graphite placé dans le réseau U2 et au centre de ce réseau non perturbé. Ces résultats sont présentés dans le tableau V.

TABLEAU V : COMPARAISON CALCUL EXPERIENCE DES INDICES DE SPECTRE

Indice	Valeur mesurée	Rapports calcul expérience	
		Bloc de graphite	Réseau U2
$\overline{\sigma_{f8}}/\overline{\sigma_{f5}}$	0,0161 ± 0,0002	0,92 ± 0,01	0,94 ± 0,01
$\overline{\sigma_{f9}}/\overline{\sigma_{f5}}$	0,98 ± 0,01	1,01 ± 0,01	1,00 ± 0,01
$\overline{\sigma_{c8}}/\overline{\sigma_{f5}}$	0,234 ± 0,006	1,08 ± 0,03	0,94 ± 0,03

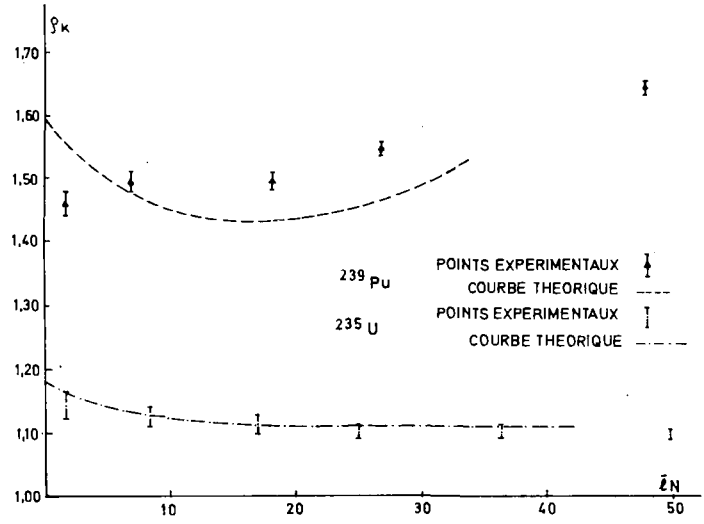

FIG.3. Effets en réactivité.

b) Effets en réactivité de l'uranium 235 et du plutonium 239

L'effet en réactivité étant à la base de toutes les méthodes, il est intéressant de comparer à ce stade le calcul et l'expérience. Les effets mesurés étant relatifs, il a été choisi comme normalisation commune du calcul et de l'expérience le résultat obtenu avec l'échantillon d'uranium 235 Ø 4 mm. Les courbes de la figure 3 permettent de faire deux constatations :

- Le rapport plutonium sur uranium est en moyenne en bon accord, à l'exception du plus petit échantillon.

- La courbe expérimentale de ^{235}U, en fonction de la taille des échantillons, est voisine de la courbe calculée alors que pour le plutonium le désaccord est important, en particulier au voisinage de l'origine où on ne constate pas par l'expérience une remontée semblable à celle de la courbe calculée.

c) Valeurs de α_5 et α_9

Sur les courbes des figures 4 et 5, on compare l'expérience et le calcul pour les variations de α en fonction de la taille des échantillons. Les valeurs expérimentales sont calculées avec le jeu CADARACHE dans sa version la plus récente [10], la capture du plutonium étant basée essentiellement sur les résultats des mesures de GWIN [11]. Les barres d'erreurs apparaissant sur ces courbes sont uniquement celles à prendre en compte pour la comparaison des différents points entre eux.

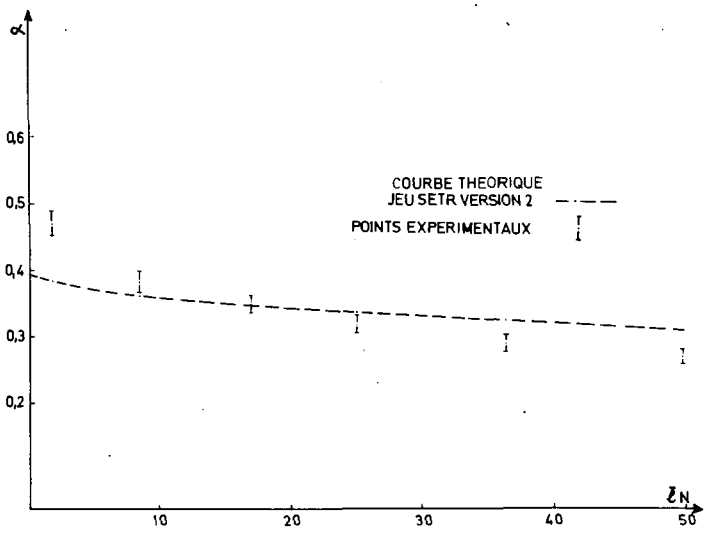

FIG.4. Valeurs de α (uranium-235).

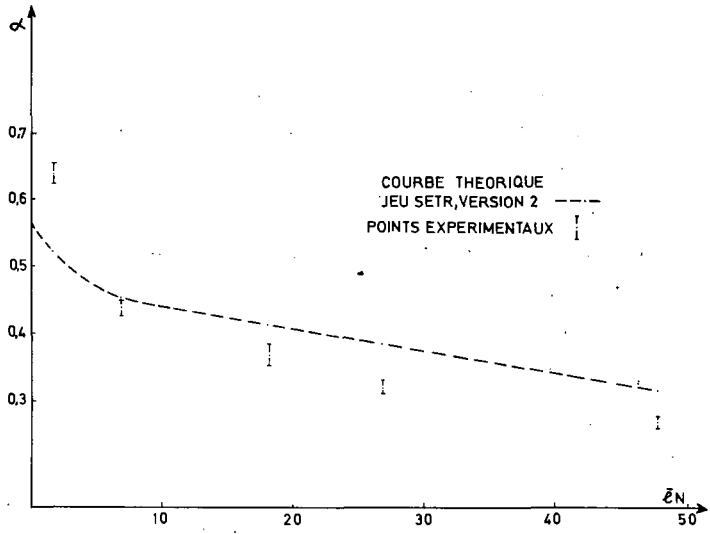

FIG.5. Valeurs de α (plutonium-239).

Le recoupement entre les trois méthodes a été effectué après extrapolation des résultats à dilution infinie. Les valeurs relatives obtenues pour les deux autres méthodes par rapport aux résultats du signal local sont données dans le tableau VI et on constate que ce recoupement est satisfaisant, compte tenu des précisions.

Les incertitudes totales à prendre en compte pour comparer chacune des valeurs de α à des valeurs obtenues à partir des mesures différentielles ou d'autres mesures intégrales sont données dans le tableau VII qui résume les résultats.

Des différents résultats apparaissant ici, on peut déduire plusieurs conclusions :

- le recoupement satisfaisant des trois méthodes justifie les ordres de grandeur adoptés pour les différentes incertitudes et exclut une explication expérimentale d'écarts dépassant notablement les barres d'erreurs sauf, bien sûr, si cette explication peut être trouvée dans la réactivité, ce qui paraît peu probable compte tenu des nombreux recoupements qui ont été effectués.

- On constote que les valeurs obtenues pour α_5 sont compatibles avec les valeurs calculées, dans la limite des barres d'erreurs, à l'exception de celle correspondant au plus petit échantillon.

TABLEAU VI : RECOUPEMENT DES TROIS METHODES DE MESURE

	Uranium 235	Plutonium 239
bore	$0,98 \pm 0,12$	$1,04 \pm 0,12$
étalonnages absolus	$0,90 \pm 0,12$	$0,96 \pm 0,12$

TABLEAU VII : VALEURS DE α MESUREES DANS ERMINE

^{235}U				^{239}Pu			
Echantillon				Echantillon			
Ø ou e	$\bar{I}$ N	α_5 mesuré	α_5 calc.	Ø ou e	$\bar{I}$ N	α_9 mesuré	α_9 calc.
0,1	1,79	$0,47 \pm 0,05$	0,385	0,1	1,70	$0,64 \pm 0,07$	0,521
1,9	8,43	$0,38 \pm 0,05$	0,360	1,9	6,9	$0,44 \pm 0,05$	0,457
4	17,0	$0,35 \pm 0,04$	0,347	4	18,2	$0,37 \pm 0,04$	0,414
6	25,0	$0,32 \pm 0,04$	0,336	6	26,8	$0,32 \pm 0,04$	0,384
9	36,4	$0,29 \pm 0,04$	0,323	12,1	47,8	$0,27 \pm 0,04$	0,318
12,7	49,8	$0,27 \pm 0,04$	0,311				

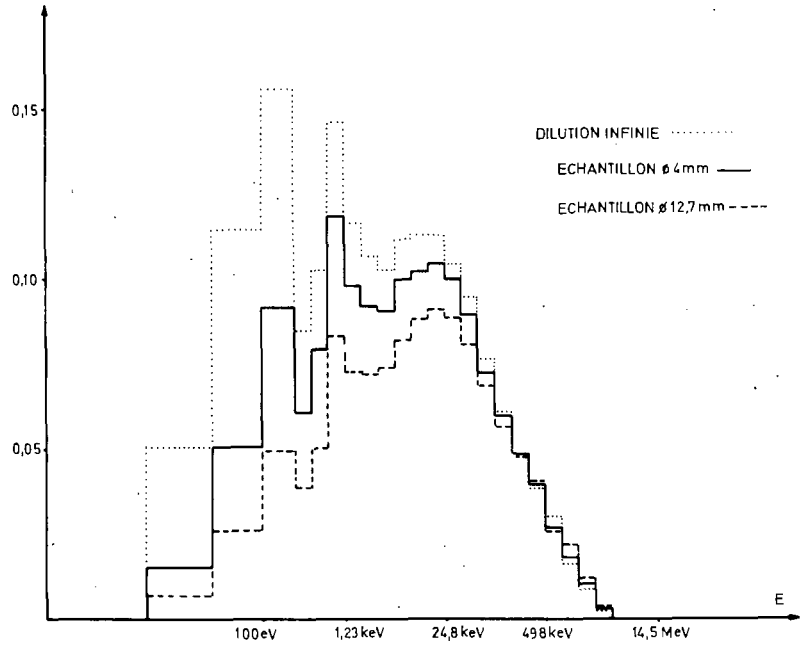

FIG. 6. Taux de capture de l'uranium-235.

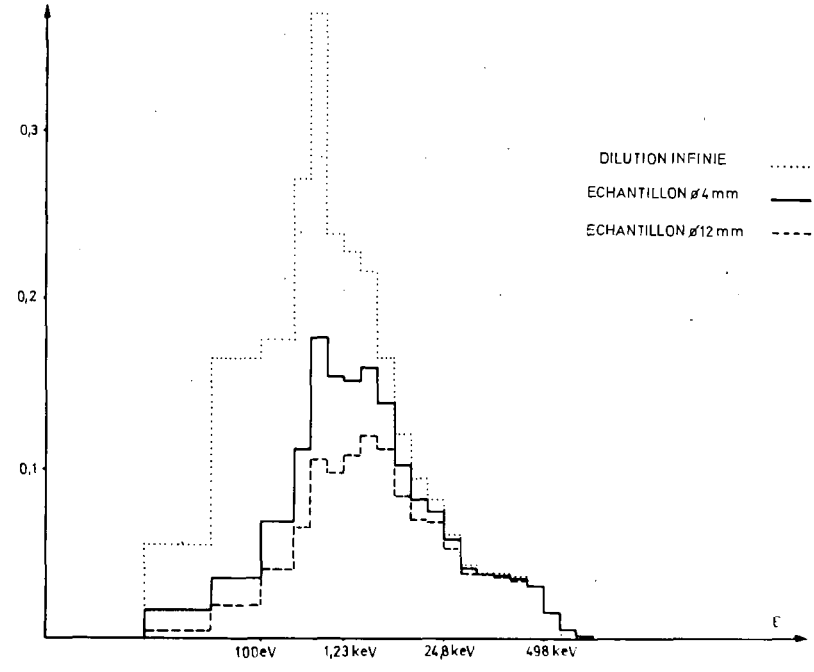

FIG. 7. Taux de capture du plutonium-239.

- Pour le plutonium 239, la variation de α_9 en fonction de la taille des échantillons est beaucoup plus importante dans les résultats expérimentaux que pour les valeurs calculées.

- En fait la variation de taille des échantillons entraîne, non seulement une variation de dilution, mais également une variation du spectre sur lequel est déterminé α. Ceci ressort nettement dans la comparaison de la répartition des taux de capture présentée sur les figures 6 et 7. On constate que pour une très grande dilution, comme c'est le cas pour le plus petit échantillon de ^{235}U ou de ^{239}Pu, les absorptions au dessous de 1 keV, et plus particulièrement au voisinage de 200 eV, sont très importantes. Les méthodes de calcul et le jeu de constantes utilisé ne sont pas spécialement bien adaptés dans ce domaine d'énergie qui intéresse peu les réacteurs rapides.

- Les résultats les plus importants sont ceux des échantillons de diamètre au moins égal à 4 mm pour lesquels la part du taux de capture entre 1 et 20 keV est supérieure à 40%. Ces résultats traduisent pour le ^{235}U un accord satisfaisant avec le calcul, cependant que pour le ^{239}Pu, les valeurs expérimentales sont dans l'ensemble plus faibles que les valeurs calculées, l'écart, voisin de 15%, dépassant légèrement l'incertitude de mesure ou l'écart plus faible, 7% en moyenne, constaté sur α_5.

II - DETERMINATION DE α PAR IRRADIATIONS

La possibilité d'obtenir α_5 et α_9 par analyses de combustibles irradiés dans RAPSODIE, aussi intéressante qu'elle soit par les informations qu'elle procure sur les sections efficaces à haute énergie, ne répondait pas entièrement au problème posé, la participation du domaine 1 - 20 keV aux taux de réaction étant alors très faible. C'est pourquoi, parallèlement à cette étude des combustibles de RAPSODIE, on a effectué une irradiation sous filtre de bore dans le réacteur thermique OSIRIS.

Ces expériences d'irradiation permettent d'obtenir de très bonnes précisions : ce sont toutefois des méthodes très délicates et le risque d'erreurs systématiques y est particulièrement élevé. C'est pourquoi nous nous sommes attachés, ici encore, à multiplier les déterminations indépendantes d'un même paramètre, chaque fois que nous en avions la possibilité.

Les paramètres que l'on atteint aisément par examen des combustibles irradiés ne sont pas les mêmes que ceux que l'on peut obtenir sans grande difficulté par des mesures de taux de réaction classiques en expérience critique. Il nous est apparu qu'une combinaison des deux pourrait être fructueuse et les résultats qui sont présentés ici y font largement appel.

II.1 - Principe des déterminations de α

Pour déterminer les taux de capture, on utilise, pour l'uranium 235 la variation de la teneur en ^{236}U, et pour le plutonium 239 la variation de la teneur en ^{240}Pu. Il faut que les teneurs initiales, respectivement en ^{236}U ou en ^{240}Pu, soient suffisamment faibles et que le taux d'irradiation soit compatible avec la précision des mesures de teneur isotopique. Ces conditions ont pu être remplies aussi bien pour OSIRIS que pour RAPSODIE.

En ce qui concerne le taux de fission, la détermination est plus compliquée et dans l'examen de ces irradiations nous avons retenu trois solutions pour l'atteindre :

a) Formation de Néodyme 148

L'analyse par la méthode de double dilution isotopique permet d'obtenir le rapport de la quantité de ^{148}Nd formée à la quantité d'un des isotopes fissiles présent dans le combustible.

Si le combustible ne contient qu'un élément fissile, noté X, et si le rendement en ^{148}Nd de la fission, pour cet isotope et pour les conditions de fission correspondant à l'irradiation, est γ_X, on peut alors écrire en négligeant tous les termes de second ordre

$$\sigma_{fX}\tau = \frac{1}{\gamma_X} \frac{N_{148}}{N_X}$$

τ étant le flux intégré.

b) Disparition de l'uranium 235

On effectue deux analyses isotopiques, l'une à l'état initial, l'autre à l'état irradié, d'un échantillon d'uranium enrichi en ^{235}U. On a, en première approximation :

$$\sigma_{f5}\tau = \frac{\left(\frac{1-N_8}{N_8}\right)_0 - \left(\frac{1-N_8}{N_8}\right)_F}{\left(\frac{N_5}{N_8}\right)_0 + \left(\frac{N_4}{N_8}\right)_0 \frac{\sigma_{f4}}{\sigma_{f5}} + \left(\frac{N_6}{N_8}\right)_0 \frac{\sigma_{a6}}{\sigma_{f5}} - \left(\frac{1-N_8}{N_8}\right)_F \frac{\sigma_{a8}}{\sigma_{f5}}}$$

les indices 0 et F désignant respectivement les valeurs initiales et finales.

Les termes correctifs, en $(\frac{N_4}{N_8})_0 \frac{\sigma_{f4}}{\sigma_{f5}}$ et $(\frac{N_6}{N_8})_0 \frac{\sigma_{a6}}{\sigma_{f5}}$ sont faibles si le combustible initial est bien choisi ; par contre le rapport σ_{a8}/σ_{f5} a une contribution plus importante puisque l'on mesure la variation du ^{235}U par rapport à celle du ^{238}U et il est souhaitable de l'obtenir expérimentalement.

Cette méthode, qui pose surtout des problèmes de précision, n'est pas applicable pour le ^{239}Pu, d'une port parce que les analyses isotopiques du plutonium n'atteignent pas la très forte précision nécessaire pour utiliser cette méthode, et d'autre part parce qu'il faudrait alors prendre comme référence le ^{240}Pu dont nous ne pouvons pas encore déterminer la disparition.

Par contre en mesurant le rapport σ_{f9}/σ_{f5} par une autre méthode, on déduit :

$$\sigma_{f9}\,\tau = \sigma_{f5} / \frac{\sigma_{f9}}{\sigma_{f5}}$$

c) Capture de l'uranium 238

La détermination du taux de capture du ^{238}U est obtenue par la mesure sur un échantillon d'uranium appauvri irradié, du rapport Pu/U par double dilution isotopique.

Si on dispose de la valeur expérimentale du rapport σ_{c8}/σ_{fX}, indice de spectre qui se mesure assez couramment en expérience critique, on obtient :

$$\sigma_{fX}\,\tau = \sigma_{c8}\,\tau\,\frac{\sigma_{fX}}{\sigma_{c8}}$$

d) Discussion de ces méthodes

La méthode du néodyme n'est pratiquement applicable qu'à des combustibles "purs", ne contenant qu'un seul élément fissile. De plus, son principal inconvénient réside dans les rendements de fission, qui sont connus avec une assez bonne précision pour la fission par des neutrons thermiques, mais demeurent encore très imprécis pour la fission par des neutrons rapides.

En fait la mesure du néodyme dans les irradiations considérées ici apporte deux éléments :

- des mesures relatives du taux de fission entre les différents échantillons de même nature irradiés simultanément,

- une amélioration de la connaissance des rendements de cet élément dans les différentes fissions pour deux spectres de neutrons rapides qui couvrent à peu près

le domaine d'énergie correspondant aux réacteurs expérimentaux et aux réacteurs de puissance.

La mesure de la disparition de l'U 235, lorsqu'on dispose d'irradiations suffisamment longues pour que l'incertitude sur la variation des teneurs isotopiques n'affecte pas trop la précision du résultat, permet une détermination directe de α_5 dans un combustible quelconque, même s'il est mixte comme celui de RAPSODIE. Elle nécessite par contre des analyses très soignées des échantillons avant et après irradiation.

L'utilisation d'indices de spectre, mesurés au point d'irradiation ou en un point équivalent, que nous introduisons dans la seconde méthode pour obtenir un taux de fission autre que celui du ^{235}U, et qui constitue la base de la troisième méthode, est la plus intéressante car la plus précise pour le développement des mesures intégrales par irradiation dans le domaine des réacteurs à neutrons rapides.

Il se trouve en effet que certains rapports, comme σ_{f9}/σ_{f5} par exemple, se mesurent avec une bonne précision à l'aide de chambres à fission, alors que pour les déduire de l'analyse d'échantillons irradiés on rencontre de grosses difficultés. Par contre l'irradiation permet d'obtenir dans de bonnes conditions les taux de capture des éléments fissiles qui sont très difficiles à atteindre en expérience critique, si on excepte celui de l'U 238. La combinaison de ces deux techniques que nous présentons ici constitue une solution séduisante susceptible de nombreuses autres applications.

e) Précision des mesures

Dans la présentation des résultats de ces irradiations nous utilisons pour le calcul des précisions les erreurs de mesure regroupées dans le tableau VIII. [13]

TABLEAU VIII - PRECISION DES ANALYSES

PARAMETRE LIMITES DE PRECISION	$\frac{N_6}{N_5}$	$\frac{N_8}{1-N_8}$	$\frac{N_0}{N_9}$	$\frac{N_9}{N_8}$	$\frac{N_{148}}{N_X}$
RELATIVE (%)	0,5	0,1	0,5	0,7	1,5
ABSOLUE (ppm)	30		30		

II.2 - Irradiation OSIRIS

OSIRIS est un réacteur d'irradiation, d'une puissance de 70 MW, du type piscine, installé au Centre de SACLAY. Ce réacteur est pourvu de canaux expérimentaux dans le coeur et les réflecteurs. L'irradiation " α " a été effectuée dans un canal

central, les échantillons étant disposés dans une capsule en carbure de bore enrichi à 90 % en bore 10, d'épaisseur 1 cm environ.

Ce réacteur dispose à ses côtés d'une maquette, ISIS, de plus faible puissance, qui simule exactement le coeur d'OSIRIS, y compris, si nécessaire, avec les éléments combustibles irradiés. La présence de cette maquette nous a apporté deux possibilités très importantes :

- la mesure des indices de spectre qui, combinés avec les résultats d'analyses, permettent d'obtenir les valeurs de α par les méthodes décrites auparavant,

- la réalisation d'un certain nombre de mesures destinées à vérifier les calculs de spectre à l'intérieur de la capsule de bore.

En effet le choix d'un dispositif expérimental relativement simple, comme celui qui a été adopté ici, n'a de valeur que dans la mesure où on est à même de vérifier le calcul que l'on en fait et, au besoin, de modifier les méthodes utilisées pour que ce calcul soit aussi représentatif que possible. Ce n'est qu'à cette condition que les valeurs de α mesurées peuvent constituer une contribution intéressante.

a) Vérification du spectre calculé

On a mesuré sur ISIS plusieurs indices de spectre, dans les conditions exactes de l'irradiation, à l'intérieur d'une capsule de bore identique à celle d'OSIRIS. Les résultats sont présentés dans le tableau IX et comparés avec les valeurs calculées et le rapport calcul/expérience est confronté avec ceux obtenus par les mêmes méthodes dans différents réseaux étudiés dans MASURCA ou dans ERMINE. On constate que l'approximation du calcul est tout à fait du même ordre pour ISIS que pour les autres expériences.

TABLEAU IX - INDICES DE SPECTRE MESURES DANS ISIS

Indice	Mesure	Calcul	Rapport calcul/expérience	
			ISIS	autres expériences
σ_{f8}/σ_{f5}	0,0885 ± 0,0008	0,0818	0,92 ± 0,01	0,92 à 1,05
σ_{f9}/σ_{f5}	1,096 ± 0,010	1,101	1,005 ± 0,010	0,98 à 1,03
σ_{f3}/σ_{f5}	1,47 ± 0,02	1,53	1,04 ± 0,02	
σ_{f0}/σ_{f5}	0,394 ± 0,016	0,467	1,18 ± 0,05	0,96 à 1,10
σ_{f1}/σ_{f5}	1,36 ± 0,03	1,50	1,10 ± 0,03	1,13 à 1,22
σ_{c8}/σ_{f5}	0,134 ± 0,004	0,127	0,95 ± 0,03	0,91 à 0,98

On a aussi vérifié que ces indices variaient peu entre un coeur neuf et un coeur irradié, ainsi que le calcul le prévoyait, et que le spectre au point d'irradiation n'était pas sensible aux mouvements des barres de compensation du réacteur.

On a également effectué des mesures de spectre, à l'aide d'un spectromètre à protons de recul, dans une capsule de plus grandes dimensions mais de même épaisseur [14] . Les résultats sont également en bon accord avec le spectre calculé, ce qui constitue une vérification intéressante, même si le domaine d'énergie contrôlé n'est pas exactement celui qui correspond au maximum du taux de capture de l'uranium 235 ou du plutonium 239.

b) Echantillons irradiés

On a irradié de petits échantillons d'oxyde d'uranium appauvri et enrichi et de plutonium à différentes compositions isotopiques. Les quantités d'oxyde étaient de l'ordre de quelques dizaines de mg à un g, et l'irradiation a fourni un flux intégré, à l'intérieur du filtre de bore, de l'ordre de 5.10^{21} n/cm^2, ce qui correspond à un taux de combustion légèrement supérieur à 1 % pour l'uranium 235.

Il y avait deux ou trois échantillons de chaque nature, de manière, d'une part à recouper les résultats et d'autre part à obtenir la courbe de répartition de flux à l'intérieur de la capsule.

Le détail des échantillons est donné dans le tableau X

c) Résultats

Les différents taux de réaction obtenus à partir des analyses sont présentés dans le tableau XI.

La valeur de σ_{c8}/σ_{f5} , mesurée dans ISIS, telle qu'elle apparaît dans le tableau IX doit être augmentée de 3,5 % pour prendre en compte :

TABLEAU X : ECHANTILLONS IRRADIES DANS OSIRIS ET RAPSODIE

Nature	Composition initiale
U enrichi à 90 %	U 234 : 1,06 %, U 235 : 90,12 %, U 238 : 8,81 %
U enrichi à 80 %	U 234 : 0,58 %, U 235 : 79,32 %, U 238 : 20,10 %
U enrichi à 60 %	U 234 : 0,38 %, U 235 : 59,86 %, U 236 : 0,47 %, U 238 : 39,29 %.
Pu à 0,1 %	Pu 240/Pu 239 = 1350 ppm
Pu à 1 %	Pu 239 : 98,52 %, Pu 240 : 1,41 %, Pu 241 : 0,07 %
U oppauvri	U 235/U 238 : 370 ppm

TABLEAU XI : RESULTATS D'ANALYSES OSIRIS

Echantillons	Nombre	Taux de réaction	Résultat
Uranium enrichi	5	$\sigma_{c5}\,\tau$	1990 ± 40 ppm
Plutonium	3	$\sigma_{c9}\,\tau$	1890 ± 60 ppm
Uranium appauvri	3	$\sigma_{c8}\,\tau$	1205 ± 10 ppm
Uranium enrichi	5	$\gamma_5\ \sigma_{f5}\,\tau$	137,4 ± 2,7 ppm

TABLEAU XII : α MESURES DANS OSIRIS

Paramètre	Mesure	Calcul
α_5	0,230 ± 0,012	0,227
α_9	0,199 ± 0,012	0,215

TABLEAU XIII : DECOMPOSITION DES ERREURS

Cause d'erreur	Incertitude
Détermination de $\sigma_{c8}\,\tau$	0,7 %
Equivalence capsules OSIRIS et ISIS	2 %
Mesure de σ_{c8}/σ_{f5} dans ISIS	3 %
Mesure de σ_{f9}/σ_{f5} dans ISIS	1 %
Détermination de $\sigma_{c5}\,\tau$	2 %
Détermination de $\sigma_{c9}\,\tau$	3 %
Détermination de $\gamma_5\ \sigma_{f5}$ avec correction du Nd formé dans l'U 238 et U 234	2 %

- la dilution de l'U 238 de la pastille d'oxyde irradiée qui n'est pas exactement la même que celle du détecteur utilisé pour les mesures d'ISIS

- la température dans l'échantillon irradié qui était de 600 °C, alors que la mesure dans ISIS a été faite à la température normale.

Les valeurs de α_5 et α_9 obtenues sont données dans le tableau XII, avec la décomposition des différentes erreurs dans le tableau XIII.

On constate un très bon accord avec le calcul pour α_5 cependant que la valeur obtenue pour α_9 est surestimée par le calcul, d'environ 8 % c'est-à-dire un peu plus que l'erreur expérimentale.

II.3 - Irradiation RAPSODIE

a) Conditions de mesure

L'irradiation de petits échantillons dans des aiguilles spéciales disposées à l'intérieur de certains assemblages de RAPSODIE nous a permis d'obtenir les valeurs de α_5 et α_9 pour le spectre de ce réacteur.

Le problème de la validité du spectre calculé ne se pose évidemment pas comme dans le cas de la capsule d'OSIRIS. Par contre il n'a pas été possible de mesurer dans RAPSODIE les indices de spectre, $\overline{\sigma_{f9}}/\overline{\sigma_{f5}}$ et $\overline{\sigma_{c8}}/\overline{\sigma_{f5}}$, et nous n'avons donc pas pu utiliser dans ce cas la méthode basée sur la capture de U 238.

Le taux d'irradiation atteint étant très élevé, la détermination de la disparition de U 235 par fission a été précise et c'est à partir de cette détermination et de celle de la capture par la teneur en U 236 que l'on obtient α_5. Pour le Pu 239 on a mesuré la formation de Pu 240 et on a déterminé α_9 à partir de α_5 en utilisant le rapport $\overline{\sigma_{f9}}/\overline{\sigma_{f5}}$ calculé.

Les échantillons irradiés étaient à quelques exceptions près les mêmes que dans OSIRIS (voir tableau X).

b) Résultats

Les valeurs qui apparaissent dans le tableau XIV correspondent à des résultats préliminaires, toutes les analyses sur les échantillons irradiés dans RAPSODIE n'étant pas achevées. Elles sont, en particulier, affectées de marges d'erreur qui devraient être réduites en tenant compte de tous les résultats.

TABLEAU XIV : α MESURES DANS RAPSODIE

Paramètre	Mesure	Calcul
α_5	$0,190 \pm 0,008$	0,203
α_9	$0,099 \pm 0,007$	0,108

La décomposition des erreurs est voisine de celle donnée dans le tableau XIII pour les résultats d'OSIRIS, à l'exception de la détermination directe de $\sigma_{f5}\,\tau$ qui est affectée d'une incertitude de 3 % et de la valeur de $\overline{\sigma_{f9}}/\overline{\sigma_{f5}}$ pour laquelle on a estimé une erreur possible de 3 % sur la valeur calculée.

Les résultats du tableau XIV font apparaître des valeurs expérimentales plus faibles que les valeurs calculées, de 6 % pour α_5 et 9 % pour α_9.

II.4 - Rendement de fission du Nd 148 :

La mesure de la formation de Nd dans les échantillons d'uranium enrichi irradiés dans OSIRIS et RAPSODIE nous a permis de déterminer le rendement de cet isotope pour la fission de U 235 dans des spectres voisins de ceux des réacteurs de puissance à neutrons rapides. La valeur obtenue :

$$\gamma_5 = 1,65 \pm 0,06$$

est identique à celle que nous avons obtenue dans les irradiations par des neutrons thermiques. Nous la comparons dans le tableau XV à celles qui ont été précédemment publiées pour un spectre thermique et pour un spectre de fission [15].

TABLEAU XV : RENDEMENTS DE FISSION DU Nd 148

Conditions de fission	γ_5	Référence
Neutrons thermiques	1,67	[15]
Neutrons de fission	1,75	[15]
Neutrons de réacteur thermique ou rapide	1,65 ± 0,06	ce rapport

CONCLUSION

Les mesures effectuées dans ERMINE ont permis d'obtenir dans un délai assez court, et avec une expérience peu coûteuse, des résultats avec une précision de 10 %. La méthode du signal local, mise au point pour ces expériences, permet d'obtenir des valeurs du rapport capture sur fission pour un échantillon de dimensions quelconques dans un spectre que l'on choisit en fonction de la valeur cherchée.

Les analyses sur des échantillons irradiés, combinées avec des mesures d'indices de spectre, nous conduisent à des valeurs de α plus précises, environ 5 %, mais constituent des expériences plus coûteuses dans l'interprétation desquelles la connaissance du spectre sur lequel est mesuré α est plus délicate, excepté le cas où ces irradiations sont faites dans le spectre caractéristique d'un réacteur à neutrons rapides, comme pour RAPSODIE.

L'ensemble des résultats ne traduit que des écarts assez faibles par rapport aux valeurs calculées à partir des dernières évaluations effectuées sur la base des mesures différentielles les plus récentes [12]. Il faut toutefois noter que les trois résultats concernant le Pu 239 traduisent tous une surestimation de α_9 par le calcul,

d'environ 10 %, cependant que pour α_5 les valeurs théoriques et expérimentales sont beaucoup plus proches, excepté dans le cas de RAPSODIE c'est-à-dire du spectre le plus dur.

La détermination du rendement du Nd 148 pour la fission de U 235 conduit à la même valeur que dans le cas de la fission par des neutrons thermiques, valeur nettement plus basse que celle mesurée précedemment pour un spectre de fission [15].

REMERCIEMENTS

Le succès des expériences d'irradiation est dû en grande partie aux analyses effectuées par le Laboratoire de Spectrométrie de Masse que nous tenons à associer à ce travail, en particulier Melle LUCAS et M. FREJAVILLE, pour leur excellente collaboration.

Nous tenons aussi à remercier MM. GUERY et GOURDON pour la préparation des échantillons et des irradiations.

Enfin le concours de Mme KATZ nous a été très précieux pour la présentation de ce rapport.

REFERENCES

[1] BOUCHARD, J., MOUGNIOT, J.C., VIDAL, R., Etude expérimentale des caractéristiques neutroniques des milieux multiplicateurs rapides dans l'assemblage critique thermique-rapide ERMINE "Fast reactor physics, IAEA Symposium (Karlsruhe 1967)" Proceedings vol I (1968) 309.

[2] BOUCHARD, J. and al., Fast integral experiments : with thermal driver zone in MINERVE - exponential experiments with HARMONIE - pulsed experiments in collaboration with the Germans - BNES Conference LONDON (1969).

[3] TILL, C.E., DAVEY, W.G., LEWIS, R.A., PALMER, R.G., The Argonne National Laboratory Critical Experiment Programme, BNES Conference, LONDON (1969).

[4] ADAMSON, J., and al., ZEBRA VI - A dilute Plutonium Fuelled Assembly-Conference on fast critical experiments and their analysis, ANL 7320 (1966).

[5] ANDERSSON, T.L. and al., Measurement of the effective capture to fission ratio in Pu 239 and U 235 in two different fast reactor spectra. "Fast reactor physics, IAEA Symposium (Karlsruhe, 1967)" Proceedings, Vol II (1968) 171.

[6] CARRE, J.C., Pilote automatique pour les mesures précises de faibles variations de réactivité. Note CEA N 1139, (1969).

[7] GUERY, M., MENESSIER, P., Description et utilisation des chambres à fission miniatures pour la mesure d'indices de spectre, Note CEA (à paraître).

[8] "Neutron monitoring", AIEA Symposium (Vienne 1966). Communication SM 76/64

[9] DARROUZET M, Mesure du rapport capture sur fission du Pu 239 dans l'assemblage critique thermique-rapide ERMINE, Thèse de 3e cycle - Faculté des Sciences d'ORSAY (1970).

[10] BARRE, J.Y., HEINDLER, M., LACAPELLE, J., RAVIER, J., Lessons drawn from integral experiments on a set of multigroup cross sections. BNES conference LONDON (1969).

[11] GWIN R., Communication au meeting de spécialistes sur les valeurs de α du Pu 239 - IAEA NPR/5 - Juin 1969.

[12] BARRE, J.Y., BOUCHARD, J., Rôle complémentaire des expériences intégrales par rapport aux mesures différentielles pour un projet de réacteur à neutrons rapides. Cas des isotopes du plutonium - Communication à cette conférence - CN 26/73.

[13] Rapport final du contrat CEA - EURATOM - Recyclage du plutonium - EUR 2853 f (1966).

[14] LERIDON., SCHMITT, A., Communication personnelle.

[15] MEEK, M.E., RIDER, B.F., Summary of fission products yields for U 235, U 238, Pu 239 and Pu 241 at thermal, fission spectrum and 14 MeV neutron energies, APED 5398 A, (1968).

DISCUSSION

TO PAPERS IAEA-CN-26/73, 96

W. P. POENITZ: In connection with the reactor calculations at Cadarache, Dr. Barré reports the use of low ^{238}U capture cross-sections as measured by Moxon and by Menlove and Poenitz. ^{238}U data of this type are also used at Karlsruhe, as reported by Dr. Küsters. On the other hand, Cadarache uses the high fission cross-section of White. I think it is well established that these data sets are inconsistent.

H. HÄGGBLOM: I would like to mention that in our calculations we did not use the fission cross-sections of White. In fact, about two years ago we realized that our fission cross-sections had to be decreased in order to improve the integral data. Quite arbitrarily, therefore, we decreased the cross-section below 40 keV by 10%. The adjustment calculations indicate a positive adjustment in this region by about 2% but also a negative adjustment by about 5-6% in the higher energy region.

J. L. ROWLANDS: The dominant energy range for fission in a typical fast reactor is 100 keV to 300 keV, while the dominant energy range for capture is 10 keV to 30 keV. It would not be inconsistent to use the low (Moxon's) capture data and the high (White's) fission data if an energy-dependent systematic error were present between the two energy ranges.

W. G. DAVEY: I would like to draw attention to two integral measurements of α for ^{239}Pu. These were made at Argonne National Laboratory and will be reported at the American Nuclear Society Meeting at Los Angeles in June 1970. They were carried out by Kato et al. and Bretscher et al. The assembly used, ZPR-3/57, was a small fast critical with the flux minimized in the region 1 to 30 keV. The neutron spectrum was measured at Gulf General Atomic by a sub-critical method and at ANL by the proton-recoil method. One of the measurements in particular, is still in a developmental stage and both are subject to uncertainties due to heterogeneity, so that the results must be considered preliminary. However, it is interesting to note that they do not indicate a reduction in α ^{239}Pu below the measurements of Gwin et al. but rather an increase.

H. CEULEMANS: Does Dr. Barré know whether there are any integral measurements that are comparable and have been reported at different laboratories? If so, did they show complete agreement or did they, as I suspect, also suffer from the same kind of inconsistencies or systematic errors that affect several differential measurements?

J. Y. BARRÉ: The techniques for the measurement of spectral indexes, for example, are intercalibrated between various laboratories. This comparison is the best means of eliminating systematic errors in respect of these parameters. Moreover, the fact that a given laboratory uses several independent methods in carrying out each technique helps to eliminate possible systematic errors.

It is for the same reason that CEA employs two independent techniques in making buckling measurements, namely, flux mapping and substitution.

The critical mass is not subject to large systematic errors for cores comparable to PHENIX (presently studied in MASURCA) because the heterogeneity effects are small.

So far, I do not think that the main parameters measured in the fast critical experiments (buckling, spectral index, critical mass) suffer from the same kind of systematic errors that now affect differential measurements.

The main purpose of integral measurements is to find differences between two measurements. This is the philosophy underlying the second method for the analysis of integral experiments described in paper CN-26/73. The present MASURCA program will show the variation of buckling and spectral indexes as a function of the enrichment and the differences in these parameters between uranium and plutonium cores. As a result of the measurement of such differences, a number of possible systematic errors (e. g. in connection with the enrichment of the fuel) have vanished.

C. G. CAMPBELL: The point of the question being asked is whether integral experiments have been conducted in different laboratories using the same composition of test assembly. I think it is important to make such tests and I suggest that a suitable composition is that adopted in the recent ZEBRA assembly of unit k-infinity. This is an assembly composed of ^{238}U metal and ^{235}U metal with a small amount of structural steel. Integral checks of the important reaction-rate ratios, of the proton-recoil spectrum and of the composition to yield unit k-infinity would be possible. The assembly could be built by a number of laboratories from their existing fuel inventories.

B. ROSE: I should like to express my full support of Dr. Campbell's remarks. On the question of repeating integral experiments to establish reproducibility (and therefore - by implication - absolute accuracy), I do not consider it adequate to have these repeats carried out in the same laboratory, by the same team and presumably by the same methods. It is essential to have them carried out by different people, different methods, different laboratories, as is routine in the differential case. As an example, I can quote a serious discrepancy over the spectrum from a Vera assembly, carried out at both Harwell and Aldermaston, which it took several years to resolve. Errors in technique were revealed in both experiments.

J. J. SCHMIDT: I would like to have a comment on the following question. I think it is fair to say that quite a number of differential capture and fission cross-sections measurements agree fairly well in shape, but disagree in absolute magnitude by unknown systematic errors. Besides acknowledging the necessity of solving systematic discrepancies by a careful evaluation of the differential measurements themselves, I would like to ask whether integral experiments could help in determining reliable absolute values of differential cross-section shapes.

J. Y. BARRÉ: I do not see things this way because I think that, as reactor physicists, we must not go from integral experiments to differential measurements but vice versa. I believe nevertheless that integral experiments should enable us to determine an absolute value, a standard, for ^{238}U capture, to take one example. This, in fact, is what was done in the case of thermal energies when the resonance integral was adjusted. I think that this can be true for other cases as well, e. g. ^{239}Pu fission. However, I have the impression that, for the entire range of energies of interest to us, the differential measurements are not unique but correspond to two or more types of measurements and that often the shape itself is not satisfactory, that is to say, in the region of overlap there are serious problems. Many of these have been mentioned in the course of this Conference.

C. G. CAMPBELL: In answer to Dr. Schmidt, I think that the data-fitting techniques can be developed to help to answer these questions, provided that the integral information is sufficiently sensitive and provided that the random uncertainties and the possible systematic uncertainties and ranges of these are defined in the group-averaged differential data. I think, too, that it is important in this to identify further constraints that may be applied by differential ratio measurements. If all this is put together properly in the fitting program it might well be that evidence for systematic errors in the differential data would emerge.

CALCULATIONS OF JEZEBEL AND GODIVA WITH RECENT ENDF/B MICROSCOPIC DATA

G.H. BEST, M.E. BATTAT, R.J. LABAUVE, R.E. SEAMON
University of California,
Los Alamos Scientific Laboratory,
Los Alamos, N. Mex.
United States of America

Abstract

CALCULATIONS OF JEZEBEL AND GODIVA WITH RECENT ENDF/B MICROSCOPIC DATA.

Accurate predictions of reactor-design parameters, such as critical mass, material worths, and spectral response, require the development and maintenance of up-to-date basic microscopic nuclear data files. To meet this need, a national co-operative program is in progress in the United States to prepare an evaluated nuclear data file (ENDF/B). The large amount of experimental data which is becoming available, together with theoretical data, makes the maintenance of ENDF/B a continuing task. In addition, a large effort is needed in testing the microscopic data prior to use in reactor-design calculations.

Testing of the original ENDF/B data has indicated deficiencies in the microscopic data for some materials. As a result, a re-evaluation of the data for selected materials, including fissile and fertile nuclides, was performed by the ENDF/B working group. The experimental fast critical assemblies JEZEBEL and GODIVA were used as the calculational models for the initial testing of the re-evaluated data files. To minimize uncertainties in the model specifications, the geometry and material specifications for these assemblies were based on a recent re-evaluation by Hansen and Paxton, which resulted in modest changes in the critical masses of homogeneous spheres of the appropriate alloys.

Multigroup constants were generated from the microscopic data using the MC^2 data processing code. The criticality calculations assumed spherical geometry and used isotropic transport theory. The effects of higher-order anisotropic scattering and quadrature order were taken into account in arriving at the final comparison. Central reactivity worths were computed using a perturbation-theory calculation.

Certain physics parameters are calculated better with the re-evaluated data, but the general lack of agreement between measured and calculated parameters indicates that deficiencies remain in the cross-section data.

INTRODUCTION

In this study several physics parameters of the small fast critical assemblies JEZEBEL and GODIVA were calculated using evaluated microscopic cross sections for comparison with the experimentally determined values of the parameters These assemblies emphasize neutron energies above about 100 keV, and they have a minimum of extraneous materials and of heterogeneities. The principal comparisons are based on k_{eff}, central fission ratios, and central reactivity worths. This study indicates the level of confidence that can be placed in the higher energy portion of the cross-section data by reactor designers.

CALCULATIONAL MODELS

The critical specifications used in the calculations are shown in Tables I and II. These are derived from Hansen and Paxton's recent re-evaluation of

TABLE I. CRITICAL SPECIFICATIONS OF ISOLATED BARE U(94) SPHERE DERIVED FROM GODIVA ASSEMBLY

A. Critical Configuration	
Mass, kg	52.42 ± 0.3%
Density, g/cm^3	18.74
Radius, cm	8.741

B. Composition

Isotope	Weight per cent	Atom Density atoms/cm^3
^{234}U	1.02	4.92×10^{20}
^{235}U	93.71	4.50×10^{22}
^{238}U	5.27	2.498×10^{21}

TABLE II. CRITICAL SPECIFICATIONS OF ISOLATED BARE PLUTONIUM SPHERE DERIVED FROM JEZEBEL ASSEMBLY

A. Critical Configuration (Pu alloy)	
Mass, kg	17.02 ± 0.6%
Density, g/cm^3	15.61
Radius, cm	6.385

B. Composition of Alloy

Element	Concentration	Atom Density atoms/cm^3
^{239}Pu	95.2 at.% Pu	3.705×10^{22}
^{240}Pu	4.5 at.% Pu	1.751×10^{21}
^{241}Pu	0.3 at.% Pu	1.17×10^{20}
Gallium	1.02 wt.% alloy	1.375×10^{21}

the JEZEBEL and GODIVA assemblies [1]; changes from previously published specifications resulted from improvement of the data used as a basis for corrections and from more careful accounting of actual dimensions than seemed previously justified.

CALCULATIONAL METHOD

Isotropic transport theory calculations were made with the DTF-IV code [2]. Both the regular and adjoint options were used with spherical geometry, S_{16} quadrature, twenty-six energy groups, and a convergence criterion of 10^{-5}. The k_{eff} values were calculated for the solid homogeneous spheres specified in

Tables I and II. The regular and adjoint angular fluxes, along with the model descriptions, were used in the DAC1 perturbation code [3] to obtain various physics parameters.

The calculated values of k_{eff} were adjusted for the finite orders of the angular quadrature and for the spatial mesh according to studies by Lathrop [4]. His investigation considered GODIVA, but, in the absence of a similar specific study, these results were used for extrapolating the JEZEBEL multiplication factor also. GODIVA was calculated with 30 spatial intervals, and JEZEBEL with 25. Adjustments were also made, according to the work of Cremer et al. [5], for the differences in k_{eff} due to the use of isotropic transport theory instead of explicitly including anisotropic scattering in the calculations. In the case of JEZEBEL, the gallium was not explicitly included in these calculations, but an adjustment was made based on previous (unreported) studies made at the Los Alamos Scientific Laboratory.

The multigroup constants were generated from the microscopic data by use of the MC^2 code [6]. MC^2 was run with the all-fine-group option, using 0.25 lethargy widths from 10 MeV and using constant flux weighting for the fine-group cross sections. An infinite homogeneous medium P_1 calculation was iterated on buckling to attain criticality, and then the spectrum was used for weighting the fine-group cross sections to get 0.5 lethargy-width cross sections (26 groups). The ^{239}Pu fission spectrum was used for JEZEBEL calculations, and the ^{235}U fission spectrum was used for GODIVA calculations.

NUCLEAR DATA

The two models were calculated using multigroup constants derived from the ENDF/B library [7] and using re-evaluated data prepared in the ENDF/B format. The ^{235}U re-evaluation was done by Alter and Dunford [8] for energies above 15 keV, which is the range of particular interest here. In brief, Davey's [9,10] evaluated fission cross-section data were used from 15 keV to 10 MeV, and the data of Henkel, Nobles, and Smith, as corrected by Hansen and McGuire [11], were used above 10 MeV; the alpha data of de Saussure [12], Weston [13], Diven [14], and Hopkins [15] were used between 15 keV and 1 MeV, and the Schmidt evaluation [16] was used above 1 MeV. This evaluation of alpha agrees with the Schmidt evaluation from 15 to 40 keV, makes a smooth transition to values 5 to 7% higher than Schmidt's between 60 and 200 keV, and then rejoins the Schmidt evaluation at about 400 keV. The capture cross section was obtained by multiplying the fission data by the alpha data. The ^{235}U ENDF/B and re-evaluated fission and capture cross sections are shown in Figs. 1 and 2, respectively.

The ^{238}U capture cross sections for the energy range of interest here were re-evaluated by Pitterle (unpublished) and are shown in Fig. 3. Between 1 and 100 keV, the re-evaluated data are based on the Moxon shape [17] normalized by a factor of 1.08 which was obtained by an average of all available data at 30 keV. For the higher energies, the re-evaluation presumably rests heavily on the data of Barry, Bunce, and White [18]. The fission cross section supposedly follows Davey's 1968 evaluation [10].

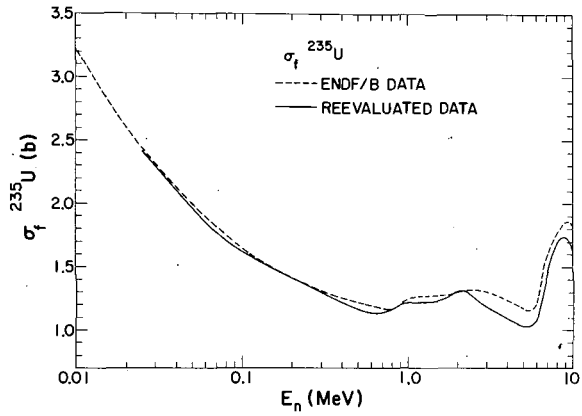

FIG. 1. Fission cross-section of ^{235}U.

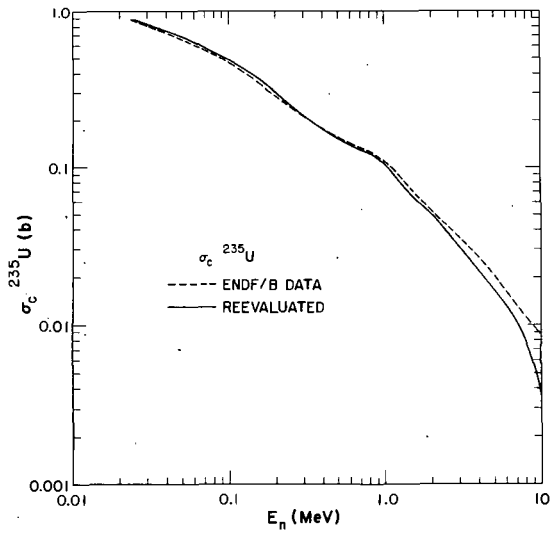

FIG. 2. Capture cross-section of ^{235}U.

The re-evaluation of the ^{239}Pu data above 25 keV was performed by Craven et al. [19]. Fission ratio data, $\sigma_f(^{239}Pu)/\sigma_f(^{235}U)$, were fit by high-order polynomials, using a weighted least-squares technique, and the ^{235}U data cited above were used to generate ^{239}Pu fission cross sections. The Davey ratio evaluation [10] agrees well with Craven's below 0.6 MeV, the Craven evaluation shows structure and oscillates about Davey's straight line between 0.6 and 6.0 MeV, and the two evaluations show similar sharp drops between 6 and 10 MeV.

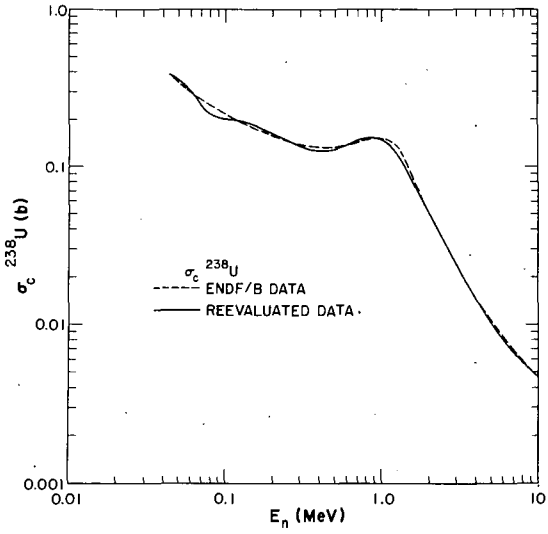

FIG.3. Capture cross-section of ^{238}U.

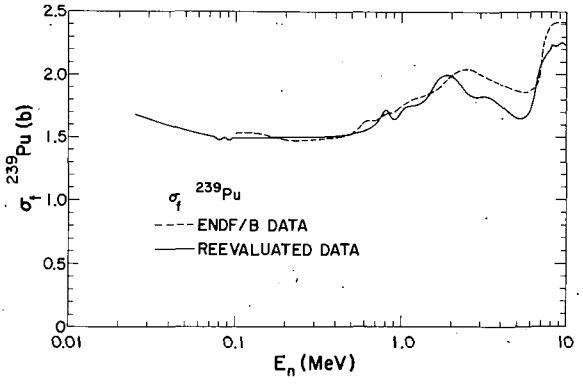

FIG.4. Fission cross-section of ^{239}Pu.

The ENDF/B and re-evaluated fission cross sections for ^{239}Pu are shown in Fig. 4. The capture cross sections, Fig. 5, were based on a fit to the experimental alpha data where they exist, i.e., up to 1 MeV, and were given an $E^{-3/2}$ extrapolation (by BNL) above 1 MeV. The re-evaluated inelastic scattering data, Fig. 6, are the result of BNL model calculations [20] based on recently reported scattering measurements [21].

The fission cross sections for ^{240}Pu and ^{241}Pu are based on Davey's evaluation [10]. The capture cross sections for iron and nickel, which are shown in Figs. 7 and 8, were re-evaluated by Azziz and Connelley [22].

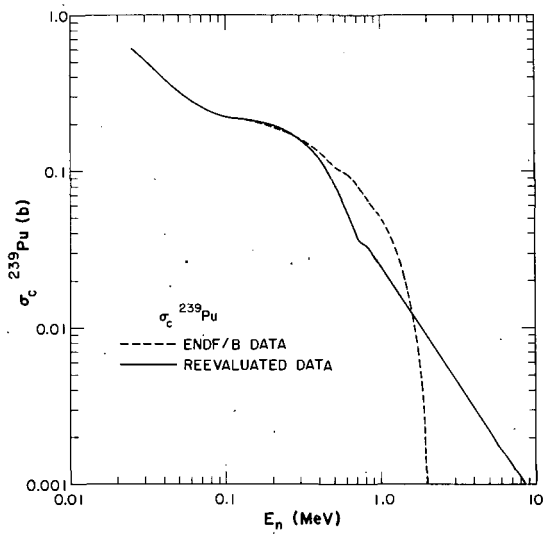

FIG. 5. Capture cross-section of ^{239}Pu.

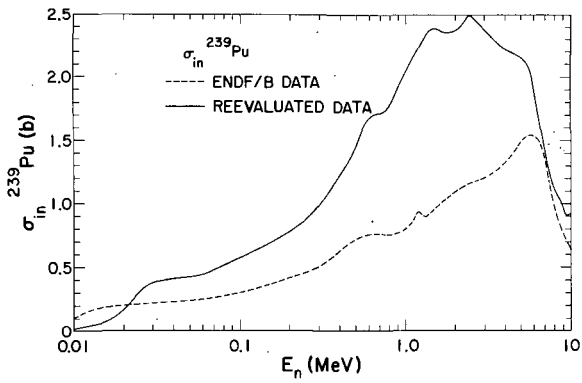

FIG. 6. Inelastic scattering cross-section of ^{239}Pu.

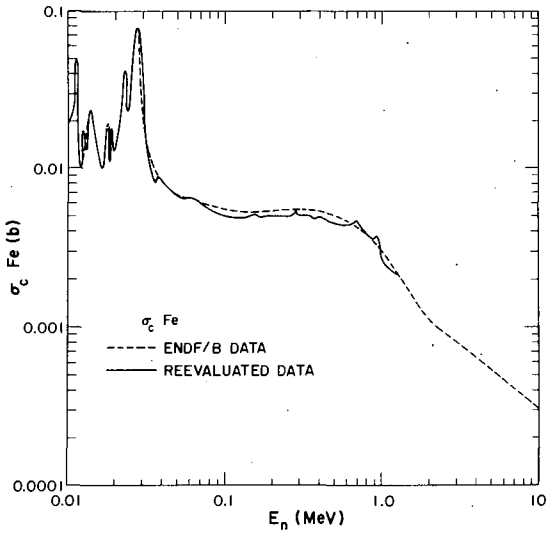

FIG.7. Capture cross-section of iron.

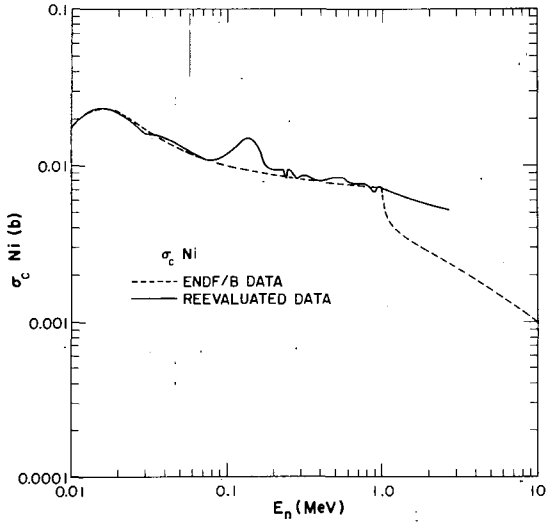

FIG.8. Capture cross-section of nickel.

RESULTS AND CONCLUSIONS

Calculated regular and adjoint central fluxes for GODIVA are presented in Figs. 9 and 10, and those for JEZEBEL are given in Figs. 11 and 12. The adjoint fluxes are relatively constant but are plotted with a suppressed zero, in order to display the modest differences obtained in the individual groups

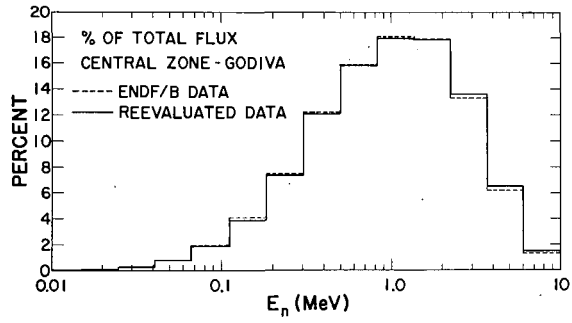

FIG. 9. Central regular fluxes of GODIVA with ENDF/B and re-evaluated data.

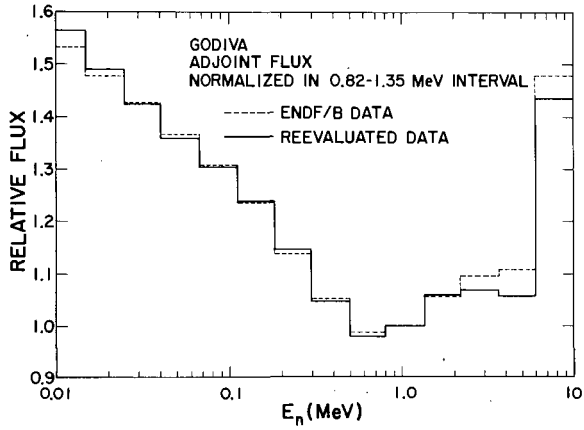

FIG. 10. Central adjoint fluxes of GODIVA with ENDF/B and re-evaluated data.

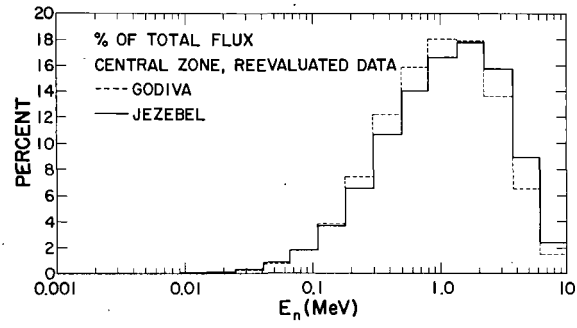

FIG. 11. Central regular fluxes of JEZEBEL with ENDF/B and re-evaluated data.

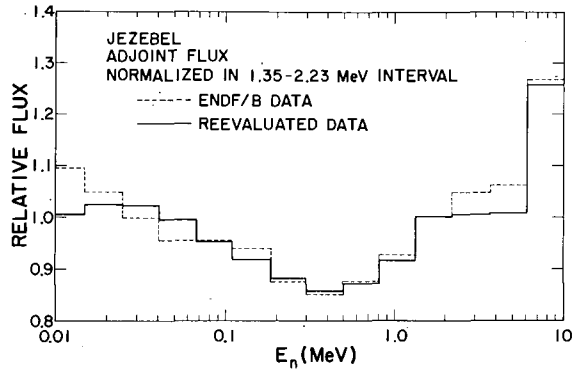

FIG. 12. Central adjoint fluxes of JEZEBEL with ENDF/B and re-evaluated data.

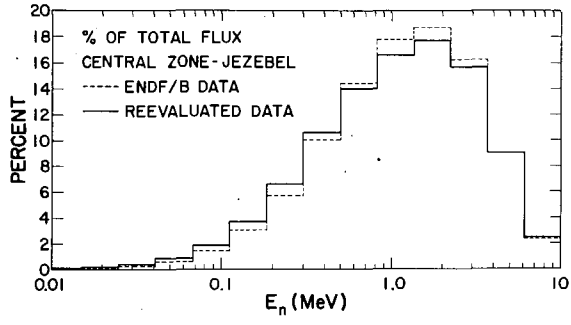

FIG. 13. Central regular fluxes of GODIVA and JEZEBEL with re-evaluated cross-sections.

with the two data sets. The re-evaluated cross sections produced little change in GODIVA spectra, but there is a noticeable softening in the JEZEBEL regular spectrum. Figure 13 shows that the regular flux spectrum for GODIVA with the re-evaluated data is somewhat softer than that for JEZEBEL.

The calculated and measured parameters for GODIVA are presented in Table III, and those for JEZEBEL are given in Table IV. For GODIVA, the improvement in k_{eff} is impressive; however, there are no significant changes in the other calculated parameters. In particular, the capture-to-fission ratio for ^{238}U shows no improvement nor does the central reactivity worth, and neither of these is calculated as well as would be hoped.

TABLE III. CALCULATED AND MEASURED PARAMETERS FOR GODIVA

	ENDF/B Data	Experimental Value [23]	Re-evaluated Data
k_{eff} (DTF-IV)	1.02694		1.00229
Corrections:			
$S_\infty - S_{16}$ -0.00080			
P_3 - Iso. Tr. -0.002			
-0.00280			
Corrected k_{eff}	1.02414	1.000 ± 0.003	0.99949
β_{eff}	0.00658	0.00659	0.00664
Lifetime	5.16×10^{-9} s	5.99×10^{-9} s	5.20×10^{-9} s
Rossi α	-1.27/μs	-1.10/μs	-1.28/μs
Central Capture and Fission Ratios			
$(^{238}U)_F/(^{235}U)_F$	0.156	0.156 ± 0.005	0.155
$(^{239}Pu)_F/(^{235}U)_F$	1.35	1.42 ± 0.02	1.36
$(^{238}U)_C/(^{238}U)_F$	0.553	0.47 ± 0.02	0.553
Central Reactivity Worths		(¢/g-atom)	
^{239}Pu	278	285	286
^{240}Pu	166	170	
^{235}U	149	149	150
^{238}U	21.5	24.3	21.6
Fe	-1.35	-0.2	-0.778
Ni	-5.48	-4.4	-5.06

For JEZEBEL, the deviation of k_{eff} from critical has changed sign but not size. The $^{238}U/^{235}U$ fission ratio, as calculated with the re-evaluated data, is farther from the experimental value than is the case for the ENDF/B data. The ^{238}U central reactivity worth is still quite far from the experimental value.

The iron and nickel central worths in JEZEBEL, as calculated with the re-evaluated data, are in better agreement with the experimental values than are those using the ENDF/B data.

The improvements noted in these comparisons are encouraging; however, for the energy region considered in this study, i.e., above about 100 keV, it seems evident that there remain deficiencies in the uranium and plutonium cross sections.

TABLE IV. CALCULATED AND MEASURED PARAMETERS FOR JEZEBEL

		ENDF/B Data	Experimental Value [23]	Re-evaluated Data
k_{eff} (DTF-IV)		1.01093		0.98846
Corrections:				
Ga effect	+0.0035			
$S_\infty - S_{16}$	-0.00085			
P_3 - Iso. Tr.	-0.002			
	+0.00065			
Corrected k_{eff}		1.01158	1.000 ± 0.003	0.98911
β_{eff}		0.00183	0.00194	0.00186
Lifetime		2.90×10^{-9} s	2.98×10^{-9} s	3.12×10^{-9} s
Rossi α		-63/μs	-65/μs	-60/μs
Central Fission Ratios				
($^{239}Pu/^{235}U$)		1.38	1.49 ± 0.03	1.37
($^{238}U/^{235}U$)		0.192	0.205 ± 0.008	0.181
Central Reactivity Worths			(¢/g-atom)	
^{239}Pu		1670	1592	1666
^{240}Pu		1028	1038	975
^{235}U		874	804	873
^{238}U		77.9	114	83.9
Fe		-26.0	-21.5	-21.2
Ni		-60.7	-48.0	-50.7

REFERENCES

1. HANSEN, G. E. and PAXTON, H. C., "Reevaluated Critical Specifications of Some Los Alamos Fast-Neutron Systems," LA-4208, Los Alamos Scientific Laboratory (1969).
2. LATHROP, K. D., "DTF-IV, a FORTRAN-IV Program for Solving the Multigroup Transport Equation with Anisotropic Scattering," LA-3373, Los Alamos Scientific Laboratory (1965).
3. CARMICHAEL, B. M., "DAC1, a One-Dimensional S_n Perturbation Code," LA-4342, Los Alamos Scientific Laboratory (1969).
4. Argonne Code Center: Benchmark Problem Book, Numerical Determination of the Space, Time, Angle, or Energy Distribution of Particles in an Assembly, ANL-7416, Argonne National Laboratory (1968).

5. CREMER, C. C. et al., "Comparison of Calculations with Integral Experiments for Plutonium and Uranium Critical Assemblies," LA-3529, Los Alamos Scientific Laboratory (1968).
6. TOPPEL, B. J. et al., "MC^2, A Code to Calculate Multigroup Cross Sections," ANL-7318, Argonne National Laboratory (1967).
7. "Version I, ENDF/B Data Tapes Numbered 114, 115, 116, 117, and 999," distributed by Brookhaven National Laboratory (1967).
8. ALTER, H. and DUNFORD, C. L., "An Evaluation of Uranium-235 Neutron Cross Section Data for Energies Above 15 kev," AI-AEC-MEMO-12916, Special Distribution, Atomics International (1970).
9. DAVEY, W. G., Nucl. Sci. Engng. 26 149 (1966).
10. DAVEY, W. G., Nucl. Sci. Engng. 32 35 (1968).
11. HANSEN, G., McGUIRE, S., and SMITH, R. K., Los Alamos Scientific Laboratory, private communication with H. Alter (see Ref. 8).
12. de SAUSSURE, G. et al., "Nuclear Data for Reactors," Vol. II, IAEA, Vienna 233 (1967).
13. WESTON, L. W. et al., Nucl. Sci. Engng. 20 80 (1964).
14. DIVEN, B. C. et al., Phys. Rev. 109 144 (1958).
15. HOPKINS, J. C. and DIVEN, B. C., Nucl. Sci. Engng. 12 169 (1962).
16. LANGNER, I., SCHMIDT, J. J., WOLL, D., "Tables of Evaluated Neutron Cross Sections for Fast Reactor Materials," KFK 750 (1968).
17. MOXON, M. C., "The Neutron Capture Cross Section of ^{238}U in the Energy Region 0.5 to 100 keV," AERE-R-6074, Harwell, England (1969).
18. BARRY, J. F., BUNCE, J., WHITE, P. H., J. Nucl. Energy A/B 18 (1964).
19. GREENE, N. M., LUCIUS, J. L., CRAVEN, JR., C. W., "An Evaluation and Compilation of the Fission and Capture Cross Sections of ^{239}Pu in the Energy Range 25 kev - 15 Mev," ORNL-TM-2797 (ENDF-131), Oak Ridge National Laboratory (1970).
20. DRAKE, M., private communication.
21. KNITTER, H. H., COPPOLA, M., "Elastic Neutron Scattering Measurements on ^{239}Pu in the Energy Range Between 0.19 and 0.38 MeV," (EURATOM, Geel, Belgium), Z. Phys. 228 286-94 (1969).
22. AZZIZ, N. and CONNELLEY, J. W., WCAP 7281 (1969).
23. ENGLE, L. B., HANSEN, G. E., and PAXTON, H. C., "Reactivity Contributions of Various Materials in Topsy, Godiva, and Jezebel," Nucl. Sci. Engng. 8 543 (1960).

DISCUSSION

A. M. FABRY: I might point out that the measured $^{239}Pu(n,f)/^{235}U(n,f)$ average cross-section ratios as reported in Table II of our paper (CN-26/39) tend to be higher than the computed ones, which is similar to what you observed in the centre of the GODIVA core. I would also like to ask if you could comment on the discrepancy between the measured and the computed Rossi α for GODIVA?

G. H. BEST: We have been unable to explain the discrepancy between the computed and measured Rossi α for GODIVA.

J. L. ROWLANDS: I would like to ask two questions. First, have the new ENDF/B data taken account of discrepancies between integral measurements and calculations made using the first version of ENDF/B.

G. H. BEST: It is the intention of ENDF/B to present the results of evaluations of differential cross-section measurements, and, therefore, no adjustments have been made to reflect such discrepancies.

J. L. ROWLANDS: Secondly, how is it proposed to allow for discrepancies between calculation and integral measurements in fast reactor design calculations?

G. H. BEST: The neutron spectra in GODIVA and JEZEBEL peak in the vicinity of 1 MeV and show relatively few neutrons at or below a few hundred keV. Typical FBR-spectra peak below these lower energies, so I suspect that the FBR-designers will note the discrepancies shown in this paper but take little action as a result of them.

THE INFLUENCE OF THE UNCERTAINTIES OF σ_{25}^{f} IN THE MONTE-CARLO CALCULATIONS OF SMALL CRITICAL ASSEMBLIES

V. BENZI, E. CUPINI, A. De MATTEIS
Comitato Nazionale Energia Nucleare,
Centro di Calcolo, Bologna,
Italy

Abstract

THE INFLUENCE OF THE UNCERTAINTIES OF σ_{25}^{f} IN THE MONTE-CARLO CALCULATIONS OF SMALL CRITICAL ASSEMBLIES.

Recent measurements of the fission cross-section of ^{235}U in the energy range ~100 keV – 1 MeV, give values ~15% lower than the results previously obtained. A Monte-Carlo analysis of some fully enriched small fast critical assemblies shows that such a reduction gives critical mass values which are in strong disagreement with the experimental ones.

The possible influence of variations in the elastic and inelastic cross-sections is also discussed.

1. INTRODUCTION

A few years ago, extensive calculations on small critical assemblies were performed at the Centro di Calcolo-C.N.E.N. using the Monte Carlo method. The purpose of these calculations was twofold:

a) to test the reliability of the M.C. method for criticality calculations,

b) to test the reliability of the cross sections adopted in the fast neutron energy range.

Details of these calculations are given in refs. 1 and 2.

For thirty-one bare and reflected critical assemblies of enriched Uranium, a quite good agreement was found between calculations and experiments.

The largest discrepancies in K_{eff} (about 3-4%) were found for four assemblies with a rather thick reflector of graphite. This may be due to the fact that in these assemblies the low energy end of the spectrum contains an appreciable number of neutrons, so that a much more detailed group structure should be adopted than the twenty groups used in the calculations. In addition, it must be mentioned that a recent test on the elastic scattering cross sections for carbon leads to the conclusion that the existing data should be re-examined [3].

2. MONTE CARLO CALCULATIONS

The results mentioned in §. 1 suggest the reliability of the method and cross sections adopted.

For the σ_f of U-235 the nuclear data file from which the multigroup set was derived was based on the well-known experimental data of White [4].

More recently, preliminary data on the σ_f of U-235 obtained with a new set of measurements have been published by Poenitz [5].

These data are shown in fig. 1 where the solid line represents the σ_f adopted for the M.C. calculations mentioned above. The data of Poenitz are about 15% lower than those adopted over a wide energy range. To test the reliability of these data, a few calculations on U-235 fast critical assemblies were performed, using a σ_f multigroup set based on the dashed line shown in fig. 1.

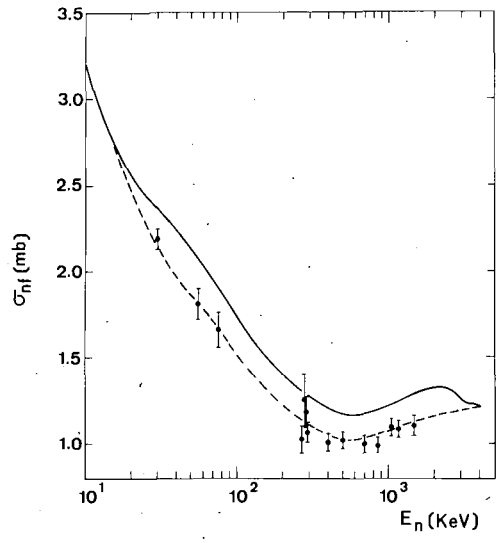

FIG. 1. Adopted σ_{nf} for ^{235}U. Solid line based on White's data. Dashed line based on Poenitz' data.

TABLE I. CRITICALITY MONTE-CARLO CALCULATIONS

No.	Geometry	Radius (cm)	Height (cm)	Enrichment (%)	Density (gm/cm^3)	K_{eff} (±0.004)				
						(a)	(b)	(c)	(d)	(e)
1	Sphere	8.718	-	93.8	18.75	1.018	0.938	0.949	1.037	1.008
2	Cylinder	6.90	24.3	93.5	18.8	1.002	0.919	0.930	1.013	0.978
3	Cylinder	7.98	15.2	93.5	18.8	1.005	0.924	0.935	1.014	0.985

TABLE II. LEAKAGE PROBABILITY FOR BARE ^{235}U ASSEMBLIES

Assembly No.	Leakage Probability	
	White σ_f	Poenitz σ_f
1	0.556	0.583
2	0.560	0.591
3	0.560	0.588

To avoid uncertainties due to other nuclei, bare U-235 assemblies were selected. The results are given in table I. In column (a) the values of K_{eff} obtained using White's data are given. Column (b) gives the results obtained with Poenitz's data. It can be seen that they are considerably lower than unity. An analysis of the M.C. results revealed that this was mainly due to an increase in leakage, as shown in table II.

The overall reduction in K_{eff} was about 8% in all three cases considered. About 2% was lost in K_∞, and ~6% in leakage. The relatively small effect in K_∞ can be understood if one considers a one-group definition of K_{eff}

$$K_{eff} = \frac{\nu\Sigma_f}{(\Sigma_f+\Sigma_a)} \cdot \mathcal{L} = K_\infty \cdot \mathcal{L}$$

where $\mathcal{L}$ represents the non-leakage probability. Due to the fact that

$$\Sigma_a << \Sigma_f$$

it follows immediately that a change in Σ_f does not affect K_∞ very much, as long as $\Sigma_f \gg \Sigma_a$.

Additional calculations based on Poenitz's data were performed, in which the elastic scattering cross section of U-235 was increased over the entire energy range.

Column (c) in table I gives the effect of a 10% increase of σ_{el}, a variation which can be accepted as an upper limit within the uncertainties of the experimental data at present available. The value of K_{eff} is again too low. The elastic scattering cross section was then doubled, giving an acceptable K_{eff} value for cilinders, as shown in column (d) of table I. However, such a drastic increase in σ_{el} is not acceptable; among the other things, it would imply an increase of ~60% in σ_T.

Column (e) gives the results obtained by using the inelastic cross sections as obtained from the KEDAK [6] nuclear data file. The other data adopted were the same as in column (a). It is clear that the adoption of these data for the inelastic scattering cross sections, cannot compensate the effect of the lower Poenitz's σ_f.

On the basis of the above mentioned results, it seems rather difficult to predict the experimental critical masses of bare U-235 critical assemblies by using the Poenitz data on σ_f without assuming sensible changes in the other parameters.

REFERENCES

[1] BENZI, V., CUPINI, E., DE MATTEIS, A., J. Nucl. Energy (Parts A-B), 20 (1966) 17.

[2] BENZI, V., CUPINI, E., DE MATTEIS, A., ANL-7320 (1967).

[3] DUNFORD, C.L., ALTER, H., AI-AEC-MEMO 12915 (1970).

[4] WHITE, P.H., J. Nucl. Energy (Parts A-B), 19 (1965) 423.

[5] POENITZ, W.P., NBS/SP-299, Vol. I (1968) 503.

[6] LANGNER, I., SCHMIDT, J.J., WOLL, D., KFK-750 (1968).

DISCUSSION

W. P. POENITZ: At Argonne, reactor calculations have been carried out by Kallfelz and Zolotar for 10 different critical assemblies including GODIVA. Three different sets of data have been used: the old and the new version of ENDF(B) and a set modified by lower absolute fission cross-sections, as indicated by the capture cross-sections. The difference obtained for the old and new ENDF(B) data was in very good agreement with the results reported in your paper. However, a much smaller difference has been obtained for the modified set than you report. In fact your difference is larger by a factor 2-3.

In addition, it should be realized that your calculations may not allow any conclusion to be drawn concerning the fission cross-section in the energy range below 1 MeV because the use of the data above 1.5 MeV is open to question. As recently pointed out by Hart, the Los Alamos data on which ENDF(B) relies in this range do not fit the well-known 14 KeV cross-section.

V. BENZI: To answer your question, it would be necessary to know the calculation method used by the authors you mentioned. As regards the data above 1.5 MeV, I can mention that our Monte-Carlo calculations reproduce reasonably well the GODIVA leakage spectrum, the shape of which is rather sensitive to the shape of σ_f.

H. W. KÜSTERS: Could you comment on how the picture of GODIVA prediction changes with the introduction of harder fission spectra, such as those measured by Fabry, and higher $\bar{\nu}$ (E)-values, such as those which have been reported at this Conference?

V. BENZI: In our experience, a harder fission spectrum implies a reduction in k_{eff} for assemblies like GODIVA. As far as the influence of $\bar{\nu}$ is concerned, I remember that calculations carried out by Pendlebury and presented at the 1961 Vienna Seminar on Fast Reactors, showed that an increase of 7.5% on $\bar{\nu}$ over the entire energy range would imply a variation of -23% in critical mass for GODIVA. This corresponds, more or less, to +5% in k_{eff}.

IMPLICATIONS OF FUNDAMENTAL INTEGRAL MEASUREMENTS ON HIGH-ENERGY NUCLEAR DATA FOR REACTOR PHYSICS

A. FABRY, M. DE COSTER, G. MINSART,
J.C. SCHEPERS, P. VANDEPLAS
SCK/CEN Mol, Belgium

Abstract

IMPLICATIONS OF FUNDAMENTAL INTEGRAL MEASUREMENTS ON HIGH-ENERGY NUCLEAR DATA FOR REACTOR PHYSICS.

Among the recent specific results obtained in the course of the SCK-CEN program of clean integral experiments, much attention is paid to new measurements of absolute average fission-spectrum cross-sections; an original procedure is described, which allows minimization and control of the sources of systematic errors; it is shown that this is probably the most precise and powerful method ever employed for this type of experiment, especially when reactions without threshold are investigated. A recommended set of data is tentatively presented and discussed for some high-energy nuclear reactions and for the ^{235}U-thermal-fission-neutron spectrum. This set is based on the requirement to fit simultaneously, whenever possible, within their respective confidence intervals, the most accurate differential measurements as well as the integral experiments performed in Belgian and other laboratories. The energy range extends from about 100 keV up to 10 MeV and the reactions include fission in ^{235}U, ^{238}U, ^{239}Pu, ^{232}Th, capture in a few important nuclides, inelastic scattering and charged-particle production in materials commonly used for reactor dosimetry. The long-standing reactor-theoretic underestimation of the ^{238}U-fission rates relative to ^{235}U- is also discussed.

1. SCOPE OF THE WORK

1.1. Foreword

The CEN-activities in the field of fast-reactor physics involve specific responsibility with respect to nuclear constants. The work presented in this paper is part of a long-standing program of clean integral experiments [1, 2] aimed at improving nuclear data as well as experimental and computational methods relevant to fast-reactor design and operation.

Although the scope of this paper is limited to high-energy cross-sections – by high energy is meant here the range 100 keV - 10 MeV – and to the debated question of fission-neutron spectra, it is believed that it offers a typical illustration of how clean integral experiments may and must supplement differential work, a topic which has become more and more pressing since the IAEA Paris Conference in 1966. Also evidenced is the benefit of what may be termed a fundamental approach to clean integral experiments, i.e. an approach where attention is paid to using as much physical insight as possible for designing the measurements as well as to the later stage of their interpretation and the critical appraisal of their implications.

1.2. Guiding lines

This work is an attempt to understand a number of conflicting results about high-energy integral and differential nuclear data. Two quantities of

paramount importance in this analysis are the ^{235}U thermal fission-neutron spectrum $\chi_5(E)$ and the ^{235}U fission cross-section σ_{f5} (E) in the specified energy range: they are interrelated in a manner which will be explained immediately. Throughout this paper, the symbol $\bar{\sigma}_i$ is used, unless otherwise specified, to denote fission-spectrum average cross-sections:

$$\bar{\sigma}_i = \int_0^\infty \sigma_i\ (E)\ \chi_5\,(E)\ dE$$

Any representation $\chi_5\,(E)$ is normalized such that

$$\int_0^\infty \chi_5\,(E)\ dE = 1$$

Experimentally, a consistent set of suitably selected integral cross-section ratios or absolute spectral indices $\bar{\sigma}_i\ /\bar{\sigma}_{f5}$ is derived with great care. If it is assumed provisionally that the differential-cross-section ratios $\sigma_i\ (E)/\sigma_{f5}\,(E)$ are perfectly well fixed, the interrelation referred to above will become more apparent after considering Figs 1 and 2, where the WATT-type [3] representation of the fission spectrum has been used, expressed as a function of two parameters ν, β:

$$\chi_5^W\ (E) = \frac{2}{\sqrt{\pi}}\ \frac{\beta^{3/2}}{\nu}\ e^{-\nu^2/4\beta}\ \sinh\ \nu\sqrt{E}\ e^{-\beta E}$$

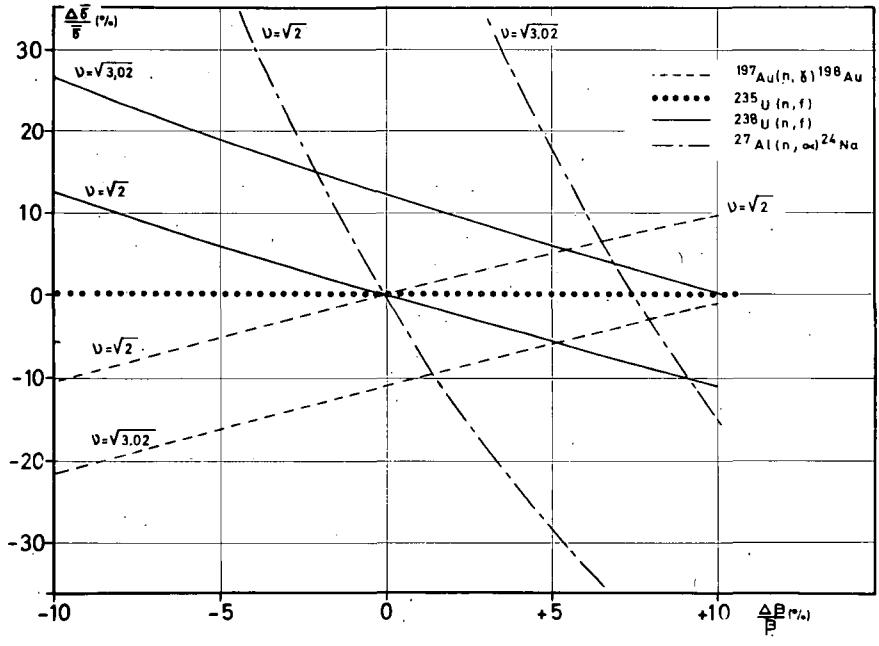

FIG.1. Sensitivity of integral cross-sections to the representation of fission-neutron spectra.

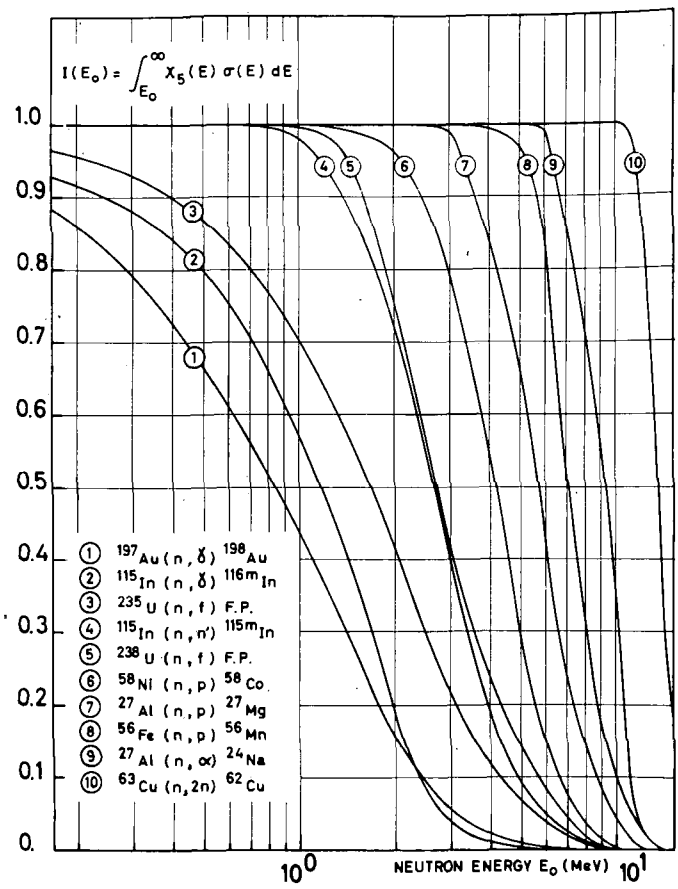

FIG.2. Integral response functions of a few nuclear reactions in the ^{235}U-thermal-fission-neutron spectrum.

On the provisional assumption made, the consistent set of spectral indices places, in principle, a serious constraint upon the energy dependency of the two basic quantities $\chi_5(E)$ and $\sigma_{f5}(E)$, provided that the energy coverage of the selected cross-sections $\sigma_i(E)$ is sufficient. If the shape of the excitation function $\sigma_{f5}(E)$ is fixed, then $\chi_5(E)$ might be derived accurately, but not conversely, as $\bar{\sigma}_{f5}$ is highly insensitive to the spectrum shape. Therefore, the absolute spectral indices $\bar{\sigma}_i/\bar{\sigma}_{f5}$ are mostly very sensitive indicators of the adequacy of the representation $\chi_5(E)$, but even if the cross-section ratios $\sigma_i(E)/\sigma_{f5}(E)$ are known to a high degree of accuracy, any serious error in the shape of $\sigma_{f5}(E)$ would be reflected by $\chi_5(E)$ in an unfolding procedure; although this propagation of error is minimized by the choice of ^{235}U fission as monitoring reaction it must, nevertheless, be considered once reactions without threshold, like $^{197}Au(n,\gamma)^{198}Au$, are used in order to attempt an unfolding significantly sensitive also to the low-energy part of the fission spectrum (see section 1.3). Further, it results from Fig.1 that a precise absolute measurement of $\bar{\sigma}_{f5}$ is a valuable integral constraint

upon $\sigma_{f5}(E)$. The same statement applies to the critical mass of the elemental assembly GODIVA [4], also considered in a later part of this paper. Now, if the cross-section ratios $\sigma_i(E)/\sigma_{f5}(E)$ have been reasonably specified, and under the assumption that $\chi_5(E)$ does not differ much for incident thermal and fission neutrons, any choice of an energy dependency $\sigma_{f5}(E)$ in the energy range concerned results in a representation $\chi_5(E)$ which, when used for a transport-theory computation of Lady GODIVA, should restitute correctly the core-centre spectral indices and neutron spectrum.
A further point must be explained. Although the greatest effort has been made to select a priori the most reliable sets of ratios $\bar{\sigma}_i/\bar{\sigma}_{f5}$ and $\sigma_i(E)/\sigma_{f5}(E)$, placed on the best consistent scale with respect to each other, and although the uncertainties associated with such ratios are generally expected to be distributed more randomly and to be smaller than the energy-correlated absolute errors in $\sigma_{f5}(E)$, the analysis has been carried out such as to avoid too much confidence in the input data at the expense of the output.

Thus, an emphasis has been laid in this work on reconciling as many data as possible while remaining, whenever reasonably acceptable, within the respective confidence intervals.

1.3. The main dilemmas under study

Recent differential experiments supply some direct or indirect evidence to be discussed more fully, towards a reduction of $\sigma_{f5}(E)$ between 10 keV and 1 MeV. The implications of fluctuations observed in fission cross-sections up to a few hundred keV and generally attributed to the intermediate class-two states [5] are far from being clarified and anyway might be a serious source of trouble for the reactor physicist concerned with nuclear data. Opposite to such possible lowering trends is the absolute value of 1335 mb [6] determined at CEN for $\bar{\sigma}_{f5}$ in 1968 in agreement with a value of 1330 ± 50 mb measured by Andreev [7] and supplied by the new experiments to be described hereafter, whose absolute accuracy is believed to be better than ± 5%. Older absolute measurements of $\bar{\sigma}_{f8}$ by Leachman and Schmitt [8] and by Richmond [9], when combined with the consistent set of spectral indices of the present work, lead to $\bar{\sigma}_{f5}$ = 1190 ± 10 mb, which, in turn, favours the lowering trends and just implies considerable distortion of $\sigma_{f5}(E)$ with respect to the choice fitting best our measurements: if we anticipate later results, we can say that this distortion may very schematically be regarded as due to the existence of two energy regions in $\sigma_{f5}(E)$, the first one extending from about 2 MeV up to 10 MeV, and the second one below 1 MeV, the critical point for the present analysis being the problem how to join them.

This dilemma is also significant with respect to $\chi_5(E)$. Thus, any change in $\sigma_{f5}(E)$ has a correlated influence on all other cross-sections measured directly or indirectly relative to it, but also on $\chi_5(E)$ and finally, on all other fission neutron spectra, $\chi_9(^{239}Pu)$ and $\chi_8(^{238}U)$ being especially important for fast-reactor physics. Once the wave of contest reaches the $\sigma_{f5}(E)$ data which are due to White [10] and have been valid for a long time, it will presumably also affect the long-standing semi-empirical models of Terrell [11] for the fission spectra. According to Greebler [12] hardening $\chi_5(E)$ by about 8% might produce a 2% reduction in fissile mass and an increase in the breeding ratio for a large fast power reactor. The analysis [13] of earlier integral data from Los Alamos [14] and CEN [15, 6],

has revealed a noticeable spectral depletion below 1.4 MeV in $\chi_5(E)$ compared to the Maxwellian representation with an average energy $\bar{E} = 1.935$ MeV; such an effect, as well as high-energy distortions, resulted in average energies varying from 2.11 [16] up to 2.24 MeV [13], depending upon the analysis. This was pointed out by Staub [17] and by Hardy [18] to be highly inconsistent with the Fermi age to indium resonance in water as well as with the eigenvalues of a collection of homogeneous uranium-water spheres.

A further point to be understood is the usual underestimation of the ^{238}U fission rates relative to ^{235}U by reactor theory. This may be related [19] to uncertainties either in $\chi_5(E)$ or in the ^{238}U down-scattering matrix [16].

2. A CONSISTENT SET OF AVERAGE CROSS-SECTION RATIOS IN THE ^{235}U THERMAL-FISSION-NEUTRON SPECTRUM

2.1. Introduction

The whole program of these measurements has been governed by the idea of randomizing, to a certain extent, the potential sources of systematic uncertainties, which means, first, that they must be seriously identified, then, that suitable methods must be found to deal with them, and, finally, that the correction factors must be subjected to sizeable perturbations so as to check how far they may be determined properly. For about one year, efforts have been made to develop these methods. The accuracy goals for absolute spectral indices in the ^{235}U-thermal-fission-neutron spectrum had been fixed to $\pm$ 2-3%. The presently well-developed method will in future be applied to the study of other fission-neutron spectra as $\chi_9(E)$ as well as to systematic integral tests of poorly known nuclear cross-sections [6].

2.2. Production of fission neutrons

The fission neutrons are produced by means of a "converter" arrangement (Fig.3) within a 50-cm-diameter spherical cavity located at the external edge of BR1-horizontal-graphite thermal column. This facility has been described elsewhere [1, 16]. It may accommodate various experimental devices, the most important one being the CEN-secondary-intermediate-standard-neutron-spectrum assembly $\Sigma\Sigma$ [16, 20]. Grundl has extensively discussed the problems in the production of cavity fission spectra [14, 21]. Four main sources of perturbation leading to correction factors must be considered:

a) Epithermal- and fast-neutron leakage from the core of the feeding reactor;
b) elastic and inelastic neutron scattering within the source-detector assembly;
c) axial and radial flux profiles within the source-detector assembly;
d) wall return background.

Our cavity has been located such as to render the first type of correction entirely negligible (< 0.1%). In doing so, much attention had to be paid to

the case of nuclear reactions without threshold, especially when the resonance integrals were large compared with the high-energy part of the cross-section curve. In some cases, it has also been observed that thermal-neutron perturbation through cadmium wrappings might lead to observable reaction rates; on the other hand, increasing the cadmium thicknesses enhances the corrections of types b and c so that a suitable compromise had to be determined experimentally. The corrections b have been computed in the DS4-approximation through simulation of the source-detector assembly by a homogeneous sphere of equivalent composition and average chord length [22]. These calculations reveal slight softening of the neutron spectrum compared with the ideal point-source spectrum. The corrections are small.

The detector foils have been sandwiched together by using various orders of combination such as to ensure an overall optimum control of axial-flux-profile effects, which never exceeded 2% in the geometrical arrangement of Fig.3. Radial flux profiles are important only when relating measurements of reaction rates performed by the track-recorder technique to activation measurements; they will be considered in further detail in section 2.

It should be noted that the distance x (Fig.3) between the 90%-enriched uranium-oxide-source pellets must be kept highly reproducible, as it affects the wall return background. This last contribution is, by far, the largest effect to be dealt with when studying reactions without threshold, and will be discussed more fully. The trend in this laboratory has been towards determining wall return backgrounds experimentally rather than computing them. The method described previously [6] was felt to have, at least, two weak points:

a) The closest effective distance to the neutron source was not the minimum distance, and the statistical accuracy was neither ideal since one had to measure steeply varying geometrical flux attenuations which gave rise to flat wall return backgrounds of variable intensity level;

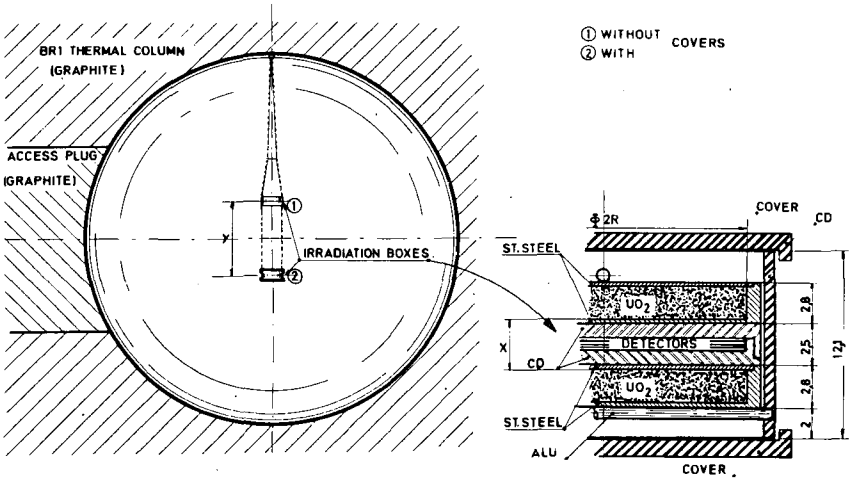

FIG.3. Irradiation device for integral cross-section measurements in thermal-fission-neutron spectra.

b) the self-shielding of wall-return-neutron spectra in the source-detector assembly was treated somewhat arbitrarily.

These shortcomings are avoided by means of the double source-detector assembly device illustrated in Fig.3. Here, too, use is made of the fundamental property of wall-return-neutron spectra in spherical cavities [23]:

$$\Phi_W(E;\ r_s,\ r_D) = \Phi_W(E) \quad r_s \leq 0.9\ R_0$$

where R_0 denotes the cavity radius, r_s the radial position of the fission source and r_D the radial position of the point where the wall return is observed.

The distance $y = \overline{r_s} - \overline{r_D}$ is chosen such that the direct contribution from the first source cap to the second (cadmium-covered) one is negligible with respect to the wall-return contribution.

It may then be shown [23] that, to a good approximation, the activation rates in cap 2 just provide a reliable determination of the wall-return contributions in cap 1, including any self-shielding effects both within detector foils and from traverse of the source pellets.

The amount of wall-return background depends on many, sometimes unexpected details of the irradiation geometry, as, e.g. the angular distribution of the incident thermal neutrons.[1] A suitable selection of the foil thicknesses may improve the signal-to-background ratio, as is illustrated in Table I. However, the most important parameter is, of course, the effective source-to-detector distance $\overline{X}$, i.e. a distance such that an equivalent point source would produce the same reaction rate within an equivalent point detector as is actually observed. This effective distance $\overline{X}$ is a sensitive function of X, and even more of R (Fig.3); its influence is also shown in Table I, where the effective cross-section is simply the absolute reaction rate observed in cap 1 divided by the absolute fission flux, before any wall-return correction has been applied.

2.3. Discussion of measurements and their accuracy

The reaction rates have been measured either by the activation technique or by means of track recorders.

In the first case, a variety of methods have generally been used according to the peculiarities of the radioactive nuclide under study. It is outside the scope of this paper to enter into these details which may be found in earlier internal documents or in progress reports to the EANDC or to the Euratom Working Group for Reactor Dosimetry. Only a few relevant comments will be given here. Generally speaking, interlaboratory exchanges have been organized whenever possible. For nuclides with rather short half-lives, this was limited to the CEN-absolute-measurement group of R. Jacquemin and to the neighbouring CBNM institute, where the kind ability of R. Vaninbrouckx was always highly appreciated. Very good agreement with our independently calibrated gamma-ray spectrometer [26] has been found most often.

---

[1] In the course of this systematic optimization study, it has been possible to understand more fully why the Monte-Carlo-correction factors determined by Bresesti et al.[24] for their irradiations in the converter facility of the ISPRA-I reactor are not to be applied to the collimated-beam geometry of Fabry [15].

TABLE I. SOME DETAILS OF THE MEASUREMENTS FOR (n, γ) REACTIONS

Reaction	Source Diameter					
$^{197}Au(n,\gamma)^{198}Au$	2 R = 9.68 ± 0.02 mm			2 R = 19.50 ± 0.02 mm		
	Effective cross-section (mb)	Wall-return correction (%)	Average fission-spectrum cross-section (mb)	Effective cross-section (mb)	Wall-return correction (%)	Average fission-spectrum cross-section (mb)
y = 10 cm	131	25	98	163	45	89
0.03 mm	131	21	105	161	45	89
thick foil	132	26	98	179	50	89
	132	24	101	185	49	95
	135	31	94	164	46	89
y = 20 cm	115	18	94	173	52	83
0.127 mm	114	18	93	181	51	90
thick foil				186	47	98
$^{115}In(n,\gamma)^{116m}In$						
y = 10 cm	186	17	155			
0.127 mm	183	16	152			
thick foil	193	20	155			
	192	20	153			
	189	17	156			
				238	31	164
0.1 mm				238	33	160
thick foil				217	31	149
y = 20 cm	188	16	157	225	32	153
0.127 mm	186	16	156	230	31	161
thick foil						

Use has also been made of standard sources supplied by the IAEA. A recent example is the circulation of ^{32}P-calibrated pellets organized by W. Köhler. The unactive samples have been irradiated in the fission spectrum and compared to better than ± 0.2% with the active standards using both plastifluor counters and the gas-flow high-stability proportional counter developed by Grundl [21]; this last counter has been operated very successfully at CEN for more than one year in the framework of our collaboration. The monitoring reactions $^{56}Fe(n,p)^{56}Mn$, $^{27}Al(n,\alpha)^{24}Na$ and $^{58}Ni(n,p)^{58}Co$ yielded typical fluence values of 1.005, 0.985 and 0.988 on the relative scale; this gives an indication on the degree of consistency in our routine procedures, i.e. better than ± 1%,[2] which is considered sufficient at present. When interpreted in terms of absolute flux values based on the beam-converter arrangement described by Depuydt [27] and

[2] The slight deviation for $^{56}Fe(n,p)$ is related to the fact that the measurements were performed with our calibrated spectrometer [26], which does not lead to high accuracies for ^{56}Mn owing to Compton contributions from γ-rays with greater energies than the main peak. This reaction is not a routine reaction used in this way.

further investigated by Fabry [15], an absolute average fission-spectrum cross-section of 72.7 mb results, to be compared with our published value of 74 ± 3 mb. In the case of the $^{115}In(n,\gamma)^{116m}In$ reaction, calibration has been performed as previously [15] by irradiation in a known thermal flux, but the 2200 m/s cross-section is here taken equal to 157 b. A similar procedure [6] is followed for all fission-cross-section measurements performed by means of the track-recorder technique. The fissile and fertile foils are 0.1 mm thick alloys with aluminum, supplied and assessed by R. Van Audenhove and his colleagues of CBNM. Various weight per cents of fissionable materials in the alloys, ranging from 1 up to 23%, are used to allow a check for systematic errors; none has been found. More details about this method are given in Refs [28-31]. The calibration procedure has been extensively investigated and verified at CEN [32].

At this stage, it might be of significance to emphasize that, at least for $\bar{\sigma}_{f5}$, many sources of systematic errors tend to cancel out or to be very small in the CEN methodology, as is easy to see with the help of relation (3) of Ref. [15]; schematically, if F denotes the number of fragment tracks counted per unit area, we have:

$$\sigma_{f5} = \frac{F_f}{F_{th}} \frac{1}{\bar{\nu}_5}$$

(The indices f, th denote fission- and thermal-flux irradiations, respectively)[3]

where $\bar{\nu}_5$ is the average number of prompt-plus-delayed neutrons per thermal fission of ^{235}U, taken equal to 2.422 ± 0.005 [33]. The combined error due to the assessment of converter plate and fission foils is believed to exceed hardly 1%. The reproducibility of $\bar{\sigma}_{f5}$ measurements in the facility presented in section 2.2. has been found exceptionally good, the statistical spread in about 10 runs being only of the order of 1% for a confidence level of 90%. This is in contrast to $\bar{\sigma}_{f8}$ measurements where the statistics are enigmatically poorer as yet. For $\bar{\sigma}_{f5}$ runs in the two types of caps (section 2.2), the corrections are as follows:

reactor background : < 0.1%;
^{238}U- and ^{234}U-contribution to ^{235}U-response : -2.5%;
perturbation by source-detector assembly : + 0.1%;
wall return background : - 2 ± 1%;
radial-flux-profile effect : - 26 ± 1.5%.

This last correction is the most serious. It does not play any role as far as fission-cross-section ratios are concerned, but must be established carefully when relating to each other track-recorder and activation measurements, which is needed for defining the wanted consistent set of spectral indices $\bar{\sigma}_i/\bar{\sigma}_{f5}$, as well as for deriving the absolute ^{235}U-fission cross-section because the beam-converter-plate facility is not suited to

[3] The geometrical factor G(x) describing in Ref. [15] the fission-flux attenuation with distance to converter plate has been experimentally checked many times to high accuracy and re-computed by S. De Leeuw (CEN) by a new general and very critical approach.

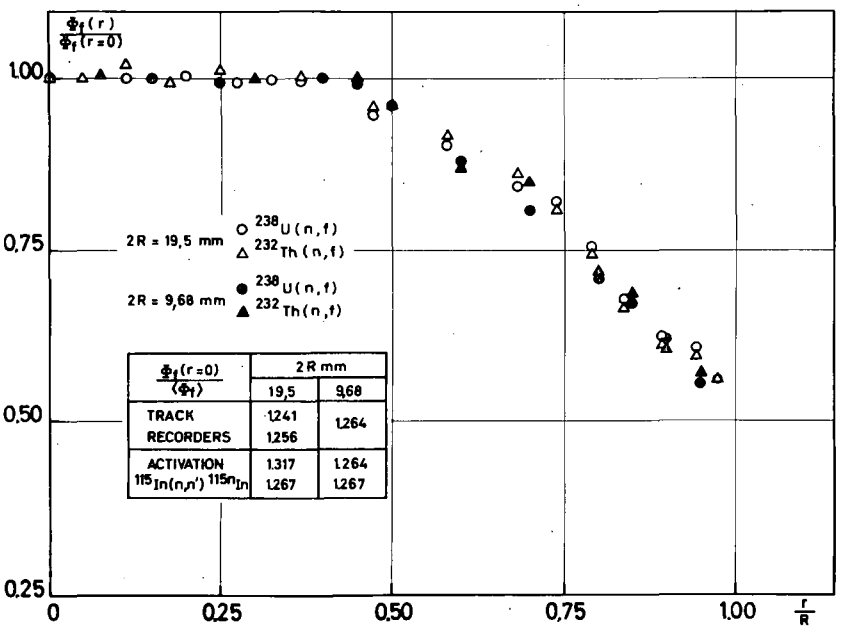

FIG.4. Radial fission-flux distribution in irradiation caps.

TABLE II. ABSOLUTE FISSION CROSS-SECTIONS (mb) MEASURED IN THE FISSION SPECTRUM $\chi_5(E)$[a]

$^{235}U(n,f) : \bar{\sigma}_{f_5}$	$^{239}Pu(n,f) : \bar{\sigma}_{f_9}$	$^{238}U(n,f) : \bar{\sigma}_{f_8}$	$^{232}Th(n,f) : \bar{\sigma}_{f_2}$
1340 ± 40	1985 ± 100	374 ± 30	87.5 ± 3.5

Cross-section ratios $\bar{\sigma}_{f_9}/\bar{\sigma}_{f_5}$		Cross-section ratios $\bar{\sigma}_{f_2}/\bar{\sigma}_{f_8}$	
This measurement :	1.48 ± 0.03	Measurements : this work	: 0.234
Evaluations: Parker 63 [34], Douglas 64 [35]	1.45	present $\bar{\sigma}_{f_2}$, earlier σ_{f_8} [6]	: 0.248
Schmidt 68 [36]	1.42	Barrall 68 [39] [b,c]	0.223
Hart 69 [37]	1.44	McElroy 70 [40] [d,c]	0.282
Greene 70 [38]	1.44	McElroy 70 [40] [e,c]	0.232
		Rago 70 [29] [f]	0.222
		Evaluation : Hart 69 [37]	0.232

[a] See also discussion in section 1.3.
[b] In the core of homogeneous water reactor.
[c] Based on ^{99}Mo fission-yield values of 2.7% and 6.3%, respectively, for $^{232}Th(n,f)$ and $^{238}U(n,f)$.
[d] Core centre of Lady GODIVA.
[e] GODIVA escape spectrum.
[f] Track-recorder technique.

direct study of reactions without threshold. The reaction $^{115}In(n,n')^{115m}In$ usually serves as a monitor for such purposes at CEN. Figure 4 illustrates the measurements performed to establish this correction, for the two types of source caps. The overall agreement between all experiments is satisfactory.

2.4. Presentation of results

The integral data obtained in this work are gathered in Tables II and III. Table II only gives four results which, with the exception of $\bar{\sigma}_{f5}$, have not been used in the analysis described in subsequent sections, for reasons which will now be outlined. The ^{239}Pu result is not final because the available data about the isotopic composition of the foils are preliminary (1% accuracy). The number of runs, although of exceptionally good reproducibility ($\sim$ 0.1 - 0.2%), is still rather limited: three runs only, but companion ^{235}U foils provided $\bar{\sigma}_{f5}$ values in perfect agreement (0.1%) with the bulk of the data discussed in section 2.3. Inasmuch as $\bar{\sigma}_{f9}$ is insensitive to the shape of $\chi_5(E)$, there is much incentive to treat $\bar{\sigma}_{f9}/\bar{\sigma}_{f5}$ as an integral constraint upon $\sigma_{f9}(E)/\sigma_{f5}(E)$; this is attempted on the left-hand side of Table II, where use has been made of a few evaluated cross-section files. The measured ratio is a little higher than all the computed ones, the discrepancy perhaps lying just at the limit of the respective errors. The accurate figure of (1340 ± 40) mb obtained for $\bar{\sigma}_{f5}$ is in excellent agreement with the value of (1335 ± 130) mb previously obtained [6], while the present $^{238}U(n,f)$-result is higher, but not strictly discrepant with our earlier value of (353 ± 30) mb, which seems to be preferable. Only the rather old measurements of Henkel [41] are available to specify the absolute $^{232}Th(n,f)$ differential cross-section in the energy range of interest here; clearly, the present integral result can primarily be used to check Henkel rather than to be part of the consistent set of spectral indices in the fission spectrum. The cross-section ratio $\bar{\sigma}_{f2}/\bar{\sigma}_{f8}$ is also considered in Table II because it is not very sensitive to the shape of neutron spectra, because of the similar behaviour of the two excitation functions. No attempt has been made to interpret these results any further at the present stage of the work. In Table III the recommended set of spectral indices and uncertainties is derived for the subsequent tentative analysis of high-energy nuclear data. These experiments which are believed to be the most reliable and complete ones have only been considered for combination with our own results. The reactions have been selected on the basis of straightforward criteria. The two reported capture cross-sections require a brief discussion since they disagree by as much as 30% with earlier preliminary values obtained at this laboratory [15]; the approach followed in the preliminary work was similar to that illustrated later on in Ref. [6], but the experimental arrangement was less refined. To assure more confidence in the data and to understand the discrepancy, two additional runs have been conducted with the device used in Ref. [6]; the cross-sections obtained for the $^{197}Au(n,\gamma)^{198}Au$ reaction are, respectively, 92.7 and 95.7 mb, now in very good agreement with the weighted mean value of 94 ± 5 mb given in Table III.

TABLE III. CONSISTENT SET OF SPECTRAL INDICES IN THE ^{235}U THERMAL-FISSION-NEUTRON SPECTRUM

Reaction	Boldeman 64 [42]		Grundl 68 [14]		Bresesti 70 [25]		This work		Recommended set
	$\bar{\sigma}$ [a]	$\bar{\sigma}/\bar{\sigma}_{f5}$ [b]	$\bar{\sigma}$	$\bar{\sigma}/\bar{\sigma}_{f5}$ [b]	$\bar{\sigma}$ [a]	$\bar{\sigma}/\bar{\sigma}_{f5}$ [b]	$\bar{\sigma}$ [a]	$\bar{\sigma}/\bar{\sigma}_{f5}$	$\bar{\sigma}/\bar{\sigma}_{f5}$
$^{197}Au(n,\gamma)^{198}Au$	-	-	-	-	-	-	94 ± 5	0.0704	0.0704 ± 2%
$^{115}In(n,\gamma)^{116m}In$	-	-	-	-	-	-	156 ± 6	0.117	0.117 ± 2%
$^{235}U(n,f)F.P.$	-	-	1250 [c]	0.996	-	-	1335 ± 55	1.000 [e]	1.000 [e]
$^{237}Np(n,f)F.P.$	-	-	1365 ± 95	1.088	-	-	-	-	1.088 ± 4%
$^{115}In(n,n')^{115m}In$	-	-	-	-	177 ± 6	0.150	200 ± 8	0.150	0.150 ± 2% [f]
$^{238}U(n,f)F.P.$	-	-	325 ± 19	0.259	308 ± 15	0.262	353 ± 30	0.264	0.260 ± 3%
$^{31}P(n,p)^{31}Si$	30.5 ± 1.2	0.0287	38.7 ± 2.7	0.0308	-	-	-	-	0.030 ± 3%
$^{32}S(n,p)^{32}P$	60 ± 1.2	0.0564	-	-	-	-	73 ± 3	0.0547	0.055 ± 2%
$^{58}Ni(n,p)^{58}Co$	105 ± 5	0.0987	-	-	104.5 ± 4	0.0888	120 ± 6	0.0899	0.090 ± 3%
$^{27}Al(n,p)^{27}Mg$	2.9 ± 0.5	0.00273	4.70 ± 0.33	0.00374	-	-	4.35 ± 0.20	0.00326	0.00325 ± 10%
$^{56}Fe(n,p)^{56}Mn$	0.90 ± 0.05	0.000846	1.15 ± 0.08	0.000916 [d]	1.06 ± 0.04	0.000901	1.15 ± 0.04	0.000861	0.000865 ± 6%
$^{27}Al(n,\alpha)^{24}Na$	0.60 ± 0.03	0.000564	0.752 ± 0.05	0.000599	0.695 ± 0.02	0.000590	0.78 ± 0.03	0.000584	0.000590 ± 2%
$^{63}Cu(n,2n)^{62}Cu$	-	-	0.123 ± 0.009	0.0000980	-	-	-	-	0.000098 ± 7%

[a] As reported originally by the authors.
[b] Fitted to the spectral indices scale of this work.
[c] Normalization. The cross-section scale chosen by Grundl 68 has been preserved, except for d.
[d] See text.
[e] Normalization value.
[f] The error band does not include the uncertainties in the internal-conversion coefficient. The γ-ray intensity for the 335-keV isomeric transition is fixed to 46% throughout this work, including the evaluation of σ(E).

3. SELECTION OF DIFFERENTIAL-CROSS-SECTION DATA FOR THE ANALYSIS OF INTEGRAL MEASUREMENTS IN THE HIGH-ENERGY RANGE

3.1. Foreground

Three input sets of differential cross-sections, labelled as sets 1, 2 and 3, have been used for the present analysis of integral data. They only differ (section 1.2) by the choice of $\sigma_{f5}(E)$; all the cross-section ratios $\sigma_i(E)/\sigma_{f5}(E)$ are kept constant, except for the analysis of Lady GODIVA where various subsets of our main set 2 have also been tried (section 5.2). Furthermore, all three sets are identical at neutron energies above 2.2 MeV.

3.2. Background

It must be understood that the present effort to evaluate input-data sets has been kept as limited as possible, i.e. it has been attempted to draw maximum benefit from existing evaluations, which were first of all critically reviewed and confronted with each other. As far as fissile and fertile nuclides are concerned, this mainly includes the old [34, 35] and new DFN [37, 53], the ENDF/B [54] and the KEDAK [36] files as well as recent Los Alamos [55, 56] and Argonne [57, 58] work.

The $\sigma_{f9}(E)/\sigma_{f5}(E)$ and $\sigma_{c8}(E)/\sigma_{f5}(E)$ ratios have finally been taken, respectively, from Greene [38] and from Davey [58]; $\alpha_5(E)$, $\sigma_{in5}(E)$ and the ^{235}U-down-scattering matrix pertain to the various subsets used for the analysis of GODIVA, as is briefly commented in section 5.2. Our standard choices are, respectively, Berlijn [55] for $\alpha_5(E)$ and Parker for the ^{235}U-down-scattering data, except in the case of set 2 where $\alpha_5(E)$ is taken from KEDAK. The ^{238}U-down-scattering matrix and the total inelastic-scattering cross-section of Parker [34] seem, at present, the less bad choice; the $\sigma_{in8}(E)$ curve of Parker is supported by current CEN spherical-shell-transmission measurements [16], in contrast to the new DFN [59], ENDF/B [60] and KEDAK selections, which appear to have weighted too heavily the time-of-flight measurements of Barnard [61] and to lead towards the prediction of too high down-scattering from above to below 1 MeV: this might be one of the reasons for the difficulties in computing ^{238}U-to-^{235}U-fission ratios in fast reactors [19]. The transport cross-sections have finally been taken from KEDAK [36] and $\bar{\nu}(E)$ from Fillmore [33]. In all the GODIVA calculations, the elastic, transport-corrected, cross-sections are always left free so as to compensate the modifications of other data while preserving the transport cross-sections.

The ratio $\sigma_{f8}(E)/\sigma_{f5}(E)$ has received particular attention and will be further discussed; the conclusion of our literature appraisal has been to follow the recommendation of Grundl-67 [62] as input selection. The cross-section-ratio scale when analysing Grundl's work [14, 52, 62] can be chosen arbitrarily, but an appropriate scale is needed to combine his data with other ones (i.e. Tables III and VII) and the suggestion of the author for this scale (Table III of Ref. [62]) has been estimated suitable, except for the ^{31}P(n, p)^{31}Si and ^{56}Fe(n, p)^{56}Mn reactions; for the first one, serious doubts existed, but no other choice was possible a priori; for the second one, there is a systematic discrepancy between the Chalk River [63] and the CBNM

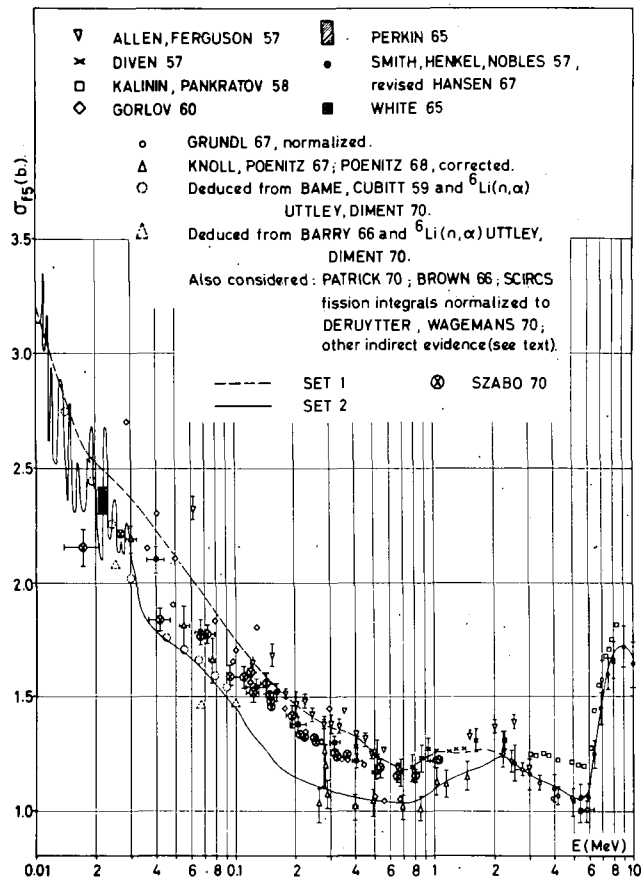

FIG. 5. The neutron-induced ^{235}U-fission cross-section at high energy.

[64, 65] measurements: this discrepancy of (10.5 ± 1)% is also found for the ^{59}Co(n,α)^{56}Mn reaction in the extensive studies of these two laboratories and is tentatively attributed [65] to the measurement of absolute reaction rates rather than to the flux monitoring; the Chalk River data have been lowered by 10.5%, for various reasons, including the CEN absolute integral results. With this exception in mind and as far as spectral indicators are concerned, the overall conclusion of our initial survey has been to follow Grundl's $\sigma_i(E)/\sigma_{f5}(E)$ data [62] as input selection, and to re-evaluate the reactions not considered by this author. This re-evaluation is reported in Figs 6 to 8 and in Table VIII which is to be considered here as supplementary to Table III of Ref. [62]. The absolute scale in Table VIII is that of our set 3, but attention must be paid to the fact that the absolute scale for the best curves in Figs 7 and 8 is that of our set 2. Not illustrated is the reaction ^{32}S(n,p)^{32}P for which the recommendation of CBNM [66] may consistently be followed all throughout this work. The detailed ingredients of our tentative evaluations are to be found elsewhere [67, 68].

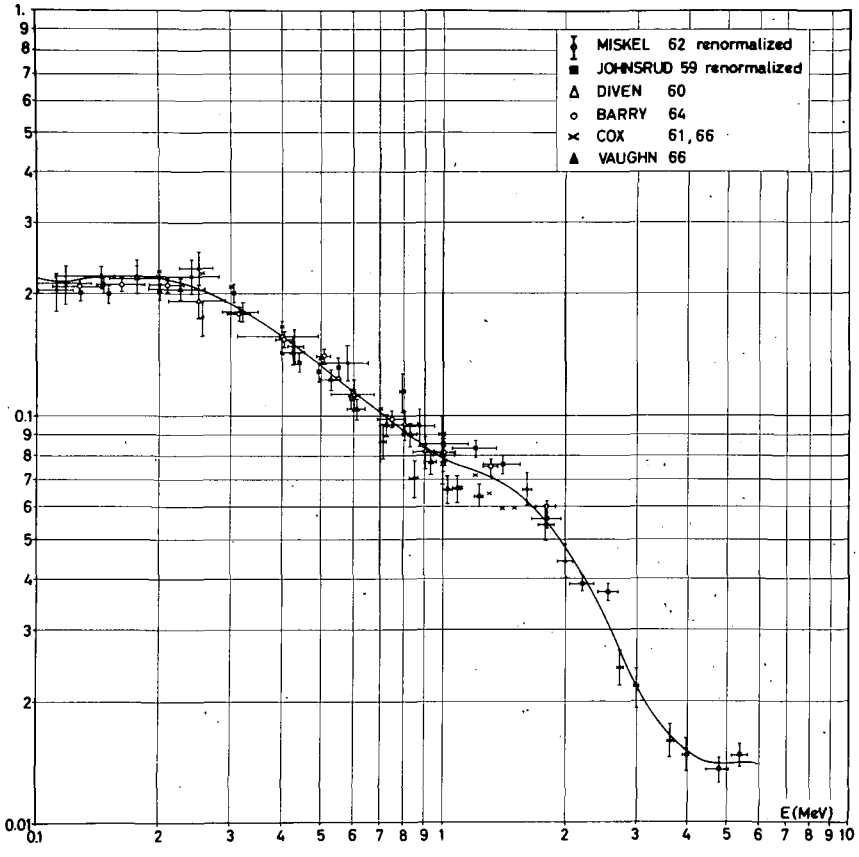

FIG.6. $^{197}Au(n,\gamma)^{198}Au$ to ^{235}U fission cross-section ratio.

3.3. Specification of $\sigma_{f5}(E)$ for the three data sets used in this analysis

At neutron energies greater than 2.2 MeV, the absolute measurements of Smith, Henkel and Nobles [69], as corrected by Hansen et al.[70] for scattering effects in proton-recoil telescope, are preferred to the higher-lying data of Kalinin and Pankratov [71] (Fig.5).

Hinging on the 2.2 MeV point are drawn three $\sigma_{f5}(E)$-curves down to 10 keV, which constitute the basis of our differential data sets 1, 2 and 3. Set 1 simply follows Parker 63 [34] below 1 MeV and is essentially identical with the selection of Grundl 67 [62] (Fig.5). It provides $\bar{\sigma}_{f5}$ = 1250 mb. Note that accepting Parker's data over the whole energy range leads to $\bar{\sigma}_{f5}$ = 1300 mb and about an increase of 1.8% in k_{eff} for GODIVA. Set 2, on the other hand, is the lowest, but still acceptable from the point of view of the conflicting absolute average fission-spectrum cross-section measurements: it gives $\bar{\sigma}_{f5}$ = 1157 mb, i.e. is in substantial agreement with Leachman and Schmitt [8], as pointed out in section 1.3., but presents a 15% discrepancy with the absolute scale of the present measurements (section 2.3). $\sigma_{f5}(E)$ for set 2 has been patterned according to what might be called a number of direct and indirect suggestive evidences. Among

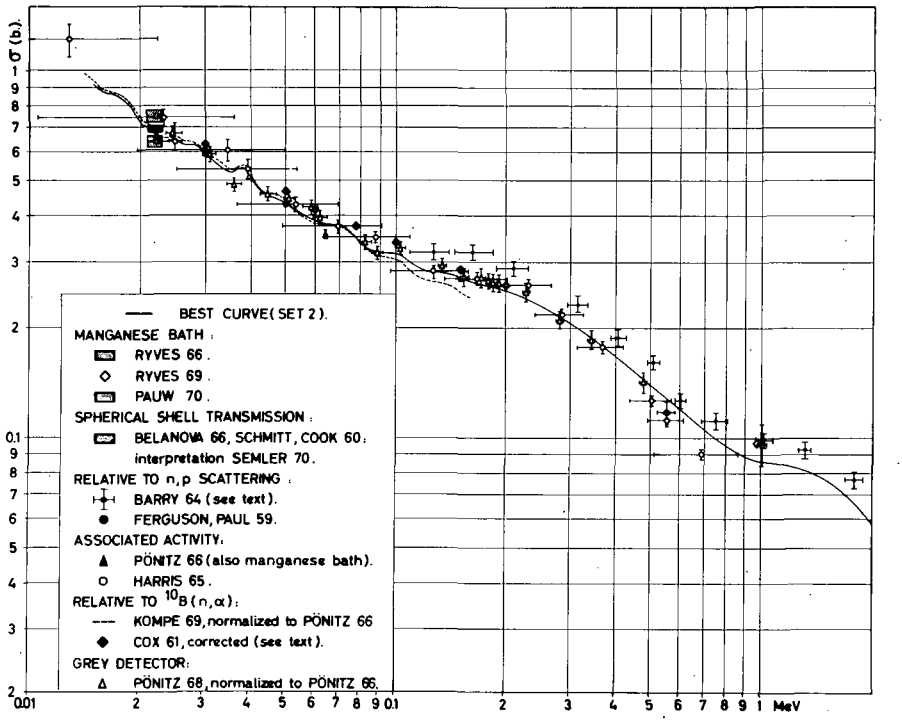

FIG. 7. The high-energy neutron-capture cross-section of gold.

the direct evidences, there is the famous Poenitz [72] grey-detector-cross-section-shape measurement,[4] corrected according to Ref. [73] and normalized to the Knoll-Poenitz [74] absolute point at 30 keV; this is partly supported, too, by Gorlov's [76] data, and by the recent high-resolution time-of-flight measurements of Patrick et al. [77] which, when increased by 5%, just constitute our set-2 curve between 10 and 30 keV (Fig. 5); the pronounced intermediate structure (section 1.3) observed in this energy range casts some doubt on the reliability of the careful Sb-Be source measurement of Perkin et al. [78]; this structure has also been observed in the Petrel nuclear-explosion time-of-flight measurements of Brown et al. [79]; once renormalized according to Deruytter, Wagemans 70 [80], the data of Brown lead to a fission integral between 10 and 20 keV of 2768 mb, in perfect agreement with a similar manipulation of the Saclay data (2801 mb; deduced from SCIRCS files [81][5] and only 5.5% higher than according to our set-2 curve (2625 mb), i.e. in agreement within combined uncertainties.

[4] Shape agrees with Allen and Ferguson [75].

[5] The corresponding Dubna [81] figure is 3300 mb.

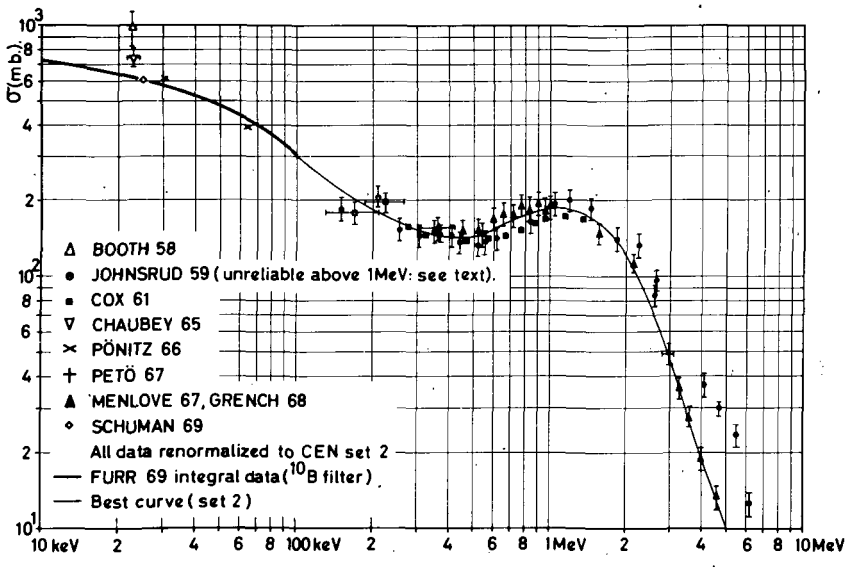

FIG.8. The high-energy cross-section of the reaction $^{115}In(n,\gamma)^{116m1}In$.

Among the indirect evidences, the $^{6}Li(n,\alpha)$ cross-section deduced below 100 keV from accurate ^{6}Li total [82-84] and scattering [85] cross-section measurements may be compared to data obtained relatively to $\sigma_{f5}(E)$ with a view to contesting this last cross-section. The dashed circles [86][6] and the triangles [87] in Fig.5 are obtained in this way. As suggested elsewhere [72], a similar treatment may be applied to the gold capture cross-section data and this has been done too in the energy range 30-500 keV, using Fig.6; the absolute gold capture cross-section accepted for this game (Fig.7) relies upon Refs [89-94].

Note that a kind of breaking-off in the shape of $\sigma_{f5}(E)$ between 100 and 200 keV is needed to keep the Cox [95] gold capture results below 200 keV in line with the overall shape displayed in Fig.7, once the $^{10}B(n,\alpha)$ cross-section recommended by Sowerby et al. [88] is preferred to other evaluations [96, 97], a choice which also improves the consistency between the gold shapes as measured by Kompe [98] and by Poenitz [99]. Indications for such a breaking-off in $\sigma_{f5}(E)$ may also be seen in the higher-lying data of White [10] and of Szabo et al. [100]. When combined with the $\sigma_{c8}(E)/\sigma_{f5}(E)$ evaluation of Davey [58], our $\sigma_{f5}(E)$ set-2 curve throws us back perfectly upon the low but careful $\sigma_{c8}(E)$ measurements of Moxon [101] below 100 keV, which might be considered consistent with the resolved resonance range data of Glass [102].

Set 3 has to some extent been derived from the previous one as far as a number of shape features is concerned: so the breaking-off between 100 and 200 keV is preserved, and no modification at all is made below 30 keV, but the absolute scale from 30 keV up to 2.2 MeV has been largely influenced by the recent $\sigma_{f5}(E)$ and even more the $\sigma_{f9}(E)$ measurements of

[6] Neglecting possible multiple-scattering errors in the calibration of the ^{6}Li glass scintillator used.

Szabó et al.[100] below 1 MeV. This set is not shown in Fig.5, but is given in Table VIII. Probably the weakest point in $\sigma_{f5}(E)$ for the present analysis is how to join data between 2.2 and about 1.5 MeV, where the Diven [103] measurements cease to exist.

4. INTERPRETATION OF INTEGRAL MEASUREMENTS IN THE ^{235}U THERMAL-FISSION-NEUTRON SPECTRUM

4.1. Method

The two sets of data $r_i = \bar{\sigma}_i/\bar{\sigma}_{f5}$ and $\sigma_i(E)/\sigma_{f5}(E)$ are constrained to fulfill the relations

$$r_i = \frac{\int_0^\infty \sigma_i(E)\,\chi_5(E)\,dE}{\int_0^\infty \sigma_{f5}(E)\,\chi_5(E)\,dE} = R_i, \quad i = 1, \ldots, N$$

where all quantities $\sigma_i(E)$, $\sigma_{f5}(E)$, r_i and $\chi_5(E)$ are subjected to statistical spreads as well as to possible systematic errors. The problem is considered to delineate all these uncertainties better. To manage this, a physically reasonable analytical approximation to $\chi_5(E)$ is needed so as to reflect all uncertainties in $\chi_5(E)$ upon a limited number of underlying parameters p_K. This approximation must be reasonably simple, but also sufficiently grounded to avoid misleading conclusions.

A FORTRAN-IV least-squares fit program has been written [104] which basically minimizes the expression

$$\sum_i W_i \left[\frac{r_i - R_i(p_K)}{r_i}\right]^2 \qquad (W_i \text{ are weight factors})$$

with respect to the parameters p_K. Using the resulting p_K^0 values, the percent deviations $\delta_i = (r_i - R_i(p_K^0))/r_i$ are computed. If $\delta_i \gg \delta r_i$ where δr_i is the confidence interval of r_i, a hidden error may then be suspected either in r_i or in $\sigma_i(E)/\sigma_{f5}(E)$ or in both of them. This is confirmed, first, by repeating the least-squares fit with the corresponding weight W_i set up to zero. When reasonably justified, according to the evaluation work in previous sections, the cross-section ratio $\sigma_i(E)/\sigma_{f5}(E)$ may be modified, or the integral figure definitely rejected. It must be emphasized that only gross errors are sought, and that no effort has been undertaken to optimize the ratios $\sigma_i(E)/\sigma_{f5}(E)$ in all details, as yet. The least-squares procedure has been run for the three choices of the functional dependency $\sigma_{f5}(E)$ outlined in section 3.3.

4.2. Theoretical models of prompt-fission-neutron emission and selection of parameters.

In view of the importance of this phenomenon, the theory of prompt-fission-neutron emission is still a matter of embarrassment. Rather sophisticated calculations of the total neutron spectrum have been performed [11, 105-107] in which account is taken of the frequency of occurrence

of individual primary-fission fragments, the distribution of their excitation energy, the saw-tooth mass dependence of the number of emitted neutrons, and many other known peculiarities of the fission process. Most often, it is assumed [11] that all neutrons are evaporated isotropically in the centre-of-mass system from moving fragments after they have reached their full velocities; a few authors [108, 109] have explored the suggestion by Bohr and Wheeler [110] that some fraction of the total number of neutrons might be emitted at or very nearly close to the moment of scission. The existence of these scission or "central" neutrons is far from being unambiguously established, but seems to be supported by a number of experimental studies (i.e. [43-46], [111-113]). The spectral depletion in $\chi_5(E)$ below 1.4 MeV suggested by the integral data of Grundl [14] was a further incentive to consider scission neutrons in the present analysis.[7] The selected representation $\chi_5(E)$ is given by the expression:

$$\chi_5(E) = \frac{1}{\sqrt{\pi}} \sum_{K=L,H} \nu_K \frac{e^{-\frac{E_f^K}{T_K}}}{\sqrt{T_K E_f^K}} e^{-\frac{E}{T_K}} \sinh \frac{2}{T_K} \sqrt{E_f^K E} + \nu_C \frac{E}{T_c^2} e^{-\frac{E}{T_c}}$$

where L, H mean the light and heavy fragment groups, respectively. The first two terms in the summation correspond to the simplifying assumption that the mean spectra of neutrons evaporated from the light and heavy fragment in the pairs are emitted isotropically in the centre-of-mass system with an essentially Maxwellian-type energy distribution

$$\Phi_K(\eta) = \frac{2}{\pi^{1/2} T_K^{3/2}} \eta^{1/2} e^{-\eta/T_K}$$

where η denotes the centre-of-mass neutron energy.

Such an assumption is just a plausible special case of the cascade-emission statistical model of Le Couteur and Lang [114]; however, the detailed distribution of the nuclear temperatures of the fission fragments is ignored and replaced by a mean temperature T_K. Measured centre-of-mass neutron spectra agree roughly with this picture or, at least, are not felt to disagree enough for the present analysis of integral experiments to be made unvalid. The choice of an evaporation-type distribution for the central component is somewhat arbitrary, but usually accepted.[8]

A further advantage of the selected representation is that putting ν_c equal to zero is just equivalent to trusting the recommendation of Terrell (Ref. [47], page 900) in his variance analysis of neutron-emission spectra, i.e. to testing directly the usual semi-empirical single Maxwellian representation of fission-neutron spectra (corresponding to $\bar{\eta}_L - \bar{\eta}_H \simeq 0.85$ MeV).

---

[7] Another approach, considered less attractive and grounded, would be to introduce a centre-of-mass anisotropy of neutron emission.

[8] It fits experiment within the rather large error bands once isotropic emission of scission neutrons in the laboratory system is assumed; ν_C is deduced in this way from angular distributions of neutrons with respect to fragments.

TABLE IV. LITERATURE DATA RELEVANT TO FISSION NEUTRONS FROM THERMAL-NEUTRON-INDUCED FISSION OF ^{235}U

Authors	ν_L/ν_H	$\bar{\eta}_L$ (MeV) [a]	$\bar{\eta}_H$ (MeV) [a]	$\bar{\eta}$ (MeV) [c]	ν_C/ν [e]	T_C
Skarsvåg, Bergheim 63 [43]	1.45 ± 0.12	1.19	1.23	1.21 ± 0.03	15%	0.92
Kapoor 63 et al. [44]	1.30 ± 0.07	1.36	1.03	1.21 ± 0.06	~ 10%	1.60
Blinov 65 et al. [45]	1.10	1.28 [b]	1.26 [b]	1.27 ± 0.03	≤ 10%	-
Milton, Fraser 65 [d] [46]	1.50	1.32	1.26	1.30	20%	1.07
Terrell 62 [47]	1.0 ± 0.1	-	-	1.21 ± 0.05	-	-
Apalin 64 et al. [48]	1.15	-	-	-	-	-
Maslin 67 et al. [49]	1.27	-	-	-	-	-

[a] Eventually computed from original data when the representation $\chi_5(E)$ used differs from the one accepted in this paper.

[b] Estimated. Authors only state that $\bar{\eta}_L - \bar{\eta}_H < 0.02$ MeV.

[c] $\bar{\eta} = \dfrac{\nu_L \bar{\eta}_L + \nu_H \bar{\eta}_H}{\nu_L + \nu_H}$

[d] Fit number 8 in Table I of original paper.

[e] $\nu = \nu_L + \nu_H + \nu_C$.

In the present analysis, the free parameters p_K (section 4.1) are T_L, T_H, and T_C; however, ν_c has been varied by steps until optimum conditions were found for one of the cross-section sets defined in section 3. The finally accepted value is $\nu_C/\nu_L + \nu_H + \nu_C = 0.18$, which is quite reasonable, as may be seen from Table IV. The ratio ν_L/ν_H has been fixed at 1.30, also after scanning the field of possibilities by steps. The average fragment kinetic energies per nucleon are taken to be [47]

$$E_f^L = 1.01 \pm 0.02 \text{ MeV}$$

$$E_f^H = 0.48 \pm 0.01 \text{ MeV}$$

4.3. Implications of the least-squares fit

Tables V and VI show the output data. The analysis has revealed a number of remarkable features which are now shortly discussed.

First of all, it seems quite well established by this work that the simple semi-empirical Maxwellian representation of fission neutron spectra as suggested by Terrell [11] and widely used between 1958 and 1970 is inadequate for correlating differential and integral cross-section ratios in the energy range concerned here: such a simple representation is unable to achieve this while preserving simultaneously the fission age to indium resonance in water. The clarification of the age dilemma (section 1.3) is perhaps the most enjoyable result of this study from the standpoint of reactor physics; indeed, the age is essentially sensitive to the mean energy and not to the higher moments of the fission neutron spectra so that the apparently conflicting items have now been reconciled at the expense of some distortion in the spectrum shape. The cross-section set 2, however, does not seem to be ideal with respect to age, but this conclusion is not really clear-cut because of the present lack of a reasonable scheme for error propagation in the analysis; furthermore, the accuracy of the theoretical age calculations might be overestimated.

The Watt formula $\chi_5^W(E)$, with $\nu = \sqrt{2}$ and $\beta = 1$ (section 1.2), has been recommended by one of the authors of this paper since early 1966 [115]. It is seen that such a selection is a more or less reasonable approximation, except at very high energy where it predicts too few neutrons; a similar result has been obtained recently by Steen [116] from consideration of the $^{16}O(n,p)^{16}N$ reaction rates. For the Watt formula the average energy in the system $\bar{\eta}$ largely disagrees with the data in Table IV, which is not the case with any of the three other representations.

Less satisfactory is the difference between the average temperatures for the heavy and the light fragments: although such a result would be physically easier to understand [117], it is reproduced only by one of four differential experiments [44][9] (Table IV). If ν_C is put equal to zero, a poorer but still quite acceptable fit results, with $\bar{\eta} = 1.21$ MeV, $\bar{E} = 1.986$ MeV and $\bar{\eta}_L - \bar{\eta}_H = 0.48$ MeV (instead of 0.23 MeV) for cross-section set 3; the value for the simple Maxwellian representation is 0.85 MeV which confirms

[9] in which the selected range of fragment masses might be too restricted.

TABLE V. FISSION-SPECTRUM AVERAGE CROSS-SECTION RATIOS FOR VARIOUS REPRESENTATIONS OF $\chi_5(E)$ AND THE FISSION AGE TO INDIUM RESONANCE IN WATER (τ_f)

Reaction	Measured	Computed							
		Set 1		Set 2		Set 3		Set 3 (Watt)	
	$\bar{\sigma}/\bar{\sigma}_{f5}$	$\bar{\sigma}/\bar{\sigma}_{f5}$	Deviation (%)[d]	$\bar{\sigma}/\bar{\sigma}_{f5}$	Deviation (%)[d]	$\bar{\sigma}/\bar{\sigma}_{f5}$	Deviation (%)[d]	$\bar{\sigma}/\bar{\sigma}_{f5}$	Deviation (%)[d]
$^{197}Au(n,\gamma)^{198}Au$	0.0704	0.0734	- 4.2	0.0720	- 2.3	0.0730	- 3.7	0.0739	- 5.0
$^{115}In(n,\gamma)^{116m}In$	0.117	0.110	+ 6.0	0.109	+ 6.8	0.110	+ 6.0	0.110	+ 6.0
$^{237}Np(n,f)$ F.P.	1.088	1.046	+ 3.9	1.058	+ 2.8	1.051	+ 3.4	1.102	- 1.3
$^{115}In(n,n')^{115m}In$	0.150	0.152	- 1.3	0.155	- 3.3	0.152	- 1.3	0.152	- 1.3
$^{238}U(n,f)$ F.P.[b]	0.260	0.244	+ 6.2[a]	0.248	+ 4.6[a]	0.244	+ 6.2[a]	0.244	+ 6.1[a]
$^{31}P(n,p)^{31}Si$ [b]	0.030	0.0266	+ 11	0.0270	+ 10	0.0264	+ 12	0.0267	+ 11
$^{32}S(n,p)^{32}P$	0.0552	0.0541	+ 1.9	0.0547	+ 0.9	0.0537	+ 2.7	0.0542	+ 1.8
$^{58}Ni(n,p)^{58}Co$	0.0897	0.0901	+ 0.4	0.0912	- 1.7	0.0894	- 0.3	0.0900	- 0.3
$^{27}Al(n,p)^{27}Mg$	3.26, -3	3.21, -3	+ 1.5	3.20, -3	+ 1.8	3.17, -3	+ 2.8	3.11, -3	+ 4.6
$^{56}Fe(n,p)^{56}Mn$	8.61, -4	8.97, -4	- 4.2	8.87, -4	- 3.0	8.84, -4	- 2.7	8.33, -4	+ 3.2
$^{27}Al(n,\alpha)^{24}Na$	5.91, -4	6.07, -4	- 2.7	6.00, -4	- 1.5	5.99, -4	- 1.4	5.50, -4	+ 6.9
$^{63}Cu(n,2n)^{62}Cu$	9.80, -5	9.73, -5	- 0.7	9.54, -5	+ 2.7	9.6, -5	+ 2.0	6.93, -5	+ 29.0
T_L (MeV)		0.979		0.966		0.977		-	
T_H (MeV)		0.725		0.648		0.700		-	
T_C (MeV)		0.879		0.809		0.854		-	
$\bar{\eta}$ (MeV)		1.303		1.242		1.280		1.5	
$\bar{E}$ (MeV)		2.024		1.948		1.999		2.000	
τ_f (cm^2)[c]		26.62		25.73		26.33		26.30	

[a] Using $\sigma_{f8}(E)/\sigma_{f5}(E)$ ratios recommended in this paper; the deviations amount to about 11% for more conventional choices of these ratios below 2 MeV.

[b] Finally taken with weight zero in least-squares fitting.

[c] Most probable experimental value: (26.5 ± 0.2) cm^2.

[d] Deviation: (measured-computed)/measured.

TABLE VI. SEVEN-GROUP DISPLAY OF VARIOUS REPRESENTATIONS $\chi_5(E)$

Energy groups (MeV)	This work			Grundl 68 [14]	Watt [3]
	Set 1	Set 2	Set 3		
0 - 0.6	0.1583	0.1690	0.1617	0.373	0.1682
0.6 - 1.4	0.2755	0.2863	0.2790		0.2718
1.4 - 2.2	0.2125	0.2121	0.2124	0.360	0.2087
2.2 - 3.0	0.1405	0.1353	0.1388		0.1399
3.0 - 6.0	0.1850	0.1716	0.1806	0.241	0.1864
6.0 - 11.0	2.743, -2	2.501, -2	2.6667, -2	2.57, -2	2.546, -2
11.0 - 20.0	7.900, -4	7.157, -4	7.7314, -4	6.9, -4	5.517, -4

this representation to be grossly in error. These comments suggest a repetition of the fits with the restriction that $T_L = T_H$ and perhaps ν_L/ν_H left entirely free.[10] However, not too much physical meaning should be expected from fits to integral data. Also quite interesting is the systematic observation of anomalous deviations (> 10%) for the spectral indices involving $^{238}U(n,f)$ and $^{31}P(n,p)$: this was true in all fits attempted, whatever the value for ν_C was and whatever cross-section set was used. Table III suggests that this should be attributed to errors in $\sigma_i(E)/\sigma_{f5}(E)$ rather than to uncorrect integral data. As far as $^{31}P(n,p)$ is concerned, this is instantaneously confirmed [118] by the existence of serious doubts on the absolute scale for $\sigma_i(E)/\sigma_{f5}(E)$ as well as discrepant shapes between the threshold and 2.5 MeV; thus, this reaction has been rejected from analysis.

Figure 9 displays the present situation for $\sigma_{f8}(E)/\sigma_{f5}(E)$. The accurate data from Refs [62, 69, 70, 119, 120] hamper any contest for energies above 2.5 MeV. Below 2 MeV, it is customary to trust the very detailed measurements of Lamphere [121], renormalized to the other precise data in the first plateau above this energy. The present work strongly suggests a systematic unsuspected error in the Lamphere data: although the energy resolution is of the order of 50-60 keV, the simplest improvement would be to assume an error in the neutron-energy calibration, and it seems appropriate to shift all the points by about 100 keV towards lower energies. Such a correction associated to a better depiction of fission-neutron spectra is believed to help improve the computations of ^{238}U- to ^{235}U-fission ratios in reactors.

[10] A manageable improvement would be to allow a linear distribution of temperatures for both fragment groups up to a cut-off value taken as parameter.

TABLE VII. SPECTRAL INDICES[a] AT CORE CENTRE OF LADY GODIVA

Reaction	Computed			Measured		
	Set 1	Set 2	Set 3	Hansen 62 [50] Byers 60[b] [51]	Grundl 66 [52]	McElroy 70 [40]
$^{197}Au\,(n,\gamma)^{198}Au$	0.105	0.106	0.104	0.105	-	0.115
$^{115}In\,(n,\gamma)^{116m}In$	0.130	0.131	0.130	0.126	-	-
$^{238}U\,(n,\gamma)^{239}U$	0.0885	0.0892	0.0884	0.0734	-	0.0835
$^{239}Pu\,(n,f)$ F.P.	1.351	1.347	1.367	1.420	-	-
$^{115}In\,(n,n')^{115m}In$	0.102	0.101	0.102	-	-	0.117
$^{238}U\,(n,f)$ F.P.	0.148	0.146	0.149	0.156	0.161[c] ± 0.002	0.168
$^{32}S\,(n,p)^{32}P$	0.0331	0.0324	0.0331	-	-	0.0379
$^{58}Ni\,(n,p)^{58}Co$	0.0552	0.0540	0.0551	-	-	0.0591
k_{eff}	1.018	0.963	1.008			

[a] Relative to $^{235}U\,(n,f)$.
[b] Renormalized.
[c] Mean between activation-foil and fission-chamber measurements.

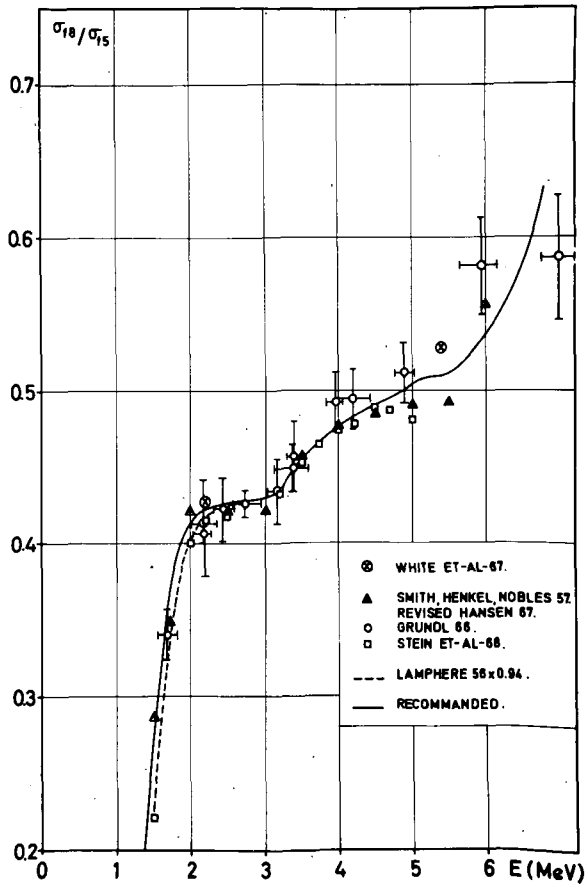

FIG. 9. ^{238}U-to-^{235}U-fission-cross-section ratio as a function of neutron energy.

5. TENTATIVE ANALYSIS OF LADY GODIVA

5.1. Purpose

It is now attempted to derive further evidence (section 1.2) for better discrimination between the three sets of nuclear data previously described (section 3) and used (section 4). This is done by applying them to the elemental critical assembly GODIVA. It is assumed that $\chi_5(E)$ is not markedly different for thermal- and fast-neutron-induced fission, in accordance with Grundl [122].

5.2. Method

The geometry and composition of Lady GODIVA has been taken from Ref.[123], which also provided a comprehensive guide for fixing calculational details such as the suitable number of mesh points, the accuracy needed upon weighing spectra, etc. The computations have been performed

by means of the GMS-II code [124] in the DS8-approximation. To each set of cross-sections described in section 3 the corresponding $\chi_5(E)$-representation taken in Table V has been associated.

A number of variational calculations has been performed in the case of set 2, by defining various subsets characterized by different selections for α_5 and the down-scattering data: $\sigma_{in5}(E)$ has, for instance, been increased so as to fit a composite of the data points from Refs [125, 126]. The maximum gain in reactivity obtained in this way does not exceed 1.5%. The results discussed hereafter pertain to the three basic sets fully described in section 3.

5.3. Results and discussion

The experimental data considered for comparison with theory include the critical mass, the core-centre spectral indices and the time-of-flight spectrum measurements performed at Gulf General Atomics [127] on the APFA-III duplication of GODIVA.

The spectral indices and k_{eff} are summarized in Table VII. It is useful to point out some features deduced from the neutron balances. Since lower $\alpha_5(E)$ data have been used with set 2, a higher k_∞-value is obtained: k_∞ amounts to 2.305, 2.339 and 2.307 for sets 1, 2 and 3, respectively.

However, the leakage is also larger for set 2: 59.2% of the fission source, as compared to 56.1% for set 1, and 56.9% for set 3. This increase in leakage is the main reason for which k_{eff} in set 2 is markedly too low. The leaking fraction of the fission neutrons is a very sensitive parameter (1% leak $\approx$ 2.3% $\Delta k/k$) and could be affected, for instance, by the treatment of the anisotropy in neutron scattering which has still to be investigated so that no clear-cut conclusion may yet be drawn from the absolute values obtained in this work for k_{eff}; there is only an indication that set 2 might be under-reactive.

The core-centre spectral indices are not more helpful than k_{eff}.

Maybe, the leakage-neutron spectrum from Lady GODIVA provides the most meaningful indications for selecting an optimum data set. The GGA time-of-flight measurements agree reasonably well with Frye's photoplate data [128] and seem to be a reliable basis for comparison although room-scattered neutron effects might somewhat obscure the conclusions. An encouraging and striking feature is that the deviations between the time-of-flight measurements and our calculations for any of the three cross-section sets considered here behave very similarly at the core centre and for escape neutrons. As is also seen from the spectral indices in Table VII, too few neutrons are always found by theory at neutron energies above 1 MeV. The deviation increases with increasing energy. In this respect, set 1 is the most satisfactory one, but is followed closely enough by set 3 so as to hamper any decisive choice between them. However, set 2 leads to incredibly large deviations at high energy, which might only be understood if the measurements of neutron spectra were grossly in error. A similar conclusion is reached if the Watt representation is associated with any of the three sets instead of their corresponding $\chi_5(E)$ as given in Table V.

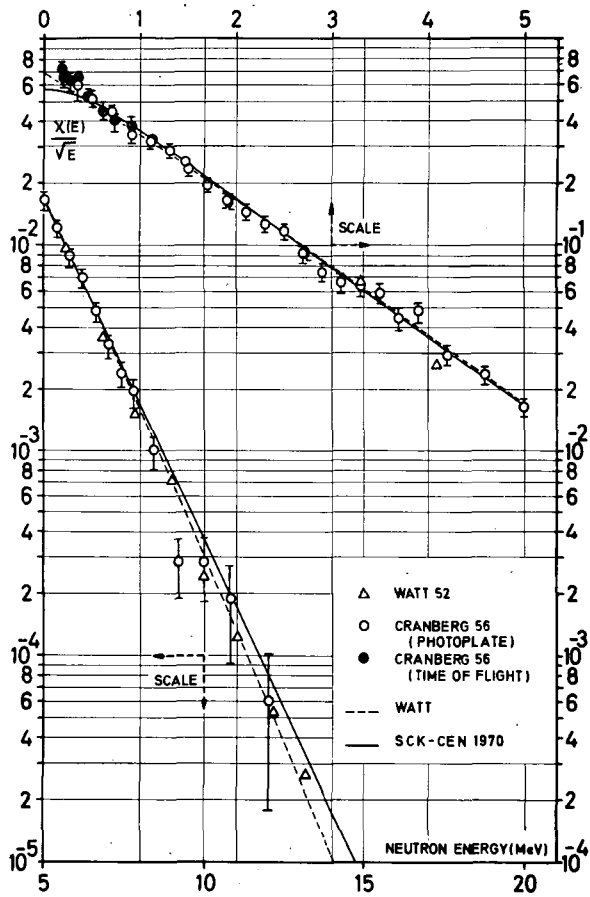

FIG. 10. The neutron-flux spectrum from thermal-neutron-induced ^{235}U-fission.

6. OUTSTANDING CONCLUSIONS

6.1. According to the present analysis, the failure of the latest time-of-flight measurements [129, 130] to define reliably the total prompt-fission-neutron spectrum of ^{235}U and the inadequacy of the simple Maxwellian-type representations widely used under the marked influence of Terrell's masterful work cast serious doubts on our present knowledge of fission-neutron spectra for such important nuclides as ^{239}Pu and ^{238}U. The possible implications for fast-reactor physics are difficult to delineate decisively as long as no more reliable data are available. An integral approach to this problem has been shown to be a valuable tool provided it is based on reasonable theoretical grounds and on careful evaluations of differential cross-sections. Anyway, earlier interpretations of integral comparisons of fission-neutron spectra [14, 131] should be revised and possibly new measurements should be undertaken.

TABLE VIII. FIVE-GROUP RECOMMENDED CROSS-SECTIONS WITH FISSION SPECTRUM AVERAGING (mb)

Energy division (MeV)	$^{115}In(n,\gamma)^{116m}In$	$^{197}Au(n,\gamma)^{198}Au$	$^{235}U(n,f)$	$^{115}In(n,n')^{115m}In$	$^{238}U(n,f)$	$^{58}Ni(n,p)^{58}Co$	$^{56}Fe(n,p)^{56}Mn$
0.01	673.5	746.6	2608	0	0	0	0
0.02	589.0	596.4	2085	4.690, -3	0	0	0
0.04	510.0	457.0	1823	8.939, -3	0	0	0
0.06	439.3	410.3	1777	1.296, -2	0	0	0
0.08	377.3	359.5	1674	1.701, -2	0	0	0
0.1	268.8	323.6	1496	0.15 3.078, -2	0	0	0
0.2	184.4	240.0	1289	0.3 0.08 8.389, -2	0.06362	0	0
0.4	165.9	159.1	1191	0.5 2.576, 0	0.7942	0	0
0.6	184.1	120.0	1173	0.7 15.53	3.901	0	0
0.8	204.1	102.1	1207	0.9 51.17	16.46	0	0
1.0	205.4	94.58	1250	98.53	39.42	2.324	0
1.2	194.2	89.11	1260	148.3	156.1	8.564	0
1.4	180.8	82.31	1266	194.8	355.2	16.38	0
1.6	162.4	74.60	1278	Co 3% too low 238.4	463.1	20.03	0
1.8	138.7	65.36	1273	275.5	515.5	32.33	0
2.0	114.4	55.89	1260	300.2	528.9	52.48	0
2.2	94.70	47.07	1238	315.1	517.2	83.66	0
2.4	78.37	37.71	1208	324.7	509.4	114.0	0
2.6	64.37	32.33	1185	328.9	504.1	144.8	0
2.8	52.10	27.21	1166	330.1	499.0	205.9	0

TABLE VIII (cont.)

Energy division (MeV)	$^{115}In(n,\gamma)^{116m}In$	$^{197}Au(n,\gamma)^{198}Au$	$^{235}U(n,f)$	$^{115}In(n,n')^{115m}In$	$^{238}U(n,f)$	$^{58}Ni(n,p)^{58}Co$	$^{56}Fe(n,p)^{56}Mn$
3.0	42.33	23.83	1154	331.0	496.7	268.0	0.01963
3.2	34.91	21.27	1140	331.0	504.9	236.2	0.05962
3.4	29.40	19.44	1134	331.0	514.3	207.5	0.09961
3.6	24.79	18.06	1124	331.0	520.0	284.7	0.1396
3.8	20.93	17.06	1111	331.0	524.9	422.7	0.1796
4.0	18.17	16.38	1105	331.0	529.9	445.0	0.2196
4.2	15.92	15.71	1095	331.0	534.3	461.4	0.2596
4.4	13.87	15.28	1085	331.0	535.0	478.0	0.2996
4.6	12.17	15.05	1079	331.0	535.6	495.4	0.4400
4.8	10.76	14.90	1070	331.0	539.3	513.0	0.7326
5.0	9.709	14.83	1061	330.5	540.0	530.2	1.434
5.2	8.933	14.85	1061	329.5	540.0	546.4	2.707
5.4	8.183	15.00	1065	328.5	541.8	560.4	4.738
5.6	7.556	15.07	1070	327.5	555.7	571.4	7.854
5.8	7.080	15.27	1091	326.5	579.7	583.5	11.93
6.0	6.537	15.40	1207	323.6	665.3	600.9	17.58
6.5	6.060	14.55	1399	318.1	844.9	621.0	25.43
7.0	5.792	13.70	1550	311.5	940.5	635.6	32.80
7.5	5.642	12.85	1660	304.0	965.1	645.3	40.66
8.0	5.600	12.10	1709	296.1	969.6	651.9	44.74
8.5	5.600	11.45	1720	286.1	970.0	654.5	52.47

TABLE VIII (cont.)

Energy division (MeV)	$^{115}In(n,\gamma)^{116m}In$	$^{197}Au(n,\gamma)^{198}Au$	$^{235}U(n,f)$	$^{115}In(n,n')^{115m}In$	$^{238}U(n,f)$	$^{58}Ni(n,p)^{58}Co$	$^{56}Fe(n,p)^{56}Mn$
9.0	5.616	10.94	1720	272.9	970.0	652.2	58.44
9.5	5.665	10.59	1720	254.5	970.0	647.7	64.57
10.0	5.730	10.16	1720	233.6	970.0	639.0	71.12
10.5	5.795	9.637	1720	210.4	970.0	627.0	78.22
11.0	5.858	9.117	1720	185.3	-	610.6	85.70
11.5	5.918	8.597	1734	157.6	-	590.7	93.24
12.0	6.002	7.869	1860	121.0	-	553.7	103.8
13.0	6.109	6.830	2061	89.17	-	484.9	110.5
14.0	6.186	5.790	2246	72.27	-	385.9	101.0
15.0	6.233	4.751	2446	65.03	-	296.6	87.87
16.0	6.272	3.712	2646	62.60	-	255.6	74.41
17.0	6.322	2.672	2846	61.37	-	231.4	63.16
18.0	6.374	1.321	3106	60.23	-	214.9	51.56
20.0							

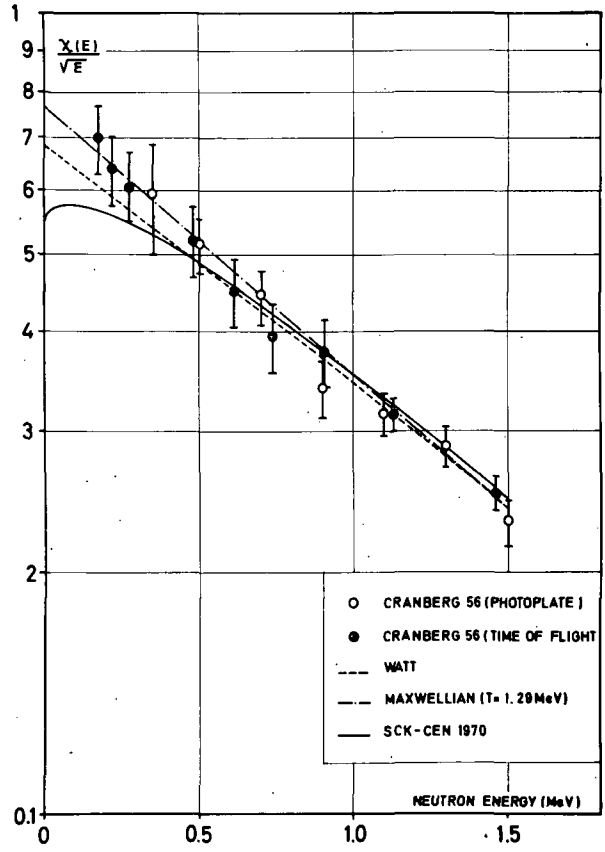

FIG. 11. The low-energy behaviour of the neutron-flux spectrum from thermal-neutron-induced ^{235}U fission.

6.2. Figures 10 and 11 illustrate the neutron-flux spectrum from thermal-neutron-induced ^{235}U fission. The deviation of the CEN-representation with respect to the classical low-energy $E^{1/2}$-dependence must not be taken too seriously: other acceptable (although a little less satisfactory) fits are easily possible to our data when scission neutrons are ignored. However, it is believed appropriate to remind sometimes nuclear physicists of the long-ago issued challenge [110] about the origin of fission neutrons.

6.3. Another rather well established conclusion of this work is that the ^{238}U to ^{235}U-fission-cross-section ratio is presumably taken too low by the evaluators of nuclear data in the energy range below about 2.5 MeV. This affects the computations of integral ratios of these cross-sections in fast reactors.

6.4. The ^{235}U fission cross-section between 10 keV and 10 MeV might well be uncertain by as much as 15%. The present integral study seems to favour somewhat higher values than are generally accepted at present in

the range from 30 keV up to a few MeV. Although any selection is likely to remain a matter of contest for some time, a recommended set of data for the analysis of high-energy integral experiments is tentatively given in Table VIII. This set is believed reliable as far as cross-section ratios $\sigma_i(E)/\sigma_{f5}(E)$ are concerned.

ACKNOWLEDGEMENTS

The continuous assistance of a number of people of the SCK-CEN Reactor Study Department has enabled us to realize this work. This is especially true for members of the BR1-staff as well as of the applied-mathematics section. We are even more indebted to F. Cops for his help in the fission-spectrum irradiations and the interpretation of activation measurements while the competence and the patience of D. Langela in scanning and analysing track-recorder data must be emphasized. To the same extent, we appreciate the enlightened and persistent support of J. Lacroix in the evaluation of cross-sections and of M. Dandoy in the preparation of the transport-theory calculations. Finally, the appropriate issue of this paper in due time would have been impossible without the faithful collaboration of Mrs. P. Rans and Miss E. Umans, of L. Buve and V. Grailet as well as the editorial staff of H. Fredrix.

REFERENCES

[1] FABRY, A., VANDEPLAS, P., in Fast Reactor Physics (Proc. Symp. Karlsruhe, 1967) 1 (1968) 389.
[2] FABRY, A., SCHEPERS, J.C., VANDEPLAS, P., Report EACRP-A-97 (1969).
[3] WATT, B.E., Phys. Rev. 87 (1952) 1037; See also Report LA-935.
[4] PETERSON, R.E., NEWBY, G.A., Nucl. Sci. Engng 1 (1956) 112.
[5] STRUTINSKY, V.A., Nucl. Phys. A95 (1967) 420.
[6] FABRY, A., DECOSTER, M., Neutron Cross-Sections and Technology NBS Special Publication 299 (Proc. Conf. Washington) 2 (1968) 1263.
[7] BONDARENKO, I.I., KOVALEV, V.P., in Pile Neutron Research in Physics (Proc. Symp. Vienna, 1960) IAEA, Vienna (1962) 159.
[8] LEACHMAN, R.B., SCHMITT, H.W., J. nucl. Energy 4 (1957) 38.
[9] ALLEN, W.D., HENKEL, R.L., Progress in Nuclear Energy, Series 1, 2, (1958) 29, 34.
[10] WHITE, P.H., J. nucl. Energy A/B, 19 (1965) 325.
[11] TERRELL, J., Phys. Rev. 113 (1959) 527.
[12] GREEBLER, P., HUTCHINS, B.A., Trans. Am. nucl. Soc. 9 (1966) 453.
[13] McELROY, W.N., Nucl. Sci. Engng 36 (1969) 109.
[14] GRUNDL, J.A., Nucl. Sci. Engng 31 (1968) 191.
[15] FABRY, A., Nukleonik 10 (1967) 280.
[16] FABRY, A., DECOSTER, M., DE LEEUW, G. and S., SCHEPERS, J.C., VANDEPLAS, P., Russian-Dutch-Belgian Meeting on Fast-Reactor Physics, Melekess, 23-27 February (1970) (to be published).
[17] STAUB, A., SWAJA, R.E., Trans. Am. nucl. Soc. 12 (1969) 2, 748.
[18] HARDY, J., (unpublished).
[19] KALLFELZ, J.M., ZOLOTAR, B.A., SEHGAL, B.R., Report EACRP-L-77 (1969).
[20] FABRY, A. et al., (work to be published).
[21] GRUNDL, J.A., Report LAMS-2883 (1963).
[22] CASE, K.M., de HOFFMANN, F., PLACZEK, G., Introduction to the Theory of Neutron Diffusion, 1 USAEC (1953).
[23] FABRY, A., private communication. Oversimplification to shorten presentation.
[24] BRESESTI, A.M., BRESESTI, M., RYDIN, R.A., Nucl. Sci. Engng 29 (1967) 7.
[25] BRESESTI, A.M., BRESESTI, M., RYDIN, R.A., Nucl. Sci. Engng 40 (1970) 331.

[26] FABRY, A., DEWORM, J.P., unpublished communication to the Euratom Working Group for Reactor Dosimetry (1964).
[27] DEPUYDT, H., NEVE de MEVERGNIES, M., J. nucl. Energy A/B 16 (1962) 447.
[28] PRETRE, S., TOCHILIN, E., GOLDSTEIN, N., Report USNRDL-TR-1089 (1966).
[29] RAGO, P.F., GOLDSTEIN, N., TOCHILIN, E., Nucl. Appl. Techn. 8 (1970) 302.
[30] MORY, J., Report CEA-R 2846 (1965).
[31] GOLD, R., ARMANI, R.J., ROBERTS, J.H., Nucl. Sci. Engng 34 (1968) 13.
[32] DECOSTER, M., private communication (1970).
[33] FILLMORE, F.L., J. nucl. Energy 22 (1968) 79.
[34] PARKER, K., Report AWRE 082/63 (1963).
[35] DOUGLAS, A.C., BARRY, J.F., Report AWRE 079/64 (1964).
[36] SCHMIDT, J.J., Report KFK 120 (1966); Numerical values in KFK-750 (1968).
[37] HART, W., Report AHSB (S) R 169 (1969).
[38] GREENE, N.M., LUCIUS, J.L., CRAVEN, C.W., Jr., Report ORNL-TM-2797 (ENDF-131) (1970).
[39] Private communication to FABRY, A., (1968).
[40] McELROY, W.N., ARMANI, R.J., TOCHILIN, E., Trans. Am. nucl. Soc. 12, 2, 757-759 (1969) and private communication (1970).
[41] HENKEL, R.L., Report LA-2114 (1957).
[42] BOLDEMAN, J.W., J. nucl. Energy A/B, 18 (1964) 417.
[43] SKARSVÅG, K., BERGHEIM, K., Nucl. Phys. 45 (1963) 72.
[44] KAPOOR, S.S., RAMANNA, R., RAMA RAD, P.N., Phys. Rev. 131 (1963) 283.
[45] BLINOV, M.V., KAZARINOV, N.M., PROTOPOPOV, A.N., Atomn. Energ. 18 (1965) 108.
[46] MILTON, J.C.D., FRASER, J.S., in Physics and Chemistry of Fission (Proc. Conf. Salzburg, 1965) 2 (1965) 39, IAEA, Vienna; see also report KR-64 (1963).
[47] TERRELL, J., Phys. Rev. 127 (1962) 880.
[48] APALIN, V.F., GRITSYUK, Y.N., KUTIKOV, I.E., LEBEDEV, V.I., MIKAELIAN, L.A., Nucl. Phys. 55 (1964) 249.
[49] MASLIN, E.E., RODGERS, A.L., CORE, W.G.F., Phys. Rev. 164 (1967) 1520.
[50] HANSEN, G.E., in Physics of Fast and Intermediate Reactors (Proc. Sem. Vienna, 1961) 1, IAEA, Vienna (1962) 445.
[51] BYERS, C.C., Nucl. Sci. Engng 8 (1960) 608.
[52] GRUNDL, J.A., HANSEN, G.E., in Nuclear Data for Reactors (Proc. Conf. Paris, 1966) 1, IAEA, Vienna (1967) 321.
[53] JAMES, G.D., PATRICK, B.H., Report AERE, M 2065 amended (1968).
[54] ENDF/B Cross Section Evaluation Center, Brookhaven, Report BNL 50066 (T-467).
[55] BERLIJN, J.J.H., CREMER, C.C., HUNTER, R.E., Report LA-3527 (1968).
[56] HUNTER, R.E., BERLIJN, J.J.H., CREMER, C.C., Report LA-3528 (1968).
[57] DAVEY, W.G., Nucl. Sci. Engng 32 (1968) 35.
[58] DAVEY, W.G., Nucl. Sci. Engng 39 (1970) 337.
[59] VASTEL, M., Report HX-1/1375 (1968) EDF. See also NBS special publication 299 2 (1968) 1129.
[60] WITTKOPF, W.A., ROY, D.H., LIVOLSI, A.Z., Report ENDF-103 (1967).
[61] BARNARD, E., FERGUSON, A.T.G., McMURRAY, W.R., VAN HEERDEN, I.J., Nucl. Phys. 80 (1966) 46.
[62] GRUNDL, J.A., Nucl. Sci. Engng 30 (1967) 39.
[63] SANTRY, D.C., BUTLER, J.P., Can. J. Phys. 42 (1964) 1030.
[64] LISKIEN, H., PAULSEN, A., J. nucl. Energy A/B 19 (1965) 73.
[65] LISKIEN, H., PAULSEN, A., Nukleonik 8 6 (1966) 315.
[66] SPAEPEN, J., Report IAEA-107 (1968).
[67] FABRY, A., SCHEPERS, J.C., Communication to the EURATOM Working Group for Reactor Dosimetry (1970).
[68] FABRY, A., private communication (1970).
[69] SMITH, R.K., HENKEL, R.L., NOBLES, R.A., Bull. Amer. Phys. Soc. 2 (1957) 196.
[70] HANSEN, G., McGUIRE, S., SMITH, R.K., work to be published.
[71] KALININ, S.P., PANKRATOV, V.M., in 2nd. Int. Conf. peaceful Uses atom. Energy (Proc. Conf. Geneva) 16 (1958) 136.
[72] POENITZ, W.P., NBS special publication 299 2 (1968) 503.
[73] POENITZ, W.P., Nucl. Instrum. Meth. 72 (1969) 120.
[74] KNOLL, G.F., POENITZ, W.P., J. nucl. Energy A/B 21 (1967) 643.
[75] ALLEN, W.D., FERGUSON, A.T.G., Proc. Phys. Soc. Lond. A70 (1957) 575.

[76] GORLOV, G.V., GOKHBERG, B.M., MOROZOV, B.M., OSTROSHENKO, V.M., SHIGIN, G.A., J. nucl. Energy A12 (1960) 79.
[77] PATRICK, B.H., SOWERBY, M.G., SCHOMBERG, M.G., Report AERE-R 6350 (1970).
[78] PERKIN, J.L., WHITE, P.H., FIELDHOUSE, F., AXTON, E.J., CROSS, P., ROBERTSON, J.C., J. nucl. Energy A/B 19 (1965) 423.
[79] BROWN, W.K., BERGEN, D.W., CRAMER, J.D., Conf. 660303 (1966) 971.
[80] DERUYTTER, A.J., WAGEMANS, C., Report EANDC(E) 129 AL (1970).
[81] JAMES, G.D., SCHOMBERG, M.G., Report AERE-M2157 revised (1969).
[82] HIBDON, C.T., MOORING, F.P., NBS special publication 299, 2 (1968) 159.
[83] FARRELL, J.A., PINEO, W.F.E., ibid., 153.
[84] UTTLEY, C.A., DIMENT, K.M., quoted in Ref.[88].
[85] ASAMI, A., MOXON, M.C., quoted in Ref.[88]; see also AERE-PR/NP15 (1969).
[86] BAME, S.J., CUBITT, R.L., Phys. Rev. 114 (1959) 1580.
[87] BARRY, J.F., Conf. 660303 book 2 (1966) 763.
[88] SOWERBY, M.G., PATRICK, B.H., UTTLEY, C.A., DIMENT, K.M., Report AERE-R 6316 (1970) and these Proceedings, papers CN-26/26, 25.
[89] HARRIS, K.H., GRENCH, H.A., JOHNSON, R.G., VAUGHN, F.J., Nucl. Phys. 69 (1965) 37.
[90] PÖNITZ, W., J. nucl. Energy A/B 20 (1966) 825.
[91] FERGUSON, A.T.G., PAUL, E.B., J. nucl. Energy 10 (1959) 19.
[92] SEMLER, T.T., Nucl. Sci. Engng 39 (1970) 259.
[93] RYVES, T.B., ROBERTSON, J.C., AXTON, E.J., GOODIER, I., WILLIAMS, A., J. nucl. Energy 20 (1966) 249.
[94] PAUW, H., Communication to the EURATOM Working Group for Reactor Dosimetry (1970).
[95] COX, S.A., Phys. Rev. 122 (1961) 1280 and unpublished results (1966).
[96] BOGART, D., NICHOLS, L.L., Nncl. Phys. A125 (1969) 463.
[97] GUBERNATOR, K., MORET, H., Report EUR. 3950e (1968).
[98] KOMPE, D., Nucl. Phys. A133 (1969) 513.
[99] POENITZ, W.P., KOMPE, D., MENLOVE, H.O., J. nucl. Energy 22 (1968) 505.
[100] SZABO, I., MARQUETTE, J.P., FORT, E., LEROY, J.L., these Proceedings, paper CN 26/69, 70 (1970).
[101] MOXON, M.C., Report AERE-R 6074 (1969).
[102] GLASS, N.W., SCHELBERG, A.D., TATRO, L.D., WARREN, J.H., NBS special publication 299 2 (1968) 573.
[103] DIVEN, B.C., Phys. Rev. 105 (1951) 1350 and Report LA-1336 (1953).
[104] VANDEPLAS, P., private communication (1970).
[105] NEBENZAHL, I., RAKAVY, G., Report IA-1007 (1965).
[106] IYER, M.R., GANGULY, A.K., Nukleonik 8 7 (1966) 408.
[107] KLUGE, G.Y., in Physics and Chemistry of Fission (Proc. 2nd. Symp. Vienna, 1969) IAEA, Vienna (1969) 927 (abstract).
[108] STAVINSKII, V.S., Soviet Phys. JETP 36 (1959) 629.
[109] FULLER, R.W., Phys. Rev. 126 (1962) 684.
[110] BOHR, N., WHEELER, J.A., Phys. Rev. 56 (1939) 426.
[111] BISHOP, C.J., Thesis, Report RLO-1388-99 (1969).
[112] BOWMAN, H.R., THOMPSON, S.G., MILTON, J.C.D., ŚWIĄTECKI, W.J., Phys. Rev. 126 (1962) 2120.
[113] CHEIFETZ, E., FRAENKEL, Z., Phys. Rev. Letts 21 (1968) 36.
[114] LE COUTEUR, K.J., LANG, D.W., Nucl. Phys. 13 (1959) 32.
[115] FABRY, A., Radiation Measurements in Nuclear Power (1966) 322.
[116] STEEN, N.M., Report WAPD-TM-691 (1969).
[117] GINDLER, J.E., HUIZENGA, J.R., in Nuclear Fission in Nuclear Chemistry (YAFFE, L., Ed.) 2, Academic Press (1968).
[118] LISKIEN, H., PAULSEN, A., Report Eur. 119e, updated 1968.
[119] WHITE, P.H., WARNER, G.P., J. nucl. Energy 21 (1967) 671.
[120] STEIN, W.E., SMITH, R.K., SMITH, H.L., NBS Special Publication 299 2 (1968) 627.
[121] LAMPHERE, R.W., Phys. Rev. 104 (1956) 1654.
[122] GRUNDL, J.A., USNER, A., Nucl. Sci. Engng 8 (1960) 598.
[123] CREMER, C.C., HUNTER, R.E., BERLIJN, J.J.H., WORLTON, D.R., Report LA 3529 (1969).
[124] GRATTON, C.P., SMITH, P.E., Report AEEW-M 458 (1965).
[125] BATCHELOR, R., Report AWRE-005/69 (1969).

[126] ARMITAGE, B.H., FERGUSON, A.T.G., MONTAGUE, J.H., STARFELT, N., in Nuclear Data for Reactors (Proc. Conf. Paris, 1966) 2, IAEA, Vienna (1967) 383.
[127] NEILL, J.M., CROSBIE, K.L., RUSSELL, J.L., Jr., Trans. Am. nucl. Soc. 12 (1969) 202.
[128] FRYE, G.M., GAMMEL, J.H., ROSEN, L., Report LA-1670 (1954).
[129] CONDÉ, H., DURING, G., Ark. Fysik 29 (1965) 313.
[130] BARNARD, E., FERGUSON, A.T.G., McMURRAY, W.R., VAN HEERDEN, I.J., Nucl. Phys. 71 (1965) 228.
[131] KOVALEV, V.P., ANDREEV, V.N., NIKOLAEV, M.N., GUSEINOV, A.G., JETP 33 (1957) 1069.

DISCUSSION

J.Y. BARRÉ: I should like to minimize the importance of the absolute value of the fission spectrum to the overall balance, as far as fast power reactors of the PHENIX type are concerned. Very simple calculations show that a 10% increase in the average energy of the fission spectrum is reflected in an increase of 10% in the σ_{f8}/σ_{f9} index but of only 1% over k (only the factor E, the fertile fission factor, varies significantly). Moreover, the σ_{f8}/σ_{f9} index is measured with an accuracy of ±1.5%. Measurements of this index carried out systematically in MASURCA on very similar uranium and plutonium cores show that the ratio of the mean fission energies of ^{239}Pu and ^{238}U could be 1.04. On the other hand, these measurements do not enable us to confirm the proposed increase in the absolute value of $\overline{E}_f$.

A.M. FABRY: The parameters to which you refer are not the only important ones. I should mention that it is also necessary to have a better understanding of the origin of fission neutrons both in relation to $\bar{\nu}$ data and to the correlation of the fission neutron spectra induced in ^{239}Pu, ^{235}U and ^{238}U at incident neutron energies relevant to fast breeders.

L.A.R. DIERCKX: For your calculation you make use of DS4 techniques. However, I have doubts about the validity of the quantitative results that can be obtained by such a calculation. I would prefer to use Monte-Carlo techniques, taking into account the exact geometry.

A.M. FABRY: As shown by the CEN work, the treatment of perturbation correction factors in integral fission spectrum cross-section measurements is strongly related to the angular distribution of neutrons inducing fission. This is the main reason for apparent disagreements between the findings of various authors on this question.

FISSION-SPECTRUM-AVERAGED NEUTRON CROSS-SECTIONS FOR SOME THRESHOLD DETECTORS †

M. NAJŽER, J. RANT, H. ŠOLINC
Institut "Jožef Stefan",
Ljubljana, Yugoslavia

Abstract

FISSION-SPECTRUM-AVERAGED NEUTRON CROSS-SECTIONS FOR SOME THRESHOLD DETECTORS.

Neutron-activation cross-sections averaged over the ^{235}U fission spectrum for $^{115}In(n, n')^{115}In$, $^{64}Zn(n, p)^{64}Cu$, $^{27}Al(n, p)^{27}Mg$, $^{56}Fe(n, p)^{56}Mn$, $^{24}Mg(n, p)^{24}Na$ and $^{19}F(n, 2n)^{18}F$ reactions have been measured relative to the $^{27}Al(n, \alpha)^{24}Na$ reaction for which the averaged cross-section of 0.61 mb was assumed. The values obtained are 156 ± 5, 25.2 ± 1.3, 2.9 ± 0.3, 0.85 ± 0.05, 1.31 ± 0.05 and 0.0053 ± 0.0005 mb, respectively. A standard fission-neutron source made of a 20% enriched uranium disk placed in the thermalizing column neutron beam was used for the irradiations. The converter was suspended in the exposure room in the reconstructed shielding facility of the TRIGA Mark II reactor. The large distance between the neutron source and the room walls makes fission-spectrum distortions due to scattered neutrons negligible. The induced gamma or positron-annihilation radiation was measured by a calibrated 3-in. diameter × 3-in. thick NaI(Tl) scintillation spectrometer. To obtain the activities, the spectra were unfolded by a technique similar to Heath's technique. The measured cross-section values are compared with the results obtained by other authors as well as with values calculated by the available cross-section data and the fission spectrum given by $\Phi E = 0.513 \exp(-1.013 E) \sinh(1.93 E)^{\frac{1}{2}}$.

1. INTRODUCTION

It is well-known that the errors in the absolute values of the neutron activation cross-sections involve large uncertainties in the neutron spectra measured by threshold-activation detectors. These errors can be appreciably reduced if precise fission-spectrum-averaged cross-sections are available. There exists a number of data from different authors [1-5, etc.]. In some cases, rather large discrepancies can be found, so it can be of interest to measure some commonly used activation cross-sections in good experimental conditions.

2. IRRADIATIONS

The scheme of the irradiation equipment is shown in Fig. 1. A standard fission-neutron source facility was installed in the exposure room of the Ljubljana TRIGA Mark II reactor. It consists of a 260-mm dia. 1.5-mm thick converter plate made of 20% enriched uranium cladded by 0.8 mm

† Work partially supported by the International Atomic Energy Agency, Vienna, under the Research Contract No. 536/RB.

TABLE I. DETECTOR CROSS-SECTION DATA

Reaction	γ-ray energy (MeV)	γ-rays per decay (%)	σ (mb) present work	Bresesti et al. [1] (1967)	Boldeman [2] (1964)	Hogg et al. [3] (1962)	Passell [4] (1961)	calculated value
$^{27}Al(n, \alpha)$	1.368 + 2.75	100 100	0.61	0.61	0.60	0.57	0.60	0.65
$^{24}Mg(n, p)$	1.368 + 2.75	100 100	1.31 ± 0.05	1.26	1.31	1.1	1.2	1.35
$^{115}In(n, n')$	0.335	46	156 ± 5	155				170
$^{64}Zn(n, p)$	0.510 (β^+)	38	25.2 ± 1.3		27	25	28	28
$^{19}F(n, 2n)$	0.510 (β^+)	194	$(5.3 \pm 0.5) \times 10^{-3}$					0.0083
$^{27}Al(n, p)$	0.835 + 1.015	100	2.9 ± 0.3		2.9			3.8
$^{56}Fe(n, p)$	0.850	99	0.85 ± 0.05	0.93	0.90	0.71	0.82	0.99

of aluminium. The converter was placed approximately in the middle of the exposure room at a distance of about 110 cm from the thermalizing column. In this way, the distortion of the fission spectrum due to the scattering of fast neutrons from the surrounding walls was minimized at the expense of the source intensity which was about $1.5 \cdot 10^7$ n cm^{-2} s^{-1} at the converter surface. For the same reason, the supports for the converter and detectors were of a "material-free" construction.

All detectors except the fluorine ones were made of grade-1 metallic foils supplied by Johnson Matthey and Co. Instead of fluorine, GAFLON C_2F_4 obtained from Appareil Gachot was used. The detectors were in the form of disks with diameters of 5 cm, and thicknesses from 0.1 mm to 2 mm. The irradiations were performed on the converter axis at two positions, nominally 26 and 41 mm from the converter surface. Normally, several detectors were sandwiched between two aluminium foils whose activities were used to monitor the fast-neutron flux. Parasitic activities due to thermal-neutron capture were suppressed by putting the detectors into a cylindrical cadmium box of 150 mm diameter and 200 mm length with 1-mm-thick walls.

The distortion of the fission spectrum due to scattering of fast neutrons was checked by comparing measured and calculated values of the fast-neutron flux at different distances from the converter. $^{115}In(n, n')$, $^{64}Zn(n, p)$ and $^{27}Al(n, \alpha)$ detectors were irradiated at nine equidistant 15.5 mm positions along the converter axis. The calculations were done for the same positions, taking into account the distribution of neutron sources in the converter and the detector thicknesses. Relative differences between measured and calculated values, which were previously normalized at the third detector position, were taken as percent distortion of the activation integral of the respective detector. No detectable effects were observed at the positions close to the converter used for detector intercalibration.

The fast-neutron background due to the fast-neutron component from the reactor core was determined by measuring the activity of detectors irradiated in the converter out of beam condition. It was found to be between 2% and 10%, depending on the threshold reaction and irradiation position.

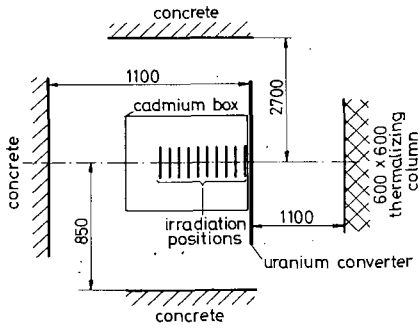

FIG. 1. Irradiation equipment.

3. MEASUREMENT OF ACTIVITIES

The gamma activities induced in irradiated detectors were measured by a low-background gamma-ray spectrometer consisting of a 3-in.-dia. 3-in.-high NaI(Tl) scintillator and multichannel analyser. The detectors were counted at a standard position 12.5 mm in front of the scintillator. The spectra were unfolded by a technique similar to Heath's [6] technique. No significant overlap of parasitic activities and gamma-rays of interest was observed owing to good energy resolution of the spectrometer and favourable fast-to-thermal-neutron flux ratio.

The spectrometer response function was measured using gamma sources ^{203}Hg, ^{52}Cr, ^{198}Au, ^{18}F, ^{137}Cs, ^{54}Mn, ^{65}Zn, ^{22}Na, ^{88}Y, and ^{24}Na. Some of them which were calibrated by the 4π β-γ coincidence method were also used to determine the spectrometer efficiency at gamma-ray energies of 0.279, 0:323, 0.412, 0.835, 1.117, and 2.75 MeV. The efficiency curve was interpolated between the calibration points by using the tabulated values given by Heath [7].

4. RESULTS AND DISCUSSION

Measured activities have to be converted into specific activities proportional to the cross-sections. The data needed to calculate the conversion factors were taken from the Nuclear Data Sheets [8] for all detectors except ^{115}In(n, n'). For ^{115}In(n, n') Misra's [9] results were used. The energy and intensity of measured gamma-rays are given in the second and third columns of Table I. All cross-sections were evaluated relative to the activity of the ^{27}Al(n, α) monitor for which a cross-section of 0.61 mb was assumed. In the fourth to ninth columns of Table I we give the cross-sections obtained in the present work, cross-sections published in some recent publications and cross-sections calculated from BNL cross-section data using a fission spectrum given by $E = 0.513 \exp(-1.013\,E) \sinh(1.93\,E)^{\frac{1}{2}}$. Very good agreement with the results given in the most recent references [1, 2] is obtained for ^{27}Al(n, α), ^{24}Mg(n, p), ^{115}In(n, n'), ^{27}Al(n, p) and ^{64}Zn(n, p) activation cross-sections. The ^{56}Fe(n, p) value is slightly lower but it is still in the range of estimated experimental errors. The ^{19}F(n, 2n) cross-section shows large discrepancy with the value of 0.0083 mb found by Zijp [5]. The agreement with the calculated values is rather good except for the ^{19}F(n, 2n) and ^{27}Al(n, p) reactions.

REFERENCES

[1] BRESESTI, A.M., BRESESTI, M., RYDIN, R.A., Nucl. Sci. Engng 29 (1967) 7.
[2] BOLDEMAN, J.W., J. Nucl. Energy Parts A/B 18 (1964) 417.
[3] HOGG, C.H., WEBER, L.D., USAEC Rep. IDO-16744 (1962).
[4] PASSELL, T.O., HEATH, R.L., Nucl. Sci. Engng 10 (1961) 308.
[5] ZIJP, W.L., RCN Rep RCN-37 (1965).
[6] HEATH, R.L., HELMER, R.G., SCHMITTROTH, L.A., CAZIER, G.A., USAEC Rep. IDO-17017 (1965).
[7] HEATH, R.L., USAEC Rep. IDO-16880 (1964).
[8] Nuclear Data Sheets, National Academy of Sciences, National Research Council, Washington, D.C. (1965).
[9] MISRA, S.C., MERITT, J.S., AECL Rep. AECL-2044 (1964).

DISCUSSION

L. A. R. DIERCKX: I would like to comment on the neutron spectrum in a converter facility. I calculated the perturbation of the fission spectrum in the Ispra facility by Monte-Carlo techniques and found a negative perturbation at high energies (10% between 6 and 10 MeV) due to cladding material. Could Dr. Najžer comment on how he calculates the perturbation in his facility?

M. NAJŽER: We measured the perturbation of the neutron spectrum in our facility comparing the activities of $^{115}In\ (n, n')$, $^{64}Zn\ (n, p)$ and $^{27}Al\ (n, \alpha)$ detectors irradiated at different distances from the converter. No effects exceeding the experimental errors, which were between 1 and 2%, were observed.

НЕКОТОРЫЕ ИНТЕГРАЛЬНЫЕ ХАРАКТЕРИСТИКИ УРАНА-235 В ПРОМЕЖУТОЧНОМ СПЕКТРЕ НЕЙТРОНОВ

Г. М. ВЕСЕЛОВА, С. М. ЗАХАРОВА, В. А. КУЗНЕЦОВ, А. Г. КАЛАШНИКОВ, А. И. МОГИЛЬНЕР, В. Н. ОСИПОВ, Г. И. ТОШИНСКИЙ, Г. Н. ФОКИН, Л. А. ЧЕРНОВ
Физико-энергетический институт, Обнинск,
Союз Советских Социалистических Республик

Presented by S.I. Sukhoruchkin

Доклад представлен С.И. Сухоручкиным

Abstract — Аннотация

SOME INTEGRAL DATA FOR URANIUM-235 IN INTERMEDIATE NEUTRON SPECTRUM.

The paper gives the results of measuring, on a PF-4 unit, the spectrum-average values of $\bar{\nu}_{eff}$ in intermediate uranium-beryllium physical assemblies with $\rho_{Be}/\rho_{235U} = 84$. The work was performed as part of the programme for improving the constants needed for building fast reactors. $\bar{\nu}_{eff}$ was measured by two methods. One of these made use of relationships which link the total statistical weight of the core and reflector components with the quantity K_∞. The expression used had the form: $S = 2(1/K_{eff} - 1/K^+)$, where S is the total statistical weight of the core and reflector components, K_{eff} is the effective multiplication factor, and $K^+ \approx K_\infty$. This method was used for measurements in the PF-4 (F-8) assembly, the structure of which has been described in studies published earlier. In this assembly the core having the dimension diam. 60 x 86 cm was surrounded with a steel reflector. In the PF-4 (F-9) assembly, where the core of the same composition but having the dimensions diam. 40.2 x 86 cm was surrounded with a two-layer beryllium and steel reflector, work was performed by a method in which the values of neutron flux attenuation were measured by means of uranium and boron chambers in boron-10 and uranium-235 filters, respectively. The experimental values of $\bar{\nu}_{eff}/\nu_T = (\overline{\sigma_f \sigma_B})/(\overline{\sigma_a \sigma_B})$ were measured at the centre and at the boundary of the core with the beryllium lateral reflector. The paper briefly describes the method used and the results of a multigroup calculation of these quantities employing three systems of constants used at the Institute of Physics and Power Engineering. The results of the calculation are compared with the experimental data.

НЕКОТОРЫЕ ИНТЕГРАЛЬНЫЕ ХАРАКТЕРИСТИКИ УРАНА-235 В ПРОМЕЖУТОЧНОМ СПЕКТРЕ НЕЙТРОНОВ.

В докладе приводятся результаты экспериментов по измерению на стенде ПФ-4 средних по спектру значений $\bar{\nu}_{эфф}$ в промежуточных уран-бериллиевых физических сборках с отношением $\rho_{Be}/\rho_{235U} = 84$. Работа предпринята по программе уточнения констант, необходимых для сооружения быстрых реакторов. Измерения $\bar{\nu}_{эфф}$ выполнены двумя методами. В одном из методов использованы соотношения, связывающие суммарный статистический вес компонент активной зоны и отражателей с величиной K_∞. Используемое выражение имеет вид: $S = 2(1/K_{эфф}^{\dagger} - 1/K^+)$, где S — суммарный статистический вес компонент активной зоны и отражателей, $K_{эфф}$ — эффективный коэффициент размножения, $K^+ \approx K_\infty$. Метод использован для измерений в сборке ПФ-4 (Ф-8), состав которой приведен в опубликованных ранее работах. В сборке активная зона с размером $\phi 60 \times 86$ см была окружена стальным отражателем. Для измерений в сборке ПФ-4 (Ф-9), в которой активная зона с тем же составом и размером $\phi 40{,}2 \times 86$ см окружалась двуслойным отражателем из бериллия и стали, был использован метод, состоящий в измерении величин ослабления нейтронного потока с помощью урановых и борных камер в фильтрах из бора-10 и урана-235, соответственно. Получаемые из экспериментов величины $\bar{\nu}_{эфф}/\nu_T = (\overline{\sigma_f \sigma_B})/(\overline{\sigma_a \sigma_B})$ измерены для центра активной зоны и на ее границе с боковым бериллиевым отражателем. Кратко описывается методика и приводятся результаты многогрупповых расчетов этих величин с применением трех систем констант, используемых в ФЭИ. Приводится сравнение результатов расчета с экспериментами.

ВВЕДЕНИЕ

Несмотря на многочисленные исследования детального хода сечений деления и захвата нейтронов урана-235, нет полного согласия между имеющимися экспериментальными данными в области промежуточных энергий нейтронов. Это приводит к существенному различию в усредненных по спектру реактора величинах α и $\nu_{эфф}$ урана-235, рассчитанных по многогрупповым системам констант, составленным с использованием различных исходных данных. В данной работе изложены результаты измерения и расчета некоторых интегральных величин для урана-235 в спектре промежуточного реактора. Сравнение полученных экспериментальных значений с расчетными дает возможность сделать некоторые выводы относительно констант урана-235, используемых в расчетах.

1. ИНТЕГРАЛЬНОЕ ИЗМЕРЕНИЕ $\nu_{эфф}$ МЕТОДОМ ПРОПУСКАНИЯ

Для измерений была использована методика, описанная в работе [1], которая заключается в относительных измерениях по методу пропускания величин, пропорциональных значениям $\overline{\sigma_f \sigma_B}$ и $\overline{\sigma_a \sigma_B}$, где σ_f – сечение деления, а σ_a – полное сечение поглощения в уране-235, σ_B – сечение бора. Измерения проводились на стенде ПФ-4 [2] в изотропном потоке нейтронов вблизи центра и на границе физической уран-бериллиевой сборки ПФ-4Ф-9 [3] с отношением $\rho_{Be}/\rho_{^{235}U} = 87$. Если поглощение в чехле, окружающем камеру, невелико ($n \bar{d} \sigma_a \ll 1$), разность в счете урановой камеры с борным чехлом и без него можно представить в виде:

$$\Delta N_U^B = B \int_0^\infty \sigma_f(E)\, \Phi(E)\, \sigma_B(E)\, n_B\, \bar{d}_B\, dE$$

а разность в счете борной камеры с урановым чехлом и без него в виде:

$$\Delta N_B^U = A \int_0^\infty \sigma_a(E)\, \Phi(E)\, \sigma_B(E)\, n_U\, \bar{d}_U\, dE$$

где n_B, n_U – ядерная плотность бора-10 и урана-235 в борном и урановом чехлах, соответственно, $\bar{d}_{U,B}$ – толщина чехлов для изотропного потока.

Нетрудно убедится в справедливости следующего соотношения:

$$\frac{\sigma_{aT}}{\sigma_{BT}} \cdot \frac{\dfrac{\Delta N_U^B}{N_U n_B \bar{d}_B}}{\dfrac{\Delta N_B^U}{N_B n_U \bar{d}_U}} \cdot \frac{\dfrac{N_U}{N_B}}{\left(\dfrac{N_U}{N_B}\right)_T} \cdot g_{f(T)} = \frac{\int_0^\infty \sigma_f(E)\, \sigma_B(E)\, \Phi(E)\, dE}{\int_0^\infty \sigma_a(E)\, \sigma_B(E)\, \Phi(E)\, dE} \cdot \frac{\sigma_{aT}}{\sigma_{fT}}$$

где N_U и N_B – счет урановой и борной камер в спектре реактора, $(N_U/N_B)_T$ – отношение счетов этих камер в калибровочном тепловом спектре нейтронов. $g_{f(T)}$ – фактор Вескотта для сечения деления урана-235 [4].

Правую часть этого равенства можно рассматривать как определение некоторой величины $\tilde{\nu}_{эфф}/\nu_T$, поскольку зависимостью ν_f от энергии для спектра нейтронов рассматриваемой сборки можно пренебречь.

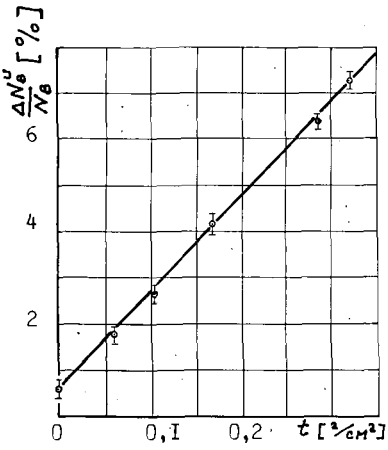

Рис. 1. Поглощение в ^{235}U-фильтрах в зависимости от их толщины, измеренное ^{10}B камерой. Центр активной зоны.

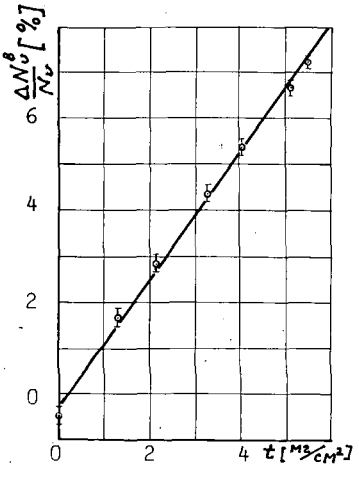

Рис. 2. Поглощение в ^{10}B фильтрах в зависимости от их толщины, измеренное ^{235}U камерой. Центр активной зоны.

В эксперименте находилась зависимость относительного изменения счета камер от оптической толщины чехлов. Чехлы имели цилиндрическую форму ϕ11,5 мм и ℓ = 142 мм. Диаметр камер по активному слою составлял 6 мм [5]. Результаты измерений приведены на рис. 1-4. Величины $(\Delta N/n\bar{d}N)_{d=0}$ для урановой и борной камер определялись по начальному наклону кривой, проведенной через экспериментальные точки методом наименьших квадратов. Калибровочные измерения в тепловом спектре производились в парафиновом блоке диаметром 150 мм и длиной 500 мм с $R_{Cd}{}^{U-235}$ = 65. Установление в таких блоках теплового

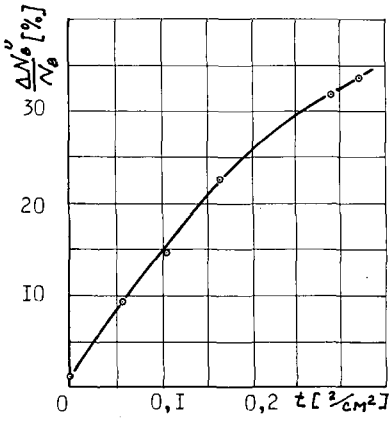

Рис.3. Поглощение в ^{235}U фильтрах в зависимости от их толщины, измеренное ^{10}B камерой. Периферия активной зоны.

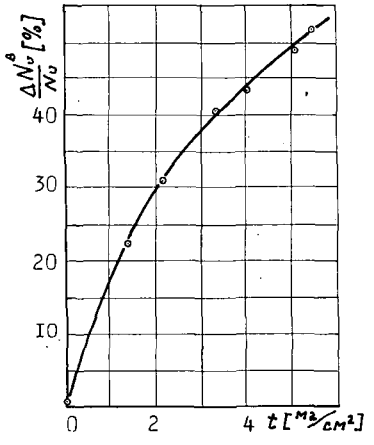

Рис.4. Поглощение в ^{10}B фильтрах в зависимостн от их толщины, измеренное ^{235}U камерой. Периферия активной зоны.

максвелловского спектра нейтронов с температурой, равной температуре замедлителя, показано в работах [6] и [7]. В результате измерений были получены следующие значения $\widetilde{\nu}_{эфф}/\nu_T$:

$$\text{центр } \widetilde{\nu}_{эфф}/\nu_T = 0{,}894 \pm 0{,}020$$

$$\text{периферия } \widetilde{\nu}_{эфф}/\nu_T = 1{,}010 \pm 0{,}030 .$$

С целью проверки многогрупповых ядерно-физических констант [8 - 10], величина $\widetilde{\nu}_{эфф}/\nu_T$ для реактора ПФ-4Ф-9 была получена расчетным путем. Вычисление производилось по формуле:

$$\frac{\widetilde{\nu}_{эфф}}{\nu_T} = \frac{\sum_{j=1}^{n} \sigma_{fi}^{5}\, \sigma_{aj}^{B}\, \Phi_j(r)}{\sum_{j=1}^{n} \sigma_{aj}^{5}\, \sigma_{aj}^{B}\, \Phi_j(r)} \cdot \frac{\sigma_{aT}^{5}}{\sigma_{fT}^{5}}$$

ТАБЛИЦА 1. СРАВНЕНИЕ РАСЧЕТНЫХ ЗНАЧЕНИЙ $\widetilde{\nu}_{эфф}/\nu_T$ С ЭКСПЕРИМЕНТАЛЬНЫМИ ЗНАЧЕНИЯМИ

Система констант	Расчет				Эксперимент
	[8]	[9]	[10]	[10']а	
Число групп	21	21	26	26	
E(эв) (50% делений в центре активной зоны)	247	317	340	270	
$\widetilde{\nu}_{эфф}/\nu_T$					
а) центр активной зоны	0,925	0,884	0,837	0,887	0,894 ± 0,020
б) периферия	0,995	0,994	0,995	1,00	1,01 ± 0,03
$\widetilde{\alpha} = (\nu_T/\widetilde{\nu}_{эфф}) - 1$ центр активной зоны	0,290	0,355	0,405	0,330	0,315 ± 0,09

[a] Система констант [10] с использованием сечений урана-235, приведенных в данной работе (см. Приложение).

Многогрупповые сечения деления и поглощения урана-235 вычислялись с учетом самоэкранирования резонансов, поток нейтронов рассчитывался в P_1-приближении.

В табл. 1 расчетные значения величины $\widetilde{\nu}_{эфф}/\nu_T$, полученные для центра активной зоны и на границе с отражателем, сравниваются с экспериментальными значениями.

2. ИНТЕГРАЛЬНОЕ ИЗМЕРЕНИЕ ВЕЛИЧИНЫ $\nu_{эфф}$ МЕТОДОМ СТАТИСТИЧЕСКИХ ВЕСОВ

В данном разделе приводится описание измерения величины $\nu_{эфф}$ методом статвесов. В достаточно гомогенной сборке, где горючим является высокообогащенный уран и количество поглощающих материалов сведено к минимуму, основным поглотителем служит делящееся вещество, и значение K_∞ близко по величине к $\nu_{эфф}$.

Метод статистических весов [11-13] дает возможность измерения величины K^+:

$$K^+ = \frac{\iiint \sum_f (r, u') \Phi(r, u') \nu(u') \chi(u', u) \Phi^+(r, u)\, du'\, du\, dV}{\iint \Phi^+(r, u) \sum_{tot} (r, u) \Phi(r, u)\, du\, dV - \iiint \sum_s (r, u' \to u) \Phi(r, u') \Phi^+(r, u)\, du\, du'\, dV}$$

где пространственные интегралы берутся по всему объему реактора, включая отражатель. Удовлетворительной аппроксимацией величины K^+, как показано в работе [12], служит величина K_∞. Необходимые поправки могут быть вычислены по рекомендациям работы [13].

Опыты по измерению $\nu_{эфф}$ описанным методом выполнялись на стенде ПФ-4 [2], где была собрана сборка ПФ-4Ф8М с физически гомогенной уран-бериллиевой активной зоной (отношение ядерных концентраций Be: $^{235}U \sim 87$), окруженной стальным отражателем.

ТАБЛИЦА 2. СРАВНЕНИЕ РАСЧЕТА И ЭКСПЕРИМЕНТА

Система констант	[8]	[9]	[10]	[10¹]
Число групп	21	21	26	26
E [эв] (50% делений в центре активной зоны)	247	317	340	270
K_∞ расчетное	1,64	1,48	1,56	1,64
b расчетное	1,106	1,0792	1,0632	1,0801
K_∞ эксп[a]	1,685±0,04	1,655±0,04	1,655±0,04	1,685±0,04
$\nu_{эфф}$ расчетное	1,81	1,59	1,66	1,77
$\nu^{эксп}_{эфф} = K_{\infty эксп} \cdot b^a$	1,800±0,046	1,734±0,04	1,719±0,04	1,767±0,04
$\alpha_{расч}$	0,362	0,532	0,462	0,367
$\alpha_{эксп}$[a]	0,367±0,09	0,401±0,09	0,408±0,08	0,380±0,09
$\nu^{расч}_{эфф}/\nu_T$	0,866	0,773	0,810	0,862
$\nu^{эксп}_{эфф}/\nu_T$[a]	0,861±0,02	0,842±0,02	0,839±0,02	0,857±0,02

[a] Приведенные значения величин различны для разных систем констант в связи с введением в экспериментальные величины расчетных значений $\beta_{эфф}$ и "b".

ТАБЛИЦА 2а. ДОЛЯ ДЕЛЕНИЙ В НЕСКОЛЬКИХ ИНТЕРВАЛАХ ЭНЕРГИЙ

Интервал энергий	Доля делений			
	[8]	[9]	[10¹]	[15]
Выше 10 кэв	15%	15%	14%	11%
10 кэв ÷ 4 эв	78%	80%	80%	74%
ниже 4 эв	7%	5%	6%	15%

Использовался уран 90%-го обогащения изотопом ^{235}U. Статистический вес измерялся по методике, описанной в [3].

Полный статвес всех материалов реактора связан с величиной K^+ соотношением [12]: $S + 2\rho = 2\rho^+$, где $\rho = 1 - (1/K_{эфф})$ – реактивность реактора и $\rho^+ = 1 - (1/K^+)$.

Всего было выполнено две серии измерений при реактивности $\rho \approx 0{,}45\beta_{эфф}$. Среднее значение из двух серий составило $\overline{S + 2\rho} = (118{,}6 \pm 3{,}0)\beta_{эфф}$. Для перевода статвеса в абсолютные единицы использовалось полученное из расчета [14] значение $\beta_{эфф}$: $\beta_{эфф} = 0{,}7053$ [8] и $\beta_{эфф} = 0{,}693$ [9]. Соответствующее значение K^+ оказалось равным:

$$K^+_{эксп} = 1{,}72 \pm 0{,}04 \\ K^+_{расч} = 1{,}67 \quad [8]; \qquad K^+_{эксп} = 1{,}69 \pm 0{,}04 \ [9].$$

Расчетная оценка показала, что в рассматриваемом случае $K^+/K_\infty = 1{,}021$. Следовательно, в качестве экспериментальной величины K_∞ следует считать величину:

$$K_\infty = 1{,}685 \pm 0{,}04 \ [8] \\ K_\infty = 1{,}655 \pm 0{,}04 \ [9].$$

Использование в данных опытах бериллия в качестве замедлителя потребовало учета реакции (n, 2n), а в величине θ – реакции (n, α). Поэтому в нашем случае $\nu_{эфф}$ связано с K_∞ следующим соотношением:

$$\nu_{эфф} = K_\infty b, \text{ где:}$$

$$b = \frac{1}{(\mu_8 + \mu_{n,\,2n})\theta} \qquad \theta = \frac{\sum_{j=1}^{n} \Sigma_{aj}^{5}\,\Phi_j}{\sum_{j=1}^{n} \Sigma_{aj}^{a.3}\Phi_j}$$

$$\mu_8 = 1 + \frac{\sum_{j=1}^{n} (\nu_f\,\Sigma_f)_j^8\,\Phi_j}{\sum_{j=1}^{n} (\nu_f\,\Sigma_f)_j^5\,\Phi_j} \qquad \mu_{n,2n} = \frac{\sum_{j=1}^{n} \Sigma_{n,\,2n\,j}\,\Phi_j}{\sum_{j=1}^{n} (\nu_f\,\Sigma_f)_j^5\,\Phi_j}$$

Сравнение расчета и эксперимента приводится в табл. 2.

3. ИЗМЕРЕНИЕ $\bar{\alpha}_{U\text{-}235}$ МЕТОДОМ ОТРАВЛЕНИЯ БОРОМ [15]

В работе [15] приводятся экспериментальные и расчетные значения величины $\bar{\alpha}$ для урана-235, полученные в спектре промежуточного реактора HECTOR. Нами проведен расчет по определению $\bar{\alpha}_{U\text{-}235}$ в реакторе HECTOR на системах констант [8, 9, 10¹]. Для получения расчетного спектра, близкого к спектру в центральной зоне реактора HECTOR, был рассчитан спектр в бесконечной среде, состоящей из смеси урана с 90%-обогащением по изотопу уран-235 и графита с соотношением ядер $\rho_B/\rho_{^{235}U} = 300$, а также естественного бора. Концентрация бора $\rho_B/\rho_{^{235}U}$ была выбрана из условия $K_\infty = 1$. Полученный расчетный спектр имеет распределение по числу делений, близкое к значениям, приведенным в работе [15].

ТАБЛИЦА 3. СРАВНЕНИЕ РЕЗУЛЬТАТОВ РАСЧЕТА $\bar{\alpha}_{U\text{-}235}$ ПО СИСТЕМАМ КОНСТАНТ [8, 9, 10, 10¹] С ДАННЫМИ РАБОТЫ [15].

Характеристика спектра	$\bar{\alpha}_{U\text{-}235}$						
	Расчет						Эксперимент
	[8]	[9]	[10]	[10¹]	[15][a] (1)	[15][a] (2)	[15]
Спектр в центре активной зоны реактора HECTOR	0,46	0,58	–	0,51	0,48	0,64	0,53 ± 0,06
1/E спектр выше 0,5 эв	0,48	0,62	0,62	0,5	0,5	0,67	

[a] Многогрупповые вычисления [15] были сделаны с использованием двух систем данных по урану-235 с величинами эпитеплового $\alpha_{U\text{-}235}$ для спектра 1/E выше 0,5 эв, приведенными в табл. 3.

ТАБЛИЦА 4. ОТКОРРЕКТИРОВАННЫЕ СЕЧЕНИЯ σ_f, σ_c и σ_{tot} ДЛЯ УРАНА-235

i	E_n	Δu	σ_t	σ_f	ν	σ_c	σ_{in}	σ_e	μ_e	ξ	σ_3(c)
1	6,5 - 10,5 Мэв	0,48	6,3	1,67	3,40	0,02	1,03	3,58	0,84	0,0013	0,024
2	4,0 - 6,5 Мэв	0,48	7,4	1,12	3,04	0,03	1,92	4,33	0,80	0,0017	0,025
3	2,5 - 4,0 Мэв	0,48	7,7	1,22	2,79	0,04	1,91	4,53	0,71	0,0024	0,027
4	1,4 - 2,5 Мэв	0,57	7,0	1,29	2,63	0,06	1,76	3,89	0,55	0,0038	0,026
5	0,8 - 1,4 Мэв	0,57	6,7	1,21	2,52	0,12	1,38	3,99	0,45	0,0046	0,032
6	0,4 - 0,8 Мэв	0,69	7,7	1,16	2,46	0,17	1,20	5,17	0,35	0,0054	0,040
7	0,2 - 0,4 Мэв	0,69	9,5	1,32	2,47	0,25	1,00	6,93	0,23	0,0064	0,064
8	0,1 - 0,2 Мэв	0,69	11,6	1,52	2,45	0,38	0,60	9,10	0,13	0,0073	0,096
9	46,5 - 100 кэв	0,77	13,0	1,80	2,44	0,58	0,18	10,44	0,07	0,0078	0,106
10	21,5 - 46,5 кэв	0,77	14,0	2,26	2,43	0,80	0,06	10,88	0,04	0,0081	0,114
11	10,0 - 21,5 кэв	0,77	15,5	2,87	2,42	1,05	–	11,58	0,02	0,0082	0,123
12	4,65 - 10,0 кэв	0,77	17,0	3,6	2,42	1,4	–	12	0,01	0,0083	0,129
13	2,15 - 4,65 кэв	0,77	19,3	5,2	2,42	2,1	–	12	0,00	0,0084	0,131
14	1,0 - 2,15 кэв	0,77	22,7	7,4	2,42	3,3	–	12	0,00	0,0084	0,131
15	465 - 1000 эв	0,77	28,6	11,6	2,42	5,0	–	12	0,00	0,0084	0,131
16	215 - 465 эв	0,77	37,6	16,7	2,42	8,9	–	12	0,00	0,0084	0,131
17	100 - 215 эв	0,77	45,2	21,3	2,42	11,9	–	12	0,00	0,0084	0,131
18	46,5 - 100 эв	0,77	62,4	34,5	2,42	15,9	–	12	0,00	0,0084	0,131
19	21,5 - 46,5 эв	0,77	79	43	2,42	24	–	12	0,00	0,0084	0,131
20	10,0 - 21,5 эв	0,77	104	50	2,42	42	–	12	0,00	0,0084	0,131
21	4,65 - 10,0 эв	0,77	94	45	2,42	37	–	12	0,00	0,0084	0,131
22	2,15 - 4,65 эв	0,77	36	17	2,42	7	–	12	0,00	0,0084	0,131
23	1,0 - 2,15 эв	0,77	59,5	35	2,42	12	–	12,5	0,00	0,0084	0,136
24	0,465 - 1,0 эв	0,77	84	64	2,42	8	–	12	0,00	0,0084	0,131
25	0,215 - 0,465 эв	0,77	205	155	2,42	36	–	14	0,00	0,0084	0,153
T	0,0252 эв	–	696	580	2,42	98	–	18	0,00	–	–

Расчет $\bar{\alpha}_{U\text{-}235}$ производился по формуле:

$$\bar{\alpha} = \frac{\sum_{j=1}^{n} \Sigma_{cj}^{5} \Phi_j}{\sum_{j=1}^{n} \Sigma_{fj}^{5} \Phi_j}$$

где Σ_{cj}^{5} и Σ_{fj}^{5} – макросечения радиационного захвата и деления урана-235 с учетом самоэкранирования резонансов.

В табл.3 результаты расчета $\bar{\alpha}_{U\text{-}235}$ по системам констант [8, 9] и [10] сравниваются с данными работы [15].

4. ОБСУЖДЕНИЕ РЕЗУЛЬТАТОВ

При анализе результатов следует иметь в виду, что использованные в данной работе системы многогрупповых констант [8], [10] и [9] составлены на основании экспериментальных и теоретических данных по сечениям взаимодействия нейтронов с ядрами, опубликованных соответственно до 1962 г., 1964 г. и 1966 г. Система констант [10'] отличается от [10] групповыми сечениями урана-235 (см. Приложение), которые получены на основании данных, опубликованных до 1970 г. Следует также отметить, что при составлении системы констант [8] в групповые сечения вносились эмпирические поправки, обеспечившие удовлетворительное согласие расчетных величин $K_{эфф}$ с экспериментальными для широкого класса критических сборок, хотя в ряде случаев энергетическая зависимость таких "подогнанных" сечений и не соответствовала фактической энергетической зависимости сечений отдельных элементов.

Анализ результатов, приведенных в табл. 1, 2 и 3 показывает следующее:

Метод измерений, описанный в разделе 1 подчеркивает низкоэнергетическую область спектра нейтронов из-за усреднения сечений с весом 1/v, поэтому вблизи границы активной зоны с замедляющим отражателем (в реакторе ПФ-4Ф-9 отражатель – бериллий), где спектр нейтронов определяется в основном тепловыми нейтронами, расчетная величина $\nu_{эфф}/\nu_T$ для рассмотренных систем констант фактически не изменяется и находится в полном согласии с экспериментом, поскольку сечения захвата и деления урана-235 определены здесь достаточно точно. Для центра активной зоны, где спектр нейтронов оказывается промежуточным, наилучшее согласие с экспериментом показывают системы констант [9] и [10']. То же самое наблюдается и при сравнении результатов табл.3. Сравнение с экспериментом расчетных результатов, приведенных в табл. 2, говорит в пользу систем констант [8] и [10']. Для этих систем констант $\bar{\alpha}_{U\text{-}235}$ на спектре Ферми ниже, чем в системах [9], [10] (см. табл.3). Поскольку методика, описанная в разделе 1, подчеркивает низкоэнергетическую часть спектра нейтронов по сравнению с методикой раздела 2, величины $\nu_{эфф}/\nu_T$ табл.2 меньше соответствующих значений $\widetilde{\nu}_{эфф}/\nu_T$ табл. 1.

В системе констант [8] в низкоэнергетической части промежуточного спектра величина $\alpha_{U\text{-}235}$ несколько занижена (см. табл. 1 и 3). Систе-

мы констант [9], [10] дают завышенное значение величины $\alpha_{U\text{-}235}$ по сравнению с экспериментом, причем особенно завышается величина $\alpha_{U\text{-}235}$ в жесткой части промежуточного спектра, рассчитанная по системе констант [9].

Относительно $\alpha_{U\text{-}235}$ системы констант [9] можно сказать, что отличие от эксперимента раздела 2 (табл. 2) должно быть того же порядка, как и для системы констант [10], поскольку величины $\bar{\alpha}_{U\text{-}235}$ на спектре Ферми для систем констант [9] и [10] равны (см. табл. 3). Наблюдаемое различие в величинах $\alpha_{U\text{-}235}$ систем констант [9] [и [10] в табл. 2 можно объяснить тем, что величина $\alpha_{U\text{-}235}$, полученная методом, изложенным в разделе 2, включает в себя также погрешности констант других элементов, так как коэффициент θ составляет $\sim 0{,}87$ и в значительной степени обусловлен поглощением нейтронов в стальной облицовке урановых дисков стенда ПФ-4. По-видимому, групповые сечения захвата железа в системе констант [9], принятые по данным работы [25], являются завышенными и требуют корректировки.

Результаты, полученные по системе констант [10] после ее корректировки [10'], значительно лучше согласуются со всей совокупностью экспериментальных данных. Аналогичная корректировка констант урана-235 в системе [9], по-видимому, также улучшит согласие расчета с экспериментом. В заключение следует заметить, что сделанные выводы имеют в некоторой степени вероятностный характер в связи со значительными величинами ошибок экспериментальных данных.

Авторы благодарят Б. Ф. Громова и М. Ф. Троянова за полезное обсуждение результатов работы.

ПРИЛОЖЕНИЕ

В табл. 4 приводятся откорректированные сечения σ_f, σ_c, σ_{tot} для урана-235 [10'] системы констант [10], составленные Л. П. Абагян, Л. В. Антоновой, Н. О. Базазянц, М. Н. Николаевым, Л. В. Петровой с использованием данных работ [16-24]. Остальные сечения табл. 4 не отличаются от приведенных в [10], факторы самоэкранирования f_f, f_c, f_t, f_ℓ также остаются прежними [10]. Пересмотренные авторами сечения будут опубликованы в специальном выпуске Бюллетеня ИЦЯД Атомиздата в 1970 г.

ЛИТЕРАТУРА

[1] НИКИТИН, С. Я., СУХОРУЧКИН, С. И. и др., "Материалы сессии АН СССР по мирному использованию атомной энергии", 1955 г.
[2] ЛЕЙПУНСКИЙ, А. И. и др., "Экспериментальное исследование некоторых физических особенностей промежуточных реакторов с бериллиевым замедлителем". Physics of Fast and Intermediate Reactors, IAEA, Vienna 1 1962, p. 327.
[3] МОГИЛЬНЕР, А. И., ОСИПОВ, В. А., ФОКИН, Г. Н., Атомная энергия 24 (1968) 42.
[4] Reactor Physics Constants, ANL-5800, 1963.
[5] МАЛЫШЕВ, Е. К., ДМИТРИЕВ, А. Б., РЕФОРМАТСКАЯ, И. А., "Малогабаритные импульсные камеры деления", ПТЭ, 4 (1968).
[6] ТОЛСТОВ, К. Д., ШАПИРО, Ф. Л., "Материалы сессии АН СССР по мирному использованию атомной энергии", 1955 г.
[7] БУРКАРТ, К., РЕЙХАРДТ, В., из книги "Термализация нейтронов", Атомиздат, 1964.

[8] МАРЧУК, Г.И., КОЧЕРГИН, В.П., НЕВИННИЦА, А.И., УЗНАДЗЕ, О.П., "Критические параметры гомогенных размножающих систем", Атомиздат, 1965.
[9] ЗАХАРОВА, С.М., СИВАК, Б.Н., ТОШИНСКИЙ, Г.И., "Ядернофизические константы для расчета реакторов". Бюллетень ИЦЯД, выпуск III (приложение), Атомиздат, 1967.
[10] АБАГЯН, Л.П., БАЗАЗЯНЦ, Н.О., БОНДАРЕНКО, И.И., НИКОЛАЕВ, М.Н., "Групповые константы для расчета ядерных реакторов", Атомиздат, 1964.
[11] МОГИЛЬНЕР, А.И., Атомная энергия 21 (1966) 127.
[12] МОГИЛЬНЕР, А.И., Атомная энергия 24 (1968) 78.
[13] МОГИЛЬНЕР, А.И., Атомная энергия (1970) (в печати)
[14] ТОШИНСКИЙ, Г.И., БУЛАВИН, П.Е., Атомная энергия 23 (1967) 2.
[15] FOX, W.W., KINCHIN, G.H., SANDERS, J.E., "Measurement of U-235 in an Intermediate Energy Neutron Spectrum", Transaction ANS 10 (1967) 231.
[16] HART, W., AHSB(S)R 169, Warrington, 1969.
[17] DAVEY, W.G., Nucl.Sci.Eng. 26 (1966) 149.
[18] JAMES, G.D., SCHONBERG, M.S., AERE-M-2157, Harwell, 1969.
[19] SAUSSURE, G. de, GWIN, R., WESTON, L.W., INGLE, R.W., ORNL-TM-1804, 1967; Nucl. Sci. and Eng. 23 (1965) 45.
[20] SCHMIDT, J.J., "Neutron Cross Section for Fast Reactor Materials", Part I; Evaluation, KFK 120 (EA NDC-E-350), February, 1966.
[21] DRAUWBAUGH, D.W., GIBSON, G., Nucl. Data for Reactors, IAEA, Vienna 2 (1967) 251.
[22] BNL-325, Second Edition, Supplement N2, III, Z = 80 to 98, 1965.
[23] SAUSSURE, J. de, WESTON, L.W. et al., WASH-1068 (1966) 131.
[24] РЯБОВ и др., Атомная энергия 24 (1968) 351.
[25] MOXON, M.C., Intern. Conf. on the Study of Nuclear Structure with Neutrons, N 88, Antwerp, Belgium, 1965.

MEDIDAS DE INTEGRALES DE RESONANCIA DE ACTIVACION A DILUCION INFINITA CON UN ESPECTROMETRO DE RAYOS GAMMA DE Ge-Li Y COMPARACION CON LOS VALORES CALCULADOS

G.H. RICABARRA, R. TURJANSKI, M.D. RICABARRA
Comisión Nacional de Energía Atómica,
Buenos Aires, Argentina

Abstract — Resumen

MEASUREMENT OF ACTIVATION RESONANCE INTEGRALS AT INFINITE DILUTION WITH A LITHIUM-DRIFTED GERMANIUM GAMMA-RAY SPECTROMETER AND COMPARISON WITH CALCULATED VALUES.

Activation resonance integrals are cross-sections which can be used to confirm the accuracy of microscopic neutron cross-sections and neutron resonance parameters in the evaluation of reactor-neutron cross-sections. In the past the accuracy of neutron cross-sections has been frequently limited by the poor resolution of the measuring instruments used and the consequent inability to separate completely the desired activity from other activities in the sample. The high resolution attainable with a lithium-drifted germanium gamma-ray spectrometer makes it possible by activation analysis of the samples to select an energy region which is completely free from contaminants and furthermore to include the standard in the sample so as to avoid, by simultaneous measurement of photo-peaks relating to the standard and the unknown, the need for weight calibrations and corrections due to slight differences in irradiation position and counter geometry.

The flux in the RA-1 reactor where the irradiations were made was sufficiently large (2×10^{12} n/cm^2 s) to permit the use of samples with negligible self-shielding correction. The reactor spectrum at the irradiation site was calculated by means of multi-group diffusion theory and a correction factor allowing for the slight deviation from the 1/E spectrum was applied to the resonance integral.

In consequence the systematic errors which have been common in the majority of previous resonance integral determinations, such as insufficient discrimination of spurious activities, self-shielding of epithermal neutrons and uncertain or incomplete description of the thermal spectrum at the irradiation site have been carefully avoided in the present method. This technique has been used to obtain an accurate determination of the ratio of the activation resonance integral to the thermal cross-section either by measurement of the cadmium ratio or by comparing the ratios in a reactor spectrum and in a quasi-thermal spectrum in respect of 28 isotopes (of mass number less than 220).

Where serious doubts exist on the accuracy of the published values for thermal activation cross-sections, an absolute determination of the activation resonance integral was performed. Up-to-date neutron resonance parameters have also been used to calculate the resonance integrals for 23 isotopes. From the final results presented a better agreement is observed with the calculated values than in previous experimental determinations. Serious deviations from previous determinations are discussed in the light of present data on neutron resonance parameters.

MEDIDAS DE INTEGRALES DE RESONANCIA DE ACTIVACION A DILUCION INFINITA CON UN ESPECTROMETRO DE RAYOS GAMMA DE Ge-Li Y COMPARACION CON LOS VALORES CALCULADOS.

Integrales de resonancia de activación son secciones efectivas que pueden ser usadas para comprobar la exactitud de las secciones eficaces neutrónicas microscópicas y los parámetros neutrónicos de resonancia por los evaluadores de secciones eficaces neutrónicas para reactores. En el pasado la exactitud de las secciones eficaces neutrónicas ha estado a menudo limitada por la pobre resolución de los instrumentos de medición usados, que impedía la completa separación de la actividad analizada de otras actividades en las muestras. La alta resolución alcanzable con un detector de rayos gamma de Ge con litio difundido permite, mediante análisis de activación de las muestras, seleccionar una región de energía que este completamente libre de contaminantes y, además, incluir el standard dentro de las muestras, por lo que la simultánea medición de los fotopicos del standard y la incógnita eliminan calibraciones de peso y corrección debidas a ligeras diferencias en la posición de irradiación y contaje.

El flujo en el reactor RA-1 donde las irradiaciones fueron hechas era lo suficientemente grande (2.10^{12} n/cm^2 s) para permitir el uso de muestras con corrección de «self-shielding» despreciable. El

espectro del reactor en el lugar de irradiación fue calculado con teoría de difusión a multigrupos y un factor de corrección que tiene en cuenta la pequeña desviación del espectro del reactor del espectro 1/E fue aplicada a la integral de resonancia.

Por lo tanto errores sistemáticos que son comunes a la mayoría de las determinaciones previas de integrales de resonancia como deficiente discriminación de actividades espúreas, «self-shielding» de neutrones epitérmicos y descripción incierta o incompleta del espectro epitermal en el lugar de irradiación han sido cuidadosamente evitados por la técnica presente. Esta técnica ha sido usada para hacer determinaciones exactas de la relación de la integral de resonancia a la sección eficaz térmica midiendo ya sea la relación de Cd o las relaciones relativas en el espectro de un reactor y un espectro «cuasi» térmico para 28 isótopos (con número de masa menor que 220).

En algunos casos que existían serias dudas sobre la exactitud de las determinaciones publicadas de secciones eficaces térmicas de activación se hizo una determinación absoluta de la integral de resonancia de activación. Igualmente, parámetros de resonancia neutrónicas puestos al día se usaron para hacer cálculos de las integrales de resonancia para 23 isótopos. Los resultados finales son presentados, y se observa que el acuerdo con los valores calculados son mayores que los resultados experimentales anteriores de otros investigadores, las discrepancias serias con los valores anteriores son discutidas teniendo en cuenta el actual conocimiento de los parámetros de resonancia neutrónica.

INTRODUCCION

Las secciones eficaces efectivas, ya sea la integral de resonancia o la relación de la integral de resonancia a la sección eficaz térmica, son magnitudes experimentales útiles para comprobar la exactitud de los parámetros neutrónicos obtenidos por los espectrocopistas neutrónicos. Además, puesto que estas secciones eficaces efectivas son aplicadas, en definitiva, por los calculistas y usuarios de reactores, su importancia práctica es evidente.

DISCUSION DE ERRORES

Las principales dificultades inherentes al método de medición de las integrales de resonancia de activación han consistido fundamentalmente en la inadecuada capacidad para separar la actividad deseada de las actividades de contaminantes en la muestra irradiada. El procedimiento usual para resolver este problema consistía en el estudio de los períodos de las actividades pertinentes.

Este procedimiento puede ser bastante exacto si la diferencia entre los períodos es suficientemente grande y si el período de la actividad de interés es conocido con exactitud.

Además si se desea medir actividades de período mayor que 10 días las mediciones se hacen prohibitivamente largas y exigen una estabilidad excepcional de los equipos electrónicos.

La alta resolución de un espectrómetro de rayos gamma de Ge con Li difundido nos ha permitido resolver las actividades en estudio de manera que podemos aislar un fotopico identificado sin ninguna ambigüedad como perteneciente a la actividad producida por captura neutrónica en el elemento cuya integral de resonancia queremos medir.

Este fotopico se caracteriza por tener fuera de él un razonable número de canales con una distribución satisfactoriamente constante de cuentas debido al efecto Compton de picos de mayor energía y, mediante una simple interpolación lineal a ambos lados del fotopico, podremos substraer cómodamente y con exactitud las actividades debidas al efecto Compton de otros rayos gamma.

CUADRO I. ESTIMACION DE ERRORES Y CORRECCIONES

Isótopo	Desviación «standard» (%)	Corrección, autoprotección, resonancia (%)	Corrección por espectro (%)
^{64}Zn	0,9	< 0,1	- 12%
^{68}Zn	2,5	< 0,1	- 10
^{74}Ge	1,0	0,7	- 12
^{76}Ge	0,5	1,5	- 10
^{74}Se	0,5	< 0,1	- 3
^{78}Se	1,4	< 0,1	- 10
^{80}Se	0,5	< 0,1	- 13
^{81}Br	0,3	1,0	- 9
^{85}Rb	2,2	< 0,1	- 9,8
^{84}Sr	0,8	< 0,1	- 9,7
^{94}Zr	0,4	< 0,1	- 13
^{96}Zr	0,1	2,0	- 10
^{100}Mo	1,2	< 0,1	- 10
^{102}Ru	3,0	< 0,1	- 9
^{113}In	0,6	< 0,1	- 1,8
^{124}Sn	0,4	2,4	- 6,6
^{121}Sb	2,1	< 0,1	- 1
^{123}Sb	2,1	< 0,1	- 3,5
^{127}I	1,0	2,0	- 4
^{138}Ba	0,5		
^{140}Ce	0,4		
^{142}Ce	0,3		
^{159}Tb	2,1	< 0,1	- 1
^{180}Hf	3,1	< 0,1	- 7

Otra posibilidad de este método que hemos utilizado consiste en la introducción del «standard» (Au) en la muestra. Estas muestras están preparadas mediante soluciones en las cuales la relación de concentraciones del elemento a medir y el standard es la misma.

La medida final no depende, por lo tanto, ni de los pequeños gradientes de flujo que podrían existir en el lugar de irradiación ni de las calibraciones en peso o de pequeñas diferencias que podría haber en la geometría del contaje.

La reproducibilidad estadística de las medidas es por lo tanto mejorada substancialmente debido a la mucha mejor resolución y a la medida e irradiación simultáneas del «standard» y del elemento a medir.

En el cuadro I se consignan las desviaciones standards en por ciento que hemos obtenido para la R_{Cd} (x)/R_{Cd} (Au) de diversos elementos.

Otra fuente de error sistemático importante en la determinación de la integral de resonancia consiste en la autoprotección de los neutrones epitérmicos en las resonancias. Si las muestras son gruesas desde el punto de vista neutrónico la corrección teórica de la autoprotección puede resultar inexacta, particularmente si las resonancias en cuestión son resonancias en donde la dispersión predomina sobre la captura.

El procedimiento que hemos adoptado para evitar este error sistemático consistió en preparar soluciones suficientemente diluidas de manera que las muestras preparadas a partir de ella tuvieran una autoprotección casi despreciable. En el cuadro I están especificadas las correcciones de «self-shielding» para los espesores usados en nuestras medidas; se observa que para la casi totalidad de los elementos es menor que 0,1%.

Otra fuente importante de errores sistemáticos es la incompleta o incierta descripción del espectro de la zona de irradiación en la cual se ha medido la integral de resonancia.

En un trabajo previo [32] se muestran las distribuciones de flujo en la zona de irradiación del Reactor Argentino 1. El R.A.1 es un reactor anular compacto con ^{235}U al 20% moderado con agua ligera, y el reflector interno de 17 cm de diámetro es de grafito. Las muestras eran irradiadas en el reflector interno a 2 cm del núcleo. El flujo epitérmico medido con hojas de Mn bajo cadmio es plano desde el centro del anillo a través del reflector; existe por lo tanto una región de flujo epitérmico constante de alrededor de 20 cm.

Axialmente el índice epitermal es constante en una región de 20 cm. Como se irradió en el centro del reactor los gradientes de flujo térmico son pequeños (1% cada 3 cm).

Irradiando en una zona como la indicada se consigue, en primer lugar, que no haya variación del índice epitermal entre la muestra desnuda y bajo cadmio y, en segundo lugar, puesto que la distribución de flujo epitermal es plana, no hay variación de la forma del flujo de moderación en la zona de irradiación ya que el escape de los neutrones es nulo sobre una amplia zona.

El espectro de moderación ha sido calculado con un código a 54 grupos de difusión [32]. Este espectro señala una desviación apreciable del comportamiento 1/E, que a la energía de 2 keV es del 13% debido a la captura de los neutrones epitérmicos en la zona de resonancia del ^{238}U.

Con el flujo calculado se ha corregido la integral de resonancia medida, y estas correcciones se presentan tabuladas en por ciento para los diversos elementos consignados en el cuadro I.

Resumiendo, los errores sistemáticos que son comunes a la mayoría de las determinaciones previas, como pobre discriminación de las actividades contaminantes, autoprotección de los neutrones epitérmicos y descripción inadecuada del espectro en el lugar de irradiación, han sido cuidadosamente corregidos.

PROCEDIMIENTO EXPERIMENTAL Y RESULTADOS

El análisis detallado de nuestra técnica experimental ha sido descripto en trabajos previos [32, 33, 34].

Brevemente, consiste en irradiar en el flujo neutrónico del reactor R.A.1 muestras especialmente preparadas a base de soluciones en las cuales se incluye el standard (Au).

Dos muestras son irradiadas, una desnuda y otra bajo cadmio, o en dos espectros distintos. Después de la irradiación son medidas en forma alternada con un cambiador automático en un espectrómetro de Ge con Li difundido. El número de cuentas sobre el fotopico es calculado y la doble relación de actividades corregidas da:

$$R_{Cd}(x)/R_{Cd}(Au) = \frac{(A(x)/A(Au))_{\text{desnuda}}}{(A(x)/A(Au))_{\text{cadmio}}}$$

La relación de cadmio del oro $R_{Cd}(Au)$ fué medida en forma independiente y dió $R_{Cd}(Au) = 1,684 \pm 0,003$ y el índice epitermal de Westcott $r\sqrt{T/T_0} = 0,0794 \pm 0,0003$.

En algunas mediciones se usó el método de irradiar una muestra en el espectro del reactor y otra muestra en la columna térmica.

Se obtuvo la siguiente relación

$$R = \frac{(A(x)/A(Au))_{\text{espectro del reactor}}}{(A(x)/A(Au))_{\text{columna térmica}}}$$

De las cantidades medidas $R_{Cd}(x)/R_{Cd}(Au)$ y R es posible obtener el valor de I'/σ_0 del elemento estudiado donde I' es la integral de resonancia reducida definida como:

$$I' = \int_{\mu kT}^{\infty} \left[\sigma(E) - g\sigma_0\sqrt{\frac{E_0}{E}}\right] \frac{dE}{E}$$

y donde σ_0 es la sección eficaz de absorción a la energía $E_0 = 0,025$ eV y μkT es la energía de corte equivalente de un espectro $1/E$.

La notación y los factores correctivos definidos en el formalismo de Westcott se han seguido consistentemente en todo el análisis [32, 35, 36].

Nuestro procedimiento general para obtener el valor de I' ha consistido básicamente en normalizar el valor de I'/σ_0 medido por nosotros a mediciones de σ_0 (sección eficaz térmica de activación) efectuadas por otros autores.

En general se han adoptado los valores de secciones eficaces térmicas recomendados en BNL-325 [1].

En algunos casos se han elegido otros valores cuando resultados mejores han aparecido en la literatura de los recientes años.

Solamente en el caso del ^{94}Zr y del ^{96}Zr se midió en forma absoluta el valor de I' y de σ_0 debido a que las mediciones previas de la sección eficaz de activación térmica de estos elementos habían sido hechas en el espectro de un reactor.

El cálculo de la integral de resonancia se realizó mediante la ecuación de Breit-Wigner para las resonancias resueltas y se estimó la contribución de las resonancias no resueltas mediante el formalismo de Dresner.

Los parámetros de resonancia recomendados en BNL-325 [1] han sido usados en general, aunque también han sido usados datos recientes provenientes de varios laboratorios.

Los detalles experimentales y el análisis de las mediciones de las integrales de resonancia para cada elemento están descriptos en trabajos publicados y por publicarse [32, 33, 34].

CUADRO II. INTEGRALES DE RESONANCIA EN BUEN ACUERDO CON LOS VALORES CALCULADOS

Isótopo	σ_0 [a] (barns)	I/σ_0 [b]	I'_{exp} (barns)		I' calculado [a] (barns)	Comentarios
			Este trabajo	Otros autores		
^{68}Zn	1,095 ± 0,150	3,30 ± 0,12	3,61 ± 0,51		3,0	
^{74}Se	50 ± 7 [3]	9,13 ± 0,09	456 ± 64		530 607 [2]	
^{78}Se	0,42 ± 0,05	10,9 ± 0,3	4,58 ± 0,60	4,49 [5]	5,8 3,3 [2] 4,5 [4]	Mejor acuerdo obtenido con ref. [4]
^{81}Br	3,1 ± 0,4	21,5 ± 0,4	67 ± 10	41 [6]	63,0	
^{84}Sr	0,49 ± 0,10	13,6 ± 3,0	6,7 ± 1,3		8,6	
^{94}Zr	0,063 ± 0,008 [c] 0,058 [d]	5,87 ± 0,05	0,37 ± 0,04		0,28 [f]	
^{102}Ru	1,44 ± 0,16 [3]	3,33 ± 0,03	4,8 ± 0,5	4,4 ± 0,4 [10]	5,4 [31]	
^{113}In	11,1 ± 1,3 [23]	21,9 ± 0,4	243 ± 29		259 [3]	
^{124}Sn	0,13 ± 0,02	53,1 ± 1,3	6,9 ± 1,0		10,7 6,3 [4]	Discrepancia en Γ_n entre [1] y [4]
^{121}Sb	6,56 ± 0,81	27,2 ± 0,1	178 ± 26	145 [12]	191	
^{123}Sb	4,50 ± 0,14 [e]	25,1 ± 1,9	113 ± 9	138 [15]	114	

CUADRO II. (cont.)

^{127}I	6,2 ± 0,2	24,6 ± 0,4	153 ± 6	130 [15] 106 ± 13 [16] 183 ± 3 [17]	156	
^{159}Tb	22 ± 2 [23]	15,6 ± 0,8	343 ± 35	440 ± 50 [23]	382	
^{168}Yb	5500 ± 2600	6,49 ± 0,13	35706 ± 17139		30950 [18]	Medido en dos espectros
^{180}Hf	12,6 ± 0,7	1,92 ± 0,08	24,3 ± 1,6	11 ± 6 [19] 43 ± 8 [20] 15,5 [15]	29,6	

[a] Cuando no se indica otra procedencia, los valores de sección eficaz térmica y de los parámetros de resonancia son los recomendados en la referencia [1].

[b] Medido en este trabajo.

[c] Deducido por los autores de los valores medidos de I' e I'/σ_0.

[d] De la referencia [9] corregido por contribución epitérmica.

[e] Promedio de las secciones eficaces térmicas de las referencias [13] y [14].

[f] Se usaron los parámetros de la referencia [7] para resonancias entre 2,2 keV y 14,2 keV; para energías mayores se usaron los valores de Γ_n de la referencia [8] y Γ_γ = 0,300 eV [7].

CUADRO III. INTEGRALES DE RESONANCIA PARA ISOTOPOS CUYOS PARAMETROS DE RESONANCIA SON MAL CONOCIDOS

Isótopo	σ_0 [a] (barns)	I'/σ_0 [b]	I' exp. (barns)	
			Este trabajo	Otros autores
^{96}Ru	0,21 ± 0,02 [29]	31,8 ± 4,1	6,67 ± 0,11	
^{104}Ru	0,47 [23]	9,28 ± 0,54	4,36	4,6 [30]
^{138}Ba	0,35 ± 0,15	0,575 ± 0,04	0,20 ± 0,09	
^{140}Ce	0,60 ± 0,06	0,422 ± 0,03	0,25 ± 0,03	0,255 [30]
^{142}Ce	0,95 ± 0,05	0,767 ± 0,04	0,73 ± 0,04	

[a] Cuando no se indica otra procedencia, los valores de sección eficaz térmica son los recomendados en la referencia [1].

[b] Medido en este trabajo.

CUADRO IV. INTEGRALES DE RESONANCIA ANOMALAS

Isótopo	σ_0 [a] (barns)	I'/σ_0 [b]	I' exp. (barns)		I' calculado [a] (barns)	Comentarios
			Este trabajo	Otros autores		
^{64}Zn	0,47 ± 0,05	1,83 ± 0,03	0,86 ± 0,09	0,67 [21]	0,59	
^{74}Ge	0,45 ± 0,20	1,35	0,61		0,22 [22]	
^{76}Ge	0,166	12,07	2,01		1,20 [22]	
^{76}Ge→m	0,11	10,93	1,20			
^{76}Ge→g	0,056 [23]	14,35	0,80			
^{80}Se	0,61 ± 0,05	2,35 ± 0,02	1,43 ± 0,16		0,56	Probable captura p
^{85}Rb	0,45 ± 0,04 [24]	16,31 ± 0,53	7,34 ± 0,68	24,5 [25]	2,77	
^{96}Zr	5,7 ± 1 mb. [c]	879 ± 96	4,97 ± 0,50		5,61 0,90 [d]	Valor anómalo de I'/σ_0
^{100}Mo	0,199 ± 0,003 [27]	19,24 ± 0,71	3,82 ± 0,15	3,71 ± 0,2 [27]	8,04	
^{130}Te	0,26 ± 0,08	1,86 ± 0,06	0,48 ± 0,14	4,06 [28]	0,17	

[a] Cuando no se indica otra procedencia, los valores de sección eficaz térmica y de los parámetros de resonancia, son los recomendados en la referencia [1].

[b] Medido en este trabajo.

[c] Deducido por los autores de los valores medidos de I' e I'/σ_0.

[d] La primera resonancia se calculó con los parámetros de la referencia [26]. Para las resonancias de energía mayor que 2 keV, se usaron los valores de Γ_n de [8] y Γ_γ = 0,300 eV [7].

En este trabajo sólo se hace una presentación global de estos resultados para su mejor evaluación y discusión con respecto a los valores calculados a partir de los datos microscópicos.

En el cuadro II se muestran los resultados de las integrales de resonancia en que se observa un acuerdo razonable con los resultados calculados mediante los parámetros de resonancia.

En el cuadro III están tabulados los resultados para los cuales no existen parámetros de resonancia confiables.

En el cuadro IV están tabulados aquellos resultados que podríamos llamar «anómalos» puesto que difieren en forma sustancial de los resultados calculados con los parámetros de resonancia.

Igualmente en todos los cuadros se han incluído los resultados de la integral de resonancia medida por otros autores normalizando sus resultados a la sección térmica adoptada por nosotros y se ha substraído la parte 1/V en caso de que la integral de resonancia citada la incluyera.

El standard al cual todas nuestras medidas han sido referidas es el Au; los valores de secciones eficaces adoptados para el Au en este trabajo son los siguientes: I'_{Au} = 1551 barns, σ_0 = 98,8 ± 0,3 barns y I'/σ_0 = 15,69.

DISCUSION DE LOS RESULTADOS DE I'_{exp} EN RELACION A LAS INTEGRALES DE RESONANCIA CALCULADAS

En el cuadro II se puede observar que de los 15 elementos medidos, 11 coinciden con los valores calculados dentro del 15% y los cuatro restantes concuerdan dentro del 15 al 30%.

El error de I'_{exp} para los diversos elementos es alrededor del 10% fluctuando los valores de acuerdo al error con que ha sido medida la sección eficaz térmica que es el valor con que hemos normalizado el valor de I'/σ_0 medido en el presente trabajo para obtener el I' experimental.

Por otro lado, el error citado para los parámetros de resonancia en BNL-325 [1] varía entre un 10% y un 20% aparte de las discrepancias de mayor importancia provenientes de los datos de diversos laboratorios.

Por lo tanto es posible ver que el acuerdo de los valores que hemos medido con los valores calculados es excelente y confirma en general los parámetros recomendados en BNL-325 [1].

Las únicas excepciones podrían ser el ^{78}Se y el ^{124}Sn en que nuestros resultados confirman aparentemente como mejores resultados los del grupo de Saclay (ver cuadro II).

En cuanto a los valores consignados en el cuadro III los valores de las integrales de resonancia experimental difieren entre un 60% y un 200% de los valores calculados. Igualmente se ha incluido en este cuadro el ^{96}Zr a pesar que el I'_{exp} coincide con el valor de I' calculado, ya que el I'/σ_0 experimental es un valor realmente «anómalo» puesto que es más grande por un orden de magnitud que el I'/σ_0 calculado o experimental de cualquiera de los elementos de la tabla periódica. Estos elementos están caracterizados por tener sus resonancias más importantes de 0,3 keV en adelante.

Dos efectos pueden explicar la discrepancia: por un lado, la incertidumbre en el valor de Γ_γ que es una magnitud sujeta a errores en su determinación cuando $\Gamma_n \gg \Gamma_\gamma$ y, por otro lado, el efecto de la captura p en la zona de energía de los keV.

Por ejemplo los resultados para el ^{74}Ge y el ^{76}Ge fueron calculados con los valores de Maletzki et al. [22]; Γ_γ = 0,120 eV obtenido por estos autores para el ^{76}Ge es por lo menos un factor de dos más bajo que los valores de Γ_γ obtenidos por Julien et al. [4] para el ^{74}Se y el ^{76}Se. Si se usaran los resultados obtenidos en la sistemática de los anchos radiativos del grupo de Saclay, se obtendría un acuerdo mucho mejor de la integral de resonancia calculada con la experimental.

Igualmente Maletzki et al. [22] han observado una variación de la función fuerza (strength function) S_0 entre el intervalo de $0 < E < 15$ keV y el intervalo de $15 < E < 30$ keV de un factor de 40 para el ^{76}Ge que podría ser explicado por un aumento de interacciones p entre el intervalo de 0-15 keV y el intervalo de 15-30 keV.

El ^{80}Se muestra una discrepancia considerable y en este caso la suposición de una incertidumbre en Γ_γ no puede explicar la discrepancia. El valor de Γ_γ = 0,250 keV para las resonancias de energía de los keV es una suposición razonable en vista de los valores obtenidos de los isótopos par del Se y de la sistemática de los anchos radiativos. Una estimación hecha con el modelo estadístico de la probable contribución de la captura p en la integral de resonancia del ^{80}Se pondría en buen acuerdo el valor calculado con el valor experimental [32].

Un caso interesante es el ^{96}Zr, el valor de I'/σ_0 experimental es de 979, que es un orden de magnitud más grande que cualquier valor esperado y por otro lado el valor de I' calculado coincide con el valor de I'_{exp}. La sección eficaz térmica de activación resulta ser entonces de 5 mb, mientras que la sección eficaz térmica de absorción calculada a partir de los parámetros de resonancia da 200 mb. Esto sugiere que casi el 100% de las capturas neutrónicas en la integral de resonancia del ^{96}Zr son debidas a capturas p.

Este hecho no puede ser explicado en base al conocimiento actual de las funciones fuerzas p en esa región de masa, puesto que habría que admitir que la función de fuerza p podría tomar un valor de $30,10^{-4}$ para el ^{96}Zr.

Esta anomalía confirma resultados anteriores de Newson et al. [37] Biggerstaff et al. [38] y Good and Kim [8], de que la sección eficaz y los anchos neutrónicos reducidos para los núcleos par del Zr subían mucho más rápidamente en función de la energía que lo esperado para una interacción de onda s. La explicación propuesta por el grupo de Oak Ridge a este fenómeno implica que la función fuerza s tendría que variar en función de la energía, o que la función fuerza p podría tomar valores anómalamente altos. Nuestros resultados para el I'/σ_0 del ^{96}Zr aparentemente confirman la segunda parte de la explicación propuesta por el grupo de Oak Ridge.

La integral de resonancia del ^{100}Mo difiere también sustancialmente del valor calculado. En este caso el valor Γ_γ = 0,260 eV supuesto en nuestros cálculos puede ser más alto por un factor de 2 o más si los resultados obtenidos para los isótopos del Mo de Julien et al. [4] son ciertos. Por otro lado las experiencias efectuadas con filtros de boro de Baumann [28] nos muestran que una contribución significante a la integral de resonancia proviene de resonancias mucho más altas que 364 eV, y esto no está de acuerdo con el valor obtenido por el cálculo que indica que solamente el 30% de las capturas neutrónicas proviene de energías más altas. Es posible pues para el ^{100}Mo dos efectos que pueden obrar en

sentido opuesto, por un lado un valor mucho más bajo de Γ_γ que el supuesto y por otro lado capturas neutrónicas adicionales en la zona de los keV.

Finalmente para el ^{85}Rb, ^{64}Zn, y ^{130}Te estimaciones aproximadas de la posible contribución de la captura de onda neutrónica p a la integral de resonancia [39] nos muestra que su contribución sería significativa, pero dado el pobre conocimiento que existe de las funciones fuerzas p, estos cálculos sólo tienen un significado cualitativo.

Concluyendo, los valores de I'_{exp} concuerdan satisfactoriamente con los valores calculados a partir de los parámetros de resonancia. Las discrepancias signficativas pueden ser cualitativamente explicadas y provienen de que el actual conocimiento de los parámetros de resonancia en la zona de los keV tiene una doble incertidumbre: el valor de Γ_γ y la contribución de capturas de neutrones de momento angular igual a 1.

Nuestros resultados experimentales sugieren que esa contribución puede como en el caso del ^{96}Zr llegar hasta ser el 100% de la integral de resonancia.

AGRADECIMIENTOS

Este trabajo ha sido parcialmente apoyado por el Organismo Internacional de Energía Atómica, Viena y se agradece la dirección y entusiasmo del Dr. C. B. Bigham que trabajó inicialmente en este proyecto bajo los auspicios del OIEA.

BIBLIOGRAFIA

[1] GOLDBERG, M.D., MUGHABGHAB, S.F., PUROHIT, S.N., MAGURNO, B.A., MAY, V.M., BNL Rep. BNL-325, 2ª ed. supl. 2 (1966).
[2] MALETSKI, Kh., PIKELNER, L.B., SALAMATIN, I.M., SHARAPOV, E., INDC (CCP)-7/U (1970) 56.
[3] HUGHES, D.J., SCHWARTZ, R.B., BNL Rep. BNL-325, 2ª ed. (1958).
[4] JULIEN, J., ALVES, R., DE BARROS, S., HUYNH, V.D., MORGENSTERN, J., SAMOUR, C., Nucl. Phys. A132 (1969) 129.
[5] KRAMER, H.H., WAHL, W.H., Nucl. Sci. Engng 22 (1965) 373.
[6] EMERY, J.F., J. inorg. nucl. Chem. 27 (1965) 903.
[7] BARTOLOME, Z.M., HOCKENBURY, R.W., MOYER, W.R., TATARCZUK, J.R., BLOCK, R.C., Nucl. Sci. Engng 37 (1969) 137.
[8] GOOD, W.M., KIM, H., Phys. Rev. 20 (1968) 1329.
[9] LYON, W.S., Nucl. Sci. Engng 8 (1960) 378.
[10] LANTZ, P.M., ORNL Rep. ORNL-3832 (1965).
[11] MURADYAN, G.V., ADAMCHUK, Yu.G., SHCHEPKIN, Yu,G., INDC-260 E (1969) 64.
[12] HARRIS, S.P., MUEHLHAUSE, C.O., THOMAS, G.E., Phys. Rev. 79 (1950) 11.
[13] COURTEMANCHE, R., EASTWOOD, T.A., WERNER, R.D., Can. J. Phys. 44 (1966) 2956.
[14] SIMS, G.H.E., JUHNKE, D.G., J. inorg. nucl. Chem. 30 (1968) 349.
[15] MACKLIN, R.L., POMERANCE, H.S., Prog. nucl. Energy, Ser. I, 1 (1956).
[16] KLIMENTOV, V.B., GRIAZEV, V.M., Atomn. Energ. (traducción inglesa) 3 (1957) 1387.
[17] TATTERSALL, R.B., ROSE, H., PATTENDEN, S.K., JOWITT, D., J. nucl. Energy 12 (1960) 32.
[18] MUGHABGHAB, S.F., CHRIEN, R.E., Phys. Rev. 174 (1968) 1400.
[19] SCOVILLE, J.J., FAST, E., ROGERS, J.W., AEC Rep. WASH-1053 (1964).
[20] FULMER, C.B., AEC Rep. WASH-E 20 (1968).
[21] BRUNE, D., JIRLOW, K., J. nucl. Energy, A y B 17 (1963) 350.
[22] MALETSKI, Kh., PIKELNER, L.B., SALAMATIN, I.M., SHARAPOV, E.I., Atomn. Energ. (traducción francesa) 24 (1968) 173.
[23] WALKER, W.H., AECI-3037, Parte I (1969).
[24] KEISCH, B., Phys. Rev. 129 (1963) 769.

[25] SIMS, G.H.E., JUHNKE, D.J., J. inorg. nucl. Chem. 29 (1967) 2031.
[26] MORGENSTERN, J., Centre d'études nucl. Saclay, Rep. CEA-R-3609 (1968).
[27] CABELL, M.J., Nucl. Energy, A12 (1960) 172.
[28] BAUMANN, N.P., AEC Rep. DP-817 (1963).
[29] HUGHES, D.J., MAGURNO, B.A., BRUSSEL, M.K., BNL Rep. BNL-325 2ª ed. supl. 1 (1960).
[30] LANTZ, P.M., BALDOCK, C.R., IDOM, L.E., Nucl. Sci. Engng 20 (1964) 302.
[31] BOLOTIN, H.H., CHRIEN, R.E., Nucl. Phys. 42 (1963) 676.
[32] RICABARRA, M.D., TURJANSKI, R., RICABARRA, G.H., BIGHAM, C.B., Can. J. Phys. 46 (1968) 2473.
[33] RICABARRA, M.D., TURJANSKI, R., RICABARRA, G.H., Can. J. Phys. 47 (1969) 2031.
[34] RICABARRA, M.D., TURJANSKI, R., RICABARRA, G.H., present. para public. en Can. J. Phys. (1970).
[35] WESTCOTT, C.H., WALKER, W.H., ALEXANDER, T.K., «Effective cross-sections and cadmium ratios for the neutron spectra of thermal reactors», Int. Conf. peaceful Uses atom. Energy (Proc. Conf. Geneva, 1958) 1b, UN, New York (1958) 70.
[36] WALKER, W.H., COPLEY, L.A., Can. J. Phys. 44 (1966) 1985.
[37] NEWSON, H.W., BLOCK, R.C., NICHOLS, P.F., TAYLOR, A., FURR, A.K., MERZBACHER, E., Ann. Phys. 8 (1959) 218.
[38] BIGGERSTAFF, J.A., GOOD, W.M., KIM, H., Proc. Internat. Conf. Study of Nuclear Structure with Neutrons, paper 76, Antwerp (1965).
[39] MUSGROVE, A.R. de L., Australian AEC Rep AAEC/E198 (1969).

INTEGRAL MEASUREMENT OF FISSION-PRODUCT REACTIVITY WORTHS IN SOME FAST REACTOR SPECTRA

T.L. ANDERSSON
AB Atomenergi, Studsvik, Nyköping,
Sweden

Abstract

INTEGRAL MEASUREMENT OF FISSION-PRODUCT REACTIVITY WORTHS IN SOME FAST REACTOR SPECTRA.

The reactivity worth per atom for a number of fission-product isotopes relative to that of ^{235}U was measured in three various fast-reactor spectra. The following isotopes were studied: ^{95}Mo, ^{97}Mo, ^{99}Tc, ^{101}Ru, ^{102}Ru, ^{104}Ru, ^{103}Rh, ^{133}Cs, ^{147}Pm and ^{149}Sm. A fission product mock-up sample was also included in the measurements.

The reactivity worths were measured by the pile-oscillator technique. The fundamental mode amplitude of the perturbation signal was obtained through Fourier analysis.

The experimental results are compared with calculated values obtained from perturbation calculations using published cross-sections for the sample materials. From a comparison between the measured and the calculated reactivity worths it is concluded that only the ^{95}Mo, ^{104}Ru and ^{149}Sm worths are well predicted in all three systems. For the other samples, the calculated values are generally too high.

1. INTRODUCTION

There is a considerable lack of experimental cross section information for fission products over the energy range of interest in typical fast reactors. Furthermore, despite the fact that many of the important fission products are radioactively stable the difficulty in obtaining pure samples of separated isotopes in large quantities and the full programme of higher priority at the large cross section measuring centres make it unlikely that the situation will be substantially improved within a near future. Under these circumstances integral data as obtained from reactivity worth measurements in a fast reactor should be of value.

A series of measurements was therefore initiated at the fast critical assembly FR0 at Studsvik. A list of important fission products as calculated from current cross section sets was prepared and about ten isotopes were selected as being of special interest. Most of these could by courtesy of the USAEC be obtained as a loan from the Research Inventory Pool at Oak Ridge. In total the following isotopes were studied: ^{95}Mo, ^{97}Mo, ^{99}Tc, ^{101}Ru, ^{102}Ru, ^{104}Ru, ^{103}Rh, ^{133}Cs, ^{147}Pm, and ^{149}Sm. Of these materials only ^{99}Tc and ^{147}Pm are radioactive. Some samples of a fission product mock-up prepared at Karlsruhe [1] were also included in the study.

2. EXPERIMENTAL

2.1 Description of core arrangement

In order to allow more definite conclusion concerning the cross sections to be drawn from the experiment, measurements were performed in three cores - Nos. 3, 5 and 8 - with widely different spectra. The dimensions and compositions of the three assemblies are specified in Table I. The calculated central neutron spectra for the cores are shown in Fig. 1.

TABLE I. COMPOSITION AND DIMENSIONS OF THE FRO CORES

Core No.	Atomic densities, 10^{22} atoms/cm^3								Core height (cm)	Core radius (approx.) (cm)
	^{235}U	^{238}U	C	H	Fe	Cr	Ni	Al		
3	.568	2.234	2.47	-	.408	.096	.048	-	38.7	21.5
5	.498	1.963	2.77	.604	.408	.096	.048	-	38.7	19.5
8	.498	1.963	2.55	.151	.408	.096	.048	.34	38.7	23.0

The cores were surrounded by at least 30 cm copper reflector in axial and radial direction.

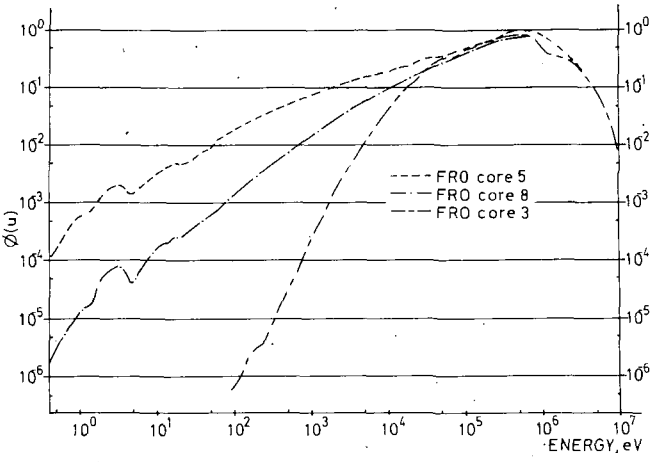

FIG. 1. Calculated central neutron spectra for FRO cores 3, 5 and 8.

The central part of each core was built as a "pseudo-homogeneous" zone by using thin plates of uranium (0.06 cm), graphite (0.06 cm), polythene (0.01-0.005 cm) and aluminium (0.005 cm). Heterogeneity effects in the core region close to the sample thereby became negligible.

2.2 Experimental arrangement

2.2.1 Oscillator

The experimental set up is shown in Figs. 2 and 3. The pile oscillator rod was extending horizontally through the centre of the core. The oscillator channel including the guide tube (aluminium) had a cross sectional area of 2.85x2.85 cm^2. The rod dimension (2.4x2.4 cm^2) was chosen to fit closely into the channel, leaving space only for a thin teflon lining (low friction) in the reflector parts of the guide tube. The rod was made of solid aluminium with two pockets (2.15x2.15x11 cm^3) for the samples. The sample changer, which could serve one of the two pockets, could be loaded with eight samples.

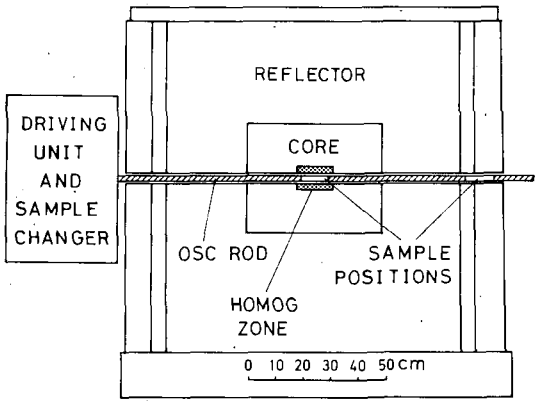

FIG. 2. Pile oscillator arrangement at the FRO assembly.

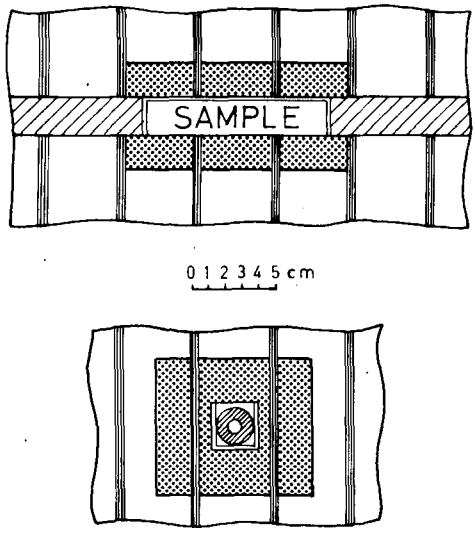

FIG. 3. Details of the central core region.

In the cores 5 and 8, which had comparatively soft neutron spectra, measurements were made with as well as without a copper layer between the oscillator rod and the core. The former arrangement was used in an attempt to reduce the effect of neutrons being moved into the resonance dips of the unperturbed core spectrum by scattering events in the sample. This particular scattering effect is difficult to treat in the perturbation calculation. Complementary measurements of the ^{238}U and ^{235}U reaction rates in the fuel surrounding the sample position has clearly demonstrated the effectiveness of the copper layer in this respect [2]. On the other hand, the copper introduces a substantial heterogeneity close to the sample that must be taken into account in the calculation of the real and adjoint spectra.

The thickness of the copper lining was 1.4 cm in core 5 and 0.7 cm in core 8.

2.2.2 Samples

Data for the samples are given in Table II. The fission product samples were in most cases in elemental form but for the cesium and the rare earths chemical compounds (oxide, fluoride, carbonate) had to be used due to difficulties to prevent oxidizing. Some special samples were included in order to make experimental corrections for the carbon, oxygen and fluorine contents. A uranium sample (93 % ^{235}U) was used as a reference.

TABLE II. LIST OF SAMPLES

Sample No.	Material	Mass[a] (g)	Enrichment (atom %)	Cyl. sample diam. (cm)	Flat sample thickness (cm)	Mean[c] chord length (cm)
1	^{133}CsF	8.83	100	.62		.601
2	$^{133}Cs_2CO_3$	12.80	100	.81		.778
21	$^{133}Cs_2CO_3$	2.86	100	.40		.392
5	^{99}Tc	1.99	100	.41		.139
6	$^{149}Sm_2O_3$	1.01	97.72	.25		.247
7	$^{149}Pm_2O_3$	2.33	100	.45		.440
8	^{95}Mo	2.27	96.47	.60		.300
9	^{95}Mo	7.69	96.47	1.10		.579
10	^{101}Ru	2.41	97.73	.30		.105
11	^{102}Ru	3.90	99.53	.30		.296
12	^{104}Ru	2.41	99.7	.30		.150
13	^{97}Mo	1.90	92.70	.60		.166
14	^{97}Mo	8.00	92.70	1.10		.495
19	F.P.mock-up	3.24	-	.55		.535
20	F.P.mock-up	10.02	-	.95		.907
70	^{103}Rh	1.26	100		.005	.010
71	^{103}Rh	2.49	100		.010	.020
72	^{103}Rh	3.72	100		.015	.030
73	^{103}Rh	4.95	100		.020	.040
54	^{235}U	2.298	92.99		.0065	.0130
57	Al_2O_3[b]	53.55		o.d.2.05 i.d.1.50		
58	CF_2[b]	22.68		o.d.1.50 i.d.1.00		
59	C	19.83		1.20		
65	Al[b]	30.52		o.d.1.80 i.d. .75		

Cylindrical samples: Length 10.45 cm. Flat samples: Length 10.45 cm; width 1.90 cm

a) Total mass. Corresponding masses corrected for impurities etc. are listed in Tables 6-8

b) Cylindrical annular samples. The central volume was filled with aluminium.

c) For various practical reasons it was necessary at the preparation of some of the samples to place thin (diam. 0.1-0.5 cm) aluminium pins inside the "sample volume". Hence the mean chord length can have different values for samples with the same diameter.

Most samples had a cylindrical form but a few were flat. The cans had the same outer dimensions for all the samples (length 11 cm, diam. 2.15 cm). The canning material was aluminium.

Some special problems had to be solved when the sample cans were designed. The enriched isotope samples are extremely expensive and furthermore they are in many cases available only in very small amounts even at the Research Inventory Pool. Hence large efforts had to be devoted to the handling of the different materials. The sample can must be designed in such a way that it could be filled, tightened and (after completion of the experiment) opened and emptied again without losing any significant amount of the sample material or causing any contamination of the sample.

All the cylindrical samples were canned in a container of the type shown in Fig. 4a. The can was made of a cylindrical aluminium rod through which a hole was drilled with a diameter chosen to accommodate the desired amount of a given sample. Both ends of the cylinder were tightened by screw lids. Just around the hole at the two ends of the cylinder there were circular sharp edges which were allowed to cut into the lids when these were screwed on. Hereby the container was generally tight enough that changes in the sample due to absorption of moisture from the air could be avoided. The container was fixed inside a thin-walled cylindrical aluminium tube.

The flat samples were placed in an aluminium casette which was pressed into a slit through a solid aluminium cylinder (Fig. 4b).

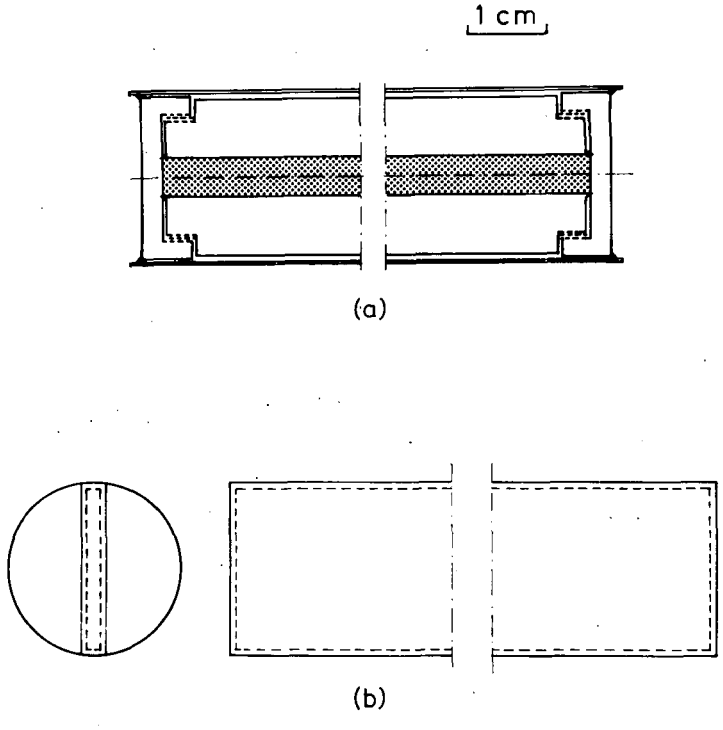

FIG. 4. Sample cans: a) cylindrical sample; b) flat sample.

TABLE III. CALCULATED REGULAR AND ADJOINT 25-GROUP SPECTRA.
(u = LETHARGY)

Group No.	Lower group limit E_L	Regular flux $[\phi(u)\cdot\Delta u)]$					Adjoint flux $[\phi^*(u)]$				
		Core 3	Core 8	Core 8/Cu	Core 5	Core 5/Cu	Core 3	Core 8	Core 8/Cu	Core 5	Core 5/Cu
1	6.5 MeV	3.53,E-4	2.57,E-4	2.01,E-4	1.57,E-4	1.23,E-4	1.948	2.002	1.786	1.806	1.606
2	4.0	1.73,E-3	1.26,E-3	9.67	7.66	5.93	1.455	1.524	1.414	1.387	1.283
3	2.5	3.64	2.66	2.11,E-3	1.60,E-3	1.28,E-3	1.409	1.480	1.376	1.354	1.256
4	1.4	6.57	4.88	4.35	2.88	2.59	1.319	1.391	1.309	1.282	1.202
5	0.8	9.33	6.68	6.42	3.68	3.59	1.127	1.215	1.164	1.140	1.086
6	0.4	1.94,E-2	1.31,E-2	1.30,E-2	6.30	6.38	1.146	1.238	1.184	1.175	1.116
7	0.2	2.09	1.35	1.35	5.74	5.92	1.221	1.303	1.241	1.247	1.181
8	0.1	1.65	1.05	1.05	4.23	4.32	1.259	1.336	1.265	1.290	1.217
9	46.5 keV	1.25	8.22,E-3	8.36,E-3	3.30	3.41	1.252	1.334	1.256	1.306	1.225
10	21.5	7.14,E-3	5.35	5.34	2.42	2.41	1.248	1.339	1.259	1.323	1.238
11	10.0	2.95	3.16	3.04	1.73	1.62	1.231	1.330	1.231	1.320	1.211
12	4.65	9.91,E-4	1.82	1.99	1.32	1.32	1.287	1.387	1.296	1.364	1.259
13	2.15	3.02	1.13	1.25	1.05	1.05	1.362	1.449	1.372	1.401	1.309
14	1.0	6.27,E-5	6.00,E-4	7.64,E-4	7.51,E-4	8.42,E-4	1.491	1.548	1.425	1.458	1.334
15	465 eV	1.02	3.12	3.23	5.33	5.02	1.536	1.613	1.360	1.495	1.265
16	215	1.48,E-6	1.57	1.66	3.63	3.51	1.713	1.642	1.423	1.502	1.310
17	100	1.95,E-7	7.27,E-5	8.12,E-5	2.26	2.31	1.402	1.412	1.320	1.357	1.265
18	46.5	2.49,E-8	2.65	3.13	1.16	1.24	1.439	1.487	1.386	1.426	1.325
19	21.5	3.84,E-9	9.29,E-6	1.04	5.31,E-5	5.42,E-5	1.369	1.323	1.237	1.280	1.193
20	10.0	5.4,E-10	5.27	5.72,E-6	3.54	3.60	1.424	1.544	1.386	1.525	1.366
21	4.65	1.9	3.40	3.33	2.39	2.25	1.293	1.309	1.190	1.378	1.238
22	2.15	3.8	2.36	2.26	1.91	1.75	1.599	1.912	1.610	1.959	1.640
23	1.00	5.8,E-11	1.13	1.15	1.17	1.10	1.778	2.165	1.739	2.192	1.756
24	0.465	3.5,E-12	2.65,E-7	2.47,E-7	4.16,E-6	3.50,E-6	2.592	2.701	2.015	2.586	1.943
25	0.215	0	1.01	9.00,E-8	2.28	1.83	2.603	2.599	1.785	2.504	1.748

There were two main reasons for choosing an arrangement with thick-walled aluminium cans. The experimental geometry was easy to describe in the spectrum calculations. The amount of aluminium in the sample pocket was very similar to that in the rest of the oscillator rod so that the whole rod could be regarded as homogeneous. Furthermore, the thick-walled cans were expected to have an advantageous effect similar to that of the copper lining (cf. Sect. 2.2.1).

2.3 Measurements

The electronics equipment for the pile oscillator measurements was conventional. An ion chamber placed just outside the reflector gave a signal proportional to the reactor power. The signal was amplified and the major part of its DC component was compensated through a "backing-off-voltage". The excess signal was fed to a voltage-to-frequency converter and then to a scaler system.

The oscillator period was 60 sec. The scaler integrated the pulse rate during 1.0 sec intervals and the results were fed to a punching unit, where a computer tape was produced.

A computer programme [3] was used for the fundamental mode analysis of the perturbation signal.

Each sample was oscillated for 1-2 hours with the reactor well stabilized. The average reactor power level was about 4 Watts, which was somewhat low with regard to the noise, but a higher power level would give a too high induced activity in the fuel plates rendering a core reloading difficult.

The reproducibility of an oscillator measurement was typically about 2 to 3×10^{-7} in $\Delta k/k$ when the measurements were made during the same reactor run (same day). However, it turned out that this reproducibility could not be kept when a sample was remeasured several times during a period of some weeks. The resulting errors are specified in the tables presented in Sect. 4. These errors are based on the observed scatter of the data and they also include estimated uncertainties in the corrections for carbon, fluorine, oxygen, impurities and for other isotopes than the main one (cf. Sect. 3.3).

3. CALCULATIONS

3.1 Calculation of the regular and adjoint spectra

Fine group spectra were produced by the SPENG programme [4], which calculates the spectrum in the fundamental mode approximation for a homogeneous medium. The fine group spectra were used for production of group cross sections for the various core materials in the different cores. Regular and adjoint 25 group spectra valid for the sample position (i.e. with the oscillator rod and the copper layer, if any, taken into account) were then produced by the diffusion code MONDAY [5]. The spectra are listed in Table III.

The energy group structure was chosen to be the same as that of the ABN set [17], which was considered suitable as it has a large number of groups in the low energy region where the effect of resonances in the sample material is important.

3.2 Calculation of group cross sections for the sample materials

For the resonance region fine group cross sections were calculated by the DORIX [6] programme, using published resonance parameters (resolved and for some isotopes also statistical ones). The resonance data were taken mainly from the compilations by Goldberg et al. [7] and by J J Schmidt [8]. The fine group cross sections were tabulated in the SPENG library for a discrete number of background cross sections (self shielding). The shielded cross sections for the samples were then obtained by interpolation. For the energy regions below and above that energy region point by point cross sections were introduced directly into the SPENG library. Above about 1 keV the capture cross sections were mainly obtained from a recently published paper by Benzi and Reffo [9].

25 group cross sections for the sample materials were produced by the SPENG programme. The SPENG spectrum for core 5 was used as weighting spectrum. The cross section for the ^{235}U sample was shielded to the same extent as for the ^{235}U present in the various cores, except for the copper lined cases where unshielded ^{235}U data was used (cf. Sect. 3.3).

The references from which the cross section information for the sample isotopes (including the important impurities) were taken are specified in Table IV.

TABLE IV. REFERENCE LIST ON THE CROSS-SECTION DATA USED IN THE PERTURBATION CALCULATIONS

Isotope	Above res. region			Res. Region[a] res. par.	Below res. region		Lowest inelastic threshold (MeV)
	σ_{tot}	σ_c	$\sigma_{inel.}$		$\sigma_{el.}$	σ_c	
^{95}Mo	[10]	[9]	[10]	[7]	[10]	[10]	.190
^{96}Mo	[10]	[9]	[10]	[7]	[10]	[7]	.778
^{97}Mo	[10]	[9]	[10]	[7]	[10]	[7]	.704
^{98}Mo	[10]	[9]	[10]	[8]	[10]	[7]	.788
^{99}Tc	[7]	[11]	E[b]	[12]	C[c]	[7]	.180
^{101}Ru	[7]	[9]	E	[7]	C	[7]	.127
^{102}Ru	[7]	[9]	E	[7]	C	[7]	.474
^{104}Ru	[7]	[9]	E	[7]	C	[7]	.358
^{103}Rh	[7]	[9]	[13]	[8]	[8]	[7]	.040
^{133}Cs	[7]	[9]	[14]	[8]	[8]	[7]	.081
^{147}Pm	[7]	[11]	E	[15]	[15]	[7]	.090
^{147}Sm	[7]	[9]	[14]	[7]	C	[7]	.120
^{148}Sm	[7]	[9]	[14]	-[d]	C	[11]	.550
^{149}Sm	[7]	[9]	[14]	[7]	C	[7]	.022
^{150}Sm	[7]	[9]	[14]	[7]	C	[7]	.330
^{152}Sm	[7]	[9]	[14]	[8]	[8]	[7]	.120

a) Here the term resonance region means the energy region within which resolved or statistical parameters are given in the quoted references.

b) E indicates estimated data based on threshold energies from [16].

c) C indicates calculated data based on $\sigma_{pot} = 4\pi R^2$, $R \approx 1.35 \cdot A^{1/3}$.

d) No resonance parameters found in the literature.

For the fission product mock-up sample the cross sections and self shielding factors were taken from the ABN-set [17]. The data valid for fission fragments of ^{239}Pu was used.

The difficulty in producing correctly shielded group cross sections for the samples containing strong resonance absorbers is obvious. This is particularly serious in "soft" neutron spectra like that of core 5, where the low energy neutrons give a comparatively large contribution to the sample reactivity. The problem can not be avoided because dilute samples can not be used (cf. Sect. 5).

3.3 Calculation of sample reactivity worths

Perturbation calculations were made for samples of the size used in the experiments with a second order version of the perturbation programme SHOP, which is a modified version of PERS [18].

The calculations were performed for spherical samples with radii chosen to give the same mean chord lengths as those of the cylindrical or flat samples. Perturbed group fluxes were applied for those energy groups where unshielded sample cross sections were used.

Separate calculations were made for the actual isotope mixture in the samples as well as for "purified" samples containing the main isotope only. Thereby correction factors were obtained, which could be used to convert the experimental reactivity worths into values valid for pure samples of the isotopes under consideration.

Calculations were also performed for infinitely small samples using a first order version of SHOP. The ratio between the calculated reactivity worth per atom of the real sample and that for an infinitely small one can be regarded as the total sample size correction factor. It includes the resonance self shielding in the sample as well as the perturbation of the flux due to the presence of the sample.

The calculated reactivity worths for zero sample size are listed in Table V. The various contributions to the reactivity due to production, absorption and scattering are also specified there. From Table V it may be seen that the reactivity effect of the fission product isotopes is strongly dominated by the absorption for all the three spectra. The relative reduction of the scattering contribution with the softening of the neutron spectrum is also clearly demonstrated.

Since it is difficult to estimate the self shielding in the ^{235}U sample when the copper layer was surrounding the oscillator channel, perturbation calculations for that sample were made using both core shielded and unshielded ^{235}U data. However, it appeared - due to compensating effects - that only a very small change was obtained in the calculated reactivity worth. Hence it was concluded that unshielded cross sections could be used for the ^{235}U standard sample in the copper lined case without introducing any significant systematic error.

4. RESULTS AND DISCUSSION

The reactivity worth per atom of the fission products relative to that of ^{235}U is listed together with the corresponding calculated quantities in Tables VI-VIII for cores No. 3, 8 and 5, respectively. The figures are valid for the sample size used. The sample size correction factors as defined in Sect. 3.3 are included in the tables.

TABLE V. CALCULATED REACTIVITY WORTHS PER ATOM FOR INFINITELY THIN SAMPLES. NORMALIZED TO UNITY FOR THE ^{235}U SAMPLE

Material	Core 3			Core 8			Core 5		
	Total	Absorption	Scattering	Total	Absorption	Scattering	Total	Absorption	Scattering
^{95}Mo	- .080	- .071	- .009	- .133	- .124	- .009	- .294	- .288	- .006
^{97}Mo	- .089	- .084	- .005	- .142	- .138	- .004	- .224	- .221	- .003
^{99}Tc	- .238	- .229	- .009	- .295	- .288	- .007	- .514	- .509	- .005
^{101}Ru	- .196	- .186	- .010	- .329	- .320	- .009	- .587	- .581	- .006
^{102}Ru	- .096	- .088	- .008	- .150	- .144	- .006	- .350	- .345	- .005
^{104}Ru	- .042	- .034	- .008	- .057	- .050	- .007	- .096	- .091	- .005
^{103}Rh	- .177	- .173	- .004	- .260	- .256	- .004	- .652	- .653	+ .001
^{133}Cs	- .140	- .131	- .009	- .213	- .206	- .007	- .504	- .500	- .004
^{147}Pm	- .249	- .239	- .010	- .774	- .765	- .009	-4.42	-4.42	- .00
^{149}Sm	- .364	- .365	+ .001	- .899	- .900	+ .001	-3.52	-3.53	+ .008
F.P.mixture	- .156	- .131	- .025	- .232	- .212	- .020	- .501	- .490	- .011
^{235}U	+1.000[a]	- .908	- .012	+1.000[b]	-1.028	- .010	+1.000[c]	-1.375	- .006

a) Production contribution in core 3 : +1.920

b) " " " " 8 : +2.038

c) " " " " 5 : +2.381

TABLE VI. MEASURED AND CALCULATED REACTIVITY WORTHS PER ATOM RELATIVE TO THAT OF ^{235}U IN FRO CORE 3

Sample			Sample size correction factor	ρ/ρ_{25} core 3	
No.	Material	Mass (g)		exp.	calc.
1	^{133}CsF	7.72	.991	.085±.007	.136
2	$^{133}Cs_2CO_3$	10.44	.992	.059±.005	.136
21	$^{133}Cs_2CO_3$	2.34	.994	.068±.024	.136
5	^{99}Tc	1.99	.996	.116±.020	.233
6	$^{149}Sm_2O_3$	.836	.990	.425±.068	.362
7	$^{147}Pm_2O_3$	1.40	.995	.140±.042	.243
8	^{95}Mo	2.17	.995	.063±.017	.078
9	^{95}Mo	7.34	.994	.074±.005	.078
10	^{101}Ru	2.31	.989	.165±.017	.191
11	^{102}Ru	3.82	.996	.048±.011	.094
12	^{104}Ru	2.36	.997	.058±.017	.041
14	^{97}Mo	7.34	.992	.075±.005	.087
20	F.P.mock-up	3.24	.998	.042±.008	.153
73	^{103}Rh	1.23	.992	.173±.009	.173
54	^{235}U	2.134	1.017	1.000	1.000

Sample masses are referring to the amount of the studied isotope

The results could also be presented as effective one group perturbation cross sections for the different isotopes relative to that of ^{235}U. This implies in principle only a different way of normalizing the data and has been omitted.

The final errors in the measured reactivity worths are rather large. This is particularly true for core 3. The main reason for the large errors in the latter core was that so limited amounts of the enriched samples were available that large enough samples could not be made. A contributing factor was also that these isotopes were obtained on loan for a limited time period only, which did not allow sufficient time to be spent on each sample.

From a comparison between the experimental and calculated values some general statements can be made concerning the cross section sets used. The difficulty in being more specific is due to several interdependent factors. The experimental information gained is integral in nature. Lack in agreement between experiment and calculation may be due to errors in the cross section data over the whole energy range or over only a limited part of it. Furthermore, for the hard spectrum core the reactivity signal for the samples used is, as mentioned, small and the relative errors of the experimental values become large. The conditions are more favourable in this respect for the softer cores No. 8 and 5. For these, however, the calculated values sometimes include large corrections for self shielding in the samples, corrections that are highly dependent on the resonance parameters used. The calculated results for the soft cores should also be more dependent on the number of groups used and their distribution in energy. Some tests have been made to study this effect [19] but additional work has to be made.

TABLE VII. MEASURED AND CALCULATED REACTIVITY WORTHS PER ATOM RELATIVE TO THAT OF ^{235}U IN FRO CORE 8

Sample			Sample size correction factor	ρ/ρ_{25} core 8		ρ/ρ_{25} core 8/Cu	
No.	Material	Mass (g)		exp.	calc.	exp.	calc.
1	^{133}CsF	7.72	.841	.135±.008	.177	.141±.009	.178
2	$^{133}Cs_2CO_3$	10.44	.840	.111±.006	.177	-	-
21	$^{133}Cs_2CO_3$	2.34	.875	.103±.026	.184	.103±.025	.185
5	^{99}Tc	1.99	.960	.179±.023	.280	.169±.022	.281
6	$^{149}Sm_2O_3$	.836	.799	.725±.077	.714	.820±.068	.728
7	$^{147}Pm_2O_3$	1.40	.798	.368±.049	.609	.412±.043	.601
8	^{95}Mo	2.17	.880	.097±.020	.115	-	-
9	^{95}Mo	7.34	.860	.113±.006	.112	.103±.006	.115
10	^{101}Ru	2.31	.905	.247±.020	.294	.252±.018	.299
11	^{102}Ru	3.82	.880	.053±.012	.130	.069±.012	.134
12	^{104}Ru	2.36	.993	.046±.020	.056	.077±.019	.054
13	^{97}Mo	1.75	.964	.075±.025	.135	-	-
14	^{97}Mo	7.34	.934	.102±.006	.131	.095±.006	.136
20	F.P.mock-up	10.02	.986	.100±.009	.226	.119±.009	.224
70	^{103}Rh	1.23	.922	.235±.037	.237	-	-
71	^{103}Rh	2.46	.906	.250±.019	.232	.247±.018	.239
54	^{235}U	2.134	1.013[a] 1.008[b]	1.000	1.000	1.000	1.000

Sample masses are referring to the amount of the studied isotope

[a] Core 8 ; [b] Core 8/Cu

For core 3 (Table VI) a comparison of the data shows that the reactivity effect is strongly overpredicted for ^{133}Cs, ^{99}Tc, ^{147}Pm, ^{102}Ru and for the fission product mock-up, whereas for the other isotopes the agreement is good or the disagreement is too small to be significant. Because of the hard neutron spectrum in this core only a very small contribution to the reactivity will be due to neutrons below the keV-region. Hence it is mainly the cross section data above the resonance region which is tested.

For core 8 (Table VII) results are given for the arrangement with as well as without a copper lining around the oscillator channel. For all samples the experimental data are not significantly changed in going from one arrangement to the other. The measured reactivity signal for all samples including the ^{235}U reference sample decreased with a few per cents when the copper lining was introduced. Thus only slight changes in the resulting ratios were obtained. A perusal of Table VII reveals that - as for core 3 - the reactivity of the ^{133}Cs, ^{99}Tc, ^{147}Pm, ^{102}Ru and fission product mock-up samples is overpredicted. This is also true for the ^{101}Ru and the ^{97}Mo data.

A comparison of measured and calculated data for core 5 (Table VIII) shows a similar situation as for cores 3 and 8 except that the ^{133}Cs worth is now rather well predicted. The ^{103}Rh worth, on the other hand, which was well calculated in cores 3 and 8, is underestimated in core 5. As for core 8 the experimental relative reactivity worths do not change significantly for most samples when the copper lining is added around the oscillator channel.

TABLE VIII. MEASURED AND CALCULATED REACTIVITY WORTHS PER ATOM RELATIVE TO THAT OF ^{235}U IN FRO CORE 5

Sample			Sample size correction factor	ρ/ρ_{25} core 5		ρ/ρ_{25} core 5/Cu	
No.	Material	Mass (g)		exp.	calc.	exp.	calc.
1	^{133}CsF	7.72	.534	.251±.006	.286	.252±.006	.250
2	$^{133}Cs_2CO_3$	10.44	.532	.224±.005	.267	.240±.004	.249
21	$^{133}Cs_2CO_3$	2.34	.602	.235±.019	.302	-	-
5	^{99}Tc	1.99	.774	.322±.017	.396	.293±.018	.373
6	$^{149}Sm_2O_3$	.836	.504	2.04±.06	1.78	1.93±.06	1.65
7	$^{147}Pm_2O_3$	1.40	.474	.99±.04	2.09	.92±.04	1.75
8	^{95}Mo	2.17	.633	.223±.015	.185	.164±.015	.182
9	^{95}Mo	7.34	.590	.172±.005	.173	.157±.005	.169
10	^{101}Ru	2.31	.797	.368±.015	.463	.339±.015	.440
11	^{102}Ru	3.82	.704	.074±.011	.245	.069±.009	.242
12	^{104}Ru	2.36	.982	.093±.016	.094	.059±.026	.089
13	^{97}Mo	1.75	.923	.130±.019	.206	.156±.019	.201
14	^{97}Mo	7.34	.863	.129±.005	.193	.133±.005	.188
19	F.P.mock-up	3.24	.949	.387±.021	.472	.288±.021	.444
20	F.P.mock-up	10.02	.941	.323±.007	.468	.286±.007	.440
70	^{103}Rh	1.23	.583	.589±.028	.378	.478±.028	.334
71	^{103}Rh	2.46	.552	.522±.015	.358	.432±.015	.316
73	^{103}Rh	4.92	.520	-	-	.378±.007	.298
54	^{235}U	2.134	1.006[a] .982[b]	1.000	1.000	1.000	1.000

Sample masses are referring to the amount of the studied isotope

a) Core 5 ; b) Core 5/Cu

As a summary it may be concluded that the ^{95}Mo, ^{104}Ru and ^{149}Sm reactivity worths were well predicted in all the three systems. For the other isotopes the calculated values were generally overpredicted indicating that the cross sections (mainly absorption) entering into the perturbation calculation were too high.

It may be noted that a typical neutron spectrum of a sodium cooled fast reactor has more low energy neutrons than that of core 3 but less than that of core 8. Hence the results from these two FRO cores should be of more practical interest than those from core 5. The latter core has a spectrum similar to that in a steam cooled fast reactor, which is now less interesting as a reactor type.

A more detailed account of the experiments, the analysis and the perturbation calculations will be given in a forthcoming AE-report.

ACKNOWLEDGEMENTS

The author would like to express his thanks to Dr. E. Hellstrand for guidance throughout the work and helpful criticism on the manuscript, to Mr. R. Håkansson for introducing the fission product cross sections into the

SPENG library and for performing the perturbation calculations, to Mr. I. Gustafsson for design of the pile oscillator and preparation of the samples, to Mr. S. Sjööquist for design of the experimental instrumentation and to Messrs. B. Karmhag, E. Nerentorp and A. Pettersson for operation of the FRO reactor and for great help with the tedious oscillator measurements.

The loan of the enriched stable isotopes from the USAEC Research Inventory Pool is gratefully acknowledged.

REFERENCES

1. SCHRÖDER,R., Private communication. 1970

2. QAZI M.N., AB Atomenergi Sweden, Internal Report RF-70-89 (1970)

3. SOKOLOWSKI E.K. and LISSING C., AB Atomenergi Sweden, Internal Memo TPM-FFR-149 (1968)

4. NYMAN K., AB Atomenergi Sweden, Internal Report RFN-279 (1967)

5. LINDE S., AB Atomenergi Sweden, Internal Memo TPM-RFN-259 (1967) (In Swedish)

6. HÄGGBLOM H., AE-334 (1968)

7. GOLDBERG M.D. et al., BNL-325, Second Ed, Suppl. No. 2 (1966)

8. CONNOLLY T.J., de KRUIJF F. and SCHMIDT J.J., KFK 718 (1968)

9. BENZI V. and REFFO G., CCDN-NW/10 (1969)

10. SCHMIDT J.J., KFK 120, Part II (1962)

11. JOANOU G.D. et al., GA-2451 (1961)

12. WATANABE T. and REEDER S., WASH-1124 (1968)

13. HOWERTON R.J., UCRL-5226 (1959)

14. HOWERTON R.J., UCRL-5351 (1958)

15. KIROUAC G.J. et al., Total Neutron Cross Section and Resonance Parameters for ^{147}Pm. The 2:nd Conf. on Neutron Cross Section Data and Technology. Washington D.C. (1968) E4

16. LEDERER C.M. et al., Tables of Isotopes, 6th Ed. (1968) John Wiley & Sons

17. BONDARENKO I.I. (Ed.), Group Constants for Nuclear Reactor Calculations (1964). Consultants Bureau, New York

18. AHLIN Å. and LÖNDEN S-O., AB Atomenergi Sweden, Internal Report FFX-29 (1965)

19. ANDERSSON T.L. et al., Fast Reactor Physics (Proc. Conf. Karlsruhe, 1967) Vol. II p. 171. Vienna (1968) IAEA

CLOSING REMARKS BY CHAIRMAN

Y. F. CHERNILIN (Chairman): It has long been known - and the fact has emerged even more clearly at this Conference - that there are fairly important differences in the experimental results of concern to us. There are also differences of opinion as to the role of integral experiments and their relationship with differential measurements. Against this background, I should like to make the following comments:

First, international co-operation between the experimentalists engaged in the measurement of important cross-sections, for the purpose of analyzing their own systematic errors, could constitute a new method of evaluation and one which might probably be made more precise and useful.

Second, it is not enough to have evaluation efforts just on a national basis. It is very important that there should be a truly international approach. As an example of this I might mention the well-known studies - now completed - on the 2200 m/s-data, which were organized by the IAEA. Along similar lines, the Agency is now trying to organize studies on α ^{239}Pu and $\bar{\nu}$-values for the main fissile isotopes. It is very much to be hoped that the Agency will be able to bring these studies to a successful conclusion. To this end, it might be useful if it could convene a meeting of the experimentalists directly involved to discuss the problems which arise and to summarize the results of these studies. Before such a meeting is held, there should be consultations and close collaboration between the experimentalists concerned.

Section VIII

EVALUATION PROBLEMS AND METHODS I

Chairman
J.S. STORY (UK)

Invited Paper

PROGRESS IN INTERNATIONAL NUCLEAR DATA COMPILATION AND EXCHANGE
A Report of the four Neutron Data Centers

S. PEARLSTEIN
Director, NNCSC

Abstract

PROGRESS IN INTERNATIONAL NUCLEAR DATA COMPILATION AND EXCHANGE.

There are now four neutron data centers in the world, each responsible for collecting data from a particular geographic area. (A data collection is determined by where the measurements are performed, not where they are published.) The National Neutron Cross Section Center (NNCSC), supported by the United States Atomic Energy Commission and located at the Brookhaven National Laboratory, collects data measured in the USA and Canada. The Neutron Data Compilation Center (CCDN), operated by the European Nuclear Energy Agency and located at the Saclay Laboratory near Paris, France, collects data measured in Austria, Belgium, Denmark, France, Germany, Italy, Japan, The Netherlands, Norway, Spain, Sweden, Switzerland, and the United Kingdom. The Centr Po Jadernym Dannym (CJD), or Nuclear Data Center in translation, is the new name for the center located at Obninsk, USSR, and is responsible for collecting data from the Soviet Union. The Nuclear Data Section (NDS) of the International Atomic Energy Agency, Vienna, Austria, collects data from the remaining countries and to date has acted as liaison between the CJD and other centers.

During the past year, the 4-Centers have arrived at a neutron reaction classification scheme, dictionaries of related quantities, and a detailed format for the exchange of experimental data between Centers. Trial exchanges have already taken place and final details decided. Much of this progress has been an outgrowth of the IAEA Panel meeting on Nuclear Data Compilation, held at Brookhaven National Laboratory in February 1969.

The formal agreements for the exchange of experimental and evaluated data between Centers will be reviewed. Individual reports covering the activities of each Center will also be presented.

1. BACKGROUND OF THE FOUR NEUTRON DATA CENTERS

There are now four neutron data centers in the world, each responsible for collecting data from a well-defined geographic area. [Data collection is determined by where the measurements are performed --- not where they are published.] The National Neutron Cross Section Center (NNCSC), supported by the United States Atomic Energy Commission and located at the Brookhaven National Laboratory, collects data measured in the U.S. and Canada. The Neutron Data Compilation Centre (CCDN), operated by the European Nuclear Energy Agency and located at the Saclay Laboratory near Paris, France, collects data measured in Austria, Belgium, Denmark, France, Germany, Italy, Japan, The Netherlands, Norway, Spain, Sweden, Switzerland, and the United Kingdom. The Centr Po Jadernym Dannym (CJD), or Nuclear Data Center in translation, is the new name for the center located at Obninsk, U.S.S.R., and

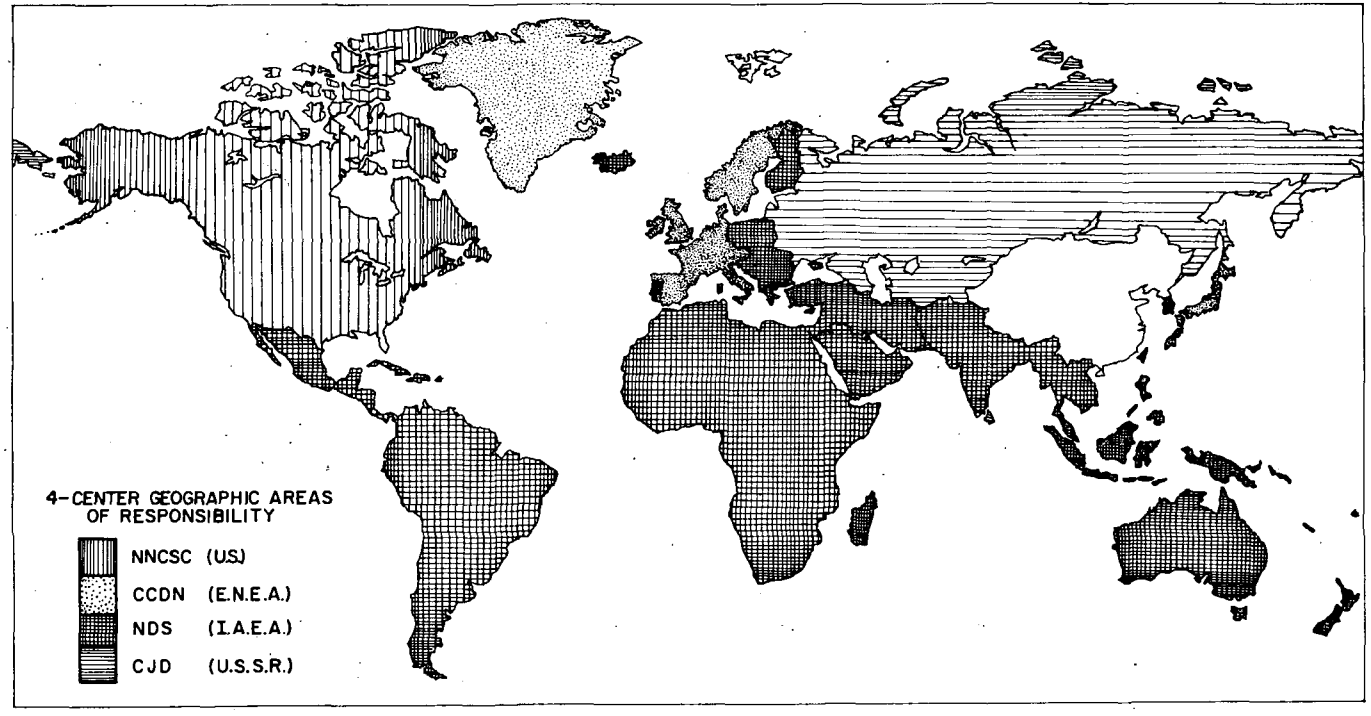

FIG. 1. 4-Center geographic areas of responsibility.

is responsible for collecting data from the Soviet Union. The Nuclear Data Section (NDS) of the International Atomic Energy Agency, Vienna, Austria, collects data from the remaining countries and to date has acted as liaison between the CJD and other centers. The geographic coverage of each of these centers is illustrated in Fig. 1.

Throughout this paper, the four neutron data centers will be referred to collectively as the "4-Centers."

2. EXCHANGE AGREEMENTS

There now exist formal agreements to exchange all published and author-released experimental neutron data between the 4-Centers. Requested experimental data to and from the Soviet Union are transmitted through the NDS in Vienna. A regular exchange of data sets in the format of the Evaluated Nuclear Data File takes place between the NNCSC and CCDN and, by special bilateral agreement, also between the NNCSC and Australia, India, and Israel. There is also a limited exchange of evaluated data between CCDN, NDS, and CJD. Although a formal mechanism does not now exist, an exchange of evaluated data could conceivably take place between the NNCSC and the remaining centers.

Evaluated data may be defined as the documented analysis of experimental data and/or nuclear model studies to provide a data set useful for characterizing nuclear properties in physics or engineering calculations.

3. 4-CENTER MEETINGS

Arranged and, for the most part, financed by the IAEA, meetings are held about once a year at the site of one of the centers. These meetings are attended by personnel or representatives from each of the 4-Centers and serve to coordinate the international effort in the collection, compilation, and dissemination of neutron data information. To date there have been five such meetings, the most recent of which was hosted by the CJD in Moscow. In addition, a "workshop" meeting of 4-Center programming personnel was held recently in order to further coordinate the computer problems associated with international data exchange.

During the past year the 4-Centers have arrived at a neutron reaction classification scheme, dictionaries of related quantities, and a detailed format, called EXFOR, for the exchange of experimental data between Centers. Trial exchanges have already taken place and final details decided. Much of this progress has been an outgrowth of the IAEA Panel meeting on Nuclear Data Compilation, held at Brookhaven National Laboratory in February 1969.

The progress in the exchange of experimental data is expected to continue as greater and varied amounts of data are stored in the files of each Center. The demand for exchange of evaluated data is increasing. By holding regular get-togethers of 4-Center personnel (one has just taken place at this conference), a profitable exchange of ideas occurs, leading to better services to the users of each neutron data center.

Following are brief reports that describe the scope and activities of each of the 4-Centers.

4. NATIONAL NEUTRON CROSS SECTION CENTER (NNCSC)

4.1. Background

Neutron data compilation was started at BNL in 1951 by D. J. Hughes as a supplementary activity to the neutron measurement program in the Physics Department. Upon his death in 1960 the compilation activity was moved to what is now the Department of Applied Science (DAS) and organized as the Sigma Center. At the same time, a companion group, specializing in cross section theory and data evaluation, was organized and later became known as the Cross Section Evaluation Center.

In September 1967 these two centers were merged to form the National Neutron Cross Section Center. In order to strengthen its ability to meet the expanding data requirements of the US AEC and contractors, this new Center was given the status of a Division within the Department of Applied Science at BNL. An advisory committee was appointed by BNL to assist the NNCSC in defining a program to meet the continuing needs of the neutron cross section community. The members of this committee are R. Ehrlich (Knolls Atomic Power Laboratory), H. Goldstein (Columbia University), P. Greebler (General Electric Co.), G. C. Hanna (Chalk River Nuclear Laboratory, Canada), R. Lazarus (Los Alamos Scientific Laboratory), and A. B. Smith (Argonne National Laboratory). They meet regularly with the NNCSC staff to review the administrative and technical progress of the Center.

Many in the scientific community are perhaps most familiar with the Center through its publication of the widely used compilations Neutron Cross Sections (BNL-325) and Angular Distributions of Neutron-Induced Reactions (BNL-400). [See also Section 4.6.]

4.2. Organization and facilities

The NNCSC is organized into four main technical groups---Cross Section Theory, Cross Section Compilation, Cross Section Evaluation, and Computer Programming Applications--- plus an administrative staff. The

personnel consists of 12 scientists, 5 professionals, and 5 non-professionals. For the last two years there have also been one or two industrial physicists resident at the NNCSC for an extended period while developing nuclear analysis techniques under the auspices of the US AEC Industrial Participation Program.

Recently a computer facility was installed at the Center. The fact that the NNCSC has exclusive use of this machine ensures reliable and efficient handling of the Center's large store of data.

4.3. Experimental data library

The experimental neutron data library already exceeds 1,000,000 points and, as a result of automated experimental techniques, is expanding rapidly at a rate of approximately 120,000 points a year. The neutron data library consists mainly of resonance parameters and energy- and angle-dependent cross sections, although other types of information are also stored. An automated storage and retrieval system [1] has been in use since 1964, but only recently have all available data been entered into the system. Information can be selected according to element, isotope, reaction type, energy range, reference, laboratory, and other criteria. Descriptive text and comments about the data are also part of the library.

This system, however, is being superseded by an improved version which operates with a greater degree of flexibility. In addition it can retrieve many more types and combinations of information than was previously possible. The new system's requirements have placed a greater burden on the Center's scientific staff, whose members must now make far more detailed specifications of the experimental information that is constantly received. This new system is in trial use at the present time; when fully operational, it will be linked to the NNCSC's automated publication of data.

An important adjunct to the Center's storage and retrieval system is the "author proof" system. Basically, this procedure works as follows: After data have been received from an experimenter and coded in the storage format, a listing and plot of his data are produced by computer and sent to him for comment. In this way the experimenter is given an opportunity to contribute to the accuracy and reliability of the data library. To date there has been excellent cooperation between the experimenter and the NNCSC in the review of proof material.

Through 4-Center meetings sponsored by the IAEA, a format common to all Centers was constructed for the exchange of experimental data. A computer programming effort to support this exchange has been completed and trial exchanges have already taken place.

4.4. Evaluated data library

The Evaluated Nuclear Data File (ENDF) was started at BNL in 1964 by Henry Honeck. The purpose of this library is to place data sets from many different sources into a common format for use in neutronics calculations, thus establishing a link between the data library and processing codes. A flexible format [2] is used which permits data to be specified in tabular form, power series, and nuclear model formulas. A series of file maintenance programs [3] in machine-compatible language is available to create library tapes and to check, correct, and convert the data into readable forms such as expanded text listings and plots.

The ENDF library is divided into two parts, ENDF/A and ENDF/B, each using the same format. The ENDF/A library consists of data sets that may or may not have been extensively tested. For each isotope there can be more than one data set for a particular reaction from which to choose, but there may not be data sets for all important reactions through the energy range of interest.

The ENDF/B library is intended to provide a reference set of data for use in nuclear calculations. Data for approximately 80 isotopes are recommended for all significant neutron-induced reactions in the energy range 10^{-5} eV to 20 MeV. Included are some thermal scattering data, as well as photon interaction and production data. The library contains approximately 300,000 tabulated data points, with parametric representations of other data as well. After a one- or two-year period the data sets are revised on the basis of new information available. The use of a well-documented, single data set per isotope which can be used over an extended period of time permits comparisons of calculations to be made without ambiguity. Development of this library takes place through working arrangements with other U.S. laboratories.

4.5. Cross Section Evaluation Working Group

The Cross Section Evaluation Working Group (CSEWG) was organized in 1966 by the U. S. Atomic Energy Commission, Division of Reactor Development and Technology. Its membership consists of representatives from the data evaluation and/or user groups of approximately twenty laboratories, most of which are under AEC contract. CSEWG meetings are held at BNL about twice annually, with NNCSC personnel directing the proceedings. The main objective of CSEWG is to generate and test (both microscopically and macroscopically) new and revised data for the ENDF/B library. In support of the Liquid Metal Fast Breeder Reactor (LMFBR) program, CSEWG devotes considerable effort to the comparison of calcu-

lated results with those from carefully selected integral experiments. In addition, ENDF/B data are tested in thermal reactors and in shielding and space applications.

There are many problems arising in the use of data to which CSEWG members have devoted attention, such as code compatibility, cross section formalisms, documentation standards, etc. Much of this work is accomplished by special subcommittees within CSEWG---namely, the Resonance Region, Codes and Formats, Data Testing, Shielding, and Normalization and Standards Subcommittees. In addition to the CSEWG meetings held regularly at BNL, separate subcommittee meetings are held at other times to explore problems in greater detail than is possible at the general meetings.

Another important CSEWG activity has been the review of data sets for the fissile elements. Before they can be considered reliable for calculation purposes, it is absolutely necessary that (1) the data in each set be consistent (i.e., the partial cross sections for any one isotope should be consistent with the total cross section), and (2) the ratios of a data set relative to another corroborate those ratios that are independently determined. To ensure consistency in some of these data sets, the NNCSC recently called together a group of experimenters to join CSEWG evaluators in making necessary revisions.

4.6. Automation

The NNCSC activities strongly emphasize the computerization of data processing. Computer codes perform comprehensive checks for consistency of the evaluated data by comparing the data with well-known empirical limits and theoretical values. Other codes are developed that perform least-squares fitting of the experimental data [4, 5].

The publication of neutron data compilations is now automated. An edition of BNL-400, Angular Distributions in Neutron-Induced Reactions, will appear in 1970, the contents of which will be produced almost entirely by a computer. The graphics portion is photographed on 35-mm film with use of a cathode-ray tube device---a process that is 100 times faster than mechanical plotting. Publication proceeds directly from the film.

In the future the Center plans to implement a system that will permit scientists to analyze data by means of display tools. One such example of an interactive display system already using the NNCSC data files is SCORE [6].

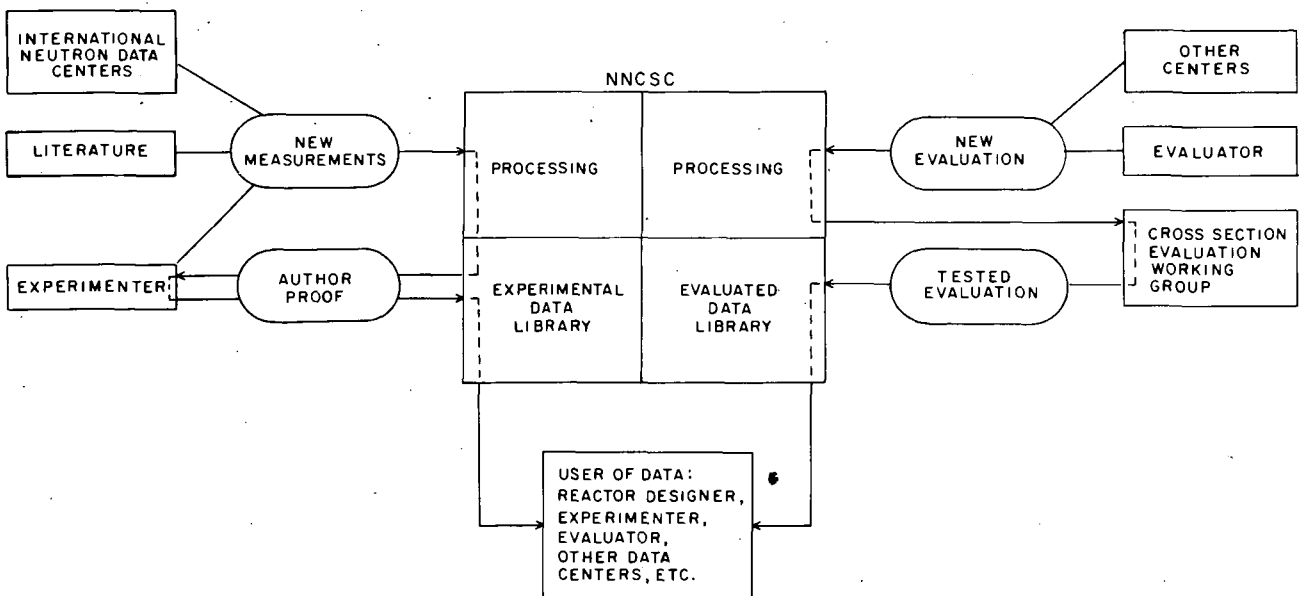

FIG. 2. The relationship of NNCSC to other centers, experimenters and evaluators.

4.7. Summary

In brief, the NNCSC is a US AEC-supported information center whose functions include the following:

1. Compiling experimental and evaluated neutron data.
2. Disseminating information through regular publications and in answer to specific requests.
3. Developing new methods of neutron data analysis.
4. Coordinating neutron data activities through working arrangements with other laboratories.
5. Developing computerized systems for the storage, retrieval, analysis, and publication of neutron data.

The relationship of the NNCSC to other Centers, experimenters, and evaluators is shown in Fig. 2.

REFERENCES

[1] FRIEDMAN, J.M., PLATT, M., "SCISRS - Sigma Center information storage and retrieval system," Brookhaven National Laboratory Rep. BNL 833 (1964).

[2] HONECK, H., "ENDF/B Specifications for an evaluated nuclear data file for reactor applications," Brookhaven National Laboratory Rep. BNL 50066 (1966).

[3] HONECK, H., FELBERBAUM, J., "Description of the ENDF/B processing codes CHECKER, CRECT, DAMMET, PLOTFB, and retrieval subroutines," Brookhaven National Laboratory Informal Rep. ENDF-110 (Revised 1969).

[4] AUERBACH, E.H., "ABACUS-II," Brookhaven National Laboratory Informal Rep. BNL 6562 (1962).

[5] BHAT, M., "SIGTEST, a rapidly convergent program to least-squares fit experimental data using the Adler-Adler formalism," Brookhaven National Laboratory Rep. (to be published).

[6] DUNFORD, C.L., BERLAND, R.F., CREASY, R.J., "SCORE - an automated cross section evaluation system," Atomics International Rep. NAA-SR-MEMO-12527 (1968).

5. NEUTRON DATA COMPILATION CENTRE (CCDN)

5.1. Experimental data

CCDN introduced its NEUDADA data storage and retrieval system [1] in order to make the fullest use of the direct access storage features of its IBM 360/30 computer. At present this system is used with two

libraries coded to SCISRS specifications: the Internal File contains all data compiled from laboratories in the CCDN responsibility area (European OECD countries plus Japan), while the External File contains data received from other laboratories, mainly those compiled by the NNCSC.

Dissemination of data retrievals from these libraries was started in January 1969 covering a basic range of physical parameters, while with effect from July 1969 the programmes were extended to allow selection of data by bibliographic parameters also. Index listings for all data available through the CCDN were published as CCDN Newsletters [2-5]. For data exchange between the main data centres a Translation Programme NEUDADA→EXFOR exists, while the inverse Translation Programme is being written.

The current compilation work covers several problems besides that of coding recently published work in EXFOR-compatible format: the existing entries for work from the CCDN area are being checked, and this includes modifying the comments to make them EXFOR-compatible. The recent implementation of multiprogramming with two IBM 2260 terminals used in foreground facilitates this task. In addition, a start has been made to catch up on the very large backlog of earlier work still to be coded. It is hoped to obtain feedback about errors and help in coding data not yet in the file by directing all communications through liaison officers for those laboratories which are willing to appoint one. Several have already done so, and we hope to extend this practice.

5.2. CINDA

CCDN's double task in CINDA is to prepare entries for its service area and to carry out computer operations on behalf of the three centres on the European continent. While only minor changes have been made in computer operations, work on the entries has continued with the aim of producing a file as complete and error-free as possible. In the last four years special effort has been expended successively on correcting formally inadequate entries, collating all entries referring to essentially the same work and sending out the results to be checked in the laboratory where the work was done, and then trying to fill the gaps known to exist in the coverage of literature before about 1960.

Many CINDA users have asked for the restoration of information on whether the data indexed are available on tape from the regional centres. Maintenance of the original hand-comparison with the SCISRS data files proved quite impracticable, but programmes being written by the CCDN should allow computer insertion in time for CINDA 71 of "DATA" tags to

CINDA entries for which the data are at least partially on file. The present contents of the CINDA master file are represented for users by the 1969 cumulation [6] plus a single supplement [7]. Due to financing difficulties, the cumulation for 1970 will be replaced by a second supplement: IAEA has agreed to take over the printing of CINDA from 1971 on, using material edited at CCDN, and it is hoped that a new cumulation can be produced as early as possible in 1971 so as to minimise the inconvenience to CINDA users.

5.3. Evaluated data

CCDN continued to collect references of evaluation work carried out in Europe. An index of evaluation work performed in different laboratories all over the world is published regularly [8-10]. The next updated index will appear in July 1970.

Most of the numerical data corresponding to this index are available through CCDN, including information from such important files as ENDF/B, KEDAK and the U.K. file. Retrievals with regard to nuclides can be made from the ENDF/B and U.K. files (the latter in direct access), while a card image copy of the KFK-KEDAK file can be obtained. In addition, GENEX tapes from the U.K. file will shortly be available. A translation programme from U.K. format to ENDF/B format has been provided by Prof. Benzi (CNEN, Bologna), while the problem of writing an inverse translation programme is under study.

CCDN support has led to the evaluation of the $^{6}Li(n,\alpha)$ [11] and various ^{3}He cross-sections [12]. Recently (n,γ) cross-sections for stable nuclei with $32 \leq Z \leq 66$ were published [13].

5.4. RENDA

CCDN has developed a general computerized bibliographic system [14] which includes the handling of conventional (upper and lower case) character strings, which is at present used for the compilation of EANDC requests [15-18] for neutron data measurements. CCDN assists the EANDC secretariat of ENEA in the operation of this request file.

REFERENCES

[1] CCDN/SYS-2 NEUADA System Description (April 1969).
[2] CCDN-NW/2 Newsletter (March 1966).
[3] CCDN-NW/4 Newsletter (December 1966).
[4] CCDN-NW/8 Newsletter (March 1969).

[5] CCDN-NW/11 Newsletter (October 1969).
[6] CINDA 69 published by ENEA/CCDN on behalf of the four participating centres (May 1969).
[7] CINDA 69 Supplement published by the USAEC/DTIE on behalf of the four participating centres (January 1970).
[8] CCDN-NW/5 Newsletter (April 1967).
[9] CCDN-NW/7 Newsletter (March 1968).
[10] CCDN-NW/9 Newsletter (April 1969).
[11] CCDN-NW/3 Newsletter (October 1966).
[12] CCDN-NW/6 Newsletter (September 1967).
[13] CCDN-NW/10 Newsletter (December 1969).
[14] CCDN/SYS-1 RENDA System Description (November 1968).
[15] RENDA EANDC 61"U" (January 1968).
[16] RENDA EANDC 62"AL" (February 1968).
[17] RENDA EANDC 78"AL" (December 1968).
[18] RENDA EANDC 85"U" (February 1970).

6. NUCLEAR DATA SECTION (NDS)

6.1. Data Centre activities

6.1.1. Experimental data compilation

One of the primary responsibilities of the NDS of the IAEA is the systematic collection and compilation of experimental neutron data from its service area which consists of all Non-EANDC countries with the exception of the USSR. In the initial stages of this activity the NDS developed and used successfully the DASTAR/CINDU system for neutron data storage and retrieval. This system allowed for ease of retrieval, without built-in sophisticated retrieval criteria, and provided the NDS users with a periodically published index called CINDU of those data available at the NDS. The growth of the DASTAR file can be judged from comparison of the volume of successive editions of the CINDU catalogue. The current catalogue CINDU-9 [2] edited in November 1969, when compared to CINDU-8 [1] shows that the number of data sets from the NDS service area entered into DASTAR has doubled since January 1969, this, however, being an exceptionally large increase. CINDU-10 [3] will be published in the course of the next few months.

Recently particular efforts have been made to complete the back coverage of literature originating from the NDS service area. For this purpose earlier journals and report series from the serviced countries are systematically scanned. In the case of some countries, such as Yugoslavia,

South Africa and Taiwan, the coverage is almost complete, in most of the remaining countries both back- and current-coverage is at least 50% complete.

DASTAR/CINDU contains also data from the other three neutron data centres, in particular also evaluated data. The CINDU-9 catalogue has reference to a total of about 1500 experimental data sets contained in DASTAR, about half of which have originated from the NDS service area. This corresponds to a total of about 150,000 experimental data lines. In addition DASTAR contains part of the UK and the complete KEDAK evaluated data libraries and Obninsk evaluated data on differential elastic and inelastic cross sections.

With the advent of EXFOR the data centre service function of the NDS will be considerably improved with regard to retrieval selectivity and completeness in the satisfaction of user requests. For this purpose the existing DASTAR/CINDU data will be transformed to the EXFOR system, supplemented by the still lacking data from the other centres; refined checking and retrieval programs will be developed in cooperation with the other centres.

As part of the overall effort to improve its data centre services, the NDS provides for one field trip every year to regions within its service area. The purpose of these field trips is to advertise the activities and services of the NDS, to stimulate the cooperation and exchange between the scientists and the NDS in general, and to encourage people in particular to send their data and auxiliary physics information to the NDS and to make use of the services of the NDS. The first of these field trips, early in 1968, covered nuclear laboratories and institutes in India, Southeast Asia and Australia. The second field trip during the summer of 1969 covered laboratories and universities in a number of countries in Latin America. A third field trip is planned for the fall of this year and will cover Eastern European countries. In addition a system of liaison officers, one in each of the serviced countries, has been established with the purpose to strengthen the cooperation between the NDS and the scientists in its service area in particular. An updated list of correspondents is published twice a year [4].

Following one of the recommendations of the IAEA Panel on Neutron Data Compilation the NDS has started a professional activity file of all neutron physicists in the NDS service area. Aside from being useful for internal NDS coordination purposes, this activity file should serve mainly as a basis for the planning of the NDS future programmes and as a potential basis for an automatic user service.

6.1.2. Data exchange and dissemination

As part of the data service to the NDS service area an average total of about 100 requests, both incoming and outgoing, are processed per year. These requests range from individual experimental data sets to complete libraries of evaluated data. In 1969 this corresponded to 350 individual sets of experimental data comprising a total number of approximately 30,000 data lines, and to 500 individual sets of evaluated data comprising a total number of approximately 320,000 data lines (where one data line corresponds to one energy, and may include from one to about ten cross sections).

Another primary function of the NDS is the exchange of neutron data between the Obninsk Nuclear Data Centre on the one side and the CCDN (Saclay) and the NNCSC (Brookhaven) on the other side. Regarding experimental neutron data a free exchange of material has been established and is functioning regularly. Through this arrangement every neutron and reactor physicist in the world has potential access to all compiled experimental neutron data. A limited amount of evaluated data exchange has taken place.

6.1.3. CINDA

Within the framework of the world coverage of the neutron data literature for CINDA the NDS scans 42 report series and 60 journals from its service area and collects CINDA entries from the USSR. In addition to this "new" CINDA input the NDS revises and completes older entries as part of its data compilation task; this in turn helps considerably to complete the data files. To quote a figure of the NDS contribution to CINDA, about 25% of the entries in CINDA 69 are of NDS origin.

Up to this year the CINDA volumes and supplements have been published alternatively by the CCDN (Saclay) and the US AEC DTIE (Oak Ridge). From 1971 on the printing of the CINDA publication will be performed by the IAEA from input produced and edited by the CCDN.

6.2. Assessment of data needs

An increasing activity of the NDS is the assessment of nuclear data needs coupled with detailed reviews of important nuclear data and surveys of experimental nuclear data activities particularly in developing countries.

6.2.1. Non-EANDC RENDA

Within the above scope the NDS has started to collect systematically contributions for a Non-EANDC request list for neutron data measurements, modelled after the existing EANDC "RENDA" request list [5]. The

Non-EANDC request list, which includes neutron data measurement requests from Non-EANDC countries and from the USSR, contains presently some 650 requests. This comprises about 250 new requests of which about 150 are from the USSR and the rest coming from 11 countries within the NDS service area. An additional 400 requests, confirming or supporting existing RENDA requests, have been received from the USSR.

6.2.2 Targets and foils

Recently, the NDS has initiated a survey among all developing countries within its service area to ascertain the needs for accelerator targets and neutron data experiment foils. A circular has been sent out to more than 50 physicists at institutions in developing countries. This has found encouraging response justifying substantial IAEA efforts to meet the needs. With possible financial aid from the IAEA it is planned to provide assistance to experimental physicists in acquiring the needed material from supplying laboratories and firms in developed countries.

6.2.3 Data for safeguards

The NDS recently also sent out a circular to all people involved in safeguards technical development asking for specific definitions and priorities of nuclear data needs for safeguards development and indications which data are either inconsistent, incomplete or unknown. The response to the circular which has been summarized in a report to the INDC [6] will serve to initiate reviews for data of prime importance.

6.2.4. Data reviews

In support of the meetings which it sponsors and in response to the evidence which has resulted from the assessment of important data needs, the NDS has continued and amplified the preparation of reviews of selected neutron data parameters of specific isotopes of particular relevance to nuclear reactor projects. The first example of such a review, which has been performed as a cooperative effort of the NDS and physicists from Canada, the U.K. and the USA was the "Survey of values of the 2200 m/sec constants for four fissile nuclides" published in 1965 [7] and updated in 1969 [8]. A few smaller reviews have been completed to-date by the NDS and submitted to the INDC: a review of the α values and fission cross sections for ^{239}Pu for fast neutron energies [9], a review of fast ^{238}U capture cross sections [10] and a review of energy dependent $\bar{\nu}$ values for the main fissile isotopes [11]. A review of threshold reactions for isotopes used as standard and in the field of dosimetry has been initiated. A review of prompt neutron fission spectrum data and a survey of data in the field of fusion reactors are planned to be started in the course of the year.

6.3 Coordination activities and meetings

Because of its position within the IAEA organisation the NDS has played a coordinating role in organising the intercentre-exchange of neutron data information and in organising and sponsoring various meetings of interest to the nuclear scientific community.

6.3.1. Four-Centre Meetings

As early as 1966 the NDS convened the first of a series of Four-Centre Meetings which had as its prime objective the formulation of an agreement to exchange experimental data between the data centre in the USSR and those of North America and Western Europe. Since then these Four-Centre Meetings held about yearly at the site of one of the centres have served to coordinate the international effort in the collection, compilation and dissemination of neutron data information. In parallel, each of the four centres has developed its individual capacity and scope to the point where a common agreement to establish a computerized system to exchange neutron data information between the centres has become feasible. At the last Four-Centre Meeting in November 1969 in Moscow [12] the four centre representatives formulated the basic framework and concept of an exchange format for the transmission of neutron data information between the four centres. The acronym for this system is EXFOR; EXFOR is designed to transmit bibliographic, data and characteristic physics information. The responsibilities of the NDS within the framework of the development and implementation of the EXFOR system are to coordinate the updating of the dictionaries and to formulate the content of the Compiler's Manual.

6.3.2. Conferences and panels

The NDS fulfills an additional coordinating function within the framework of the exchange and dissemination of nuclear data information, by sponsoring, preparing and conducting scientific meetings as part of the overall IAEA programme. Within the last four years the NDS has organized two larger Conferences, the 1966 Paris Conference on Nuclear Data for Reactors [13], the present Helsinki Conference [14], and a few smaller meetings: the 1967 Brussels Panel on Standards [15], the 1969 Brookhaven Panel on Neutron Data Compilation [16,17], and additional smaller technical meetings on α (^{239}Pu) and $\bar{\nu}$ data for fissionable nuclei (June 1970, Studsvik).

Within the next two years the NDS plans to sponsor other expert meetings which will consider "Methods of Evaluation," "Status of fission neutron spectrum data," "Standards for nuclear data measurements" and

"Status of heavy element nuclear data." A third IAEA Conference on Nuclear Data is planned for 1974.

6.3.3. INDC secretariat responsibilities

Instrumental in the coordination of the above mentioned activities and in recommending guidelines to the NDS programme is the International Nuclear Data Committee (INDC), which serves as advisory body to the Director General of the IAEA. The administrative function of the NDS with regard to the INDC consists in the operation of its secretariat. The secretariat plans and organizes the yearly meeting of the INDC, and serves as the distribution centre of INDC documents and information. In addition, in order to help in the coordination of the nuclear data efforts in the world, the INDC secretariat maintains constant contacts with the INDC liaison officers and with other groups and organisations, within and outside the IAEA.

The NDS is a section within the Division of Research and Laboratories of the IAEA; its total staff is 18 people, composed of 10 physicists, 2 programmers, 3 computer support staff and 3 secretaries.

REFERENCES

[1] CINDU-8 (January 1969).
[2] CINDU-9 (October 1969).
[3] CINDU-10 (summer 1970 - to be published).
[4] INDC Correspondents for the exchange of nuclear data information, INDC(SEC)-5/U (November 1969).
[5] Non-EANDC request list for neutron data measurements, INDC-(NDS)-20/N (May 1970).
[6] BYER, T., Nuclear data needs for safeguards technical development, INDC(NDS)-21/N (May 1970).
[7] WESTCOTT, C.H., EKBERG, K., HANNA, G.C., PATTENDEN, N.S., SANATANI, S., ATTREE, P.M., IAEA At. En. Rev. 3, (1965) 2.
[8] HANNA, G.C., WESTCOTT, C.H., LEMMEL, H.D., LEONARD, B.R. Jr., STORY, J.S., ATTREE, P.M., IAEA At. En. Rev. 7, (1969) 3.
[9] BYER, T., KONSHIN, V., "Review of the fission cross section and α for Pu^{239} in the energy region 1 keV to 10 MeV," INDC(NDS)-17/N (May 1970).
[10] KONSHIN, V., "Revised review of fast capture cross sections of U^{238}," INDC(NDS)-18/N (May 1970).
[11] MANERO, F., KONSHIN, V., "Review of energy dependent $\bar{\nu}$ data for the main fissile nuclei," INDC(NDS)-19/N (May 1970).

[12] Report of the Fifth Four-Centre Meeting, Moscow, 17-21 November 1969, INDC(NDU)-16/N (December 1969).
[13] IAEA Conference on Nuclear Data for Reactors, Paris, October 1966; Proceedings (April 1967).
[14] Second IAEA Conference on Nuclear Data for Reactors, Helsinki, June 1970 (Proceedings to be published).
[15] IAEA Panel on Nuclear Standards for Neutron Measurements, Brussels, May 1967; Technical Report IAEA No. 107 (1968).
[16] IAEA Panel on Neutron Data Compilation, Brookhaven National Laboratory, February 1969; Technical Report IAEA 111 (1969).
[17] IAEA Panel on Neutron Data Compilation, Brookhaven National Laboratory, February 1969; Technical Rep. Series No. 100 IAEA (1969).

7. CENTR PO JADERNYM DANNYM (CJD)

Since the 4-Centre meeting in Vienna in December 1968 our Centre has continued its activities according to the program described in Dr. Zolotukhin's paper at the February 1969 Panel on compilation which was held at the Brookhaven National Laboratory. The main efforts of the Centre staff have been directed toward the development of the programs for translating information from IBM tapes onto the M-220 computer tapes and vice versa, as well as to participate in the work on the exchange format which is to be specifically considered at this meeting. It should be noted that the exchange format is of particular importance to our Centre, as it is supposed to be used for our internal needs, at least at the beginning of our work.

After the spring of 1969 the 7th, 8th and 9th issues of the collection of abstracts "Nuclear Physics Research in the USSR" were published. At the present time the 6th Bulletin is being prepared for publication. We have also continued the work on our Centre Data Index which is similar to CINDU. In the field of CINDA, during 1969, 33 cards containing 624 entries had been filled in and sent to Vienna.

In exchange for information of the latest USSR measurement results and evaluations of neutron data which we have sent to the IAEA, our Centre has received a considerable amount of information on magnetic tapes which have been used for the development of the tape translation system mentioned above.

In order to improve the guidance of all the activities on the collection, handling and dissemination of neutron data information, the Nuclear Data Commission of the State Committee on the Atomic Energy Utilization was formed; it replaces the previously acting Council of the Nuclear Data

Information Centre. The director of the Institute of Physics and Power Engineering (FEI) in Obninsk, Professor V. A. Kuznetsov, was appointed chairman of this Commission. The Commission's members are physicists from different institutes of our country in which neutron data investigations are carried out; among them are the academician of the Academy of Sciences of the BSSR Professor A. K. Krasin, the academician of the Academy of Sciences of the UkSSR Professor M. V. Pasechnik, Professor F. L. Shapiro (JINR, Dubna), as well as Dr. V. I. Popov (FEI, Obninsk), Dr. S. I. Sukhoruchkin (ITEF), Mr. Yu. G. Klimov (State Committee on Atomic Energy Utilization), Dr. A. I. Abramov, and Prof. L.N. Usachev.

At the Commission's meetings, which take place several times a year, the following questions are considered: the state of the nuclear data compilation and evaluation, the needs for nuclear data for practical applications, the reports of the Nuclear Data Centre on its current activities, as well as the review of the current investigations of the most important nuclear constants. The proposals and recommendations of the Commission are taken into consideration when planning scientific research in different institutes of our country.

All of the practical work on nuclear data collection and dissemination is performed as before by the Nuclear Data Centre of the State Committee on the Atomic Energy Utilization located at the Institute of Physics and Power Engineering (FEI) in Obninsk. The staff of the Centre, headed by Dr. V. I. Popov, consists of several people working permanently; in addition a number of FEI employees take part in helping with various tasks of the Centre. The permanent working staff of the Centre is involved in the development of computer programs, in CINDA activity, in the preparation for publication of the Centre's Bulletin and collection of abstracts, as well as in carrying out of routine tasks.

The main effort in the field of nuclear data evaluation and in the analysis of nuclear data requirements is carried out in different laboratories of FEI and at other Scientific Institutes. However, the organization of the evaluation effort demands careful attention with the aim of continuous improvement.

We plan to increase the Centre staff to reinforce the above mentioned trends existing now in the Centre. Two new groups are to be organized. One of them will continue the work on neutron constants evaluation started by V. I. Popov, and the other one will ensure mathematical service of the Centre.

At present our Centre uses for its needs the M-220 computer. As it is known, the tapes for this computer are incompatible with the IBM

tapes which are used in many countries. This situation creates considerable difficulties in the exchange of information with the other data centres. Already in the course of this year we hope to receive two new tape units designed for operation with 7-track 1/2-inch tapes.

Two coordinating groups, consisting of specialists from different scientific institutes, have been formed in order to effect an efficient working relationship between our Centre and these institutes, and to coordinate the work being performed at these institutes with that of the Centre. One of these groups, headed by Dr. V. G. Zolotukhin, will be engaged in defining and making a systematic collection of the requirements in the nuclear data field, and in constructing multi-group systems of neutron constants. The other group headed by Dr. V. I. Mostovoy, will deal with the coordination of the nuclear data measurements and with the problems of experimental data compilation and evaluation. The suggestions made by these groups are to be reviewed and taken into consideration at the meetings of the Nuclear Data Committee.

DISCUSSION

P. VÉRTES: Up to now no research groups in Hungary have been engaged in the evaluation of nuclear data. However, we are deeply involved in reactor physics and other types of neutronics calculations, so that we need accurately evaluated nuclear data. For this reason the new NDS activity of IAEA represents a great help to us and I believe to other countries in a similar situation. We have received from the NDS the full KEDAK files and a large number of UK files. A system of codes for producing group constants from these evaluated data is being prepared in our laboratory.

It would be very useful if the exchange of evaluated data could be developed further so as to reach at least the present level of exchange in the case of experimental data. This would be advantageous not only to those who are not doing evaluation but also to those who are engaged in physics calculations and experiments. An increase in the number of calculations and comparisons with experiments would provide a thorough and extensive check on evaluated data sets.

S. PEARLSTEIN: There are several obstacles to the exchange of evaluated data at the present time. As is the case with computer codes, evaluated data sets are very expensive to produce. Therefore, a similar basis is used for their distribution, i.e. an exchange basis. The NNCSC receives KEDAK and UK files from the ENEA centre at Saclay in exchange for ENDF/B and the Ispra Code Library exchanges reactor and shielding codes with the Argonne Code Centre and the Radiation Shielding Information Centre, respectively.

Furthermore, the resources of a data centre are taxed considerably by the work of satisfying requests for individual evaluated data sets. Whereas experimental data are stored in a single format by a data centre, in the case of evaluated data there has been a proliferation of formats and

a data centre must have additional codes to satisfy requests for evaluated data in a usable form.

A certain amount of patience is required as far as the exchange of evaluated data is concerned. The NNCSC has been exchanging experimental data with CCDN for six years and with the NDS for three years on an unrestrictive basis and we are still working hard on the details of such exchanges. It is, therefore, not surprising that the exchange of evaluated data will still face some difficulties.

J. J. SCHMIDT: I would like to enlarge briefly on Dr. Pearlstein's statements by mentioning that, of late, the Nuclear Data Section has been receiving more and more requests for evaluated data and complete evaluated data libraries. As a general statement, I think it can be said that this conference, and particularly the present session, reflects an improvement in the quantity and quality of the evaluation work being performed in various parts of the world. I think it is reasonable to expect that in due course, owing to the growing need for and emphasis on evaluation, there will be an ever greater interest in an expanded and free exchange of evaluated data.

N. A. TUBBS: In this discussion of evaluations I think it is a mistake to overlook the question of the nature of the data to be used. I recently made a partial analysis of the material in CINDA and found that out of about 60 000 entries referring to neutron physics work, two-thirds contained some experimental information. Some of this was old material which need not have been compiled, but there is not as much of these data as one might expect, since neutron physics has been growing at an exponential rate. Accordingly, if we compare this figure with the data index we see that there is still a great deal of data remaining to be compiled, while a fair number of corrections have to be made to material already on file. Data for use in computer evaluations will cause trouble unless it is 100 per cent correct and I think this is something that has not yet been achieved.

D. W. COLVIN: In support of the remarks of Dr. Tubbs, I should like to make a statement and ask a question. In 1968-69, Dr. G. D. James was making a compilation of data, derived mainly from CCDN files. I examined the material extremely carefully and came to the conclusion that this kind of data was more or less useless for evaluation work as it stood, and also that, through no fault of his own, Dr. James had been misled in the conclusions which he had reached in his compilation. I do not have the results of my evaluation of the status of the information on data tapes with me but, if memory serves, much of the American SCISRS data was in error. I should therefore like to ask Dr. Pearlstein how much of the data in his files has been checked and how much trust he himself puts in the SCISRS files.

S. PEARLSTEIN: As far as I know, there are two ways in which the quality of the data files can be improved. One is the production of compilations such as the BNL 325 and 400, where all of the experimental data are displayed and gross errors become obvious and can thus be corrected. Another means of dealing with more subtle discrepancies is to bring compilers, evaluators and measurers together in a co-operative evaluation effort, such as that involved in assembling version II of the ENDF/B library. While not all discrepancies were resolved in that case, the simultaneous plotting of evaluations and experimental data did help prevent misinterpretation of the data.

Invited Paper

THE APPLICATION OF INTERACTIVE COMPUTER GRAPHICS TO NUCLEAR DATA EVALUATION PROBLEMS*

H. ALTER, C.L. DUNFORD
Atomics International,
A Division of North American Rockwell Corporation,
Canoga Park, Calif.,
United States of America

Abstract

THE APPLICATION OF INTERACTIVE COMPUTER GRAPHICS TO NUCLEAR DATA EVALUATION PROBLEMS.

A comprehensive semi-automated data evaluation system is being developed at Atomics International, in order to overcome many of the deficiencies associated with the application of available nuclear data evaluation methods to the more detailed, systematic, and accurate data evaluations currently required. Interactive computational techniques enable the computer to form displays on a screen, and to sense, interpret, and relate the displayed information in real time. These techniques not only permit the rapid display of data sets selected at random, but also allow the evaluator to perform a large number of sequential operations in a short time span. The evaluator can take full advantage of his experience in interpreting results at each operational step. Thus, a logical path may be followed through to conclusion, without intervening lengthy delays.

A prototype interactive data evaluation system, SCORE, is currently being used in support of the ENDF/B national neutron cross-section evaluation effort. SCORE provides a unique data storage, manipulation, and retrieval system for experimental data stored on SCISRS 1 data tapes. Other operational modules include: (1) an interactive method for fitting multilevel resonance parameters, using either Breit-Wigner or Reich-Moore theory, (2) a method for fitting analytical cubic spline curves to experimental data, and (3) a method of intercomparing, by visually displayed overlays, ENDF/B evaluated data with SCISRS 1 experimental data tapes. Other operational modules include: (1) an interactive method for fitting multilevel resonance parameters, using either Breit-Wigner or Reich-Moore theory, (2) a method for fitting analytical cubic spline curves to experimental data, and (3) a method of intercomparing, by visually displayed overlays, ENDF/B evaluated data with SCISRS I experimental data. The SCORE system is currently being further expanded in several ways. These include: (1) incorporating the Adler-Adler resonance region description and methods for obtaining model parameters from measured data, (2) developing methods to permit operation from remote graphic terminals, and (3) developing methods to produce hard-copy images of the cathode-ray tube displays. Future development includes the interfacing of SCORE with the SCISRS II experimental data files, and the incorporation of a module to perform both optical-model and compound-nucleus calculations to aid in nuclear cross-section data evaluation above the resonance region.

1. INTRODUCTION

In order to intelligently discuss problems of nuclear data evaluation, one must decide upon a definition of the term, "evaluation." In 1968, J. J. Schmidt [1] offered a description of the term, as it applies to nuclear data, which we have paraphrased: "Neutron evaluation denotes the critical judgment, comparison, and selection of information which has been compiled, and its compaction (by some averaging procedure) into a complete, easily interpolable unique set of 'best' or recommended data, for further use in reactor neutronic calculations." Within the context of this

* This work was supported by the U. S. Atomic Energy Commission under Contract AT (04-3)-701.

definition, we propose that the basic technical problem in neutron cross-section data evaluation is how to apply critical judgment to the comparison and selection of the ever-increasing amounts of nuclear data, in order to promote efficient conversion of this information to unique best sets of useful evaluated data. As a means of helping resolve this problem, we propose to utilize an interactive computing system which can provide graphic computer output on a cathode ray tube, and can accept dynamic program input while a job is continuing execution.

Communication with a computer has traditionally been limited to punched cards, magnetic or paper tape, and typewriter input, with some kind of printing device being the normal output. Interactive computer graphics, which represents the concept of man communicating with a computer by means of graphical symbols, such as lines, curves, and dots, as well as by alpha-numeric characters, now adds the dimension of sketching and drawing for both input to and output from the computer. The flexibility and high rate of information transfer (as opposed to mere data transfer) presented by such freedom of communication is not likely to be soon surpassed. These new techniques of computer science are being applied to the problem of improving the methods currently being used for the evaluation of experimental neutron cross section data.

SCORE, [2] a prototype man-machine interactive data evaluation system, under development by Atomics International, is currently being applied in support of the ENDF/B[3] national neutron cross-section evaluation effort. The SCORE system represents the results of a continuing investigation of the application of a man-machine interactive system to the resolution of nuclear data evaluation problems.

The program currently provides a module for a unique data storage, manipulation, and retrieval system for experimental data stored in the SCISRS[4] format. Other operational modules include: (1) an interactive method for fitting multilevel resonance parameters, using the theory of Reich and Moore or Breit and Wigner, (2) techniques for fitting data with piecewise linear and cubic splines, as well as a least square cubic spline fit, and (3) real-time methods for intercomparing, by visually displayed overlays, evaluated data from the ENDF/B files with experimental data from the SCISRS I files. SCORE is currently being expanded to include the development of: (1) Adler-Adler resonance region description and methods for obtaining resonance parameters from measured data, (2) methods for producing hard-copy images of displays formed on the cathode ray tube, and (3) methods permitting the operation of the system in a remote terminal mode.

2. SCORE HARDWARE AND SOFTWARE REQUIREMENTS

This system is currently operable on the IBM 360 series computer. The minimum acceptable computing configuration necessitates a machine equivalent to a Model 50 computer. Peripheral hardware requirements include two 9-track tape drives and one storage disk (storage capacity of a 2314 type disk is recommended). The graphics display device is an IBM 2250, Model I, II, or III, having the following characteristics: a 4K or 8K buffer (recommend 8K), vector generator, character generator, function keyboard, alpha-numeric keyboard, and a light-sensitive pen.

The system currently requires use of the OS-360 operating system, Release 16 or greater, and can operate in a stand-alone mode. However, such operation requires access to the entire central processing unit, and

is uneconomical. Current CPU requirements for a typical evaluation using SCORE is about 6 min/h on the IBM 360/50, somewhat less on a faster computer. It is recommended that SCORE be run in a multiprocessing or partitioned environment (i. e., the program be run concurrently with other computer jobs). In this mode, the program requires only 125K bytes of central core.

More than 90% of the program is written in Fortran IV, with all graphic displays generated by FORTRAN subroutines or FORTRAN callable subroutines. FORTRAN callable machine language subroutines provide the basic data links between the computer and graphic display.

3. EXPERIMENTAL DATA MANIPULATION

The console (Figure 1) used by the evaluator to execute SCORE consists of a cathode ray tube (CRT) on which graphical displays appear, and an alpha-numeric keyboard, a function keyboard, and a light-sensitive pen, all used to communicate with the cathode ray tube and the computer. The initial display (Figure 2) permits the evaluator to enter the case identification information via the alpha-numeric keyboard.

When the identification information has been supplied, a new display (Figure 3) is generated. This display lists all the nuclides having experimental data that are available to the system, 15 nuclides at a time. If there are experimental data files for more than 15 nuclides, the list may

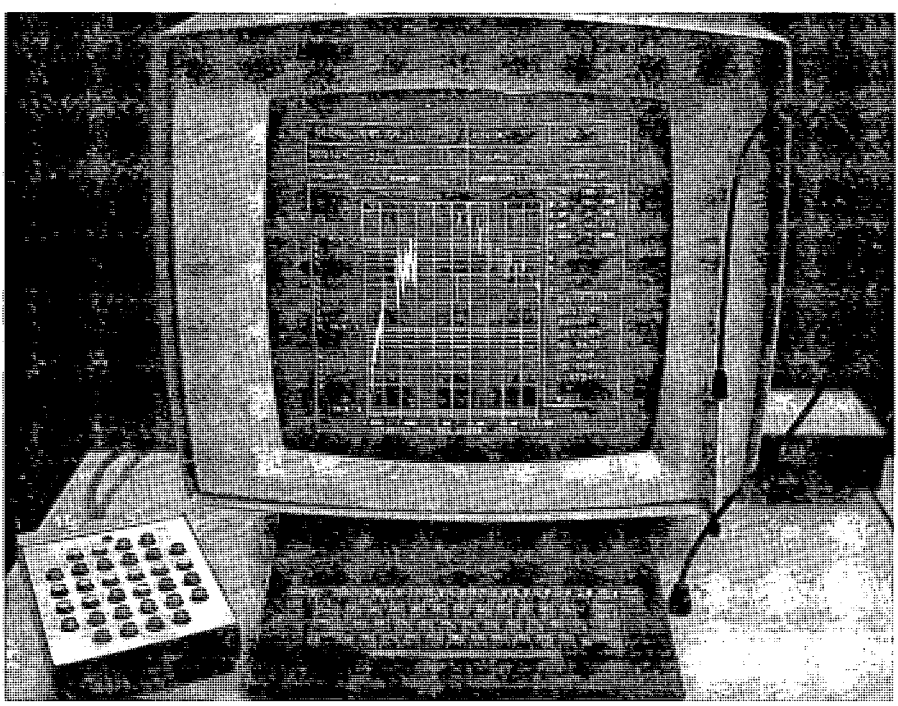

FIG. 1. An IBM 2250 graphic display terminal

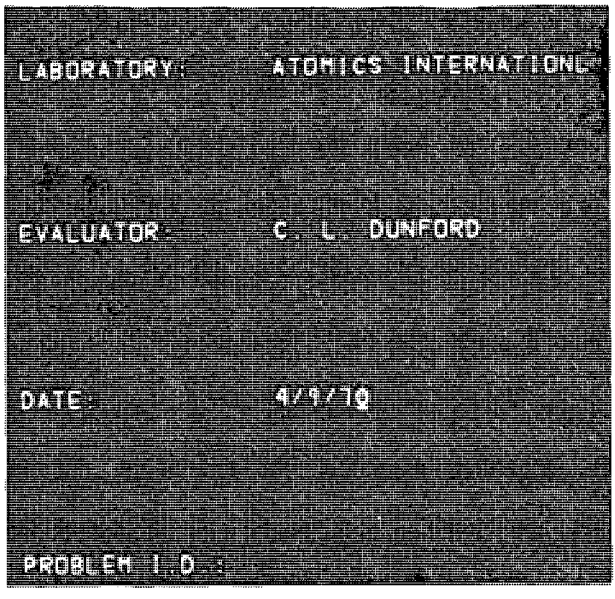

FIG. 2. Initial display for insertion of case-identifying information.

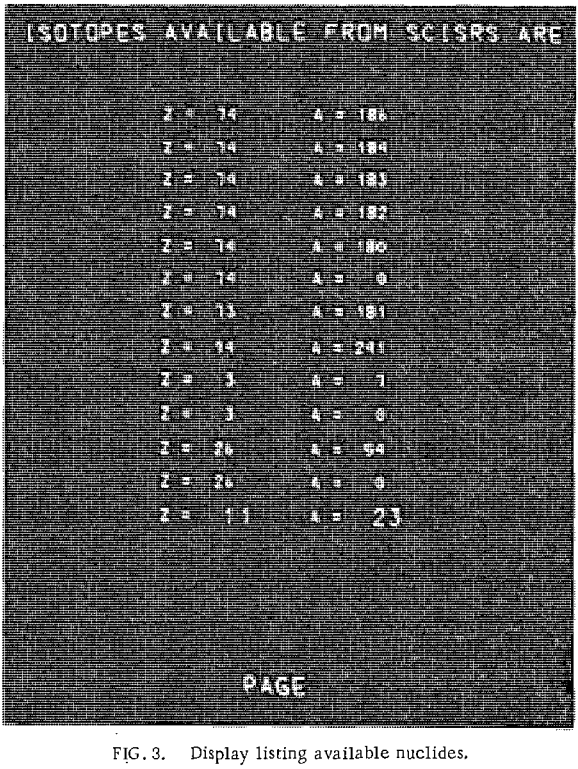

FIG. 3. Display listing available nuclides.

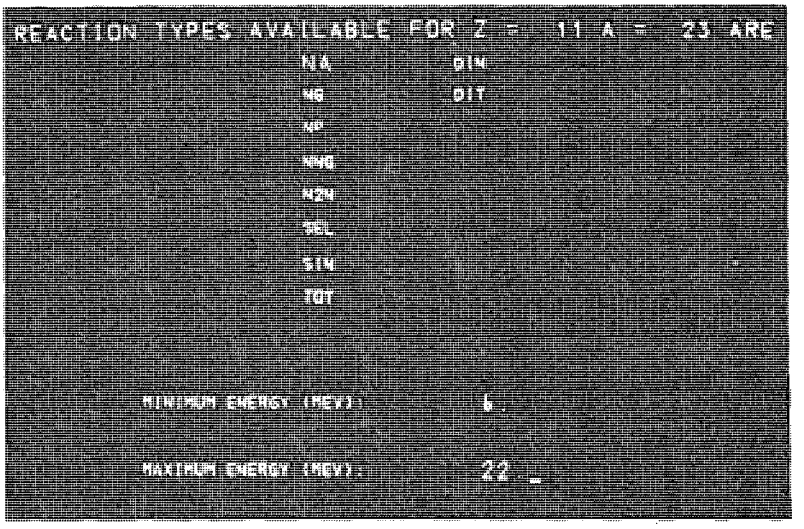

FIG. 4. Display of selected reaction-type and energy-range data.

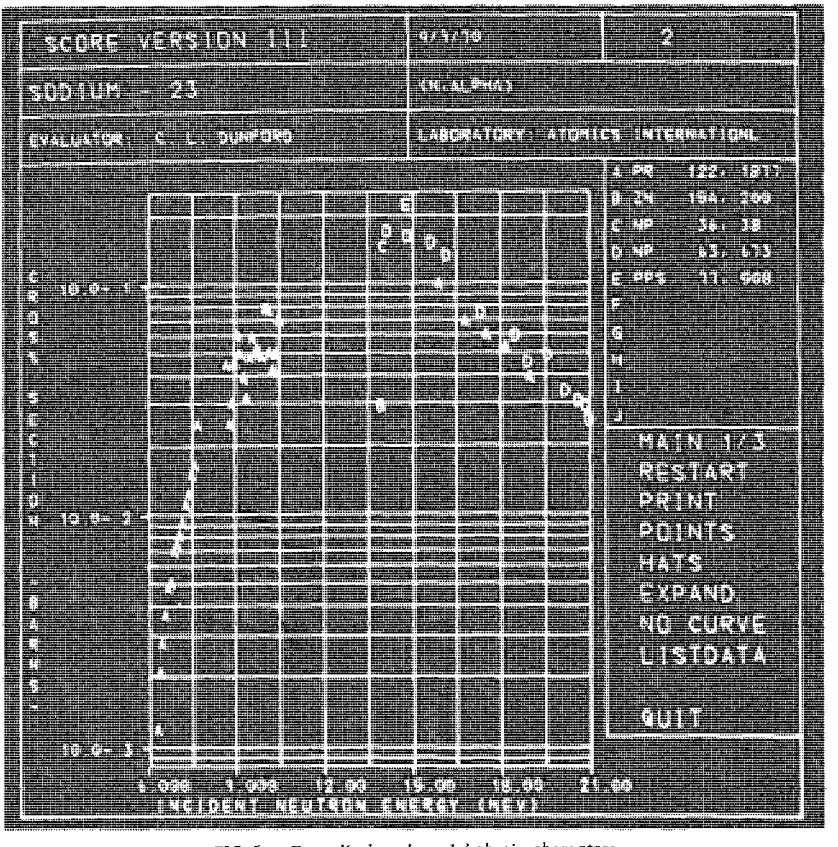

FIG. 5. Data displayed as alphabetic characters.

be paged by selecting the word PAGE with the light pen. A selected nuclide is indicated by having large characters identifying its charge and mass number.

The next display (Figure 4) presents a list of all the reaction types presently recognized by SCORE, for which data exist for the selected nuclide. The desired reaction type is then selected by the light pen, and the energy range desired is entered through the alpha-numeric keyboard. A short line, called a cursor, indicates the position at which a character entered in the keyboard will appear on the screen. This cursor may be moved to any position in the active area of the display by a key on the alpha-numeric keyboard. Thus, the evaluator is completely free to enter and correct any input data on the screen. When all specifications required for retrieval of the desired data are complete, the data are retrieved and displayed (Figure 5). Each data point is displayed, using an alphabetic character. References corresponding to these characters appear in the right center of the display. The lower right of the display contains a series of key words which indicate options that may be initiated

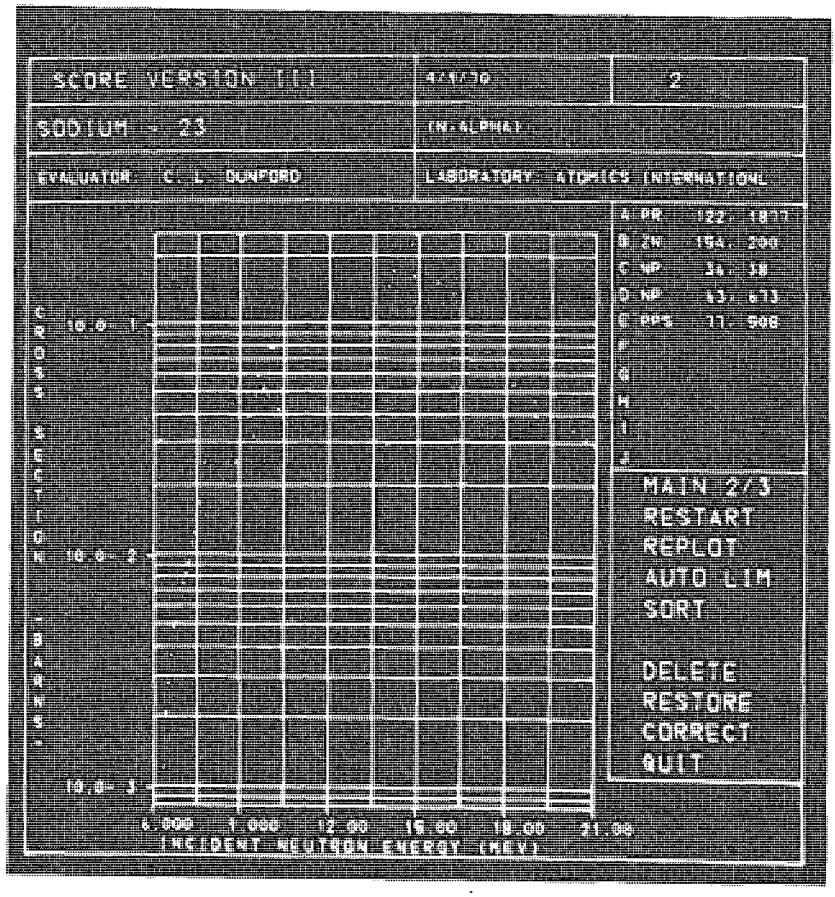

FIG. 6. Basic SCORE data display.

when that word is selected by the light pen. Several sets of options are currently available. The various options allow one to modify the grid parameters or the data units, sort the data by reference, display the data as points (Figure 6), add experimental errors to the data (Figure 7) and expand the graphical portion of the display to full screen size (Figure 8).

The basic display grid parameters are selected internally by SCORE. However, the user may wish to determine his own grid parameters, and has the option to modify any item in the display (Figure 9). The axes scaling mode, either logarithmic (LOG) or linear (LIN), may be selected by the light pen. The current selection at any time will be in large letters, and all other options in small letters. The axis units may also be modified by light pen selection. For energy-dependent cross-section data, the X or energy axis can be in MeV, keV, or eV, and the Y or cross section axis in barns (BARNS) or millibarns (MB). Angular data may be plotted in the laboratory (LAB) or center-of-mass (CM) frame of reference. The differential angular cross section can be plotted in barns per steradian (B/ST) or millibarns per steradian (MB/ST).

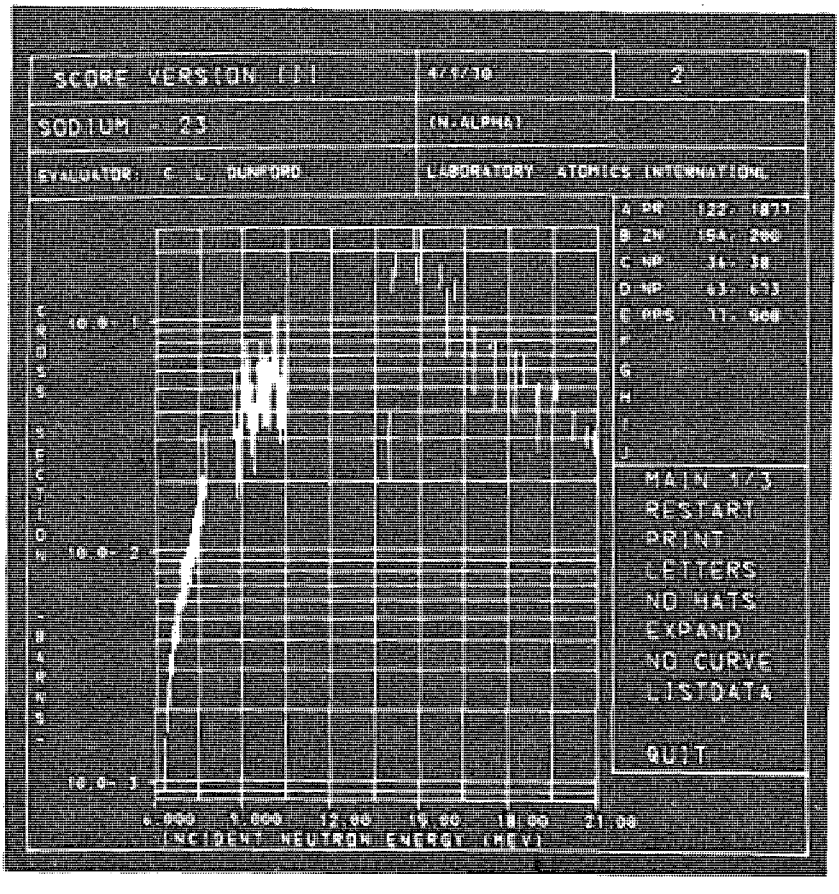

FIG. 7. Basic data display with error limits added.

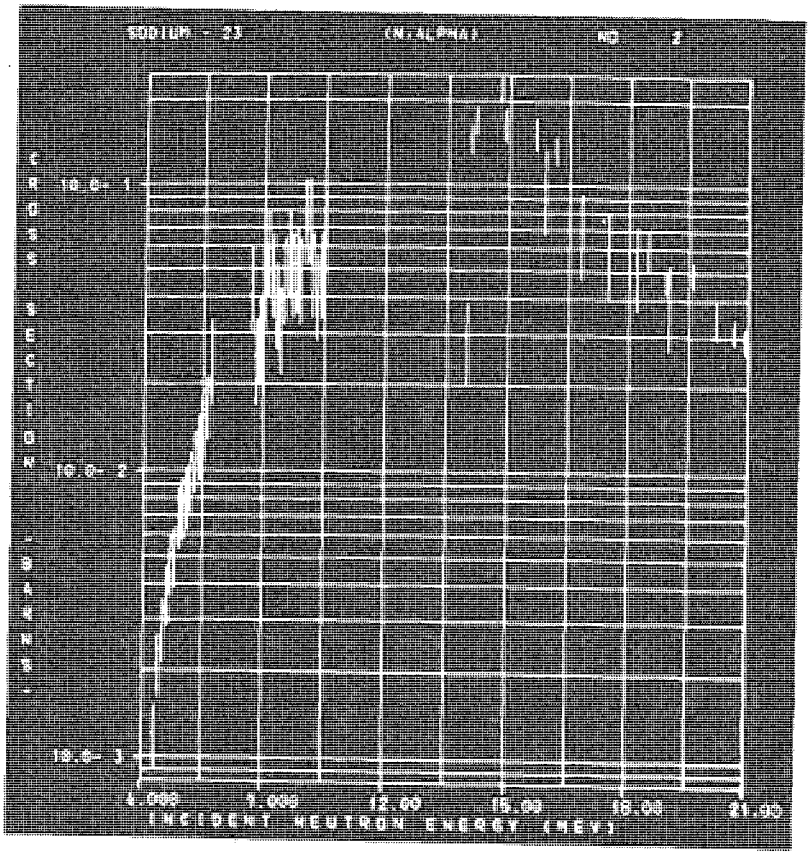

FIG. 8. Expanded data display.

Another useful option is the data correction option. If any of the data in a display are incorrect (for example, data from Reference D in Figure 10), action may be taken to correct this data. The data points are made sensitive to detection by the light pen. The evaluator detects each point he wishes to correct with the light pen; when this selection procedure is completed, the display (Figure 11) appears on the console screen. The data may be corrected by use of the cursor and alpha-numeric keyboard, as previously described for entering characters. Also, a selection of a number with the light pen causes the number to be transformed according to the linear transformation in the second line of Figure 11. When the correction procedure is completed, both the original and corrected data are shown. The result of this correction procedure is illustrated in Figure 5, in which the data from Reference D is shown as having been corrected.

It is possible to list the coordinates of all data points. The data are displayed (Figure 12) with a maximum of 20 data points at one time on the screen. The display lists the X and Y coordinates of each data point, as well as its reference and status. The status symbol meanings are: A,

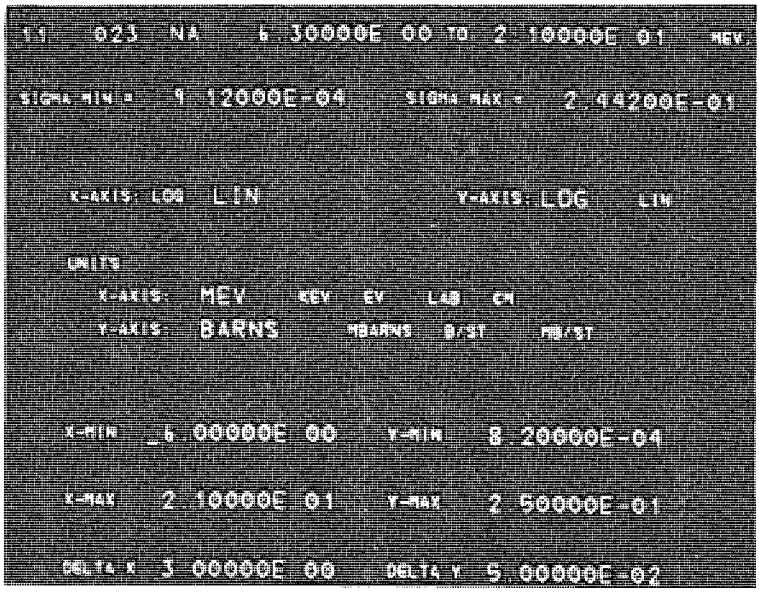

FIG. 9. Display for modifying display grid parameters.

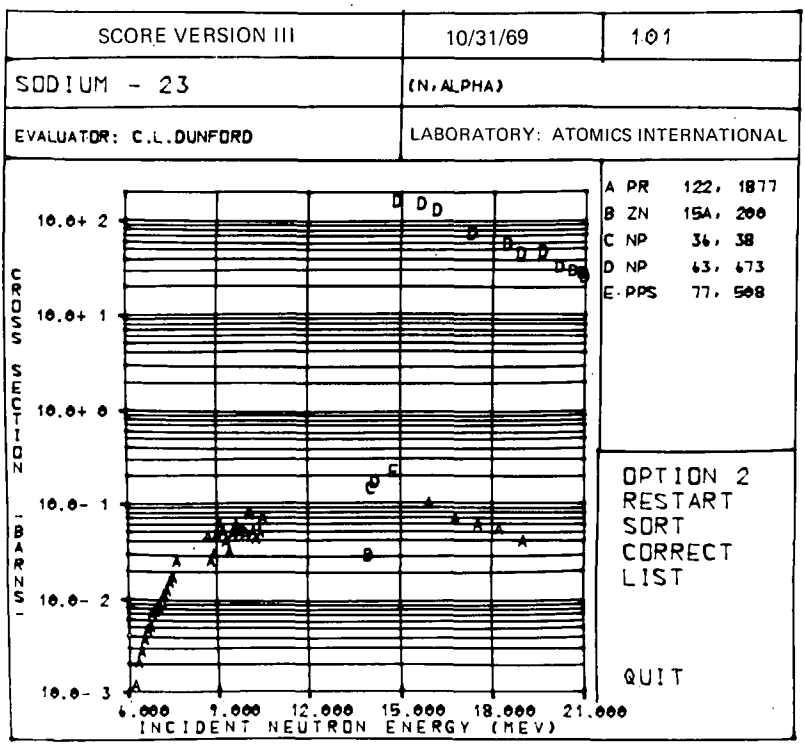

FIG. 10. Data display, alphabetic characters.

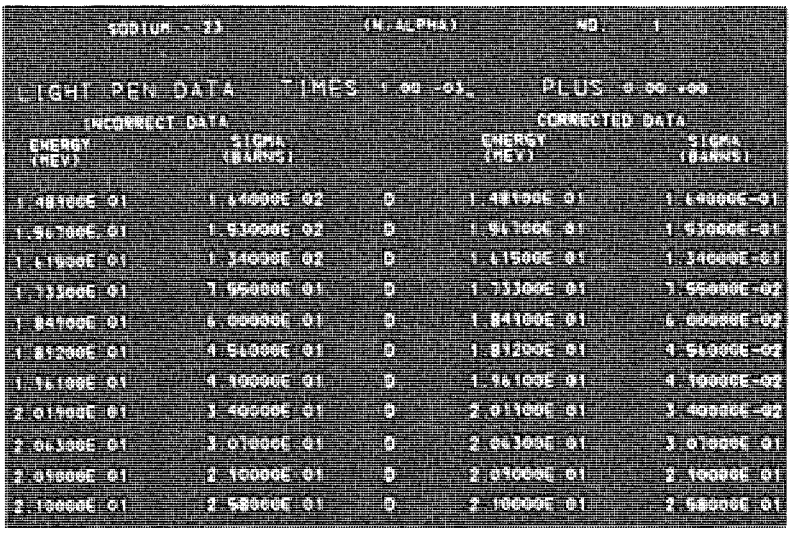

SODIUM - 23 (N,ALPHA) MD 1

LIGHT PEN DATA TIMES 1.00 -01 PLUS 0.00 +00

INCORRECT DATA ENERGY (MEV)	SIGMA (BARNS)		CORRECTED DATA ENERGY (MEV)	SIGMA (BARNS)
1.481900E 01	1.640000E 02	D	1.481900E 01	1.640000E-01
1.967300E 01	1.930000E 02	D	1.967300E 01	1.930000E-01
1.615000E 01	1.340000E 02	D	1.615000E 01	1.340000E-01
1.733000E 01	7.950000E 01	D	1.733000E 01	7.950000E-02
1.841900E 01	6.000000E 01	D	1.841900E 01	6.000000E-02
1.812000E 01	4.540000E 01	D	1.812000E 01	4.540000E-02
1.961000E 01	4.100000E 01	D	1.961000E 01	4.100000E-02
2.019000E 01	3.400000E 01	D	2.019000E 01	3.400000E-02
2.063000E 01	3.010000E 01	D	2.063000E 01	3.010000E 01
2.019000E 01	2.100000E 01	D	2.019000E 01	2.100000E 01
2.100000E 01	2.580000E 01	D	2.100000E 01	2.580000E 01

FIG. 11. Data correction display.

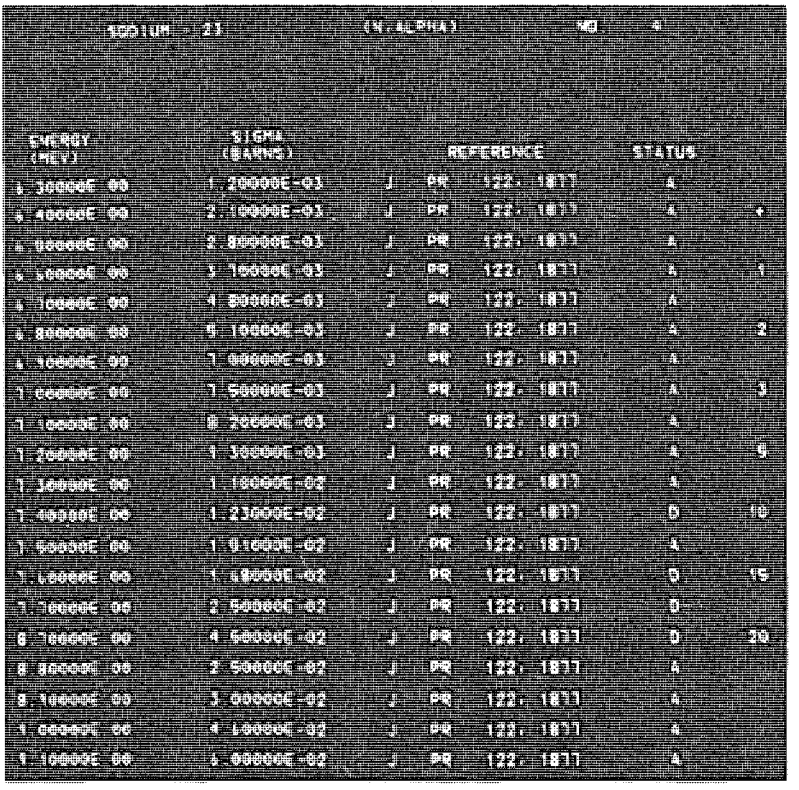

SODIUM - 23 (N,ALPHA) MD 4

ENERGY (MEV)	SIGMA (BARNS)	REFERENCE	STATUS	
6.300000E 00	1.200000E-03	J PR 122, 1877	A	
6.400000E 00	2.100000E-03	J PR 122, 1877	A	4
6.500000E 00	2.800000E-03	J PR 122, 1877	A	
6.600000E 00	3.700000E-03	J PR 122, 1877	A	1
6.700000E 00	4.800000E-03	J PR 122, 1877	A	
6.800000E 00	6.100000E-03	J PR 122, 1877	A	2
6.900000E 00	7.000000E-03	J PR 122, 1877	A	
7.000000E 00	7.500000E-03	J PR 122, 1877	A	3
7.100000E 00	8.700000E-03	J PR 122, 1877	A	
7.200000E 00	1.300000E-02	J PR 122, 1877	A	5
7.300000E 00	1.180000E-02	J PR 122, 1877	A	
7.400000E 00	1.230000E-02	J PR 122, 1877	D	10
7.500000E 00	1.010000E-02	J PR 122, 1877	A	
7.600000E 00	1.480000E-02	J PR 122, 1877	D	15
7.700000E 00	2.500000E-02	J PR 122, 1877	D	
8.700000E 00	4.600000E-02	J PR 122, 1877	D	20
8.800000E 00	2.500000E-02	J PR 122, 1877	A	
8.900000E 00	3.000000E-02	J PR 122, 1877	A	
9.000000E 00	4.600000E-02	J PR 122, 1877	A	
9.100000E 00	5.000000E-02	J PR 122, 1877	A	

FIG. 12. Data listing display.

active data point; D, data point has been deleted; and R, indicating that all data for that reference were deleted. The status of a point may be changed from A to D or D to A by selection of the symbol for that point with the light pen. The R status cannot be changed.

The display "page" can be changed, using the rightmost column. The column consists of either a plus (+) or a minus (-) and seven numbers. A plus indicates forward paging, and the minus indicates backward paging. The numbers indicate how many data points, forward or backward, should be paged.

A permanent record of a data display can be made, using the PRINT option. Only experimental data points being actively considered in the evaluation are listed, along with sufficient identifying information to provide a matchup with a hard-copy image of the data on the display screen. These two types of information can form part of the permanent record of an evaluation.

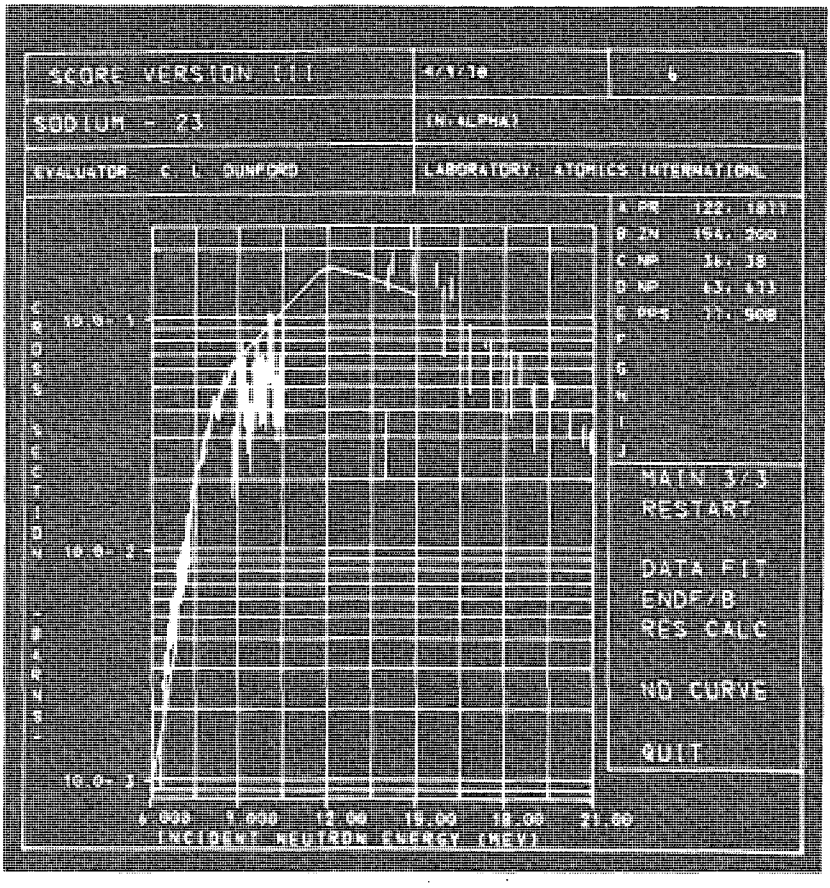

FIG. 13. Overlay of ENDF/B evaluated data.

4. EVALUATED DATA RETRIEVAL AND DISPLAY

Data from the ENDF/B evaluated neutron cross-section data files may be retrieved by SCORE, and displayed as an overlay curve on the basic experimental data display (Figure 13). The nuclide and reaction type for the retrieval are taken to be those of the experimental data currently being displayed. The energy range for energy-dependent cross sections is taken as the minimum and maximum values of the display grid. In the case of differential angular distributions, the evaluated data will be interpolated to the required incident energy. Thus, no input data are required. The overlay curve is generated by simply selecting the ENDF/B option with the light pen.

The storage and retrieval mechanism for evaluated data is similar to that for experimental data. The evaluated data resides on tapes, with one nuclide per file. A direct-access data file holding one nuclide is kept on disk. When a request is made, the direct-access data set is checked to see whether the selected nuclide is resident. If the answer is no, SCORE requests that the proper data tape be mounted, and then the requested nuclide is copied into the direct-access data set. Finally, the evaluated data is retrieved and displayed.

If data for the requested nuclide is not on the data tapes, or the reaction type or energy range has no data, then an appropriate error message is displayed, and the user may select his next step. At the present time, only data from ENDF/B Files III (smooth data), IV (angular data), and V (secondary distributions) may be retrieved and displayed. Resonance parameters from File II are stored in the direct-access data set, but are not currently used in SCORE.

5. CURVE FITTING

One end product of a data evaluation is the representation of a set of experimental data with a smooth, single-valued curve. An evaluated curve, in machine-retrievable form, consists of a series of points at which the function is specified, and an interpolation scheme for defining intermediate points. The points at which the function is specified are defined as nodes.

In order to produce a good evaluated curve, one must be able to add, move, or delete nodal points from the data fitting display. Coordinates for a nodal point could be entered from the alpha-numeric keyboard. However, without a fine mesh grid, entering nodes in this manner would involve considerable trial and error. A more efficient method is to select the desired nodal location on the cathode ray tube with the light pen. In general, this second approach is used.

The light pen can only be used to detect a bright spot on the cathode ray tube. But the desired nodal position may be in a dark location tube. Therefore, a tracking pattern was developed to allow a node to be entered at any point within the display grid. This tracking pattern (Figure 14) consists of a central point, and three concentric circles made up of points. The pattern moves from its initial location to the position of the first light detected by the light pen. Subsequent movement of the pattern is governed by the light pen also. The pattern moves toward the next point of light detected at a rate proportional to the distance between the center of the tracking pattern and the point detected. The next signal from the light

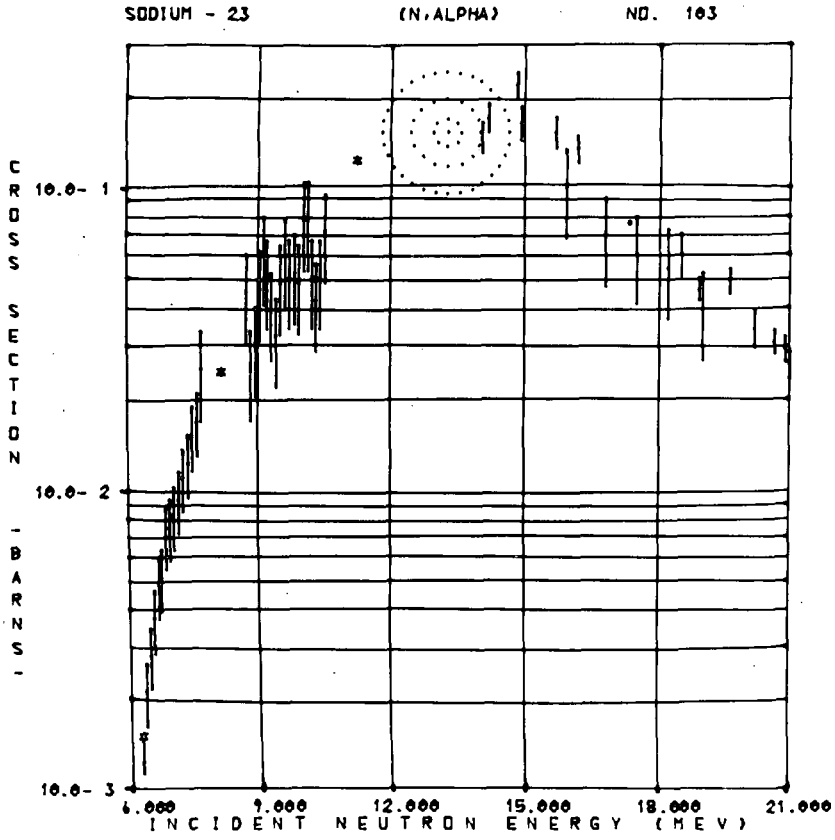

FIG. 14. Nodes (*) entered by tracking pattern.

pen causes the pattern to stop moving. Another detection of light starts the pattern moving, and another stops the motion. The tracking pattern is constructed to reflect off the sides of the display grid, and the detection of a grid line or any point outside the grid is ignored.

The small concentric circles around the central point of the tracking pattern allow the user to control accurate positioning of the tracking pattern. When the pattern center is located at the desired position, the coordinates of that location can be stored by depressing the END key.

The ADD NODE option permits the evaluator to enter new nodes in the display. The expanded data display, with a tracking pattern, appears when the light pen is used to select ADD NODE. The tracking pattern may be moved to any location within the display grid, in the manner described previously. Each time the END key is depressed, the center point of the tracking pattern becomes a node. An asterisk is then displayed at the node location. A maximum of 30 nodes can be used in an evaluation. When the evaluator feels that the nodes adequately describe the experimental data, he depresses the CANCEL key to terminate the option.

When the nodes have been supplied to the evaluator's satisfaction, an evaluated curve can be generated by selecting either the LINEAR or SPLINE options. The interpolation procedures are defined to be in the same space as the one in which the data is being displayed. That is, if the data are plotted logarithmically in Y and linearly in X, then the interpolation scheme would be defined for X versus log Y.

The LINEAR option assumes that a straight line is used to represent the function between nodes. This is the only interpolation procedure currently permitted in the ENDF/B data format. The evaluated curve appears on the data display for easy visual comparison. In the right center box, a root mean square residual (χ) is displayed when points represent the experimental data, in order to give a numerical test of the fit.

The residual is defined as follows:

$$\chi = \sqrt{\frac{1}{N}\sum_{i=1}^{N} \frac{(\sigma_{\text{calculated}} - \sigma_{\text{experimental}})_i^2}{(\Delta\sigma_{\text{experimental}})_i^2}}$$

where N is the number of experimental data points, and $\Delta\sigma$ is the reported uncertainty in the experimental data points.

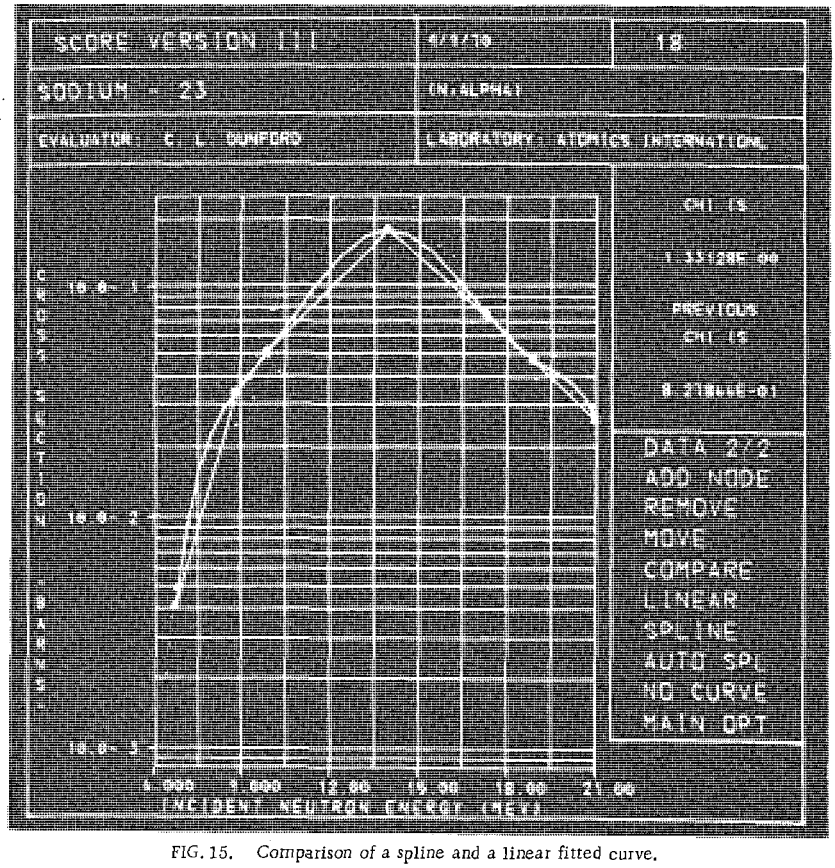

FIG. 15. Comparison of a spline and a linear fitted curve.

The SPLINE option assumes that the interpolation is given by a cubic spline curve. This interpolation procedure states that a cubic polynomial will be used to represent the curve between any pair of nodes. Furthermore, the cubic functions must be continuous at the nodes, as well as their first and second derivatives. At the two extreme nodes, the boundary conditions are that the second derivatives are zero. These conditions are sufficient to define the entire set of cubic polynomials describing the evaluated curve. A set of three values stored for each node, X, Y, and the second derivative are sufficient to define the curve for rapid digital calculations. A least square technique for cubic spline curves has been developed. [5] A subroutine to perform this calculation has been obtained from Aldermaston, and included in SCORE.

In general, the evaluator may wish to improve the fit to the data of an evaluated curve. He may do this by changing the interpolation mode, moving nodes, or both. Therefore, SCORE saves the last evaluated curve when a new one is generated. This curve can be recalled and displayed, along with the current evaluated curve, by selecting the COMPARE option. Both curves are displayed (Figure 15) for a visual test of the improved fit. The χ value for each curve is displayed in the right center box, for a numerical comparison of the fit of the two evaluated curves.

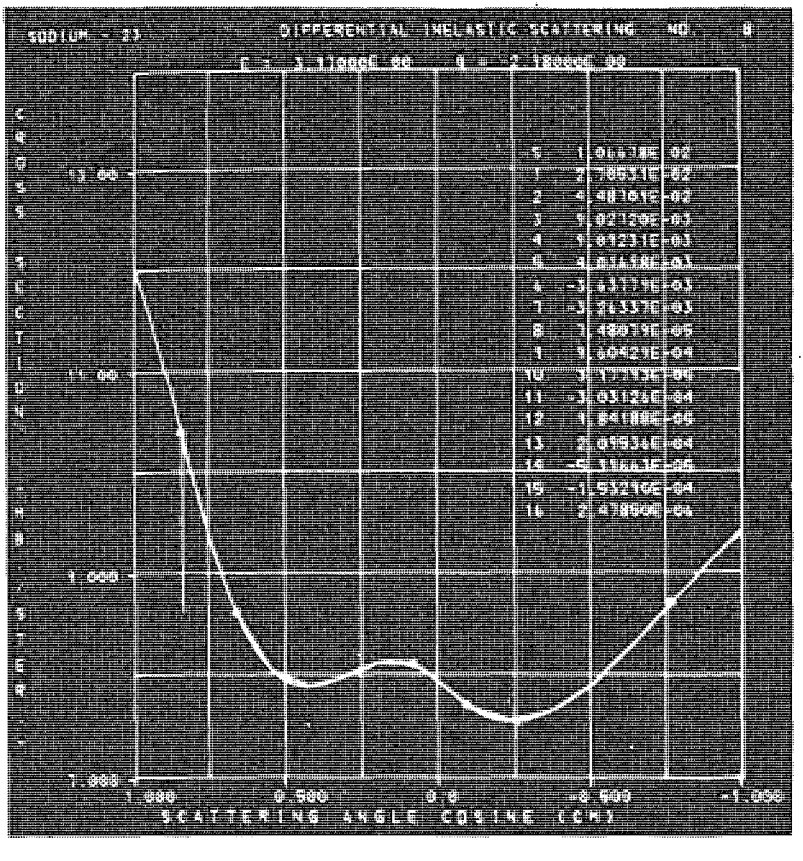

FIG. 16. A Legendre fit to an angular distribution.

6. LEGENDRE SERIES EXPANSION OF ANGULAR DATA

One method for analyzing differential angular distributions is by means of a Legendre series expansion in the cosine of the scattering angle. This series also provides a convenient storage format, one of several permitted in the ENDF/B system. Generation of Legendre Series representations for differential angular distributions is a logical extension of the data fitting methods already available.

The first step in producing a Legendre series representation of angular data is to generate a smooth evaluated curve for the experimental angular distribution data. Either linear or spline curve representations may be used. The evaluator then selects the LEG COEF option. A display appears, in which the evaluator is asked to specify the order of the fit desired. This must be 25 or less.

Legendre coefficients are generated, using the methods described in CHAD. [6] The evaluated curve is interpolated to a fine angular mesh, and Legendre coefficients extracted. A display (Figure 16) appears on the cathode ray tube when the calculation is complete. A list of the integral cross section (S) and the Legendre coefficients (1-25) appear on the right of the display. A reconstruction of the angular distribution function from the Legendre coefficients is displayed, along with the original evaluated curve, so that the evaluator may judge whether or not the order of the Legendre series was adequate to describe the curve.

7. RESONANCE REGION ANALYSIS

One of the more difficult and time-consuming problems of data evaluation is the analysis of resonance energy region data. Experimental data in this energy region consists of the desired cross section enfolded with a Doppler and a resolution function. The task of an evaluator is to unfold these effects from experimental data containing experimental uncertainties.

Nuclear reaction theory is used to aid in this analysis. Theory implies that a set of parameters can be used to describe the energy-dependent cross sections. The set of resonance region parameters provides a convenient compact storage format and a convenient starting point for the extraction of resolution and Doppler effects from experimental data.

Three models are currently available for evaluating resonance region data. These are the Breit-Wigner single-level, [7] the Reich-Moore multilevel, [8] and the Adler-Adler multilevel [9] formalisms. Any time a new resonance theory is selected, the entire case must be respecified (i.e., Doppler function, resolution function, and isotopic contents for the experimental target must be respecified). The desired model is selected by the light pen (Figure 17). A data library in the direct-access format is provided in SCORE for storage of resonance parameters for each of the three models. In addition, space is provided for several Doppler and resolution functions. The evaluator may select the model, Doppler, or resolution function to be used in a given data evaluation.

Two additional displays allow the evaluator to select his Doppler and resolution functions, respectively, and supply the necessary function parameters. Available Doppler and resolution functions are obtained from a list of the contents of the library for each of the resonance theory models. When a choice is made with the light pen, the selected function

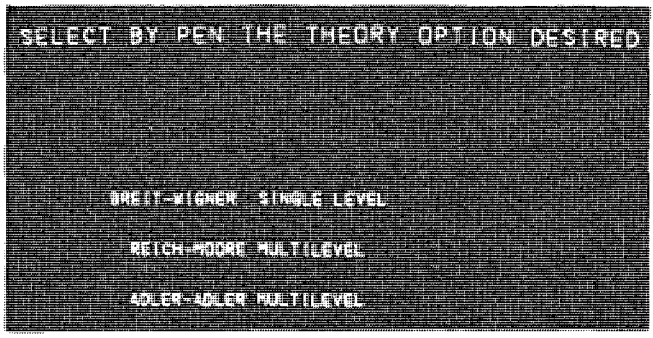

FIG. 17. Display for selection of resonance region model.

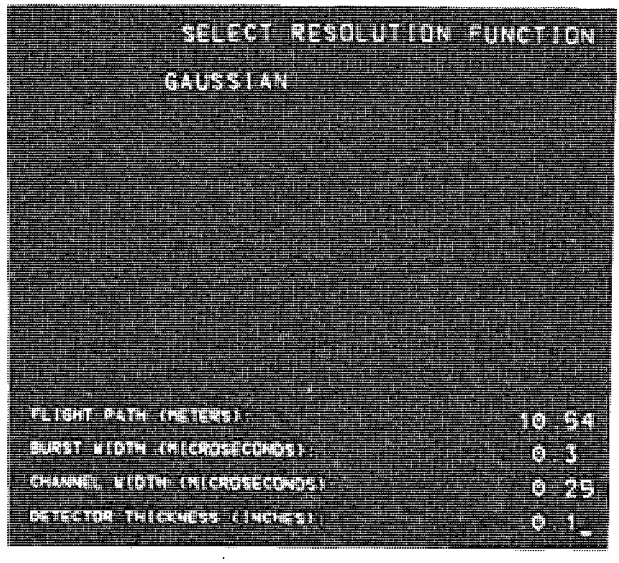

FIG. 18. Selection of resolution function and required parameters.

appears in large characters, and a list of required parameters for that particular function appears in the lower half of the display (Figure 18). The parameters may be supplied in the usual manner from the alpha-numeric keyboard.

A semiautomated fitting procedure for single-level and Reich-Moore multilevel resonance parameters is currently operational in SCORE. The methods[10] were developed by O. D. Simpson and co-workers at Idaho Nuclear Corporation. The method consists of supplying a peak point and two side points for each resonance whose parameters are to be modified to improve the fit. In addition, valley points, in between resonances, may be supplied to improve the fit to experimental data in that region. An iterative algorithm to improve the resonance parameters is executed three times, each time the FIT option is selected. A new line shape is generated, and may be compared with the previous step in the evaluation, using the COMPARE option.

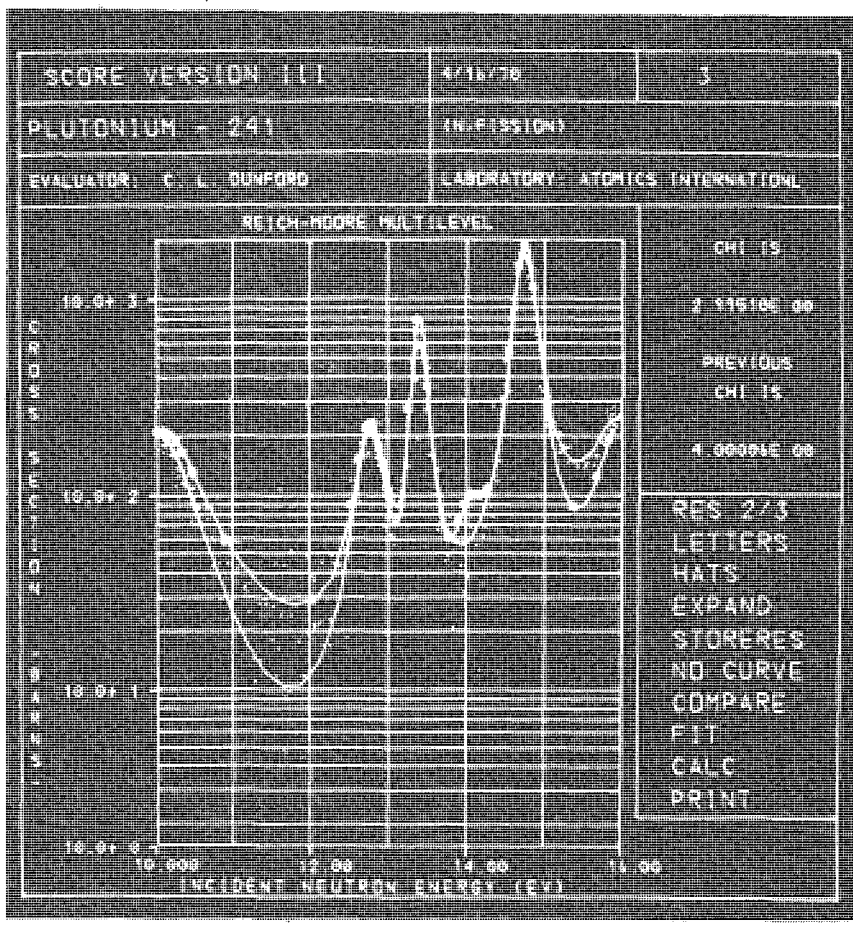

FIG. 19. Single-level and Reich-Moore calculated curves.

A Doppler and resolution broadened line shape is calculated for the selected resonance region model when the CALC option is selected by the light pen or from the function keyboard. The calculation uses the Doppler model, resolution model, and the target compositions previously requested to calculate the line shape for the reaction type and grid limits of the data being displayed. The calculated curve is overlaid on the experimental data, and the root mean square residual is displayed in the right center box (Figure 19).

If there has been a previous generation of the line shape as, for example, with a different set of resonance parameters, that line shape is stored. By using the COMPARE option as previously described, the result of the previous evaluation step can be compared with the present step.

A comparison of single-level and multilevel fits to experimental data is illustrated in Figure 19. Superposed on the measured plutonium-241 fission cross section (dots) is the curve due to a single-level analysis (curve through asterisks) and the curve obtained from a multilevel fit.

Thus, an evaluator now has the capability for improving sets of resonance parameters, by interacting with his data through the computer and the console. It is readily apparent that a task, which previously required several months to complete, can now be performed in days, and perhaps even in hours. Application of the PRINT option in SCORE allows a permanent record of the resonance evaluation steps to be made on the print file. This record consists of a list of all options and parameters used, along with a listing of the calculated line shape, the experimental data points, their weights, and residuals.

8. THE VALUE OF THE INTERACTIVE GRAPHICS MODE OF OPERATION

Advantages of an on-line or interactive computing system with the additional capability of graphical display, such as that provided by a cathode ray tube display unit with light pen and keyboard control, include:

8.1 Speed

One of the most obvious advantages of interaction, to the data evaluator who has used a batch processing environment, with its often long turnaround times, is simply that he can obtain results quickly. In fact, a system with instant (a few seconds to a few minutes) turnaround is essentially an interactive system. A well-designed interactive system can make a user aware of mistakes (while keying in numbers or instructions) before it is too late, whereas a mispunched control card in a batch processing environment costs one turnaround time. In an interactive environment, the only information needed is how to log-on (and off), and how to call the particular program. The program can then inform the user what parameters and data should be entered, when, and in what format. This type of interactive program is well suited to the evaluator who wants quick solutions to well defined and well conditioned problems.

8.2 Immediate graphical display

"One picture is worth a thousand words." The graphical display used in this work involved an IBM 2250 display unit with eight thousand bytes of memory assigned as a buffer area. With four bytes comprising one word, we have that one picture is worth 2000 words – a 100% increase, due to modern technology. In data-fitting problems, there are often characteristic maxima that are expected to appear in the fitting function. A graph of the computed fit can reveal the presence or absence of the desired character. In general, a graphical representation of a function is more revealing of its properties than a tabular representation of the same function.

The IBM 2250 is the basis for the interactive graphics discussed in this paper; however, there are other hardware units that can be used for interaction. The basic concepts do not change with the hardware, only the details of implementation. For example, a teletype could be used as an interactive-graphical terminal with a slow rate of textual output, and typewriter plots used for graphical output.

8.3 Simple control of calculations

An interactive system, using a display terminal with a light pen or similar device, can be programmed to require extremely simple actions by a user. The degree of simplicity depends on the design goals of the

system. A system designed to accept FORTRAN-like input statements requires more typing by a user than a system designed to accept only light pen, or special key interrupts and numbers entered through a keyboard. In the latter, all choices, such as which function, which numerical method, what mode of display, and what step to execute next are made by light pen selection of an option displayed on the CRT. In addition to light pen actions, other required user actions are the keyboard entry of numbers for specifying degree of fit, and, in some cases, initial values for parameters.

8.4 Various attacks on a problem

An interactive system with a variety of available options allows a user to try various methods to solve a particular problem during a single session with the computer. A data-fitting program exemplifies this aspect of on-line interactive use of a computer.

If one is given a set of raw data, for which an approximating function is desired for use in a later calculation, and there is no requirement as to what kind of function should be chosen to represent the data, an interactive data-fitting program with several built-in options for the approximating function could be very effectively employed to obtain the desired result. One would simply approximate the data with various functions of various degree and then make a final choice. The choice would probably depend on two things: (1) knowledge of the functions and their efficiency of calculation in later work, and (2) information generated by the program for each case (function and degree), such as maximum residual, sum of squares of residuals, and average error.

TABLE I. A COMPARISON OF PROBLEM SOLUTION STEPS

In a Batch Processing Environment	In an On-Line (Interactive) Environment
1. Look in program library to find appropriate program	1. Look in program library to find appropriate program
2. Obtain deck for program [or card(s) which invoke the program from an on-line storage device, e.g., disk]	2. Log on computer
3. Prepare data cards according to program writeup (prone to keypunching errors)	3. Type in instructions to execute desired program
4. Prepare system control cards (prone to keypunching errors)	4. Type in data as instructed by computer (computer will detect errors to some extent)
5. Submit job to dispatch	Not necessary
6. WAIT	Not necessary
7. Retrieve deck and listing of output.	5. Log off computer and take listing of results.

Other problem areas are also well suited to take advantage of this aspect of an on-line system. Any problem for which there are several known methods of solution could be attacked by using a computer program which allows a choice of method. The problem can then be solved in a variety of ways, and the results compared.

Table I is illustrative of how time may be allocated during a problem solution; it points out several interesting comparisons between batch processing and on-line interactive computing. Three steps in the batch environment do not exist in the interactive environment. In the interactive case, all steps can be carried out while sitting at the terminal, probably within 5 min. This allows continuation of work on a problem which required an intermediate computer solution without the loss of a train of thought. Using conventional batch methods requires going from place to place to assemble the deck for submission to the computer, and waiting an hour or so (depending on turnaround parameters) for results. This can be quite discouraging to progress on an evaluation problem which requires computer interaction at intermediate stages. The value of an interactive system lies in its capability to solve significant problems in a reasonable time. SCORE represents a "means" applied to this "end."

9. FURTHER APPLICATIONS OF SCORE

To the evaluator, an interactive graphics computing system, such as SCORE, can represent a useful tool for the solution to problems of data evaluation and dissemination. In the most simple form, SCORE could be used as an editor for the SCISRS experimental data tapes. The information stored on these tapes could be visually checked for errors by simply displaying the data. Incorrect data could be selected from the display by the light pen. These entries could be displayed on the cathode ray tube in card image form, and edited to correct any errors by entering characters through the alpha-numeric keyboard. Corrected data would then be merged into the SCISRS library.

Data displays from the SCISRS library could be generated when new experimental information becomes available. "Eye guide" curves can be rapidly fit to the data with the spline techniques currently in SCORE, or with advanced techniques planned for the future. The final displays would be transferred to 35-mm film, via a projected "hard copy" feature. Loose-leaf update pages to data evaluations, such as BNL-325 and BNL-400, could be issued with considerable savings in costs and time.

10. SUMMARY

The basic concept which makes a man-computer interactive cross-section evaluation system feasible is the availability of a rapid and convenient conversational mode between the evaluator and the computer. In the past, this conversational capability has been absent, but recent developments in auxiliary computer hardware (namely, the cathode ray tube console) now provide a conversational mechanism. By making optimum use of the cathode ray tube and computer graphics, as both a visual and digital interface between the various components of an evaluation scheme, the evaluator has a flexible and convenient tool for control of the logical flow of computer operations.

With the needed information available in digital form on tapes, disks, and/or bulk memory, the evaluator is ready to proceed with the evaluation, or to prepare or update a library. The evaluator would operate a

display console, directly linked to a high-speed digital computer. A cathode ray tube display device, with light pen, a keyboard, a set of function keys, and microfilm display screen, would be on the console. Stored on disks would be computer routines to perform calculations and other data evaluation functions, which would be activated by the function keys, keyboard, or light pen. The economy of this mode of operation is based on its time-sharing capability and its convenient output form (namely, graphic displays). The data evaluator, using the input device on a display console, can direct the processing and evaluating of experimental data by monitoring intermediate results. Errors may be corrected easily, before a large amount of computer time is consumed. In addition, the evaluator may inject his analysis of partial results (which otherwise might be very difficult or expensive to approximate, by the computer program) during execution of the program. This interaction can save computer time and turnaround time, and provides insight into the problem being solved.

Combinations of operations could be performed by the evaluator at such a console, depending on the nature of the evaluation. For example, consider that new measured values of the U^{238} fast capture cross section have been received in an update of the SCISRS tape. The evaluator could then request a display of the new data against any combination of older measurements and previous evaluations. Related documentation may be retrieved and analyzed. Numerical curve-fitting routines and/or nuclear theory could be used to generate an evaluated set of capture cross sections. The effects of various pieces of data on the final curve could be immediately visualized through the cathode ray tube display. When a newly evaluated cross-section curve is determined, programs in the computer would format the information, perform any renormalizations required to other data in the library, and store the new capture cross sections as required. When a new set of evaluated data is produced, there would be recalculations of a series of standard or benchmark problems. The results of these recalculations would tell both the evaluators and the designers how the new information would affect current reactor safety, design, and economic concepts.

REFERENCES

[1] SCHMIDT, J. J., Organizational and Technical Aspects in the Field of Neutron Nuclear Data Evaluation, KFK 791 (1968).
[2] DUNFORD, C. L., SCORE, An Interactive Nuclear Data Evaluation System, USAEC Rep. AI-AEC-12958 (1970).
[3] HONECK, H. C., "Specifications for an Evaluated Nuclear Data File for Reactor Applications," USAEC Rep. BNL 50066 (T-467) (July 1967).
[4] FRIEDMAN, J. M., PLATT, M., "SCISRS, Sigma Center Information, Storage and Retrieval System," USAEC Rep. BNL 883 (T-357) (July 1964).
[5] HORSLEY, A., et al., "Curve Fitting and Statistical Techniques for use in the mechanized evaluation of neutron cross sections," Nucl. Instr. Methods 62 (1968) 29.
[6] BERLAND, R. F., "Code to Handle Angular Data," USAEC Rep. NAA-SR-11231 (1965).
[7] WIGNER, E. P., Phys. Rev. 70 (1946) 606.
[8] REICH, C. W., MOORE, M. S., "Multilevel formula for the fission process," Phys. Rev. 111 (1958) 929.

[9] ADLER, D. B., ADLER, F. T., "Analysis of Neutron Resonances in Fissile Elements," USAEC Rep. COO 1546-3 (1966).
[10] SIMPSON, O. D., et al., "Automatic Analysis of Neutron Cross Section Data Using Interactive Graphics as an Aid," USAEC Rep. CONF-690301 (1969).

DISCUSSION

J. J. SCHMIDT: To what extent has SCORE been used in the evaluation of ENDF/B data, stage 2?

H. ALTER: SCORE has been used as an aid in the evaluation of the new tantalum files for the ENDF/B. In particular, it was applied to the tantalum capture data of Columbia, from which we received over 8000 data points describing the resonance region cross-section.

J. J. SCHMIDT: Second, I wonder whether you could comment on the status of mathematical efforts to develop automatic search procedures for optimum selection of node points for spline fits.

H. ALTER: We have had little success to date with available automatic search procedures for obtaining spline fits. SCORE does incorporate automatic search procedures for resonance parameter fitting but our experience in this area is insufficient to make definitive statements as to its capability. Eventually, one would want to be able to work with automated search procedures using cubic splines.

J. R. ASKEW: I am interested in the possiblity of applying interactive graphics to other problems of reactor physics and should like to know whether, in your experience, a light pen is essential to such studies or whether it could be considered an optional extra to input through a keyboard.

H. ALTER: Concerning the application of interactive graphics to other areas in reactor physics, I might mention that we are planning to incorporate a nuclear model module in SCORE in the near future and we eventually hope to incorporate a series of benchmark critical assemblies, against which we can evaluate new and old differential data.

As regards your specific question it is really a question of trading off the greater flexibility available with a light pen against the cost of maintaining light pen software. If such software is available or the cost can be disregarded, I highly recommend the light pen as an extremely useful addition to the function and alpha-numeric keyboards.

A. SCHETT: Do you inform the neutron data compilation centre of errors which you find in the SCISRS 1 file when doing evaluations?

H. ALTER: Yes, errors found in SCISRS 1 compilations are communicated to the NNCSC at Brookhaven. This procedure is also followed for errors found in evaluated data.

A. SCHETT: What, generally speaking, has been your experience in using the SCISRS 1 file for making evaluations by means of SCORE?

H. ALTER: At the present stage, we do not find the SCISRS 1 file to be fully adequate as a source of material for preparing data evaluations. It is believed that the SCISRS 2 file is more up to date. However, SCISRS 2 and SCORE are not as yet interfaced. They are expected to be made so during the next 12 months.

СЕЧЕНИЯ РАДИАЦИОННОГО ЗАХВАТА НЕЙТРОНОВ ЯДРАМИ УРАНА-238

Л. П. АБАГЯН, А. И. АБРАМОВ, М. Н. НИКОЛАЕВ,
Ю. Я. СТАВИССКИЙ, В. А. ТОЛСТИКОВ
Физико-энергетический институт, Обнинск,
Союз Советских Социалистических Республик

Abstract — Аннотация

CROSS-SECTIONS FOR RADIATIVE NEUTRON CAPTURE BY URANIUM-238 NUCLEI.

With a view to establishing reasonable energy resolution and measurement accuracy requirements in respect of cross-sections for the radiative capture of neutrons by uranium-238 nuclei, an analysis was made of the requests contained in RENDA and elswhere for these cross-sections in the energy range 1 eV – 15 MeV. The published results of experimental work are considered and their reliability and possible reasons for discrepancies analysed, particular attention being paid to the choice of reference cross-sections and to the calculation of the self-shielding effect. It is noted that the spread of $\sigma_\gamma(^{238}U)$ values remaining after all renormalizations far exceeds the uncertainty required by the users. The authors discuss methods of calculating cross-sections for capture in uranium-238 and present results. On the basis of selected experiments and calculations an evaluation is made of cross-sections for neutron capture by uranium-238 nuclei, the results being presented in the form of a smooth curve $\sigma_\gamma = \sigma_\gamma(E)$, recommended for use in various calculations. This curve is compared with similar curves obtained by other authors. The authors describe methods of obtaining group cross-sections and present new values of group cross-sections for neutron capture in uranium-238. These are compared with the cross-sections from the 26-group system of constants which used to be employed.

СЕЧЕНИЯ РАДИАЦИОННОГО ЗАХВАТА НЕЙТРОНОВ ЯДРАМИ УРАНА-238.

С целью определения разумных требований к энергетическому разрешению и к точности измерений сечений радиационного захвата нейтронов ядрами урана-238, проводится анализ запросов на эти сечения в интервале энергий от 1 эв до 15 Мэв, собранных в РЕНДА и в некоторых других источниках. Рассматриваются результаты опубликованных экспериментальных работ, анализируется их достоверность и возможные причины имеющихся разногласий, причем особое внимание уделяется выбору опорных сечений и учету эффекта самоблокировки. Отмечается, что остающийся после всех перенормировок разброс значений $\sigma_\gamma(^{238}U)$ намного превышает неопределенность, требуемую расчетчиками. Обсуждаются методы теоретического расчета сечений захвата для урана-238 и приводятся их результаты. На базе отобранных экспериментальных работ и теоретических расчетов производится оценка сечений захвата нейтронов ядрами урана-238, результаты которой представляются в виде плавной кривой $\sigma_\gamma = \sigma_\gamma(E)$, рекомендуемой для использования при различных расчетах. Проводится сравнение этой кривой с аналогичными кривыми из других работ. Описываются методы получения групповых сечений и приводятся новые значения групповых сечений захвата нейтронов для урана-238, которые сравниваются с использовавшимися ранее сечениями из 26-групповой системы констант.

ТОЧНОСТЬ ЗНАЧЕНИЙ $\sigma_\gamma(^{238}U)$, НЕОБХОДИМАЯ ДЛЯ РАСЧЕТА РЕАКТОРОВ

Наряду с сечениями деления, параметрами α и $\bar{\nu}$ для урана-235 и плутония-239, сечение радиационного захвата нейтронов ядрами урана-238 является одной из важнейших величин, определяющих в значительной степени перспективы развития ядерных реакторов различных типов. Особый интерес связан с сечениями захвата ядрами урана быстрых нейтронов (выше 1 кэв) в связи с возможностями процесса расширенного воспроизводства ядерного горючего в быстрых реакторах-размножителях.

Этим определяется большая заинтересованность в данных по $\sigma_\gamma(^{238}U)$ со стороны как специалистов по расчету реакторов, так и физиков, занимающихся измерениями, интерпретацией и расчетом нейтронных сечений. Отражением этой заинтересованности является большое число запросов на данные по сечениям захвата нейтронов ядрами урана-238, собранных в последних выпусках RENDA [1]. Поскольку удовлетворение потребностей реакторостроения в нейтронных константах имеет большое значение и должно осуществляться в максимальной степени и поскольку, с другой стороны, каждое уточнение физических констант требует больших усилий и средств, представляется целесообразным оценить с максимально возможной степенью объективности действительные потребности в точности величин $\sigma_\gamma(^{238}U)$, которые в настоящее время выдвигает практика.

Рассмотрение собранных в RENDA и выдвинутых в ряде других работ [2, 3] запросов показывает, что различные авторы имеют разные точки зрения на этот счет (рис. 1). Данная ситуация связана, очевидно, с различным подходом к решению вопроса о том, какие характеристики реактора считать главными (величину критмассы, длительность кампании, коэффициент воспроизводства горючего или стоимость получаемой электроэнергии), какова должна быть точность конечного результата и для какого типа реактора проводится анализ. Так или иначе, но требования на точность экспериментальных данных по $\sigma_\gamma(^{238}U)$ отличаются в отдельных энергетических интервалах до 20-50 раз даже в пределах одной 1-ой группы приоритета.

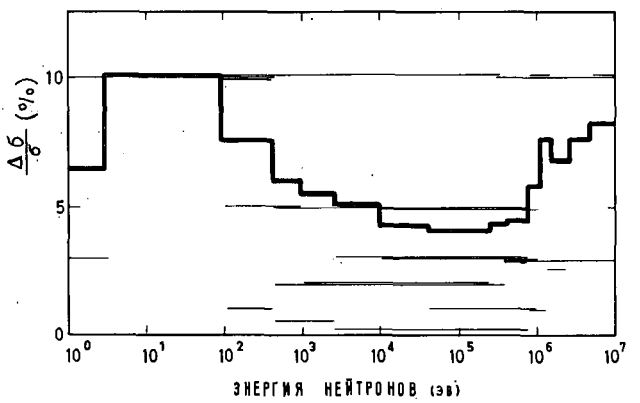

Рис. 1. Запросы на точность сечений захвата нейтронов ураном-238, требуемую для расчетов реакторов.

Совершенно ясно, что требовать от экспериментаторов немедленного удовлетворения заявок на самую высокую указанную расчетчиками точность нереально и, пожалуй, неразумно. Более оправданной представляется попытка усреднить различные запросы, чтобы дать экспериментаторам некие руководящие цифры, к которым им следует стремиться в первую очередь. Поскольку авторы многих запросов сами указывают приоритет, с которым должен выполняться их запрос (приоритет P = 1 соответствует наиболее срочным потребностям), можно провести подобное усреднение с учетом этого приоритета, считая, например, вес каждого

запроса обратно пропорциональным его приоритету. При этом среднее значение требуемой точности для каждого энергетического интервала

$$\langle \delta \rangle = \frac{\sum\left(\frac{\delta_i}{p_i}\right)}{\sum\left(\frac{1}{p_i}\right)}$$

где: δ_i – требуемая автором i – го запроса точность величины $\sigma_\gamma(^{238}U)$, p_i – приоритет этого запроса. Результат подобной обработки запросов из работ [1-3] показан гистограммой на рис. 1 (при этом детально обоснованным запросам из работы [2] приписан $p_i = 1$, а для запросов работы [3] значение $p_i = 1$ приписано более грубому, а $p_i = 3$ – более точному пределу точности). Как показывает рассмотрение рис. 1, наибольшая точность измерений величины $\sigma_\gamma(^{238}U)$ требуется в интервале энергий от 1 кэв до 1 Мэв, в котором $\langle \delta \rangle$ оказывается порядка 4-5%. При больших и меньших энергиях требования к точности $\sigma_\gamma(^{238}U)$ снижаются, однако в районе тепловых энергий нейтронов точность опять должна быть на уровне 4-5%. Следует отметить, что усреднение значений δ другими способами (например, методом наименьших квадратов) приводит примерно к таким же результатам. Это обстоятельство, а также относительно плавный характер полученной гистограммы указывают на приемлемость развитого здесь подхода. Поэтому мы склонны считать, что представленные на рис. 1 гистограммой значения $\langle \delta \rangle$ можно рассматривать, как первоочередную задачу для экспериментаторов; достижение примерно в два раза лучшей точности ($\langle \delta \rangle \sim 2\%$ при $E_n \sim 10^4$ эв) может рассматриваться в качестве второго тапа, а точность измерений лучше 1% – это задача для еще более далекого будущего.

ЭКСПЕРИМЕНТАЛЬНЫЕ ДАННЫЕ ПО $\sigma_\gamma(^{238}U)$

На рис. 2 приведены значения $\sigma_\gamma(^{238}U)$, взятые без изменений из различных экспериментальных работ. Как видно, при энергиях ниже 10 кэв имеется несколько точек, полученных методом активации [10, 34], а также имеются данные измерений на спектрометре по времени замедления в свинце [5] и усредненные результаты измерений методом времени пролета на линейном ускорителе [18] и при подземном ядерном взрыве [57]. В интервале от 10 до 200 кэв имеются данные из гораздо большего числа работ. Значительные расхождения между ними указывают, по-видимому, на существование каких-то систематических ошибок, связанных, например, с различным выбором стандартных сечений. При энергиях 0,2-1 Мэв данных существенно меньше, с чем, вероятно, связано и кажущееся уменьшение разброса между отдельными точками. Наконец, при энергиях выше 1 Мэв имеются результаты всего лишь нескольких работ, выполненных методом активации. Измерения в этой области значительно затруднены делением ядер урана-238, что требует принятия специальных мер по предотвращению влияния осколочной активности на результаты опытов.

В целом рис. 2 показывает, что разброс данных, полученных разными авторами, в различных энергетических интервалах составляет в среднем ±20% (а в отдельных точках еще больше), что намного превышает отмеченную выше точность значений $\sigma_\gamma(^{238}U)$, требуемую при расчетах.

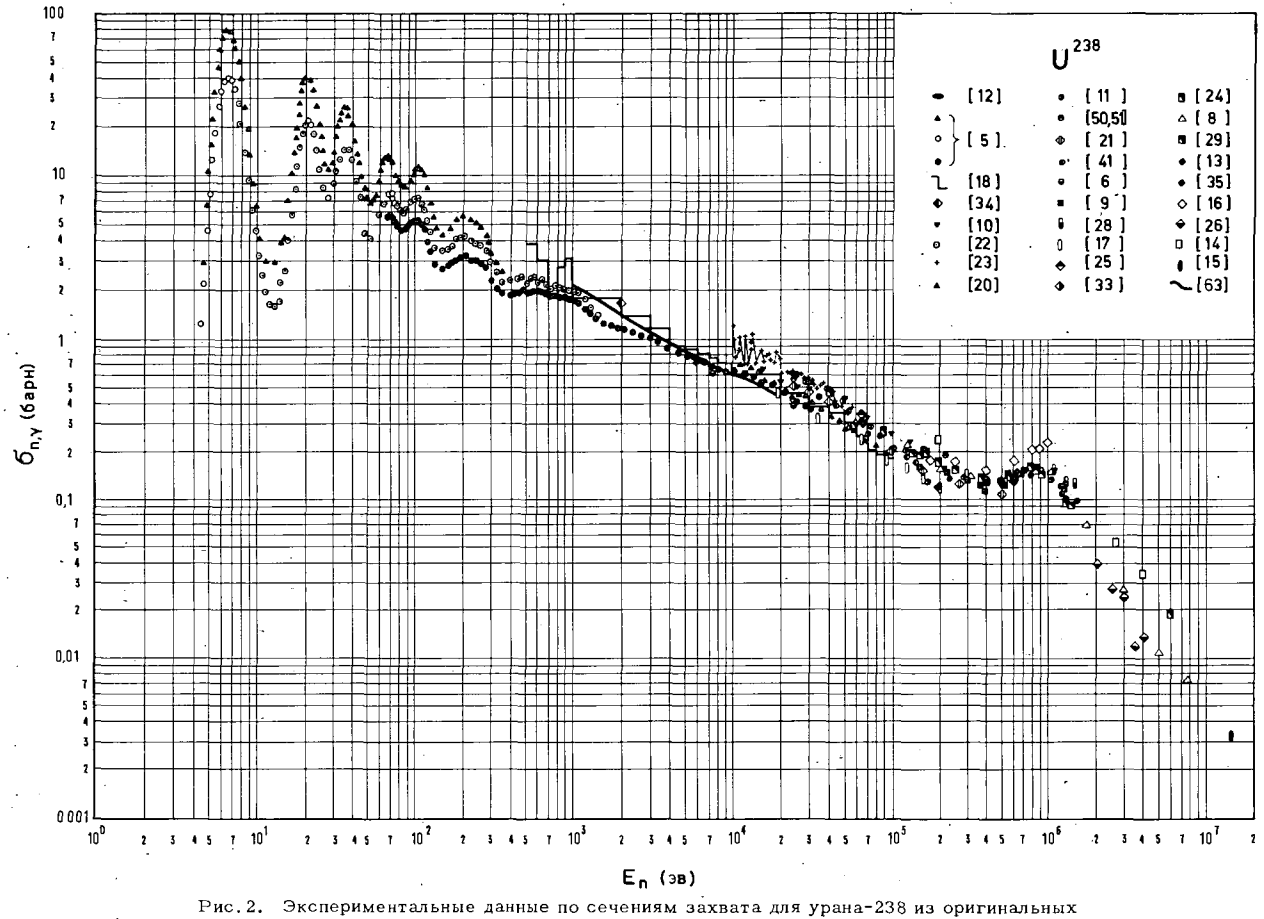

Рис. 2. Экспериментальные данные по сечениям захвата для урана-238 из оригинальных работ.

ТАБЛИЦА 1. ЭКСПЕРИМЕНТАЛЬНЫЕ ДАННЫЕ ПО СЕЧЕНИЮ ЗАХВАТА ^{238}U, ИСПОЛЬЗОВАННЫЕ В ДАННОЙ РАБОТЕ

Авторы	Год	Ссылка	Результаты оценки данных при выработке рекомендованных значений $\sigma_\gamma(^{238}U)$ с указанием критерия отбора (см. в тексте)
Broda	1945	[26]	не использовались ("б")
Lenenberger	1946	[24]	не использовались ("б")
Macklin	1957	[12]	использованы без изменений
Kafalas	1958	[28]	не использовались ("б")
Perkin	1958	[15]	использованы без изменений
Лейпунский и др.	1958	[14]	перенормированы при E = 2,7 и 4 Мэв к новым значениям $\sigma_\gamma(^{127}I)$, равным 32 и 14 мбарн соответственно; точка при 0,2 Мэв не использовалась ввиду недостаточно корректного учета поправки на "мягкую" группу нейтронов из $T(p, n)^3He$
Беланова	1958	[51]	не использовались ("а", см. [7])
Hanna	1959	[9]	использованы перенормированные данные из [40]; точка при 29 кэв не использовалась, так как она признавалась ненадежной самими авторами работы
Lyon	1959	[13]	использованы без изменения, но точка при E_n = 195 кэв не учитывалась ("в")
Беланова	1960	[50]	не использовались ("а", см. [7])
Bilpuch	1960	[10]	перенормированы к значению $\sigma_\gamma(^{238}U)$ при E = 207 кэв согласно [8]
Diven	1960	[16]	не использовались ("в", см. также [40])
Neiler	1961	[43]	см. [33]
Gibbons	1961	[42]	см. [33]
De Saussure	1962	[25]	перенормированы к современным значениям α и σ_f для урана-235 из [39]
Macklin	1963	[33]	использованы без изменения
Weston	1963	[49]	не использовались ("б")
Толстиков	1963	[11]	перенормированы к величине $\sigma_\gamma(^{238}U)$ = 495 мб при 24 кэв [31]. Точки при E_n = 53; 158 и 171 кэв не использовались, как явно заниженные ("в")
Толстиков	1963	[35]	перенормированы к новым значениям $\sigma_f(^{238}U)$ [39]
Bergqvist	1963	[17]	перенормированы по значению $\sigma_\gamma(^{238}U)$ при E_n = 207 кэв согласно [8] с экстраполяцией к энергии 200 кэв. Точка при E_n = 300 кэв не использовалась ("в")
Moxon	1963	[20]	не использовались ("а", см. [18])
Беланова	1963	[7]	не использовались
Barry	1964	[8]	при E_n < 1 Мэв использованы без изменений; при E_n > 1 Мэв перенормированы к значениям $\sigma_f(^{238}U)$ из [39]
Macklin	1964	[23]	не использовались ("б")
Беланова	1965	[4]	см. [48]
Беланова	1966	[48]	использовано исправленное на самоэкранировку значение $\sigma_\gamma(^{238}U)$ из [31]
Arai	1966	[22]	использованы значения σ_γ с учетом указанных авторами коэффициентов самоэкранировки
Королева	1966	[6]	использованы значения σ_γ, исправленные на эффект самоэкранировки в соответствии с результатами [31]
Kompe	1967	[47]	не использовались ("б")
Beckurts	1967	[46]	см. [21]
Menlove	1968	[21]	использованы без изменений
Moxon	1968	[45]	см. [18]
Schuman	1968	[44]	не использовались ("а", см. [34])
Moxon	1969	[18]	перенормированы по средневзвешенному значению $\sigma_\gamma(^{238}U)$ при 30 кэв, равному 468 мб, и введены поправки на самоэкранировку (см. в тексте)
Schuman	1969	[34]	не использовались, так как данные предварительные
Poenitz	1969	[29]	перенормированы к значениям $\sigma_f(^{238}U)$ и ^{239}Pu [39]
Паниткин	1970	[41]	использованы без изменений
Бергман	1970	[5]	использованы с коэффициентом 1,098 за счет пересмотра нормировки и введены поправки на самоэкранировку (см. в тексте)

ОЦЕНКА ЭКСПЕРИМЕНТАЛЬНЫХ ДАННЫХ ПО $\sigma_\gamma(^{238}U)$

Для уменьшения наблюдаемого разброса результатов различных работ в прошлом делались неоднократно попытки критических оценок экспериментальных данных [36, 19, 27, 30, 37, 38]. Основными элементами любой работы по оценке, как известно, являются: 1) отбор на основе тщательного анализа наиболее достоверных работ, 2) пересчет полученных в них результатов с учетом современных значений стандартных сечений и 3) проведение на основе отобранных и пересчитанных данных плавных кривых, которые могли бы быть рекомендованы для практических расчетов. Если последняя из этих операций может быть формализована и проведена с помощью ЭВМ довольно объективно, то при выполнении второй и особенно первой операции неизбежно проявление в той или иной степени субъективизма автора. Поэтому не удивительно, что полученные различными оценщиками рекомендованные кривые сами довольно сильно отличаются друг от друга (см. рис. 4): в области энергий ~ 10 кэв эти отличия от средних значений достигают 16%, в области 100 кэв – 13% и в области 550 кэв ~ 5%. Сильные расхождения результатов проведенных

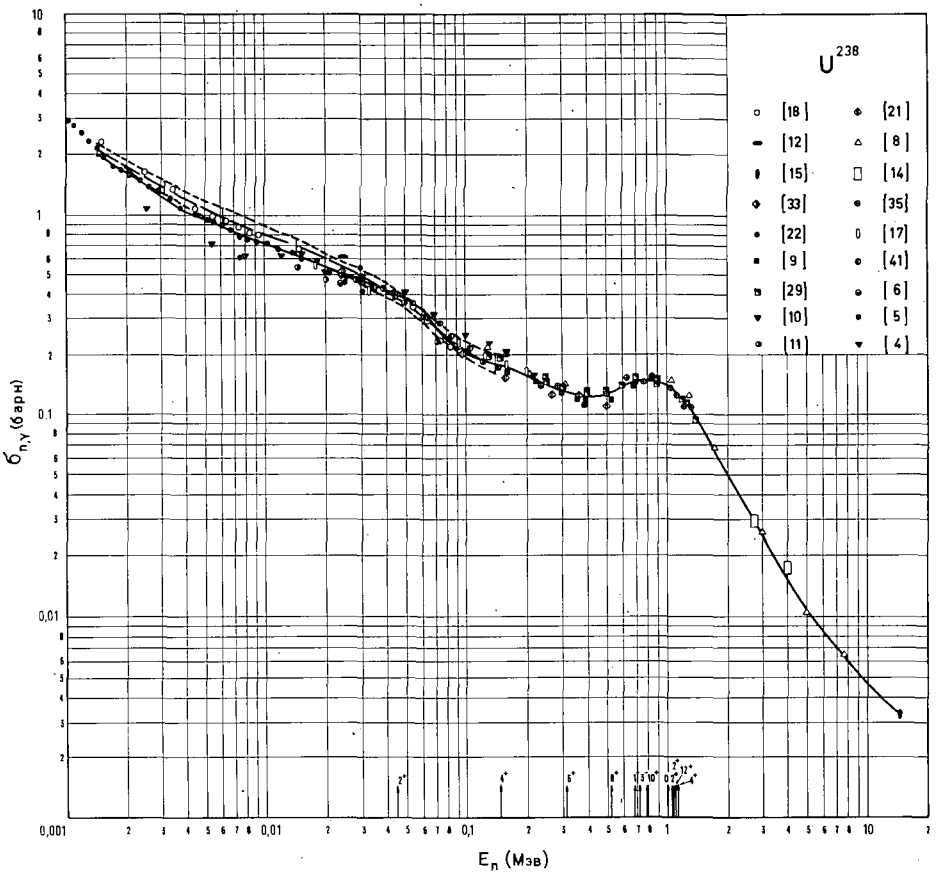

Рис. 3. Отобранные и перенормированные данные по сечениям захвата для урана-238.

ранее оценок величины $\sigma_\gamma(^{238}U)$ побудили нас сделать еще одну попытку в этом направлении. В данном докладе сообщаются результаты второго этапа этой работы, предварительные результаты которой были опубликованы ранее [8].

При отборе экспериментальных данных использовались следующие общие правила: (а) если известно несколько однотипных измерений, проведенных одними авторами на одной и той же установке, то брались результаты только последней работы; (б) не использовались работы, в которых не содержались или остались не известными авторам данного доклада (ввиду отсутствия самой работы) существенные для анализа детали эксперимента (значения опорных сечений, методы введения поправок и т.п.); (в) не использовались также работы, содержащие явные ошибки, или данные которых сильно расходятся с результатами нескольких других работ. После отбора, в случае необходимости, производилась перенормировка данных к новым значениям опорных сечений. Основные результаты этой стадии работы для интервала энергий выше 1 кэв отражены в табл. 1, а полученные значения отобранных и перенормированных сечений приведены на рис. 3.

ПОСТРОЕНИЕ УСРЕДНЕННОЙ КРИВОЙ ЗАВИСИМОСТИ $\sigma_\gamma(^{238}U)$ ОТ ЭНЕРГИИ НЕЙТРОНОВ ВЫШЕ 1 кэв

При построении усредненной кривой область энергий от 1 кэв до 1,3 Мэв была разбита на 23 неравновеликих интервала, в каждом из которых имелись близкие группировки точек. Затем определялись средние значения энергий и сечений захвата в каждом интервале, после чего строилась "грубая" кривая путем соединения соседних усредненных по интервалам точек прямыми линиями. Далее, с учетом среднего наклона кривой $\sigma_\gamma = \sigma_\gamma(E)$ производилось сведение индивидуальных сечений захвата от своих энергий к среднему значению энергии в интервале, после чего снова производилось усреднение, и вся операция повторялась снова. Обычно после 3-4 таких операций форма кривой стабилизировалась, т.е. получаемые средние значения σ_γ уже не изменялись. Тогда, по приведенным к среднему значению энергии величинам сечений, из отдельных работ находилось окончательное значение средневзвешенного среднего сечения захвата для каждого интервала и его среднеквадратичная ошибка.

При энергиях нейтронов выше 1,3 Мэв усредненная кривая проводилась по перенормированным точкам из работ [29], [8], [14] и [15].

ОЦЕНКА СРЕДНИХ РЕЗОНАНСНЫХ ПАРАМЕТРОВ ПО ДАННЫМ О РАЗРЕШЕННЫХ РЕЗОНАНСАХ

Большое число разрешенных резонансов урана-238 позволяет надеяться получить относительно надежную оценку средних резонансных параметров путем усреднения параметров разрешенных резонансов и рассчитать по ним средние характеристики сечений урана-238.

В качестве исходных данных о параметрах разрешенных резонансов были использованы рекомендации BNL-325 [19], основанные, главным образом, на результатах работ [52, 53], [54], [55], и дополненные работами [56] и [57], не учтенными в указанной компиляции. Деление на s- и p-резонансы первоначально было сделано в соответствии с данными [57].

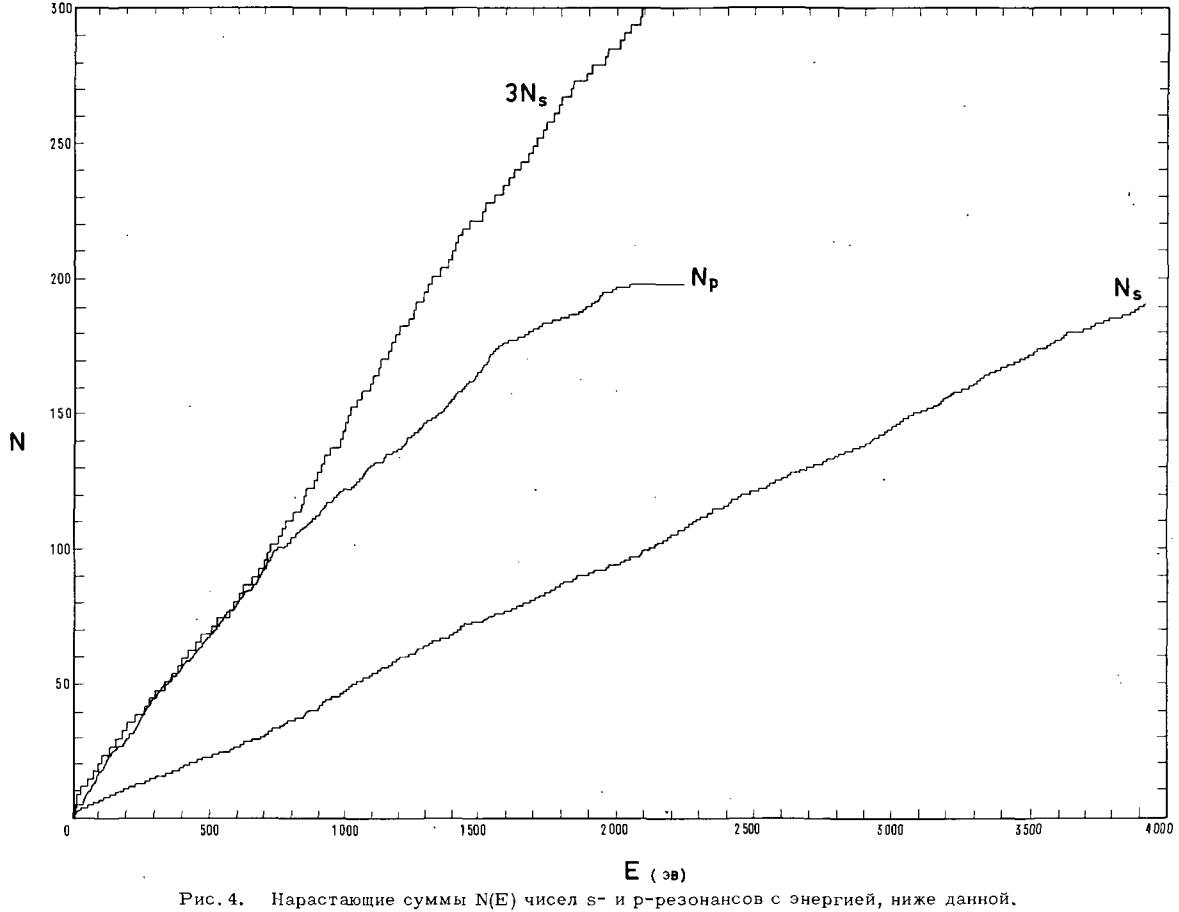

Рис. 4. Нарастающие суммы N(E) чисел s- и p-резонансов с энергией, ниже данной.

На рис. 4 приведены нарастающие суммы N(E) чисел s- и p-резонансов с энергиями, ниже данной. Линейный характер зависимости $N_s(E)$ дает основание полагать, что все или почти все s-резонансы разрешены. Дополнительная проверка этого обстоятельства может быть сделана путем сравнения наблюдаемого распределения расстояний между s-резонансами D_i и ожидаемым распределением Вигнера

$$f_B(x) = \frac{\pi}{2} x e^{-\frac{\pi x^2}{4}} \qquad (1)$$

Такое сравнение проводится на рис. 5 (пунктирная гистограмма-эксперимент). Видно, что число больших расстояний между резонансами превышает ожидаемое. Это расхождение можно устранить, если предположить, что относительно широкие резонансы при 1363,4 эв, 1854,7 эв и 2051,1 эв, идентифицированные в [57] как p-уровни, в действительности являются узкими s-резонансами. Кроме того, наблюдается некоторый недостаток малых расстояний между уровнями ($0 \div 0{,}2\bar{D}$) и избыток средних расстояний ($\sim 0{,}7\bar{D}$). Следует отметить, что в распределении приведенных нейтронных ширин также наблюдаются аналогичные систематические расхождения (см. рис. 6): резонансов с малыми ширинами ($< 0{,}016\bar{\Gamma}_n^0$) наблюдается как будто меньше, а с ширинами $\sim 0{,}06\,\bar{\Gamma}_n^0$ – больше, чем это ожидается из распределения Портера-Томаса. Естественно предположить, что причиной этого расхождения является ошибочная идентификация очень узких s-резонансов как p-резонансы. Оказалось, что расхождения в распределениях ширин и расстояний между уровнями можно существенно уменьшить путем замены всего лишь пяти (из 150) s-резонансов p-уровнями. Именно, резонансы при E = 721,8 эв, 779,1 эв, 909,6 эв, 1550 эв, 1797,7 эв были заменены на резонансы при E = 729,9 эв, 787,4 эв, 918,2 эв, 1527,1 эв и 1803,5 эв, соответственно.

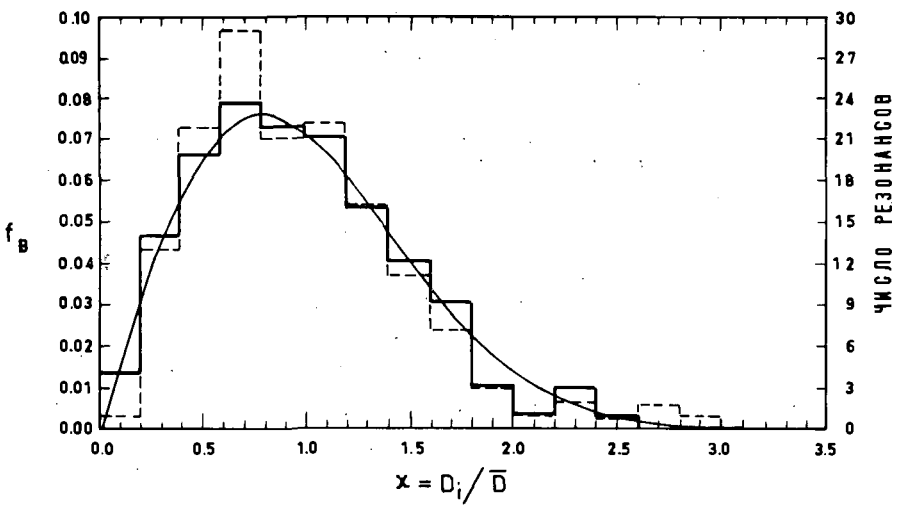

Рис. 5. Распределение расстояний между уровнями для первых 150 s-резонансов урана-238, (– – – исходный вариант, —— окончательный вариант) в сравнении с распределением Вигнера (кривая).

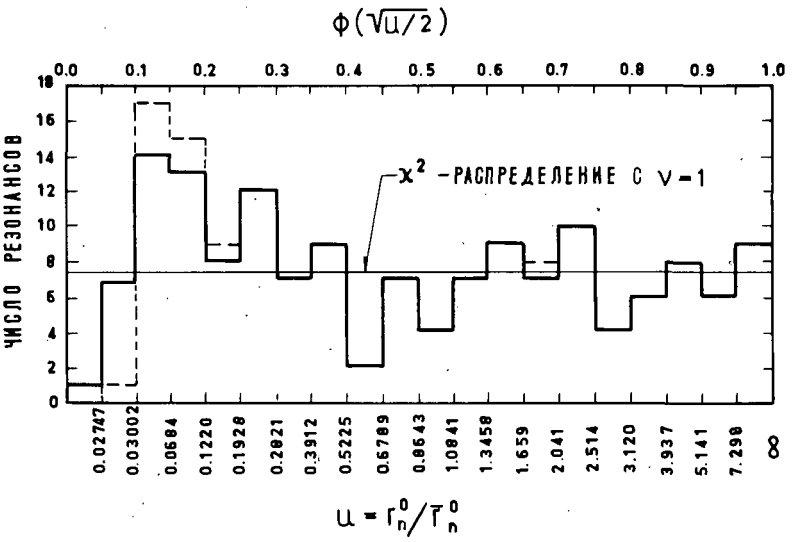

Рис. 6. Распределение приведенных ширин первых 150 s-резонансов урана-238 (--- исходный вариант,—— окончательный вариант) в сравнении с распределением Портера-Томаса.

Распределения D_i и Γ^0_{ni} после внесения всех изменений на рис. 5 и 6 приведены сплошными гистограммами. На остальных рисунках (в том числе и на рис. 4) все приводимые данные соответствуют измененной системе резонансов урана-238.

Определение среднего расстояния между s-резонансами проводилось трояким образом:

а) путем простого усреднения наблюдаемых расстояний

$$\bar{D}_1 = \frac{\sum_{i=1}^{N_s} (E_{i+1} - E_i)}{N_s} \qquad (2)$$

б) по наклону кривой зависимости $N_s(E)$, определявшемуся методом наименьших квадратов

$$\bar{D}_2 = \frac{\sum_{i=1}^{N_s} E_i^2 - \frac{1}{N_s}\left(\sum_{i=1}^{N_s} E_i\right)^2}{\sum_{i=1}^{N_s} i E_i - \frac{N_s+1}{2}\sum_{i=1}^{N_s} E_i} \qquad (3)$$

в) путем пересчета из среднеквадратичного расстояния

$$\bar{D}_3 = \sqrt{\frac{\pi}{4N_s}\sum_{i=1}^{N_s} (E_{i+1} - E_i)^2} \qquad (4)$$

где N_s – число рассматриваемых резонансов.

Дисперсия оценки D_1, связанная с конечностью рассматриваемого числа расстояний, равна $D_1^2/10N_s$ [58]. Аналогичная дисперсия для $\bar{D}_2$ оценивалась по сумме квадратов отклонений между наблюдаемой зависимостью $N_s(E)$ и наилучшей линейной $(a + E_i/D_2)$

$$\delta^2(\bar{D}_2) = \frac{S_{min}}{(N_s - 1)} \cdot \frac{\bar{D}_2^2}{N_s \sum_{i=1}^{N_s} E_i^2 - \left(\sum_{i=1}^{N_s} E_i\right)^2} \qquad (5)$$

где:

$$S_{min} = \sum_{i=1}^{N_s} \left[\left(i + \frac{1}{2}\right) - \left(a + \frac{E_i}{D_2}\right)\right]^2 \qquad (6)$$

К указанным дисперсиям добавлялись дисперсии в N_s числе рассматриваемых уровней, связанные с неопределенностью идентификации s-резонансов. По нашим оценкам, эта неопределенность составляет примерно 5 резонансов. Оценка $\bar{D}_3$, более чувствительная к пропуску резонансов, чем предыдущие [58], использовалась для дополнительного контроля несущественности пропуска s-резонансов.

Расчеты показали, что при учете нескольких (3 ÷ 5) десятков резонансов, оценки $\bar{D}_1$ и $\bar{D}_2$ еще заметно различаются, но для ≥ 100 практически совпадают. $\bar{D}$ не зависит от числа рассмотренных резонансов вплоть до $N_s \sim 150$. При учете большого числа уровней наблюдается падение $\bar{D}$, что может быть связано с тем, что при энергиях выше 3 кэв часть широких p-резонансов ошибочно идентифицирована как s-уровни. Поэтому для оценки мы ограничивались рассмотрением 150 s-резонансов ($E < 3100$ эв). При этом $\bar{D}_1 = 20{,}6 \pm 0{,}8$ эв; $\bar{D}_2 = 20{,}6 \pm 0{,}8$ эв; $\bar{D}_3 = 20{,}5$ эв. То обстоятельство, что $\bar{D}_3$ не превышает $\bar{D}_2$ и $\bar{D}_1$, свидетельствует о несущественности пропуска s-резонансов.

В случае p-резонансов, как видно из рис. 4, пропуск уровней становится ощутимым, начиная, по крайней мере, с $\sim 0{,}8$ кэв. Для учета пропущенных резонансов использовалась методика, развитая в работе [60] для случая, когда энергетическая зависимость известна и имеет вид $\delta(E) \sim aE^b$. Поскольку разрешение экспериментов, результаты которых мы использовали, не было нам известно достаточно хорошо, параметры разрешения определялись нами путем подбора. Для этого зависимость $N_p(E)$ аппроксимировалась формой

$$N_p(E) \simeq \frac{E}{\bar{D}_p}\left[1 + AE^b + BE^{2b}\right] \qquad (7)$$

в которой параметры $\bar{D}_p$ – среднее расстояние между p-резонансами, A, B и b определялись методом наименьших квадратов. При включении в анализ до 200 p-резонансов $\bar{D}_p$ оказывается слабо зависящим от их числа и равным 6,7 эв. Погрешность $\bar{D}_p$ оценена равной 0,3 эв.

Отношение $\bar{D}_s/3\bar{D}_p = 1{,}02 \pm 0{,}06$. Это подтверждает предположение о том, что плотность уровней со спином I пропорциональна 2I+1 (при малых и близких между собой I). В дальнейшем при расчете сечений мы будем исходить из этого предположения. Здесь же воспользуемся им, чтобы оценить возможную ошибку в числе s-уровней, обусловленную неопределен-

ностью идентификации наблюдаемых резонансов как s-уровней. Полагая $\overline{D}_s = 3\overline{D}_p$ и рассматривая полученную оценку $\overline{D}_p$ как независимую, имеем:

$$\overline{D}_{1/2} = \frac{\overline{D}_s/\delta^2(\overline{D}_s) + 3\overline{D}_p/9\delta^2(\overline{D}_p)}{1/\delta^2(\overline{D}_s) + 1/9\delta^2(\overline{D}_p)} = 20{,}4 \text{ эв} \tag{8}$$

с ошибкой

$$\delta(\overline{D_{1/2}}) = \left[1/\delta^2(\overline{D}_s) + 1/9\delta^2(\overline{D}_p)\right]^{-1/2} = 0{,}6 \text{ эв} \tag{9}$$

Здесь $\delta^2(\overline{D_{1/2}})$ – дисперсия $\overline{D}_{1/2}$.

Оценка средних нейтронных ширин и силовых функций

Распределение приведенных ширин первых 150-ти s-резонансов показано на рис. 6 в сравнении с распределением Портера-Томаса. По оси x отложены границы групп, делящих площадь под χ^2-распределением с одной степенью свободы на 20 равных частей. Прямая, проходящая через 7,5 (150 резонансов: 20), соответствует теоретическому распределению. Сплошными прямыми изображена гистограмма после внесения описанных выше изменений.

Так как согласие между наблюдаемым и ожидаемым распределением удовлетворительно, Γ_n^0 оценивалась как

$$\overline{\Gamma}_n^0 = \frac{\sum_{i=1}^{N_s} \Gamma_{ni}^0}{N_s} \tag{10}$$

Эта оценка подчиняется χ^2-распределению с n степенями свободы, которое при большом n близко к гауссовому с дисперсией $2\overline{\Gamma}_n^{0\,2}/N_s$. В результате усреднения получено $\overline{\Gamma}_n^0 = 1{,}86 \pm 0{,}20$ эв. Отсюда, используя найденную выше оценку для $\overline{D}_{1/2}$, находим для силовой функции s-волны:

$$S_0 = \frac{\overline{\Gamma}_n^0}{\overline{D}_{1/2}} = (0{,}91 \pm 0{,}11)\cdot 10^{-4} \tag{11}$$

При оценке ошибки в $\overline{\Gamma}_n^0$ мы не учитывали возможный пропуск или неправильную идентификацию s-уровней, поскольку эта ошибка меньше, чем та, которая обусловлена конечностью выборки Γ_{ni}^0.

Приведенные нейтронные ширины для p волны рассчитывались по формуле:

$$g\Gamma_n^1 = g\Gamma_n E_0^{-3/2}(E_0 + 3\cdot 10^5) \tag{12}$$

E_0 – энергия резонанса в эв.

Для расчета $\overline{\Gamma}_n^1$ – средней приведенной нейтронной ширины были взяты первые 100 p-резонансов (до энергии 743 эв), так как из анализа расстояний между p-уровнями можно полагать, что в этой области энергий пропущено в среднем лишь 10 p-уровней.

Силовая функция p-волны, рассчитанная как

$$S_1 = \frac{\sum_{i=1}^{N_p} g\Gamma_{ni}^1}{N_p \cdot \overline{D}_{1/2}} \tag{13}$$

при $N_p = 100$ оказалась равной $2{,}2 \cdot 10^{-4}$. Учет пропуска 10 слабых уровней не повлияет на $\sum_{i=1}^{N_p} g\Gamma_{ni}^1$, но уменьшит S_1 за счет увеличения N_p в знаменателе. С учетом пропуска уровней $S_1 = (2{,}0 \pm 0{,}3) \cdot 10^{-4}$, где ошибка определяется статистической погрешностью в сумме ширин.

К сожалению, полученная таким образом ошибка недостаточна для оценки надежности полученной силовой функции для p-волны. Дело в том, что наблюдаемое суммарное распределение приведенных ширин двух систем p-резонансов (с $I = 1/2$ и $I = 3/2$) сильно отличаются от теоретического χ^2-распределения с числом степеней свободы $\nu = 3/2$. Сравнение этих распределений на рис. 7 показывает, что, помимо нехватки резонансов с малыми нейтронными ширинами, наблюдается недостаток относительно широких уровней. (с $\Gamma_n^1 \sim 6\overline{\Gamma}_n^1$). Устранить это расхождение путем разумного перевода части узких s-резонансов в разряд p-уровней не удалось. Отмечаемое расхождение понижает надежность оценки S_1 по параметрам разрешенных резонансов. Для отражения этого обстоятельства мы повысили погрешность S_1 до 25%, т.е. приняли $S_1 = (2{,}0 \pm 0{,}5) \cdot 10^{-4}$.

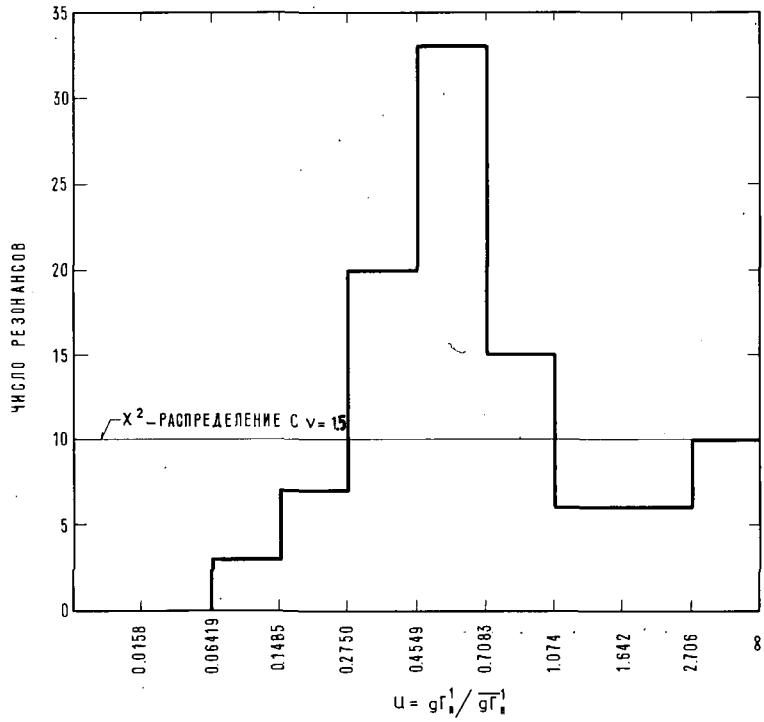

Рис. 7. Распределение приведенных ширин первых 100 p-резонансов урана-238 в сравнении с χ^2-распределением с $\nu = 1{,}5$.

Оценка средней радиационной ширины

Данные о радиационных ширинах имеются для 72 резонансов урана-238, причем для 31 из них известны результаты двух или большего числа работ. Сравнение данных различных авторов между собой показало, что расхождения между ними очень часто намного превышают величину приписываемых авторами ошибок. Поэтому они не являются мерой точности этих результатов и их нельзя использовать для вычисления статистических весов при усреднении. Явное наличие систематических ошибок в результатах отдельных авторов не позволяет использовать в качестве меры точности и число резонансов, для которых определены радиационные ширины в той или иной работе. В связи с этим мы не нашли лучшего способа оценки $\overline{\Gamma}_\gamma$, чем простое усреднение результатов, полученных для этой величины в 7 работах, выполненных после 1956 года:

ТАБЛИЦА 2. ВЕЛИЧИНЫ СРЕДНИХ РАДИАЦИОННЫХ ШИРИН $\overline{\Gamma}_\gamma$, ПО ДАННЫМ РАЗЛИЧНЫХ АВТОРОВ

Bollinger [55]	24 ± 2
Rosen [54]	24,7
Moxon [45]	23,2
Firk [53]	27,6 ± 1,3
Garg [52]	25
Asghar [56]	23,7 ± 1,1
Glass [57]	19,1 ± 2
среднее	$\overline{\Gamma}_\gamma = 23,9 \pm 0,9$

Ошибка среднего значения Γ_γ оценена по среднеквадратичному разбросу данных различных авторов. Наибольшее расхождение с этой средней величиной наблюдается для данных Гласса [57]. Наряду с низким значением Γ_γ в этой работе обнаружены значительные флуктуации радиационной ширины, носящие характер некоторой промежуточной структуры. Природу этих флуктуаций трудно объяснить. Если же принять, как это следует из представления о радиационном захвате как о многоканальном процессе, что Γ_γ флуктуирует слабо, то обнаруженные в [57] флуктуации следует рассматривать как аппаратурный эффект, резко снижающий надежность данных. Если при усреднении Γ_γ данные работы [57] не учитывать, то получится $\overline{\Gamma}_\gamma = 24,7 \pm 0,7$ эв, т. е. учет данных Гласса и др. влияет как на величину, так и на точность $\overline{\Gamma}_\gamma$. Окончательно нами была выбрана величина $\overline{\Gamma}_\gamma = 24,3 \pm 0,9$ эв.

РАСЧЕТ СЕЧЕНИЙ РАДИАЦИОННОГО ЗАХВАТА ПО СРЕДНИМ РЕЗОНАНСНЫМ ПАРАМЕТРАМ

Расчет сечений урана-238 по оцененным резонансным параметрам $\overline{D}_{1/2} = 20,4 \pm 0,6$ эв; $S_0 = (0,91 \pm 0,11)\,10^{-4}$; $S_1 = (2,0 \pm 0,5)\,10^{-4}$; $\overline{\Gamma}_\gamma = 24,3 \pm 0,9$ Мэв проводился с помощью программы УРАН [62]. Среднее сечение (соответствующее бесконечному разбавлению или с учетом резонансной самоэкранировки в приближении узких резонансов) в каждой

энергетической точке получалось в результате соответствующего усреднения детального хода сечений в окрестности двадцати эффективных резонансов. Параметры этих резонансов были подобраны таким образом, чтобы результат усреднения правильно учитывал флуктуации ширин и расстояний [61]. Эта квазислучайная последовательность резонансов отличалась следующими свойствами.

1. Распределение приведенных нейтронных ширин двадцати резонансов обеспечивало сохранение $\bar{\Gamma}_n^0$ – точно; $(\bar{\Gamma}_n^0)^{1/2}$ – с точностью до 3%, $(\bar{\Gamma}_n)^{3/2}$ – с точностью до 1,6%; $(\bar{\Gamma}_n^0)^2$ – с точностью 5,6%. Точность учета флуктуаций нейтронных ширин при расчете радиационного захвата для бесконечного разбавления лучше 1% при любом отношении $\Gamma_\gamma/\bar{\Gamma}_n^0$.

2. Распределение расстояний между резонансами квазислучайной последовательности описывает распределение Вигнера с еще лучшей точностью, чем распределение нейтронных ширин – распределение Портера-Томаса.

3. Последовательность ширин резонансов выбрана таким образом, чтобы отношения нейтронных ширин соседних резонансов удовлетворяли теоретическому распределению, полученному в предположении о независимости флуктуаций ширин соседних резонансов.

4. Последовательность расстояний между резонансами выбрана так, чтобы описывалось теоретическое распределение отношений ширин и расстояние между уровнями (полученное в предположении о их независимости).

Принимавшаяся нами квазислучайная последовательность резонансов приведена в табл. 3. Ее использование позволяет достаточно корректно производить учет распределений ширин и расстояний между уровнями для вычисления средних сечений с помощью программы расчета сечений по известным резонансным параметрам.

ТАБЛИЦА 3. КВАЗИСЛУЧАЙНАЯ ПОСЛЕДОВАТЕЛЬНОСТЬ РЕЗОНАНСОВ ДЛЯ УЧЕТА ФЛУКТУАЦИИ ШИРИН И РАССТОЯНИЙ МЕЖДУ УРОВНЯМИ

i	$x = \frac{\Gamma_{ni}^0}{\bar{\Gamma}_n^0}$	$y = \frac{E_{i+1} - E_i}{\bar{D}}$	i	$x = \frac{\Gamma_{ni}^0}{\bar{\Gamma}_n^0}$	$y = \frac{E_{i+1} - E_i}{\bar{D}}$
1	0,00134	0,7728	11	0,5112	1,822
2	5,577	1,492	12	1,476	0,1694
3	3,203	1,282	13	0,1763	1,0436
4	0,04922	1,197	14	0,1241	0,3142
5	0,08217	0,7070	15	1,174	0,8400
6	0,6376	1,378	16	0,2392	0,5692
7	0,02502	0,4952	17	0,7881	0,9732
8	0,9704	1,628	18	0,4071	0,6404
9	0,3151	1,119	19	1,846	0,4110
10	0,00915	0,9060	20	2,368	2,240

Важным моментом при расчете сечений в области неразрешенных резонансов является правильный учет вкладов различных систем уровней в среднее сечение, вычисляемое с учетом резонансной самоэкранировки. В приближении узких резонансов эффективное сечение захвата в среде при разбавлении барн на атом поглотителя равно:

$$\bar{\sigma}_c = \frac{\langle \sigma_c/(\sigma_t+\sigma_0)\rangle}{\langle 1/(\sigma_t+\sigma_0)\rangle} \tag{14}$$

где угловые скобки означают усреднение по энергии в некотором интервале Δu. Фигурирующие здесь средние значения могут быть выражены через функции пропускания

$$T(t) = \frac{1}{\Delta u}\int e^{-\sigma_t(E)\,t}\cdot\frac{dE}{E} \tag{15}$$

следующим образом:

$$\langle \sigma_c/(\sigma_t+\sigma_0)\rangle = \int_0^\infty T_c(t)\,e^{-\sigma_0 t}\cdot dt; \quad \langle 1/(\sigma_t+\sigma_0)\rangle = \int_0^\infty T(t)\,e^{-\sigma_0 t}\cdot dt \tag{16}$$

Энергетические зависимости $\sigma_t(E)$ и $\sigma_c(E)$ представляют собой суммы флуктуирующих функций энергетических зависимостей сечений для отдельных систем резонансов, отличающихся спином и четностью. Пользуясь независимостью положений и ширин уровней разных систем, получим:

$$T(t) = \prod_{m=1}^{M} T_m(t); \quad T_c(t) = \sum_{m=1}^{M}\left[T_{cm}(t)\prod_{m\neq m'} T_{m'}(t)\right] \tag{17}$$

где T_{cm} и T_m – функции пропускания, рассчитанные для m-й системы резонансов в предположении об отсутствии других систем; M – полное число систем. Функции $T_{cm}(t)$ и $T_m(t)$ вычислялись по детальному ходу сечений в окрестности квазислучайной последовательности 20 резонансов, генерируемой при каждой энергии для каждой системы уровней. Значение этих функций позволило рассчитать полные функции пропускания, а через них и эффективные сечения с учетом самоэкранировки. Усреднение этих сечений по групповым интервалам позволило получить групповые средние сечения и факторы самоэкранировки, которые приведены в табл. 3 (для температуры 300°K).

РЕКОМЕНДУЕМЫЕ СЕЧЕНИЯ

Результаты оценки сечения радиационного захвата в области энергий выше 1 кэв приведены на рис. 3.

Как уже отмечалось, сплошная линия получена путем усреднения отобранных и перенормированных экспериментальных данных о сечениях.

Точность этой оценки определяется разбросом данных различных авторов и составляет в области энергий (16 эв – 1,5 Мэв) 5%-8%. При больших энергиях ошибки, согласно оценкам самих авторов экспериментальных работ возрастают до 20%-30%.

Точность приводимой расчетной кривой (жирный пунктир на рис. 3) оценивалась в предположении о независимости ошибок средних резонансных параметров. Коридор ошибок изображен тонкими пунктирными линиями.

Как видно из рис. 3, результаты двух независимых оценок согласуются между собой в пределах ошибок.

В табл. 3 приведены окончательные рекомендуемые значения сечений захвата для урана-238.

В области энергий ниже 1 кэв сечение захвата рассчитывалось по известным параметрам разрешенных резонансов. В области энергий от 1 кэв до 10 ÷ 20 кэв, где в экспериментальные данные вносились существенные поправки на самоэкранировку сечений в образце, сплошная кривая на рис. 3 имеет относительно меньшую надежность. Поэтому в этой области в качестве рекомендованных данных использовались результаты расчета по средним параметрам.

При энергиях выше 30 кэв результаты обеих оценок совпадают.

В табл. 4 приводятся среднегрупповые сечения радиационного захвата в интервалах 26-групповой системы констант [32] и их ошибок. Там же даны параметры резонансной самоэкранировки, определенные согласно [32].

Рекомендации данной работы сравниваются на рис. 8 с оценками других авторов.

ТАБЛИЦА 4. СРЕДНЕГРУППОВЫЕ СЕЧЕНИЯ РАДИАЦИОННОГО ЗАХВАТА В ИНТЕРВАЛАХ 26-ГРУППОВОЙ СИСТЕМЫ КОНСТАНТ [32] И ИХ ОШИБОК. ПАРАМЕТРЫ РЕЗОНАНСНОЙ САМОЭКРАНИРОВКИ

	E_n	Δu	σ_c	$\Delta\sigma_c$	f_c при σ_0, равной:				
					10^4	10^3	10^2	10	0
1	6,5 - 10,5 Мэв	0,48	0,007						
2	4,0 - 6,5 Мэв	0,48	0,012						
3	25 - 4,0 Мэв	0,48	0,024						
4	1,4 - 2,5 Мэв	0,57	0,06						
5	0,8 - 1,4 Мэв	0,57	0,13						
6	0,4 - 0,8 Мэв	0,69	0,13						
7	0,2 - 0,4 Мэв	0,69	0,14						
8	0,1 - 0,2 Мэв	0,77	0,18	0,02	1,000	1,000	0,999	0,994	0,989
9	46,5 - 100 кэв	0,77	0,29	0,02	1,000	1,000	0,997	0,986	0,977
10	21,5 - 46,5 кэв	0,77	0,48	0,04	1,000	0,999	0,991	0,960	0,936
11	10,0 - 21,5 кэв	0,77	0,70	0,06	1,000	0,997	0,975	0,905	0,857
12	4,65 - 10,0 кэв	0,77	0,98	0,09	0,999	0,990	0,934	0,802	0,727
13	2,15 - 4,65 кэв	0,77	1,36	0,10	0,994	0,969	0,833	0,628	0,537
14	1,0 - 2,15 кэв	0,77	2,1	0,12	0,990	0,917	0,665	0,420	0,340
15	465 - 1000 эв	0,77	3,2	0,2	0,978	0,839	0,462	0,222	0,166
16	215 - 465 эв	0,77	4,4	0,2	0,961	0,745	0,343	0,150	0,112
17	100 - 215 эв	0,77	20	1	0,811	0,390	0,129	0,058	0,048
18	46,5 - 100 эв	0,77	17	2	0,800	0,373	0,124	0,055	0,044
19	21,5 - 46,5 эв	0,77	57	3	0,601	0,203	0,071	0,038	0,031
20	10,0 - 21,5 эв	0,77	83	5	0,677	0,230	0,061	0,025	0,019
21	4,65 - 10 эв	0,77	174.	3	0,703	0,263	0,082	0,037	0,028
22	2,15 - 4,65 эв	0,77	0,68	0,02					
23	1,0 - 2,15 эв	0,77	0,48	0,01					
24	0,465 - 1,0 эв	0,77	0,52	0,01					
25	0,215 - 0,465 эв	0,77	0,76	0,01					
T	0,0252		2,73	0,04					

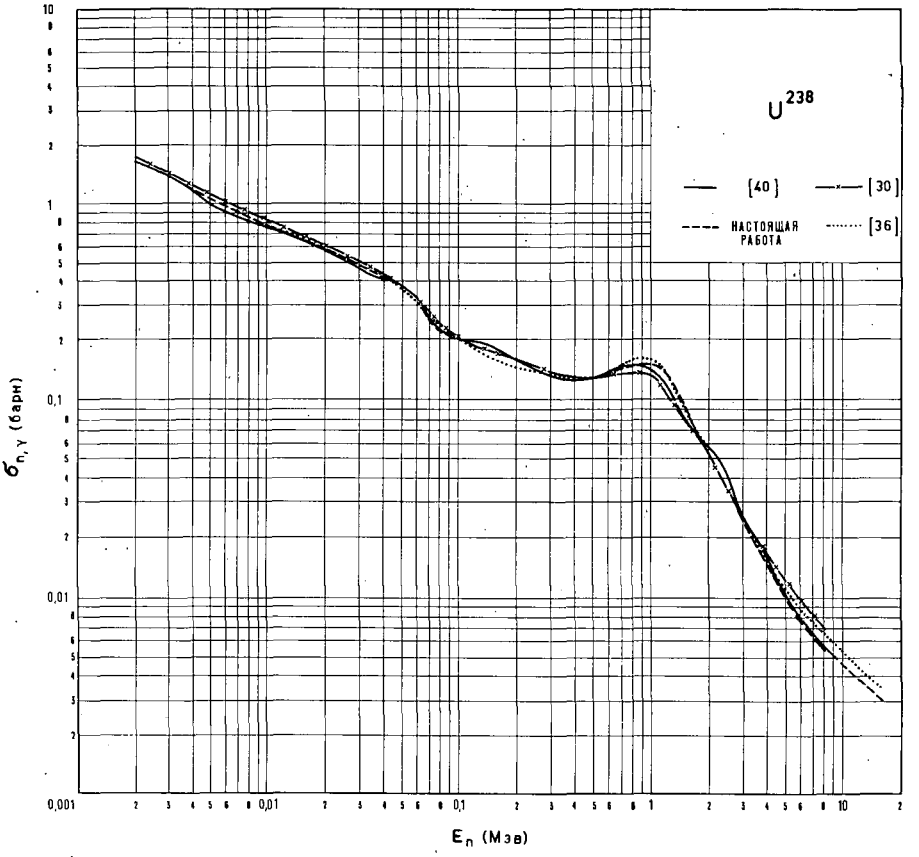

Рис. 8. Сравнение результатов данной работы с оценками других авторов.

ЛИТЕРАТУРА

[1] RENDA, INDC/226, IAEA, Vienna, 1968.
[2] GREEBLER, P. et al., Neutron Cross Sections and Technology, Washington, 1 (1968) 291.
[3] ЗАРИЦКИЙ, С.М., ТРОЯНОВ, М.Ф., Доклад на конф. по физике быстрых реакторов, Лондон, июнь 1969.
[4] БЕЛАНОВА, Т.С. и др., Атомиая энергия, 19 (1965) 3.
[5] БЕРГМАН, А.А. и др., Доклад CN-26/78, Хельсинки, 1970.
[6] КОРОЛЕВА, В.П., СТАВИССКИЙ, Ю.Я., Атомная энергия 20 (1966) 431.
[7] БЕЛАНОВА, Т.С., Атомная энергия 8 (1960))549.
[8] BARRY, J.F. et al., J. Nucl. Energy, A/B 18 (1964).
[9] HANNA, R.C., ROSE, B., J. Nucl. Energy 8 (1958) 2197.
[10] BILPUCH, E.G. et al., Ann. Phys. 10 (1960) 455.
[11] ТОЛСТИКОВ, В.А., ШЕРМАН, Л.Е., СТАВИССКИЙ, Ю.Я., Атомная энергия 15 (1963) 414.
[12] MACKLIN, R.L., LAZAR, N.H., LYON, W.S., Phys. Rev. 107 (1957) 504.
[13] LYON, W.S., MACKLIN, R.L., Phys. Rev. 114 (1959) 1619.
[14] ЛЕЙПУНСКИЙ, А.И. и др., Вторая Женевская конф. 1958, доклад № P/2219.
[15] PERKIN, J.L., O'CONNOR, L.R., COLEMAN, P.F., Proc. Phys. Soc. 72 (1958) 505.

[16] DIVEN, B.C., TERREL, J., HEMMENDINGER, A., Phys. Rev. 120 (1960) 556.
[17] BERGQVIST, J., Ark. f. Fysik 23 (1963) 425.
[18] MOXON, M.C., AERE-R 6074 (1969).
[19] STEHN, J.R. et al., BNL-525, Second Edition, Suppl. 2 3 (1965).
[20] MOXON, M.C., CHALLEY, C.M., Частное сообщение, 1963 (см. [19]).
[21] MENLOVE, H.O., POENITZ, W.P., Nucl. Sci. Eng. 33 (1968) 24.
[22] ARAI, E., MIESSNER, H., BECKURTS, K.N., Nucl. Sci. Eng. 26 (1966) 573.
[23] MACKLIN, R.L., GIBBONS, J.H., Частное сообщение, 1964 (см. [19]).
[24] LINENBERGEN, G.A., MISKEI, J.A., LA-647 (1946).
[25] SAUSSURE, G. de et al., ONRL-3360 (1962).
[26] BRODA, E., BR-574 (1945). Данные приведены в [8].
[27] SCHMIDT, J.J., KFK-120 (1966).
[28] KAFALAS, P., HEINREICH, R.R., ANL-5924 (1958). Данные см. в [27].
[29] POENITZ, W.P., Trans. Am. Nucl. Soc. 12 (1969) 279. см. также ссылку [1] в работе [30].
[30] KONSHIN, V.A., The Present Status of Sigma Capture for ^{238}U at 2 keV-5 MeV, IAEA, Vienna, Dec. 1969.
[31] MILLER, L.B., POENITZ, W.P., Nucl. Sci. Eng. 35 (1969) 259.
[32] АБАГЯН, Л.П. и др., "Групповые константы для расчета ядерных реакторов", Атомиздат, М., 1964.
[33] MACKLIN, R.L. et al., Phys. Rev. 129 (1963) 2695.
[34] SCHUMAN, R.P., Предварительное сообщение, 1969.
[35] ТОЛСТИКОВ, В.А., (1963). Данные см. в [38].
[36] PARKER, K., AWRE-0 82/63 (1963).
[37] VASTEL, M., RAVIES, J.,2 nd Conf. on Neutron Cross Sections and Technology, Washington, 2 (1968) 1129.
[38] АБРАМОВ, А.И., ТОЛСТИКОВ, В.А., Сообщение во время тематической дискуссии на 2-м совещании МКЯД в БНЛ (1969).
[39] HART, W., Англо-советский семинар, Дубна 1968. Доклад UK/10.
[40] DAVEY, W.G., "An Analysis of the Capture Cross Section of ^{238}U between 1 keV and 15 MeV", ANL, 1969.
[41] ПАНИТКИН, Ю.Г., ТОЛСТИКОВ, В.А., СТАВИССКИЙ, Ю.Я., Доклад CN-26/77, Хельсинки 1970.
[42] GIBBONS, J.H. et al., Phys. Rev. 122 (1961) 182.
[43] NEILER, J.H., 61 Vienna, IAEA, 1 (1961) 91.
[44] SCHUMAN, R.P., Предварительное сообщение, 1968.
[45] MOXON, M.C., Thesis M. Sc., Harwell, 1968.
[46] BECKURTS, K.H. et al., 67 Karlsruhe 1 (1968) 67.
[47] KOMPE, D., KFK-635 (1967).
[48] БЕЛАНОВА, Т.С. и др., Nuclear Data for Reactors, Vienna, 1 (1967) 455.
[49] WESTON, L.W. et al., EANDC-33U (1963) 64.
[50] БЕЛАНОВА, Т.С., Атомная энергия 8 (1960) 549.
[51] БЕЛАНОВА, ЖЭТФ 34 (1958) 574.
[52] GARG, J.B., RAINWATER, J., PETERSON, J.S., HAVENS, W.W., Jr. Phys. Rev. 134 (1964) B 985.
[53] FIRK, F.W.K., LYNN, J.E., MOXON, W.C., Nucl. Phys. 41 (1963) 614.
[54] ROSEN, J.L., DESJARDINS, J.S., RAINWATER, J., HAWENS, W.W., Jr., Phys. Rev. 118 (1960) 687.
[55] BOLLINGER, L.M., COTE, R.S. et al., Phys. Rev. 105 (1957) 661.
[56] ASGHAR, M., CHAFFEY, C.M., MOXON, M.C., Nucl. Phys. 85 (1966) 305.
[57] GLASS, N.W., THEOBALD, J.K., SCHELBEY, A.D., Conf. on Neutron Cross Section Technology II (1966) 766.
[58] МАЛЕЦКИ, Х., ПИКЕЛЬНЕР, Л.Б., САЛАМАТИН, И.М., ШАРАПОВ, Э.И., Препринт Р3-4484, Дубна, 1969.
[59] PORTER, Ch.E., J. Math. Phys. 4 (1963) 1039.
[60] FUKETA, T., HARVEY, J.A., Nucl. Instr. and Methods 33 (1965) 107.
[61] НИКОЛАЕВ, М.Н., АБАГЯН, Л.П. и др., Докл. на советско-бельгийско-голландском симп. по некоторым проблемам физики быстрых реакторов, Мелекесс, 1970.
[62] АБАГЯН, Л.П., НИКОЛАЕВ, М.Н., ПЕТРОВА, Л.В., Бюллетень ИЦЯД, вып. 4 (1967) 392.
[63] КОНЬШИН, В.А., Сечение захвата для ^{238}U. INDC(NDU)-14/N, октябрь 1969.

EVALUATION OF ^{238}U NEUTRON CROSS-SECTIONS FOR THE ENDF/B FILE*

T.A. PITTERLE
Westinghouse Electric Corporation,
Advanced Reactors Division,
Madison, Pa.,
United States of America

Presented by S. Pearlstein

Abstract

EVALUATION OF ^{238}U NEUTRON CROSS-SECTIONS FOR THE ENDF/B FILE.

Neutron cross-section data for ^{238}U between 0.00001 eV and 15 MeV, available through August 1969, have been evaluated in order to revise the ^{238}U file in the United States ENDF/B data library. Neutron data reevaluated are σ_t, σ_γ, σ_f, $\sigma_{nn'}$, σ_{ne}, σ_n, $\sigma_{n,2n}$, $\sigma_{n,3n}$ and $\bar{\nu}$. Emphasis in this paper is placed on the capture, fission and inelastic cross-section evaluations and existing experimental discrepancies. Resolved resonance parameters were re-evaluated to include more p-wave resonances and recent radiation width measurements which lead to an average radiation width of 0.0235 eV for this evaluation. Measurements reported since the previous evaluation have resulted in the following qualitative changes to the data relative to the previous ENDF/B ^{238}U evaluation: the capture cross-section is lower by 5 - 15% between 1 and 100 keV, the fission cross-section is consistently lower by 4 - 8%, the inelastic scattering cross-section, particularly for excited levels above 0.15 MeV, is lower by 5 - 15% between 1.3 and 2 MeV, and the total cross-section differs by up to ± 10% above 100 keV. Uncertainties of at least 10% still exist in the capture cross-section below 150 keV. While the ^{238}U/^{235}U fission ratio is reasonably well known, uncertainties in the absolute ^{238}U fission cross-sections are relatively large owing to discrepancies in the ^{235}U fission cross-section above 2 MeV. Large discrepancies in the ^{238}U data have not been adequately resolved by recent measurements and the existing uncertainties, particularly for the capture cross-section, are probably the most important data problem for fast-reactor applications at the present time.

1. INTRODUCTION

Neutron cross section data for ^{238}U between 0.00001 eV and 15 MeV, available through August 1969, have been evaluated for Version II of the United States ENDF/B data library. Neutron data evaluated are resolved and average unresolved resonance parameters, σ_t, σ_γ, σ_f, $\sigma_{nn'}$, σ_{ne}, σ_n, $\sigma_{n,2n}$, $\sigma_{n,3n}$, and $\bar{\nu}$. Data for cross section below 0.5 eV and for $\bar{\nu}$ were taken from evaluations by members of the Cross Section Evaluation Working Group for the ENDF/B File. New measurements and revised normalizations of older measurements lead to significant changes in the evaluated neutron cross sections relative to the previous ^{238}U ENDF/B evaluation [1]. Consistent normalization of the experimental data, particularly for capture and fission measurements relative to ^{235}U fission, has been stressed in this evaluation. Emphasis, in this paper, is on the capture, fission and inelastic scattering evaluations and current experimental discrepancies. Existing uncertainties in the neutron data, particularly for the capture and fission cross sections, are considerably larger than desired for fast reactor analysis. Additional details on the present evaluation will be published as WARD-4181-1.

* Work supported by the US Atomic Energy Commission.

2. RESONANCE PARAMETERS

2.1 Resolved Resonances

Resolved resonance parameters were evaluated for 188 s-wave resonances and 210 p-wave resonances up to 3.9 keV based on measurements by Garg [2], Glass [3], and Asghar [4] as well as other data given in BNL-325 [5]. The assignments of resonances to p-waves follow principally the recommendations of Glass based on resonance size and shape considerations. Uncertainties in the s- and p-wave resonance assignments can influence the average resonance parameters obtained as:

$D = 20.8$ eV, $S_o = 0.90 \times 10^{-4} eV^{-1/2}$, $S_1 = 1.6 \times 10^{-4} eV^{-1/2}$ and $\Gamma\gamma = 23.5$ meV.

Due to uncertainties in the p-wave assignments, and large experimental errors on the small neutron width measurements, the p-wave strength function of 1.6×10^{-4} $eV^{-1/2}$ is not considered reliable and was not used in this evaluation.

The radiation widths, $\Gamma\gamma$, determined by Glass [3] for 62 resonances yield an average $\Gamma\gamma = 19.1 \pm 2$ meV and show large fluctuations from resonance to resonance. Glass used the neutron widths of Garg [2] in analyzing his measurements of capture areas for radiation widths. Since this procedure could lead to inconsistencies, the Glass values were given low weighting in the determination of the average $\Gamma\gamma = 23.5$ meV which was obtained as an average over 21 resonances each having at least two measured values with consistency within the error bounds. This average $\Gamma\gamma$ was used for all other resonances, thus neglecting the measurements of Glass above 1 keV.

Glass's $\Gamma\gamma$ data indicate considerable variation from resonance to resonance and an approximate tendency toward lower $\Gamma\gamma$ at higher energies up to the 2.0 keV upper limit of the measurements. The structure in $\Gamma\gamma$ found by Glass below 800 ev is not found in the data of Asghar. Glass notes that the radiation width fluctuations could be considered as arising from the total radiation widths consisting of a constant plus a fluctuating part from high energy gamma-ray transitions which vary in intensity from resonance to resonance. To test potential implications of this mechanism, statistical calculations were made using a constant $\Gamma\gamma = 12$ meV plus a fluctuating $\Gamma\gamma = 11.5$ meV having a chi-squared distribution with $\nu = 4$. It was found that this distribution leads to effects of less than 2% on infinite dilution cross sections and 1 - 10% effects on the temperature derivative (related to reactor Doppler coefficients) of the self-shielded cross sections, when compared to totally constant $\Gamma\gamma$ calculations. At this time, it is felt that additional verification of the magnitudes and fluctuations of the radiation widths found by Glass is required before incorporating these data into evaluated data files.

A possible mechanism for apparent fluctuations in the measured radiation widths could be random overlap of s- and p-wave resonances. Such overlap would contribute little to the neutron width of the s-wave resonance but could make a significant contribution to the measured capture area and hence the radiation width. Durston and James [6] have examined random overlap between s- and p-wave resonances in U-238 using a set of resonances up to 2.0 keV generated by random sampling from statistical distributions. Based on examination of the 100 s-wave and 269 p-wave resonance sample, about 20% of the p-wave resonances would be partially hidden (within 1.6 eV of an s-wave resonance as found for the closest s- and p-wave resonances in the Glass data) by s-wave resonances thus contributing to larger capture areas for the s-wave resonances. About 11% of the s-wave resonances could be mistaken for p-wave resonances or small enough to be hidden by p-wave resonances while only

around 1 - 2% of the p-waves would likely be mistaken for s-waves. These effects indicate that the s-wave level spacing of 20.8 eV obtained from the resolved resonances could be overestimated by approximately 7%.

Since many p-wave resonances and perhaps a few s-wave resonances below 3.9 keV have not been resolved, it is necessary to estimate the capture cross section contribution from the missed levels. Based on average level spacing considerations, it appears reasonable for the background cross section estimation, to assume that all s-wave resonances up to 3.91 keV and all p-wave resonances up to 600 eV have been resolved. The background capture cross section was then estimated as approximately the difference between the p-wave cross section obtained from a statistical calculation (D = 20.8 eV, $S_o = 0.9 \times 10^{-4}$, $S_1 = 2.0 \times 10^{-4}$, and $\Gamma\gamma$ = 23.5 meV) and that calculated from the p-wave parameters. Table I gives the contributions to the net σ_γ (column 6 of Table I) along with the results of the statistical calculations and the measurements of Moxon [7]. Agreement of the net σ_γ with the Moxon data is about 5% except for the intervals 0.5 - 0.6 and 0.9 - 1.0 keV where the Moxon data are lower by 20 - 25%. Both of these intervals have large resonances within 10 eV of the top of the interval so that resolution differences could be significant in the Moxon data comparisons for these intervals. Table I separates the resolved p-wave resonances into contributions from the largest 62 resonances and the remaining 148 resonances. To reduce computation time in applying the ENDF/B file to reactor applications, only the 62 large p-wave resonances were included as resonance parameters in the ENDF/B file while a calculated pointwise capture cross section is included for the remaining 148 resonances.

2.2 Unresolved Resonance Parameters

Unresolved resonance parameters are required within the ENDF/B file for use in resonance self-shielding calculations for reactor applications. Current ENDF/B formats permit energy variations in the strength functions in order to permit adjustment to gross structure and shape in low resolution experimental data without introduction of large negative, background cross sections. For this evaluation, the p-wave strength function was adjusted to fit the evaluated smooth (n, γ) cross section (see section 3.2) at energies between 3.9 and 45.0 keV. Other parameters assumed constant in the fitting were $S_o = 0.9 \times 10^{-4}$, $S_2 = 1.5 \times 10^{-4}$ and $\Gamma\gamma$ = 23.5 meV. The fitting procedure yielded an average $S_1 = 1.97 \times 10^{-4}$ with fluctuations of up to 10%. The nuclear radius to be used with this strength function for penetration factor calculations is 0.84×10^{-12}cm. If a nuclear radius of 0.9184×10^{-12}cm, as required to obtain the desired potential scattering cross section of 10.6 barns, were used in the fitting, the resulting S_1 would be about 1.65×10^{-4}.

3. NEUTRON CROSS SECTIONS

3.1 Cross Sections Below 5.0 eV

Cross sections from 10^{-5} to 5.0 eV were obtained from an evaluation by Leonard [8] conducted concurrently with the present evaluation above 5.0 eV. The 0.0253 eV capture cross section is 2.72 b. based primarily on the measurement of Bigham [9]. The shape of the cross sections is deduced from the positive energy levels of the current evaluation, four negative levels including one with parameters determined by the simultaneous requirement of the normalization value of 2.72 b. and a fit to the total cross section data of Bollinger [10] in the region 1 - 5 eV, and a potential scattering cross section of 10.6 b. Resonance parameters for the 6.67 eV resonance which strongly influences the thermal cross sections are Γn = 1.50 meV and $\Gamma\gamma$ = 25.6 meV.

TABLE I. CONTRIBUTIONS TO (n, γ) CROSS-SECTION IN RESOLVED ENERGY RANGE

ΔE keV	Resolved Resonances			Background Estimation	Net σ_γ	Statistical Calculation			Measurements of Moxon [7]+
	s-wave 188 Res.	p-wave 62 Res.*	p-wave 148 Res.			s-wave	p-wave	Total σ_γ	
0.0-0.1	45.65	0.008	0.019	0.0	45.68				
0.1-0.2	16.35	0.015	0.027	0.0	16.39	10.5	0.101	10.60	
0.2-0.3	8.05	0.156	0.060	0.0	8.27	7.08	0.130	7.21	
0.3-0.4	2.52	0.036	0.056	0.0	2.61	5.41	0.153	5.56	
0.4-0.5	2.17	0.109	0.064	0.0	2.34	4.41	0.173	4.58	
0.5-0.6	4.47	0.074	0.057	0.0	4.60	3.73	0.191	3.92	3.85 ± .13
0.6-0.7	3.02	0.112	0.075	0.017	3.22	3.25	0.206	3.46	3.00 ± .11
0.7-0.8	1.39	0.082	0.077	0.065	1.61	2.89	0.221	3.11	1.71 ± .08
0.8-0.9	2.64	0.084	0.070	0.090	2.88	2.60	0.234	2.83	2.78 ± .10
0.9-1.0	3.68	0.062	0.085	0.092	3.92	2.37	0.246	2.62	3.12 ± .11
1.0-2.0	1.55	0.087	0.078	0.138	1.85	1.61	0.275	1.89	1.77 ± .08
2.0-3.0	1.01	0.028	0.007	0.320	1.37	1.04	0.360	1.40	1.37 ± .07
3.0-3.9	0.83	0.015	0.0	0.380	1.23	0.773	0.397	1.17	1.16 ± .06

* Approximately the 62 largest p-wave reduced neutron widths.

+ A normalization of 1.09 not given in this column, was applied to Moxon data in this evaluation. See Section 3.2.

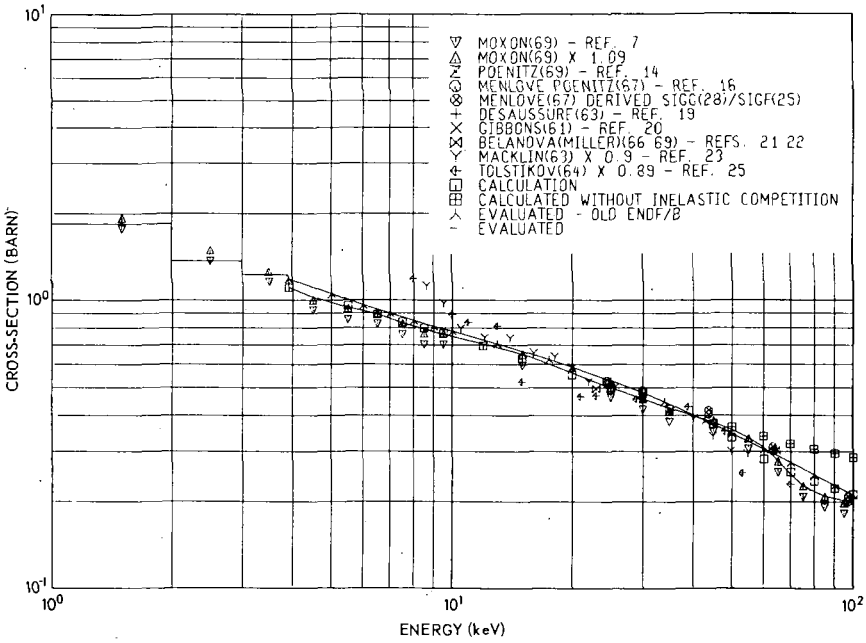

FIG. 1. Comparison of experimental and evaluated capture cross-sections between 1 and 100 keV.

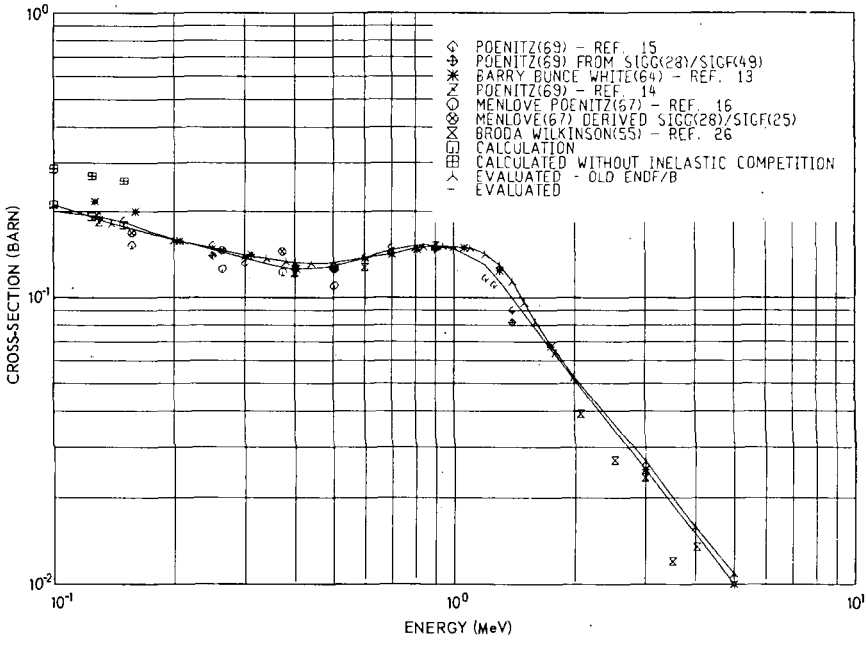

FIG. 2. Comparison of experimental and evaluated capture cross-sections between 0.1 and 10 MeV.

TABLE II. SUMMARY OF 30-keV (n, γ)-DATA USED IN EVALUATION

Experiment	Type and Value of Measurement	Adjusted σ_γ*
Poenitz (1969)[14]	$\sigma_\gamma^{28}/\sigma_f^{25}$ = .205 ± .008	0.459 ± .022
de Saussure (1963)[19]	$\sigma_\gamma^{28}/\sigma_a^{25}$ = .150 ± .012	0.461 ± .040
Gibbons, et. al. (1961)[20]	σ_γ^{28}= .473 ± .05 relative In = .763	0.473 ± .06
Menlove (1968)[16]	Absolute .473 ± .015	0.473 ± .02
Belanova (Miller)(1966, 1968)[21, 22]	Absolute σ_γ^{28}(23 keV) = .495 ± .04, $\frac{\sigma_\gamma(30)}{\sigma_\gamma(23)}$ = .91	0.450 ± .04
Macklin (1963)[23]	Relative Ta - Davey [12] = .507 ± .051	0.507 ± .08
Moxon, Chaffee (1966)[24]	Relative $B^{10}(n,\alpha)$, σ_γ^{28} = .403 ± .062	0.403 ± .062
Moxon (1969)[7]	Relative $B^{10}(n,\alpha)$, σ_γ^{28} = .418 ± .029	0.418 ± .029
Average	Reciprocal Weighting by (uncertainty)^2	0.456

*Normalization Values

σ_f^{25} = 2.24 ± .05

σ^{25} = .372 ± .03

$\sigma_{n,\alpha}^{B10}$ = 3.41 ± .07

3.2 Capture Cross Section

In Version II of the ENDF/B file, emphasis has been placed on consistent normalization of the experimental data with ^{235}U fission from the evaluation of Davey [11] adopted as the primary standard cross section. In addition, the $^{10}B(n, \alpha)$ cross section, as by Moxon [7], has been used for normalization in this evaluation. Davey [12] has reported a ^{238}U capture evaluation emphasizing ^{235}U fission normalization. The selection of reliable experimental data in the present evaluation follows closely that of Davey [12] although differing somewhat in final data adjustments.

Above 100 keV, the majority of accurate capture measurements are relative to ^{235}U fission, such as Barry [13], Poenitz [14,15], while the Menlove and Poenitz [16] data can be placed relative to ^{235}U fission by use of the fission cross section of Poenitz [17] obtained by the same experimental techniques. These four sets of data were normalized to the ENDF/B [11,18] ^{235}U fission cross section and are shown in Figure 1. In general, the data are in agreement within experimental errors ($\sim$5%) between 0.2 and 1.0 MeV. The discrepancy of up to 15% between Barry [13] and Poenitz [15] above 1.0 MeV is significant as it could extend beyond 1.5 MeV where the only reliable data is that of Barry. The discrepancy of 10 - 15% between 0.12 and 0.16 MeV is particularly notable in that the lower limits of the data at these energies is required for consistent extrapolation to the capture data below 100 keV (Moxon [7]) measured relative to $^{10}B(n, \alpha)$.

Below 100 keV, the experimental data on ^{238}U capture is highly discrepant as shown in Figure 2. The most accurate shape measurement of the cross section is that of Moxon [7] between 0.5 and 100.0 keV. This measurement, relative to $^{10}B(n, \alpha)$, is also one of the most accurate measurements with a quoted accuracy of 3 - 6%. Other measurements of significant accuracy ($\lesssim$ 10%) are those given in Table II at 30 keV with additional measurements by de Saussure [19] and Gibbons [20] at 64 keV and Menlove [16] at 24.4, 43.8, 63.3, and 97.3 keV. The latter measurements can at least be traced to ^{235}U fission normalization and tend to be 10 - 15% higher than the Moxon [7] data which alone supports very low capture cross sections. Similarly the Moxon data at 100 keV is lower than the evaluated cross section above 100 keV for which the ^{238}U capture/^{235}U fission ratio appears to be well established. Unfortunately, accurate ^{235}U fission/$^{10}B(n, \alpha)$ measurements, which could help to resolve the present discrepancies, are not available.

The relatively large number of 30 keV measurements permit a "best estimate" for further normalizations of the data. The most reliable 30 keV measurements, given in Table II, were averaged to obtain 0.456 b. for the 30 keV cross section. Data offering significant shape information, of which the Moxon data is clearly the most accurate, were normalized to 0.456 b. at 30 keV. For the Moxon data, the normalization factor is 1.09 and the evaluated curve is based primarily on the normalized Moxon data from 3.9 to 100.0 keV as shown in Figure 2.

The Moxon data shows a drop in the cross section above 50 keV most likely resulting from inelastic scattering competition from the 45 keV level. This drop in the cross section was examined by statistical calculations using the average parameters given in Section 2.2 plus inelastic widths estimated by assuming the inelastic strength function for each open channel to be the same as the corresponding p- and d-wave strength functions for elastic scattering. Chi-squared distributions for the inelastic widths were assigned using ν values equal to the number of open channels. Penetration factors for the inelastic widths were also obtained similarly to elastic widths but were calculated using the excess energy above the inelastic threshold. Results of the calculations both with and without inelastic scattering are shown in Figures 2 and 3. The statistical calculations confirm the magnitude of the drop in the cross section found

by Moxon above 45 keV although the relatively simple calculational model differs somewhat in the shape of the cross section.

3.3 Fission Cross Section

The most accurate ^{238}U fission data have been measured as $^{238}U/^{235}U$ fission ratios by Lamphere [27], Stein [28], and White and Warner [29]. Measurements by Smith et. al. [30] of absolute ^{238}U and ^{235}U fission cross sections have recently been revised by Hansen et. al. [31] on the basis of calculated scattering corrections to the original measurements. Fission ratios obtained from the Hansen data are shown with other ratio data in Figure 3. The original Lamphere data [27] have been decreased by 6%, following the recommendation of Davey [11], based on normalization to the more accurate (± 1%) measurements of Stein [28] at 1.5, 2.0, 2.5, and 3.0 MeV. In the overlapping energy range between 2.0 and 5.0 MeV, the ratios obtained from the Hansen data are in excellent agreement with the data of Stein. At 5.4 and 14.1 MeV, discrepancies between White [29] and Hansen are 5% and 3% respectively.

The fission ratio data were evaluated to obtain the curve given in Figure 3. Accuracy of the evaluated fission ratio is about 5% below 2 MeV, 2% between 2 and 5 MeV, and 5% between 5 and 15 MeV. The evaluated fission ratio was combined with the ENDF/B ^{235}U fission cross section [11,18] to obtain the ^{238}U fission cross section. Other ^{238}U fission measurements such as Kalinin and Pankratov [32] or the shape measurements of Henkel [33] and Pankratov [34] are not sufficiently accurate to resolve remaining discrepancies in the fission cross section.

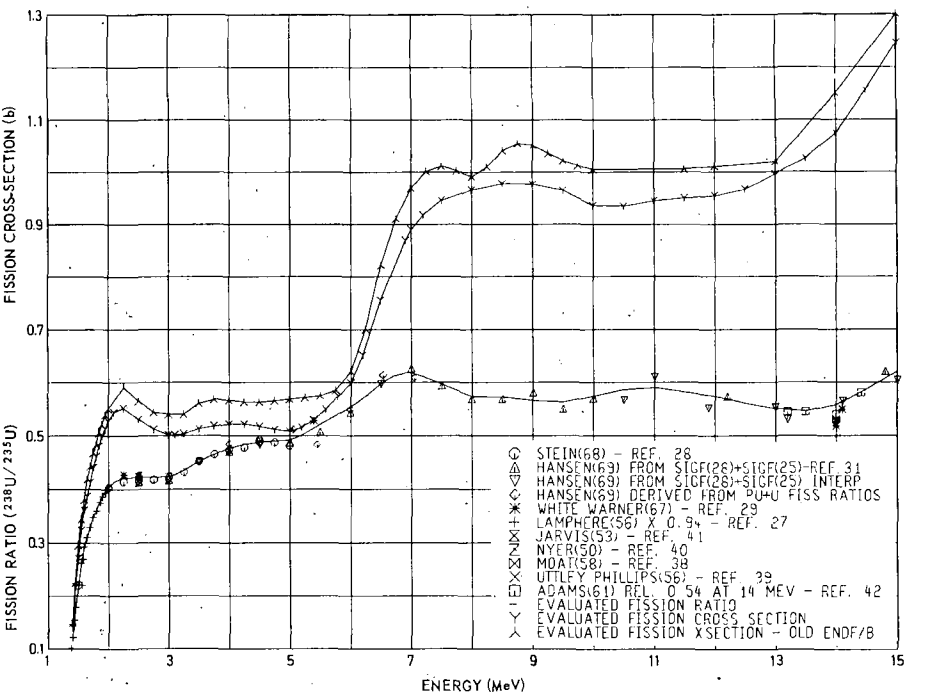

FIG.3. Comparison of experimental and evaluated fission ratio and of evaluated fission cross-sections.

An average of the evaluated fission cross section over the Watt spectrum for thermal ^{235}U fission yields 0.284 b. which is about 8% lower than experimental values of 0.304 ± 0.007 [35], 0.310 ± 0.004 [36], and 0.31 ± 0.01 [37]. The 14 MeV cross section in the present evaluation is 1.075 b. compared to an average value of 1.13 b. indicated by absolute measurements [38,39,40]. These comparisons, as well as numerous integral experiment analyses which yielded good agreement between calculation and experiment with about 5 - 10% higher fission cross sections than the present evaluation, tend to indicate that the presently evaluated fission cross section may be too low by 5 - 8%. A discrepancy of this size appears to be outside the range of uncertainty in the $^{238}U/^{235}U$ fission ratio and is likely, at least in part, due to an underestimation of the ^{235}U fission cross section, particularly above 2.5 MeV where the Hansen data [31] was used for the ENDF/B ^{235}U evaluation.

3.4 Inelastic Scattering Cross Section

Recent measurements of the ^{238}U inelastic scattering cross section by Smith [43] provide a check against the extensive measurements of Barnard [44] and other measurements by Smith [45], Cranberg [46] and Glazkov [47]. Smith [43] determined cross sections for 14 levels between 0.045 and 1.27 MeV with some measurements up to neutron energies of 1.69 MeV while Barnard reports cross sections for 22 levels between 0.045 and 1.47 MeV with measurements to 1.62 MeV neutron energy. Agreement between Smith [42] and Barnard is generally good for the first 6 levels at 0.0447, 0.148, 0.310, 0.681, 0.732 and 0.840 MeV. Experiment and evaluation are compared in Figure 4 for the 0.0447, 0.148 and 0.680 MeV levels.

Smith obtained cross sections for a level at 0.945 MeV which represents the sum of the 0.939 and 0.968 MeV levels measured by Barnard. A level found by Smith at 0.995 Mev corresponds to the 1.006 MeV level of Barnard. Experimental and evaluated data for this level, the sum of the 0.945 and 0.995 levels of Smith and the sum of the 0.939 + 0.968 + 1.006 MeV levels of Barnard are compared in Figure 4. For these levels, as well as higher energy levels, Barnard's data consistently indicates higher cross sections above 1.5 MeV than Smith's data.

Above 1.0 MeV, the Smith and Barnard data are generally more consistent as sums over levels than for individual levels. Evaluation of the sums over levels was performed simultaneously with evaluation of the individual levels to maintain consistency. Figure 4 compares the sum of the Smith data for 1.04 + 1.085 + 1.115 + 1.165 MeV with the Barnard data for 1.047 + 1.076 + 1.123 + 1.15 + 1.19 MeV and with evaluated levels for 1.045 + 1.080 + 1.12 + 1.17 MeV. Also shown are the Smith data for a 1.22 MeV level compared to the sum of the 1.210 and 1.246 MeV levels of Barnard and the evaluation for a 1.22 MeV level.

Smith measured a cross section of 0.21 ± .086 at 1.69 MeV for a level at 1.27 MeV while Barnard obtained cross sections at 1.62 MeV for levels at 1.272, 1.313, 1.361, 1.401, 1.437 and 1.47 MeV. Barnard's values for the 1.272 and 1.313 MeV levels are 0.12 ± .02 and 0.16 ± .02 b. respectively so that Smith's 1.27 MeV value appears to be a partial resolution of the Barnard's 1.272 + 1.313 MeV levels. For this evaluation, cross sections were estimated for levels above 1.22 MeV at 1.27, 1.31, 1.36, 1.40 and 1.45 based primarily on the lower limits of the 1.62 MeV values of Barnard.

The total inelastic cross section up to 1.55 MeV neutron energy is treated as completely resolved and defined by the sum of 19 level cross sections. Above 1.55 MeV, the inelastic cross section is obtained as the difference between the evaluated non-elastic cross section and the capture, fission, (n,2n) and (n,3n) cross sections. No reliable measurements of either total inelastic or non-elastic cross sections have been made below the 2.0 MeV measurements of Batchelor [48] who measured elastic

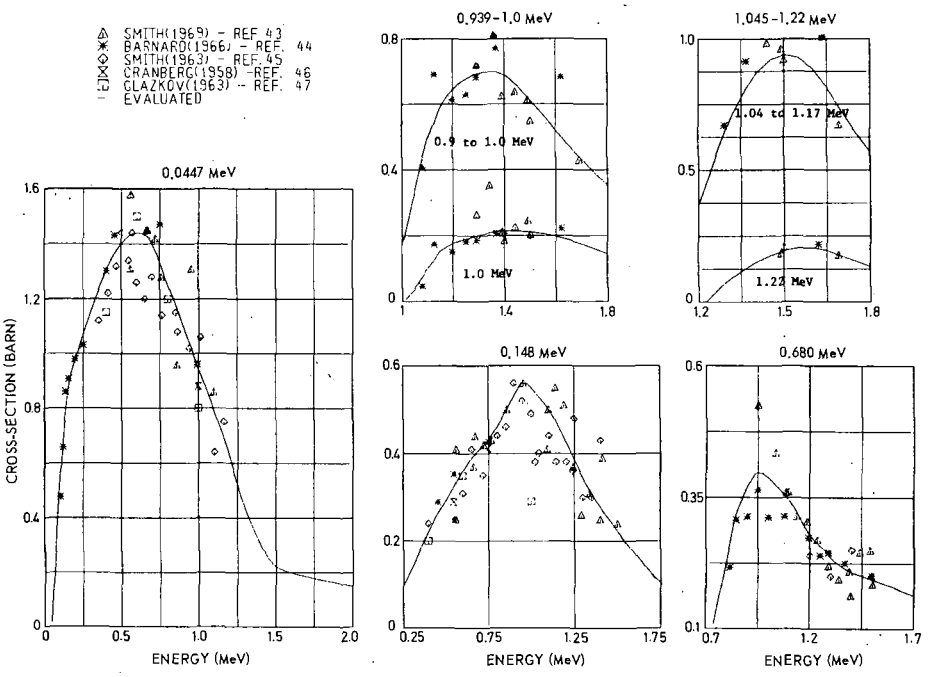

FIG. 4. Comparison of experimental and evaluated level excitation cross-sections.

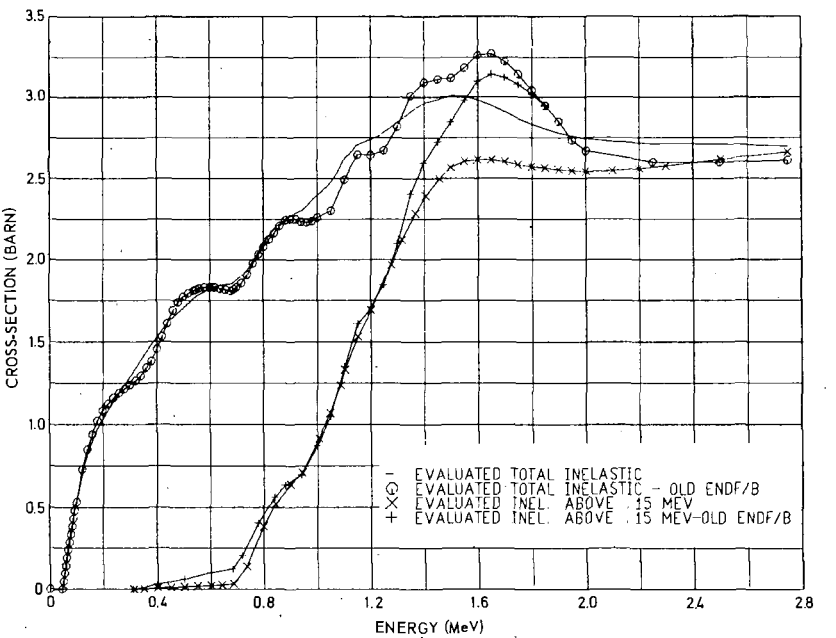

FIG. 5. Comparison of evaluated inelastic scattering cross-sections.

scattering and inelastic scattering for excitation of levels between 0.57 and 1.38 MeV. From a total cross section of 7.45 b., Batchelor determined a non-elastic cross section of 3.38 b. and an inelastic cross section for levels above 0.57 MeV of 2.79 b. It is not clear from Batchelor's paper [48] whether the total cross section of 7.45 b. was measured or evaluated as no uncertainties are assigned to this value. In this evaluation, non-elastic and inelastic cross sections of 3.08 b. and 2.50 b. were obtained using Batchelor's elastic scattering cross section of 4.07 ± 0.2 b. and evaluated total (7.15 b.), capture and fission cross sections. The evaluated inelastic cross section for levels above 0.57 MeV was then smoothly extrapolated (assuming the total compound reaction cross section to be nearly constant in this energy range) above 1.55 MeV to obtain a value of 2.54 b. at 2.0 MeV. With this procedure, the peak in the inelastic cross section near 1.6 MeV found in many previous ^{238}U evaluations, reference 49 for example, is not found in this evaluation. However, the principal cause for the reduction in the peak inelastic cross section is lower weighting of the 1.62 MeV measurements of Barnard [44] in this evaluation.

The total inelastic cross section including levels below 0.15 MeV is highly sensitive to extrapolation of the 0.0447 and 0.148 MeV levels above the last measured values at 1.15 and 1.5 MeV respectively. Optical model calculations including direct interaction effects (references 50, 51, for example) indicate that the direct interaction contributions to excitation of these levels could lead to a net cross section of the order of 0.5 b. above 2.0 MeV. Assessment of a direct interaction cross section of this magnitude would require detailed comparisons with measured scattering angular distribution which has not been done in the present evaluation. For reactor applications of the inelastic data, the separation of elastic scattering and direct interactions for the first two levels is not important provided, of course, that direct interaction contributions are assigned to level excitations rather than statistical secondary distributions. At this time, it is felt that direct interaction contributions as large as 0.5 b. above 2.0 MeV are not sufficiently verified and the cross sections for the 0.0447 and 0.148 MeV levels were extrapolated to zero at 3.0 and 2.5 MeV, respectively.

Figure 5 compares the present evaluation and previous ENDF/B evaluation [1] (based on Schmidt [49]) for the total inelastic cross section and the cross section for excitation of levels above 0.15 MeV. The primary difference in the evaluations is the reduction in this evaluation of the high energy level excitation between 1.3 and 2.1 MeV. In addition, the 0.148 MeV level cross section is up to 20% higher between 0.9 and 1.3 MeV in the present evaluation.

The secondary distribution for the statistical inelastic scattering is represented by a Maxwellian distribution with temperature $\theta = (E/a)^{1/2} = 0.206\ E^{1/2}$ based on a fit to the measurements of Batchelor [48].

3.5 Total Cross Section

The evaluated total cross section is based primarily on the measurements of Uttley [52] between 6.5 keV and 8 MeV, Whalen [53] between 0.1 and 1.5 MeV, and Foster [54] between 2.2 and 15 MeV along with the measurements of Henkel [55] and Batchelor [48]. Figure 6 compares experimental data with the present and previous ENDF/B evaluations for the total cross section.

3.6 Non-elastic Cross Section

The non-elastic cross section up to 1.55 MeV was obtained as a summation of the capture, fission and inelastic scattering cross sections. Between 1.55 and 2.0 MeV, the non-elastic cross section for

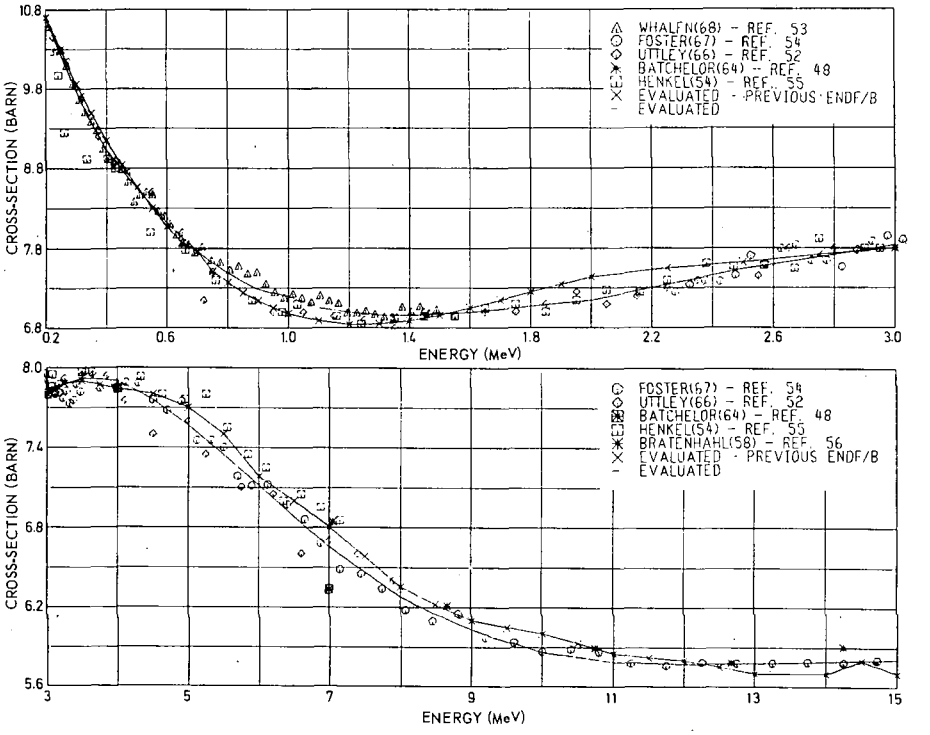

FIG. 6. Comparison of experimental and evaluated total cross-sections.

levels above 0.15 MeV was smoothly extrapolated through a value of 2.54 b. at 2.0 MeV as discussed in Section 3.4. Above 2.0 MeV, the evaluation is based primarily on the measurements of MacGregor [57], Degtyarev [58], Batchelor [48], Beyster [59], and Bethe [60]. The present evaluation is in good agreement above 2.5 MeV with the previous ENDF/B evaluation [1] and the evaluation of Schmidt [49] with maximum deviations of about 3%.

3.7 (n,2n) and (n,3n) Cross Sections

Measurements of the (n,2n) cross section by Knight [61] and Graves [62] were corrected by Barr [63] leading to adjustments of +10% to the data of Knight and ± 10% to the data of Graves. However, the normalization of the corrected data is unknown. For this evaluation, ratios relative to ^{238}U fission were obtained using the fission measurements of Smith, Henkel and Nobles [30] and renormalized to the presently evaluated fission cross section. These renormalized data along with the 14 MeV measurement of Mather [64] form the basis of the present evaluation. Figure 7 compares the experimental data with the present evaluation and the previous ENDF/B evaluation [1].

The evaluated (n,3n) cross section is based primarily on the 14 MeV measurement of Mather [64] and is shown in Figure 7.

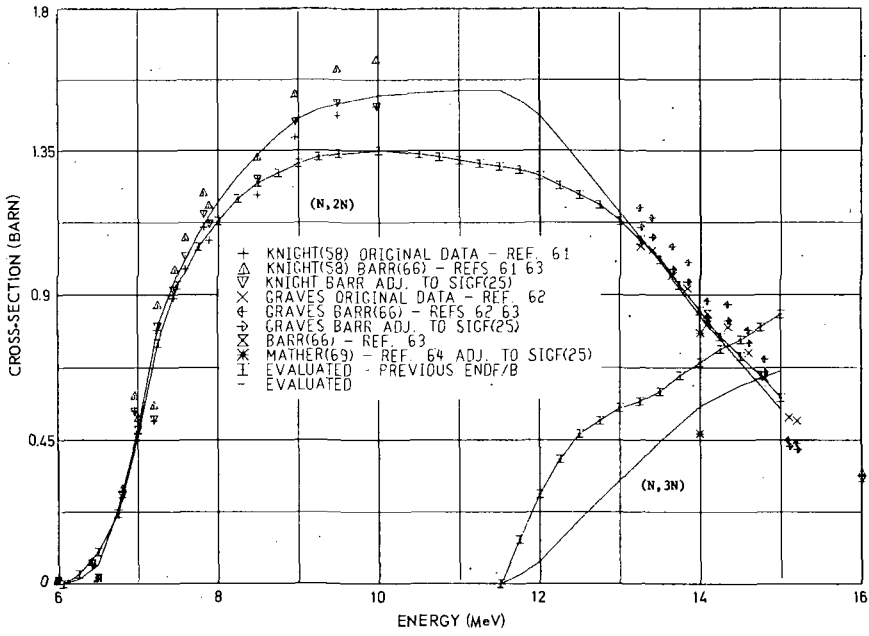

FIG. 7. Comparison of experimental and evaluated (2, 2N) and (N, 3N) cross-sections.

3.8 Elastic Scattering

The cross section for elastic scattering was obtained as the difference between the total and non-elastic cross sections. In general, the agreement with other evaluations such as references 1 and 49 is within about 5% although somewhat larger differences arise between 1.5 and 2.5 MeV due to variations in the separation between elastic scattering and inelastic scattering to the 0.0447 and 0.148 MeV levels.

3.9 Average Number of Neutrons per Fission - $\bar{\nu}$

The average number of total neutrons per fission is given by $\bar{\nu}$ = 2.337 + 0.1521E(MeV) based on an evaluation by Drake [65] which included the recent measurements of Soleilhac [66]. Normalization for $\bar{\nu}$ is based on the 1969 evaluation of Hanna, et. al. [67].

4. CONCLUSIONS

The most important differences between the present evaluation and the previous ENDF/B evaluation [1] or the evaluation of Schmidt [49] are: the capture cross section is lower by 5 - 15% between 1 and 100 keV; the fission cross section is consistently lower by 4 - 8%; and the inelastic scattering cross section for levels above 0.15 MeV is lower by 5 - 15% between 1.3 and 2.0 MeV. Integral testing of the Version I ENDF/B data tends to support reductions in the capture and inelastic cross sections similar to or larger than the present evaluation. However, the reductions in the fission cross section relative to Version I data of more than a few percent do not appear to be supported by integral testing.

Estimates of the current uncertainties in the evaluated data are: capture--about 5 - 10% below 2 keV, 10% between 2 and 150 keV, 5% between 0.15 and 2 MeV, and 10% above 2 MeV; fission--5% below 2.5 MeV and 4 - 8% above 2 MeV although the accuracy of the $^{238}U/^{235}U$ fission ratio is known to about 2% between 2 and 5 MeV; total inelastic scattering--5% below 1 MeV, 5 - 10% between 1 and 6 MeV, 10 - 15% between 6 and 12 MeV and 50% above 12 MeV; total--approximately 5% over the entire energy range; non-elastic--typically about 5 - 10%; (n,2n) and (n,3n)--about 10% although the accuracy would be near 5% with better knowledge of the fission cross section and experimental details on the (n,2n) measurements; elastic scattering--typically about 10%; and $\bar{\nu}$--about 2 - 3%.

The present uncertainties in the ^{238}U data, particularly for the capture and fission cross sections, do not meet the accuracy requirements of a few percent required for reliable fast reactor analysis. Uncertainties in the capture cross section between 1 and 200 keV is one of the most important data problems for fast reactor applications.

REFERENCES

[1] WITTKOPF, W. A., ROY, D. H., LIVOLSI, A. Z., ENDF-103(BAW-316), May, 1967.
[2] GARG, J.B., et. al., Phy. Rev. 134 5B (1964) 985.
[3] GLASS, N. W., et. al, Neutron Cross Sections and Technology (Proc. Conf. Washington, D. C., 1968) NBS Special Pub. 299 1 (1968) 573.
[4] ASGHAR, M., CHAFFEY, C. M., MOXON, M. C., Nuc. Phy. 85 (1966) 305.
[5] GOLDBERG, M. D., et. al., BNL-325 2nd Ed. Supp. 2 Vol. III (1965).
[6] DURSTON, C. JAMES, G. D., private communication (1970).
[7] MOXON, M. C., AERE-R6074 (1969).
[8] LEONARD, B. R., private communication (1969).
[9] BIGHAM, C. B., DURHAM, R. W., UNGRIN, J., Can J. Phys. 47 (1969) 1317.
[10] BOLLINGER, L. M., et. al., Phy. Rev. 105 (1957) 661.
[11] DAVEY, W. G., Nucl. Sci. Engng. 32 (1968) 35.
[12] DAVEY, W. G., Nucl. Sci. Engng. 39 (1970) 337.
[13] BARRY, J. F., BUNCE, J., WHITE, P.H., J. Nucl. Energy A/B 18 (1964) 481.
[14] POENITZ, W. P., Trans. Am. Nucl. Soc., 12 (1968) 279.
[15] POENITZ, W. P., Nucl. Sci. Engng. 40 (1970) 383.
[16] MENLOVE, H. O., POENITZ, W. P., Nucl. Sci. Engng. 33 (1968) 503.
[17] POENITZ, W. P., Neutron Cross Sections and Technology (Proc. Conf. Washington, D. C., 1968) NBS Special Pub. 299 1 (1968) 503.
[18] ALTER, H., DUNFORD, C. L., AI-AEC-MEMO-12916 (1970).
[19] DESAUSSURE, G., et. al., ORNL-3360 (1963) 51.
[20] GIBBONS, J. H., et. al., Phys. Rev. 122 (1961) 182.
[21] BELANOVA, T. S., et. al., J. Nucl. Energy 20 (1966) 411.
[22] MILLER, L. B., POENITZ, W. P., Nucl. Sci. Engng. 35 (1968) 295.
[23] MACKLIN, R. L., GIBBONS, J. H., PASMA, P. J., WASH-1046 (1963) 88.
[24] MOXON, M. C., CHAFFEY, C. H., TRDWP/P8 (1966).
[25] TOLSTIKOV, V. A., SHERMAN, L. E., STAVISKII, Y. Y., J. Nucl. Energy A/B 18 (1964) 599.
[26] BRODA, E., WILKINSON, D. H., BR-574 reported by B. ROSE, AERE NP/R 1743 (1955).
[27] LAMPHERE, R. W., Phys. Rev. 104 (1956) 1654.
[28] STEIN, W. E., SMITH, R. K., SMITH, H. L., Neutron Cross Sections and Technology (Proc. Conf. Washington, D. C., 1968) NBS Special Pub. 299 9 (1968) 627.
[29] WHITE, P. H., WARNER, G. P., J. Nucl. Energy 21 (1967) 671.
[30] SMITH, R. K., HENKEL, R. L., NOBLES, R. A., Bull. Am. Phys. Soc. 2 (1957) 196.

[31] HANSEN, G., MCGUIRE, S., SMITH, R. K., Private communication from L. STEWART (LASL) - 1969.
[32] KALININ, S. P., PANKRATOV, V. M., Second Int. Conf. Peaceful Uses of Atomic Energy, 16, UN, New York (1959) 136.
[33] HENKEL, R. L., LA-2122 (1957).
[34] PANKRATOV, V. M., J. Nuc. Energy A/B 18 (1964) 215.
[35] RICHMOND, R., quoted by W. D. ALLEN and R. L. HENKEL, Progress in Nuclear Energy, Series I, Permagon Press 2 (1957) 38.
[36] LEACHMAN, R. B., SCHMITT, H. W., J. Nucl. Energy 4 (1957) 38.
[37] NIKOLAEV, M. N., GOLUBEV, V. I., BONDARENKO, I. I., J. Expt. Theoret. Phys. 7 (1958) 517.
[38] MOAT, A., quoted by K. PARKER in AWRE 0-79/63 (1963).
[39] UTTLEY, C. A., PHILLIPS, J. A., AWRE-NP/R 1996 (1956).
[40] NYER, W., LAMS-938 (1950).
[41] JARVIS, G. A., LA-1571 (1953).
[42] ADAMS, B., BATCHELOR, R., GREEN, T. S., Reactor Sci. Tech. 14 (1961) 85.
[43] SMITH, A. B., Private communication (1969).
[44] BARNARD, E., et. al., Nuc. Phys. 80 (1966) 46.
[45] SMITH, A. B., Nuc. Phys. 47 (1963) 633.
[46] CRANBERG, L., LEVIN, J. S., Phys. Rev. 109 (1958) 2063.
[47] GLAZKOV, N. P., Atomnaya Energiya 14 (1963) 400.
[48] BATCHELOR, R., GILBOY, W. B., TOWLE, J. H., Nuc. Phy. 65 (1965) 236.
[49] SCHMIDT, J. J., KFK 120, Part I (1966).
[50] DUNFORD, C. L,, Nuclear Data for Reactors, Vol. I (1966) 429.
[51] PRINCE, G., Private communication (1969) (See paper CN 26/91, this meeting).
[52] UTTLEY, C. A., Private communication (1967).
[53] WHALEN, J., private communication A. B. SMITH (1965).
[54] FOSTER, D. G., unpublished.
[55] HENKEL, R. L., et. al., Phys. Rev. 94 (1954) 141.
[56] BRATENAHL, A., et. al., Phys. Rev. 110 (1958) 921.
[57] MACGRAGOR, M. H., BOOTH, R., BALL, W. P., Phy. Rev. 130 (1963) 1471.
[58] DEGTYAREV, Y. G., Atomnaya Energiya 19 (1965) 456.
[59] BEYSTER, J. R., et. al., Phys, Rev. 104 (1956) 1319.
[60] BETHE, H. A., et. al., LA-1939 (1959).
[61] KNIGHT, J. D., SMITH, R. K., WARREN, B., Phys. Rev. 112 (1958) 259.
[62] GRAVES, CONNER, FORD, WARREN, unpublished, quoted by KNIGHT.
[63] BARR, D., unpublished (1966), private communication L. STEWART (1969).
[64] MATHER, D. S., PAIN, L. F., AWRE-0-47/69 (1969).
[65] DRAKE, M., et. al., private communication (Nov. 1969).
[66] SOLEILHAC, M., FREHAUT, J., GAURIAU, J., J. Nucl. Energy, 23 (1969) 257.
[67] HANNA, G. C., et. al., Atomic Energy Review, Vol. VII, No. 4, IAEA (1969).

A SIMULTANEOUS EVALUATION OF THE FISSION CROSS-SECTIONS OF ^{235}U, ^{239}Pu AND ^{238}U AND THE CAPTURE CROSS-SECTION OF ^{238}U IN THE ENERGY RANGE 100 eV TO 20 MeV

M.G. SOWERBY, B.H. PATRICK
UKAEA, AERE Harwell, Didcot, Berks,
United Kingdom

Abstract

A SIMULTANEOUS EVALUATION OF THE FISSION CROSS-SECTIONS OF ^{235}U, ^{239}Pu AND ^{238}U AND THE CAPTURE CROSS-SECTION OF ^{238}U IN THE ENERGY RANGE 100 eV TO 20 MeV.

Among the most important cross-sections required for the calculation of fast reactor properties are the fission cross-sections of ^{235}U, ^{239}Pu and ^{238}U and the capture cross-section of ^{238}U. Many experimental determinations of these quantities have been made and several evaluations have been performed. These evaluations in general suffer from the following defects:

(a) account is taken only of the cross-section measurements or their ratio relative to the ^{235}U fission cross-section and hence all the data are not used to full advantage;
(b) it has always been assumed that the average fission cross-sections have a smooth energy dependence in the keV region. Recent measurements indicate that this is not in general true;
(c) recommended values have usually been obtained from a curve drawn by hand through the data and so tend to be subjective.

In order to overcome these defects a simultaneous evaluation of the cross-sections and their ratios is being performed. The experiments providing the data have been critically examined so that doubtful experiments can be detected and their results eliminated or have their errors increased. For this purpose an abstract of each experiment has been prepared and examples of these are given. Account has been taken in the evaluation of the structure observed in the keV fission cross-sections. To make the evaluation objective the cross-sections are found by a least-squares minimization procedure which has the advantage of allowing new data to be rapidly incorporated.

1. INTRODUCTION

Among the most important cross-sections required for the calculation of fast reactor properties are the fission cross-sections of U-235, Pu-239 and U-238 and the capture cross-section of U-238. There are now many measurements of these quantities and their ratios over the energy range of interest for fast reactor design and evaluations of the data are required for two purposes. The first is to provide the best values of the cross-sections so that data files can be constructed for use in reactor calculations. The second reason is to see that the accuracy achieved in the experiments satisfies the requests of the reactor physicists.

There have been a number of evaluations of these cross-sections and in general these have tended to show that the required accuracies have not been met. Recently there have been a number of new measurements of fission and capture cross-sections which need to be considered. In addition the $^{10}B(n,\alpha)$ cross-section which is the standard for many measurements below 30 keV has been shown [1] to depart from 1/v energy dependence and structure has been

observed in the U-235 fission cross-section [2] in the keV energy region. In the light of these factors it has become clear that new evaluations are necessary.

Previous evaluations have in general suffered from at least one of the following defects. It has been normal to consider only one cross-section at a time. For example the fission cross-section of U-235 is evaluated first and then the other cross-sections are taken in turn. However, since the measurements of cross-sections and their ratios form a highly inter-related set, this method does not take full advantage of the data. Again the best values of any cross-section have usually been taken from a curve drawn by hand through the data and so tend to be subjective. With this technique it is difficult to update satisfactorily an existing evaluation as new data become available and to take account adequately of the assigned weights of a large number of experiments.

In this work we are attempting to remedy these defects by making a simultaneous evaluation of the cross-sections and their ratios over the energy range 100 eV to 20 MeV. In this the best curve through the data will probably be obtained by using a modified version of the cubic spline fitting programme of Horsley et al. [3]. However, this paper is essentially only a progress report and this stage has not yet been reached.

The remainder of the paper will be divided into four sections. In the first of these the techniques of the evaluation will be briefly considered. This will be followed by two sections dealing with the energy regions below and above 30 keV respectively. The final section will summarise the conclusions that have been reached to date.

2. TECHNIQUE OF EVALUATION

As there are usually several measurements of a cross-section or ratio covering a given energy region and there are often serious discrepancies between their results, it is necessary to examine critically the experiments so that doubtful ones can be detected and their results eliminated or increased errors assigned. For this purpose an abstract of each experiment is being prepared using a standardised format and examples of these are given in the appendix. Abstracts are produced by at least two of the authors in each case and the use of these makes comparison of experiments much easier.

The energy regions above and below 30 keV have essentially to be considered separately because below 30 keV most of the data are continuous time-of-flight data while above, the values are mainly "spot points". (Of course, in any evaluation the cross-section curve must have no discontinuity at 30 keV). In the energy range below 30 keV true average cross-sections over specified energy intervals can be obtained. There are very few measurements of cross-section ratios in this energy region and essentially the cross-sections can be evaluated independently. Above 30 keV true average cross-sections cannot be obtained because measurements are made with monoenergetic neutron sources. Therefore the data have to be handled in a different way.

In this energy range there are in general measurements of several cross-sections and their ratios and hence the cross-sections are over determined. The procedure adopted is to take each cross-section or ratio and make a plot of the appropriate data and examples of these are shown in Figs. 1-3. Curves are then drawn through the data and the values of the cross-sections and ratios at given energies are extracted and reasonable

errors estimated. These data are then used as the starting values in the following minimisation procedure. A computer programme obtains the best values of the cross-sections (σ) at a given energy (E) by finding the minimum value of F(E) where F(E) is given by

$$F(E) = G(E) + H(E) \tag{1}$$

The value of G(E) is given by

$$G(E) = \sum \left(\frac{x_i - \sigma_i}{\Delta x_i} \right)^2 \tag{2}$$

where the sum is taken over all the directly measured cross-sections and x_i and Δx_i are the starting value and error of the i^{th} cross-section. The quantity H(E) is defined by

$$H(E) = \sum \left(\frac{R_{kl} - \sigma_k/\sigma_l}{\Delta R_{kl}} \right)^2 \tag{3}$$

where the sum is taken over all available combinations of the ratios of the cross-sections σ_k and σ_l and R_{kl} and ΔR_{kl} are the starting value and error of the ratio.

3. CROSS-SECTIONS BELOW 30 keV

In this section we shall consider measurements below 30 keV and discuss some of the associated difficulties.

Almost all data in this energy range are measured relative to the $^{10}B(n,\alpha)$ or $^{6}Li(n,\alpha)$ cross-sections. It has generally been assumed that the $^{10}B(n,\alpha)$ cross-section varies as 1/v. Recent measurements of the ratio of the $^{6}Li(n,\alpha)$ to $^{10}B(n,\alpha)$ cross-sections and their total and scattering cross-sections have shown [1] that this is not true. It is therefore necessary to correct the data for the revised cross-sections which are now known to better than $\pm 2\%$ over most of this energy range. It is also to be noted that many measurements of the incident neutron spectrum are made with copper-walled BF_3 counters and it is conceivable that the resonances in the total cross-section of copper could affect the efficiency. Indeed in their measurements, Sowerby et al. [1] observed a 4% decrease in the efficiency averaged over the energy range 532 eV to 612 eV due to the resonance at 577 eV. It is therefore necessary for further experimental work on this problem to be done to check that data based on flux measurements using copper bodied $^{10}BF_3$ counters are reliable. Until this has been done it is probably wise to down weight the affected experiments.

Measurements of the fission cross-section of U-235 and Pu-239 providing data in the energy range 100 eV to 30 keV are usually normalised in the energy range near 10 eV. Some experiments are normalised at thermal energies but these are in a minority. Table I gives the integrated fission cross-sections in the energy ranges 5-10 eV and 10-15 eV for the important experiments. When all experiments are effectively normalised to 582 b at 0.0253 eV the spread in data between 5 and 10 eV means that the best primary normalisation of the low energy U-235 fission cross-section measurements is not known to better than $\sim \pm 3\%$. Further work is obviously desirable. Although the situation appears to be better in the case of Pu-239, there are only two acceptable measurements [11, 12] which give average cross-sections in the energy range 10 to 20 eV of 103.8 and 105.6 barns respectively.

TABLE I. NORMALIZATION OF MEASUREMENTS OF THE ^{235}U FISSION CROSS-SECTION

Experiment	Normalisation	$\int_{E_1}^{E_2}\sigma(E)dE$ (barns.eV) E_1=5 eV E_2=10eV	E_1=10eV E_2=15eV
Van Shi-Di et al. [4]	582b at 0.0253 eV	256.3	205.9
De Saussure et al. [5]	$\int_{0.45}^{10}\sigma(E)dE/E$ = 127.9 as given by Bowman et al.	281.4	216.7
Bowman et al. [6]	577.1 b at 0.0253 eV	292.1	220.0
Brooks et al. [7]	η = 2.084 at 0.06 eV	258.0	197.7
Shore and Sailor [8]	Effectively to 582b at 0.0253 eV	272.4	
Michaudon [9]	to Shore and Sailor between 8 and 10 eV	277.8	218.7
Deruytter et al. [10]	580.2b at 0.0253 eV	282.1	214.4

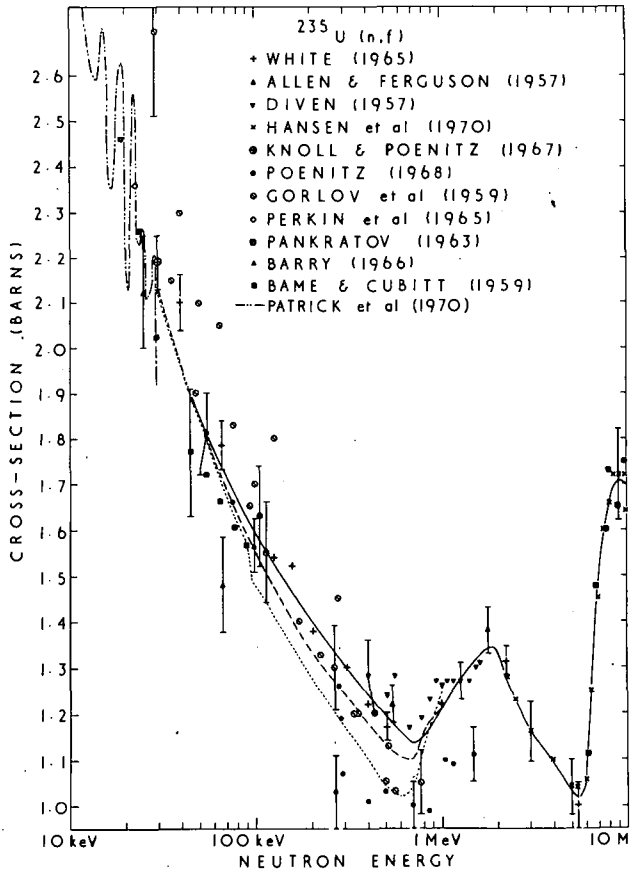

FIG.1. ^{235}U fission cross-section.

TABLE II. ^{238}U CAPTURE CROSS-SECTION AT 30 keV

Experiment	Energy (keV)	Cross-section (mb)	Comments
Moxon [17]	30 ± 8	425 ± 31	
Hanna and Rose [18]	30 ± 8	375 ± 51	Flux from $^{7}Li(p,n)$ reaction obtained from ^{7}Be associated activity
Gibbons et al. [19]	30 ± 8	473 ± 47	
Menlove and Poenitz [20]	30 ± 8	492 ± 17	Relative to Au(n,γ)
		473 ± 15	Flux from $^{7}Li(p,n)$ reaction obtained from ^{7}Be associated activity
Belanova [21]	30	427 ± 39	Corrected value of Miller and Poenitz [22]. Cross-section extrapolated to 30 keV using shape data of Moxon [17]
Mean value		468 ± 10	(Internal Error)
		± 13	(External Error)

Recent high resolution measurements of the U-235 fission cross-section [2,13,14] have shown that there is pronounced structure up to at least 166 keV. In Fig. 1 the data of Patrick et al. [2] in the energy range 10 to 30 keV are shown; the plotted curve has been renormalised upwards by 4.5% to give agreement with our provisional evaluated cross-section in this energy range. The fluctuations in the cross-section, which are probably due to intermediate structure in sub-threshold fission, make it important that the energy spectrum of the incident neutrons in any fission cross-section determination must be known precisely. For instance the mean energy of neutrons produced by an Sb-Be source, which is 22.8 keV with an uncertainty of ±1 keV [15], happens to lie in the region of very pronounced structure. The average cross-section over the source spectrum varies by ~8% when the mean energy changes from 22.5 to 24 keV. This is unfortunate since it makes the measurement of Perkin et al. [16], which is the most accurate in this energy region, of limited value until the Sb-Be neutron source spectrum is better known.

The measurements of the U-238 capture cross-section are mainly concerned with the energy range above 30 keV and it is convenient to normalise relative data at 30 keV where there are a number of absolute determinations. Some of the values that have been used to obtain absolute data at 30 keV are measured relative to the U-235 fission cross-section but because of the presence of the structure it is necessary to ignore these. Table II gives the values at or near 30 keV which at the present time we consider to be reliable. The estimated best value is 468±13 mb and the best cross-section curve below 30 keV is provided by the data of Moxon normalised to this value.

4. CROSS-SECTIONS ABOVE 30 keV

Fig. 1 shows our accepted U-235 fission cross-section data from 20 keV to 10 MeV. In the case of Allen and Ferguson [23] only the absolute values at 550 keV and 1.8 MeV were accepted. Their relative measurements were made

with a multiplate chamber with a spacing of 5 mm between the plates and it is possible that the efficiency of the chamber could change if the angular distribution of the fission fragments altered as a function of neutron energy. The data of Henkel [24] have been omitted because of uncertainties in the various corrections which have been made since the results were first published. The results of Kalinin and Pankratov [25] have been neglected because of uncertainties in the available values due to later changes [26] in the efficiency of their long counter. Since the main purpose of the experiment of Smirenkin et al. [27] was to investigate correlations between structure in the angular anisotropy of fission fragments and the fission cross-section rather than to make an accurate measurement of the cross-section, their results have been neglected.

Also plotted in Fig. 1 are the data of Barry [28] and Bame and Cubitt [29] which are more conventionally thought of as giving information on the $^{6}Li(n,\alpha)$ cross-section. There is no doubt that the $^{6}Li(n,\alpha)$ cross-section is known to much higher accuracy than the fission cross-section of U-235 and therefore we have chosen to use these data as determinations of the U-235 fission cross-section based upon the $^{6}Li(n,\alpha)$ cross-section of Uttley and Diment [30].

A search of the literature revealed only three acceptable absolute determinations of the fission cross-section of Pu-239 below 14 MeV. These are the value at 22.8 keV measured by Perkin et al. [16] and values at 550 keV and 1.5 MeV obtained by Allen and Ferguson. Almost all other data on this cross-section are measurements relative to the fission cross-section of U-235. There are two experiments which have measured the ratio of the cross-section to $^{238}U(n,f)$. This means that we cannot use the simultaneous evaluation technique for this cross-section below 1 MeV and it would be desirable to have further absolute measurements in this region.

In the case of the measurements of the ratio of the Pu-239 to U-235 fission cross-sections, we have accepted all known data without alteration except for those of Gilboy and Knoll [3]. The lack of consistency between the results from their Methods A and B suggests that the data should be down weighted.

Since we have not yet completed our assessment of the available fission cross-section data for U-238, we shall concentrate on the region below 1 MeV in this paper.

The experiments which have measured the capture cross-section of U-238 can be divided into two classes; those which are relative to the U-235 fission cross-section and others. We are still in the process of assessing these and so far have tended to agree with the assessment of Davey [32]. However at the present time we are rejecting the values of Macklin et al. [33,34] and Bergquist [35] because they were measured relative to tantalum, iodine and silver respectively. The presently accepted data are shown in Fig. 2.

The solid lines drawn in the figures are used to provide the starting values of the cross-sections and ratios for use in the minimisation procedure discussed in Section 2. In drawing the curves the following points should be noted. The high resolution measurements of $^{235}U(n,f)$ below 30 keV discussed in the previous section suggest that the cross-section may be falling quite rapidly above 30 keV. This is supported by the data of Barry and Bame and Cubitt and is therefore in disagreement with the 40 keV and perhaps the 67 keV values of White. Although the presence of structure is now well established up to ~100 keV, at the time of writing there are no

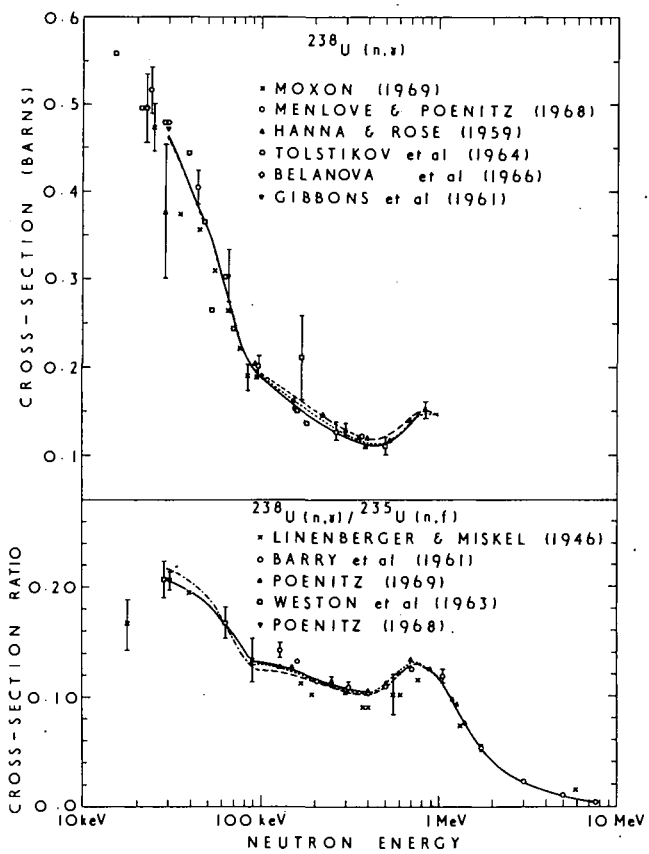

FIG.2. ^{238}U (n, γ) and ^{238}U(n, γ)/^{235}U(n, f).

detailed cross-section data above 30 keV and clearly there is a great need for further measurements. Around 500 keV the data of Poenitz [36] are significantly lower than the data of White [37] and Allen and Ferguson. This may be due to the structure in the cross-section at 30 keV where the data of Poenitz are normalised. The solid curve was therefore drawn giving greater weight to the White values. In the case of the ^{239}Pu(n,f) to ^{235}U(n,f) ratio data, the values of White et al. [32] and Gilboy and Knoll disagree with the data of Pfletschinger and Kappeler [39] and Allen and Ferguson. The data of Pfletschinger and Kappeler show no sign of the known structure in the ^{235}U(n,f) cross-section, particularly in the region 70 to 120 keV, whereas those of Gilboy and Knoll and Allen and Ferguson show the expected shoulder in this region. The data of Gilboy and Knoll appear to be low below 30 keV where the cross-section ratio is reasonably well known from other data and this suggests that their data may require to be renormalised upwards by ~10%. We believe that the best ratio values probably lie between the data of White et al. and those of Pfletschinger and Kappeler. The data involving the ^{238}U(n,γ) cross-section appear to be very consistent except for those of Barry et al. [40] between 100 and 200 keV.

Because of the structure in the ^{235}U(n,f) cross-section, it is doubtful that the simultaneous evaluation below 100 keV has great value at present.

TABLE III. PERCENTAGE ERRORS IN THE STARTING VALUES OF THE CROSS-SECTIONS AND RATIOS

Energy (keV)	U-235 (n,f)	Pu-239 (n,f)	$\frac{^{239}Pu(n,f)}{^{235}U\ (n,f)}$	U-238 (n,γ)	$\frac{^{238}U(n;\gamma)}{^{235}U(n,f)}$	Au-197 (n,γ)	$\frac{^{197}Au(n,\gamma)}{^{235}U(n,f)}$
30	10	10	5	3	10		
40	10	10	5	4	10		
50	10	10	5	4	10		
60	7	10	4	4	10		
70	7	10	4	4	10		
80	7	10	4	4	10		
90	7	10	4	4	10		
100	5	10	4	4	7	4	5
200	5	10	4	6	4	4	5
300	5	10	4	6	3	4	5
400	5	10	4	6	3	4	5
500	5	10	4	6	3	4	5
600	5	10	4	6	3	4	5
700	5	10	4	6	3	4	5
800	5	10	5	6	3	4	5
900	5	10	5	6	3	4	5
1000	5	10	5	6	3	4	5

However, for the sake of completeness, we have made a simultaneous evaluation assuming smooth cross-sections. The dashed curves shown in the figures are the results of the minimisation procedure discussed in Section 2, using the errors given in Table III. The only significant departures from the starting values occur in the fission cross-section of U-235 which is required to be consistently lower and in the $^{238}U(n,\gamma)$ cross-section which is raised in the 200-700 keV region. This suggests that the $^{235}U(n,f)$ cross-section may be even lower. The amount by which the programme will alter any cross-section or ratio is governed to a large extent by the error attributed to the particular quantity. Accordingly we increased the error in the $^{235}U(n,f)$ cross-section to 10% at all energies and found that the computed values decreased even further while the $^{238}U(n,\gamma)$ cross-section values came into better agreement with their starting values. The values of the $^{235}U(n,f)$ cross-section resulting from the minimisation procedure thus tend to agree with the data of Poenitz who suggested in his paper that a similar conclusion can be drawn from measurements of the $^{197}Au(n,\gamma)$ cross-section and the $^{197}Au(n,\gamma)/^{235}U(n,f)$ ratio.

We have, therefore, examined the data on $^{197}Au(n,\gamma)$ and Fig. 3 shows the accepted values of both the cross-section and its ratio to $^{235}U(n,f)$. By including these data in the minimisation procedure the dotted curves on Figs. 1-3 are obtained and it is found that the U-235 fission cross-section values are required to be reduced even further.

From the above discussion it can be seen that there is strong evidence that between 30 keV and 700 keV the fission cross-section of U-235 is 10 to 15% lower than given by the measurements of White and Allen and Ferguson.

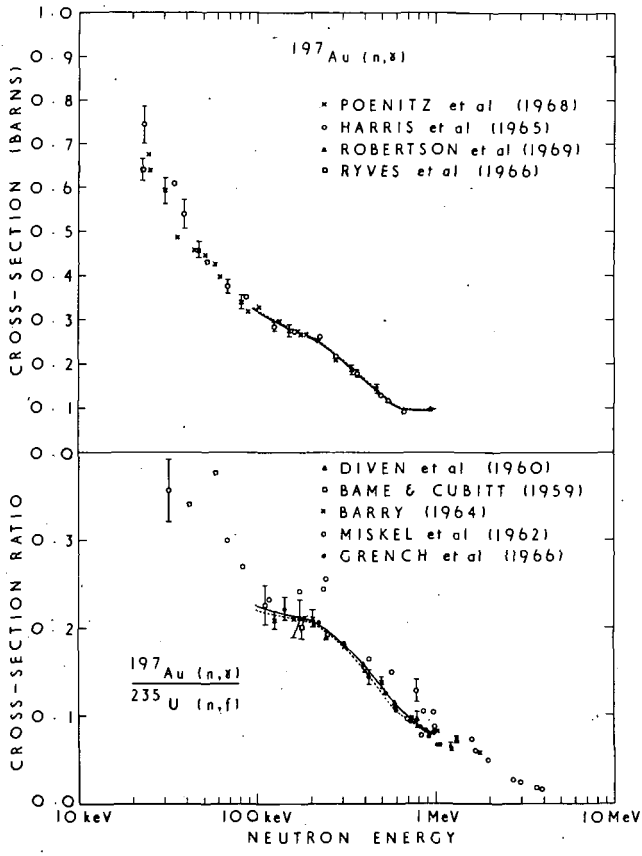

FIG.3. $^{197}Au(n, \gamma)$ and $^{197}Au(n, \gamma)/^{235}U(n, f)$.

This conclusion is supported between 300 and 700 keV by the direct measurements of Poenitz using a grey neutron detector. Between 30 keV and ~100 keV the situation is complicated by the existence of structure. However, from 100 keV to 700 keV it is not possible to obtain values which simultaneously fit all the available data. The measurements on $^{197}Au(n,\gamma)$ and $^{238}U(n,\gamma)$, which togethe with ratio measurements suggest that the $^{235}U(n,f)$ cross-section is low, are made using a variety of neutron flux measuring techniques. The relevant experiments are listed below, together with their accuracy at 500 keV:

(a)	$^{238}U(n,\gamma)$ Menlove and Poenitz [20]	± 10%	Grey neutron detector
(b)	$^{238}U(n,\gamma)$ Hanna and Rose [18]	± 7%	Proton recoil
(c)	$^{197}Au(n,\gamma)$ Poenitz et al [41]	± 6%	Grey neutron detector
(d)	$^{197}Au(n,\gamma)$ Harris et al. [42]	± 3.5%	Associated activity

These data are supported below 100 keV by the data of Moxon ($^{238}U(n,\gamma)$) and Kompe [43] ($^{197}Au(n,\gamma)$), at 22.8 keV by the shell transmission measurement ($^{238}U(n,\gamma)$) of Belanova [21] and the determinations ($^{197}Au(n,\gamma)$) using calibrated sources of Ryves et al. [44] and Robertson et al. [45] at 22.8 and 966 keV. The variation of the efficiency of the grey detector as a

function of neutron energy is usually calculated. However, Poenitz [46] has made measurements which show that the calculated curve is good to ~ ±2% below 600 keV.

The measurements of White and Allen and Ferguson, which at ~500 keV are accurate to ±2.5% and ±3.5% respectively, used the proton recoil technique to measure the neutron flux. Allen and Ferguson [47] checked the technique by calibrating a long counter using a proton recoil detector and calibrated neutron sources and found excellent agreement. It is interesting to note that the results of Barry [28] and Bame and Cubitt [29] tend to support the low values. Since these were measured relative to a cross-section which has a similar energy dependence, this might indicate that the discrepancy may be caused by low energy neutrons which would not be detected by a proton recoil detector. Both White and Allen and Ferguson used D.C. neutron beams and so did not have the advantage of the time-of-flight technique. Poenitz [48] in measuring the $^{239}Pu(n,f)/^{235}U(n,f)$ ratio using the time-of-flight technique has noted that integrating the counts over the whole time-of-flight range yields results which differ by up to 10% with the results of the time-of-flight peak only.

It is obvious from this discussion that further accurate measurements are required on $^{235}U(n,f)$ in the energy range 30 keV to 1 MeV and that these must use the time-of-flight technique or some equally good neutron energy selection technique. Since the present evaluation is not complete we do not at this time need to select the best value of the U-235 fission cross-section. However, the values of the $^{239}Pu(n,f)$ and $^{238}U(n,\gamma)$ cross-sections depend upon the choice. The U-235 fission cross-section is not known to better than ±10% between 30 keV and 700 keV at the present time and the uncertainties for $^{239}Pu(n,f)$ (from 30 keV to 700 keV) and $^{238}U(n,\gamma)$ (above 100 keV) must be similar. Below 100 keV the $^{238}U(n,\gamma)$ curve does not depend so strongly on the fission data and the cross-section is known to 3-4%. It is therefore recommended that further absolute and accurate $^{239}Pu(n,f)$ and $^{238}U(n,\gamma)$ cross-section measurements should be made so that the effects of the structure in $^{235}U(n,f)$ are minimised and the simultaneous evaluation technique can be used to full advantage.

5. CONCLUSIONS

This paper reports the status of a simultaneous evaluation of the fission cross-sections of U-235, Pu-239, U-238 and the capture cross-section of U-238 in the energy range 100 eV to 20 MeV. Though the evaluation is not complete a number of important points can be made:-

(1) The U-235 fission cross-section is not as well known as previously thought (Hart [49] suggested ~±5% and ~±2% below and above 40 keV). There are uncertainties of ~±3% in the cross-section at ~10 eV where many experiments are normalised. Structure in the cross-section in the keV region makes the accurate value of Perkin et al. at 22.8 keV of little use until the energy spectrum of Sb-Be source neutrons is well known. It has also been shown that the $^{235}U(n,f)$ data of White and Allen and Ferguson are not consistent with the measurements of $^{238}U(n,\gamma)$ and the $^{238}U(n,\gamma)/^{235}U(n,f)$ ratio. By taking advantage of the simultaneous evaluation technique, it has been possible to include $^{197}Au(n,\gamma)$ data which have been obtained by a variety of techniques. Again it is found that the $^{235}U(n,f)$ cross-section values of White and Allen and Ferguson are not in agreement with the absolute measurements of $^{197}Au(n,\gamma)$ and those relative to $^{235}U(n,f)$. It appears therefore that the $^{235}U(n,f)$ measurements are the likely cause of the discrepancies between 100 keV and 800 keV and these are eliminated if the $^{235}U(n,f)$ cross-section is reduced by ~10% in this region.

It would also appear likely that the $^{235}U(n,f)$ cross-section between 30 keV and 100 keV is lower than is usually assumed. The time-of-flight measurements, which show structure in the keV region, suggest that the cross-section at 40 keV is lower than the value of White. Another indication that this may be the case arises from the $^{6}Li(n,\alpha)$ cross-section measurements of Barry and Bame and Cubitt made relative to the $^{235}U(n,f)$ cross-section. By reducing the $^{235}U(n,f)$ cross-section by ~10%, their $^{6}Li(n,\alpha)$ cross-section values agree well with the latest best estimate of this cross-section. In the light of these statements, we recommend that further accurate, absolute measurements of the $^{235}U(n,f)$ cross-section be made between 30 keV and 1 MeV using the time-of-flight technique.

(2) The present accuracy of evaluated $^{239}Pu(n,f)$ and $^{238}U(n,\gamma)$ cross-sections is intimately connected with the choice of the $^{235}U(n,f)$ cross-section curve. Above 30 keV virtually all our knowledge of the $^{239}Pu(n,f)$ cross-section arises from measurements of the ratio to the $^{235}U(n,f)$ cross-section. This ratio is probably known to ~3% above 100 keV but in view of the possible uncertainties in the $^{235}U(n,f)$ cross-section, there is clearly a great need for further absolute measurements of the $^{239}Pu(n,f)$ cross-section in the energy range 30 keV to 15 MeV. In the case of the $^{238}U(n,\gamma)$ cross-section, the situation is somewhat better. Up to 1 MeV, there are a number of measurements which do not rely on the $^{235}U(n,f)$ cross-section and these are in reasonable agreement. However, these data do not agree with the measurements relative to $^{235}U(n,f)$ using, for example, the cross-sections of White. Between 100 keV and 1 MeV, the $^{238}U(n,\gamma)$ cross-section is known to ~6% if we neglect the ratio data. Further work is clearly required to improve the accuracy of this cross-section.

6. ACKNOWLEDGEMENTS

The authors wish to express their sincere appreciation to Dr. D. S. Mather for his work and co-operation in the performance of this evaluation. The authors are also indebted to R. Batchelor, A. T. G. Ferguson, E. D. Pendlebury, E. R. Rae, J. S. Story and P. H. White for useful discussions and advice. The work of V. Sherriffs in collecting and processing the data is gratefully acknowledged.

7. REFERENCES

[1] SOWERBY, M. G., Patrick, B. H., Uttley, C. A. and Diment, K. M. CN-26/26 (1970).
[2] PATRICK, B. H., Sowerby, M. G. and Schomberg, M. G. UKAEA Report AERE - R 6350 (1970).
[3] HORSLEY, A., Parker, J. B., Parker, K. and Price, J. A. Nuc. Inst. and Meth. 62, 29 (1968).
[4] VAN SHI-DI, Van Yun-chan, Dermendzhiev, E. and Ryabov, Yu. A. Phys. and Chem. of Fission 1, 287 (IAEA Vienna) (1965).
[5] DE SASUSSURE, G., Gwin, R., Weston, L. W., Ingle, R. W., Fullwood, R. R. and Hockenbury, R. W. ORNL-TM-1804 (1967).
[6] BOWMAN, C. D., Auchampaugh, G. F., Fultz, S. C., Moore, M. S. and Simpson, F. B. UCRL-14606 (1966).
[7] BROOKS, F. D., Jolly, J. E., Schomberg, M. G. and Sowerby, M. G. UKAEA Report AERE - M 1670 (1966).

[8] SHORE, F. J. and Sailor, V. L. Phys. Rev. 112, 191 (1958).
[9] MICHAUDON, A. CEA - R 2552 (1964).
[10] DERUYTTER, A. J. and Wagemans, C. EANDC (E) 129 AL (1970).
[11] GWIN, R., Weston, L. W., De Saussure, G., Ingle, R. W., Todd, J. H., Gillespie, F. E., Hockenbury, R. W. and Block, R. C. ORNL-TM-2598 (1969).
[12] BOLLINGER, L. M., Cote, R. E. and Thomas, G. E. Proc. 2nd U.N. Int. Conf. P.U.A.E. 15, 127 (1958).
[13] VAN HEMERT, R. L. UCRL - 50501 (1968)
[14] BLONS, J. Private communication (1970).
[15] RYVES, T. B. and Beale, D. W. Int. J. App. Radiation and Isotopes 18, 204 (1967).
[16] PERKIN, J. L., White, P. H., Fieldhouse, P., Axton, E. J., Cross, P. and Robertson, J. C. J. Nuc. En. 19, 423 (1965).
[17] MOXON, M. C. UKAEA Report AERE - R 6074 (1969) and Private communication (1970).
[18] HANNA, R. C. and Rose, B. J. Nucl. En. 8, 197 (1959).
[19] GIBBONS, J. H., Macklin, R. L., Miller, P. D. and Neiler, J. H. Phys. Rev. 122, 182 (1961).
[20] MENLOVE, H. O. and Poenitz, W. P. Nuc. Sci. and Eng. 33, 24 (1968).
[21] BELANOVA, T. S., Van'kov, A. A., Mikhailus, F. F. and Staviskii, Yu. Ya. J. Nuc. En. 20, 411 (1966).
[22] MILLER, L. B. and Poenitz, W. P. Nuc. Sci. and Eng. 35, 295 (1969).
[23] ALLEN, W. D. and Ferguson, A. T. G. Proc. Phys. Soc. A70, 573 (1957).
[24] HENKEL, R. L. LA-1495 (1952), LA-2113 (1957) and LA-2122 (1957).
[25] KALININ, S. P. and Pankratov, V. M. Proc. 2nd Int. Conf. P.U.A.E. 16, 136 (1958).
[26] PANKRATOV, V. M. J. Nuc. En. 18, 215 (1964).
[27] SMIRENKIN, G. N., Nesterov, V. G. and Bondarenko, I. I. Atomnaya Energiya 13, 366 (1962).
[28] BARRY, J. F. Proc. Conf. on Neutron Cross-sections and Technology, Washington, p.763 (1966).
[29] BAME, S. J. and Cubitt, R. L. Phys. Rev. 114, 1580 (1959).
[30] UTTLEY, C. A. and Diment, K. M. To be published.
[31] GILBOY, W. B. and Knoll, G. KFK-450 (1966).
[32] DAVEY, W. G. Nucl. Sci. and Eng. 39, 337 (1970).
[33] MACKLIN, R. L., Gibbons, J. H. and Pasma, P. J. WASH-1046, p.88 (1963).
[34] MACKLIN, R. L., Lazar, N. H. and Lyon, W. S. Phys. Rev. 107, 504 (1957).
[35] BERGQUIST, I. Arkiv for Fysik 23, 425 (1963).
[36] POENITZ, W. P. Proc. 2nd Conf. on Neutron Cross-sections and Technology Washington, 1, 503 (1968).
[37] WHITE, P. H. J. Nucl. En. 19, 325 (1965).
[38] WHITE, P. H., Hodgkinson, J. G. and Wall, G. J. Phys. and Chem. of Fission 1, 219 (I.A.E.A. Vienna) (1965).
[39] PFLETSCHINGER, E. and Kappeler, F. Unpublished.
[40] BARRY, J. F., Bunce, J. and White, P. H. J. Nucl. En. 18, 481 (1964).
[41] POENITZ, W. P., Kompe, D. and Menlove, H. O. J. Nucl. En. 22, 505 (1968).
[42] HARRIS, K. K., Grench, H. A., Johnson, R. G. and Vaughn, F. J. Nuc. Phys. 69, 37 (1965).
[43] KOMPE, D. Nuc. Phys. A133, 513 (1969).
[44] RYVES, T. B., Robertson, J. C., Axton, E. J., Goodier, I. and Williams, A. J. Nuc. En. 20, 249 (1966).
[45] ROBERTSON, J. C., Ryves, T. B., Axton, E. J., Goodier, I. and Williams, A. J. Nuc. En. 23, 205 (1969).
[46] POENITZ, W. P. Nuc. Inst. and Meth. 72, 120 (1969).
[47] ALLEN, W. D. and Ferguson, A. T. G. Proc. Phys. Soc. 70A, 639 (1957).
[48] POENITZ, W. P. To be published (1969).
[49] HART, W. UKAEA Report AHSB(S)R-169 (1969).

APPENDIX

Abstract 1

Author	:	B. C. Diven
Reference	:	Phys. Rev. 105, 1350 (1957)
Establishment	:	Los Alamos
Quantities Measured	:	U-235 absolute σ_{nf} at 1.272 MeV. Variation of U-235 σ_{nf}, normalised at 1.272 MeV, at 13 points between 0.40 and 1.62 MeV
Accuracy	:	3.5% at 1.272 MeV, errors increase away from normalisation point to a maximum of 6.2%
Standard	:	H(n,n)
Neutron Source	:	2.5 MV Van de Graaff, T(p,n) gas target. Energy spread ±30 to 41 keV
Fission and Flux Detector	:	Fission foil and a proton radiator of same diameter mounted back to back in the same envelope so that fission fragments detected in an ionisation chamber and the proton recoils in a proportional counter. Outer container thin steel surrounded by Cd.
Sample Details	:	U-235 foils of thickness 38-95 $\mu g/cm^2$ on 0.013 cm Pt prepared by electroplating. Assay by quantitative electroplating and weighing. Relative masses checked by α-counting and foils compared with other standard foils at LASL. Proton radiators (12-120 $\mu g/cm^2$) of glycerol tristearate. Assay by weighing and hydrogen content analysed.
Flux Measurement:		Neutron flux deduced from proton recoil spectrum fitted according to methods of Rossi and Staub.
Experimental Arrangement	:	No information on target-counter geometry.
Corrections and Errors	:	The principal corrections and errors at 1.27 MeV are U-235 foil thickness and extrapolation to zero bias <2.0 ±1.1%; angular distribution of fragments (C. of M. motion only) 0.6 ± 0.1%; error in extrapolating proton recoil spectrum to zero bias ± 2.6%; error in weight of radiator and fitting proton recoil curves ±1.5%; correction for thickness of radiator 5.0 ± 0.5%; hydrogen contamination of proportional counter gas (Expt) 4 ± 0.5%; room background (Expt) 1.3 ± 0.2%; counter scattering (Expt) 1.3 ± 0.4%; error in assay of fission foils ±1%; composition of proton radiator ±0.5%; correction for scattering in U-235 foil backing and increasing neutron path length in radiator 0.5 ± 0.3%.
Authors Comments:		A generous estimate of the error associated with the extrapolation of the recoil proton pulse height distribution has been allowed.
Abstractors Comments	:	The advantage of this experiment in that the flux and fissions are measured simultaneously at the same position is somewhat offset by the inability to interchange the foil and radiator. Although the correction for the extrapolation of the recoil proton pulse height distribution is not given it appears to be ~30% and the error estimate of ±2.6% does not appear to be "overgenerous".

Abstract 2

Authors	:	P. H. White, J. G. Hodgkinson and G. J. Wall
Reference	:	Phys. and Chem. of Fission 1, 219 (IAEA Vienna) (1965).
Establishment	:	A.W.R.E. Aldermaston
Quantities Measured	:	Ratio of σ_{nf} for U-233, U-234, U-236, Np-237, Pu-239 and Pu-241 to σ_{nf} U-235.
Energy Range	:	40 to 505 keV, 3 to 6 points for each element.
Accuracy	:	U-233 2.2%, U-234 4-16%, U-236 10-50%, Np-237 2.5-8%, Pu-239 2.2%, Pu-241 2.5%.
Standard	:	Relative to U-235 σ_{nf}. Since measurements made at same nominal energies and with same foils and chambers as U-235 measurements of White [1] absolute measurements based on H(n,n) are deduced.
Neutron Sources	:	3 MV Van de Graaff, ^{7}Li(p,n), energy spread $\pm$7 to $\pm$10 keV.
Fission chamber	:	See White [1]
Samples	:	Thickness of foils mainly 0.5 mgm/cm^2, assay error typically 0.8% except Pu-239 (0.5%) and Pu-241 (2.0%). Isotopic composition and impurities in painted foils given in Table I.
Experimental Arrangement	:	Back to back fission chambers with one containing U-235 foil. Measurements made at 14 and 40 cm from source. Two runs with chambers interchanged. Background by $1/r^2$ technique.
Corrections and Errors	:	Foil thickness correction calculated, similar for all foils, error $\pm$0.5-1.0%; extrapolation to zero bias, error $\pm$0.2-0.5%; assay error see above; correction for flux and neutron energy variation across the foil <0.2% except threshold isotopes at 40 and 67 keV where <2%, error $\pm$0.1%; statistical error for both isotope and standard $\pm$0.7%; scattering in neutron source and fission chambers calculated. Since back to back geometry correction very small and neglected.
Authors Comment	:	Below 100 keV the present ratio measurements on U-233, Pu-239 and Pu-241 are consistently lower than previous results. A background of low energy neutrons may be the cause of this for U-233 and Pu-239 since they have a higher epithermal to fast fission cross-section ratio than U-235.
Abstractors Comments	:	It is to be noted that the U-235 σ_{nf} measurements of White [1] and these ratio determinations were made with different energy spreads. This means that, because of the structure in U-235, the absolute cross-sections deduced from the two sets of measurements particularly at the low energies may be in error.
Associated Papers	:	[1] WHITE, P. H. J. Nucl. En. 19, 325 (1965). [2] WHITE, P. H. and Warner, G. P. J. Nucl. En. 21 671 (1967). [3] PERKIN, J. L. et al. J. Nucl. En. 19, 423 (1965). [4] WHITE, P. H. Nucl. Inst. and Meth. 79, 1 (1970). [5] WHITE, P. H. Nucl. Inst. and Meth. 39, 256 (1966).

DISCUSSION

TO PAPERS IAEA-CN-26/80, 83, 34

W. P. POENITZ: First, I should like to make a remark concerning the evaluation of the capture cross-section for ^{238}U as presented in the first two papers. If one starts out with the intention of obtaining data consistent with the ^{235}U fission cross-section of White, as Pitterle did, then it is proper to use the measured ratios to obtain $\sigma_\gamma(^{238}U)$. For an independent evaluation, however, one should avoid reintroducing the White fission cross-section into the evaluation with each measured ratio. A more proper approach would be to evaluate first the ratio data and then to take the absolute values of the fission cross-section into account just once.

I have one further comment on the paper of Dr. Pitterle, which was presented by Dr. Pearlstein. In the evaluation of the ^{238}U fission cross-section the data measured by Lamphere have been multiplied by a factor of 0.94. This is a procedure which has been used by Dr. Davey. I am wondering what is the basis for this normalization. It seems to me that if there are no indications of errors, the proper course is to base the evaluation on the original values as presented. The only argument ever mentioned in support of a renormalization of the Lamphere data was a 6% discrepancy between the Lamphere and White data for ^{233}U. It would appear, however, that there is now satisfactory confirmation of the Lamphere data in the case of ^{233}U.

J. J. SCHMIDT: You seem to be suggesting that the Lamphere data are right and not the White data. Can you give the reasons for this?

W. P. POENITZ: There are four new sets of data $\sigma_f(^{233}U)/\sigma_f(^{235}U)$ which are now available. The measurements by Letho confirm the Lamphere data in the low-energy range, and those of Nesterov and Smirenkin are in very good agreement with them in the high-energy region. The new Karlsruhe measurements show very good agreement within error bars. And clearly, the very careful measurements by Meadows in connection with mass assignment and the use of the time-of-flight method for background-suppression agree very well with the Lamphere data. (This can be seen in Fig. 9 of my contribution to this Conference [CN-26/111].)

A. M. FABRY: I would like first to make a brief comment on Dr. Poenitz's remarks concerning the ^{238}U fission cross-section. If Davey's 6% reduction of the Lamphere data is inappropriate and the original results of Lamphere are therefore correct, they would agree with the integral measurements discussed in our paper (CN-26/39) without requiring the suggested error in neutron energy calibration below 2.5 MeV.

I would then like to ask a question of Dr. Sowerby: in using the $^{6}Li(n,\alpha)/^{235}U(n,f)$ data of Bame and Cubbitt (CN-26/34, Ref. [29]), have you made allowance for multiple scattering corrections in the glass scintillator used for the measurements? Such corrections would have the effect of raising the inferred values for the ^{235}U fission cross-section.

M. G. SOWERBY: We have not made multiple scattering corrections for these data. However, I think that the measurements were made not with a glass scintillator but with a LiI(Eu) crystal.

J. L. ROWLANDS: We have made a cross-section adjustment study starting from the preliminary recommendations of Dr. Sowerby: that is,

^{235}U and ^{239}Pu fission cross-sections about 10% to 15% lower than those in White's data, together with consistent ^{238}U capture data. The cross-sections were adjusted back to the White data. I understand that the integral data studies made by Professor Benzi and Dr. Küsters also support the White data. Unless some other cross-sections are changed to compensate for the reduction in fission cross-sections these are not consistent with the integral measurements. Would Dr. Sowerby like to comment on this? Are further cross-section revisions implied by his recommended data?

M. G. SOWERBY: We have not made any recommendations on cross-section values in our paper but we thought it was important that Mr. Rowlands should try the adjustment he described. Many measurements of capture cross-sections above 100 keV are based on the ^{235}U fission cross-section, and all these data should be modified before the adjustment procedure is carried out.

J. L. LEROY: I would like to ask the authors of the papers under discussion whether their evaluations of ^{238}U capture cross-sections lead to the same value.

M. G. SOWERBY: I have not had an opportunity to make a comparison as I saw the paper of Dr. Pitterle for the first time at the start of the present session.

P. H. RIBON: I have made such a comparison: Dr. Abramov gives a value of 0.20, Dr. Pitterle 0.21 and Dr. Sowerby 0.185. Thus, there is a discrepancy of 10-12%.

W. P. POENITZ: I think it is very obvious why different results have been obtained in the three evaluations of ^{238}U. If one performs an evaluation based on a certain ^{235}U fission cross-section one will obtain for ^{238}U a cross-section corresponding to the absolute input value.

Dr. Sowerby's paper shows the result of another possible approach: the simultaneous use of the absolute cross-sections of ^{238}U and ^{235}U necessarily carries with it a lowering of the input values of the ^{235}U fission cross-section.

J. J. SCHMIDT: The two most comprehensive transmission measurements on ^{238}U resonances at present available are those of Garg et al. from Columbia University and those performed recently at BCMN Geel, as reported at this Conference (CN-26/18). Both measurements cover something like 200 to 300 s-wave resonances and might thus be expected to give fairly similar values for the s-wave strength function. However, the values obtained differ by almost 20%; the Columbia value used in the evaluations of Dr. Abramov and Dr. Pitterle was about 0.91×10^{-4} and the BCMN Geel value was 1.09×10^{-4}. I wonder whether a systematic comparison of both measurements has been performed and whether someone could comment on this discrepancy.

W. HAVENS: The resonance parameters of ^{238}U measured at Geel were not available until this meeting so I have not had a chance to examine them in detail. I will certainly do this when I return home. A quick examination of the parameters indicates that they agree up to an energy of 1 keV but there are unexpectedly large disagreements above 1 keV. I would like to mention that the Columbia Γ_γ values were not published by Garg et al. in 1964 but were obtained by Rosen et al. using a self-detection technique and were published in 1960. We have just finished a velocity selector run at Columbia in which the transmission and capture of ^{238}U were measured with several sample thicknesses and several detectors. The data obtained look

very much better than any we have obtained previously and we hope to have a new better set of resonance parameters on ^{238}U in about one year.

A. I. ABRAMOV: It is possible that the differences in the strength functions to which Dr. Schmidt referred are due to incorrect identifications of individual resonances. In our paper it is shown that the transfer of 3-5 resonances from the group of s-wave levels to p-wave levels and vice versa significantly improves the agreement between the experimental results and the theoretical distributions for the mean distances and neutron widths, which is of course also reflected in the values of the corresponding strength functions.

D. W. COLVIN: I should like to try and connect the work of the previous speakers this morning with the last paper. In principle, I think the method of evaluation used by Sowerby is different from that described in the earlier papers. If I understood his paper correctly, he appears to be using his own types of program for compilation and evaluation and I am curious to know how much use he made of Data Centre files and the SCORE program. It would be interesting to hear his opinion of the usefulness of SCORE in evaluations of this type? By way of a comment, I think it is important to bear in mind that if evaluations of Sowerby's type (which he tells us are provisional) find their way into complete files of evaluations, great care must be exercised to avoid cross-correlations with other evaluations.

M. G. SOWERBY: We made a limited use of the Data Centre files and used the same program to get listings of some of the data. We do not think that SCORE is of much use for evaluations of our type.

K. H. BÖCKHOFF: I would like to come back to the total cross-section of ^{238}U. As indicated in the Geel paper (CN-26/18), our data may be considered as preliminary. Up to now, we have measured with only one sample thickness but we intend to extend the measurements to other thicknesses. At high energies there may be a prompt gamma effect on the results. These will be checked quantitatively in the near future. It is not to be expected, however, that this effect will explain the discrepancies.

EVALUATION OF NEUTRON NUCLEAR DATA FOR SEVERAL ACTINIDES IN THE ENERGY RANGE FROM THERMAL TO 10 MeV

B. HINKELMANN
Institut für Neutronenphysik und Reaktortechnik,
Kernforschungszentrum Karlsruhe,
Federal Republic of Germany

Abstract

EVALUATION OF NEUTRON NUCLEAR DATA FOR SEVERAL ACTINIDES IN THE ENERGY RANGE FROM THERMAL TO 10 MeV

This paper presents the results of a first evaluation of the still very scarce experimental data on $^{231}_{91}$Pa, $^{232}_{92}$U, $^{234}_{92}$U, $^{236}_{92}$U, $^{237}_{92}$U, $^{237}_{93}$Np, $^{238}_{93}$Np, $^{236}_{94}$Pu, $^{238}_{94}$Pu, $^{241}_{95}$Am, $^{242}_{96}$Cm. Radiative capture cross-sections, fission cross-sections, (n, 2n)-cross-sections and $\bar{\nu}$, the mean number of secondary neutrons per fission, have been evaluated and transformed into 5-group cross-sections.

1. INTRODUCTION

The following types of microscopic neutron nuclear data have been evaluated and transformed into 5-group cross-sections:

σ_γ – radiative capture cross-section,

σ_f – fission cross-section,

σ_{2n} – cross-section for the (n, 2n)-process,

$\bar{\nu}$ – mean number of secondary neutrons per fission.

The investigations were carried out for the isotopes:

$^{231}_{91}$Pa; $^{232}_{92}$U, $^{234}_{92}$U, $^{236}_{92}$U, $^{237}_{92}$U; $^{237}_{93}$Np, $^{238}_{93}$Np; $^{236}_{94}$Pu, $^{238}_{94}$Pu; $^{241}_{95}$Am; $^{242}_{96}$Cm

This report presents the results of a first evaluation of the still very scarce experimental data information for the isotopes investigated. The large gaps in the basic experimental data in many cases necessitated the use of nuclear systematics. Here, rather simple considerations and methods had to be applied because of the limited amount of time available on the part of the Karlsruhe safeguard project for the evaluation of the required data. Table I gives a complete survey about the computed 5-group constant values for a typical thermal reactor, and Table II for a typical fast reactor.

TABLE I. 5-GROUP AVERAGED VALUES OF $\sigma(n,f)$, $\sigma(n,\gamma)$, $\sigma(n,2n)$ and $\bar{\nu}\sigma(n,f)$ FOR THE CASE OF A THERMAL REACTOR SPECTRUM (CROSS-SECTIONS IN BARN)

Energy group	5 thermal group			4 0.5 eV - 1 keV			3 1 keV - 46.5 keV			2 46.5 keV - 800 keV			1 800 keV - 10 MeV			
Isotope	$\langle\sigma_\gamma\rangle$	$\langle\sigma_f\rangle$	$\langle\bar{\nu}\sigma_f\rangle$	$\langle\sigma_\gamma\rangle$	$\langle\sigma_f\rangle$	$\langle\bar{\nu}\sigma_f\rangle$	$\langle\sigma_\gamma\rangle$	$\langle\sigma_f\rangle$	$\langle\bar{\nu}\sigma_f\rangle$	$\langle\sigma_\gamma\rangle$	$\langle\sigma_f\rangle$	$\langle\bar{\nu}\sigma_f\rangle$	$\langle\sigma_\gamma\rangle$	$\langle\sigma_f\rangle$	$\langle\bar{\nu}\sigma_f\rangle$	$\langle\sigma_{2n}\rangle$
^{231}Pa	200	0	-	61	0	-	3.5	0	-	0.43	0.18	0.46	0.05	1.2	4.2	2.96 10^{-2}
^{232}U	78	77	188	20	39	95	0.7	5.0	12	0.16	1.9	4.6	0.06	1.9	7.3	1.495 10^{-3}
^{234}U	95	0	-	91	0	-	1.4	0	-	0.31	0.29	0.70	0.14	1.3	4.9	8.875 10^{-4}
^{236}U	5.6	0	-	54	0	-	1.4	0	-	0.31	0.004	0.01	0.14	0.69	3.5	6.01 10^{-3}
^{237}U	480	2	4.8	37	0	-	2.2	0	-	0.18	0.67	1.7	0.07	0.68	3.1	2.85 10^{-2}
^{237}Np	170	0	-	122	0	-	4.6	0	-	0.96	0.28	0.76	0.17	1.57	6.2	4.79 10^{-3}
^{238}Np	43	2200	6094	3.7	191	528	0.16	8.1	22	0.30	1.2	3.5	0.12	1.3	6.0	1.58 10^{-2}
^{236}Pu	33	162	465	25	123	353	1.0	4.8	14	0.30	2.5	7.4	0.12	2.6	9.7	6.66 10^{-5}
^{238}Pu	547	16	45	18	2.8	7.9	2.4	0.64	1.8	0.14	1.1	3.0	0.03	2.3	9.0	3.48 10^{-4}
^{241}Am	582	3	9.3	208	1.1	3.4	4.5	0.02	0.07	0.30	0.07	0.22	0.12	1.5	8.1	5.81 10^{-3}
^{242}Cm	20	0.8	2.6	87	3.9	12.4	2.9	0.13	0.41	0.30	2.7	8.8	0.12	2.7	11.6	3.21 10^{-4}

TABLE II. 5-GROUP AVERAGED VALUES OF $\sigma(n,f)$, $\sigma(n,\gamma)$, $\sigma(n,2n)$ and $\bar{\nu}\sigma(n,f)$ FOR THE CASE OF A FAST REACTOR SPECTRUM (CROSS-SECTIONS IN BARN)

Energy group	5 thermal group			4 0.465 eV - 1 keV			3 1 keV - 46,5 keV			2 46,5 keV - 800 keV			1 800 keV - 10 MeV			
Isotope	$\langle\sigma_\gamma\rangle$	$\langle\sigma_f\rangle$	$\langle\bar{\nu}\sigma_f\rangle$	$\langle\sigma_\gamma\rangle$	$\langle\sigma_f\rangle$	$\langle\bar{\nu}\sigma_f\rangle$	$\langle\sigma_\gamma\rangle$	$\langle\sigma_f\rangle$	$\langle\bar{\nu}\sigma_f\rangle$	$\langle\sigma_\gamma\rangle$	$\langle\sigma_f\rangle$	$\langle\bar{\nu}\sigma_f\rangle$	$\langle\sigma_\gamma\rangle$	$\langle\sigma_f\rangle$	$\langle\bar{\nu}\sigma_f\rangle$	$\langle\sigma_{2n}\rangle$
^{231}Pa	200	0	-	10,6	0	-	3,0	0	-	0,53	0,11	0,28	0,07	1,1	4,2	9,40 10^{-4}
^{232}U	78	77	188	3,7	10,3	25	0,8	2,2	5,3	0,18	1,9	4,7	0,07	1,9	7,3	4,64 10^{-4}
^{234}U	95	0	-	5,8	0	-	0,9	0	-	0,33	0,19	0,46	0,18	1,3	4,9	2,84 10^{-4}
^{236}U	5,6	0	-	4,9	0	-	0,9	0	-	0,33	0,0015	0,0036	0,19	0,62	3,5	1,95 10^{-3}
^{237}U	480	2	4,8	16	0	-	3,9	0	-	0,07	0,67	1,7	0,18	0,68	3,1	9,91 10^{-3}
^{237}Np	170	0	-	15,3	0	-	3,3	0	-	1,14	0,18	0,49	0,22	1,5	6,2	1,54 10^{-3}
^{238}Np	43	2200	6094	2,1	18,3	51	0,54	7,8	22	0,12	1,2	3,4	0,30	1,3	6,0	5,51 10^{-3}
^{236}Pu	33	162	465	4,7	8,8	25	1,0	2,0	5,8	0,12	2,5	7,3	0,30	2,6	9,7	2,08 10^{-5}
^{238}Pu	547	16	45	6,9	1,6	4,5	1,2	0,28	0,78	0,16	0,88	2,5	0,03	2,2	9,0	1,10 10^{-4}
^{241}Am	582	3	9,3	15,7	1,4	4,4	3,1	0,59	1,8	0,12	0,05	0,16	0,30	1,4	8,1	1,97 10^{-3}
^{242}Cm	20	0,8	2,6	7,5	0,32	1,0	1,6	0,066	0,21	0,12	2,7	8,8	0,30	2,7	11,6	1,02 10^{-5}

TABLE III. PREFERRED THERMAL σ_γ- AND σ_f-VALUES

Isotope / Cross-section	^{231}Pa	^{232}U	^{234}U	^{236}U	^{237}U	^{237}Np	^{238}Np	^{236}Pu	^{238}Pu	^{241}Am	^{242}Cm
σ_γ (barn)	200 [1,2]	78 [1,2]	95 [1,3]	5,6 [1,4,5,6]	480 [4]	170 [4,7]	43 a	33 a	547 [1,4,8]	582 [1]	20 [7]
σ_f (barn)	0 [1,2]	77 [1,2]	0 [9]	0 [4,9]	2 [4]	0 [4,7]	2200 [4]	162 [10]	16 [4,8]	3 [11]	0,8 [12]

a Estimated from $\sigma_{\gamma\,therm} = (\bar{\Gamma}_\gamma/\bar{\Gamma}_f)\sigma_{f\,therm}$

TABLE IV. AVERAGE RESONANCE PARAMETERS FOR THE EVEN NUCLEI INVESTIGATED

Isotope	$\overline{\Gamma}_\gamma$ (MeV)	$S_0 \times 10^{+4}$	$\overline{D}_{obs}$ (eV)	$\overline{\Gamma}_f$ (MeV)	$\overline{\Gamma}^{(0)}_{n\ell=0}$ $J=1/2$ (MeV)	$\overline{D}^{J=3/2}_{\ell=1}$ (eV)	$\overline{\Gamma}^{(0)}_{n\ell=1}$ $J=1/2$ (MeV)	$\overline{\Gamma}^{(0)}_{n\ell=1}$ $J=3/2$ (MeV)
^{232}U	50 [1]	1.0 [15]	13.1 [1]	360 [1]	1.31	7.20	2.62	1.44
^{234}U	25 [1]	1.2 [16]	19.1 [1]	- g	2.29	10.50	3.82	2.10
^{236}U	23 [6]	1.3 [16]	17.3 [1,6]	- g	2.25	9.50	3.46	1.90
^{238}Np	40 b	1.3 d	6.76 [17] f	2040 h	0.88	3.72	1.35	0.74
^{236}Pu	40 b	1.0 e	7.35 [17] f	195 h	0.735	4.04	1.47	0.808
^{238}Pu	38 [13]	1.1 [13]	13.5 [13]	10.4 [18]	1.49	7.41	2.70	1.48
^{242}Cm c	40 [14]	0.76 [14]	8.8 [17] f	1.8 i	0.669	4.83	1.76	0.966

b Mean value assumed for fissile nuclei.

c The average resonance parameters for ^{242}Cm have been assumed to be the same as for ^{244}Cm.

d Calculated from $RI_f^\infty \cong \frac{4\pi^2 \lambda\!\!\!^{-2}_0}{\sqrt{E^*}} S_0$, where E^* is the cutoff energy, and $\lambda\!\!\!^{-}_0$ reduced neutron wave-length.

e Assumed value from systematics of neighbouring nuclei.

f Obtained from $\rho_J = 1/\overline{D}_J$ with $\rho_J = \rho_0 (2J+1)$ and ρ_0 given in Ref [17], for nuclei with even Z as a function of the neutron binding energy.

g Negligible subthreshold fission.

h Calculated from $\sigma_{f\,therm} = \frac{\pi \lambda\!\!\!^{-2}_0}{\sqrt{E_{therm}}} S_0 \cdot \frac{\overline{\Gamma}_f}{E^*}$ where E^* is the energy of the lowest resonance.

i Calculated from $RI_\gamma^\infty / RI_f^\infty \cong \overline{\Gamma}_\gamma / \overline{\Gamma}_f$.

2. NEUTRON CROSS-SECTIONS AT THERMAL ENERGY (0.025 eV)

Experimental and even evaluated capture and fission cross-sections are available for all the isotopes studied with the exception of the thermal capture cross-section of ^{238}Np and ^{236}Pu. Because of the limited length of the paper only preferred σ_γ- and σ_f-values could be quoted in Table III together with the literature references for the data values taken into account.

The determination of the mean number of neutrons produced by thermal fission $\bar{\nu}_{therm}$ is described in section 4.

3. NEUTRON CROSS-SECTIONS IN THE RESONANCE REGION

The experimental information in this energy range consists of measured resonance integrals and resolved resonance measurements. The latter kind of information is available for all isotopes except ^{237}U, ^{238}Np, ^{236}Pu and ^{242}Cm, but only for a part of them given up to several hundreds of eV.

The resonance integrals offer an opportunity of directly determining group-averaged cross-sections weighted with a thermal reactor spectrum, after having derived average resonance parameters.

A survey of the average resonance parameters used here is given in Table IV for the even nuclei and in Table V for the odd nuclei studied. If no contrary comment is made in the tables the parameters have been determined from resolved resonance parameters given in the reference work quoted. For the average level spacing the J-dependence predicted by the Fermi-gas model has been used. The preferred values of the infinite-dilution resonance integrals for capture and fission as well as the references of the reports considered are summarized in Table VI.

In the case of the fast-reactor spectrum, statistical microscopic fission and capture cross-section values have been determined by using the NEARREX-Code [26]. The group-averaged cross-sections are given in Table I and Table II, respectively.

4. NEUTRON CROSS-SECTIONS IN THE FAST REGION

In this energy range, microscopic cross-section values have been available in a pointwise form for a large part of the isotopes considered.

Literature references concerning the available data information for the radiative-capture cross-sections are listed in Table VII. For the isotopes ^{237}U, ^{238}Np, ^{236}Pu, ^{241}Am, ^{242}Cm, for which the capture cross-section has not been measured hitherto, only group-averaged σ_γ-values have been determined relative to the corresponding group values for ^{238}U according to the approximately valid relation

$$\langle \sigma_\gamma^k \rangle_i = \frac{\bar{\Gamma}_\gamma^k}{\bar{\Gamma}_\gamma^{238}U} \langle \sigma_\gamma^{238}U \rangle_i \qquad (1)$$

where i denotes the energy group considered and k the isotope studied.

TABLE V. AVERAGE RESONANCE PARAMETERS FOR THE ODD NUCLEI INVESTIGATED

Isotope		^{231}Pa	^{237}U	^{237}Np	^{241}Am
$\bar{\Gamma}_\gamma$ (MeV)		48 [1]	24 [a]	44 [20]	40 [1]
$S_0 \times 10^{+4}$		0.60 [1]	1.0 [b]	1.0 [20]	1.1 [21]
$\bar{D}_{obs}$ (eV)		0.44 [1]	[c] [17]	0.67 [20]	0.81 [1]
$\bar{\Gamma}_f$ (MeV)		-	-	-	0.21 [9]
I		3/2 [1]	1/2 [19]	5/2 [2]	5/2 [1]
J($\ell = 0$)		1;2	0;1	2;3	2;3
J($\ell = 1$)		0;1;2;3	0;1;2	1;2;3;4	1;2;3;4
$\bar{D}_{\ell=0}$ (eV)	J_1	1.09	14	1.45	1.73
	J_2	0.74	4.7	1.25	1.50
$\bar{D}_{\ell=1}$ (eV)	J_1	3.07	14	2.13	2.54
	J_2	1.09	4.7	1.45	1.73
	J_3	0.74	2.8	1.25	1.50
	J_4	0.65	-	1.25	1.50
$\bar{\Gamma}^{(0)}_{n\ell=0}$ (MeV)	J_1	0.0655	1.40	0.145	0.190
	J_2	0.042	0.470	0.125	0.165
$\bar{\Gamma}^{(0)}_{n\ell=1}$ (MeV)	J_1	0.614	2.80	0.426	0.508
	J_2	0.218	0.94	0.29	0.346
	J_3	0.148	0.56	0.25	0.30
	J_4	0.130	-	0.25	0.30

[a] Average from ^{234}U, ^{236}U, ^{238}U.

[b] Assumed value from systematics of neighbouring nuclei.

[c] Only $\bar{D}^{J=0}_{\ell=0}$ and $\bar{D}^{J=1}_{\ell=0}$ have been determined from $\rho_J = 1/\bar{D}_J$ with $\rho_J = \rho_0\,(2J+1)$ and ρ_0 given in Ref. [17] for nuclei with even Z as a function of the neutron binding energy.

As to the fission cross-section, evaluated microscopic data based on measurements already exist for some isotopes in question. The corresponding references are given in Table VIII. For the other isotopes ^{232}U, ^{237}U, ^{238}Np, ^{236}Pu, ^{242}Cm with lacking data information, microscopic fission cross-section values have been determined by fission systematics developed by Zamyatnin [35]. It is based on the description of the fission process by the compound-nucleus model. In spite of Drake's evaluation [2], these systematics have also been applied to ^{232}U, because in this energy range. experimental values do not exist for ^{232}U and crude estimates not described in detail have been made by Drake. The $\sigma_f(E)$-curves determined are plotted in Fig. 1 for the isotopes under consideration.

Calculations of the (n, 2n) cross-section have already been performed for several isotopes studied here. Authors and methods are given in

TABLE VI. PREFERRED VALUES FOR THE INFINITE-DILUTION RESONANCE INTEGRALS

Isotope	^{231}Pa	^{232}U	^{234}U	^{236}U	^{237}U	^{237}Np	^{238}Np	^{236}Pu	^{238}Pu	^{241}Am	^{242}Cm
RI_γ^∞(barn)	480 [22]	220 [22]	700 [3, 9]	417 [1, 6, 9, 23, 4]	290 [4]	945 [4, 9, 22, 24]	29 c	197 d	148 [4, 8, 9, 25]	1600 [9]	670 e [8, 9, 12]
RI_f^∞(barn)	0 a	320 [22]	0 a [9]	0 a [9]	b	0 [4]	1500 [4]	960 c	2.4 [4, 8, 9]	8.5 [9]	30 e [8, 12]

a Negligible subthreshold fission.

b Unknown value, assumed to be 0.

c Calculated according to $RI_\gamma^\infty/RI_f^\infty \cong \frac{\overline{\Gamma}_\gamma}{\overline{\Gamma}_f}$

d Calculated with average resonance parameters.

e The resonance integrals of ^{242}Cm have been assumed to be the same as those of ^{244}Cm.

TABLE VII. REFERENCES FOR CAPTURE CROSS-SECTION DATA IN THE FAST-ENERGY RANGE

Isotope	References	Comments
^{231}Pa	[2]	Calculated from unresolved resonance parameters without taking into account competing processes; above 0.2 MeV a 1/E-dependence was assumed for $\sigma_\gamma(E)$.
^{232}U	[2]	
^{234}U	[5]	The results of calculations with unresolved resonance parameters have been extrapolated above 1 keV by assuming a shape similar to that measured for σ_γ of ^{236}U because of the rather similar s-wave resonance parameters.
^{236}U	[5]	1 keV - 0.3 MeV calculated from unresolved resonance parameters; 0.3 - 4 MeV smooth curve through experimental data points; above 4 MeV 1/E-dependence assumed.
^{237}Np	[27]	Measurements with the activation technique at 8 neutron energies between 0.15 and 1.5 MeV.
^{238}Pu	[8]	Below 2 MeV calculated with statistical theory with the basic value $\langle\Gamma_\gamma/D\rangle_0 = 2.54 \times 10^{-3}$; Above 2 MeV the σ_γ-shape was obtained by comparison with ^{238}U.

TABLE VIII. REFERENCES FOR FISSION CROSS-SECTION DATA IN THE FAST-ENERGY RANGE

Isotope	References	Comments
^{231}Pa	[2]	Up to 3 MeV smooth curve through measured data points; above 3 MeV the authors say that there they have assumed the σ_f-shape to be the same as that of similar isotopes.
^{234}U	[28]	Measured fission ratios of ^{234}U/^{235}U have been given, the revised values [28] have been taken.
^{236}U	[28, 29]	Measurements of fission cross-sections for ^{236}U relative to ^{235}U in the energy range from 1.0 to 5.0 MeV have been carried out recently by Stein et al. [29]. Therefore, the fission cross-sections for ^{236}U selected by Davey [28] had to be revised in that range. Absolute fission cross-section data have been obtained by using ^{235}U fission cross-section values recommended by Davey [28].
^{237}Np	[28]	The same as for ^{234}U; most recent experimental values of Stein et al. [29] are in good agreement with the revised data of Davey based on earlier measurements of Stein et al. in the range from 1.0 to 5.0 MeV.
^{238}Pu	[8]	Based on recent experiments of D. Barton not specified in greater detail.
^{241}Am	[30, 31]	Measurements in the energy range 20 eV-1 MeV and 550 keV - 6 MeV respectively.
	[32, 33]	Measurements at 14.6 MeV and 14.5 MeV, respectively.
	[34]	Measurements at 2.5 MeV and 14.5 MeV.

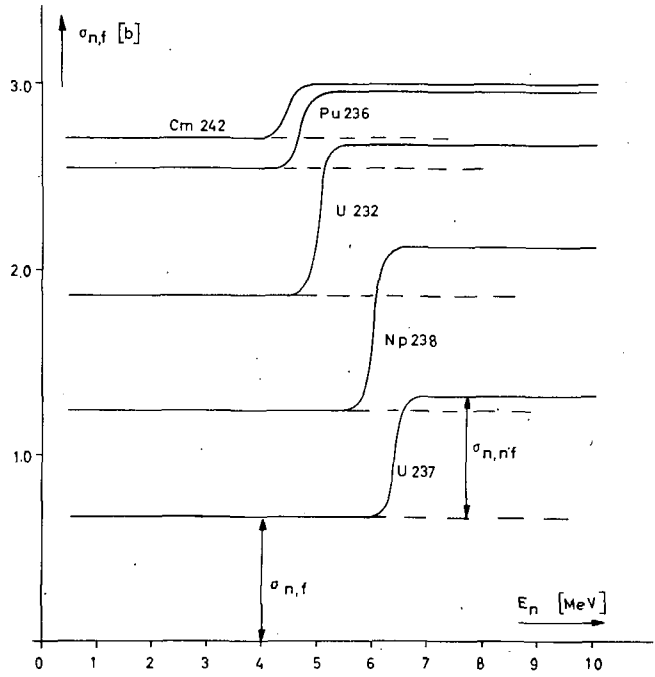

FIG. 1. The fission cross-section in the fast-energy region for the isotopes ^{232}U, ^{237}U, ^{236}Pu, ^{238}Np, ^{242}Cm.

TABLE IX. REFERENCES FOR (n, 2n) CROSS-SECTION DATA

Isotope	Threshold	Author	Comment
^{231}Pa	6.64 MeV	Drake, Nichols [2]	Statistical method described by Pearlstein [36]
^{232}U	7.32 MeV		
^{234}U	6.80 MeV	Drake, Nichols [5]	Evaluation by Parker [37] based on cross-sections for similar nuclides and optical-model calculations
^{236}U	6.43 MeV		
^{238}Pu	6.93 MeV	Dunford, Alter [8]	Statistical method [36]; curves given

Table IX. For the isotopes ^{237}U, ^{237}Np, ^{238}Np, ^{236}Pu, ^{241}Am and ^{242}Cm (n, 2n) cross-section data have not been available and have, therefore, been calculated with the method indicated by Pearlstein [36]. For ^{237}Np, contrary to the other isotopes mentioned, a single measurement of the (n, 2n) cross-section at 14.5 MeV [38] exists which has served to fit the (n, 2n) shape due to Pearlstein. The (n, 2n) cross-section curves for the above isotopes are shown in the Figs 2a and 2b.

With regard to the isotopes studied here the mean number of neutrons per fission $\bar{\nu}$ has hitherto been measured only for ^{234}U at several energy points. Fillmore [39] has fitted these data points by the following equation

$$\bar{\nu}_p(E) = 2.371 + 0.1353E \text{ (MeV)} \quad (2)$$

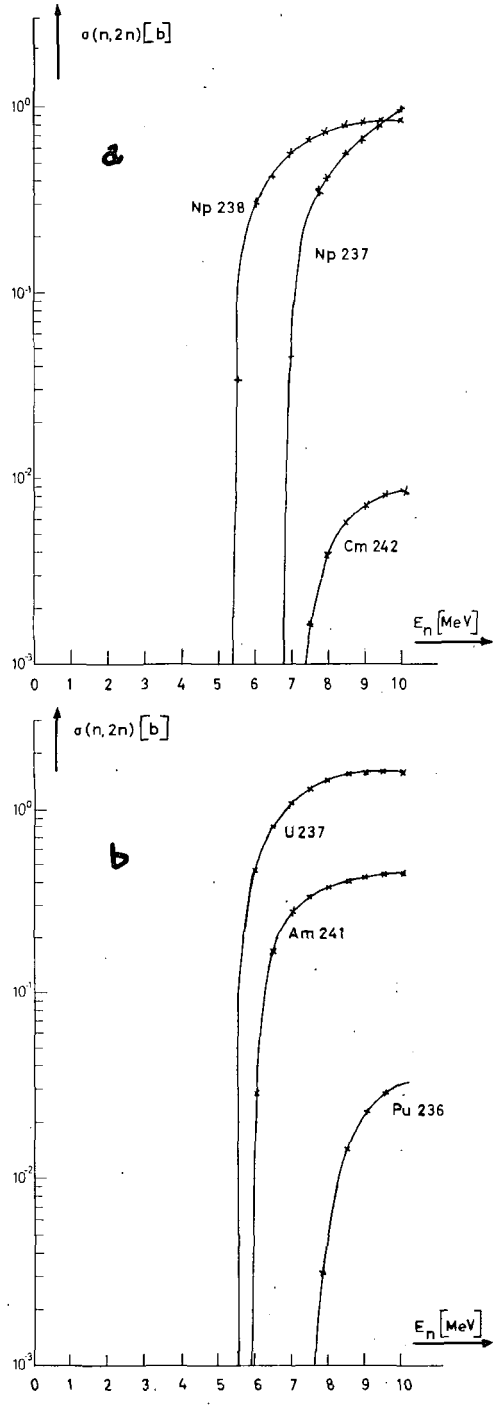

FIG. 2. The energy dependence of σ(n, 2n) for the isotopes ^{237}Np, ^{238}Np, ^{242}Cm (a) and ^{237}U, ^{236}Pu, ^{241}Am (b).

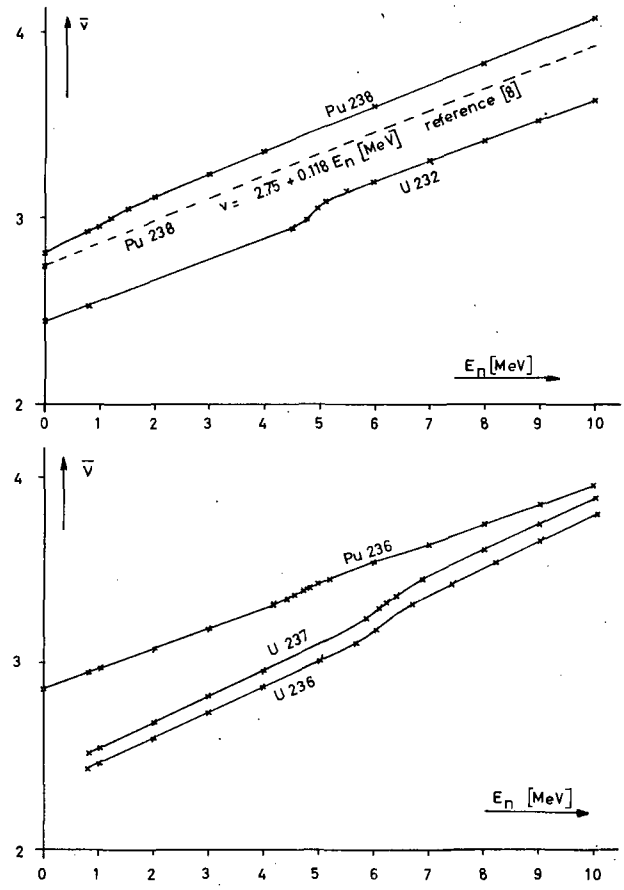

FIG. 3. $\bar{\nu}$ as a function of the neutron energy for ^{232}U, ^{236}U, ^{237}U, ^{236}Pu, ^{238}Pu.

with normalization to $\bar{\nu}_p(^{252}Cf) = 3.782$. This relationship was used to determine the $\bar{\nu}$-values for ^{234}U in the whole energy range above the fission threshold. For ^{231}Pa the $\bar{\nu}$-values given in the evaluation of Drake [28] have been adopted. To the other isotopes in study systematics have been applied in order to derive $\bar{\nu}(E)$.

For the U- and Pu-isotopes the systematics of Schuster and Howerton [40] have been used, as the calculated results of these authors for ^{235}U, ^{238}U, ^{233}U compare favourably with experimental data. Schuster and Howerton have modified the linear energy dependence of $\bar{\nu}(E)$ by taking into account the various fission modes, i.e. the standard (n, f) process, the (n, n'f) fission and the (n, 2n'f) fission. The resulting variation in $\bar{\nu}$ as a function of neutron energy is shown in Fig. 3 for the U- and Pu-isotopes under consideration.

For the rest of the studied isotopes, namely ^{237}Np, ^{238}Np, ^{241}Am and ^{242}Cm because of lack of data, the linear energy dependence of $\bar{\nu}$ has been assumed valid. To determine the $\bar{\nu}$-values at thermal energy a general correlation given by Gordeeva and Smirenkin [41] has been used. It

represents $\nu_{thermal}$ as linear function of the mass number A and the charge number Z. For the slope ν_1 of $\bar{\nu}(E)$ the value $\nu_1 = 0.15\ MeV^{-1}$ as quoted by Terrell [42] has been adopted for the isotopes considered here, except ^{237}Np. For ^{237}Np, three experimental data points and the calculated thermal value have been used to determine the slope. The deduced straight-line functions $\bar{\nu}(E)$ for the abovementioned isotopes are the following:

$$^{237}Np : \bar{\nu}(E) = 2.67 + 0.13E(MeV) \quad (3)$$

$$^{238}Np : \bar{\nu}(E) = 2.77 + 0.15E(MeV) \quad (4)$$

$$^{241}Am : \bar{\nu}(E) = 3.08 + 0.15E(MeV) \quad (5)$$

$$^{242}Cm : \bar{\nu}(E) = 3.19 + 0.15E(MeV) \quad (6)$$

5. FINAL CONSIDERATION

In the final phase of the investigations reported here an evaluation of cross-section data for ^{237}Np carried out by the Idaho Nuclear Corporation has been published [43] which has not been regarded. The two evaluations differ considerably from each other only in the (n, 2n) cross-sections and the assumed energy dependence of $\bar{\nu}$. The (n, 2n) cross-section values are determined in both reports according to the procedure given by Pearlstein [36]. The values reported in the Idaho evaluation, however, are much lower than our results. This is mainly due to the fact that in the Idaho evaluation the shape of $\sigma(n, 2n)$ has not been fitted to the experimental value at 14.5 MeV [38].

For the mean number of neutrons per fission of ^{237}Np the Idaho evaluation gives

$$\bar{\nu}(E) = 2.61 + 0.16E \quad (7)$$

This energy dependence has been determined by assuming a slope of $0.16\ MeV^{-1}$ and passing through the average of the two measurements of Hansen [44]. In this report the measurements of Hansen have been used together with a Russian measurement to fix the slope of the straight-line function $\bar{\nu}(E)$, while the thermal $\bar{\nu}$-value has been taken from a systematic formula (see section 4). The last procedure for the deduction of $\bar{\nu}(E)$ has to be preferred because the slope for $\bar{\nu}(E)$ assumed in the Idaho evaluation for ^{237}Np is not characteristic of this isotope.

As to the energy dependence of $\bar{\nu}$ the straight-line function given by Dunford and Alter [7] for ^{238}Pu,

$$\bar{\nu}(E) = 2.75 + 0.118E(MeV) \quad (8)$$

has not been adopted in this report either. The energy dependence derived here allows for the multiplicities of fission modes. Both functions $\bar{\nu}(E)$ are displayed in Fig. 3.

The average resonance parameters for ^{236}U reported here are based on preliminary results of Carlson obtained from 17 positive resonances between 5.45 eV and 272.8 eV. His finally published results [6] based on resonance measurements for a single negative resonance at -9.7 eV and 28 positive resonances up to an energy of 415 eV could not be taken into account. They show that we have assumed too large values for S_0 and $\overline{D}_{obs}$ and too small values for $\overline{\Gamma}_\gamma$ and S_1. In a later re-evaluation this defect has to be corrected.

ACKNOWLEDGEMENTS

I wish to express my appreciation to Dr. J.J. Schmidt for his close collaboration during the entire course of this work.
Dr. A. Sauer and Dr. K.E. Schroeter deserve thanks for making available the thermal and fast-reactor weighting spectra.

REFERENCES

[1] STEHN, R., GOLDBERG, M.D. et al.; BNL-325, 2nd ed. suppl.2 3 (1965).
[2] DRAKE, M.K., NICHOLS, P.F., GA-7462 (1967).
[3] HALPERIN, J., STOUGHTON, R.W., 2nd Int. Conf. peaceful Uses atom. Energy (Proc. Conf. Geneva 1958) 16 (1958) 64.
[4] HENNELLY, E.J., CORNMAN, W.R., BAUMANN, N.P., in Neutron Cross-Section Technology (Proc. Conf. Washington) 2 (1968) 1271.
[5] DRAKE, M.K., NICHOLS, P.F., GA-8135 (1967).
[6] CARLSON, A.D. et al., Wash. 1093 (1968) 54; to be published as GA-9057 (1968).
[7] HUGHES, D.J., SCHWARTZ, R.B., BNL-325, 2nd ed. (1958).
[8] DUNFORD, C.L., ALTER, H., NAA-SR-12271 (1967) 13.
[9] PEARLSTEIN, S., BNL-982 (1966) 22.
[10] HULET, E.K., WEST, H.I., COOPS, M.S., Wash-1033 (1961) 28.
[11] HULET, E.K., HOFF, R.W., BOWMAN, H.R., MICHEL, M.C., Phys.Rev. 107 (1957) 1294.
[12] FOLGER, R.L. et al., in Neutron Cross-Section Technology (Proc. Conf. Washington) 2 (1968) 1279.
[13] YOUNG, T.E., SIMPSON, F.B., BERRETH, J.R., COOPS, M.S., Nucl. Sci. Engng 30 (1967) 335.
[14] COTE, R.E., BARNES, R.F., DIAMOND, H., Phys.Rev. 134B (1964) 1281.
[15] JAMES, G.D., Nucl. Phys. 55 (1964) 517.
[16] PILCHER, V.E., HUGHES, D.J., HARVEY, J.A., Bull. Am. Phys. Soc. 1 (1956) 187.
[17] MOORE, M.S., SIMPSON, O.D., Fission Cross-Sections, unpublished.
[18] STUBBINS, W.F., BOWMAN, C.D., AUCHAMPAUGH, G.F., COOPS, M.S., Phys.Rev. 154 (1967) 1111.
[19] BANANOV, S.A. et al., Soviet Phys. J. nucl. Physics 1 (1965) 397.
[20] PAYA, D., BLONS, J., DERRIEN, H., FUBINI, A., MICHAUDON, A., RIBON, P., Journal de physique 29 suppl. No. 1 (1968) 159.
[21] SLAUGHTER, G.G., HARVEY, J.A., BLOCK, R.C., ORNL 3085 (1961) 42.
[22] DRAKE, M.K., Nucleonics 24 (1966) 108.
[23] BAUMANN, N.P., HALFORD, J.D., PELLARIN, D.J., Nucl. Sci. Engng 32 (1968) 265.
[24] TATTERSALL, R.B., ROSE, H., PATTENDEN, S.K., JOWITT, D., J. nucl. Energy A12 (1960) 32.
[25] BUTLER, J.P., LOUNSBURY, M., MERRITT, J.S., Can. J. Phys. 35 (1957) 147.
[26] MOLDAUER, P.A., ENGELBRECHT, C.A., DUFFY, G.J., ANL-6978 (1964).
[27] STUPEGIA, D.C., SCHMIDT, M., KEEDY, C.R., Nucl. Sci. Engng 29 (1967) 218.
[28] DAVEY, W.G., Nucl. Sci. Engng 26 (1966) 149 and Nucl. Sci. Engng. 32 (1968) 35.
[29] STEIN, W.E., SMITH, R.K., SMITH, H.L., in Neutron Cross-Section Technology (Proc. Conf. Washington) 1 (1968) 627.
[30] SEEGER, P.A., HEMMENDINGER, A., DIVEN, B.C., LA-3586 (1966) 86.

[31] BOWMAN, C.D., HOFF, R.W., AUCHAMPAUGH, G.F., FULTZ, S.C., Wash 1071 (1966) 84 (unpublished).
[32] PROTOPOPOV, A.N., SELITSKII, Yu.A., SOLOVEV, S.M., Soviet Phys.: Atomic Energy 6 (1959) 36.
[33] FOMUSHKIN, E.F. et al., Soviet Phys.: Nucl. Physics 5 (1967) 689.
[34] KAZARINOVA, M.I., ZAMYATNIN, Yu.S., GORBACHEV, V.M., Soviet Phys.: Atomic Energy 8 (1967) 125.
[35] ZAMYATNIN, Yu.S., Soviet Phys.: Atomic Energy, Suppl. 1 (1957) 26.
[36] PEARLSTEIN, S., BNL-897 (1964).
[37] PARKER, K., AWRE-O-37/64 (1964).
[38] PERKIN, J.L., COLEMAN, R.F., J. nucl. Energy A&B Reactor Science 14 (1961) 69.
[39] FILLMORE, F.L., J. nucl. Energy 22 (1968) 79.
[40] SCHUSTER, S.H., HOWERTON, R.J., Journ. Nucl. Energy Parts A/B 18 (1964) 125.
[41] GORDEEVA, L.D., SMIRENKIN, G.N., Soviet Phys.: Atomic Energy 14 (1963) 562.
[42] TERRELL, J., Phys. Rev. 113 (1959) 527 and Phys. Rev. 108 (1957) 783.
[43] SMITH, J.R., GRIMESEY, R.A., IN-1182 (1969).
[44] HANSEN, G.E. et al., Los Alamos unpublished report (1958); quoted in LEACHMAN, R.B., 2nd Int. Conf. peaceful Uses atom. Energy (Proc. Conf. Geneva 1958) 15 (1958) 335.

DISCUSSION

J. STORY (Chairman): I think this tour de force continues the demonstration of what has otherwise been becoming more and more apparent during the course of this meeting, namely, that experimental physicists really are not needed very much longer.

W.G. DAVEY: It is interesting to note your use of Schuster and Howerton's systematics because I have also used them in an evaluation of $\bar{\nu}$ of my own and I think they are applicable.

I cannot agree with the Chairman's comment that experimental phycisists are not needed since I believe that the systematics do not fit too well and it is possible that this is due to errors or insufficient precision in the experimental data.

B. HINKELMANN: I agree. The systematics of Schuster and Howerton give good agreement with experimental data only above 5 MeV; below this energy it is not so good.

L. WALLIN: I have a question concerning the correlation between fission cross-sections at 3 MeV. If I understood your slide correctly, you were showing points taken from evaluations. However, it may be dangerous to infer the validity of the correlation from this as the evaluators may already have taken the correlation into account, in which case the good agreement would be only apparent.

B. HINKELMANN: The evaluated data lie within the experimental data and so the scattering around this linear curve is the same as if I had taken the experimental values directly.

CALCULATION OF ^{240}Pu NEUTRON CROSS-SECTIONS IN THE keV-RANGE

M. CANER, S. YIFTAH
Israel Atomic Energy Commission,
Soreq Nuclear Research Centre
Yavne, Israel

Abstract

CALCULATION OF ^{240}Pu NEUTRON CROSS-SECTIONS IN THE keV-RANGE

A cross-section calculation for ^{240}Pu in the keV-range is presented. There are no experimental data in this region except for the fission cross-section. In addition to the experimental data evaluation, calculations are made by means of the optical model and the Hauser-Feshbach model; optical parameters are obtained from a fit to the ^{238}U cross-sections. The recommended curves are compared with the values in the ENDF/B library.

1. Introduction

We are conducting an evaluation of the nuclear data for the higher plutonium isotopes in order to update our 1967 evaluation [1]. In this context, we present here a calculation of the neutron cross sections of ^{240}Pu from 1 keV to MeV.

For our computations we use the optical model code ABACUS-2 [2], whose Hauser-Feshbach subroutine was replaced by the code NEARREX [3].

Since our previous evaluation there has been an increase in the number of ^{240}Pu resonances observed; 264 resonances have been analyzed with respect to Γ_n [4], compared with the 43 we recommended before. Also, interesting data on s-wave fission width bunching has come forth [5], as well as a lower average capture width [6]. In the keV and MeV ranges not much new data have been reported: only σ_f has been measured so far; it is expected that this situation will improve in the near future [7].

In the previous evaluation, heavy reliance was put on systematics - whenever no data was available for ^{240}Pu, ^{238}U came to the rescue. Here we still do this, but on a quantitative as opposed to a qualitative fashion, i.e. instead of just saying that the total and elastic cross sections of the two isotopes are similar, we say that the optical model parameters which describe the scattering and absorption interaction are the same. We then go on to use these parameters to calculate the ^{240}Pu cross sections utilizing the statistical model of Hauser-Feshbach [8] and Moldauer [9] plus the ^{240}Pu average resonance parameters. It is hoped that this procedure will give a more accurate description of the partial cross sections, particularly the inelastic scattering.

2. The optical model calculation

The code ABACUS-2 is described in refs. [2] and [10]. We use a complex potential of the form used by Auerbach and Moore [11].

The parameters used are discussed in section 4. Although ^{240}Pu is, like ^{238}U, a deformed nucleus, it is felt that the spherical potential can fit sufficiently well the scattering data with the present experimental accuracy of about 10%. For ^{238}U spherical [11] and deformed potentials [12] have been used. Smith et al. [13], report calculations for the deformed nuclei hafnium, gadolinium and samarium using both approaches: they conclude there is a slightly better agreement for the deformed potential results. The spherical potential calculation has the advantage of being much less machine-time-consuming which allows a least squares fit to be performed.

3. The statistical model calculation

The code NEARREX is described in ref. [3]. We have done calculations with the statistical factor Q=0, so that we use the Hauser-Feshbach equations modified to take account of capture and fission competition to inelastic scattering and of the width fluctuation correction.

An addition was made so that the code would calculate the differential compound elastic cross section $\sigma_{CE}(\theta)$. This is done by assuming the shape of the partial cross section $\sigma_{CE}(\ell,j,\ell',j',J;\theta)$ to be the same as in the simple Hauser-Feshbach theory.

For the calculation of the fission cross section the linear dependence of the fission width on energy was replaced by the expressions of the channel theory of fission [14].

3.1 Calculation of the fission cross section.

A Hill-Wheeler penetration factor was assumed:

$$T_f(J,\ \Pi,\ K,\ M) = T_f = \left[1 + \exp\left(2\pi\ \frac{E_f - E}{\hbar\omega_f}\right)\right]^{-1}$$

- E = entrance channel energy
- E_f = fission threshold
- $\hbar\omega_f$ = curvature of the potential barrier peak
- K = component of total angular momentum J along the body axis of symmetry
- M = component of J along a space axis
- Π = parity

The fission channels are assumed to have characteristics similar to that of low-lying rotational states of deformed nuclei [15].

The parameters E_f and $\hbar\omega_f$ are dependent on the quantum numers J, Π, K. In the present analysis we neglect this dependence and we take

$$N_f(J,\Pi) = \sum_{K,M} T_f(J,\ \Pi,\ K,\ M) = n(J,\Pi) \times T_f$$

- $N_f(J,\Pi)$ = effective number of fission channels of given J,Π
- $n(J,\Pi)$ = total number of fission channels of given J,Π

From previous analyses [16], the K-bands observed in the fit of the angular distribution of fission fragments are $K\Pi = \frac{1}{2}^-, \frac{3}{2}^-$, which are mainly p-wave fission. The work of Migneco et al., [5] as well as the Byers data [17] indicate s-wave fission and consequently a $K\Pi = \frac{1}{2}^+$ band.

In the calculation of the number of channels we include all the levels compatible with angular momentum conservation up to $\ell=4$.

The values of K-rotational bands are determined by analyses of the fission fragment angular distributions [16,18]. However, as mentioned by Ermagambetov et al., [19], it is hard to assign the parity of the $K=\frac{1}{2}$ as well as to distinguish between contributions of the $\frac{3}{2}^+$ and $\frac{5}{2}^-$ bands. We calculated the number of fission channels $n(J,\Pi)$ under the assumption that all the possible K-bands ($K \leq J$) are present. To each state of angular momentum J corresponds a twofold degeneracy due to $M = \pm 1/2$. The following sequence is obtained:

J	Π	n(J,Π)
1/2	+	2
1/2	-	2
3/2	+	4
3/2	-	4
5/2	+	6
5/2	-	6
7/2	+	8
7/2	-	8
9/2	+	10

E_f was taken, as a first guess, to be the energy at which the fission cross section attained one half of its value after the threshold ($E_f \cong 700$ keV).

The curvature $\hbar\omega_f$ was obtained by fitting the average s-wave parameters (see section 5).

$$\frac{2\pi \langle \Gamma_f \rangle^{\ell=0}_{J=1/2}}{\langle D \rangle_{J=1/2}} = N_f(J\Pi=1/2+) = \frac{2}{1 + \exp\left(2\pi \frac{E_f}{\hbar\omega_f}\right)}$$

The best overall fit was obtained with the values: $E_f = 840$ keV; and $\hbar\omega = 703$ keV. Compare with Migneco et al. [5] values of 710 and 650 keV respectively. We assumed the above parameters to be the same for all channels; this is certainly not true for E_f which depends mainly on K, so our E_f is an effective value.

The width fluctuation correction was calculated assuming one degree of freedom.

4. Fit to ^{238}U

A fit was done to the cross sections of ^{238}U in order to obtain an optical model parameter set which could be later used for ^{240}Pu. ^{239}Pu was not used as a reference because it was felt to be more appropriate to extrapolate from one even-even nucleus to another.

The fit was done in the range from 50 keV to 1 MeV to the following cross sections: total (σ_T), total elastic (σ_n), differential elastic ($\sigma_n(\theta)$), and total inelastic ($\sigma_{n'}$). The ^{238}U cross sections, average resonance parameters and energy levels were taken from refs. [20,21]. The fission cross section was neglected in this range.

The starting point of the optical model parameter search was the set of Auerbach and Moore [11]. The parameters adopted are as follows (the Auerbach-Moore value, if different, is enclosed in parentheses):

VRE = 40.3 MeV (39.8)
VIM = 7.0 MeV (6.9)
VSR = 15 MeV
a = 0.67F (0.47)
R_o = 1.32F
b = 1.0F

The main change is in the diffusion parameter a; our value is within the spread of values used by other investigators, as compiled in ref. [22]. The change in VIM is not significant. The parameter b was kept constant.

5. Average resonance parameters

The average level spacing value of Kolar et al., [4] as quoted in ref. [5] based on 102 resonances was used

$$\langle D \rangle_{J=1/2} = 14.9 \pm 0.8 \text{ eV}$$

From the data of Asghar et al., [23] we obtain a value of 19.9 eV from 72 resonances. It appears that resonances of small neutron width were not detected. This would make the average $\langle \Gamma_n^o \rangle$ larger: that this is the case is seen in the fact that their recommended s-wave strength function agrees with the Kolar value.

For the average capture width Weigman and Schmid [6] report a value of 23.2 ± 2.0 meV based on 32 resonances. Asghar et al., [23] report a value of 21 ± 2 (statistical) ± 1.2 (systematic) meV. Apparently, the systematic error is due to the uncertainty in the composition of the ^{240}Pu samples. We assumed all the errors to be of

a statistical nature and calculated weighted averages; from this method we obtain the following value, which we adopt:

$$\langle \Gamma_\gamma \rangle_{J=1/2}^{\ell=0} = 22.6 \pm 2.9 \text{ meV}$$

For the average fission width the value of Migneco and Theobald [5] is adopted

$$\langle \Gamma_f \rangle_{J=1/2}^{\ell=0} = 3.5 \text{ meV}$$

This value is based on 17 fission widths but averaged over the whole 450 eV to 4 keV range.

The level scheme of Lederer et al.,[24] below 1 keV is used, with the addition of an assumed (3-) level at 640 keV: the following sequence results: (E (keV), JΠ) = (0,0 +); (42.88, 2 +) ; (141.7, 4 +) ; (296, 6 +) ; (599,1 -) ; (640, 3 -) ; (863, 0 +) ; (903, 2 +) ; (945, 2 +).

We take from the analysis of Facchini et al. [27] the values for the level density parameter $\underline{a}$ = 29.76 MeV^{-1} and the pairing energy Δ = 0.61 MeV. The neutron binding is 5.39 MeV. The neutron width is assumed to follow a χ^2 distribution with one degree of freedom.

Kolar and Bockhoff [4] obtain from resonance analysis, the s-wave strength function $S_o = (1.05 \pm 0.16) \times 10^{-4}$. Asghar et al. [23] get a similar value: $(1.03 \pm 0.20) \times 10^{-4}$. From our calculation for E = 1 keV we deduce $S_o^{1/2^-} = 1.10 \times 10^{-4}$ which is in excellent agreement with the resonance data and consequently we can take it as a recommended value. Similarly, we calculate the p-wave strength functions: $S_1^{1/2} = 1.08 \times 10^{-4}$; $S_1^{3/2} = 2.39 \times 10^{-4}$; $S_1 = 1.95 \times 10^{-4}$. In our previous work [1] we recommended the value $S_1 = 2.5 \times 10^{-4}$.

6. Calculated cross sections

The computed cross sections are shown in figures 1 - 3. In figure 1 we show our fit to the experimental evaluated fission cross section as evaluated by Davey [25] which is based on a simultaneous evaluation of fission for several fissile and fertile nuclei. In the 1 - 10 keV range the average cross section from Byers et al., [17] is followed: These measurements, together with those of Migneco et al., agree with the notion that s-wave fission is indeed allowed, in contradiction to previous assumptions. Above 800 keV the calculated σ_f falls below the experimental curve: the same situation was in Ref.[19]. In figure 2 we compare our calculated cross sections with the evaluation of Pitterle et al. [26]. Our σ_T and σ_n are higher in the 10 - 100 keV range. The more significant discrepancy is in the calculation of the inelastic scattering. In figure 3 we display our 5 lowest calculated excitation curves; the 3 lowest excitation curves of ref. [26] are included for comparison. Below 600 keV the (42.88 keV, 2 +) curves agree; above that Pitterle's is lower. The (296 keV, 6 +) curve we calculate is

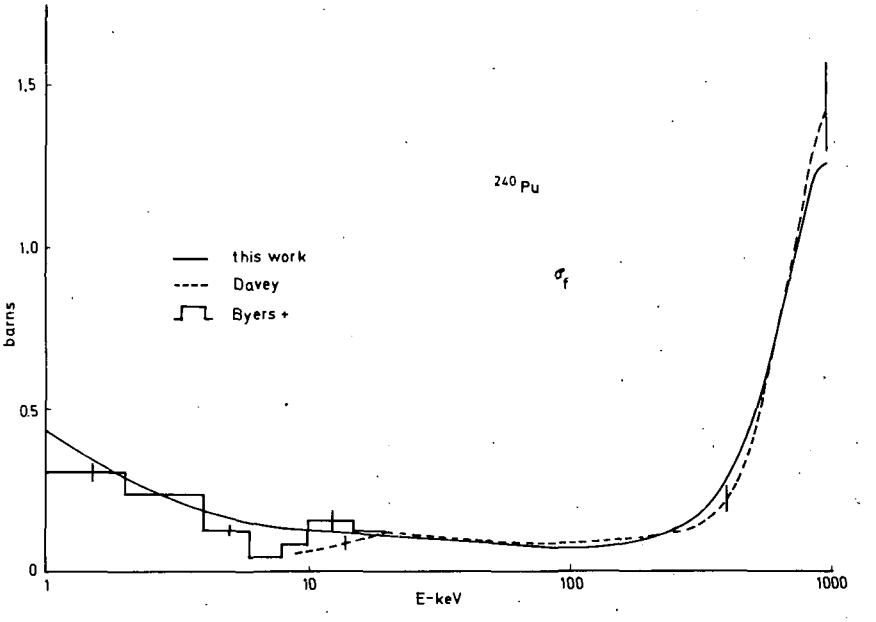

FIG. 1. ^{240}Pu fission cross-section.

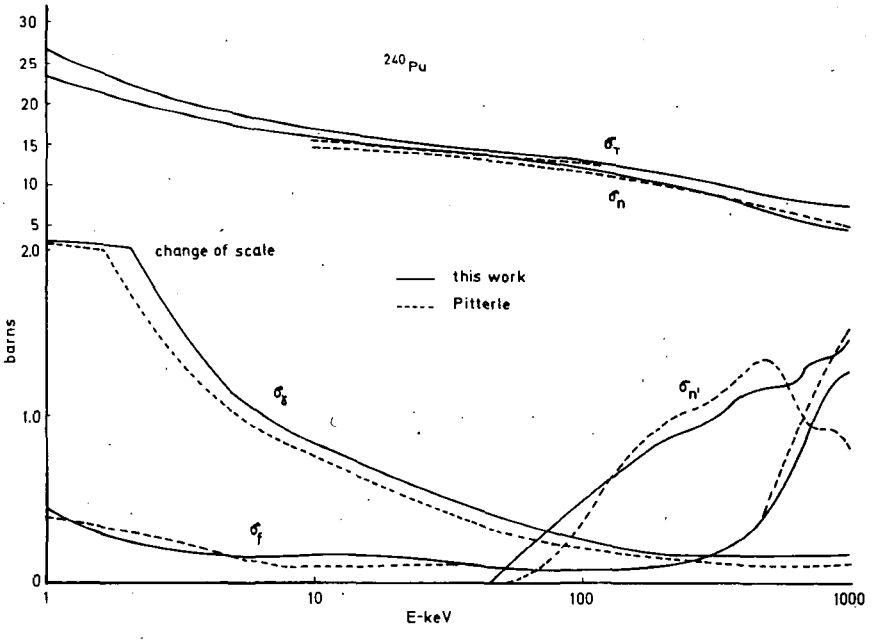

FIG. 2. ^{240}Pu total and partial cross-sections.

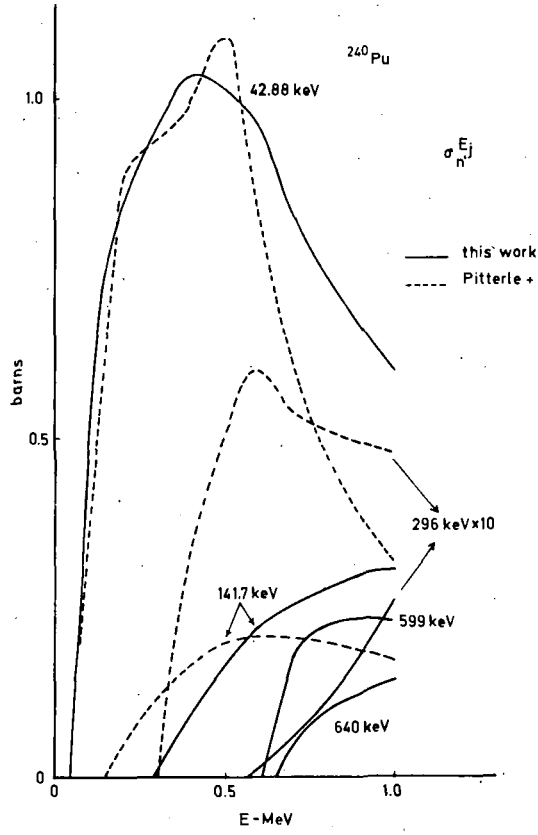

FIG. 3. ^{240}Pu excitation curves.

smaller by a factor of 2 from the curve of Pitterle, which is based on ^{238}U. It must be said that the same effect is evident when we compare our calculation of the (310, 6 +) level of ^{238}U with the evaluated curve of Schmidt [21]; but the expeimental data there are sparse and with large errors and we do not place much weight on it.

7. Conclusion

The evaluating procedure which evolves from these calculations is as follows.

First, the best experimental data is to be selected; if the calculated data falls within the assigned errors it will be recommended; if not, the experimental data should be preferred and corrections applied to the calculated values. In this spirit, to obtain a recommended set from our calculated cross sections, we will adjust slightly σ_f above 250 keV ($\sim$0.1 b) and compensate by renormalizing σ_n, and $\sigma_n^{E_j}$; all other cross sections will remain as calculated.

We believe that in the absence of sufficient experimental data and of a parameter-free theory of nuclear reactions, our procedure of obtaining optical model parameters by fitting the ^{238}U cross sections and then using them for ^{240}Pu (and ^{242}Pu) is the best we can do, and superior to simple systematics as in our previous evaluation.

If we compare our present calculation with our previous evaluation, we see that our new σ_γ is lower below 500 keV (this has been introduced into the KEDAK file); σ_f below 10 keV is higher now; σ_T is lower now in the 1 - 100 keV region by about 5%; σ_n is substantially the same throughout, within a few percent. Comparing the excitation curves, we see that the 42.88 keV level is down by 20%; the 141.7 keV level is down by 20%; and the 296 keV level is down by a factor of 3 (see section 6).

Acknowledgements

The ABACUS-2 code was received from Dr. Scheffel and Dr.E.H. Auerbach of the Brookhaven National Laboratory.

Our thanks are due to Dr. J.J. Schmidt for discussions and suggestions.

This research is partly supported by the Gfk, Kernforschungszentrum, Karlsruhe.

References

[1] YIFTAH, S., SCHMIDT, J.J., CANER, M. and SEGEV, M., Fast Reactor Physics, IAEA (Vienna, 1968), Vol, p. 123. Also, Israel AEC Rep. IA-1152 (1967).
[2] AUERBACH, E.H., U.S. Rep. BNL 6562 (preprint) (1964).
[3] MOLDAUER, P.A. and ENGELBRECHT, C.A., USAEC Rep. ANL-6978 (1964).
[4] KOLAR, W. and BOCKHOFF, K.H., J. Nucl. En. 22 (1968) 299.
[5] MIGNECO, E. and THEOBALD, J.P., Nucl. Phys. A112 (1968) 603.
[6] WEIGMANN, H. and SCHMID, H., J. Nucl. En. 22 (1968) 317.
[7] SMITH, A. et al., WASH-1136 (1969).
[8] HAUSER, W. and FESHBACH, H., Phys. Rev. 87 (1952) 366.
[9] MOLDAUER, P.A., Rev. Mod. Phys. 36 (1964) 1079.
[10] AUERBACH, E.H. et al., USAEC Rep. KAPL-3020 (1964).
[11] AUERBACH, E.H. and MOORE, S.O., Phys. Rev. B135 (1964) 895.
[12] DUNFORD, C.L., Nucl. Data for Reactors, IAEA (Vienna, 1967) Vol. I, p.429.
[13] SMITH, A.B. and SHERWOOD, G., USAEC Rep. ANL-7410 (1969) p.11.
[14] WHEELER, J.A., Fast Neutron Physics, Vol. II, MARION, J.B. and FOWLER, J.L., ed., John Wiley & Sons (1963).
[15] DAVIDSON, J.P., Collective Models of the Nucleus, Academic Press, N.Y. (1968).
[16] LAMPHERE, R.W., Phys. & Chem. of Fission, IAEA, (Vienna, 1965) Vol. I, p.63.
[17] BYERS, D.H. et al., U.S. Rep. LA-3586 (1966).
[18] HUIZENGA, J.R. et al., 2nd Symp. Phys. & Chem. of Fission, IAEA (Vienna, 1969) p. 403.
[19] ERMAGAMBETOV et.al., Sov. J. Nucl. Phys. 8 (1969) 409.
[20] LANGNER, I., SCHMIDT, J.J. and WOLL, D., KFK 750 (1968).

[21] SCHMIDT, J.J., KFK 120/I (1966).
[22] VASTEL, M., Report, Electricite de France, Direction des Etudes et Recherches (Feb.1968): Evaluation des donnees neutroniques de l'uranium 238, etc.
[23] ASGHAR, M. et al., EANDC (UK) 103AL (1968).
[24] LEDERER, C.M. et al., Table of Isotopes, John Wiley & Sons (1968).
[25] DAVEY, W.G., Nucl. Sci. Eng. 32 (1968) 35.
[26] PITTERLE, T.A. and YAMAMOTO, M., APDA-218 (1968).
[27] FACCHINI, U. and SAETTA-MENICHELLA, E., Energia Nucleare 15 (1963) 54.

DISCUSSION

J.J. SCHMIDT: The inelastic excitation cross-sections you showed for ^{240}Pu are substantially lower than those of ^{238}U. Is this due to higher fission competition in ^{240}Pu than in ^{238}U?

M. CANER: Yes, since the gross fission threshold for ^{240}Pu is about 700 keV, as against about 1 MeV for ^{238}U.

MULTILEVEL RESONANCE ANALYSIS OF THE TOTAL NEUTRON CROSS-SECTION OF ^{23}Na AND Ca BELOW 1 MeV

J. NEBE, G.J. KIROUAC
Institut für Angewandte Kernphysik,
Kernforschungszentrum Karlsruhe,
Federal Republic of Germany

Abstract

MULTILEVEL RESONANCE ANALYSIS OF THE TOTAL NEUTRON CROSS-SECTION OF ^{23}Na AND Ca BELOW 1 MeV.

The total neutron cross-sections of ^{23}Na and Ca have been analysed below 1 MeV in order to provide neutron resonance parameters. The analysis uses the standard multilevel R-matrix formulas for a single open channel. A chi-squared fitting procedure is used for shape analysis. Resonance widths and energies have been assigned for ^{23}Na up to 900 keV. The values of ℓ and J have been determined up to 439 keV; above this energy the inelastic channel opens and the assigned J values are only lower limits. In the case of Ca, the parameters of resonances between 0.5 and 1.2 MeV have been determined. In many cases we have used new differential data for Ca to verify the ℓ-value obtained by fitting the resonance. The channel radii and s and p-wave strength function of these nuclei are also discussed.

1. INTRODUCTION

The neutron total cross-section of Na is of obvious importance for fast-reactor calculations. In recent years, several new measurements have been performed [1 - 6]. In this work, these measurements are compared, and our results are analysed by the multilevel one-channel R-matrix formalism. In spite of the wealth of data for Na, there appears to be a paucity of detailed analysis, the work of Stelson and Preston [7] and of Hibdon [8] being exceptions. At least for high neutron energies, (E > 0.432 MeV), this is due to the lack of a reliable two-channel multilevel fitting program. This work attempts an extension of the one-channel description to higher energies where it is clearly an incorrect description. The first excited state of the ^{23}Na nucleus occurs at 0.432 MeV, but the "elastic-scattering-only" description has been pushed to 1 MeV. It was hoped that the failure of the description could also provide some indication of the extent and influence of inelastic scattering in this region. In fact, it has been found that the elastic scattering picture does provide a fairly good phenomenological description up to 1 MeV. The interpreted J-values must be taken as lower limits and one must be very careful about reading too much physical meaning into the results above 0.5 MeV.

The ^{40}Ca results may be of interest because the ℓ- and J-values reported were determined from our high-resolution, differential elastic-scattering cross-section measurements. The assignments were accomplished by studying the resonance shapes as a function of the scattering angle. The formalism required has been highly developed by Blatt and

Biedenharn [9]. This work is currently in press. The results of a preliminary study [10] and some differential-scattering measurements and analysis of ^{12}C [11] have already been published.

Calcium also provides an example of a clean nucleus for the single-channel description. The inelastic channel is not open until 3.354 MeV and the ground-state spin is zero, making the channel spin unique. Furthermore, a quick view of any high-resolution data for calcium above a few hundred keV indicates that multilevel interference will be important. For these reasons, analysis of this neutron cross-section is discussed here.

In the following sections, the Karlsruhe experimental set-up is reviewed and the R-matrix formulae used in this work are summarized. Both the experimental details [12] and the theory [13 - 15] are covered in much more detail elsewhere. Resonance parameters are given for Na and Ca. In the case of sodium some previous assignments are corrected. The calcium results considerably extend previous analysis.

2. EXPERIMENTAL DESCRIPTION

The total neutron cross-sections of sodium and calcium were measured with the neutron time-of-flight facility at the Karlsruhe Isochronous Cyclotron and were previously published [5, 6]. The detailed description of the spectrometer has been given elsewhere [12], and hence only features pertinent to these measurements will be described here. These data were obtained for the energy range from 290 keV (500 keV Ca) to 40 MeV by transmission measurements with good geometry. Neutrons were produced in bursts of $\approx$ 1 ns duration by bombarding a uranium target with deuterons of the internal cyclotron beam at a repetition rate of 19.13 kHz. Standard time-of-flight techniques were used for data collection. A liquid scintillator (NE-213), 9 cm in diameter by 1 cm thick, mounted on a XP-1040 photomultiplier was used for neutron detection. The incident neutron beam was monitored by a γ-pulse-shape discriminating detector placed at 6° to the beam at a distance of 11 m from the source. About 8200 time channels were analysed by a Laben UC-KB and recorded in a CDC on-line computer.

With a flight path of about 57 m, an overall resolution of better than 0.05 ns/m was achieved. This corresponds to an energy resolution of 0.22 keV at 300 keV and 2.5 keV at 1.5 MeV. The scattering sample for sodium was a high-purity (99.998%) metal slab[1], 0.2323 atoms/barn, sealed in an aluminum can. The calcium sample had a thickness of 0.2133 atoms/barn and consisted of granulated metal enclosed in a cylindrical aluminum container with thin end windows. In both cases, an identical empty can was put into the open beam position for background compensation. Spectra were measured with the sample in place and with sample removed in a typical cycle time of 20 min. Uncertainties in the calcium cross-section due to counting statistics varied from 5% at 800 keV to 3% at 1.5 MeV. The sodium data have a statistical uncertainty of less than 0.3% between 600 and 900 keV and smaller than 1% between 420 and 600 keV. Corrections for background and dead-time effects were applied. The combined

[1] The machining and canning of this sample was performed by the CBNM, Geel.

corrections were typically a few percent of the open beam counting rate and did not exceed 20% below 1 MeV. Corrections for in-scattering were less than 0.01% and were not performed.

3. SINGLE-CHANNEL MULTILEVEL DESCRIPTION

Since resonance widths are approaching the level spacings for Na and Ca in the energy region investigated, the usual Breit-Wigner single-level formulae are not applicable. An appropriate formalism is the multilevel R-matrix description with a single open channel for elastic scattering. This description will be exact for Ca and Na below the thresholds for inelastic scattering, assuming γ-ray channels to be negligible.

Of course, much has been written about the R-matrix formalism [13 - 16]. The following is only intended to summarize the formulae used in this analysis. According to Lane and Thomas [13], the R-function can be split up into an explicit multilevel sum $R'_{\ell Js}$ and a background term $R^0_{\ell Js}$:

$$R_{\ell Js} = R^0_{\ell Js} + \sum_{\lambda} \frac{\gamma^2_{\lambda \ell Js}}{(E_\lambda - E)}$$

where the sum is over λ levels of total angular momentum J, orbital momentum ℓ and channel spin s. The quantities E_λ are the eigenvalues of the internal nuclear energy and the reduced widths $\gamma_{\lambda \ell Js}$ are given by the projection of the internal wave functions onto the channel surface. The R-function is related to the collision function, $U_{\ell Js}$, by

$$U_{\ell Js} = \exp(-2i\varphi'_\ell)\,(1 + 2i\,P'_\ell \frac{R'_{\ell Js}}{1 - L'_\ell R'_{\ell Js}})$$

where the newly introduced quantities contain the background term $R_{\ell Js}$. These are defined as

$$L'_\ell = S'_\ell + i\,P'_\ell$$
$$S'_\ell = [S_\ell(1 - R^0_{\ell Js} S_\ell) - R^0_{\ell Js} P^2_\ell]/d$$
$$P'_\ell = P_\ell / d, \quad d = (1 - R^0_{\ell Js} S_\ell)^2 + (R^0_{\ell Js} P_\ell)^2$$
$$\varphi'_\ell = \varphi_\ell - \arctan [R^0_{\ell Js} P_\ell / (1 - R^0_{\ell Js} S_\ell)]$$
$$S_\ell = S^0_\ell - B_\ell$$

where S^0_ℓ, P_ℓ and φ_ℓ are the usual shift factor, the penetration factor and the potential-scattering phase shift, respectively.
The total neutron cross-section is given by

$$\sigma_t = \frac{2\pi}{k^2} \sum_{\ell Js} g_J (1 - \mathrm{Re}\, U_{\ell Js})$$

where g_J is the spin weight factor.

Since the R-matrix formulation does not directly specify the eigenvalues E_λ and internal eigenfunctions, the boundary condition B_ℓ is arbitrary. The total cross-section is independent of the choice of this quantity. It is

convenient to choose B_ℓ such that the level-shift factor vanishes. Then, without strong resonance-potential interference, the physical resonance peaks occur at the energies E_λ. The level-shift factor can be made zero by choosing $B_\ell = S_\ell(E)$, but the price of this energy-dependent boundary condition is that the parameters E_λ and $\gamma_{\lambda \ell J s}$ are no longer simply related to the eigenvalues of the internal energy and the projection of the eigenfunctions on the channel surface. The level shift is identically zero for s-wave neutrons and there is no change in interpretation from the usual energy-independent boundary condition $B = 0$. It can also be shown that for higher ℓ-values the energy dependence introduced into E_λ and $\gamma_{\lambda \ell J s}$ is small [14].

Another important quantity to be considered in practical application of the R-matrix formulae is the channel radius which is closely related to the treatment of resonances outside the region of analysis. Detailed parameters can only be obtained for an energy range which includes a restricted number of local levels. Nevertheless, the influence of levels outside this range is not negligible. This may be accounted for by an expansion of the $R^0_{\ell J s}$ background term about the median energy E_m of the region of analysis [17],

$$R^0_{\ell J s} = A_{\ell J s} + B_{\ell J s}(E - E_m) + C_{\ell J s}(E - E_m)^2 + \ldots .$$

The coefficients A, B and C may be ℓ-and J-dependent and represent parameters to be determined as well as the resonance energies and widths.

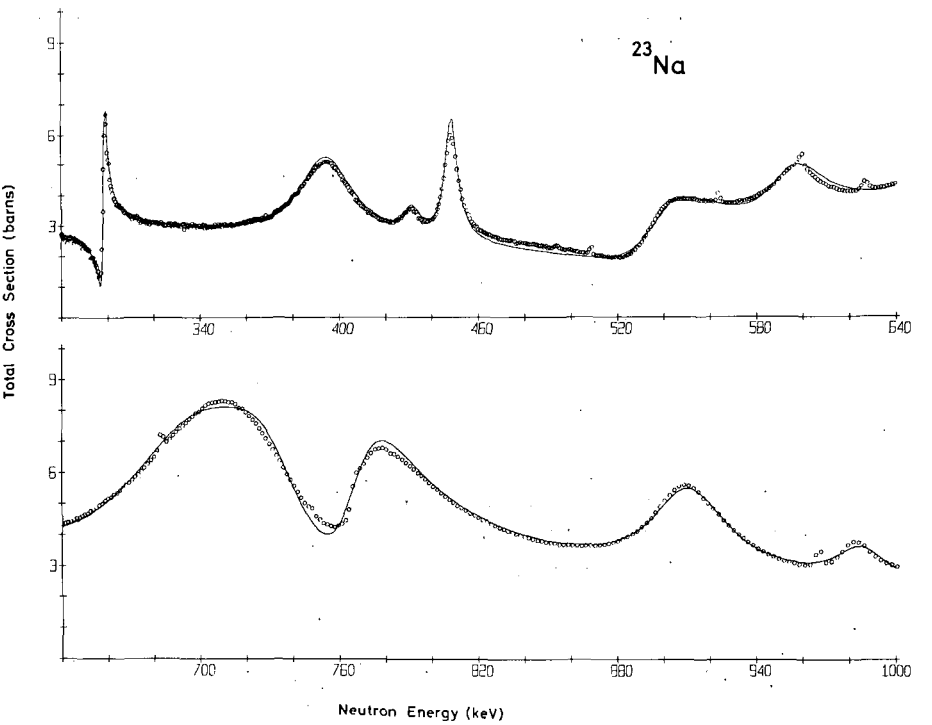

FIG. 1. Experimental and calculated total neutron cross-section of ^{23}Na from 0.28 to 1.02 MeV.

Their influence and interpretation depend strongly on the nucleus and energy region.

The constant term $A_{\ell J s}$ may be understood as a representation of the effect of very-far-away resonances in the energy region of interest. Such would be the case, for example, for a far-removed "giant resonance" containing many individual levels. At low energies, it can be interpreted as a channel-radius correction which makes the total cross-section independent of the assumed channel radius. The effect is mainly seen in the potential-scattering cross-section. The coefficient $B_{\ell J s}$ has been shown to be directly related to the corresponding strength function [17]. In particular, it contains that fraction of the total strength not arising from the local levels which have been explicitly included in the level sum.

The above formulation has been programmed [18]. The code operates by a χ^2-minimization, given a particular input set of resonance assignments (ℓ-and J-values). The results obtained are the E_λ, Γ_λ, A, B and C parameters for all possible ℓ-and J-values. The experimental resolution function cn also be folded with the theoretical cross-section to better represent the experimental data.

TABLE I. RESONANCE PARAMETERS[a] FOR THE ^{23}Na TOTAL NEUTRON CROSS-SECTION

E_R(keV)	$\Gamma_n(E_R)$ (keV)	ℓ	J	Γ_{obs} (keV)
298.4	1.9	0	2	
393.8	25.8	1	1	
431.2	7.8	1	0	
448.4	5.7	2	2	
508.8				
536.6	35.3	0	1	
564.1				
597.8	25.8	(1)	1	21
599.8				
627.0				
683.4				
697.2	60.	(2)	(4)	72
726.6	45.	(1)	(3)	
748.3				
766.4				
780.5	43.6	(2)	(4)	38
911.2	40.1	(2)	(3)	32
968.0				
985.1	27.2	(2)	(1)	16

	$\ell = 0$		$\ell = 1$				$\ell = 2$				
J	1	2	0	1	2	3	0	1	2	3	4
$A_{\ell J}$	0.139	-0.143	-0.329×10^{-1}	0.630×10^{-1}	-	0.254×10^{-1}	-	-0.512×10^{-2}	0.171×10^{-3}	0.749×10^{-1}	0.139×10^{-1}
$B^R_{\ell J}$	0.434×10^{-3}	0.490×10^{-3}	0.986×10^{-3}	0.679×10^{-4}	-	0.590×10^{-4}	-	-	-	-	-

[a] Analysis performed with $S_\ell = B_\ell$ and channel radius a = 4.26 f.

4. CROSS-SECTIONS AND RESONANCE PARAMETERS

Cross-section data and resonance parameters are given here for sodium and calcium. The total neutron cross-section for Na from 0.28 to 1.02 MeV is shown in Fig. 1. The solid curve was calculated using the parameters listed in Table I. The first four columns of the table give the analysed resonance energy, the fitted neutron width and the ℓ-and J-values. These parameters are based on a one-channel description. Column five gives the observed total width which is different from the fitted neutron width only for the five cross-section fluctuations observed above 500 keV. The A and B parameters discussed previously are shown at the bottom of the table. Several smaller resonances are also identified in the table; owing to their size and narrowness, no attempt has been made to analyse these levels. The assignments and parameters are discussed later.

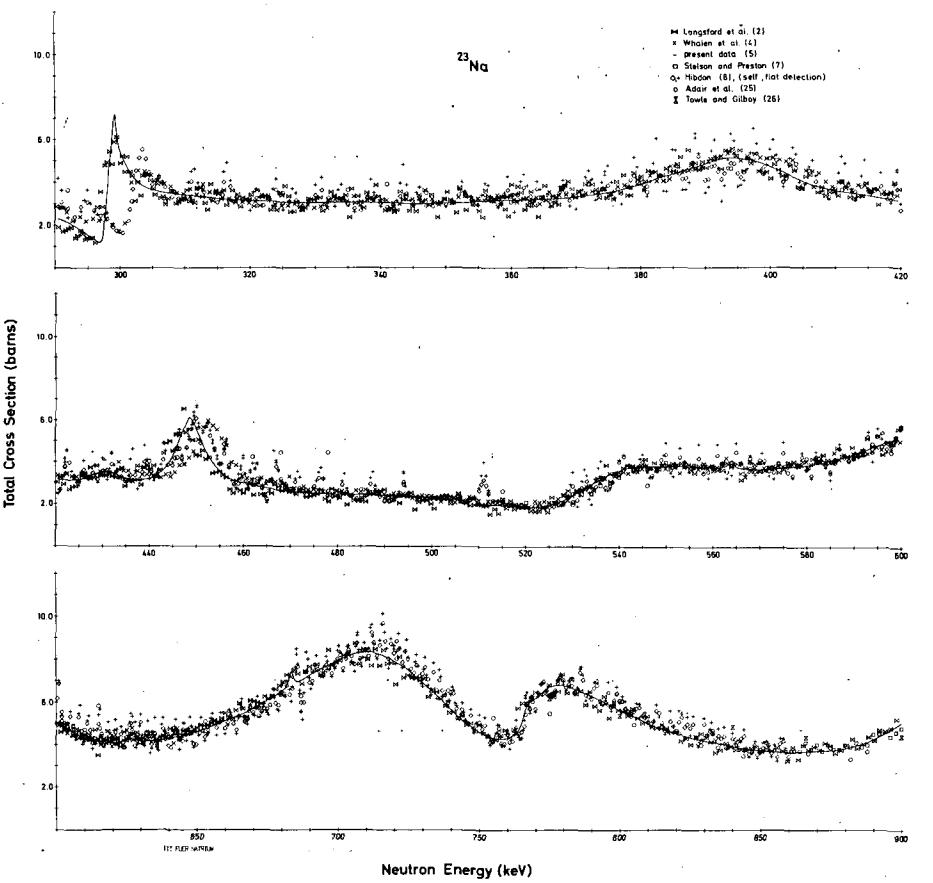

FIG. 2. Comparison of ^{23}Na total neutron cross-section data available from CCDN in the energy range from 290 to 900 keV.

Figure 2 compares these data with other total cross-section data available from CCDN. Nearly all data lie in a band which is approximately 15% of the cross-section value. The data of Hibdon [8] and Whalen [4] demonstrate a significant shift of resonance peaks to higher energies. This is clearly seen for the 300 keV resonance. In general, we agree best with the Langsford data [2], but neglecting the energy shift there is also excellent agreement in the regions between resonances with the Whalen data. Considering the point scatter of some of the earlier measurements the overall agreement is very satisfactory.

The total neutron cross-section for calcium from 0.56 to 1.26 MeV is shown in Figs 3 and 4. The solid curve again illustrates the calculation. Only those resonances sufficiently resolved for analysis were included in the calculation. In this energy range, this unfortunately eliminates many narrow resonances. The ^{40}Ca resonance parameters are listed in Table II. In nearly all cases, the ℓ-and J-values were obtained by analysis of our differential scattering cross-section data. The total cross-section alone does not permit a clear separation of p- and d-wave resonances or of the appropriate J-values for narrow resonances.

The calcium resonance parameters have been further analysed for the level spacing and s-wave strength function. An s-wave spacing of (38.6 ± 7.6)keV and a strength function of (2.8 ± 1.0) × 10^{-4} are found. These values are in good agreement with other results [19, 20].

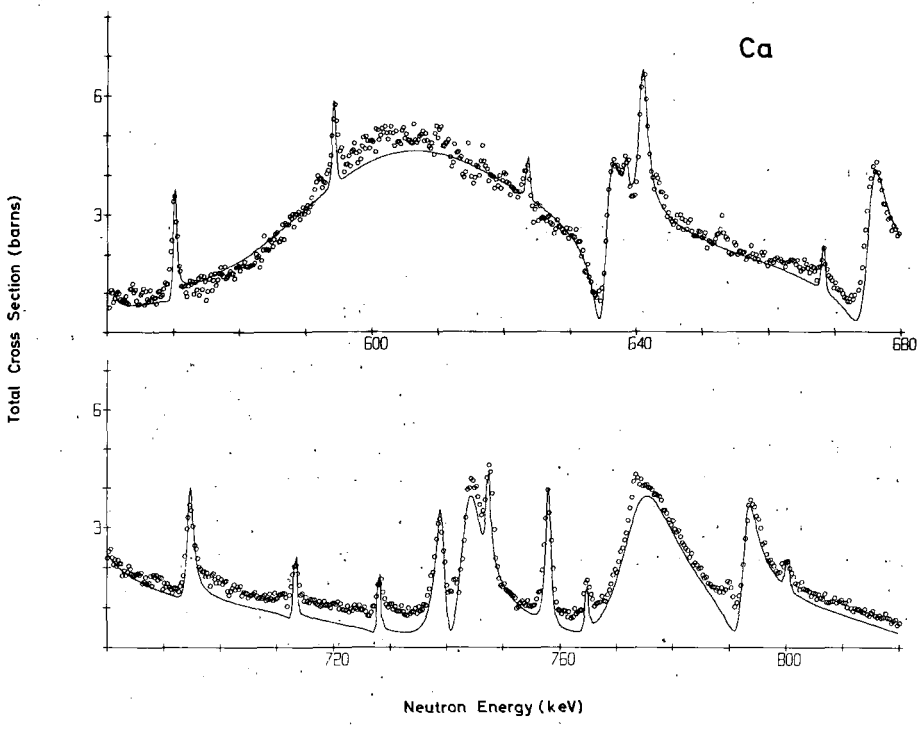

FIG. 3. Experimental and calculated total neutron cross-section of Ca from 560 to 820 keV.

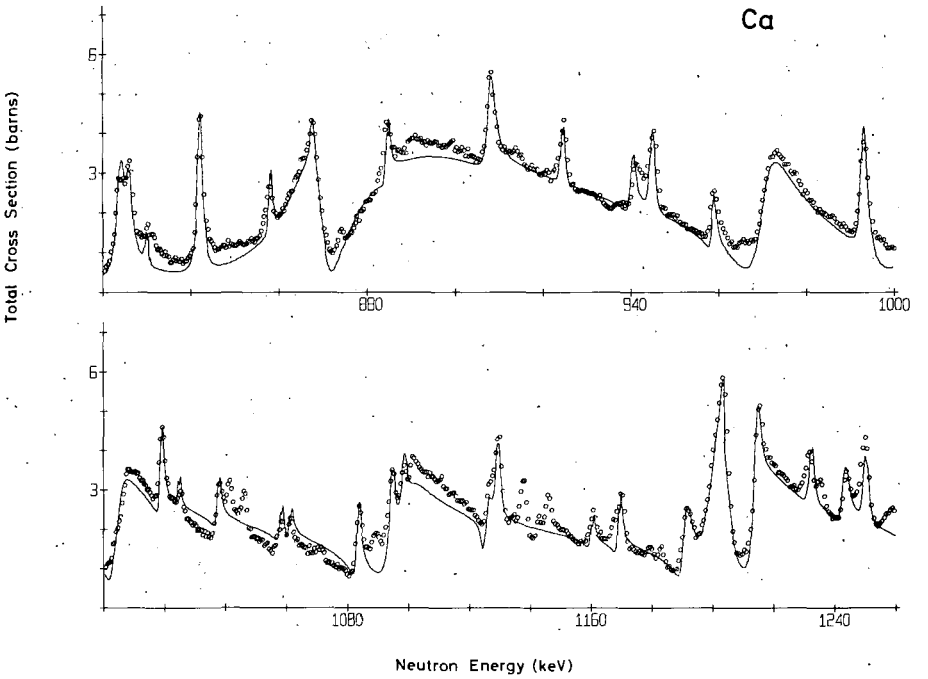

FIG. 4. Experimental and calculated total neutron cross-section of Ca from 820 to 1260 keV.

5. DISCUSSION

5.1. Analysis of Na-resonances

The resonance parameters obtained for ^{23}Na have been given in Table I. In this section, the analysis is discussed in further detail. The inelastic-scattering cross-section is not very large below 1 MeV. Recommended values for $\sigma_{n,n'}$ indicate about 300 mb [21]. Since a satisfactory two-channel fitting procedure has not been available we decided to try to extend the elastic-scattering formulae. However, above 500 keV, the reported J-values must be understood as lower limits. The true total cross-section is reduced from that given by the one-channel formalism by approximately a factor $\Gamma_n/(\Gamma_n + \Gamma_{n'})$ due to inelastic scattering.

298 keV: Because of a pronounced interference shape, this level is assigned to s-wave neutrons. The J-value of 2 is also clear. This analysis yields a neutron width of 1.9 keV rather than 4 keV as reported previously [7]. It seems that just this problem of experimental resolution is the cause of the previous assignment to J = 1. No evidence was seen for the J-dependence of the s-wave potential scattering reported by Stelson and Preston.

394 keV: The parameters obtained for this level agree with those previously reported. Only slight changes in the resonance energy and neutron width have resulted from this analysis.

TABLE II. RESONANCE PARAMETERS[a] FOR ^{40}Ca (n, n)

E_R (keV)	Γ_n^b (E_K)(keV)	ℓ	J	E_R (keV)	Γ_n^b (E_R) (keV)	ℓ	J
570.1	0.2	1	3/2	924.6	0.2	2	5/2
591.3	55.	0	1/2	940.5	0.6	1	1/2
594.2	< 0.1	2	5/2	945.1	0.5	2	(3/2)
623.5	< 0.1	2	(5/2)	958.8	0.4	1	3/2
635.5	2	0	1/2	970	7.2	0	1/2
638.4	< 0.1	2	5/2	993.3	1.1	(2)	(3/2)
640.9	1.3	1	1/2	1003.9	11	0	1/2
668.1	<0.1	2	(5/2)	1018.7	0.5	1	(3/2)
675	2.7	0	1/2	1025.2	0.3	(1)	(1/2)
694.6	0.9	1	1/2	1037.4	0.7	1	1/2
713.2	0.1	1	3/2	1058	0.4	(1)	1/2
728	<0.1	1	3/2	1061.5	0.4	(1)	1/2
738.2	3.2	0	1/2	1083.2	0.7	(1)	3/2
742.8	4.4	0	1/2	1094.4	0.6	2	(3/2)
747.3	0.3	1	1/2	1094.9	1.2	0	1/2
758	0.6	2	(3/2)	1097.7	0.2	2	5/2
764.8	0.1	(2)	3/2	1126	0.5	(0)	1/2
771.5	12	0	1/2	1129.2	0.7	2	3/2
792.5	2.4	0	1/2	1160.2	0.2	(2)	3/2
800.2	<0.1	2	5/2	1169	0.7	1	3/2
823	3.5	0	1/2	1189.4	3	0	1/2
826	0.4	(1)	1/2	1202.6	4	(2)	5/2
830	0.1	2	(5/2)	1210.8	15	0	1/2
842.2	0.9	1	3/2	1214	1	1	3/2
857.2	0.3	2	(3/2)	1232	1	2	3/2
861.8	29	0	1/2	1242.9	1.5	1	1/2
867.6	0.3	1	(1/2)	1250	0.5	2	(5/2)
878.7	31	0	1/2	1262	0.5	(2)	(3/2)
884.8	0.3	1	3/2	1284	15	0	1/2
908.1	1.5	1	1/2				

0.82 - 1 MeV $\ell = 0$	$\ell = 1$		$\ell = 2$	
J	1/2	1/2	3/2	3/2	5/2
$A_{\ell J}$	0.238	-0.467	-0.504	0.586×10^{-2}	0.345×10^{-2}
$B_{\ell J}$	0.337×10^{-4}	0.189×10^{-3}	0.107×10^{-3}	-	-
$C_{\ell J}$	0.250×10^{-6}	0.430×10^{-6}	0.770×10^{-6}	-	-

[a] Analysis performed with $S_\ell = B_\ell(E)$ and channel radius a = 3.59 f.

[b] Owing to the effects of resolution, the accuracy of neutron widths $0 \leq .5$ keV is estimated to be 20%.

431 keV: This small level is assigned to p-wave neutrons with $J = 0$; it had not been seen in previous cross-section measurements. The J-value is certain for this 8 keV resonance width since the narrow 1.9 keV level at 298 keV was fully resolved in our data.

449 keV: This resonance is assigned to p- or d-wave neutrons and is well fitted by $J = 2$. We find a width of 5.8 keV rather than the previously reported value of 9 keV for $J = 1$. This again seems to be explicable by the experimental resolution. A value of $J = 2$ is favoured by the differential data obtained by Chein [22].

537 keV: Because of the interference pattern, this level is certainly due to s-wave formation. The value of $J = 1$ gives an excellent description. In principle, the J-value could be higher since inelastic scattering can occur. However, this is extremely unlikely since the inelastic neutron would have only about 100 keV and a small penetrability compared with a 537 keV s-wave neutron. The first excited level of ^{23}Na has been assigned $5/2^+$; thus, the inelastically scattered neutron must have an orbital momentum $\ell \geq 2$ and a low penetrability.

597 keV: The cross-section at this resonance agrees well with $\ell \geq 1$, $J = 1$. Again the inelastic-scattering width must be very large in order to permit an assignment $J = 2$. However, this argument is less convincing for this $\ell \geq 1$ resonance than for the previous s-wave level.

710 keV and 780 keV: The J-values assumed for these levels are only lower limits. Comparing the elastic-scattering cross-section based on these J-values with the measured total cross-section, we see that appreciable inelastic scattering is indicated. The situation is further complicated by the fact that the lower resonance is almost certainly a superposition of two non-interfering levels. We have assumed $\ell \geq 1$, $J = 3$ at 697 keV and $1 = 2$, $J = 4$ at 727 keV. These assignments give a reasonably good fit in a one-channel description. Such "assignments" are useful only for an empirical description and should not be taken as a correct physical interpretation. However, such parameters may be useful for reactor calculations. In this case, it is also unlikely that a two-channel description would yield unique parameters.

911 keV and 985 keV: These two levels are reasonably fitted by $\ell = 2$, $J = 3$ and $\ell = 2$, $J = 1$ respectively. Since the calculated elastic-cross-section peak is lower than the total cross-section a larger J-value is indicated. A J-value larger than 4 cannot be caused by d-wave neutrons. If the $J = 4$ assignment is correct, an inelastic reaction width of about 10 keV is indicated for the 910 keV level. For increasingly higher J-values the inelastic width will increase accordingly.

5.2. Analysis of Ca-resonances

A superficial examination of the Ca cross-section reveals regions of slowly varying cross-section at the lower energies and an increasing density of resonances at higher energy. Many of the resonances appear to be broad and overlapping. Nearly 60 resolved resonances were analysed between 0.56 and 1.26 MeV. For analysis, the entired region was subdivided into four intervals. No attempt was made to fit the structure above 1.26 MeV. Good agreement is obtained for nearly all analysed resonances. In between the resonances the calculation is not satisfactory. This is due in part to the presence of unresolved resonance structure. Definite assignments and

parameters for these levels are impossible though their existence is regarded as certain.

At the beginning of this analysis several difficulties were encountered. The high background cross section value in the minima of broad resonances suggested unusually large p-wave scattering. Shortcomings in the experimental data could be excluded by careful examination of our cross-section data and detailed comparison with recent high-resolution results from other laboratories. In some cases, the resonances seemed to be better described by assuming p-wave formation. This assumption yields an unreasonable high density of p-wave levels and p-wave strength. Furthermore, all of the broad resonances have been assigned to $J = 1/2$. The assignment of these resonances to s-wave formation has been confirmed by recent differential scattering measurements [23].

The A and B coefficients obtained for p-waves indicate a large R^0 component in this region. Undoubtedly, some of this background comes from unresolved local levels. The remaining background must be assumed to come from an energy region containing large p-wave strength, probably below the neutron binding energy. The implications of this interpretation are under investigation [24].

In view of the limited success in representing the non-resonant part of the cross-section, this analysis provides detailed resonance parameters for calcium, but a full description of the cross section requires further investigation.

6. SUMMARY

New assignments of Na resonances based on high-resolution total neutron cross-section data are given for the energy range between 280 keV and 1 MeV. A satisfactory phenomenological description of the data is presented using a one-channel description even above the inelastic-scattering threshold. However, the uncertainty in the J-values emphasizes the need for measurements of the differential elastic scattering and a suitable two-channel multilevel code. For calcium, a resonance-parameter analysis was performed using highly resolved total neutron cross-sections. Level assignments were mostly obtained from differential scattering cross-section data. Evidence is found for a large p-wave strength in the energy region investigated.

REFERENCES

[1] DECONNINCK, G., DE VROEY, M., MEULDERS, J.P., Rep. EANDC(E)-49 "L" (1963).
[2] LANGSFORD, A., BOWEN, P.H., COX, G.C., FIRK, F.W.K., McCONNELL, D.B., ROSE, B., SALTMARSH, M.J., Nuclear Structure Study with Neutrons (Proc. Conf. Antwerp, 1965). North-Holland Publishing Company, Amsterdam (1966) 529.
[3] GARG, J.B., RAINWATER, J., WYNCHANK, S., HAVENS, W.W., Jr., Nuclear Structure Study with Neutrons (Proc. Conf. Antwerp, 1965), North-Holland Publishing Company, Amsterdam (1966) 526.
[4] WHALEN, J., data referenced in CCDN-NW/11 (1969).
[5] CIERJACKS, S., FORTI, P., KOPSCH, D., KROPP, L., NEBE, J., UNSELD, H., Rep. KFK-1000 (1968).
[6] CIERJACKS, S., FORTI, P., KOPSCH, D., KROPP, L., NEBE, J., Phys. Letts 29B (1969) 417.
[7] STELSON, P.H., PRESTON, W.M., Phys. Rev. 88 (1952) 1354.

[8] HIBDON, C.T., Phys. Rev. 118 (1960) 514;
HIBDON, C.T., Phys. Rev. 122 (1961) 1235;
HIBDON, C.T., Phys. Rev. 124 (1961) 500.
[9] BLATT, J.M., BIEDENHARN, L.C., Rev. mod. Phys. 24 (1952) 258.
[10] KIROUAC, G.J., NEBE, J., Rep. KFK-1069 (1969).
[11] NEBE, J., KIROUAC, G.J., Rep. KFK-1189 (1970).
[12] CIERJACKS, S., DUELLI, B., FORTI, P., KOPSCH, D., KROPP, L., LOSEL, M., NEBE, J., SCHWEICKERT, H., UNSELD, H., Rev. scient. Instrum. 39 (1968) 1279.
[13] LANE, A.M., THOMAS, R.G., Rev. mod. Phys. 30 (1958) 257.
[14] LYNN, J.E., The Theory of Neutron Resonance Reactions, Clarendon Press, Oxford (1968).
[15] WIGNER, E.P., EISENBUD, L., Phys. Rev. 72 (1947) 29.
[16] WIGNER, E.P., Phys. Rev. 70 (1946) 15.
[17] FIRK, F.W.K., LYNN, J.E., MOXON, M.C., Proc. Phys. Soc. 82 (1963) 477.
[18] NEBE, J., Internal Rep. Karlsruhe (1968).
[19] BOWMAN, C.D., BILPUCH, E.G., NEWSON, H.W., Ann. Phys. 17 (1962) 319.
[20] WILENZICK, R.M., MITCHELL, G.E., SETH, K.K., LEWIS, H.W., Phys. Rev. 121 (1960) 1150.
[21] SCHMIDT, J.J., Rep. KFK-120 (1966).
[22] CHIEN, J.P., SMITH, A.B., Nucl. Sci. Engng 26 (1966) 500.
[23] KIROUAC, G.J., NEBE, J., submitted for publication in Nucl. Phys. (1970).
[24] NEBE J., thesis in preparation (1970).
[25] ADAIR, R.K., BARSCHALL, H.H., BOCKELMANN, C.K., SALA, O., Phys. Rev. 75 (1949) 1124.
[26] TOWLE, J.H., GILBOY, W.B., Nucl. Phys. 32 (1962) 610.

DISCUSSION

J.S. STORY (Chairman): You are extending resonance analysis to quite high energies. Do you think it will be sufficient at these energies to continue calculating the potential scattering from the usual hard-sphere phase-shifts, or do you expect that it will be necessary to use instead the potential scattering calculated from a typical optical-model potential (i.e. from a well with a rounded edge) - as was done, for instance, by Slaggie and Reynolds at KAPL some years ago in their resonance analysis for carbon and/or for oxygen.

J. NEBE: No such calculations were performed in this case. In these calculations, the potential scattering phase shift is not assumed to be caused by pure hard-sphere scattering. The effect of a realistic potential is represented by the energy-dependent expansion of the R^{∞} term. Since for sodium the inelastic channel is open, the description is really phenomenological, and a more realistic calculation of the potential phase shift may not be very useful.

MULTILEVEL ANALYSIS OF THE ^{233}U AND ^{235}U CAPTURE AND FISSION CROSS-SECTIONS AND STATISTICAL PROPERTIES OF THE KAPUR-PEIERLS-TYPE RESONANCE PARAMETERS FOR THE S-WAVE CROSS-SECTIONS OF THE FISSILE ISOTOPES*

G. de SAUSSURE, R. B. PEREZ
Oak Ridge National Laboratory Oak Ridge, Tenn.,
United States of America
H. DERRIEN
Centre d'Etudes Nucléaires de Saclay,
France

Abstract

MULTILEVEL ANALYSIS OF THE ^{233}U AND ^{235}U CAPTURE AND FISSION CROSS-SECTIONS AND STATISTICAL PROPERTIES OF THE KAPUR-PEIERLS-TYPE RESONANCE PARAMETERS FOR THE S-WAVE CROSS-SECTIONS OF THE FISSILE ISOTOPES.

At the 1966 Conference on Nuclear Data for Reactors, simultaneous measurements of the capture and fission cross-sections of ^{233}U and ^{235}U were presented. Those measurements have now been analysed with the multilevel formalism developed by Adler and Adler. To obtain consistent sets of resonance parameters the capture and fission data were least-square fitted simultaneously. This analysis was carried out to 60 eV for ^{233}U and to 100 eV for ^{235}U.

The main purpose of this analysis was to provide a simple and precise analytical description of the very complex structure of the fission and capture cross-sections of ^{233}U and ^{235}U at low energy. Such an analytical description should be useful to calculate reaction rates in nuclear reactors and to compare experimental data taken with different energy resolutions or at different sample temperatures.

For the low-energy resonances of ^{233}U and ^{235}U, the neutron width is always smaller, by at least two orders of magnitude, than the total width. Thus, the total cross-section, for those isotopes, can be approximated as the sum of the absorption cross-section and the potential scattering cross-section. Hence it is possible to compute the total cross-section from the resonance parameters obtained by fitting the fission and capture cross-sections. The total cross-section of ^{235}U computed by this method is compared to the data from a transmission measurement done at Saclay, with the sample at 77° K. The computed total cross-section of ^{233}U is compared with transmission data obtained at Oak Ridge National Laboratory and at the Material Testing Reactor. Such comparisons between data obtained by different experimental techniques illustrate the internal consistency of the low-energy cross-sections of the two main uranium fissile isotopes.

The pyhsical interpretation of the resonance parameters is somewhat ambiguous, because such multilevel fits are by no means unique. This is particularly true for ^{233}U since, for this nucleus, the resonances are not well resolved even at low energies. The fact that multilevel analyses are not unique will be illustrated by comparing parameters obtained in this investigation with parameters obtained by other workers, for the same cross-sections. Finally the distribution of the Adler parameters obtained in this investigation will be compared with distributions derived from the partial-width distribution laws of Porter and Thomas.

Three different multilevel formalisms have been extensively used to describe the low-energy neutron cross-sections of the fissile nuclei. Those formalisms are specializations of the R-matrix theory of Wigner and Eisenbud.

* Research sponsored by the US Atomic Energy Commission under contract with the Union Carbide Corporation.

In the Vogt and Reich and Moore formalisms, the cross-sections are expressed in terms of the R-matrix level parameters: the eigenvalues E_λ, and the partial widths $\Gamma_{\lambda c}$. The statistical properties of those parameters have been studied extensively. Unfortunately, the functional dependence of the cross-sections on the level parameters is very complicated so that these formalisms are cumbersome to use in reactor calculations or data evaluations.

The Adler and Adler formalism is a generalized Kapur-Peierls formalism. It leads to cross-section expressions which have a simple functional form particularly suitable for reactor calculations and for the fitting of experimental data, but it requires a re-definition of the level parameters. Apparently there is no theory yet which gives directly the statistical behaviour of the parameters used in the Adler and Adler formulation.

The R-matrix theory and the generalized Kapur-Peierls theory are complementary in that the statistical properties of the R-matrix parameter are much better known, but the Kapur-Peierls formulation is best suited to a variety of applications. Techniques have been developed to obtain the distribution of the generalized Kapur-Peierls parameters using the known distribution of the R-matrix parameters and the mathematical connection between the R-matrix and the Kapur-Peierls cross-section formalisms.

This paper describes such a technique, based on the direct partial fraction expansion of the Reich-Moore cross-section formulae. This technique is particularly useful for the low-energy cross-sections of the usual fissile isotopes where many levels but only a few fission channels need to be considered. The technique was used for an extensive study of the statistical distribution of the Adler-Adler parameters as a function of the known distributions of the R-matrix parameters.

Among the various results obtained, it was found that the computation of average cross-sections utilizing a single-level formalism, that is neglecting interference effects, may lead to errors as large as 30% in the estimation of the average capture-to-fission ratio.

1. INTRODUCTION

At the 1966 IAEA Conference on Nuclear Data for Reactors, simultaneous measurements of the capture and fission cross sections of ^{233}U and ^{235}U were presented.[1-3] This paper discusses a multilevel analysis of a part of these data. The low-energy capture and fission cross sections were "least square-fitted" simultaneously using the multilevel formalism developed by Adler and Adler.[4]

In order to compare the Kapur-Peierls parameters obtained with the Adler formalism to the R-matrix parameters obtained by others, for the same cross sections, a method was developed to convert a set of R-matrix parameters into an equivalent set of Kapur-Peierls parameters. This same method was also used to numerically investigate the distributions of the Kapur-Peierls parameters by selecting R-matrix parameters from the appropriate distributions and converting those into equivalent Kapur-Peierls parameters.

2. METHOD OF ANALYSIS

Three different multilevel formalisms have been extensively used to describe the low-energy neutron cross sections of the fissile nuclei. Those formalisms are specializations of the R-matrix theory of Wigner and Eisenbud.[5,6]

In the Vogt[7] and Reich and Moore[8] formalisms, the cross sections are expressed in terms of the R-matrix level parameters: the level energies, E_λ, and partial widths, $\Gamma_{\lambda c}$. The Adler and Adler[4] formalism is a generalized Kapur-Peierls[9] formalism in which the cross sections are given in terms of Kapur-Peierls poles μ and ν and residues G and H.

Those different formalisms have been reviewed by Harris[10,11] and described in some detail in the excellent review of Moore.[12] The relations of the multilevel formalisms to the different nuclear-reaction theories have been discussed by Adler and Adler.[13] Complete reviews of the formal nuclear-reaction theories have been given by Lane and Thomas[14] and by Lynn.[15]

In the Adler and Adler multilevel formalism, the general expression for the resonance part of the reaction cross section is given by:

$$\sigma^{(x)}(E)\ E^{\frac{1}{2}} = \sum_k \frac{G_k^{(x)}\ \nu_k + H_k^{(x)}\ (\mu_k - E)}{(\mu_k - E)^2 + \nu_k^2} \qquad (1)$$

where $\sigma^{(x)}(E)$ is the cross section for reactions (x) as a function of neutron energy, E, and G, H, μ, and ν are resonance parameters which have only a weak energy dependence and hence have been treated here as constants.

If the Doppler and instrumental resolution broadening can be approximated by Gaussian kernels, the Doppler and instrumental broadened cross section corresponding to Eq. (1) is:[2,16,17]

$$\sigma_\Delta^x(E)\ E^{\frac{1}{2}} = \sum_k \frac{1}{\nu_k}\left\{G_k^{(x)}\ \psi(\beta_k,\ x_k) - H_k^{(x)}\ \varphi(\beta_k,\ x_k)\right\} \qquad (2)$$

where Δ^2 is the sum of the squares of the Doppler width and of the instrumental resolution width, $\beta = (\Delta/\nu)$, $x = (E - \mu)/\nu$, and

$$\psi(\beta,x) = \frac{1}{\beta\pi^{\frac{1}{2}}} \int \frac{e^{-(x-y)^2/\beta^2}\ dy}{1 + y^2}$$

$$\varphi(\beta,x) = \frac{1}{\beta\pi^{\frac{1}{2}}} \int \frac{ye^{-(x-y)^2/\beta^2}\ dy}{1 + y^2}$$

To obtain the best possible parameters from the simultaneous measurements of the capture and fission cross sections, it is desirable to fit simultaneously the two cross sections. A computer program[18] was written to minimize the quantity:

$$S = \sum_i \left\{\left[(\sigma_f\sqrt{E})_e - (\sigma_f\sqrt{E})_c\right]_i^2 \omega_{fi} + \left[(\sigma_c\sqrt{E})_e - (\sigma_c\sqrt{E})_c\right]_i^2 \omega_{ci}\right\} \qquad (3)$$

where σ_f and σ_c represent the fission and capture cross sections, respectively, ω_{fi} and ω_{ci} are statistical weights appropriate to the ith channel of the fission or capture measurement, and the subscripts e and c refer to the experimental data and the computed values (Eq. 2), respectively.

3. RESULTS AND COMPARISON WITH OTHER DATA

The statistical errors and the resolution function associated with the data have been discussed elsewhere.[2-3] The cross sections of ^{233}U were analyzed up to 60 eV, those of ^{235}U up to 100 eV. The resonance parameters obtained are given in Table I for ^{233}U and Table II for ^{235}U. The ^{233}U cross sections computed with the parameters of Table I are compared with the experimental data on Figs. 1, 2, and 3. Similarly the ^{235}U cross sections computed with the parameters of Table II are compared with the experimental data on Figs. 4, 5, and 6. The figures illustrate that there are no significant discrepancies between the cross sections obtained from the resonance parameters and the experimental data on which those parameters are based.

TABLE I. MULTILEVEL RESONANCE PARAMETERS FOR FOR ^{233}U UP TO 60 eV*

μ(eV)	ν(eV)	G^f(barn·eV$^{3/2}$)	H^f(barn·eV$^{3/2}$)	G^c(barn·eV$^{3/2}$)	H^c(barn·eV$^{3/2}$)
−2.81	0.36	−2349.03	−551.99	143.16	0.48
0.15	0.05	−0.23	−0.20	0.16	−0.09
1.43	0.29	50.86	−18.87	1.80	−6.47
1.78	0.12	114.26	−0.23	26.09	6.00
2.29	0.05	42.74	18.48	37.30	2.07
3.63	0.08	22.02	6.80	9.66	1.46
4.61	0.40	62.53	−35.08	3.90	−1.53
3.37	0.35	28.12	−13.61	0.0	0.0
6.80	0.09	176.62	31.33	58.51	2.68
5.80	0.15	20.14	−17.06	3.61	−0.72
7.47	0.10	6.78	−0.67	1.87	0.75
8.69	0.28	22.67	4.82	2.95	−1.21
9.14	0.15	17.48	−20.48	3.44	−0.94
10.35	0.16	275.89	0.42	54.43	2.34
11.30	0.20	33.41	8.67	3.14	−2.59
12.76	0.17	238.89	49.43	33.10	3.01
13.45	0.20	41.96	14.53	9.93	−3.89
13.65	0.14	44.99	−26.72	2.52	0.89
15.28	0.12	119.77	−35.47	45.86	−3.91
16.13	0.22	101.25	−4.79	4.90	−2.93
16.52	0.13	94.54	26.62	19.87	4.42
17.93	0.12	43.16	4.22	9.76	1.49
18.42	0.21	58.68	1.83	5.11	−1.07
18.86	0.15	216.24	−46.49	35.50	4.50
20.53	0.20	111.51	6.53	18.95	0.82
21.85	0.13	130.22	86.08	35.27	13.30
22.23	0.24	532.22	−77.59	60.93	−6.79
22.94	0.38	96.58	3.64	0.0	0.0
23.54	0.32	65.49	−94.87	5.63	−4.16
25.13	0.19	80.77	−38.01	14.67	−0.98
26.19	0.18	−0.73	16.46	−4.89	−1.13
26.57	0.24	70.76	19.32	13.92	7.55
27.18	0.77	14.32	−42.57	8.52	−4.99
28.31	0.11	13.54	14.45	7.93	−1.55
29.05	0.27	176.58	48.21	15.60	−2.47
29.60	0.08	12.87	10.80	3.00	−1.21
30.81	0.14	25.10	63.80	11.55	4.79
31.11	0.57	182.38	−101.63	13.07	−16.72
32.00	0.12	85.57	21.77	19.23	−4.06
32.95	0.30	52.95	−17.16	3.37	−5.34
33.95	0.61	168.77	74.72	−19.29	−24.05
34.46	0.40	188.57	−42.32	0.91	11.08
35.19	0.12	35.51	−3.87	−7.56	0.88
35.40	0.15	0.87	−36.07	4.36	8.90
36.54	0.11	64.42	18.68	21.24	6.02
37.44	0.27	91.39	9.81	6.14	1.57
39.14	0.60	106.60	−100.30	−1.64	−2.13
40.46	0.42	49.81	27.85	1.32	9.81
41.03	0.09	25.66	8.29	11.87	1.69
42.63	0.12	62.48	21.92	17.58	4.72
43.46	0.18	41.15	5.38	8.49	−0.59
44.57	0.46	62.05	9.81	4.04	2.25
45.19	0.53	2.71	−30.08	−0.57	−4.14
46.02	0.08	26.31	−12.60	14.34	−2.60
47.22	0.24	76.28	6.91	3.47	−2.19
48.66	0.12	167.58	−0.15	79.66	10.28
49.06	0.14	18.21	−17.49	−1.53	−8.29
50.25	0.46	64.02	−25.22	−0.73	−2.51
51.16	0.28	17.38	9.23	2.78	−3.97
51.87	0.73	34.99	−71.95	−13.89	−1.13
52.89	0.25	42.86	−77.74	9.20	0.40
53.96	0.11	48.00	−22.96	9.75	1.26
54.80	0.10	58.90	16.76	19.93	5.42
56.08	0.27	63.92	132.05	5.89	6.59
56.35	0.30	224.78	−56.42	28.62	1.05
57.48	0.49	288.74	17.40	19.66	−0.68
58.51	0.23	91.26	23.33	10.78	−4.40
61.30	0.40	132.80	46.89	−0.55	−11.66
62.50	0.20	107.86	−14.96	56.08	−2.62
64.30	0.40	228.02	−22.05	35.51	−16.18

* The parameters are defined by Eq. (1).

TABLE II. RESONANCE PARAMETERS FOR ^{235}U UP TO 100 eV*

μ (eV)	ν (eV)	G_c (beV$^{3/2}$)	H_c (beV$^{3/2}$)	G_f (beV$^{3/2}$)	H_f (beV$^{3/2}$)
−1.05	0.10	355.17	19.22	1170.15	19.31
0.29	0.06	1.12	−0.10	2.35	−1.19
1.14	0.08	2.32	−0.28	6.69	2.79
2.03	0.03	2.80	0.12	0.83	0.15
2.73	0.07	0.23	0.06	−0.76	−0.59
3.16	0.08	2.03	0.31	5.90	2.45
3.61	0.05	6.53	0.19	9.95	3.21
4.84	0.02	16.14	0.19	1.73	0.11
5.42	0.16	0.57	−0.22	3.01	−1.99
6.23	0.10	1.85	−0.93	10.07	5.68
6.38	0.03	55.42	1.68	16.61	0.64
7.08	0.04	16.80	0.25	14.11	1.09
7.77	0.17	−0.12	−0.34	−1.44	0.95
8.44	0.18	−0.26	−0.97	−0.20	−3.19
8.77	0.07	61.63	0.51	177.22	−14.87
9.29	0.05	8.62	2.31	15.93	1.59
9.92	0.31	−0.19	3.75	−0.68	22.94
10.16	0.07	5.00	−0.10	9.60	−2.95
10.76	0.44	−1.94	1.92	11.56	5.53
11.66	0.03	97.29	3.58	13.89	3.91
12.40	0.04	133.06	5.85	103.06	14.61
12.86	0.10	3.59	−0.24	10.57	2.40
13.30	0.12	2.46	0.56	9.19	2.87
13.65	0.14	3.24	−1.60	9.18	−6.90
14.00	0.26	3.42	−0.42	79.98	2.54
14.55	0.04	12.47	0.18	6.09	4.39
15.42	0.06	17.41	0.64	22.70	5.30
16.09	0.04	38.70	1.66	23.95	3.43
16.66	0.09	10.72	0.70	35.34	−5.40
18.04	0.09	11.11	1.40	41.49	−4.07
18.98	0.08	8.68	−2.18	6.68	0.45
19.30	0.07	166.92	7.26	291.05	9.72
20.21	0.13	3.63	−0.57	7.23	7.86
20.61	0.07	9.49	−3.64	15.35	1.92
21.07	0.05	114.73	8.92	91.02	6.25
22.94	0.06	25.52	1.68	35.91	1.80
23.43	0.05	88.22	10.87	25.93	3.31
23.63	0.12	15.51	−5.08	85.95	−9.17
24.23	0.08	27.79	−1.69	22.44	−16.81
25.65	0.35	6.43	−0.66	138.42	83.69
26.44	0.16	11.22	0.41	69.42	−30.40
27.21	0.04	2.51	0.90	3.52	3.63
27.81	0.10	23.73	−0.35	69.31	−2.60
28.35	0.11	4.26	−0.08	16.91	−4.40
28.77	0.04	0.76	0.53	1.05	0.63
29.68	0.05	10.92	1.42	7.56	1.63
30.59	0.09	1.41	−0.99	12.53	−3.72
30.91	0.07	44.76	10.44	21.95	11.46

*The parameters are defined by Eq. (1).

TABLE II. (cont.)

μ (eV)	ν (eV)	G_c (beV$^{3/2}$)	H_c (beV$^{3/2}$)	G_f (beV$^{3/2}$)	H_f (beV$^{3/2}$)
32.10	0.08	83.36	5.24	135.24	12.63
33.55	0.07	123.20	14.48	95.21	4.06
34.39	0.09	142.82	20.02	139.89	− 8.19
34.85	0.14	51.16	− 30.97	113.40	− 18.75
35.21	0.11	133.79	10.35	344.31	− 2.53
35.75	0.49	− 13.41	− 14.72	22.87	− 2.86
37.06	0.06	0	0	− 0.69	0.13
38.42	0.19	2.37	− 1.73	29.38	19.08
39.44	0.09	100.65	8.57	173.72	8.47
39.92	0.10	5.13	− 2.73	19.61	− 4.82
40.51	0.15	6.93	0.17	30.59	− 15.07
41.39	0.14	4.04	6.14	28.45	15.81
41.64	0.06	8.12	5.79	22.59	9.43
41.91	0.08	116.62	8.35	55.77	3.87
42.16	0.13	6.34	− 24.56	25.90	− 27.25
42.70	0.06	19.46	− 8.75	1.98	0.91
43.41	0.04	37.32	− 2.68	16.39	− 3.96
44.04	0.04	3.71	2.05	16.03	9.45
44.75	0.15	28.04	18.97	44.47	77.33
44.97	0.28	0.48	− 18.58	115.80	− 25.84
45.79	0.17	4.62	− 2.13	19.94	0.81
46.92	0.06	23.63	46.08	76.90	122.36
46.98	0.05	18.05	− 45.31	44.67	− 112.13
48.06	0.12	63.65	15.86	57.16	27.75
48.35	0.20	0.34	− 31.20	111.16	− 31.57
48.82	0.03	12.20	2.97	24.51	− 17.36
49.51	0.06	62.25	16.21	20.95	8.17
50.24	0.19	50.92	10.29	45.88	− 11.55
50.45	0.02	17.73	− 14.09	17.13	− 18.65
51.37	0.13	95.45	11.14	219.55	95.05
51.68	0.11	7.72	− 5.29	38.42	− 18.29
52.27	0.25	13.54	− 0.52	234.92	12.25
53.56	0.14	14.61	9.56	50.23	20.72
53.98	0.23	6.83	− 9.89	31.35	− 16.34
55.16	0.12	140.49	20.04	178.46	60.80
55.87	0.33	45.26	− 47.31	369.01	− 178.43
56.58	0.07	110.91	13.74	195.16	36.97
57.83	0.10	13.87	3.20	70.75	− 9.76
58.15	0.08	60.82	0.75	69.04	9.23
58.68	0.12	22.27	− 5.35	88.98	− 34.96
59.75	0.28	4.39	− 4.99	35.72	− 67.35
60.25	0.10	7.56	− 0.43	35.51	− 8.03
60.76	0.05	0.96	− 1.35	6.99	− 10.52
61.10	0.12	12.44	2.61	13.09	− 0.97
62.03	1.03	− 4.42	− 2.60	− 8.48	23.61
62.49	0.10	2.13	− 0.79	2.53	2.04
63.64	0.32	4.81	− 2.67	65.30	10.05
64.31	0.08	81.38	2.17	15.31	5.56

TABLE II. (cont.)

μ (eV)	ν (eV)	G_c (beV$^{3/2}$)	H_c (beV$^{3/2}$)	G_f (beV$^{3/2}$)	H_f (beV$^{3/2}$)
65.81	0.09	16.50	−0.82	12.70	−0.64
66.39	0.10	14.02	−2.27	13.74	3.02
67.29	0.03	−0.62	0.77	0.74	0.74
68.66	0.10	1.11	0.25	3.08	0.10
69.37	0.11	2.24	5.28	34.43	−0.41
70.54	0.26	97.61	7.57	276.76	9.37
70.80	0.16	1.00	−0	59.35	0.72
71.61	0.25	2.97	−0	8.33	−0
72.45	0.12	45.39	3.70	157.02	−0.91
72.91	0.16	0	−0	7.81	−0
74.62	0.14	95.32	11.38	153.92	−2.18
75.24	0.16	15.90	−9.64	58.38	0.78
75.62	0.09	3.69	−5.33	59.40	−0.24
76.94	0.15	1.71	−1.24	8.86	−1.93
77.62	0.17	26.06	−3.08	63.33	−3.83
78.18	0.03	13.25	−3.45	37.05	−2.14
78.51	0.16	3.35	5.18	11.20	−9.70
79.75	0.18	20.99	0.34	42.27	−1.66
80.45	0.12	9.03	0.44	36.86	0.17
80.95	0.16	7.30	0	0	0
81.49	0.12	16.84	0.41	46.71	0.32
82.06	0.16	2.61	−0	0	−0
82.73	0.14	90.59	4.23	42.63	−10.52
83.68	0.14	47.34	−0.91	54.65	16.13
84.06	0.09	0	−0	72.13	12.36
84.39	0.16	24.65	1.94	153.16	−2.97
85.08	0.33	9.59	−1.06	123.68	−12.55
85.75	0.16	−0.79	0.92	17.65	7.88
86.14	0.16	3.01	−0	0	−0
86.95	0.06	6.27	2.58	15.80	−0.34
87.72	0.35	11.52	3.55	56.54	3.12
88.72	0.22	−1.75	4.71	130.24	10.74
89.10	0.16	20.53	6.88	55.09	−4.85
89.90	0.16	37.91	6.33	55.82	−3.85
90.44	0.10	263.08	−2.56	56.92	−26.97
91.32	0.16	10.85	−19.53	128.32	−7.41
92.25	0.16	20.66	1.32	40.27	13.21
92.68	0.11	76.76	−0.11	74.11	4.36
93.30	0.16	0	−0	6.04	−0
94.16	0.14	222.21	7.08	40.04	−0.13
94.89	0.16	3.73	−0	27.21	−2.84
95.66	0.20	2.09	−4.90	57.80	−5.30
96.50	0.20	1.24	−5.78	44.65	8.82
98.16	0.21	29.27	−1.57	150.43	0.51
99.69	0.16	8.54	−2.01	23.96	−1.42
100.48	0.16	18.89	−0	28.24	0.98
101.07	0.16	37.23	−0	27.96	−5.73

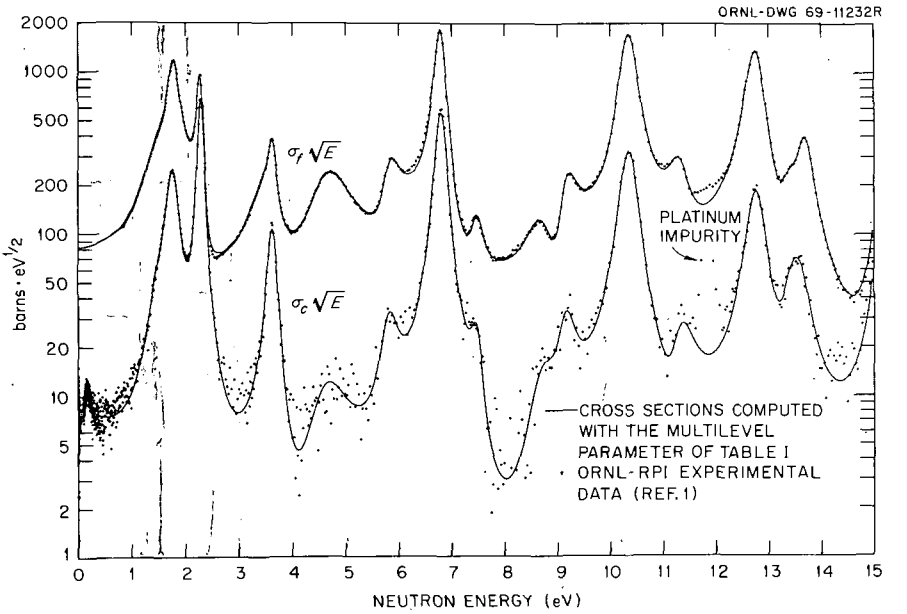

FIG. 1. Fission and capture cross-sections of ^{233}U up to 15 eV. The dots are the experimental data from the ORNL-RPI measurement (Ref. [1]). The solid lines are the resolution-broadened cross-sections computed with the parameters of Table I. The resonance at 11.9 eV in the capture cross-section is due to a Pt impurity in the sample used in the ORNL-RPI measurement.

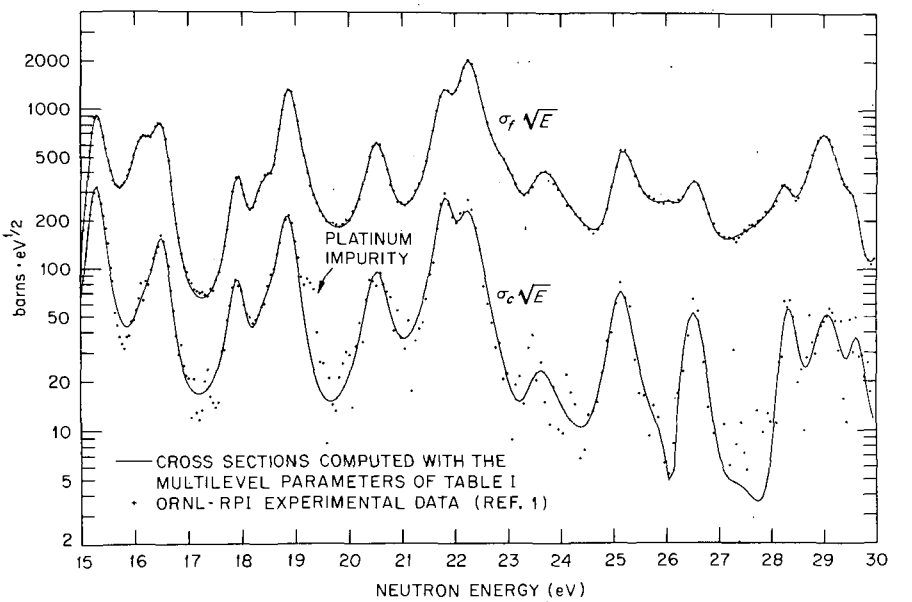

FIG. 2. Fission and capture cross-sections of ^{233}U from 15 to 30 eV. The dots are the experimental data from the ORNL-RPI measurement (Ref. [1]). The solid lines are the resolution-broadened cross-sections computed with the parameters of Table I. The resonance at 19.6 eV in the capture cross-section is due to a Pt impurity in the sample used in the ORNL-RPI measurement.

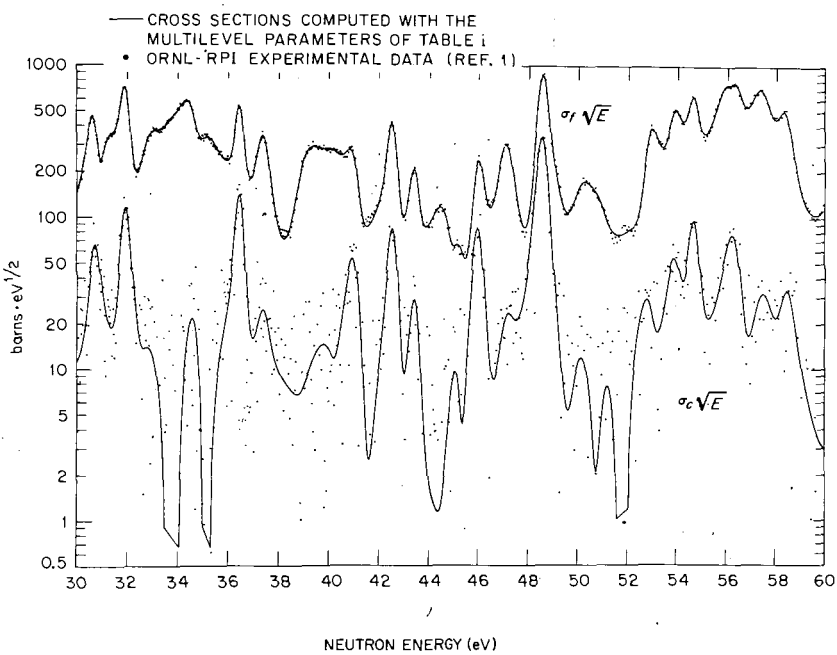

FIG. 3. Fission and capture cross-sections of ^{233}U from 30 to 60 eV. The dots are the experimental data from the ORNL-RPI measurement (Ref. [1]). The solid lines are the resolution-broadened cross-sections computed with the parameters of Table I.

Nevertheless, the parameters of Tables I and II are not unique; other sets of parameters approximate the cross sections with comparable accuracy. For this reason, meaningful standard deviations cannot be assigned to the parameters. The parameters are intended to provide an analytical representation of the cross sections. The uncertainties associated with the use of this representation can best be obtained from comparison between the computed cross sections and experimental data from various sources.

Such comparisons are illustrated in Figs. 7, 8, 9, 10, and 11. In Figs. 7 and 8 the data from three different measurements[3,19-21] of the fission cross section of ^{233}U are compared with the cross sections computed with the parameters from Table I and broadened with the resolution function corresponding to each measurement.

The scattering cross sections of ^{233}U and ^{235}U have been measured by Simpson et al.[22] and Sauter and Bowman.[23] Those measurements indicate that the resonance scattering cross section is, at most, a few percent of the total cross section, and, except at a few resonance energies, it never exceeds a few barns at energies below 100 eV. Hence, the total cross section can be very well approximated as the sum of the potential scattering and of the absorption cross section. Figures 9 and 10 illustrate comparisons between the total cross sections computed from the parameters of Tables I and

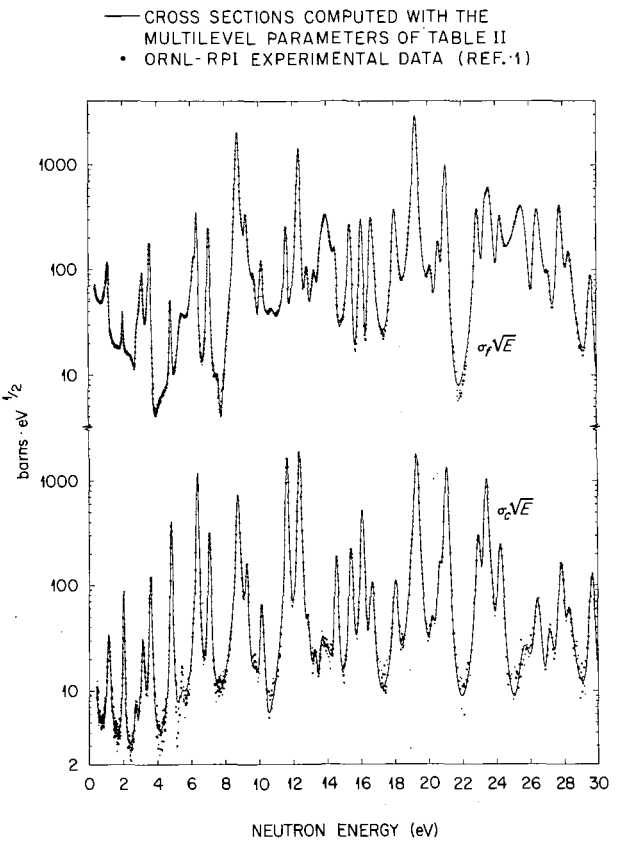

FIG. 4. Fission and capture cross-sections of ^{235}U up to 30 eV. The dots are the experimental data from the ORNL-RPI measurement (Ref. [1]). The solid lines are the resolution-broadened cross-sections computed with the parameters of Table II.

II, neglecting the resonance scattering contributions, and various sets of experimental data obtained from transmission measurements.[24-26] The total cross section measurement of ^{235}U, done at Saclay,[26] was done at a sample temperature of 77°K, that is considerably lower than the temperature (298°K) of the measurements on which the parameters of Table II are based. The usual uncertainties in "unfolding" the resolution and Doppler broadenings may explain the discrepancies between the measurement and the calculation shown on Fig. 10.

Figure 11 illustrates a comparison between two direct measurements[27,28] of η and the values obtained for η with the parameters of Table I, assuming a constant value of 2.5 for ν over the energy range 0-10 eV. Weinstein et al.[29] have measured the variation of ν for ^{233}U and found that at low energies the variation of this parameter did not exceed 1%; this variation is negligible compared to the uncertainties in the direct measurements of η.

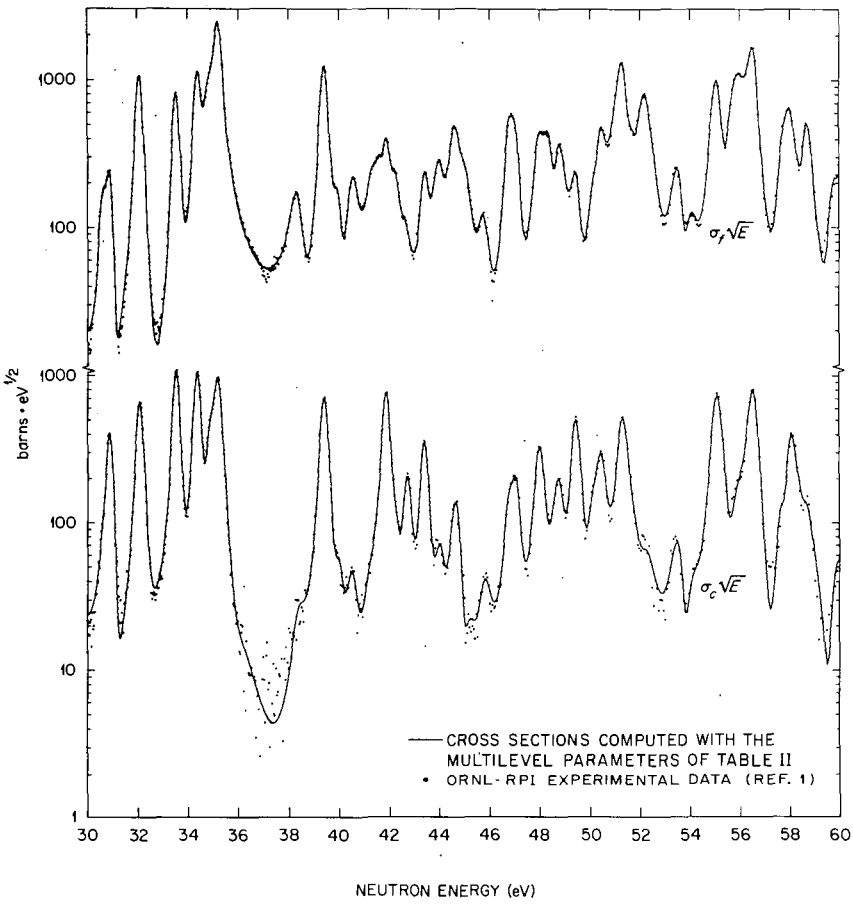

FIG. 5. Fission and capture cross-sections of ^{235}U from 30 to 60 eV. The dots are the experimental data from the ORNL-RPI measurement (Ref. [1]). The solid lines are the resolution broadened cross-sections computed with the parameters of Table II.

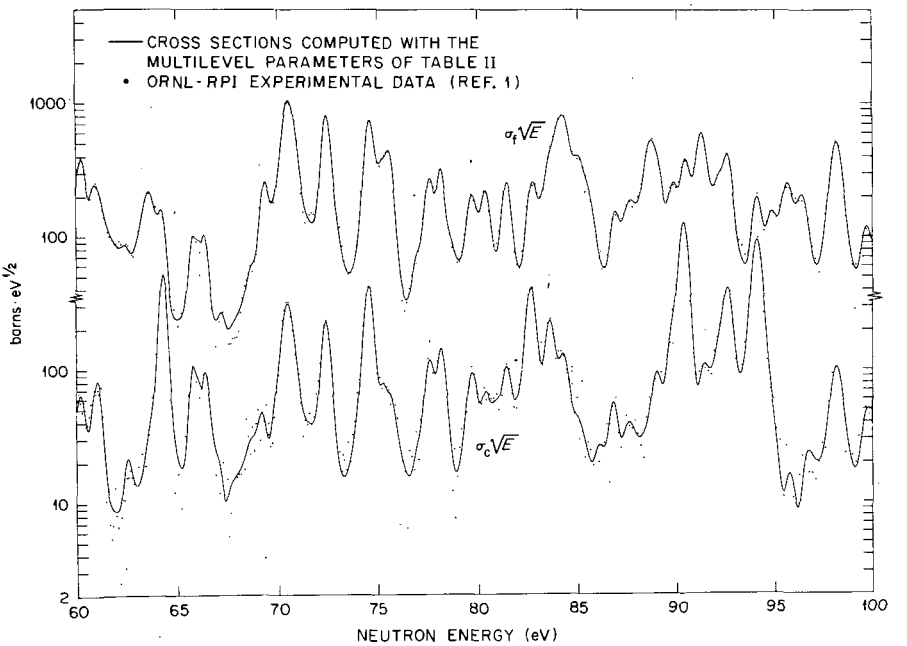

FIG. 6. Fission and capture cross-sections of ^{235}U from 60 to 100 eV. The dots are the experimental data from the ORNL-RPI measurement (Ref. [1]). The solid lines are the resolution-broadened cross-sections computed with the parameters of Tabel II.

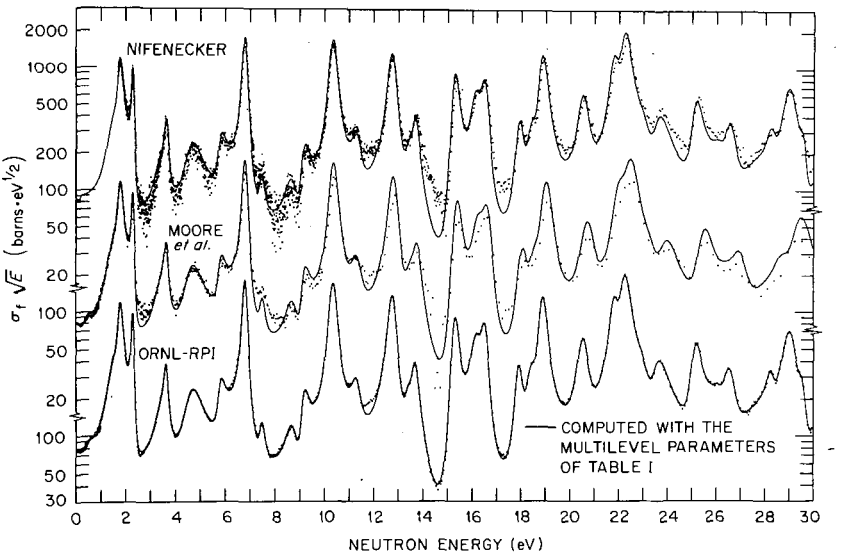

FIG. 7. Comparison of fission cross-sections of ^{233}U up to 30 eV. The upper curve shows the data of Nifenecker (Ref. [19]). The center curve shows the data of Moore, Miller, and Simpson (Ref. [25]). The lower curve shows the ORNL-RPI data (Ref. [1]). The solid lines were computed with the parameters of Table I. The differences in the three solid lines are due to differences in the resolution broadening associated with the three experiments.

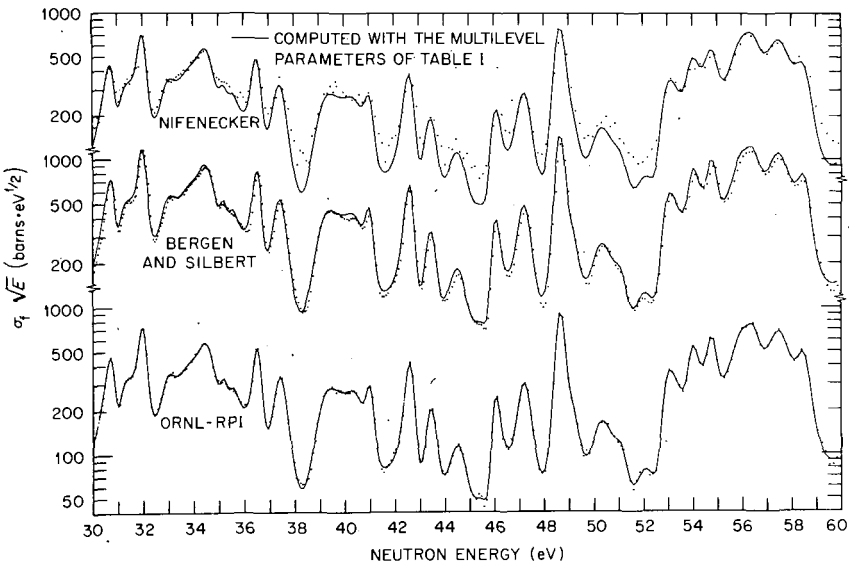

FIG. 8. Comparison of fission cross-sections of ^{233}U from 30 to 60 eV. The upper curve shows the data of Nifenecker (Ref. [19]). The central curve shows the data of Bergen and Silbert (Ref. [21]). The lower curve shows theORNL-RPI data (Ref. [1]). The solid lines were computed with the parameters of Table I. The differences in the three solid lines are due to the differences in the resolution broadening associated with the three experiments. The central line was multiplied by a factor 1.6 because in this energy region three is a systematic discrepancy of this magnitude between the data of Bergen and Silbert and the two other sets of data (see Ref. [21]).

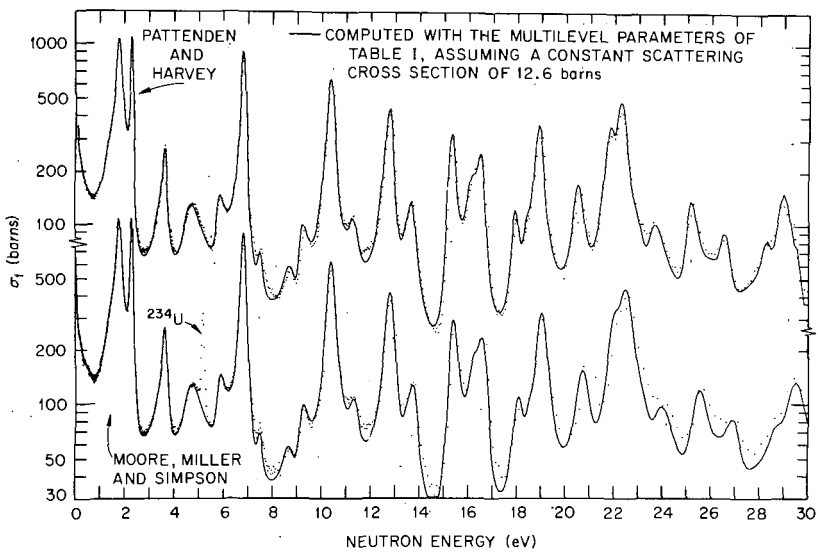

FIG. 9. Total cross-section of ^{233}U up to 30 eV. The upper curve shows the data of Pattenden and Harvey (Ref. [24]). The lower curve shows the data of Moore, Miller, and Simpson (Ref. [25]). The solid line was obtained by computing the resolution-broadened absorption cross-section with the parameters of Table I, and adding to it a constant potential scattering cross-section of 12.6 barns. The resonance at 5.19 eV in the data of Moore et al. is associated with a ^{234}U contamination in the sample used for the measurement.

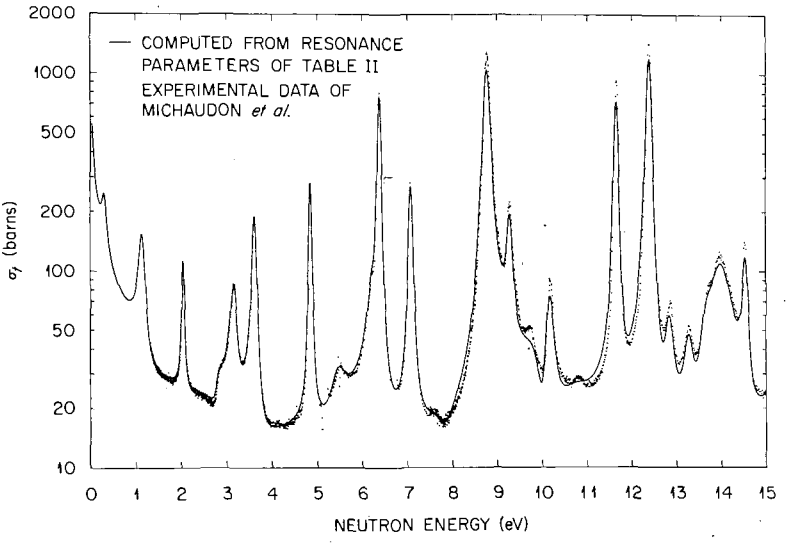

FIG. 10. Total cross-section of ^{235}U up to 15 eV. The solid line was obtained by computing the resolution-broadened absorption cross-section with the parameters of Table II and adding to it a constant potential scattering cross-section of 11.7 barns. The data are from the transmission measurement at 77°K of Michaudon et al. (Ref. [26]).

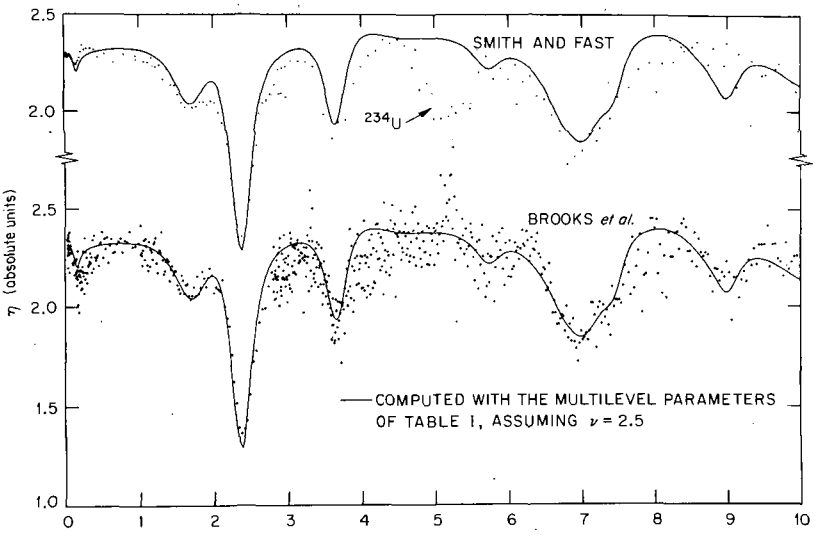

FIG. 11. Eta for ^{233}U below 10 eV. The upper curve shows the data of Smith and Fast (Ref. [27]). The lower curve shows the data of Brooks et al. (Ref. [28]). The solid lines were computed with the resonance parameters of Table I, using a constant value of $\nu = 2.5$. The dip at 5.19 eV in the data of Smith and Fast is associated with a ^{234}U contamination in the sample used for the measurement.

IV. COMPARISON WITH R-MATRIX RESONANCE PARAMETERS

Bergen and Silbert[21] and Cramer[30] have analyzed their measurements of the fission cross sections of ^{233}U and ^{235}U and the ORNL-RPI capture cross section measurements and have obtained multilevel R-matrix parameters with the Reich-Moore[8] formalism. In order to compare the R-matrix parameters of Bergen and Silbert and Cramer with the Kapur-Peierls parameters listed in Tables I and II, a program was written to transform a set of R-matrix parameters into an equivalent set of Kapur-Peierls parameters. The technique used in this program is described below. The Kapur-Peierls parameters are obtained by the direct partial fraction expansion of the Reich-Moore cross-section formulae. For instance, the S-wave fission cross section can be expressed as:

$$\sigma_f = C.g. \sum_c \frac{1}{E} \left| \frac{m_{nc}}{\Delta} \right|^2 = \frac{1}{\sqrt{E}} \sum_{\lambda,c} \left(\frac{R_{\lambda,c}}{d_\lambda - E} + \text{complex conjugate} \right) \qquad (4)$$

where $C = 6.52 \times 10^5$ b·eV, g is the spin statistical factor, the sum on the LHS of Eq. (4) is over the channels leading to fission, m_{nc} is the cofactor of element n,c, and Δ is the determinant of the matrix[8]

$$(I - K)_{cc'} = \delta_{cc'} - \frac{i}{2} \sum_\lambda \frac{(\Gamma_{\lambda c} \Gamma_{\lambda c'})^{1/2}}{E_\lambda - E - (i/2)\Gamma_{\lambda\gamma}}$$

It is easy to see that, if the energy variation of the total width is neglected, the LHS of Eq. (4) can be expressed as the ratio of two polynomials in E; hence the validity of the partial fraction expansion given in the RHS of Eq. (4). This expansion is clearly identical with the generalized Kapur-Peierls expansion of the Adler and Adler formalism [Eq. (1)]. Similar expansions can be obtained for the other cross sections.[31] Other techniques to transform R-matrix parameters into equivalent Kapur-Peierls parameters have been described by Moldauer et al.,[32] Alder and Adler,[33] and Harris.[34]

TABLE III. COMPARISON OF RESONANCE PARAMETERS FOR ^{235}U*

μ(eV)		ν(eV)		G^c(barn·eV$^{3/2}$)		H^c(barn·eV$^{3/2}$)		G^f(barn·eV$^{3/2}$)		H^f(barn·eV$^{3/2}$)	
16.67	16.66	.06	.09	10.23	10.72	−.03	.70	28.98	35.34	−5.73	−5.40
18.05	18.04	.08	.09	11.03	11.11	.01	1.40	52.37	41.49	7.85	−4.07
18.97	18.98	.05	.08	18.21	8.68	−.01	−2.18	24.10	6.68	−.43	.45
19.30	19.30	.05	.07	111.39	166.92	−.08	7.26	245.44	291.05	−9.09	9.72
20.19	20.21	.04	.13	2.02	3.63	.00	−.57	3.52	7.23	.96	7.86
20.67	20.61	.03	.07	12.77	9.49	.01	−3.64	12.54	15.35	4.29	1.92
21.08	21.07	.03	.05	102.93	114.73	−.04	8.92	81.50	91.02	−1.83	6.25
22.95	22.94	.03	.06	26.88	25.52	−0.4	1.68	34.52	35.91	−2.33	1.80
23.44	23.43	.02	.05	65.17	88.22	.03	10.87	30.97	25.93	3.08	3.31
23.63	23.63	.06	.12	21.52	15.51	−.09	−5.08	61.07	85.95	−12.46	−9.17
23.97		.07		3.04		.00		6.69		.42	
24.25	24.23	.04	.08	14.15	27.79	−.17	−1.69	20.60	22.44	−18.54	−16.81
25.67	25.65	.34	.35	7.02	6.43	−.07	−.66	139.11	138.42	69.97	83.69
26.14		.04		.82		.27		−.24		.87	
26.46	26.44	.11	.16	8.61	11.22	.00	.41	51.05	69.42	−30.05	−30.40
27.18	27.21	.05	.04	1.94	2.51	.00	.90	5.02	3.52	2.13	3.63
27.80	27.81	.05	.10	21.43	23.73	−.12	−.35	53.90	69.31	−6.88	−2.60
28.42	28.35	.07	.11	4.62	4.26	.03	−.08	12.98	16.91	3.74	−4.40
28.72	28.77	.05	.04	1.44	.76	.08	.53	2.62	1.05	.64	.63
29.16		.08		.29		−.05		−.19		−.87	
29.68	29.68	.04	.05	11.14	10.92	.04	1.42	8.42	7.56	2.59	1.63

*For each parameter, the first column gives parameters obtained from the R-Matrix parameters of Cramer, the second column gives parameters from Table II.

A comparison of the Kapur-Peierls parameters obtained from the parameters of Cramer,[30] and of the parameters of Table II, is given in Table III for the range 15 to 30 eV. There are large differences in the two sets of parameters of Table III, yet both fit the experimental data fairly well. This illustrates the nonuniqueness of multilevel resonance analysis. For ^{233}U the analysis is even more ambiguous since, even at low energy, the resonances are not fully resolved.[35]

V. MULTILEVEL EFFECTS IN THE CROSS SECTIONS OF FISSILE ELEMENTS

The technique described in the previous section, to convert R-matrix parameters into equivalent Kapur-Peierls parameters, was used to study the magnitude of the multilevel effects in the cross sections of the fissile isotopes. Average cross sections are often computed in the single level approximation:[36]

$$\langle \sigma_f \sqrt{E} \rangle = \frac{2\pi}{\langle D \rangle} \cdot Cg \, \langle (\Gamma_n^o \, \Gamma_f)/\Gamma \rangle \quad \text{(for S-wave neutrons)} \tag{5}$$

where $\langle D \rangle$ is the average level spacing and C and g are defined after Eq.(4). This approximation is used because the exact relation between the average value of the R-matrix parameters and the average value of the cross sections is very complicated. On the other hand, as Moldauer[37] and Hwang[38] have pointed out, the R-matrix parameters can be transformed into equivalent Kapur-Peierls parameters and the magnitude of the interference effect may then be numerically investigated, since the relation between the average cross sections and the average value of the Kapur-Peierls parameters is very simple:

TABLE IV. MULTILEVEL EFFECTS IN FISSILE CROSS-SECTIONS

Average Resonance Parameters Assumed:

$\langle D \rangle$ + 1. eV; $\langle \Gamma_n^o \rangle$ = 0.1 mV; Γ_γ = 50 mV; g = $\frac{1}{2}$

$$\langle \Gamma_f \rangle = \frac{\langle D \rangle}{2\pi} \sum_{n=1}^{\nu_f} P_n \text{ with } P_n = 1$$

ν_f, Number of Fission Channels Open	1	2	3	4
$\langle G_f \rangle / 2Cg \, \langle \frac{\Gamma_n^o \, \Gamma_f}{\Gamma} \rangle$	0.93 ±0.03	0.945 ±0.02	0.96 ±0.02	0.97 ±0.02
$\langle G_\gamma \rangle / 2Cg \, \langle \frac{\Gamma_n^o \, \Gamma_\gamma}{\Gamma} \rangle$	1.075 ±0.02	1.15 ±0.02	1.20 ±0.02	1.23 ±0.02
$\frac{\langle \alpha \rangle \text{ multilevel}}{\langle \alpha \rangle \text{ single level}}$	1.15 ±0.03	1.22 ±0.03	1.26 ±0.03	1.27 ±0.03
$\frac{\langle \Gamma \rangle^2}{\langle \nu \rangle^2} \cdot \frac{\text{variance } \nu}{\text{variance } \Gamma}$	1.22 ±0.03	1.33 ±0.03	1.32 ±0.03	1.39 ±0.02

$$\langle \sigma_f \sqrt{E} \rangle = \frac{\pi}{\langle D \rangle} \langle G^f \rangle \qquad (6)$$

This relation can be obtained immediately from Eq. (1).

The ratio between the correct value of the average cross sections and the value given by the single level approximation [Eq. (5)] was computed for various degrees of interference. Table 4 gives the result of such a computation for typical values of the resonance parameters and for 1, 2, 3, and 4 fission channels fully open. The second and third lines of Table 4 show that the single-level approximation overestimates the average fission and underestimates the average capture. The value of $\alpha = \sigma_c/\sigma_f$ obtained from the single-level approximation may be too low by 20% or more. Lynn[39] had already noted this effect. The results of Table 4 were obtained by transforming ten sets of 100 levels with spacings and widths selected by the Monte Carlo technique[40] from the usual distributions.[41] The standard deviation was obtained by comparing the results from the ten sets.

VI. CONCLUSION

The parameters of Tables I and II provide an accurate analytical description of the cross sections of ^{233}U up to 60 eV and of ^{235}U up to 100 eV. The computed cross sections are consistent with many experimental measurements. Such an analytical description should be useful to calculate reaction rates in nuclear reactors and in evaluating experimental data.[42] The physical interpretation of the resonance parameters is ambiguous because the multilevel fits are not unique. The ambiguity is due to the complexity of the low-energy nuclear structure of ^{233}U and ^{235}U and also, in part, to the lack of precise experimental data, particularly concerning the spin of the low-energy resonances.

Numerical investigations done by transforming R-matrix parameters into equivalent Kapur-Peierls parameters indicate that multilevel effects in the usual fissile nuclei are small but not entirely negligible. The single-level approximation may be as much as 20% in error in estimating the value of the capture to fission ratio, α.

REFERENCES

[1] de SAUSSURE, G., et al., "Nuclear Data for Reactors," Proc. Conf. IAEA, Vienna, 1967, vol. II, p. 233.

[2] de SAUSSURE, G., et al., "Simultaneous Measurements of the Neutron Cross Section for ^{235}U for Incident Neutron Energies from 0.4 eV to 3 keV." ORNL-TM-1804 (1967). This memorandum contains a listing of the ^{235}U data.

[3] WESTON, L. W., et al., "Measurement of the Neutron Fission and Capture Cross Sections for ^{233}U in the Energy Region 0.4 to 2000 eV," ORNL-TM-2140 and Nucl Sci. Eng. 34, 1 (1968). WESTON, L. W., et al., "Neutron Fission and Capture Cross Section Measurements of ^{233}U in the Energy Region 0.02 to 1 eV," ORNL-TM-2353 (1969). The ORNL-TM Memos contain listsings of the ^{233}U data.

[4] ADLER, D. B., ADLER, F. T., Proc.Conf. on Breeding Economics and Safety in Large Fast Power Reactors, Argonne, Oct. 7-10, 1963, ANL-6792, 695 (1963).

[5] WIGNER, E. P., EISENBUD, L., Phys. Rev. 72, 29 (1947).

[6] BREIT, G., WIGNER, E. P., Phys. Rev. 49, 519 (1936).

[7] VOGT, E., Phys. Rev. 112, 203 (1958).

[8] REICH, C. W., MOORE, M., Phys. Rev. 111, 929 (1958).

[9] KAPUR, P. L., PEIERLS, R., Proc. Roy. Soc. (London) A166, 277 (1938).

[10] HARRIS, D. R., Trans. Am. Nucl. Soc. 8, 216 (1965).

[11] HARRIS, D. R., Conf. on Neutron Cross Section Technology, March 22-24, 1966, Washington, CONF-660303, Book 2, 823 (1967).

[12] MOORE, M. S., "Low Energy Neutron Spectroscopy Measurements on Fissile Nuclides," IN-1222 (1969), p. 199.

[13] ADLER, F. T., ADLER, D. B., Conf. on Neutron Cross Section Technology, op. cit., Book 2, 873 (1967).

[14] LANE, A. M., THOMAS, R. G., Rev. Mod. Phys. 30, 257 (1958).

[15] LYNN, J. E., "The Theory of Neutron Resonance Reactions," Clarendon Press, Oxford, 1968.

[16] SOLBRIG, A. W., Am. J. Phys. 29, 257 (1961).

[17] FROHNER, F. M., Nucl. Instr. and Methods 49, 89 (1967).

[18] de SAUSSURE, G., "Neutron Physics Division Annual Progress Report for Period Ending May 31, 1967," ORNL-4134, p. 1.

[19] NIFENECKER, H., Le Journal de Physique, Tome 25, Oct. 1964, p. 877.

[20] MOORE, M. S., REICH, C. W., Phys. Rev. 118, 718 (1960).

[21] BERGEN, D. W., "The ^{233}U Fission and Capture Cross Sections and Their Analysis at Low Energies," LA-3676-MS (1967); BERGEN, D. W., SILBERT, M. G., Phys. Rev. 166, 1178 (1968).

[22] SIMPSON, F. B., et al., to be published. Data shown in Fig. 15 of Ref. 12.

[23] SAUTER, G. D., BOWMAN, C. D., Phys. Rev. 174, 1413 (1968).

[24] PATTENDEN, N. J., HARVEY, J. A., Nucl. Sci. Eng. 17, 404 (1963). See also PATTENDEN, N. J., HARVEY, J. A., "Tabulation of the Neutron Total Cross Section of ^{233}U from 0.07 to 10,000 eV Measured with the ORNL Fast Chopper," ORNL-TM-556.

[25] MOORE, M. S., MILLER, L. G., SIMPSON, O. D., Phys. Rev. 118, 714 (1960)

[26] MICHAUDON, A., et al., Nucl. Phys. 69, 545 (1965).

[27] SMITH, J. R., FAST, E., "Conference on Neutron Cross Section Technology," op. cit. in Ref. 11, p. 919.

[28] BROOKS, F. D., et al., "Eta and Neutron Cross Sections of ^{239}Pu and ^{233}U," AERE M-1709. Also BROOKS, F. D., "Reactor Physics in the Resonance and Thermal Regions," op. cit. in Ref. 36, vol. II, p. 193.

[29] WEINSTEIN, S., REED, R., BLOCK, R. C., "Neutron Multiplicity Measurements for ^{233}U, ^{235}U, and ^{239}Pu Resonance Fission," Second Symposium on the Physics and Chemistry of Fission, Vienna, 1969 (Proc. Conf. IAEA, Vienna, 1969, p. 477).

[30] CRAMER, J. D., Nuclear Physics A126, 471 (1969).

[31] de SAUSSURE, G., PEREZ, R. B., "POLLA, A Fortran Program to Convert R-Matrix-Type Multilevel Resonance Parameters for Fissile Nuclei into Equivalent Kapur-Peierls-Type Parameters," ORNL-TM-2599 (1969).

[32] MOLDAUER, P. A., HWANG, R. N., GARBOW, B. S., "MATDIAG, A Program for Computing Multilevel S-Matrix Resonance Parameters," ANL-7590 (1969) (see also Ref. 37).

[33] ADLER, D. B., ADLER, F. T., "LEMA: A Program for Calculating Neutron Cross Sections with the R-Matrix Formalism and with the Complex Pole Expansion of the Collision Matrix," COO-1546-4 (1967).

[34] HARRIS, D. R., "Perturbation Transformation of Nuclear Cross-Section Parameters Between Wigner-Eisenbud and Kapur-Peierls Formalisms: The PERTA Program," LA-4327, 1970.

[35] The authors of Ref. 7, 8, and 21 were very successful in representing the cross sections of ^{233}U with multilevel formulae but they all conclude from their analysis that "a variety of equally simple fits appear possible."

[36] For instance, SCHMIDT, J. J., "Reactor Physics in the Resonance and Thermal Region," Proc. National Topical Meeting of ANS, San Diego, February 7-9, 1966, vol. II, p. 223.

[37] MOLDAUER, P. Phys. Rev. 136, B947 (1964).

[38] HWANG, R. N., Nucl. Sci. Eng. 36, 67 (1969).

[39] LYNN, J. E., "Nuclear Data for Reactors," Proc. Conf. IAEA, Vienna, 1967, vol. II, p. 89.

[40] MOORE, M. SIMPSON, O. D., Conference on Neutron Cross Section Technology, March 22-24, 1966, Washington, D. C., Conf-660303, Bk. 2, p. 840.

[41] PORTER, C. E., THOMAS, R. G., Phys. Rev. 104, 483 (1956).

[42] A more detailed discussion of the analysis of the ^{233}U cross section can be found in de SAUSSURE, G., "Analytical Description of the Neutron Cross Sections of ^{233}U Below 60 eV," ORNL-TM-2745 (1969) unpublished. The use of the parameters to evaluate data is discussed by STEEN, N. M., "An evaluation of the Neutron Reaction Cross Sections and Fission Spectrum of ^{233}U for ENDF/B," WAPD-TM-691, unpublished.

CORRELATED ANALYSIS OF FISSILE-ELEMENT CROSS-SECTIONS AND INTERPRETATION IN TERMS OF R-MATRIX PARAMETERS†

F. T. ADLER, D.B. ADLER
Department of Physics,
University of Illinois, Urbana, Ill.,
United States of America

Abstract

CORRELATED ANALYSIS OF FISSILE-ELEMENT CROSS-SECTIONS AND INTERPRETATION IN TERMS OF R-MATRIX PARAMETERS.

Fission, capture, and total cross-sections of ^{235}U in the energy region below 50 eV have been analysed by least-squares procedures with a multilevel expansion of the Kapur-Peierls type. The simultaneous analysis of three data sets allows constraints to be imposed which reflect the unitarity of the formalism, thus achieving compatibility among the resonance parameters and limiting uncertainties arising from possible quasi-resonances or hidden small levels. In a manner analogous to those earlier applied to the analysis of η in ^{239}Pu, the energy dependence of α can readily be interpreted.

The multilevel parameters derived from data analysis cannot be used for statistical studies, however, as the pertinent distribution laws are as yet unknown. This fact makes it desirable to complement the analysis by deriving compatible R-matrix parameters, for which the distribution laws are well known. For this purpose, three independent approaches have been investigated: (1) direct data fitting in terms of the complex amplitudes of the theory; (2) a perturbation method; and (3) an analysis of the mathematical structure of the transformations governing the relation of R-matrix and multilevel expansions. Numerical results for R-matrix parameters obtained in these ways and of the uncertainties involved will be illustrated by examples based on the numerical analysis of theoretically prescribed cross-sections and by results obtained from the analysis of representative low-energy fissile-element cross-sections in the region below 50 eV.

1. Introduction

The R-matrix theory of nuclear reactions[1] has been used in various forms for the analysis of low energy cross sections of fissile elements.[2] The results of an R-matrix analysis, based either on the Vogt[3] or on the Reich and Moore[4] approach can always be recast into the equivalent multilevel expansion of a generalized Kapur-Peierls type.[1,5] This formalism provides a flexible tool for data analysis with least squares techniques[6,7] readily applicable to the simultaneous treatment[8] of several cross section sets.[1] Yet, R-matrix parameters are essential not only for nuclear physics investigations, but also because of their well-established statistical properties[10] relevant for the treatment of the unresolved resonances.

Mathematical methods to extract R-matrix from the multilevel parameters are presented here, and illustrative numerical results obtained by means of the computer program Gamplex are given. In section 2 some of the basic relations connecting R-matrix and multilevel formalisms are recalled.[2]

† This work was supported in part by the US Atomic Energy Commission under Contract AEC(11-1)-2022.

[1] A comparison of results obtained from R-matrix and multilevel approaches for the low energy Pu^{239} cross sections has been presented elsewhere.[9]

[2] A detailed derivation, which includes an explicit treatment of the effects of the distant resonances and the k dependence of the s-wave penetration factor will be given elsewhere.[11]

The mathematical formalism underlying the process of extraction of R-matrix parameters is described in sections 3 and 4. Resonance energies and partial widths of R- matrix theory are derived in section 5. Numerical results are given in section 6, while computer programs and procedures will be described separately.

2. Multilevel Expansion

For a given spin-parity state, the collision matrix can be written as

$$U = e^{i\Omega}(1 + T)e^{i\Omega} \tag{1}$$

where the matrix T satisfies the generalized optical theorem [12]:

$$T + T^{*} + TT^{*} = 0. \tag{2}$$

Two alternative expansions of T will be used here:

$$T_{cc'} = i \sum_{\lambda\lambda'} A_{\lambda\lambda'} \sqrt{\Gamma_{\lambda c} \Gamma_{\lambda' c'}} = i \sum_{k} \tilde{\gamma}_{kc} \tilde{\gamma}_{kc'}/(c_k - E) \tag{3}$$

where A is the Wigner level matrix,[1] and $\Gamma_{\lambda c}$ the R-matrix partial widths.

The multilevel expansion shown in (3) follows from the diagonalization of A^{-1} by a complex orthogonal transformation S:

$$(\tilde{S}\, A^{-1} S)_{kk'} = D_{kk} \equiv \delta_{kk'}(c_k - E) \tag{4}$$

where c_k denote the complex eigenvalues of A^{-1}. The residues

$$\tilde{\gamma}_{kc} = \sum_{\lambda} S_{\lambda k} \sqrt{\Gamma_{\lambda c}} \tag{5}$$

can be interpreted as the complex width amplitudes in the multilevel expansion. For low-energy neutron resonances in fissile elements the poles c_k can be regarded as energy independent over a finite energy interval so that S and $\tilde{\gamma}_c$ are energy independent as well.[3]

The unitarity of U(optical theorem) provides the relation:

$$\tilde{\gamma}_{kc} = i \sum_{k'} \tilde{\gamma}^{*}_{k'c} \sum_{c''} \tilde{\gamma}_{kc''} \tilde{\gamma}^{*}_{k'c''} /(c^{*}_{k'} - c_k) \tag{6}$$

Here the channel summation extends over all the open channels, and the level indices k,k' include all the interfering levels of the same spin and parity. In applying (6) to data analysis it is convenient to define the auxiliary hermitean matrix

$$X_{kk'} \equiv \sum_{c''} \tilde{\gamma}_{kc''} \tilde{\gamma}^{*}_{k'c''} = i(c_k - c^{*}_{k'}) \sum_{\lambda} S_{\lambda k} S^{*}_{\lambda k'} = \sum_{(x)} X^{(x)}_{kk'} \tag{7}$$

where, (x) referring to a specific reaction:

$$X^{(x)}_{kk'} = \sum_{c(x)} \tilde{\gamma}_{kc} \tilde{\gamma}^{*}_{k'c} \tag{8}$$

---

[3] This approach differs from the Humblet-Rosenfeld theory where the poles of the collision matrix are defined in the momentum plane, and are therefore rigorously constant.

Furthermore, (6) can be written in the compact form:

$$\tilde{Y}_{kc} = \sum_{k'} Y_{kk'} \tilde{Y}^{*}_{k'c} \tag{9}$$

where the matrix

$$Y_{kk'} \equiv iX_{kk'}/(c^{*}_{k'} - c_k) = \sum_{\lambda} S_{\lambda k} S^{*}_{\lambda k'} \tag{10}$$

is complex orthogonal and hermitean. From (9) one proves the sum rule:

$$\sum_{k} \tilde{Y}_{kc} \tilde{Y}_{kc'} = \sum_{k'} \tilde{Y}^{*}_{kc} \tilde{Y}^{*}_{k'c} = \sum_{\lambda} \sqrt{\Gamma_{\lambda c} \Gamma_{\lambda c'}} \tag{11}$$

that is, the sum of products of the complex width amplitudes over the interfering levels is real and equals the corresponding sum in terms of R-matrix partial width amplitudes.[4]

In particular (for c = c') (11) gives:

$$\sum_{k} \sum_{c(x)} \tilde{Y}^{2}_{kc} \equiv \sum_{k} \tilde{\Gamma}_{k(x)} = \sum_{\lambda} \Gamma_{\lambda(x)} \tag{12}$$

showing that the average of the complex partial width $\tilde{\Gamma}_{k(x)}$ equals the corresponding R matrix average.

The line shape parameters $G_k^{(x)}$, $H_k^{(x)}$, $\alpha_k^{(o)}$, $\beta_k^{(o)}$ of the cross section expansions [5,11] in the multilevel formalism are defined and calculated in terms of the poles c_k, the matrices $X^{(x)}$, and the complex neutron widths $\tilde{\gamma}_{kn}$. Multilevel parameters for U^{235} obtained from the simultaneous triple fit of total fission and capture cross sections have been reported elsewhere.[8] A correlated analysis of this type is as yet not practical with procedures based directly on R-matrix theory. Several avenues have been explored to obtain R-matrix parameters from the results of a data analysis based on the multilevel expansion. In one, the matrices $X^{(x)}$ are determined by a second least squares calculation, after the line shape parameters are obtained from the experimental data. While the matrices $X^{(x)}$ thus obtained reproduce the original line shape parameters, they do not lend themselves always to a direct physical interpretation. An alternative approach consists in utilizing all the mathematical properties of the matrix Y to supplement the physical information embodied in the line shape parameters. This approach is followed here.

3. Mathematical Properties of S and Y

The complex orthogonal transformation S of (4), according to a general theorem of Gantmacher[14], can be represented in the form:

$$S = R \exp(-iK) \tag{13}$$

where R is a real orthogonal matrix and K is a real skewsymmetric matrix. The matrix Y, defined in (10), can thus be written as

$$Y \equiv \tilde{S} S^{*} = \exp(2iK) = \exp(iG) \tag{14}$$

---

[4] A similar relation for two interfering levels with the Humblet-Rosenfeld formalism is discussed in reference 13.

where G = 2K is real skewsymmetric, and the symbol ~ indicates transposition.

The matrix Y can be brought to the quasi-diagonal form[14] by the real orthogonal transformation 0, where the symbol {a,b,...} denotes a block-diagonal matrix with submatrices a,b,.. of rank 2 or 1 ranged along the diagonal:

$$Y = 0\left\{\begin{Vmatrix} s_1 & it_1 \\ -it_1 & s_1 \end{Vmatrix}, \ldots, \begin{Vmatrix} s_q & it_q \\ -it_q & s_q \end{Vmatrix}, \; s_{q+1}, \ldots s_N \right\} 0^{-1} \quad (15)$$

The same matrix 0 transforms as well the matrix

$$C = \exp(-iK) \quad (16)$$

appearing in (13) into the form

$$C = 0\left\{\begin{Vmatrix} a_1 & ib_1 \\ -ib_1 & a_1 \end{Vmatrix}, \ldots, \begin{Vmatrix} a_q & ib_q \\ -ib_q & a_q \end{Vmatrix}, a_{q+1}, \ldots a_N \right\} 0^{-1} \quad (17)$$

where

$$a_k^2 + b_k^2 = s_k, \; 2a_k b_k = -t_k, k=1,\ldots q \quad (18)$$

Indicating with Y^{BD} and C^{BD} the block-diagonal forms of Y and C respectively, one has from (14)

$$Y^{BD} C^{BD} = C^{BD^*} \quad (19)$$

Thus the columns of C^{BD*} form a set of base vectors of Y^{BD} in each subspace j of the block-diagonal representation. The transformed vector

$$\bar{\gamma}_{n,k} = (\tilde{0}\,\tilde{\gamma}_n)_k = u_k + iv_k \quad (20)$$

is here decomposed into subvectors having the dimensions of the corresponding blocks of Y^{BD}, as seen from (9). Denoting these subvectors of two or one components by $\vec{X}_j$, and with Y_j^{BD} the corresponding blocks of Y^{BD}, one has from (9)

$$Y_j^{BD} \vec{X}_j^* = \vec{X}_j \qquad j = 1,\ldots,N \quad (21)$$

The system of interfering levels is here decomposed into isolated pairs of interfering resonances (j = 1,q) and possibly in some isolated non-interfering levels (j = q + 1, ...,N). Moreover, for each pair

$$\sum_k u_k v_k = 0 \quad (22)$$

with k = 1,2 in each subspace j. Each $\vec{X}_j$ can be expanded as

$$\left(\vec{X}_j\right)_k = \eta_1^{(j)} \left(C_j^{BD*}\right)_{k1} + \eta_2^{(j)} \left(C_j^{BD*}\right)_{k2} \quad (23)$$

where the $\eta^{(j)}$ are real coefficients, and C_j^{BD} the blocks of C^{BD}. Because Y^{BD} is invariant under rotations of the form

$$\rho_j = \begin{pmatrix} \cos\varphi_j & -\sin\varphi_j \\ \sin\varphi_j & \cos\varphi_j \end{pmatrix} \quad (24)$$

applying to the jth block, one can choose to align $\vec{X}_j$ to one of the base vectors, thus simplifying $\bar{\gamma}_n$ and bringing it to the form

$$\bar{\gamma}_{n,k} = \text{real for k odd, pure imaginary for k even.} \quad (25)$$

4. Construction of the Matrix Y

In the original representation, Y contains N^2 real unknowns, where N is the number of interfering resonances belonging to the same spin-parity state. In order to construct Y, its block-diagonal form Y^{BD} would naturally be most suitable, as the number of unknowns reduces in this case to N. The rotation O of (15) leading to Y^{BD} is, however, not known a priori.

An intermediate representation, having some of the advantages of the block-diagonal representation that reduces the number of unknowns of Y to N(N + 1)/2, can, nevertheless be constructed. For this purpose, successive elementary rotations are applied to the (known) vector $\tilde{\gamma}_n$, reducing it into a form structurally equivalent to the one of (25).

4.1. Elementary Rotations

By successive application of elementary rotations, $^{15}\tau_{ij}$, an orthogonal transformation Q is constructed[5] so that the transformed vector

$$\bar{\gamma} = Q\,\tilde{\gamma} \tag{26}$$

has the structure given by (25), and moreover satisfies the condition that in pairs the resonances mutually interfere (eq. 22). It should be noted that Q does not necessarily coincide with $\tilde{O}$ of eq.(15), neither does $\bar{\gamma}$ of (26) reproduce the vector defined in (25). The matrix

$$\bar{Y} = Q\,Y\,\tilde{Q} \tag{27}$$

thus has not the block-diagonal form, yet it has a simpler structure than Y has in the original representation. Using (9) for $\bar{Y}$ and $\bar{\gamma}$ one can show that $\bar{Y}$ has the form

$$\bar{Y}_{ij} = \text{real for } i + j \text{ even}, \quad \bar{Y}_{ij} = \text{pure imaginary for } i + j \text{ odd},$$

that is, it contains N(N + 1)/2 independent, real elements. The orthogonal transformation O_1 from Y to Y^{BD} cannot be determined unless $\bar{Y}$ is known, although its structure is well defined in terms of elementary rotations; e.g., for

$$N = 3,\ O_1 = \tau_{12};\ \text{for } N = 4,\ O_1 = \tau_{13}\,\tau_{24},\ \text{etc...}$$

4.2. Methods of Solution for Y

In the Q representation the number of (real) unknowns equals the number of equations provided by the orthogonality conditions for $\bar{Y}$. These equations however, are nonlinear, so that in general the elements of $\bar{Y}$ will not be determined uniquely. Some of these nonlinear equations need not be used; they can be replaced by N-1 linear equations provided by (9), and in special cases, by additional 2N-1 relations derived from the capture line shape parameters.[6]

---

[5] τ_{ij} only affects the axes i,j, so that $(\tau_{ij})_{ii} = (\tau_{ij})_{jj} = \cos\psi$ and $(\tau_{ij})_{ij} = -(\tau_{ij})_{ji} = \sin\psi$.

[6] The sum rule (12) and the corresponding condition $\sum_k (G_k^{(x)} + iH_k^{(x)}) = \text{real}$, induce in fact a linear dependence and thus reduce the number of independent equations.

As a consequence, only for N = 2,3,4 the use of the nonlinear equations can be avoided, thus obtaining for $\bar{Y}$ a mathematically unique solution. The actual numerical calculations necessary for constructing Y can be based on different procedures:

(1) An approximate treatment of $\bar{Y}$ in which small off-diagonal elements of $\bar{Y}$ are neglected in the first approximation. A system of linear equations in this case is sufficient to determine $\bar{Y}$ to an accuracy higher than that of a second order perturbation procedure.[5,6] By iteration the approximation can be further improved.[7]

(2) A nonlinear procedure, expanding exp(iG) of (14) and using the Hamilton-Cayley theorem. The number of unknowns is reduced to N(N-1)/2 and the nonlinearity is of the order N-1. Preliminary numerical studies indicate however a slow convergence of the series in G, and the first method appears preferable.

(3) Wherever it is physically reasonable[17] to postulate a constant value of Γ for the group of resonances investigated, the line-shape parameters $G^{(\gamma)}{}_{H}(\gamma)$ can be used to provide an additional set of linear equations so that for N = 3,4 the problem becomes a straightforward linear problem, and $\bar{Y}$ is determined exactly.

(4) The orthogonality conditions can be used to complement available linear relations. This avenue has not been fully explored at this time.

These procedures are sufficient for determining Y^{BD} from $\bar{Y}$, and the transformation $\tilde{O} = O_1 Q$. The calculation of the matrices C^{BD}, C and Y is hence straightforward.

5. Derivation of R-matrix Parameters

5.1. Determination of the Transformation S

The real orthogonal transformation R of eq.(13) is determined from Y and the poles c_k, as follows:

The matrix X follows directly from eq.(10). Indicating now with

$$A^{-1} = E_r - i\Gamma \tag{28}$$

the inverse level matrix, one can relate X explicitly to the matrix Γ, using (7)

$$X = \tilde{S}\, 2\Gamma\, S^{*} \tag{29}$$

Applying the transformation C to X one calculates the matrix

$$Z \equiv C\, X\, C = 2\tilde{R}\, \Gamma\, R \tag{30}$$

which is directly related to A^{-1}. Using eq.(4),(13), and (28), one has

$$\tilde{R} A^{-1} R = \tilde{R} E_r R - iZ/2 = CD\tilde{C} \tag{31}$$

where the last matrix is calculated from the poles c_k, thus defining

$$\mathcal{C} \equiv \tilde{R} E_r R \tag{32}$$

[7] It is easily seen that N = 2 is a degenerate case in which Y is in block diagonal form in the original representation. Cases of closely spaced resonances and quasi-resonances[16] can be treated exactly as isolated pairs.

as a real symmetric matrix with the level matrix resonance energies as eigenvalues. The transformation R follows as the matrix of the corresponding eigenvectors, so that S is readily obtained through (13).

5.2. Determination of the R-matrix Partial Widths

The matrix Γ of (28) is derived immediately from R and Z, using (30), thus completing the determination of the elements of A^{-1}.

It should be noted that, apart from an involutory transformation associated with the sequencing of the eigenvalues E_λ, the matrix R is uniquely defined in all those cases in which $\bar{Y}$ is obtained from a linear system of equations, as discussed in 4.2. If this is not the case, R, and therefore Γ are no longer uniquely determinable: each possible level matrix thus deduced should however remain compatible with the original set of line shape parameters and poles, i.e., with the cross section curves represented by them.

While the neutron partial width follows in a straight-forward manner from the relation (5), the partial capture width is obtained through a system of linear equations involving the line shape parameters G_k^γ and H_k^γ. For radiative capture it is usually assumed that

$$\sum_{c(\gamma)} \sqrt{\Gamma_{\lambda c}\,\Gamma_{\lambda' c}} = \Gamma_{\lambda\gamma}\,\delta_{\lambda\lambda'} \tag{33}$$

so that one has[11]

$$G_k^\gamma + iH_k^\gamma = \sum_\lambda \sum_{k'} \left\{ i\tilde{\gamma}_{kn}\,\tilde{\gamma}^*_{k'n}\,S_{\lambda k}\,S^*_{\lambda k'} / (c^*_{k'} - c_k) \right\} \Gamma_{\lambda\gamma} \tag{34}$$

providing a system of N linear equations in the N unknowns $\Gamma_{\lambda\gamma}$.

Combining $\Gamma_{\lambda\lambda}$ with $\Gamma_{\lambda\gamma}$, and $\Gamma_{\lambda n}$, the fission widths are calculated by difference, while from the off-diagonal elements of Γ one can determine[3]

$$\cos\theta_{\lambda\lambda'} = (2\Gamma_{\lambda\lambda'} - \sqrt{\Gamma_{\lambda n}\,\Gamma_{\lambda' n}}) \Big/ \sqrt{\Gamma_{\lambda f}\,\Gamma_{\lambda' f}} \tag{35}$$

as a measure of the fission channel interference. Hence, the complex partial widths of the multilevel formalism can be deduced, as

$$\tilde{\Gamma}_{kf} = \sum_{\lambda\lambda'} S_{\lambda k}\,S_{\lambda' k} \sqrt{\Gamma_{\lambda f}\,\Gamma_{\lambda' f}}\,\cos\theta_{\lambda\lambda'} \tag{36}$$

and

$$\tilde{\Gamma}_{k\gamma} = \sum_\lambda S_{\lambda k}\,S_{\lambda k}\,\Gamma_{\lambda\gamma} \tag{37}$$

6. Numerical Results

6.1. Numerical Experiments

The mathematical procedures presented here have been incorporated into the computer program GAMPLEX. To test the significance of the approach, preliminary numerical experiments have been carried out using as input multilevel parameters and poles, which were deduced from a prescribed set of R-matrix parameters by means of the independent program LEMA-CHAMA,[18] Illustrative examples are given in Tables I and II.

The three resonances shown in Table I were selected from Farrell's compilation[17] for Pu^{239}, with g = 3/4 and a constant capture width of 0.040eV. Although the first and the second resonance are close enough that through resolution and Doppler broadening they might coalesce into one apparent peak, the corresponding complex poles $c_k = \mu_k - i\nu_k$ differ by a negligible amount from the R-matrix resonance energies and half-widths $E_\lambda - i\Gamma_{\lambda\lambda}$ because the level spacing is still larger than the half-widths.[λ] The results shown in Table I were obtained from GAMPLEX, using the first-order approximation described under (1), and the exact calculation discussed under (3) in Section 4.2.

The effects of the assumption that Γ_γ is constant for a group of resonances of the same spin-parity state can also be investigated with the program GAMPLEX. For the data shown in Table I, parametric studies have been made varying Γ_γ from 0.038eV to 0.042 eV, bracketing the Farrell value of 0.040 eV. Using the procedure described under (3) in Section 4.2, for each

TABLE I. ILLUSTRATIVE RESULTS OF NUMERICAL EXPERIMENTS WITH THREE INTERFERING RESONANCES OF ^{239}Pu

(1) R-matrix parameters for Pu^{239} from Farrell's compilation[17]

E_λ(eV)	$\Gamma_{\lambda\lambda}$(eV)	$\Gamma^o_{\lambda n}$(eV)$^{\frac{1}{2}}10^3$	$\Gamma_{\lambda f}$(eV)	$\Gamma_{\lambda\gamma}$(eV)	$\epsilon_\lambda^{(*)}$
41.43	0.0400	0.1515	0.03935	0.040	+
41.72	0.0600	0.1680	0.07920	0.040	-
44.51	0.0326	0.3300	0.02375	0.040	+

(2) Multilevel parameters calculated from (1) with Program LEMA-CHAMA

μ_k(eV)	ν_k(eV)	α^o_k 10^3	β^o_k 10^4	G^F_k 10^3	H^F_k 10^4	G^γ_k 10^3	H^γ_k 10^4
41.432	0.03979	0.1536	-0.2841	0.0685	-0.2675	0.0835	-0.202
41.718	0.06017	0.1659	0.2713	0.1041	0.2531	0.0606	0.202
44.510	0.03260	0.3301	0.0128	0.1201	0.0144	0.2025	0.0

(3) R-matrix parameters calculated from (2) with Program GAMPLEX in first approximation

E_λ(eV)	$\Gamma_{\lambda\lambda}$(eV)	$\Gamma^o_{\lambda n}$(eV)$^{\frac{1}{2}}$ 10^3	$\Gamma_{\lambda f}$(eV)	$\Gamma_{\lambda\gamma}$(eV)	$\epsilon_\lambda^{(*)}$
41.430	0.03994	0.1519	0.03889	0.04033	(+)
41.720	0.06003	0.1676	0.07885	0.04078	(-)
44.510	0.03260	0.3301	0.02374	0.04000	(+)

(4) R-matrix parameters calculated with prescribed value of Γ_γ from (2) [exact calculation]

E_λ(eV)	$\Gamma_{\lambda\lambda}$(eV)	$\Gamma^o_{\lambda n}$(eV)$^{\frac{1}{2}}$ 10^3	$\Gamma_{\lambda f}$(eV)	$\Gamma_{\lambda\gamma}$(eV)	$\epsilon_\lambda^{(*)}$
41.430	0.0400	0.1515	0.03935	0.040	(+)
41.720	0.0600	0.1680	0.07920	0.040	(-)
44.510	0.0326	0.3300	0.02375	0.040	(+)

$^{(*)}\epsilon_\lambda$ = sign of the fission channel interference for a 2-channel model.

α^o_k, β^o_k, G^F_k, H^F_k, G^γ_k, H^γ_k in $(eV)^{\frac{1}{2}}$.

parameter value of Γ_γ, R-matrix resonance energies and half-widths were calculated with GAMPLEX. The results proved to be highly sensitive to the choice of Γ_γ. In particular, the elementary trace relations that

$$\sum_\lambda E_\lambda = \sum_k \mu_k; \quad \sum_\lambda \Gamma_{\lambda\lambda} = \sum_k \nu_k \tag{38}$$

appear[8] to be violated for any Γ_γ differing from the "exact" value (here, $\Gamma_\gamma = 0.040$ eV). In Fig. 1 and 2, the calculated differences

$$\Delta_\mu \equiv \sum_\lambda E_\lambda - \sum_k \mu_k; \quad \Delta_\nu \equiv \sum_\lambda \Gamma_{\lambda\lambda} - \sum_k \nu_k \tag{39}$$

are shown as functions of Γ_γ. Thus, in data fitting parametric studies using GAMPLEX could easily indicate the appropriate common value of Γ_γ, provided such an assumption is physically compatible with the data.

Table II presents results for three well-spaced levels with different values of Γ_γ. The results were obtained from GAMPLEX using the approximate method discussed under (1) in Section 4.2. Since the level spacing is larger, the agreement with the input data is even better than that shown

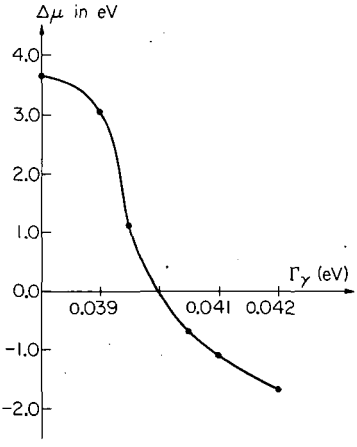

FIG. 1. Difference Δ_μ between the sums of the R-matrix and multilevel resonance energies as function of Γ_γ.

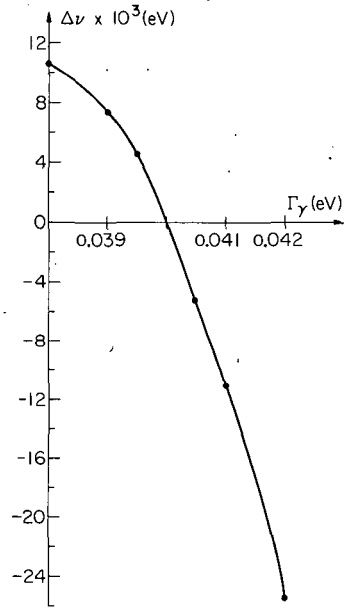

FIG. 2. Difference Δ_ν between the sums of R-matrix and multilevel resonance widths as function of Γ_γ.

[8] Within the multilevel formalism the trace relation is, of course, valid. The apparent violation discussed here is due to making an arbitrary choice of Γ_γ, imposing a value that is not compatible with the other parameters used in the multilevel expansion.

TABLE II. NUMERICAL EXPERIMENT FOR THREE WELL-SPACED INTERFERING LEVELS WITH DIFFERENT VALUES OF Γ_γ

(1) R-matrix parameters used to generate multilevel parameters (input to LEMA-CHAMA)

E_λ (eV)	$\Gamma_{\lambda\lambda}$ (eV)	$\Gamma^o_{\lambda n}$ (eV)$^{\frac{1}{2}}$ 10^3	$\Gamma_{\lambda f}$ (eV)	$\Gamma_{\lambda\gamma}$ (eV)	ϵ_λ (*)
41.43	0.0428	0.1515	0.03935	0.0450	(+)
42.72	0.0610	0.1680	0.0792	0.0420	(-)
44.51	0.0291	0.3300	0.02375	0.0330	(+)

(2) Multilevel parameters calculated from (1) with Program LEMA-CHAMA

μ_k (eV)	ν_k (eV)	α^o_k 10^3	β^o_k 10^4	G^F_k 10^3	H^F_k 10^4	G^γ_k 10^3	H^γ_k
41.43	0.0425	0.1516	-0.0453	0.0698	-0.0466	0.0806	0.0
42.72	0.0610	0.1678	0.0126	0.1086	0.0119	0.0582	0.0
44.51	0.0291	0.3301	0.0327	0.1344	0.0347	0.1873	0.0

(3) R-matrix parameters calculated from (2) with Program GAMPLEX in first approximation

E_λ (eV)	$\Gamma_{\lambda\lambda}$ (eV)	$\Gamma^o_{\lambda n}$ (eV)$^{\frac{1}{2}}$ 10^3	$\Gamma_{\lambda f}$ (eV)	$\Gamma_{\lambda\gamma}$ (eV)	ϵ_λ (*)
41.43	0.0426	0.1516	0.03922	0.0451	(+)
42.72	0.0610	0.1678	0.07900	0.0423	(-)
44.51	0.0291	0.3301	0.02372	0.0330	(+)

(4) Multilevel parameters recalculated from the results given under (3)

α^o_k 10^3	β^o_k 10^4	G^F_k 10^3	H^F_k 10^4	G^γ_k 10^3	H^γ_k
0.1516	-0.0453	0.0698	-0.0468	0.0806	0.0
0.1678	0.0126	0.1086	0.0120	0.0582	0.0
0.3301	0.0327	0.1344	0.0348	0.1873	0.0

(*) ϵ_λ = sign of the fission channel interference for a 2-channel model.

α^o_k, β^o_k, G^F_k, H^F_k, G^γ_k, H^γ_k in $(eV)^{\frac{1}{2}}$.

in Table I. Finally, the multilevel parameters are recalculated within GAMPLEX. The agreement for the line shape parameters G^F_k and G^γ_k is perfect, while slight deviations occur between the original and the recalculated values of H^F_k and H^γ_k. These deviations provide a measure for the inherent numerical accuracy of the procedure.

6.2. Illustrative Results from Experimental Data

In Table III are listed R-matrix parameters for six J = 1 resonances of Pu^{239} between 6 and 20 eV. The results were obtained with program GAMPLEX, using as input multilevel parameters derived from the triple fit of total[19] fission and capture[20] data. These multilevel parameters agree closely with those previously obtained by correlating total and fission data with η/ν values.[9] A comparison is made with existing R-matrix analysis, showing over-all agreement, except for a few values of the widths and signs of the interferences.

TABLE III. ILLUSTRATIVE RESULTS FOR ^{239}Pu FOR J = 1 LEVELS BELOW 20 eV

E_λ(eV)	$\Gamma_{\lambda f}$(eV)	$\Gamma_{\lambda\gamma}$(eV)	$\Gamma_{\lambda n}$(mV)	$2g\Gamma_{\lambda n}\sqrt{E}\ 10^{-3}(eV)^{\frac{1}{2}}$	ϵ_λ	Source
7.80	0.0472	0.0398	0.797	0.427	(+)	A
7.84	0.035	0.040	0.88	0.47	(-)	B
7.90	0.042	0.038	-	0.47	(-)	C
10.93	0.155	0.0351	1.824	0.827	(+)	A
10.95	0.081	0.040	1.44	0.83	(-)	B
11.0	0.147	0.032		0.83	(-)	C
11.892	0.0194	0.0331	0.950	0.413	(-)	A
11.95	0.023	0.040	0.90	0.135	(+)	B
14.312	0.0653	0.0360	0.601	0.238	(+)	A
14.25	0.034	0.040				B
14.29	0.067	0.040		0.275	(-)	D
14.673	0.0293	0.0324	1.907	0.747	(+)	A
14.70	0.023	0.040				B
14.68	0.068	0.040		0.644	(+)	D
17.647	0.0320	0.0366	1.807	0.646	(-)	A
17.70	0.029	0.040	1.47	2.20		B
17.65	0.0684	0.040		0.585	(-)	D

A = this calculation
B = Ignatiev[21]
C = Vogt[3]
D = Farrell[17]

REFERENCES

1. LANE, A.M., THOMAS, R.F., Rev. Mod. Phys. 30 (1958) 257.
2. MOORE, M.S.,"Low energy neutron spectroscopy,"IN-1222(1969) TID 4500.
3. VOGT, E., Phys. Rev. 112 (1958) 203.
4. REICH, C.W., MOORE, M.S., Phys. Rev. 111 (1958) 929.
5. ADLER, D.B., ADLER, F.T., Proc. of the Conf. on Breeding,Econ. and Safety in Large Fast Power Reactors (1963) 695. USAEC Rept.ANL-6792. ADLER, F.T., ADLER, D.B.,Trans.Am.Nucl.Soc.5 (1962) 53; 5 (1962) 407. ADLER, F.T., ADLER, D.B., Proc. of the Conf. on Neutron Cross Section Technology, Washington, D.C. (HEMMIG, P.B., Ed.) (1966) 873. USAEC Rept. CONF.-660303.
6. ADLER, D.B., ADLER, F.T., USAEC Rept. BNL-50045 (1967) T-455; Rept. COO-1546-7.(1967).
7. DE SAUSSURE, G., ORNL-4280 UC-34 Physics (1968).
8. ADLER, D.B., ADLER, F.T., Trans. Am. Nucl. Soc. 12 (1969) 287.
9. ADLER, F.T., ADLER, D.B., Proc. of Conf. on Neutron Cross Section Technology, NBS Spec.Pub., II (1968) 967 (GOLDMAN, D.T., Ed.).
10. PORTER, C.E., "Statistical theory of spectra," Acad.Press,N.Y. (1965).
11. ADLER, D.B., ADLER, F.T.,"Multilevel description of low-energy neutron reactions in fissile elements," Rept. COO-2022-4, submitted for publication to Nuclear Phys.

12. NEWTON, R.G., "Scattering theory of waves and particles," McGraw-Hill Book Co., New York (1966).
13. LYNN, J.E., "Interpretation of neutron-induced fission cross sections and related data," Nucl. Data for Reactors II IAEA, Vienna (1967) 89-115.
14. GANTMACHER, F.T., "Applications of the theory of matrices," Interscience Publishers, New York (1959).
15. FADDEEV, D.K., FADDEEVA, V.N., "Computational methods of linear algebra," W.H. Freeman and Co., San Francisco (1963).
16. LYNN, J.E., "Nuclear structure study with neutrons," (M. Neve de Mevergnies, et al, Eds.) North Holland, Amsterdam (1965a) 125.
17. FARRELL, J.A., Phys. Rev. 175 (1968) 1371.
18. ADLER, D.B., ADLER, F.T., "LEMA," Rept. 300-1546-5 (1967). ADLER, D.B., "Program LEMA-CHAMA," Rept. COO-2022-5 (1970).
19. DERRIEN, H., BLONS, J., EGGERMANN, C., MICHAUDON, A., PAYA, D., RIBON, P., "Proc. of IAEA Symposium on Nucl. Data, Paris (1966), Vol. II IAEA, Vienna (1967) 195.
20. GWIN, R., et al, ORNL-TM-2598 (1969).
21. IGNATEV, K.G., KIRPICHNIKOV, I.V., SUKHORUCHKIN, S.I., J. Nuc. Eng. A/B-18 (1964) 719,523.

METHODE D' ANALYSE DE FORME DES SECTIONS EFFICACES DES NOYAUX FISSILES

J. KREBS, G. LE COQ,
J. P. L' HERITEAU, P. RIBON
CEA, Centre d' études
nucléaires de Saclay,
France

Abstract — Résumé

METHOD OF SHAPE ANALYSIS OF CROSS-SECTIONS OF FISSILE NUCLEI.

First, the authors present the comparisons which they have carried out between different experimental data and the corrections which they have applied. Then they give the characteristics of a program permitting, by a least-squares method, the resonance parameters of fissile nuclei to be determined; it performs the shape analysis of several experiments simultaneously. The inferences between the levels are treated as corrections and not taken into account in the least squares. A visualization unit allows simultaneous representation of theoretical curves and experimental points which permits the evolution of the calculation to be followed and, if necessary, the data with variable parameters to be modified. An example is given for some resonances of ^{235}U.

METHODE D' ANALYSE DE FORME DES SECTIONS EFFICACES DES NOYAUX FISSILES.

Les auteurs exposent d' abord les comparaisons qu' ils ont effectuées entre différentes données expérimentales et les corrections qu' ils ont apportées. Puis ils présentent les caractéristiques d' un programme permettant, par une méthode de moindres carrés, la détermination des paramètres des résonances de noyaux fissiles; il effectue simultanément l' analyse de forme de plusieurs expériences. Les interférences entre niveaux sont traitées comme des corrections et ne sont pas prises en compte dans les moindres carrés. Une unité de visualisation permet de représenter simultanément les courbes théoriques et les points expérimentaux, ce qui permet de se rendre compte de l' évolution du calcul et de modifier les données en paramètres variables si nécessaire. Un exemple est donné pour quelques résonances de ^{235}U.

INTRODUCTION

Notre but est de constituer un jeu cohérent de paramètres de résonances pour un noyau fissile. Par jeu cohérent nous entendons :

- les mêmes hypothèses et les mêmes méthodes de calcul sont appliquées à toute la zone analysée
- les sections efficaces moyennes calculées à partir des paramètres sont égales aux sections moyennes expérimentales, aux erreurs expérimentales près.

Nous expliquons notre méthode en l' appliquant aux données du ^{235}U entre 22 et 37 eV.

1. EXAMEN DES DONNEES EXPERIMENTALES

1.1. Etalonnage en énergie

Nous avons adopté l' étalonnage donné par le BCMN (Ca 68) à Geel, car ce laboratoire y porte une grande attention et nous avons constaté un bon accord entre ses énergies et celles de Saclay en transmission (Mi 65).

Les corrections qui doivent être apportées aux données fournies par les autres laboratoires entre 22 et 37 eV sont :

LASL (Br 66a)	$E=E'_{ap}\ (1+2,4\cdot10^{-4}\ \sqrt{E})$	
ORNL-RPI (De 67)	$E=E'_{ap}\ (1+1,85\cdot10^{-3}-3,93\cdot10^{-4}\ \sqrt{E})$	$22 < E < 27,5$
	$E=E'_{ap}\ (1-3,5\cdot10^{-3}+3,27\cdot10^{-4}\ \sqrt{E})$	$27,5 < E < 28,5$
	$E=E'_{ap}\ (1+1,85\cdot10^{-3}-4,8\cdot10^{-4}\ \sqrt{E})$	$28,5 < E < 37$
Harwell (Br 66)	$E=E'_{ap}\ (1-9\cdot10^{-3}+1,9\cdot10^{-3}\ \sqrt{E})$	
Doubna (Wa 65)	$E=E'_{ap}\ (1-9,5\cdot10^{-4}\ \sqrt{E})$	
Kurchatov (Mo 66)	$E=E'_{ap}\ (1-5\cdot10^{-3}+8\cdot10^{-4}\sqrt{E})$	

1.2. Sections efficaces moyennes

Comme indiqué par Ribon (Ri 70) nous avons élargi les sections efficaces de fission expérimentales par une gaussienne d'écart-type $\sigma = 0,15\sqrt{E}$. A partir de celles-ci nous avons calculé une moyenne $\bar{\sigma}$;

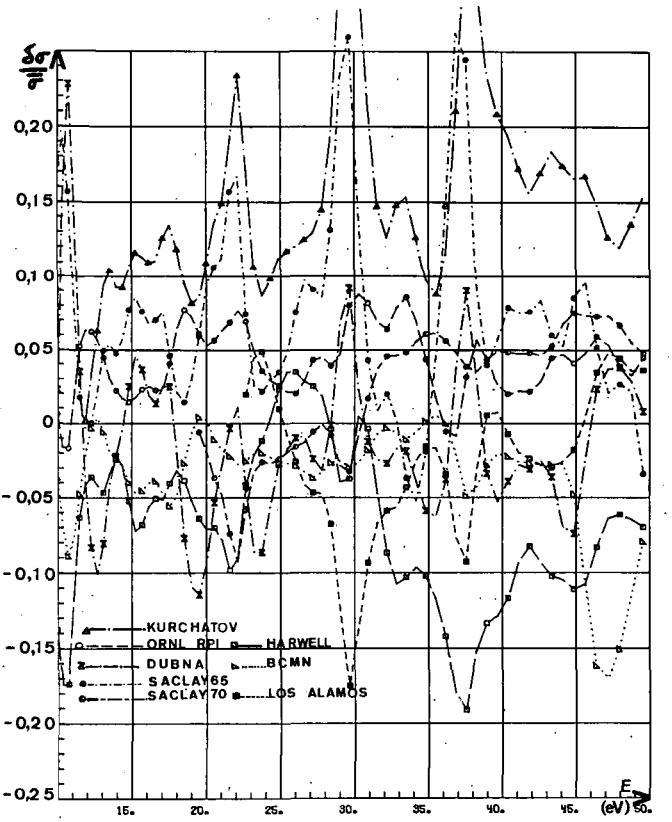

FIG. 1. Uranium-235 : Valeur de $\delta\sigma_f = \sigma_f - \bar{\sigma}_f$ (après élargissement) pour huit expériences entre 10 et 50 eV.

la figure 1 représente $(\sigma_i - \bar{\sigma})/\bar{\sigma}$. Les écarts sont considérables; néanmoins pour BCMN et ORNL-RPI on remarque que les courbes sont parallèles : elles présentent les mêmes fluctuations à une constante de normalisation près ($\sim 6\,\%$), sauf à 48 eV où BCMN présente un creux dû à une résonance du tungstène. Nous nous baserons donc sur ces deux expériences. Pour LASL la courbe présente un creux vers 30 eV; ceci est inexpliqué (mais on doit remarquer qu'à cette énergie, il en est de même pour les données du ^{239}Pu, mesurées par ce laboratoire). Ailleurs les fluctuations sont similaires à celles de BCMN et ORNL-RPI. Pour Saclay 70 (Bl 70) l'accord est bon au-dessus de 35 eV, mais nous constatons certaines irrégularités en dessous de 30 eV, zone dans laquelle Blons ne recommande pas ses données. Les fluctuations des résultats des autres expériences (celles de Kurchatov, de Doubna, de Saclay 65 (Mi 65) et de Harwell) sont très grandes. On remarque qu'elles sont souvent soit en opposition aux variations de $\bar{\sigma}$ (Kurchatov, Doubna, Saclay 65) soit en phase (Harwell).

Nous retiendrons donc pour la détermination des paramètres de résonances dans la zone de 22 à 37 eV les expériences de fission de BCMN, LASL et ORNL-RPI et de transmission de Saclay.

1.3. Section efficace de fission résiduelle

Ainsi qu'il en a déjà été discuté (Ri 70) les sections efficaces résiduelles données par LASL sont inférieures à toutes les autres, et probablement plus proches de la vérité.

1.4. Résolution

Nous supposons que la fonction de résolution est une gaussienne de largeur Δ_{eff}.

$$\Delta^2_{eff} = \Delta^2_{Doppler} + R^2 = a\,E + b\,E^2 + c\,E^3$$

A titre d'exemple, nous présentons au tableau I quelques valeurs numériques.

TABLEAU I. VALEURS NUMERIQUES

Exp.		a ($\times 10^4$)	b ($\times 10^6$)	c ($\times 10^{10}$)
σ_t Saclay		1,36	0,16	12
σ_f	BCMN	4,41	0,3	8,78 E < 26,3 6,4 E < 26,3
	LASL	4,4	-	350
	ORNL-RPI	4,37	1,71	325 E < 27,5 222 27,5 < E < 28,5 174 E < 28,5

TABLEAU II. COMPARAISON DES AVANTAGES ET DES INCONVENIENTS DES DIFFERENTS FORMALISMES UTILISES

	Breit-Wigner 1 niveau	Méthode Vogt	Méthode Reich-Moore	Développement en série	Méthode Adler-Adler
Exactitude du formalisme	Non	Oui	Oui	Non (traitement approché des interférences)	Oui (en fait petites) approximations)
Analyse par moindres carrés	Oui	Non	Oui si peu de voies	Oui	Oui
Paramètres de la matrice R	Oui	Oui	Oui	Oui	Non
Détermination des résonances interférentes	/	Oui	Oui	Oui	Non
Analyse en principe sans ambiguïté	Oui (?)	Non	Non	Non	Oui
Prise en compte aisée de l'effet Doppler	Oui	Non	Non	Oui	Oui

1.5. Conclusion

L'examen des données que nous retenons nous conduit à conclure que :
- la section efficace moyenne de fission n'est pas définie à mieux que 5 %
- les sections efficaces résiduelles sont surestimées de 2 à 15 barns $eV^{1/2}$.

2. FORMALISME

Le tableau II montre les avantages et les inconvénients des différents formalismes couramment utilisés.

Compte tenu de l'imprécision des données expérimentales, nous avons pensé qu'un formalisme approché pourrait être suffisant si l'erreur résultant de l'approximation effectuée est inférieure à l'erreur sur les données.

2.1. Principe

Notre méthode peut être expliquée à partir de celle de Vogt (Vo 58, La 58). Cette dernière nécessite l'inversion de la matrice des niveaux A^{-1} d'éléments.

$$A^{-1}_{\lambda\lambda'} = (E_\lambda - E)\,\delta_{\lambda\lambda'} - \frac{i}{2}\sum_c (\Gamma_{\lambda c})^{\frac{1}{2}}(\Gamma_{\lambda' c})^{\frac{1}{2}}$$

On peut écrire :

$$D^{-1}_{\lambda\lambda'} = (E_\lambda - E - \frac{i}{2}\sum_c \Gamma_{\lambda c})$$

et

$$N^{-1}_{\lambda\lambda'} = \frac{i}{2}(1 - \delta_{\lambda\lambda'})\sum_c (\Gamma_{\lambda c})^{\frac{1}{2}}(\Gamma_{\lambda' c})^{\frac{1}{2}}$$

$$A = D + D\,N^{-1}\,D + D\,N^{-1}\,D\,N^{-1}\,D + \ldots$$

On peut montrer que ce développement est toujours convergent. Les éléments diagonaux sont grands, les non diagonaux sont petits, et l'on peut limiter le développement à quelques termes. Le premier (D) correspond à la formule de Breit et Wigner multiniveau. Le second terme ($D\,N^{-1}\,D$) peut s'écrire sous la forme :

$$\sum_\lambda \frac{C\,P\,S_\lambda}{\mathscr{E}_\lambda - E}$$

et les troisième et quatrième sous la forme :

$$\sum_\lambda \left(\frac{C\,P\,S\,D_\lambda}{\mathscr{E}_\lambda - E} + \frac{C\,P\,D\,D_\lambda}{(\mathscr{E}_\lambda - E)^2}\right)$$

De même les cinquième et sixième termes feraient intervenir des termes de la forme $CPTT/(\mathscr{E}_\lambda - E)^3$.

Finalement les sections efficaces pourront s'écrire sous la forme

$$\sigma = \sigma_{\substack{\text{Breit} \\ \text{Wigner}}} + \sum_{\lambda} \left(\frac{C\,S_\lambda}{E - \mathscr{E}_\lambda} + \frac{C\,D_\lambda}{(E - \mathscr{E}_\lambda)^2} \right)$$

Les coefficients CS, CD, ... étant indépendant de E (tout au moins dans la mesure où Γ_n est indépendant de E).

2.2. Précision

Celle-ci sera évidemment d'autant meilleure que le développement sera poussé plus loin; nous nous limitons actuellement au quatrième ordre. En pratique l'erreur sera inférieure à ~ 1 % dès que :

$$\left| \frac{\Sigma (\Gamma_{\lambda c})^{\frac{1}{2}} (\Gamma_{\lambda' c})^{\frac{1}{2}}}{E_\lambda - E_{\lambda'}} \right| < 0,5$$

La figure 2 représente l'erreur commise sur σ_t de ^{235}U selon l'ordre du développement en prenant comme référence la valeur calculée à l'aide du programme MUFLE (Pr 65). Alors que l'erreur résultant de la

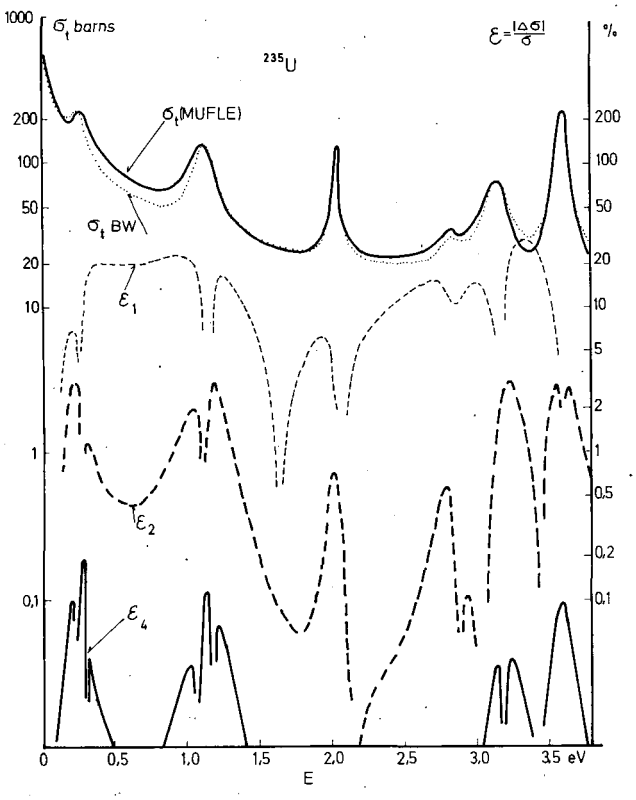

FIG. 2. Valeur de σ_t ou de $\epsilon = (\sigma_t$ approché/σ_t exact)-1 d'après différentes formules.

formule de Breit et Wigner atteint 30 %, celles résultant des développements aux deuxième et quatrième ordres atteignent respectivement 3 % et 0,2 %. Les calculs sont effectués sans tenir compte de l'effet Doppler : celui-ci aura pour effet de diminuer encore l'erreur.

2.3. Effet Doppler

Le produit de convolution de ces fonctions par une gaussienne est une somme de fonctions ψ, ϕ ou de leurs dérivées.

Le calcul est nécessaire pour les moindres carrés : la prise en compte des interférences n'entraîne donc pas une augmentation importante des temps de calcul.

2.4. Moindres carrés

Il est aisé d'effectuer l'analyse de forme par une méthode de moindres carrés en ne calculant que la dérivée du terme Breit et Wigner. Les interférences sont considérées comme des termes correctifs; le fait de ne pas les prendre en compte dans la dérivation peut diminuer la rapidité de la convergence, mais n'influe pas sur la qualité de celle-ci.

Les coefficients CS_λ et CD_λ sont recalculés à chaque itération.

3. PROGRAMME D'ANALYSE DE FORME

Nous mettons au point un programme permettant l'analyse simultanée de huit expériences indépendantes (σ_t, σ_f, σ_c ou transmission). Les points expérimentaux situés dans les ailes des résonances sont regroupés pour le calcul. Le nombre de points analysés (regroupés ou non, est au plus égal à 4000.

Le programme est conçu pour une IBM 360-91 avec une unité IBM 22-50 qui permet de visualiser jusqu'à 1500 points (théoriques ou expérimentaux).

En principe, nous traitons rarement les 4000 points simultanément car le temps de calcul serait prohibitif. Le programme permet de choisir une ou plusieurs séries de données, et une zone d'énergie restreinte, que nous analysons; puis nous changerons de zone d'énergie, de données, de paramètres variables.

Temps de calcul

Il dépend assez peu du nombre de paramètres variables, mais est directement proportionnel au nombre de points et d'itérations et à peu près proportionnel au nombre de résonances. Par point et par itération il vaut respectivement 14 et 18 ms pour 3 et 13 paramètres variables. Il est surtout dû au temps de calcul des fonctions ψ, ϕ et de leurs dérivées.

4. EXEMPLE D'ANALYSES

Nous considérons les valeurs de σ_t(Mi 65) et de σ_f(Ca 68) entre 22 et 37 eV.

1) Analyse un niveau avec seulement les grandes résonances. Cette analyse est effectuée en partant d'un jeu de paramètres complet (Sc 66).

Un premier calcul montre un désaccord très important. Nous ne conservons que les grandes résonances dont nous ajustons les paramètres : la figure 3 montre le meilleur accord que nous ayons pu obtenir.

2) Analyse un niveau avec des résonances supplémentaires. Nous n'avons pas réussi à améliorer sensiblement l'analyse en introduisant un nombre raisonnable de résonances supplémentaires. Ceci serait évidemment possible, ainsi que l'ont montré Drawbaugh et Gibson (Dr 66) en introduisant un grand nombre de celles-ci.

3) Analyse multiniveaux. Nous avons essayé d'améliorer l'analyse en introduisant des interférences, d'abord entre les résonances à 23,5 et 26,5 eV $(\Gamma_f)^{1/2}$ de même signe (c'est-à-dire interférences destructives entre les résonances), puis entre ces deux résonances et celle à 24,3 eV (signe opposé pour $(\Gamma_f)^{1/2}$). Il en résulte une nette amélioration (fig. 3).

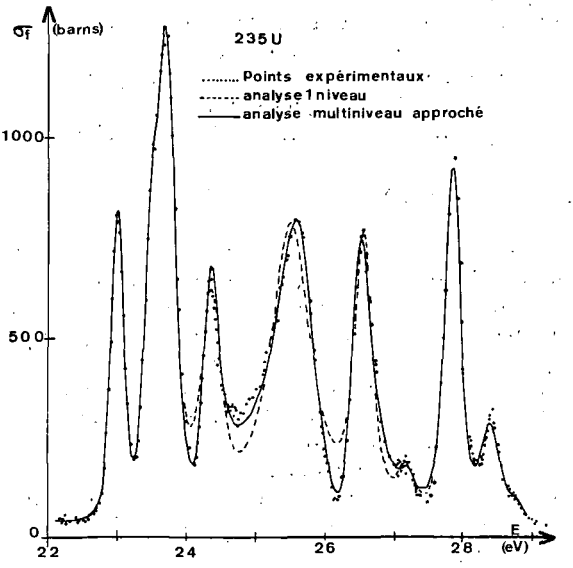

FIG. 3. Analyse de forme de σ_f [Mi 65 et Ca 68] d'après des formalismes à un niveau et multiniveau approché.

CONCLUSION

Une analyse des sections efficaces de noyaux fissiles dans le domaine des résonances ne peut ignorer les interférences. Mais il faut introduire celles-ci avec prudence; les données expérimentales sont insuffisamment précises pour en permettre une bonne détermination.

Nous proposons l'utilisation d'un formalisme approché qui permet de combiner les avantages des analyses à un niveau et multiniveaux. L'utilisation d'une unité de visualisation permet de fractionner les cas du calcul (gain de temps machine) et de les enchaîner (gain de temps physicien).

REFERENCES

Br 66 F. BROOKS et al, Report AERE - N 1670 (1966)

Br 66a W. K. BROWN et al, Neutron Cross Section Technology Washington 1966, Volume I p. 971

Bl 70 J. BLONS - Communication privée

Ca 68 M. G. CAO et al, Conference Cross Section and Technology Washington D. C. Mars 1968

De 67 G. DE SAUSSURE et al - Conference on Nuclear Data for Reactors PARIS 1967 (IAEA), Volume 2 p. 233

Dr 66 D. W. DRAWBAUGH et G. GIBSON - Conference IAEA on Nuclear Data for Reactors PARIS 1967, Volume 2 p. 251

La 58 A. M. LANE et R. G. THOMAS - Rev. Mod. Phys. 30 (1958) 257

Mi 65 A. MICHAUDON - Thèse rapport CEA - R. 2552
A. MICHAUDON et al, Nuclear Pysics. 69 (1965) 545

Mo 66 T. MOSTOVAYA et al, INDC - 152 E

Pr 65 C. A. PRESKITT - ORNL - TM - 1180 (1965)

Ri 70 P. RIBON - Cette conference

Sc 66 J. J. SCHMIDT - Rapport KFK 120 - EANDC (E) 135 U

Vo 58 E. VOGT, Phys. Rev. 112 (1958) 203

Wa 65 WANG-Shi di et al, Physics and Chemistry of Fission Salzburg 1965 (IAEA)

DISCUSSION

TO PAPERS IAEA-CN-26/94, 50, 65

J. GARRISON: I would like to comment on two subjects. I have been working on the effect of interference on the average cross-sections of fissile nuclei. The results of this research, which have been submitted to Nuclear Physics for publication, are in agreement with those presented in Table IV of the paper of Dr. de Saussure. Some of these results are shown in the figures and tables below.

Figure A shows the ratio of the average capture cross-section including interference to the cross-section not including interference. These results were obtained by a Monte-Carlo calculation using a modification of the approach of Adler and Adler for generating the cross-sections. The average resonance parameters were those appropriate to ^{233}U or ^{235}U at 7000 eV. The abscissa is the number of levels included in the matrices used to calculate the average cross-sections. The numbers on the right in the figure are an extrapolation to infinite matrix size. About 10^4 levels contributed to the results shown in the figure.

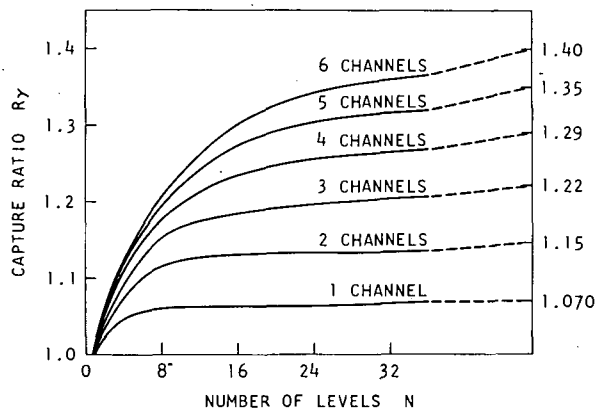

FIG. A. Calculation of the capture ratio R_γ as a function of the number of open fission channels and the number of levels N for $\langle \Gamma_n \rangle / D_J = 0.009$ and $\Gamma_\gamma / D_J = 0.04$.

Figure B shows the same kind of results for the ratio of the average fission cross-section including interference to the cross-section not including interference. These results differ from de Saussure somewhat because resonance scattering is greater at 7000 eV. Table 1 shows the effective number of levels with which a given level interferes as a function of the number of open fission channels. This result was obtained by a simple calculation connected with the saturation effect shown in the first two figures. It can be seen that each level interferes with quite a large number of other levels. Moldauer has indicated a larger number. For ^{233}U, which has three or four open fission channels, approximately 8 or 10 levels are involved.

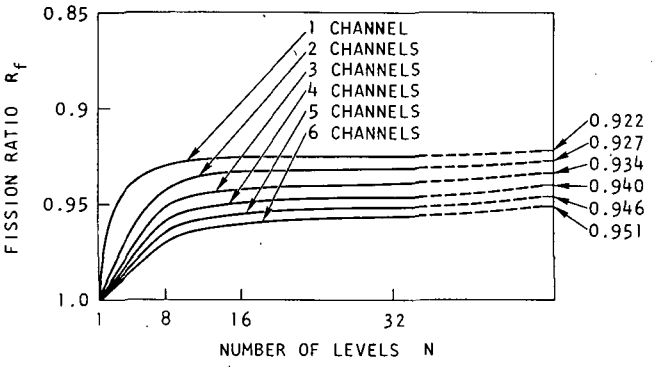

FIG. B. Calculation of the fission ratio R_f as a function of the number of open fission channels and the number of levels N for $\langle \Gamma_n \rangle / D_J = 0.009$ and $\Gamma_\gamma / D_J = 0.04$.

TABLE 1. EFFECTIVE NUMBER OF INTERFERING LEVELS

Open fission channels n	Interfering levels n
1	3
2	6
3	8
4	10
5	11
6	12

Table 2 shows the results obtained for the three fissile nuclei ^{233}U, ^{235}U and ^{239}Pu. The effect of interference and the $(n, \gamma f)$-process are shown at three energies for each nucleus. This result was obtained by statistical fitting of the average capture and fission cross-section up to 100 keV.

My second comment concerns the analysis of the low-energy cross-sections of fissile nuclei. Because of the large number of missed resonances and the lack of uniqueness in any multi-level fitting of the cross-sections, it is desirable to use a complementary approach to the analysis of the low-energy cross-sections. The multi-level fitting is useful for reproducing the cross-sections, but it is not of value in obtaining the average resonance parameters which are of interest theoretically or in the calculation of average cross-sections. Together with William Martin, one of my students, I have statistically analysed the fission cross-sections of ^{233}U by an autocorrelation method (short range correlation) and also by measuring the widths of the observable resonances. By making comparisons with statistically calculated cross-sections, we have been able to deduce the average total width, the number of missed levels and the mean observed

TABLE 2. CROSS-SECTION RATIOS INDICATING THE EFFECT OF THE (n, γ f) PROCESS AND INTERFERENCE

Nucleus	Energy (keV)	Capture ratios			Fission ratios		
		(n, γf)	Rγ	combined	(n, γf)	Rγ	combined
$^{233}_{92}U$	0.5	0.86	1.23	1.06	1.02	0.95	0.97
	7.0	0.84	1.21	1.02	1.02	0.95	0.97
	100.0	0.76	1.15	0.87	1.06	0.92	0.98
$^{235}_{92}U$	0.5	0.87	1.11	0.97	1.04	0.94	0.98
	7.0	0.88	1.09	0.96	1.04	0.94	0.98
	100.0	0.92	1.09	1.00	1.03	0.92	0.95
$^{239}_{94}Pu$	0.5	0.89	1.00	0.89	1.15	0.99	1.14
	7.0	0.88	1.01	0.89	1.10	0.97	1.07
	100.0	0.81	1.09	0.88	1.04	0.94	0.97

level spacing (both spin states). The preliminary results for the cross-section up to 100 eV were $\langle\Gamma\rangle \cong 650$ meV, missed levels about 45% and D_{obs} slightly less than 0.5 eV. This method is also being applied to ^{235}U, ^{239}Pu and ^{241}Pu.

M. S. MOORE: I should like to congratulate the Drs Adler on addressing themselves to a difficult problem with such remarkable success. As a note of caution, however, I would add that this technique cannot be expected to give uniqueness for many resonances when a two-fission-channel analysis is required. Numerical experiments by Auchampaugh at Los Alamos have shown that here the phase relationships between the fission width vectors are not invariant in an R-matrix description.

D. B. ADLER: In the case of 3 or 4 resonances, the solution is obtained from a set of linear equations and the calculation produces $\cos_{\lambda\lambda'}$ which are independent of the channel number (i. e. consines à la Vogt, which can of course be transformed into a Reich-Moore formalism). For a larger number of resonances the problem is non-linear, there is an entire family of solutions and we have not yet investigated whether all of them are physically meaningful.

The case of two resonances is degenerate, and can always be solved. The 2-level results (especially for statistics) cannot necessarily be generalized to a larger number of levels.

F. T. ADLER: I would like to ask Dr. Ribon whether his elegant perturbation procedure is more economical in computing time. As a comment, I would add that the perturbation method presented reminds me somewhat of a method introduced for a different purpose by Wigner in 1946 or thereabouts. Could Dr. Ribon comment on this point, too?

P. H. RIBON: It is difficult to answer this question because it would be necessary to know the time required for the other methods. I can merely state that the length of one iteration is practically the same, regardless of whether or not one introduces interferences between levels - i. e. it is the same as for a 1-level analysis. However, the explicit formulation of the interferences requires the performance of several experiments. I am not acquainted with the method proposed by Wigner.

Section IX

EVALUATION PROBLEMS AND METHODS II

Chairman

A.I. ABRAMOV (USSR)

FAST-NEUTRON CAPTURE CROSS-SECTIONS OF Cr, Fe, Ni AND Mo

K. NISHIMURA, T. ASAMI, S. IGARASI, M. HATCHYA,
H. NAKAMURA
Japan Atomic Energy Research Institute,
Tokai-mura, Naka-gun,
Ibaraki-ken, Japan

Abstract

FAST-NEUTRON CAPTURE CROSS-SECTIONS OF Cr, Fe, Ni AND Mo.

In the keV-energy region, neutron radiative capture cross-sections for such reactor materials as Cr, Fe, Ni and Mo have been measured by a number of authors. A variety of standard cross-sections used in different groups of measurements makes a systematic comparison among their results difficult. In the present work, the measurements of the Au(n,γ) cross-section curve by Poenitz et al. are adopted as a common standard cross-section. By multiplying the normalization factors to each (n,γ) cross-section in different groups of measurements, the renormalized (n,γ) cross-sections for Cr, Fe, Ni and Mo have been obtained. By the use of the results of the systematic study of level density parameter a and strength function $1/\xi^{\circ}$, statistical model calculations have been performed up to the region of about a few MeV. Calculations are made by the use of a computer code RACY. Collective and direct model calculations have been performed in the region above a few MeV. The results of calculations from 10 keV to 20 MeV are adjusted to the renormalized (n,γ) cross-sections for Cr, Fe, Ni and Mo, and are compared with the curves of ENDF/B, KFK 750 and UK data.

1. INTRODUCTION

Stainless steel is one of the important materials for reactors, and it consists mainly of Cr, Fe, Ni and Mo nuclides. The radiative capture cross-sections of these nuclides have been measured in the energy region up to a few MeV by using different kinds of standard cross-section. The standard cross-sections used in the measurements are radiative capture cross-sections of In, Ta, Ag and Au, as well as fission (or capture-plus-fission) cross-sections of ^{235}U. To remove an ambiguity originating from the use of the different kinds of standard cross-sections, it would be necessary to use a common standard cross-section.

Poenitz et al. [1] have recently obtained the Au(n,γ) cross-section with the good accuracy of 3.9-5.9% in the energy region of 25 to 500 keV. In the present work, therefore, the Au(n,γ) cross-section of Poenitz et al. is adopted as the common standard cross-section, and a normalization factor is determined by comparing the Au(n,γ) cross-section obtained in a particular measurement with the standard Au(n,γ) cross-section adopted. Then the renormalized (n,γ) cross-sections of Cr, Fe, Ni and Mo were obtained here in the energy region from 10 keV to a few MeV.

The statistical model calculations of the radiative capture cross-sections for Cr, Fe, Ni and Mo have been carried out up to a few MeV, by taking into account the competition of inelastic scattering. The level density parameter a and strength function $1/\xi^0 = 2\pi\Gamma_\gamma(B_n)/D^0(B_n)$ have been systematically investigated over a wide mass-number range, since the value of the (n,γ) cross-section is affected by these parameters in

the statistical model calculations. The calculated cross-section curves are fitted to the renormalized cross-sections obtained above, by means of the adjustment of a constant factor included in ξ^0.

To estimate the unknown (n,γ) cross-sections of these nuclides in the MeV region, calculations have been performed on the basis of collective and direct capture models, as well as the statistical model. The (n,γ) cross-section curves of Cr, Fe, Ni and Mo thus obtained are compared with those of ENDF/B, KFK 750, and UK data in the energy region from 10 keV up to 20 MeV.

2. RENORMALIZATION OF ORIGINAL DATA

The $Au(n,\gamma)$ cross-section is not always adopted for the standard cross-section of neutron radiative-capture measurements, as mentioned in the introduction. In many cases, however, $Au(n,\gamma)$ cross-sections have been measured in the same experiments as the (n,γ) cross-section measurements of Cr, Fe, Ni or Mo [2-5]. A comparison has then been made among these $Au(n,\gamma)$ cross-sections in the present work, and the result is shown in Fig. 1.

Recently, Poenitz et al. [1] have measured the $Au(n,\gamma)$ cross-section shape in the energy region of 25 to 500 keV and normalized to a best fit-value of 596 ± 12 mb at 30 keV. The result is also shown in Fig. 1. The final error originates from those errors as statistical error, error of detector efficiency, correction for elastically or inelastically scattered neutrons, correction for resonance self-shielding, γ-spectrum normalization error at 30 keV, etc. The contributions of those errors to the final error of 3.9-5.9% are extensively examined in their article. The absolute

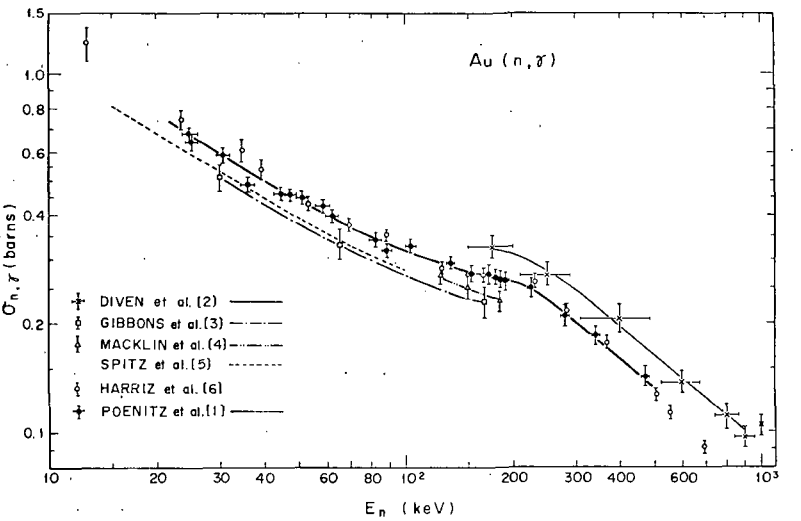

FIG. 1. Comparison of $Au(n,\gamma)$ cross-sections, which have been measured in the same experiment as the (n,γ) cross-section measurements of Cr, Fe, Ni or Mo [2-5]; curves have been drawn smoothly through the experimental data, except for the curve of Poenitz et al. [1], adopted as a common standard cross-section; the absolute cross-section measurement of Harris et al. [6] is also shown.

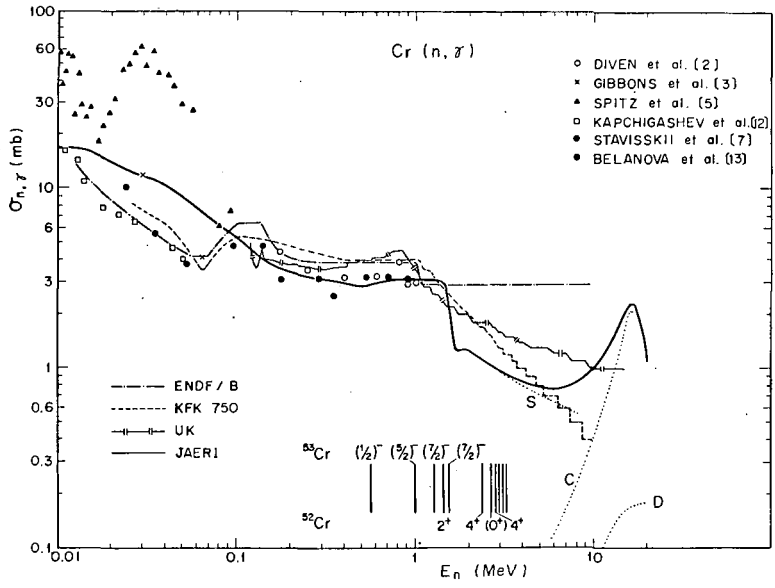

FIG. 2. Renormalized Cr(n,γ) cross-sections, which are obtained by adopting the Au(n,γ) cross-section curve of Poenitz et al. [1] as the common standard; the result of the present calculation is shown by a solid curve; the dotted curves with the symbols S, C or D stand for the (n,γ) cross-sections calculated by statistical, collective or direct models, respectively.

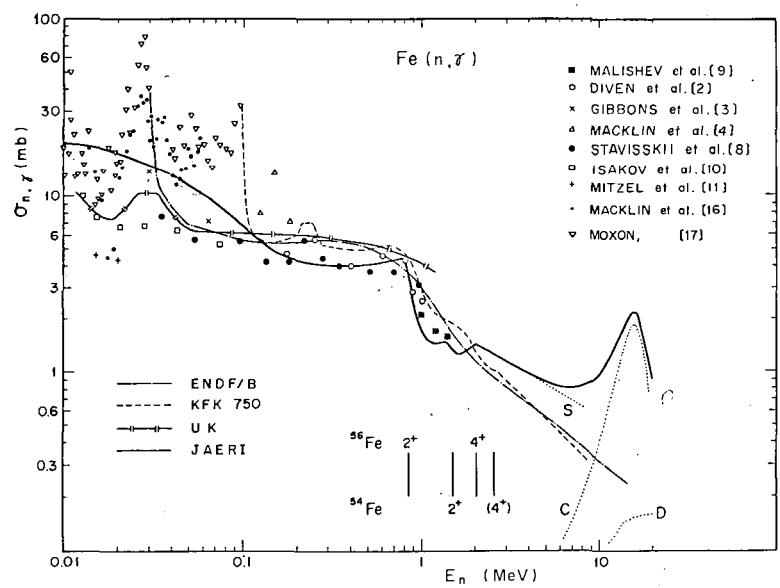

FIG. 3. Renormalized Fe(n,γ) cross-sections, which are obtained by adopting the Au(n,γ) cross-section curve of Poenitz et al. [1] as the common standard; the notation of curves is the same as in Fig. 2.

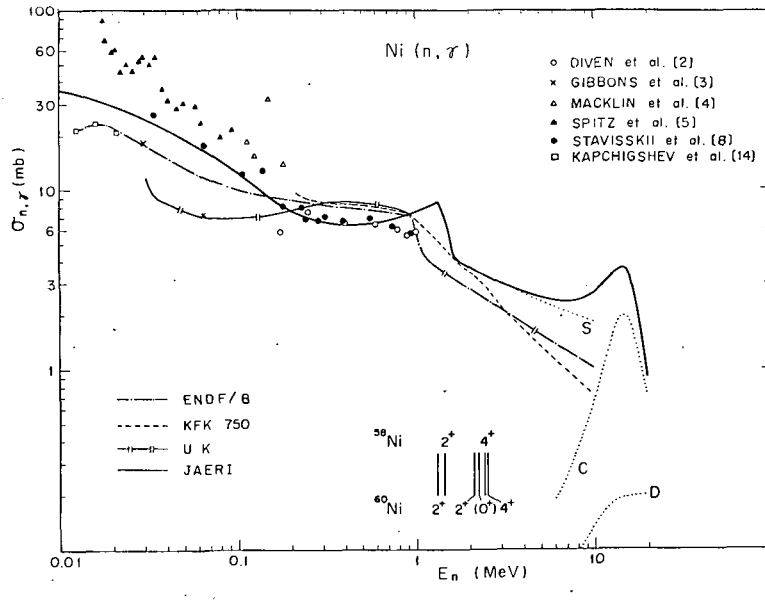

FIG. 4. Renormalized Ni(n,γ) cross-sections, which are obtained by adopting the Au(n,γ) cross-section curve of Poenitz et al. [1] as the common standard; the notation of curves is the same as in Fig. 2.

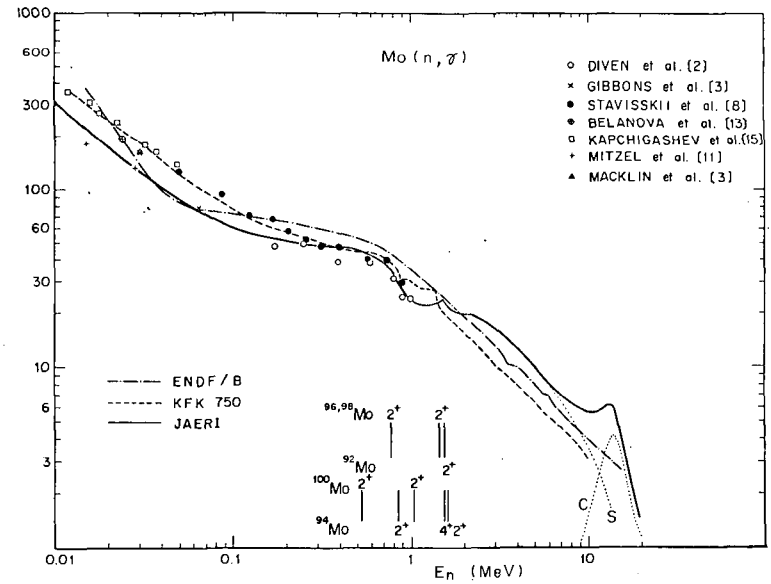

FIG. 5. Renormalized Mo(n,γ) cross-sections, which are obtained by adopting the Au(n,γ) cross-section curve of Poenitz et al. [1] as the common standard; the notation of curves is the same as in Fig. 2.

measurements by Harris et al. [6] agree very well with the results of Poenitz et al., and support the reliability of Poenitz data, as shown in Fig. 1. We therefore adopted the Au(n,γ) cross-section of Poenitz et al. as the common standard for the renormalization.

Original data of (n,γ) cross-sections for Cr, Fe, Ni and Mo are renormalized by comparing the (n,γ) cross-sections obtained in the measurements with the standard Au(n,γ) cross-section adopted. Present renormalizations are made only by multiplying all the results of a particular experiment by a constant factor, which are determined by comparing each Au(n,γ) cross-section with the standard one adopted. Magnitudes of the cross-section are affected, but not the shapes of the cross-section versus energy. The renormalizing factors thus obtained are about 0.806 for Diven et al. [2], Stavissky et al. [7,8], Malishev et al. [9], and about 1.16 for Gibbons et al. [3], Macklin et al. [4], and about 1.13 for Spitz et al. [5].

The renormalized results for the (n,γ) cross-sections of Cr, Fe, Ni and Mo are shown in Figs 2-5, respectively. The results of Isakov et al. [10], Mitzel et al. [11] and others [12-17] have been plotted in the figures without any normalization, since either the energy region of their measurements on the Au(n,γ) cross-section does not overlap with that of Poenitz et al., or else the Au(n,γ) cross-section was not measured in their experiments.

3. CALCULATIONS OF RADIATIVE CAPTURE CROSS-SECTIONS

The radiative capture cross-sections via the compound nucleus and direct kinds have been calculated by many authors [18-20]. On the basis of the statistical model, the radiative capture cross-section through the compound nucleus process can be written as follows

$$\sigma_{n\gamma}(E) = \frac{\pi\lambda^2}{2(2I+1)} \sum_{\ell} T_{\ell}(E) \sum_{J} \frac{\epsilon^{J}_{s',\ell'} (2J+1)\, f(E,E)}{1+\xi^{J} f(E,0) \sum_{i} \sum_{\ell} \epsilon^{J}_{s\ell}\, T_{\ell}(E-E_i)} \tag{1}$$

where

$$f(E,X) = \frac{\int_{X}^{B_n+X} E_\gamma^3 \rho_{0c}(B_n+X-E_\gamma)\, dE_\gamma}{\int_{0}^{B_n+E} E_\gamma^3 \rho_{oc}(B_n-E_\gamma)\, dE_\gamma} \tag{2}$$

$$1/\xi^{J} = 2\pi\Gamma^{J}_{\gamma}(B_n)/D^{J}(B_n) \tag{3}$$

In Eqs (1) to (3), an incident neutron with energy E and angular momentum ℓ is captured by a target nucleus with spin I, and forms a compound nucleus with spin J. The compound nucleus is disintegrated by the emissions of neutron or photon. In the above equations, the neutron with angular momentum ℓ' (channel spin s') is emitted and the residual nucleus is left

the i^{th} excited state of energy E_i; $T_\ell(E)$ is the neutron transmission coefficient and ϵ_s^J is accessible channel number. The photon is emitted with energy $E_\gamma \sim E_\gamma + dE_\gamma$ and the compound nucleus is de-excited to the region of the excitation energy $(E + B_n - E_\gamma)\, dE_\gamma$; B_n is the neutron binding energy. Quantities $1/\xi^J$ and ρ_{oc} are the strength function of the gamma-ray emission and the level density of the compound nucleus, respectively. These two quantities play an important role in the radiative capture. Therefore, some systematic trends of these quantities were investigated before the calculations of the radiative capture cross-sections in this work. Detailed descriptions of these systematics will be presented elsewhere [21]. A brief description of the systematics of the level density ρ_{oc} and the strength function $1/\xi^J$ is presented here.

On the basis of the free-gas model [22], the level density $\rho_0(U)$ for zero-spin state is expressed as follows

$$\rho_0(U) = C(a^{1/2}/A^{5/2}) \exp[2(aU)^{1/2}]/U^2, \quad U = E - \delta \tag{4}$$

where C, a, A and δ are constant, level density parameter, mass number and pairing energy, respectively. In the lower-excitation energy, the constant temperature model is fairly valid [23-25], and the level density is given as follows

$$\rho_0(U) = C' \exp(U/T) \tag{5}$$

The values of constant C' and temperature T are determined by the smooth fitting of Eqs (4) and (5) at the energy of break-down point U_c.

In the present work, the systematics of the level density parameter a in ρ_0 is calculated by using the observed spacing D_{obs} compiled by Baba and Baba [26]. The pairing energy δ is obtained by the similar method of Kümmel et al. [27], with the back-shifted gas model [28]. The values of U_c are calculated by using Lang's formula [24].

To estimate the level density parameter a for those nuclides having no experimental data of D_{obs}, a semi-empirical formula

$$a/A = 0.1 + S(Z, N, \alpha) \tag{6}$$

is used. Here, $S(Z, N, \alpha)$ is the shell-correction term of Myers and Swiatecki [29] in their mass formula; Z, N and α are proton number, neutron number and deformation parameter of nucleus, respectively.

Assuming $D^J(B_n) = D^\circ(B_n)/(2J+1)$ and J-independence of Γ_γ^J in Eq. (3), $1/\xi^\circ$ can be expressed as $1/\xi^\circ(B_n) = 2\pi\Gamma_\gamma(B_n)/D^\circ(B_n)$. Then the following equation is derived by Lane and Lynn [19]

$$1/\xi^\circ = C_0 \frac{NZ}{A} \int_0^{B_n} E_\gamma^3\, g(E_\gamma)\, \rho_{oc}(B_n - E_\gamma)\, dE_\gamma \tag{7}$$

where C_0, N, Z and A are constant, neutron number, proton number and mass number of the target nucleus. $g(E_\gamma)$ is the profile function for photon absorption cross-section of photon energy E_γ.

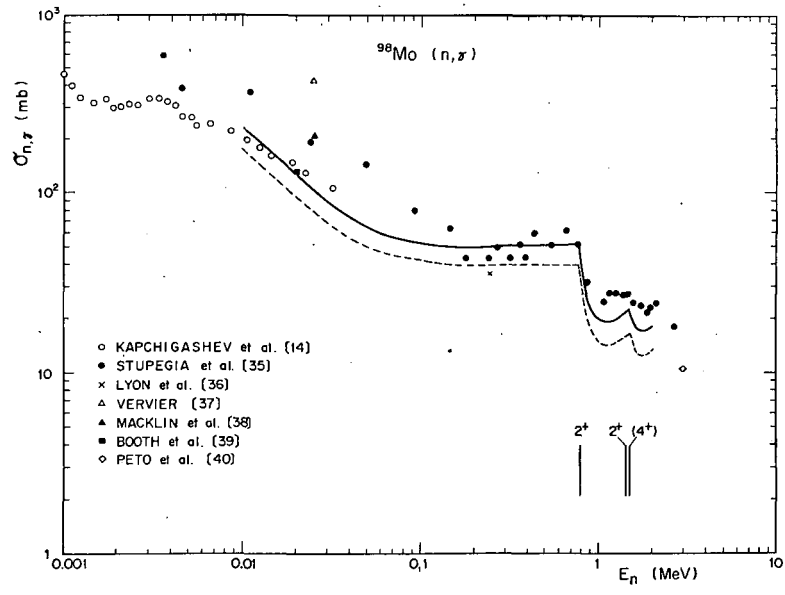

FIG. 6. ^{98}Mo(n,γ) cross-sections are compared with the calculated curves obtained by the two methods of estimation for the level density parameter a; the dashed and solid lines represent the calculated (n,γ) cross-section curves obtained by using (1) the observed level spacing D_{obs}, and (2) the semi-empirical formula of Eq.(6), respectively.

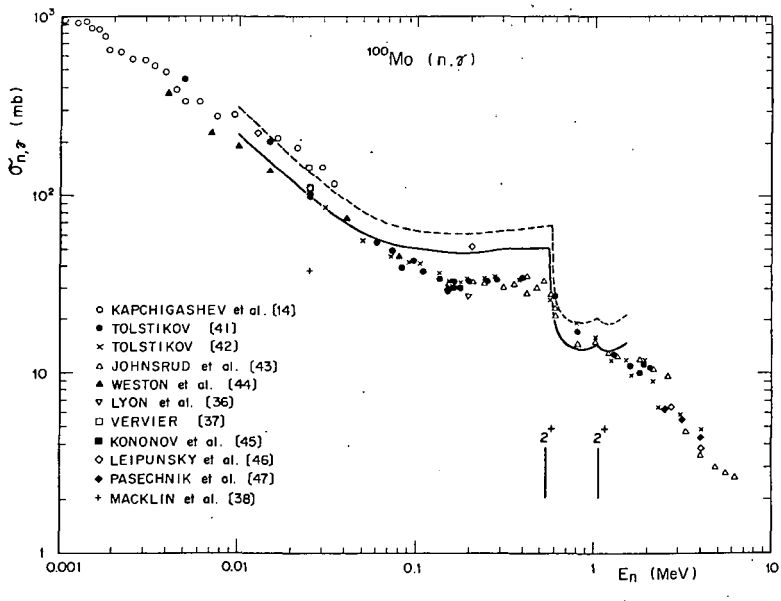

FIG. 7. ^{100}Mo(n,γ) cross-sections are compared with the calculated curves obtained by the two methods of estimation for the level density parameter a; the notation of curves is the same as in Fig. 6.

When energies of incident neutrons increase more than several MeV, the contribution of the collective capture [30] to the (n,γ) cross-section becomes important. In the collective model calculation, the values of iso-spin part V_1 of the average nuclear potential are taken to be 130 MeV for Cr, Fe and Ni, and 200 MeV for Mo.

Finally, the calculated cross-section curve for a natural element is obtained by the summation of cross-sections for each isotope weighted by relevant isotopic abundances, where the values of constant C_0 in Eq.(7) are taken to be the same for all isotopes of the natural element. The constant C_0 is determined by fitting the calculated cross-section curve of the natural element to the renormalized cross-section obtained in section 2.

In the present calculations, neutron-transmission coefficients $T_\ell(E)$, the values of neutron binding energy B_n, and level schemes of isotopes are taken from Refs [31-33], respectively.

4. RESULTS AND DISCUSSION

Results of calculations of radiative capture cross-sections for natural elements of Cr, Fe, Ni and Mo are presented in Figs 2-5, as well as those of the renormalized experimental data. In the figures, the solid lines represent the capture cross-sections obtained in the present work; the dotted lines with the marks of S, C or D stand for the capture cross-sections calculated by statistical, collective or direct models, respectively. Calculations were done by using a computer code RACY [34].

Owing to competition with inelastic scattering, the radiative capture cross-section decreases rapidly at threshold energies of the target nucleus. This fact is clearly seen in the experimental data for the isotopes of ^{98}Mo [14,35-40] and ^{100}Mo [14,36-38, 41-47], as shown in Figs 6 and 7. The present results of RACY calculation reproduce this decrease in the (n,γ) cross-section, and are in good agreement with the experimental data for ^{98}Mo and ^{100}Mo, as well as for Fe (see Fig.3).

The cross-section values of Spitz et al. [5] for Cr and Ni in the resonance region below about 60 keV are rather high as compared with the present cross-section curves (see Figs 2 and 4). However, good agreement may be expected if a multiple scattering correction is properly applied to the experimental data in that resonance region.

Looking at the resonance-energy region of Fe below 100 keV in Fig.3, the calculated $Fe(n,\gamma)$ cross-section curve seems to represent approximately a similar behaviour to the smooth cross-section which may be obtained by averaging the high resolution measurements of Macklin et al. [16] and Moxon [17].

The calculated (n,γ) cross-section curves for Fe, Ni and Mo, except for Cr, are higher than those of ENDF/B, KFK 750 and UK data in the energy region above 2-3 MeV, since other charged-particle channels, for example the (n,p) reaction are not taken into account in the statistical-model calculation of RACY.

Because of the ambiguity of the values of V_1, there is an uncertainty of a factor of about two in the present results of the collective capture cross-sections. The (n,γ) cross-section measurements around 14 MeV are, therefore, needed for the comparison with the collective-model calculations.

In the case of ^{98}Mo and ^{100}Mo, where the experimental data of both the (n,γ) cross-sections and D_{obs} are available, two methods for estimating the level density parameter a are carried out so as to determine a proper approach to the problem. The results are shown in Figs 6 and 7. The dashed and solid lines represent the calculated (n,γ) cross-section curves obtained by using the observed level spacing D_{obs}, and the semi-empirical formula of Eq.(6), respectively. The agreement of the solid curves with the experimental data of ^{98}Mo and ^{100}Mo is better than that of the dashed curves. The results of both $Mo(n,\gamma)$ cross-section curves obtained by the weighted summation of seven isotopes, including ^{98}Mo and ^{100}Mo, are in good agreement with the renormalized $Mo(n,\gamma)$ cross-section data, while the constants C_0 in Eq.(7) are somewhat different.

The strength function $1/\xi^\circ$ of Eq.(7) is important not only for the shape but also for the absolute value of the radiative capture cross-section, and it includes the constant C_0 and the level density ρ_{oc}. In the present work, the systematic trend for the level density ρ_{oc} has been studied, but not for the constant C_0. Therefore, it will be necessary for an advanced study of the radiative capture cross-section to investigate the systematic trend of the constant C_0 in Eq.(7).

REFERENCES

[1] POENITZ, W.P., KOMPE, D., MENLOVE, H.O., J. nucl. Energy 22 (1968) 505.
[2] DIVEN, B.C., TERRELL, J., HEMMEDINGER, A., Phys. Rev. 120 (1960) 556.
[3] GIBBONS, J.H., MACKLIN, R.L., MILLER, P.D., NEILER, J.H., Phys. Rev. 122 (1961) 182; MACKLIN, R.L., GIBBONS, J.H., INADA, T., Phys. Rev. 129 (1963) 2695, Nucl. 43 (1963) 353.
[4] MACKLIN, R.L., GIBBONS, J.H., Phys. Rev. 159 (1967) 1007.
[5] SPITZ, L.M., BARNARD, E., BROCKS, F.D., Nucl. Phys. A121 (1968) 655.
[6] HARRIS, K.K., GRENCH, H.A., JOHNSON, R.G., BAUGAN, F.J. et al., Nucl. Phys. 69 (1965) 37.
[7] STAVISSKY, Yu.Ya., SHAPAR, A.V., Sov. atom. Energy 12 (1962) 545.
[8] STAVISSKY, Yu.Ya., SHAPAR, A.V., Sov. atom. Energy 10 (1960) 255.
[9] MALISHEV, A.V., STAVISSKY, Yu.Ya., SHAPAR, A.V., Sov. atom. Energy 17 (1965) 1277; J. nucl. Energy, Pt A/B, 19 (1965) 918.
[10] ISAKOV, A.I., POPOV, Yu.P., SHAPITO, F.L., Sov. Phys. JETP 11 (1960) 712.
[11] MITZEL, F., PLENDL, H.S., Nukleonik 6 (1964) 371.
[12] KAPCHIGASHEV, S.P., POPOV, Yu.P., Sov. atom. Energy 16 (1964) 306.
[13] BELANOVA, T.S., VAN'KOV, A.A., MIKHAILUS, F.F., STAVISSKY, Yu.Ya., Atomn. Energ. 19 (1965) 3.
[14] KAPCHIGASHEV, S.V., POPOV, Yu.P., Sov. atom. Energy 15 (1964) 808.
[15] STAVISSKY, Yu.Ya., SHAPAR, A.V., Soviet Progress in Neutron Physics, (1961) 227.
[16] MACKLIN, R.L., PASMA, P.J., GIBBONS, J.H., Phys. Rev. 136 (1964) B695.
[17] MOXON, M.C., "The neutron capture cross-sections of Iron and Cobalt", Study of Nuclear Structure with Neutrons, EANDC-50-S (Proc. Int. Conf. Antwerp, 1965) 1 CEN, Mol (1965) paper 88.
[18] LANE, A.M., Nucl. Phys. 11 (1959) 625.
[19] LANE, A.M., LYNN, J.E., Nucl. Phys. 11 (1959) 646.
[20] BENZI, V., BORTOLANI, M.V., Nuovo Cim. 38 (1965) 216.
[21] NAKAMURA, H., to be published.
[22] ERICSON, T., Advances Phys. 9 (1960) 425.
[23] GILBERT, A., CAMERON, A.G.W., Can. J. Phys. 43 (1965) 1446.
[24] LANG, E.W., Nucl. Phys. 42 (1963) 397.
[25] SANO, M., YAMASAKI, S., Prog. theor. Phys. 29 (1963) 353.
[26] BABA, H., BABA, S., JAERI-1183 (1969).

[27] KÜMMEL, H., MATTAUCH, J.H.E., THIELE, W., WAPSTRA, A.H., Nucl. Phys. 81 (1966) 129.
[28] HUIZENGA, J.R., VONACH, H.K., KATSANOS, A.A., GORSKI, A.J., STEPHAN, C.J., Phys. Rev. 182 (1969) 1149.
[29] MYERS, W.D., SWIATECKI, W.J., Nucl. Phys. 81 (1966) 1.
[30] CLEMENT, C.F., LANE, A.M., ROOK, J.R., Nucl. Phys. 66 (1965) 293.
[31] IGARASI, S., JAERI Memo. 3368 (1969).
[32] MATTAUCH, J.H.E. et al., Nucl. Phys. 67 (1965) 32.
[33] LEDERER, M.C., HOLLANDER, J.M., PERLMAN, I., Table of Isotopes, 6th Edn, John Wiley & Sons Inc. (1967).
[34] NAKAMURA, H., HATCHYA, M., JAERI Memo. 3300 (1968).
[35] STUPEGIA, D.C., KEEDY, C.R., SCHMIDT, M., MADSON, A.A., ANL-7105, (1965) 38.
[36] LYON, W.S., MACKLIN, R.L., Phys. Rev. 114 (1959) 1619.
[37] VERVIER, J.F., Nucl. Phys. 9 (1958/59) 569.
[38] MACKLIN, R.L., LAZAR, N.H., LYON, W.S., Phys. Rev. 107 (1957) 504.
[39] BOOTH, R., BALL, W.P., MACGREGOR, M.H., Phys. Rev. 112 (1958) 226.
[40] PETŐ, G., MILIGY, X., HUNYADI, I.J., Nucl. Energy 21 (1967) 797.
[41] TOLSTIKOV, V.A., KOLESOV, V.E., DOVBENKO, A.G., STAVISSKY, Yu.Ya., Sov. atom. Energy 17 (1965) 1272.
[42] TOLSTIKOV, V.A., STAVISSKY, Yu.Ya., Soviet Progress in Neutron Physics, (1961) 229.
[43] JOHSRUD, A.E., SILBERT, M.G., BARSCHALL, H.H., Phys. Rev. 116 (1959) 927.
[44] WESTON, L.W., SETH, K.K., BILPUCH, E.G., NEWSON, H.W., Annls Phys. 10 (1960) 477.
[45] KONONOV, V.N., STAVISSKY, Yu.Ya., TOLSTIKOV, V.A., J. nucl. Energy 11 (1959/60) 46.
[46] LEIPUNSKY, A.I. et al., "Measurements of radiative capture cross-sections for fast neutrons", Int. Conf. peaceful Uses atom. Energy (Proc. Conf. Geneva, 1958) 15 UN, Geneva (1958) 50.
[47] PASECHNIK, M.V. et al., "Fast neutron scattering and capture by atomic nuclei", Int. Conf. peaceful uses atom. Energy (Proc. Conf. Geneva, 1958) 15 UN, Geneva (1958) 18.

DISCUSSION

M.P. FRICKE: I would like to ask three questions. First, how was the lower limit on the integral of the partial radiation widths calculated? I think you called it X in your first slide. In other words, how was the cascade capture treated?

K. NISHIMURA: We did not take account of cascade capture or second particle emission in our calculations.

M.P. FRICKE: Did you make a correction for width fluctuations?

K. NISHIMURA: No, we did not.

M.P. FRICKE: What spin dependence was used for the level density?

K. NISHIMURA: We assumed (2J+1) dependence for the level density.

CAPTURE CROSS-SECTIONS OF STRUCTURAL MATERIALS

M.C. MOXON
UKAEA, AERE, Harwell, Didcot, Berks,
United Kingdom

Abstract

CAPTURE CROSS-SECTIONS OF STRUCURAL MATERIALS.

The improvements in the cross-section data for fissile and fertile materials contrast strongly with the large discrepancies between different measurements of the absorption cross-sections of some of the elements used for fuel cladding and in the structure of nuclear reactors. The available data on the neutron absorption in these materials will be examined, especially the more recent capture measurements which have shown the presence of many narrow capturing resonances in most of these elements. These results also indicate that in some cases the capture cross-section in the region of the large s-wave resonances could be an order of magnitude higher than the older results from the slowing-down spectrometer. Comment is about the corrections used to obtain the cross-sections from the γ-ray yield data, which in some cases can be very large.

1. INTRODUCTION

Most of the elements that have been used as fuel cladding and as structural materials in nuclear reactors occur in the mass region around that of iron. Considering the importance of these elements, there is a surprising lack of good cross-section data. This is especially true for the capture cross-section, where very large discrepancies can be seen in certain neutron energy regions for most of these elements. The earlier capture data in the keV region, obtained mainly using the lead slowing-down-time spectrometer [1-7], followed the total cross-section and gave average radiation widths in general agreement with values expected for this mass region. The recent high resolution capture measurements [8,9,10] have, however, shown up some large discrepancies as well as showing a much more complex resonance structure. Narrow capturing resonances are superimposed on the underlying capture cross-section due to the broad s-wave structure that is observed in total cross-section measurements. The presence of these narrow resonances makes analysis, interpretation and correction of the observed data much more difficult. Some of the disagreement between different sets of poor resolution data could possibly be accounted for by a lack of knowledge of these resonances, which would result in inadequate corrections for multiple scattering and self-screening.

2. EXPERIMENTAL PROBLEMS

Besides the problems of measuring the neutron flux incident on the sample and the efficiency of the neutron capture detector, there are several other problems that are more important in capture measurements on the light elements than in those on the heavier elements.

In general the capture cross-sections are small, and due to the high scattering cross-section only thin samples can be used. Even so corrections for multiple scattering and self-screening can be large. An example of the

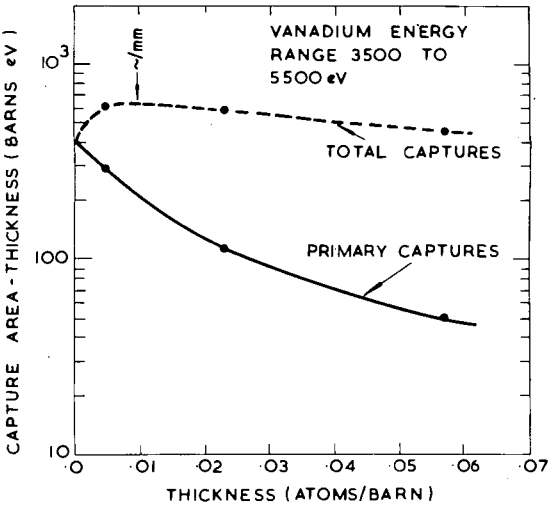

FIG. 1. Effect of multiple scattering.

effect of multiple scattering is shown in Fig. 1. This is the result of a Monte-Carlo calculation of the area under the observed cross-section* curve in the energy region 3.5 keV to 5.5 keV for vanadium plotted as a function of sample thickness. Also plotted is the cross-section area for the fraction of neutrons that are captured on their initial collision. The primary area decreases with increasing sample thickness, whereas the total capture area increases rapidly with sample thickness to a broad maximum some 50% above the zero thickness value and then slowly decreases with increasing sample thickness. The multiple scattering and self-screening corrections require accurate values of the total cross-section in order to avoid further uncertainties in the interpretation of the observed data. But in the case of some of the elements in the mass region 50 to 60 the total cross-section data are poor and show large discrepancies between the results of different measurements.

The large scattering to capture ratio in neutron interactions with most light elements (~1000 to 1) requires a neutron capture detector that is very insensitive to the scattered neutrons. Hockenbury et al [9] at RPI gave a value of 10^{-5} for the efficiency of detecting scattered neutrons with a bias set at ~3 MeV on the pulse height distribution from their 400 litre boron loaded liquid scintillator. A measurement [11] of the neutron detecting efficiency of a 'Moxon-Rae' capture gamma-ray detector on IBIS at Harwell gave a value of ~4×10^{-6} at 30 keV. This is ~1.5×10^{-4} down in efficiency on the detection efficiency for a typical capture gamma-ray cascade. Activation measurements are free from the effects of scattered neutrons but care must be taken that the neutron monitor cannot see the neutrons scattered by the sample being activated.

The relatively small number of initial gamma-ray transitions following neutron capture in light elements could lead to large fluctuations in the

* The observed capture cross-section can be defined as the number of neutrons captured in the sample per incident neutron, divided by the sample thickness in atoms per barn.

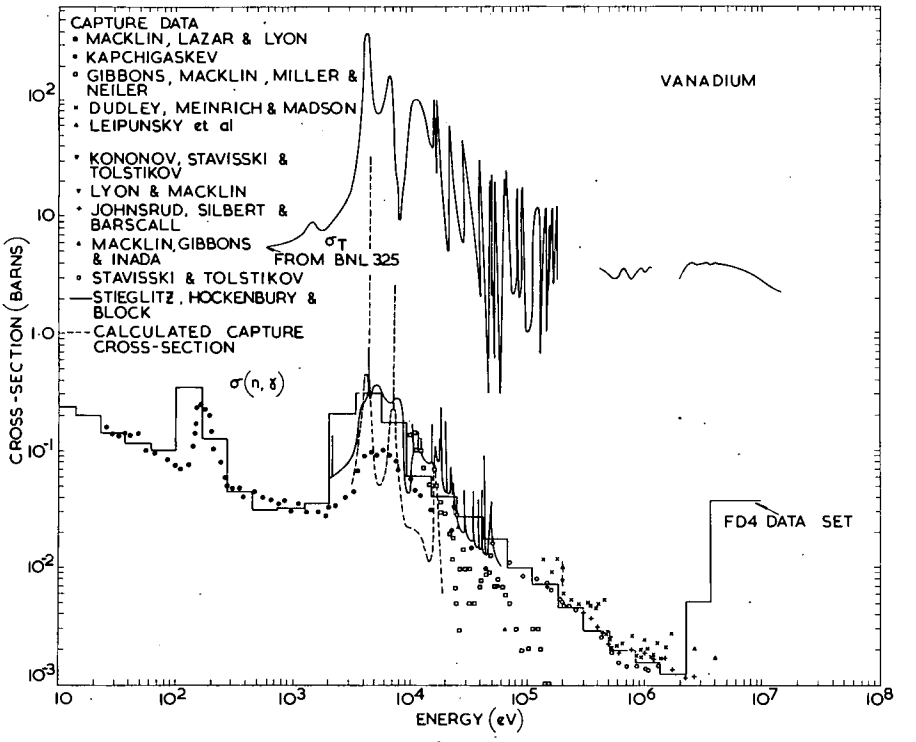

FIG. 2. Vanadium cross-sections.

gamma-ray spectra from resonance to resonance, and to obtain meaningful results from measurements using the prompt gamma-rays requires a gamma-ray detector that is insensitive to these variations. A large liquid scintillator overcomes this problem by absorbing nearly all the prompt gamma-ray energy emitted when a neutron is captured. Another method is to have a detector such as a 'Moxon-Rae', whose efficiency is small but proportional to the total prompt gamma-ray energy emitted when a neutron is captured. Activation measurements will avoid this problem but require a knowledge of the decay of the active nucleus produced, and cannot be used on several major isotopes in this mass region as capture produces another stable isotope.

3. AVAILABLE DATA

During the past few years several sets of high resolution capture measurements on the elements in the mass region from 50 to 60 have been carried out. Much of these data are in disagreement with the older measurements and in most cases they reveal a much more complex resonance structure. This is best illustrated by the examples of the data on V, Fe and Ni as there is very little information on the other elements in this mass region.

3.1 Vanadium

The total cross-section (Fig. 2) shows the broad s-wave resonances with large interference effects and an average level spacing of 4.2 keV in the energy range up to 100 keV.

The capture data can be divided into two energy regions above and below approximately 100 keV. The data below 100 keV are mainly obtained using the prompt capture gamma-rays, while those above have been measured using activation techniques.

Below 1 keV there are only the data of Kapchigashev [7], who used the lead slowing-down-time spectrometer and normalised the data to the extrapolation of the thermal cross-section using the 1/v law. In the energy region between 1 and 10 keV there is only one set of published data other than those of Kapchigashev, namely the high resolution data of Stieglitz et al. [10] at RPI. These data are not true capture cross-sections, but capture yield divided by sample thickness and are uncorrected for multiple scattering or self-screening. From 10 keV to 100 keV the data of Stieglitz et al. clearly indicate many more resonances than the data of Gibbons et al. [12] and tend to give a higher cross-section. In the region above 100 keV there are several activation measurements [13,14,15] all of which are in fairly good agreement amongst themselves but which indicate an even higher cross-section than an extrapolation of the RPI data.

TABLE I. RESONANCE PARAMETERS

E_R (keV)	J	Γ_n (keV)	Γ_γ (eV)
4.162	4	(0.51)	0.65
4.38	—	— $\Gamma_n\Gamma_\gamma/\Gamma$ =	0.16eV
6.84	3	(1.28)	1.45
7.35	—	— $\Gamma_n\Gamma_\gamma/\Gamma$ =	0.10eV
11.75	3	(5.50)	(1.5)
16.20	4	(0.35)	(1.5)

The dashed curve between 3 keV and 20 keV is a preliminary attempt to obtain the true capture cross-section using the resonance parameters given in Table I. These were calculated from area data obtained from capture measurements on a 0.01 inch vanadium sample. These measurements were carried out on the Harwell 45 MeV electron linac neutron time-of-flight spectrometer using a 'Moxon-Rae' detector at 32.54 m from the neutron source. Details of the detector and measurement are given in reference [11].

A comparison of the capture yield curves with Monte-Carlo calculations using the parameters given in the table shows that there is a low energy tail on the capture due to the broad s-wave resonances at 4.16 keV and 6.84 keV. This is very similar to that observed in sodium at 2.8 keV with the same equipment. This is still under investigation and at present there is no experimental evidence to show that it is not due to capture of neutrons in the sample at their correct times of arrival.

3.2 Iron

Iron is one of the elements most widely used as a structural material in both fast and thermal nuclear reactors. In the total cross-section of

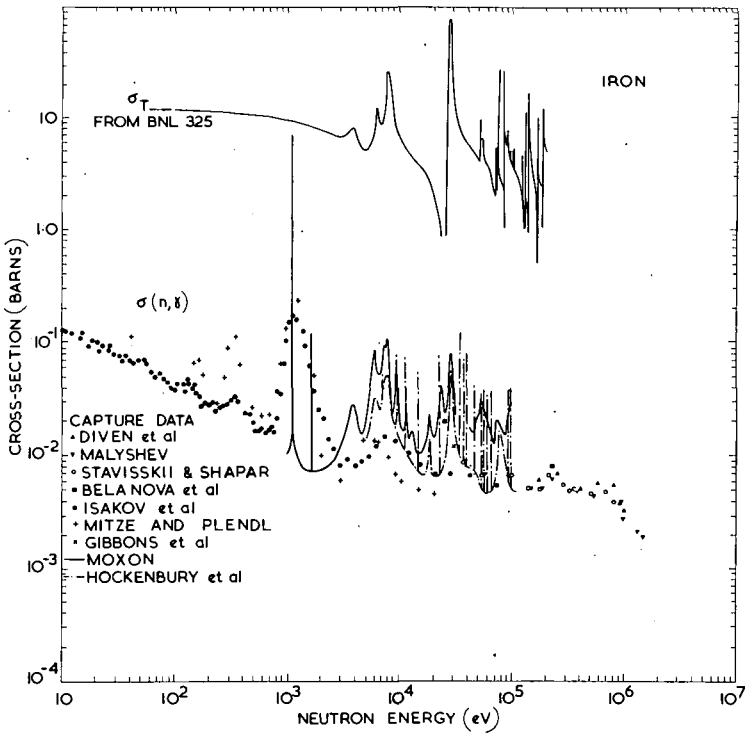

FIG.3. Iron cross-sections.

iron several s-wave resonances are observed below 100 keV; the only p-wave resonance identified with any certainty is at 1.1 keV. The spread in the capture data [2,6,9,16-24] shown in Fig. 3 is not as great as for other elements in this mass region, and the resonance parameters obtained from the capture data [9,11] are also in reasonable agreement. A summary of all the observed resonance parameters for iron up to ~100 keV is given in Table II. Where there is more than one value a weighted mean has been calculated. The observed capture cross-section in the region of the resonances is reasonably represented by the parameters given in Table II, but in the region between resonances the observed values (uncorrected for multiple scattering) are about a factor of ten higher than the calculated ones. Monte-Carlo calculations of the multiple scattering effects between the resonances indicate that even when these effects are taken into account the observed value may still be as much as a factor of five higher than that calculated from the resonance parameters. Several possibilities suggest themselves to explain this discrepancy.

(i) Since the capture yield in the region between resonances is very low, the discrepancy may be caused by the background being underestimated.

(ii) The effect may be due to the existence of a long tail on the spectrometer resolution function. But to explain the observed inter-resonance yield the tail would have to extend for a few μs and contain as many neutrons as are present in the main pulse. This is certainly not true for the RPI Linac.

TABLE II. SUMMARY OF RESONANCE PARAMETERS

Isotope	E_R (keV)	Γ_n (eV)	Γ_γ (eV)	$g\Gamma_n\Gamma_\gamma/\Gamma$ (eV)	$\sigma_o\Gamma_\gamma$ (b.eV)	Isotope	E_R (keV)	Γ_n (eV)	Γ_γ (eV)	$g\Gamma_n\Gamma_\gamma/\Gamma$(eV)	$\sigma_o\Gamma_\gamma$ (b.eV)
58	0.230	-	-	0.0065±0.0014	74.1	57	28.3	-	-	-	-
58	0.359	-	-	0.017 ±0.005	124.0	57	29.0 J=1	3000	4±1	-	-
56	1.167	0.056±0.006	0.673±0.1	-	-	56	34.1	-	-	0.59±0.07	44.1±5.0
57	1.62	-	-	0.050 ±0.01	79.6±16.0	56	36.6	-	-	0.30±0.032	21.4±2.2
56	2.35	-	-	0.0004	0.42	56	38.3	-	-	0.46±0.05	30.1±3.0
58	2.82	-	-	-	-	57	40.0	-	6±2	-	-
57	3.96 J=0	177	1.14 ±0.06	-	-	56	45.8	-	-	0.32±0.04	18.7±2.0
57	4.75	-	-	0.051 ±0.01	28±5	56	51.9	-	-	0.51±0.05	25.6±2.6
58	4.96	-	-	-	-	54	52.0	2100±300	-	-	-
58	6.16	-	-	-	-	56	53.3	-	-	0.54±0.06	26.4±2.8
57	6.21 J=1	396	1.32 ±0.15	-	-	56	55.0	-	-	0.14±0.04	6.7±2.0
57	7.22	-	-	0.36 ±0.09	132±33	56	59.0	-	-	0.54±0.06	24.2±2.6
54	7.825	1000±50	<3.0	-	-	56	63.1	-	-	-	-
57	7.90	-	-	0.18 ±0.05	60±18	54	72.1	1600±400	-	-	-
58	9.29	-	-	-	-	56	72.6	-	-	-	-
54	9.48	-	-	0.53 ±0.05	-	56	74.0	505±36	-	-	-
58	10.4	-	-	-	-	56	76.7	-	-	-	-
56	11.2	-	-	0.043 ±0.007	10.2±1.5	56	80.4	-	-	-	-
57	12.8	-	-	0.46 ±0.15	-	56	82	-	-	-	-
57	13.9	-	-	0.7 ±0.2	-	56	83.5	970±65	-	-	-
54	14.4	-	-	0.53 ±0.14	97 ±25	56	90.2	<50	-	-	-
57	17.5	-	-	0.71 ±0.35	-	56	92.1	-	-	-	-
57	21.3	-	-	1.09 ±0.28	135 ±32	56	95.9	-	-	-	-
56	22.7	-	-	0.191 ±0.02	21.9±2.0	54	98.5	400	-	-	-
56	27.9	1670±200	1.44 ±0.14	-	-	56	102	-	-	-	-

(iii) The between-resonance cross-section may be due to the presence of a small amount of heavy element contamination. This explanation, however, is not valid, since the measurements [9] made use of ARMCO iron whose impurity levels are known to be extremely low. The effect calculated for the known impurities could not account for any more than ~0.5 mb out of the observed inter-resonance cross-section of ~4 mb at ~50 keV.

(iv) The effect may be due to missed levels. Since the smallest observed resonance near 50 keV has an area of the same order of magnitude as the mean area expected for p- and d-wave resonances in this energy region, assuming the strength function for even parity is 1.6×10^{-4} and for odd parity is 0.1×10^{-4} with average radiation widths of 1.4 eV and 0.6 eV respectively and a mean level spacing for J = 0 of 45 keV, a rough calculation gives an average capture cross-section of ~14 mb at 50 keV, slightly higher than the experimental results, but much higher than the value of ~6 mb given by the known resonance parameters in this region. The calculated value is dependent on the average radiation width and in reference [21] a fit to experimental data in the energy region 150 to 1400 keV gives an average radiation width of 0.45 eV. Using this value an average capture cross-section of ~10 mb at 50 keV is still considerably higher than the value given by the resonance parameters but in reasonable agreement with the experimental data.

(v) Contribution from other isotopes. The other isotopes may be expected to contribute ~10% of the mean capture cross-section. Since it would be unlikely that dips in the ^{56}Fe cross-section would coincide with dips in the cross-section due to the other isotopes, we can assume a smooth underlying cross-section due to this effect which will then contribute ~1 mb near 50 keV.

The latter two possibilities may be the major causes of the discrepancies, (i) and (iii) may also contribute a small amount while it is thought that very little can be attributed to (ii).

The conclusions that can be drawn about the iron capture cross-section are that the capture cross-section below about 30 keV is reasonably represented by the resonance parameters given in Table II. The fit to the observed data between 30 keV and 100 keV is reasonably satisfactory in the region of the strong resonances; between resonances the fit is poor, but this is probably due mainly to small p- and d-wave resonances being missed in the experiments.

A correction based on our poor knowledge of the parameters for resonances with $l > 0$ and on the effect of other isotopes accounts qualitatively for the discrepancy, but a better knowledge of these parameters would be required to give full confidence in the results. The uncertainty on the mean capture cross-section in the energy range below 100 keV is estimated at $\pm 30\%$.

Above 100 keV the effect of unresolved resonances becomes dominant and the uncertainty in the parameters for $l > 0$ enters directly into the cross-section. The uncertainty on the calculated cross-section could be as large as $\sim \pm 50\%$ in the energy region from ~100 keV to ~1 MeV. To improve the situation both here and in the lower energy region, a better knowledge of the p- and d-wave parameters is essential. Above 100 keV this is the most promising way to a better knowledge of the capture cross-section since its small value makes direct measurement very difficult. The most promising line of attack would appear to be via high resolution transmission data which would yield information on neutron widths, level spacings and strength functions. Radiation widths would have to be obtained from capture measurements at the lower end of the range.

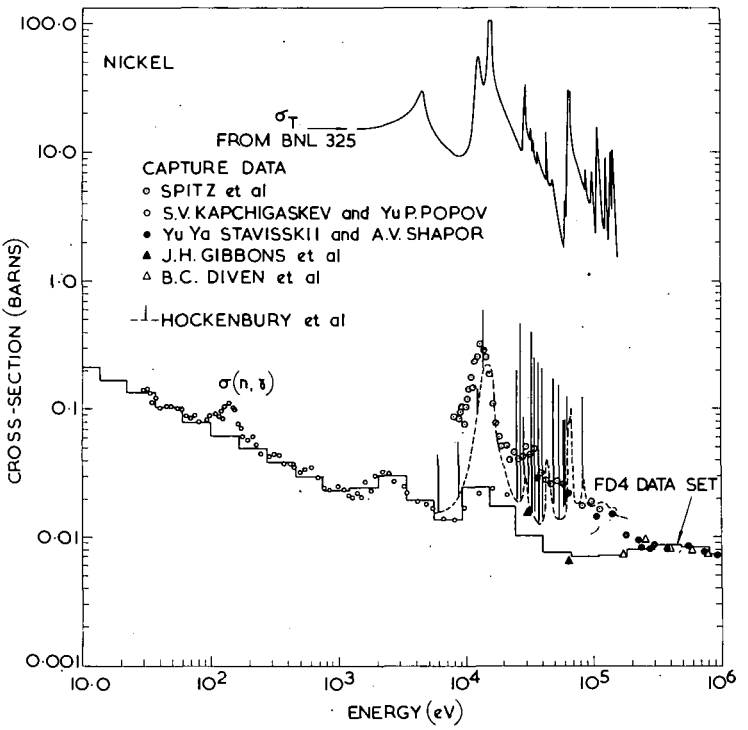

FIG.4. Nickel cross-sections.

3.3 Nickel

Until very recently there existed only four measurements [4,17,18,19] of the capture cross-section of nickel. In the energy region below 30 keV, there were the data of Kapchigashev and Popov [4] (lead slowing-down-time spectrometer). In the energy region above 30 keV there were some spot points by Gibbons et al. [19] and Diven et al. [17], together with some widely spaced data by Stavisskii and Shapar [18]. In the past year two sets of data on nickel covering the energy range ~10 to ~100 keV have been published. The first was by Spitz et al. [8] and indicated that the capture cross-section was much higher than that given by Kapchigashev and Popov, especially in the region 10 to 20 keV where it was an order of magnitude higher. These data were confirmed by some measurements carried out at RPI by Hockenbury et al. [9], who used much higher resolution and were able to resolve many resonances in the energy region up to 100 keV (Fig.4).

Some preliminary results of a measurement of the capture yield for several samples of nickel, carried out at Harwell, agree in general with these last two sets of data, but confirm the higher cross-section given by Spitz et al. on the lower energy side of the group of resonances near 15 keV. This feature (the low energy tail) was not observed in the RPI data, but is analogous to the low energy tails observed at Harwell in the resonances in sodium and vanadium. It may be significant that Spitz et al. also used a Moxon-Rae type detector.

4. GENERAL COMMENTS ABOUT THE AVAILABLE DATA

In general the capture cross-section data for the elements in the mass region between 50 and 60 are poor. Very few radiation widths have been determined and in the case of cobalt [23] where several have been measured, there is a large spread in the values, which can also be expected to occur in the other elements. This spread will put large uncertainties on average cross-section calculations based on the few radiation widths that have been determined. The fact is that we know very little about the capture cross-section of most of these elements. There are often only a few discrepant measurements existing, covering only limited energy regions and only in the case of iron does the uncertainty on the capture cross-section approach the accuracy required by the reactor designers.

The capture measurements from the lead slowing-down-time spectrometer all give lower results in the resonance region than any of the other data, and as in the case of the heavy elements, the activation measurements give results which are higher than those using prompt capture gamma-ray detectors.

The recent high resolution capture measurements have revealed a much more complex structure than is indicated by the total cross-section data. Some of the discrepancies in the poorer resolution data could be explained by a lack of knowledge of this fine structure causing inadequate corrections to the observed data. Even extrapolation to zero thickness can lead to erroneous results as is shown in Fig. 1. The extrapolation of the calculation to zero thickness from the points above an n value of 0.01 will give a zero thickness value some 60% above the true value. This suggests that some high resolution capture measurements should be carried out on 'thin samples', in order to avoid large corrections to the observed data. Good total cross-sections are also required for the accurate calculation of these corrections and this is especially true for the energy region below 100 keV.

REFERENCES

[1] STAVISSKII, Yu. Ya. and Tolstikov, V. A. Atomnaya Energiya 9, 401 (1960).
[2] ISAKOV, A. I., Popov, Yu. P. and Shapiro, F. L. JETP 11, 712 (1960).
[3] STAVISSKII, Yu. Ya. and Tolstikov, V. A. Atomnaya Energiya 10, 508 (1961).
[4] KAPCHIGASHEV, S. P. and Popov, Yu. P. Atomnaya Energiya 15, 120 (1963).
[5] KAPCHIGASHEV, S. P. and Popov, Yu. P. Atomnaya Energiya 16, 256 (1964).
[6] MITZEL, F. and Plendl, M. S. Nukconik 6, 371 (1964).
[7] KAPCHIGASHEV, S. P. Atomnaya Energiya 19, 294 (1965).
[8] SPITZ, L. M., Barnard, E. and Brooks, F. D. Nuc. Phys. A121, 655 (1968).
[9] HOCKENBURY, R. W., Bartolome, Z. M., Tatarczuk, J. R., Moyer, W. R. and Block, R. C. Phys. Rev. 178, 1746 (1969).
[10] STIEGLITZ, R. G., Hockenbury, R. W. and Block, R. C. RPI Linear Accelerator Project, Annual Technical Report RPI-328-171.
[11] MOXON, M. C. The measurement of average neutron capture cross-sections in the mass region above 100 (1968) HL 68/3739.
[12] GIBBONS, J. H., Macklin, R. L., Miller, P. D. and Neiler, J. H. Unpublished data given in BNL-325.
[13] MACKLIN, R. L., Lazar, N. H. and Lyon, W. S. Phys. Rev. 107, 504 (1957).
[14] JOHNSRUD, A. E., Silbert, M. G. and Barschall, H. H. Phys. Rev. 116, 927 (1959).
[15] DUDEY, N. D., Heinrich, R. R. and Madson, A. A. J. Nuc. Energy 23, 443 (1969).
[16] BELANOVA, T. S. Atomnaya Energiya 8, 549 (1960).

[17] DIVEN, B. C., Terrell, J. and Hemmendinger, A. Phys. Rev. 120, 556 (1960).
[18] STAVISSKII, Yu. Ya. and Shapar, A. V. Atomnaya Energiya 10, 264 (1961).
[19] GIBBONS, J. H., Macklin, R. L., Miller, P. D. and Neiler, J. H. Phys. Rev. 122, 182 (1961).
[20] MACKLIN, R. L., Gibbons, J. H. and Inada, T. Phys. Rev. 129, 2695 (1963).
[21] MALYSHEV, A. V., Stavisskii, Yu. Ya. and Shapar, A. V. Atomnaya Energiya 17, 508 (1964).
[22] MACKLIN, R. L., Pasma, P. J. and Gibbons, J. H. Phys. Rev. 136, B695 (1964).
[23] MOXON, M. C. Conf. on Study of Nuclear Structure with Neutrons (Antwerp) (1968) Paper 88.
[24] MACKLIN, R. L. and Gibbons, J. H. Phys. Rev. 159, 1007 (1967).
[25] STAVISSKII, Yu. Ya. and Shapar, A. V. Atomnaya Energiya 12, 514 (1962).

ANALYSIS OF HIGH-ENERGY NEUTRON CROSS-SECTIONS FOR FISSILE AND FERTILE ISOTOPES*

A. PRINCE
Brookhaven National Laboratory,
Upton, N.Y.
United States of America

Abstract

ANALYSIS OF HIGH-ENERGY NEUTRON CROSS-SECTIONS FOR FISSILE AND FERTILE ISOTOPES.

Based on the results of differential and integral data testing and the appearance of new signficant experimental data, a program was established to revise the Evaluated Nuclear Data File (ENDF/B) on the major fissile and fertile isotopes.

This paper will outline the various theoretical methods employed in calculating the total (σ_T), elastic (σ_{el}), inelastic ($\sigma_{nn'}$), radiative capture ($\sigma_{n\gamma}$), and fission (σ_{nf}) neutron cross-sections in the energy range of 10 keV to 15 MeV for ^{238}U, ^{239}Pu, ^{240}Pu, and ^{241}Pu. Heretofore, most calculations have employed a spherical optical potential with the various reaction cross-sections being interpreted as arising only from compound nucleus formation. Since these nuclides are deformed, a high degree of anisotropy in the direct inelastic component is caused by the strong coupling between the ground and low-lying levels, making it very difficult to predict differential elastic and inelastic scattering cross-sections.

Thus, to describe the experimental data adequately, a deformed optical model potential was used in which the first three levels were coupled, i.e. ^{239}Pu ($1/2^+$, $3/2^+$, $5/2^+$), ^{241}Pu ($5/2^+$, $7/2^+$, $9/2^+$), and ^{240}Pu, ^{238}U (0^+, 2^+, 4^+). An equivalent local potential with the appropriate deformation was chosen so as to satisfy four important experimental constraints, i.e., the total scattering cross-section σ_T, the potential scattering cross-section σ_{pot}, and the s- and p-wave strength functions.

The compound nuclear reactions were determined by employing a combined spherical potential and modified statistical model to describe the compound elastic, compound inelastic, radiative capture, and fission cross-sections.

The application of the aforementioned phenomenological models, using a single set of parameters for each isotope, produced very good agreement with the experimental data at both low and high energies. The methods were extended into areas where no experimental data exist to provide a consistent set of nuclear data that promise to be very useful in reactor analysis.

INTRODUCTION

As part of the program to revise the Evaluated Nuclear Data Files (ENDF/B) at Brookhaven National Laboratory, an effort was undertaken to re-evaluate the major fissile and fertile isotopes. This decision was based on the results of differential and integral data testing programs and the acquisition of new and significant experimental data.

The importance of these data in analyzing nuclear reactors predicated that analyses as complete and thorough as possible be used based on the most recent acceptable theories combined with the most accurate experimental data. This paper will outline

* Work supported by the US Atomic Energy Commission.

the various theoretical methods employed in calculating the total, elastic, inelastic, capture, and fission neutron cross sections in the energy range of 10 keV to 15 MeV for ^{238}U, ^{239}Pu, ^{240}Pu, and ^{241}Pu.

Heretofore most calculations used in evaluating these nuclides have employed a spherical optical potential with the various reaction cross sections being interpreted as arising only from compound nucleus formation. However, since these nuclides are known to exhibit a high degree of deformity, the scattering of neutrons cannot be described adequately by the conventional optical model, which does not take the direct coupling between the incident neutron motion and the nuclear surface rotation, thereby resulting in a direct excitation of the rotational levels by inelastic scattering.

While these previous analyses have provided fairly good agreement between calculated and experimental angular distributions, the magnitude of the diffraction minima and maxima has not been well produced. As has been pointed out by others [1,2], neglecting the high degree of anisotropy exhibited by the direct inelastic component can lead to serious errors in the prediction of the differential elastic and inelastic cross sections. These errors manifest themselves in two major areas. In the low energy region ($E < 1.0$ MeV) where discrete excitation energies are observed, the direct interaction can be very significant and ignoring its presence can produce erroneous results in the prediction of the individual level excitations and the total inelastic cross section. At higher energies where the resolution of the experimental apparatus exceeds that of the low-lying rotational states, the true shape and magnitude of the differential elastic cross section might differ from that observed due to the inelastic scattering contamination arising from these lower rotational levels.

In order to describe this strong coupling between the ground and low-lying levels, a non-spherical energy-dependent optical model potential with spin-orbit coupling was used, with the three low-lying states of each nuclide being coupled---namely, ^{239}Pu ($1/2^+$, $3/2^+$, $5/2^+$), ^{241}Pu ($5/2^+$, $7/2^+$, $9/2^+$), and ^{240}Pu, ^{238}U (0^+, 2^+, 4^+).

To adequately describe the compound nuclear reactions such as compound elastic σ_{ce}, compound inelastic $\sigma_{nn'}$(comp.), radiative capture $\sigma_{n\gamma}$, and fission σ_{nf} cross sections, a combination of an optical model, employing a spherical potential, and a statistical model, based on Hauser-Feshbach theory modified by Moldauer to take width fluctuations into consideration, was used.

To portray the level excitations in the discrete region, twenty-three levels were used in ^{239}Pu; for ^{238}U, ^{240}Pu, and ^{241}Pu, twelve, eleven, and fifteen were employed, respectively.

In applying a deformed optical potential, the form factors, which were based on a generalization of the equivalent local potential and the degree of deformity, were chosen so as to satisfy four important experimental constraints; namely, the total cross section σ_T, the potential scattering cross section σ_{pot}, and the s- and p-wave strength functions (S_0 and S_1). This restriction was successful in providing a consistent set of parameters that enabled calculations to be performed that gave very good agreement with all available experimental data from 10 keV to 15 MeV.

THEORY

Since these nuclides are deformed, the neutron interactions were analyzed in terms of a spherical and rotational-optical model, which permitted the investigation of not only compound nuclear reactions but also the direct excitation of the rotational levels by inelastic scattering due to the existence of a direct coupling between the incident particle and the nuclear surface.

The differential cross sections for shape elastic scattering (σ_{SE}), the total reaction cross section (σ_R), and the direct inelastic scattering ($\sigma_{(rot)}$) were calculated using the Coupled Channel Code JUPITER I by Tamura [4]. The cross sections for excitation by way of the compound nucleus (inelastic $\sigma_{nn'}$, radiative capture $\sigma_{n\gamma}$, compound elastic σ_{CE}, and fission σ_{nf}) were calculated using the ABACUS-NEARREX [5,6] computer code, which is a combination of an optical model that assumes spherical potentials and the statistical theory of Hauser-Feshbach [7].

In the phenomenological description it is assumed that the whole interaction to which the neutron is subjected may be described by an optical-model potential $V(r,\theta,\varphi)$ which is complex and includes spin orbit coupling. Its radial dependence is of the Saxon-Woods form and its derivative [5]. $V(r,\theta,\varphi)$ is assumed to be, in general, non-spherical and is defined as [4]:

$$V(r,\theta,\varphi) = -(V+iW)\frac{1}{1+\exp[(r-R)/a]} - 4iW_D\frac{\exp[(r-\bar{R})/a]}{\{1+\exp[(r-\bar{R})/a]\}^2} - V_{SO}(d\cdot l)\,\lambda_\pi^2\frac{1}{ar}\frac{\exp[(r-R)/a]}{\{1+\exp[(r-R)/a]\}^2} + V_{Coul} \quad (1)$$

(λ_π = π-meson Compton wavelength)

(V_{Coul} = 0 for neutrons).

When R and $\bar{R}$ are assumed to be independent of angle, Eq. (1) becomes the usual optical model potential. R and $\bar{R}$ are made to

be dependent on ϑ and φ according to the collective nature of the target nucleus.

The rotational deformation is defined as

$$R = R_0 \left(1 + \sum_\lambda \beta_\lambda Y_{\lambda 0}(\theta')\right) \tag{2a}$$

and

$$\bar{R} = \bar{R}_0 \left(1 + \sum_\lambda \beta_\lambda Y_{\lambda 0}(\theta')\right) \tag{2b}$$

where β is the usual nuclear deformation parameter.

The compound nuclear processes were calculated using the statistical theory for the decay of the compound nucleus [6,8] with

$$\langle \sigma_{cc'} \rangle = \pi \lambda_c^2 \left[\frac{\langle \theta_{\lambda c} \rangle \langle \theta_{\lambda c'} \rangle}{\langle \theta_\lambda \rangle} W_{cc'} - \frac{\delta_{cc'}}{4} Q_c \langle \theta_{\lambda c} \rangle^2 \right]$$

where

$$\theta_\lambda = \sum_\alpha \langle \theta_{\lambda \alpha} \rangle \qquad \alpha \equiv \text{all open channels}$$

$$W_{cc'} = \left\langle \frac{\theta_{\lambda c} \theta_{\lambda c'}}{\theta_\lambda} \right\rangle \Big/ \frac{\langle \theta_{\lambda c} \rangle \langle \theta_{\lambda c'} \rangle}{\langle \theta_\lambda \rangle}$$

and

$$\langle \theta_{\lambda c} \rangle = T_c + \frac{1}{Q_c} \left[1 - \sqrt{1 - Q_c T_c}\right]^2$$

T_c is the optical model penetrability for channel c, and Q_c is the statistical parameter with range $0 \leq Q_c \leq 2$.

The neutron capture cross section was defined in terms of the emission of dipole radiation in the compound nucleus given by

$$\langle \theta_{\lambda \gamma} \rangle = 2\pi \left\langle \frac{\Gamma_\gamma}{D} \right\rangle_0 \rho(A,J,E)$$

where ρ is the density of levels at excitation energy E.

The fission cross section (used for ^{238}U only) [9] was interpreted in terms of the Hill-Wheeler [10] model with

$$\langle \theta_{\lambda f} \rangle^{J\pi} = \frac{N^{J\pi}}{2\pi}$$

where $N^{J\pi}$ is the effective number of fission channels and is dependent upon the penetrability factor P_i by

$$N^{J\pi} = \sum_i P_i$$

and

$$P_i = \frac{1}{1 + \exp\left[\frac{2\pi(E_{fi}^{J\pi} - E)}{\hbar\omega}\right]}$$

E_{fi} is the fission threshold, and $\hbar\omega$ the characteristic energy of the barrier curvature.

Combining the coupled-channel calculations with the statistical model produced the following interaction cross sections:

σ_T = total cross section
σ_{SE} = shape elastic cross section
σ_{CE} = compound elastic cross section
σ_{el} = $\sigma_{SE} + \sigma_{CE}$ total elastic
σ_R = reaction cross section
σ_C = compound formation cross section
$\sigma_{nn'}$,(comp.) = compound inelastic cross section
$\sigma_{nn'}$,(rot.) = direct inelastic cross section.

PROCEDURAL ANALYSIS

The Optical Model parameters used in both the coupled-channel and the spherical potential model are essentially the same as those used in Refs. [2] and [3], except that the interaction radius was varied so as to obtain better agreement with experiment. A spin orbit contribution was also included. These values, along with those employed in the statistical analyses of the compound nuclear processes, are given in Tables I-A and I-B.

The binding energies in Table I-B were taken from Ref. [11]. The average radiation widths and spacings are those recommended by Ref. [12] for ^{238}U, Refs. [13] and [14] for ^{239}Pu, Ref. [15] for ^{240}Pu, and Ref. [16] for ^{241}Pu. The parameter δ was determined from the neutron and pairing energies as determined by Cook, et al. [17]. The quantities E_{f1} and E_{f2} and $\hbar\omega$ were used in the calculation of the fission cross section for ^{238}U only [9].

TABLE I-A. OPTICAL-MODEL PARAMETERS

$V_0 = 46.53 - 0.29E$ (all energies in MeV)

$$W_D = \begin{cases} 4.27 + 0.756E + 24.4E^2 & 0 < E \leq 0.1 \\ 4.27 + 3.64E - 4.35E^2 & 0.1 < E \leq 0.5 \\ 4.27 + 1.89E - 0.86E^2 & 0.5 < E \leq 1.0 \\ 5.0 + 0.36E & 1.0 < E \leq 4.0 \\ 5.54 + 0.202E & 4.0 < E \leq 10.0 \\ 6.16 + 0.138E & 10.0 < E \leq 20.0 \end{cases}$$

$$R_0 = \begin{cases} 1.28\ f & \text{Coupling } (0^+, 2^+) & E < 1.0 \\ 1.2\ f & \text{Coupling } (0^+, 2^+, 4^+) & 1.0 \leq E \leq 2.0 \\ 1.28\ f & \text{Coupling } (0^+, 2^+, 4^+) & 2.0 < E \leq 5.0 \\ 1.24\ f & \text{Coupling } (0^+, 2^+, 4^+) & E > 5.0 \end{cases} \quad \left.\begin{matrix} \\ \\ \\ \\ \end{matrix}\right\} \text{U-238, Pu-240}$$

$$R_0 = \begin{cases} 1.28\ f \\ 1.24\ f \end{cases} \text{Coupling } (1/2^+, 3/2^+, 5/2^+) \begin{cases} 0 < E \leq 5.0 \\ 5.0 < E \leq 20.0 \end{cases} \text{Pu-239}$$

$$R_0 = \begin{cases} 1.28\ f \\ 1.24\ f \end{cases} \text{Coupling } (5/2^+, 7/2^+, 9/2^+) \begin{cases} 0 < E \leq 5.0 \\ 5.0 < E \leq 20.0 \end{cases} \text{Pu-241}$$

$a = 0.65$ f

$b = 0.47$ f

$V_{SO} = 7.0$ MeV

Deformation Parameters

$\beta = 0.24$ { U-238, Pu-240

$\beta = 0.26$ { Pu-239, Pu-241

TABLE I-B. STATISTICAL-MODEL PARAMETERS

Isotope	B_n (meV)	$\langle\Gamma_\gamma\rangle$ (meV)	$\langle D\rangle_o$ (eV)	δ	Q_c	E_{f1} (MeV)	E_{f2} (MeV)	$\hbar\omega$ (MeV)
U-238	4.803	23.0	20.8	0.0599	$\begin{cases} 1 & E \leq 1.0 \\ 0 & E > 1.0 \end{cases}$	6.04	6.85	0.57
Pu-239	6.524	40.0	9.5	0.0556	$\begin{cases} 1 & E \leq 1.0 \\ 0 & E > 1.0 \end{cases}$	----	----	----
Pu-240	5.243	23.2	14.7	0.0545	$\begin{cases} 1 & E \leq 1.0 \\ 0 & E > 1.0 \end{cases}$	----	----	----
Pu-241	6.305	40.0	2.5	0.0544	$\begin{cases} 1 & E \leq 1.0 \\ 0 & E > 1.0 \end{cases}$	----	----	----

TABLE II. ENERGY LEVEL SCHEME

Level	U-238		Pu-239		Pu-240		Pu-241	
	I^π	Excitation (MeV)	I^π	Excitation (MeV)	I^π	Excitation (MeV)	I^π	Excitation (MeV)
0	0^+	0.0000	$1/2^+$	0.0000	0^+	0.0000	$5/2^+$	0.0000
1	2^+	0.0450	$3/2^+$	0.0080	2^+	0.0430	$7/2^+$	0.0400
2	4^+	0.1480	$5/2^+$	0.0570	4^+	0.1420	$9/2^+$	0.0950
3	6^+	0.3080	$7/2^+$	0.0760	6^+	0.2960	$1/2^+$	0.1630
4	1^-	0.6540	$9/2^+$	0.1640	1^-	0.5990	$3/2^+$	0.1690
5	3^-	0.7100	$11/2^+$	0.1930	0^+	0.8630	$7/2^+$	0.1740
6	5^-	0.7280	$5/2^+$	0.2860	2^+	0.9030	$9/2^+$	0.2310
7	0^+	0.9350	$7/2^+$	0.3300	2^+	0.9450	$7/2^+$	0.2450
8	2^+	0.9860	$9/2^+$	0.3880	3^+	1.0200	$11/2^+$	0.3000
9	2^+	1.0300	$7/2^-$	0.3920	4^+	1.4200	$9/2^+$	0.3350
10	3^+	1.1100	$5/2^+$	0.4320	3^+	1.5300	$5/2^+$	0.4480
11	4^+	1.1130	$9/2^-$	0.4340	2^+	1.6200	$1/2^+$	0.7530
12	4^+	1.1700	$11/2^+$	0.4630			$1/2^-$	0.8280
13			$1/2^-$	0.4700			$3/2^+$	0.8940
14			$7/2^+$	0.4800			$5/2^+$	0.9180
15			$11/2^-$	0.4860			$7/2^+$	0.9410
16			$3/2^-$	0.4920				
17			$5/2^-$	0.5050				
18			$7/2^+$	0.5120				
19			$7/2^-$	0.5560				
20			$3/2^+$	0.7350				
21			$5/2^+$	0.7590				
22			$7/2^+$	0.8000				
23			$9/2^+$	0.8490				

TABLE III. COUPLED-CHANNEL CALCULATIONS AT 10 keV

Isotope	$S_0 \times 10^4$	$S_1 \times 10^4$	σ_{pot} (b)	σ_T (b)
U-238	1.03	1.93	9.70	14.66
Pu-239	1.17	1.68	9.60	15.10
Pu-240	1.03	1.98	9.50	14.50
Pu-241	1.31	2.30	9.32	15.94

The energy levels involved in the calculations of the inelastic (direct and compound) are shown in Table II. For ^{238}U the level scheme is the same as that used by Moóre, et al. [18] to describe inelastic scattering in ^{238}U using a spherical potential. The levels of rotational excitation present at 0.520 MeV (8^+), 0.790 MeV (10^+), and 1.100 MeV (12^+) determined from Coulombic excitation [19] exhibited negligible cross sections and were ignored in this analysis.

TABLE IV. HIGH-ENERGY NEUTRON CROSS-SECTIONS FOR ^{238}U

Energy (MeV)	σ_{tot}	σ_{el}	σ_{non}	$\sigma_{n\gamma}$	σ_{nf}	Comp. $\sigma_{nn'}$	σ_{rot}	Total $\sigma_{nn'}$	$\sigma_{n,2n}$	$\sigma_{n,3n}$	$\bar{\mu}$	$\xi \times 10^3$
0.0010	23.8700	21.1400	2.7300	2.7300	0.0000	0.0000	0.0000	0.0000	0.0000	0.0000	0.0028	8.3800
0.0050	16.4100	15.3800	1.0300	1.0300							0.0028	8.3800
0.0100	14.7000	13.9390	0.7610	0.7610							0.0170	8.2620
0.0300	13.8000	13.3210	0.4790	0.4790							0.0446	8.0300
0.0500	13.2000	12.7900	0.4010	0.3560		0.0450		0.0450			0.0709	7.8080
0.0600	12.9000	12.5000	0.4000	0.3100		0.0900		0.0900			0.0839	7.7000
0.0800	12.4000	11.9500	0.4500	0.2170		0.2330		0.2330			0.1090	7.4900
0.1000	12.0000	11.4860	0.5140	0.2000		0.3140		0.3140			0.1327	7.2900
0.2000	10.5100	9.4999	1.0101	0.1600		0.8501		0.8501			0.2350	6.4300
0.3000	9.6500	8.2418	1.4082	0.1350		1.2732		1.2732			0.3130	5.7700
0.5000	8.5400	6.3817	2.1583	0.1290	0.0006	1.9487	0.0800	2.0287			0.4230	4.8500
0.8000	7.5200	4.9886	2.5314	0.1520	0.0050	2.1564	0.2180	2.3744			0.5340	3.9100
1.0000	7.2000	4.2440	2.9559	0.1480	0.0156	2.5033	0.2890	2.7923			0.6300	3.1000
1.1000	7.0900	4.0379	3.0521	0.1350	0.0220	2.5771	0.3180	2.8951			0.6430	2.9970
1.2000	7.0300	3.9980	3.0320	0.1300	0.0375	2.5175	0.3470	2.8645			0.6550	2.8980
1.3000	7.0000	3.8660	3.1340	0.1130	0.0537	2.5933	0.3740	2.9673			0.6660	2.8100
1.4000	7.0000	3.7680	3.2320	0.1000	0.1410	2.5930	0.3980	2.9910			0.6760	2.7200
1.5000	7.0100	3.7400	3.2700	0.0870	0.2710	2.4880	0.4240	2.9120			0.6860	2.6400
1.6000	7.0300	3.7120	3.3180	0.0800	0.3610	2.4290	0.4480	2.8770			0.6950	2.5600
1.7000	7.0700	3.7180	3.3520	0.0600	0.4140	2.4100	0.4680	2.8780			0.7047	2.4800
1.8000	7.1100	3.7260	3.3840	0.0600	0.4620	2.3750	0.4870	2.8620			0.7140	2.4000
2.0000	7.2200	3.7540	3.4660	0.0515	0.5280	2.3615	0.5250	2.8865			0.7320	2.2500
2.5000	7.5200	3.6700	3.8500	0.0210	0.5300	2.7270	0.5720	3.2990			0.7710	1.9300
3.0000	7.7900	3.7900	4.0000	0.0250	0.5010	2.9050	0.5690	3.4740			0.7185	2.3700
4.1000	7.7700	3.9600	3.8100	0.0140	0.5220	2.7438	0.5302	3.2740			0.7780	1.8600
5.0000	7.7200	4.0000	3.7200	0.0100	0.5080	2.6857	0.5163	3.2020			0.8060	1.6300
7.0000	6.7300	3.2800	3.4500	7.5 (-3)	0.8900	1.7390	0.4630	2.2020	0.3500		0.8060	1.6300
8.0000	6.3600	3.0000	3.3600	6.4 (-3)	0.9660	0.8104	0.4376	1.2480	1.1400		0.8010	1.6700
10.0000	5.8800	2.6500	3.2300	4.7 (-3)	0.9360	0.3689	0.3901	0.7590	1.5300		0.7810	1.8400
14.1000	5.8500	2.8200	3.0300	3.3 (-3)	1.0900	0.1936	0.3234	0.5170	0.8400	0.5800	0.8495	1.2600
15.0000	5.9200	2.9400	2.9800	3.1 (-3)	1.2460	0.2025	0.3085	0.5110	0.5600	0.6600	0.8640	1.1400

TABLE V. HIGH-ENERGY NEUTRON CROSS-SECTIONS FOR ^{239}Pu

Energy (MeV)	σ_{tot}	σ_{el}	σ_{non}	$\sigma_{n\gamma}$	σ_{nf}	Comp. $\sigma_{nn'}$	σ_{rot}	Total $\sigma_{nn'}$	$\sigma_{n,2n}$	$\sigma_{n,3n}$	$\bar{\mu}$	$\xi \times 10^3$
0.0010	24.0000	16.7700	7.2300	3.9000	3.3300	0.0000	0.0000	0.0000	0.0000	0.0000	0.0028	8.4152
0.0050	16.7000	12.1000	4.6000	1.9000	2.7000	0.0000	0.0000	0.0000			0.0028	8.4152
0.0100	15.1000	11.7350	3.3650	1.1800	2.1650	0.0200	0.0000	0.0200			0.0028	8.4152
0.0300	13.6400	11.1024	2.5376	0.5096	1.6480	0.3780	0.0020	0.3800			0.0600	8.0400
0.0500	13.0400	10.7301	2.3099	0.3249	1.5580	0.4210	0.0060	0.4270			0.0882	7.6943
0.0600	12.7800	10.5174	2.2626	0.2841	1.5350	0.4350	0.0085	0.4435			0.1050	7.5500
0.0800	12.3395	10.0411	2.2984	0.2409	1.4980	0.5015	0.0185	0.5200			0.1320	7.2700
0.1000	11.8900	9.5916	2.2984	0.2249	1.4970	0.5450	0.0315	0.5765			0.1623	7.0700
0.2000	10.5301	8.0428	2.4873	0.1973	1.5030	0.6870	0.1000	0.7870			0.2750	6.1500
0.3000	9.7200	7.0680	2.6520	0.1608	1.5030	0.8252	0.1630	0.9882			0.3500	5.5200
0.5000	8.6550	5.6007	3.0543	0.0842	1.5290	1.1581	0.2830	1.4411			0.4506	4.6373
0.8000	7.6561	4.1254	3.5307	0.0338	1.7170	1.3319	0.4480	1.7799			0.5600	3.7500
1.0000	7.2520	3.4900	3.7620	0.0255	1.7000	1.5065	0.5300	2.0365			0.6046	3.3420
1.2000	7.0700	3.0640	4.0060	0.0192	1.7550	1.6358	0.5960	2.2318			0.6300	3.0000
1.5000	7.0580	2.7900	4.2680	0.0138	1.8650	1.7231	0.6661	2.3892			0.7002	2.5435
1.8000	7.1680	2.8030	4.3650	0.0104	2.0000	1.6426	0.7120	2.3546			0.7500	2.1500
2.0000	7.2970	2.9070	4.3900	0.0089	2.0040	1.6429	0.7342	2.3771			0.7740	1.9318
2.5000	7.6420	3.3160	4.3260	0.0064	1.8560	1.7066	0.7570	2.4636			0.8155	1.5911
3.0000	7.9130	3.6990	4.2140	0.0048	1.8310	1.6208	0.7574	2.3782			0.8517	1.3013
4.0000	7.9899	4.0020	3.9879	0.0030	1.7570	1.5274	0.7005	2.2279			0.8824	1.0660
5.0000	7.7320	3.9200	3.8120	0.0022	1.6540	1.4837	0.6721	2.1558			0.9002	0.9374
7.0000	6.7420	3.1890	3.5530	0.0013	2.0630	0.8180	0.5887	1.4067	0.0820		0.9166	0.8701
8.0000	6.3970	2.9470	3.4500	0.0011	2.2140	0.5735	0.5354	1.1089	0.1260		0.9150	0.9000
10.0000	5.9520	2.6590	3.2930	0.0008	2.2270	0.4407	0.4685	0.9092	0.1560		0.9078	1.0829
14.1000	5.8780	2.8040	3.0740	0.0005	2.2710	0.2685	0.3790	0.6475	0.0970	0.0580	0.9200	1.1340
15.0000	5.9630	2.9350	3.0280	0.0004	2.3210	0.1963	0.3623	0.5586	0.0530	0.0950	0.9261	1.1337

TABLE VI. HIGH-ENERGY NEUTRON CROSS-SECTIONS FOR ^{240}Pu

Energy (MeV)	σ_{tot}	σ_{el}	σ_{non}	$\sigma_{n\gamma}$	σ_{nf}	Comp. $\sigma_{nn'}$	σ_{rot}	Total $\sigma_{nn'}$	$\sigma_{n,2n}$	$\sigma_{n,3n}$	$\bar{\mu}$	$\xi \times 10^3$
0.0010	25.3000	22.3922	2.9078	2.7478	0.1600	0.0000	0.0000	0.0000	0.0000	0.0000	0.0028	8.3802
0.0050	17.5100	16.0500	1.4600	1.3500	0.1100						0.0028	8.3802
0.0100	14.5500	13.6180	0.9320	0.8410	0.0910						0.0185	8.2484
0.0300	13.6745	13.0655	0.6090	0.5030	0.1060						0.0500	8.0250
0.0500	13.0630	12.4493	0.6137	0.3800	0.0883	0.1438	0.0016	0.1454			0.0750	7.7500
0.0600	12.7932	12.0109	0.7823	0.3430	0.0838	0.3498	0.0057	0.3555			0.0918	7.6325
0.0800	12.1781	11.2065	0.9716	0.2970	0.0773	0.5800	0.0173	0.5973			0.1194	7.4006
0.1000	11.9080	10.7918	1.1162	0.2650	0.0813	0.7388	0.0311	0.7699			0.1149	7.1860
0.2000	10.5138	9.1098	1.4040	0.1940	0.1043	1.0050	0.1007	1.1057			0.2443	6.3515
0.3000	9.6676	8.0847	1.5829	0.1720	0.1342	1.1191	0.1576	1.2767			0.3104	5.7959
0.5000	8.4120	6.4050	2.0070	0.1590	0.3700	1.2242	0.2538	1.4780			0.4011	5.0342
0.8000	7.5314	4.4964	3.0350	0.1280	1.1100	1.4110	0.3860	1.7970			0.5250	3.9500
1.0000	7.2237	3.7135	3.5102	0.1080	1.4300	1.5260	0.4462	1.9722			0.5864	3.4821
1.2000	7.0980	3.3080	3.7900	0.0910	1.5030	1.7100	0.4860	2.1960			0.6250	3.3000
1.5000	7.0767	3.4476	3.6291	0.0730	1.4300	1.6001	0.5260	2.1261			0.6535	2.9241
1.8000	7.2402	3.5919	3.6483	0.0595	1.5070	1.5308	0.5510	2.0818			0.6700	2.7700
2.0000	7.3793	3.7240	3.6553	0.0525	1.5860	1.4568	0.5600	2.0168			0.6767	2.7339
2.5000	7.5983	3.6925	3.9058	0.0392	1.6180	1.6758	0.5728	2.2486			0.7101	2.4660
3.0000	7.8533	3.8322	4.0211	0.0297	1.5630	1.8586	0.5698	2.4284			0.7380	2.2465
4.1000	7.9889	4.0054	3.9835	0.0184	1.5150	1.9179	0.5322	2.4501			0.7886	1.8428
5.0000	7.7115	3.9297	3.7818	0.0124	1.4460	1.8058	0.5176	2.3234			0.8166	1.6281
7.0000	6.7335	3.4057	3.3278	0.0076	1.7900	0.9123	0.4639	1.3762	0.1540		0.8279	1.5744
8.0000	6.3607	3.1075	3.2532	0.0063	1.8050	0.6211	0.4388	1.0599	0.3820		0.8450	1.4000
10.0000	5.9634	2.6858	3.2776	0.0048	1.6400	0.6126	0.3932	1.0058	0.6270	0.0000	0.9078	1.0829
14.1000	5.8645	2.8315	3.0330	0.0032	2.0200	0.0600	0.3268	0.3868	0.3210	0.3020	0.9250	0.8000
15.0000	5.9263	3.0049	2.9214	0.0030	2.1300	0.0662	0.3116	0.3778	0.0760	0.4030	0.9261	0.7500

TABLE VII. HIGH-ENERGY NEUTRON CROSS-SECTIONS FOR ^{241}Pu

Energy (MeV)	σ_{tot}	σ_{el}	σ_{non}	$\sigma_{n\gamma}$	σ_{nf}	Comp. $\sigma_{nn'}$	σ_{rot}	Total $\sigma_{nn'}$	$\sigma_{n,2n}$	$\sigma_{n,3n}$	$\bar{u}$	$\xi \times 10^3$
0.0010	27.4870	10.2490	17.2380	5.3980	11.8400	0.0000	0.0000	0.0000	0.0000	0.0000	0.0028	8.2760
0.0050	18.1820	10.6300	7.5520	2.5520	5.0000						0.0028	8.2760
0.0100	16.5140	10.7540	5.7600	1.8200	3.9400						0.0028	8.2760
0.0300	14.4980	10.5300	3.9680	1.0180	2.9500						0.0067	7.8000
0.0500	13.8845	10.4000	3.4845	0.7530	2.6000	0.1307	0.0008	0.1315			0.1071	7.4100
0.0600	13.7477	10.3891	3.3586	0.6410	2.4800	0.2357	0.0019	0.2376			0.1252	7.2596
0.0800	13.2456	10.1056	3.1400	0.4850	2.3200	0.3300	0.0050	0.3350			0.1457	7.0890
0.1000	12.9380	9.8206	3.1174	0.4000	2.2200	0.4883	0.0091	0.4974			0.1877	6.7412
0.2000	11.6057	8.4684	3.1373	0.1850	1.8800	1.0161	0.0562	1.0723			0.3093	5.7320
0.3000	10.6977	7.2500	3.4477	0.1307	1.6800	1.5300	0.1070	1.6370			0.4048	4.9400
0.5000	9.6445	5.8345	3.8100	0.1030	1.5000	2.0100	0.1970	2.2070			0.5196	3.9864
0.8000	8.5572	5.0000	3.5572	0.1000	1.5000	1.6912	0.2660	1.9572			0.5952	3.3592
1.0000	8.0039	4.4819	3.5220	0.1050	1.5700	1.5320	0.3150	1.8370			0.6179	3.1711
1.2000	7.6630	4.1500	3.5130	0.1100	1.6300	1.4100	0.3630	1.7730			0.6500	2.9500
1.5000	7.3284	3.9879	3.3405	0.1090	1.6935	1.1100	0.4280	1.5380			0.6742	2.7040
1.8000	7.2600	3.9000	3.3600	0.0970	1.7400	1.0400	0.4830	1.5230			0.7000	2.5000
2.0000	7.3335	3.8528	3.4807	0.0900	1.7600	1.1170	0.5137	1.6307			0.7147	2.3679
2.5000	7.6016	3.9092	3.6924	0.0754	1.6550	1.4000	0.5620	1.9620			0.7404	2.1541
3.0000	7.7218	4.0321	3.6897	0.0560	1.5000	1.5557	0.5780	2.1337			0.7668	1.9351
4.1000	7.8187	4.2124	3.6063	0.0500	1.4500	1.5600	0.5463	2.1063			0.8243	1.4583
5.0000	7.5700	4.1762	3.3938	0.0420	1.4100	1.4411	0.5007	1.9418			0.8476	1.2635
7.0000	6.7730	3.3880	3.3850	0.0300	1.8500	0.5014	0.3956	0.8970	0.6080		0.8673	1.1016
8.0000	6.4138	3.1219	3.2919	0.0260	2.1100	0.0990	0.3739	0.4729	0.6830		0.8609	1.1542
10.0000	5.9450	2.8046	3.1404	0.0200	2.1000	0.0792	0.3312	0.4104	0.6100	0.0000	0.8471	1.2687
14.1000	5.7407	2.9393	2.8014	0.0140	2.3200	0.0080	0.2574	0.2654	0.0820	0.1200	0.8779	1.0134
15.0000	5.7533	3.0380	2.7153	0.0130	2.3400	0.0060	0.2403	0.2463	0.0310	0.0850	0.6882	0.9275

TABLE VIII. INELASTIC CROSS-SECTIONS FOR THE FIRST TWO EXCITED STATES IN ^{238}U

Energy (MeV)	Comp. (2^+) 0.0450	Rot. (2^+) 0.0450	Total (2^+) 0.0450	Comp. (4^+) 0.1480	Rot. (4^+) 0.1480	Total (4^+) 0.1480
0.0452	0.0000	0.0000	0.0000	0.0000	0.0000	0.0000
0.0500	0.0450		0.0450			
0.0600	0.0900		0.0900			
0.0700	0.1000		0.1000			
0.0800	0.2330		0.2330			
0.1000	0.3140		0.3140			
0.1486	0.4800		0.4800			
0.2000	0.8452		0.8452	0.0049		0.0049
0.3000	1.2388		1.2388	0.0344		0.0344
0.3093	1.2450		1.2450	0.0400		0.0400
0.4000	1.4700	0.0010	1.4800	0.1080		0.1080
0.5000	1.6000	0.0800	1.6800	0.2027		0.2027
0.6000	1.6320	0.1280	1.7600	0.3130		0.3130
0.6567	1.4900	0.1500	1.6400	0.3420		0.3420
0.7000	1.3478	0.1640	1.5110	0.3588	0.0120	0.3708
0.7130	1.3100	0.1660	1.4760	0.3610	0.0150	0.3760
0.7310	1.2500	0.1750	1.4250	0.3660	0.0180	0.3840
0.8000	1.0452	0.1900	1.2352	0.3702	0.0280	0.3982
0.9000	1.0243	0.2120	1.2363	0.4347	0.0420	0.4767
0.9390	0.9800	0.2200	1.2000	0.4300	0.0470	0.4770
0.9900	0.9200	0.2320	1.1520	0.3860	0.0520	0.4380
1.0000	0.9000	0.2340	1.1340	0.3854	0.0550	0.4404
1.0340	0.8600	0.2400	1.1000	0.3700	0.0570	0.4270
1.1000	0.7190	0.2540	0.9730	0.3220	0.0640	0.3860
1.1150	0.6900	0.2550	0.9450	0.3190	0.0650	0.3840
1.1180	0.6700	0.2560	0.9260	0.3100	0.0670	0.3770
1.1750	0.5200	0.2670	0.7870	0.2920	0.0700	0.3620
1.2000	0.4500	0.2740	0.7240	0.2833	0.0730	0.3563
1.3000	0.2900	0.2940	0.5840	0.2400	0.0800	0.3200
1.4000	0.0000	0.3100	0.3100	0.2030	0.0880	0.2910
1.5000		0.3300	0.3300	0.1660	0.0940	0.2600
1.6000		0.3480	0.3480	0.1300	0.1000	0.2300
1.7000		0.3650	0.3650	0.0960	0.1030	0.1990
1.8000		0.3800	0.3800	0.0640	0.1070	0.1710
1.9000		0.3960	0.3960	0.0320	0.1120	0.1440
2.0000		0.4100	0.4100	0.0000	0.1150	0.1150
2.2000		0.4280	0.4280		0.1210	0.1210
2.4000		0.4380	0.4380		0.1260	0.1260
2.5000		0.4420	0.4420		0.1300	0.1300
2.6000		0.4400	0.4400		0.1320	0.1320
2.8000		0.4360	0.4360		0.1350	0.1350
3.0000		0.4320	0.4320		0.1370	0.1370

The level scheme of ^{239}Pu was derived from Schmidt [13], Baranov, et al. [20], and Ref. [21]. For ^{240}Pu the level structure is that of Refs. [20,21], with spin assignments of the 1.42, 1.53, and 1.63 MeV levels being taken to be the same as that of ^{228}Th. An additional level at 1.02 MeV was also included [22,23] and given a spin assignment of 3^+. Data for the level structure and spin assignments for ^{241}Pu were determined from data in Refs. [20-24].

TABLE IX. INELASTIC CROSS-SECTIONS FOR THE FIRST TWO EXCITED STATES IN ^{239}Pu

Energy (MeV)	Comp. $(3/2^+)$ 0.0080	Rot. $(3/2^+)$ 0.0080	Total $(3/2^+)$ 0.0080	Comp. $(5/2^+)$ 0.0570	Rot. $(5/2^+)$ 0.0570	Total $(5/2^+)$ 0.0570
0.0080	0.0000	0.0000	0.0000	0.0000	0.0000	0.0000
0.0090	0.0120	0.0000	0.0120			
0.0120	0.0380	0.0001	0.0381			
0.0140	0.0600	0.0002	0.0602			
0.0160	0.0900	0.0003	0.0903			
0.0180	0.1250	0.0004	0.1254			
0.0200	0.1650	0.0005	0.1655			
0.0250	0.3000	0.0012	0.3012			
0.0300	0.3780	0.0020	0.3800			
0.0500	0.4210	0.0060	0.4270			
0.0573	0.4275	0.0075	0.4350			
0.0764	0.4320	0.0120	0.4440	0.0580	0.0041	0.0621
0.0900	0.4220	0.0150	0.4370	0.0930	0.0090	0.1030
0.1000	0.4120	0.0180	0.4300	0.1130	0.0135	0.1265
0.1400	0.3965	0.0275	0.4240	0.1650	0.0310	0.1960
0.1600	0.3950	0.0325	0.4275	0.1840	0.0400	0.2240
0.1647	0.3945	0.0340	0.4285	0.1885	0.0425	0.0231
0.1800	0.3960	0.0375	0.4335	0.2010	0.0490	0.2500
0.1940	0.3970	0.0405	0.4370	0.2110	0.0550	0.2660
0.2000	0.3980	0.0420	0.4400	0.2160	0.0580	0.2740
0.2400	0.4060	0.0520	0.4580	0.2400	0.0740	0.3140
0.2600	0.4140	0.0570	0.4710	0.2500	0.0820	0.3320
0.2873	0.4220	0.0630	0.4850	0.2610	0.0930	0.3540
0.3000	0.4250	0.0650	0.4900	0.2660	0.0980	0.3640
0.3200	0.4285	0.0700	0.4985	0.2720	0.1060	0.3780
0.3314	0.4295	0.0730	0.5025	0.2755	0.1105	0.3860
0.3600	0.4305	0.0795	0.5100	0.2825	0.1215	0.4040
0.3897	0.4310	0.0860	0.5170	0.2880	0.1330	0.4210
0.3937	0.4310	0.0870	0.5180	0.2895	0.1345	0.4240
0.4200	0.4305	0.0930	0.5235	0.2940	0.1440	0.4380
0.4338	0.4300	0.0960	0.5260	0.2960	0.1495	0.4455
0.4369	0.4300	0.0970	0.5270	0.2965	0.1505	0.4470
0.4400	0.4295	0.0980	0.5275	0.2970	0.1520	0.4490
0.4630	0.4285	0.1030	0.5315	0.2990	0.1600	0.4590
0.4720	0.4280	0.1050	0.5330	0.2995	0.1630	0.4625
0.4800	0.4275	0.1065	0.5340	0.3000	0.1660	0.4660
0.4820	0.4270	0.1070	0.5340	0.3000	0.1665	0.4665
0.4880	0.4265	0.1082	0.5347	0.3000	0.1685	0.4685
0.5000	0.4260	0.1110	0.5370	0.3000	0.1720	0.4720
0.5070	0.4240	0.1120	0.5360	0.2995	0.1750	0.4745
0.5142	0.4220	0.1130	0.5360	0.2990	0.1770	0.4760
0.5400	0.4155	0.1190	0.5345	0.2960	0.1860	0.4820
0.5584	0.4095	0.1230	0.5325	0.2930	0.1910	0.4840
0.5800	0.4020	0.1280	0.5300	0.2860	0.1990	0.4850
0.6000	0.3935	0.1320	0.5255	0.2780	0.2060	0.4840
0.7000	0.3280	0.1540	0.4820	0.2230	0.2400	0.4630
0.7381	0.2985	0.1620	0.4605	0.2085	0.2540	0.4625
0.7630	0.2830	0.1670	0.4500	0.2005	0.2620	0.4625
0.7800	0.2735	0.1700	0.4435	0.1965	0.2670	0.4635
0.8040	0.2620	0.1740	0.4360	0.1915	0.2740	0.4655
0.8200	0.2550	0.1770	0.4320	0.1880	0.2790	0.4670
0.8530	0.2425	0.1820	0.4245	0.1835	0.2880	0.4715
0.8800	0.2335	0.1870	0.4205	0.1800	0.2950	0.4750
0.9000	0.2280	0.1900	0.4180	0.1780	0.3000	0.4780
0.9400	0.2170	0.1960	0.4130	0.1750	0.3120	0.4870
0.9800	0.2080	0.2020	0.4100	0.1730	0.3220	0.4950
1.0000	0.1990	0.2040	0.4030	0.1660	0.3270	0.4930
1.2000	0.1510	0.2280	0.3790	0.1430	0.3680	0.5110
1.5000	0.0990	0.2550	0.3540	0.1110	0.4110	0.5220
1.7000	0.0740	0.2670	0.3410	0.0900	0.4310	0.5210
2.0000	0.0360	0.2800	0.3160	0.0580	0.4540	0.5120
2.5000	0.0015	0.2865	0.2880	0.0140	0.4710	0.4850
3.0000	0.0000	0.2841	0.2841	0.0070	0.4730	0.4800

TABLE X. COMPOUND INELASTIC CROSS-SECTIONS ABOVE THE FIRST TWO EXCITED STATES IN ^{238}U

Energy (MeV)	(6^+) 0.3080	(1^-) 0.6540	(3^-) 0.7100	(5^-) 0.7280	(0^+) 0.9350	(2^+) 0.9860	(2^+) 1.0300	(3^+) 1.1100	(4^+) 1.1130	(4^+) 1.1700	$\sigma_{nn'}$ Continuum
0.3093	0.0000	0.0000	0.0000	0.0000	0.0000	0.0000	0.0000	0.0000	0.0000	0.0000	0.0000
0.4000	0.0001										
0.5000	0.0015										
0.6000	0.0037										
0.6567	0.0070										
0.7000	0.0094	0.3312									
0.7130	0.0100	0.3800									
0.7310	0.0110	0.4000	0.0600								
0.8000	0.0133	0.4924	0.2300	0.0053							
0.9000	0.0242	0.5329	0.3293	0.0117							
0.9390	0.0250	0.5700	0.3750	0.0130							
0.9900	0.0270	0.6190	0.4380	0.0150	0.0700						
1.0000	0.0279	0.6264	0.4390	0.0156	0.0850	0.0240					
1.0340	0.0290	0.6170	0.4200	0.0170	0.1040	0.1000					
1.1000	0.0310	0.5672	0.4072	0.0220	0.1350	0.2340	0.1397				
1.1150	0.0315	0.5660	0.4050	0.0230	0.1349	0.2400	0.1410				
1.1180	0.0320	0.5650	0.4030	0.0250	0.1347	0.2450	0.1460				
1.1750	0.0325	0.5200	0.4000	0.0280	0.1340	0.2750	0.2200	0.0770	0.0200		
1.2000	0.0330	0.5180	0.3872	0.0318	0.1307	0.2846	0.2467	0.0977	0.0330	0.0098	0.0117
1.3000	0.0362	0.4940	0.3759	0.0432	0.1308	0.3023	0.2845	0.1638	0.0724	0.0572	0.1030
1.4000	0.0405	0.4330	0.3380	0.0494	0.1241	0.2962	0.2861	0.1874	0.0900	0.0840	0.4613
1.5000	0.0450	0.3743	0.3000	0.0550	0.1160	0.2890	0.2800	0.1960	0.1050	0.0970	0.4647
1.6000	0.0500	0.3330	0.2800	0.0590	0.1104	0.2820	0.2750	0.2020	0.1120	0.1080	0.4876
1.7000	0.0550	0.3000	0.2550	0.0630	0.1040	0.2700	0.2680	0.2080	0.1140	0.1190	0.5580
1.8000	0.0570	0.2650	0.2350	0.0660	0.0960	0.2650	0.2600	0.2120	0.1150	0.1240	0.6160
1.9000	0.0590	0.2350	0.2150	0.0662	0.0830	0.2540	0.2540	0.2100	0.1150	0.1250	0.7018
2.0000	0.0590	0.2000	0.1950	0.0670	0.0770	0.2450	0.2450	0.2080	0.1130	0.1260	0.8265
2.2000	0.0570	0.1500	0.1650	0.0650	0.0540	0.2250	0.2300	0.2000	0.1080	0.1230	1.0830
2.4000	0.0500	0.0900	0.1350	0.0630	0.0310	0.2000	0.2100	0.1920	0.1020	0.1180	1.4340
2.5000	0.0480	0.0600	0.1200	0.0610	0.0200	0.1930	0.2030	0.1870	0.0980	0.1140	1.6230
2.6000	0.0430	0.0400	0.1050	0.0590	0.0080	0.1800	0.1950	0.1800	0.0940	0.1100	1.7760
2.8000	0.0420	0.0000	0.0750	0.0550	0.0000	0.1580	0.1780	0.1680	0.0850	0.1000	2.0240
3.0000	0.0370	0.0000	0.0450	0.0490	0.0000	0.1350	0.1580	0.1540	0.0750	0.0900	2.1620

TABLE XI-A. COMPOUND INELASTIC CROSS-SECTIONS ABOVE THE FIRST TWO EXCITED STATES IN ^{239}Pu

Energy (MeV)	$(7/2^+)$ 0.0760	$(9/2^+)$ 0.1640	$(11/2^+)$ 0.1930	$(5/2^+)$ 0.2860	$(7/2^+)$ 0.3300	$(9/2^+)$ 0.3880	$(7/2^-)$ 0.3920	$(5/2^+)$ 0.4320
0.0764	0.0000	0.0000	0.0000	0.0000	0.0000	0.0000	0.0000	0.0000
0.0900	0.0115							
0.1000	0.0200							
0.1400	0.0460							
0.1600	0.0560							
0.1647	0.0605							
0.1800	0.0645	0.0001						
0.1940	0.0697	0.0003						
0.2000	0.0725	0.0004	5.0(-5)					
0.2400	0.0845	0.0016	3.7(-4)					
0.2600	0.0895	0.0024	6.2(-4)					
0.2873	0.0965	0.0041	0.0011					
0.3000	0.0975	0.0044	0.0013	0.0310				
0.3200	0.1015	0.0056	0.0020	0.0630				
0.3314	0.1045	0.0064	0.0025	0.0760				
0.3600	0.1100	0.0083	0.0035	0.1010	0.0086			
0.3897	0.1155	0.0106	0.0045	0.1200	0.0190			
0.3937	0.1160	0.0109	0.0046	0.1221	0.0210	0.0001		
0.4200	0.1200	0.0131	0.0053	0.1341	0.0304	0.0010	0.0048	
0.4338	0.1215	0.0142	0.0056	0.1395	0.0346	0.0017	0.0084	
0.4369	0.1220	0.0145	0.0057	0.1405	0.0356	0.0018	0.0069	0.0025
0.4400	0.1225	0.0148	0.0058	0.1415	0.0364	0.0018	0.0091	0.0040
0.4630	0.1242	0.0169	0.0063	0.1478	0.0423	0.0030	0.0123	0.1750
0.4720	0.1245	0.0178	0.0063	0.1494	0.0445	0.0034	0.0134	0.0225
0.4800	0.1250	0.0185	0.0066	0.1502	0.0460	0.0038	0.0143	0.0270
0.4820	0.1251	0.0187	0.0067	0.1504	0.0465	0.0040	0.0145	0.0275
0.4880	0.1252	0.0194	0.0067	0.1511	0.0478	0.0043	0.0151	0.0320
0.5000	0.1255	0.0205	0.0069	0.1521	0.0500	0.0050	0.0153	0.0385
0.5070	0.1255	0.0210	0.0071	0.1523	0.0512	0.0054	0.0169	0.0425
0.5142	0.1255	0.0213	0.0072	0.1525	0.0522	0.0058	0.0175	0.0460
0.5400	0.1246	0.0227	0.0075	0.1523	0.0554	0.0072	0.0193	0.0590
0.5584	0.1232	0.0238	0.0078	0.1522	0.0570	0.0082	0.0205	0.0670
0.5800	0.1210	0.0245	0.0080	0.1521	0.0588	0.0096	0.0217	0.0760
0.6000	0.1182	0.0253	0.0082	0.1520	0.0600	0.0107	0.0228	0.0830
0.7000	0.1013	0.0294	0.0091	0.1513	0.0642	0.0164	0.0269	0.1070
0.7381	0.0988	0.0311	0.0095	0.1507	0.0648	0.0184	0.0283	0.1125
0.7630	0.0982	0.0324	0.0099	0.1499	0.0651	0.0196	0.0291	0.1152
0.7800	0.0984	0.0334	0.0102	0.1492	0.0653	0.0204	0.0296	0.1165
0.8040	0.0997	0.0353	0.0108	0.1486	0.0659	0.0215	0.0304	0.1180
0.8200	0.1004	0.0366	0.0112	0.1480	0.0663	0.0222	0.0308	0.1185
0.8530	0.1023	0.0392	0.0122	0.1468	0.0675	0.0239	0.0318	0.1195
0.8800	0.1042	0.0417	0.0132	0.1456	0.0690	0.0253	0.0324	0.1198
0.9000	0.1058	0.0432	0.0140	0.1448	0.0701	0.0264	0.0329	0.1199
0.9400	0.1090	0.0468	0.0157	0.1420	0.0730	0.0285	0.0339	0.1198
1.0000	0.1135	0.0520	0.0186	0.1375	0.0795	0.0317	0.0354	0.1190
1.2000	0.1211	0.0592	0.0243	0.1216	0.0888	0.0361	0.0381	0.1127
1.4000	0.1243	0.0621	0.0276	0.1007	0.0891	0.0383	0.0391	0.1034
1.5000	0.1246	0.0627	0.0284	0.0888	0.0882	0.0389	0.0390	0.0968
1.6000	0.1242	0.0626	0.0288	0.0758	0.0868	0.0392	0.0388	0.0903
1.8000	0.1211	0.0613	0.0290	0.0558	0.0837	0.0387	0.0373	0.0746
2.0000	0.1152	0.0587	0.0284	0.0397	0.0792	0.0370	0.0351	0.0578
2.2000	0.1068	0.0547	0.0267	0.0217	0.0738	0.0343	0.0318	0.0432
2.5000	0.0888	0.0466	0.0234	0.0128	0.0638	0.0290	0.0253	0.0251
3.0000	0.0500	0.0303	0.0158	0.0000	0.0428	0.0163	0.0158	0.0051
3.2000	0.0322	0.0233	0.0122		0.0328	0.0100	0.0122	0.0003
3.5000	0.0060	0.0123	0.0067		0.0168	0.0000	0.0067	0.0000
4.0000	0.0000	0.0000	0.0000	0.0000	0.0000	0.0000	0.0000	0.0000

TABLE XI-B. COMPOUND INELASTIC CROSS-SECTIONS ABOVE THE FIRST TWO EXCITED STATES IN ^{239}Pu

Energy (MeV)	$(9/2^-)$ 0.4340	$(11/2^+)$ 0.4630	$(1/2^-)$ 0.4700	$(7/2^+)$ 0.4800	$(11/2^-)$ 0.4860	$(3/2^-)$ 0.4920	$(5/2^-)$ 0.5050	$\sigma_{nn'}$ Continuum*
0.0764	0.0000	0.0000	0.0000	0.0000	0.0000	0.0000	0.0000	
0.0900								
0.1000								
0.1400								
0.1600								
0.1647								
0.1800								
0.1940								
0.2000								
0.2400								
0.2600								
0.2873								
0.3000								
0.3200								
0.3314								
0.3600								
0.3897								
0.3937								
0.4200								
0.4338								
0.4369								
0.4400	0.0002							
0.4630	0.0013							
0.4720	0.0017	8.0(-5)						
0.4800	0.0020	1.6(-4)	0.0032					
0.4820	0.0021	1.8(-4)	0.0041					
0.4880	0.0023	2.4(-4)	0.0067	0.0008				
0.5000	0.0027	3.6(-4)	0.0124	0.0028	1.0(-5)			
0.5070	0.0030	4.4(-4)	0.0163	0.0041	2.0(-5)	0.0141		
0.5142	0.0032	5.2(-4)	0.0206	0.0054	3.0(-5)	0.0198	0.0022	
0.5400	0.0040	8.3(-4)	0.0326	0.0098	6.0(-5)	0.0353	0.0097	
0.5584	0.0045	1.1(-3)	0.0393	0.0130	9.0(-5)	0.0431	0.0143	
0.5800	0.0050	1.4(-3)	0.0458	0.0168	1.4(-4)	0.0507	0.0197	
0.6000	0.0055	1.7(-3)	0.0507	0.0203	1.9(-4)	0.0563	0.0242	
0.7000	0.0074	3.4(-3)	0.0646	0.0362	5.2(-4)	0.0716	0.0399	
0.7381	0.0081	4.1(-3)	0.0657	0.0408	6.4(-4)	0.0738	0.0436	
0.7630	0.0085	4.5(-3)	0.0654	0.0436	7.3(-4)	0.0741	0.0456	
0.7800	0.0088	4.9(-3)	0.0651	0.0456	7.9(-4)	0.0754	0.0467	
0.8040	0.0092	5.2(-3)	0.0647	0.0476	8.8(-4)	0.0759	0.0482	
0.8200	0.0095	5.6(-3)	0.0642	0.0496	9.7(-4)	0.0762	0.0490	
0.8530	0.0101	6.4(-3)	0.0635	0.0527	0.0012	0.0766	0.0507	
0.8800	0.0106	7.0(-3)	0.0627	0.0552	0.0014	0.0768	0.0518	
0.9000	0.0109	7.4(-3)	0.0623	0.0570	0.0016	0.0769	0.0526	
0.9400	0.0117	8.4(-3)	0.0613	0.0602	0.0019	0.0768	0.0537	
1.0000	*For E ≥ 1.0 MeV these levels are included in the continuum							0.5533
1.2000								0.7399
1.4000								0.9032
1.5000								0.9458
1.6000								0.9581
1.8000								1.0020
2.0000								1.0980
2.2000								1.2182
2.5000								1.3758
3.0000								1.4401
3.2000								1.4446
3.5000								1.4757
4.0000								1.4979

TABLE XI-C. COMPOUND INELASTIC CROSS-SECTIONS ABOVE THE FIRST TWO EXCITED STATES IN ^{239}Pu

Energy (MeV)	$(7/2^+)$ 0.5120	$(7/2^-)$ 0.5560	$(3/2^+)$ 0.7350	$(5/2^+)$ 0.7590	$(7/2^+)$ 0.8000	$(9/2^+)$ 0.8490	$\sigma_{nn'}$ Continuum*
0.0764	0.0000	0.0000	0.0000	0.0000	0.0000	0.0000	
0.0900							
0.1000							
0.1400							
0.1600							
0.1647							
0.1800							
0.1940							
0.2000							
0.2400							
0.2600							
0.2873							
0.3000							
0.3200							
0.3314							
0.3600							
0.3897							
0.3937							
0.4200							
0.4338							
0.4369							
0.4400							
0.4630							
0.4720							
0.4800							
0.4820							
0.4880							
0.5000							
0.5070							
0.5142							
0.5400	0.0044						
0.5584	0.0075						
0.5800	0.0113	0.0019					
0.6000	0.0147	0.0036					
0.7000	0.0304	0.0114					
0.7381	0.0354	0.0142					
0.7630	0.0383	0.0159	0.0097				
0.7800	0.0402	0.0170	0.0162	0.0036			
0.8040	0.0427	0.0185	0.0256	0.0097			
0.8200	0.0444	0.0193	0.0316	0.0141	0.0022		
0.8530	0.0476	0.0210	0.0442	0.0240	0.0070		
0.8800	0.0502	0.0220	0.0537	0.0318	0.0108	0.0017	
0.9000	0.0520	0.0232	0.0603	0.0374	0.0136	0.0030	
0.9400	0.0557	0.0249	0.0721	0.0477	0.0193	0.0054	
1.0000	*For E ≥ 1.0 MeV these levels are included in the continuum						0.5533
1.2000							0.7399
1.4000							0.9032
1.5000							0.9458
1.6000							0.9581
1.8000							1.0020
2.0000							1.0980
2.2000							1.2182
2.5000							1.3758
3.0000							1.4401
3.2000							1.4446
3.5000							1.4757
4.0000							1.4979

CALCULATIONS

The calculated cross sections for ^{238}U, ^{239}Pu, ^{240}Pu, and ^{241}Pu are given in Tables III-XI. Although the fission cross sections were calculated for ^{238}U based on a two-barrier Hill-Wheeler formalism, they are not included, since the apparent structure evident in the experimental data [13,25] at energies $E < 1.3$ MeV were not duplicated. Instead, the recommended values suggested by Pitterle [12] which were based on data contained in Refs. [25-29] were used.

The capture cross sections were also calculated for ^{238}U using the parameters listed in Table III and differed very little from those in Table IV. However, in order to mitigate the heretofore systematic discrepancies in this reaction and also to be consistent with the suggested fission cross sections, the selected values derived from Refs. [30-33] by Pitterle were used.[1]

In a similar fashion, the fission and capture cross sections for ^{239}Pu contained in Table V were taken from Craven, et al. [34].

The fission cross sections for ^{240}Pu and ^{241}Pu (Tables VI and VII) are based on experimental data as analyzed by Davey [29].

The capture cross section for ^{240}Pu was calculated by the statistical method and then adjusted so as to be consistent with those based on resolved resonance parameters [35].

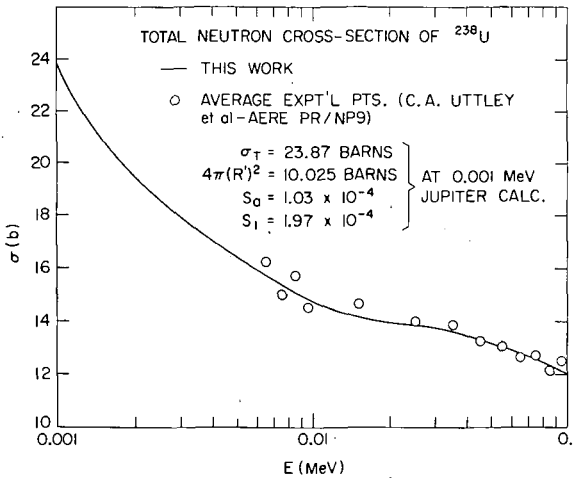

FIG. 1. Total neutron cross-section of ^{238}U ($0.001 \leq E \leq 0.1$ MeV).

[1] Values of $\sigma_{n\gamma}$ for $E < 50$ keV in Table IV are based on the statistical model calculations.

The capture data in Table VI for ^{240}Pu for E < 50 keV are model calculations, while all data on radiative capture for ^{241}Pu in Table VII are model calculations.

The inelastic cross sections for direct and compound reactions involving the first two excited states of each nuclide are given in Tables VIII - IX. Cross sections for the higher excited states and continuum are contained in Tables X-XI(A,B,C). These tables on the inelastic excitation cross sections have been constituted such that the threshold energy for each of the excited states is included and the density of points chosen so as to allow adequate interpolation.

The $\sigma_{n,2n}$ and $\sigma_{n,3n}$ cross sections were readjusted from those recommended in ENDF/B so as to be consistent with the threshold energies based on the more recent data on nuclidic masses contained in Ref. [11]. These threshold energies are given below:

^{238}U = $E_{thr}(n,2n)$ = 6.17 MeV
$E_{thr}(n,3n)$ = 11.32 MeV

^{239}Pu = $E_{thr}(n,2n)$ = 5.68 MeV
$E_{thr}(n,3n)$ = 12.71 MeV

^{240}Pu = $E_{thr}(n,2n)$ = 6.55 MeV
$E_{thr}(n,3n)$ = 12.23 MeV

^{241}Pu = $E_{thr}(n,2n)$ = 5.27 MeV
$E_{thr}(n,3n)$ = 11.80 MeV.

COMPARISON WITH EXPERIMENT

U-238

The total cross section for $0.001 \leq E \leq 0.1$ MeV is shown in Fig. 1 and is compared with the average experimental points given by Uttley [36]. As can be seen, the calculated values are in general agreement with the experimental data, and the s-wave strength function $S_0 = 1.03 \times 10^{-4}$ is in agreement with Uttley's also. The p-wave strength function of $S_1 = 1.97 \times 10^{-4}$ lies between that recommended by Uttley ($S_1 = 2.3 \times 10^{-4}$) and ENDF/B [37] ($S_1 = 1.58 \times 10^{-4}$).

Figure 2 shows the experimental total cross sections for $0.1 \leq E \leq 1.0$ MeV. These data include the most recent data of Smith [38]. The high density of points makes it impractical to draw a curve; however, a least-squares fit to these data compared favorably with Table IV.

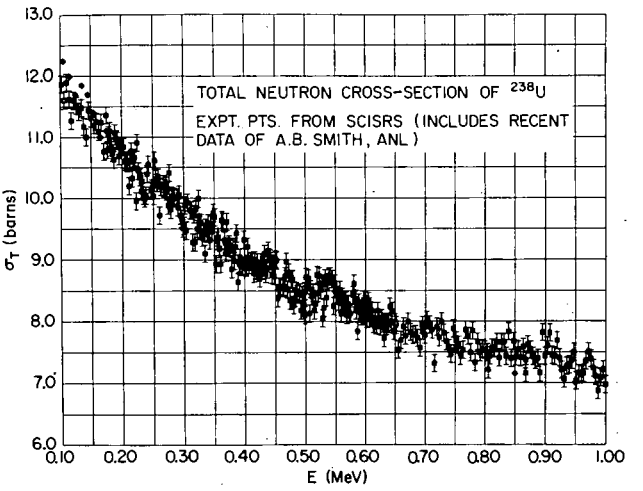

FIG.2. Total neutron cross-section of ^{238}U ($0.1 \leq E \leq 1.0$ MeV).

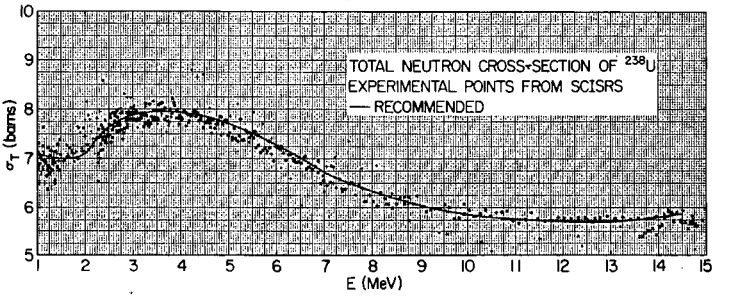

FIG.3. Total neutron cross-sections of ^{238}U ($1.0 \leq E \leq 15.0$ MeV).

Figure 3 contains experimental data points for $1.0 \leq E \leq 15.0$ MeV from the BNL SCISRS data file along with the calculated values of σ_T.

The calculated elastic scattering cross section $0.2 < E < 1.6$ MeV is compared with the empirical data in Fig. 4. The dashed line represents the sum of the shape and compound elastic contributions. However, since these experimental points may include the direct 0.045 (2^+) component, a second curve (solid line) is shown.

Figure 5 displays the scattering cross sections at higher energies, and since it is definite that this contains contamination not only from the first direct excitation but also from the second excited state [0.148 (4^+)], three calculated curves are presented (see Fig. 6).

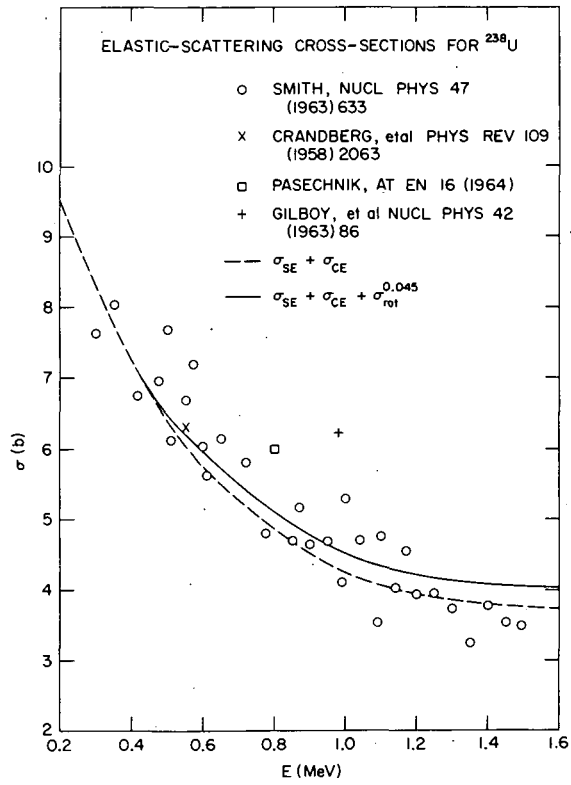

FIG. 4. Elastic scattering cross-sections for ^{238}U ($0.2 \leq E \leq 1.6$ MeV).

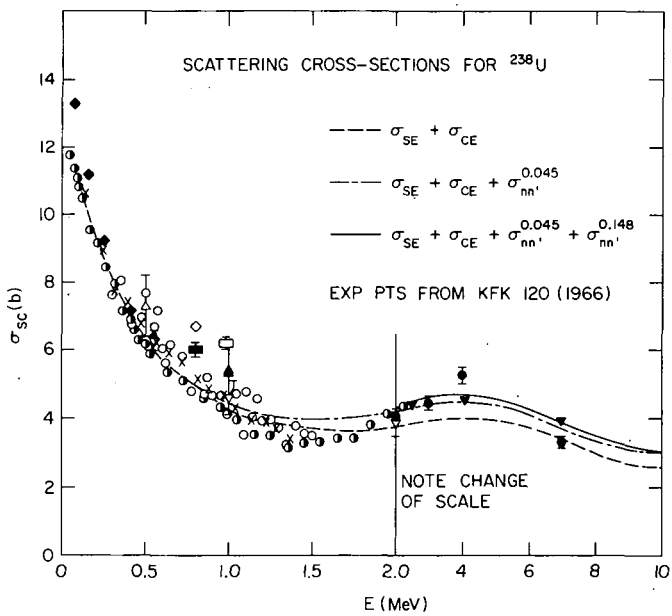

FIG. 5. Scattering cross-sections for ^{238}U ($0.1 \leq E \leq 10$ MeV).

The angular distribution at 7.0 MeV is given in Fig. 6. This curve definitely points out the necessity for including the direct excitation of the rotational levels.

One of the most elusive reactions that has defied coherent description has been the inelastic scattering cross section for ^{238}U. Therefore an attempt has been made hopefully to resolve some of this dilemma. In Figs. 7a and 7b the results of this analysis are presented in comparison with the two lowest-lying levels. Shown are the sums of the direct and compound inelastic contributions. As can be seen, while the compound component fits the data fairly well for energies $E \leq 0.7$ MeV, at higher energies consideration of the direct component permits a more favorable comparison. This is even more succinctly displayed in Fig. 8, where the total inelastic cross section given by $\sigma_{nn'}(\text{total}) = \sigma_{nn'}(\text{comp.}) + \sigma_{nn'}(\text{rot.})$. The separate components are also presented primarily to show their relative magnitudes. (The experimental and evaluated data points are from Ref. [13].)

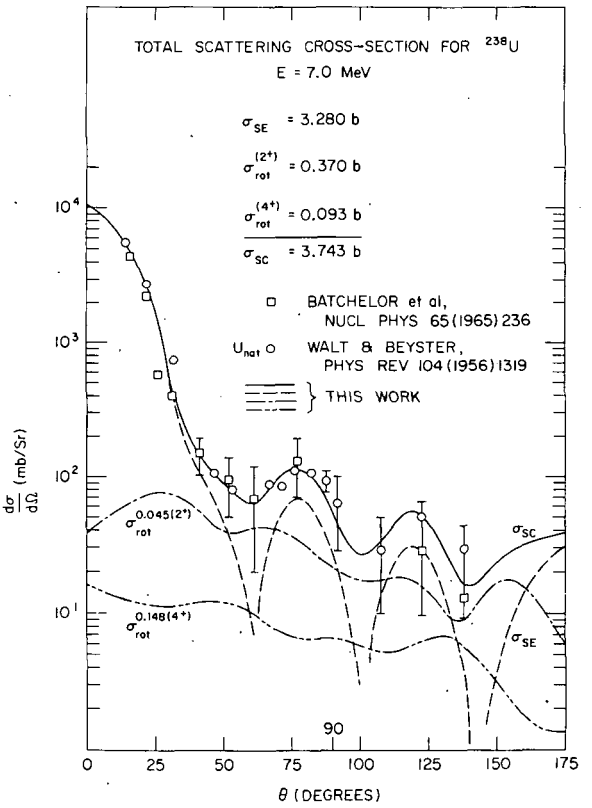

FIG. 6. Total differential scattering cross-section for ^{238}U (E = 7.0 MeV).

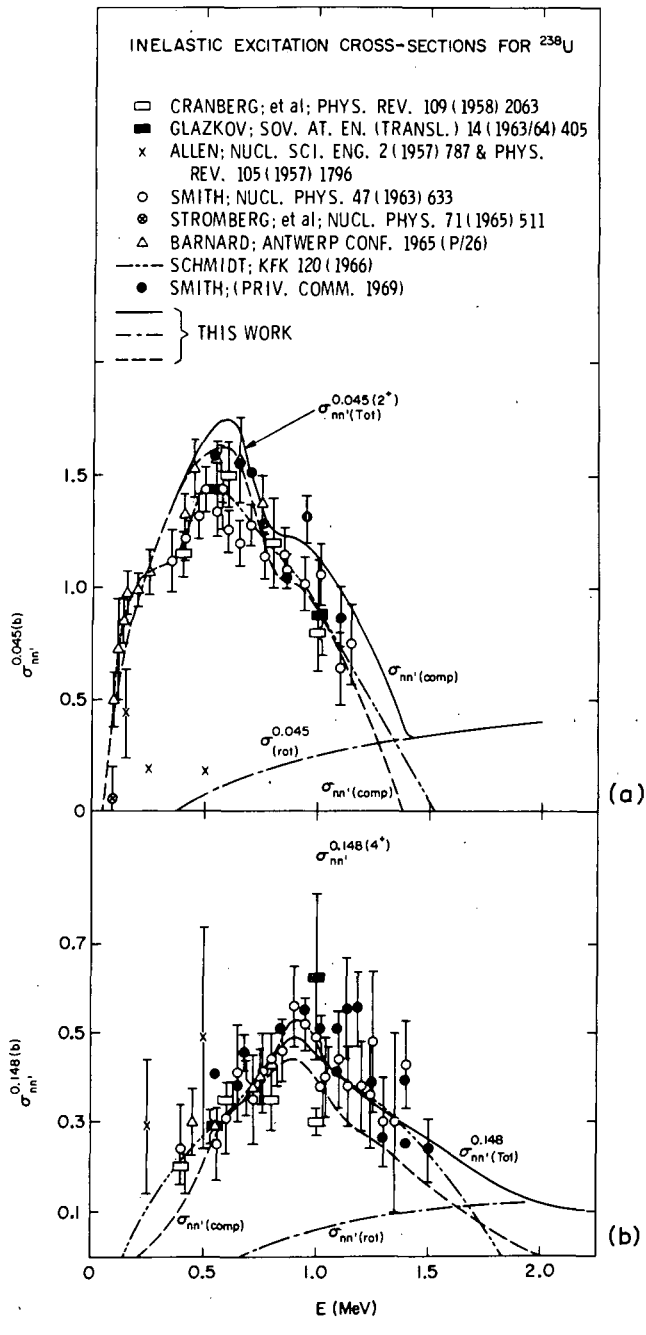

FIG. 7. a) Inelastic cross-sections for ^{238}U (0.045 level) (Threshold ≤ E ≤ 2.0 MeV);
b) Inelastic cross-sections for ^{238}U (0.148 level) (Threshold ≤ E ≤ 2.0 MeV).

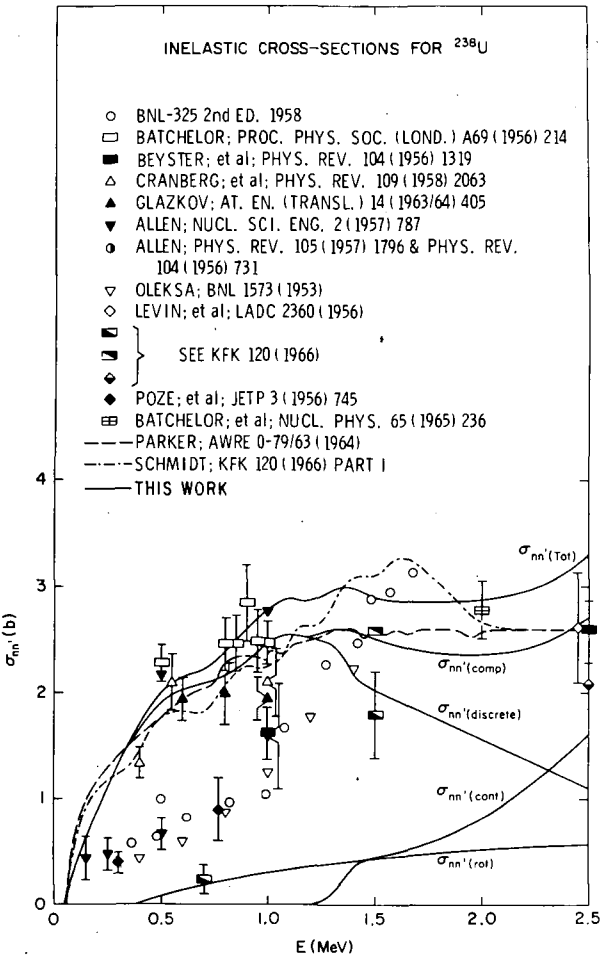

FIG.8. Inelastic cross-sections for ^{238}U (Threshold $\leq E \leq 2.5$ MeV).

Figure 9 shows the non-elastic cross sections from Table IV in the same energy range where $\sigma_{non} = \sigma_{n\gamma}+\sigma_{nf}+\sigma_{nn'(comp.)}+\sigma_{rot}$. ($\sigma_{n,2n} = \sigma_{n,3n} = 0$ in this range.)

The non-elastic cross section in Fig. 10 includes the $\sigma_{n,2n}$ and $\sigma_{n,3n}$; however, in most scattering experiments the direct reactions of the 2^+ and 4^+ levels are not resolved. Therefore, it was deemed more advisable to display σ_{non} with the σ_{rot} contributions subtracted out. This also permits consistency in analyzing the experimental data by $\sigma_{el}(expt'l) = \sigma_T - \sigma_{non}$.

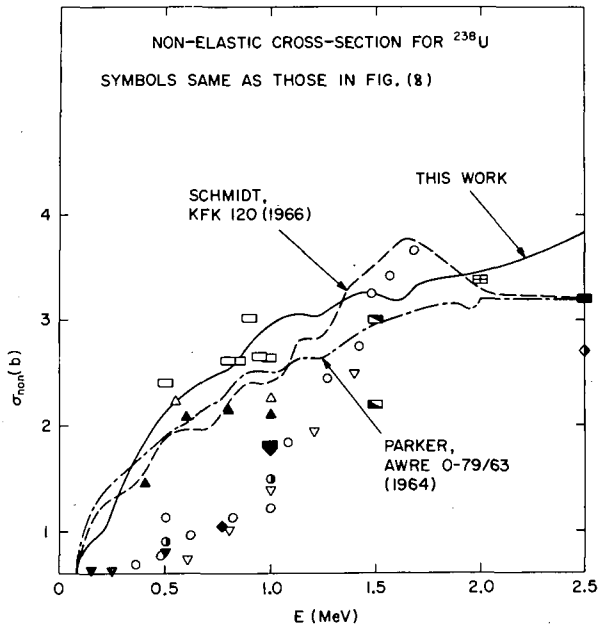

FIG. 9. Non-elastic cross-section for ^{238}U ($0.1 \leq E \leq 2.5$ MeV).

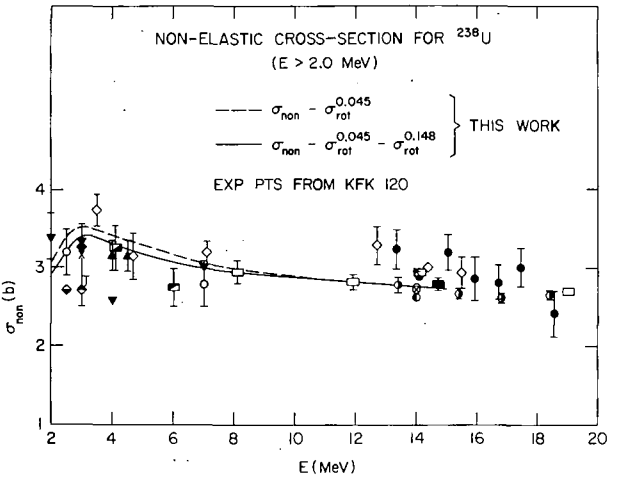

FIG. 10. Non-elastic cross-section for ^{238}U ($2.0 \leq E \leq 19.0$ MeV).

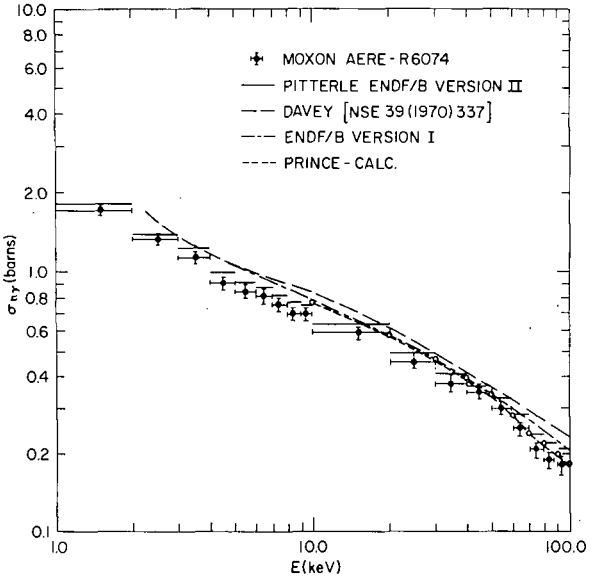

FIG. 11. Radiative capture cross-section of ^{238}U ($0.001 \leq E \leq 0.1$ MeV).

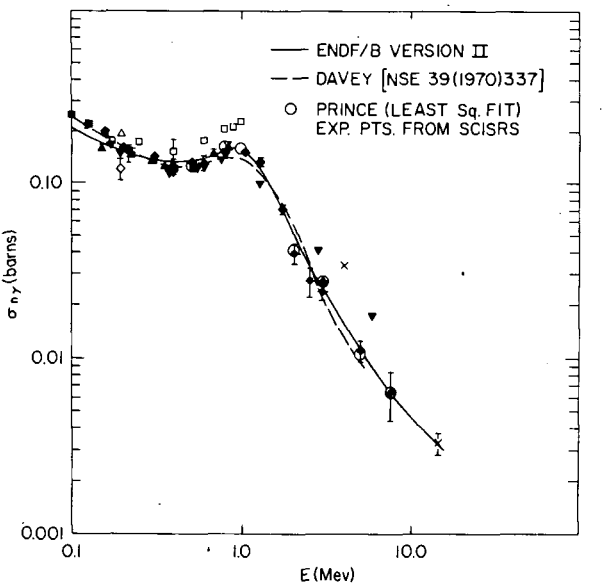

FIG. 12. Radiative capture cross-section of ^{238}U ($0.1 \leq E \leq 15$ MeV).

In Figs. 11 and 12 the capture cross section is shown based on several evaluations and calculations using the statistical model. As mentioned earlier, the calculated values were sacrificed so as to maintain consistency, and they are shown only for comparison.

Pu-239

The total cross section for ^{239}Pu in the energy range 0.001 MeV $\leq$ E $\leq$ 0.1 MeV is shown in Fig. 13 and is compared with the experimental data of Uttley [39]. Along with the calculated values of this work is the evaluation due to Barre, et al.[40]. In both cases the agreement with Uttley's experimental points is very good, deviating only slightly around 50 keV.

The s- and p-wave strength functions at 1 keV were calculated to be 1.19×10^{-4} and 1.71×10^{-4}, respectively, which may be compared with the values given below:

Energy Region	$S_0 \times 10^4$	$S_1 \times 10^4$	References
0-450 eV	1.33±0.14		Derrien, et al. [41]
0-205 eV	1.24±0.17		Ryabov, et al. [42]
100-200 eV	1.04		Uttley [43] a)
	1.15		Uttley [39] b)
200-300 eV	1.27		Uttley [43] a)
	1.54		Uttley [39] b)
1-130 keV	1.07	2.5±5	" "
0- 70 eV	1.0 ±0.3		Bollinger, et al. [44]
100 eV-10 keV	1.2 ±0.4		Hughes, et al. [45] b)

a) Based on resonance parameters.

b) Based on $\langle \sigma_T \rangle$.

As pointed out by Barre, et al. [40], the deviations in the experimentally determined s-wave strength functions are probably due to the local fluctuations in S_0; however, an error of 5% could cause an error as much as 10% in α. Therefore it is obvious that a more concise knowledge of this quantity is necessary.

Also shown in Fig. 13 is the calculated potential scattering cross section, whose value at 1 keV was σ_{pot} = 9.96 b ($R' = 8.9 \times 10^{-13}$ cm) which might be compared to Uttley's [39] value of σ_{pot} = 10.3±0.15 b ($R' = 9.054 \times 10^{-13}$ cm).

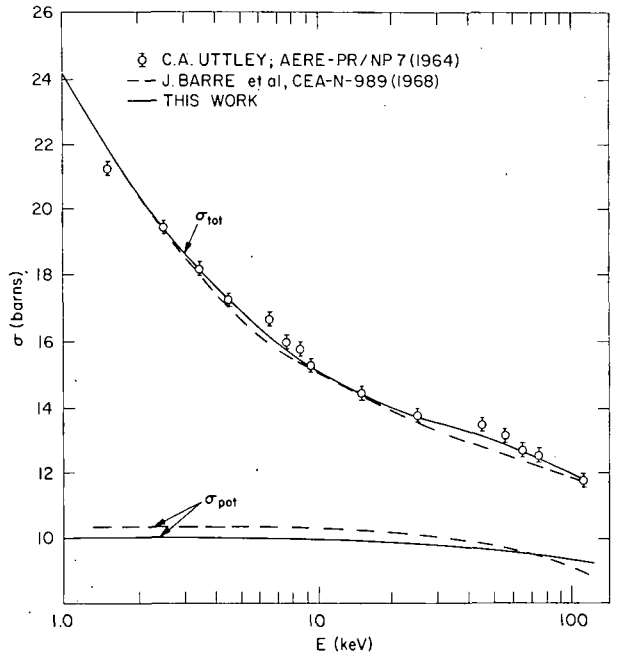

FIG. 13. Total and potential scattering cross-sections for ^{239}Pu ($0.001 \leq E \leq 0.1$ MeV).

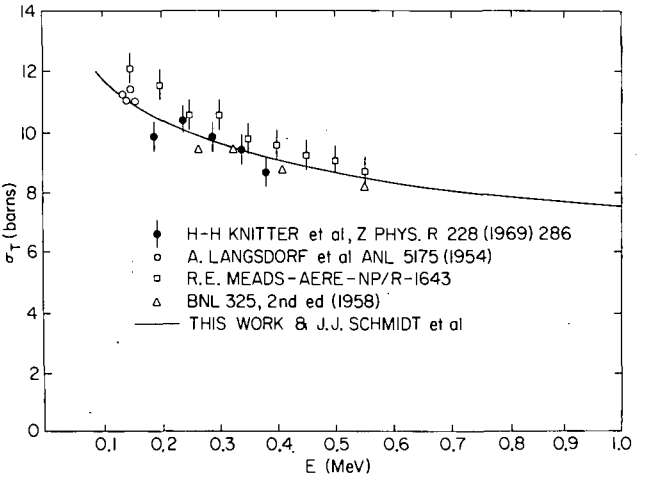

FIG. 14. Total cross-sections of ^{239}Pu ($0.1 \leq E \leq 1.0$ MeV).

Figure 14 shows the total cross section along with the recent empirical data of Knitter, et al. [46] in the range $0.1 \leq E \leq 1.0$ MeV. The calculated values and the evaluation of Schmidt [13] could not be distinguished from each other. Therefore, the full curve represents both.

The high-energy total cross sections are given in Fig. 15 compared with the experimental data from SCISRS. A least-squares fit of this experimental data and the recommended curve were concurrent.

Figure 16 points out rather succinctly the importance of the methods in which an experimenter's scattering data are interpreted. The dashed line represents "pure" elastic scattering

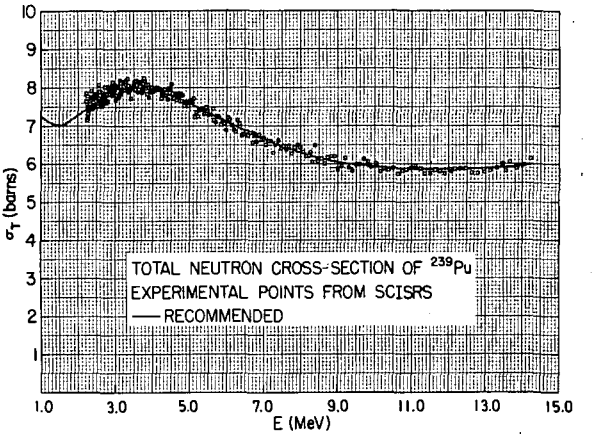

FIG.15. Total neutron cross-section of ^{239}Pu ($1.0 \leq E \leq 15.0$ MeV).

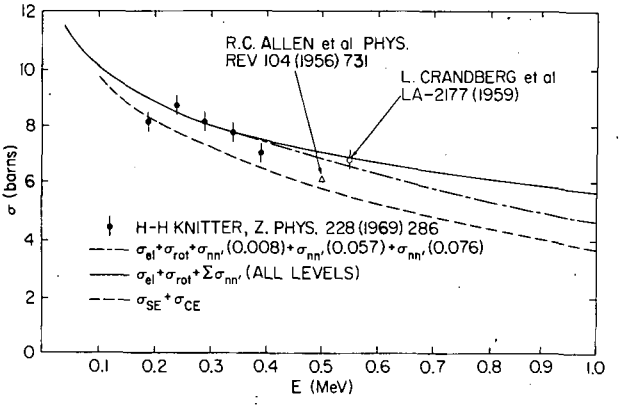

FIG.16. Scattering cross-sections of ^{239}Pu ($0.1 \leq E \leq 1.0$ MeV).

TABLE XII. COMPARISON OF CALCULATIONS AND REF. [45] FOR ^{239}Pu. E = 0.149 ± 0.005 MeV

θ in degrees	$d\sigma_{SE}/d\Omega$ (mb/sr)	$d\sigma_{CE}/d\Omega$ (mb/sr)	$d\sigma_{nn'}/d\Omega$ (mb/sr)	This Work $d\sigma_{Sc}/d\Omega$ [a] (mb/sr)	Ref. [45] $d\sigma/d\Omega$ (mb/sr)
0	1108	216	31.0	1355	----
20	1043	115		1189	1113±78
30	982	108		1121	984±58
40	909	101		1041	963±52
50	828	93		952	913±47
60	743	85		859	885±29
70	659	79		769	733±24
80	579	75		685	619±22
90	507	74		612	520±17
110	389	79		499	441±17
120	345	85		461	----
130	309	93		433	439±16
150	263	109		403	----
180	243	121		395	----

[a] $\frac{d\sigma_{nn',(rot.)}\ (0.008)}{d\Omega}$ < 3 mb over angular range and was not included.

($\sigma_{el} = \sigma_{SE} + \sigma_{CE}$). However, as pointed out by Knitter, the experimental points include the inelastic scattering cross sections to the levels with Q = -0.008 MeV, Q = -0.057 MeV, and Q = -0.076 MeV, which is shown as the dash-dot curve.

Another case in point is in the analysis of the scattering data on ^{239}Pu by Cavanagh, et al. [47]. These authors carried out measurements in which the 0.008-MeV level could not be resolved. Therefore, its contribution must be considered in an optical model analysis. Table XII will serve to illustrate this fact.

The 2.0-MeV scattering data of Batchelor, et al. [48] are presented in Fig. 17 and show that the contributions of the direct reactions for the first two excited levels were necessary to duplicate the experiment, since the compound elastic and inelastic cross sections were negligible at this energy. This is a clear demonstration of the importance of using a coupled-channel analysis to analyze deformed nuclei.

An adequate interpretation by means of model calculations of the experimental data on the inelastic cross sections in ^{239}Pu still remains in a state of quandary. Firstly, the amount of

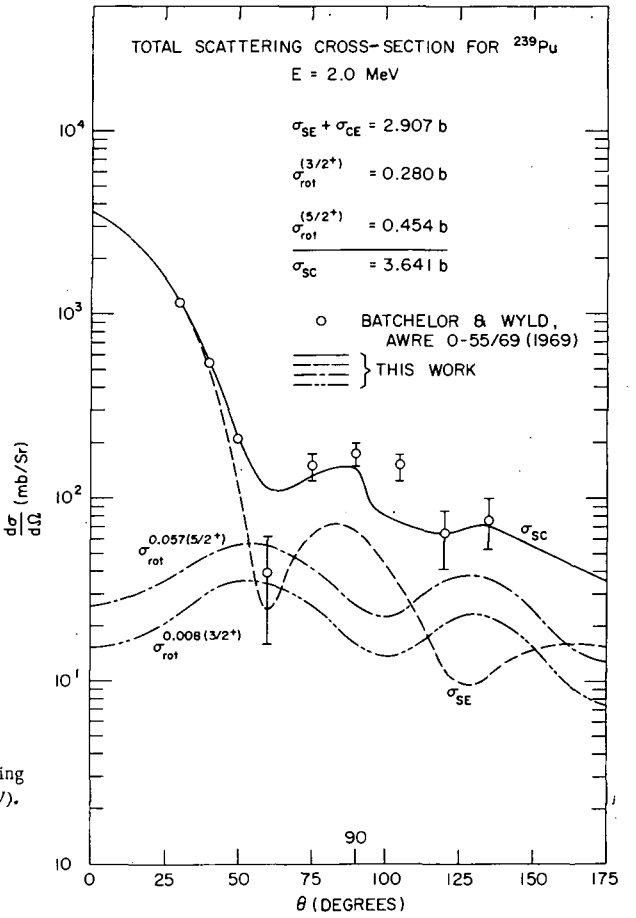

FIG. 17. Total differential scattering cross-section for ^{239}Pu (E = 2.0 MeV).

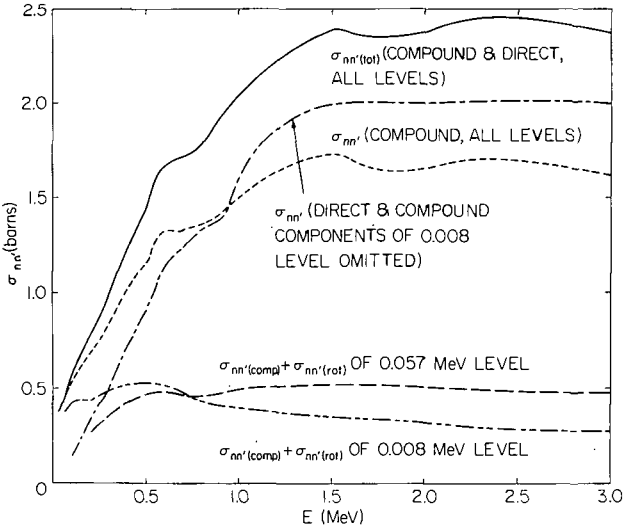

FIG. 18. Calculated inelastic cross-sections for ^{239}Pu (Threshold ≤ E ≤ 3.0 MeV).

TABLE XIII. INTERCOMPARISON OF EXPERIMENTAL AND THEORETICAL CROSS-SECTIONS OF THE INELASTIC NEUTRON SCATTERING BY ^{239}Pu

Primary Neutron Energy (MeV)	-Q (keV)	Inelastic Scattering Cross Sections for Pu-239 (barns)						
		Experimental				Theoretical		
		Cranberg Ref. [53]	Allen Ref. [54]	Cavanagh Ref. [47]	Batchelor Ref. [48]	Moldauer Ref. [50]	Bazazyants Ref. [49]	This Work
0.250	≥40	---	0.56±0.4	0.18±0.05	---	0.19	---	0.568
0.500	≥40	---	0.16±0.4	0.50±0.04	---	0.44	0.75	0.904
0.500	≥75	---	0.09±0.4	0.15±0.03	---	0.17	0.26	0.306
0.550	90→200	0.13±0.05	---	0.02±0.015	---	0.016	0.006 (500 keV)	0.030
0.550	200→300	0.10±0.05	---	0.09±0.015	---	0.096	0.18 (500 keV)	0.160
1.000	≥150	---	0.77±0.3	0.59±0.08	---	---	---	1.028
1.000	150→500	0.16±0.06	---	0.17±0.03	---	---	---	0.685
1.000	500→750	<0.06	---	0.19±0.04	---	---	---	0.206
2.000	≥75	---	---	---	1.47±0.49	---	---	1.55[a]
3.000	≥75	---	---	---	1.58±0.61	---	---	1.61
4.000	≥75	---	---	---	1.81±0.69	---	---	1.53

a) The direct inelastic components are assumed to be part of Batchelor's σ_{el} (see Fig. 17).

TABLE XIV. THEORETICAL INELASTIC CROSS-SECTIONS FOR ^{239}Pu. E = 0.5 MeV

Level No.	Energy (MeV)	Bazazyants Ref. [49]	Moldauer Ref. [50]	This Work
1	0.008	0.51	0.307	0.537[a]
2	0.057	0.36	0.191	0.300
3	0.076	0.13	0.08	0.126
4	0.164	0.004	0.016	0.020
5	0.193	0.0024	---	0.007
6	0.286	0.18	0.096	0.152
7	0.330	0.053	0.036	0.050
8	0.388	0.00048	---	0.005
9	0.392	0.014	0.023	0.015
10	0.434	0.005	---	0.039
		$\Sigma\sigma_{nn'} = 1.26$		$\Sigma\sigma_{nn'} = 1.25$

a) Includes $\sigma_{nn'}$ (rot.) (0.008).

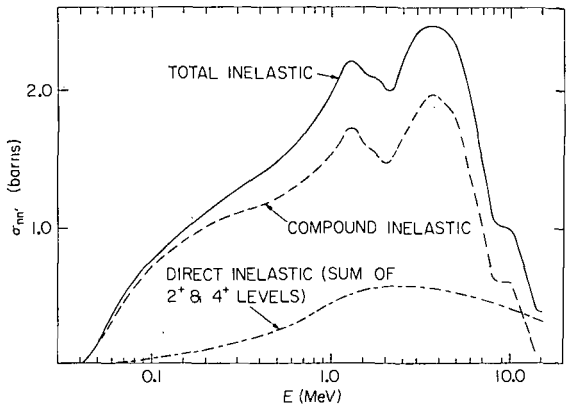

FIG. 19. Inelastic cross-sections of ^{240}Pu (Threshold ≤ E ≤ 15 MeV).

empirical data on inelastic scattering to discrete levels is still very scarce. Another factor which contributes to this dilemma is that the levels at energies of E ≈ 0.5 MeV are so dense that in most experiments only the sums of the various levels can be interpreted.

Figure 18 presents the calculations on this reaction for energies up to E = 3.0 MeV. Actually, the calculations were performed only up to 2.0 MeV for the compound processes and extrapolated to 3.0 MeV with proper cognizance of the competition of the last discrete level at 0.85 MeV and the competition that

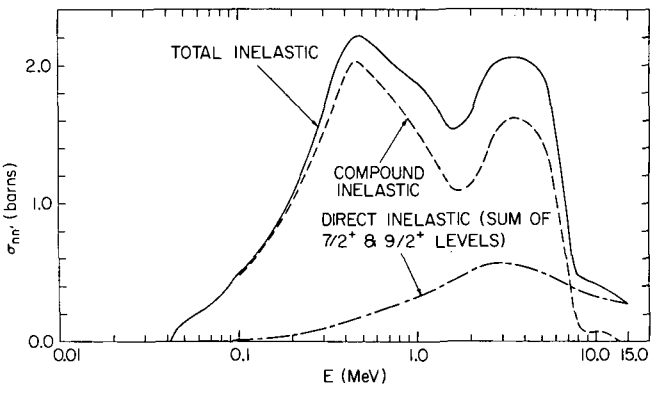

FIG. 20. Inelastic cross-sections of ^{241}Pu (Threshold ≤ E ≤ 15 MeV).

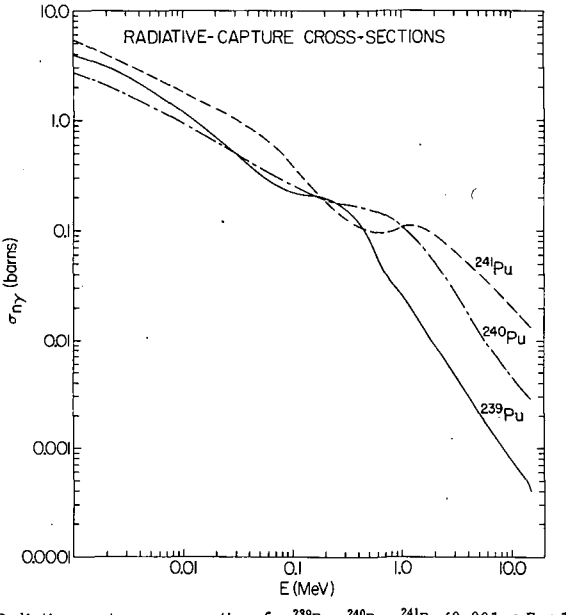

FIG. 21. Radiative capture cross-sections for ^{239}Pu, ^{240}Pu, ^{241}Pu (0.001 ≤ E ≤ 15.0 MeV).

ensues with levels entering at energies around 1.0 MeV. No data points were placed on Fig. 18 because of the diffidence in the interpretation of an experimenter's data. However, an attempt has been made to compare the analysis of this work with the quoted results of others as given in Tables XIII and XIV.

In Table XIII we see an intercomparison of experimental and theoretical analyses of the ^{239}Pu inelastic cross sections. While there are areas of general agreement, there are also areas of wide fluctuations which again serve to demonstrate the dilemma that presents itself in the interpretation of the inelastic data for this isotope.

Table XIV shows the comparison between some theoretical calculations. It is interesting to note that although Bazazyants [49] used a spherical potential (as did Moldauer [50]), his results are much closer to this work.

The capture cross section for ^{239}Pu was based on the most recent α measurements [34] and is shown in Fig. 21.

Pu-240 and Pu-241

The cross sections for these two isotopes were calculated in the same manner as those of ^{238}U and ^{239}Pu (i.e., the three low-lying levels were coupled so as to produce the direct inelastic excitations as well as the compound processes).

The strength functions of $S_0 = 1.03 \times 10^{-4}$ and $S_1 = 1.98 \times 10^{-4}$ for ^{240}Pu are consistent with those of Uttley [51] ($S_1 = 2.0 \times 10^{-4}$) but are somewhat lower than those recommended by Yiftah, et al. [22], who state that $S_0 = (1.37\pm0.51) \times 10^{-4}$ and $S_1 = 2.5 \times 10^{-4}$.

For ^{241}Pu the calculated strength functions $S_0 = 1.31 \times 10^{-4}$ and $S_1 = 2.30 \times 10^{-4}$ may be compared with that of Uttley [52], who quotes $S_0 = (1.3\pm0.3) \times 10^{-4}$ and a potential scattering cross section of $\sigma_{pot} = 8.0\pm4$ b, which certainly are within the calculated value of $\sigma_{pot} = 9.32$ b of this work. Yiftah, et al. [23] quote values of $S_0 = (1.3\pm0.75) \times 10^{-4}$ and $S_1 = 2.5 \times 10^{-4}$ for ^{241}Pu which compare very favorably with the calculated values.

Unlike ^{238}U and ^{239}Pu the amount of experimental data for ^{240}Pu and ^{241}Pu is practically nil, so no real comparison in the high energy region could be made. Figures 19 and 20 show the inelastic cross sections over the entire energy region from threshold to 15 MeV.

CONCLUSION

It is hoped that the theoretical treatment described herein for these deformed nuclides will clear up some of the discrepancies that have existed. This is especially true in the analyses of the elastic and inelastic scattering cross sections for ^{238}U and ^{239}Pu.

Previous evaluations have ignored the strong coupling of the 148-keV (4^+) state in ^{238}U, and the compound inelastic treatment always underestimates this reaction.

The possibility of coupling the 6^+ state in ^{238}U was considered, but as pointed out by Bühler [55], this changed the potential scattering cross section insignificantly and the integrated inelastic 6^+ contribution was nil.

It has been firmly established that in describing the experimental angular distribution scattering data, one should include the effects of the direct rotational components.

A satisfactory interpretation of the ^{239}Pu experimental inelastic data still remains somewhat of an enigma, and while there is agreement in many areas, much still remains to be done.

Ideally all the competing compound nuclear processes should be handled in a concurrent manner. However, until our knowledge of the fission reaction improves, one must rely on the experimental fission data. Some efforts are already underway in this area [56-60] and show great promise for improving our comprehension of this phenomenon.

REFERENCES

[1] CHASE, D.M., WILETS, L., Phys. Rev. 110 (1958) 1080.
[2] BALDONI, B., SARUIS, A.M., Nuovo Cim. 33 4 (1964) 1145.
[3] DUNFORD, C.L., Int. Conf. Nuclear Data for Reactors (Proc. Conf. Paris, 1966) I, IAEA, Vienna (1967) 429.
[4] TAMURA, T., Computer Program JUPITER I for Coupled Channel Calculations, ORNL Rep. ORNL 4152 (1967); see also TAMURA, T., Rev. Mod. Phys. 37 (1965) 679.
[5] AUERBACH, E.H., ABACUS-II, BNL Informal Rpt. BNL 6562 (1962, unpublished).
[6] MOLDAUER, P.A., et al., NEARREX, A Computer Code for Nuclear Reaction Calculations, ANL Rep. ANL 6978 (1964); see also MOLDAUER, P.A., Rev. Mod. Phys. 36 (1964) 1079.
[7] HAUSER, W., FESHBACH, H., Phys. Rev. 87 (1952) 366.
[8] MOLDAUER, P.A., Phys. Rev. 136B (1964) 947.
[9] DUNFORD, C.L., Atomics International (private communication).
[10] HILL, D.L., WHEELER, J.A., Phys. Rev. 89 (1953) 1102.
[11] WAPSTRA, A.H., et al., Third Int. Conf. Atomic Masses (Proc. Conf. Winnipeg, Canada, 1967), Univ. Manitoba (1967) 153.
[12] PITTERLE, T. (Westinghouse Electric Corp., private communication).
[13] SCHMIDT, J.J., KFK Rep. KFK-120, Pt. I (1966), EANDC-E-35"U".
[14] HUTCHINS, B.A., (General Electric Co., private communication).
[15] KOLAR, W., BÖCKHOFF, K.H., J. Nucl. Energy 22 (1968) 299.
[16] DOHERTY, G., UKAEA Rep. AEEW-M-714 (1967).
[17] COOK, J.L., et al., Austral. J. Phys. 20 (1967) 477.
[18] MOORE, S.O., AUERBACH, E.H. BNL Rep. BNL 818 (1963).
[19] STEPHENS, F.S., Jr., et al., Phys. Rev. Letters 3 (1959) 435.
[20] BARANOV, S.A., et al., Sov. J. Nucl. Phys. 4 (1967) 798.
[21] LEDERER, C.M., et al., Table of Isotopes, 6th Ed., Wiley, New York (1967).
[22] DOUGLAS, A.C., UKAEA Rep. AWRE O-101/64 (1965).
[23] YIFTAH, S., et al., Israel At. Energy Comm. Rep. IA-1152 (1967).
[24] BRAID, T.H., et al., Phys. Letters 18 (1965) 149.
[25] LAMPHERE, R.W., Phys. Rev. 104 (1956) 1654.

[26] STEIN, W.E., et al., Conf. Neutron Cross Sections and Technology (Proc. Conf. Washington, D.C., 1968) I, NBS Special Pub. 299 (1968) 627.
[27] WHITE, P.H., et al., J. Nucl. Energy 21 (1967) 671.
[28] SMITH, R.K., et al., Bull. Amer. Phys. Soc. 2 (1967) 196.
[29] DAVEY, W.G., Nucl. Sci. Engng. 32 (1968) 35.
[30] MOXON, M.C., UKAEA Rep. AERE-R-6074 (1969).
[31] POENITZ, W.P. (to be published).
[32] BARRY, J.F., et al., J. Nucl. Energy 18 (1964) 481.
[33] PERKIN, J.L., et al., Proc. Phys. Soc. London 72 (1958) 505.
[34] CRAVEN, C.L., Jr., et al., ORNL Rep. ORNL-TM-2797 (1970).
[35] MATHEWS, D.R. (Gulf General Atomic, private communication).
[36] UTTLEY, C.A., UKAEA Rep. AERE-PR/NP-9 (1965).
[37] WITTKOPF, W.A., et al., Babcock & Wilcox Rep. BAW-316 (1967), ENDF-103.
[38] SMITH, A.B. (Argonne Nat'l. Lab., private communication).
[39] UTTLEY, C.A., Rep. EANDC(UK)40"L" (1964).
[40] J.-Y. Barre, et al., CEA Rep. CEA-N-989 (1968), EANDC(EUR)-111.
[41] DERRIEN, H., Int. Conf. Nuclear Data for Reactors (Proc. Conf. Paris, 1966) II, IAEA, Vienna (1967) 195.
[42] RYABOV, Yu. V., Sov. J. Nucl. Phys. 5 (1967) 657.
[43] UTTLEY, C.A., Int. Conf. Study of Nuclear Structure with Neutrons (Individual Contributions to Conf., Antwerp, 1965), EANDC Rep. EANDC-50-S, Vol. I (1965), Paper 98.
[44] BOLLINGER, L.M., et al., Int. Conf. Peaceful Uses Atomic Energy (Proc. Conf. Geneva, 1958) 15, UN, New York (1958) 127.
[45] HUGHES, D.J., et al., Phys. Rev. Letters 1 (1958) 461.
[46] KNITTER, H.-H., COPPOLA, M., Z. Phys. 228 (1969) 294.
[47] CAVANAGH, P.E., et al., UKAEA Rep. AERE-R-5972 (1969).
[48] BATCHELOR, R.A., UKAEA Rep. AWRE O-55/69 (1969).
[49] BAZAZYANTS, N.O., Sov. J. At. Energy 13 (1963) 931.
[50] MOLDAUER, P.A., IAEA Seminar Physics of Fast and Intermediate Reactors (Proc. Seminar Vienna, 1961) I, IAEA, Vienna (1962) 171.
[51] UTTLEY, C.A., UKAEA Rep. AERE-PR/NP-7 (1964).
[52] UTTLEY, C.A., UKAEA Rep. AERE-PR/NP-6 (1963).
[53] CRANBERG, L., LASL Rep. LA-2177 (1959).
[54] ALLAN, R.C., Nucl. Sci. Engng. 2 (1957) 787.
[55] BÜHLER, F., Z. Naturforsch. 24a (1969) 52.
[56] BJORNHOLM, S., STRUTINSKY, V.M., Nucl. Phys. A136 (1969) 1.
[57] RABOTNOV, N.S., Sov. J. Nucl. Phys. 9 (1969) 451.
[58] GAI, E.V., et al., Sov. J. NUcl. Phys. 10 (1970) 311.
[59] ERMAGAMBETOV, S.B., et al., Sov. J. Nucl. Phys. 8 (1969) 409.
[60] Second Int. Symp. Physics and Chemistry of Fission (Proc. Conf. Vienna, 1969), IAEA, Vienna (1970).

DISCUSSION

A.I. ABRAMOV (Chairman): In your opinion, what is the degree of reliability of the values which you obtained for the strength functions in the case of s- and p-neutrons, and what are the probable errors in the values of S_0 and S_1 for ^{238}U?

A. PRINCE: It is rather difficult to give an estimate of the reliability, since there is such a wide divergence in the quoted experimental results based on resonances in the resolved region.

As I pointed out in my presentation, the model calculations produced values of $S_0 = 1.03 \times 10^{-4}$, which are in agreement with Uttley's value, and also with the value of $S_0 = (0.91 \pm 0.11) \times 10^{-4}$, which you yourself quoted in the presentation of paper CN-26/80. The calculated value of the p-wave strength function ($S_1 = 1.97 \times 10^{-4}$) lies between that recommended by Uttley ($S_1 = 2.3 \times 10^{-4}$) and ENDF/B ($S_1 = 1.58 \times 10^{-4}$), and is in excellent agreement with Abramov's value of $S_1 = (2.0 \pm 0.3) \times 10^{-4}$.

Of course, if no experimental data existed, then I would say that the calculated values are 100% accurate, but since empirical data do exist I feel that it would be rather risky to assign error bars to an evaluation.

STUDY OF THE ^{239}Pu ANGULAR DISTRIBUTIONS IN THE ENERGY RANGE 0.2 - 5.5 MeV

V. BENZI, L. ZUFFI
Comitato Nazionale Energia Nucleare, Centro di Calcolo, Bologna, Italy
M. COPPOLA, H.H. KNITTER
Central Bureau for Nuclear Measurements, EURATOM, Geel, Belgium

Abstract

STUDY OF THE ^{239}Pu ANGULAR DISTRIBUTIONS IN THE ENERGY RANGE 0.2 – 5.5 MeV.

The ^{239}Pu nucleus presents a structure in the low-lying nuclear levels which indicates a deformation of the collective type. The effects of such a deformation on the neutron-scattering angular distributions are studied by means of a non-spherical optical potential using the coupled-channel method, and the results of these calculations are compared with recently measured experimental values.

1. INTRODUCTION

The neutron scattering cross section analysis is generally performed according to the central optical model in order to obtain sets of potential parameters which can be used to fill the gaps in the experimental data. Several "recommended" sets are available to-day. Such sets were obtained on the basis of systematic analysis of a large amount of experimental data, such as angular distributions, polarization, total cross sections, etc. These recommended sets can be confidently used at least for a first approximation in particular analyses of neutron scattering, if the scattering nucleus is not very deformed.

On the other hand, if the nucleus is strongly deformed, the recommended sets generally provide theoretical results which are not in agreement with the experimental data. Even in this case, however, it is possible to find some agreement between theory and experiment by assuming "ad hoc" parameters, which generally largely differ from the recommended ones. It is evident, by definition, that such "ad hoc" parameters cannot be adopted for nuclei differing from the nucleus for which they were obtained. Therefore, they can be only used for purposes of interpolation. Extrapolation is in fact seriously questionable when not supported by any systematic behaviour inferrable from the neighbouring nuclei.

A clear example of the above mentioned situation is provided by Pu-239. Measured angular distributions in the energy range 0.19÷5.5 MeV were analysed by Coppola and Knitter [1,2] in terms of central potential, by using different sets of recommended parameters.

In all the cases considered, no acceptable agreement was reached. On the other hand, Boyce et al. [3] were able to obtain a good fit of their data within the 0.15÷1.5 MeV range by using rather unusual parameters.

The purpose of this paper is to show how the above mentioned experimental results on Pu-239 can be reproduced by the optical model by using a generalized deformed potential instead of a central one.

Such a result is obtained by adopting parameters which are very similar to those successfully used in the analysis of neighbouring nuclei.

2. ADOPTED MODEL

The neutron scattering angular distributions considered in the present analysis are those reported in ref. [1,2]. The neutron energy interval to be considered ranges from 0.19 up to 5.5 MeV. All the data include some inelastic scattering. More precisely, below 0.38 MeV there is a contribution due to the first three excited levels, within the 1.5÷2.3 MeV range there are all the levels up to 0.286 MeV, and within the 4.0÷5.5 MeV range all the levels below 1 MeV provide a contribution to the observed values.

The level structure of Pu-239 cannot be interpreted in terms of pure rotational states. It is felt, however, that a better agreement between experiment and theory can be obtained if at least a certain amount of coupling among levels of the ground state rotational band is taken into account.

The model here adopted is based on the coupled channel theory as developed by Tamura [4]. In the low energy range, i.e. between 0.19 and 0.38 MeV, all the states up to the $7/2^+$ level (0.076 MeV) were assumed to be strongly coupled with the ground state. Above 1.5 MeV the so called adiabatic approximation was assumed. All the states belonging to the ground state band were consequently automatically coupled.

The adopted potential was a Saxon-Woods of the type

$$V(r,\theta,\phi) = -(V+iW)\frac{1}{1+\exp[(r-R)/a]} - 4iW_D\frac{\exp[(r-R)/b]}{\{1+\exp[(r-R)/b]\}^2}$$

$$- V_{SO}(\sigma.\ell)\,\lambda^2\frac{1}{ar}\cdot\frac{\exp[(r-R)/a]}{\{1+\exp[(r-R)/a]\}^2}$$

where

$$R = R_o(1+\beta Y_{2o}(\theta'))$$

The potential was expanded in Legendre polynomials $P_\lambda(\cos\theta')$ up to $\lambda = 4$.

All the notations adopted are in ref. [4]

3. RESULTS AND DISCUSSION

Calculations were carried out on an IBM 7094 computer, using the codes "Jupitor" [5] and "ADAPE" [6] (the last one for the adiabatic model). The generalized optical potential parameters used are shown in Table I. They are the same parameters which were successfully adopted in the total cross section analysis of Th-232 above 2 MeV, the only exceptions being: deformation β, for which the value of 0.22 was adopted, and the absorptive part W_D which was assumed as free parameter.

TABLE I. OPTICAL-MODEL PARAMETERS USED IN THE CALCULATIONS

$V(E) = 47 - 0.5\,E(MeV)$	$W_D = 3.52 + 0.52\,E(MeV)$
$W = 0$	$V_{SO} = 6.5$ MeV
$a = 0.65$ fm	$b = 0.47$ fm
$R_0 = 1.25\,A^{1/3}$	$\beta = 0.22$

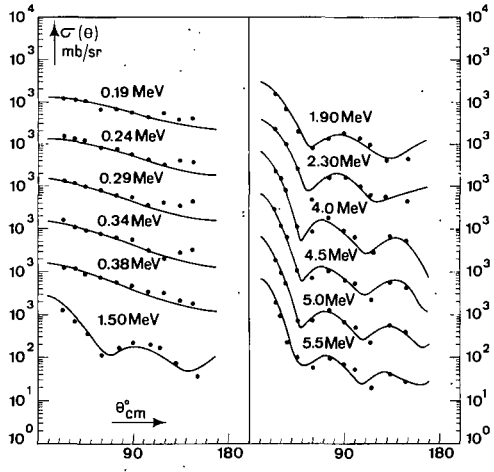

FIG.1. Comparison between the theoretical result (solid line) and the experimental data of Refs [1] and [2] (solid points).

The choice of W_D as a free parameter was suggested by the fact that this quantity takes into account processes which strongly depend on the particular structure of the nucleus considered.

The comparison between theory and experiment is shown in Fig. 1. The contribution of the direct inelastic scattering from the $(3/2^+)$, $(5/2^+)$ and $(7/2^+)$ levels is contained within the solid line curves, whereas the contributions due to compound nucleus processes were neglected. The calculations performed showed that the magnitude of the direct processes was, at low energy, strongly influenced by the number of coupled channels considered. The values obtained for these quantities must, therefore, be accepted with caution.

The value of W_D too strongly depends on the particular coupling adopted. The Hauser-Feshbach calculations of compound processes seem consequentially devoid of any meaning. In other words, the present results below 1 MeV, where big discrepancies are found by using central potential with recommended parameters, merely show the capability of the generalized optical model to achieve reasonable fits.

The most pronounced discrepancies were found in the backward scattering at low energies, while at higher energies discrepancies were found at the minima. The first kind of discrepancies could be removed by considering a more or less isotropic contribution due to the compound processes. As far as higher energy minima are concerned, it was found that the corresponding experimental values are strongly influenced by the multiple scattering correction technique adopted. The data shown in Fig. 1 were corrected by using a modified version of the code "Maggie" [7]. Somewhat different results were obtained by using two different programmes: one based on the Monte Carlo technique [8], as adopted in "Maggie", and the other one based on the linear programming technique [9]. The main reasons of these differences seem to be the following. Multiple scattering corrections are essentially based on perturbation theory concepts. It is assumed that a Legendre polynomial fit of the uncorrected data can be used as a first guess of the angular distribution, provided the condition

$$\sigma(\theta) = \sum_{0}^{N}{}_{\ell}\, a_\ell\, P_\ell(\theta) \geq 0$$

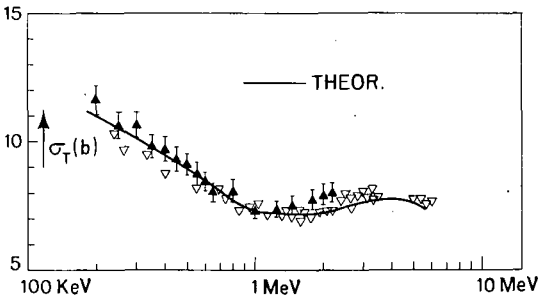

FIG.2. Comparison between the theoretical total cross-section (solid line) and experimental data in the 0.2-5.5 MeV energy range.

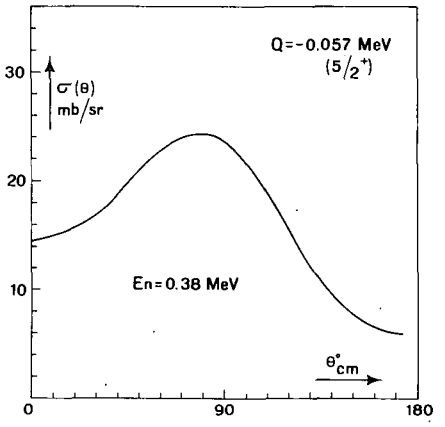

FIG.3. Theoretical differential cross-section for direct inelastic scattering of 0.38 MeV neutrons from the $5/2^+$ (0.057 MeV) level.

is fulfilled. Now, for a given set of experimental points the above condition can be generally satisfied by using different values of the maximum degree N of the Legendre polynomials considered. A different choice of N does not change very much the behaviour of $\sigma(\theta)$, except at the minima, where variations by a factor 2-3 can be obtained by changing N of one unity.

As a consequence, the basic assumptions of the perturbative methods are frequently unfulfilled, and the "corrected" experimental values near the minima strongly depend on the particular polynomial fit adopted.

The existing data on the total cross section in the energy range 0.19--5.5 MeV have been compared with the theoretical ones in order to find additional evidence of the generalized optical model capability to reproduce the experimental situation. The satisfactory agreement existing over the entire range considered is shown by Fig. 2.

As an example, the calculated differential cross section for direct inelastic scattering of 0.38 MeV neutrons from the $5/2^+$ (0.057 MeV) level is shown in Fig. 3. The curve, which is sensibly asymmetric around 90°, has to be considered as qualitative only. A different choice of level coupling would result in different absolute values.

4. CONCLUSIONS

From the previous considerations, it seems that the following conclusions can be drawn

i) The generalized optical model provides a reasonable fit for the observed angular distributions of neutron scattered by Pu-239 over a wide energy range. This can be obtained by using parameters in agreement with those adopted for neighbouring nuclei.

ii) At low energies, the absolute values of the direct inelastic scattering cross sections and the choice of the imaginary part of the potential are strongly influenced by the particular coupling adopted. To have an unambiguous estimate of these quantities, it would be necessary to couple a very large number of channels. Such an endeavour would be a time consuming one even using a very large computer.

iii) Multiple scattering corrections near minima must be considered with caution. It would be highly desiderable to perform measurements of angular distributions in correspondence of the zeroes of the Legendre polynomial expansions assumed, rather than at arbitrarily selected angles.

iv) The angular distributions of the neutrons inelastically scattered by the low energy levels are probably quite asymmetric around 90°. Excitation functions estimated by multiplying by 4π the result obtained at a given angle must be considered as a rough first approximation.

REFERENCES

[1] KNITTER, H.H., COPPOLA, M., Z. Physik 228 (1969) 286.

[2] COPPOLA, M., KNITTER, H.H., Z. Physik 232 (1970) 286.

[3] BOYCE, D.A., CAVANAGH, P.E., COLEMAN, C.F., GARD, G.A., HARDACRE, A.G., KERR, J.C., TURNER, J.F., Unpublished (1969).

[4] TAMURA, T., Rev. Mod. Phys., 37 (1965) 679.

[5] TAMURA, T., Unpublished.

[6] FABBRI, F., ZUFFI, L., CNEN Report RT/FI(69)7 (1969).

[7] SCHMIDT, H., HORSTMANN, H., CBNM Internal Communication.

[8] HOLMQVIST, B., GUSTAVSSON, B., WIEDLING, T., Arkiv för Fysik, 34 (1967) 481.

[9] GIOVANNINI, R., MARSEGUERRA, M., Unpublished.

DISCUSSION

C.M. NEWSTEAD: I see that you have obtained quite a good fit to the total cross-section of ^{239}Pu. I recall that in a previous calculation of your group concerned with ^{238}U, you were not able to obtain such a good fit, particularly near 1 MeV. Could you comment on this improvement? Is it connected with the use of both the NACC-(non-adiabatic coupled-channel) and the ACC-(adiabatic coupled-channel) approach in the present work or was this done mainly to save computing time?

V. BENZI: A similar improvement was obtained for ^{238}U when more coupled channels were considered (see the Proceedings of Tokyo Conference on Nuclear Structure, for example). In the calculation you mentioned, only the coupling of the first 2^+ excited level was considered. The ACC approach was used in the higher-energy range, because it is believed to give better results when many excited levels are involved. Of course, the ACC-approach saves a lot of computer time, too.

ANALYSIS OF NEUTRON INELASTIC SCATTERING BY ^{238}U

S. IGARASI, H. NAKAMURA, T. MURATA, K. NISHIMURA
Japan Atomic Energy Research Institute,
Tokai-mura, Naka-gun,
Ibaraki-ken, Japan

Abstract

ANALYSIS OF NEUTRON INELASTIC SCATTERING BY ^{238}U.

Total and partial inelastic scattering cross-sections of ^{238}U are being investigated in the range of neutron energy from 50 keV to 15 MeV, consistency being taken into account among total, elastic, inelastic and reaction cross-sections. In the present status there are few data to obtain a reliable data set from the experimental inelastic scattering cross-section. The optical model and Hauser-Feshbach's formula are mainly used in the energy range from 50 keV to 1.5 MeV and the evaporation model is used above 1.5 MeV. Values and trends of optical-potential parameters and level density parameters are sought by fitting the calculated values of the inelastic scattering cross-sections and the emitted neutron spectra to the experimental data. In order to obtain a curve of the inelastic scattering cross-section, detailed information is needed for spin, parity and energy of excited states from 1 MeV to 1.5 MeV. After surveying experimental and theoretical information, and comparing results of calculations with experimental data for excitation functions, values of these level parameters are tentatively determined. Calculations are performed by using a computer code ELIESE in the lower energy region. Effects of competitive processes, such as (n, γ), (n, f), etc. are taken into account in the calculations. Above the 1.5-MeV region, inelastic scattering cross-sections are obtained by using Hauser-Feshbach's model which includes contribution from the continuous state of the target nucleus, and by using cross-sections for compound formation and experimental data for (n, f), (n, 2n), (n, 3n) and (n, γ) cross-sections.

1. INTRODUCTION

There have been many attempts to investigate neutron cross-sections of ^{238}U, some of which are works of evaluation [1-3]. In the present report, total and partial inelastic scattering cross-sections for ^{238}U are analysed in the range of neutron energy from 50 keV to 15 MeV, and a method is illustrated by which a curve of the inelastic scattering cross-section is obtained from the lower energy region, 50 keV to 1.5 MeV, to the higher energies between 1.5 MeV and 15 MeV.

The energy range considered here is divided into three regions. The first region, from 50 keV to 1.5 MeV, is referred to as the "discrete region". The second region is that from 1.5 MeV to 3.0 MeV. The level scheme above 1.5 MeV is not yet clearly assigned. Distribution of the levels is assumed to be continuous in this region, and there are two components of the inelastic scattering cross-section, one for excitation of the discrete levels and the other for excitation of the continuous state. They are superposed on each other to obtain a smooth curve of the cross-section, so this region is here called the "joint region".

For the third region, namely above 3.0 MeV, the usual level density approximations are used in the calculations. This region is referred to as the "continuous region".

2. REVIEW OF EXPERIMENTAL DATA

2.1. Level scheme

There are two kinds of data on the level scheme for ^{238}U. One is measured by using neutron inelastic scattering and the other is obtained from measurements of Coulomb excitation. Of the former type are the data measured by Barnard et al.[4], who separated the levels up to about 1.5 MeV and assigned spin and parity below about 1.0 MeV. Diamond and Stepens [5] proposed a level scheme up to about 1.4 MeV based on the Coulomb excitation. Agreement of both measurements is good below about 1.0 MeV, except for high-spin states. Above 1.0 MeV, level assignments of both measurements do not correspond clearly with each other. It seems, however, that there are a considerable number of low-spin states in this energy region.

2.2. Inelastic scattering cross-section

Measurements of the excitation functions for discrete levels have been performed by several authors [4, 6, 7]. Smith [7] showed the cross-sections integrated by scattering angle. Cranberg and Levin [6] and Barnard et al.[4] presented the data measured at 90°. Agreement among their data is satisfactory for the excitations of the levels below 730 keV. There are some discrepancies among the excitation functions of the levels above 730 keV. The measurements of Barnard et al.[4] are considered to be reliable from the viewpoint of energy resolution and error assignment. Strőnberg and Schwarz [8] measured the excitation function of the first level at 95-keV incident energy. Measurements were performed by Batchelor et al.[9] at 2, 3, 4, and 7 MeV.

2.3. Elastic scattering cross-section

There are several measurements in which the inelastic scattering is not separated from the elastic scattering. Below 1.5 MeV, Smith [7] presented well separated data. Barnard et al.[4] also measured the elastic scattering cross-sections in the same energy region. Agreement between both measurements is good for the shape of the angular distributions, but it is not satisfactory for elastic scattering cross-sections. Batchelor et al.[9] and Voignier [10] have measured elastic scattering in the higher-energy region.

2.4. Other reaction cross-sections

Data for (n,γ), (n,f), (n,3n) reactions are compiled in BNL-325 [11]. Menlove and Poenitz [12] measured the radiative capture cross-section in the energy region from 25 to 500 keV. The cross-section of the (n,2n) reaction was measured by Knight et al.[13].

3. CALCULATIONS IN THE DISCRETE REGION

Excitation functions for each level are calculated by using the Hauser-Feshbach method. The total inelastic scattering cross-section is a summation of these excitation functions. Calculations are performed by using computer codes ELIESE-2 [14] and ELIESE-3 [15].

TABLE I. LEVEL SCHEME FOR ^{238}U USED IN THIS PAPER

Energies, spins and parities are the same as those recommended by J.J. Schmidt [1], except for spins and parities above 1.0 MeV; these spins and parities are tentatively assigned

Level No.	Excitation energy (keV)	Spin	Parity
Ground	0.0	0	+
1	44.7	2	+
2	148.0	4	+
3	301.0	6	+
4	520.0	8	+
5	680.0	1	-
6	732.0	3	-
7	790.0	10	+
8	838.0	5	-
9	939.0	2	+
10	968.0	2	+
11	1006.0	0	+
12	1047.0	2	+
13	1076.0	2	+
14	1100.0	12	+
15	1123.0	1	-
16	1150.0	2	-
17	1190.0	3	-
18	1210.0	2	+
19	1246.0	4	-
20	1272.0	5	-
21	1313.0	2	+
22	1361.0	2	+
23	1401.0	2	+
24	1437.0	14	+
25	1470.0	1	-

The level scheme used here is shown in Table I. Below 1.0 MeV, energies, spins and parities have been given for many levels by several authors [4, 5, 16, 17]. Above 1.0 MeV, level assignment is far from complete. In the present paper, values of the energies, spins and parities recommended by J.J. Schmidt [1] are used. For levels above 1.0 MeV, however, spin and parity are not assigned in Ref. [1]. Therefore, spins and parities for the levels above 1.0 MeV are tentatively assigned by comparing results of preliminary calculations with experimental data.

Radiative capture is the main competitive process in this region. The fission cross-section is also taken into account as competitive above 1.0 MeV. Effects of these competitive processes are taken into account in the calculations as branching ratio, $\alpha_{J\Pi}$. The formula including these effects is written as

$$\sigma_{in}(E, I, \pi \rightarrow E', I', \pi') = \frac{\pi}{k^2} \frac{1}{2(2I+1)} \sum_{J\Pi} \frac{2J+1}{\sigma_{J\Pi}}$$

$$\times \sum_{} \omega(\Pi, \pi, \ell) T_{\ell}^{j}(E, I, \pi) \times \sum_{} \omega(\Pi, \pi', \ell') T_{\ell'}^{j'}(E', I', \pi') \qquad (1)$$

and

$$\sigma_{J\Pi} = \sum \omega(\Pi, \pi'', \ell'') T_{\ell''}^{J''}(E'', I'', \pi'')/(1 - \alpha_{J\Pi})$$

where (T_ℓ^J)s are transmission coefficients and ωs are parity-conservation factors. The branching ratio, $\alpha_{J\Pi}$, is estimated from experimental data of the radiative capture and fission cross-sections [11, 12], and from the compound formation cross-section obtained by the optical-model calculations. Trend of the branching ratio, $\alpha_{J\Pi}$, is shown in Fig.1, assuming that $\alpha_{J\Pi}$ does not depend on J and Π.

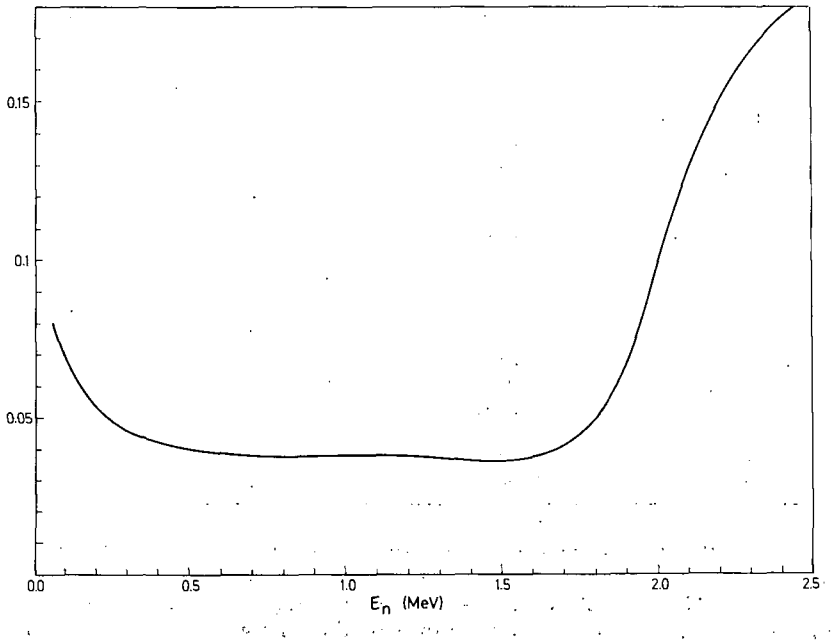

FIG. 1. Trend of the parameter $\alpha_{J\Pi}$ used in Eqs (1) and (3); dependence on J and Π is not taken into account.

Optical potential used here is written as follows:

$$V(\gamma) = V_0 \frac{1}{1+\exp\{(\gamma - \gamma_0 A^{1/3})/a_0\}} + iW_s \frac{4\exp\{(\gamma-\gamma_s A^{1/3})/a_s\}}{[1+\exp\{(\gamma-\gamma_s A^{1/3})/a_s\}]^2}$$

$$+ V_{s0}\left(\frac{\hbar}{m_\pi C}\right)^2 \frac{1}{\gamma a_{s0}} \frac{\exp\{(\gamma-\gamma_{s0} A^{1/3})/a_{s0}\}}{[1+\exp\{(\gamma-\gamma_{s0} A^{1/3})/a_{s0}\}]^2} (\vec{\sigma}\cdot\vec{\ell}), \qquad (2)$$

Values of the parameters used are listed in Table II. The depth of the imaginary potential, W_s, is chosen to be larger than that of Auerbach

TABLE II. OPTICAL POTENTIAL PARAMETERS

V_0	40.5 MeV
W_s	9.0 MeV
V_{so}	15.0 MeV
γ_0	1.32 Fm
γ_s	1.32 Fm
γ_{so}	1.32 Fm
a_0	0.47 Fm
a_s	0.47 Fm
a_{so}	0.47 Fm

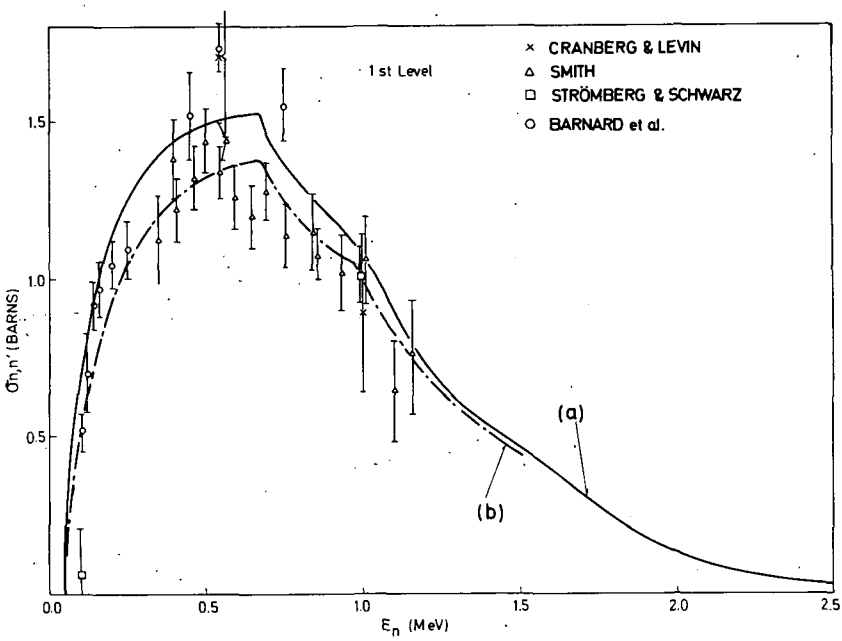

FIG. 2. Calculated and experimental inelastic scattering cross-sections for first level. Curve (a) is obtained by using the potential parameters listed in Table II and Eq.(2). Curve (b) is calculated by using the Gaussian form for imaginary potential with V_0 =40.0 MeV, W_s =9.0 MeV and a_s =1.0 Fm.

and Moore [18], because of taking into account the effects of the competitions. A larger value than theirs [18] is also used for the depth of the real potential, V_0, because better fits to the excitation functions of the levels are obtained above the second excited state.

Angular distributions of the elastic scattering cross-sections are compared with experimental data at 350 keV and 415 keV [7], for testing the reliability of the set of parameters. Results of fitting are good. Excitation functions through collective motion [19] are also calculated at 200, 300, 400, 500 and 600 keV using the same potential parameters as in Table II. The nuclear deformation parameter β is taken as 0.33. Results illustrate that the effects of the collective process are one or more orders lower than those of the compound process. Therefore, the effects of the collective motion are neglected.

In Figs 2-5, calculated and experimental excitation functions are shown for 12 levels. For the first, second, fifth and sixth levels, curves (a) are obtained by using the parameters listed in Table II, and Eq.(2). For the same levels, curves (b) are obtained in preliminary work by using V_0 = 40 MeV, Gaussian form for the imaginary potential with width parameter 1.0 Fm and $\alpha_{1/2} = \alpha_{3/2} = 0.1$ for all energy points. For the other levels, results obtained are illustrated in Figs 4 and 5.

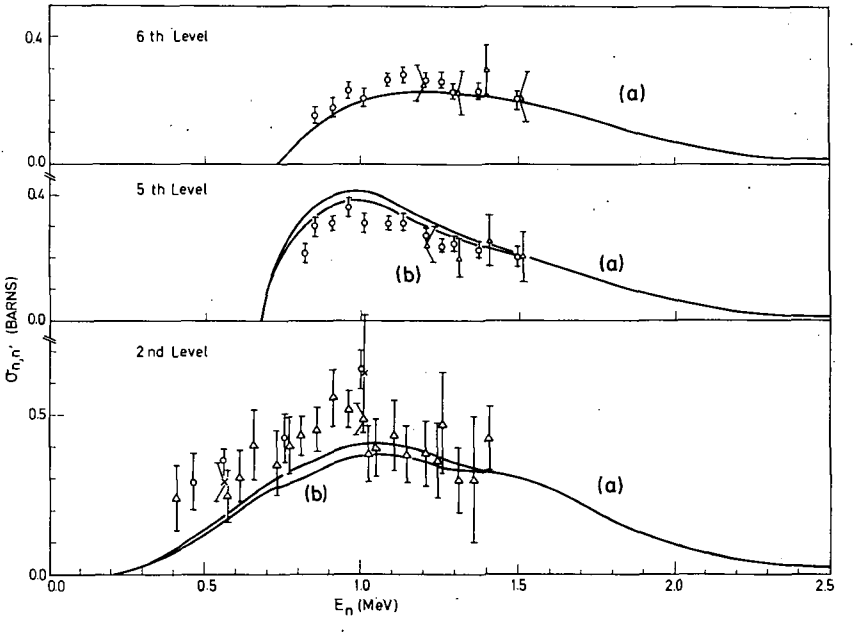

FIG.3. Calculated and experimental inelastic scattering cross-sections for second, fifth and sixth levels. Curves (a) are obtained by using the potential parameters listed in Table II and Eq.(2). Curves (b) are calculated by using the Gaussian form for imaginary potential with V_0=40.0 MeV, W_s=9.0 MeV and a_s=1.0 Fm. Symbols for experimental data are the same as in Fig.2.

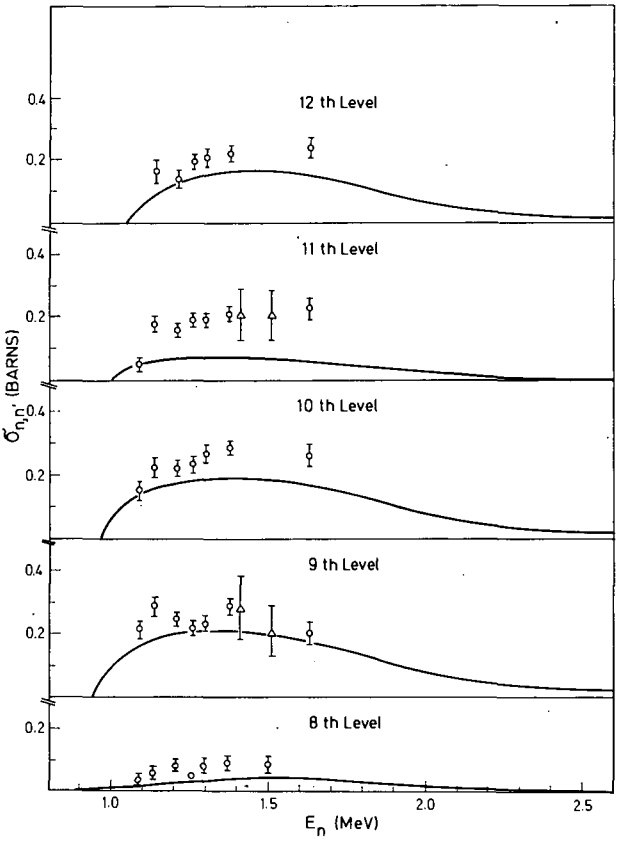

FIG.4. Calculated and experimental inelastic scattering cross-sections for eighth, ninth, tenth, eleventh, and twelfth levels. Calculations are performed by using the potential parameters listed in Table II and Eq.(2). Symbols for experimental data are the same as in Fig.2.

4. CALCULATIONS IN THE JOINT AND CONTINUOUS REGIONS

Excitation of the continuous state competes gradually with excitation of the discrete levels, and suppresses the latter above about the 2-MeV energy region. Excitation functions for the discrete levels are calculated by using Eq.(1) with a modified denominator which includes effects of competition with excitation of the continuous state. The modified denominator is described by the following formula

$$\sigma_{J\Pi} = \sum_{I''\pi''j''\ell''} \left\{ \sum_{E''} \omega(\Pi, \pi'', \ell'') T^{j''}_{\ell''}(E'', I'', \pi'') + \int_0^{Q_c} \rho(U, I'') T^{J''}_{\ell''}(E'', I'', \pi'') dE'' \right\} / (1 - \alpha_{J\Pi}) \qquad (3)$$

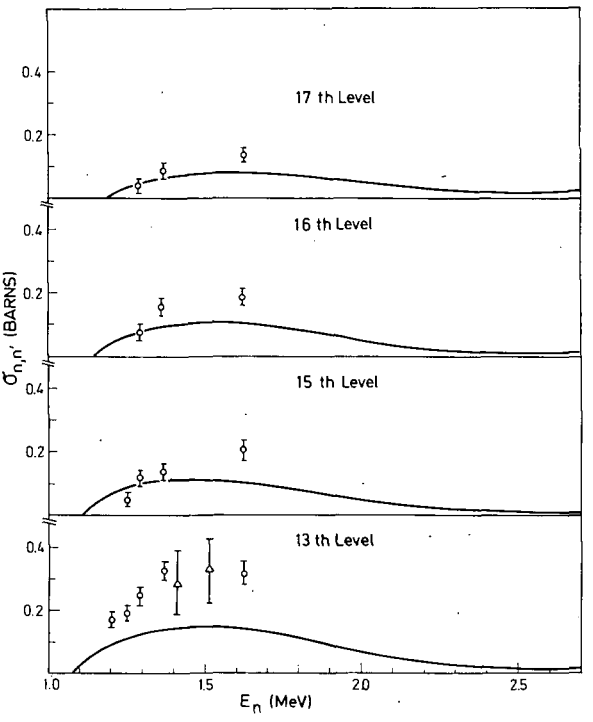

FIG.5. Calculated and experimental inelastic scattering cross-sections for thirteenth, fifteenth, sixteenth and seventeenth levels. Calculations are performed by using the potential prameters listed in Table II and Eq.(2). Symbols for experimental data are the same as in Fig.2.

where $\rho(U,I)$ is the level density of the residual nucleus at the excitation energy U. The interval of integration, Q_c, is equal to $(E-E_c)$, the difference between incident energy, E, and the lowest energy of this joint region, E_c. Curves in Figs 2-5 decrease with increasing energy owing to the competitive processes, and their values are negligibly small at about 3 MeV. The trends of this decrease depend strongly on the level density.

A reasonable choice of the level density is an important problem in the joint region. Continuity of the emitted neutron spectrum is used in order to determine the level density. The level density at higher excitation energy is written as [20]

$$\rho_0(U) = C \exp(2\sqrt{aU})/U^2 \tag{4}$$

where C is a constant. At lower excitation energy, the constant nuclear temperature model is fairly valid [21-23]. The level density is given, below a break-down point U_0, as

$$\rho_0(U) = C' \exp(U/T) \tag{5}$$

Constant C' and T are determined from the conditions of continuity at U_c between the two formulae, Eqs (4) and (5).

Usually the excitation energy U is shifted from the real excitation energy by the pairing energy δ. Here we adopted the "back-shifted" model in which $\delta = 0$ is taken for an even-even nucleus and $\delta \neq 0$ for the others. The value of the parameter a is taken from its systematics [24], and $a = 24.96\ MeV^{-1}$ is given for ^{238}U. The break-down point U_c is determined so that reasonable connection between the two spectra of emitted neutrons is made; one leaves the residual nucleus in the discrete levels and the other in the continuous state. The value of U_c obtained here is 2 MeV. By using these values of parameters, good agreements are obtained between the neutron spectra calculated by the use of Eqs (4) and (5) and those of the experimental data [9].

The values of the level density parameters used in Eq.(3) are those obtained by the above-mentioned procedure. The level density used in Eq.(3) has the form of Eq.(5). The component of the inelastic scattering cross-section for excitation of the continuous state is obtained here by subtracting the component for excitation of the discrete levels from the total inelastic scattering cross-section. The total inelastic scattering cross-section in the joint and the continuous regions is calculated as follows

$$\sigma(n, n') = \sigma(\text{total}) - \sigma(n, n) - \sigma(n, f) - \sigma(n, \gamma) - \sigma(n, 2n) - \sigma(n, 3n) \qquad (6)$$

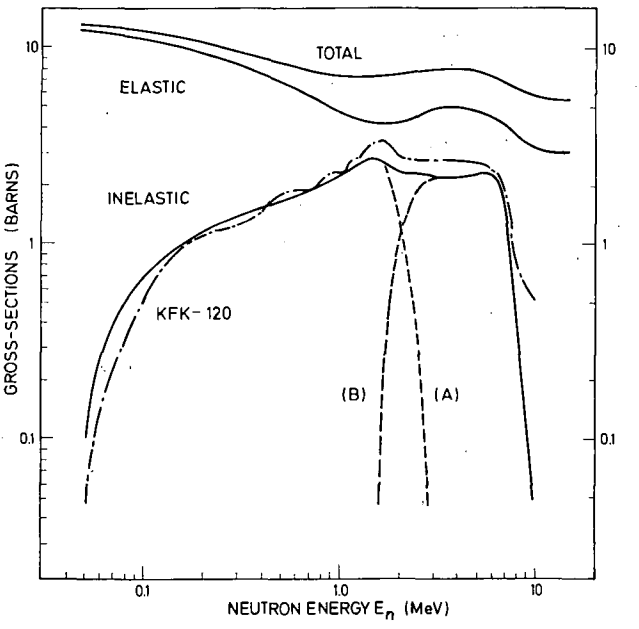

FIG.6. Total, elastic scattering and inelastic scattering cross-sections. Curves (A) and (B) indicate the two components of the inelastic scattering cross-section in the joint region. The inelastic scattering cross-section curve taken from KFK-120 is also shown.

where the total cross-section σ(total) and the elastic scattering cross-section σ(n, n) are obtained from the optical model calculations, and other reaction cross-sections are taken mainly from BNL-325 [11]. Parameters shown in Table II are testified for their reliability by comparisons between calculated and experimental angular distributions for elastic scattering at 2, 3, 4, 7 and 14.1 MeV. In Fig.6, the total inelastic scattering cross-section, the elastic scattering cross-section and the total cross-section are given in the full energy range considered in this work.

5. DISCUSSIONS AND REMARKS

Below 1.5 MeV, the Hauser-Feshbach method is used to calculate the inelastic scattering cross-section. It is difficult to obtain good fits between experimental data and the calculated cross-sections for all the excited states considered here, if one uses only one set of the optical potential parameters. Curves (a) for the first and fifth levels are rather larger than the experimental data, but seem to be smaller in the case of the second and sixth levels. Curves (b) give better fitting than curves (a) for the first level, but not so good for the second level. There will be, however, possibilities for better fitting. For example, effects of the level-width fluctuation and the resonance interference [25] seem to be worth taking into consideration in order to obtain more desirable results for the excitation functions. In such a case, values of the optical potential parameters may be different from those values as shown in Table II.

The best set of potential parameters is not sought in this work. The systematic trend of the potential parameters is needed to get more reliable results than those obtained here. The inelastic scattering cross-section shown in Fig.6 is, however, comparable to that presented in KFK-120 [1].

The excitation curves shown in Figs 2-4 decrease more rapidly above 1.5 MeV than those expected in this region. This comes from the somewhat large contribution of the continuous state to the excitation functions for each discrete level. The level density in Eq.(3) has the same form as that in Eq.(5). Therefore, more reasonable excitation functions will be obtained above 1.5 MeV, provided that somewhat small values of the constant C' are adopted in the level density of Eq.(3).

A suitable choice of the level scheme and the level density is necessary for obtaining a proper curve of the inelastic scattering cross-section. As one of the means in helping to make this suitable choice, a connection between the two spectra of the emitted neutrons is adopted here; one leaves the residual nucleus in the discrete levels and the other in the continuous state. A proper correlation between the two spectra has been made by searching for the break-down point U_c, while the level scheme is fixed as shown in Table II. Precise information about the level scheme between 1.0 and 1.5 MeV is necessary to get a closer correlation between the two spectra than that obtained in this work.

REFERENCES

[1] SCHMIDT, J.J., Neutron cross sections for fast reactor materials, KFK-120 (1966).

[2] VASTEL, M., Evaluation des données neutroniques de l'uranium 238 dans le domaine d'énergie 10 keV-15 MeV, HX-1/1375/CL RA-FI-04 (1968).

[3] PARKER, K., Neutron cross sections of ^{235}U and ^{238}U in the energy range 1 keV-15 MeV, AWRE-0-79/63 (1963).
[4] BARNARD, E., FERGUSON, A.T.G., McMURRAY, W.R., VAN HEERDEN, I.J., nucl. Phys. 80 (1966) 46.
[5] DIAMOND, R.M., STEPHENS, F.S., Ark. Fys. 36 (1967) 221.
[6] CRANBERG, L., LEVIN, J.S., Phys. Rev. 109 (1958) 2063.
[7] SMITH, A.B., Nucl. Phys. 47 (1963) 633.
[8] STRÖNBERG, L.G., SCHWARZ, S., Nucl. Phys. 71 (1965) 511.
[9] BATCHELOR, R., GILBOY, W.B., TOWLE, J.H., Nucl. Phys. 65 (1965) 236.
[10] VOIGNIER, J., CEA-R-3503 (1968).
[11] BNL-325, 2nd Edn, Supplement No.2, Vol. III (1965).
[12] MENLOVE, H.L., POENITZ, W.P., Nucl. Sci. Engng 33 (1968) 24.
[13] KNIGHT, J.D., SMITH, R.K., WARREN, B., Phys. Rev. 112 (1958) 259.
[14] IGARASI, S., JAERI-1169 (1968).
[15] IGARASI, S., to be published.
[16] DRESNER, L., Nucl. Sci. Engng 10 (1961) 142.
[17] LEDERER, C.B., HOLLANDER, J.M., PERIMAN, I., Table of Isotopes, 6th Edn (1967).
[18] AUERBACH, E.H., MOORE, S.O., Phys. Rev. 135 (1964) B895.
[19] TAMURA, T., ORNL-4152 (1967); revised version is presented for FACOM 230-60, IBM 360/175 and HITAC-5020E computers by WAKAI, M., IGARASI, S., MIKOSHIBA, S., YAMAJI, S., JAERI Memo 3833 (1969).
[20] ERICSON, T., Advanced Phys. 9 (1960) 425.
[21] LANG, D.W., Nucl. Phys. 42 (1963) 353.
[22] SANO, M., YAMASAKI, S., Prog. theor. Phys. 29 (1963) 397.
[23] GILBERT, A., CAMERON, A.G.W., Can. J. Phys. 43 (1965) 1446.
[24] NAKAMURA, H., to be published.
[25] MOLDAUER, P.A., Phys. Rev. 135 (1964) B642.

COMPOUND-NUCLEUS CALCULATIONS OF LOW-ENERGY NEUTRON REACTION CROSS-SECTIONS USING LEVEL DENSITIES FROM EXACT COUNTING OF SHELL-MODEL STATES

J.R. ERIKSSON
Neutron Physics Section, AB Atomenergi, Studsvik, Nyköping, Sweden

Abstract

COMPOUND-NUCLEUS CALCULATIONS OF LOW-ENERGY NEUTRON REACTION CROSS-SECTIONS USING LEVEL DENSITIES FROM EXACT COUNTING OF SHELL-MODEL STATES.

The proton and alpha-particle production in neutron chain reactors appears to be a most important long-term property leading to brittleness in supporting materials. Since the (n, p) and (n, α) cross-sections are difficult to measure it is of interest to treat these processes theoretically.

The prediction of the energy-dependent (n, p) and (n, α) cross-sections from the compound-nucleus model is usually based on the assumption that the level density of the residual nucleus is of the Fermi-gas form $\rho_{FG}(E, I)$, where E is the nuclear excitation energy, and I is the spin. With this assumption, the integral mean of the (n, p) (or (n, α)) production cross-section $\langle \sigma_{n,p} \rangle_{\Phi}$ over a thermal-reactor neutron-flux distribution $\Phi(E)$ shows that the most important part of the level density is the residual excitation below 5 MeV.

The level density $\rho(E, I)$ is calculated at low excitation energies E by the method of exactly counting the spherical-model states. The single-particle shell-model levels are subject to a modified BCS calculation after which the quasi-particle states obtained are used as input in a level-counting program giving the level density $\rho(E, I)$. The resulting $\rho(E, I)$ shows pronounced effects arising from the specific neutron and proton single-particle-level schemes up to energies above 10 MeV. Despite this low-energy picture and the overall scatter of the values of $\rho(E, I)$ an adequate $\rho_{FG}(E, I)$ can always be obtained at higher energies. It turns out that, except for a few cases, the Fermi-gas ground state lies above the ground state of the model nucleus indicating that $\rho_{FG}(E, I)$ tends to underestimate the low-energy level density.

1. INTRODUCTION

The purpose of this investigation (as yet incomplete) is to improve the calculation of reaction cross sections by applying a physically more satisfactory model to get nuclear level densities. Usually level densities which have a smooth monotonic dependence on the excitation energy, like the Fermi-gas model result, are used in calculations of the compound nucleus cross section. To those who have calculated (n, p) and (n, α) cross sections, such level densities with no energy dependent structure will have appeared improper in the energy range of say the lowest hundred levels of the excited rest nuclei. Because of the relatively low energies of the fission neutrons an improvement in the description of the lower energy part of the level density distribution is of primary interest when making theoretical predictions of nuclear data for reactors. It is worth mentioning that for a large number of fission products, estimates of reaction cross sections from calculation will be the only ones which can be simply obtained.

2. THEORETICAL METHOD

The angle integrated cross section $\sigma_{n,x'}(E)$ with the incident neutron n leading to an emitted particle x' from the compound nucleus formed, may be given by the Hauser-Feshbach formula [1]

$$\sigma_{n,x'}(E) = \frac{\pi}{k_n^2} \sum_{J\Pi} \frac{(2J+1)}{(2I+1)(2i+1)} \sum_{sl} T_l(n) \frac{\sum_{s'l'} T_{l'}(x')}{\sum_{x'',s''l''} T_{l''}(x'')} \qquad (1)$$

with the sum in the denominator running over all possible exit channels x''. The channels index $x = (\alpha, I, i, s, l, J, \Pi)$ is taken to be in the channel-spin picture and in common notations. In two cases in which there is an adequate knowledge of spin, parity and energy of the low lying excited states of all rest nuclei involved, Buthler and Santry [2] obtained good agreement between (n, p) and (n, α) cross sections calculated from eq. (1) and experimental results. However a detailed knowledge of the level structure over some MeV excitation energy and simultaneously for at least three rest nuclei is quite rare. Thus the Weisskopf-Ewing [3] evaporation formula written in the form

$$\sigma_{n,x'}(E) = \sigma_{c,n}(E) \frac{g_{x'} \int_0^{\epsilon_{max}^{x'}} p_{x'}^2 \sigma_{c,x'}(\epsilon_{x'}) \rho(U_{x'})\, d\epsilon}{\sum_{x''} g_{x''} \int_0^{\epsilon_{max}} p_{x''}^2 \sigma_{c,x''}(\epsilon_{x''}) \rho(U_{x''})\, d\epsilon} \qquad (2)$$

replaces the eq. (1) for the purpose of estimating (n, p) and (n, α) cross sections. Eq. (2) does not cope with the spin- and parity-distributions of the residual excited nuclei. Furthermore, almost always the Fermi-gas model level density [4]

$$\rho_{FG}(U) = \frac{\pi^{1/2}}{12} \frac{\exp(2\sqrt{aU})}{a^{1/4} \cdot U^{5/4}} \frac{1}{(2\pi)^{1/2}\sigma} \qquad (3)$$

is used in connection with eq. (2). In eq. (3) the standard notation a is used for the density parameter and U is the excitation energy of the Fermi gas.

The most promising way to obtain level density expressions which are an improvement on eq. (3) is by the use of the shell model [5]. Taking the neutron (or proton) shell-model levels of a nucleus including a sufficiently large energy interval around the Fermi energy λ, excitations will be schematically constructed by redistribution of the neutrons over the shells. The spin and parity of such an excited state are given by simple sums over the particle occupations of the shells. On the other hand, the energy of a particular configuration must at least involve intershell effects from the pairing force. We do, however neglect the pairing force between neutrons and protons. We have used the standard pairing Hamiltonian

$$H' = H - \lambda n = \sum \epsilon_k a_k^+ a_k - G \sum a_k^+, a_{-k}^+, a_k a_{-k} \qquad (4)$$

where G is the pairing force parameter, $\epsilon_k = E_k - \lambda$ is the shifted single particle energy, E_k is the energy of the shell (j, l) and the index k stands for j, l and m_l. In eq. (4) a^+ and a are the creation- and annihilation-oper-

rators respectively of real nucleons. As a consequence of eq. (4) the excitation energies will be obtained in the quasi-particle picture and we shall use the Hamiltonian

$$H' = 2 \sum_{k>0} \epsilon_k V_k^2 + \sum_{k>0} \epsilon_k (U_k^2 - V_k^2)(\alpha_k^+ \alpha_k + \alpha_{-k}^+ \alpha_{-k}) +$$

$$+ G \sum_{\substack{k>0 \\ k'>0}} \Big\{ U_k V_k U_{k'} V_{k'} \Big[-1 + (\alpha_k^+ \alpha_k + \alpha_{-k}^+ \alpha_{-k}) + (\alpha_{k'}^+ \alpha_{k'} + \alpha_{-k'}^+ \alpha_{-k'}) -$$

$$- (\alpha_k^+ \alpha_k + \alpha_{-k}^+ \alpha_{-k})(\alpha_{k'}^+ \alpha_{k'} + \alpha_{-k'}^+ \alpha_{-k'}) \Big] -$$

$$- U_k^2 U_{k'}^2 \alpha_k^+ \alpha_{-k}^+ \alpha_{-k'} \alpha_{k'} - V_k^2 V_{k'}^2 \alpha_{-k} \alpha_k \alpha_{k'}^+ \alpha_{-k'}^+ \Big\} \qquad (5)$$

with α^+ and α as the quasi-particle creation and annihilation operators. The ground state is the quasi-particle vacuum. In eq. (5) all quasi-particle number-conserving terms obtained from eq. (4) by the standard quasi-particle transformation are kept and thus eq. (5) has more terms than the free quasi-particle Hamiltonian. The reason for taking the extended form eq. (5) is that up to 20 MeV excitation of heavier nuclei the number of contributing quasi-particles will exceed 10. It has been numerically verified against the BCS-solution [6] including the blocking effect that eq. (4) gives a good approximation to the excitation energy if the U's and V's are kept fixed at their ground state values but a shift in λ is allowed due to the non-conservation of the real particle number in quasi-particle excitations.

Spin and energy summation of the independently calculated neutron and proton level distributions gives the spin dependent level density $\rho(E, I)$ of the whole nucleus. Fig. 1 shows a plot of the spin-independent level density $\rho(E)$ of both parities of ^{48}Ca showing distinct irregularities at lower energies. Since this nucleus is doubly magic, the first excited shell model state lies at a few MeV.

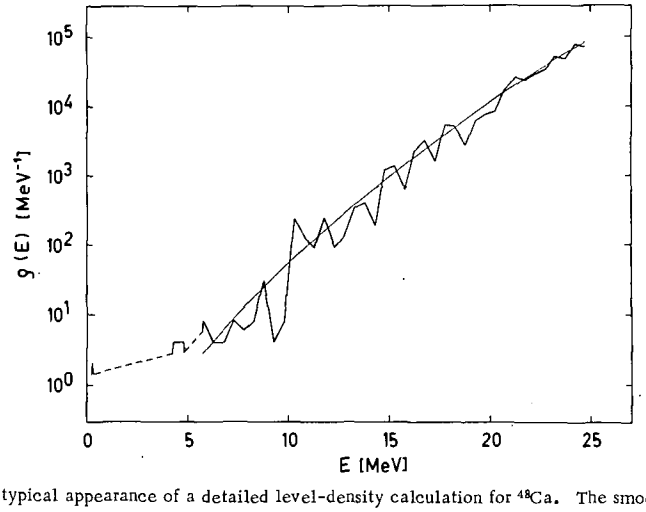

FIG. 1. The typical appearance of a detailed level-density calculation for ^{48}Ca. The smooth curve is the best fit of $\rho_{FG}(U)$.

3. CONCLUDING REMARKS

Separate investigations on nuclei in the Ca, Sn and Pb-region have demonstrated that the model of detailed level density can be fitted by a high energy behaviour of the form eq. (3) with level density parameter values a in good agreement with results of experiment analysis [7]. An essential point, however, is that low lying collective states should be included. Tests on (n, p) and (n, α) cross sections of ^{27}Al and ^{59}Co show that rotational states may not be neglected at low energies. A further detail which will have to be considered is the Moldauer correction [8] which accounts for the fact that the compound nucleus state is actually not a measured one.

ACKNOWLEDGEMENT

The author would like to acknowledge the contribution of Dr. S. Jägare, who has worked with the author on the problem of detailed nuclear level densities.

REFERENCES

[1] LANE, A.M., THOMAS, R.G., Rev. Mod. Phys. 30 (1958) 259.

[2] BUTHLER, J.P., SANTRY, D.C., Phys. Rev. 152 (1966) 1034.

[3] WEISSKOPF, V.F., EWING, D.H., Phys. Rev. 57 (1939) 472.

[4] GILBERT, A., CAMERON, A.G.W., Can. J. Phys. 43 (1965) 1446.

[5] HILLMAN, M., GROVER, J.R., Phys. Rev. 185 (1969) 1303.
MARAYAMA, M., Nucl. Phys. A131 (1969) 145.

[6] BARDEEN, COOPER, SCHRIEFFER, Phys. Rev. 108 (1957) 1195.

[7] CINDRO, N., Rev. Mod. Phys. 38 (1966) 391.

[8] MOLDAUER, P.A., Rev. Mod. Phys. 36 (1964) 1079.

DISCUSSION

M.P. FRICKE: Do you think your method would give a level density which is very different from the Gilbert and Cameron formulas for a heavy, vibrational, odd-odd nucleus between, say, 3 MeV and the neutron separation energy?

J.R. ERIKSSON: As I said in my presentation, I have so far not developed a complete theory for treating different types of collective states.

ПЛОТНОСТЬ ВОЗБУЖДЕННЫХ СОСТОЯНИЙ АТОМНЫХ ЯДЕР

А.В. ИГНАТЮК, В.С. СТАВИНСКИЙ,
Ю.Н. ШУБИН
Физико-энергетический институт, Обнинск,
Союз Советских Социалистических Республик

Presented by A.I. Abramov

Доклад представлен А.И. Абрамовым

Abstract — Аннотация

DENSITY OF EXCITED STATES OF ATOMIC NUCLEI.

In order to evaluate average neutron cross-sections it is necessary to have detailed and reliable information on the widths of the processes involved. In statistical theories of nuclear reactions these are expressed in terms of the excited state density of the final reaction products. Since high degrees of accuracy and reliability are required in evaluating reactor constants, it is essential to develop new methods of calculating the energy dependence of nuclear level density. The average values of excited nuclei and of neutron cross-sections cannot be represented consistently with the generally accepted Fermi-gas model. The paper discusses the results of calculations of the level density of atomic nuclei, in which systematic account is taken of the individual properties of nuclei associated with their shell structure. The calculations are based on the superfluid-nucleus model, which is at present being used with success in analysing the properties of low-lying excited states of nuclei. The calculations do not involve the use of additional parameters and provide a means based on a single approach for correlating the properties of highly excited nuclei and those of nuclei in the ground and weakly excited states. The calculations performed show that the discrete structure of the single-particle spectrum leads to substantial changes in the energy dependence of level density as compared with the Fermi-gas model, provides a natural explanation for the anomalies observed in the spectra of inelastically scattered neutrons and yields a qualitative description of the main characteristics of the nuclear fusion process, phase-transition range and so on. The spin dependence of nuclear level density and the dependence of the equilibrium deformation of nuclei on excitation energy are also considered. The internal consistency of the model and the fact that it explains the different average characteristics of excited nuclei justify the hope that the proposed method will provide a reliable basis for calculating and evaluating nuclear data.

ПЛОТНОСТЬ ВОЗБУЖДЕННЫХ СОСТОЯНИЙ АТОМНЫХ ЯДЕР.

Для оценки средних нейтронных сечений необходима детальная и надежная информация о ширинах соответствующих процессов, которые в статистической теории ядерных реакций выражаются через плотность возбужденных состояний конечных продуктов реакции. Высокие требования к точности и надежности оценки реакторных констант делают необходимым развитие новых методов расчета энергетической зависимости плотности ядерных уровней. Использование общепринятой модели ферми-газа не дает последовательного описания свойств возбужденных ядер. В данной работе рассмотрены результаты расчетов плотности уровней, в которых учтены индивидуальные свойства ядер, связанные с их оболочечной структурой. Расчеты основаны на модели сверхтекучего ядра, успешно применяемой в настоящее время при анализе свойств низколежащих состояний ядер. Они не содержат дополнительных параметров и позволяют связать в едином подходе свойства высоковозбужденных ядер со свойствами ядер в основном и слабо возбужденном состояниях. Проведенные расчеты показали, что дискретная структура одночастичного спектра приводит к существенным изменениям энергетической зависимости плотности уровней по сравнению с моделью ферми-газа, дает естественное объяснение аномалий, наблюдаемых в спектрах неупруго рассеянных нейтронов, приводит к качественному описанию основных особенностей процесса деления ядер, области фазового перехода и т.д. Исследована спиновая зависимость плотности ядерных уровней и зависимость равновесной деформации ядер от энергии возбуждения. Внутренняя согласованность модели, объяснение различных средних характеристик возбужденных ядер позволяют надеяться, что предложенный метод расчета плотности уровней даст надежную основу для расчета и оценки ядерных данных.

ВВЕДЕНИЕ

Применение статистического подхода для расчетов сечений реакций, ширин различных процессов, спектров частиц, испущенных в реакциях, и т. д., требует знания плотности возбужденных состояний ядер в широком интервале энергий возбуждения. Простые аналитические выражения для этой величины, полученные впервые Бете [1] в модели ферми-газа, в настоящее время широко используются при анализе экспериментальных данных [3-5]. При этом фактически пренебрегают двумя важными эффектами: наличием дискретной структуры спектра одночастичных состояний и влиянием остаточных взаимодействий. Качественному рассмотрению этих эффектов был посвящен целый ряд работ. Влияние вырождения уровней модели оболочек было исследовано Розенцвейгом [6] в рамках модели невзаимодействующих частиц с периодическим одночастичным спектром. Эффекты остаточных взаимодействий корреляционного типа были рассмотрены в приближении непрерывного спектра в работах [7]. Однако применение этих результатов, полученных на упрощенных моделях, для описания свойств реальных ядер является затруднительным.

В работе [8] были получены термодинамические характеристики возбужденных ядер в рамках модели сверхтекучего ядра при строгом учете структуры одночастичного спектра. В данной работе показано, что такой подход позволяет проследить за влиянием оболочечной структуры на плотность возбужденных состояний ядер и оценить точность приближений, используемых при различных упрощенных рассмотрениях. Представленные результаты описывают широкий круг явлений, связанных с поведением высоко возбужденных ядер.

1. ОСНОВНЫЕ СООТНОШЕНИЯ

Общее выражение для плотности возбужденных состояний ядер может быть получено с помощью хорошо известного в статистической физике метода Дарвина-Фаулера [1-5]. Для системы, состоящей из Z протонов и N нейтронов и обладающей энергией E и проекцией M момента количества движения на выбранное направление, можно записать плотность возбужденных состояний в виде:

$$\rho(E, Z, N, M) = (2\pi i)^{-\nu} \int_{\gamma_1-i\infty}^{\gamma_1+i\infty} d\beta \int_{\gamma_2-i\infty}^{\gamma_2+i\infty} d\alpha_M \int_{\gamma_3-i\infty}^{\gamma_3+i\infty} d\alpha_Z \int_{\gamma_\nu-i\infty}^{\gamma_\nu+i\infty} d\alpha_N \times \exp\{\beta(E-\Omega) - \alpha_Z Z - \alpha_N N - \alpha_M M\} \quad (1)$$

Здесь: Ω – термодинамический потенциал системы; $\beta = t^{-1}$; $\alpha_k = \lambda_k t^{-1}$; t – термодинамическая температура и λ_k – химический потенциал, обеспечивающий сохранение в системе соответствующего интеграла движения (Z, N и M). Используя для вычисления интегралов метод седловой точки, имеем:

$$\rho(E, Z, N, M) = (2\pi)^{-2} \left| \det \frac{\partial^2 \alpha_0 \Omega}{\partial \alpha_i \partial \alpha_j} \right|^{-1/2} \exp\{S(\alpha_{i0})\}; \quad (2)$$

$$i = 0, 1, 2, 3; \quad \alpha_0 \equiv \beta;$$

где $S(\alpha_{i0})$ – значение логарифма подинтегральной функции, вычисленное в седловой точке, определяемой уравнением:

$$\frac{\partial S}{\partial \alpha_i}\Big|_{\alpha_i=\alpha_{i0}} = 0. \tag{3}$$

Выражение (1) можно рассматривать как определение плотности возбужденных состояний системы. Оно получено обращением статистической суммы и не связано с использованием каких-либо модельных представлений о системе. Выражение (2) содержит, однако, неточности, связанные с использованием метода седловой точки для вычисления интегралов. Точность метода седловой точки для ряда примеров обсуждалась в литературе [9, 10]. Для области энергий возбуждения, представляющих интерес для ядер, эта неточность не превышает нескольких процентов.

Модельные представления о системе приходится привлекать при вычислении термодинамического потенциала. В модели невзаимодействующих ферми-частиц двух сортов имеем:

$$\begin{aligned} -\beta\Omega &= -\beta(\Omega_Z + \Omega_N) \\ -\beta\Omega_Z &= \sum_i g_i \ln\left\{1 + \exp[\beta(\lambda_Z + m_i\lambda_M - \epsilon_i)]\right\} \end{aligned} \tag{4}$$

и аналогично для Ω_N. Здесь: ϵ_i – энергия одночастичных состояний; m_i – проекция момента количества движения частицы в этом состоянии и g_i – кратность вырождения i-того состояния.

Чтобы получить выражение для плотности уровней (2) в явном виде, необходимо вычислить (4). Обычно при этом используют приближение непрерывного спектра, т.е. предполагают, что плотность одночастичных состояний можно описать плавной функцией $g(\epsilon)$ и заменить суммирование по одночастичным состояниям интегрированием. Модель невзаимодействующих частиц в приближении непрерывного спектра мы будем называть моделью ферми-газа. Для вычисления возникающих интегралов используют еще два дополнительных приближения: 1) приближение низких температур $t\lambda_N^{-1} \ll 1$ и 2) приближение малых моментов $\overline{m}\lambda_M \ll \lambda_N$. Для плотности уровней при этом получим хорошо известный результат:

$$\rho(U,Z,N,M) = \frac{\sqrt{2}}{24a^{1/4}U^{5/4}\sigma}\exp\left\{2\sqrt{a(U - M^2/2F)}\right\} \tag{5а}$$

В приближении малых моментов $U \gg M^2/2F$ имеем:

$$\rho(U,Z,N,M) = \frac{\sqrt{2}}{24a^{1/4}U^{5/4}\sigma}\exp\left\{2\sqrt{aU} - M^2/2\sigma^2\right\} \tag{5б}$$

Для термодинамических функций системы имеем:

$$\begin{aligned} U &= at^2 + M^2/2F \\ S &= 2at = 2\sqrt{a(U - M^2/2F)} \approx 2\sqrt{aU} - M^2/2\sigma^2 \\ \sigma^2 &\equiv Ft = g\overline{m_f^2}t \qquad F = g\overline{m_f^2} \end{aligned} \tag{6}$$

Здесь: U – энергия возбуждения, S – энтропия, F – момент инерции ядра, σ^2 называют параметром спиновой зависимости плотности уровней. Основными параметрами этих выражений являются a и $\overline{m_f^2}$, определенные как:

$$a = \frac{\pi^2}{6} g = \frac{\pi^2}{6} (g_Z + g_N)$$
$$\overline{m_f^2} = \frac{\overline{m_{fZ}^2} g_Z + \overline{m_{fN}^2} g_N}{g_Z + g_N} \qquad (7)$$

где: g_Z и g_N – плотности одночастичных состояний на поверхности Ферми, а $\overline{m_f^2}$ – средний квадрат проекции момента нуклонов в этих состояниях.

Плотность уровней ядра с энергией возбуждения U и моментом количества движения I можно получить из (5б) в виде [1]:

$$\rho(U,Z,N,M) = \frac{2I+1}{24\sqrt{2}\, a^{1/4} U^{5/4} \sigma^3} \exp\left\{ 2\sqrt{aU} - \frac{(I+1/2)^2}{2\sigma^2} \right\} \qquad (8)$$

Каждый из этих уровней 2I + 1 – кратно вырожден по проекции момента. Полную плотность состояний можно получить, суммируя (5б) по всем значениям проекции момента или (8) по всем значениям момента, с учетом их вырождения:

$$\rho(U,Z,N) = \frac{\sqrt{\pi}}{12\, a^{1/4} U^{5/4}} \exp\left[2\sqrt{aU} \right] \qquad (9)$$

Плотность уровней ядра в модели невзаимодействующих ферми-частиц можно вычислить без использования приближения непрерывного спектра [8,11]. В этом случае система уравнений (3), определяющих седловую точку, имеет вид:

$$E = \sum_i \epsilon_{iZ} g_{iZ} \bar{n}_{iZ} + \sum_i \epsilon_{iN} g_{iN} \bar{n}_{iN}$$
$$Z = \sum_i g_{iZ} \bar{n}_{iZ} \qquad N = \sum_i g_{iN} \bar{n}_{iN} \qquad (10)$$
$$M = \sum_i m_{iZ} g_{iZ} \bar{n}_{iZ} + \sum_i m_{iN} g_{iN} \bar{n}_{iN}$$

где средние числа заполнения протонных одночастичных состояний определены как:

$$\bar{n}_{iZ} = \{ 1 + \exp(\beta \epsilon_{iZ} - \alpha_Z - m_{iZ} \alpha_M) \}^{-1} \qquad (11)$$

Аналогичные выражения имеем для n_{iN}. В качестве m_i удобно выбрать проекцию одночастичного момента количества движения на ось симметрии ядра. Для ядер с аксиальной симметрией одночастичные состояния $|m_i\rangle$ вырождены по знаку проекции на ось симметрии, поэтому можно провести суммирование по знаку m_i в приближении малых моментов:

$$\bar{n}_{i+} + \bar{n}_{i-} \simeq 2\bar{n}_i - m_i^2 \alpha_M^2 \bar{n}_i (1 - \bar{n}_i)(1 - 2\bar{n}_i)$$
$$\bar{n}_{i+} - \bar{n}_{i-} \simeq 2m_i \alpha_M \bar{n}_i (1 - \bar{n}_i) \qquad (12)$$

и получить выражение для α_M в виде:

$$\alpha_M = \frac{M}{2\sum_{N,Z}\left\{\sum_i m_i^2 g_i \bar{n}_i (1 - \bar{n}_i)\right\}} \qquad (13)$$

В этом случае система четырех уравнений (10) для седловой точки сводится к системе трех уравнений:

$$E = \sum_{N,Z}\left\{2\sum_i \epsilon_i g_i \bar{n}_i\right\} + M^2/2F_{\perp}$$
$$Z = 2\sum_i g_{iZ}\bar{n}_{iZ} \qquad N = 2\sum_i g_{iN}\bar{n}_{iN} \qquad (14)$$

Для энтропии имеем:

$$S = \sum_{N,Z}\left\{2\sum_i\left[\beta(\epsilon_i - \lambda)\bar{n}_i + \ln(1 + \exp\{\lambda - \beta\epsilon_i\})\right]\right\} - \frac{\beta M^2}{2F_{\perp}} \qquad (15)$$

Здесь момент инерции ядра относительно оси симметрии определен как:

$$F_{\perp} = \beta\sum_{N,Z}\left\{2\sum_i m_i^2 g_i \bar{n}_i (1 - \bar{n}_i)\right\} \qquad (16)$$

В (12) – (16) средние числа заполнения (11) взяты при $\alpha_M = 0$.

Решив систему уравнений (14) относительно β, λ_Z и λ_N с помощью (15) и (2), можно вычислить $\rho(U,Z,N,M)$. Связь полной энергии E с энергией возбуждения U имеет вид:

$$U = \sum_{N,Z}\left\{2\sum_i \epsilon_i g_i (n_i - n_{i0})\right\} + M^2/2F_{\perp} \qquad (17)$$

где n_{i0} – числа заполнения в основном состоянии (t = 0)

Приведенные соотношения позволяют для заданной схемы одночастичных состояний найти термодинамические характеристики и плотность состояний возбужденного ядра в модели невзаимодействующих частиц без введения каких-либо параметров. Полученные при этом результаты могут быть также использованы для оценки точности асимптотических выражений модели ферми-газа (7).

Реальное взаимодействие между нуклонами в ядре не сводится к одному самосогласованному полю, и поэтому движение нуклонов в ядре не описывается только движением невзаимодействующих частиц в самосогласованном потенциале. После выделения самосогласованной части потенциала остается некоторое взаимодействие между частицами. Такое остаточное взаимодействие может быть слабым, но оно имеет принципиальное значение для многих ядерных явлений. Было показано [12,13], что для

основных и первых возбужденных состояний ядер остаточное взаимодействие имеет много общего с силами спаривания в теории сверхпроводимости. Для учета этого взаимодействия был применен математический аппарат, разработанный Бардиным, Купером, Шриффером и Боголюбовым [14,15] (БКШ). Этот аппарат может быть использован для описания термодинамических характеристик возбужденных ядер. Влияние парных корреляций на плотность возбужденных состояний ядер в приближении непрерывного спектра было исследовано в работах [7]. Для последовательного учета влияния оболочечной структуры одночастичного спектра и парных корреляций на свойства возбужденных ядер необходимо вычисление термодинамических характеристик и плотности уровней ядер без использования приближения непрерывного спектра [8,11].

Если матричный элемент парного взаимодействия в модели сверхтекучего ядра выбрать следующим образом:

$$G_{k\,k'} = \begin{cases} 0 & k, k' < f \quad \text{или} \quad k, k' > f' \\ G_Z & f \leqslant k, k' \leqslant f' \end{cases} \tag{18}$$

то система уравнений, определяющая термодинамические функции, для протонной компоненты имеет вид:

$$\begin{aligned} \frac{2}{G_Z} &= \sum_{k=f}^{f'} \frac{\mathrm{th}(\beta E_k/2))}{E_k} \\ Z &= 2\left\{ \sum_{k=1}^{f-1} \bar{n}_k + \sum_{k=f'+1}^{\infty} \bar{n}_k \right\} + \sum_{k=f}^{f'} \left(1 - \frac{\epsilon_k - \lambda}{E_k} \,\mathrm{th}\, \frac{\beta E_k}{2} \right) \\ E_Z &= 2\left\{ \sum_{k=1}^{f-1} \epsilon_k \bar{n}_k + \sum_{k=f'+1}^{\infty} \epsilon_k \bar{n}_k \right\} \\ &\quad + \sum_{k=f}^{f'} \epsilon_k \left(1 - \frac{\epsilon_k - \lambda}{E_k} \,\mathrm{th}\, \frac{\beta E_k}{2} \right) - \frac{\Delta_Z^2}{G_Z} \end{aligned} \tag{19}$$

$$\begin{aligned} S_Z &= 2\left[\sum_{k=1}^{f-1} + \sum_{k=f'+1}^{\infty} \right] \left\{ \beta(\epsilon_k - \lambda)\bar{n}_k + \ln\left[1 + \exp\beta(\lambda - \epsilon_k)\right] \right\} \\ &\quad + 2 \sum_{k=f}^{f'} \left\{ \beta E_k (1 + \exp \beta E_k)^{-1} + \ln\left[1 + \exp(-\beta E_k)\right] \right\} \end{aligned} \tag{20}$$

где:

$$E_k = \sqrt{(\epsilon_k - \lambda)^2 + \Delta_Z^2} \tag{21}$$

и n_k определено в (11). Для основного состояния ($t = 0$) уравнения БКШ имеют вид:

$$\frac{2}{G_Z} = \sum_{k=f}^{f'} \frac{1}{E_k}$$

$$Z = 2(f - 1) + \sum_{k=f}^{f'} \left(1 - \frac{\epsilon_k - \lambda}{E_k} \right) \qquad (22)$$

$$E_{Z0} = 2 \sum_{k=1}^{f-1} \epsilon_k + \sum_{k=f}^{f'} \epsilon_k \left(1 - \frac{\epsilon_k - \lambda}{E_k} \right) - \frac{\Delta_{Z0}^2}{G_Z}$$

Эффекты парных корреляций исчезают при температурах выше критической температуры, определяемой уравнениями:

$$\frac{2}{G_Z} = \sum_{k=f}^{f'} \frac{\text{th}\, \beta(\epsilon_k - \lambda)/2}{\epsilon_k - \lambda}$$

$$Z = 2 \sum_{k=1}^{\infty} \bar{n}_k \qquad (23)$$

и поведение термодинамических функций совпадает с их поведением в модели невзаимодействующих с частиц. В этих уравнениях предполагается, что одночастичные уровни двукратно вырождены.

Для нейтронной компоненты уравнения имеют вид, аналогичный (18-23).

Уравнения (19-23) написаны для равной нулю проекции полного момента количества движения. В приближении малых моментов спиновая зависимость плотности уровней в модели БКШ была исследована Каммури [16]. Для энтропии и энергии возбуждения ядра в этом случае имеем:

$$S = S_Z + S_N - M^2/2\sigma^2$$

$$U = E_Z - E_{Z0} + E_N - E_{N0} + M^2/2F_{\perp} \qquad (24)$$

где:

$$F_{\perp} \equiv \beta\sigma^2 = \sum_{N,Z} \left\{ 2 \left[\sum_{k=1}^{f-1} + \sum_{k=f'+1}^{\infty} \right] m_k^2 \bar{n}_k (1 - \bar{n}_k) + \sum_{k=f}^{f'} m_k^2 / 2 \, \text{ch}^2 \frac{\beta E_k}{2} \right\} \qquad (25)$$

Соотношение (18-25) позволяют вычислить при заданной схеме одночастичных уровней термодинамические характеристики и плотность уровней в модели сверхтекучего ядра.

2. ВЛИЯНИЕ ДИСКРЕТНОЙ СТРУКТУРЫ ОДНОЧАСТИЧНОГО СПЕКТРА НА ТЕРМОДИНАМИЧЕСКИЕ ХАРАКТЕРИСТИКИ ЯДЕР

Наиболее наглядно влияние дискретной структуры можно проследить на примере однокомпонентной системы в модели невзаимодействующих частиц. Чтобы показать отличие соотношений (6) модели ферми-газа от точного решения задачи, введем следующие величины:

$$\bar{a} = \frac{\pi^2}{6}\beta\sum_k g_k\bar{n}_k(1-\bar{n}_k)$$
$$a' = S^2/4U \qquad a'' = U/t^2 \qquad a''' = S/2t \tag{26}$$

$$\overline{m^2} = \frac{\sum_k m_k^2 g_k \bar{n}_k(1-\bar{n}_k)}{\sum_k g_k\bar{n}_k(1-\bar{n}_k)} \tag{27}$$

Эти соотношения выбраны таким образом, что в модели ферми-газа все величины в (26) переходят в параметр a плотности уровней, а (27) – в параметр $\overline{m_f^2}$.

Результаты расчетов этих величин представлены на рис. 1, показана также зависимость термодинамической температуры и момента инерции системы от энергии возбуждения. Сплошной кривой показаны результаты для магического числа нуклонов Z = 82. Одночастичный спектр в этом случае имеет ярко выраженную оболочечную структуру. Пунктиром даны результаты расчетов со схемой уровней, типичной для деформированных ядер (Z = 92).

Величины, определенные в (26), не являются постоянными и не равны друг другу. Однако, для схемы, соответствующей деформированным ядрам, зависимость от энергии возбуждения слабая, и различия между разными a невелики. В этом случае для описания термодинамических функций системы можно использовать параметр a модели ферми-газа с точностью порядка 10% и параметр $\overline{m_f^2}$ с точностью $< 5\%$. Для магического числа неуклонов все величины a в (26) сильно зависят от энергии возбуждения и заметно отличаются друг от друга по абсолютной величине. Поведение термодинамической температуры и момента инерции $F_{\parallel}$ также значительно отличается от ферми-газового. Следует отметить, что здесь проявляется принципиально важный эффект – зависимость средней плотности однонуклонных состояний вблизи энергии Ферми от энергии возбуждения, который отсутствует в модели ферми-газа.

При наличии сильного вырождения одночастичных уровней поведение термодинамических функций существенно зависит от степени заполнения последней подоболочки в основном состоянии. На рис. 2 показаны результаты расчетов энергетической зависимости температуры, энтропии и величины a' для подоболочки $1g_{9/2}$ (Z = 40-50). Характер зависимости a' при небольших энергиях возбуждения различен для наполовину заполненной и полностью заполненной (или свободной) подоболочки. Видна симметрия относительно наполовину заполненной подоболочки в поведении термодинамических функций. Влияние вырождения одночастичных уров-

ней на плотность состояний ядер рассматривалось Розенцвейгом [6] на модели периодической одночастичной схемы. Такой подход дает качественное описание оболочечных эффектов, подобных представленным на рис. 2, однако, он не применим для реальной схемы уровней модели оболочек, где нет строгой периодичности в положении и кратности вырождения подоболочек [17].

Для реальных ядер наложение протонной и нейтронной компонент может приводить как к усилению, так и к ослаблению указанных эффектов [8]. Это можно проследить на рис. 3 и 4, где представлены результаты расчетов a', $\bar{a}$, $\overline{m^2}$, F_n в модели невзаимодействующих частиц с потенциалом

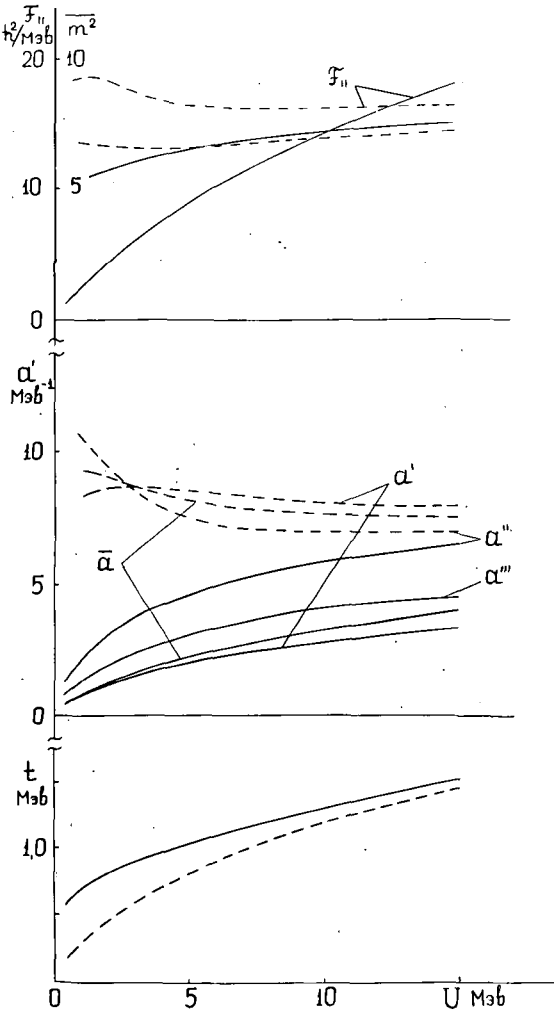

Рис. 1. Термодинамические характеристики однокомпонентной системы. Сплошная кривая – расчеты с одночастичной схемой магического ядра (Z = 82), пунктирная – со схемой деформированных ядер (Z = 92, ϵ = 0,25). Для Z = 92 отложена величина $F_n/2$.

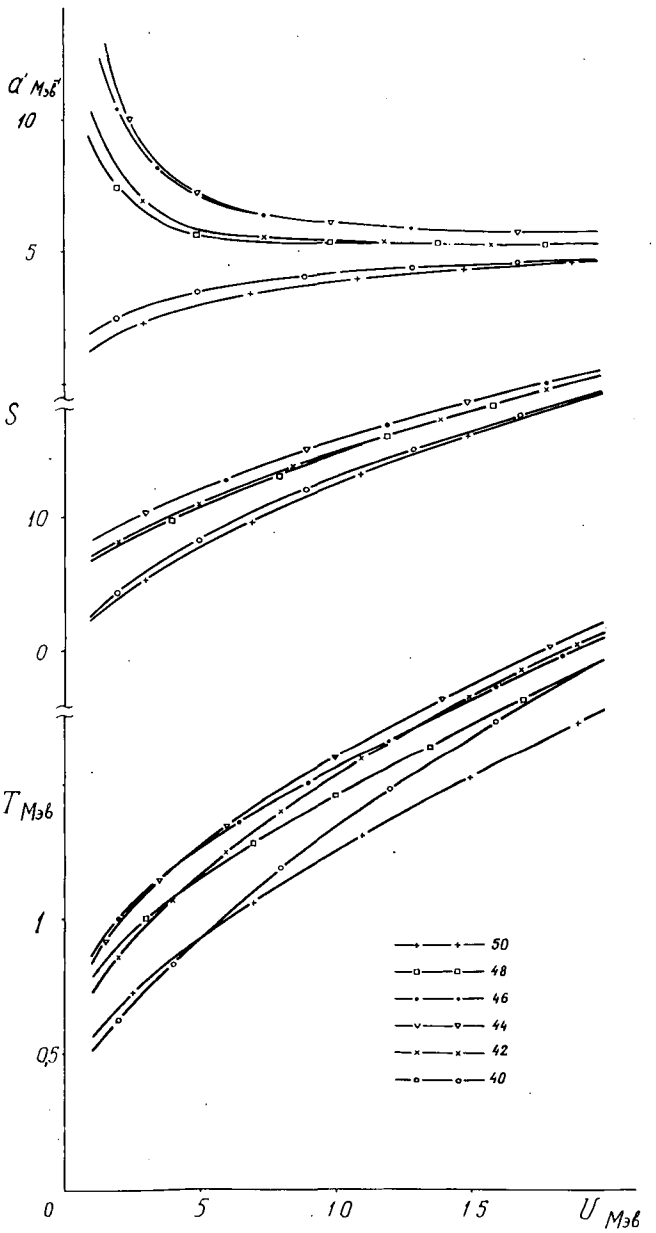

Рис. 2. Зависимость термодинамических функций модели невзаимодействующих частиц от степени заполнения подоболочки $1g_{9/2}$.

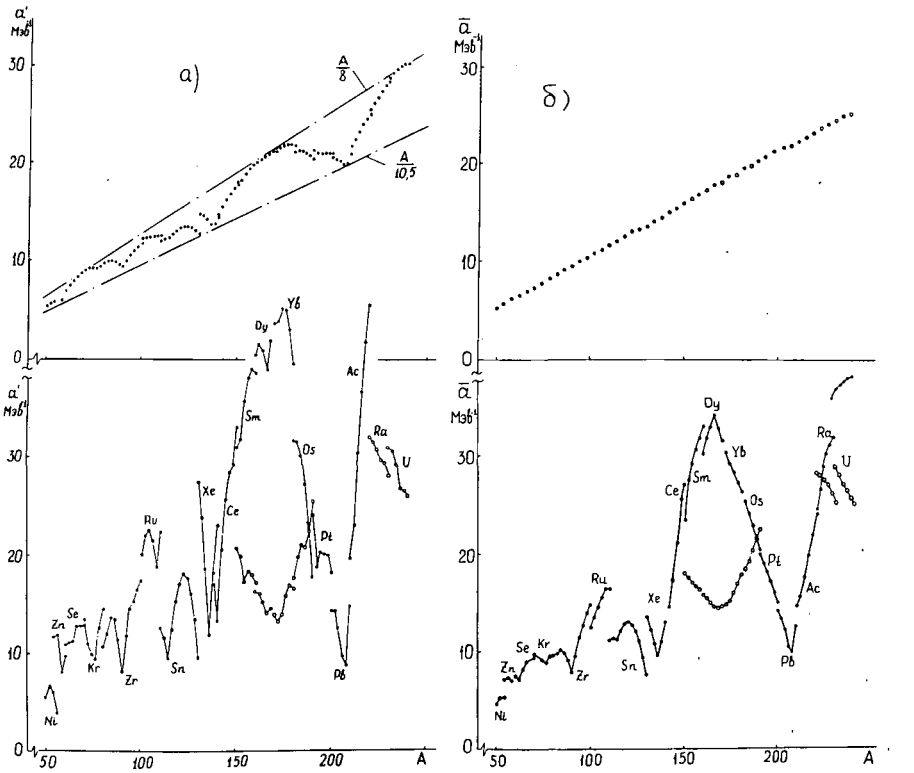

Рис. 3. "Параметры" a' и ā модели невзаимодействующих частиц для энергий возбуждения 7 Мэв (нижняя часть рисунков) и 100 Мэв (верхняя часть). Темными кружками показаны результаты расчетов для сферических ядер, светлыми – для деформированных ($\epsilon = 0{,}3$ в области редких земель и $\epsilon = 0{,}2$ для актинидов).

Нильссона [18] для ядер в широком интервале массовых чисел [19]. При энергии возбуждения 7 Мэв в поведении a' и ā отчетливо проявляется хорошо известный экспериментально эффект – уменьшение параметра плотности уровней вблизи магических ядер. Аналогичная зависимость имеет место для $\overline{m^2}$ и $F_{\parallel}$. При достаточно больших энергиях возбуждения (100 Мэв) оболочечные неоднородности одночастичного спектра уже не оказывают заметного влияния на термодинамические характеристики системы; полученную в расчетах зависимость рассматриваемых величин от массового числа можно представить в простом виде:

$$\begin{aligned} \bar{a} &= (0{,}105 \pm 0{,}005)\, A \text{ Мэв}^{-1} \\ \overline{m^2} &= (0{,}290 \pm 0{,}005)\left(1 - \frac{2}{3}\epsilon\right) A^{2/3} \\ F &= (0{,}0185 \pm 0{,}0005)\left(1 - \frac{2}{3}\epsilon\right) A^{5/3}\, \hbar^2 \text{ Мэв}^{-1} \end{aligned} \qquad (28)$$

где ϵ – параметр квадрупольной деформации ядра [18].

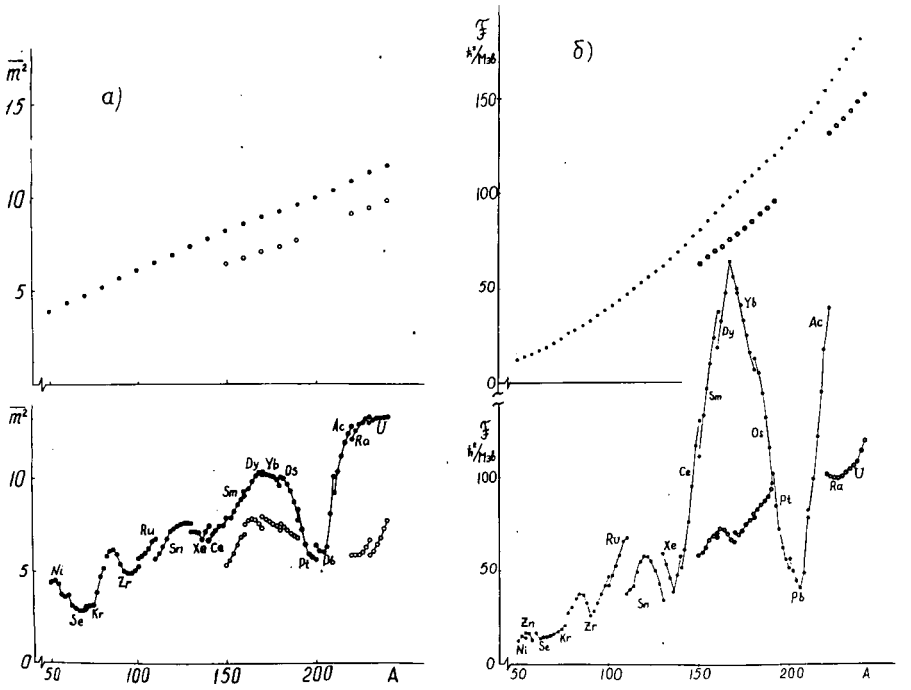

Рис. 4. "Параметры" $\overline{m^2}$ и F_{II} модели невзаимодействующих частиц для энергий возбуждения 7 Мэв (нижняя часть рисунков) и 100 Мэв (верхняя часть). Темными кружками показаны результаты расчетов для сферических ядер, светлыми – для деформированных ($\epsilon = 0{,}3$ в области редких земель и $\epsilon = 0{,}2$ для актинидов).

Исчезновение оболочечной структуры с ростом энергии возбуждения не учитывается моделью ферми-газа, и в ряде случаев это должно приводить к заметному отличию ее предсказаний от экспериментальных значений плотности уровней при высоких энергиях возбуждения.

3. ВЛИЯНИЕ ПАРНЫХ КОРРЕЛЯЦИЙ

Наличие парных корреляций приводит к важному отличию поведения термодинамических функций по сравнению с моделью невзаимодействующих частиц. Результаты расчетов термодинамических функций ^{176}Hf и ^{236}U на основе соотношений (19-25) представлены на рис. 5. В этих расчетах была использована схема уровней, соответствующая деформированным ядрам, где эффекты неоднородности одночастичного спектра очень слабы, и роль парных корреляций видна наиболее наглядно. Величина a' определена так же, как и в модели невзаимодействующих частиц (26), а величина $\overline{m^2}$ определена как $\overline{m^2} = \sigma^2/(A - \bar{A})^2$:

$$(A - \bar{A})^2 = \sum_{N,Z} \left\{ 2 \left[\sum_{k=1}^{f-1} + \sum_{k=f'+1}^{\infty} \right] \bar{n}_k (1 - \bar{n}_k) + \sum_{k=f}^{f'} \frac{1}{2\,\mathrm{ch}^2 \dfrac{\beta E_k}{2}} \right\} \qquad (29)$$

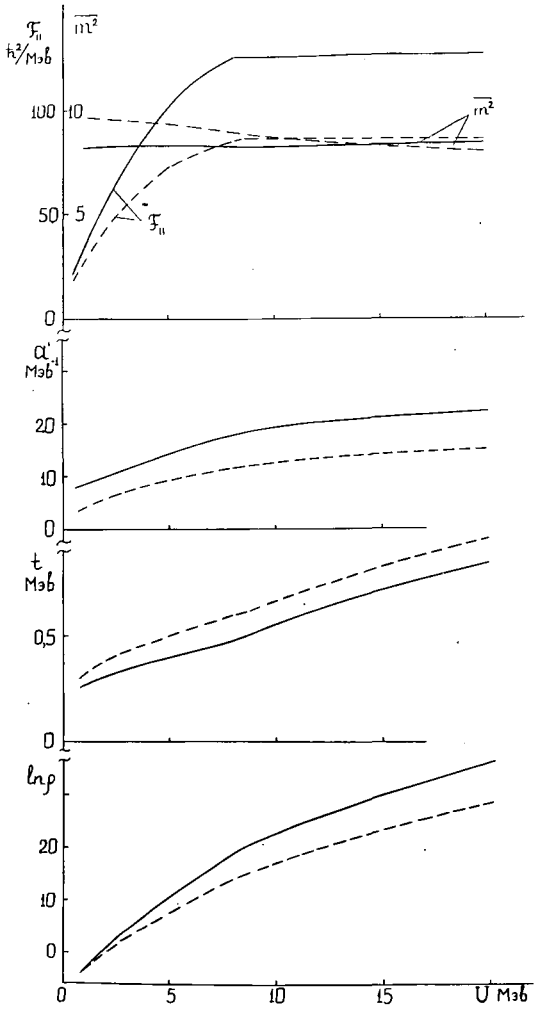

Рис. 5. Термодинамические функции ^{176}Hf (пунктир) и ^{236}U (сплошная кривая) в модели сверхтекучего ядра.

Такое определение $\overline{m^2}$ аналогично определению $\overline{m_f^2}$ в приближении непрерывного спектра, и при температуре, выше критической (29), тождественно (27). Видны типичные особенности, обусловленные парными корреляциями: излом в зависимости плотности уровней и термодинамической температуры от энергии возбуждения ниже точки фазового перехода из сверхпроводящего состояния в нормальное, резкое уменьшение момента инерции.

Выше критической энергии поведение термодинамических функций описывается моделью невзаимодействующих частиц с энергией возбуждения, сдвинутой на величину энергии конденсации, так что:

$$\rho_{БКШ}(U) = \rho_{невз}(U - E_{конд}) \qquad (30)$$

где энергия конденсации определяется как разность энергий основных состояний ядра без учета и с учетом парных взаимодействий. В приближении непрерывного спектра:

$$E_{конд} = \frac{1}{4}(g_Z \Delta_{ZO}^2 + g_N \Delta_{NO}^2) \qquad (31)$$

Ниже критической энергии влияние парных корреляций не сводится к перенормировке энергии возбуждения. Например, зависимость момента инерции от энергии возбуждения является характерным свойством модели сверхтекучего ядра.

Для деформированных ядер, какими являются Hf и U, одночастичная схема достаточно однородна, поэтому влияние парных корреляций может быть описано в приближении непрерывного спектра [7]. Однако, во многих случаях, особенно для сферических ядер, происходит наложение эффектов парных корреляций и оболочечных эффектов, и приближение непрерывного спектра оказывается некорректным.

4. ВЛИЯНИЕ СПЕКТРА ОДНОЧАСТИЧНЫХ СОСТОЯНИЙ

В настоящее время для описания свойств ядер широко используется одночастичный потенциал анизотропного осциллятора, предложенный Нильссоном [18]. Такой потенциал удобен для использования, однако, он недостаточно корректно передает ряд свойств самосогласованного поля ядра: конечную глубину и диффузность потенциальной ямы. Рассмотрим влияние выбора одночастичного потенциала на результаты расчетов термодинамических функций ядер. На рис. 6 показаны схемы одночастичных уровней в потенциале Нильссона и потенциале Саксона-Вудса [20] для ядра ^{208}Pb. Последовательность уровней близка в обеих схемах, но имеется некоторое отличие в величине оболочечной щели. Кроме того, в схеме Саксона-Вудса отсутствуют уровни положительной энергии с малыми моментами. Параметры потенциала взяты из [21].

Результаты расчетов термодинамических характеристик возбужденного ядра ^{208}Pb для обеих схем показаны на рис. 7. Так как для дважды магических ядер корреляционные функции $\Delta_{ZO} = \Delta_{NO} = 0$ уже для основного состояния, то поведение соответствующих характеристик описывается моделью невзаимодействующих частиц.

Как было показано выше, при больших энергиях возбуждения ($\sim$ 100 Мэв) оболочечные эффекты не проявляются, и для потенциала Саксона-Вудса соотношения, аналогичные (28), имеют вид:

$$\begin{aligned} \tilde{a} &= (0{,}090 \pm 0{,}005)\ A\ \text{Мэв}^{-1} \\ \overline{m^2} &= (0{,}263 \pm 0{,}005)\left(1 - \frac{2}{3}\epsilon\right) A^{2/3} \\ F_{II} &= (0{,}0144 \pm 0{,}0005)\left(1 - \frac{2}{3}\epsilon\right) A^{5/3}\ \hbar^2\ \text{Мэв}^{-1} \end{aligned} \qquad (32)$$

Отличие коэффициентов в (28) и (32) связано с конечностью глубины и диффузностью потенциальной ямы.

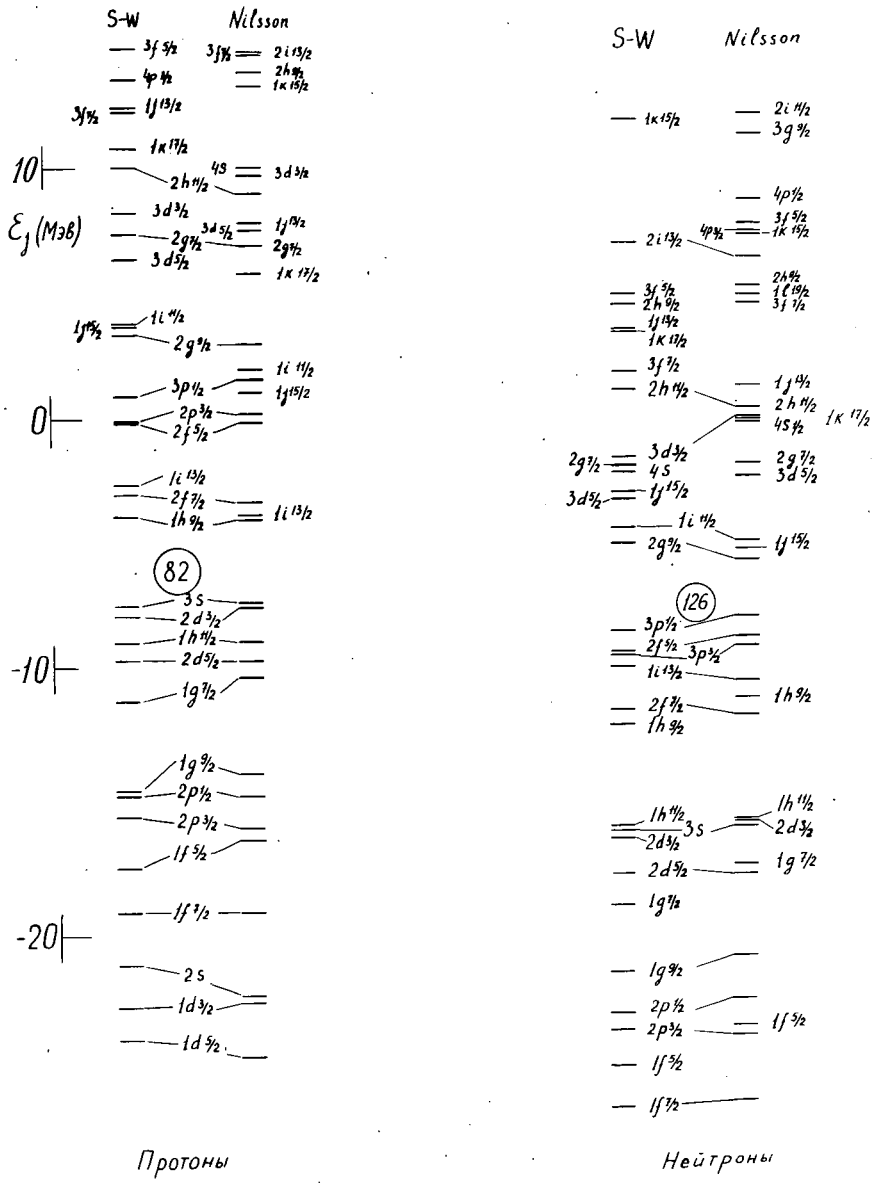

Рис. 6. Схемы одночастичных состояний Саксона-Вудса и Нильссона для ядра ^{208}Pb.

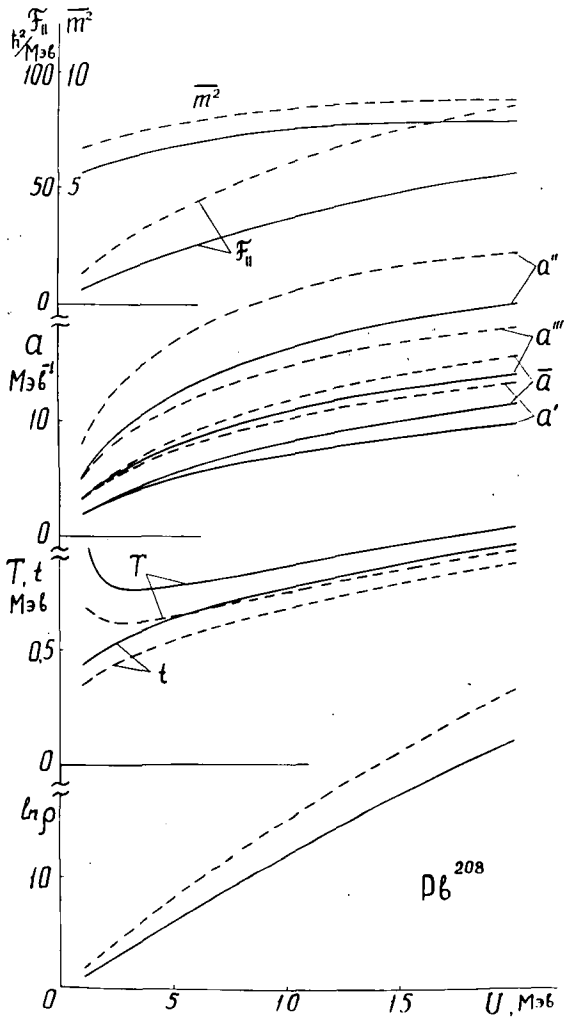

Рис. 7. Термодинамические функции ^{208}Pb для схемы Саксона-Вудса (сплошные кривые) и схемы Нильссона (пунктир).

5. ПЛОТНОСТЬ УРОВНЕЙ ЯДЕР С ЧЕТНЫМ И НЕЧЕТНЫМ ЧИСЛОМ НУКЛОНОВ

Хорошо известным экспериментальным фактом является значительное различие плотностей уровней ядер, отличающихся четностью числа нейтронов или протонов. Для объяснения этого различия в модели ферми-газа вводится эффективная энергия возбуждения:

$$U_{эфф} = U - \begin{cases} 0 \text{ для неч.-неч. ядер} \\ \delta_Z \text{ или } \delta_N \text{ для неч. ядер} \\ \delta_Z + \delta_N \text{ для чет.-чет. ядер} \end{cases} \qquad (33)$$

Из анализа плотности нейтронных резонансов было найдено, что величины δ можно отождествить с энергией спаривания [35]. Для протонов энергию спаривания обычно определяют в виде:

$$P_Z(Z,N) = -\frac{1}{2}\left\{E(Z,N) - 2E(Z,-1,N) + E(Z-2,N)\right\} \qquad (34)$$

где $E(Z,N)$ – энергия связи ядер; аналогичное выражение имеется для нейтронов. Несколько иное определение энергий спаривания использовано в работе [22], где учтены плавные измерения энергии связи для соседних ядер. Неопределенность в выборе величины δ приводит к заметному отличию параметров a плотности уровней, определяемых различными авторами в модели ферми-газа [3-5].

Четно-нечетные различия в плотности уровней ядер можно объяснить на основе модели сверхтекучего ядра. Выше критической энергии фазового перехода плотность уровней описывается моделью невзаимодействующих частиц с перенормированной энергией возбуждения (30). Присутствие неспаренной частицы заметно уменьшает энергию конденсации нечетной

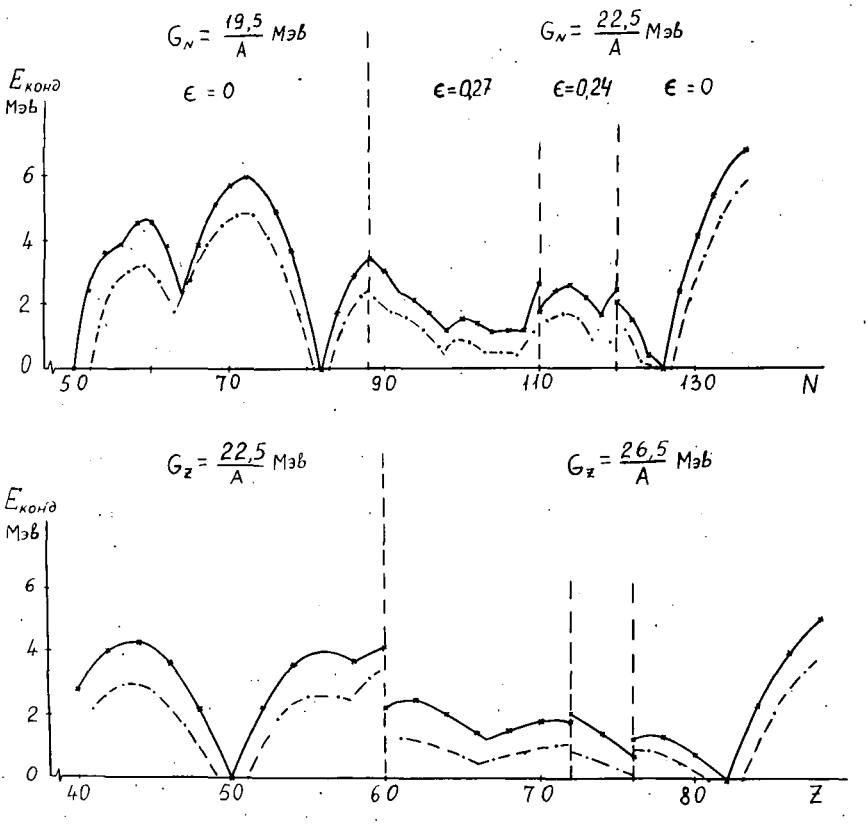

Рис. 8. Энергии конденсации четных (сплошная кривая) и нечетных (штрих-пунктир) систем для нейтронов и протонов. Для соответствующих областей нуклонов указаны константы парного взаимодействия и параметры деформации потенциала Нильссона.

системы по сравнению с системой с четным числом частиц. Такое явление получило название эффекта блокировки и подробно рассмотрено во многих работах [13,23]. Результаты вычислений энергий конденсации систем с четным и нечетным числом нуклонов представлены на рис. 8. Параметры одночастичных схем соответствуют равновесным деформациям ядер с данными Z и N, а константы парного взаимодействия определены при суммировании по 42 уровням среднего поля в (22) [23]. Видно систематическое отличие энергий конденсации для четного и нечетного числа нуклонов, и эта разность близка по величине к энергиям спаривания (34). В большинстве случаев энергии фазового перехода близки к энергиям связи нейтрона, так что наблюдаемое четно-нечетное различие в плотности нейтронных резонансов получает естественное объяснение на основе соотношения (30). Ниже критической энергии влияние неспаренной частицы имеет более сложный характер.

Следует иметь в виду, что имеется существенное различие в описании остаточных взаимодействий в модели сверхтекучего ядра и их феноменологическом учете в модели ферми-газа (33). В большинстве нечетно-нечетных ядер энергия конденсации отлична от нуля (рис. 8) и может значительно превышать величину δ. Это должно привести к заметному увеличению плотности одночастичных состояний, извлекаемой из эксперимента на основе сверхтекучей модели. Такое определение параметра a было бы более последовательным по сравнению с проводимым в настоящее время.

6. СРАВНЕНИЕ С ЭКСПЕРИМЕНТОМ

Наиболее прямая и надежная информация о плотности возбужденных состояний ядер получается из экспериментальных данных по плотности нейтронных резонансов. Анализ этих данных проводится на основе соотношений модели ферми-газа (5-7) и (33) [3-5]. Извлекаемый при этом параметр a плотности уровней показан на рис. 9. Поведение параметра a в зависимости от массового числа подобно поведению величин a' и $\bar{a}$ на рис. 3, рассчитанных для энергии возбуждения 7 Мэв; видны провалы в области ядер с магическим числом нуклонов, значения a', $\bar{a}$ и a близки по абсолютной величине. Детальное сравнение этих величин не имеет смысла, поскольку a' и $\bar{a}$ зависят от энергии возбуждения. Наличие парных корреляций и отличие энергии конденсации от феноменологически учитываемой энергии спаривания требует переоценки экспериментально извлекаемого параметра a.

Представляет интерес непосредственно сравнить экспериментальные и теоретические значения плотности уровней при энергии возбуждения, равной энергии связи нейтрона B_n. Такое сравнение результатов, полученных для ряда ядер в расчетах со схемой Нильссона, проделано в [8]. Результаты расчетов со схемой Саксона-Вудса для сферических четно-четных ядер представлены в табл. 1. Экспериментальные данные и используемые при их обработке параметры взяты из работы [4] (верхняя строка для каждого элемента) и [5] (нижняя строка). Экспериментальное значение плотности возбужденных состояний получено согласно (9) для указанных параметров. В работе [5] принято $\overline{m_f^2} = 0{,}146\,A^{2/3}$, тогда как в [4] $\overline{m_f^2} = 0{,}24\,A^{2/3}$. Вместе с различием в величине δ это приводит к заметной неопределенности в величине $\ln \rho_{экс}$. Результаты вычислений

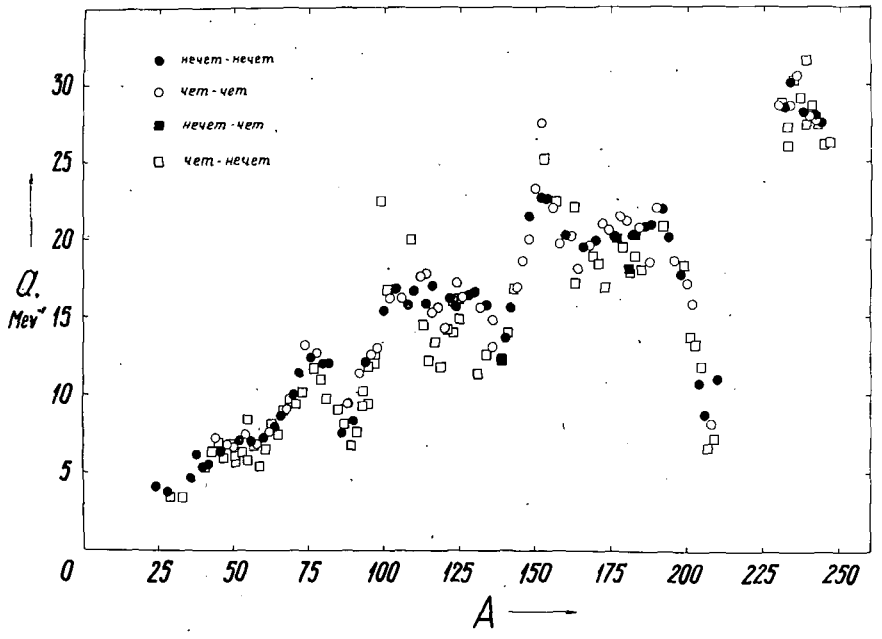

Рис. 9. Экспериментальные значения параметра a, полученные из плотности нейтронных резонансов [5].

$\overline{m^2}/m_f^2$ при больших энергиях возбуждения (28,30) указывают, что значения $\overline{m^2}/m_f^2$ следует выбирать при анализе экспериментальных данных близкими к используемым в [4]. Согласие экспериментальных и расчетных $\ln \rho(B_n)$ достаточно хорошее для ядер, тяжелее Te, но имеется систематическое отличие для более легких ядер.

Аналогичные расхождения имеются и для деформированных ядер редких земель и трансурановой области. При вычислении характеристик деформированных ядер существенным является выбор параметра деформации одночастичного потенциала. Исследование этого вопроса показало, что как для невзаимодействующих частиц, так и с учетом парных корреляций величина наиболее вероятной деформации возбужденных ядер совпадает с их равновесной деформацией в основном состоянии. Как видно из рис. 3, величины a' и $\tilde{a}$ для деформированных ядер несколько ниже экспериментальных параметров a (рис. 9). Это означает, что плотность возбужденных состояний ядер при энергии связи нейтрона, вычисленная в модели невзаимодействующих частиц, ниже экспериментально наблюдаемой, и при учете парных корреляций это различие увеличится.

Информация о плотности возбужденных состояний ядер, полученная из ядерных реакций, является менее надежной, по сравнению с данными о нейтронных резонансах, так как при этом используется ряд предположений о механизме реакций. Например, анализ спектров испарения позволяет получить энергетическую зависимость плотности уровней в широком интервале энергий возбуждения, но на эти результаты заметно влияет выбор сечения обратного процесса. Результаты измерения спектров неупруго рассеянных нейтронов показали [24], что в ряде случаев, осо-

ТАБЛИЦА 1. РЕЗУЛЬТАТЫ РАСЧЕТОВ СО СХЕМОЙ САКСОНА-ВУДСА ДЛЯ СФЕРИЧЕСКИХ ЧЕТНО-ЧЕТНЫХ ЯДЕР

Элемент	$\bar{D}_{obs}$ Мэв	a $Мэв^{-1}$	δ Мэв	B_n Мэв	$\ln \rho_{эксп}$	$\ln \rho_{расч}$
$^{74}_{32}Ge$	$7{,}7 \cdot 10^{-5}$	13,07 13,2	3,24 3,04	10,2 10,1	14,1	9,8
$^{88}_{38}Sr$	$2{,}3 \cdot 10^{-4}$ $2{,}6 \cdot 10^{-4}$	9,4 9,4	2,17 2,93	11,1	13,1 11,4	10,6
$^{92}_{40}Zr$	$2{,}3 \cdot 10^{-4}$ $3{,}0 \cdot 10^{-4}$	12,39 11,40	1,92 2,13	8,64	13,3 12,35	10,6
$^{96}_{42}Mo$	$5{,}7 \cdot 10^{-5}$ $1{,}5 \cdot 10^{-4}$	12,87 12,55	2,40 2,72	9,16	13,66 13,13	12,5
$^{98}_{42}Mo$	$8 \cdot 10^{-5}$ $1{,}6 \cdot 10^{-4}$	15,45 13,00	2,57 2,38	8,64 8,5	14,51 13,0	12,4
$^{102}_{44}Ru$	$2{,}8 \cdot 10^{-5}$ $1{,}7 \cdot 10^{-5}$	15,34 16,2	2,22 2,85	9,22 9,32	15,68 15,46	14,00
$^{106}_{46}Pd$	$1{,}33 \cdot 10^{-5}$ $0{,}9 \cdot 10^{-5}$	16,7 16,2	2,6 2,5	9,55 9,4	16,46 16,1	12,5
$^{112}_{48}Cd$	$3{,}3 \cdot 10^{-5}$	17,06 17,6	2,5 2,8	9,4 9,05	16,56 16,08	12,8
$^{114}_{48}Cd$	$2{,}7 \cdot 10^{-5}$	18,7 17,8	2,7 2,9	9,05	16,68 16,08	12,8
$^{116}_{50}Sn$	$5 \cdot 10^{-5}$	15,3	2,5	9,5	15,67	11,8
$^{118}_{50}Sn$	$4{,}5 \cdot 10^{-5}$ $5 \cdot 10^{-5}$	16,43 15,6	2,3 2,8	9,33 9,36	16,36 15,25	12,1
$^{120}_{50}Sn$	$5{,}2 \cdot 10^{-5}$ $1{,}8 \cdot 10^{-4}$	16,88 14,3	2,43 2,8	9,11	16,2 14,1	12,2
$^{126}_{52}Te$	$6{,}0 \cdot 10^{-5}$ $5 \cdot 10^{-5}$	16,32 13,3	2,23 2,65	9,1	16,18 15,56	15,4
$^{130}_{54}Xe$	$3 \cdot 10^{-5}$	16,6	2,6	9,3	16,0	16,8
$^{132}_{54}Xe$	$4 \cdot 10^{-5}$	15,1	2,26	8,9	15,4	15,7
$^{136}_{56}Ba$	$3{,}7 \cdot 10^{-5}$ $5 \cdot 10^{-5}$	15,98 14,8	2,28 2,45	9,2	16,07 15,03	15,4
$^{138}_{56}Ba$	$4 \cdot 10^{-4}$	13,7	2,43	8,54	13,47	12,1
$^{144}_{60}Nd$	$2{,}6 \cdot 10^{-5}$ $5 \cdot 10^{-5}$	18,24 16,9	1,94 2,36	7,8	16,53 14,46	14,7
$^{146}_{60}Nd$	$2 \cdot 10^{-5}$ $2{,}5 \cdot 10^{-5}$	20,1 18,6	2,1 2,2	7,6	16,2 15,26	14,7
$^{148}_{62}Sm$	$7{,}7 \cdot 10^{-6}$ $7{,}0 \cdot 10^{-6}$	20,36 20,0	2,14 2,4	8,14	17,20 16,5	15,4
$^{200}_{80}Hg$	$9{,}0 \cdot 10^{-5}$ $6{,}5 \cdot 10^{-5}$	17,62 17,1	1,7 1,73	8,0	16,2 15,8	15,8
$^{202}_{80}Hg$	$9{,}0 \cdot 10^{-5}$ $8{,}5 \cdot 10^{-5}$	16,8 15,8	1,58 1,7	7,78	15,5 14,8	14,4
$^{208}_{82}Pb$	$2 \cdot 10^{-2}$ $1{,}9 \cdot 10^{-2}$	7,31 8,1	1,21 1,1	7,7 7,4	9,0 9,5	8,5

бенно для ядер с числом нуклонов, близким к магическим, энергетическая зависимость плотности уровней не может быть описана моделью ферми-газа. Наблюдаемое в этом случае поведение плотности уровней характеризуется в диапазоне энергий возбуждения от 2 до 8 Мэв постоянной ядерной температурой, которая определяется соотношением:

$$\frac{1}{T} = \frac{d \ln \rho}{dU} \tag{35}$$

Этот результат можно объяснить рассмотренной выше зависимостью величин a' и ã от энергии возбуждения. Это наглядно видно на рис. 7, где представлены результаты расчетов ядерной температуры T для ядра ^{208}Pb. Аналогичный результат имеет место и для других околомагических ядер [25].

Влияние парных корреляций наиболее отчетливо наблюдается в поведении параметра K_0^2, определяющего угловое распределение осколков деления:

$$K_0^2 = \frac{t}{\hbar^2} \frac{F_\parallel F_\perp}{F_\perp - F_\parallel}$$

Здесь $F_\perp$ – момент инерции ядра относительно оси, перпендикулярной оси симметрии. Так как $F_\perp \gg F_\parallel$, то $K_0^2 \approx \sigma^2$ и резкое уменьшение $F_\parallel$ ниже критической энергии фазового перехода (рис. 5) непосредственно проявляется в поведении K_0^2. Величина критической энергии, получаемая в расчетах для тяжелых ядер при деформации, соответствующей положению барьера деления, удовлетворительно согласуется с экспериментальной [26].

Результаты расчетов в данном подходе указывают на существенную зависимость плотности уровней возбужденных ядер от их деформации. Непосредственная проверка этих эффектов по области стабильных ядер невозможна, поскольку она требует данных о ядре при разных деформациях. Ряд возможностей для изучения такой зависимости представляет процесс деления. Расчеты выходов продуктов деления в рамках статистического подхода позволили качественно объяснить основные особенности деления тяжелых ядер: ассиметрию выходов масс, провал средних кинетических энергий в область симметричного деления, пилообразную зависимость среднего числа нейтронов, испущенных осколками [27]. Определяющим эффектом при этом явилась зависимость плотности возбужденных состояний осколков от их деформации.

Подводя итог этому краткому обсуждению, можно сказать, что рассмотренная схема вычислений плотности возбужденных состояний ядер объясняет многие закономерности в экспериментальных данных в широкой области массовых чисел.

Для проведения расчетов необходимо знание одночастичных уровней среднего поля, особенно вблизи поверхности Ферми, и констант парного взаимодействия. В настоящее время эти величины выбираются, исходя из спектроскопических характеристик основных и первых возбужденных состояний ядер. В этом смысле расчеты плотности уровней возбужденных ядер не требуют дополнительных параметров. Однако остается неясным, в какой мере схема одночастичных уровней высоко возбужденных ядер совпадает со схемой одночастичных уровней, выбранной для основных состояний. Отличие может быть связано с изменением вклада ос-

новной части нуклон-нуклонного взаимодействия в формирование самосогласованного одночастичного потенциала. Такое изменение может возникать из-за ослабления влияния принципа Паули для высоко возбужденных ядер.

Отмеченное выше систематическое превышение экспериментальных значений плотности возбужденных состояний ядер над теоретическими для легких и деформированных ядер может быть устранено некоторым изменением параметров одночастичного потенциала. Например, увеличение ширины потенциальной ямы приведет к систематическому сгущению одночастичных состояний и, тем самым, к увеличению рассчитываемой плотности уровней. Такие изменения затрагивают, однако, широкий круг ядерных явлений и требуют детальных исследований.

ЗАКЛЮЧЕНИЕ

Обсудим теперь возможности применения информации о плотности возбужденных состояний ядер для оценки ядерных данных. Используемые в настоящее время параметры плотности уровней a и m_f^2 опираются, в основном, на результаты измерений плотности нейтронных резонансов. Параметризация этих результатов на основе модели Ферми-газа является весьма наглядной и удобной и успешно используется для экстраполяции плотности уровней в области энергий возбуждения, не слишком удаленных от энергии связи нейтрона. Однако применение этой модели для более широкого диапазона энергий возбуждения не следует считать обоснованным. Модель Ферми-газа сохраняет оболочечные эффекты при сколь угодно высоких энергиях возбуждения, что противоречит основным физическим представлениям о природе оболочек, не согласуется с экспериментальными данными о характеристиках околомагических ядер, и поведение плотности уровней при малых энергиях возбуждения не в состоянии объяснить наблюдаемое уменьшение моментов инерции.

Рассмотренные в данной работе методы расчетов плотности уровней дают естественное объяснение этих эффектов. Несмотря на некоторую громоздкость таких вычислений по сравнению с простыми аналитическими выражениями модели ферми-газа, их проведение является необходимым как при исследовании целого ряда физических явлений, так и для удовлетворения постоянно растущих требований к точности и надежности ядерных данных.

В заключение авторы хотят выразить искреннюю признательность сотрудникам Объединенного института ядерных исследований С. П. Ивановой и Н. Ю. Широковой за предоставление программ и помощь в проведении расчетов уровней в потенциале Саксона-Вудса.

ЛИТЕРАТУРА

[1] BETHE, H., Rev. mod. Phys. 9 (1937) 69.
[2] ERICSON, T., Adv. Phys. 9 (1960) 425.
[3] GILBERT, A., CAMERON, A.G.W., Can. J. Phys. 43 (1965) 1446.
[4] FACCHINI, V., SAETTA-MENICHELLA, E., Energia nucl. 15 (1968) 54.
[5] МАЛЫШЕВ, А.В., "Плотность уровней и структура атомных ядер", Атомиздат, М., 1969.
[6] ROSENZWEIG, N., Phys. Rev. 108 (1958) 817; Nuovo Cim. 43 (1966) 227.

[7] LONG, D.W., Nucl. Phys. 42 (1963) 353;
SANO, M., YAMASAKI, S., Prog. theor. Phys. 29 (1963) 397;
ГРИНЬ, Ю.Т., СТРУТИНСКИЙ, В.М., Ядерная физика 1 (1965) 420.
[8] ИГНАТЮК, А.В., ШУБИН, Ю.Н., Ядерная физика 8 (1968) 1135.
[9] SNEDDON, I.N., TOUSCHEK, B.F., Proc. Camb. phil. Soc. 44 (1947) 391.
[10] LANG, J.M., CONTEUR, K.Le, Proc. phys. Soc. A67 (1954) 585.
[11] DECOVSKI, P. et al., Nucl. Phys. A110 (1968) 129.
[12] BELYAEV, S.T., Mat. Fys. Medd. Dan. Vid. Selsk. 31 (1959) 11.
[13] СОЛОВЬЕВ, В.Г., "Влиянне парных корреляций сверхпроводящего типа на свойства атомных ядер", Атомиздат, 1963.
[14] BARDEEN, J., COOPER, L., SCHRIFFER, J., Phys. Rev. 108 (1958) 1175.
[15] БОГОЛЮБОВ, Н.Н., ДАН АН СССР 119 (1958) 244.
[16] KAMMURI, T., Prog. theor. Phys. 31 (1964) 595.
[17] KAHN, P., ROSENZWEIG, N., Phys. Rev. 187 (1969) 1193.
[18] NILSSON, S.G., Mat.-fys. Medd. Dan. Vid. Selsk. 29 (1955) 16;
GUSTAFSON, C., LAMM, I., NILSSON, B., NILSSON, S.G., Ark.Fys. 36 (1967) 613.
[19] ИГНАТЮК, А.В., СТАВИНСКИЙ, В.С., Ядерная физика 11 (1970) 1213.
[20] ШИРИКОВА, Н.Ю., Препринт ОИЯИ Р5-3712, 1968.
[21] НЕМИРОВСКИЙ, П.Э., ЧЕПУРНОВ, В.А., Ядерная физика 3 (1966) 998.
[22] NEMIROVSKY, P.E., ADAMCHUK, Yu.V., Nucl.Phys. 39 (1962) 553.
[23] МАЛОВ, Л.А., СОЛОВЬЕВ, В.Г., ХРИСТОВ, И.Д., Ядерная физика 6 (1967) 1186.
[24] MARUJAMA, M., Nucl. Phys. A131 (1969) 145.
[25] ИГНАТЮК, А.В., СТАВИНСКИЙ, В.С., ШУБИН, Ю.Н., Ядерная физика 11 (1970) 1012.
[26] СМИРЕНКИН, Г.Н., НЕСТЕРОВ, В.Г., ТИШИН, А.С., Ядерная физика 6 (1967) 921.
[27] ИГНАТЮК, А.В., ЯФ 9 (1969) 357.

СРЕДНИЕ РАДИАЦИОННЫЕ ШИРИНЫ ПРИ ЭНЕРГИИ ВОЗБУЖДЕНИЯ ПОРЯДКА ЭНЕРГИИ СВЯЗИ НЕЙТРОНА

С. М. ЗАХАРОВА, В. С. СТАВИНСКИЙ,
Ю. Н. ШУБИН

Физико-энергетический институт, Обнинск,
Союз Советских Социалистических Республик

Presented by A.I. Abramov

Доклад представлен А.И. Абрамовым

Abstract — Аннотация

AVERAGE RADIATION WIDTHS FOR EXCITATION ENERGIES OF THE ORDER OF NEUTRON BINDING ENERGY.

The behaviour of the average radiation width is studied as a function of the number of nucleons in a nucleus. Nuclear level density is calculated in terms of the Fermi-gas model, allowance for residual interactions being made on a phenomenological basis. It is shown that the ratio of the average radiation width obtained from the experimental data on neutron resonances in the low-energy range to the average radiation width calculated with the Weisskopf model depends on the shell structure and correlates with the behaviour of the width of a dipole giant resonance. Analytical treatment of the data yielded a semi-empirical expression for the average radiation width which can be used for calculating this quantity, in the case of a nuclear excitation energy of the order of neutron binding energy, to within ± 40% in the range of A = 60 to A = 200.

СРЕДНИЕ РАДИАЦИОННЫЕ ШИРИНЫ ПРИ ЭНЕРГИИ ВОЗБУЖДЕНИЯ ПОРЯДКА ЭНЕРГИИ СВЯЗИ НЕЙТРОНА.

В работе исследуется поведение средней радиационной ширины в зависимости от числа нуклонов в ядре. Плотность ядерных уровней рассчитывается в рамках модели ферми-газа с феноменологическим учетом остаточных взаимодействий. Показано, что отношение средней радиационной ширины, полученной из экспериментальных данных по нейтронным резонансам в области низких энергий, к средней радиационной ширине, рассчитанной в рамках модели Вайскопфа, зависит от оболочечной структуры и коррелирует с поведением ширины дипольного гигантского резонанса. На основании проведенного анализа получено полуэмпирическое выражение для средней радиационной ширины, позволяющее вычислить эту величину при энергии возбуждения ядра порядка энергии связи нейтрона с точностью не хуже 40% в области массовых чисел от A = 60 до A = 200.

1. Сечение радиационного захвата нейтронов является важнейшей ядерной характеристикой, необходимой для проектирования и расчета реакторов различных типов. Имеющихся в настоящее время экспериментальных данных для этой цели явно недостаточно. Для нестабильных ядер, особенно для таких, как осколки деления, прямые измерения $\sigma(n, \gamma)$ вообще отсутствуют.

В такой ситуации разработка теоретических методов расчета $\sigma(n, \gamma)$ представляет большой практический интерес. С другой стороны, такие расчеты могут дать дополнительную информацию о важной проблеме взаимодействия электромагнитного излучения с атомными ядрами.

Наиболее простой метод оценки $\sigma(n, \gamma)$ основан на предположении о том, что радиационный захват нейтронов идет через стадию составного

ядра. Надежность таких расчетов связана с оценкой зависимости средней по резонансам радиационной ширины Γ_γ от энергии возбуждения составного ядра и его структуры, определяемой числом протонов Z и нейтронов N. В настоящее время для расчета Γ_γ применяются, главным образом, два метода. Один из них [1] основан на допущении Вайскопфа о том, что средний квадрат матричного элемента мультипольных переходов, в которых участвуют сильно возбужденные состояния, обратно пропорционален плотности этих состояний при данной энергии возбуждения. Так как оценки Вайскопфа не претендуют на хорошую точность в определении абсолютной величины Γ_γ, то рассчитанные значения этой величины обычно нормализуются по известным значениям средних ширин Γ_γ нейтронных резонансов [2].

Второй метод основан на использовании сечения обратной реакции $\sigma(\gamma, n)$. При этом предполагается, что сечение фотопоглощения возбужденными ядрами совпадает с сечением поглощения фотонов невозбужденными ядрами, в частности, имеет характерный резонанс, отвечающий поглощению дипольных электрических квантов. Для проверки надежности этого предположения мы также можем использовать данные по средним радиационным ширинам нейтронных резонансов. В том и в другом случае зависимость Γ_γ от энергии возбуждения и от массового числа в значительной степени определяется плотностью уровней составного и конечного ядер.

В данной работе на основании анализа средних радиационных ширин нейтронных резонансов исследуется вопрос о надежности этих методов оценки Γ_γ в связи с прогрессом в области количественных оценок плотности ядерных уровней [3] и характеристик дипольного резонанса в фотозахвате [4]. Это также необходимо сделать, потому что в последнее время накоплено большое количество данных по средним радиационным ширинам нейтронных резонансов в интервале атомных весов от 20 до 240.

2. Из принципа детального равновесия следует, что средняя по резонансам с данным значением полного момента J ширина по отношению к испусканию дипольного излучения с энергией ϵ_γ есть

$$\Gamma(\epsilon_\gamma, E) = \frac{\epsilon_\gamma^2 \sigma_\gamma(\epsilon_\gamma, E - \epsilon_\gamma)\, \rho(E - \epsilon_\gamma, 0)}{(\pi\hbar c)^2\, \rho(E, 0)} \qquad (1)$$

Здесь: E – энергия возбуждения ядра, $\sigma_\gamma(\epsilon_\gamma, E - \epsilon_\gamma)$ – сечение поглощения дипольного электрического кванта с энергией ϵ_γ, ядром с энергией возбуждения $E - \epsilon_\gamma$.

При получении (1) предполагалось, что зависимость плотности возбужденных состояний от энергии и момента количества движения J имеет вид:

$$\rho(E, J) = \rho(E, 0)\,(2J + 1)\, e^{-\frac{(J + 1/2)^2}{2\sigma^2}} \qquad (2)$$

В этом предположении $\Gamma(\epsilon_\gamma, E)$, определяемая соотношением (1), не зависит от J с точностью до членов $1/\sigma^4$.

С другой стороны, для дипольного электрического излучения [1]

$$\Gamma(\epsilon_\gamma, E) = \frac{16\pi}{3}\, \frac{\epsilon_\gamma^3}{(\hbar c)^3}\, |Q_1|^2 \qquad (3)$$

где $Q_1(\epsilon_\gamma, E)$ – матричный элемент соответствующего перехода. Рассматривая среднюю вероятность перехода из группы возбужденных состояний при энергии E на определенное конечное состояние с энергией $E - \epsilon_\gamma$, Вайскопф делает предположение:

$$\langle |Q_1|^2 \rangle = \frac{q}{\rho(E, 0)} \tag{4}$$

где q = const при $E < E_{max}$ и q = 0 при $E > E_{max}$. Значение E_{max} определяется из соответствующего правила сумм для $|Q_1|^2$. Грубая оценка для $|Q_1|^2$ дает [1]:

$$q \simeq \frac{e^2}{4\pi}\left(\frac{3}{4}\right)^2 \frac{R^2}{D(0)} \tag{5}$$

где R – радиус ядра. D(0) – среднее расстояние между низколежащими уровнями ядра, между которыми возможны переходы данной мультипольности. Из оценки (5) и правил сумм для $|Q_1|^2$ следует, что

$$E_{max} \simeq Z\,D(0)$$

Сравнивая (1) и (3), приходим к выводу, что предположение Вайскопфа эквивалентно утверждению, что $\sigma_\gamma(\epsilon_\gamma, E - \epsilon_\gamma) \sim \epsilon_\gamma$ при $\epsilon_\gamma < E_{max}$ и $\sigma_\gamma(\epsilon_\gamma, E - \epsilon_\gamma) = 0$ при $\epsilon_\gamma > E_{max}$. Опыт показывает, что в сечении $\sigma_\gamma(\epsilon_\gamma, 0)$ имеется характерный гигантский резонанс. Такая же энергетическая зависимость должна наблюдаться и для $\sigma_\gamma(\epsilon_\gamma, E - \epsilon_\gamma)$, по крайней мере для малых значений $E - \epsilon_\gamma$.

В настоящее время форма сечения фотопоглощения апроксимируется следующими способами.

Форма Коши:

$$\sigma_\gamma(\epsilon_\gamma, 0) = \frac{\sigma}{2\pi} \cdot \frac{\epsilon_\gamma \Gamma_R}{\epsilon_R [(\epsilon_\gamma - \epsilon_R)^2 + 1/4\ \Gamma_R^2]}$$

где Γ_R – ширина гигантского резонанса, ϵ_R – его положение. Видно, что при $\epsilon_\gamma \ll \epsilon_R$ $\sigma_\gamma \sim \epsilon_\gamma$ и q ~ Const. При $\epsilon_\gamma \gg \epsilon_R$ $\sigma_\gamma \sim 1/\epsilon_\gamma$ и q уменьшается как $1/\epsilon_\gamma^2$.

Однако, форма Коши дает слишком медленное падение $\sigma_\gamma(\epsilon_\gamma, 0)$ с уменьшением ϵ_γ в области $\epsilon_\gamma < \epsilon_R$, особенно важной для расчета Γ_γ в области нейтронных резонансов. Более подходящей для наших целей является форма Лоренца:

$$\sigma_\gamma(\epsilon_\gamma, 0) = \frac{1.3A}{100\,\Gamma_R} \frac{\epsilon_\gamma^2 \Gamma_R^2}{[(\epsilon_\gamma^2 - \epsilon_R^2)^2 + \epsilon_\gamma^2 \Gamma_R^2]} \tag{6}$$

В этом случае при $\epsilon_\gamma \ll \epsilon_R$ $\sigma_\gamma \sim \epsilon_\gamma^2$ и $q \sim \epsilon_\gamma$. При $\epsilon_\gamma \gg \epsilon_R$ $\sigma_\gamma \sim 1/\epsilon_\gamma^2$ и $q \sim 1/\epsilon_\gamma^3$.

Ниже будет представлен результат анализа экспериментальных данных по средним радиационным ширинам нейтронных резонансов как в приближении Вайскопфа с оценкой q согласно (5), так и с учетом более реальной энергетической зависимости $\sigma_\gamma(\epsilon_\gamma, 0)$ (6).

3. В соответствии с (1) Γ_γ в области энергий возбуждения, близких к энергии связи нейтрона B_n, имеет вид:

$$\Gamma_\gamma = \frac{D(B_n, 0)}{(\pi\hbar c)^2} \int_0^{B_n} \epsilon_\gamma^2 \sigma_\gamma(\epsilon_\gamma, B_n - \epsilon_\gamma)\, \rho(B_n - \epsilon_\gamma, 0)\, d\epsilon_\gamma \qquad (7)$$

Плотность уровней оценивалась по модели ферми-газа с учетом энергии спаривания и группировки вырожденных одночастичных уровней в оболочки [3].

На рис. 1 представлены экспериментальные данные $\overline{\Gamma}_\gamma$ нейтронных резонансов в зависимости от массового числа A. Видно, что с ростом A Γ_γ уменьшается почти на порядок в интервале A от 30 до 200. Однако эта зависимость не является монотонной. Так, в области ядер с магическим числом нуклонов наблюдается характерное возрастание Γ_γ, что особенно заметно в области $Z \approx 82$, $N \approx 126$.

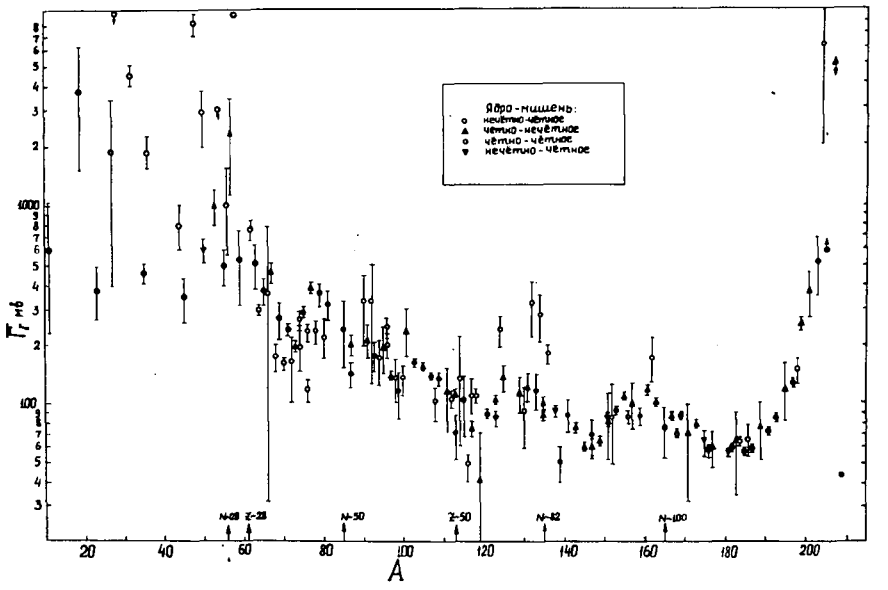

Рис. 1. Экспериментальные значения радиационных ширин нейтронных резонансов $\Gamma_\gamma^{эксп}$ в зависимости от массового числа A ядра-мишени.

Если воспользоваться для q оценкой Вайскопфа (5), то

$$\sigma_\gamma(\epsilon_\gamma) = \text{Const}\ \frac{\epsilon_\gamma}{D(0)}\, A^{2/3} \qquad (8)$$

и

$$\Gamma_\gamma = C\, \frac{A^{2/3}}{D(0)} \int_0^{B_n} \epsilon_\gamma^3\, \frac{\rho(B_n - \epsilon_\gamma, 0)}{\rho(B_n, 0)}\, d\epsilon_\gamma$$

где константа C подлежит определению из экспериментальных данных. Надо отметить, что расчеты для конкретных ядер проводились на вычислительных машинах с учетом спиновой зависимости плотности ядерных уровней согласно (2). Расстояние между одночастичными уровнями D(0), вблизи основного состояния ядра, вычислялось по формуле:

$$\frac{1}{D(0)} = \frac{6}{\pi^2}\cdot\frac{a}{2(\bar{j}_z + \bar{j}_N + 1)} \qquad (9)$$

значения параметра a, $\bar{j}_z$ и $\bar{j}_N$ брались из [3]. Структура выражения (9) связана с тем, что EI переходы между одночастичными состояниями в пределах группы с заданным j запрещены правилами отбора по четности.

На рис. 2 представлено отношение $\Gamma_\gamma^{эксп}/\Gamma_{\gamma w}$, где:

$$\Gamma_{\gamma w} = A^{2/3}\frac{a}{2(\bar{j}_z + \bar{j}_N + 1)}\,\frac{1}{2}\sum_{J=I-\frac{1}{2}}^{I+\frac{1}{2}} D(U,J)\int_0^U \epsilon_\gamma^3 \sum_{i=(J-1)}^{J+1} \rho(U-\epsilon_\gamma, i)\,d\epsilon_\gamma \qquad (10)$$

при $I \neq 0$,

и

$$\Gamma_{\gamma w} = A^{2/3}\,\frac{a}{2(\bar{j}_z + \bar{j}_N + 1)}\,D(U,1/2)\int_0^U \epsilon_\gamma \sum_{i=1/2}^{3/2} \rho(U-\epsilon_\gamma, i)\,d\epsilon_\gamma \qquad (11)$$

При $I = 0$.

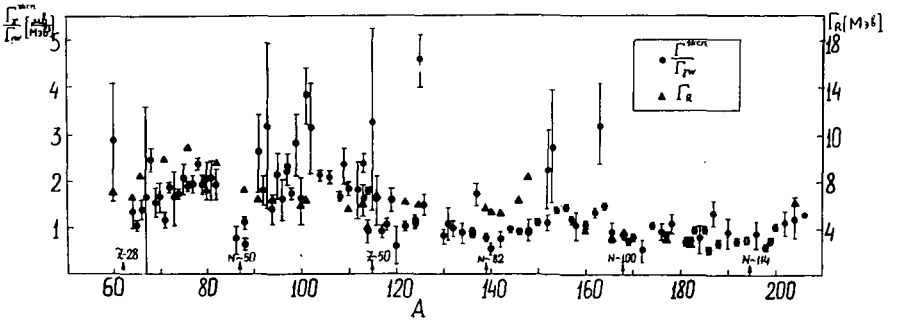

Рис. 2. Отношение $\Gamma_\gamma^{эксп}/\Gamma_{\gamma w}$ в зависимости от массового числа A составного ядра. Треугольники – экспериментальные значения ширин дипольного гигантского резонанса Γ_R.

Здесь I – спин мишени, $U = B_n - \Delta$, а Δ – величина, определенная в работе [5]. Согласно приближению Вайскопфа, это отношение не должно зависеть от A. Однако из рис. 2 видно, что это отношение заметно коррелирует с оболочечной структурой ядер – факт, который ранее был отмечен в работе [6]. Обращает на себя внимание также и то, что это отношение коррелирует с наблюдаемым поведением ширин гигантского дипольного резонанса Γ_R [4], которые представлены на том же рис. 2. Это связано с тем, что приближение Вайскопфа игнорирует факт наличия

гигантского резонанса в сечении фотопоглощения, а наблюдаемые резонансные ширины чувствительны к этому эффекту. Чтобы учесть нерегулярности в поведении $\Gamma_\gamma^{эксп}/\Gamma_{\gamma w}$, нами предлагается следующая апроксимация:

$$\frac{\Gamma_\gamma^{эксп}}{\Gamma_{\gamma w}} = C\left(1 + X_n \operatorname{Sin}\frac{\pi(N - N_i)}{(N_{i+1} - N_i)}\right)^2\left(1 + X_z \operatorname{Sin}\frac{\pi(Z - Z_i)}{(Z_{i+1} - Z_i)}\right)^2 \qquad (12)$$

где N_i и Z_i – границы выбранных интервалов изменения N и Z, которые совпадают с магическими числами протонов и нейтронов, кроме области ядер с $82 < N < 126$, где оказалось необходимым ввести три области $82 \leqslant N \leqslant 100$, $100 < N \leqslant 114$ и $114 < N \leqslant 126$. Формулы (10) и (12) с константой, определяемой (12), описывают эксперимент в области $60 < A < 200$ со среднеквадратичной ошибкой ~0,3 (рис. 3). Только в восьми случаях из 104 расчетные значения выходят за указанные пределы, однако во всех этих случаях экспериментальные данные недостаточно надежны.

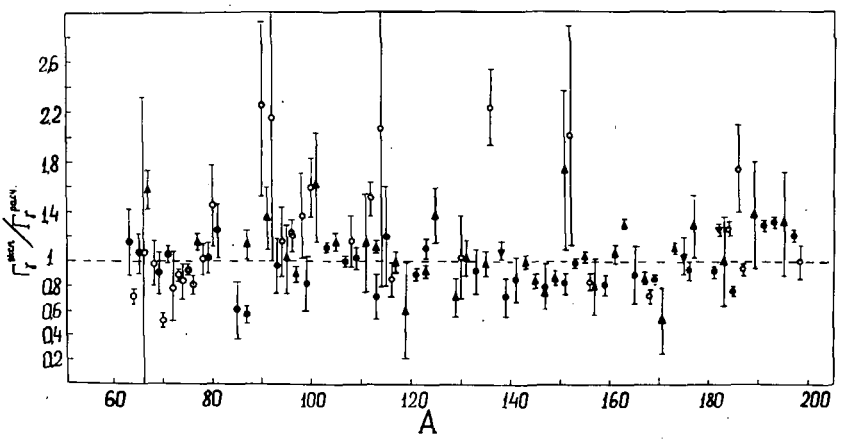

Рис. 3. Величина $\Gamma_\gamma^{эксп}/\Gamma_\gamma^{расч}$ как функция массового числа A ядра-мишени.

Радиационные ширины легких ядер ($A < 60$) и ядер, расположенных вблизи дважды замкнутой оболочки $N = 126$ и $Z = 82$ ($A > 200$), несколько хуже укладываются в эту систематику. Это связано, во-первых, с большими неопределенностями в экспериментальных данных и, во-вторых, с возможным вкладом прямых процессов, которые в данном подходе не учитываются.

4. Корреляция отношения $\Gamma_\gamma^{эксп}/\Gamma_{\gamma w}$ с Γ_R говорит о необходимости более точной оценки $\sigma_\gamma(\epsilon_\gamma)$, которая бы учитывала наличие гигантского резонанса. Если σ_γ имеет форму кривой Лоренца, то в приближении $\epsilon_\gamma < \epsilon_R$ и $\epsilon_R > \Gamma_R$

$$\Gamma_{\gamma R} = \text{Const}\sum_{J=I-\frac{1}{2}}^{I+\frac{1}{2}} D(U,J)\int_0^U \frac{\epsilon_\gamma^4 \sigma_R \Gamma_R}{(\epsilon_\gamma^2 - \epsilon_R^2)^2}\sum_{i=J-1}^{J+1}\rho(U - \epsilon_\gamma, i)\,d\epsilon_\gamma \qquad (13)$$

На рис. 4 приведено рассчитанное с помощью (13) отношение $\Gamma_\gamma^{\text{экпс}}/S$, где:

$$S = \frac{NZ}{A}\sum_{J=I-\frac{1}{2}}^{I+\frac{1}{2}} D(U,J)\int_0^U \frac{\sum_{i=|J-1|}^{J+1}\epsilon_\gamma^4\,\rho(U-\epsilon_\gamma,\,i)\,d\epsilon_\gamma}{(\epsilon_\gamma^2-\epsilon_R^2)^2} \qquad (14)$$

При этом предполагалось, что сечения поглощения в максимуме резонанса $\sigma_R \sim NZ/A$. Видно, что это отношение, пропорциональное в соответствии с (13) ширине гигантского резонанса, зависит от A таким же образом, как и отношение $\Gamma_\gamma^{\text{расч}}/\Gamma_{\gamma w}$ (рис. 2).

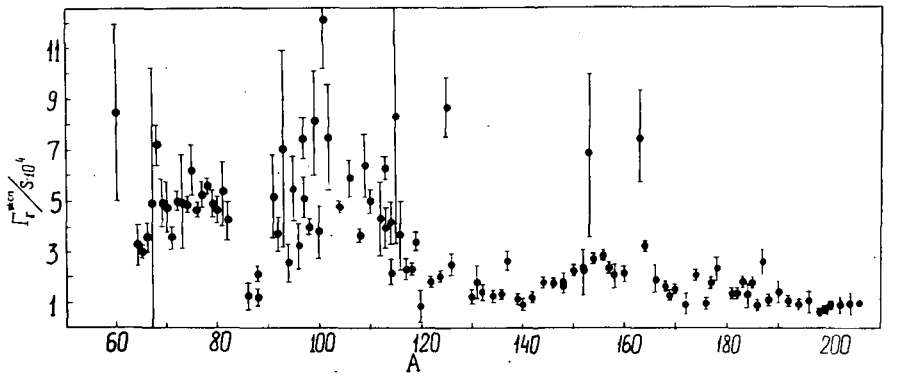

Рис. 4. Отношение $\Gamma_\gamma^{\text{эксп}}/S\cdot 10^4$ в зависимости от массового числа составного ядра.

Таким образом, в тех случаях, когда отсутствует экспериментальная информация о величине Γ_R, ее можно определить из систематически радиационных ширин нейтронных резонансов.

5. Приведенные результаты показывают, что оба рассматриваемых выше метода оценки радиационных ширин нейтронных резонансов могут быть использованы в практических расчетах. Вследствие того что экстраполяция $\sigma_\gamma(\epsilon_\gamma)$ в области $\epsilon_\gamma < B_n$ является довольно произвольной, наиболее надежную оценку дает систематика, основанная на приближении Вайскопфа. При этом необходимо учитывать вариации матричного элемента Q_1, связанные с резонансным характером $\sigma_\gamma(\epsilon_\gamma, E-\epsilon_\gamma)$. Полученное таким образом выражение для Γ_γ позволяет, на основе имеющейся надежной информации о плотности уровней возбуждаемых ядер [3], вычислять эту величину с точностью, близкой к экспериментальной, для широкого интервала атомных весов.

Наблюдаемая корреляция Γ_γ с Γ_R дает новые возможности для изучения процесса фотопоглощения на основании анализа характеристик обратного процесса.

ЛИТЕРАТУРА

[1] БЛАТТ, Дж., ВАЙСКОПФ, В., "Теоретическая ядерная физика", ИЛ, Москва, 1954.
[2] МАЛЫШЕВ, А.В., "Плотности уровней и структура атомных ядер", Атомиздат, Москва, 1969.
[3] ШУБИН, Ю.Н., МАЛЫШЕВ, А.В., СТАВИНСКИЙ, В.С., Proceedings of a Conference on Nuclear Data (Paris, 17-21 October 1966) INDC/156, CN-23/106.
[4] GORJACHEV, B.V., Atomic Energy Review 2, 3 (1964).
[5] NEMIROVSKY, P.E., ADAMCHUK, Ju.V., Nucl. Phys. 39 (1962) 553.
[6] ZAKHAROVA, S.M., MALYSHEV, A.V., Int. Conf. Phys. Nucl., 4a(1)/C394, Paris, 1964.

CLOSING REMARKS BY CHAIRMAN:

A. I. ABRAMOV: The papers presented at this session and the preceding one, on the subject of the evaluation of nuclear constants, reflect the most recent achievements in all the important lines of research in this field. They cover the evaluation of neutron data proper and of a number of physical parameters, such as nuclear level density, radiation widths etc., which are used extensively in neutron cross-section work. Besides being of great practical value because of the information which they contain, these papers are important in that they give an indication of the problems that remain to be solved in the near future, e. g. standardization of evaluation methods, minimizing the subjective element in the selection and renormalization of experimental data, and others. In the matter of organizing a wide international exchange of evaluated data, it will be necessary to solve a number of practical problems relating to the choice of formats and the compatibility of computers in various countries. It is to be hoped that the Nuclear Data Section of the IAEA will be able to do a great deal in the years ahead towards finding solutions to these urgent problems.

PANEL DISCUSSION

Friday, 19 June 1970

Chairman: G.C. HANNA (Canada)

Members of the Panel:

H. Condé (Sweden)
W.G. Davey (USA)
W. Havens (USA)
R.L. Joly (France)
G.H. Kinchin (UK)
E.R. Rae (UK)
P.H. Ribon (France)
R.F. Taschek (USA)
S.I. Sukhoruchkin (USSR)

G.C. HANNA: I propose to ask each member of the Panel to summarize one of the conference topics. After each summary there will be time for one or two questions from the floor. I shall now call on Dr. Taschek, who will discuss the first topic, General Aspects of the Needs and Uses for Nuclear Data.

R.F. TASCHEK: The session devoted to this topic covered a very wide range, attempting to show the extensive nature of requirements. The first paper presented was that of Dr. Schmidt, which defined the main business of the conference, namely, the status of the general data requirements in connection with the basic problem of applications to reactor systems. He paid considerable attention to the matter of standards, a question which was not much discussed during the rest of the conference. He drew attention to a certain lack of confidence prevailing in the general area of standards. In a way, this is the most difficult problem of all, as far as the qualitative aspect of neutron and nuclear data measurements are concerned. This question deserves to be mentioned because it is a very important one.

Dr. Schmidt then proceeded to enumerate the most urgent problems and these were emphasized time and again throughout the conference. One of these problems was the plutonium alpha: this has now been measured and those concerned are fairly satisfied with the results. This value is of great importance for the design of fast reactor systems and will necessarily have to be emphasized in the future. Another question with which Dr. Schmidt dealt extensively was that of the basic $\overline{\nu}$ of californium, if we can describe anything of that kind as basic. He also referred to the energy dependence of $\overline{\nu}$, particularly the question – discussed earlier at Studsvik – of the low-energy region in which there now seems to be an accumulation of data indicating that, indeed, there is perhaps a variation in $\overline{\nu}$. Except for a comment by Dr. Moore, there was not much theoretical speculation on what might be the cause of this. One other point that was made was the occurrence of fission fluctuations at low energies. A matter that was not mentioned at the meeting was that the fluctuations found on the Livermore cyclotron have also been found in a recent underground nuclear test and have been verified, I believe, in detail. I have seen Diven's plots superposed on Bowman's data and indeed there are real fluctuations that are reproduced by quite different experimental methods. Personally, I do not agree with Bowman's conclusion: I believe that we could have difficulties in the

normalization of fission cross-sections in this general energy range (24 keV) and that these might indeed be the cause of some of our discrepancies.

The next paper was the excellent, thoroughly quantitative study of Dr. Hutchins. Among other things, he drew attention — at least by implication — to a difference in philosophy which seems to characterize the approach of the United States and that of certain other countries to the relationship between the integral and microscopic data. At least it seemed to me that the point of view he was putting forward was somewhat different from that expressed by Dr. Campbell in his subsequent discussion of essentially the same subject. That is to say, there was a difference in emphasis on the need for getting accurate data: in particular, Dr. Hutchins took a strong position regarding the need to obtain good data on the fissile and fertile nuclides, a view which seemed to be the opposite of that of Dr. Campbell.

In addition to the outstanding problems listed by Dr. Schmidt, Dr. Hutchins referred to the matter of the ^{238}U radiative capture cross-section, which he considered to be the most important uncertainty at present, and I am inclined to agree with him. There seems to be an implication that people have already made up their minds about the ^{235}U fission cross-section, which obviously is in much worse shape, but this depends on one's original premises.

Next, there was the very interesting paper of Dr. Clayton on thermonuclear power sources and their origin; I mean real thermonuclear power sources that actually work. The point he made, with respect to neutron cross-section measurements, was that the capture cross-sections above iron are a very important consideration as far as nucleogenesis and perhaps even gravitational theory are concerned. Of course, you also have to know the neutron capture for the elements below iron because, although they may be produced through cycles that are charged-particle cycles, neutrons are nevertheless present and neutrons become a part of any gains and losses and chains of element growth.

Dr. Chernilin brought up a question which has gained very considerable significance in the last 18 months, namely, how one might build a controlled thermonuclear reactor that could be used as a power source. This is looking a very long way ahead. You probably realize that the main reason for studies on this subject is that even if you were able to prove the scientific feasibility — to use a word that is now employed in the CTR programs — of a thermonuclear reactor, it would not mean that you could make one that was economic. Obviously, one has to worry nowadays about whether money is being allocated in the general direction of fast-reactor programs and whether some of it can be reserved for a long shot of this kind. There are still a large number of unresolved questions concerning the nature of the core of the thermonuclear device (a subject on which very little is known), the economics involved in the construction of the remainder of the reactor and also, of course, the metallurgy neutron interactions, nuclear physics and so forth. I am glad to say, however, that at present it does look as if it will be possible to make an economic CTR reactor, something which was not true a few years ago. Another matter to which Dr. Chernilin attributed great importance in this connection was the $^{7}Li(nn't)$ reaction. This is for the production of tritons. Lithium is almost certainly going to serve as both a coolant and a fuel as well as a device for multiplying tritium.

Dr. Crocker made a more detailed analysis of some of the nuclear cross-section requirements for thermonuclear devices and emphasized

many of the same points as did Dr. Chernilin, particularly the (n, n') and (n,n't) reactions, regardless of where the tritium comes from. He placed considerable emphasis on the fact that the thermonuclear reactor was not going to have a fission spectrum in it but would start out with 14-MeV neutrons. There is really no doubt about that. It is unlikely that a DD reactor will be built before a DT reactor. All this means that one is dealing with fast neutron spectra and one has to understand the nature of all these neutron and gamma interactions.

Dr. Lynn presented an excellent discussion of the status of theoretical nuclear physics as it interacts with experiment and he pointed up the view, to which I think we all subscribe, that theory must go along with the experiment. The theoreticians, like the experimentalists, perhaps unlike some of the reactor people, are interested in obtaining good data. He put special emphasis on what one might call special dynamic nuclear states that add to and improve our understanding of nuclear physics and of fine structure. In particular, he drew attention to the enhancement of our understanding of the fission process during the last two or three years, thanks to a shell model that has affected a marriage between charge-particle fission physics and neutron physics.

J. L. ROWLANDS: I would like to try to clarify the United Kingdom position on the relationship between integral and differential data. Perhaps I can illustrate it by means of an example. Two or three years ago we were saying that we required an accuracy of $\frac{1}{2}$% in fission cross-sections to enable us to predict reactivity to 1%. We are now saying that we think the main requirement is for the shape of the fission cross-section to be determined accurately to about 3% accuracy and that we can supplement such accurate shape measurements with integral data to enable us to get the accuracy we need. So the emphasis is changing. We are looking to the differential measurements to give us the accuracy in structure of cross-sections and to the integral measurements to give us the absolute accuracy in the prediction of reactor properties.

G. C. HANNA: As no one else wishes to comment at this point, I shall call on our next panel speaker, Dr. Rae, who will speak about Cross-sections and Techniques for High-Precision Neutron Nuclear Data Measurements.

E. R. RAE: This topic was concerned essentially with what is normally called neutron nuclear standards, that is, with the accurate measurements of neutron fluxes and of certain cross-sections used as standards against which other cross-sections are measured.

Dr. Deruytter (BCMN) started the session with an excellent review of this topic, He listed the cross-sections currently used as standards, ^{6}Li(n, α), ^{10}B(n, α), ^{3}He(n, p) and H(n, p), and reviewed the present status of the accuracy with which these cross-sections are known. He noted that the fluctuations suggested in the H(n, p) cross-sections had not been observed in detailed observations at NBS, BCMN and AERE, so that this cross-section remained the standard at energies above a few hundred keV. At lower energies he conceded the virtues of ^{6}Li(n, α) as a standard due to the absence of competing reactions and the simplicity of the structure, but he favoured the ^{10}B(n, α) cross-section as the practical standard in view of its convenience of use in practical detectors and the fact that it is currently the best determined. In his opinion the ^{10}B(n, α) cross-section was now known to 1% to 1 keV, 2% to 10 keV and 3% to 100 keV. He regarded ^{3}He as a useful standard below a few keV.

Papers by Sowerby, Asami and Moxon (AERE and JAERI) and Leroy et al. (Cadarache) showed the progress being made in the consolidation of the (n, α) cross-sections of ^{6}Li and ^{10}B. The departure from the 1/v law of the $^{10}B(n, \alpha)$ cross-section below 100 keV now seems to be well established, and the discrepancies in the $^{6}Li(n, \alpha)$ cross-section in the region of the 250 keV resonance appear slowly to be evaporating. A direct measurement with a ^{6}Li glass scintillator at Cadarache, where the ^{6}Li content was determined by transmission and where the multiple scattering effects were carefully assessed, gives a considerably higher-peak cross-section than was earlier observed by Schwartz et al. This value now lies closer to that calculated by Uttley and Diment from high-resolution total cross-section measurements. A similar result was reported by Coates et al. (AERE) from a preliminary measurement using a thin (1/8 in.) ^{6}Li glass scintillator where the neutron flux was determined using a flat response ^{10}B-vaseline sphere detector.

Deryutter also discussed the use of fission cross-sections as a standard, particularly that of ^{235}U, and showed that these cross-sections are particularly useful because of their high Q-values, so that their accurate measurement is most important in the field of nuclear standards. He touched on the status of the 2200 m/s values of the fission cross-sections, and Leroy et al. presented a new determination of the fission cross-sections of ^{235}U and ^{239}Pu in the energy range 15 keV to 1 MeV, where great care had been taken with all aspects of the experiment, especially the neutron flux measurements. Three different methods had been used: the associated particle technique, the manganese bath, and proton recoil detectors. The results for ^{235}U supported the cross-section shape of White above 100 keV but below this energy the new data tended to lie significantly below those of White.

Other papers on neutron flux measurement were presented by Käppeler and by Rae. The former author described a carefully designed proton recoil detector having a small solid angle and low efficiency (4×10^{-5}) but eliminating pulse height extrapolation problems. The latter described the Harwell ^{10}B-vaseline sphere flat-response detector. This device, which as an efficiency constant to 4% over the energy range 10 eV to 700 keV is also fast enough (full width of half maximum of time response $\sim$150 ns) to be used in time-of-flight experiments. It is anticipated that this detector will be useful in bridging the energy gap between the $^{10}B(n, \alpha)$ detectors and the $H(n, p)$ detectors.

The ^{12}C total and scattering cross-sections (which are essentially identical) and which are used as a standard in low-energy scattering measurements, were discussed by Knitter in papers from BCMN and AERE. The status of this cross-section as a standard at least up to $\sim$1 MeV appears to be very satisfactory and the cross-section shape is well understood theoretically.

Finally, the session included a pair of papers presented by Fröhner (KFK). One of these described a re-evaluation of the 24 keV capture cross-section of Au by Schmitt and Cook. This work confirms the normalization recommended by Poenitz for the Au cross-section which is frequently used as a sub-standard. The other paper did not relate to the field of standards, but was concerned with fluctuations in the Au total cross-section in the keV range and the effect of this on the temperature dependence of leakage through thick shields.

G. C. HANNA: Our next topic is Nuclear Data in the Thermal and Resonance Energy Region for A > 220 and two members of the Panel will deal with this subject. Dr. Sukhoruchkin will speak first.

S.I. SUKHORUCHKIN: The third session opened with a review paper summarizing the state of the art of nuclear data in the thermal neutron region. This very interesting study, presented by Dr. James, dealt with certain aspects of the measurement of fission cross-sections and total cross-sections of heavy elements. It seems to me that one of the most interesting points he made had to do with the constant nature of the radiation widths of ^{238}U, which have already been confirmed by the results obtained at two other laboratories. A great deal of material has been accumulated on the analysis of fission cross-sections and in my opinion this demonstrates very convincingly the presence of a structure connected with a two-hump potential barrier. This had originally been predicted by Strutinsky and at present is being observed in many sub-threshold fission cross-sections.

The next paper was that of Dr. Hanna et al. from Chalk River, which concerned thermal measurements of α for ^{233}U, ^{235}U and ^{239}Pu. I must say that as a result of these measurements the accuracy with which the thermal values of α are being determined has been increased by a factor of two and some experimentalists may take pride in the fact that their contributions to such fundamental constants for reactor design have been of such decisive importance.

In my own review paper, I listed the main recommendations of the Studsvik panel with respect to the α values of ^{239}Pu and compiled a table summarizing the most recent results, including those obtained by Dr. Farrell et al. at Los Alamos and those we ourselves obtained in Moscow. This table will be included in the published version of my paper. The participants in the Studsvik panel came to the conclusion that after refinement of the normalization procedure and the introduction of some other corrections – all of which can be done by the group of Dr. Schmidt at the Agency – it will be possible to evaluate α ^{239}Pu with an accuracy of $\pm$ 10%. Although the experimental results had been subjected to a very thorough analysis by physicists dealing with integral measurements, they have been the object of a certain amount of criticism. I would like to ask those who are concerned with such integral measurements to consider not only the discrepancies in the microscopic data but also the large area where there is agreement in the results.

The part of the session on which I am reporting ended with two studies which are very interesting from the physics point of view. The first was the excellent paper by Dr. Rae et al. at Harwell, who observed a very interesting effect when the shape of one of the strong resonances of ^{238}U proved to be distorted. This distortion was identified as a result of a delayed decay with a half-life of about 1 microsecond. It seems to me that this study can be considered a genuinely pioneering work. The second paper to which I refer is that of Chrien et al. at Brookhaven, who were the first to obtain capture gamma spectra from fissile nuclei. Although the capture spectra for ^{235}U were not found to be very suitable for analysis, plutonium in this case again turned out to be an exception and very strong gamma capture lines were observed in this nucleus. This study, like many others that have been presented at this conference, is an example of how neutron physics is building bridges from pure nuclear physics to the applications of nuclear data for reactor design.

G.C. HANNA: I shall now call upon Dr. Joly to conclude the summary of the topic under discussion.

R.L. JOLY: In the subsequent part of the session we heard a summary of the results obtained by the groups of physicists at Saclay and Geel, who

used a linear accelerator as their neutron source, the results of the Los Alamos group, whose neutron source consisted of a nuclear explosion, and the results obtained at Bombay with a crystal spectrometer. At the conclusion of the session, Mr. Ribon discussed some of the problems posed by the analysis of the cross-sections for fissile and fertile elements in the resonance region. From the point of view of techniques, we can say that the most exact measurements and those with the best resolution are those obtained with the linear accelerator. The nuclear explosions are useful nevertheless for getting more detailed information about cross-section values in the trough between resonances. Furthermore, this technique is unmatched when it comes to the measurement of cross-sections in elements with a high specific alpha activity. The crystal spectrometer enables us to obtain data below a few electron volts with great absolute precision. Of course, these are not original conclusions but the spoken and written statements presented at this conference have placed a kind of official stamp on them.

As far as the data themselves are concerned, it may be said, generally speaking, that an effort was made by the experimentalists, in the papers which they presented, to compare their data with those of other experimentalists and I think that this is exactly in keeping with what was desired by the organizers. These comparisons were made in terms of average cross-sections. In the case of ^{235}U, such a comparison of fission cross-sections showed that there was good agreement between Saclay data presented here and the earlier data obtained in Oak Ridge. This alone should be of help to the evaluators in making a choice. Mr. Ribon, who undertook an evaluation of this kind for uranium, reached the same conclusion concerning this agreement. For this purpose he used an original method of data comparison. This method seems particularly appropriate for comparing data in resolved resonance regions and in some cases enables one to determine the causes of disagreements and to make local corrections.

To conclude the discussion on ^{235}U data, I should like to draw attention to the experiments at Geel on the determination of the spins of the resonances of this element. Although the number of resonances for which spins have been assigned is still low, these experiments nevertheless have the merit of establishing the validity of two indirect methods of spin determination, namely, studies on the multiplicity of gamma cascades and the study of the anisotropy of fission fragments emitted by aligned nuclei. These techniques should be of great value in supplementing the direct methods for obtaining information on the spin of ^{235}U resonances.

As regards ^{239}Pu, an account was given of very extensive work which has resulted in the determination of the partial fission widths and spins of practically all the resonances below 660 eV. It has been possible to find interesting correlations with the problem of the α of ^{239}Pu. On the other hand, it is striking that in the case of the average fission cross-sections for ^{239}Pu, there are important disagreements between the different experiments. As for ^{233}U, considerable progress has been made with respect to the precision and resolution of data, a fact which has emerged at this conference. However, the problem of analysing these data is still a considerable one. This difficulty is underlined by a comparison of the Geel data presented here with the earlier Oak Ridge data. The average cross-sections are generally in good agreement, i.e. $\leq 10\%$. On the other hand, analyses carried out according to the same formalism and expressed

in terms of parameters of the Kapur-Peierls type are in virtually complete disagreement.

Results relating to fission cross-sections of ^{241}Pu were presented by two laboratories. The analyses in terms of resonance parameters were not available for the conference. The mean values of the fission cross-sections are in good agreement.

Lastly, a very striking illustration of the possibilities of nuclear explosions was provided by a study made on curium isotopes. The data obtained on the parameters and cross-sections of these isotopes are sufficient in quality and quantity to permit us to affirm with reasonable certitude that, in the production of ^{252}Cf, there is nothing to be gained by going from a thermal flux to an epithermal flux. As the question of methods of analysis of cross-sections in the resonance region was dealt with much more thoroughly in other sessions, I shall merely draw attention to a proposal made by Mr. Ribon at the end of his oral presentation, namely, that a simulated cross-section should be submitted to different laboratories which would not, of course, know the parameters involved and would be asked to analyse it by means of their multilevel formalism. The results obtained would then be regrouped and compared. The progress made has been as follows: Dr. Lynn from Harwell has agreed to set the problem and to compile the results. As regards the laboratories which have agreed to participate in this game, even though I am not quite sure that I know all the details, I can nevertheless report that Messrs. de Saussure, Adler, Patrick, Derrien, Moore and, of course, Ribon are in agreement. I am convinced, after having heard the warm recommendations in favour of co-operation made by Dr. Chernilin as Chairman of Session VII that our Soviet colleagues will also want to join us.

G.C. HANNA: Does anyone wish to comment?

J.S. STORY: For my part, I am not convinced that very much is to be gained by carrying out such a resonance parameter comparison, because in reality the physical content of the resonance parameters is not very great. All that the resonance analysis does is to provide a parametric fitting of a curve and one set of parameters is as good as another if it provides a good fit.

W. HAVENS: My point of view is quite the opposite of Dr. Story's, because I think a comparison of this type is very valuable for determining what systematic errors may exist. You can fit any curve you want to by using a set of delta functions which is equal to the number of points you have to fit, and you can do a perfect job of fitting it. However, if you want to determine systematic errors you fit your data with the resonance parameters because you think there is some physical sense in this and it will determine such things as background (separating that out from fission between resonances which might be due to resonances which are not observable or to interference between resonances). So I think that the purpose of the exercise is not to supply a parametric fit to a curve but to try to determine what systematic errors exist between different experiments and to correct the systematic errors in a reasonable, logical way.

J.S. STORY: But as someone pointed out only today you do not really know how many resonances there are there. You can easily deceive yourself in this resonance analysis lark.

G.C. HANNA: I think I shall terminate the discussion at this perhaps rather unsatisfactory point, taking some consolation in the fact that our next speaker will be Dr. Havens and that he will be moving to the lower

mass range, to deal with the topic Nuclear Data in the Thermal and Resonance Energy Region, for A < 220.

W. HAVENS: Although it is the heavy elements which are of most interest to the nuclear energy business, there are a lot more elements below the fissile materials which have to be studied in order to determine the exact parameters of the structural, cooling and other types of material used in reactors as well as to gain an understanding of nuclear systematics so that information which cannot be obtained by measurement can be obtained in some other way. In the session devoted to the topic under consideration, Dr. Muradyan took a very original approach to the problem because the usual procedure has been to see what results could be obtained with the existing accelerators. He reversed the procedure and worked on the assumption of an accelerator which would give us the parameters which we need to solve all our problems. He came up with the somewhat surprising conclusion that neutron sources a couple of orders of magnitude more intense than the ones we have at present would be required for determining the parameters we need. So, even though we have obtained an enormous amount of data on a semi-infinite number of levels in the region A = 1 to A = 220 we still have to look at partial cross-sections and results are not easy to obtain. Despite the great advances that have been made as far as neutron source intensity, detectors and data-handling properties are concerned, in many cases we still do not have the intensity required to do a partial cross-section. You should be able to separate the p-levels from the s-levels and the only way you can do this experimentally is to do an angular distribution, but in most cases there is not enough intensity to do an angular distribution on a small p-resonance level with a neutron velocity selector. Dr. Muradyan's Doppler measurements to separate the p- from the s-resonances have been very effective and have given some excellent results, but there are not enough of them to enable the technique to be used for determining the systematics in the lower-atomic-weight nuclei.

The next speaker was my "opponent", Dr. Story, who gave a very interesting paper in which he pointed out how the various evaluations had shown the experimental data to be inadequate. A number of these were rather surprising because it turned out that some of the materials that have been subjects of study ever since neutron physics came into existence are still not well enough known for us to be able to use them to calculate the simplest parameters in an integral system from the differential data. He had an extremely difficult job selecting illustrative problems from the wealth of available material. His choice of topics shows that he gave a great deal of thought to the subject and I recommend that everybody read the paper in detail several times over so as to find out what are the limitations of the experimental data at the present time.

The paper on the high-resolution neutron total and capture cross-sections by Fröhner, Müller et al., and presented by Dr. Ernst, showed some of the problems encountered in the keV region when one is working with a very high resolution spectrometer. I do not know how long it will take them to parameterize all the data they have – there are so many resonances that it would seem to be a semi-infinite set and it may be that not all of them will ever be parameterized. What will probably happen is that the minute better resolutions are obtained, other resonances will be found which have affected the parameters already determined, so you will have to divide each of them up into two resonances and so on ad infinitum.

Dr. Popov described a different approach to the determination of neutron resonance parameters, consisting in a study of α-particle widths. He showed that the strength functions obtained by this technique were approximately the same as those found by the more usual methods.

I was delighted to see the results that Dr. Priesmeyer presented on the fast-chopper measurements of resonance total cross-sections for fission-product isotopes because he reported that the number of resonances observed was very much less than one would have expected for the large number of isotopes that you have in the fission-product group. Consequently the analysis of this group and the determination of what the useful parameters of this analysis will be may be a lot less difficult than originally anticipated.

The session ended with a paper by Walker on the evaluation of the fission-product yield in the thermal region. It contained very useful information and I challenge the theorists to interpret it.

G.C. HANNA: Since there are no comments, I shall ask Dr. Davey to speak on the next topic, Nuclear Data above the Resonance Energy Region of $A > 220$.

W.G. DAVEY: There were 12 papers presented on this topic, including two invited papers and one summary of a panel discussion. Unfortunately they had to be covered in too short a period to permit the discussion they deserved.

The session devoted to the topic opened with an extensive critical review by Dr. Poenitz of the recent experimental data. One important characteristic of this review was that it illustrated certain features of the experimental techniques and gave us some understanding of both the precision and the reliability of the available data. He covered total and scattering cross-sections, capture and fission cross-sections, $\bar{\nu}$ and fission neutron spectra.

With regard to the total cross-section of uranium, discrepancies of up to 15% exist between different measurements, but Dr. Poenitz stated that it is feasible to suggest cross-sections with an approximate uncertainty of 3%. The inelastic cross-section of ^{238}U was discussed in particular detail and good agreement was noted for different cross-section measurements of individual level excitations up to about 1 MeV. However, Dr. Poenitz pointed out that this might be deceptive since the sum of the elastic and inelastic data measured by one experimenter exceeded the total cross-section by a significant amount. Very extensive coverage was given to the measurements of ratios of capture and fission cross-sections and the ratios of fission cross-sections themselves, and to the particularly important problem of absolute capture and fission cross-sections. This study must be read in all its detail to appreciate its many important features, but perhaps the most significant point was the much discussed spread in the ^{235}U absolute fission cross-section above about 100 keV. I think I need not emphasize this point here since it came up many times in the course of this conference, but it is clearly of great, and perhaps extreme, importance. In conclusion, Dr. Poenitz presented some of the experimental evidence for the non-linear energy dependence of $\bar{\nu}$ for ^{235}U.

Measurements of total cross-sections were presented in other papers, e.g. by Soleilhac and by Kopsch. The measurements reported by the former concerned C, Ni, ^{235}U, ^{238}U and ^{239}Pu. Those of the latter were concerned only with uranium. The Kopsch paper concluded there was good agreement between the uranium findings and the other data, except in the case of some of the older material. It was also concluded, from an analysis of fluctuations,

that there was meaningful physical structure in the energy range of about 0.5 - 0.7 MeV, although these were of small amplitude.

Capture and fission cross-sections were the subject of three presentations in the session. There were two Russian papers on the measurement of the ^{238}U capture cross-section, presented by Abramov; a paper on fission ratio measurements of ^{241}Pu to ^{235}U by Käppeler of Karlsruhe; and a paper on high-resolution measurements of fission in ^{235}U by Bowman of Livermore, which was presented by Dr. Havens. The ^{238}U capture measurements in one case extended from 24 keV to 145 keV and in the other case, where a lead slowing-down spectrometer was used, the measurements extended from 5 eV up to 100 keV. The former measurements were of the ratio $^{238}U(n,\gamma)/^{235}U(n, f)$ and ^{238}U data were obtained using essentially White's fission data. The latter measurements were made with a slowing spectrometer, with several detector thicknesses, and there is a need to understand self-shielding effects to facilitate the comparison with other measurements. The wide energy range that may be covered with the slowing-down spectrometer was noted. The ratio measurements appear to be consistent with those made by others, for example, with Menlove and Poenitz, but the lead spectrometer data should not be assessed without careful consideration of self-shielding and perhaps energy resolution.

The $^{241}Pu/^{235}U$ ratio measurements showed quite large differences from the existing data, but since the results were stated to be preliminary this point need not be emphasized here.

The Bowman data on ^{235}U fission are of particular importance since, as is known, they do show significant structure in this cross-section which could be particularly important for lower resolution measurements. I think it also raises the question of the choice of the ^{235}U fission cross-section as a standard for other measurements. Bowman has considered this problem and he believes that the structure would not cause errors in lower-resolution measurements of more than a few per cent; but while this appears to be true for measurements above about 100 keV where some of the most significant discrepancies lie, it is perhaps a little more difficult to accept in the region of about 30 keV, where there is significant structure but where several very important measurements have been made.

Measurements of the fission neutron spectrum were presented by Jéki of Hungary and Wiedling of Sweden. The latter's measurements were of fission in ^{238}U at two neutron energies and perhaps their most significant aspect was that there appeared to be no indication that the fission spectra were harder than had been assumed in the light of some individual experiments.

Measurements on ^{238}U inelastic scattering in South Africa, presented by Reitmann, were concerned with the previously mentioned possibility of errors in this cross-section. The results, however, were in good agreement with the other data, except for the scattering from the 45-keV level. It was concluded, however, that the agreement for three other levels supported the belief that there were no large systematic errors in the technique.

A method under development in France for measurements of (n, 2n) and (n, 3n) data was described by Soleilhac. A precision of between 5 and 10% was projected. These studies were performed with a large liquid scintillator and they could be relevant to measurements of $\bar{\nu}$ with this technique. I will come back to this point very briefly later.

The session concluded with two review papers by myself and by Colvin. My own review concentrated on the absolute fission cross-section of ^{235}U, capture cross-section of ^{238}U, $\bar{\nu}$ for ^{252}Cf and the energy dependence of $\bar{\nu}$. The discrepancies and difficulties encountered in the first two subjects were discussed many times at this conference and I will merely repeat what I have said many times before, that I believe that the ^{235}U fission cross-section is the most important single unknown at present. On $\bar{\nu}$, evidence for structure and non-linear energy dependence up to 500 keV in ^{235}U was presented and the essential decoupling between the thermal $\bar{\nu}$ and that at higher energies again emphasizes the importance of the well-known $\bar{\nu}$ discrepancies, particularly those in $\bar{\nu}$ for ^{252}Cf.

The final paper was a review by Colvin of the IAEA Consultants' Meeting on $\bar{\nu}$ held at Studsvik last week. The report covered two days' discussion and I certainly cannot summarize it effectively here, particularly since many new data were presented. I will say that the question of $\bar{\nu}$ for ^{252}Cf is still an important and active one. Soleilhac showed that there may be anomalies in the detecting procedure for liquid scintillators which should be resolved. The most pressing question was that of structure in $\bar{\nu}$ and new data for ^{239}Pu were presented by Soleilhac which showed no strong evidence for structure. For ^{235}U the majority of the evidence – in a numerical sense at least – was in favour of structure, but there were definitely contradictory results, in particular those of Boldeman and co-workers in Australia, so that the question of structure is still open. Compilation and evaluation to complement the extensive experimental work are proceeding actively. Colvin concluded with eight recommendations for future work in $\bar{\nu}$ and it should be heartening to most of the participants in this conference that six of these related to the need for new experimental work.

R.F. TASCHEK: How bad do you think the situation would be with respect to the fission cross-section of ^{235}U, particularly in the 100-keV to 1-MeV range, if one were to throw out all the recent Poenitz data? Perhaps this question is unfair since Dr. Poenitz does not appear to be in the audience.

W.G. DAVEY: Well, I think it is quite clear, the measurements reported by Leroy at this conference are indeed in excellent agreement with those of White, with the exception of one point at 40 keV and one lower. These lie 6% below Allen and Ferguson's and 5% below Diven's measurements, so that the spread is approximately 6%. However, I personally believe it is anybody's guess as to whether this represents the true uncertainty.

R.F. TASCHEK: No one will ever know what the true uncertainty is, but within the errors quoted, one can draw a very fine curve that will include all these experiments. The one outstanding exception is the Poenitz experiment, and this is a very troublesome point. However, at least to me, it does not seem to be so crucial as made out in the last two years.

E.R. RAE: I think in this context one should mention the point made by Dr. Sowerby in Session VIII: if you take the gold cross-section, which has received a great deal of attention as a substandard and has been measured with great pains, and measurements which have been made relative to ^{235}U and also if you take the ^{6}Li work and turn the thing around these two pieces of evidence would not lie on this nice curve for ^{235}U. So, I think there is evidence other than Poenitz's measurement to suggest that something is not quite right.

R.F. TASCHEK: Well, I am sure something is not quite right, otherwise Poenitz's measurements would not be where they are. This is a very difficult problem but I do not think it is unique. It has happened many times. One has to try to find the source of the difficulty but in the meantime one has to keep on living with something, and gold, to the best of my recollections, has been fraught with even more discrepancies than ^{235}U in the past. I would like to point out again, as I did earlier in the meeting, that there are at least three other absolute measurements of the ^{235}U fission cross-section, which are unfortunately not reported in the standard literature, but will also fit within their approximately 5% errors into the group from about 1.3 MeV down to say 200 keV.

G.C. HANNA: Thank you gentlemen. Our next topic is Nuclear Data above the Resonance Energy Region for $A < 200$, and our speaker is Dr. Condé.

H. CONDÉ: A total of 14 papers, including two invited ones, were presented on this type of cross-section measurements. In many cases they were systematic studies covering a large number of elements and a wide energy range. As pointed out by Cierjacks in his review paper, the RENDA request list includes 343 requests in this area, half of which are concerned either with radiative capture or with charged-particle emission. A cursory examination of the papers presented at this conference shows that there is a slight disagreement between the emphasis of the experimental activities and that of the data requests.

I should like to discuss some results and trends which I think are of importance in this connection. As regards experimental facilities, the use of linear accelerators and proton or neutron cyclotrons as pulsed neutron sources represents a breakthrough, especially as far as systematic studies over a wide energy range are concerned. However, the use of Van de Graaff machines is still preferable in some experiments, because of low background and better resolution, e.g. in (n, n') and (n, n'γ) experiments. The standard cross-sections (n, p), $^{10}B(n, \alpha)$ as well as Au (n, γ) have been measured with high precision in recent years but there still exist discrepancies, especially in the Au (n, γ) cross-sections, as reported by Abramov in his review paper. At 24.5 keV, the results differ by up to as much as 15%. Total cross-sections are measured in this energy range with quoted errors of 2-3%. Systematic differences which have existed between the findings of certain laboratories have in some cases, as pointed out by Cierjacks, gradually disappeared when new measurements have been undertaken with better resolution, and the older data have thus been superseded.

Concerning elastic and inelastic scattering of neutrons, papers were presented describing interesting experiments from Obninsk, Tokai-Mura and Studsvik. Their experimental differential elastic scattering data are fitted to optical model calculations and in general a good agreement is obtained. As observed by Holmquist and Wiedling, the optical model parameters as a function of mass number at 8-MeV incident neutron energy show a smooth behaviour for mass numbers higher than about 55, while below this number the imaginary potential depths exhibit pronounced fluctuations. On the other hand, Tsukada et al. calculated the energy dependence of the optical model parameters for aluminium, copper and zinc, and the energy dependence was found not to be monotonic.

For the inelastic scattering data, the cross-sections calculated from the Hauser-Feshbach theory, including the Moldauer and Smith fluctuation corrections, do not agree with the experimental data in many cases, both

for light and heavy elements. In general, the calculated values are larger than the experimental ones, in many cases by as much as a factor of two. More work, and preferably systematic work, is needed in the (n, n') and (n, n'γ) field.

A large number of requests is concerned with radiative neutron capture in the fast energy range. As pointed out by Abramov, the accuracy of the existing data (15-20%) is far from fulfilling the requested accuracy of 5-10%. In the very interesting work of Lopez et al. from Gulf General Atomic, measurements were reported on eight different elements in the energy region from 1 keV to 1 MeV. Above 100 keV the data for most of the elements disagree with earlier measurements by Diven et al., Gibbons et al., and by Kononov and Stavissky. More work is needed to solve these disagreements.

A better understanding of the reaction mechanism in fast neutron capture has been obtained in recent years by introducing the qualitative or semi-direct capture theory of Lane and Lynn and of Brown. The theory can predict fairly well the shape of the cross-section curve but does not predict the absolute values, which in some cases are off by an order of magnitude.

Finally, I would like to say a few words about the (n, x) cross-sections, where x stands for a charged particle such as a proton or alpha or for the two neutrons emitted in (n, 2n) reactions. For these cross-sections there exists a large amount of data centred around 14 MeV and only very few experiments in the energy region below that energy. This is partly because of the difficulties in producing neutrons in the energy range from the threshold of these reactions up to 14 MeV. However, systematic trends have been found by Chatterjee in the (n, 2n) cross-sections as a function of the neutron excess in the residual nucleus. A smooth curve with depths corresponding to the magic numbers has been reported. Systematic trends have also been found in the (n, p) and (n, α) cross-sections, but there are still large uncertainties in the reported cross-sections. In conclusion, let me say that there is a need for more experiments, especially relating to the (n, p) and (n, α) cross-sections, but also to the (n, 2n) cross-section below 14 MeV neutron energy.

G.C. HANNA: Our next topic is Relationships of Microscopic and Integral Data and our speaker is Dr. Kinchin.

G.H. KINCHIN: I am fortunate – or unfortunate, as the case may be – in being the rapporteur for one of the sessions of the conference which aroused a great deal of interest and discussion. We had reports on a number of resonance integral measurements. These are perhaps one of the oldest types of integral measurement and they have the advantage that they can be made practically independent of the choice of other cross-sections. We also had reports on the fission-spectrum averaged cross-sections and here there is the relation between the fission spectrum and the cross-sections. The two are not entirely independent. As regards the capture-to-fission determinations, reported in the Kuznetsov paper, these are not independent of other cross-sections, and this also applies to the studies of the GODIVA reactor with different data sets. In the latter case there was an indication from the Monte Carlo work of the best choice of fission cross-section above 100 keV, although some unresolved problems clearly remain with the calculations of these small, highly leaking assemblies.

The Andersson paper on fission-product cross-sections casts a gleam of light in suggesting that the measured cross-sections of a number of important

fission products, and of a mock fission-product sample, are lower than the calculated values. If these results are substantiated by the further work in progress, they will make a welcome contribution to fast-reactor reactivities and breeding gains, both of which have suffered in the last few years from the upward trends in capture to fission ratios.

However, I would like to spend most of the short time at my disposal on the papers by Dr. Campbell, Dr. Küsters and Dr. Barré and on the discussion which followed, on the question of the relative roles of differential and integral data. In doing this I shall take the opportunity of adding some remarks of my own to the dialogue between the two faces of Janus to which Dr. Schmidt referred in his oral presentation at the opening of the conference. Traditionally the two faces are tragic and comic but I shall not attempt to say which is which.

I would like for a moment to refer to the paper presented by Dr. Hutchins in the first session and just remind you – for it is a point which has been made before – that not all of the difference in generating costs ascribable to data uncertainties can be recovered by removing these uncertainties. To take an example which I have already mentioned, we cannot – unfortunately – change the yields and cross-sections of the fission products of ^{235}Pu by measuring them more accurately. We will know more accurately what penalty to ascribe to the existence of fission products but we will not be able to avoid the penalty. The savings to be made by forewarnings are the smaller ones of being able the better to predict and provide for operational fuel management procedures. This sort of argument, and the fact that the existence of integral measurements is not taken into account quantitatively in Dr. Hutchins' paper, although they are indeed referred to, means that the cost uncertainties must be treated with some reserve. That does not mean that there are no savings but the numbers must be used with care. The last point about the integral experiments is illustrated in Dr. Campbell's paper in which he demonstrates that the initial reactivity uncertainty for the Prototype Fast Reactor (PFR) is reduced from ± 5% to ± 0.5% by the use of integral measurements. This is of very topical interest in the United Kingdom since we have to decide <u>now</u> on the enrichment of the first charge of the PFR.

The arguments on the relative value of differential and integral data are familiar ones to me, since the subject was debated in the United Kingdom at length before we decided, a year or two ago, not to attempt differential measurements of very high accuracy, by which I mean ± 1% or better. Instead, we would relax the accuracy requirements for differential measurements and tune up the data by adjustment to fit integral experiments. Our recent requests have been put forward on that basis, with the assumption that the major parameters, such as the fission cross-section of ^{235}U would be shown to be known to a sufficient accuracy in the important energy range.

Although not everyone might agree with this approach, I think that there is a measure of agreement with Dr. Küsters' suggestion that the widening discrepancies, notably in the fission cross-section of ^{235}U, will not be resolved by repetition of the measurements using the same techniques and claiming the same high accuracies. Rather, one should look critically at the existing experiments or "evaluate" them in the broad sense defined by Professor Havens, to identify the reasons for discrepancies and to eliminate the incorrect measurements. Detailed discussions by small groups of experimenters are called for, and the exercise must be an international one.

If an acceleration of the convergence of Dr. Abramov's curves showing the spread of measurements as a function of time can be achieved by this sort of study, then the integral measurements can be of value in pointing to discrepancies in other data. Although it will rarely be the case that a single parameter will be shown to be subject to error, the exercise is useful in focusing attention on related parameters, either of which may be wrong. New differential data will be needed where none at present exist. In short, the two faces of Janus must go hand in hand.

B.A. HUTCHINS: I would like to make an observation which may shed some light on the reason for the disagreement we see as regards the need for differential data for different fast reactor programs.

There are two types of fast-reactor computations being carried out in the United States. The first is an activity concerned with building a prototype reactor in the relatively near future. The second is aimed at an evaluation of the fast reactor economy in the 1980s, or beyond. In the case of the second activity, the adjustment of data by integral measurements requires too great an extrapolation and better differential data are needed to evaluate the economics.

As for the first activity, in which a specific design is being set, the extrapolation may not be so great. However, the balance between safety and other considerations is not the same in all programs. I would not like to argue what that balance should be, as that is another matter. I do want to point out that in the United States and Germany, the scale is tipped more towards the safety side than in the United Kingdom and France. It so happens that integral measurements of safety parameters are among the most difficult to make and require the greatest extrapolations. That is an important reason why good differential measurements are needed in the United States programme.

G.H. KINCHIN: I agree with Dr. Hutchins that there are certainly some areas which are inaccessible to measurements of the integral type. These usually have to do with conditions in which one would not wish to operate a normally functioning reactor and in this case one does need to have differential measurements in order to be able to make extrapolations with confidence.

J.Y. BARRÉ: Since this conference, by definition, relates to nuclear data for reactors, I should like to emphasize two points which I think are very important and which are linked to the problem of time limits. First, reference has been made during the conference, in particular by Mr. Ribon, to the time lag occurring between requests, measurements, evaluation and use in reactor calculations. The people who make differential measurements should be aware of this time factor when they make their measurements. The second point concerns the problem of the evaluation and the use of the evaluation in a reactor calculation. Generally speaking, the reactor physicist always enters into the picture between the evaluation and the utilization of the data. On the subject of data fitting I would merely like to point out that the countries that are in the greatest hurry right now to define reactor parameters use fitting methods because in this way they can obtain results with the required precision and, in particular, within the required time limits. If, as indicated by Dr. Kinchin, the PFR enrichments are to be defined very shortly, I can say that this is also true of PHENIX, and therefore it is not possible to wait.

R.F. TASCHEK: I should like to make a very brief comment on the difficulty one can get into as a result of too much dependence on reactor physics experiments of the integral type. Dr. Best, who talked during Session VII about the GODIVA, JEZEBEL and small critical assembly calculations, may remember the time when those calculations were based on a set of group cross-sections which were quite incorrect, and it was known that they were incorrect. However, they were simply adjusted in such a way that the critical assemblies, their criticality, critical mass and other parameters were fitted by that set of incorrect constants. Gradually the quality of the differential data improved to a point where, in some cases, there were even measurements of a type which had not been made previously — for instance, of the spectra of inelastic scattering from the heavy elements — but it was found quite difficult to move the people concerned with criticality measurements away from their set of parameters. They almost preferred to use an incorrect set because it would have involved more trouble to redo all their calculations with a better set. I think that too extensive a reliance on integral experiments, even though I agree that they are necessary, can lead to your becoming penned in a corner. I am convinced that if the people stopped making neutron physics measurements for two years you would never get them started again because most of them really do not want to make these measurements which are not normally in the forefront of exciting nuclear physics work. I therefore believe it is very important to keep up the momentum that we already have in the very difficult area of measurement.

H.W KÜSTERS: I would like to support what Dr. Hutchins has said. The reactor physicists need differential nuclear data to be able to predict the neutronic properties of fast reactors. As regards the different approaches being used in the United Kingdom, France, Germany and the United States, I think that, as far as nuclear data needs are concerned, we are more or less all in the same boat, or at least we should be. It is one thing to predict the criticality or enrichment of the prototype reactor, which definitely is at a more advanced stage in Europe, but quite another thing to be able to predict the physics properties of economic fast systems of about 1000 MW(e). As indicated in my paper (CN-26/117), it is mainly the prototype reactor which is the subject of cross-section adjustment and of such activities and analysis at Karlsruhe. However, we have to be honest enough to admit that the early prototype reactors will not be economic, mainly because of high capital costs, so that the physics implications do not represent a very heavy burden. The need for differential nuclear data must, to my mind, be correlated with the requirements for larger, economic reactors. Criticality and breeding predictions can definitely be made more reliable by using critical-mass and reaction-rate ratios from clitical experiments in the cross-section fits. However, without a knowledge based on reliable differential data, it is rather difficult to make any assessment of those quantities which are related to the prediction of system behaviour after perturbation and of the very strong relationship with safety features or the long-term behaviour of a large plant with the build-up of higher plutonium isotopes and partly radioactive fission products, or the guaranteed burn-up. It is true that the calculation of reactivity coefficients can be checked in critical facilities, but one has to be aware of the fact that, due to heterogeneity effects and to effects of sample size and environment, it has not up to now been proved that adjusted cross-sections yield better results. The sodium void coefficient, for instance, is to some extent (and in large reactors to a

major extent) a spectrum effect, and the measurement of neutron spectra is not yet in a satisfactory state, a fact which is pointed out in my paper.

As shown in Karlsruhe report KFK-793 (the extended version of a paper presented at the international ANS meeting in Washington, 1968) the prediction of the steam-density coefficient of steam-cooled fast reactors is very uncertain because of partly compensating positive and negative contributions. On the other hand, the effects of higher plutonium isotopes and partly radioactive fission products should be studied in the true spectrum – but for this one has to have samples of these isotopes irradiated in the same spectrum.

Worth measurements in critical facilities, which can in principle provide information if one has the proper samples, have to be interpreted very carefully, as pointed out in my paper. We can now predict ratios of worth measurements of the heavy materials by improved theoretical methods – but material worths of medium-weight nuclei cannot be predicted satisfactorily.

In conclusion, I think these examples show that there is a need for differential data, but priority should be given to a real determination – by the experimentalists themselves – of the possible reasons for the inconsistencies in the data on the main isotopes, rather than to enlarge the data series already available. In this way it might be possible to relax some of the requests for high accuracy.

W.G. DAVEY: I agree completely with Dr. Küsters, Dr. Taschek and Dr. Hutchins, but in the United States we do have a criticals program that is really extensive. At present, we have a 1200-kg plutonium critical which is designed specifically for use in connection with the demonstration reactor under development at Argonne. This program covers both power-reactor geometry and higher-isotope effects. However, having said this, I still think we need nuclear data. Surely the point is not that one technique is better than the other but that they both have roles in a program. There may be arguments over the correct timing or the correct emphasis, but I think we would all agree that both sets, both types of experiments are needed.

G.C. HANNA: Our last report, to be given by Dr. Ribon, is on Evaluation Problems and Methods.

P.H. RIBON: This last section included 17 papers on a variety of problems. Instead of attempting to summarize them even briefly, I shall merely make a few comments. The problems I shall discuss can be divided into four groups: activities of the four centres and international co-operation; methods of evaluation; theories used for evaluation; examples of evaluation.

The theoretical models actually used by evaluators are rather limited: they are, in principle, the statistical model and the optical model. There was no paper read on the statistical model, while three papers dealt with the optical model; two of these were coupled-channel calculations leading to very good agreement with experimental data and proving that evaluators will have to use more and more such sophisticated models. Two papers were concerned with the prediction of average level spacings, a problem which has not been solved satisfactorily up to now.

A large number of examples of evaluation was given, and it was a striking fact that they related only to a very small number of nuclei, mainly structural materials, sodium, the three principal fissile nuclei, ^{238}U and ^{240}Pu. In general, capture cross-sections were stressed. But we can say that there is lack of comparison between the different data or evaluations

published, and the explanation of the disagreements was not always clear. These disagreements must not be confused with the error on the recommanded value: in the case of the capture cross-section of ^{238}U, the disagreement between four evaluations is ~ 3% at 10 keV and is very probably smaller than the error and is about 10% at 100 keV, while some evaluators give a smaller error.

Evaluators should always give errors. I realize that this is not easy to do but I think it is indispensable and that it is something reactor physicists would like to have.

The Karlsruhe paper on certain actinides inspired the jesting remark by Dr. Story that it was now no longer necessary to carry out new experiments. It is true that the evaluator must give a value, even if he knows that it has been arrived at by very coarse methods. Nevertheless, I noted that two authors, Miss Hinkelmann and Dr. Sowerby, ended their respective papers with a call for these new measurements.

Two papers related to structural materials, including nickel. In one of them, Dr. Moxon emphasized the importance of structures for an understanding and description of capture. It is legitimate to suggest that this problem deserves as much interest as that devoted to fissile nuclei. The multiplicity of evaluations on one and the same subject is related somewhat to the problem of time limits mentioned by Dr. Barré. It is conceivable that international co-operation would help solve this problem. Dr. Pearlstein, in his paper on the activities of the four nuclear data centres touched on this problem. I think that the most important progress that has been made thus far is in the definition of a unique format, EXFOR, which should facilitate exchanges between the four centres. One might hope that the same would be true of evaluated data, but it must be realized that the transformation from one format to another in the case of evaluated data is more difficult than in that of experimental data. Perhaps we should accept the fact that there must first be a proliferation of formats so as to enable the persons concerned to understand the problem and then to grasp the importance of a unique format. Like Dr. Abramov, I hope that agreement on such a single format will come to pass in a few years. The reply of Dr. Pearlstein to a question raised after the presentation of his paper shows that for this exchange there are problems other than those of technique.

We can retain two main features concerning the analysis of resonances for fissile nucleis. One is the trend to determine the R-matrix parameters by simple methods; the work concerning the possibility of obtaining them from the Adler-Adler parameters derserves attention. On the other hand, several examples show that the analysis was not unique, even with the simplest formalisms; it was shown that the different parameter sets give the same statistical laws. But the comparison of different sets will be very difficult – even impossible without comparing the cross-sections computed from these parameters.

The evaluation methods described also included the use of oscilloscopes, as Dr. Alter outlined in his paper on the SCORE program. The simultaneous analyses described by Dr. Sowerby were of interest for the energy range with which they dealt. I think it would be useful to have the specialists meet and compare the details of their methods; but most of these problems do not concern the evaluators only: the methods for handling information are often the same as those used by the experimentalists (the experimental methods were not dealt with at all at this conference) and they have the same difficulties with computers.

In conclusion, I would like to recall the point of view expressed by Dr. Rae at the Karlsruhe Conference on Data Acquisition and Processing in 1965. He showed four slides, the first showing an experimentalist processing these data by hand in 1955; the second showed the same man submerged in kilometres of perforated tape in 1960; in the third in 1965, the experimentalist was seated comfortably in a chair before a visualization unit alongside a computer operated by a very attractive person; the last slide showed the date 1970 followed by a question mark. Well, we are now in 1970 and I should like to ask whether he has any answer.

E.R. RAE: I think the situation can be illustrated by the figure appearing at the end of the record of this meeting.

G.C. HANNA: Is there any further comment?

A. PRINCE: I gather, Dr. Ribon, that you would like evaluators to put error bars on their analyses. In connection with the discussion on the paper which Dr. Abramov presented on this topic (CN-26/80), I would find it hard to justify putting error bars on an evaluation, especially where the experimental data showed such a wide divergence. Until more is known about nuclear forces in the solution to the many-body problem, I think most evaluators would feel the same way. To take the fission cross-section of ^{238}U as an example: I calculated it and would say that my finding was within 3% of the experimental values, but it could not be used because I was unable to reproduce the structure not using a Hill-Wheeler formalism. The situation is the same in the case of fission-product cross-sections, where there are some isotopes which are so short-lived that there are no experimental data on them, and for this reason people will take any information you give them. In the transuraniums and the superheavy isotopes, for example, people will accept anything, simply because there are no data and if you speak of a factor of two they will be satisfied. But I do not call that an error bar.

P.H. RIBON: I know that it is difficult but I think that it is necessary. I have taken an example at 10 keV: four evaluations with capture cross-sections of ^{238}U show agreement to within 3%. Do you think that this means that the cross-section is known to 3%? I think it would be useful for the evaluators to estimate the error. You also say that you do not call a factor of two an error bar. If it is a question of expressing this error bar in per cents, I agree with you, but I think that if you estimate that the result of your calculations can be erroneous by a factor of approximately two, you should say so.

A. PRINCE: I think the evaluator must first ask himself whether the experimenter has measured what he claims to have measured. If he decides this question in the affirmative, he then has to make the appropriate analysis and once he has done this he might possibly assign a factor of two, but never 3%. You referred to the capture cross-section for ^{238}U: if you look at Pitterle's data, which are used in ENDF B, you will find that he normalized everything to a 30-keV measurement of 479 mb. I made my own calculation and came up with a value of 478 mb but, since it had to be consistent with the fission cross-section used in the systematics of the analysis, the calculated capture cross-section had to be sacrificed. However, in my own opinion, the calculated value is as good as all the other evaluations. The only difference is that it was not used.

L.B. WALLIN: In these closing minutes of the conference, I would like to raise one small matter. I have never heard it discussed in public before, perhaps because no one wanted to show his abysmal ignorance. The question

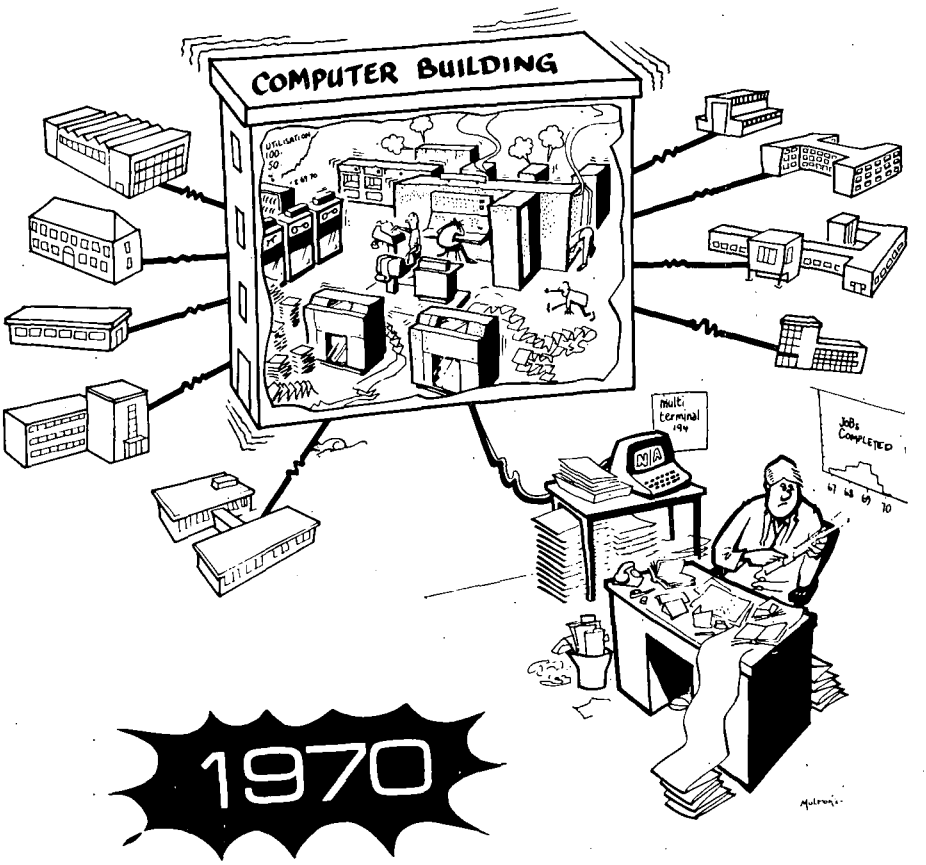

is this: we have heard a great deal from the resonance analysts about missing levels, but I wonder how they know that levels are missing. Of course, they will answer that we have the Wigner distribution and we can see that the experimental distribution does not fit the Wigner distribution. But then I would like to ask: how do you know that the experimental distributions should fit the Wigner distribution? The answer would probably be: we have made experiments which show us that we can easily fit our experimental distributions to the Wigner distributions. What is the answer, then? Could someone cast some light on my shadows?

W. HAVENS: The situation is not as bad as you paint it, because there is a lot of experimental evidence for the missing of levels. For example, every time you improve the resolution of a velocity spectrometer, you get more levels: single levels split up into two levels and so forth and so on. What you have been considering is a consistency argument with respect to the Wigner distribution, but there is no certainty that the Wigner distribution is correct. However, it is not only a question of the Wigner distribution: if you plot the square root of the Γ_n against the number and look at a Porter-Thomas distribution, you do not get a fit to the Porter-Thomas distribution

with small levels. However, there are several ways of getting it, and for this I would refer you to a paper by Michaudon on this particular subject which appeared in Physics Letters several years ago.

G.C. HANNA: Thank you, Dr. Havens. I think we can conclude the summary panel at this point. I would like to thank the members of the panel for their efforts.

A summary of the highlights of the conference has also been published in the Atomic Energy Review, Vol. 8, No. 3 (1970) 711.

CHAIRMEN OF SESSIONS

Section I	R.F. TASCHEK	United States of America
Section II	F.R. RAE	United Kingdom
Section III	S.I. SUKHORUCHKIN	Union of Soviet Socialist Republics
	R.J. JOLY	France
Section IV	W. HAVENS	United States of America
Section V	W.G. DAVEY	United States of America
Section VI	F.H. FRÖHNER	Federal Republic of Germany
Section VII	B.A. HUTCHINS	United States of America
	Yu.F. CHERNILIN	Union of Soviet Socialist Republics
Section VIII	J.S. STORY	United Kingdom
Section IX	A.I. ABRAMOV	Union of Soviet Socialist Republics

SECRETARIAT

Scientific Secretaries:	V.A. KONSHIN	Division of Research and Laboratories, IAEA
	L. HJÄRNE	
Administrative Secretary:	J.H. STORHAUG	Division of Scientific and Technical Information, IAEA
Editor:	J.W. WEIL	Division of Publications, IAEA
Records Officer:	L.S. LIEBERMANN	Division of Languages, IAEA

LIST OF PARTICIPANTS

ARGENTINA

Ricabarra, G.H.	Comisión Nacional de Energía Atómica, Buenos Aires

AUSTRALIA

Cook, J.L.	Australian Atomic Energy Commission, AEEC, Lucas Heights

AUSTRIA

Putz, F.	Österreichische Studiengesellschaft für Atomenergie, Lenaugasse 10, A-1082 Wien

BELGIUM

Bindler, L.	Belgonucléaire, S.A., 35, rue des Colonies, 1000 Bruxelles
Ceulemans, H.	SCK-CEN, Boeretang, 2400 Mol
De Coster, M.F.	Studiecentrum voor Kernenergie, Boeretang - 2400 Mol
Fabry, A.M.	SCK-CEN, Boeretang, 2400 Mol
Minsart, G.	SCK-CEN, Boeretang, 2400 Mol
Nath, M.	SCK-CEN, Boeretang, 2400 Mol
Poortmans, F.	SCK-CEN, Boeretang, 2400 Mol
Schepers, J.C.	SCK-CEN, Boeretang, 2400 Mol
Vandeplas, P.	SCK-CEN, Boeretang, 2400 Mol
Wagemans, C.	SCK-CEN, Boeretang, 2400 Mol

CANADA

Hanna, G.C.	Atomic Energy of Canada Limited, Chalk River, Ontario
Walker, W.H.	Atomic Energy of Canada Limited, Chalk River, Ontario

DENMARK

Højerup, C.F.	Danish Atomic Energy Commission, Risø, Roskilde 4000

FINLAND

Jauho, P.	Technical University, Otaniemi
Kaloinen, E.H.P.	Technical University, Otaniemi
Palmgren, A.	Technical University, Otaniemi
Saastamoinen, J.J.	Technical University, Otaniemi
Simons, L.S.	University of Helsinki, Siltavuorenpenger 20 e,Helsinki 17

FRANCE

Asghar, M.	Laboratoire de la Physique Nucléaire Université de Bordeaux, Le Haut Vigneau, 33-Gradignan
Barré, J.Y.	Centre d'Etudes Nucléaire de Cadarache, B.P. No 1 – 13 Saint-Paul lez Durance
Bouchard, J.	Commissariat à l'Energie Atomique – CEN-FAR, B.P. No 6 – 92 Fontenay-aux-Roses
Derrien, H.	Centre d'Etudes Nucléaires de Saclay, B.P. No 2 – 91 Gif-sur-Yvette
Hoffmann, A.	Centre d'Etudes Nucléaires de Saclay, B.P. No 2 – 91 Gif-sur-Yvette
Joly, R.L.	Centre d'Etudes Nucléaires de Saclay, B.P. No 2 – 91 Gif-sur-Yvette
Leroy, J.L.	Centre d'Etudes Nucléaire de Cadarache, B.P. No 1 – 13 Saint-Paul-lez-Durance
Lezer, G.	EDF-SEPTEN, 17 avenue de la Libération, 92 Clamart
Michaudon, A.M.	Centre d'Etudes Nucléaires de Saclay, B.P. No 2 – 91 Gif-sur-Yvette
Newstead, C.M.	Centre d'Etudes Nucléaires de Saclay, B.P. No 2 – 91 Gif-sur-Yvette

Perrin, A. — Centre d'Etudes Nucléaires de Limeil, B.P. No 27 – 94 Villeneuve-Saint-Georges

Racine, R. — Commissariat à l'Energie Atomique, Framatome, 107, Boulevard de la Mission Marchard - 92 - Courbevoie

Ribon, P.H. — Centre d'Etudes Nucléaires de Saclay, B.P. No 2 – 91 Gif-sur-Yvette

Soleilhac, M. — Centre d'Etudes de Bruyère le Châtel, Service P, B.P. 515, Paris

Vidal, J.C. — Commissariat à l'Energie Atomique, B.P. 27-Villeneuve-Saint-Georges

Vidal, R. — CEA - Centre de Fontenay-aux-Roses, B.P. No 6 – Fontenay-aux-Roses (92)

GERMANY, FEDERAL REPUBLIC OF

Cierjacks, S.W. — Institut für Angewandte Kernphysik, Kernforschungszentrum Karlsruhe, 7500 Karlsruhe

Eckey, H. — Kernenergieversuchsanlage der AEG, Grosswelzheim

Ernst, A. — Institut für Angewandte Kernphysik, Kernforschungszentrum Karlsruhe, 7500 Karlsruhe

Fischer, E.A. — Institut für Angewandte Kernphysik, Kernforschungszentrum Karlsruhe, 7500 Karlsruhe

Fröhner, F.H. — Institut für Angewandte Kernphysik, Kernforschungszentrum Karlsruhe, 7500 Karlsruhe

Hinkelmann, B. — Institut für Neutronenphysik und Reaktortechnik, Kernforschungszentrum Karlsruhe, 7500 Karlsruhe

Jung, H.H. — Institut für Reine und Angewandte Kernphysik der Universität Kiel, 2057 Geesthacht, Reaktorstation

Käppeler, F. — Gesellschaft für Kernforschung, 7500 Karlsruhe, Postfach 3640

Kirouac, G.J. — Institut für Angewandte Kernphysik, Kernforschungszentrum Karlsruhe, 7500 Karlsruhe

Kopsch, D. — Institut für Angewandte Kernphysik, Kernforschungszentrum Karlsruhe, 7500 Karlsruhe

Küsters, H.W.	Gesellschaft für Kernforschung, 7500 Karlsruhe, Postfach 3640
Müller, K.N.	Gesellschaft für Kernforschung, 7500 Karlsruhe, Postfach 3640
Nebe, J.	Gesellschaft für Kernforschung, 7500 Karlsruhe, Postfach 3640
Priesmeyer, H.G.	Institut für Reine und Angewandte Kernphysik der Universität Kiel, 2057 Geesthacht, Reaktorstation
Wagner, S.R.	Physikalisch-Technische Bundesanstalt, Bundesallee 100, 33 Braunschweig

HUNGARY

Csikai, G.J.	Institute for Experimental Physics, Budapest
Jéki, L.	Central Research Institute for Physics of the Hungarian Academy of Sciences, Budapest 114, P.O.B. 49
Vértes, P.	Central Research Institute for Physics, Budapest

INDIA

Ramakrishna, D.V.S.	Bhabha Atomic Research Center, Trombay - Bombay 85

ISRAEL

Caner, M.	Soreq Nuclear Research Centre, Yavne

ITALY

Accinni, F.	CISE - Casella Postale, 3986 - Milano
Benzi, V.	CNEN (National Committee for Nuclear Energy) Via Mazzini 2, 40138 Bologna
Cerullo, N.	Instituto di Impianti Nucleari, Facultà di Ingegneria, Via Diotisalvi 2, 56100 Pisa
Giacobbe, P.	CNEN, Centro di Calcolo, Via Mazzini 2, 40138 Bologna
Giannini, M.	Lab. F.N.A., C.S.N. Casaccia, CNEN, S.P. Anguillarese KN 1, 300 Roma
Motta, M.	CNEN - Centro di Calcolo, Via Mazzini 2, 40138 Bologna

Paoletti-Gualandi, M.	ENEL
Pistella, F.	CNEN, National Committee for Nuclear Energy, viale Regina Margherita, 185 Rome
Tavoni, R.	CNEN - PRV, Via Azcoveggio 56/23, Bologna

JAPAN

Nishimura, K.	Japan Atomic Energy Research Institute, Tokai-mura, Naka-Gun, Ibaraki-Ken
Oi, H.	The Tokyo Electric Power Co., Inc., No. 5-1, 1-chome, Uchisaiwaicho, Chiyoda-ku, Tokyo
Tanaka, S.	Japan Atomic Energy Research Institute, Tokai-mura, Naka-Gun, Ibaraki-Ken

NETHERLANDS

Lautenbach, G.	Reactor Centrum Netherlands, Petten

NORWAY

Skardhamar, T.	Institutt for Atomenergi, P.O. Box 40, N-2007 Kjeller

POLAND

Marcinkowsky, A.	The Institute of Nuclear Research, Warsaw, 69 Hoza Str.
Zelazny, R.	Institute of Nuclear Research at Świerk, Świerk

PORTUGAL

Martinho, E.	Laboratório de Física e Engenharia Nucleares, Sacavém

ROMANIA

Rapeanu, S.	Institute of Atomic Physics, P.O. Box 35, Bucharest

SOUTH AFRICA

Reitmann, D.	Atomic Energy Board, Private Bag 256, Pretoria

SWEDEN

Almén, E.E.A.	AB Atomenergi, Studsvik, Fack 61101, Nyköping
Andersson, T.L.	AB Atomenergi, Studsvik, S-61101, Nyköping
Condé, H.	Research Institute of National Defence, Stockholm 80
Eriksson, J.R.	AB Atomenergi, Studsvik - Nyköping
Etemad, M.A.	AB Atomenergi, Studsvik - Nyköping
Häggblom, H.	AB Atomenergi, Studsvik - Nyköping
Holmqvist, B.	AB Atomenergi, Studsvik - Nyköping
Lefvert, T.	Research Institute of Swedish National Defence, S-104 50 Stockholm
Lundberg, E.B.H.S.	Research Institute of Swedish National Defence, S-104 50 Stockholm
Stamm'ler, R.	ASEA-ATOM, Box 53, S-721 04, Vesterås
Strömberg, L.G.	Research Institute of National Defence, Stockholm 80
Wallin, L.B.	Research Institute of National Defence, Stockholm 80
Wallin, M.	AB Atomenergi, Stockholm 43, BP 43041, S-100 72 Stockholm 43
Wiedling, T.	AB Atomenergi, Studsvik-Nyköping

SWITZERLAND

Brunner, J.	Eidgenössisches Institut für Reaktorforschung, Würenlingen
Widder, F.	Eidgenössisches Institut für Reaktorforschung, Würenlingen

THAILAND

Methasiri, T.	Office of Atomic Energy for Peace, Bangkok

UNION OF SOVIET SOCIALIST REPUBLICS

Abramov, A.I.	Institute of Physics and Power Engineering, Obninsk
Muradyan, G.V.	I.V. Kurchatov Institute of Atomic Energy, Moscow
Sukhoruchkin, S.I.	Institute of Experimental and Theoretical Physics, Moscow
Tchernilin, Yu.F.	I.V. Kurchatov Institute of Atomic Energy, Moscow

UNITED ARAB REPUBLIC

Adib, M.	Institute of Theoretical and Experimental Physics, Moscow

UNITED KINGDOM

Askew, J.R.	Atomic Energy Establishment, Winfrith, Dorset
Cabell, M.J.	Atomic Energy Research Establishment, Harwell, Berks
Campbell, C.G.	U.K. Atomic Energy Authority, A.E.E., Winfrith, Dorset
Colvin, D.W.	UKAEA, Harwell, Didcot, Berks.
Crocker, V.S.	UKAEA, Harwell, Didcot, Berks.
Hunt, J.B.	National Physical Laboratory, Queens Road, Teddington, Middlesex
James, G.D.	AERE, Harwell, Didcot, Berks.
Kinchin, G.H.	UKAEA, DERE, Thurso Caithness, Scotland
Lynn, J.E.	Atomic Energy Research Establishment, Harwell, Didcot, Berks
Moxon, M.C.	Atomic Energy Research Establishment, Harwell, Didcot, Berks
Rae, E.R.	Atomic Energy Research Establishment, Harwell, Didcot, Berks
Robertson, J.C.	National Physical Laboratory, Teddington, Middlesex
Rose, B.	Atomic Energy Research Establishment, Harwell, Berks

Rowlands, J.L.	Atomic Energy Research Establishment, Winfrith, Dorset
Sowerby, M.G.	UKAEA, AERE, Harwell, Didcot, Berks
Story, J.S.	Atomic Energy Research Establishment, Winfrith, Dorset

UNITED STATES OF AMERICA

Adler, D.B.	University of Illinois, Physics Department, Urbana, Illinois 61801
Adler, F.T.	University of Illinois, Physics Department, Urbana, Illinois 61801
Alter, H.	Atomics International, 8900 Desoto Avenue, Canoga Park, Calif. 91304
Best, G.H.	University of California, Los Alamos, Scientific Laboratory, Los Alamos, N. Mex.
Clayton, D.D.	Rice University, Houston, Texas 77001
Davey, W.G.	Argonne National Laboratory, P.O. Box 2528, Idaho Falls, Idaho 83401
Farrell, John A.	University of California, Los Alamos Scientific Laboratory, Los Alamos, New Mexico 87544
Fricke, M.P.	Gulf General Atomic Inc., P.O.B. 608, San Diego, Calif. 92112
Garrison, J.	San Diego State, San Diego, Calif. 92115
Havens, W.	Columbia University, 538, West 120 Street, New York, N.Y. 10027
Hubbard, H.	Rand Corporation, 1700 Main St., Santa Monica, Calif. 90406
Hutchins, B.A.	Breeder Reactor Div. Operation, General Electric Co, 310 de Guigne, Sunnyvale, Calif.
Kolstad, G.A.	US Atomic Energy Commission, Washington, D.C.
Moore, M.S.	Los Alamos Scientific Laboratory, Los Alamos, New Mexico 87544

Pearlstein, S.	Brookhaven National Laboratory, Upton, N.Y.
Poenitz, W.P.	Argonne National Laboratory, S. Cass Avenue, Argonne, Ill.
Prince, A.	Brookhaven National Laboratory, Upton, N.Y.
Reynolds, J.T.	General Electric Co., Knolls Atomic Power Laboratory, Schenectady, N.Y.
de Saussure, G.	Oak Ridge National Laboratory, Oak Ridge, Tenn.
Taschek, R.F.	Los Alamos Scientific Laboratory, Los Alamos, N.Mex.
De Volpi, A.	Argonne National Laboratory, Argonne, Ill. 60439
Wasson, O.	Brookhaven National Laboratory, Upton, N.Y.

YUGOSLAVIA

Marković, M.	Institute of Nuclear Sciences B. Kidrič, P.O. Box 522, Beograd
Najžer, M.	Institute "Jozef Stefan", Ljubljana, Jamova 38
Rant, J.	Institute "Jozef Stefan", Ljubljana, Jamova 38

ORGANIZATIONS

ENEA/OECD

Koinig, H.G.	OECD High Temperature Reactor Project Dragon, A.E.E. Winfrith, Dorchester, Dorset
Liskien, H.O.	ENEA/CCDN, 91 Gif-sur-Yvette
Schett, A.	ENEA/CCDN, 91 Gif-sur-Yvette
Solanes, M.	European Nuclear Energy Agency, OECD, 38 Bd. Suchet, Paris XVI
Tubbs, N.A.	ENEA/CCDN, B.P.9 - 91 Gif-sur-Yvette
Valente, S.	ENEA/CCDN, P.B. 9 - 91 Gif-sur-Yvette

EURATOM

Ahmed, N.	CBNM - Geel, Steenweg naar Retie, Belgium
Aten, A.	Bureau Central des Mesures Nucléaires, Geel, Belgium
Beckev, W.	EURATOM, Geel, Weg up Retie, Belgium
Beonio-Brocchieri, F.	C.C.R. EURATOM, Ispra (Varese), Italy
Böckhoff, K.H.	Central Bureau for Nuclear Measurements, Geel, Steenweg naar Retie, Belgium
Coppola, M.	Central Bureau for Nuclear Measurements, Geel, Steenweg naar Retie, Belgium
Deruytter, A.J.	Central Bureau for Nuclear Measurements, Geel, Steenweg naar Retie, Belgium
Dierckx, L.A.R.	C.C.R., Ispra (Varese), Italy
Knitter, H.H.	Central Bureau for Nuclear Measurements, Geel, Steenweg naar Retie, Belgium
Kolar, W.	Central Bureau for Nuclear Measurements, Geel, Steenweg naar Retie, Belgium
Maracci, G.	C.C.R., Ispra (Varese), Italy
Rohr, G.	Central Bureau for Nuclear Measurements, Geel, Steenweg naar Retie, Belgium
Rustichelli, F.	C.C.R., Ispra (Varese), Italy
Theobald, J.P.	Central Bureau for Nuclear Measurements, Geel, Steenweg naar Retie, Belgium

IAEA

Schmidt, J.J.	Vienna

JINR

Florek, M.	Joint Institute of Nuclear Research, P.O.B.79, Moscow
Popov, Yu.	Joint Institute of Nuclear Research, P.O.B.79, Moscow
Stempinsky, M.	Joint Institute of Nuclear Research, P.O.B. 79, Moscow

AUTHOR INDEX

Numerals underlined refer to the first page of a paper by the author concerned.
Further numerals denote comments and questions in the discussions.

TRANSLITERATION INDEX

Абагян, Л. П.	Abagyan, L.P.
Абрамов, А. И.	Abramov, A.I.
Адамчук, Ю. В.	Adamchuk, Yu.V.
Беляев, Ф. Н.	Belyaev, F.N.
Бёмер, Б.	Böhmer, B.
Вергман, А. А.	Bergman, A.A.
Боровлев, С. П.	Borovlev, S.P.
Бродер, Д. Л.	Broder, D.L.
Ваньков, А. А.	Vankov, A.A.
Вертебный, В. П.	Vertebny, V.P.
Веселова, Г. М.	Veselova, G.M.
Власов, М. Ф.	Vlasov, M.F.
Воробьева, В. Г.	Vorobeva, V.G.
Гамалий, А. Ф.	Gamaly, A.F.
Гнидак, Н. Л.	Gnidak, N.L.
Григорев, Ю. В.	Grigorev, Yu.V.
Дьяченко, П. П.	Dyachenko, P.P.
Захарова, С. М.	Zakharova, S.M.
Замятнин, Ю. С.	Zamyatnin, Yu.S.
Игнатьев, К. Г.	Ignatev, K.G.
Игнатюк, А. В.	Ignatyuk, A.V.
Калашников, А. Г.	Kalashnikov, A.G.
Кирилюк, А. Л.	Kirilyuk, A.L.
Коллатц, З.	Kollatz, Z.
Колосов, Н. П.	Kolosov, N.P.
Колотый, В. В.	Koloty, V.V.
Кононов, В. Н.	Kononov, V.N.
Котельникова, Г. В.	Kotelnikova, G.V.
Крошкин, Н. И.	Kroshkin, N.I.
Кузьминов, Б. Д.	Kuzminov, B.D.
Кузнецов, В. А.	Kuznetsov, V.A.
Куров, М. А.	Kurov, M.A.
Лашук, А. И.	Lashuk, A.I.
Ловчикова, Г. Н.	Lovchikova, G.N.
Мельников, А. К.	Melnikov, A.K.
Могильнер, А. И.	Mogilner, A.I.
Мостовая, Т. А.	Mostovaya, T.A.
Мостовой, В. И.	Mostovoy, V.I.
Мурадян, Г. В.	Muradyan, G.V.
Нестеров, В. Г.	Nesterov, V.G.
Нефедов, В. Н.	Nefedov, V.N.
Николаев, М. Н.	Nikolaev, M.N.
Нурпеисов, Б.	Nurpeisov, B.
Осипов, В. Н.	Osipov, V.N.

Павленко, Е.А.	Pavlenko, E.A.
Павлов, В.В.	Pavlov, V.V.
Паниткин, Ю.Г.	Panitkin, Yu.G.
Парамонова, И.Н.	Paramonova, I.N.
Пасечник, М.В.	Pasechnik, M.V.
Пикельнер, Л.В.	Pikelner, L.V.
Полетаев, Е.Д.	Poletaev, E.D.
Полозов, М.В.	Polozov, M.V.
Попов, Ю.	Popov, Yu.
Прохорова, Л.И.	Prokhorova, L.I.
Прокопец, Ю.С.	Prokopets, Yu.S.
Пшитула, М.	Pshitula, M.
Разбудей, Б.Ф.	Razbudey, B.F.
Руми, Р.Ф.	Rumi, R.F.
Рябов, Ю.В.	Ryabov, Yu.V.
Садохин, И.П.	Sadokhin, I.P.
Сальников, О.А.	Salnikov, O.A.
Самсонов, А.Е.	Samsonov, A.E.
Савин, М.В.	Savin, M.V.
Сергачев, А.И.	Sergachev, A.I.
Смиренкин, Г.Н.	Smirenkin, G.N.
Смиренкина, Л.Д.	Smirenkina, L.D.
Со Дон Сик	So Don Sik
Солдатов, А.Н.	Soldatov, A.N.
Ставинский, В.С.	Stavinsky, V.S.
Стависский, Ю.Я.	Stavissky, Yu.Ya.
Стемпинский, М.	Stempinski, M.
Сухоручкин, С.И.	Sukhoruchkin, S.I.
Толстиков, В.А.	Tolstikov, V.A.
Тошинский, Г.И.	Toshinsky, G.I.
Труфанов, А.М.	Trufanov, A.M.
Турчин, Ю.М.	Turchin, Yu.M.
Федорова, А.Ф.	Fedorova, A.F.
Фетисов, Н.П.	Fetisov, N.I.
Филиппов, В.В.	Filippov, V.V.
Флорек, М.	Florek, M.
Фокин, Г.Н.	Fokin, G.N.
Фурман, В.И.	Furman, V.I.
Хохлов, Ю.А.	Khokhlov, Yu.A.
Чернилин, Ю.Ф.	Chernilin, Yu.F.
Чернов, Л.А.	Chernov, L.A.
Чиков, Н.	Chikov, N.
Челноков, В.Б.	Chelnokov, V.B.
Шубин, Ю.Н.	Shubin, Yu.N.
Щепкин, Ю.Г.	Shchepkin, Yu.G.
Яньков, Г.Б.	Yankov, G.B.

IAEA SALES AGENTS AND BOOKSELLERS

Orders for Agency publications can be placed with your bookseller or any of the addresses listed below:

ARGENTINA
Comisión Nacional de
Energía Atómica
Avenida del Libertador 8250
Buenos Aires

AUSTRALIA
Hunter Publications
23 McKillop Street
Melbourne, C.1

AUSTRIA
Publishing Section
International Atomic Energy Agency
Kärntner Ring 11
P.O. Box 590
A-1011 Vienna

BELGIUM
Office International
de Librairie
30, Avenue Marnix
Brussels 5

CANADA
Information Canada
Ottawa, Canada

C.S.S.R.
S.N.T.L.
Spolena 51
Nové Mesto
Prague 1

DENMARK
Ejnar Munksgaard Ltd.
6 Norregade
DK-1165 Copenhagen K

FRANCE
Office International de
Documentation et Librairie
48, Rue Gay-Lussac
F-75 Paris 5e

HUNGARY
Kultura
Hungarian Trading Company
for Books and Newspapers
P.O. Box 149
Budapest 62

INDIA
Oxford Book & Stationery Comp.
17, Park Street
Calcutta 16

ISRAEL
Heiliger & Co.
3, Nathan Strauss Str.
Jerusalem

ITALY
Agenzia Editoriale Commissionaria
A.E.I.O.U.
Via Meravigli 16
I-20123 Milan

JAPAN
Maruzen Company, Ltd.
P.O. Box 5050,
100-31 Tokyo International

MEXICO
Librería Internacional, S.A.
Av. Sonora 206
México 11, D.F.

NETHERLANDS
Martinus Nijhoff N.V.
Lange Voorhout 9
P.O. Box 269
The Hague

PAKISTAN
Mirza Book Agency
65, Shahrah Quaid-E-Azam
P.O. Box 729
Lahore - 3

POLAND
Ars Polona
Centrala Handlu Zagranicznego
Krakowskie Przedmiescie 7
Warsaw

ROMANIA
Cartimex
3-5 13 Decembrie Street
P.O. Box 134-135
Bucarest

SPAIN
Librería Bosch
Ronda Universidad 11
Barcelona - 7

SWEDEN
C.E. Fritzes Kungl. Hovbokhandel
Fredsgatan 2
Stockholm 16

SWITZERLAND
Librairie Payot
Rue Grenus 6
CH-1211 Geneva 11

U.S.S.R.
Mezhdunarodnaya Kniga
Smolenskaya-Sennaya 32-34
Moscow G-200

U.K.
Her Majesty's Stationery Office
P.O. Box 569
London S.E.1

U.S.A.
UNIPUB, Inc.
P.O. Box 433
New York, N.Y. 10016

YUGOSLAVIA
Jugoslovenska Knjiga
Terazije 27
Belgrade

IAEA Publications can also be purchased retail at the United Nations Bookshop at United Nations Headquarters, New York, from the news-stand at the Agency's Headquarters, Vienna, and at most conferences, symposia and seminars organized by the Agency.

In order to facilitate the distribution of its publications, the Agency is prepared to accept payment in UNESCO coupons or in local currencies.

Orders and inquiries from countries not listed above may be sent to:

Publishing Section
International Atomic Energy Agency
Kärntner Ring 11
P.O. Box 590
A-1011 Vienna, Austria

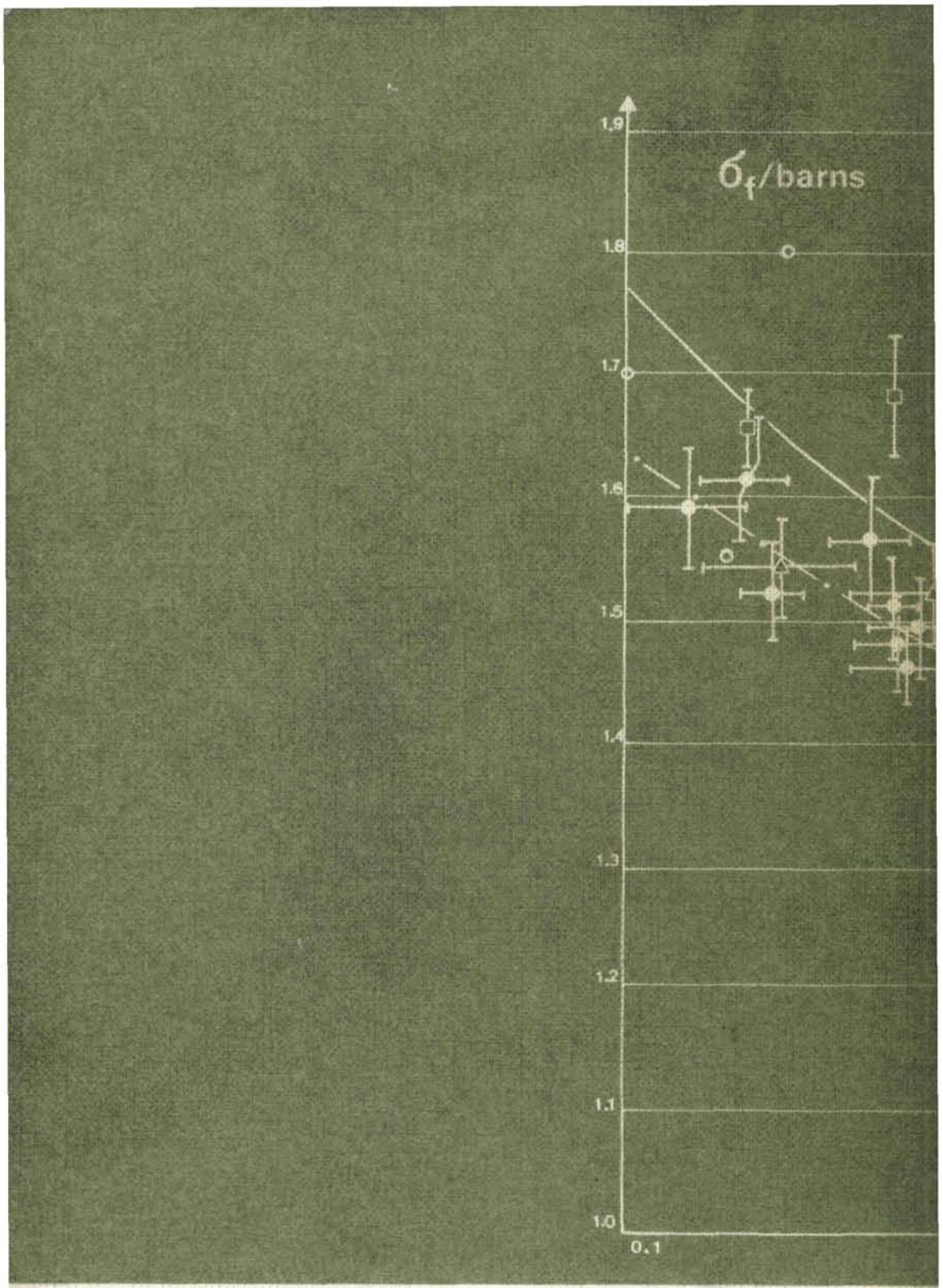

INTERNATIONAL
ATOMIC ENERGY AGENCY
VIENNA, 1970

PRICE: US $24.00
Austrian Schillings 620,-
(£10.0.0; F.Fr.133,20; DM 87,80)

SUBJECT GROUP: III
Physics/Nuclear Data